



(4)

MARINE PHYSICAL LABORATORY

SCRIPPS INSTITUTION OF OCEANOGRAPHY

San Diego, California 92152

AD-A220 173

FREELY DRIFTING SWALLOW FLOAT ARRAY: SEPTEMBER 1987 TRIP REPORT

G. L. D'Spain, W. S. Hodgkiss, and G. L. Edmonds

DTIC
ELECTED
APR 03 1990
S B D
CC

MPL TECHNICAL MEMORANDUM 413

MPL-U-60/89
August 1989

Approved for public release; distribution unlimited.

100

REPORT DOCUMENTATION PAGE

1a. REPORT SECURITY CLASSIFICATION UNCLASSIFIED		1b. RESTRICTIVE MARKINGS										
2a. SECURITY CLASSIFICATION AUTHORITY		3. DISTRIBUTION/AVAILABILITY OF REPORT Approved for public release; distribution unlimited.										
2b. DECLASSIFICATION/DOWNGRADING SCHEDULE												
4. PERFORMING ORGANIZATION REPORT NUMBER(S) MPL TECHNICAL MEMORANDUM 413 [MPL-U-60/89]		5. MONITORING ORGANIZATION REPORT NUMBER(S)										
6a. NAME OF PERFORMING ORGANIZATION Marine Physical Laboratory	6b. OFFICE SYMBOL (if applicable) MPL	7a. NAME OF MONITORING ORGANIZATION Office of Naval Research Department of the Navy										
6c. ADDRESS (City, State, and ZIP Code) University of California, San Diego Scripps Institution of Oceanography San Diego, CA 92152		7b. ADDRESS (City, State, and ZIP Code) 800 North Quincy Street Arlington, VA 22217-5000										
8a. NAME OF FUNDING/SPONSORING ORGANIZATION Office of Naval Research	8b. OFFICE SYMBOL (if applicable) ONR	9. PROCUREMENT INSTRUMENT IDENTIFICATION NUMBER N00014-87-C-0127										
8c. ADDRESS (City, State, and ZIP Code) Department of the Navy 800 North Quincy Street Arlington, VA 22217-5000		10. SOURCE OF FUNDING NUMBERS PROGRAM ELEMENT NO. PROJECT NO. TASK NO. WORK UNIT ACCESSION NO.										
11. TITLE (Include Security Classification) FREELY DRIFTING SWALLOW FLOAT ARRAY: SEPTEMBER 1987 TRIP REPORT												
12. PERSONAL AUTHOR(S) G. L. D'Spain, W. S. Hodgkiss, and G. L. Edmonds												
13a. TYPE OF REPORT tech memo	13b. TIME COVERED FROM _____ TO _____	14. DATE OF REPORT (Year, Month, Day) August 1989	15 PAGE COUNT									
16. SUPPLEMENTARY NOTATION												
17. COSATI CODES <table border="1"><tr><th>FIELD</th><th>GROUP</th><th>SUB-GROUP</th></tr><tr><td></td><td></td><td></td></tr><tr><td></td><td></td><td></td></tr></table>		FIELD	GROUP	SUB-GROUP							18. SUBJECT TERMS (Continue on reverse if necessary and identify by block number) Swallow floats, vertical line array, ocean bottom seismometer,	
FIELD	GROUP	SUB-GROUP										
19. ABSTRACT (Continue on reverse if necessary and identify by block number) Representative data collected during the 17-18 September, 1987 deployment of the Swallow floats are presented in this report. These data include those collected by the Marine Physical Laboratory's (MPL) set of 12 Swallow floats, as well as data recorded by two other concurrently-deployed sensor systems; an ocean bottom seismometer operated by Dr. L. Dorman's group at Scripps Institution of Oceanography and MPL's 900-meter-long, 120-channel, vertical line array. The deployment location, 35.0° N, 126.0° W, was about 410 km southwest of Monterey, California. The nine midwater Swallow floats were ballasted for depths starting at 400 meters and spaced every 300 meters, to 2800 meters. They were put into the water at about the geometric center of a triangle, whose sides were approximately 6.5 km in length, formed by the three remaining floats which were tethered to the ocean bottom by 4.57-meter lines. The ocean bottom seismometer (OBS) was deployed by free-fall from the research vessel Sproul												
20. DISTRIBUTION/AVAILABILITY OF ABSTRACT <input type="checkbox"/> UNCLASSIFIED/UNLIMITED <input checked="" type="checkbox"/> SAME AS RPT. <input type="checkbox"/> DTIC USERS		21. ABSTRACT SECURITY CLASSIFICATION UNCLASSIFIED										
22a. NAME OF RESPONSIBLE INDIVIDUAL W. S. Hodgkiss		22b. TELEPHONE (Include Area Code) (619) 534-1798	22c. OFFICE SYMBOL MPL									

through 4670-meter-deep water. The vertical line array (VLA) was suspended from the underside of the research platform FLIP. It spanned the depths from 400 meters to 1300 meters during the 24-hour Swallow float data recording period. Both the ocean bottom seismometer and the R/P FLIP, which was constrained by a three-point mooring, were located at the approximate center of the triangle formed by the bottom-tethered Swallow floats.

This report presents the instrument deployment locations and times, the positions and characteristics of known signal sources, environmental data such as expendable bathythermograph (XBT), conductivity-temperature-depth (CTD), and anemometer measurements as well as basic weather observations, and representative Swallow float, OBS, and VLA data. The Swallow float data include battery voltage, compass heading, and automatic gain control (AGC) measurements, the 8 kHz acoustic localization ping arrivals, and the infrasonic water particle velocity data. All 12 Swallow floats operated flawlessly, except for float 1's 8 kHz localization hydrophone which was destroyed during deployment, resulting in a 99.5 % full data set. The OBS geophone and hydrophone data and the VLA hydrophone channel data have first been resampled to 50 Hz, the Swallow float sampling frequency, so that quantitative comparisons can be made between the data sets.

A number of interesting features can be seen in a preliminary look at these data. First, the Swallow floats were clearly able to hear the 11, 16, 21, and 22 Hz tones generated by the HLF 3 source deployed at long range from the sensors. The vertical line array also appeared to hear the 16 Hz and 22 Hz tones, although a 22 Hz line occurred in many of the spectra during times when the HLF 3 was transmitting 16 Hz, and a 16 Hz line occurred when the source was transmitting 22 Hz. The origin of these contaminating lines, including an additional line at 20 Hz, is unknown. The array apparently did not detect the 11 Hz tone. The ocean bottom seismometer could hear neither the 11 Hz or the 22 Hz tones. Second, both of the 60-lb explosive charges which were detonated on the ocean bottom during the Swallow float recording period generated identifiable arrivals in the Swallow float data. The second charge, which was believed to have failed, actually partially detonated; its arrivals were much smaller in amplitude. Long-duration oscillatory signals following the detonation of the first 60-lb charge were recorded by the vertical geophone components on two of the bottom-tethered Swallow floats. These signals have been identified as the water-borne expression of the sediment-waveguide-trapped Scholte waves. Third, a seismic profiler was operating during much of the experiment. From an examination of the Swallow float data, it was located either due north or due south of the experiment site. Its signals caused an increase of up to 10 dB in the background noise levels between 6 and 16 Hz (and above 20 Hz) in both the Swallow float and the VLA spectra. The profiler signals were not detected in the OBS data. Fourth, a lump of spectral energy centered about 18 Hz, previously identified in the VLA data as strum contamination, is also present in the Swallow float and the OBS spectra. It appears to be the result of 0.5-to-1.0-second-duration "clicks" which occur every 24 to 30 seconds in the Swallow float time series. These signals have properties identical to those associated with finback whale noises. Fifth, an arrival in the Swallow float time series has tentatively been identified as the arrival of the T phase from a magnitude 4.7 earthquake in the Fox Islands in the Aleutian Island chain. The T phase has also been detected in VLA data which are not presented in this report.

Although the OBS hydrophone data appear contaminated by broadband noise of non-acoustic nature, the OBS geophone data are high in quality. The horizontal-component data are much more self consistent and less variable in time than those from the April, May, 1987 deployment at DSDP 469. A comparison of these OBS geophone data with concurrently-recorded Swallow float data show main features in common with a comparison of recently-collected Swallow float data from an infrasonic hydrophone data and from an externally-mounted geophone resting on the ocean sediment. The comparison of the vertical line array data with the Swallow float data shows that, by careful data selection, the effects of flow and strum contamination in the VLA data can be isolated to frequencies below 10 Hz.

Freely Drifting Swallow Float Array: September 1987 Trip Report

G. L. D'Spain, W. S. Hodgkiss, and G. L. Edmonds

Marine Physical Laboratory
Scripps Institution of Oceanography
San Diego, CA 92152

ABSTRACT

Representative data collected during the 17-18 September, 1987 deployment of the Swallow floats are presented in this report. These data include those collected by the Marine Physical Laboratory's (MPL) set of 12 Swallow floats, as well as data recorded by two other concurrently-deployed sensor systems; an ocean bottom seismometer operated by Dr. L. Dorman's group at Scripps Institution of Oceanography and MPL's 900-meter-long, 120-channel, vertical line array. The deployment location, 35.0° N, 126.0° W, was about 410 km southwest of Monterey, California. The nine midwater Swallow floats were ballasted for depths starting at 400 meters and spaced every 300 meters, to 2800 meters. They were put into the water at about the geometric center of a triangle, whose sides were approximately 6.5 km in length, formed by the three remaining floats which were tethered to the ocean bottom by 4.57-meter lines. The ocean bottom seismometer (OBS) was deployed by free-fall from the research vessel Sproul through 4670-meter-deep water. The vertical line array (VLA) was suspended from the underside of the research platform FLIP. It spanned the depths from 400 meters to 1300 meters during the 24-hour Swallow float data recording period. Both the ocean bottom seismometer and the R/P FLIP, which was constrained by a three-point mooring, were located at the approximate center of the triangle formed by the bottom-tethered Swallow floats.

This report presents the instrument deployment locations and times, the positions and characteristics of known signal sources, environmental data such as expendable bathythermograph (XBT), conductivity-temperature-depth (CTD), and anemometer measurements as well as basic weather observations, and representative Swallow float, OBS, and VLA data. The Swallow float data include battery voltage, compass heading, and automatic gain control (AGC) measurements, the 8 kHz acoustic localization ping arrivals, and the infrasonic water particle velocity data. All 12 Swallow floats operated flawlessly, except for float 1's 8 kHz localization hydrophone which was destroyed during deployment, resulting in a 99.5 % full data set. The OBS geophone and hydrophone data and the VLA hydrophone channel data have first been resampled to 50 Hz, the Swallow float sampling frequency, so that quantitative comparisons can be made between the data sets.

A number of interesting features can be seen in a preliminary look at these data. First, the Swallow floats were clearly able to hear the 11, 16, 21, and 22 Hz tones generated by the HLF 3 source deployed at long range from the sensors. The vertical line array also appeared to hear the 16 Hz and 22 Hz tones, although a 22 Hz line occurred in many of the spectra during times when the HLF 3 was transmitting 16 Hz, and a 16 Hz line occurred when the source was transmitting 22 Hz. The origin of these contaminating lines, including an additional line at 20 Hz, is unknown. The array apparently did not detect the 11 Hz tone. The ocean bottom seismometer could hear neither the 11 Hz or the 22 Hz tones. Second, both of the 60-lb explosive charges which were detonated on

the ocean bottom during the Swallow float recording period generated identifiable arrivals in the Swallow float data. The second charge, which was believed to have failed, actually partially detonated; its arrivals were much smaller in amplitude. Long-duration oscillatory signals following the detonation of the first 60-lb charge were recorded by the vertical geophone components on two of the bottom-tethered Swallow floats. These signals have been identified as the water-borne expression of the sediment-waveguide-trapped Scholte waves. Third, a seismic profiler was operating during much of the experiment. From an examination of the Swallow float data, it was located either due north or due south of the experiment site. Its signals caused an increase of up to 10 dB in the background noise levels between 6 and 16 Hz (and above 20 Hz) in both the Swallow float and the VLA spectra. The profiler signals were not detected in the OBS data. Fourth, a lump of spectral energy centered about 18 Hz, previously identified in the VLA data as strum contamination, is also present in the Swallow float and the OBS spectra. It appears to be the result of 0.5-to-1.0-second-duration "clicks" which occur every 24 to 30 seconds in the Swallow float time series. These signals have properties identical to those associated with finback whale noises. Fifth, an arrival in the Swallow float time series has tentatively been identified as the arrival of the T phase from a magnitude 4.7 earthquake in the Fox Islands in the Aleutian Island chain. The T phase has also been detected in VLA data which are not presented in this report.

Although the OBS hydrophone data appear contaminated by broadband noise of non-acoustic nature, the OBS geophone data are high in quality. The horizontal-component data are much more self-consistent and less variable in time than those from the April, May, 1987 deployment at DSDP 469. A comparison of these OBS geophone data with concurrently-recorded Swallow float data show main features in common with a comparison of recently-collected Swallow float data from an infrasonic hydrophone data and from an externally-mounted geophone resting on the ocean sediment. The comparison of the vertical line array data with the Swallow float data shows that, by careful data selection, the effects of flow and strum contamination in the VLA data can be isolated to frequencies below 10 Hz.

July 20, 1989

Table of Contents

- I. Introduction
- I. Deployment Geometry and Times
 - a) Swallow Float Deployment and Retrieval
 - b) OBS Deployment
 - c) R/P FLIP Vertical Line Array Deployment
 - d) Deployment Depths
- II. Sound Sources
 - a) R/V Sprout Ship Tracks
 - b) Explosive Charges
 - c) HLF 3 Source Deployed from De Steiger
 - d) Seismic Profiler
- III. Swallow Float Log Summary
- IV. Environmental Data
 - a) XBT Data from R/P FLIP
 - b) CTD Data from De Steiger
 - c) Anemometer Readings from R/V Sprout R/P FLIP
 - d) Additional Environmental Data
- V. Initial Indication of Data Integrity
 - a) Swallow Float Data
 - b) FLIP Vertical Line Array Data
- VI. Swallow Float Battery Voltage, Float Heading, and AGC Level
 - a) Battery Voltage
 - b) Float Heading
 - c) AGC Level
- VII. Swallow Float 8 kHz Surface and Bottom Bounce Data
- VIII. Swallow Float 8 kHz Interelement Range Data
- IX. Swallow Float RMS Velocity
- X. Geophone and Hydrophone Time Series
 - a) Swallow Float Data
 - b) Ocean Bottom Seismometer Data
 - c) FLIP Vertical Line Array Data
- XI. Acoustic Velocity and Pressure Autospectra and Spectral Ratios
 - a) Swallow Float Data
 - b) Ocean Bottom Seismometer Data
 - c) FLIP Vertical Line Array Data
- Acknowledgements
- References
- Appendix 1 - Swallow Float Geophone Data Acquisition System
- Appendix 2 - Calibration Curves for the OBS Instruments
- Appendix 3 - Calibration Curve for the Vertical Line Array Channels
- Appendix 4 - Differences in Navigation Position Fixes
- Figures



Accession For	
NTIS GRA&I <input checked="" type="checkbox"/> DTIC TAB <input type="checkbox"/> Unannounced <input type="checkbox"/>	
Justification	
By _____	
Distribution/ _____	
Availability Codes	
Dist	Avail and/or Special
A-1	

Introduction

This trip report presents representative data collected during the 17-18 September, 1987 deployment of the Marine Physical Laboratory's Swallow floats at 35.0° N, 126.0° W, about 410 km southwest of Monterey, California. The Swallow float deployment was part of a larger experiment involving the deployment, at the same location, of the Marine Physical Laboratory's 900-meter-long hydrophone array, suspended in the vertical direction from FLIP. The larger experiment is described in reference [1]; this report will be restricted to those data collected concurrently with the Swallow floats on 17-18 September. These data include the very low frequency (VLF) geophone data collected by the Swallow floats, low frequency (LF) hydrophone data recorded by the 120-element vertical line array (VLA) from FLIP, and both geophone and hydrophone data collected by an ocean bottom seismometer (OBS). A second OBS which was deployed did not provide useable data. Also concurrently deployed were four air-launched sonobuoys whose data were apparently not properly recorded. However, it was reported by personnel involved in real-time monitoring of the analog sonobuoy data that the sonobuoys heard the HLF 3 source deployed from the De Steiger (re Section IIc).

The 12 Swallow floats, which have been under development at the Marine Physical Laboratory, are neutrally buoyant, independently drifting, very low frequency (1-20 Hz), acoustic particle velocity sensors. They each contain within a 0.432 m diameter glass shell three orthogonally-oriented geophones for measuring infrasonic particle velocity, a magnetic compass, and the necessary hardware to record up to 25 hours of data. They also contain an 8 kHz acoustic localization system [2,3,4,5]. Figure 1 is a schematic drawing of a typical midwater float. In this experiment, twelve Swallow floats were deployed; nine were freely drifting in the water column and three were tethered to the ocean bottom by 4.57-meter lines. The nine mid-water floats were deployed in a quasi vertical line array geometry with a vertical float separation of about 300 m, starting at about 400 m depth to about 2800 m. The three bottom-tethered floats were positioned at the corners of a triangle with sides of length about 6.5 km. Except for a non-functioning 8 kHz localization hydrophone on float 1, all twelve floats operated flawlessly during the experiment.

Note that all times listed in this report are in local Pacific Daylight Time. To obtain Greenwich Mean Time, add 7 hours to the local time.

I. Deployment Geometry and Times

a) Swallow Float Deployment and Retrieval

Figure I.1 shows the NAVSAT position fixes of the R/V R. G. Sproul at those times when each of the Swallow floats were deployed and at those times when they were recovered. Both the deployment and retrieval times and the NAVSAT position fixes are listed in the Swallow float log summary in Section III. The three bottom-mounted floats, floats 9, 10 (indicated by the hexadecimal "A"), and 11 (indicated by "B"), formed a triangular array so that stable absolute position fixes could be obtained for the midwater-column buoys. The remaining nine midwater-column floats, which were ballasted for a depth spacing of about 300 m, starting at 400 m and extending to 2800 m, were deployed in the approximate center of the triangular array. The retrieval positions are all located to the east and southeast of the deployment positions.

Indicated on the figure just to the west of the mid-water float deployment positions is the position of the moored FLoating Instrument Platform (FLIP). This position fix was calculated from the range and bearing from FLIP (300 m and 145°) of the R/V Sproul at the time of the deployment of mid-water Swallow float 8. It was used instead of the Loran-C position fix or the GPS position fixes of FLIP since offsets exist between these navigation methods. The problem of consistency in the position fixes from the various navigation techniques used in the experiment is discussed in Appendix 4 and in part c below.

The Swallow floats were synchronously started and began recording data at 17:55, 17 September, but the majority of the midwater floats did not equilibrate at depth until after record 600, or about 01:30, 18 September. They recorded data until approximately record 1950, or 18:00, 18 September.

b) OBS Deployment

Also indicated on Figure I.1 using the letter "J" is the NAVSAT position fix of the Sproul during the deployment of the single properly operating ocean bottom seismometer, OBS Judy (capsule #8). The other OBS which was deployed, OBS Janice (capsule #9), did not provide any useable data. (For the actual position fixes and the times of deployment, refer to the Swallow float log summary in Section III). Note that at the time of OBS Judy's deployment, the range and bearing from R/P FLIP of the R/V Sproul was 1.090 km and 154°; therefore, the relationship between the positions of OBS Judy and FLIP in the figure is not quite correct.

The OBSs were deployed by free-fall through the water column from the R/V Sproul. OBS Judy was programmed to record 3 minutes of data every half hour on the half-hour mark. Its internal tape capacity was sufficient to record up to a total of six hours of data. The following table lists the starting times for the OBS events which were written while the Swallow floats were recording data.

OBS Judy (#8) Data Recording Times Sept, 1987

(Times are in local Pacific Daylight Time; add 7 hours to get GMT).

Event	Date	Time (hr:min:sec) of First Sample	Duration of Event (sec)	Swallow Float Record Number
901	9-18	14:59:57.504	179	1687
902	9-18	15:29:57.504	179	1727
903	9-18	15:59:57.505	179	1767
904	9-18	16:29:57.505	179	1807
905	9-18	18:29:57.506	179	1967

906

9-18

18:59:57.506

179

2007

During each 3-minute data-collection period (actually 179 sec), the OBSs sample at a 128-Hz rate. In order to make a quantitative comparison between the OBS and the Swallow float data, the OBS data were resampled to the 50-Hz sampling rate of the Swallow floats. This process is described in reference [14]. The effective bandwidth of the ocean bottom seismometers is from 0.1-30 Hz compared to an effective bandwidth for the Swallow floats of around 0.5 Hz to 20 Hz. For additional information on the OBSs, see reference [6].

c) R/P FLIP Vertical Line Array Deployment

As mentioned in the Introduction, the deployment of the Marine Physical Laboratory's 900-meter-long vertical line array (VLA) from FLIP was part of a larger experiment which is described in reference [1]. The VLA was first deployed on 10 September, 1987 and it subsequently recorded 19 days of almost continuous data. At that time, it was the longest vertical line array deployed to date. It is a 12-bit digital array composed of 12 sections with 10 hydrophone channels in each section for a total of 120 channels. The channels are equally spaced at 7.5-meter intervals, resulting in a frequency of 100 Hz for the half-wavelength criterion. During the time in which the Swallow floats were deployed, the array spanned the depths from about 400 meters to 1300 meters. The array was constrained to remain almost perfectly vertical [8] by a 420 kg weight attached to its lower end [7]. The pass band of the hydrophone channels was from 10 Hz, due to the low-frequency roll-off caused by a single high-pass resistor-capacitor circuit formed partially by the hydrophones' equivalent capacitance, to 250 Hz. The data sampling rate was 500 Hz. Each array section also contained two 12 kHz navigation channels so that the array position and shape could be determined with the help of a three-element, bottom-mounted, transponder network. Additional information on the VLA can be obtained from reference [7].

Figure 1.2 shows the FLIP position fixes obtained by Loran-C, NAVSAT, and GPS navigation methods. Since FLIP was constrained by a three-point mooring to a maximum horizontal displacement from a reference position of about 150 meters [8], the variations in position fixes shown in this figure are due to inconsistencies in the navigation methods. A further comparison between these navigation methods is presented in Appendix 4.

The VLA recorded data almost continuously during the deployment of the Swallow floats. (It stopped recording data for a short period due to overloading caused by the detonation of the first 60-lb explosive charge deployed by the OBS group). Only a very small portion of these data are examined in this report. Five 9-minute blocks of data (4220 buffers), from all 120 channels were extracted and then desampled to 50 Hz. The following table lists the time of the first sample in each block of data.

Recording Times for Desampled VLA Data Sept, 1987

(Times are in local Pacific Daylight Time; add 7 hours to get GMT).

Data Tape Number	Date	Time (hr:min:sec) of First Sample	Swallow Float Record	Comments
433	9-18	07:45:15	1107	16 Hz line from De Steiger
440	9-18	10:46:00	1348	22 Hz line from De Steiger
442	9-18	11:55:00	1440	quiet but for R/V Sproul
447	9-18	13:50:00	1593	11 Hz line from De Steiger
453	9-18	16:26:00	1801	recording time of OBS event #904

d) Deployment Depths

The simultaneous deployment of the Swallow floats, the ocean bottom seismometer, and the 900-meter vertical line array provide a unique ambient noise data set. An initial comparison between these three sets of data is given in this report. Figure I.3 illustrates the coverage with respect to depth of these three sensor systems. The circles represent the approximate depths of the 12 Swallow floats (the exact depths can be gotten from the 8 kHz localization data in Section VII), the diamond represents OBS Judy, and the vertical line array is indicated by the line extending from 400 m to 1300 m. The dashed line at 4600 m represents the ocean bottom depth at the study site. Superimposed on this figure is an average sound speed profile for the area of the experiment obtained from historical temperature and salinity measurements archived by the National Oceanographic Data Center [9] and an equation relating temperature, salinity, and depth to sound speed [10]. The average sound speed profile has been linearly extended from 4000 m to 4500 m.

II. Sound Sources

a) R/V Sprout Ship Tracks

To correctly interpret the received signals on the Swallow floats, the VLA, and the ocean bottom seismometer, the NAVSAT position fixes of the Sprout were written intermittently into the scientific log book. The positions of the ship during the period from 15:00, 17 September (as the ship approached FLIP from the east) to 20:12, 19 September (as the Sprout prepared to leave for port after recovering all instruments) are plotted in Figure II.1. Each "+" in the figure indicates a log book entry. The entries were made at irregular time intervals and therefore ship speed information cannot be obtained directly from this plot. The tortuous track of the ship can be easily unraveled by plotting the positions for shorter time intervals. For example, plotted in Figure II.2 are the ship positions during the period when the midwater Swallow floats were recording data in the water column; from 19:00, 17 September to 19:00, 18 September.

In order to estimate the frequency of some of the possible narrow band signals generated by the R/V Sprout, the following information was obtained from the ship's engineer. At a 9 knot speed, the ship's two engines rotate at 1800 rpm. At this speed, then, the diesel shaft rate is 30 Hz. The reduction gear ratio is 5.17-to-one; the corresponding shaft rate is 5.8 Hz. Since the ship has four fixed blades on each of its two props, the blade rate is 23.2 Hz at this speed. An approximately linear relationship exists between engine rpm and ship speed when both screws are engaged. Measurements of the acoustic signature of the R/V Sprout are presented in reference [5].

b) Explosive Charges

Five explosive charges of about 60 lbs each were deployed on the ocean bottom by Prof. Dorman's group in order to study Scholte wave propagation in the sediment waveguide. The positions of the five charges and OBS Judy *relative to FLIP* are plotted in Figure II.3. In this figure, the reference triangle formed by the bottom-mounted Swallow floats was determined by NAVSAT, the position of R/P FLIP was calculated by the NAVSAT location of the Sprout and the range and bearing of the Sprout from FLIP when midwater Swallow float 8 was deployed, and the OBS and explosive charge locations are referenced to the FLIP position using the range and bearing from FLIP at the time of their deployment. (Note that the relative position of OBS Judy with respect to FLIP in this figure is more accurate than that shown in Figure I.1). Both the positions and times of detonation of these ocean bottom charges are listed in the following table.

Times and Locations of the 60-lb Explosive Charges on the Ocean Bottom						
All positions are referenced to 34° N, 125° W. Times of detonation are in local Pacific Daylight Time; add 7 hours to get GMT.						
Time of Detonation	Date	Swallow Float Record	NAVSAT on Sprout	Loran-C on Sprout	Range, Bearing from FLIP	Comments
13:00	9-18	1527	58.15', 58.60'	--	1.35 km, 173°	felt
14:30	9-18	1647	58.00', 57.82'	58.00', 57.33'	2.00 km, 160°	not felt
12:00	9-19	--	57.99', 58.13'	58.02', 57.41'	2.09 km, 160°	not felt
15:00	9-19	--	57.98', 57.72'	58.08', 57.27'	2.00 km, 154°	felt
16:00	9-19	--	58.21', 57.62'	57.93', 57.08'	2.30 km, 157°	not felt

Note that only the first two explosions were scheduled to detonate during the recording period of the

Swallow floats, which ended around 19:00, 18 September. These two detonation times correspond to Swallow float records 1527 and 1647, respectively. Note also that only the first and fourth detonations were felt on board the Sprout and FLIP. However, the floats recorded an arrival (actually a series of arrivals corresponding to the direct path, the surface bounce path, the surface-to-bottom-to-float path, the surface-to-bottom-to-surface-to-float path, and possibly even two-bottom-bounce phases) at exactly the expected time of arrival from the second explosive charge. Plots of Swallow float time series showing these phases are presented and discussed in Section X.

c) HLF 3 Source Deployed from De Steiger

An HLF 3 source was deployed at 150 meters depth from the De Steiger, another ship involved in the larger experiment. This ship was located to the west of R/P FLIP's position during the Swallow float deployment. The following table lists the starting times and the duration of transmission of the 11-Hz, 16-Hz, 21-Hz, and 22-Hz monotones broadcast by the source. Other tones, 27 Hz, 41 Hz, 56 Hz, 81 Hz, 98 Hz, 115 Hz, 135 Hz, and 159 Hz, were also transmitted, but they were outside the Swallow float frequency band of 0.5 to 25 Hz. The transmission starting times at the De Steiger have been corrected to local Pacific Daylight time at FLIP by adding one hour. Also listed are the corresponding Swallow float record intervals which have been corrected for the transit time from the De Steiger to FLIP.

Starting Times and Duration for In-Band Frequencies from HLF 3 Source					
Frequency (Hz)	Starting Transmission Time (Date)	Duration (sec)	Swallow Float Record Interval	OBS	
				Event	Event
16	18:54:25 (9-17)	1200	94-120	--	
11	19:17:25 (9-17)	1200	125-151	--	
21	20:11:25 (9-17)	1200	197-223	--	
16	22:52:25 (9-17)	1200	412-438	--	
11	23:15:25 (9-17)	1200	442-468	--	
21	00:07:25 (9-18)	3600	512-591	--	
16	07:31:55 (9-18)	3600	1104-1183	--	
11	08:35:25 (9-18)	3600	1189-1268	--	
22	10:34:25 (9-18)	1200	1348-1374	--	
16	13:15:25 (9-18)	1200	1562-1588	--	
11	13:38:25 (9-18)	1200	1593-1619	--	
22	15:02:25 (9-18)	1200	1705-1731	902	
16	17:48:25 (9-18)	1200	1926-1952	--	
11	18:11:25 (9-18)	1200	1957-1983	905	

An HX 90 source deployed from the Narragansett was also used in the larger experiment, but it was not broadcasting during the Swallow float recording period.

d) Seismic Profiler

A seismic profiler used in a geophysical survey conducted on the Monterey Fan by Chevron was deployed intermittently during the larger VLA experiment. A log of the profiler deployment times and locations was obtained from Chevron in order to aid in the interpretation of the VLA data. According to their log, the profiler was not operating from about 16:30, 15 September to about 17:30, 19 September.

Also, according to a verbal communication between Chevron and one of the parties involved in the larger experiment, the profiler had malfunctioned and was in port from 15 September to the night of 18 September. However, characteristic seismic profiler signals were recorded during much of the Swallow float deployment (re Section IX). The intervals in the Swallow float data in which the profiler appears to be operating are given in the following table.

Time Periods when the Seismic Profiler appears in the Swallow Float Data		
Times are in local Pacific Daylight Time; add 7 hours to get GMT.		
Swallow Float Record Interval	Time	Date
470 - 640	23:48 - 01:55	17-18 Sept
670 - 810	02:17 - 04:03	18 Sept
1130 - 1310	08:02 - 10:18	18 Sept
1520 - end	12:55 - 19:00	18 Sept

Either the Chevron seismic profiler was operating during this time and this information was not logged possibly because it was undergoing testing, or another seismic profiler was operating. The United States Coast Guard's Local Notice to Mariners for the week of 16 September lists five other geophysical surveys being conducted during this period. Whether these surveys involved the use of a seismic profiler is unknown.

The Chevron seismic profiler generates a 30 Hz pulse every 11 to 12 seconds. Each pulse contains acoustic energy from about 10 Hz up to 200 Hz. Their profiler typically operates for 75 to 110 minutes and then is quiet for 75 minutes. Refer to Section X for plots of the time series during the recording of the seismic profiler signals.

III. Swallow Float Log Summary

Note: All times are in local Pacific Daylight Time. To obtain standard Greenwich Mean Time, add 7 hours. Note also that most ship positions in this log were obtained from a NAVSAT receiver on board the Sprout and should be corrected using the intermittent range and bearing position fixes from FLIP along with the GPS-determined FLIP positions.

15 September 1987

- 04:30 Depart Nimitz Marine Facility
- 23:45 Arrive at Port Hueneme to pick up explosives.

16 September 1987

- 00:30 Depart Port Hueneme. Greenish blue bioluminescing organisms are disturbed by the passage of the ship. Ship speed increasing to 9.0 knots.
- 20:15 Ship comes to all stop so that OBS Judy (# 8) can be removed from the OBS van. It will not be deployed since its tape formatter computer card is malfunctioning. Bring OBS Janice (# 9) into the OBS van to begin checkout procedure.

17 September 1987

- 12:20 The radio beacon wire on float 10, used for shorting out the antenna, became disconnected some time since the last radio check. Wire is re-attached.
- 16:14 Ship's position is 34° 58.42' N, 125° 59.67' W, speed is 8.4 knots and heading is 297° magnetic.
- 16:27 Ship's position is 34° 58.54' N, 125° 58.57' W, speed is 0.7 knots and heading is 339° magnetic.
- 16:50 OBS Janice is deployed. Ship's position is 34° 58.78' N, 125° 58.64' W.
- 17:15 Begin checkout of Swallow floats. The resistance of float 2's sea shunt is 85 Ω rather than 100 Ω.
- 17:55 Start all floats synchronously.
- 18:27 Deploy float 8. Ship location is 34° 58.70' N, 125° 58.45' W.
- 18:33 Deploy float 7. Ship location is 34° 58.73' N, 125° 58.46' W.
- 18:36 Float 6's ballast breaks off in initial attempt to deploy it. It will be repaired later.
- 18:39 Deploy float 5. Ship location is 34° 58.76' N, 125° 58.47' W.
- 18:42 Deploy float 4. Ship location is 34° 58.77' N, 125° 58.47' W.
- 18:46 Deploy float 3. The float is not sinking. Ship location is 34° 58.79' N, 125° 58.48' W.
- 18:52 Deploy float 2. Ship location is 34° 58.84' N, 125° 58.50' W.
- 18:55 Deploy float 1. Ship location is 34° 58.87' N, 125° 58.50' W.
- 19:02 Deploy float 0. Ship location is 34° 58.90' N, 125° 58.51' W.
- 19:03 Float 1 is not responding to the acoustic transpond command issued from the Sprout. The float may have been hit by the ship's prop.
- 19:08 Remove poleducer from water in order to retrieve float 3 which is not sinking.
- 19:20 Recover float 3. Its flasher support is broken and one of the external cables is cut. Float was probably hit by the ship's prop.
- 19:25 Begin to re-attach float 6's ballast.

19:45 Deploy float 6. Ship location is 34° 59.13' N, 125° 58.54' W.
19:59 All floats in the water except float 1 respond to acoustic transpond command.
20:05 Underway to deploy float 9.
20:23 Attaching ballast to float 3. The float was possibly resynchronized when checking resistances.
20:44 Deploy float 9. Ship location is 34° 59.69' N, 125° 56.42' W. Range and bearing to FLIP:
2.14 nmiles, 066° magnetic.
20:56 Underway to deploy float 3.
21:31 Redeploy float 3. A nylon guy wire attached to the float's radio beacon antenna was snapped
off in deployment. Ship location is 34° 58.84' N, 125° 58.82' W.
21:40 Underway to deploy float 10.
22:07 Deploy float 10. Ship location is 34° 59.85' N, 125° 59.88' W. Range and bearing to FLIP:
1.5 nmiles, 130° magnetic.
22:15 Underway to deploy float 11.
22:48 Deploy float 11. Ship location is 34° 57.14' N, 125° 58.25' W. Range and bearing to FLIP:
2.15 nmiles, 351° magnetic.
22:53 Underway for survey position A.
23:13 The OBS group reports that OBS Judy (#8) appears to be operating properly. It will be
deployed tomorrow morning before the explosives are detonated.
23:18 Ship engines stop in order to coast into survey position A.
23:20 Ship location is 34° 59.10' N, 125° 57.26' W. Ship heading is 334.9° magnetic and the speed
is 1.3 knots.
23:23 Begin to head towards survey position B conducting a Swallow float range survey. Ship loca-
tion is 34° 59.14' N, 125° 57.27' W.
23:25 Ship location is 34° 59.17' N, 125° 57.27' W.
23:28 Ship location is 34° 59.22' N, 125° 57.33' W.
23:32 Ship speed is 1.7 knots. Ship location is 34° 59.37' N, 125° 57.44' W.
23:41 Ship location is 34° 59.55' N, 125° 57.57' W.
23:50 Ship speed is 1.1 knots. Ship location is 34° 59.72' N, 125° 57.71' W.

18 September 1987

00:02 Heading to survey position C. Ship speed is 2.4 knots. Continuing to perform float range sur-
veys.
00:13 Ship location is 34° 59.31' N, 125° 57.74' W.
00:23 Ship location is 34° 59.23' N, 125° 58.24' W. Some animal is whistling into the poleducer.
00:26 Ship location is 34° 59.21' N, 125° 58.40' W.
00:45 Determine range to float 11. Ship location is 34° 59.08' N, 125° 59.25' W.
00:52 Scientific party goes to bed. The bridge will continue to record ship's position during the
night. Ship location is 34° 58.98' N, 125° 59.57' W.
01:30 Ship location is 34° 55.52' N, 125° 58.78' W.
02:00 Ship location is 34° 52.40' N, 125° 58.63' W.
02:30 Ship location is 34° 49.17' N, 125° 58.70' W.
03:00 Ship location is 34° 49.96' N, 125° 59.79' W.
03:30 Ship location is 34° 48.92' N, 126° 00.45' W.

- 03:59 Ship location is 34° 47.90' N, 125° 59.16' W.
05:00 Ship location is 34° 48.11' N, 125° 58.33' W.
05:30 Ship location is 34° 48.75' N, 125° 58.22' W.
06:00 Ship location is 34° 48.10' N, 125° 56.57' W.
06:30 Ship location is 34° 49.48' N, 125° 56.17' W.
07:00 Ship location is 34° 48.91' N, 125° 55.00' W.
07:30 The ship is underway back to the array location. Ship location is 34° 50.45' N, 125° 54.53' W.
07:51 Scientific party returns to lab. Ship's heading is 346° magnetic and speed is 6.8 knots. Ship location is 34° 51.51' N, 125° 56.86' W.
08:02 Ship's speed and heading are 6.5 knots and 338° magnetic. Ship location is 34° 52.64' N, 125° 57.29' W.
08:16 Ship's speed and heading are 6.4 knots and 337° magnetic. Ship location is 34° 54.66' N, 125° 56.53' W.
08:31 Ship's speed and heading are 6.9 knots and 338° magnetic. Ship location is 34° 56.31' N, 125° 57.39' W.
08:47 Ship's speed and heading are 7.0 knots and 328° magnetic. Ship location is 34° 57.92' N, 125° 57.99' W.
08:51 Ship is coasting to all stop.
09:20 Ship's speed and heading are 2.9 knots and 328° magnetic. Ship location is 34° 58.76' N, 125° 58.73' W.
09:24 Boston whaler launches from FLIP and heads towards the Sprout.
09:30 Boston whaler docks with the Sprout in order to exchange packages.
09:38 Boston whaler has returned to FLIP.
10:15 The P-3 aircraft passes over the Sprout.
10:18 Ship is dead in the water. Ship location is 34° 58.14' N, 125° 58.44' W.
10:20 The bridge reports that the P-3 aircraft deployed two sets of two sonobuoys. Range and bearing from FLIP are 0.75 nmiles and 245° magnetic.
10:55 The first shot is put into the water. It is 61 lbs of explosives packed into a plastic milk case. It is set to detonate at 13:00. Ship is dead in the water. The range and bearing from FLIP are 0.73 nmiles and 173.5° magnetic. Ship location is 34° 58.15' N, 125° 58.60' W.
11:32 The OBS Judy (# 8) is deployed. The range and bearing from FLIP are 0.59 nmiles and 154° magnetic. Ship location is 34° 58.46' N, 125° 58.63' W.
11:59 The ship's speed and heading are 0.4 knots and 320° magnetic. Ship location is 34° 58.03' N, 125° 58.35' W.
12:00 FLIP's Loran-C position is 34° 58.93' N, 125° 57.84' W. A P-3 aircraft passes over-head sometime around noon.
12:08 Begin a range survey of the Swallow floats.
12:24 Finish the range survey. All floats respond to the acoustic commands except float 1. The ship's speed and heading are 0.2 knots and 334° magnetic. Ship location is 34° 57.93' N, 125° 57.78' W.
13:00 The first explosive detonation is felt at 3 seconds after the hour. Note that the OBSSs are programmed to record 3 minutes of data every half-hour, starting at the half-hour mark.
13:06 Deploy the second 61-lb explosive charge. It is set to detonate at 14:30. The range and bearing from FLIP are 1.08 nmilcs and 160° magnetic. Ship location is 34° 58.00' N, 125° 57.82' W.

- 13:15 The ship is underway to the south; its speed and heading are 8.9 knots and 154° magnetic. Ship location is 34° 57.86' N, 125° 57.68' W.
- 14:00 The ship is still underway to the south; its speed and heading are 8.7 knots and 167° magnetic. Ship location is 34° 51.07' N, 125° 56.33' W.
- 14:30 The second charge, set to detonate at 14:30, apparently never exploded.
- 17:00 The ship is returning to survey position A. It spent the afternoon about 10 nmiles and a bearing of 170° from FLIP. Ship location is 34° 49.35' N, 125° 54.85' W.
- 17:50 The ship's speed and heading are 5.8 knots and 343° magnetic. Ship location is 34° 53.52' N, 125° 56.09' W.
- 18:30 The Sproul has four fixed blades on its prop. The reduction gear ratio is 5.17 : 1. At a 9-knot speed, the engines are rotating at about 1800 rpm. The captain thinks there is an approximately linear relationship between the engine rpm and the ship speed. The ship's speed and heading are 5.8 knots and 342° magnetic. Ship location is 34° 57.20' N, 125° 57.68' W.
- 18:54 The ship slows as it approaches survey position A.
- 19:02 The ship begins to travel towards survey position B with the poleducer in the water. Begin range survey of the floats. Ship's speed and heading are 0.4 knots and 320°. Ship location is 34° 58.99' N, 125° 57.04' W.
- 19:17 Ship location is 34° 59.56' N, 125° 57.52' W.
- 19:32 Ship turns towards survey position C; ship speed is 2.3 knots. Continue Swallow float range survey. Ship location is 35° 00.21' N, 125° 57.88' W.
- 20:00 Ship location is 34° 58.59' N, 125° 58.99' W.
- 20:22 Ship leave survey position C and heads toward estimated position of float 0. The ship will remain about a half mile to the south of FLIP.
- 20:34 The ship slows down from about 6.7 knots to 0.7 knots. Ship location is 34° 58.08' N, 125° 58.11' W.
- 20:38 The ship is increasing speed to about 4.1 knots. Ship location is 34° 58.14' N, 125° 58.12' W.
- 20:45 The ship's speed and heading are 1.0 knots and 065° magnetic. Ship location is 34° 58.31' N, 125° 58.36' W.
- 21:00 Range and bearing from FLIP are 0.9 nmiles and 310° magnetic.
- 21:04 Release float 0.
- 21:51 Release float 2.
- 22:10 Recover float 0. Its program is still running. Ship location is 34° 58.76' N, 125° 56.31' W.
- 22:41 Release float 3.
- 23:22 Recover float 2. Its program is still running. Ship location is 34° 58.98' N, 125° 56.48' W.
- 23:37 Release float 4.

19 September 1987

- 00:10 Release float 5.
- 00:25 Recover float 3. Its program is still running. Ship location is 34° 58.73' N, 125° 57.01' W.
- 00:31 Sproul begins revving its engines. Ship's speed and heading are 5.8 knots and 213° magnetic. Ship location is 34° 58.60' N, 125° 57.05' W.
- 00:47 Sproul stops revving its engines.
- 01:05 Release float 6.
- 02:18 Recover float 4. Its program is still running. Ship location is 34° 58.87' N, 125° 56.64' W.

02:33 Release float 7.

03:01 Release float 8.

04:42 Recover float 5. Its program is still running. Only float 5 did not have its resident ballast inside the glass sphere during this deployment. Ship location is 34° 58.27' N, 125° 57.83' W.

05:07 Recover float 1. Its program is still running. The float was listing severely to one side because the localization hydrophone was apparently hit by the ship's prop during deployment and was slung over the top of the float. The localization hydrophone has a large dent on one side. The listing of the float caused the float's radio frequency transmitter to be intermittently in and out of the water when the float was on the ocean surface. Ship location is 34° 58.52' N, 125° 56.12' W.

05:29 Recover float 6. Its program is still running. Ship location is 34° 57.96' N, 125° 56.92' W.

05:30 Recover float 7. Its program is still running. Ship location is 34° 57.96' N, 125° 56.92' W.

06:15 Release float 9.

06:27 Ship's speed is slowing from 8.1 knots as float 8 is approached. Ship's heading is 167° magnetic. Ship location is 34° 58.12' N, 125° 57.40' W.

06:39 Recover float 8. Its program is still running. Ship location is 34° 57.66' N, 125° 57.64' W.

07:15 Release float 10.

08:16 Release float 11.

10:09 A 60-lb charge of explosives (shot #3) is deployed. It is set to detonate at 12:00. Range and bearing from FLIP are 1.13 nmiles and 160° magnetic. Ship location is 34° 57.99' N, 125° 58.13' W.

10:59 Recover float 9. Its program is still running. Ship location is 34° 59.75' N, 125° 55.90' W.

12:00 Shot #3, set to detonate at noon, apparently did not explode. Note that float 9's radio beacon appears to be intermittent. It may possibly be due to a malfunctioning RF receiver.

12:27 Recover float 10. Its program is still running. Ship location is 34° 59.55' N, 125° 59.75' W.

13:32 Another 60 lbs of explosives (shot #4) is deployed. It is set to detonate at 15:00. The range and bearing from FLIP are 1.08 nmiles and 154° magnetic. Ship location is 34° 57.98' N, 125° 57.72' W.

14:08 Recover float 11. Its program is still running. Ship location is 34° 56.92' N, 125° 57.53' W.

14:34 The last 60-lb charge is deployed. It is set to detonate at 16:00. The range and bearing from FLIP are 1.24 nmiles and 157° magnetic. Ship location is 34° 58.21' N, 125° 57.62' W.

15:00 Shot #4 is felt aboard the Sprout at 4 seconds after the hour.

16:00 Shot #5 appears to not have detonated. The ship heads to the deployment locations of the two ocean bottom seismometers to begin recall.

18:27 The first OBS is recovered. The ship's position, as recorded by the bridge, is 34° 58.65' N, 125° 57.84' W.

20:12 The second OBS is recovered. The ship's position, as recorded by the bridge, is 34° 58.44' N, 125° 57.17' W. Begin to make preparations to get underway for San Diego.

IV. Environmental Data

a) XBT Data from R/P FLIP

Two expendable bathythermographs (XBT), a model T-4 (which goes to a maximum depth of just over 400 m) and a model T-7 (which goes to 700 m), were deployed each day of the larger experiment from R/P FLIP. These temperature data were used along with historical salinity data [9] and an empirical equation relating sound speed to temperature, salinity, and depth [10] to calculate sound velocity profiles. Shown in Figure IV.1 are the sound speed profiles calculated from a T-4 temperature profile measured at 06:00, 18 September (XBT 31 in the FLIP XBT log) and a T-7 profile taken at 20:00, 18 September (XBT 32 in the FLIP XBT log). The T-7 XBT deployed at 20:00, 17 September did not provide useable data. For comparision, a sound speed profile extending to 4000 m calculated from National Oceanographic Data Center historical data [8] taken in an area just east of our study site is also plotted. The XBT data show a warmer mixed layer in the uppermost few hundred meters and a possibly smaller sound speed in the sound channel than the historical data. The XBT data also show a significant amount of fine structure which is smeared out in the averaged historical data.

b) CTD Data from De Steiger

As part of the larger experiment, conductivity-temperature-depth (CTD) profiles were collected intermittently (at least one per day) from the De Steiger. Towards the end of the larger experiment, the De Steiger came within a few kilometers of FLIP to broadcast calibration signals to the vertical line array [1]. The data from a deep (almost 3900 m) CTD cast taken just prior to the calibration tests on 24 September (one week after the Swallow float deployment) were converted into a sound speed profile and are plotted in Figure IV.2. Also plotted for comparison is the historical sound speed profile from Figure IV.1. The features indicated by the XBTs, a warmer mixed layer and a smaller sound speed at the sound channel axis are also shown by the CTD data. The deviation of the two profiles below 2500 meters is due to a difference in the depth dependence in the two empirical equations used to calculate the sound velocity.

c) Anemometer Readings from R/P FLIP and R/V Sproul

Wind speed and direction, measured by the anemometer on board FLIP, were recorded approximately every hour in the scientific log. Figure IV.3 is a plot of these data for the 48 hours encompassing the Swallow float deployment period. For comparison, the anemometer readings recorded every two hours in the Sproul's ship log are plotted in Figure IV.4. Note that the wind vectors, starting at the dashed line in the plots, points in the direction the wind is blowing *from*. The vertical axis provides the scale to determine the wind velocity magnitude in m/sec.

These wind data show somewhat different features than those taken during other Swallow float deployments. In those other deployments, which were all due west of San Diego [3,4,5], the wind was blowing mainly from the west northwest, rather than from due north and north northeast as in this deployment. The average wind speed of about 6 m/sec (12 knots) (as measured on FLIP) is, however, about the same as that in the April, 1987 and August, 1988 experiments. (The wind speed was just less than 9 knots in the May, 1987 experiment).

A comparison of these two wind vector plots show that the wind speeds recorded on FLIP were generally a few m/sec *slower* than those recorded on the Sproul. This difference is contrary to that expected from a difference in anemometer height on the two vessels; the anemometer on the Sproul is about 10 meters above the water line, whereas it is approximately 18 meters above the water on FLIP. The measurements on FLIP are possibly of higher quality since the readings aboard the Sproul are many times taken while the ship is underway and must therefore be corrected for the ship's motion by the crew. The diurnal minimum in wind speed seen around 08:00 (32 hours and 56 hours) in the Sproul data is not obvious in the

FLIP data.

d) Additional Environmental Data

A large volume of environmental information in addition to those mentioned above were collected as part of the larger experiment. Expendable sound velocimeters (XSV) were deployed every 20 nautical miles from the Narragansett as it transited between FLIP and the De Steiger, air-launched expendable sound velocimeters (AXSV) and bathythermographs (AXBT) were dropped by a P-3 aircraft during the experiment, data from current meters deployed at 43 m and 90 m from FLIP were recorded, and satellite images, one per week, of the sea surface temperature were obtained. Also, basic weather information were concurrently gathered on board the Sproul, on FLIP, on the De Steiger, and on the Narragansett. These additional data include estimates of the swell height and direction, sea state, air temperature, and barometric pressure. During the Swallow float deployment, the swell was 2-4 meters from the north, the sea state decreased from rough to slight/moderate or from sea state 3-4 to sea state 2, the air temperature was 15° to 18° C, and the barometric pressure increased from 29.95 inches to 30.05 inches of mercury. To supplement the ocean wave data, wave hindcasts, which are made every 12 hours on a 2.5° spherical grid by the Fleet Numerical Oceanography Center in Monterey, may be obtained.

Finally, the locations of commercial ships were surveyed by radar on board FLIP and the Sproul. No other ships were sighted during the Swallow float deployment. The information collected by ship surveys conducted on board the P-3 aircraft appear to have been lost. Additional commercial ship position information can be obtained from the Fleet Numerical Oceanography Center (FNOC) in Monterey. The FNOC ship position data base is estimated to be about 60 to 75 % complete [Greg Schwaller of SAIC, private communication].

V. Initial Indication of Data Integrity

a) Swallow Float Data

After being synchronously started (and spending about a half second in performing an initialization), each float begins to accumulate data into a temporary buffer. Once 44 seconds of data have been accumulated, they are written to cassette tape during a one-second period in which no data are gathered by the float. This 45-second cycle, called a record, is repeated until the cassette tape is filled. Each record is composed of 7646 bytes. Appendix 1 contains a description of the record format. Each float has sufficient cassette tape capacity to store up to 2100 records, equivalent to 26 hours of data.

The first step in the data analysis of the Swallow floats is to scan all the floats' cassette tapes with a general screening program. This program checks each record for the proper location of resynchronization characters and the proper sum of byte values in a group prior to a checksum. The output from the screening program is given in Figure V.1. The cassette-tape-reading program attaches a zero-byte record with the same internal record number as the last record on the cassette tape onto the end of each float's data file; this allows the number of internal records to be determined. For example, float 0's last-written record was internal record number 1983. (The record number listed in the left-most column is assigned by the screening program itself). Since the internal record number begins with record 0, float 0 wrote 1984 records onto tape.

The number of errors detected by the screening program is slightly higher than in other Swallow float deployments [3,4,5]. Floats 2 and 6 in particular recorded a larger-than-normal percentage of bad records. The majority of float 6's screening failures occurred between external record numbers 490 to 499 and 1427 to 1463; those for float 2 showed no such clustering. However, the total number of records which failed the screening test was only 0.5 %. In addition, the greatest source of lost data in past deployments [3,4] was due to floats which quit recording prematurely or which could not be synchronously started properly. In this deployment, *all* 12 floats which were taken on the trip were deployed and all recorded full data tapes! Therefore, 99.5 % of the potential number of records which could have been recorded by 12 properly functioning floats were recorded and passed the screening test.

Although all of the Swallow floats are nearly identical in construction, the design of the experiment possibly resulted in a unique aspect being imparted to a given float. In addition, as in all deployments, unexpected events occur which may affect a float's data. The following table is a listing of some of the unique aspects of given floats in this deployment.

Unique Aspects of a Given Float in the September, 1987 Experiment

Float	Comments
1	The 8 kHz hydrophone was struck by the ship's prop during deployment and was destroyed. It caused the float to list severely to one side, apparently in a direction coincident with the geophone's y axis.
2	The sea shunt resistance was 85 ohms instead of the normal 100 ohms before deployment.

3	The float did not sink upon initial deployment. Its flasher was broken and one external cable was cut. After repairs, it was re-deployed during which its radio antenna guy wire snapped off.
5	This was the only float which did not have its resident ballast inside its glass sphere.
6	Its releasable ballast fell off during initial deployment.
7	It was equipped with an extra, expendable weight attached to a corrodable pin in order to speed its descent to depth. However, the pin broke during deployment.
8	It was equipped with an extra, expendable weight attached to a corrodable pin in order to speed its descent to depth.
9	Its radio beacon appeared to intermittently malfunction during float recovery.
3,7 - 11	FLOATS EQUIPPED WITH "NOISY" CASSETTE TAPE RECORDERS (RE SECTION XI.D OF [5]).

b) FLIP Vertical Line Array Data

The 120 channels of the vertical line array are divided into 12 sections of 10 channels each. Each section has its own processor which performs the A/D conversion, transmits the data, etc. A buffer of data is composed of 64 sampled points from each of the 120 channels. The data within a buffer are sequentially ordered according to section as they are transmitted up to the magnetic tape recording system aboard FLIP and each section data block is followed by its processor identification number. A screening program checks, among other things, that the processor ID number recorded on magnetic tape agrees with the expected value of the processor ID number in order to get some idea of the data integrity. The output from this screening program for the 9-minute periods of data (corresponding to 4220 buffers) extracted from tapes 433, 440, 442, 447, and 453 is shown in Figures V.2a and V.2b. The 12 columns in each table associated with a given tape number represent the 12 sections; information for the deepest section is contained in column 1 and that for the shallowest is in column 12. Each of the 19 or 20 rows correspond roughly to a half minute of data on the tape. For example, on tape 433, in roughly the first half minute of data in the 9-minute period, the ninth processor's data had 85 processor ID errors. The screening results show that the sixth section (the sixth column in the table) usually contains the greatest number of processor ID errors and that the data on tape 433 from the upper half of the array may be somewhat suspect. Note that the uppermost section of the array, corresponding to column 12 in the tables, did not collect useable data during the Swallow float deployment.

VI. Swallow Float Battery Voltage, Float Heading, and AGC Level

The battery voltage, the compass reading, and the automatic gain control (AGC) level, measured once during each 45-second record, are plotted in Figures VI.1 through VI.12 for all Swallow floats. The plots are ordered according to the floats' deployment depths, from the shallowest (float 0) to the deepest (bottom floats 9, 10, and 11).

a) Battery Voltage

As shown in the uppermost plot in the figures, the battery level for all floats remained constant at slightly more than 6 volts. The duration of the floats' deployment is therefore determined not by their power supply requirements, but by their recording capacity.

b) Float Heading

Installed on the inside of each of the Swallow float glass spheres, at the sphere's south pole, is a compass (re Figure 1) for determining the orientation of the horizontal components of the float's geophone with respect to magnetic north. The compass heading during each 45-second record is shown in the middle plot of Figures VI.1 through VI.12. After being put into the water, the floats typically underwent rapid rotations as they descended. Once the midwater floats stabilized at depth, they twisted back and forth at a characteristic period of between 25 minutes to an hour. The twisting is believed to be caused by internal waves. Note that float 1's compass reading remained constant at 155°. This is a result of the severe listing of the float (re Sections V, VII, and IX); the compass can only tolerate a maximum tilt of 3° from horizontal before sticking. Note also that float 8's compass heading appears to have continued to undergo relatively rapid oscillations throughout the whole period after the float released from the ocean bottom around record 1065 (re Section VII). As observed in other deployments [3,4,5], the midwater floats' headings appeared to stabilize at about 300° near the end of the experiment (float 2's heading is a possible exception). The force responsible for this asymptotic approach to 300° magnetic is believed to be due to the interaction of a small, intrinsic magnetic field of the float (possibly due to the permanent magnets inside the geophone's components) with the earth's magnetic field.

The three bottom-mounted floats, floats 9, 10, and 11, were tethered to the bottom by 4.57-meter cotton lines; their compass headings usually remained approximately constant or varied slowly due to the constraining effects of the tether and the prevailing ocean current. However, at certain times, e.g. for float 9 just after record 600, between records 1400 and 1600, and around record 1800, the heading changed significantly over a short period of time. Concurrently, the AGC level shown in the lower plot (and discussed in the next part of this section) increased to non-zero values. These periods of large changes in the bottom floats' heading, with associated increases in the AGC level, are thought to be caused by changes in the prevailing ocean current, with a resulting decrease in tether contamination.

c) AGC Level

The AGC is a variable gain amplifier, with a range of 0 to 25 dB gain, which allows the full dynamic range of the eight-bit A/D converter to be used. The AGC gain always changes by a 0.5 dB step between records. After a five-second delay in the record, if more than 1 % of the points sampled on all geophone components are clipped, then the AGC decreases by 0.5 dB. Otherwise, it increases. Because of the slow adjustment time of the AGC gain, amplitude information for large impulsive arrivals cannot be obtained.

The bottom plot in each figure shows the automatic gain control (AGC) level during every 45-second record. The first point of note is that the maximum AGC levels appear to increase slightly with increasing depth of the float. The following table shows the approximate average maximum AGC level for each of the floats (excluding float 1 because of its loss in geophone sensitivity due to its listing to one side, float 8

because it never reached stable equilibrium, and bottom floats 10 and 11 since their AGC level is dominated throughout the deployment by tether effects).

Average of Maximum AGC Level for each Float in September, 1987 Experiment

Float	Average of Maximum AGC (dB)
0	8.5
2	9.0
3	10.5
4	9.5
5	11.5
6	10.0
7	12.5
9	13.5

Some of these differences in maximum AGC gain may be due to differences in the floats' geophone channel sensitivity. Although the variation in sensitivity has not yet been measured directly, it is probably no more than ± 1 dB.

The details of the midwater floats' AGC level plots after the floats stabilized at depth are remarkably similar. Therefore, the following discussion, which refers to float 0's AGC level plot, will pertain to all midwater floats' plots. In Figure VI.1, float 0's AGC level begins to increase starting around record 270 as the float reached its equilibrium depth. At record 470, it decreases rapidly to zero and remains there until record 640. This period from record 470 to 640 of relatively high sound levels, as well as the periods from records 664 to 800, 1134 to 1306, and starting at record 1536, are all due to the operation of the seismic profiler (re Sections IIId, IX, and X).

Only the dip in AGC levels starting at about record 878 and lasting until record 894 is unexplained by the seismic profiler signals. This dip may have been partially the result of the arrival of the T phase from a body wave magnitude 4.7 earthquake in the Fox Islands in the Aleutian Islands. From the "Preliminary Determination of Epicenters" [11], the origin time of the event was 04:12:46.7 (local Pacific Daylight Time), 18 September, and the epicentral coordinates were 53.549° N, 167.369° W. The epicentral distance from the earthquake to the Swallow float array is estimated to be 34.3°, and, using an average group velocity of 1.5 km/sec for the T phase, the arrival time is predicted to be 04:55:06, local time. This time corresponds to Swallow float record 880, which agrees quite well with the beginning of the AGC decrease. Time series recorded by a Swallow float at this time are presented in Section X. Note, however, that the long duration (over 10 minutes) of decreasing AGC levels does not appear to be explainable solely in terms of a single T phase arrival (re Section IX).

During the periods of seismic profiler operation, float 1's AGC level increased intermittently when other floats' levels remained low. Since this float was listing to one side so that its y axis geophone was apparently up against its stop, these periods of AGC increase may represent times when the float rotated so that its y axis geophone was aligned with the direction from the float to the profiler. Since float 1's compass was stuck during the deployment, this hypothesis can not be tested.

VII. Swallow Float 8 kHz Surface and Bottom Bounce Data

Each Swallow float possesses an 8 kHz hydrophone suspended 1.83 m below its glass sphere (see Figure 1). The source strength of the hydrophone is 192 dB re 1 μ Pa at 1 meter. The floats periodically transmit and receive 10 msec acoustic pulses in order to measure interfloat and float-to-surface acoustic travel times. The floats normally transmit 10 seconds after the beginning of each 45 second period and since the floats ping in turn, a given float in this experiment pinged once every 12 records, i.e. once every 9 minutes. The single exception was float 1 which did not transmit at all as the result of a broken 8 kHz hydrophone (re Figure VII.2).

Figures VII.1 through VII.12 show each float's detection of its own 8kHz pulses. The vertical axes in the figures have been scaled from travel time to depth (using half of 1500 m/s) so that float depth is indicated by the leading edge of pulses propagated from the float to the ocean surface and back. The horizontal axes are in units of record number, and may be converted to elapsed time after float synchronization using the conversion factor of 80 records per hour. A line of 15 very faint dots descending from 0 range across the plot are discernible in some of the figures, e.g. Figure VII.2. They are an artifact and should be ignored.

The general features of these plots have been discussed extensively elsewhere [3,4,5]. Following an arrival at 0 depth, which corresponds to the detection of the outgoing 8 kHz ping and its reflection off the float's glass sphere, the shallower floats first detect the arrival of the reflection off the underside of the air-sea interface and then the reflection off the ocean bottom. For those floats whose equilibrium depth exceeds half the total water depth (floats 7, 8, 9, 10, and 11), the order of arrival of these two pulses is reversed. The bottom-bounce phase can, in those cases where the float depth is near half the water depth, make the identification of the first surface-bounce detection difficult. Some of the floats, e.g. float 0 (Figure VII.1), detect additional phases; the surface-to-bottom-to-float phase whose time of arrival can be used as a measure of the total water depth, and the surface-to-bottom-to-surface-to-float phase (at about 5200 m in Figure VII.1).

Note that the number of detections immediately following the 0 depth arrival is greatest when the floats are at shallow depth and decrease as the floats descend. Two reasons for this change in the number of detections with depth have previously been given; that a decrease with depth in the number of 8 kHz scatterers in the water column occurs, and that the frequency of resonance, or ringing, of the Swallow float glass sphere shifts away from 8 kHz as the float descends because of the change with temperature of the sound speed in the air enclosed by the sphere. A third possible explanation is that the 8 kHz hydrophone may decrease in sensitivity with depth (due to an increase in pressure or decrease in temperature). Evidence for this hypothesis is provided by the fact that float 0, the shallowest float, detects both the greatest number of arrivals after 0 depth and also the greatest number of multi-bounce phases.

These data contain some features unique to this deployment. Float 0 detected an arrival, starting at about record 500 in Figure VII.1, whose "depth" increased from 900 meters to almost 3600 meters (i.e., its range from float 0 increased from 1800 m to 7200 m) over the duration of the experiment. This may be the reflection of float 0's 8 kHz pulse from the body of FLIP. Also, float 6 appears to be detecting the reflection off an object at close range around record 600 and records 1200 to 1400 in Figure VII.7. This may be the reflection from another float's glass shell. Float 8 was equipped with an extra weight attached to a corrodable pin in order to speed its descent to its planned equilibrium depth of 2800 meters. However, the corrodable pin took much longer than expected to break, and, as a result, float 8 sat on the ocean bottom from just before record 500 until record 1065 (Figure VII.9). It still had not quite reached its equilibrium depth by the end of the recording period. Finally, bottom-mounted float 10 detected an unusual set of approximately three separate arrivals between the "depths" of 300 m and 600 m (i.e., ranges of 600 m to 1200 m). The arrival times of these anomalous detections remained constant over the duration of the experiment. They may represent the reflection off some unknown topographic feature near float 10's deployment position.

The surface reflection data of the bottom-mounted floats allow the total water depth to be easily determined. Accounting for the 4.57-meter-long tether attached to bottom floats 9, 10, and 11, and using an average sound speed of 1500 m/sec, the water depth has been calculated and is listed in the following table.

Total Water Depth at the Bottom Swallow Float Deployment Sites

Float	Range, Bearing from FLIP at Deployment	Water Depth
8	0.30 km, 145 deg	4670 m
9	4.00 km, 066 deg	4668 m
10	2.78 km, 309 deg	4668 m
11	3.71 km, 172 deg	4660 m

VIII. Swallow Float 8 kHz Interelement Range Data

Figures VIII.1 through VIII.12 contain the record of pulses transmitted by one float and received by another. The vertical axes have been scaled from travel time to range using 1500 m/s for the speed of sound, and the horizontal axes are time in units of Swallow float record number (80 records are written each hour). These 110 plots are provided in order to aid in the future localization of the floats in this deployment.

The general features of these plots have been discussed in the other trip reports [3,4,5] and so will not be repeated here. The plots involving float 8 (e.g., Figures VIII.8a through VIII.8j), however, are unique due to the unusual behavior of this float in the experiment. The merging of the direct and bottom-bounce interfloat arrivals as float 8 reached the bottom, and the subsequent divergence of these phases as the float ascended in the water column, in addition to the surface reflection, create the appearance of these plots. Note the gaps in the detection of the direct arrivals between floats which are near, or on, the ocean bottom; this is due to the shadow cast by the upward-refracting sound speed profile.

IX. Swallow Float RMS Velocity

In order to quickly scan the geophone data of all floats, the root mean squared velocity was calculated for all channels and are plotted in Figures IX.1 through IX.12. These RMS velocity time series have been corrected for the AGC gain, but are otherwise uncalibrated; the vertical axis is in units of volts at the A/D converter. (Refer to Appendix 1 for a block diagram of the geophone data acquisition system). Each RMS level value results from taking the square root of the average of the squared amplitude levels over a five second (or 250 point) period. Since each record is 2250 points long (which equals 45 seconds since the data sampling rate is 50 Hz), then nine RMS values are calculated for each record. The RMS value for the last five-second period of each record includes one second of zeros. The one second of zeros represents the time during which no data is sampled while data in a temporary buffer is being written to cassette tape.

Most of the following discussion will refer to float 0's RMS velocity plots in Figures IX.1a through IX.1j; the plots for the other midwater floats are quite similar.

Aspects of these plots are common to all Swallow float deployments. For example, the upward-curving part of the RMS plot over the first 25 records is due to the initial decrease of the AGC gain to 0 from its start-up value of 12 dB. Float 0 was deployed around record 80 and this is clearly indicated by the change in RMS levels at that time. It settled into stable equilibrium somewhat after record 275, as can be seen by the asymptotically decreasing RMS levels on the horizontal geophone axes. The spikes in the z axis data every 12 records, seen clearly after record 125, are the result of float 0's 8 kHz localization ping. Another source of contamination in some floats' data, e.g. float 3's data in Figures IX.4a through IX.4j, is the large impulse imparted to the float by the action of the cassette tape recorder. This causes a spike to occur once every record in the plots. In addition, data record drop-outs can be seen in float 0's data at about records 668, 1562, 1645, 1741, and 1767. These bad records were identified in the initial data screening discussed in Section V (re Figure V.1a).

A number of interesting features occur in the data. The operation of the seismic profiler is clearly indicated by a rapid oscillation with time in the horizontal geophone axes' RMS levels, between records 470 to 640, 670 to 810, 1130 to 1310, and 1520 to the end. The high frequency of the oscillations are due to the seismic profiler repetition rate (a pulse every 11-12 sec) in comparison with the RMS averaging interval of 5 sec. The change with time in the peak RMS levels from the seismic profiler on a given horizontal axis is partially due to float rotation; in many cases, a decrease on one horizontal axis corresponds to an increase on the other. Variability in levels may also be due to motion of the profiler.

The arrival identified as the T phase from an earthquake in the Fox Islands of the Aleutian Island chain (re Section VI) occurs record 879 (04:53 local time, 18 September). Subsequent arrivals which are not part of the T phase occur in records 884, 889, and 890. They may be associated with aftershocks from the main earthquake or may have some completely different source(s). A plot of the T phase time series recorded by float 0's geophone is given in the next section.

The detonation of the first explosive charge (re Section IIb) appears in record 1527. Surprisingly, an arrival corresponding to the time of the second charge, which was believed to have failed since it was not felt aboard the Sproul or FLIP, occurs in record 1648, just after the data gap in record 1645 in float 0's data. Swallow float time series recorded during the arrival of both of these explosions are given in the next section.

A number of as yet unidentified arrivals can be seen in float 0's RMS velocity plots. Some of these RMS velocity peaks probably correspond to Sproul-generated noise. The following table lists the occurrence times of several of these arrivals.

**Times of Large Peaks of Unknown Origin
in the Swallow Float RMS Velocity Plots**

Record	Local Time (Date)
336	22:07 (9-17)
347	22:15 (9-17)
373	22:35 (9-17)
377	22:38 (9-17)
529	00:32 (9-18)
589	01:17 (9-18)
605	01:29 (9-18)
634	01:50 (9-18)
635	01:51 (9-18)
756	03:22 (9-18)
884	04:58 (9-18)
889	05:02 (9-18)
890	05:03 (9-18)
1462	12:12 (9-18)
1551	13:18 (9-18)
1641	14:26 (9-18)
1654	14:36 (9-18)
1658	14:39 (9-18)
1742	15:42 (9-18)
1895	17:36 (9-18)

The RMS peaks listed in the table above are presumably of an acoustic nature since they can be seen in most (if not all) of the floats' data. However, a spike in record 1935 (18:06, 18 September) in float 0's data does not correspond to a spike in the other floats' data. It may have been caused by float 0 issuing an 8 kHz range survey ping upon acoustic command from the Sproul since it occurred near the end of the Swallow float recording period. However, the ship was returning to the array deployment site at a speed of 6 knots at this time and the 8 kHz hydrophone on board the Sproul is not deployed during ship speeds greater than a few knots. The spike therefore is possibly non-acoustic in nature.

An interesting set of small amplitude spikes appear intermittently in float 0's z axis RMS velocity plots; from records 215 to 310, 640 to 670, 950 to 1030, and 1330 to 1450. They may be present at other times (e.g., records 480 to 500), but they're readily identified only during times when the seismic profiler is not operating. The spikes occur in blocks of 10 to 12 records (7-9 minutes) duration, separated by quiescent periods of 3 to 4 records (2-3 minutes). These arrivals *may* be associated with sounds generated by whales [12]. A further discussion of this issue is given in the next section, where time series of these "clicks" are presented.

The RMS velocity plots for float 8 (Figures IX.9) show that during its stay on the bottom, its data were contaminated. This was probably caused by the rocking of the float at the end of its 8 kHz hydrophone cable; the float itself was probably sufficiently buoyant to remain off the bottom with only its 8 kHz hydrophone resting on the sediment. A sudden jump in RMS levels occurred in record 1064 as the float's corrodable pin broke and the float began to ascend in the water column. The float's geophone did not begin to collect useable acoustic data until after record 1400, judging from the z axis RMS levels.

Figures IX.10 through IX.12 show the RMS velocity plots for the bottom-mounted floats 9, 10, and 11. As can be seen from these plots, these floats' geophone data are contaminated by tether effects for much of the time after they reached the ocean bottom. However, at certain times, and on certain geophone components, useful information can be obtained. Most notable are the set of float 9's data from records 675 to 725 (02:21 to 02:59, 18 September) and 1425 to 1600 (11:44 to 13:55, 18 September); data from all three of its geophone components appear useable during these times. Float 9's z axis also records the

arrival of the first two 60-lb explosions in records 1526 and 1647.

X. Geophone and Hydrophone Time Series

a) Swallow Float Data

Selected time series recorded by the Swallow float geophones, corrected for the AGC level but otherwise uncalibrated, are presented in this section. Each figure shows the time series recorded by a given float's component over a 12-record (9 minute) period; the record numbers are given on the left hand side of the plot. The horizontal axes are in units of seconds, from 0 to 45 seconds, after the beginning of the record. The exception to this presentation are Figures X.5.1a through X.5.1c showing the stacked time series from the detonation of the first explosive charge. In these figures, the left-hand number is the Swallow float number and the horizontal axis varies from 0 to 60 seconds, rather than from 0 to 45 seconds. The geophone data are sampled at 50 Hz (see Appendix 1), so that 2200 points from each channel are collected in the 44 seconds of each record (the 45th second of the record is made up of 50 zeros). Only every other sampled point is plotted. The scale of the plots' vertical axis in volts is given at the top of each figure.

The time periods selected for plotting are:

Swallow Float Geophone Time Series				
Record Sequence	Local Time (18 Sept)	Floats	Comments	Figure Numbers
875 - 886	04:51 - 05:00	0	The Fox Islands earthquake T phase arrival.	X.1
1100 - 1111	07:40 - 07:49	0 - 7	16 Hz line from De Steiger; time of recording of VLA tape 433.	X.2
1380 - 1391	11:10 - 11:19	0 - 7, 9	Half-second clicks in the data.	X.3
1450 - 1461	12:02 - 12:11	0 - 9	Range survey pings; time of recording of VLA tape 442.	X.4
1526 - 1527	13:00	0 - 7, 9, 11	Stacked time series showing 1 min of 1st explosion arrival; seismic profiler.	X.5.1
1523 - 1534	12:57 - 13:06	9(z), 11(z)	12 records written by the bottom floats' vertical geophone which encompass the 1st explosion arrival.	X.5.2
1543 - 1554	13:12 - 13:21	0	Unknown arrival in record 1551; seismic profiler.	X.6
1640 - 1651 1648 - 1659	14:25 - 14:40	2	Arrivals from 2nd explosion; unknown arrivals in records 1641, 1653, 1657; seismic profiler.	X.7

1800 - 1811	16:25 - 16:34	0	Time of recording of OBS event 904 and VLA tape 453; seismic profiler.	X.8
-------------	---------------	---	---------------------------------------------------------------------------------	-----

The figures for this section are presented and discussed in chronological order. Features which are typical of these plots - e.g., the contamination of the geophone time series, especially the z axis time series, by the 8 kHz localization ping 10 seconds into every 12th record, and the tape-recorder-induced motion at the beginning of each record - have been discussed in the other trip reports [3,4,5]. In interpreting the plots for a given float from this deployment, it is important to note any of the float's special features (e.g., whether it is equipped with a "noisy" or "quiet" cassette tape recorder), listed in the table in Section V.

1) Records 875 - 886; T Phase Arrival

As mentioned in Sections VIc and IX, the Swallow floats detected a large amplitude signal starting about record 879 (04:54, 18 September). It has tentatively been identified as the T phase arrival from a body wave magnitude 4.7 earthquake in the Fox Islands in the Aleutian Island chain. The T phase is that portion of the seismic energy which gets coupled into (by downslope conversion), and propagates within, the deep ocean sound channel. Figures X.1.1a through X.1.1c show a 12-record sequence (9 minutes) encompassing the arrival time of this phase. The September, 1987 issue of the "Preliminary Determination of Epicenters" [11] gives the origin time of the event as 04:12:46.7 (local Pacific Daylight Time), 18 September, and the epicentral location as 53.549° N, 167.369° W. The epicentral distance, Δ , from the earthquake to the Swallow float array can be calculated using the formula;

$$\Delta = \cos^{-1}[\cos(\theta_s)\cos(\theta_r)\cos(\phi_s)\cos(\phi_r) + \cos(\theta_s)\cos(\theta_r)\sin(\phi_s)\sin(\phi_r) + \sin(\theta_s)\sin(\theta_r)]$$

where the latitude and longitude of the source are θ_s and ϕ_s , and the latitude, longitude of the receiver are θ_r and ϕ_r . The linear distance along the great circle path on the earth's surface is $R\Delta$, where R is the earth's radius. From this formula, Δ is estimated to be 34.3°, and, using an average group velocity of 1.5 km/sec for the T phase, the arrival time is predicted to be 04:55:06, local time. This time corresponds to Swallow float record 880, which agrees quite well with the first record in Figures X.1.1a through X.1.1c in which full saturation has occurred.

In all four Swallow float deployments in 1987 and 1988, arrivals from earthquakes have been identified. Therefore, as standard practice, the "Preliminary Determination of Epicenters" listing for the month of a given Swallow float experiment are obtained and scanned for interesting events. Interesting earthquakes include not only those with large magnitudes, but also those occurring along the Pacific rim, especially in the Aleutian Islands; these are most often the source of large amplitude T phases. No effort has yet been made to determine exactly how many of the earthquakes in the listings have visible arrivals in the Swallow float data. However, T phases from earthquakes in the Aleutian Islands with body wave magnitudes as small as 4.4 have been identified.

The vertical line array data recorded during the Fox Islands T phase arrival is presently being beam-formed and will be presented at a later date.

Note that after the 3.5-to-4 minute period of the T phase arrival is completed, another arrival appears in records 884 to 885. This may be the T phase from an aftershock of the Fox Islands earthquake. Since both of these signals cause clipping in the Swallow float geophone system, amplitude information is lost. In addition, since clipping results in a distortion of the autospectrum, the frequency content of the two arrivals cannot be compared. However, future analysis of the VLA data during this time may allow the second large arrival to be classified.

The 8 kHz localization ping issued by float 0 occurs 10 seconds after the beginning of record 876 in the z axis time series in Figure X.1.1c. Other one-second pulses separated by about 25 seconds also appear. These "clicks" will be discussed below in reference to the time series from records 1380 to 1391.

2) Records 1100 - 1111; Listing of Float 1

The time series for records 1100 to 1111 from floats 0 through 7 are shown in Figures X.2.1 through X.2.8. The floats on the ocean bottom, floats 8 through 11, were contaminated by tether effects during this

time and are not presented. The differences between the various floats' time series recorded near the start of a record are caused by whether or not a given float is equipped with a "noisy" cassette tape recorder; in these figures, floats 3 and 7 had noisy tape recorders (re the table in Section V and the discussion in Section XI.d of reference [5]). Because of this contamination, the first 3 seconds of data in each record are skipped in the calculation of the Swallow float spectral estimates presented in the next section. Tape-recorder-induced float rocking is the 2-3 second period oscillation seen most clearly in float 7's y axis data (Figure X.2.8b).

The occurrence of the localization ping in the z axis data appears in increasing record number in sequence with the float number, starting with record 1104 for float 0 (Figure X.2.1c), as the floats took turns issuing the 8 kHz ping. (Recall that float 1's localization hydrophone was destroyed during deployment).

For the properly functioning floats 0 and 2 through 7, the vertical axis noise levels are, in general, about 3 times smaller than the horizontal axes' levels. Because float 1 listed severely to one side, its vertical geophone was not completely vertical, and it recorded higher noise levels (re Figure X.2.2b) than the other floats' vertical geophones. In addition, its y axis was up against its stop during all except the loudest signals. Since laboratory tests have shown that the geophones can withstand a tilt of up to about 15°, float 1 must have listed by an amount greater than this angle. The autospectra estimated from float 1's y axis data agree quite well with geophone channel self noise measured in the laboratory below about 15 Hz. A spectral comparison will be presented in the next section.

An arrival of unknown source occurs in records 1100 to 1101. It is recorded predominantly on the horizontal axes and its amplitude decays with decreasing depth of the float.

3) Records 1380 - 1391; Whale(?) Clicks

Time series recorded during 11:10 to 11:19, 18 September, i.e., records 1380 to 1391, are shown next in Figures X.3.1 through X.3.9. These time series were plotted because of the unusual set of small amplitude spikes appearing in some of the z axis RMS velocity plots (e.g., Figure IX.1g). The figures clearly show the cause of the RMS velocity spikes; the vertical axis geophone data contain "clicks" which are 0.5 to 1.0 second in duration and are separated by 24 to 30 seconds. (Note that the recording of the 8 kHz localization ping should not be confused with the clicks). A gap of over 1.5 minutes in click arrivals occurs between the second click in record 1387 and the click in 1391, in accordance with the gaps of 2 to 3 minutes in the vertical component RMS velocity plots in Section IX.

The click arrivals in float 0 and 1's data appear to be longer than a half-second, but are actually composed of two arrivals. These two closely-spaced arrivals separate in time in the data recorded by deeper floats. Upon close examination, the second arrival of the pair can be seen to be a phase-reversed replica of the first arrival (e.g., the pair in record 1391 of float 2's z axis data in Figure X.3.3c). Therefore, the first arrival of the pair is the direct-path phase and the second is the surface-bounce phase. The following table lists the measured separation time in the vertical geophone time series between the two phases.

**Separation Times of Direct and Surface-Bounce Phases
of the Half-Second Clicks in Records 1380-1391**

Float	Separation Time (sec)
0	--
1	--
2	0.6
3	0.8
4	1.0
5	1.2
6	1.3
7	1.5
9	3.0(?)

If the horizontal range from the unknown source(s) to each of the floats was equal, the data above could be used to determine the range and depth of the source(s). The actual arrival time of a given click pair cannot be used easily in a preliminary look at the data to determine the source(s) positions because not only are the floats' horizontal positions unknown, but their internal clocks drift on the order of a second over 24 hours. However, the fact that the click arrivals appear to decrease in amplitude on all three geophone components as the float depth increases, at least below float 2, suggests a relatively shallow source. The fact that the click pair separate in time as the float depth increases suggests that the source range and depth are on the same order as the depth of the Swallow float array. These clicks have many of the same characteristics as the signals associated with finback whales [12]. They are of much shorter duration than the 15-to-20-second whale-associated signals recorded in the August, 1988 sea trip [5].

The second click in record 1386 is embedded within, or is closely followed by, a long-duration arrival which resulted in clipping on one or both of the floats' horizontal geophone components. Since float 6's x component was clipped by the arrival, but its y axis did not appear to detect it (Figures X.3.7a and X.3.7b), and the float's compass heading at this time was about 235° magnetic (Figure VI.7), then the source of this arrival was either to the northwest or the southeast of float 6. Float 6's time series also contain an unusual signal in record 1382. None of the other floats show a corresponding arrival at this time. Because it seems to be non-acoustic in nature, its onset was impulsive, and it set the float into rocking, it may have resulted from a small form of sea life colliding with the float.

4) Records 1450 - 1461; Range Survey Pings

Records 1450 through 1461, which were recorded at the same time as the data on VLA tape 442, are plotted in Figures X.4.1 through X.4.10. At 12:09, a range survey of the floats was started. A range survey involves the transmission, from a hydrophone suspended from the R/V Sproul, of an acoustic command coded for a specific float. The specified float then responds with an 8 kHz pulse which is five times longer in duration than the floats' localization ping. The recording of the response pulses of float 0 occur in its records 1458 and 1459. The beginning of float 2's response pulse occurs at the very end of record 1460, the response pulse from float 3 appears in record 1461, and float 4's response is recorded at the very end of record 1461. Possible whale-generated clicks occur intermittently in these time series (e.g. records 1451, 1452, 1459, and 1460). Float 8 and 9's data, especially the horizontal components, are contaminated by tether effects, but both floats' vertical axes data show some evidence of click arrivals.

5) Records 1526 - 1527; 1st Explosion and Seismic Profiler

One minute of Swallow float geophone time series, composed of the last 15 seconds of record 1526 and the whole of record 1527, is presented in Figures X.5.1a through X.5.1c. It which shows the arrival of the first 60-lb explosion. The floats' time series are ordered by increasing depth of float from the top to the bottom in the figures. Little information except the arrival time can be obtained because the loud arrival saturated the front-end geophone electronics. Even float 1's y axis geophone, up against its stop because of the severe float listing, was driven into saturation by the first arrivals (the direct and the surface-bounce paths) and it recorded about 20 seconds of signal thereafter. The Swallow float data acquisition system adapts in gain at a very slow rate of 0.5 dB every 45 seconds and is therefore poorly designed for the recording of loud, impulsive events.

The arrival time of this ocean bottom explosion does not strictly increase as the float depth decreases. This is because both the horizontal range from the charge to a float varies and the floats' internal clocks drift with respect to one another about an average of 0.5 seconds in 24 hours.

Once the geophone data acquisition system was no longer saturated, the seismic profiler signal, composed of 3.5-second pulses every 11 seconds, dominated the time series, particularly on the horizontal axes. Note that float 0's x axis barely detects the profiler signal, but the float's y axis is fully clipped by it. During this time, float 0's heading was almost 0° magnetic, implying that the profiler was located either to the south or to the north of the float.

The sound from the explosion appears to have set floats 2 and 4 into rocking, as seen by the 2.5-to-3-second oscillations on their horizontal axes. This occurs as a result of the torque applied about the float's

center of mass by the acoustic wave arrival. Such a torque is possible since a float's center of mass is displaced from its center of buoyancy in order to provide float stability in the vertical direction. The rocking motion is mechanically amplified on the geophone by the displacement of the geophone from the center of mass. Why only these two floats were set into a rocking motion remains unclear.

A few interesting features of the later arrivals from the detonation can be seen in the time series. The pair of pulses in float 3's vertical axis data at about 33 to 35 seconds are separated by 1.8 seconds. The first of the pair followed a path which bounced off the surface five times and the ocean bottom five times. The 1.8 seconds is the time necessary to travel from the float depth of about 1300 meters to the surface and back and so the second pulse of the pair interacted with the surface six times and the bottom five times. Pairs of pulses which traveled shorter paths can be identified by measuring backwards in time in steps of 6.2 seconds, the round-trip travel time from bottom to surface. (The first pulse of the third pair of arrivals is missing because of the half-second gap between records 1526 and 1527).

The vertical axes' time series of bottom floats 9 and 11 show an oscillatory tail which lasts for the full minute of data plotted in Figure X.5.1c. These oscillations, especially those recorded by float 11, are apparently not caused by tether effects as can be seen from these floats' twelve-record (9 minute) sequences in Figures X.5.2a and X.5.2b which encompass the charge arrival. The oscillations vary in frequency from 1 to about 1.5 Hz, with the lower frequencies tending to arrive before the higher frequencies. The frequency content, the change in frequency content with time, and the long duration of the oscillatory tail correspond to the properties of Scholte waves, sediment-waveguide-trapped seismic energy [13]. Also, Scholte waves are rather heavily attenuated with range [13]; float 11 was closer to the explosion than float 9 and its Scholte wave amplitude is greater than that recorded by float 9. A time series recorded by OBS Judy's vertical axis geophone of the fourth explosion on 19 September (re Section II.b) is provided in Figure X.12.1a for comparison. Note that the OBS geophone measures sediment motion whereas the bottom Swallow floats measure water-column motion. The bottom-mounted floats in this experiment were tethered to the bottom by 4.57-meter lines.

6) Records 1543 - 1554, 1640 - 1659; Unknown Arrivals and 2nd Explosion

The next three sets of time series plots, records 1543 to 1554 recorded by float 0 (Figures X.6.1), and records 1640 to 1651 (Figures X.7.1) and 1648 to 1659 (Figures X.7.2) recorded by float 2, are presented because they contain large arrivals of unknown origin (re the table in Section IX). These arrivals occur in records 1551, 1641, 1654, and 1658 and are most predominant on the horizontal axes where they result in clipping. This is evidence that these signals have traveled from long range in the deep sound channel. Further investigation may allow the sources of these signals to be identified.

An interesting set of arrival pairs occurs in record 1648, most clearly recorded on float 2's z axis (Figures X.7.1c or Figures X.7.2c). The source of these arrivals is the detonation of the second explosive charge which was not felt aboard the R/V Sproul or R/P FLIP. The first pair is the direct and the surface-bounce phases, the second pair is the surface-to-bottom-to-float phase followed by the surface-to-bottom-to-surface-to-float phase, and the barely-visible third pair, occurring just after 15 seconds into record 1648, is the pair which interacted with the ocean bottom twice. This detonation is of much lower amplitude than the first detonation discussed previously, even though both charges contained the same amount of explosives. Obviously, this charge only partially detonated.

7) Records 1800 - 1811

Finally, in Figures X.8.1a through X.8.1c are plotted the time series recorded by float 0 at the same time in which OBS event 904 (re part b of this section for a discussion of these time series) and VLA tape 453 (re part c of this section) were written. The seismic profiler signal is clearly the dominant feature in these time series, in contrast to the OBS time series from event 904.

b) Ocean Bottom Seismometer Data

The time series recorded by OBS Judy's four channels, three channels of geophone data and a single channel of hydrophone data, are presented in this section. All six events which were written while the Swallow floats were recording, events 901 through 906, have been plotted in Figures X.9 through X.11. In addition, in Figure X.12, the time series recorded on the OBS vertical geophone component on 19 September during the fourth explosion has been provided by Dr. Dorman's group. The following table lists the OBS event number, the local time, the corresponding Swallow float record numbers, and the figure numbers for these time series plots.

OBS Judy Time Series				
Event	Local Time (18 Sept)	Swallow Float Records	Comments	Figure Numbers
901	15:00 - 15:03	1687 - 1690	--	X.9
902	15:30 - 15:33	1727 - 1730	22 Hz line from De Steiger.	X.9
903	16:00 - 16:03	1767 - 1770	Anomalous spike in z axis data.	X.10
904	16:30 - 16:33	1807 - 1810	Anomalous spike in z axis data; time of recording of VLA tape 453.	X.10
905	18:30 - 18:33	1967 - 1970	11 Hz line from De Steiger.	X.11
906	19:00 - 19:03	2007 - 2010	Anomalous spike in z axis data.	X.11
Unknown	15:00 - 15:01 (19 Sept)	--	One minute of vertical geophone component data recorded during the fourth explosion arrival.	X.12

Each plot in Figures X.9 through X.11 shows the time series recorded by a given component over two adjacent 3-minute events; the event numbers are given on the left hand side of the plots. The horizontal axis is in units of seconds, from 0 to 45 seconds, in order to be consistent with the Swallow float time series plots. Note that the 180th second of each event is made up of 50 zeros. The amplitude of each of the two events' time series for a given channel has been normalized by the maximum amplitude in those two events. The maximum amplitude, in counts, is given at the top of each figure. These data have been resampled to 50 Hz from 128 Hz [14] in order that a quantitative comparison between the OBS and the Swallow float data can be made.

The vertical component time series presented in Figure X.12 has a time span of 0 to 60 seconds rather than 0 to 45 seconds.

The two horizontal geophone component time series are quite similar in appearance and the appearance and maximum amplitude does not change significantly from event to event, in contrast to much of the OBS data recorded in the April and May, 1987 experiments [14]. The horizontal axes data may therefore be of higher quality in this experiment. Likewise, the OBS hydrophone data are consistent in appearance and amplitude from event to event. These data are richer in higher frequency components than the horizontal geophone data. The vertical axis time series in events 901 and 902 (Figure X.9.1c) are different still; these time series have a low frequency component upon which a smaller, higher frequency component rides. The z axis plots for events 903-904 and 905-906 are contaminated by a large amplitude spike which occurs at exactly the same time after the start of the event, almost 2 minutes, 22 seconds, in events 903, 904, and 906. Care was taken to not include these contaminating spikes in the portion of the time series for which spectral estimates were calculated (and presented in the next section).

Note that although the midwater-column Swallow float data recorded during event 904 are dominated by the seismic profiler (see Figures X.8.1a through X.8.1c), the OBS data show no indication of this signal. To confirm that the OBS z axis did not detect the profiler, a 5-second piece of time surrounding the

contaminating spike was removed and replaced with 250 zeros. The plot of the resulting time series is shown in Figure X.10.1d.ii. (The same data with the contaminating spike is in Figure X.10.1d.i). No evidence of the profiler is seen. Note also that the source of the spike caused larger-than-normal oscillations on the vertical axis.

Figure X.12.1a shows a 60-second portion of the vertical axis time series recorded at the time of the fourth explosive arrival. As the plot indicates, the charge-to-OBS distance was about 1.0 km. The direct and surface-reflected phases are followed by the long oscillatory arrival of almost constant frequency identified as the Scholte wave. The appearance in this figure of the vertical sediment motion from the Scholte wave is quite similar to its vertical component water-borne motion recorded by the bottom floats 9 and 11; re Figure X.5.1c.

c) FLIP Vertical Line Array Data

Five 9-minute blocks of data (4220 buffers), from all 120 channels of the vertical line array were extracted, desampled from 500 Hz to 50 Hz, and plotted. The following table lists the data tape number, the local time of recording, and the Swallow float record interval corresponding to these 9-minute blocks of data.

Desampled Vertical Line Array Time Series				
Data Tape Number	Local Time (18 Sept)	Swallow Float Records	Comments	Figure Numbers
433	07:45 - 07:54	1107 - 1118	16 Hz line from De Steiger.	X.13
440	10:46 - 10:55	1348 - 1359	22 Hz line from De Steiger.	X.14
442	11:55 - 12:04	1440 - 1451	--	X.15
447	13:50 - 13:59	1593 - 1604	11 Hz line from De Steiger; seismic profiler.	X.16
453	16:26 - 16:35	1801 - 1811	Time of recording of OBS event 904; seismic profiler.	X.17

A 45-second portion of the time series in these data blocks are presented in the figures. The time of recording of the first sample in each of the plots' time series is given at the top of the plot. The numbers on the left hand side of the figures are the channel numbers which recorded the corresponding time series, where the channel numbering is done from the bottom (deepest part) of the array to the top (shallowest). Again, the horizontal axis is in units of seconds and ranges from 0 to 45 seconds. The time series are uncalibrated. The vertical axis in all the figures varies from -2000 to +2000 counts.

The most dominant features of these plots are the signals believed to be generated by R/P FLIP impulsively jerking on the array (re the plots from tape 433) and the low frequency array strum (re the plots from tape 447). These contaminating effects vary with time and with depth along the array. Their dominance masks the presence of other signals in the time series, although the seismic profiler pulses every 11 seconds can be detected in the data from tapes 447 and 453. (From examination of the Swallow float data, the profiler was not operating during the recording of tapes 433, 440, and 442). However, the flow and strum contamination appears to be isolated in frequency to below 10 Hz for most of the time, as discussed in the next section. Additional comments on array strum, including evidence for the two modes of propagation along the array, are contained in reference [7]. Future investigations into the degree of array strumming as a function of ocean current speed are planned.

Note that the uppermost section, channels 111 to 120, did not operate during the Swallow float deployment. Also, channel 21 is anomalously noisy and channel 100 appears to record unusually low signal levels.

XII. Acoustic Velocity and Pressure Autospectra and Spectral Ratios

The calibrated autospectral estimates from data collected by the Swallow floats' three orthogonally-oriented geophone components during selected periods of time are presented in Figures XI.1 through XI.7; those estimated from data collected by OBS Judy's three-component geophone and by its infrasonic hydrophone are plotted in Figures XI.9 through XI.11; and the calibrated autospectra estimated from data collected by the 120 channels of the vertical line array are shown in Figures XI.13 through XI.17. After the Swallow float spectral plots, the set of figures in Figures 8a through 8h show the ratio of each of the other floats' spectra to the spectra estimated from float 2's data. Following the OBS spectral estimate plots are plots of the ratio of the OBS-Judy-data-derived spectra to Swallow-float-data-derived spectra. These appear in Figures XI.12a through XI.12h. Plots of the ratio of the VLA-data-derived spectra to Swallow float spectra follow the VLA spectra, in Figures XI.18 through XI.22.

The Swallow float spectral estimates were made by dividing a 40.96-second (2048-point) piece of data within each record, gotten after skipping the first three seconds in the record in order to reduce tape recorder contamination, into various length segments with a 50 % overlap between segments. These segments were Fourier transformed after being windowed with a Kaiser-Bessel window of $\alpha = 2.5$. The length of each segment which was transformed is given both in seconds at the top of each figure and in sample points in the table in part a) of this section. This process was followed for a specified number of consecutive records; the number of records in each spectral estimate is given in the table in part a). The resulting individual spectra were then incoherently averaged in order to reduce the variance of the autospectral estimates; the 90 % confidence limits are typically plus or minus a dB or so. The geophone autospectra were finally properly normalized (re Appendix 1) to give units of dB re 1 (m/sec)²/Hz. By making the assumption that the average potential energy density of the sound field is equal to the average kinetic energy density (shown in [5] to be a valid assumption), an estimate of the pressure spectrum can be calculated from the individual geophone-component particle velocity autospectra. This geophone-data-derived pressure autospectral estimate is plotted in the uppermost panel of each figure in units of dB re 1 (μ Pa)²/Hz.

The OBS and VLA spectral estimates were calculated in a similar manner. However, since their time series are continuous for long durations of time, no allowance needed to be made for data gaps (as was required with the Swallow float data because of the one second of zeros every 45 seconds). Therefore, all data segments contributing to a given spectral estimate were overlapped by 50 % for these two sensor systems. Information on the length of each of the data segments which were transformed and the total duration of the time series from which the spectral estimates were made are given at the top of the figures and in the tables in part b) and c).

All of the plots in this section have an abscissa in units of frequency with a range of 0 to 25 Hz.

a) Swallow Float Data

The time periods selected for calculating the Swallow float spectral estimates are:

Times of Swallow Float Spectral Estimates

Start Record (No. of Recs)	Time (Date)	Floats	FFT Length in points (calib. curve)	Comment	Figure Nos.
515 (20)	00:21 (9-18)	0 - 9	2048 (old)	21 Hz from De Steiger	XI.1
630 (20)	01:47 (9-18)	1(y)	512 (new)	comparable to self noise	XI.2
1351 (20)	10:48 (9-18)	0 - 8	2048 (old)	22 Hz from De Steiger	XI.3
1381, 1380 (4)	11:10 (9-18)	0, 4	512, 1024 (new)	whale(?) clicks	XI.4
1565	13:29	0 - 9	2048	16 Hz from	XI.5

(20)	(9-18)		(old)	De Steiger	
1596	13:52	0 - 9	2048	11 Hz from De Steiger	XI.6
(20)	(9-18)		(old)		
1807	16:30	0, 2 - 8	512	OBS event 904, VLA tape 453	XI.7
(3)	(9-18)		(new)		

Laboratory calibration measurements made after the August, 1988 Swallow float deployment determined that some adjustments were necessary to the old Swallow float geophone calibration curve (re Appendix 1b and reference [5]). Some of the spectra presented in this section - those in Figures XI.1, XI.3, XI.5, and XI.6 - were calculated using the old calibration curve. All other spectra were obtained using the new curve. In column 4 of the table above is specified which of the two calibration curves was used in the spectral estimates. Figure A1.4 provides the correction curve needed to adjust the old spectral levels to obtain the true calibrated autospectra.

The figures in this part of this section are placed in chronological order, and in order of increasing depth of the floats.

1) Records 515 - 534, 1351 - 1370, 1565 - 1584, 1596 - 1615; Tones from the HLF 3 Source

Four tonals in the Swallow float frequency band, at 11 Hz, 16 Hz, 21 Hz, and 22 Hz, were generated by the HLF 3 deployed from the De Steiger. Figures XI.1a through XI.1j show the spectra estimated from data collected by floats 0 through 9 at a time when the 21 Hz tone was being broadcast. A line at 21 Hz, which is as much as 10 dB above the background noise (re Figure XI.1c), can be seen in the horizontal geophone-component spectra of floats 2, 3, 4, 5, and 7. Further increase in the signal-to-noise ratio can be gotten by increasing the fft length. The "lumpiness" seen in the z axis spectra is due to the fact that the floats were still descending in the water column to their equilibrium depth during this time. The quickly oscillating behavior of the spectral levels with frequency are believed due to the seismic profiler signal.

Figures XI.3a through XI.3i show the spectral estimates from floats 0 through 8 during the time of the 22 Hz broadcasting. (Float 9 was contaminated by tether effects during this time and so its spectra are not presented). All the floats, except float 8 which was still ascending (re Section VII), had by this time settled at their equilibrium depth. A line at 22 Hz, sometimes over 12 dB above the background noise, can be clearly seen in all the floats' spectra. For the shallowest floats 0 through 4, the line is present on all three geophone components; for the deeper floats 5, 6, and 7 which stabilized near the base of the ocean sound channel, it occurs predominantly on the horizontal components. However, float 8, which was below 3600 meters at this time, detected the tonal on both of its x and z axis geophones. Note that since the seismic profiler was not operating at this time, the quickly oscillating behavior seen in Figures XI.1 is not present.

The 16 Hz tone was being transmitted during the time when the data in records 1565 through 1584 were collected; the spectra estimated from these data for floats 0 through 9 are plotted in Figures XI.5a through XI.5j. The 16 Hz line shows greater variability in signal-to-noise ratio from float to float; it is not detectable in float 3's data whereas float 7's x axis recorded a strong signal, about 15 dB above the background. Note that the small horizontal offset between the vertical dotted line at 16 Hz and the peak in the spectra is explainable by the finite frequency binwidth in the spectral estimates rather than by an offset in the frequency being transmitted by the source. The seismic profiler had begun again to transmit, resulting in the "grassiness" of the spectral curves.

Finally, the Swallow float detection of the 11 Hz line transmitted by the HLF 3 is shown in Figures XI.6a through XI.6j. This line is the most difficult of the four tones to detect because of the roll-off with decreasing frequency in the source level transmitted by the HLF 3. In fact, floats 3, 4, 5, and 6 appear to not have heard this frequency. Also, no detectable line at 11 Hz occurs in any of the vertical axis spectra, except possibly that from float 8. However, the three shallowest floats, 0, 1, and 2, and the two deepest floats 7 and 8, display a distinct line in one of their horizontal axes' spectra. Note that floats 0, 7, and 8 were oriented so that their x axis geophones barely detected the seismic profiler signal, but they had excellent 11-Hz-signal-to-noise ratios. These floats' compass headings were all about 0° magnetic at this time

(re the plots in Section VI) so that their y axes were oriented north/south, in the direction of the seismic profiler (re the discussion with regard to the time series recorded during the first explosion, records 1526-1527, in Section X) and their x axes were oriented east/west, in the direction of the De Steiger.

2) Records 630 - 649; Float 1 y Axis Spectra vs Laboratory-Measured Self Noise

As mentioned repeatedly in previous sections, the 8 kHz localization hydrophone attached to float 1 is believed to have been struck by the ship's prop during float deployment. The impact knocked the hydrophone, still attached to its cable, onto the top of the float, causing the float to list substantially to one side. This listing forced the y axis geophone coil to rest against its stop for almost the whole experiment. (For an example of a time when the coil came off its stop, refer to the discussion on the first explosion arrival in the previous section). Since the y axis geophone was effectively prevented from producing a voltage in response to float motion, then any y axis voltage signal present at the A/D converter must have been generated by electronic self noise within the geophone data acquisition system. Figure XI.2 shows a comparison between the autospectrum estimated from float 1's y axis geophone data and float 11's electronic self noise data, measured in the laboratory by replacing the geophone with a resistor whose resistance was equal to the geophone coil resistance. Below about 15 Hz, both spectra agree quite well. Float 1's spectrum is the lower curve below 8 Hz in the figure; the fact that it is quieter than float 11's self noise is probably a reflection of the variation in self noise characteristics of the front-end amplifiers among the floats. Above about 15 Hz, float 1's spectrum becomes increasingly greater with increasing frequency than the self noise spectrum. The reason for this may be that higher frequency ocean noise is more effectively coupled into the geophone system when the coil is against its stop than are lower frequencies. Evidence that float 1 is detecting higher frequency ocean noise can be gotten from the peak at about 18 Hz; this peak also occurs in float 0's spectra at this time.

3) Records 1380 - 1384; Whale(?) Clicks

Spectra estimated at times when the 0.5-to-one-second-duration clicks were seen in the time series (re Figures X.3) are presented in Figures XI.4a through XI.4c. Figure XI.4a shows the 512-point spectral estimate calculated from float 0's data over a four-record interval starting with record 1381 and Figure XI.4b is a plot of the 512-point spectral estimate calculated from a four-record portion of float 4's data starting with record 1380. The data in these two estimates are offset by one record in order to avoid contamination by the localization ping; float 0 issued a range ping during record 1380 and float 4 issued a ping during record 1384. The data used in the spectral estimate in Figure XI.4c are the same as those for Figure XI.4b; the only difference is that the fft length was doubled. The clicks result in a broad hump (broad at least on plots with this scaling) centered around 18 Hz, and a possible "peakiness" at 9 Hz. However, complicating the interpretation is the fact that the R/V Sproul was rather close to the array at this time, involved in the deployments of the first explosive charge and OBS Judy (re Section III). Therefore, ship noise may result in some of the features seen in the spectra, e.g. the line at 20 Hz on the z axis in Figure XI.4c and possibly the hump at 12 Hz. In addition, the character of float 1's spectra is determined partly by clipping caused by the clicks themselves and by an anomalous arrival nine seconds after the start of record 1383.

In order to further evaluate the effect of the clicks on the spectra, the direct arrival from a single click was extracted. This was done by removing one second of data (50 points) enveloping the first arrival in the second set of arrivals in record 1380 of float 4's data. The minimum variance (i.e. maximum likelihood) technique was used to calculate a spectral estimate of this single click. The estimate showed concentrations of energy about 9 Hz and 18 Hz, confirming the observations made from the conventional spectral estimates. The results of this work will be presented at a later date.

4) Records 1807 - 1809; Seismic Profiler and General Spectral Characteristics

Spectral estimates based on 512-point FFTs of the data in records 1807 through 1809 are plotted in Figures XI.7a through XI.7h. Spectra calculated from data recorded by all properly functioning midwater floats, floats 0 and 2 through 8 (float 8 was near its equilibrium depth by this time), are presented. These data were recorded at the same time as OBS event 904 and VLA tape 453.

As mentioned previously, the seismic profiler was operating during this time. Comparison of these spectra with those estimated from data in records 1380 through 1384 (Figures XI.4a and XI.4b) show that the presence of the profiler's signals cause the background noise levels between 6 Hz and 16 Hz to increase by up to 10 dB. The increase is especially large in the horizontal axes' data, giving rise to the highly azimuthally anisotropic nature of the noise field in this deployment. Many of the details that are visible in the spectra from records 1380 through 1384 are presumably buried by the higher background levels in records 1807 - 1809 spectra.

The main features of these spectra are similar to those in spectra estimated from data collected in other Swallow float deployments (which were all located in the vicinity of Deep Sea Drilling Project hole 469) [3,4,5]. Both sets of spectra have noise levels which are approximately independent of frequency above 5 Hz, although the background level of 85 dB re 1 (μPa) $^2/\text{Hz}$ during records 1807 - 1809 is about 10 dB higher than in previous deployments. Below 5 Hz, both spectra display a slope of about -18 dB/octave (f^{-6}), representing the noise level rise towards the microseismic peak. The vertical geophone axis spectra above a few hertz are typically 6 to 10 dB lower than the horizontal geophone component spectra, although the presence of the seismic profiler signals in this deployment accentuated this difference. The increase in spectral slope below 0.5 Hz seen in all the geophone spectra is non-acoustic in nature. (Additional motion-induced contamination can be seen in the spectra of floats 3 and 5; i.e., the peak at 1.5 Hz in float 3's y axis spectra and the peak at 1.8 Hz in float 5's horizontal axes spectra).

A 9.6 Hz peak of unknown origin occurs in many of the horizontal axes' spectra in Figures XI.7a through XI.7h. Two peaks, one of slightly greater frequency than 9.6 Hz and the other of slightly smaller frequency, are present in the spectra from records 1380 through 1384. These peaks may be related to whale noise.

5) Spectral Ratios - Depth Dependence of Noise Levels

The Swallow float spectral ratio plots, presented in Figures XI.8a through XI.8g, were calculated from the spectra just discussed in part a.4 of this section, i.e., those from records 1807 through 1809. The component spectra from midwater floats 0 and 3 through 8 were normalized by float 2's component spectra. Float 2's data were chosen as a basis for the comparisons since this float was deployed at a depth approximately equal to the sound channel axis depth where the ambient noise levels may be expected to be their highest. These Swallow float spectral ratios were calculated in order to examine the possibility of a depth dependence of the ambient noise levels. No simple, consistent depth dependence of the noise field exists in these plots. However, the ratios show much greater deviations from 0 dB than the ratios of Swallow float spectra estimated from data collected by floats deployed at about the same depth [14]. The greatest deviations appear to occur at those frequencies generated by the seismic profiler, i.e., 5 Hz to 16 Hz. Confusing the comparison of the horizontal axes' spectra is the fact that the geophone axes have not been aligned and the presence of the seismic profiler results in an azimuthally anisotropic noise field.

b) Ocean Bottom Seismometer Data

The following table contains the information on the pieces of OBS Judy data chosen for spectral estimation.

Event	Time (Date)	Times of OBS Judy Spectral Estimates			Comment	Figure Nos.
		Swallow Float Records	FFT Length in Points (Total Data Length)			
902	15:30	1727 - 1731	2048		22 Hz from	XI.9

	(9-18)		(8192)	De Steiger	
904	16:30 (9-18)	1807 - 1809	512 (6912)	VLA tape 453	XI.10
905	18:30 (9-18)	1967 - 1971	2048 (8192)	11 Hz from De Steiger	XI.11

1) Events 902, 905; Tones from the HLF 3 Source

Figures XI.9 and XI.11 show the spectra estimated from the four channels of OBS Judy data during events in which the HLF 3 was broadcasting. The frequency being generated by the source is indicated by vertical dotted lines in each figure. These spectra were calculated by averaging seven 2048-point ffts overlapped by 50 %. The HLF 3 signal is not present in any of the components' spectra in either figure. (The line at 22 Hz in the hydrophone spectrum, shown in the top panel in Figures XI.9 and XI.11, is caused by a software-generated contamination occurring every half second in the pressure time series; see reference [14]). The source signal was also not present in spectra estimated using longer fft lengths. The deployment of the ocean bottom seismometer at a water depth much greater than the critical depth obviously prevented it from detecting the long range source signals.

2) Events 902, 904, and 905; General Spectral Characteristics

In Figure XI.10, the spectra estimated from 512-point ffts of event 904's data are presented. Comparison of these spectra with those calculated from data in events 902 and 905 show some interesting features. Referring first to the OBS hydrophone spectra in the uppermost panel in the figures, the aforementioned software-generated spikes are present every 2 Hz. The background hydrophone noise levels show a constant decrease with increasing frequency; a total decrease of about 7 dB from 5 Hz to 25 Hz. This frequency dependence of the noise levels is probably non-acoustic in nature.

The OBS geophone data (the lower three panels in the figures) appear to be of higher quality than the hydrophone data. The consistency from one event to the next in the noise levels reported by the horizontal geophone components suggest that the data from this instrument in this experiment are much more reliable than the horizontal-component data collected during the April - May, 1987 experiment [14]. All geophone component spectra show a lump of energy peaking at 18 Hz which corresponds to the feature in the Swallow float spectra associated with the whale clicks. However, note that a possible resonance in the OBS-to-sediment coupling exists at this frequency; a resonance in the coupling was identified in data collected at another site, DSDP 469 [18]. A set of peaks around 16 Hz and the spike at 20 Hz in the vertical geophone spectrum in event 905 (Figure XI.11) are probably the result of noise generated by the R/V Sproul; the ship was several miles to the south of OBS Judy during the recording of events 902 and 904, but was quite close (within a mile or two) and traveling at about 6 knots during event 905.

The background noise levels on the horizontal OBS geophone axes between 5 Hz and 25 Hz are about 10 to 15 dB higher than those on the vertical axis. Below 5 Hz, all geophone component spectra show a sharp rise with decreasing frequency to a peak at about 3.7 Hz. This peak is about 25 dB higher on the horizontal components than on the vertical component. Below this frequency, the geophone component spectra have a complicated (although consistent) structure, especially the horizontal component spectra. All components have approximately equal maximum noise levels of slightly greater than -105 dB re 1 (m/sec)²/Hz near the microseismic peak around 0.2 to 0.3 Hz.

3) Ratio of OBS Spectra to Swallow Float Spectra

The ratio of OBS Judy component spectra to Swallow float spectra are shown in Figures XI.12a through XI.12h. The data from which the spectral estimates were made - event 904 for the OBS data and

records 1807 to 1809 for the Swallow float data - are offset in time by less than a half minute.

The uppermost panel shows the ratio of the OBS hydrophone spectrum to the Swallow float geophone-data-derived pressure spectrum. Although the OBS hydrophone measures acoustic pressure and the Swallow float geophones measure acoustic particle velocity, this comparison is valid if the assumption is made that the average acoustic potential energy density of the ambient noise field is equal to the average kinetic energy density. Above 20 Hz, the noise levels recorded by the two sensor systems are about the same, but the OBS hydrophone detects increasingly louder noise levels with decreasing frequency. This result is contrary to that expected - sensors deployed within the sound channel should record larger ambient noise levels than sensors deployed below the critical depth. The OBS hydrophone data may be contaminated by non-acoustic turbulent pressure fluctuations, pressure fluctuations associated with sediment interface waves, or by electronic self noise.

The Swallow float geophones and the OBS geophone also measure different quantities - the former measure water particle motion whereas the latter measure sediment motion. Note also that the orientation of the two sensors' horizontal geophone components are not aligned. The lower three panels in Figures XI.12a through XI.12h show that the spectral levels of the three components of sediment motion are generally within plus or minus 10 dB of the water particle motion spectra between 5 and 15 Hz. Above 15 Hz, the OBS spectra are 5 to 10 dB quieter than the Swallow float spectra. Below 5 Hz, the OBS horizontal geophone component spectra quickly diverge from the Swallow float spectra; the noise levels recorded by the ocean bottom seismometer are more than 20 dB greater than the Swallow float noise levels. These differences are probably due to sediment-waveguide-trapped seismic waves. The differences between the vertical axes' spectra below 5 Hz are less than on the horizontal axes; the maximum differences are about 15 dB. In addition, the differences occur in peaks centered at about 0.9 and at 3.6 Hz. An additional peak in the vertical axes' spectral ratio occurs at 7.7 Hz.

In a recent (June, 1989) experiment involving the Marine Physical Laboratory's Remote Underwater Manipulator (RUM), a Swallow float geophone mounted on a PVC disk external to the glass sphere was deployed on the ocean sediment. A second concurrently-deployed float was equipped with an infrasonic ceramic hydrophone and was tethered by a half-meter line to the ocean bottom. A comparison of the spectra estimated from data collected by these two floats show the same general features as the OBS-to-Swallow-float comparisons in this report. The data from the Swallow float deployment by RUM will be presented at a later date.

c) FLIP Vertical Line Array Data

The periods of time chosen for calculating the spectral estimates from the channels of the vertical line array are:

Times of VLA Spectral Estimates					
Tape No. (Channels)	Time (Date)	Swallow Float Records	FFT Length in Points (Total Data Length)	Comment	Figure Nos.
433 1 - 120	07:45 (9-18)	1107 - 1118	2048 (26624)	16 Hz from De Steiger	XI.13
440 61 - 120	10:49 (9-18)	1352 - 1355	2048 (8192)	22 Hz from De Steiger	XI.14
442 1 - 120	12:01 (9-18)	1448 - 1451	512 (8192)	--	XI.15
447 61 - 120	13:50 (9-18)	1593 - 1603	8192 (24576)	11 Hz from De Steiger	XI.16
453 1 - 120	16:30 (9-18)	1807 - 1809	512 (6912)	OBS event 904, seismic profiler	XI.17

Note that since the uppermost section of the array, channels 111 through 120, did not operate during the Swallow float deployment, their spectral plots are nonsensical. Also, channel 21 seems to have

malfunctioed and channel 100 reports unusually low noise levels.

1) Tapes 433, 440, 447; Tones from the HLF 3 Source

The vertical line array spectral estimates, based on an incoherent average of 2048-point ffts, during periods when the HLF 3 was transmitting a 16 Hz tone and a 22 Hz tone are plotted in Figures XI.13 and XI.14, respectively. Both signals are apparently audible on many of the array channels. The 16 Hz line in tape 433's data (Figures XI.13a through XI.13k) is as much as 10 dB above the background in some spectra. It appears to be more predominant on the shallower channels, i.e., channels 50 through 100. The 22 Hz line in tape 440's data is as much as 7 dB above the background; e.g., the spectrum for channel 62 in Figure XI.14b. However, note that a 22 Hz line appears in some of the spectra from tape 433 - for example, in channel 13's spectrum in Figure XI.13c - even though only the 16 Hz tone was being broadcast at this time! Likewise, a 16 Hz line appears in some of the spectra from tape 440 (channel 62 in Figure XI.14b) during the transmission of the 22 Hz tone. The source(s) of these anomalous peaks is unknown. An additional 20 Hz spike of unknown source, possibly related to the 16 Hz and 22 Hz peaks, occurs in many of the shallower channels' spectra. (The 20 Hz spike is most likely not generated by the R/V Sproul; during the recording of tape 433, the ship was 15 km to the south of the array). The presence of these anomalous peaks complicates the interpretation of the HLF 3 signal data.

The spectral estimates which were calculated in order to look for the HLF 3-generated 11 Hz line are shown in Figures XI.16b through XI.16f. The fft length was increased to 8192 points in order to increase the signal-to-background-noise ratio. Many of the channels' spectra contain a "suggestion" of an 11 Hz line, but its actual presence is uncertain. A correlation analysis between the various channels may help to determine whether or not this tone was audible to the array.

2) Tapes 442, 453; General Spectral Characteristics

The spectral estimates from tapes 442 and 453's data were made using shorter fft lengths, 512 points, allowing a greater number of incoherent averages for statistical stability. These plots are presented in Figures XI.15 and XI.17. The background noise levels in tape 442's spectra are generally between 80 and 85 dB re 1 (μPa) $^2/\text{Hz}$ between 10 Hz and 25 Hz, whereas the background is slightly greater than 90 dB in this frequency band in tape 453's spectra. The increase in background levels is probably caused by the operation of the seismic profiler during the recording of tape 453 (re Section II d). In tape 442's spectra, a lump of energy is present between 16 Hz and 20 Hz; it peaks at 18 Hz and is about 10 dB above the background. This feature, seen in both the Swallow float data and the OBS data, has been associated with whale-generated clicks in this report. The presence of this 18 Hz lump is somewhat hidden by the higher background levels in tape 453's spectra. Because of the lower background levels during tape 442, additional spectral features, e.g., the complicated structure of the whale-generated spectral lump above 18 Hz and a peak around 11.5 Hz, are present in many of the spectra. The 11.5 Hz peak may have been generated by the R/V Sproul; it was within a few kilometers of the array during the recording of tape 442.

Below 10 Hz, the spectra show large variations in level and structure with respect to both channel number and time. This is caused by contamination from flow and strum. At times and on some channels, the degree of contamination is sufficient to appreciably affect frequencies above 10 Hz. A negative spectral slope with frequency above 10 Hz (an increase of about 10 dB in background levels from 25 Hz to 10 Hz) and a lump of energy between 10 Hz and 15 Hz in some of the spectra are probably indications of contamination. It appears that the shallower channels (with channel numbers greater than 60) suffer a greater amount of contamination than the deeper channels. Future investigations into the characteristics of the vertical line array flow and strum contamination are planned.

3) Ratio of VLA Spectra to Swallow Float Spectra

The final figures of this section, Figures XI.18 through XI.22, show plots of the ratio of averaged vertical line array pressure spectra to Swallow float geophone-data-derived pressure spectra. These ratios are indicated by the solid curve in each figure. The dashed curves in the figures will not be discussed in this report. (They are the result of estimating the vertical component particle velocity spectrum using the cross spectrum between two adjacent VLA channels' pressure time series and then normalizing by the Swallow float vertical geophone component spectrum). As mentioned previously, the conversion of the Swallow float geophone component particle velocity spectra into an equivalent pressure spectrum assumes that the average acoustic potential energy density of the sound field is equal to its average kinetic energy density.

The spectral ratios were estimated from VLA and Swallow float data collected at approximately the same time. The data were also collected at approximately the same depth; float 3 was at about the same depth in the ocean as channels 3 and 4 of the vertical line array and float 2 was at about as deep as channels 43 and 44. Since float 0 was at the same depth as the uppermost section of the array and this section did not operate properly during the Swallow float deployment, two adjacent channels, 107 and 108, from the next shallowest section were used. It is believed for various reasons [Barbara Sotirin, private communication], that the array channels with the highest quality data are those which are one or two channels removed from the center of an array section, e.g. channels 3 and 4, 7 and 8, 13 and 14, 17 and 18, etc; the channels used in this VLA-Swallow float comparison were therefore chosen from this set. Because of the problems caused by float 1's non-functioning localization hydrophone, its data were not used.

The spectral estimates in the spectral ratio calculations were obtained by incoherently averaging 512-point ffts. The VLA spectra for each channel were based on a total of 12288 points, about 4 minutes and 6 seconds of data, allowing for 47 estimates in the spectral average, whereas the Swallow float spectra were estimated from data in six consecutive records, providing 42 estimates in the average. The VLA pressure spectral estimate used in the spectral ratio calculation was the arithmetic average of the individual pressure spectra from the two adjacent channels.

These figures show that, in general, the vertical line array pressure spectra agree quite well with the Swallow float geophone-data-derived pressure spectra between 10 Hz and 24 Hz; the VLA reports an average of about 2 to 3 dB higher noise levels than the Swallow floats in this frequency range. An exception to this is the occurrence in some of the figures of a peak centered about 12.5 Hz and with spectral ratio levels as large as 16 dB (re Figure XI.19a). This peak occurs most predominantly in the ratio of channels' 107-108 spectra to float 0's spectra - i.e., in the shallowest sensors' data - and is probably the result of flow and strum contamination in the array data. This contamination is the reason that the spectral ratios quickly increase with decreasing frequency below 10 Hz. The roll-off in the spectral ratio curves above 23-24 Hz is caused by the finite transition width of the anti-aliasing filter used in desampling the VLA data.

The conclusion from this comparison of the VLA and the Swallow float spectra is that by careful selection, the flow and strum contamination in the vertical line array data can be isolated to frequencies below 10 Hz.

Acknowledgements

We would like to thank Marvin Darling at the Marine Physical Laboratory for his many contributions to the Swallow float project. The vertical line array data along with many helpful comments were provided to us by Barbara Sotirin at the Marine Physical Laboratory. Jean-Marie Tran also aided our understanding of the vertical line array data. The ocean bottom seismometer data was supplied by Dr. LeRoy Dorman's group at Scripps Institution of Oceanography. The crew of the R/V R. G. Sproul was very patient and helpful.

This work was supported by the Office of Naval Research under contract #N00014-87C-0127.

References

- [1] J. A. Hildebrand and B. J. Sotirin, "Preliminary expedition report for Fall, 1987 vertical line array experiment - R/P FLIP" Marine Physical Laboratory, Scripps Institution of Oceanography, San Diego, CA (1987).
- [2] W. S. Hodgkiss and V. C. Anderson, "Acoustic positioning for an array of freely drifting sensors" IEEE J. Oceanic Eng. 8(3), (1983).
- [3] G. L. D'Spain, R. L. Culver, W. S. Hodgkiss, and G. L. Edmonds, "Freely drifting Swallow float array: April, 1987 trip report" MPL Tech. Mem. 397, Marine Physical Laboratory, Scripps Institution of Oceanography, San Diego, CA (1987).
- [4] G. L. D'Spain, R. L. Culver, W. S. Hodgkiss, and G. L. Edmonds, "Freely drifting Swallow float array: May, 1987 trip report" MPL Tech. Mem. 402, Marine Physical Laboratory, Scripps Institution of Oceanography, San Diego, CA (1988).
- [5] G. L. D'Spain, R. L. Culver, W. S. Hodgkiss, and G. L. Edmonds, "Freely drifting Swallow float array: August, 1988 trip report" MPL Tech. Mem. 407, Marine Physical Laboratory, Scripps Institution of Oceanography, San Diego, CA (1989).
- [6] R. D. Moore, L. M. Dorman, C. Y. Huang, and D. L. Berliner, "An ocean bottom, microprocessor based seismometer" Marine Geophys. Res. 4, (1981).
- [7] B. J. Sotirin and J. A. Hildebrand, "Large aperture digital acoustic array" IEEE J. Oceanic Engin. 13 (4), (1988).
- [8] B. J. Sotirin and J. A. Hildebrand, "Acoustic navigation of a large aperture array" (in press).
- [9] J. Churgin and S. J. Haliminski, Temperature, Salinity, Oxygen, and Phosphate in Waters off the United States, Eastern North Pacific, National Oceanographic Data Center, 3, (1974).
- [10] K. V. Mackenzie, "Nine-term equation for sound speed in the oceans" J. Acoust. Soc. Am., 70 (3), (1981).
- [11] "Preliminary determination of epicenters" monthly listings from the Nat'l Earthquake Information Center, U.S. Dept. of the Interior (Sept, 1987).
- [12] W. A. Watkins, P. Tyack, and K. E. Moore, "The 20-Hz signals of finback whales (*Balaenoptera physalus*)" J. Acoust. Soc. Am., 82 (6), (1987).
- [13] A. W. Sauter, L. M. Dorman, and A. E. Schreiner, "A study of the sea floor structure using ocean bottom shots and receivers" in Ocean Seismo-Acoustics, ed. T. Akal and J. M. Berkson, Plenum Press, (1986).
- [14] G. L. D'Spain and W. S. Hodgkiss, "Comparison of Swallow float, ocean bottom seismometer, and sonobuoy data in the VLF band" Marine Physical Laboratory, Scripps Institution of Oceanography, San Diego, CA (1988).

- [15] M. Pieuchot, Seismic Instrumentation, vol. 2, from Handbook of Geophysical Exploration, Section I - Seismic Exploration, ed. K. Helbig and S. Treitel, Geophysical Press (1982).
- [16] A. B. Williams, Electronic Filter Design Handbook, McGraw-Hill (1981).
- [17] A. Antoniou, Digital Filters: Analysis and Design, McGraw-Hill (1979).
- [18] A. W. Sauter, "Studies of the upper oceanic floor using ocean bottom seismometers" Ph.D dissertation, University of California, San Diego, (1987).

Appendix 1 - Swallow Float Geophone Data Acquisition System

a) System Response

A block diagram of the Swallow float geophone electronics system appears in Figure A1.1. The water particle motion (and float rocking) is first coupled into motion at the geophone. The particle velocity at the geophone is then converted into voltages representing the three orthogonal components of particle velocity. The geophones are electromagnetic transducers in which a voltage is produced across a moving, conducting coil by its motion through the magnetic field lines produced by a permanent magnet [15]. The resulting voltage is proportional to the velocity of the coil with respect to the magnet. Constraining the coil to move in only one direction are elastic springs connecting the coil to the instrument casing. (Laboratory tests have determined that the geophones can withstand a maximum tilt from vertical of about 15°). The geophone package in each Swallow float is composed of three such transducers oriented to measure in three orthogonal directions.

The geophone amplitude and phase response was calculated using the theoretical equation of motion for this system [15]. The amplitude response curve is nearly identical to the manufacturer's calibration curve provided with the geophones. Near-critical damping of the coil is achieved using a 60 kΩ shunt resistor. An f^2 roll-off in the geophone amplitude response below the natural frequency of 8 Hz effectively pre-whitens the ocean ambient noise so that no additional pre-whitening needs to be implemented.

The three signals next undergo a fixed gain of 95 dB before being input to the automatic gain control (AGC). Included in the geophone channel circuitry are nine RC circuits. Five of these RC circuits act as high pass filters, with poles located at 0.000034, 0.034, 0.07, 0.26, and 0.47 Hz, in order to eliminate DC bias and decrease ultra-low frequency self noise. The other four RC circuits act as low pass filters, with poles at 34, 34, 72, and 337 Hz, in order to eliminate AC coupling noise (i.e. "cross-talk"). These RC circuits are lumped together with the geophone channel "fixed gain" in Figure A1.1.

The three geophone component voltages are then sent to a automatic gain control (AGC) amplifier. The AGC is a variable gain amplifier with a range of 0 to 25 dB gain which allows the full dynamic range of the eight-bit A/D converter to be used. The AGC gain always changes by a 0.5 dB step between records; if more than 1 % of all data samples from the last 40 seconds of each record are clipped, then the AGC decreases by 0.5 dB. Otherwise, it increases. Plots of the AGC level for each float during every record are given in Section VI.

Before digitizing, the signals are passed through a five-pole, four-zero, elliptic, anti-aliasing filter. Elliptic filters theoretically have the sharpest transition region for a given number of poles and circuit complexity. The filter frequency response and the pole, zero locations in the s plane are shown in Figure A1.2 [16,17]. Incoming signals are amplified by a maximum of 4.6 dB in the passband, which has a 0.28 dB equal ripple. The cut-off frequency (the highest frequency at which the amplitude gain is equal to the minimum passband gain) is 20 Hz, and the attenuation is 19.5 dB at the Nyquist frequency of 25 Hz. The maximum equal ripple level in the stop band is 50.1 dB below the level in the pass band and is first reached at 31 Hz. Before installation in the floats, all filters were adjusted so that broadband noise input to the filters yielded the same amplitude response and same null location at the filters' output.

The geophone channel response, including all components in the system except the AGC gain (which varies over the time of the experiment) is plotted in Figure A1.3.

The three signals are then digitized at a 50 Hz sampling rate and put into a temporary buffer. After 44 seconds of data (equal to one data record) have accumulated in the buffer, a one second period of writing the data to cassette tape takes place. During this time, no data is sampled. The 45 second cycle then repeats until the cassette tape is full. The cassette tape can store up to 17 Mbytes of unformatted data, which is sufficient space for up to 2100 three-component data records.

Both the RMS velocity plots presented in Section IX and the time series plots of Section X have been corrected for the variable AGC level. No other adjustments have been made in these plots. The autospectral plots of Section XI, however, have been corrected for all electronic system gains and therefore report calibrated autospectral estimates in units of dB re 1 (m/sec)²/Hz. By assuming that the average potential

energy density of the acoustic field is equal to its average kinetic energy density, an estimate of the pressure autospectrum, in units of dB re 1 (μPa)²/Hz, can be obtained from the individual geophone-component particle velocity autospectra. These estimates are plotted in the uppermost panel in Figures XI.1 through XI.7.

Excellent agreement between the laboratory-measured and theoretically-predicted amplitude and phase responses of the geophone channel circuitry, excluding the geophone itself, has been obtained. Approximate amplitude calibration of the total geophone data acquisition system has been achieved by comparing the geophone-data-derived pressure autospectra to the pressure autospectra estimated from data collected by the newly-installed Swallow float infrasonic hydrophones [5]. Additional calibration measurements of the Swallow float geophones will be conducted in the future.

b) Correction to Some of the Swallow Float Spectra

The nine RC circuits in the Swallow float geophone signal conditioning electronics had previously been assumed to have a negligible effect in the 1 to 25 Hz band. However, calibration measurements of the geophone system have shown that they actually have a significant effect at certain infrasonic frequencies. All previously reported Swallow float calibrated spectra, including those in references [3], [4], [5], and [14] have therefore under-estimated the geophone autospectral levels. In addition, some of the Swallow float spectra in Section XI - i.e., those in which a given frequency generated by the De Steiger source occurs, Figures XI.1, XI.3, XI.5, and XI.6 - were calibrated without taking the RC circuits into account. All other spectra in Section XI were properly calibrated. Figure A1.4 is a plot of the frequency-dependent correction to be added to these old spectra in order to obtain the true calibrated spectra.

c) Data Record Format

Shown in Figure A1.5 is the format of the Swallow float data records. Each record is composed of 7646 bytes, 7120 bytes of which are infrasonic acoustic data (including resynchronization and checksum bytes).

Appendix 2 - Calibration Curves for the OBS Instruments

The calibration curves for the ocean bottom seismometer geophones and the regular-type hydrophones are given in Figures A2.1 and A2.2, respectively. Each of the plots represents the frequency response of the whole instrument-amplifier-filter system. The curve for the OBS geophone was provided by Allan Sauter and Tony Schreiner. Allan Sauter also provided us with the regular OBS hydrophone system curve.

Appendix 3 - Calibration Curve for the Vertical Line Array Channels

Figure A3.1 is a hand-drawn block diagram of the vertical line array channel electronics. The channel response is approximately flat from 10 to 200 Hz, the frequency band for which the array was designed. Below 10 Hz, the roll-off in the response is provided by a single-pole RC circuit which is partially formed by the capacitance of the two hydrophones in each channel. (Two hydrophones are used in each channel in order to increase the acoustic sensitivity and decrease the sensitivity to non-acoustic accelerations). Laboratory measurements indicated that the resonant frequency of this RC circuit is around 5 Hz with a ± 1 Hz variation from channel to channel. Since the sensitivity of the hydrophones appears to be depth dependent [Barbara Sotirin, private communication], their capacitance may also be. In addition, the response of some of the electronics exposed to ambient pressures appears to be depth dependent. Therefore, a single frequency response function, calculated using a high-pass RC resonant frequency of 5 Hz, was used for all channels of the array as an approximation to the true calibration curve. This function is given in Figure A3.2 in units of dB re 1 (count/ μ Pa)². The plot represents the 0 to 25 Hz frequency response of the whole 2 hydrophone-preamplifier-line driver-variable gain amplifier-A/D converter system.

In order to quantify the comparisons between the Swallow float and the vertical line array spectral estimates, the VLA data were initially desampled from 500 Hz to 50 Hz. The transfer function of this desampling process is shown in Figure A3.3. Note that the difference above 23-24 Hz between the autospectra calculated from the VLA data and those from the Swallow float data (re Figures XI.18 through XI.22) is due to the roll-off in the anti-aliasing filters used in the desampling process. The OBS data are also resampled, from 128 Hz to 50 Hz. Information on this resampling process and a plot of the corresponding transfer function can be found in reference [14].

Appendix 4 - Differences in Navigation Position Fixes

Three different navigation techniques were used in the September, 1987 Swallow float deployment; NAVSAT, Loran-C, and GPS. The following table lists all the times and position fixes of the Sprout which were obtained by more than one navigation method at the same time;

Comparison of Sprout Position Fixes during the Sept, 1987 Experiment

All positions are referenced to 34° N, 125° W.

Times are in local Pacific Daylight Time; add 7 hours to get GMT.

Time	Date	NAVSAT on Sprout	Loran-C on Sprout bridge	Range, Bearing from FLIP from Sprout bridge	Range, Bearing from FLIP from FLIP scientific log
16:50	9-17	58.78', 58.64'	---	---	0.23 nm, 172°
18:27	9-17	58.70', 58.45'	---	---	0.16 nm, 145°
20:44	9-17	59.69', 56.42'	---	2.14 nm, 066°	2.16 nm, 066°
21:31	9-17	58.84', 58.82'	---	0.25 nm, 160°	---
22:07	9-17	59.85', 59.88'	---	1.60 nm, 309°	1.5 nm, 309°
22:48	9-17	57.14', 58.25'	---	# 2.00 nm, 173° #	# 2.0 nm, 172° #
10:55	9-18	58.15', 58.60'	---	0.73 nm, 173°	0.73 nm, 173.5°
11:32	9-18	58.46', 58.63'	58.44', ?	0.59 nm, 154°	0.59 nm, 154°
13:06	9-18	58.00', 57.82'	58.00', 57.33'	1.08 nm, 160°	1.08 nm, 160°
18:00	9-18	@ 54.44', 56.48' @	54.75', 55.75'	---	---
22:05	9-18	58.76', 56.31'	59.11', 55.09'	---	---
23:22	9-18	58.98', 56.48'	59.41', 55.39'	---	---
00:25	9-19	58.73', 57.01'	58.98', 55.88'	---	---
02:18	9-19	58.87', 56.64'	58.97', 55.61'	---	---
10:09	9-19	57.99', 58.13'	58.02', 57.41'	1.13 nm, 160°	1.13 nm, 160°
10:59	9-19	59.75', 55.90'	59.85', 55.36'	---	---
12:27	9-19	59.55', 59.75'	59.80', 58.97'	---	---
13:32	9-19	57.98', 57.72'	58.08', 57.27'	---	* 1.08 nm, 154° *
14:08	9-19	56.92', 57.53'	56.81', 57.10'	---	---
14:34	9-19	58.21', 57.62'	57.93', 57.08'	1.24 nm, 157°	1.24 nm, 157°

(#) The range-and-bearing-from-FLIP values at this time were gotten from the Sprout's bridge log and the FLIP scientific log, respectively. However, the entry in the Swallow float scientific log was a range of 2.15 nautical miles and a bearing of 171° magnetic.

(*) The time given in the FLIP scientific log for the range-and-bearing-from-FLIP-to-Sprout value for the deployment of shot #4 was 14:09, whereas the shot was actually deployed at 13:32. Although the FLIP log entry matches that of the Swallow float log entry, the Swallow float value was entered at a later time. At 14:09, the Sprout personnel recovered Swallow float 11.

(@) The NAVSAT position fix at this time was actually gotten by a linear interpolation of the position fixes entered in the log book at 17:50 and 18:16.

The least accurate of the three methods is NAVSAT. Most of the ship locations recorded in the Swallow float log were gotten from a NAVSAT receiver in the scientific laboratory of the Sprout. The crew on the bridge of the Sprout recorded position fixes from a Loran-C receiver in the ship's log. They sometimes also recorded the range and bearing to FLIP. The scientific party aboard FLIP determined the

range and bearing of the Sproul from FLIP. In conjunction with the GPS-determined FLIP positions, absolute position fixes can be derived from their measurements. Since GPS is the most accurate of the three navigation methods, these position fixes may be used in the future to correct the NAVSAT fixes recorded in the Swallow float log.

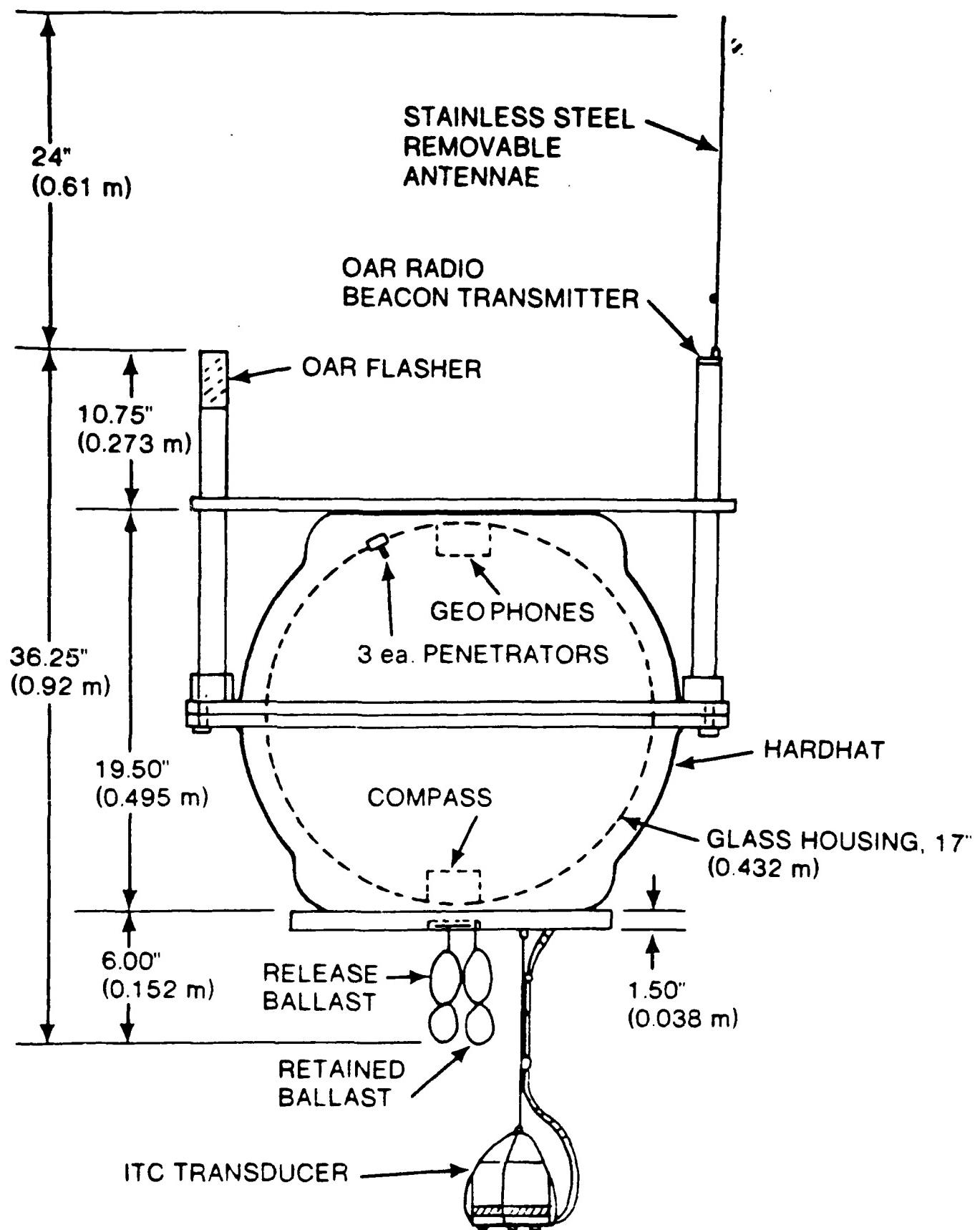


Figure 1

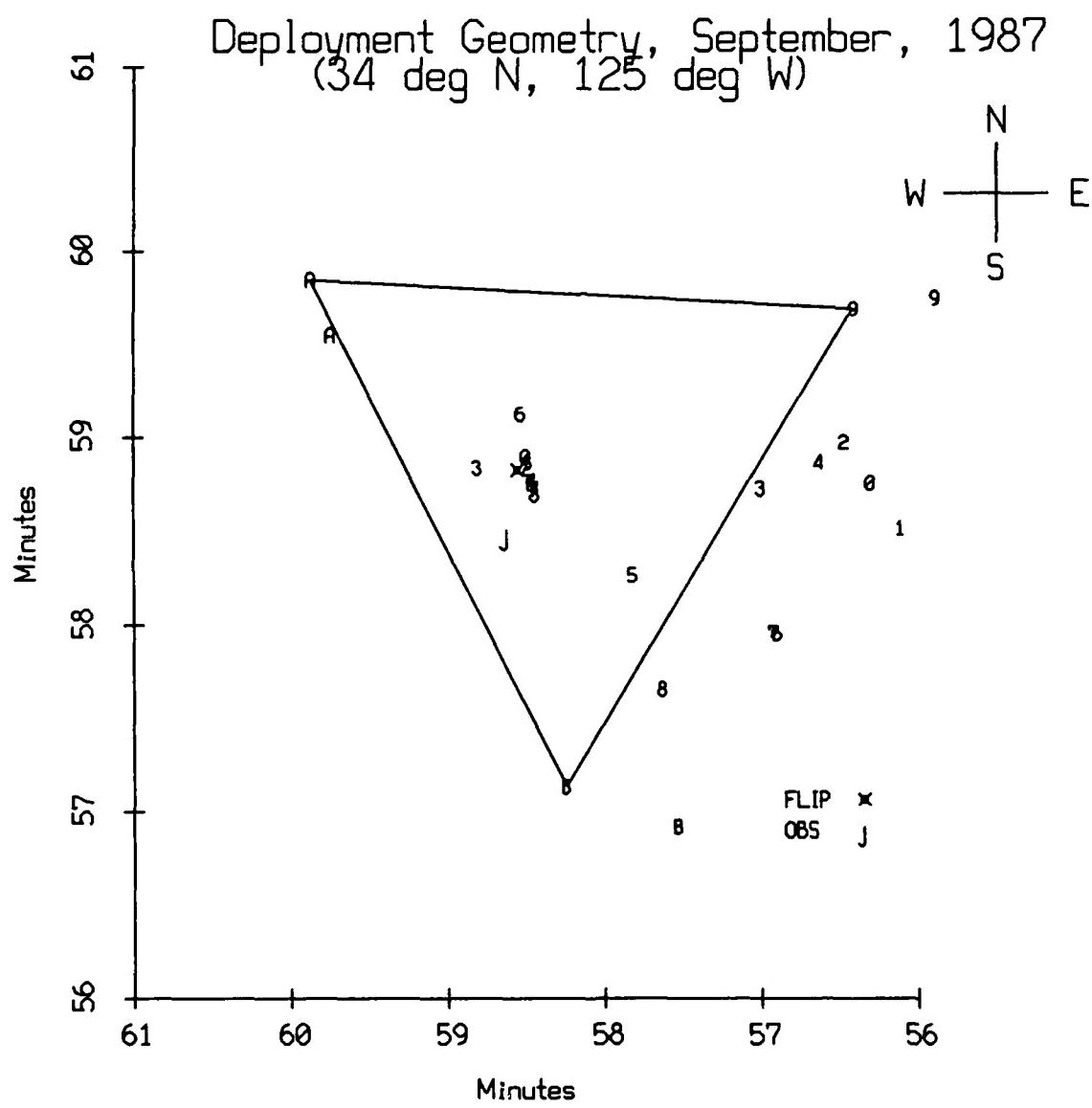


Figure I.1

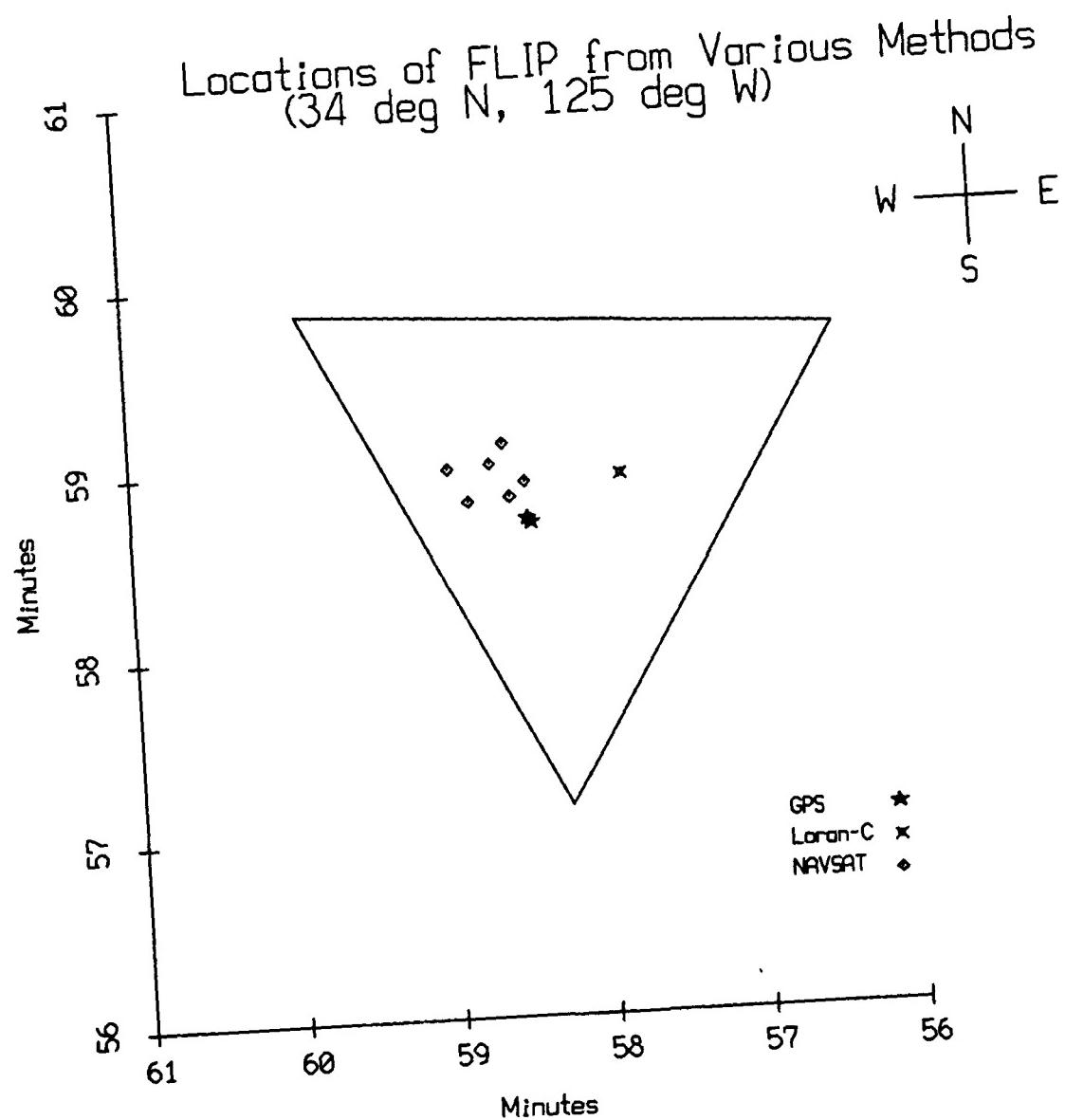


Figure 1.2

Sound Speed Profile : Area 24, Months 7-9
(34-36 deg N, 118-125 deg W)
with Instruments' Deployment Depths

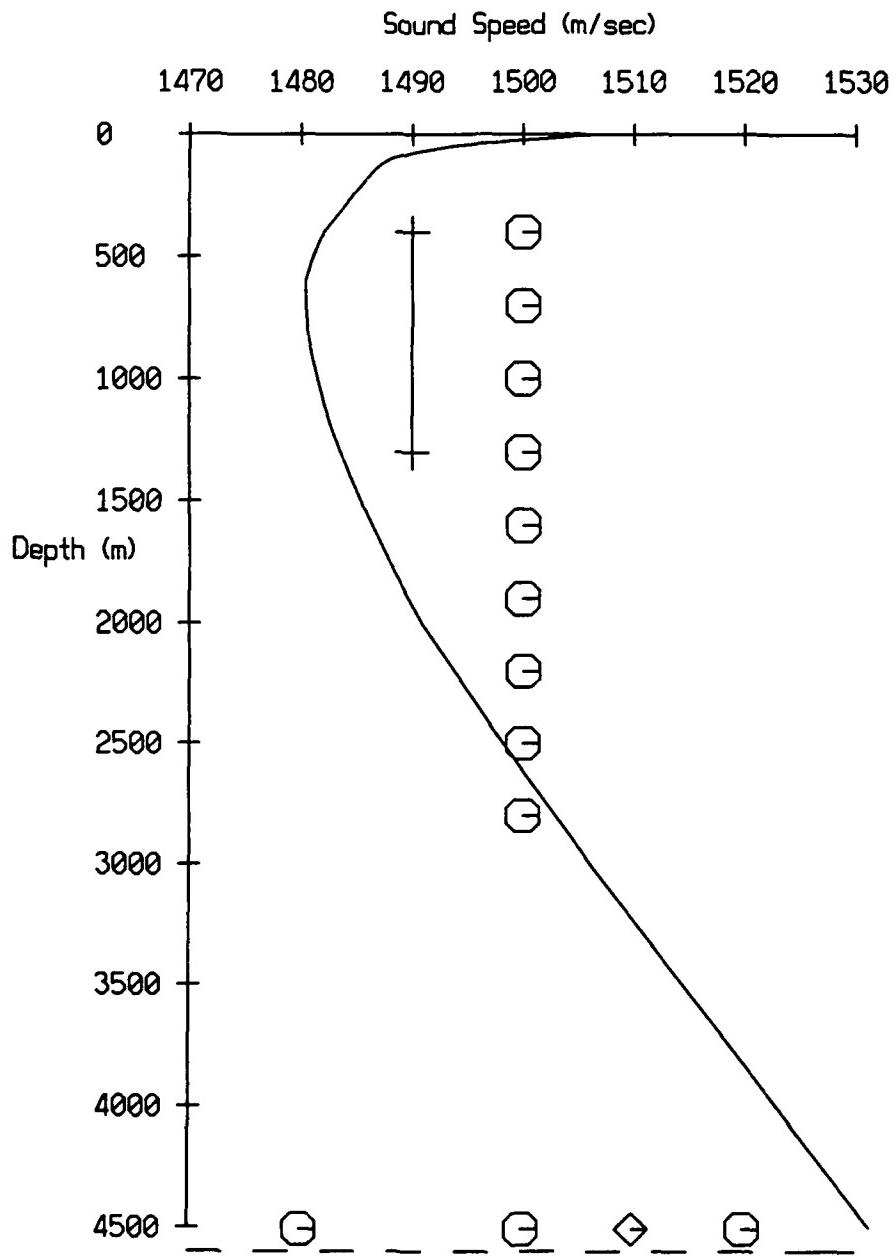


Figure I.3

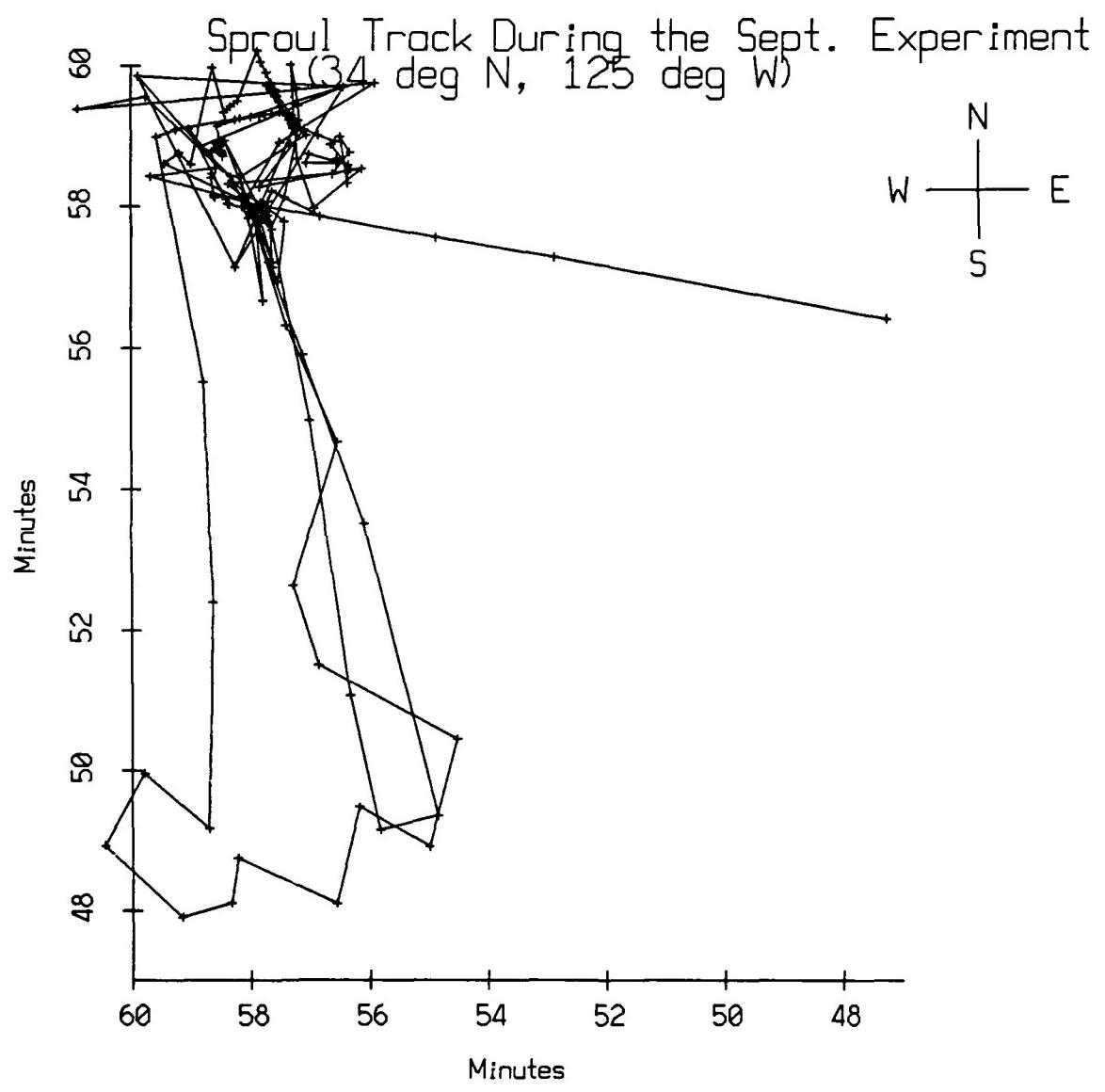


Figure II.1

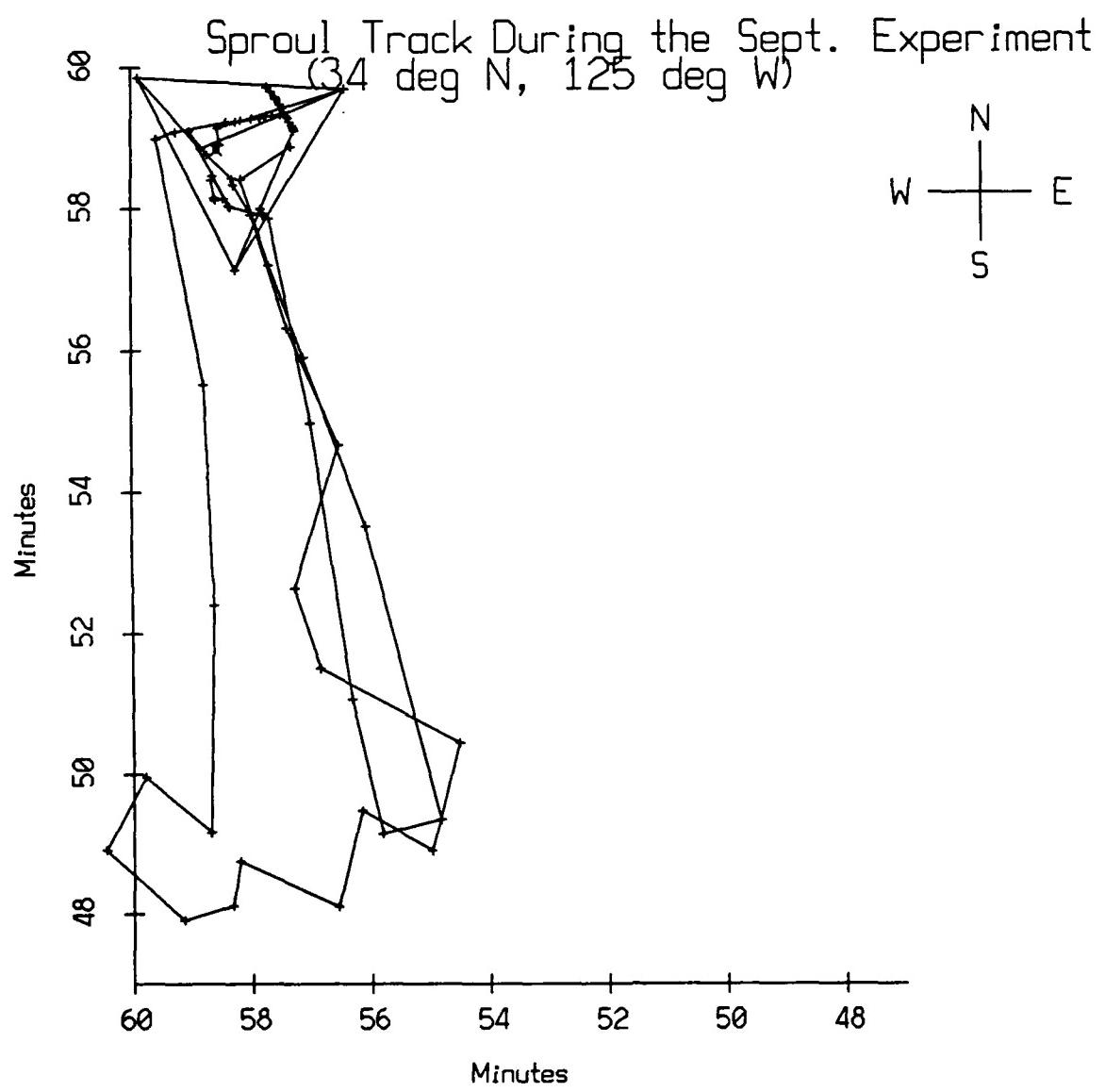


Figure II.2

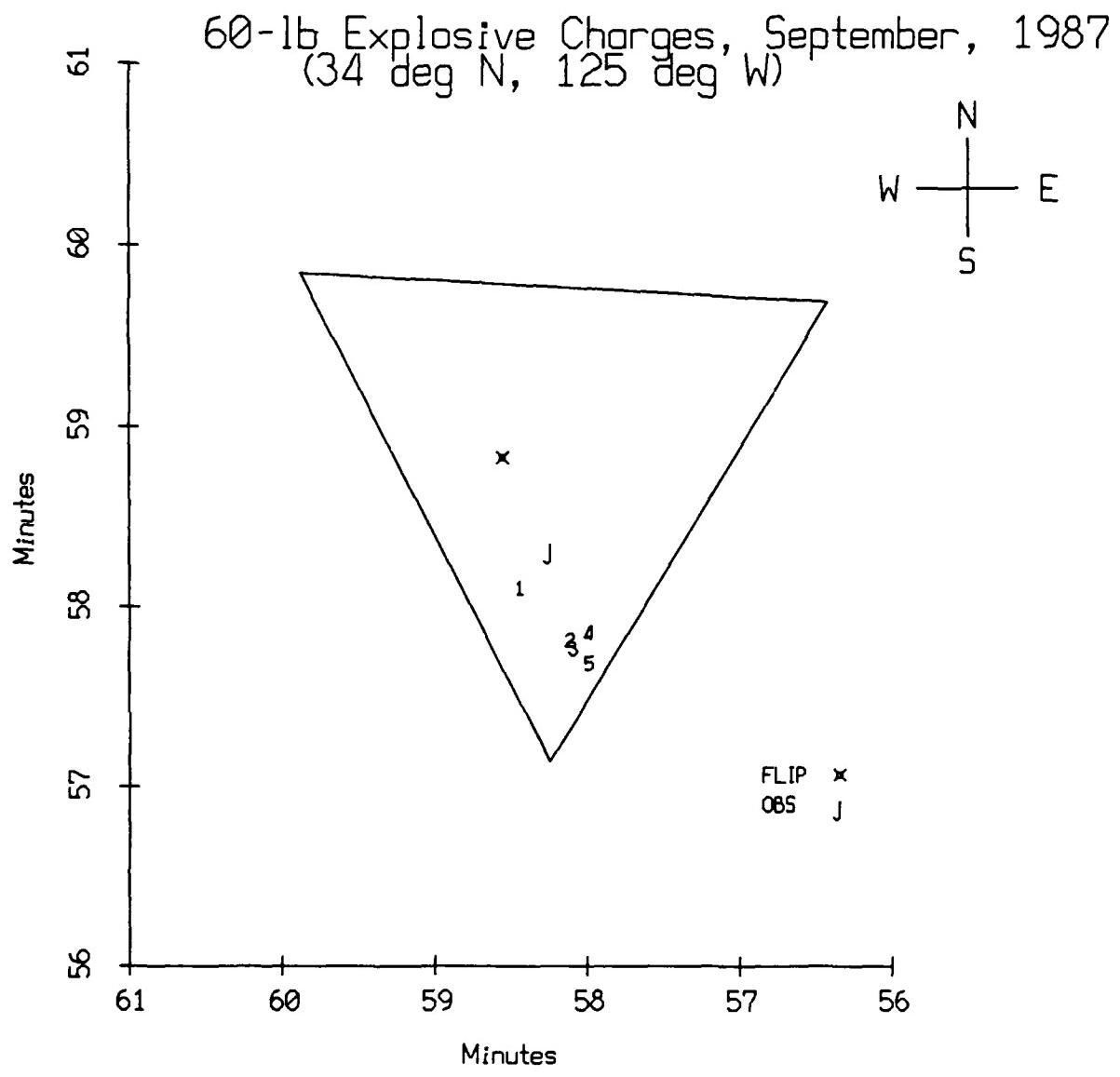


Figure II.3

Sound Speed Profile : Area 24, Months 7-9
(34-36 deg N, 118-125 deg W)
with XBT 31 (400 m) and XBT 32 (700 m)

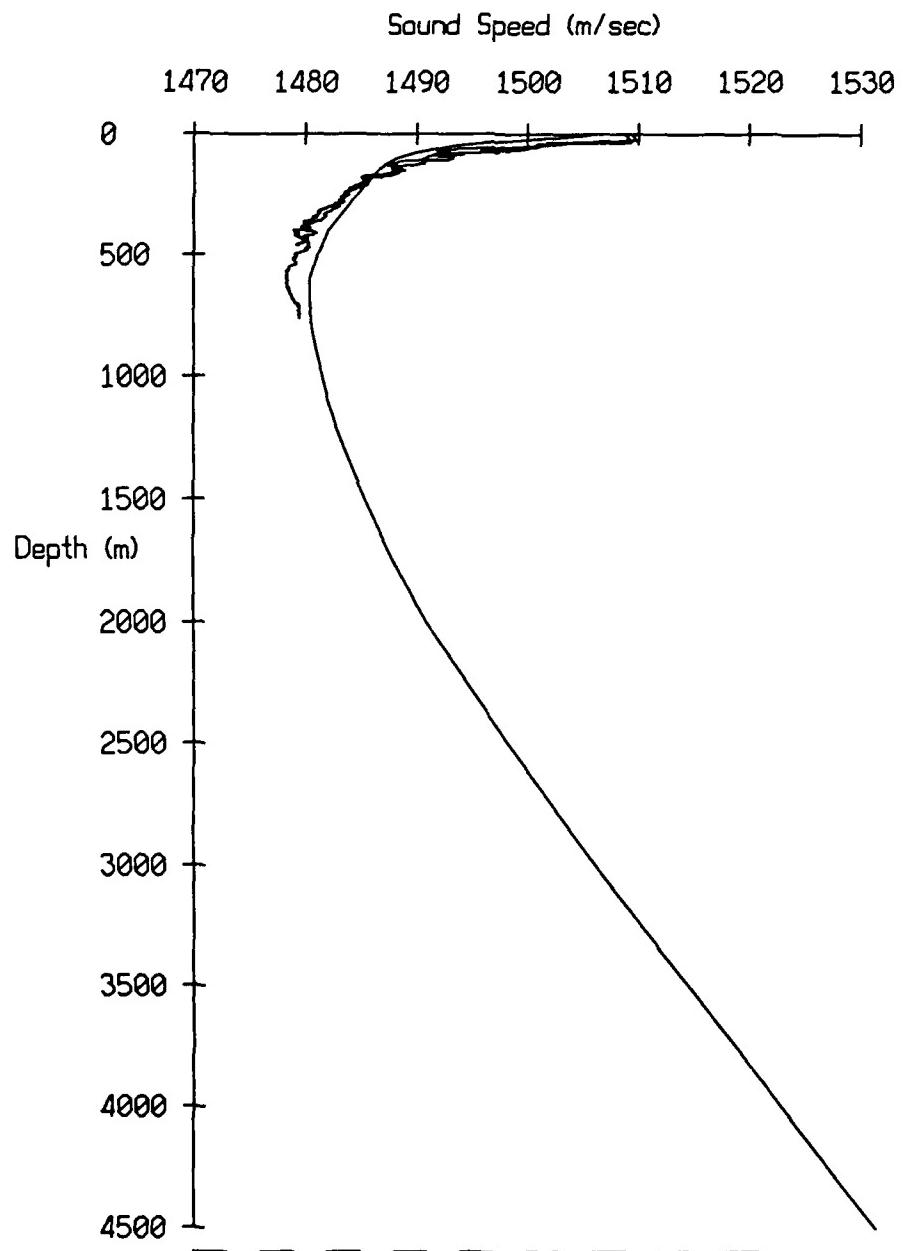


Figure IV.1

Sound Speed Profile : Area 24, Months 7-9
(34-36 deg N, 118-125 deg W)
with SSP from Deep CTD taken near FLIP

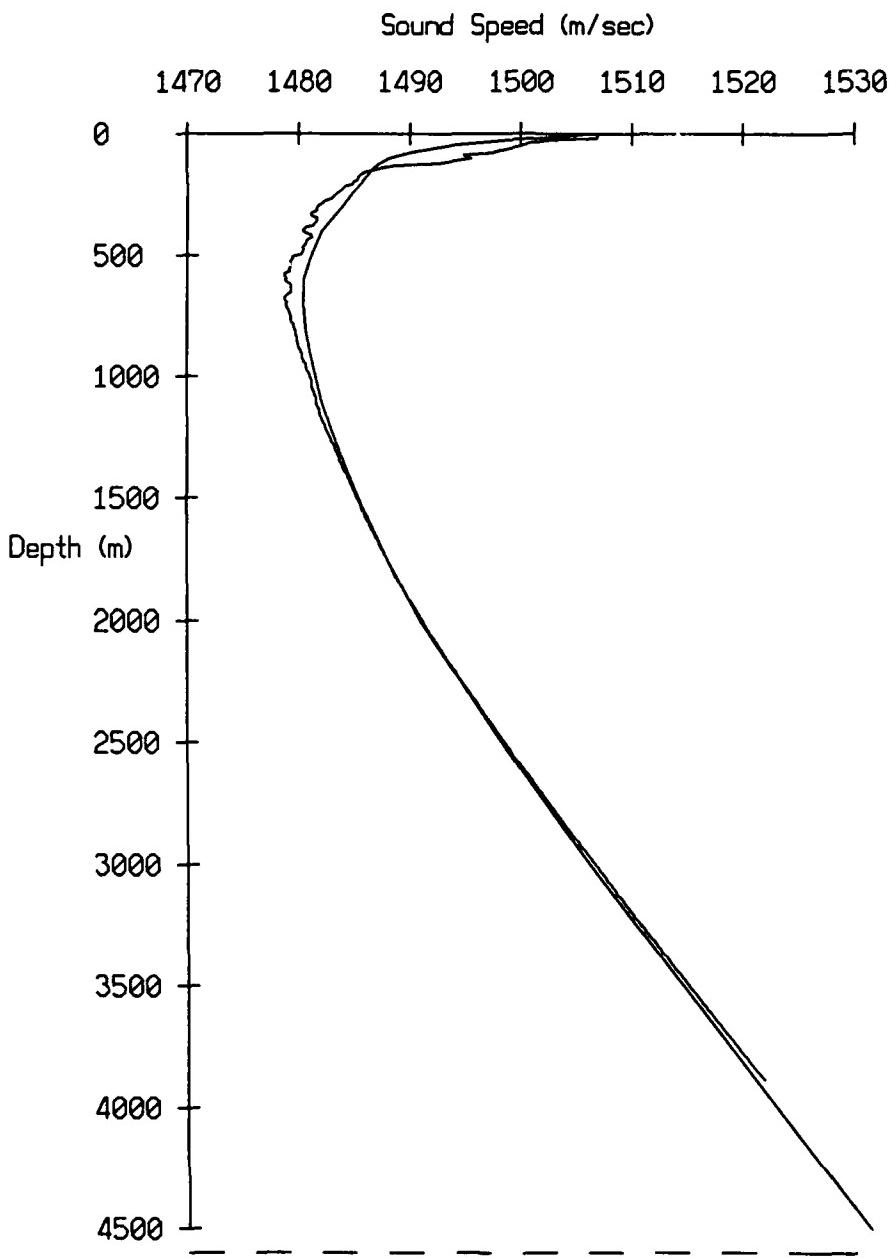


Figure IV.2

Anemometer Readings after 00:00 a.m., 9-17-87
Measurements on FLIP

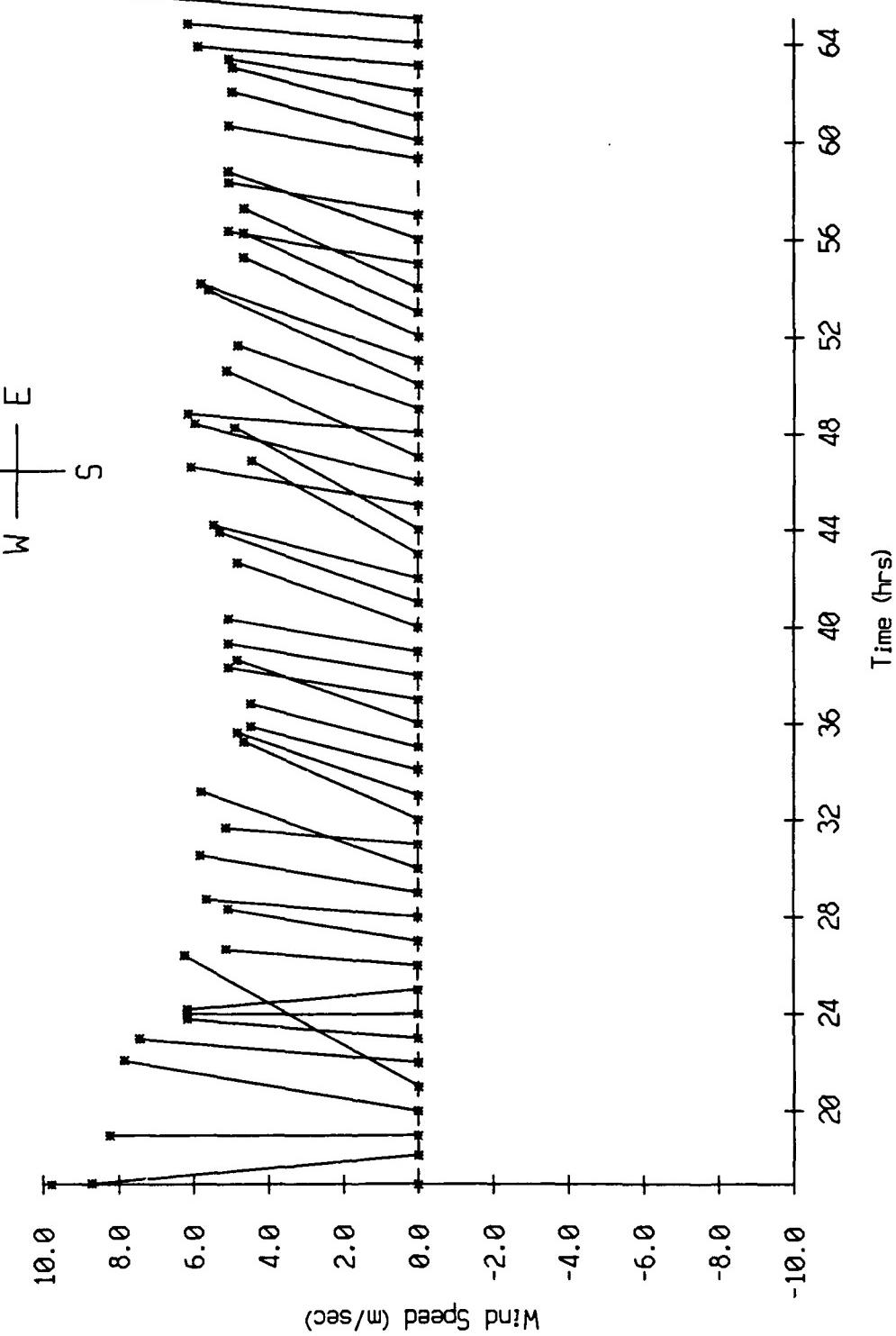


Figure IV.3

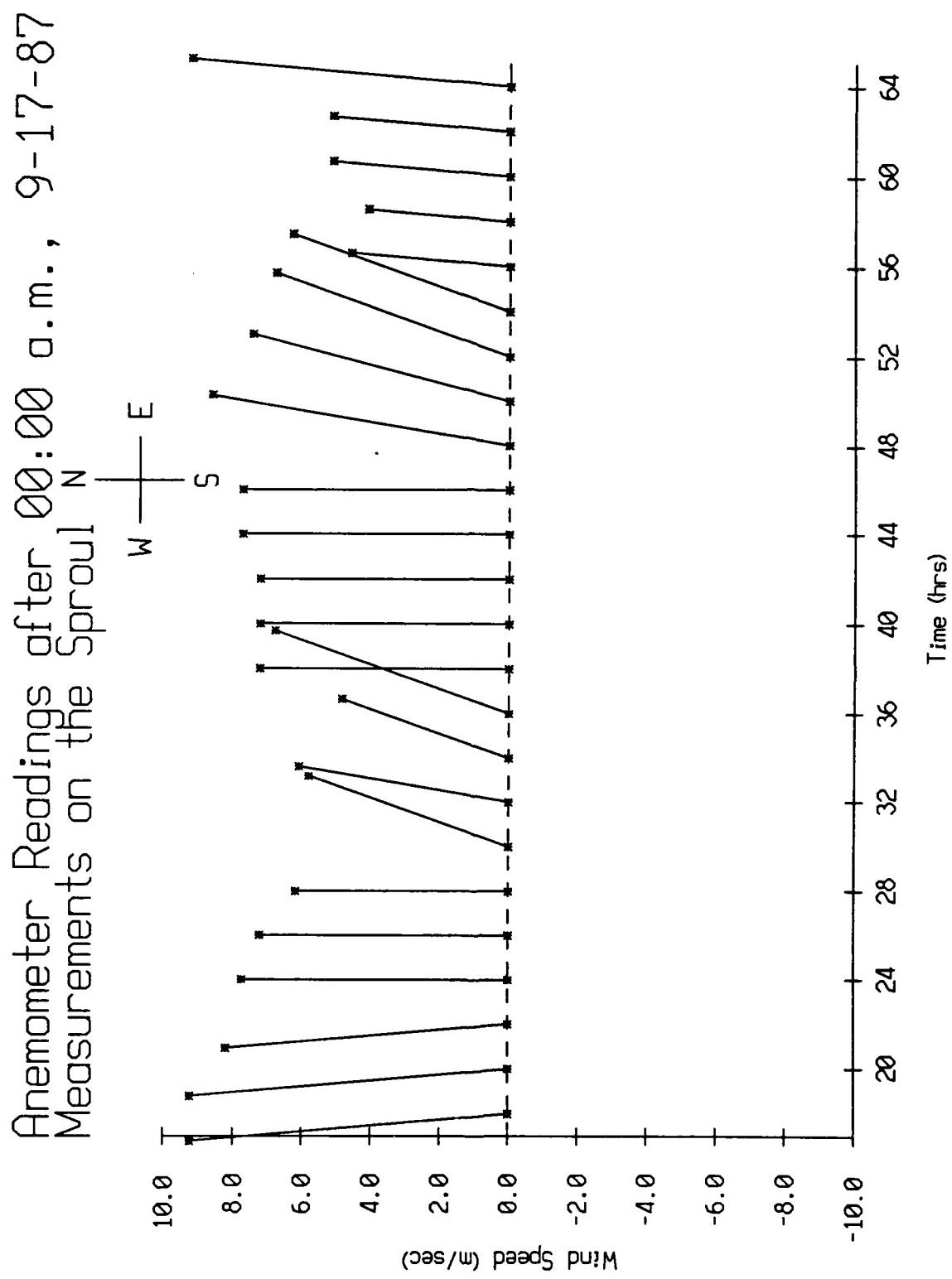


Figure IV.4

September 1987 Deployment Data Screening Results

record number	internal record number	# of bytes written	first missing resync	pass header checksum?	pass range checksum?	# of failed acoustic checksums?
Float 0						
669	-1	2	0	no	yes	0
670	****	7676	1	no	no	88
1565	1562	0	0	yes	yes	0
1566	6581	7268	1	no	no	85
1648	-1	0	0	no	yes	0
1649	6047	7676	1	no	no	88
1745	0	7646	1	no	no	88
1772	0	7646	1	no	no	88
1988	1983	0	0	yes	yes	0
Float 1						
57	0	7646	1	no	no	88
205	204	5716	0	yes	yes	1
206	****	1216	1	no	no	10
545	543	3718	0	yes	yes	1
546	510	3188	1	no	no	35
588	-1	4	0	no	yes	0
589	****	7134	1	no	no	83
894	-1	2	0	no	yes	0
895	****	7226	1	no	no	84
1100	-1	4	0	no	yes	0
1101	****	7676	1	no	no	88
1179	0	7646	1	no	no	88
1262	0	7646	1	no	no	88
1380	1373	0	0	yes	yes	0
1381	****	7086	1	no	no	82
1502	-1	2	0	no	yes	0
1503	4401	7102	1	no	no	83
1519	1510	0	0	yes	yes	0
1654	-1	0	0	no	yes	0
1655	****	7092	1	no	no	83
1690	1679	0	0	yes	yes	0
1691	-137	7166	1	no	no	83
1923	0	7644	1	no	no	88
1963	-1	2	0	no	yes	0
1964	****	7232	1	no	no	84
1990	1977	0	0	yes	yes	0
1991	-776	7188	1	no	no	84
2027	2013	0	0	yes	yes	0

Figure V.1a

September 1987 Deployment Data Screening Results

record number	internal record number	# of bytes written	first missing resync	pass header checksum?	pass range checksum?	# of failed acoustic checksums?
Float 2						
52	0	7646	1	no	no	88
54	52	-2	0	yes	yes	0
55	****	7042	1	no	no	82
79	0	7646	1	no	no	88
96	0	7644	1	no	no	88
160	-1	4	0	no	yes	0
161	****	6984	1	no	no	81
172	0	7646	1	no	no	88
231	-1	0	0	no	yes	0
232	****	7676	1	no	no	88
264	0	7648	1	no	no	88
292	0	7646	1	no	no	88
649	0	7646	1	no	no	88
761	757	2050	0	yes	yes	1
762	****	4852	1	no	no	55
814	-1	0	0	no	yes	0
815	****	7154	1	no	no	83
958	0	7646	1	no	no	88
1072	-1	0	0	no	yes	0
1073	2122	7076	1	no	no	82
1161	-1	0	0	no	yes	0
1162	****	7240	1	no	no	84
1166	-1	0	0	no	yes	0
1167	****	7070	1	no	no	82
1257	0	7648	1	no	no	88
1272	1262	0	0	yes	yes	0
1273	-521	7016	1	no	no	82
1283	0	7646	1	no	no	88
1340	****	7642	1	no	no	88
1515	0	7646	1	no	no	88
1532	-1	0	0	no	yes	0
1533	****	7288	1	no	no	85
1631	2560	7644	1	no	no	88
1837	0	7648	1	no	no	88
1858	0	7646	1	no	no	88
1940	1929	7648	0	yes	yes	0
1980	1968	0	0	yes	yes	0

Figure V.1b

September 1987 Deployment Data Screening Results

record number	internal record number	# of bytes written	first missing resync	pass header checksum?	pass range checksum?	# of failed acoustic checksums?
Float 3						
174	-1	0	0	no	yes	0
175	****	7676	1	no	no	88
274	0	7644	1	no	no	88
332	****	7644	1	no	no	88
639	****	7644	1	no	no	88
654	0	7646	1	no	no	88
715	0	7646	1	no	no	88
878	256	7644	1	no	no	88
1218	0	7646	1	no	no	88
1269	-1	0	0	no	yes	0
1270	-236	7274	1	no	no	85
1313	1309	0	0	yes	yes	0
1314	****	7120	1	no	no	83
1814	0	7646	1	no	no	88
1914	1909	0	0	yes	yes	0
Float 4						
371	0	7644	1	no	no	88
387	385	0	0	yes	yes	0
388	****	7030	1	no	no	82
1978	1975	0	0	yes	yes	0
Float 5						
354	353	7642	0	yes	yes	1
974	973	7642	46	yes	yes	45
1946	1944	0	0	yes	yes	0
Float 6						
1	0	7644	1	no	no	88
340	339	7642	0	yes	yes	1
466	465	390	0	yes	no	0
467	****	6528	1	no	no	76
472	470	7676	2	yes	no	88
490	488	6648	0	yes	yes	2
491	****	252	1	no	no	2
493	490	3456	0	yes	yes	1

Figure V.1c

September 1987 Deployment Data Screening Results

record number	internal record number	# of bytes written	first missing resync	pass header checksum?	pass range checksum?	# of failed acoustic checksums?
494	-769	3456	1	no	no	37
495	491	2252	24	yes	yes	16
496	-782	6384	1	no	no	77
498	493	5040	0	yes	yes	1
499	****	2622	1	no	no	28
518	512	7642	2	yes	no	88
526	520	7642	74	yes	yes	17
633	627	7642	0	yes	yes	1
832	826	7642	10	yes	yes	81
1030	0	7646	1	no	no	88
1427	1421	7642	0	yes	yes	1
1428	1422	376	0	yes	no	1
1429	****	6450	1	no	no	75
1434	1427	4106	0	yes	yes	1
1435	****	2728	1	no	no	29
1437	1429	868	2	yes	no	5
1438	-3	54	1	no	no	5
1439	7455	5164	1	no	no	58
1441	1431	3864	29	yes	yes	17
1442	****	2128	1	no	no	37
1443	****	114	1	no	no	37
1448	1436	7642	42	yes	yes	49
1449	1437	7642	10	yes	yes	81
1456	1444	6106	0	yes	yes	1
1457	****	1058	1	no	no	8
1460	1447	7638	55	yes	yes	36
1462	1449	6320	0	yes	yes	2
1463	****	554	1	no	no	3
1530	1516	4570	0	yes	yes	1
1531	****	2322	1	no	no	24
1795	1780	4532	0	yes	yes	2
1796	****	2380	1	no	no	26
1797	1781	7642	0	yes	yes	1
1928	1911	0	0	yes	yes	0

Float 7

263	0	7646	1	no	no	88
286	0	7646	1	no	no	88
332	0	7648	1	no	no	88
500	0	7646	1	no	no	88
644	0	7646	1	no	no	88
721	-1	0	0	no	yes	0

Figure V.1d

September 1987 Deployment Data Screening Results

record number	internal record number	# of bytes written	first missing resync	pass header checksum?	pass range checksum?	# of failed acoustic checksums?
722	-595	7266	1	no	no	85
813	0	7646	1	no	no	88
910	0	7646	1	no	no	88
942	0	7646	1	no	no	88
1024	1022	3982	0	yes	yes	1
1025	****	2864	1	no	no	31
1943	1939	0	0	yes	yes	0
Float 8						
482	****	7644	1	no	no	88
549	****	7644	1	no	no	88
668	0	7646	1	no	no	88
950	949	7642	0	yes	yes	1
1005	1004	7648	0	yes	yes	0
1185	0	7646	1	no	no	88
1513	****	7644	1	no	no	88
1845	****	7644	1	no	no	88
1888	****	7644	1	no	no	88
1906	1904	0	0	yes	yes	0
Float 9						
1962	1960	0	0	yes	yes	0
Float 10						
112	111	7648	0	yes	yes	0
1558	0	7648	1	no	no	88
1917	1915	0	0	yes	yes	0
Float 11						
1912	1910	0	0	yes	yes	0

Figure V.1e

May 10, 1989 header page 1

May 10 10:13 1989 header page 2

Table 433

Figure V.2a

Tape 447

ט' טבת

卷之三

Tape 453

Tape 442 33 PID Errors in 20 intervals:
 * 1 0 0 0 0
 * 3 0 0 0 0
 * 4 0 0 0 0
 * 8 0 0 0 0

Tape 44

May 10 10:13 1989 header Page 3

#15	0	0	0	0	5	0	0	0	0	0	0
#16	0	0	0	0	2	0	0	0	0	0	0
#18	0	0	0	0	4	0	0	0	0	0	0
#19	0	0	0	0	5	0	0	0	0	0	0
#20	0	0	0	0	2	0	0	0	0	0	0
	29	22	18	30	23	70	28	29	30	28	30

Figure V.2b

AGC Level and Buoy Heading, Float 0, September 1987 Sea Trip

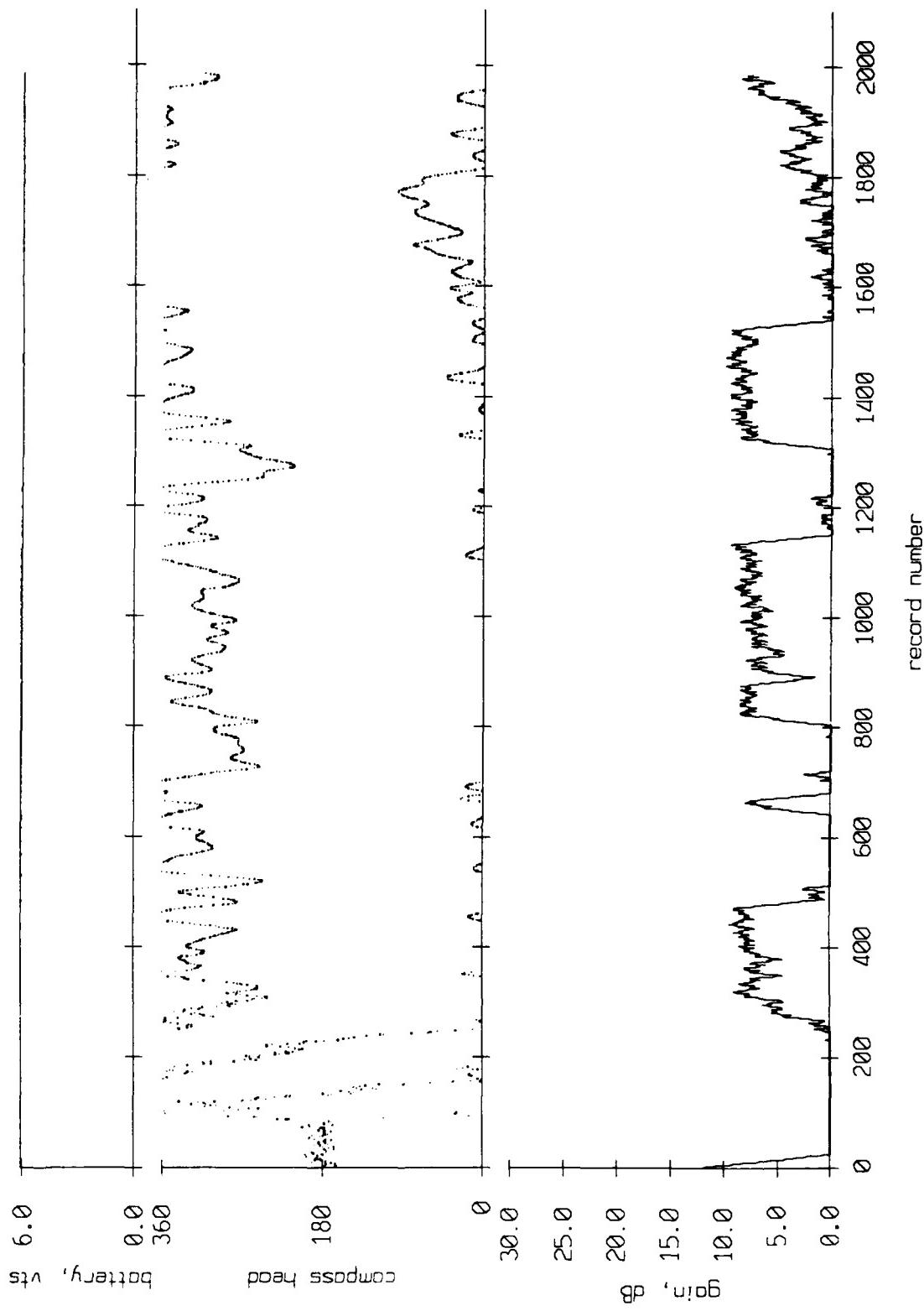


Figure VI.1

AGC Level and Buoy Heading, Float 1, September 1987 Sea Trip

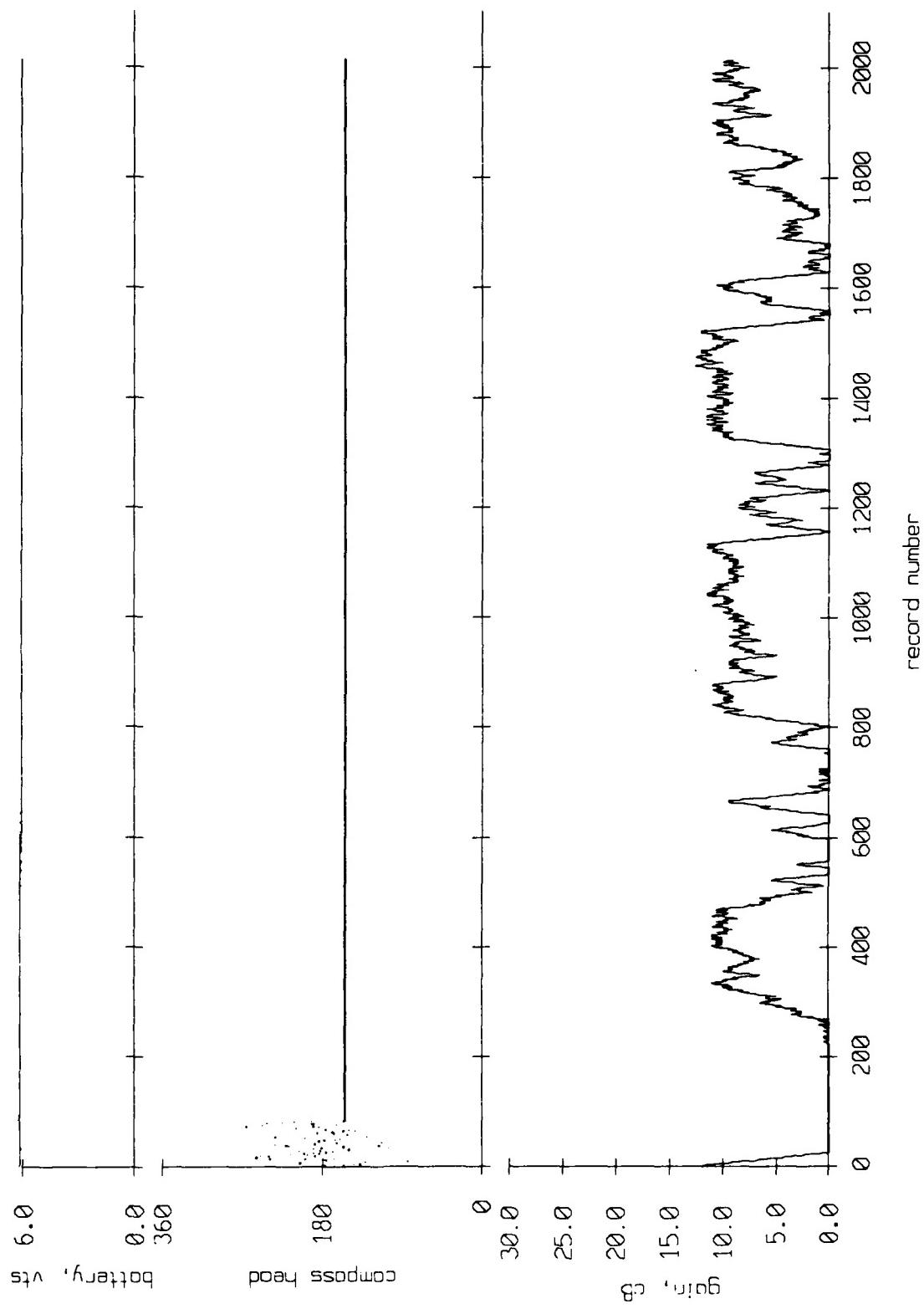


Figure VI.2

AGC Level and Buoy Heading, Float 2, September 1987 Sea Trip

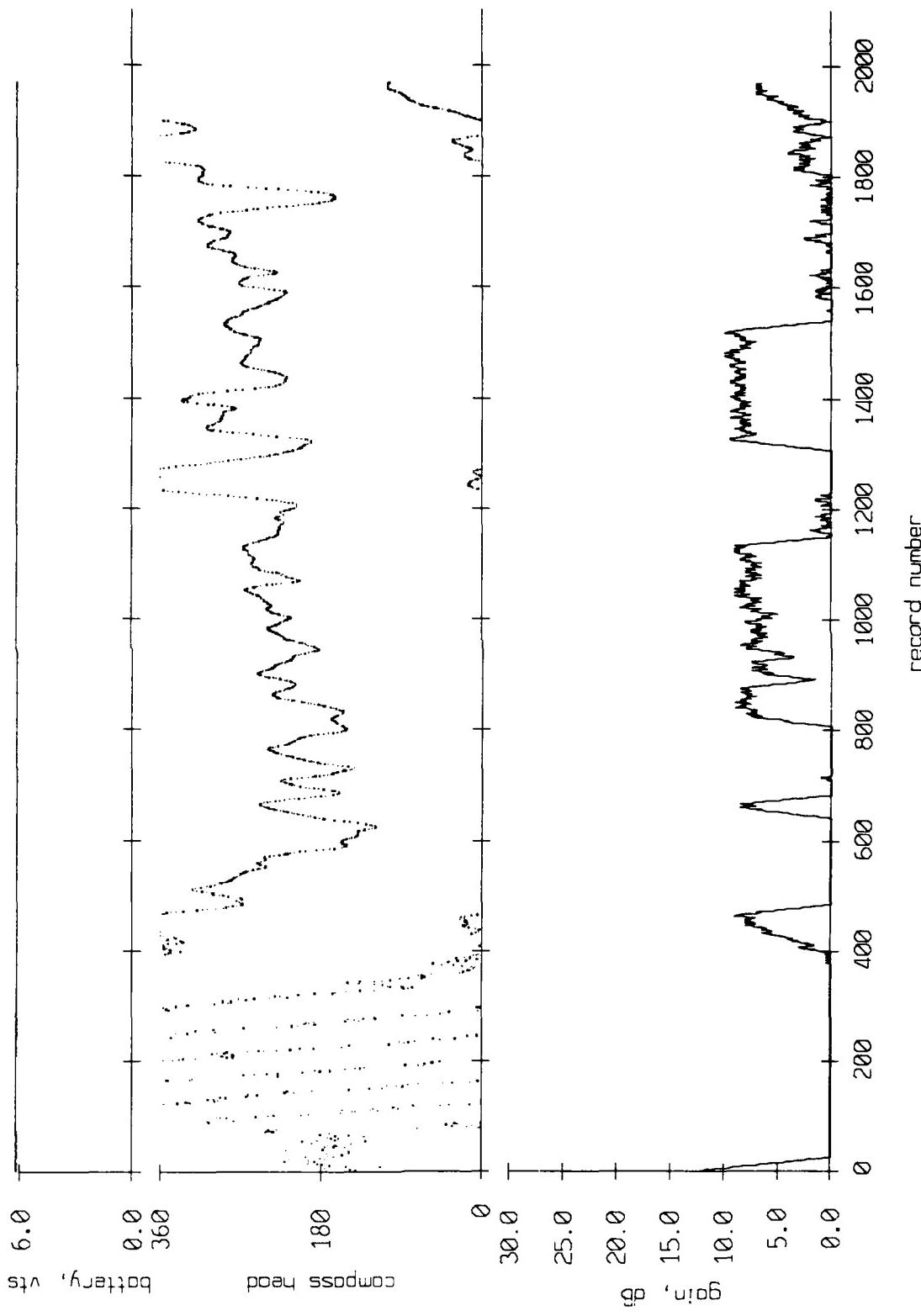


Figure VI.3

AGC Level and Buoy Heading, Float 3, September 1987 Sea Trip

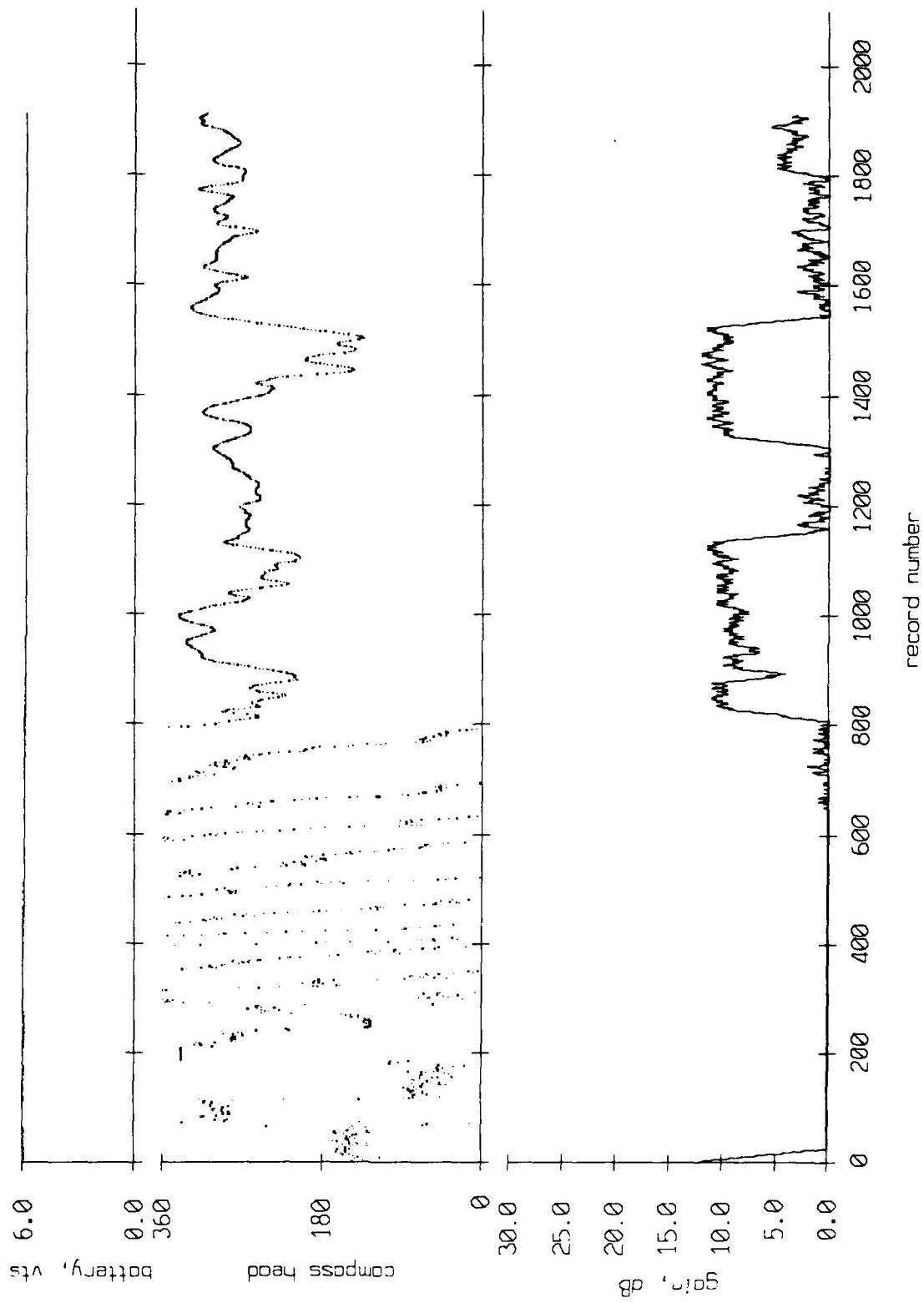


Figure VI.4

AGC Level and Buoy Heading, Float 4, September 1987 Sea Trip

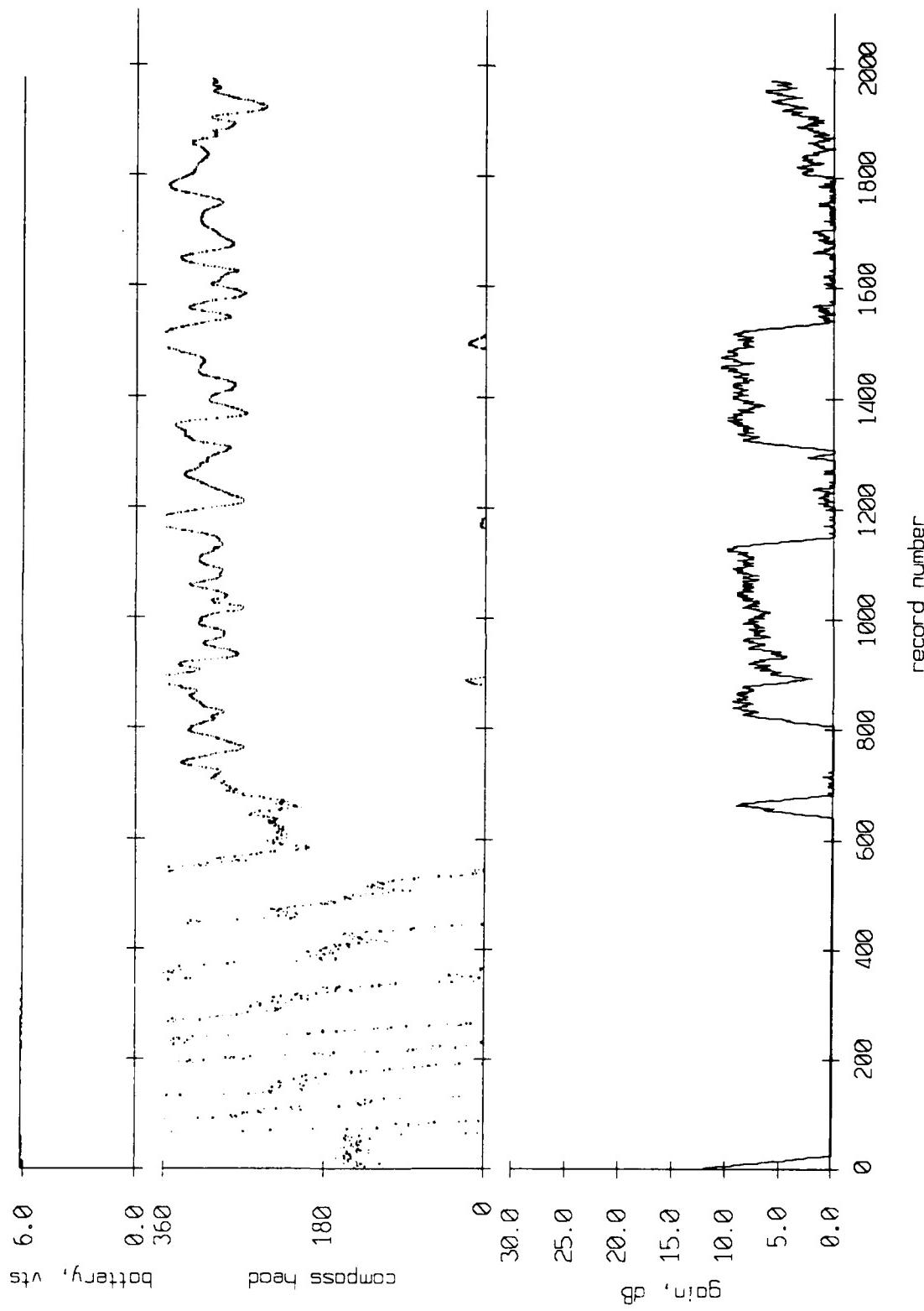


Figure VI.5

AGC Level and Buoy Heading, Float 5, September 1987 Sea Trip

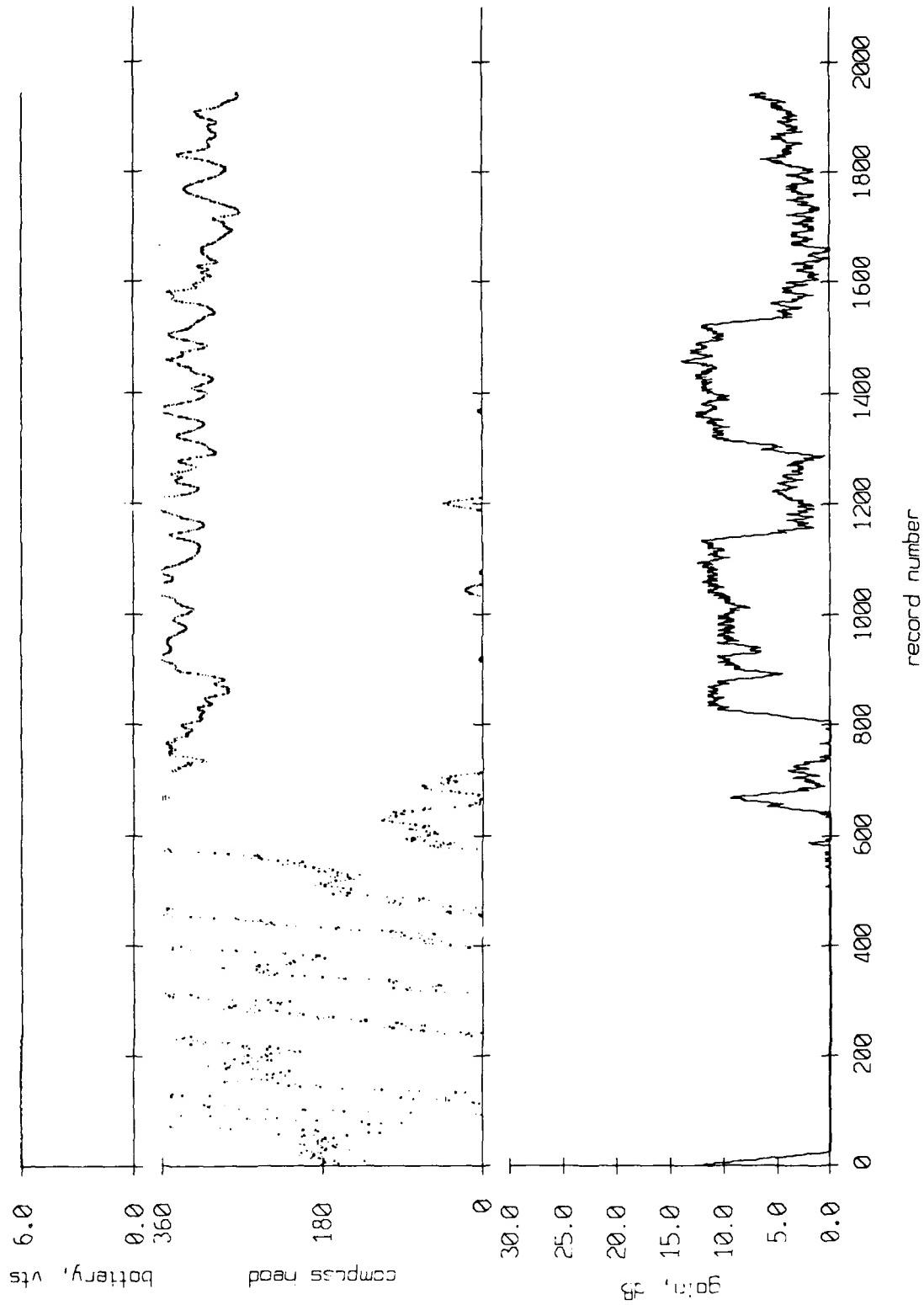


Figure VI.6

AGC Level and Buoy Heading, Float 6, September 1987 Sea Trip

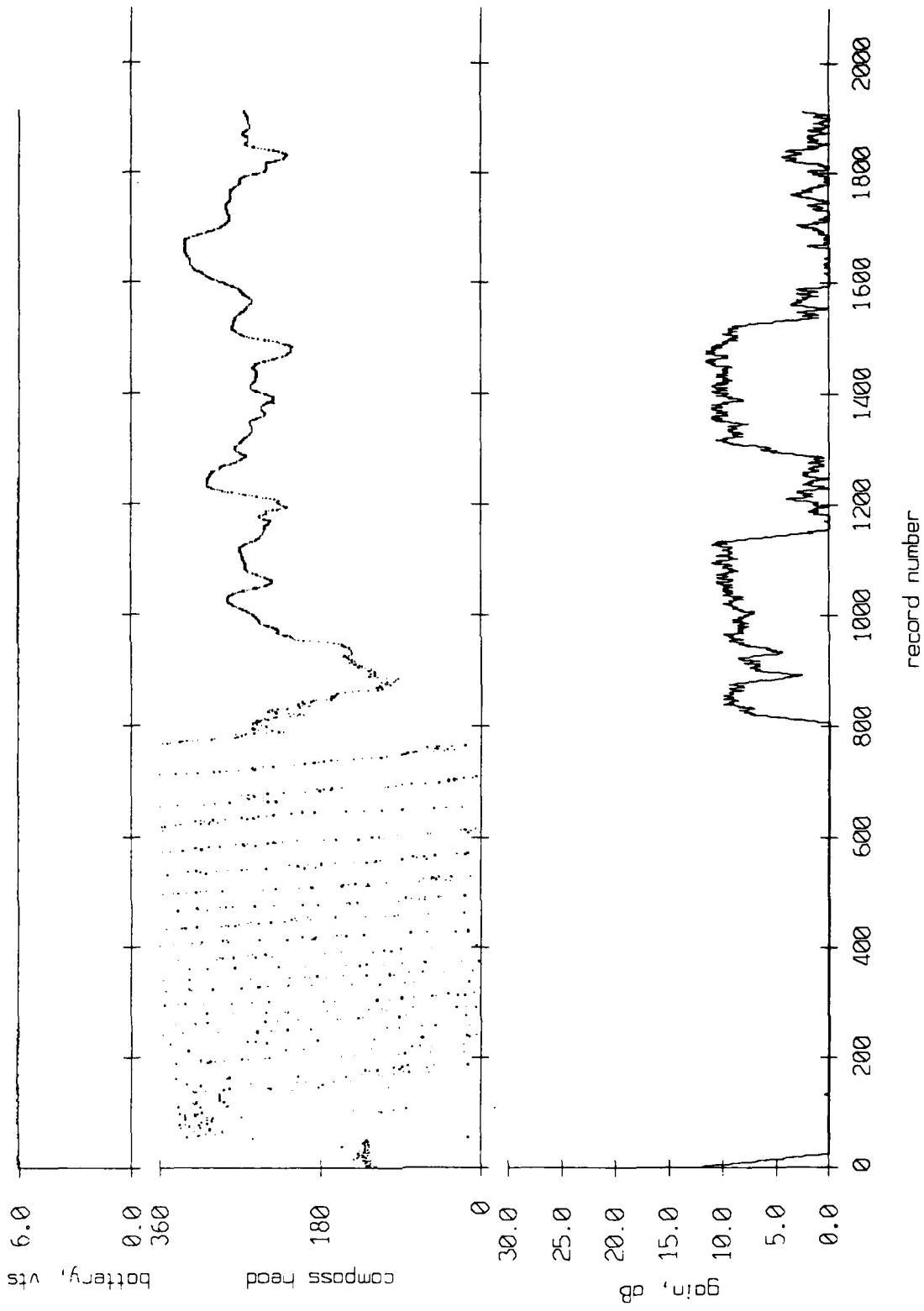


Figure VI.7

ACC Level and Buoy Heading, Float 7, September 1987 Sea Trip

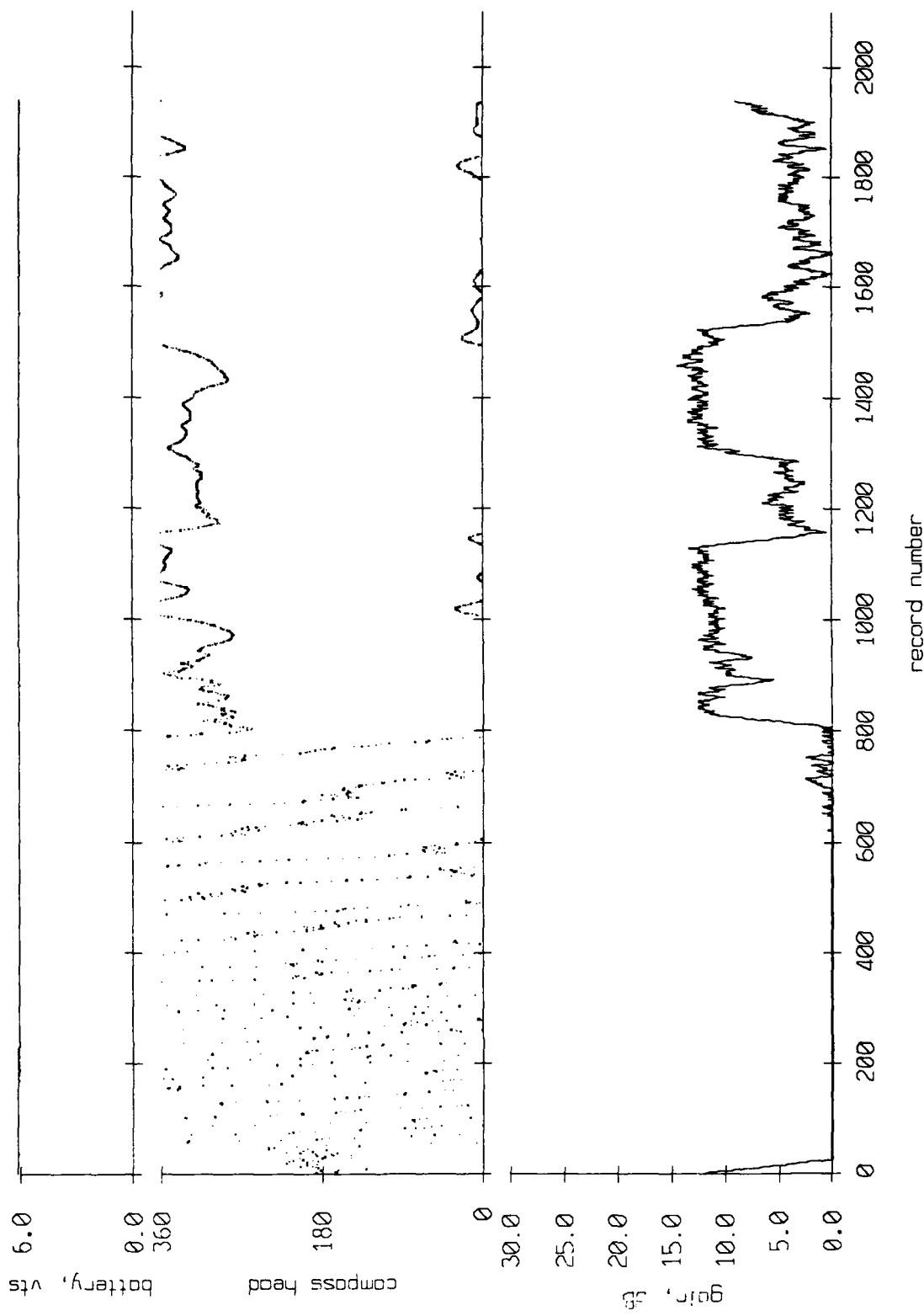


Figure VI.8

AGC Level and Buoy Heading, Float 8, September 1987 Sea Trip

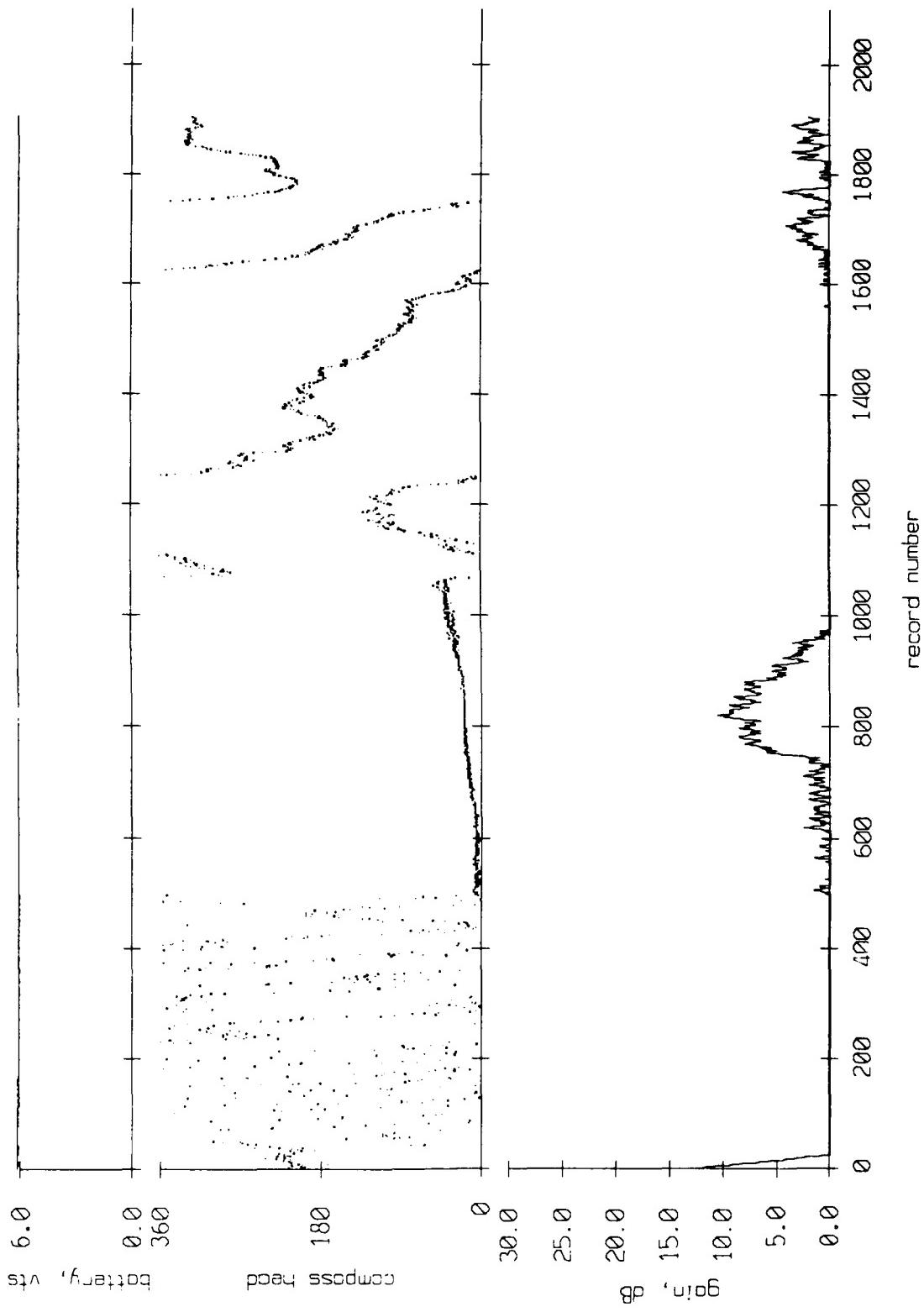


Figure VI.9

AGC Level and Buoy Heading, Float 9, September 1987 Sea Trip

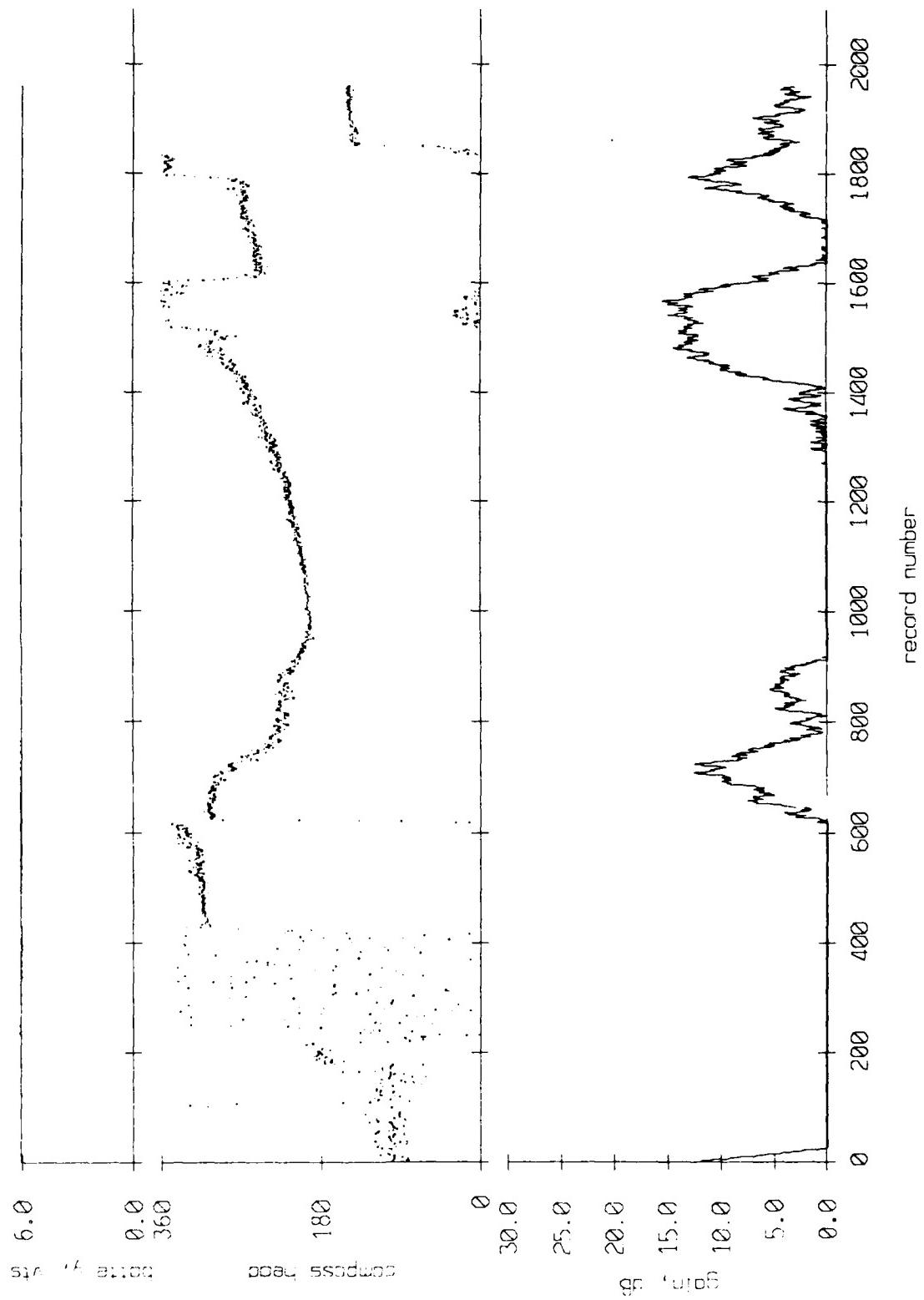


Figure VI.10

AGC Level and Buoy Heading, Float 10, September 1987 Sea Trip

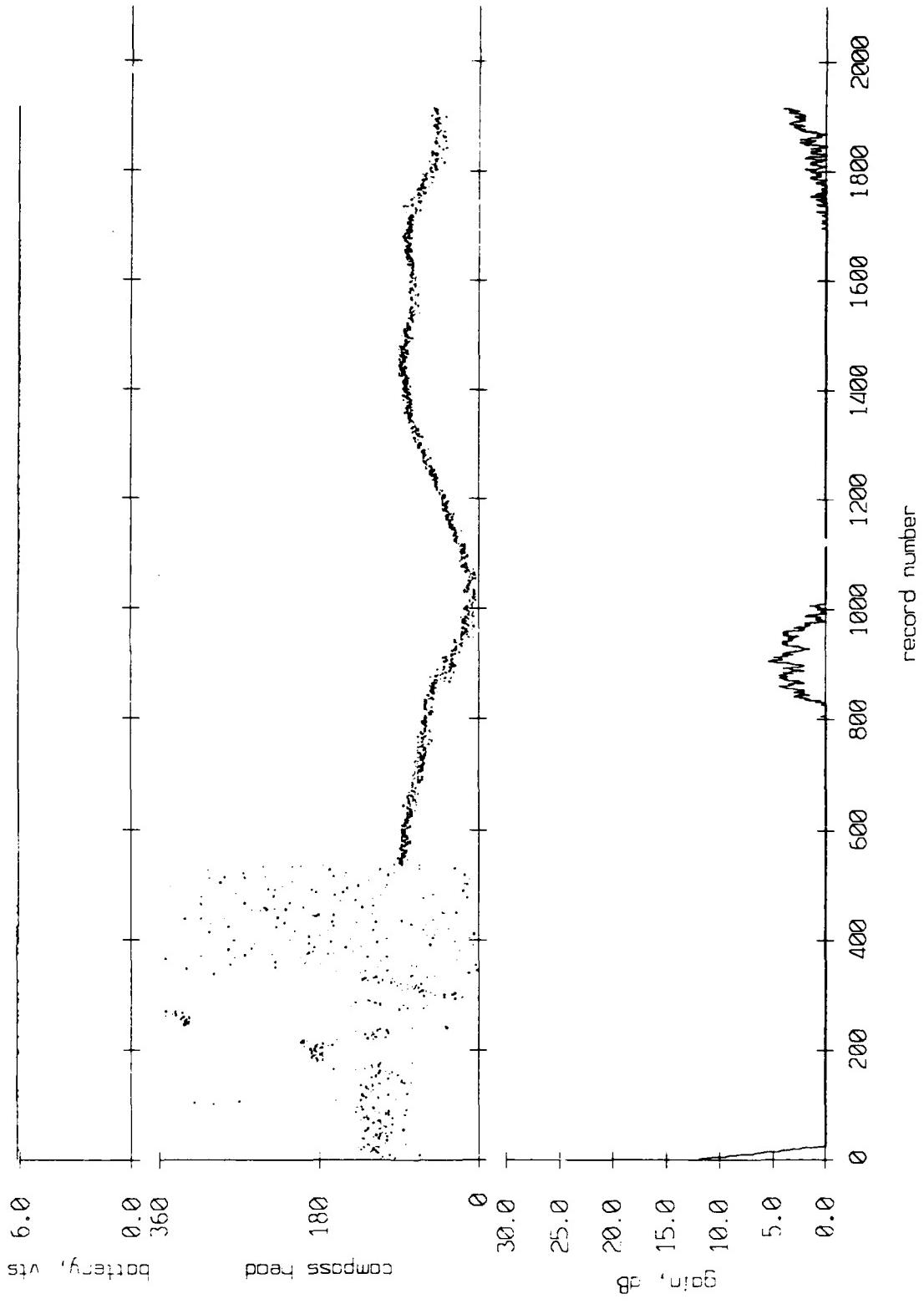


Figure VI.11

AGC Level and Buoy Heading, Float 11, September 1987 Sea Trip

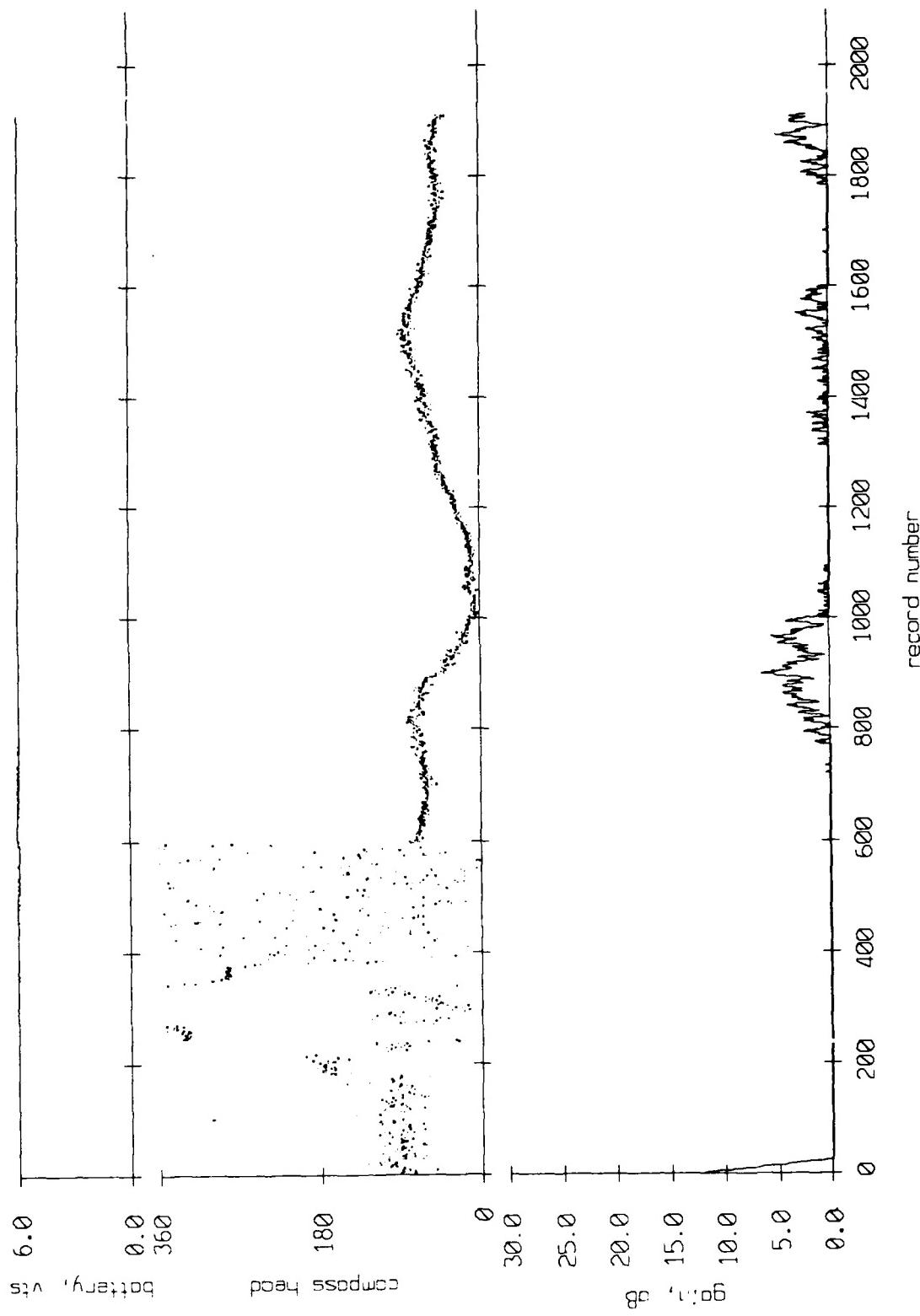


Figure VI.12

Float 0, September 1987 Sea Trip: surface & bottom bounces

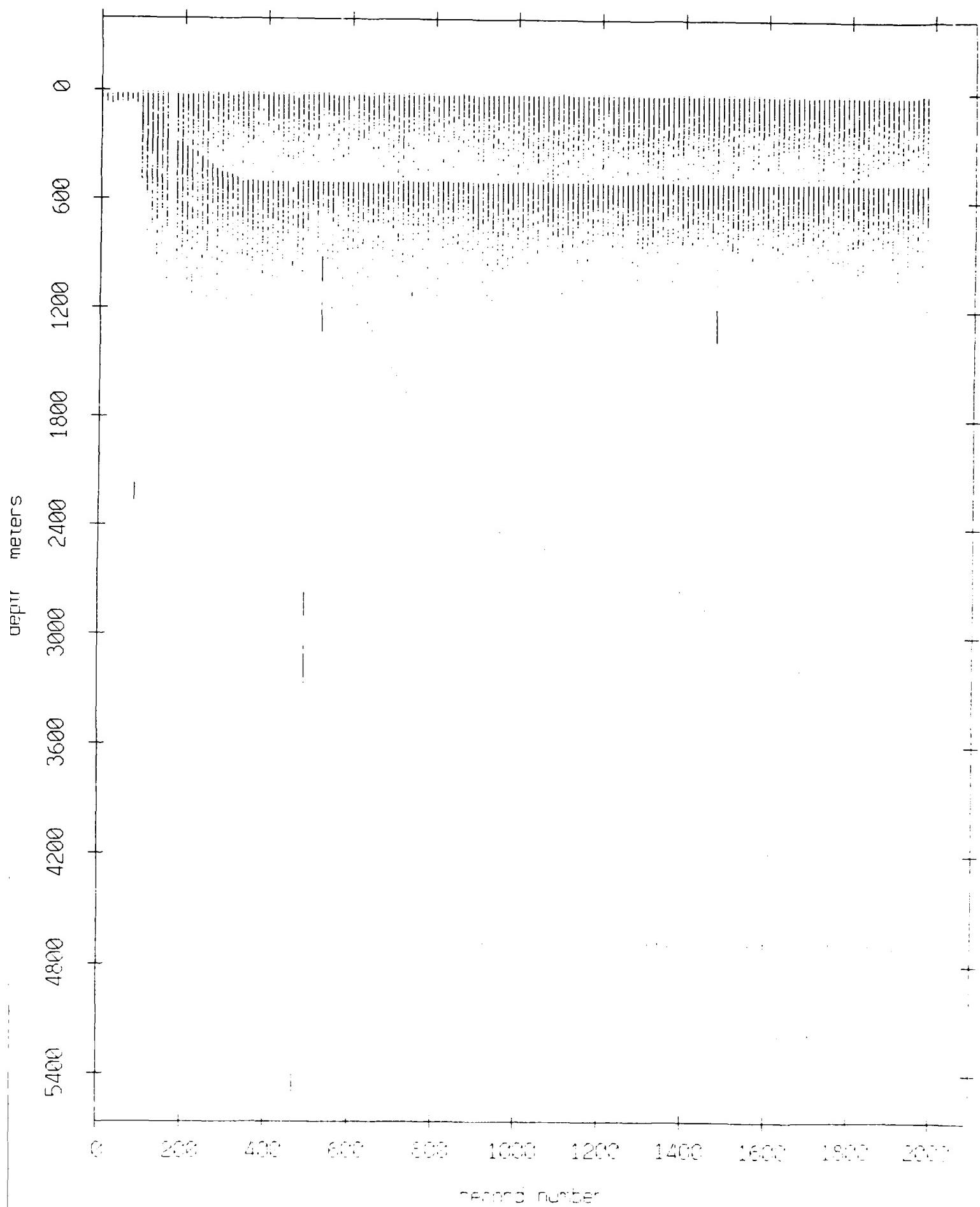


Figure VII.1

Float 1, September 1987 Sea Trip: surface & bottom bounces

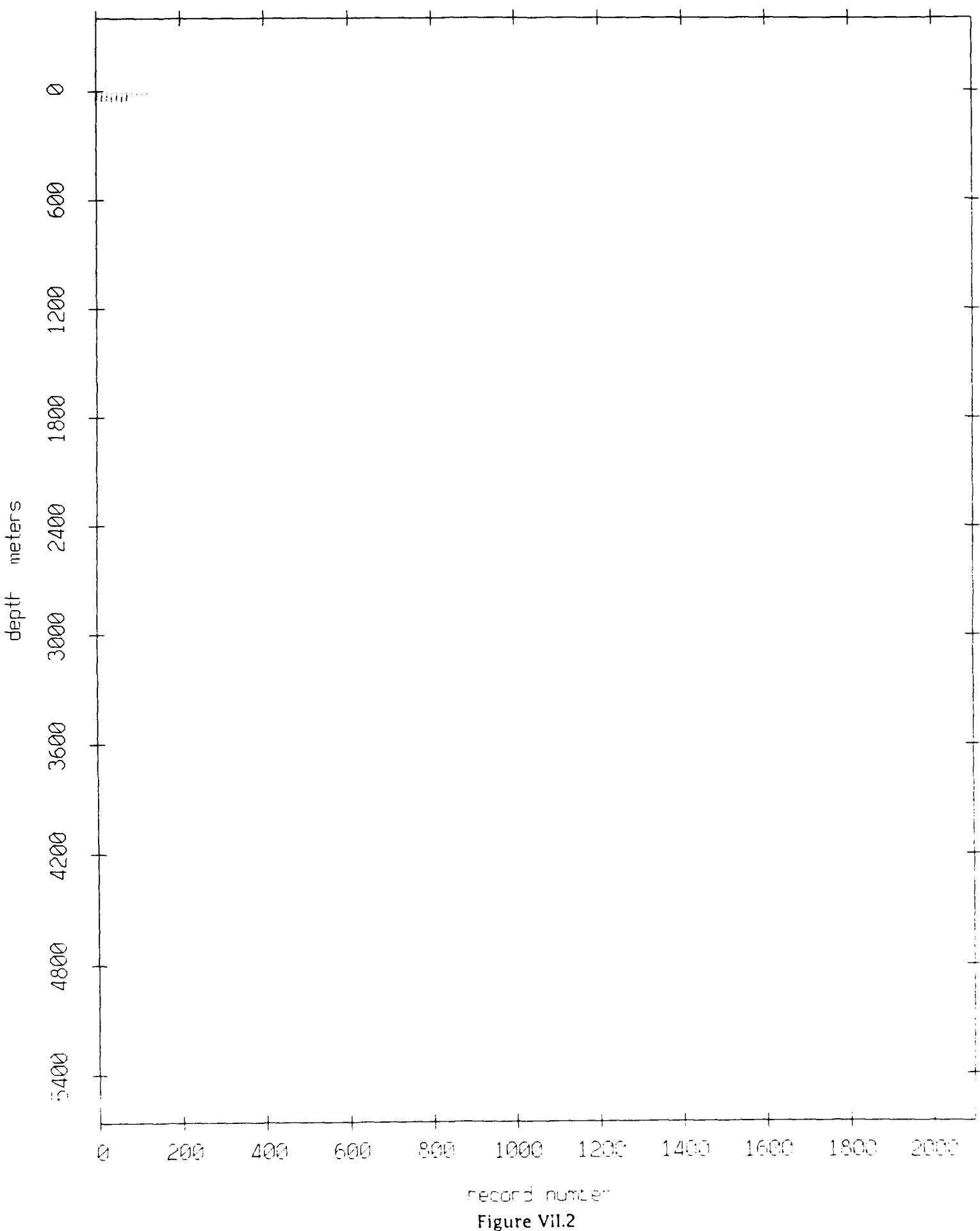
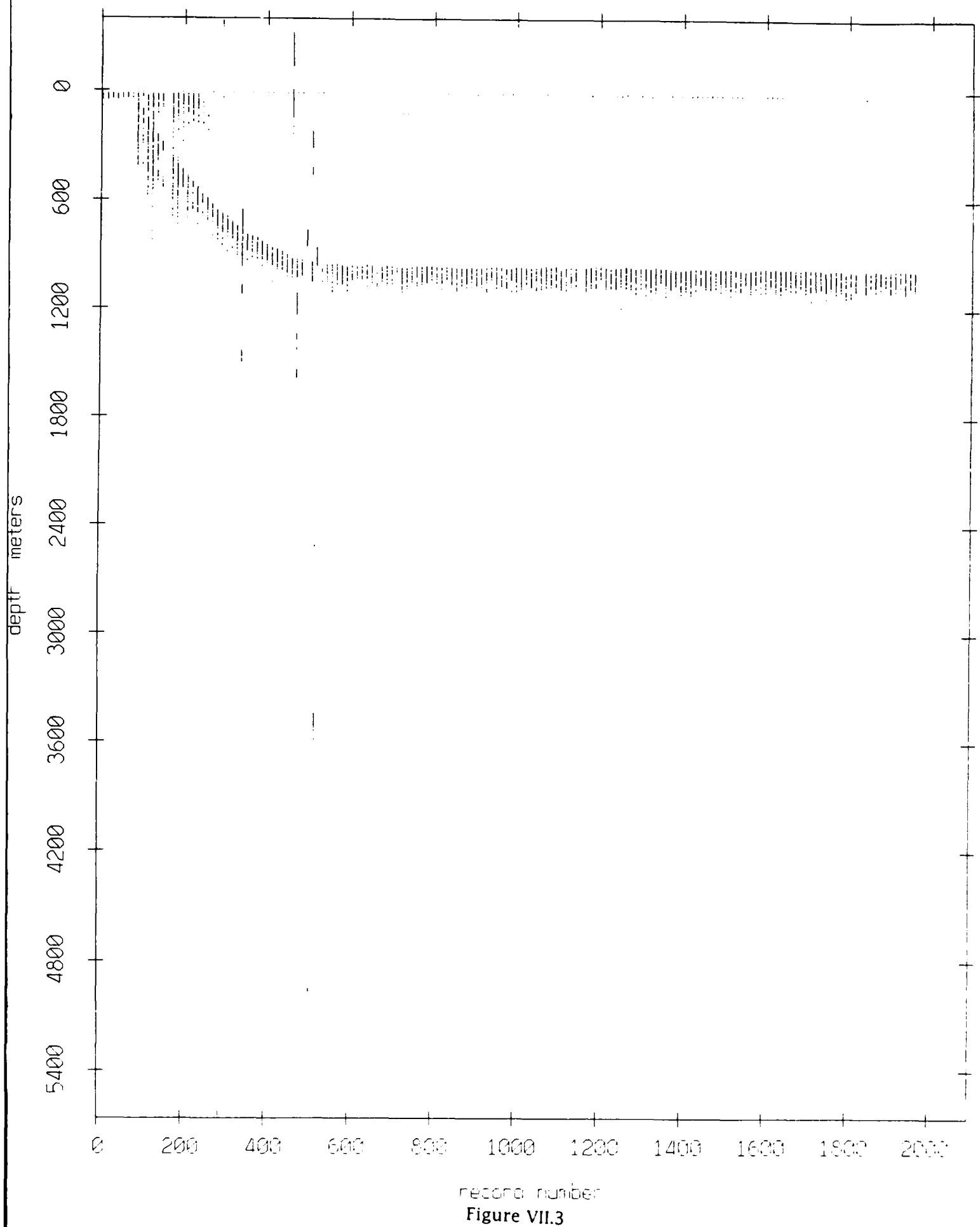


Figure VII.2

Float 2, September 1987 Sea Trip: surface & bottom bounces



record number

Figure VII.3

Float 3, September 1987 Sea Trip: surface & bottom bounces

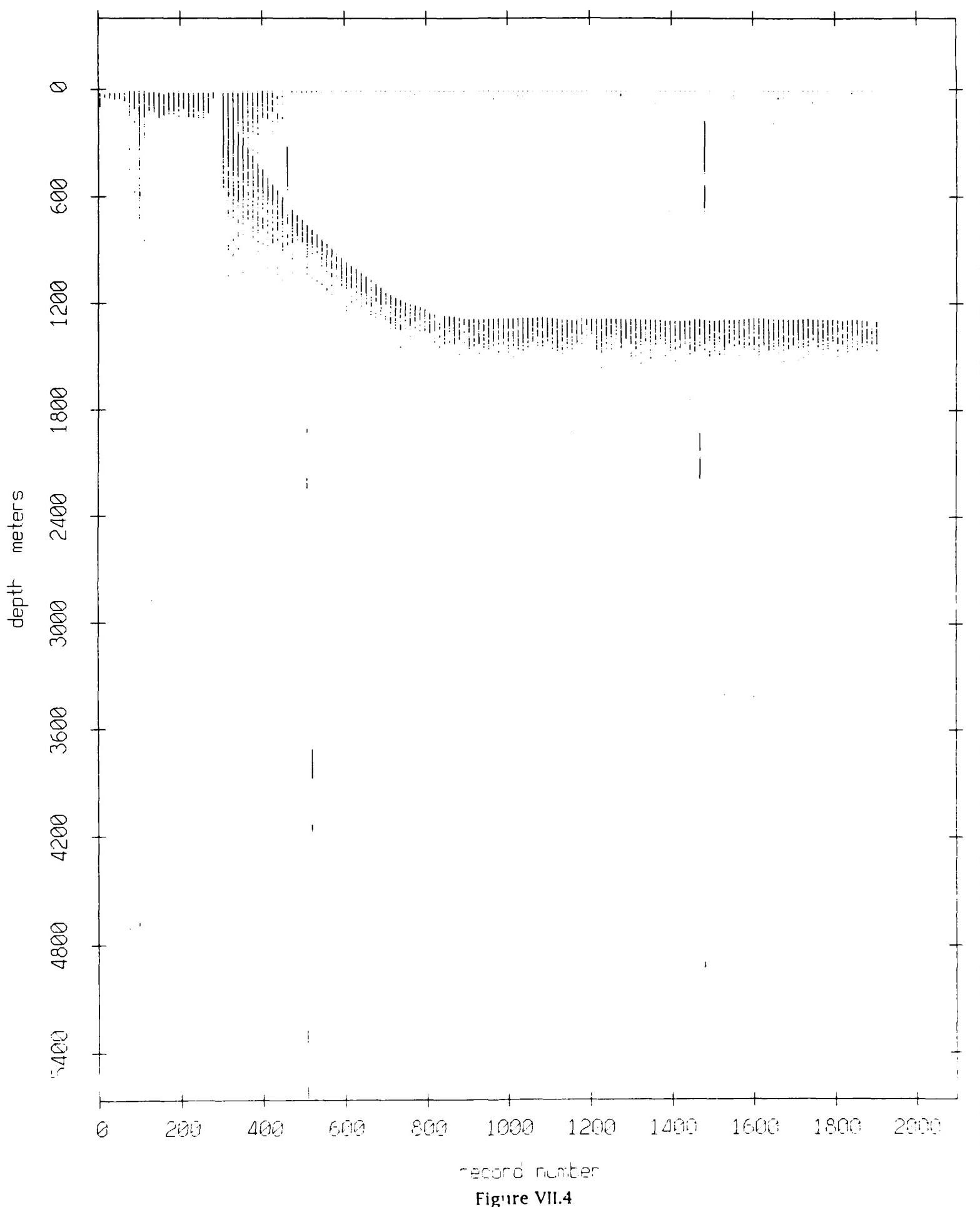


Figure VII.4

Float 4, September 1987 Sea Trip: surface & bottom bounces

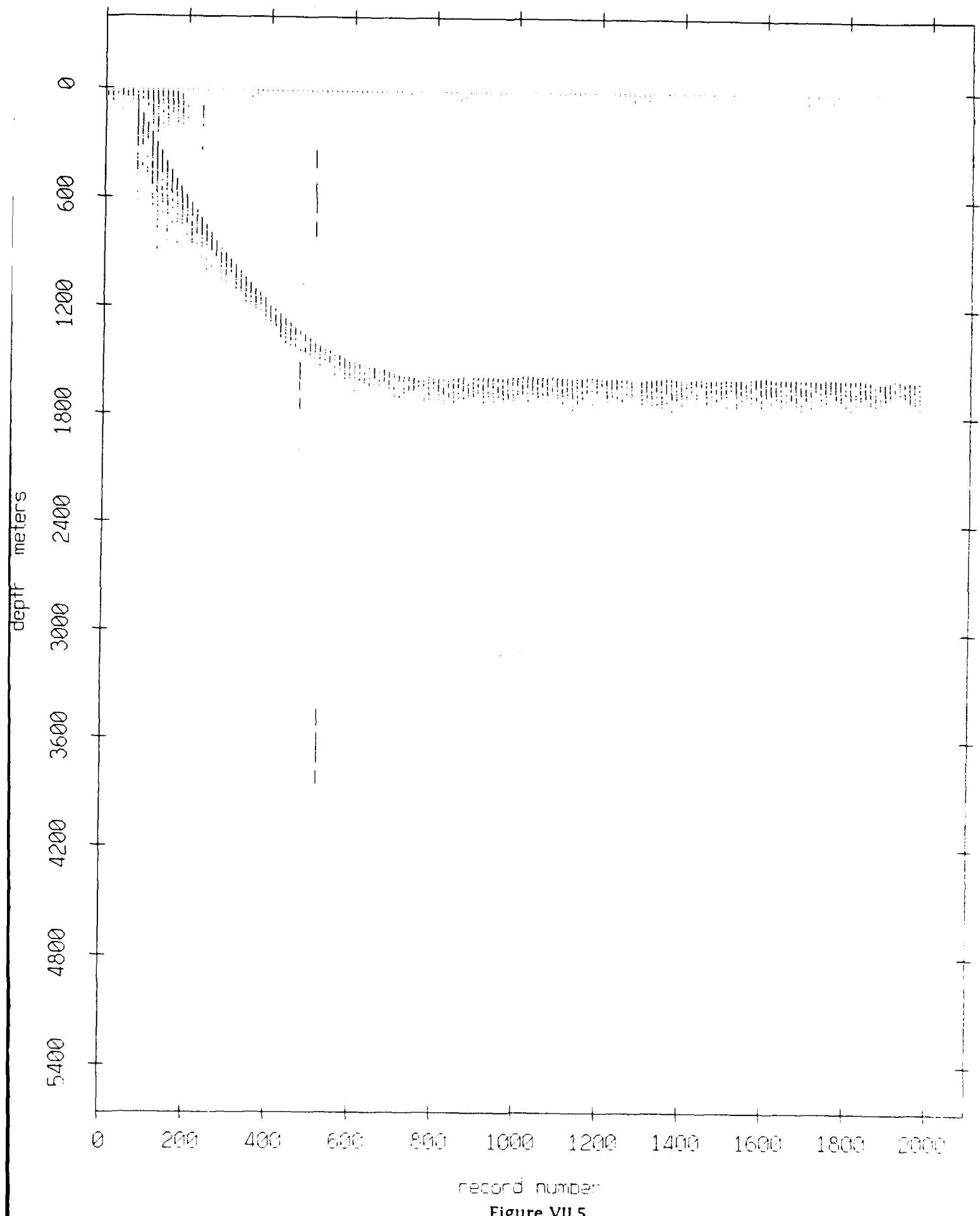


Figure VII.5

Float 5, September 1987 Sea Trip: surface & bottom bounces

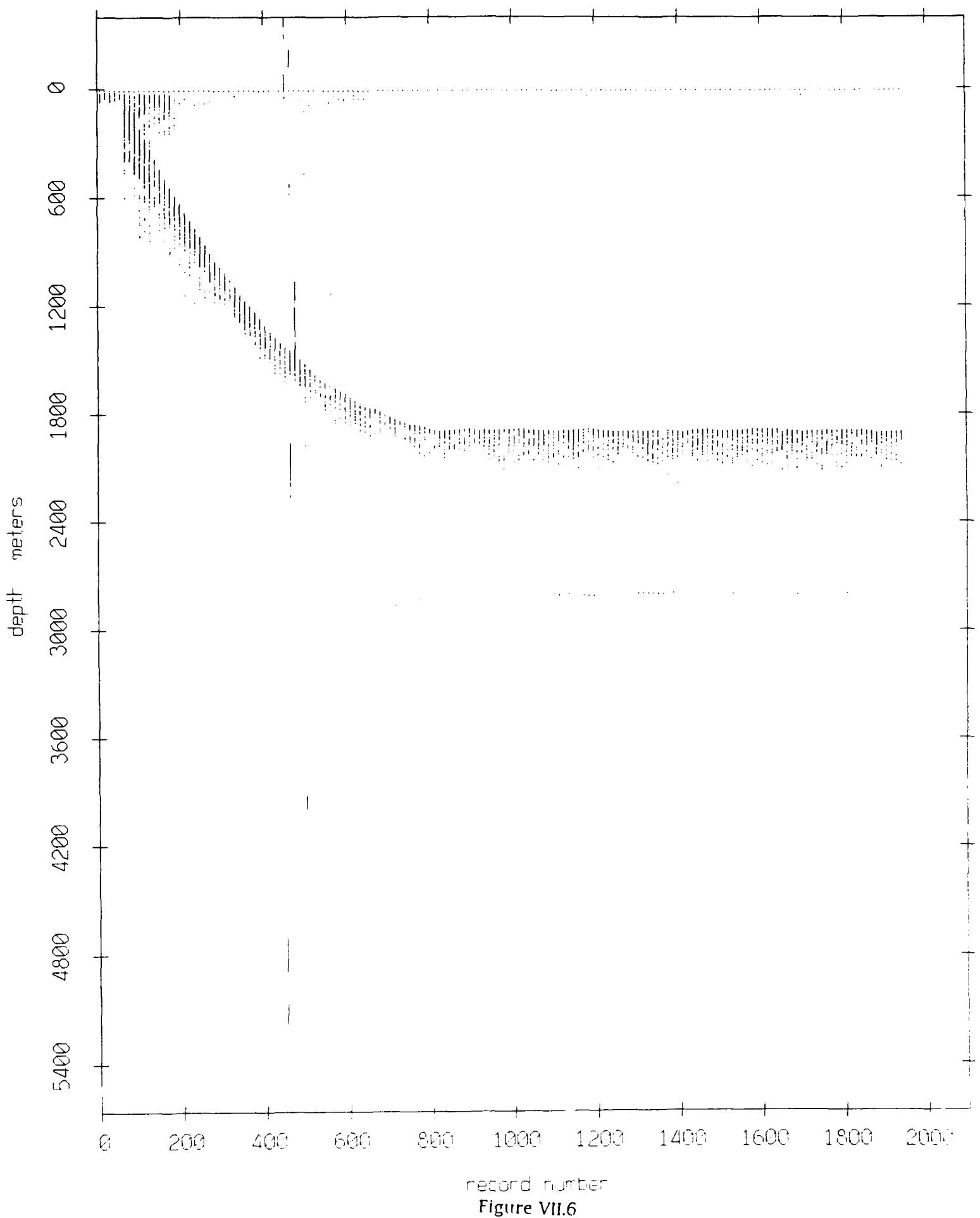


Figure VII.6

Float 6, September 1987 Sea Trip: surface & bottom bounces

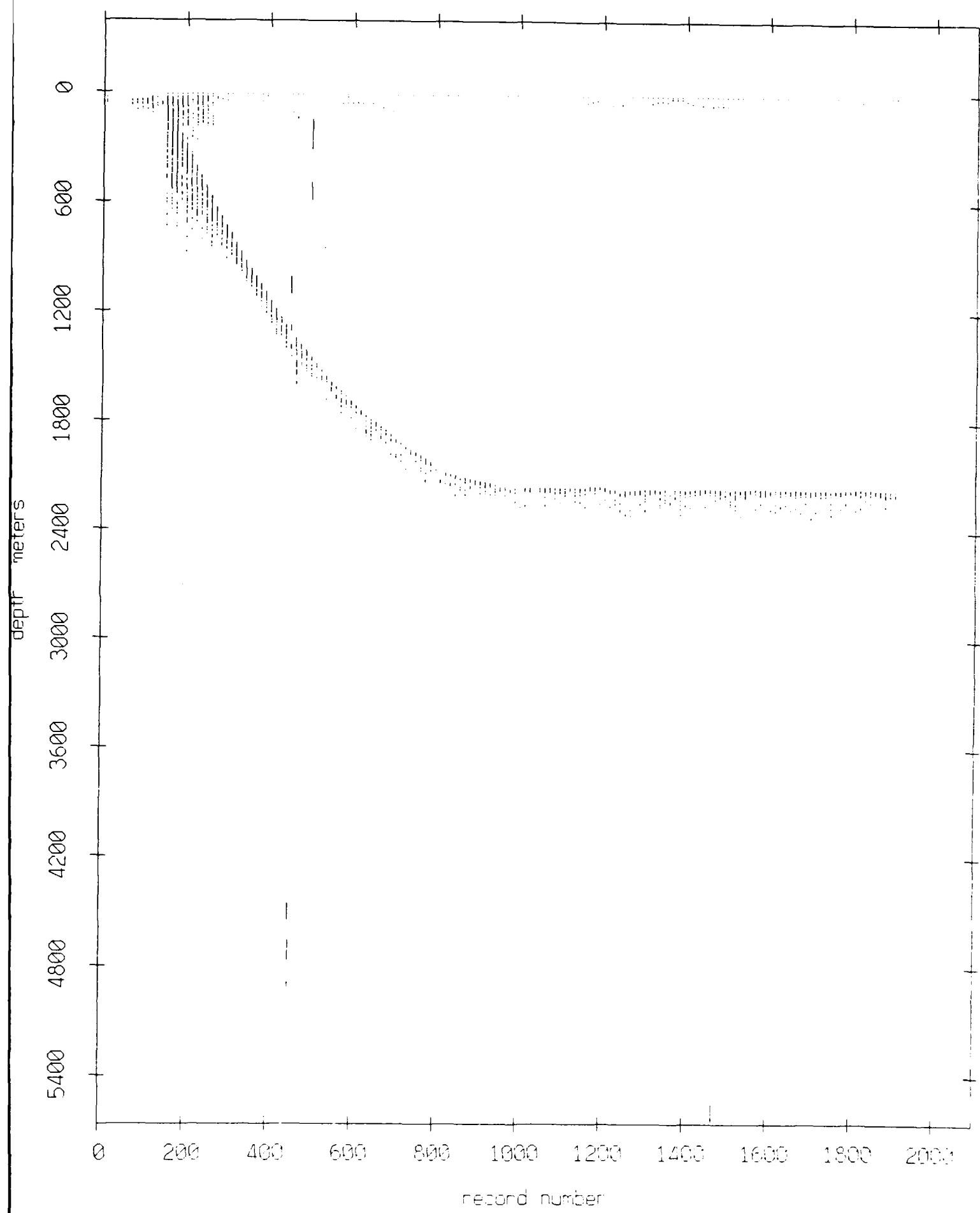


Figure VII.7

Float 7, September 1987 Sea Trip: surface & bottom bounces

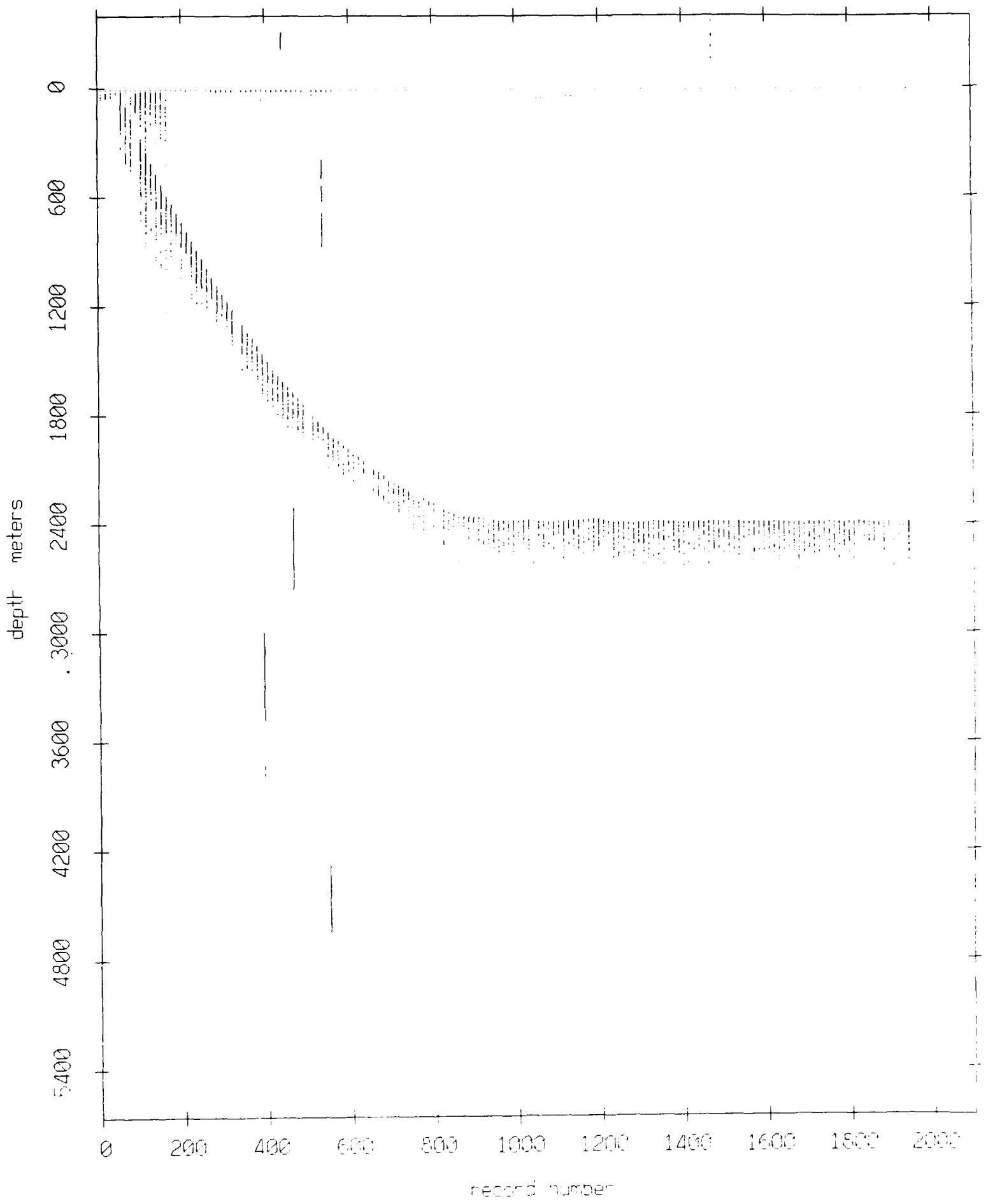


Figure VII.8

Float 8, September 1987 Sea Trip: surface & bottom bounces

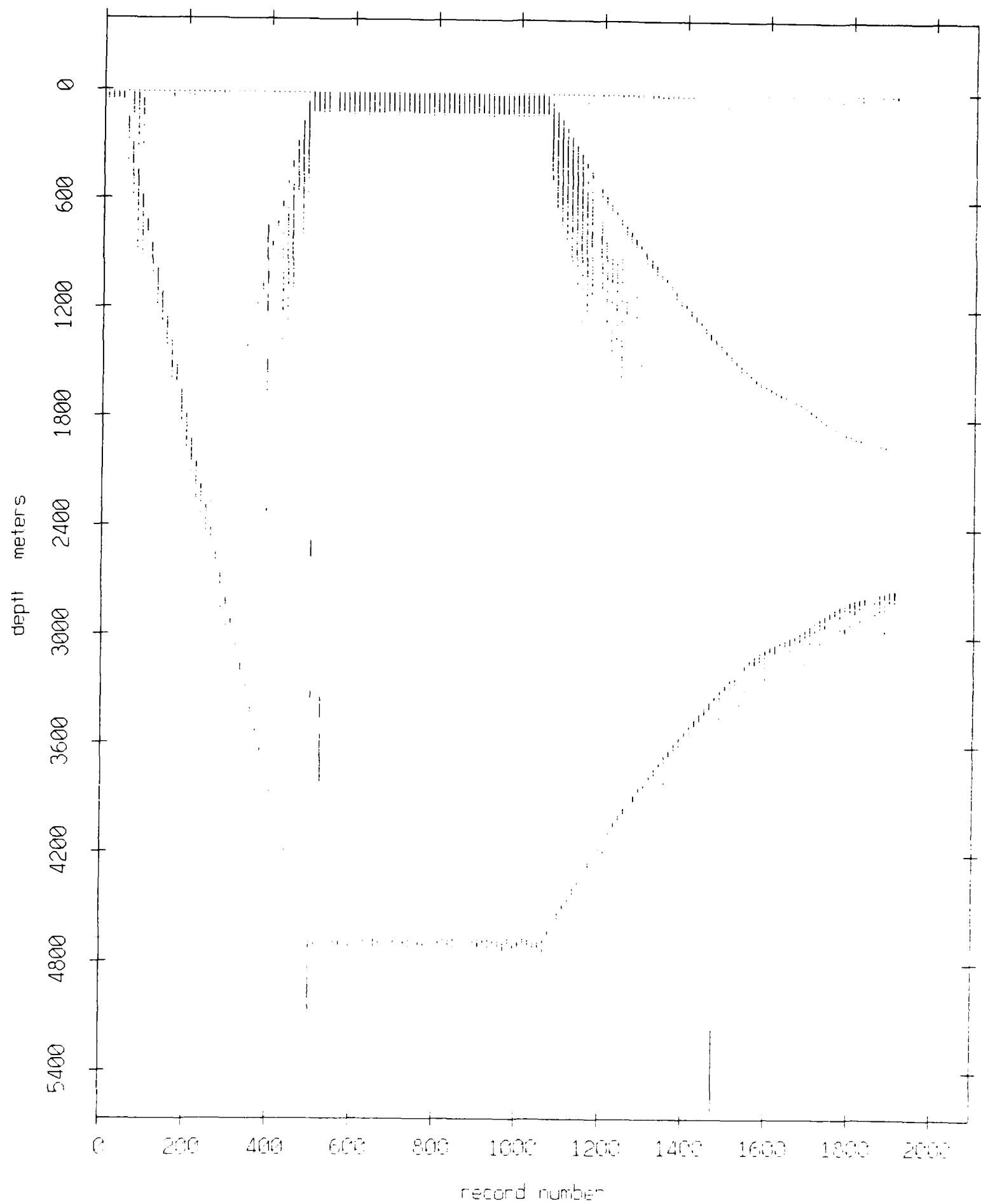


Figure VII.9

Float 9, September 1987 Sea Trip: surface & bottom bounces

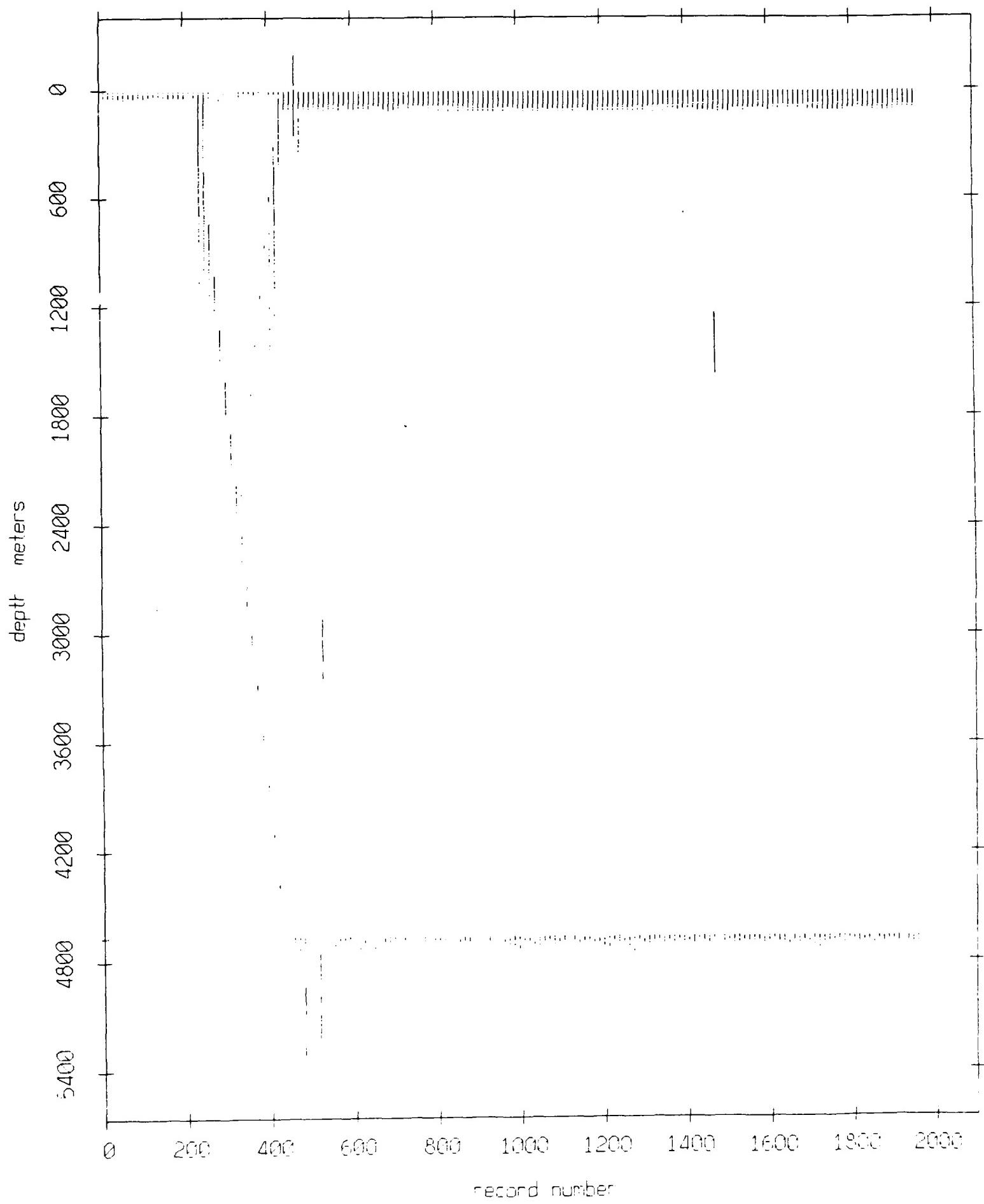


Figure VII.10

Float 10, September 1987 Sea Trip: surface & bottom bounces

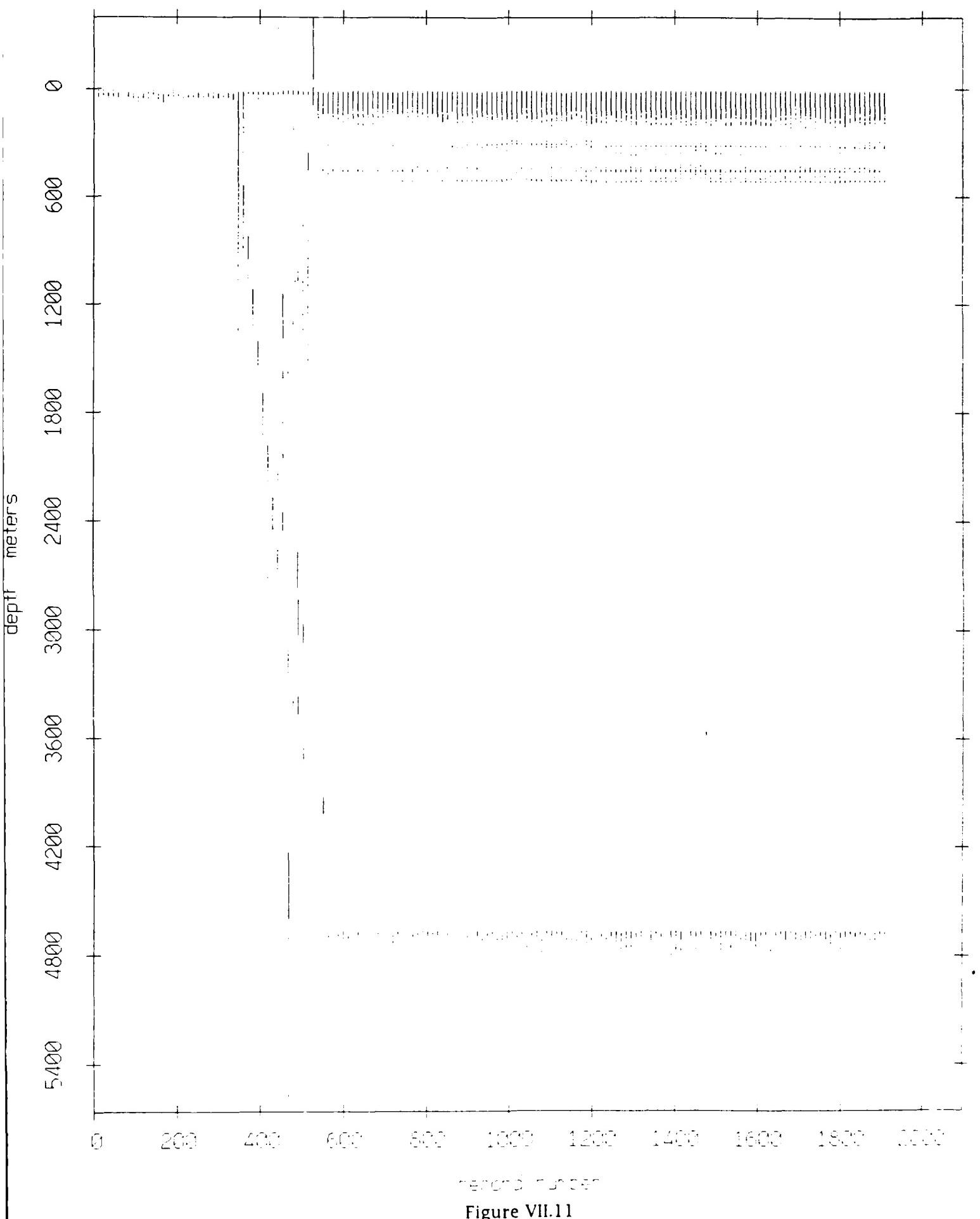


Figure VII.11

Float 11, September 1987 Sea Trip: surface & bottom bounces

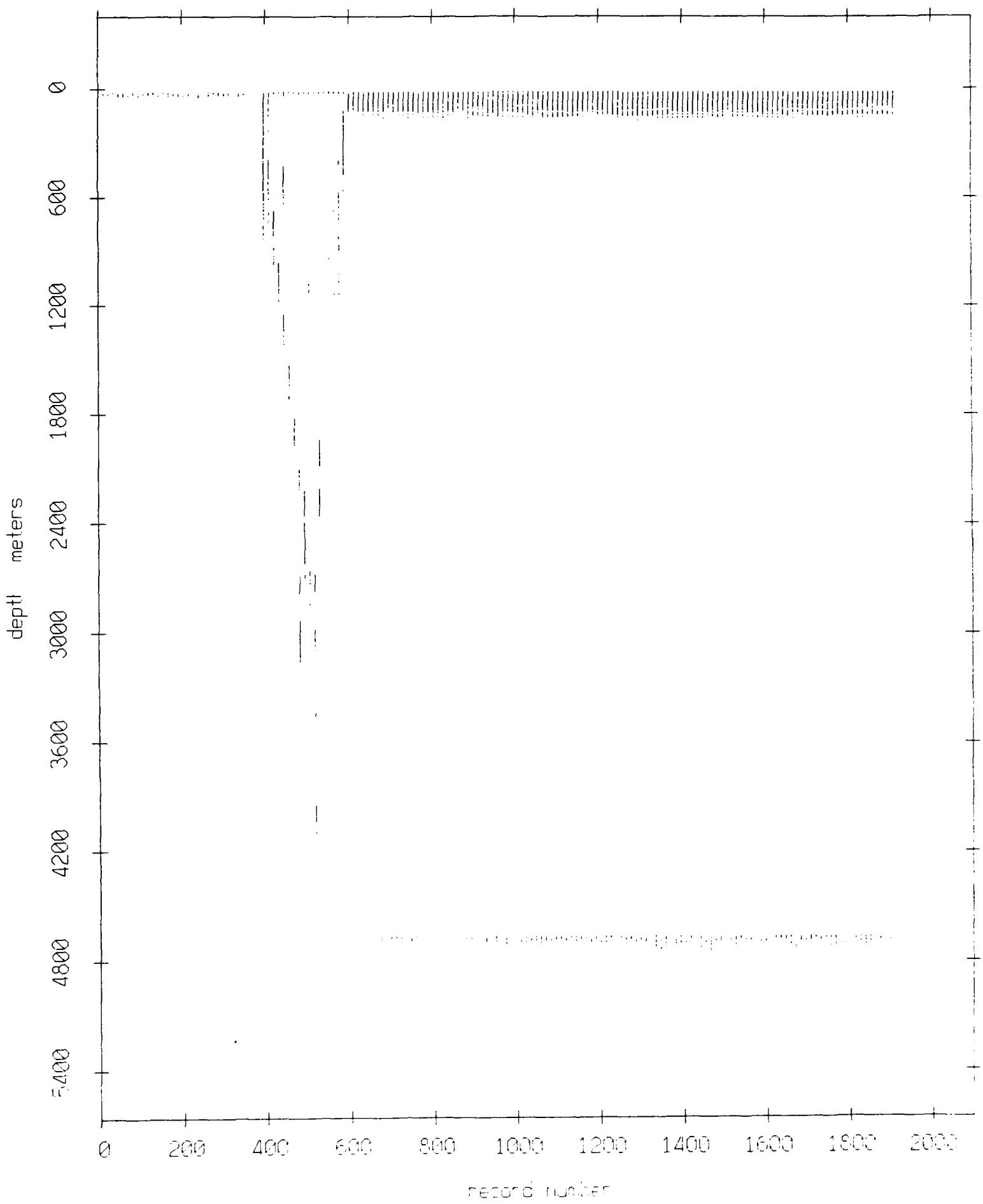


Figure VII.12

Float 0, September 1987 Sea Trip: range from float 2

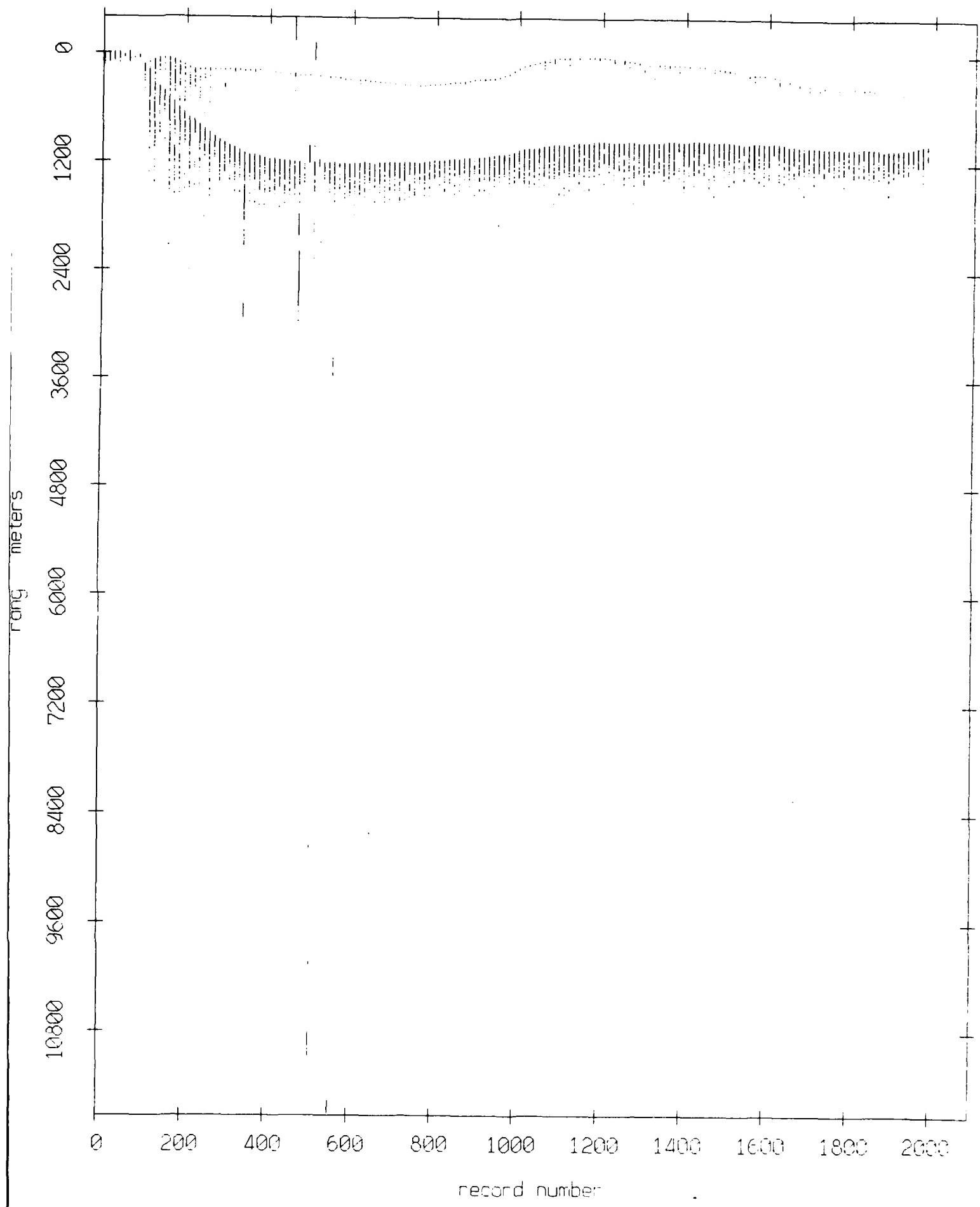


Figure VIII.1a

Float 0, September 1987 Sea Trip: range from float 3

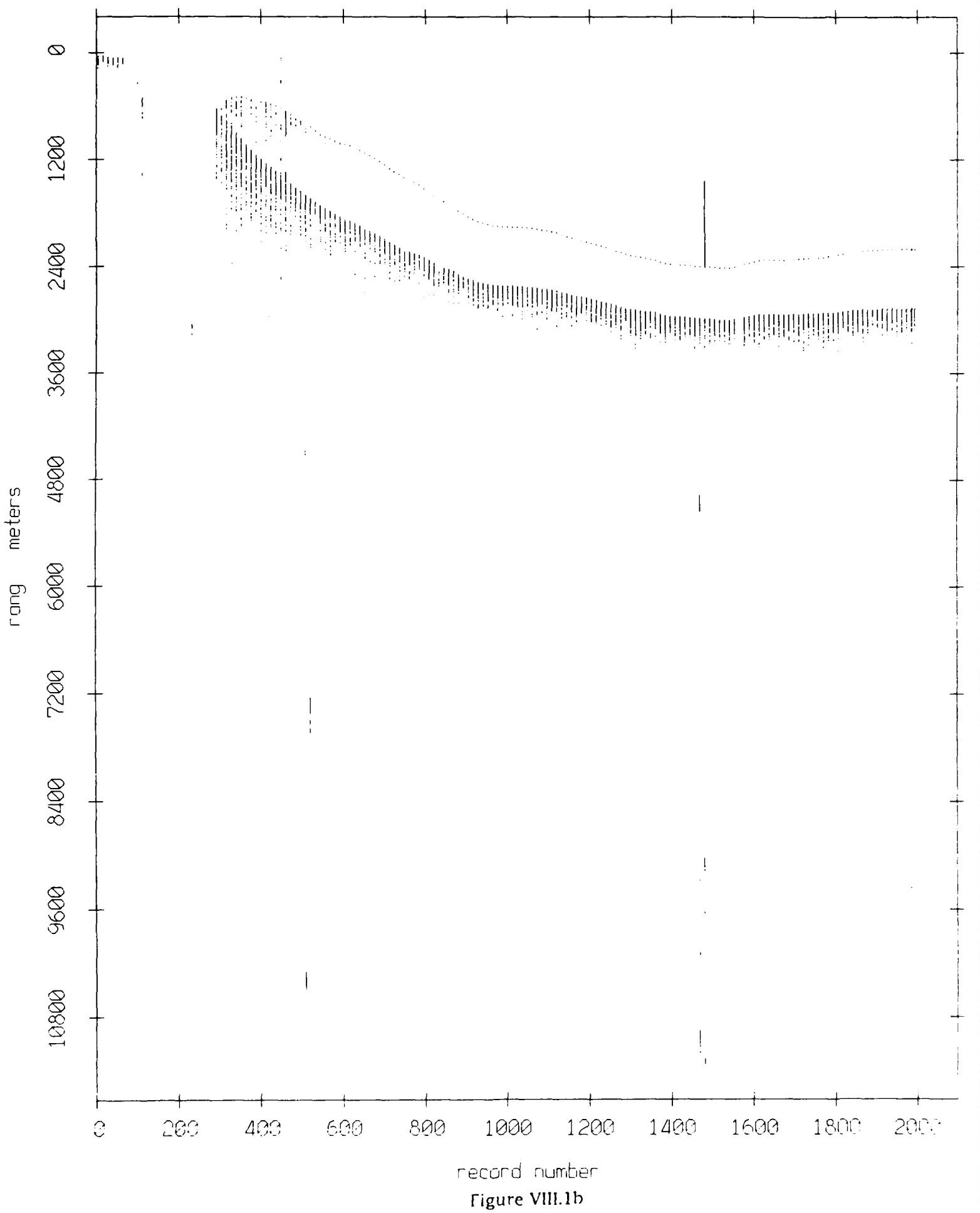
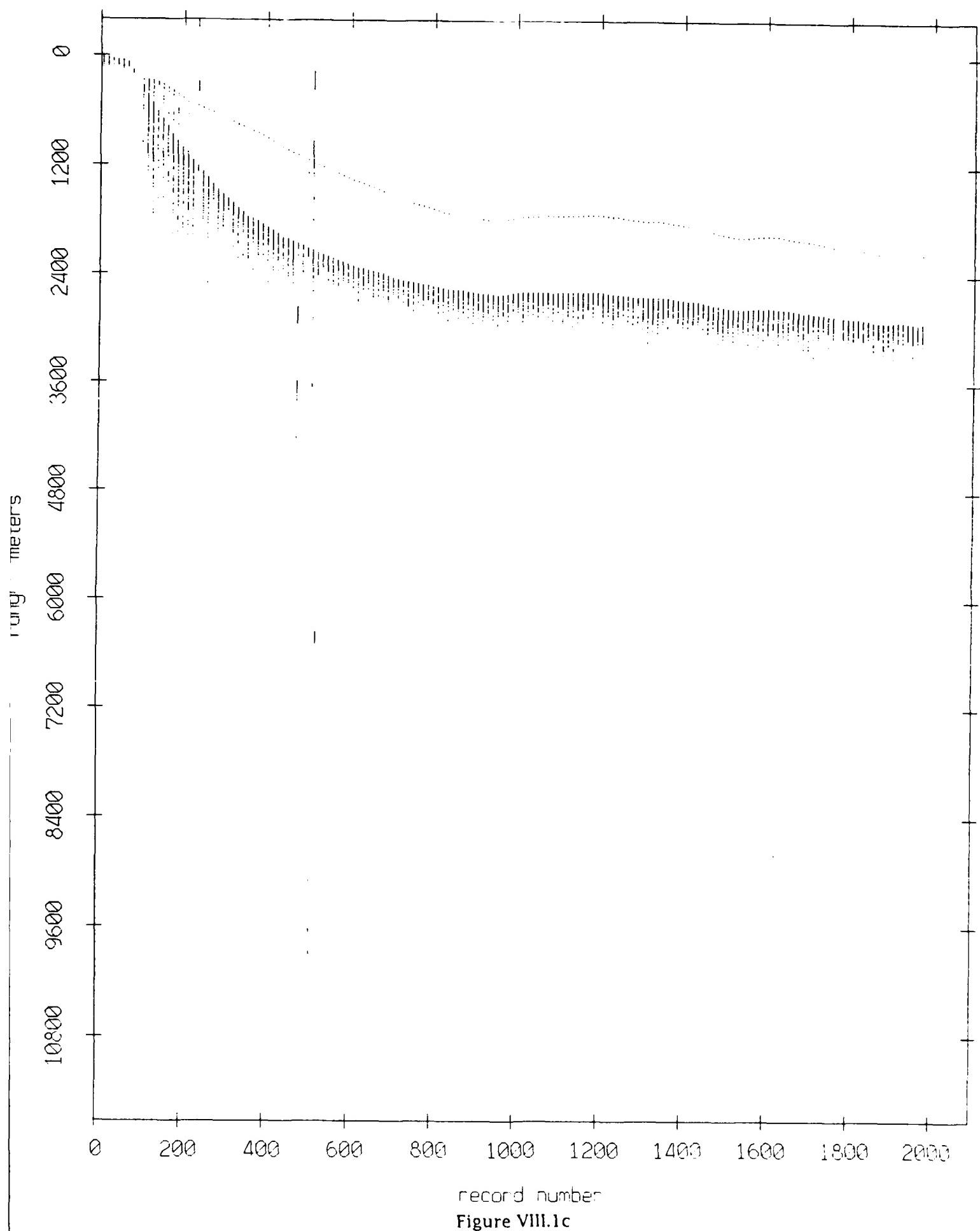


Figure VIII.1b

Float 0, September 1987 Sea Trip: range from float 4



record number
Figure VIII.1c

Float 0, September 1987 Sea Trip: range from float 5

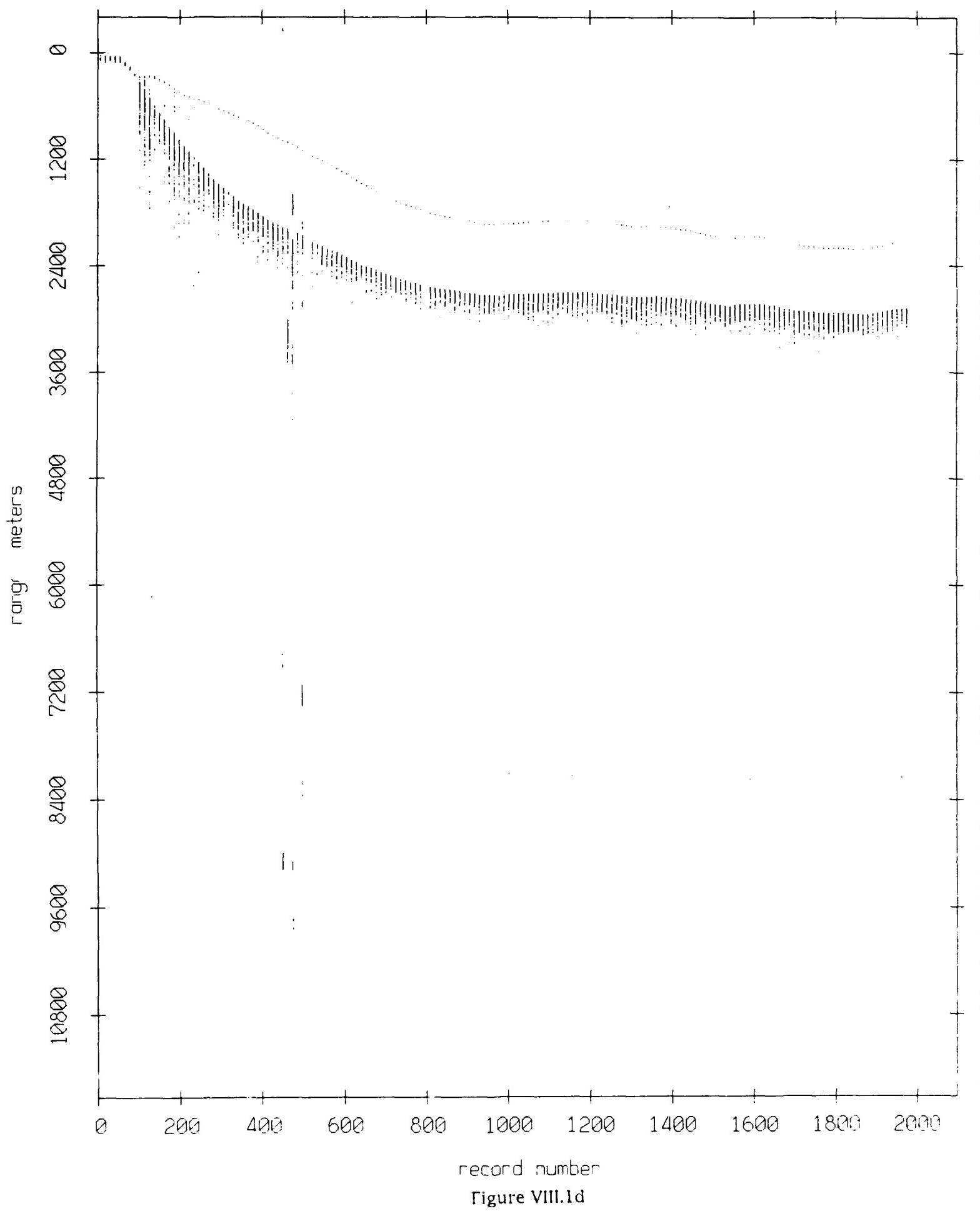
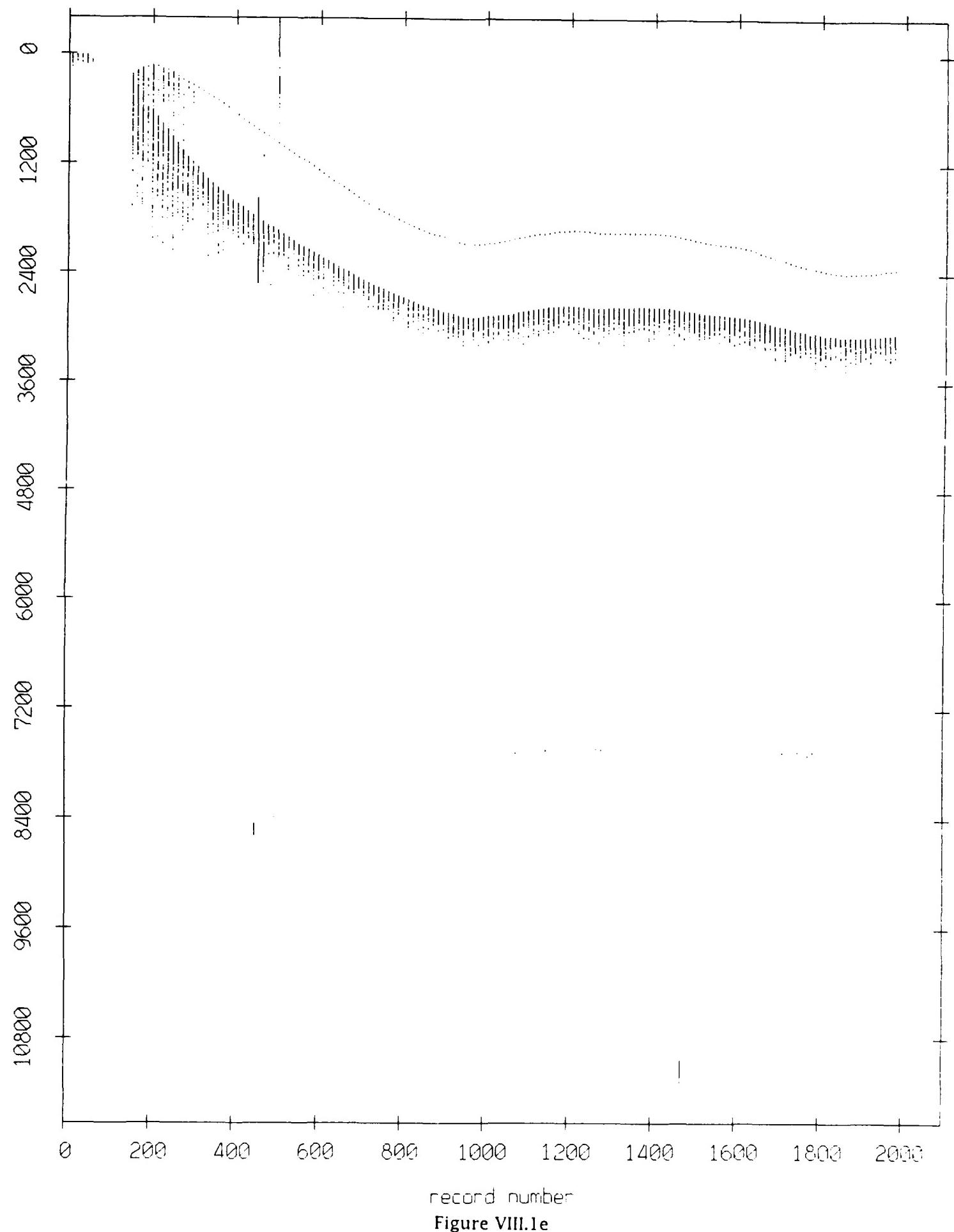


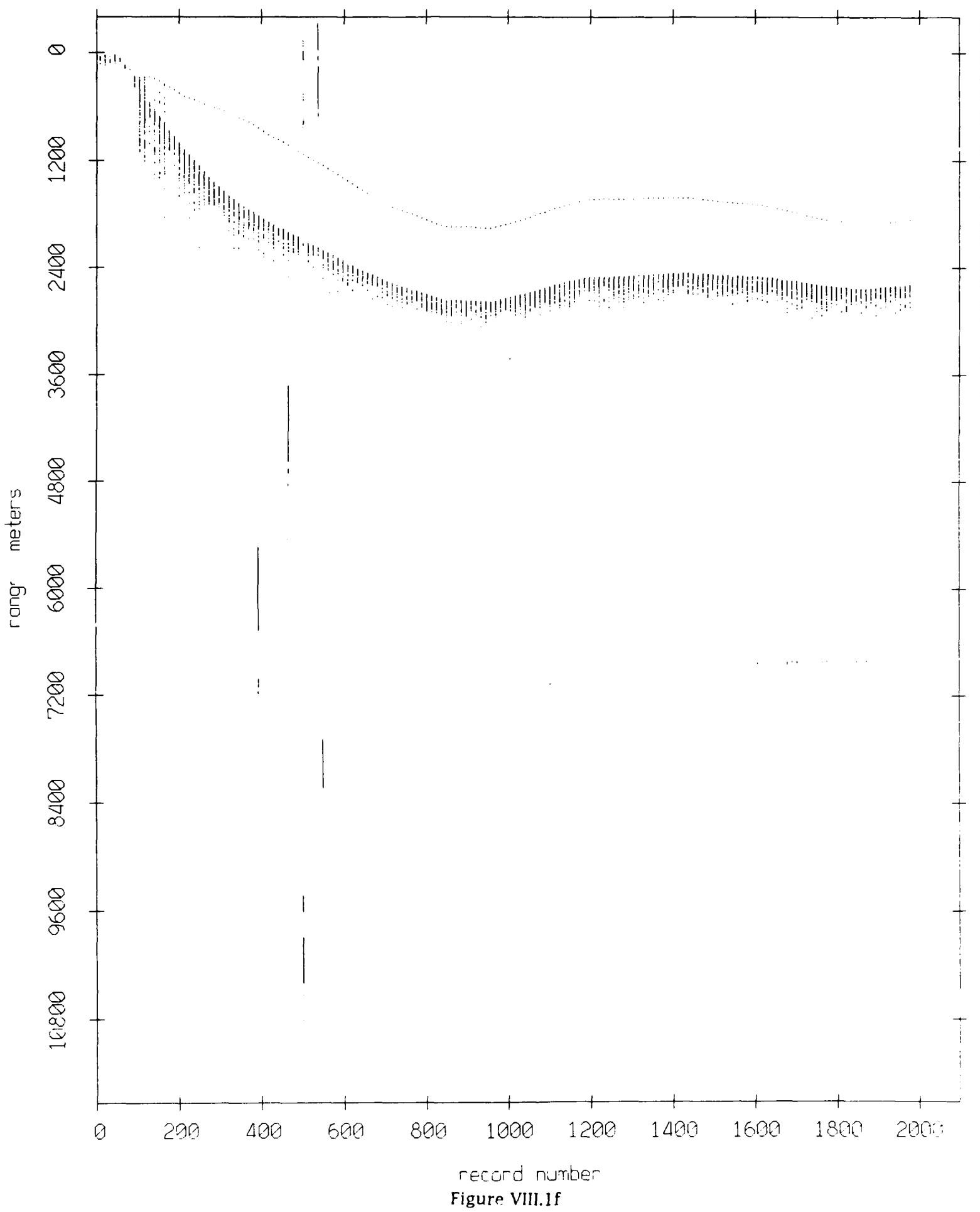
Figure VIII.1d

Float 0, September 1987 Sea Trip: range from float 6



record number
Figure VIII.1e

Float 0, September 1987 Sea Trip: range from float 7



record number
Figure VIII.1f

Float 0, September 1987 Sea Trip: range from float 8

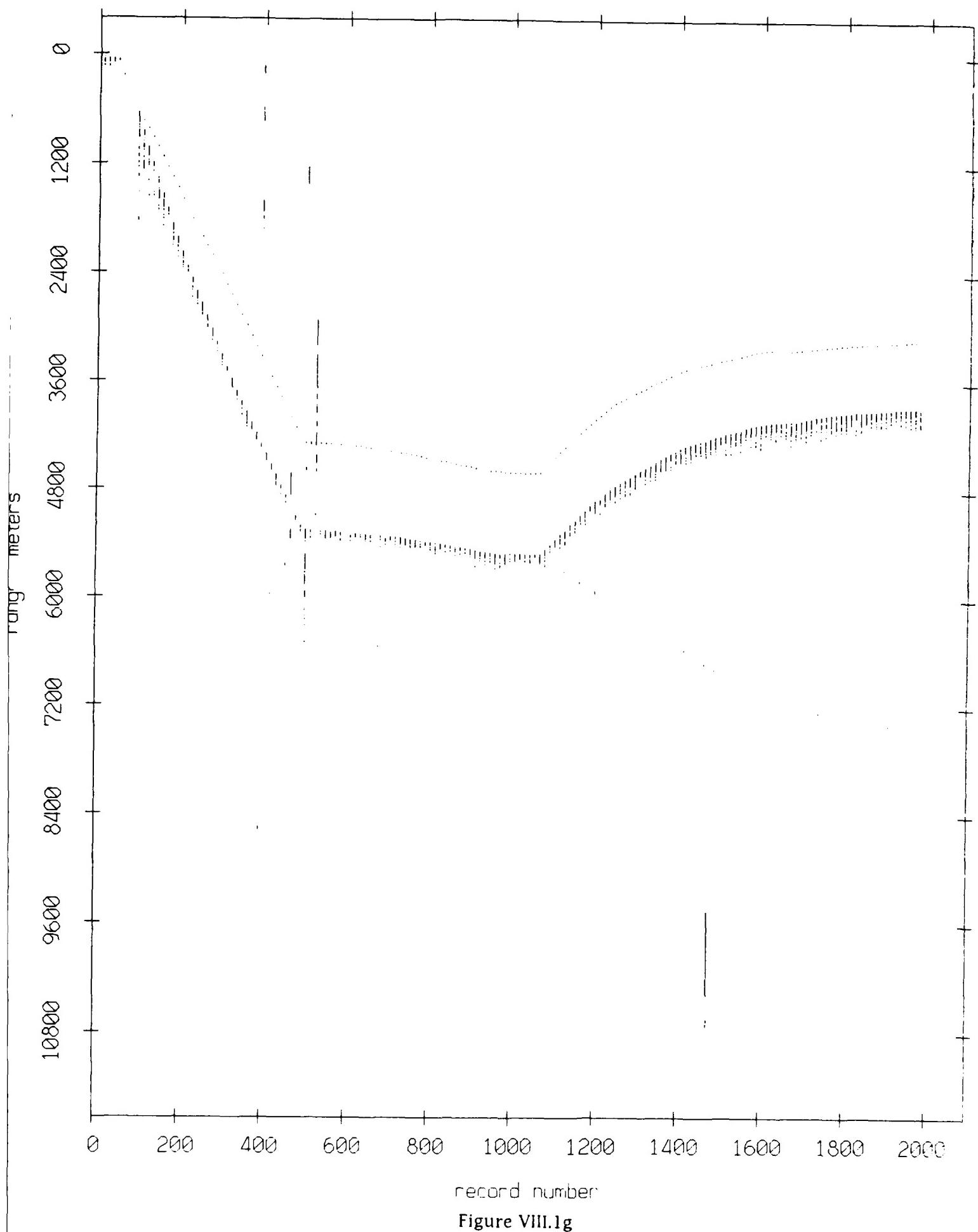


Figure VIII.1g

Float 0, September 1987 Sea Trip: range from float 9

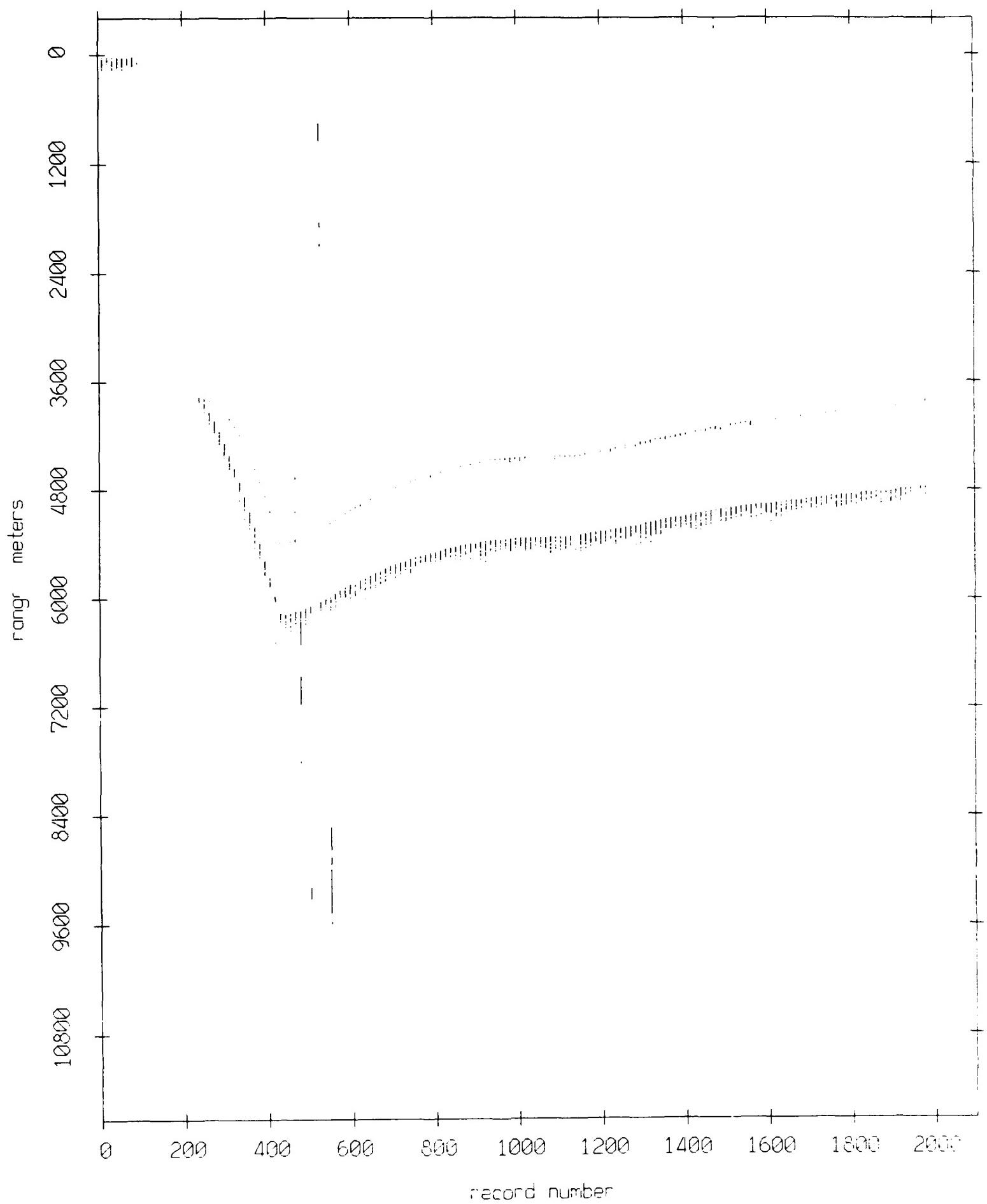


Figure VIII.1h

Float 0, September 1987 Sea Trip: range from float 10

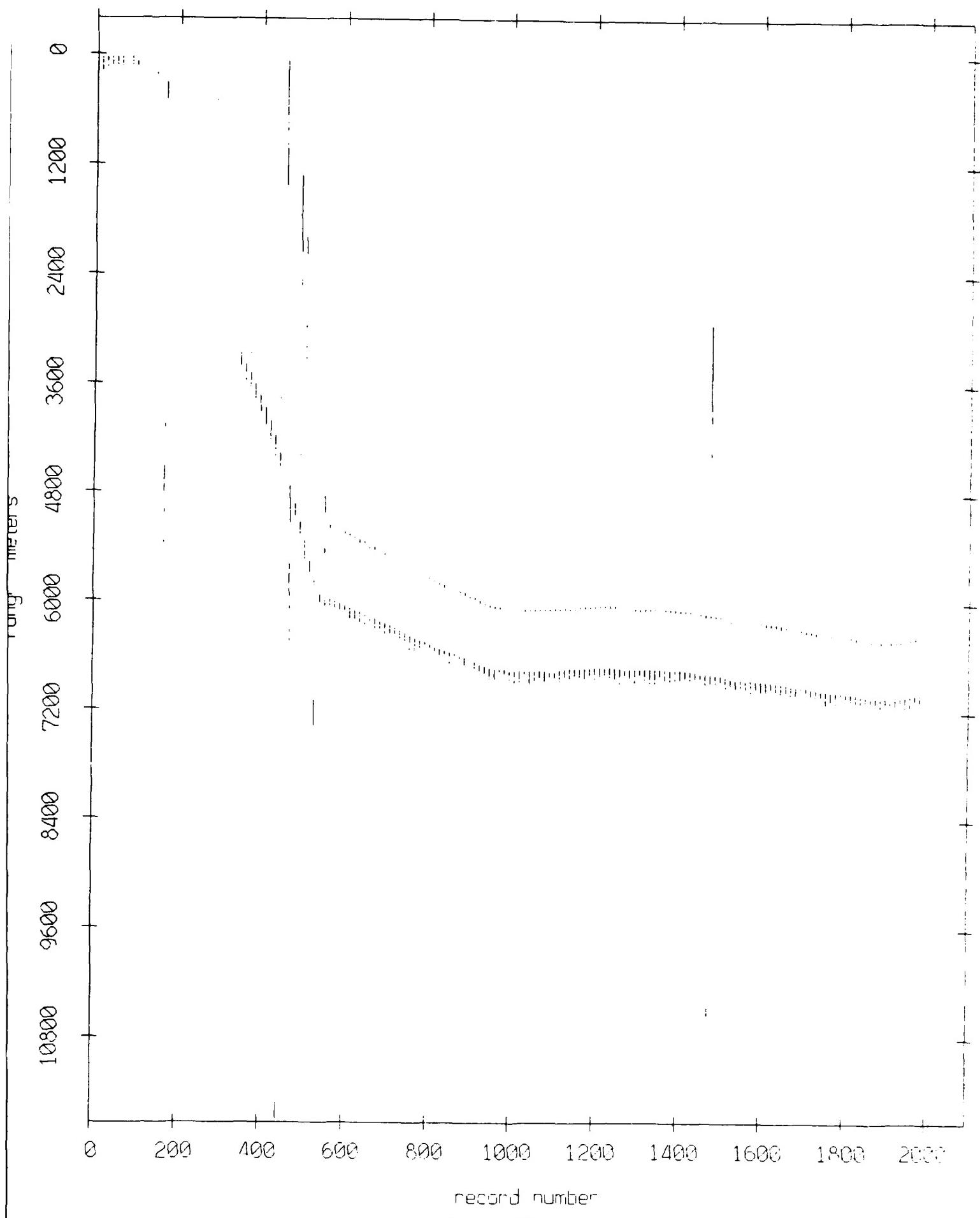


Figure VIII.1i

Float 0, September 1987 Sea Trip: range from float 11

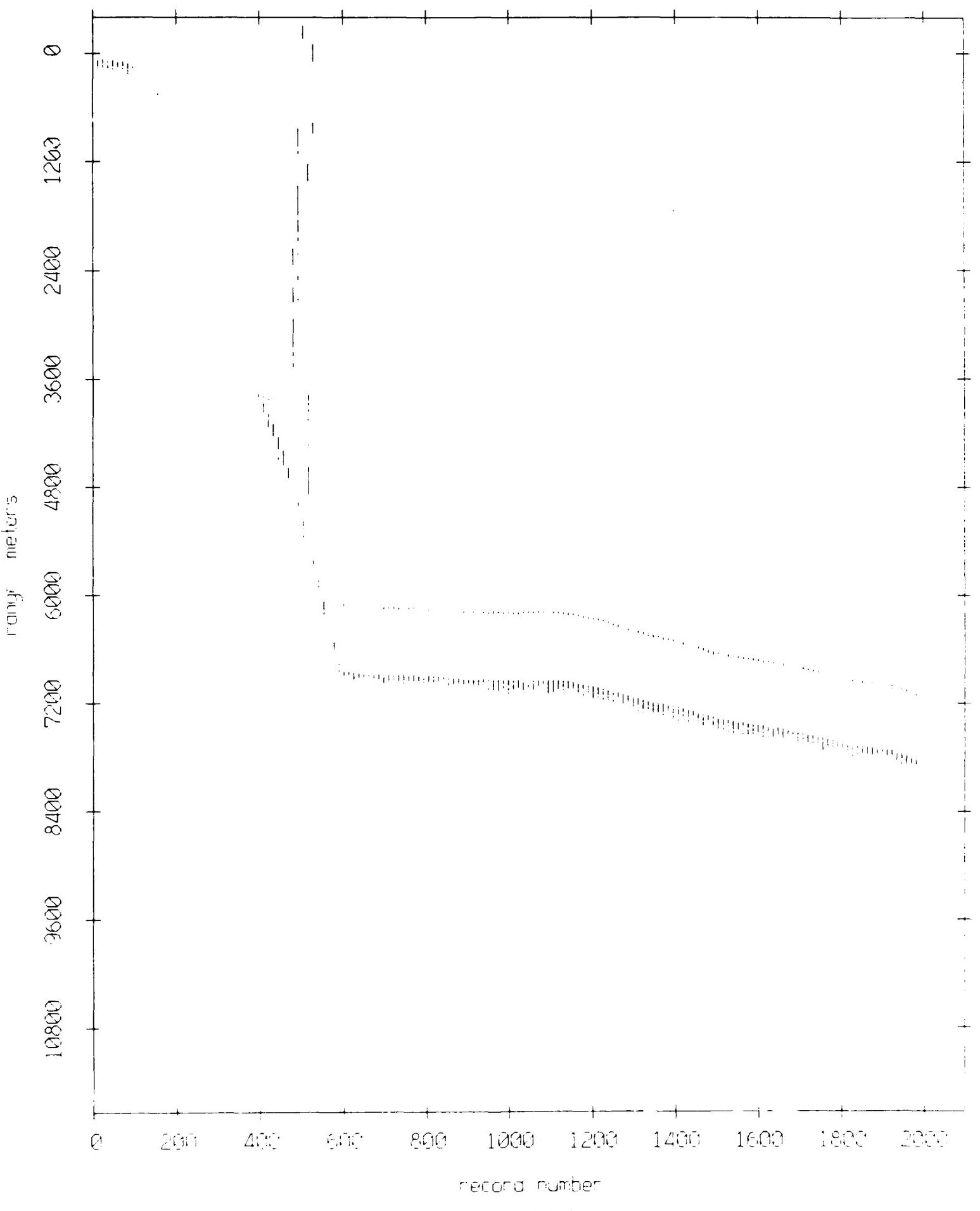


Figure VIII.1j

Float 2, September 1987 Sea Trip: range from float 0

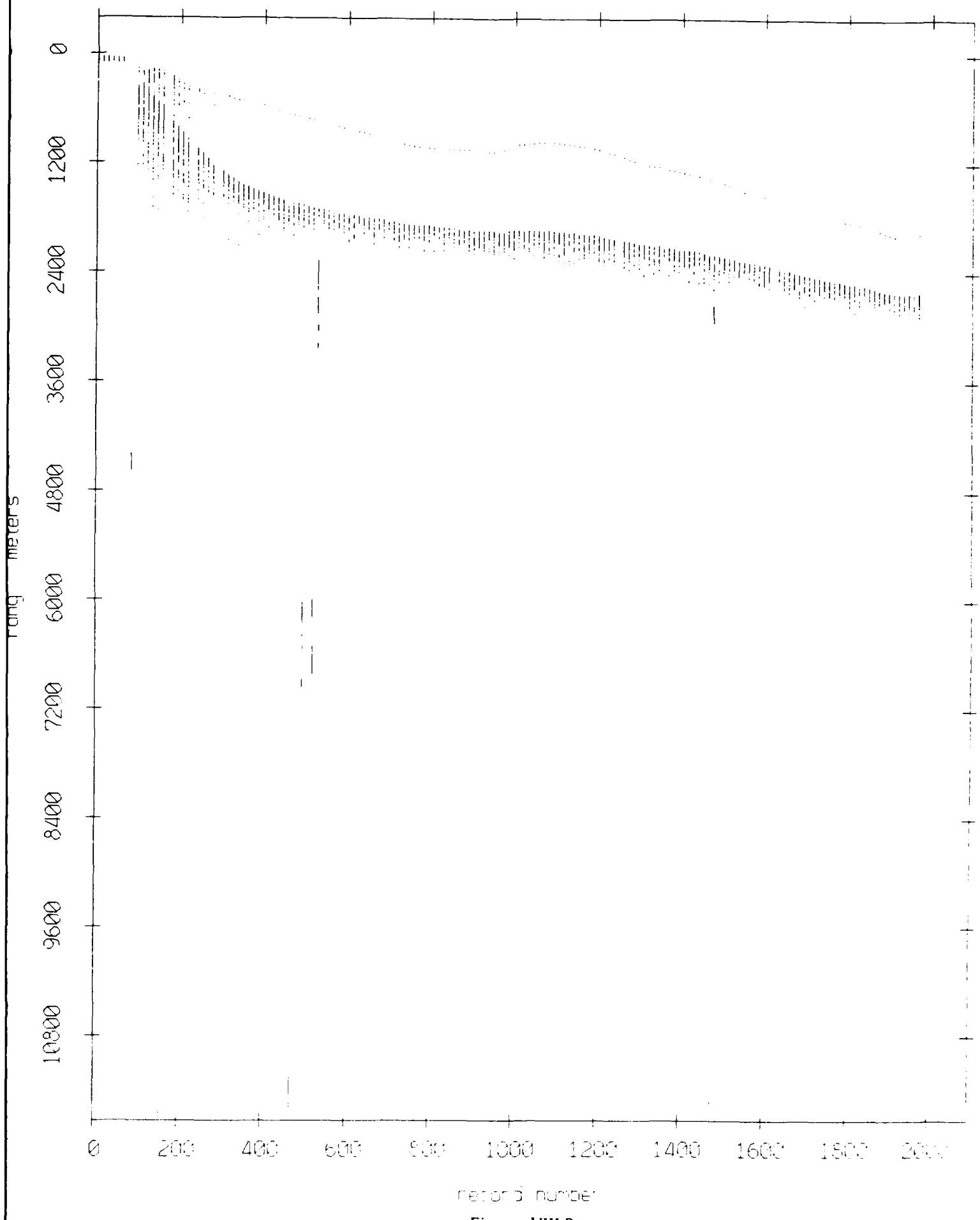


Figure VIII.2a

Float 2, September 1987 Sea Trip: range from float 3

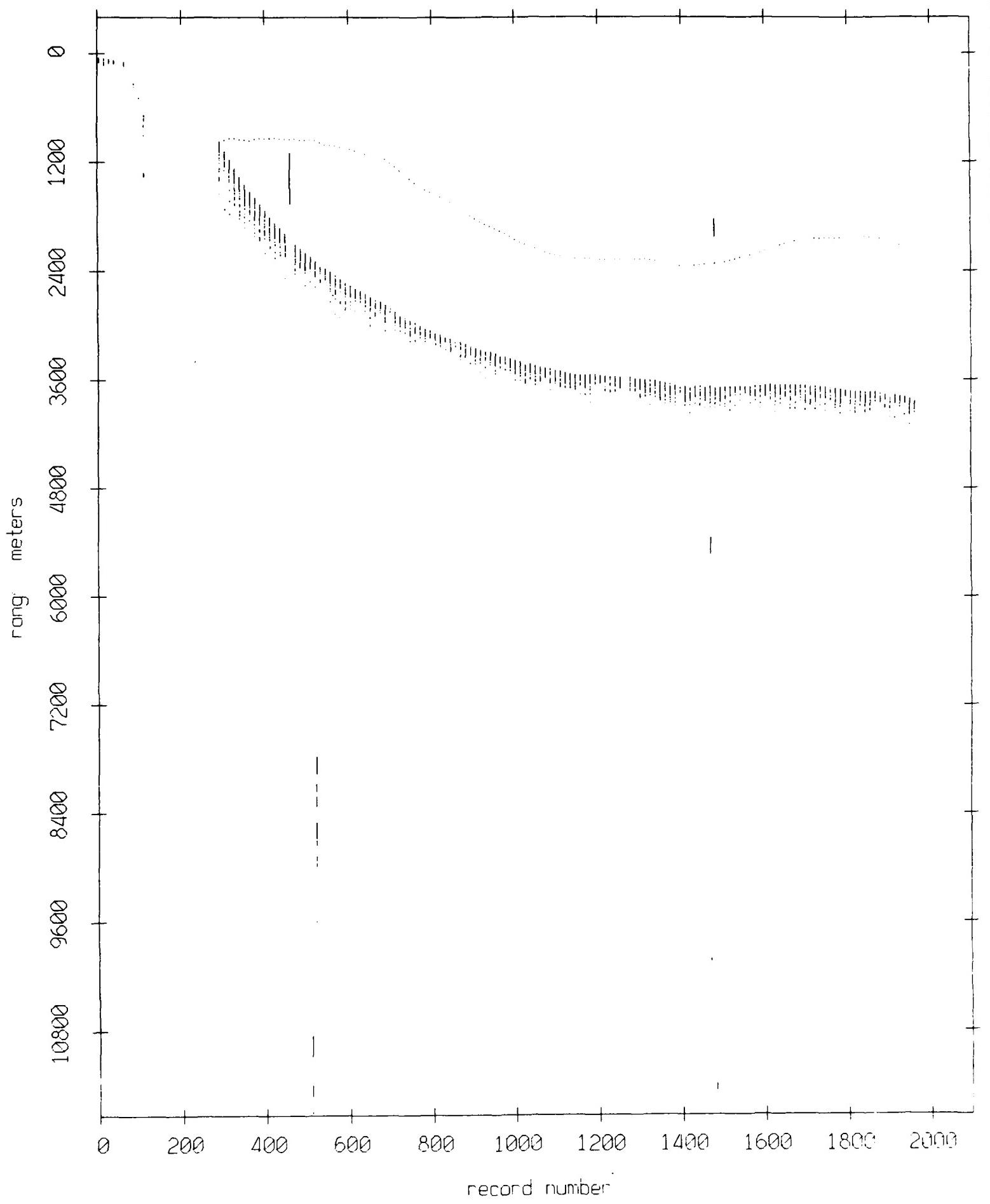


Figure VIII.2b

Float 2, September 1987 Sea Trip: range from float 4

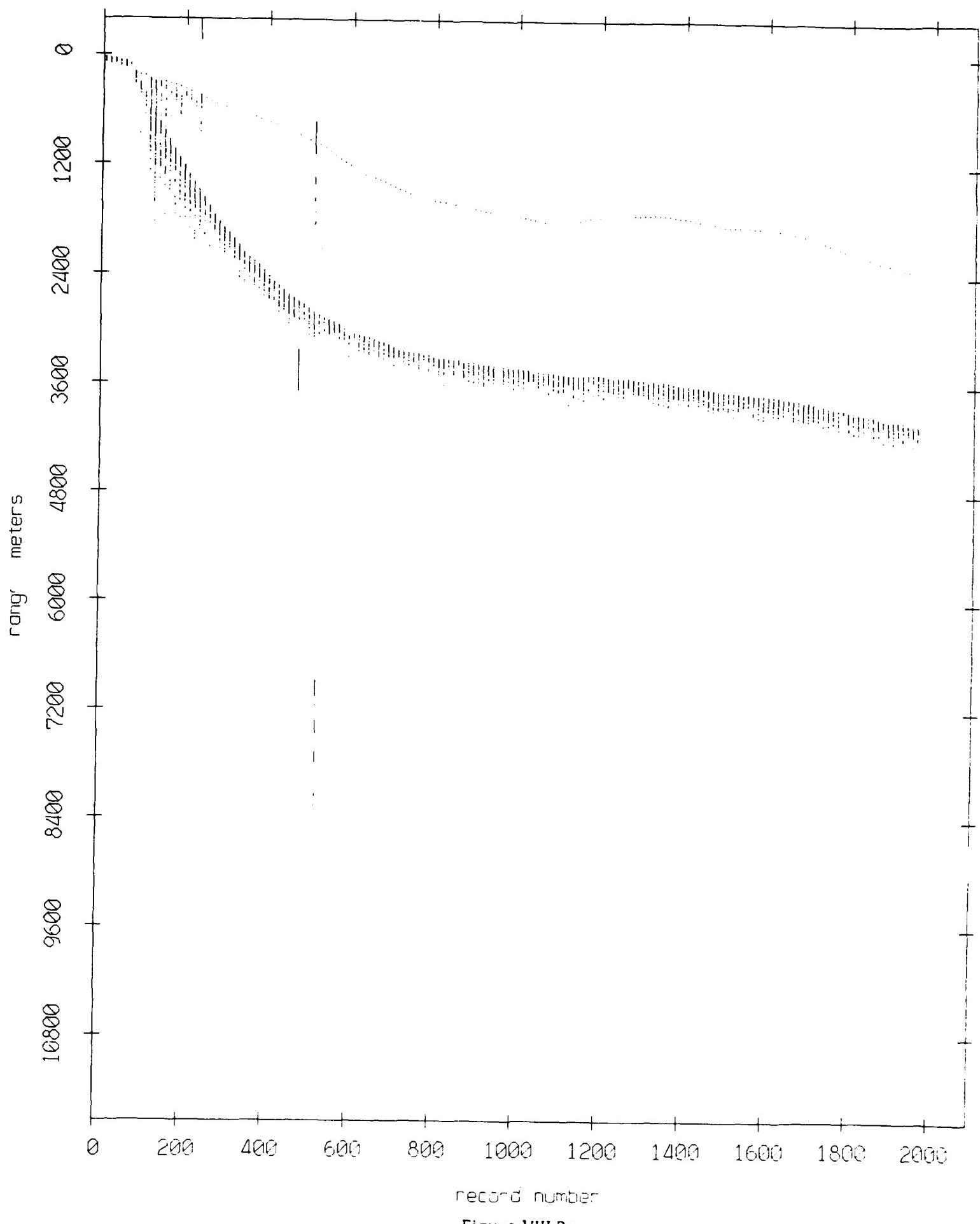


Figure VIII.2c

Float 2, September 1987 Sea Trip: range from float 5

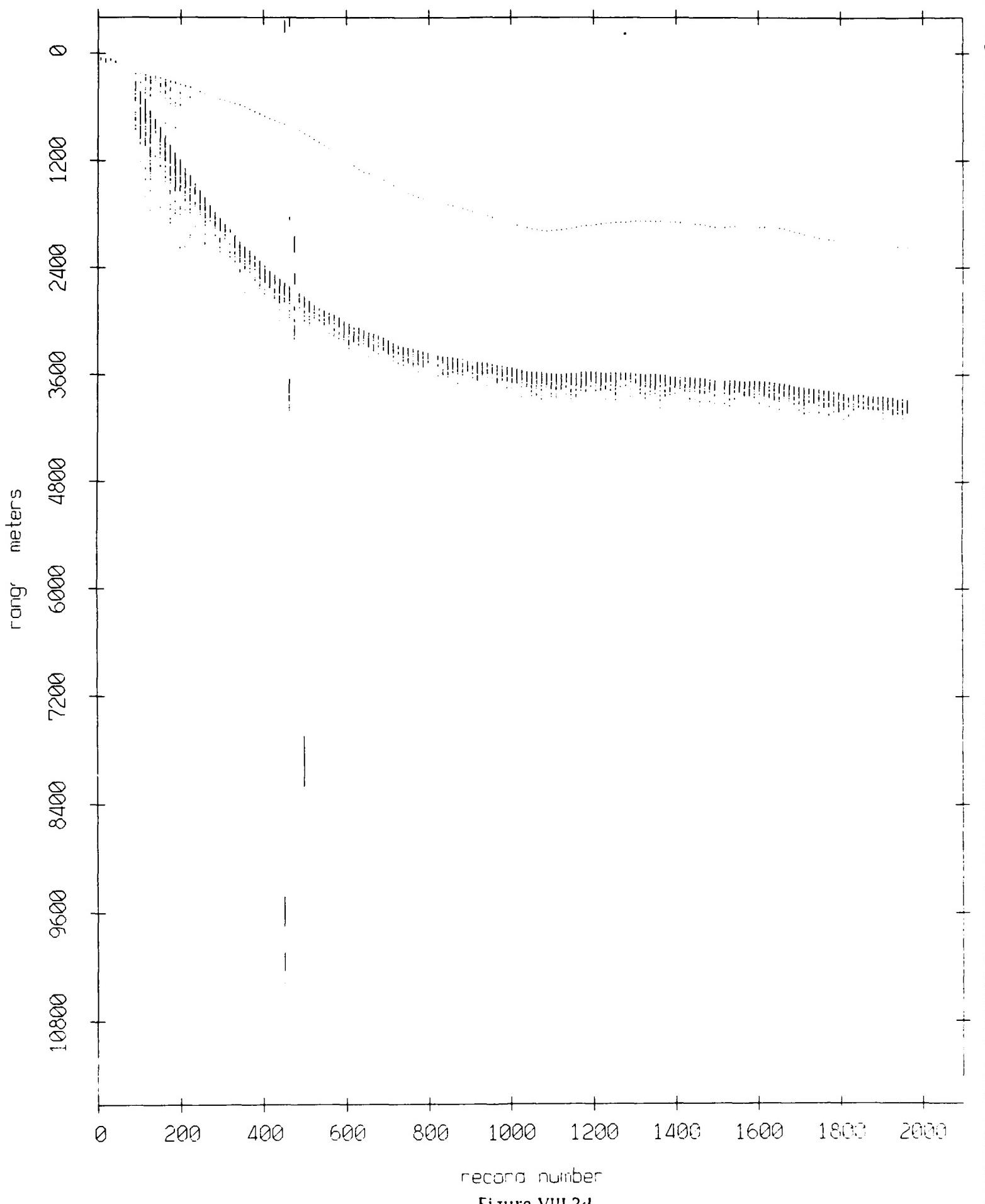


Figure VIII.2d

Float 2, September 1987 Sea Trip: range from float 6

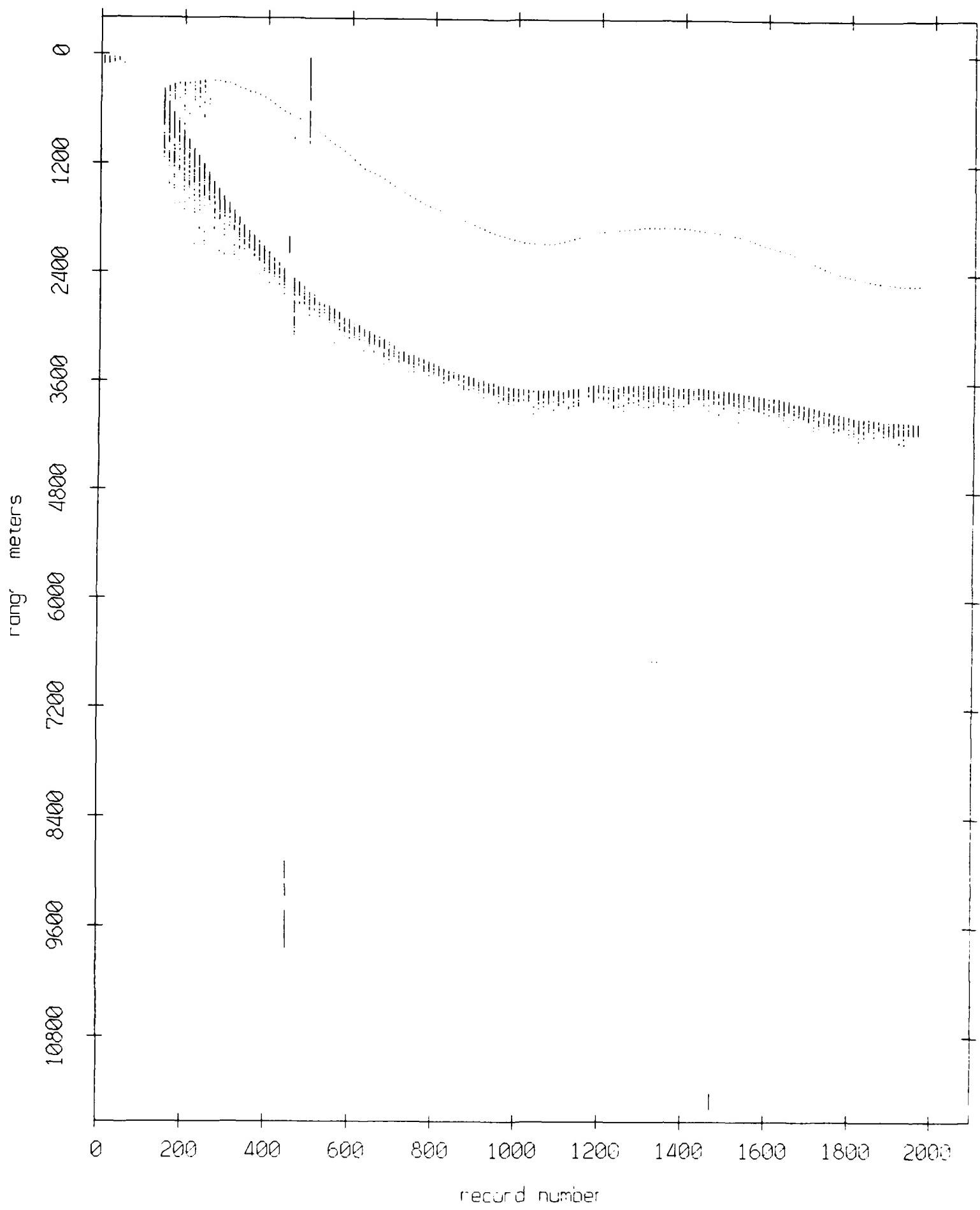


Figure VIII.2e

Float 2, September 1987 Sea Trip: range from float 7

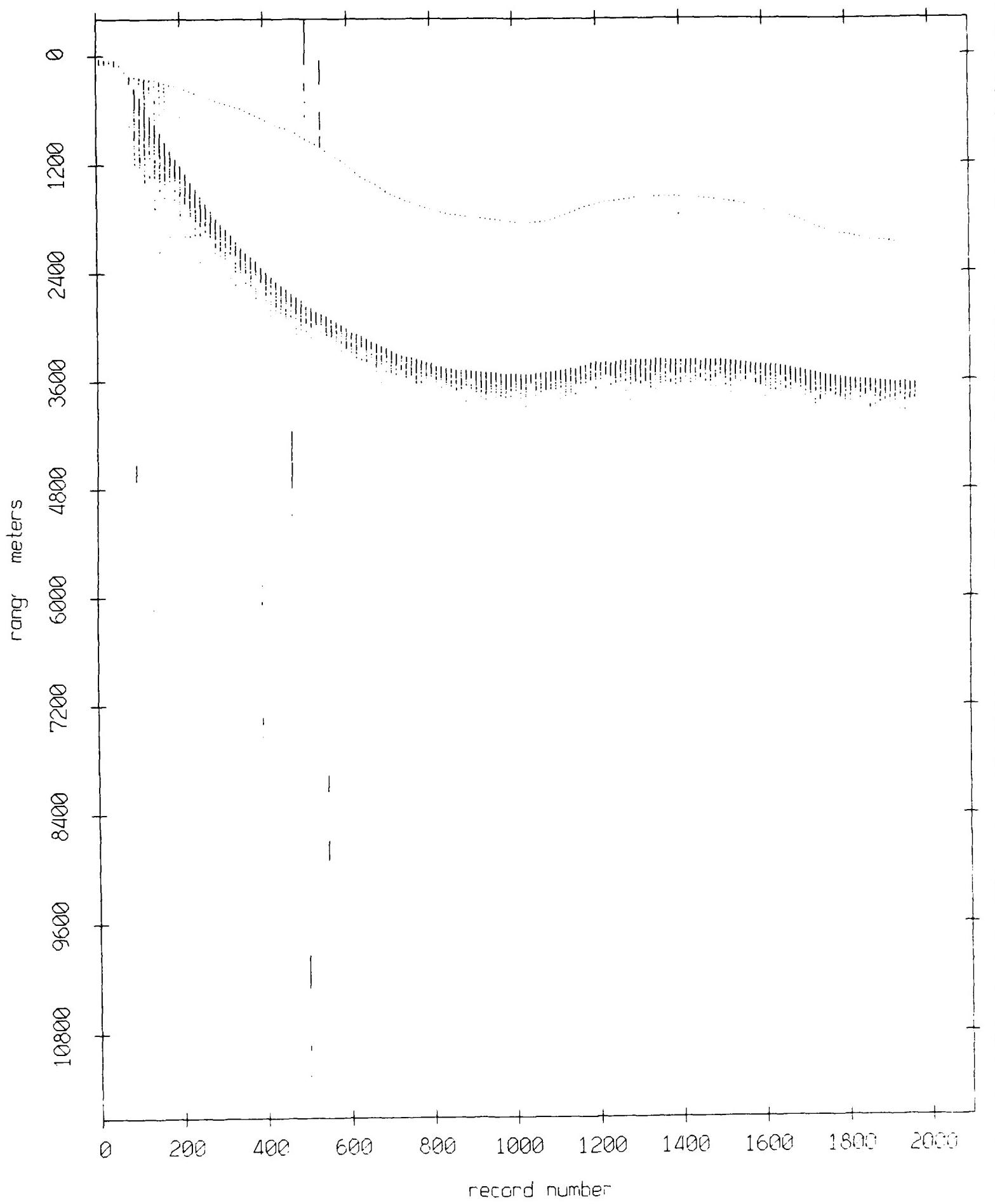


Figure VIII.2f

Float 2, September 1987 Sea Trip: range from float 8

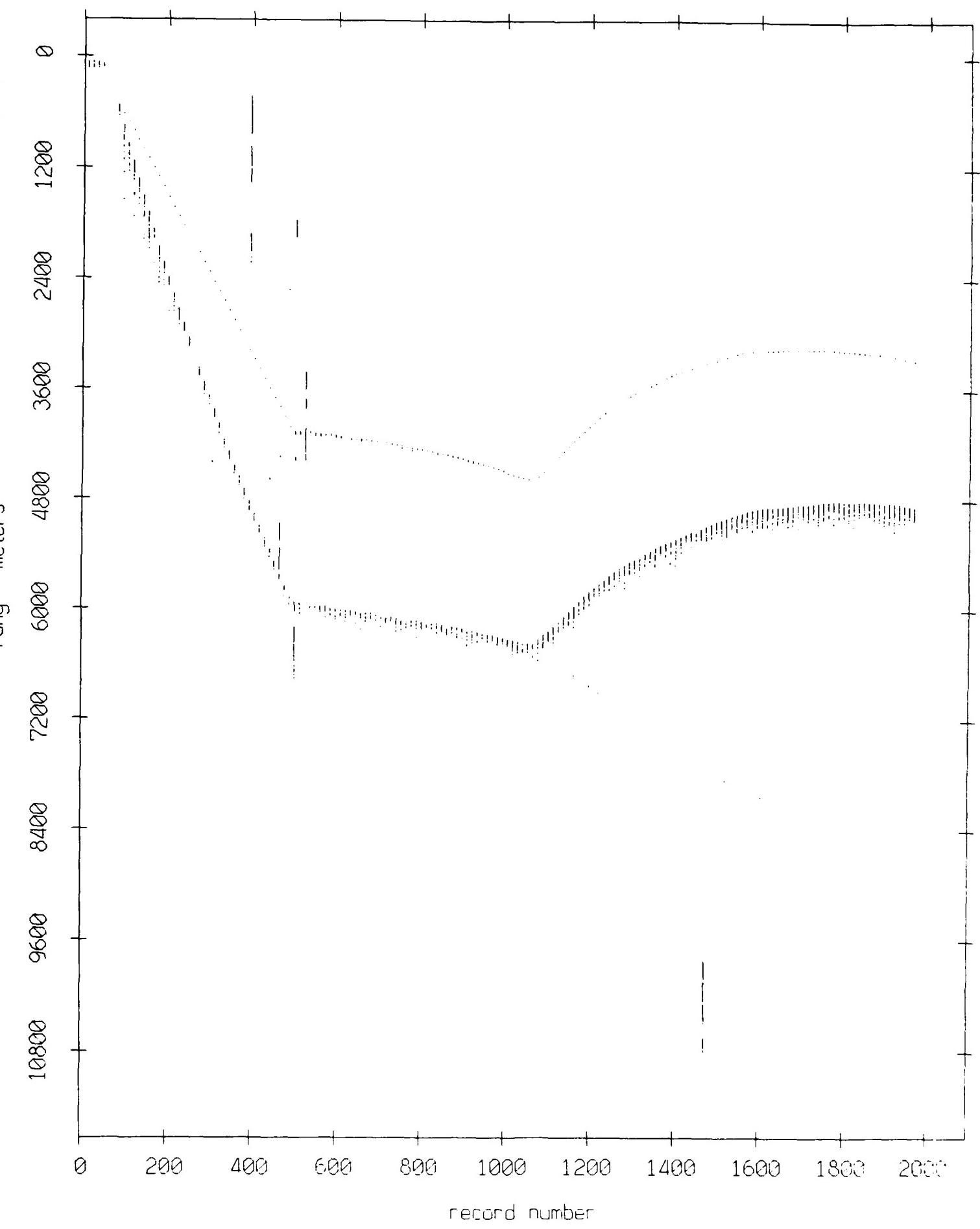


Figure VIII.2g

Float 2, September 1987 Sea Trip: range from float 9

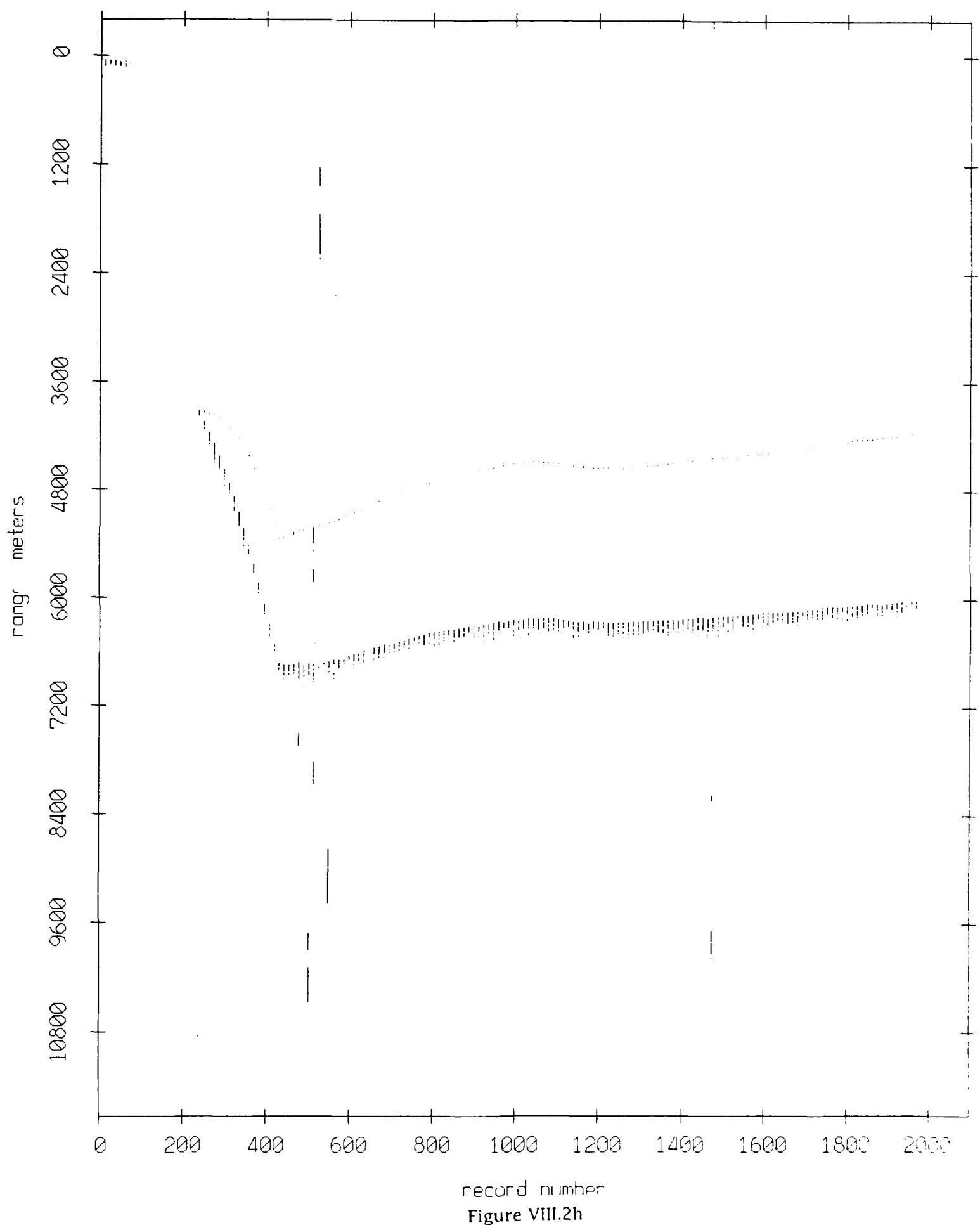
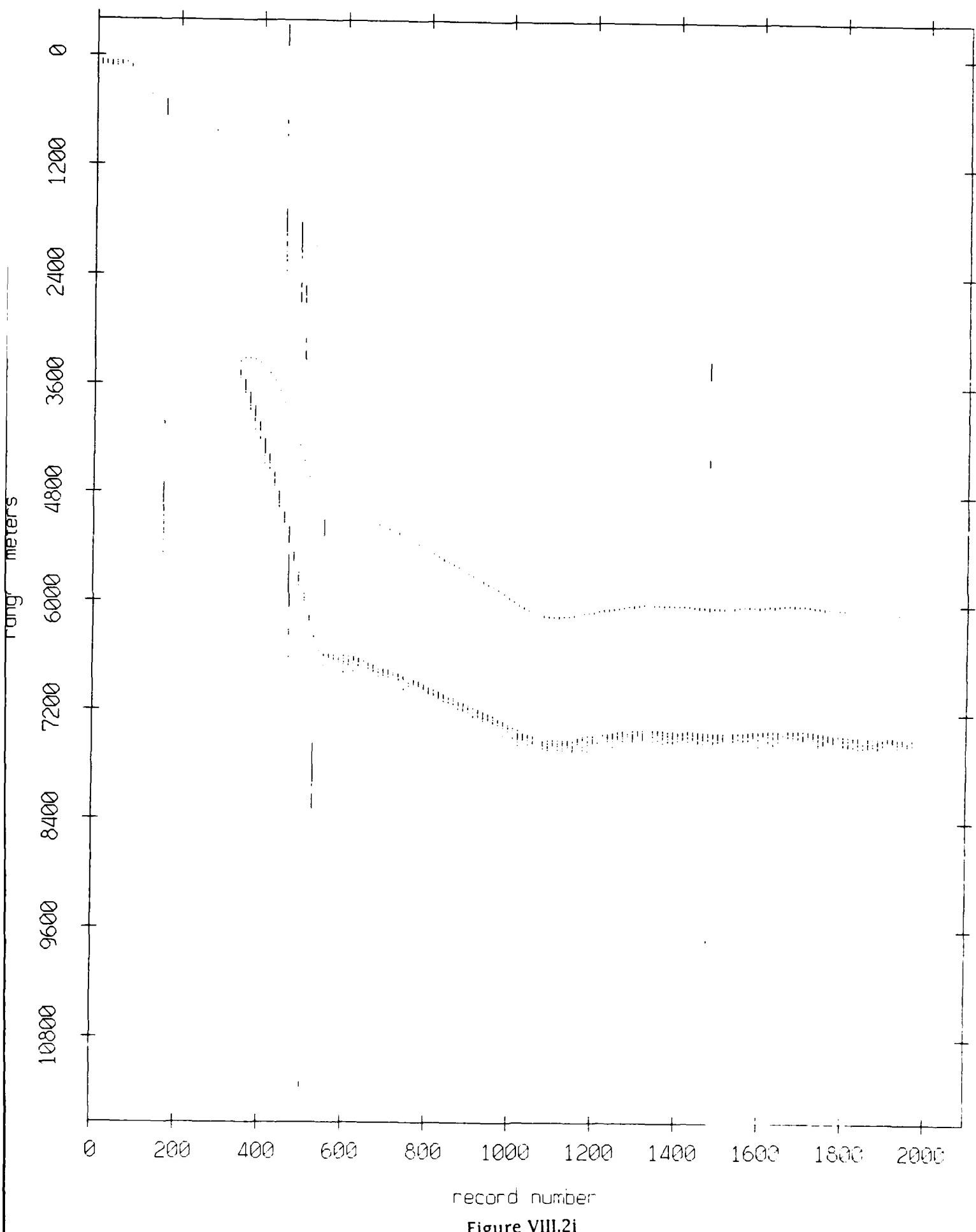


Figure VIII.2h

Float 2, September 1987 Sea Trip: range from float 10



record number

Figure VIII.2i

Float 2, September 1987 Sea Trip: range from float 11

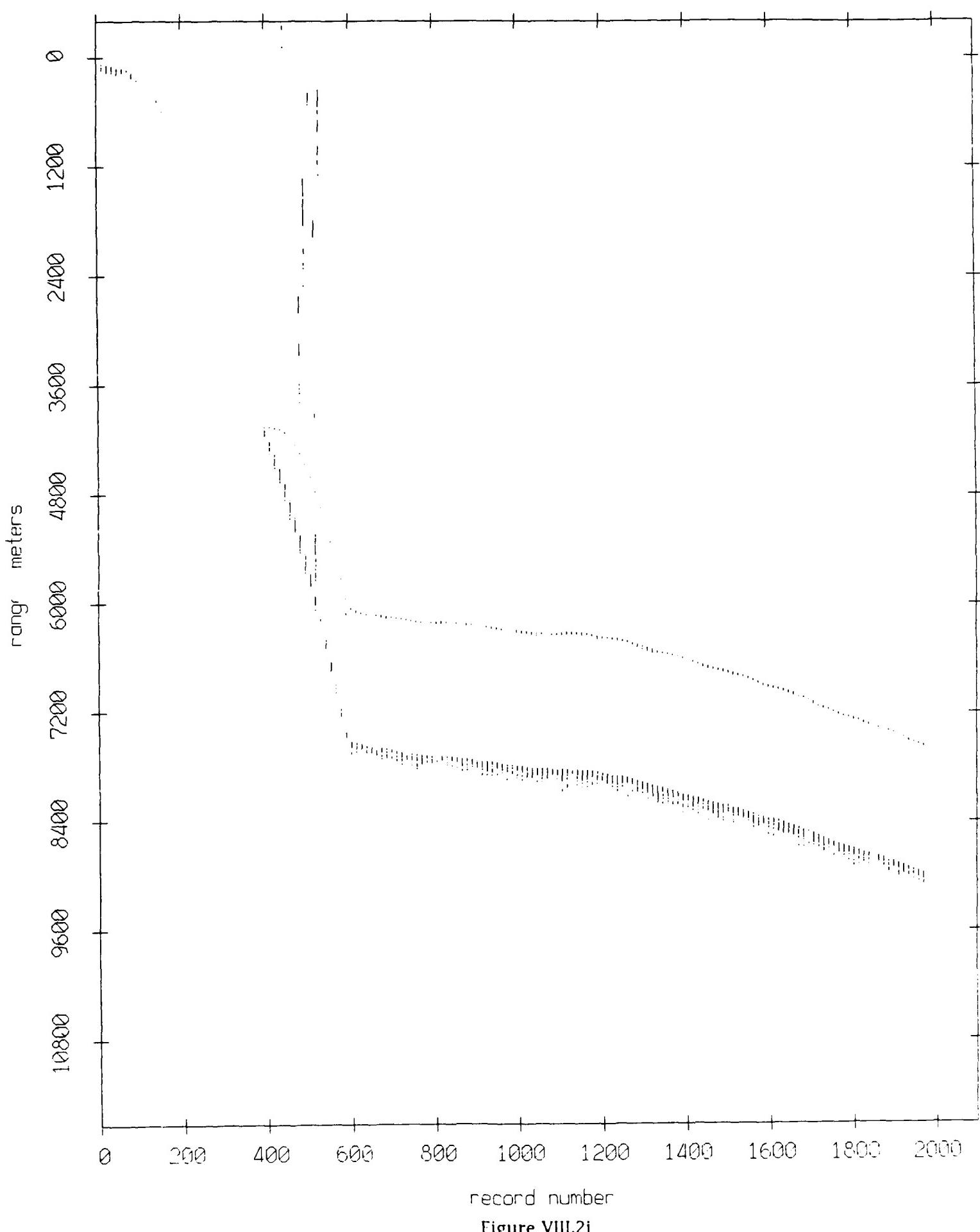


Figure VIII.2j

Float 3, September 1987 Sea Trip: range from float 0

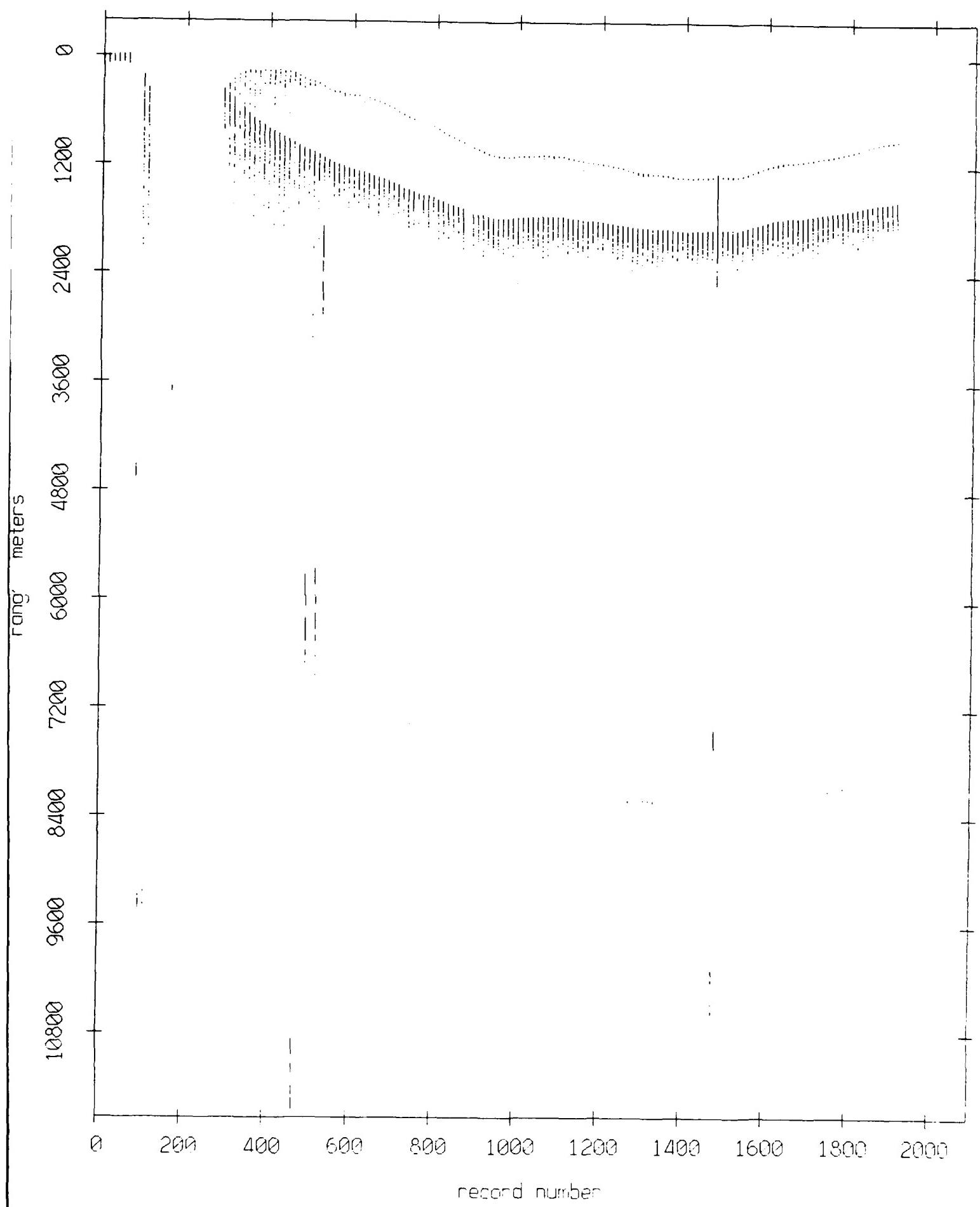


Figure VIII.3a

Float 3, September 1987 Sea Trip: range from float 2

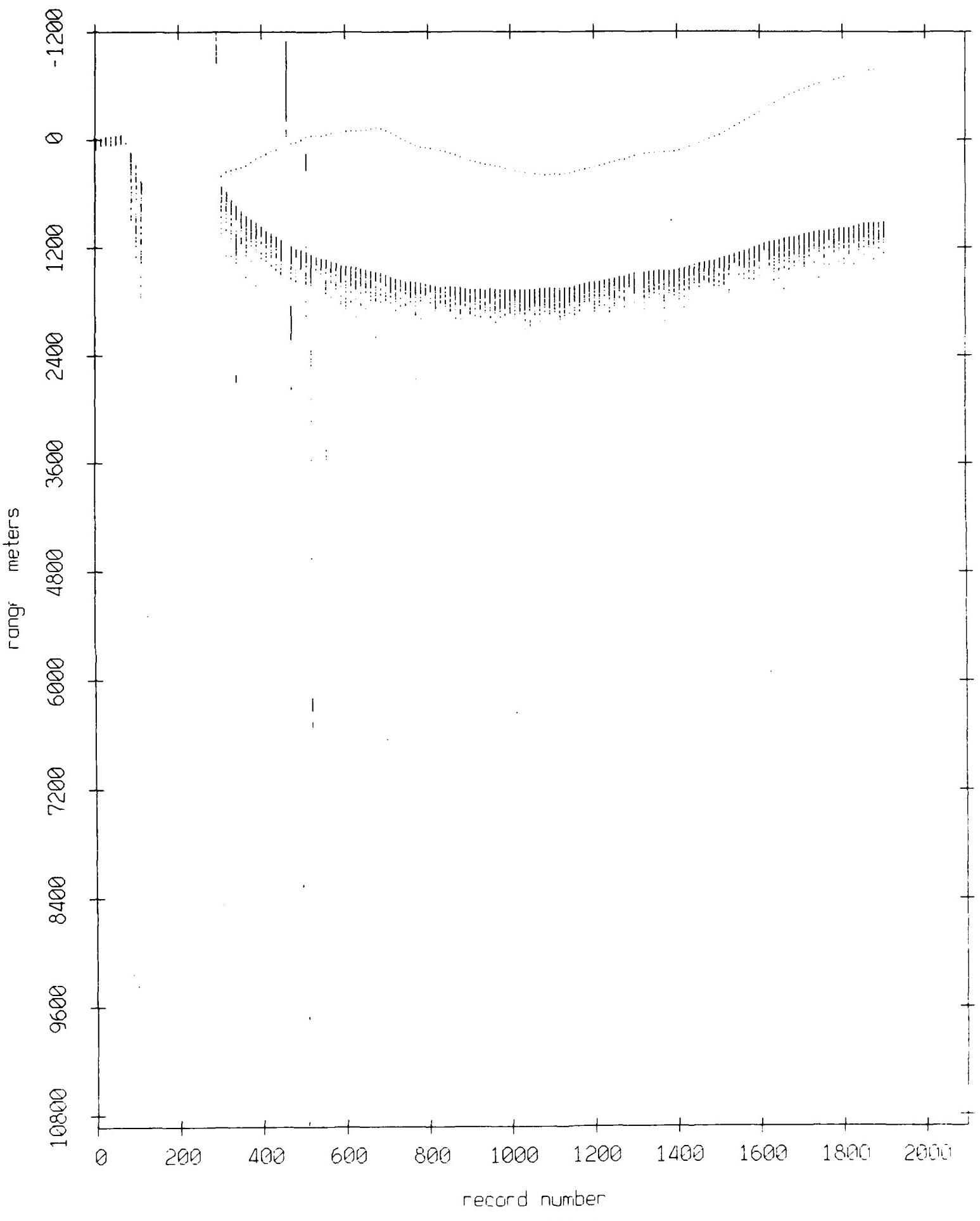


Figure VIII.3b

Float 3, September 1987 Sea Trip: range from float 4

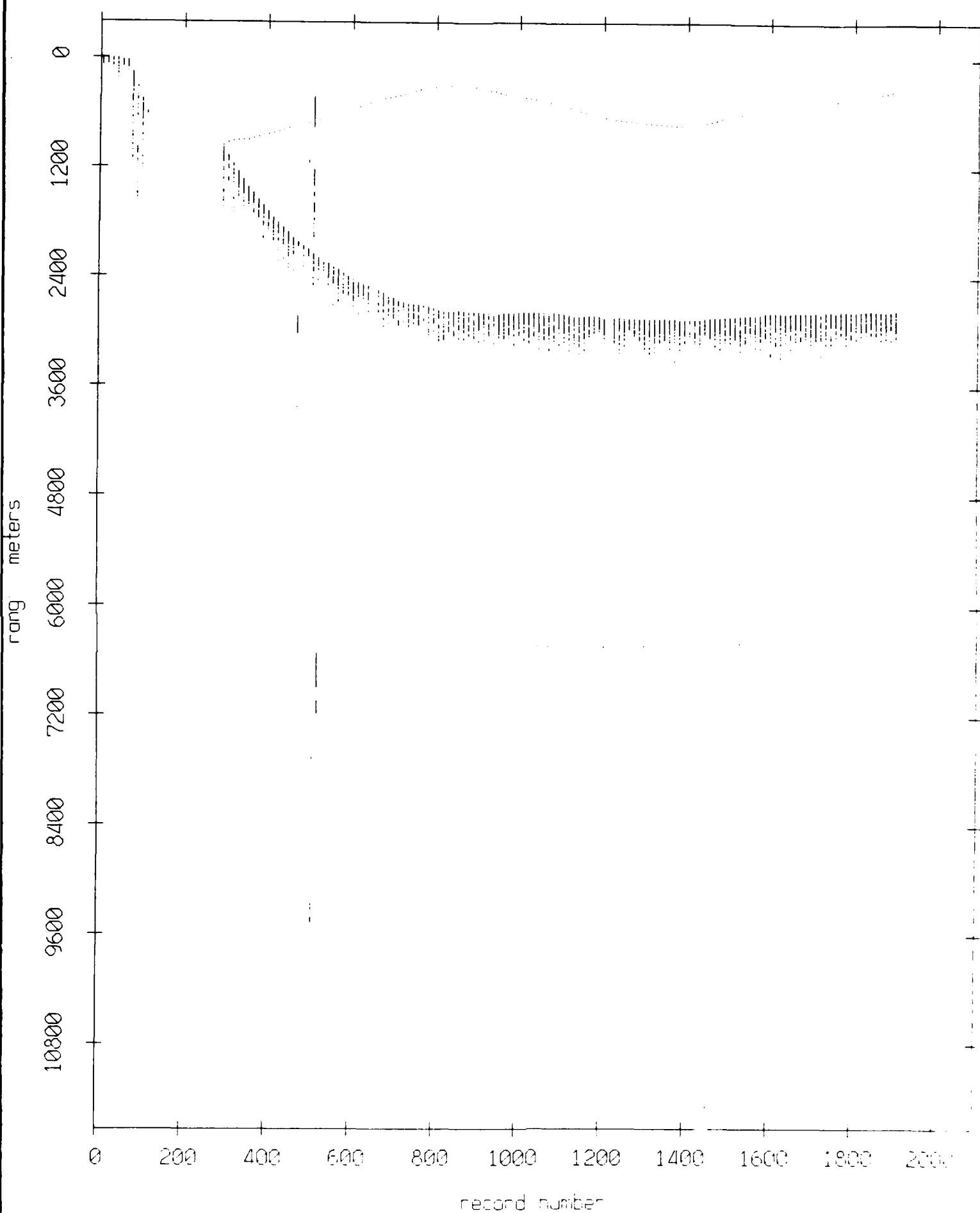


Figure VIII.3c

Float 3, September 1987 Sea Trip: range from float 5

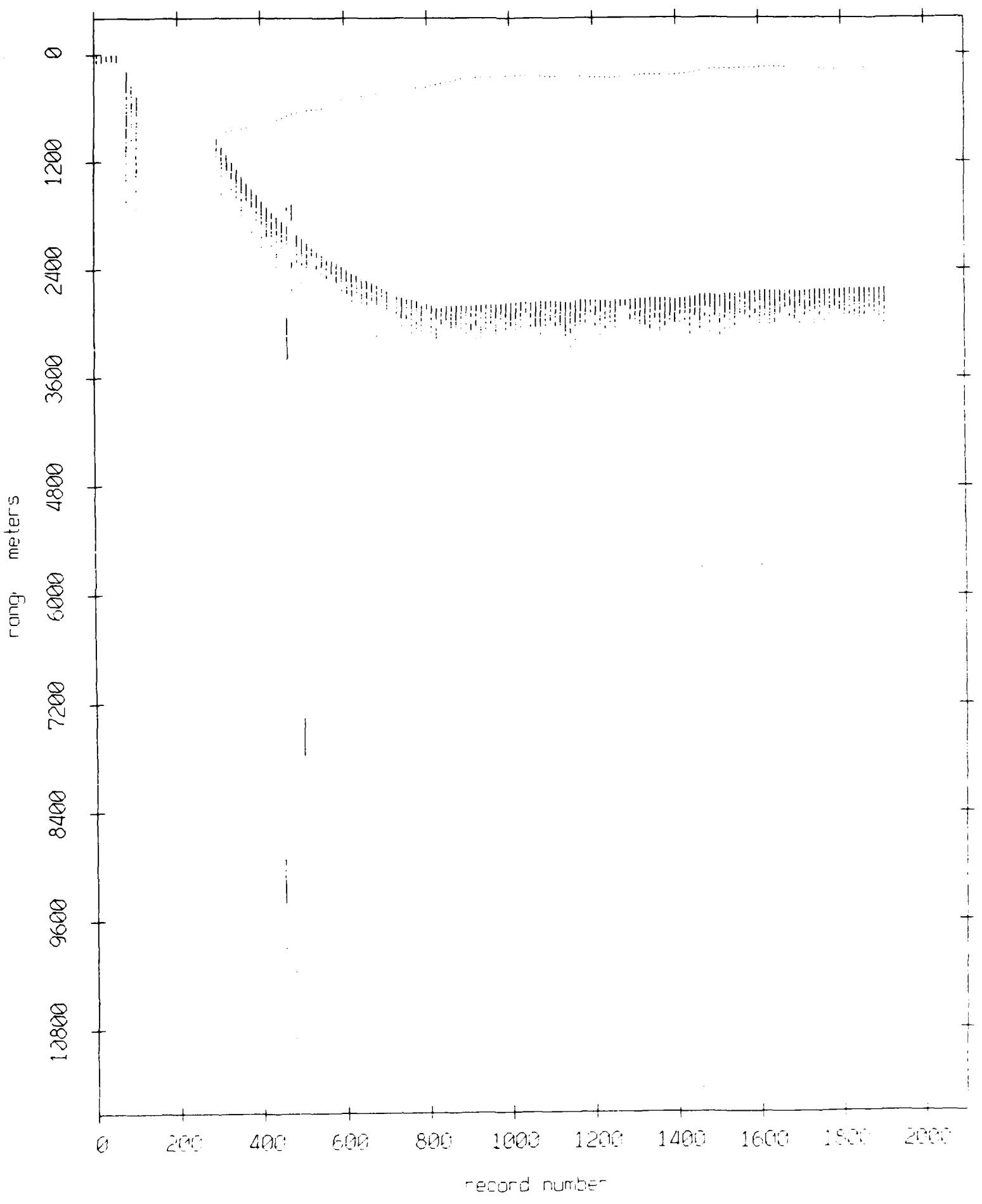


Figure VIII.3d

Float 3, September 1987 Sea Trip: range from float 6

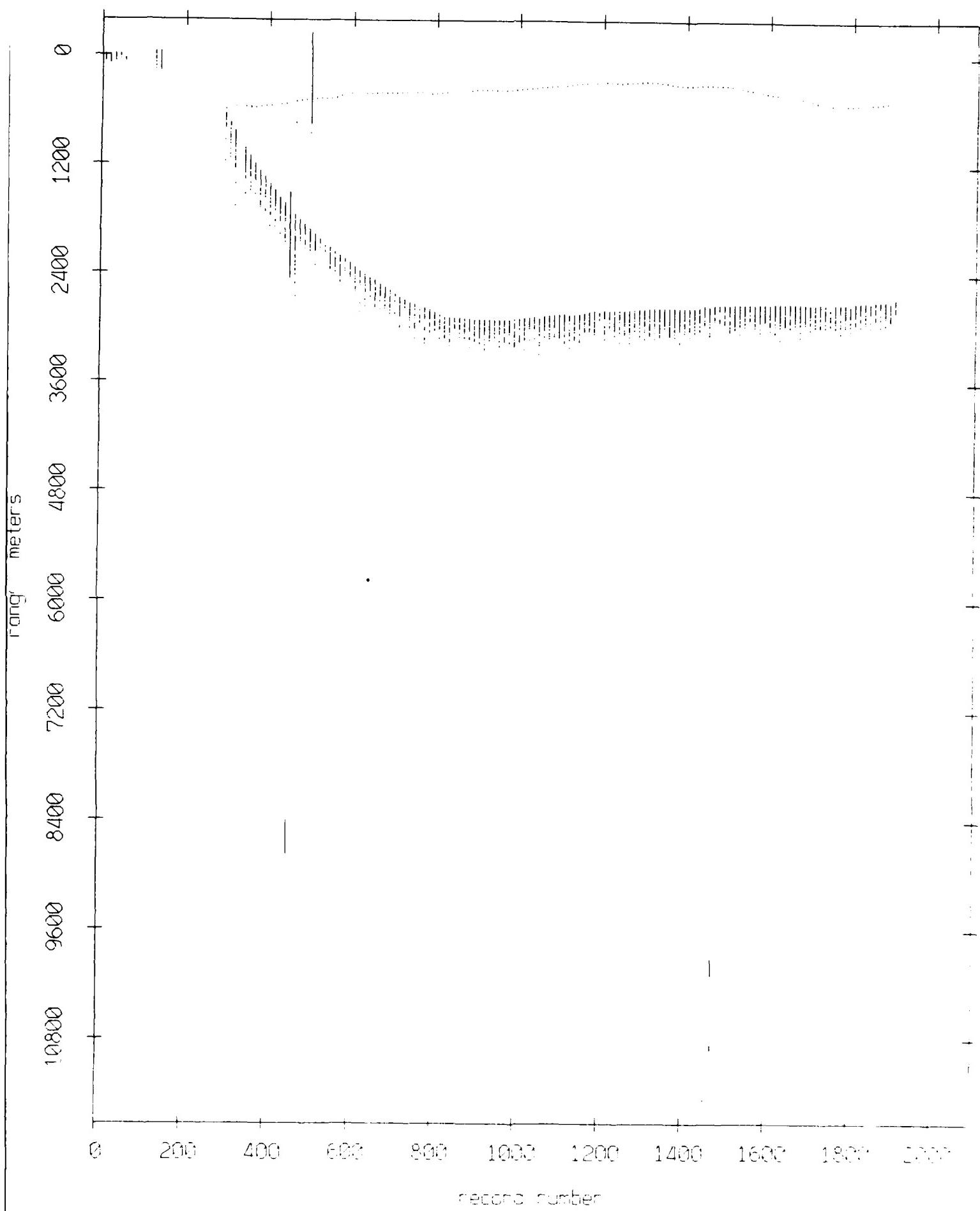
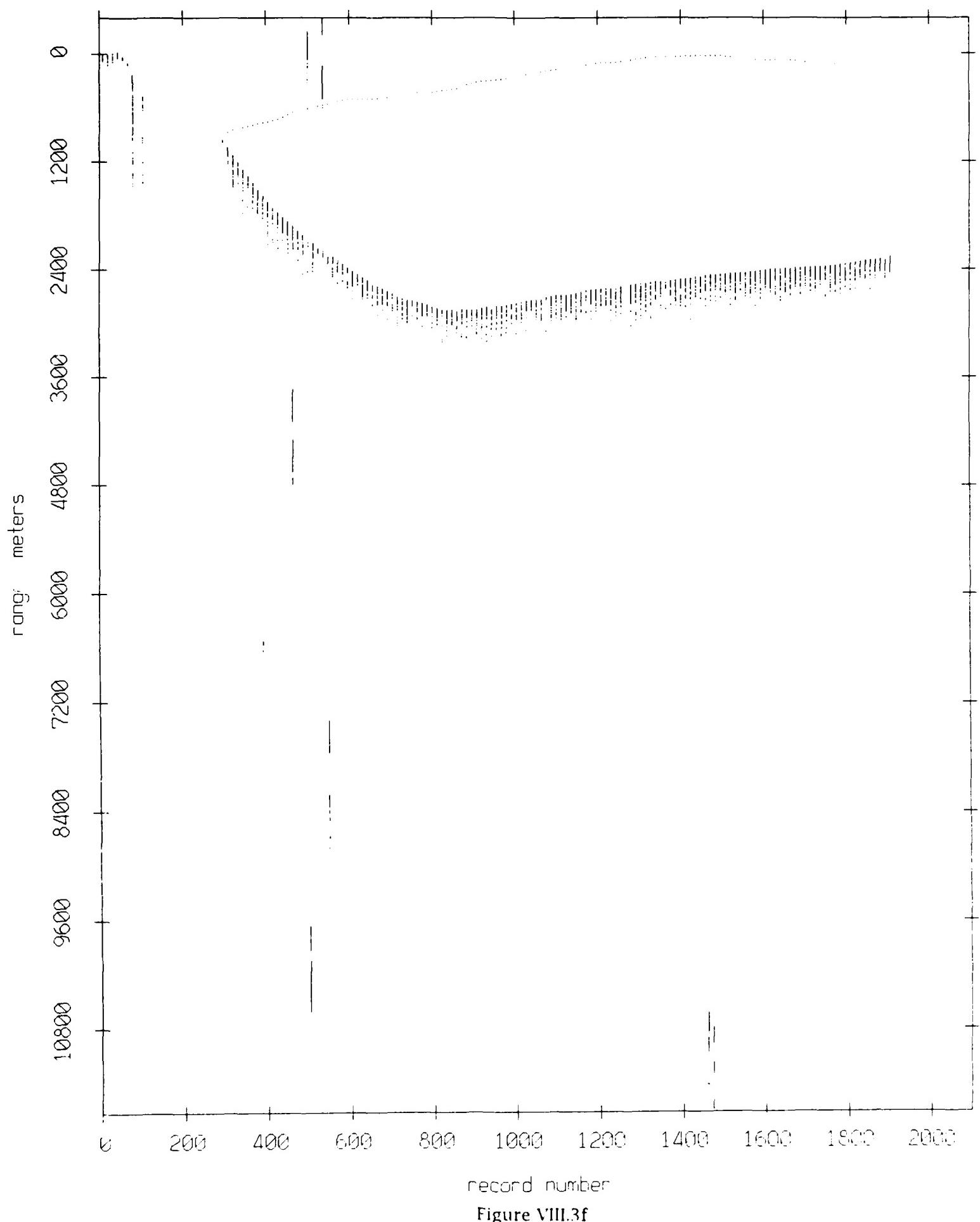


Figure VIII.3e

Float 3, September 1987 Sea Trip: range from float 7



record number

Figure VIII.3f

Float 3, September 1987 Sea Trip: range from float 8

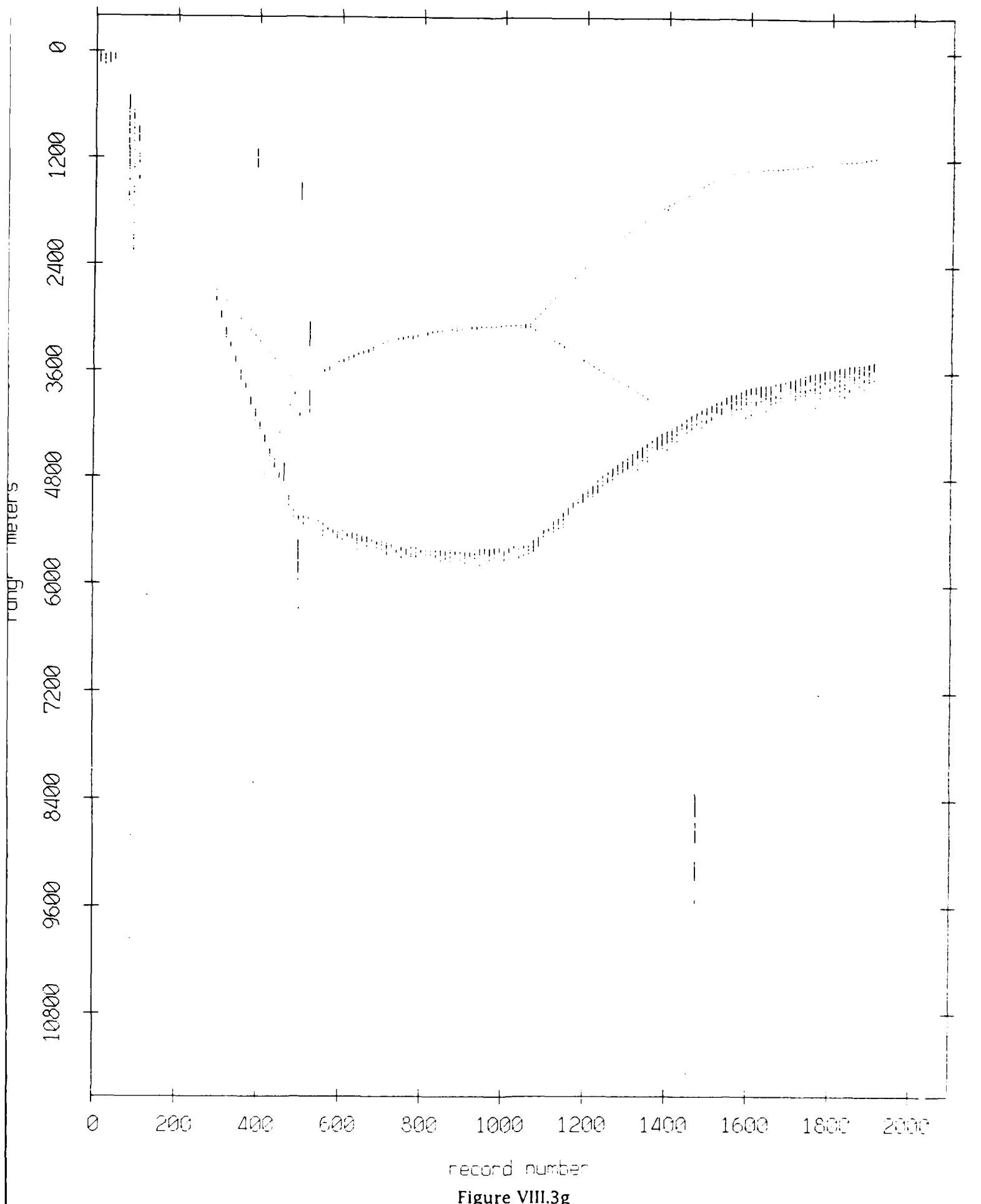


Figure VIII.3g

Float 3, September 1987 Sea Trip: range from float 9

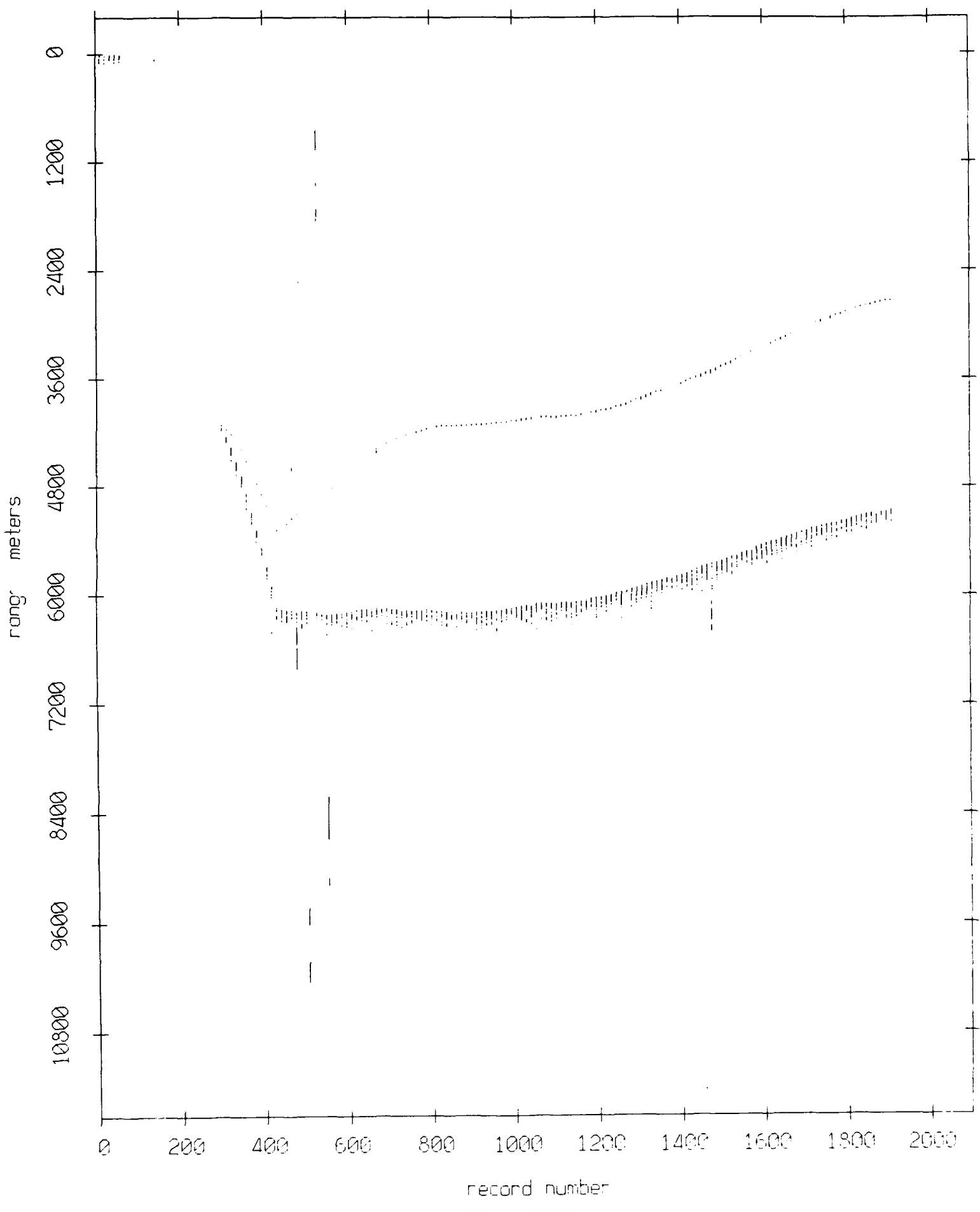


Figure VIII.3h

Float 3, September 1987 Sea Trip: range from float 10

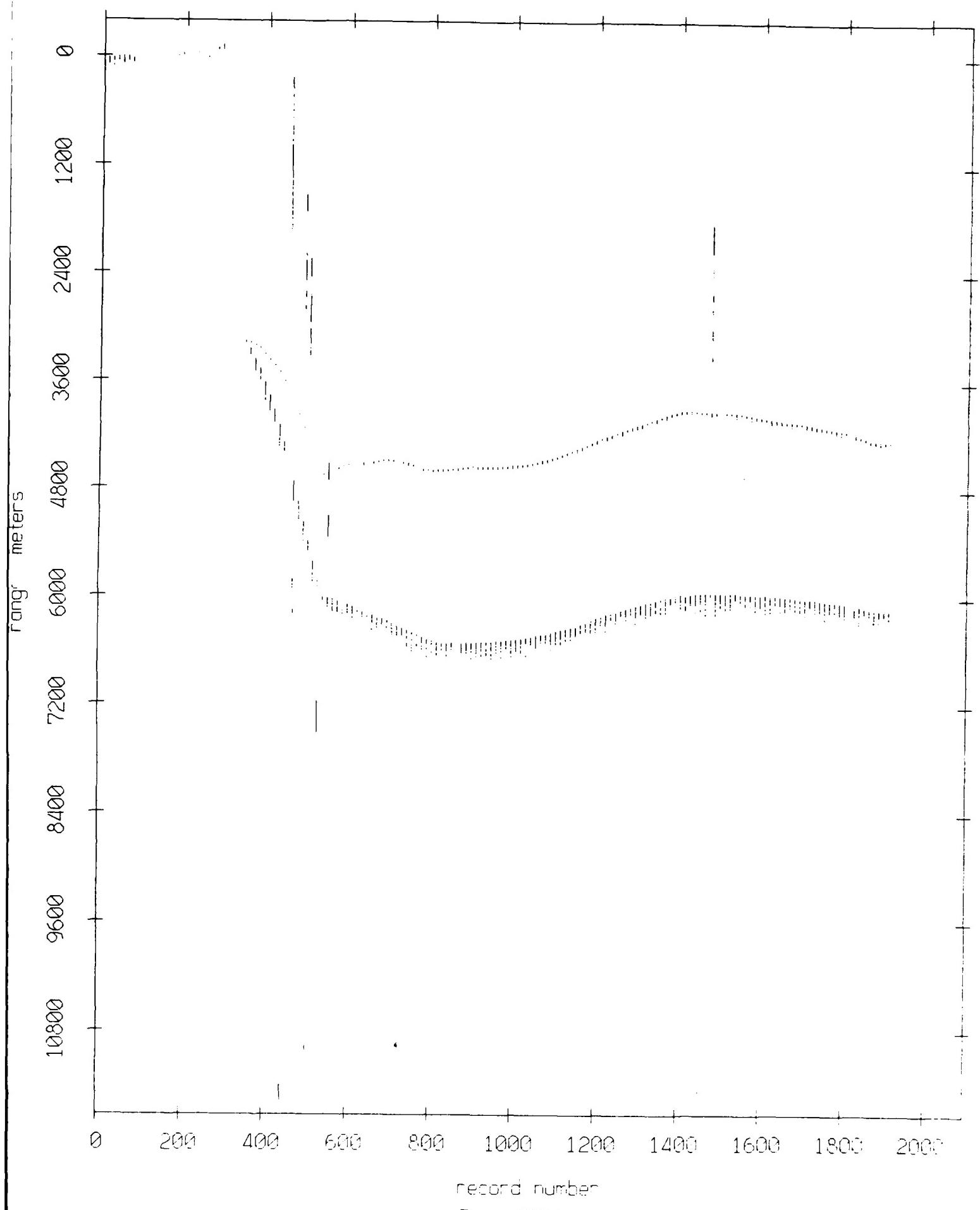


Figure VIII.3i

Float 3, September 1987 Sea Trip: range from float 11

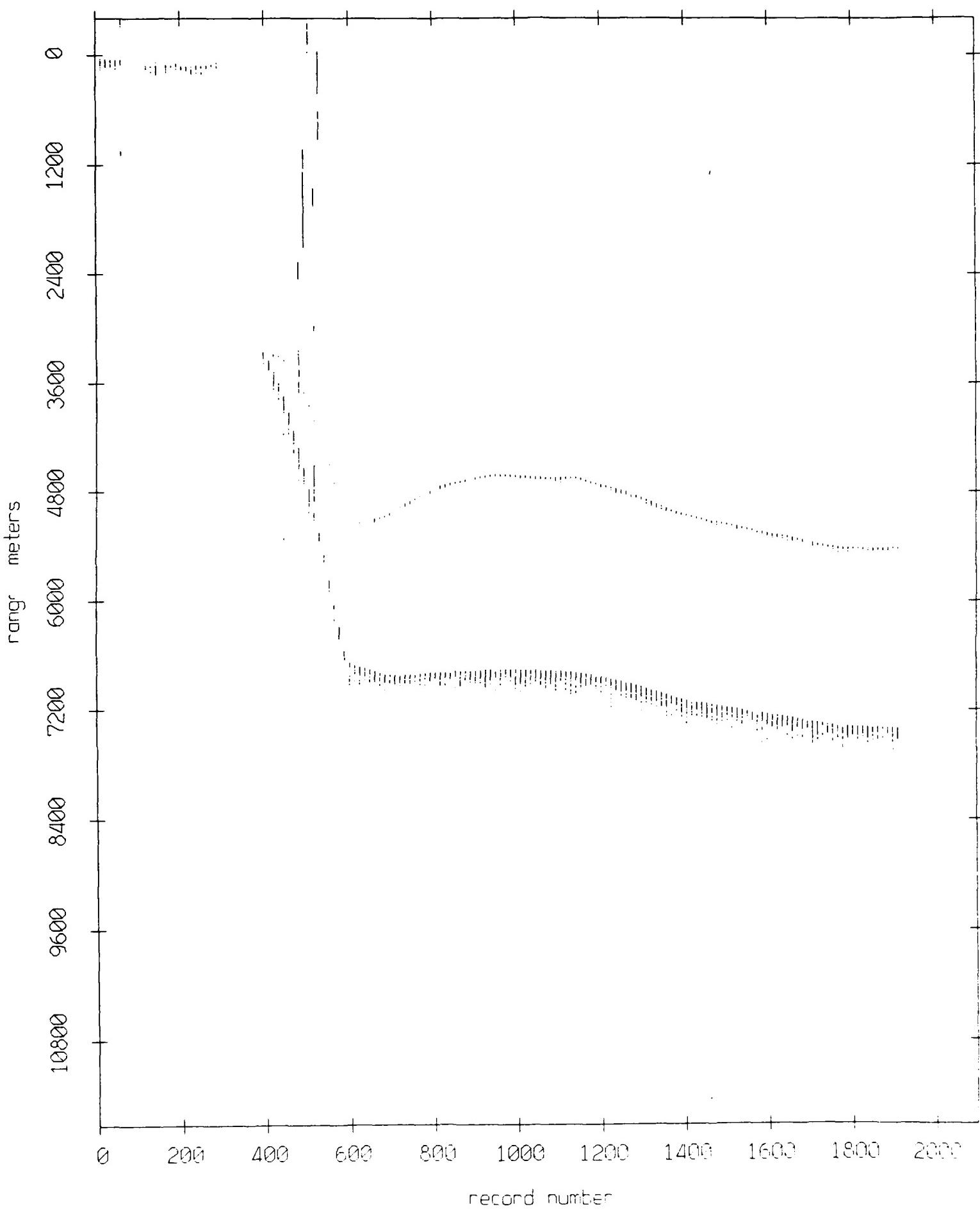


Figure VIII.3j

Float 4, September 1987 Sea Trip: range from float 0

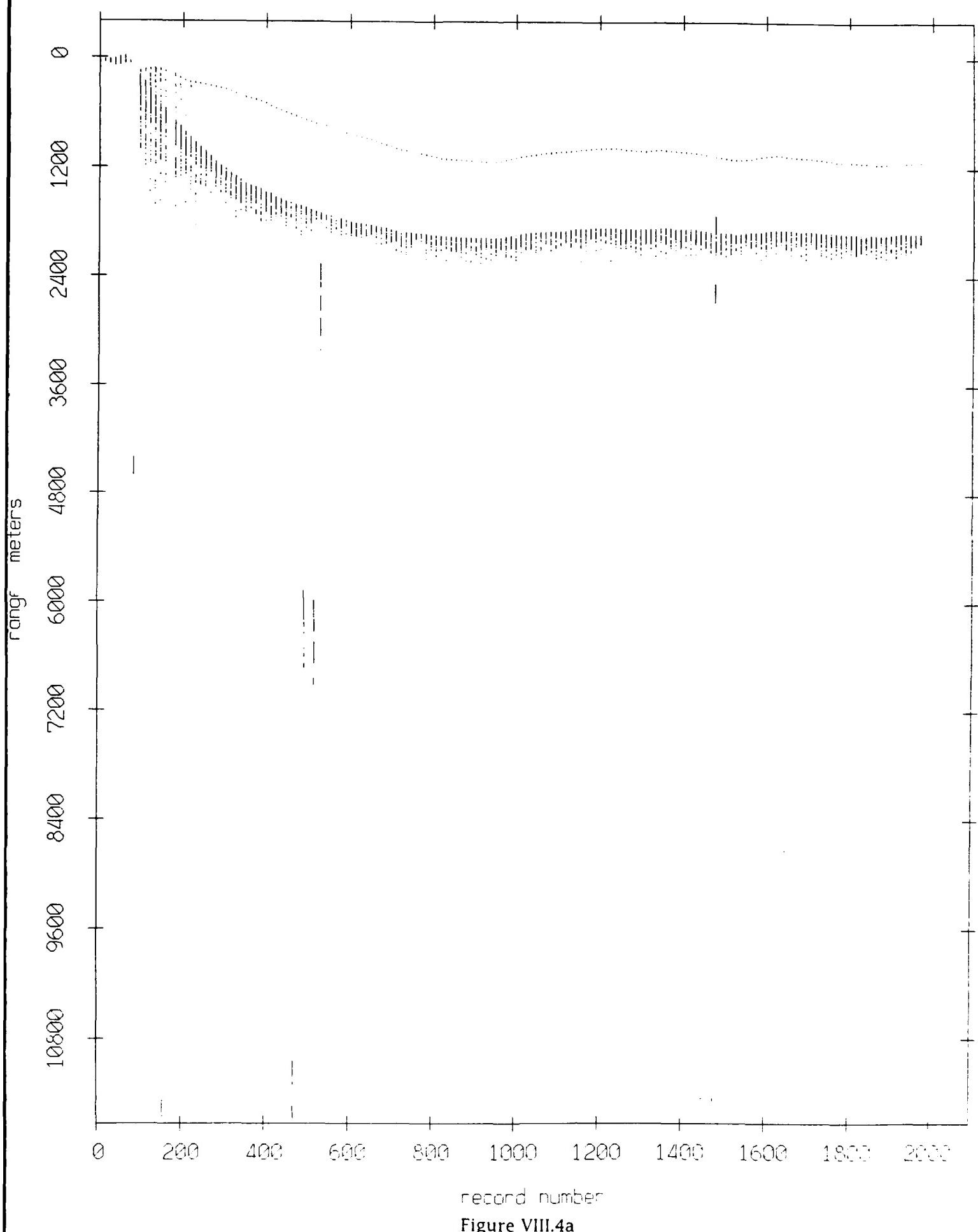
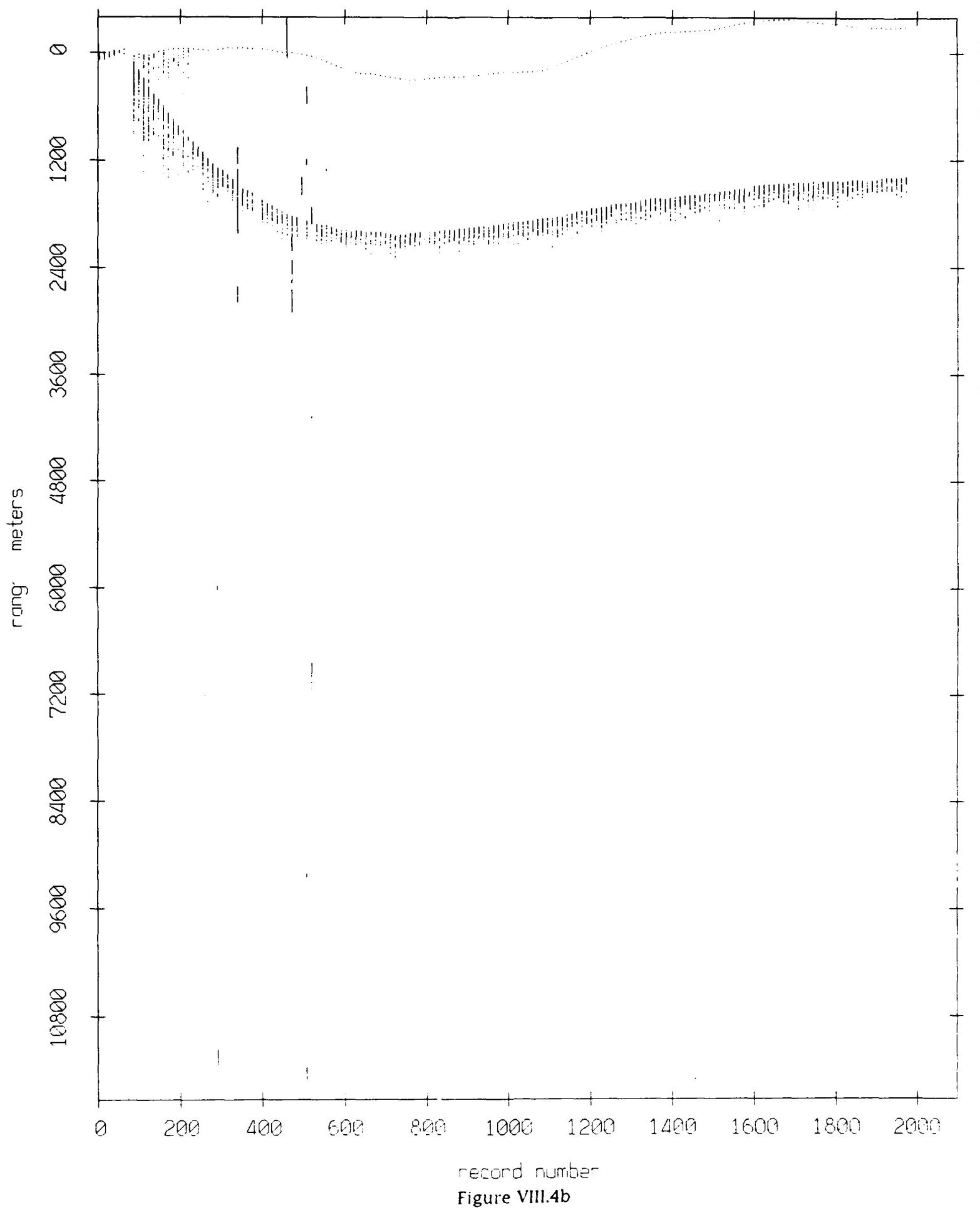


Figure VIII.4a

Float 4, September 1987 Sea Trip: range from float 2



Float 4, September 1987 Sea Trip: range from float 3

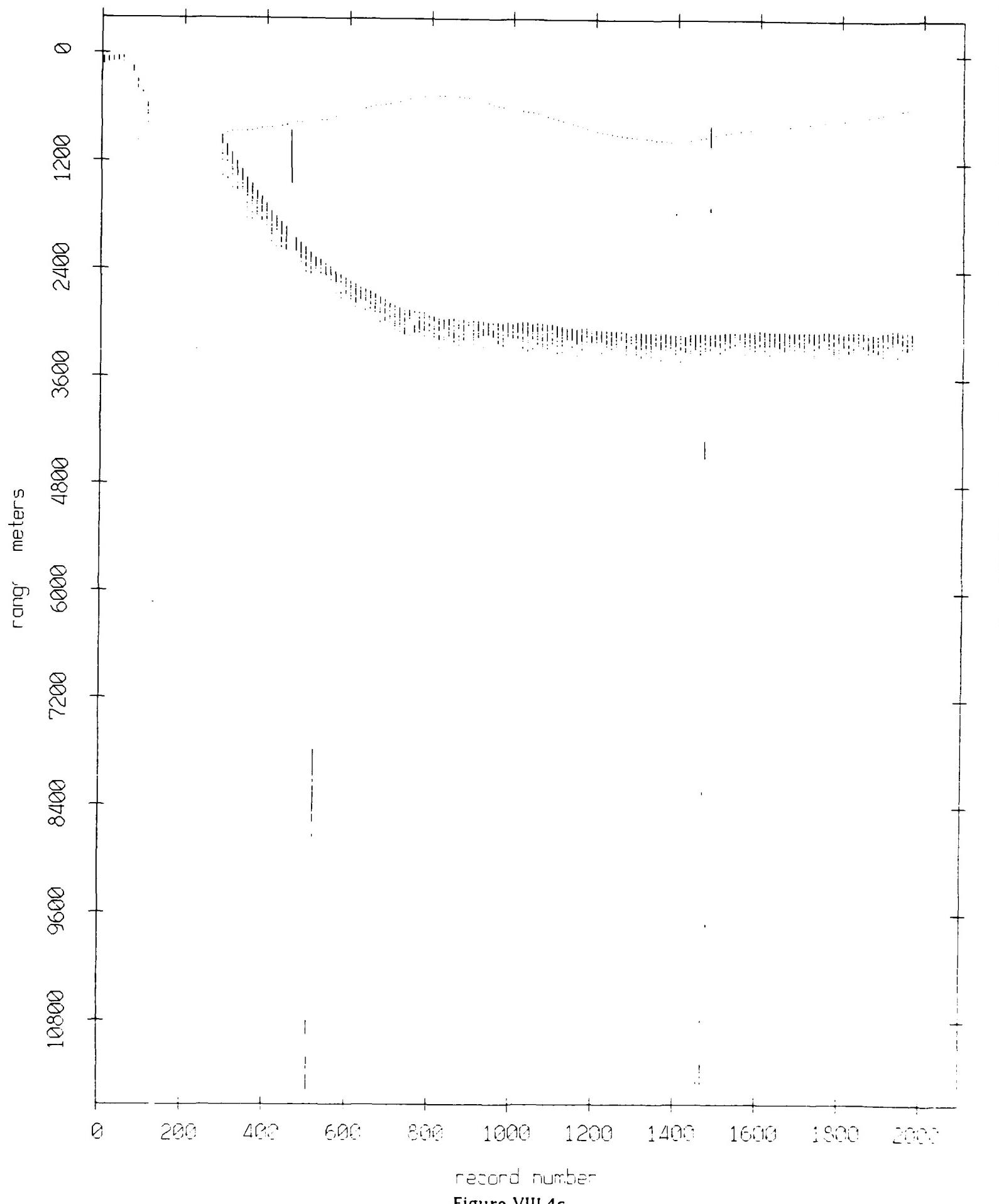


Figure VIII.4c

Float 4, September 1987 Sea Trip: range from float 5

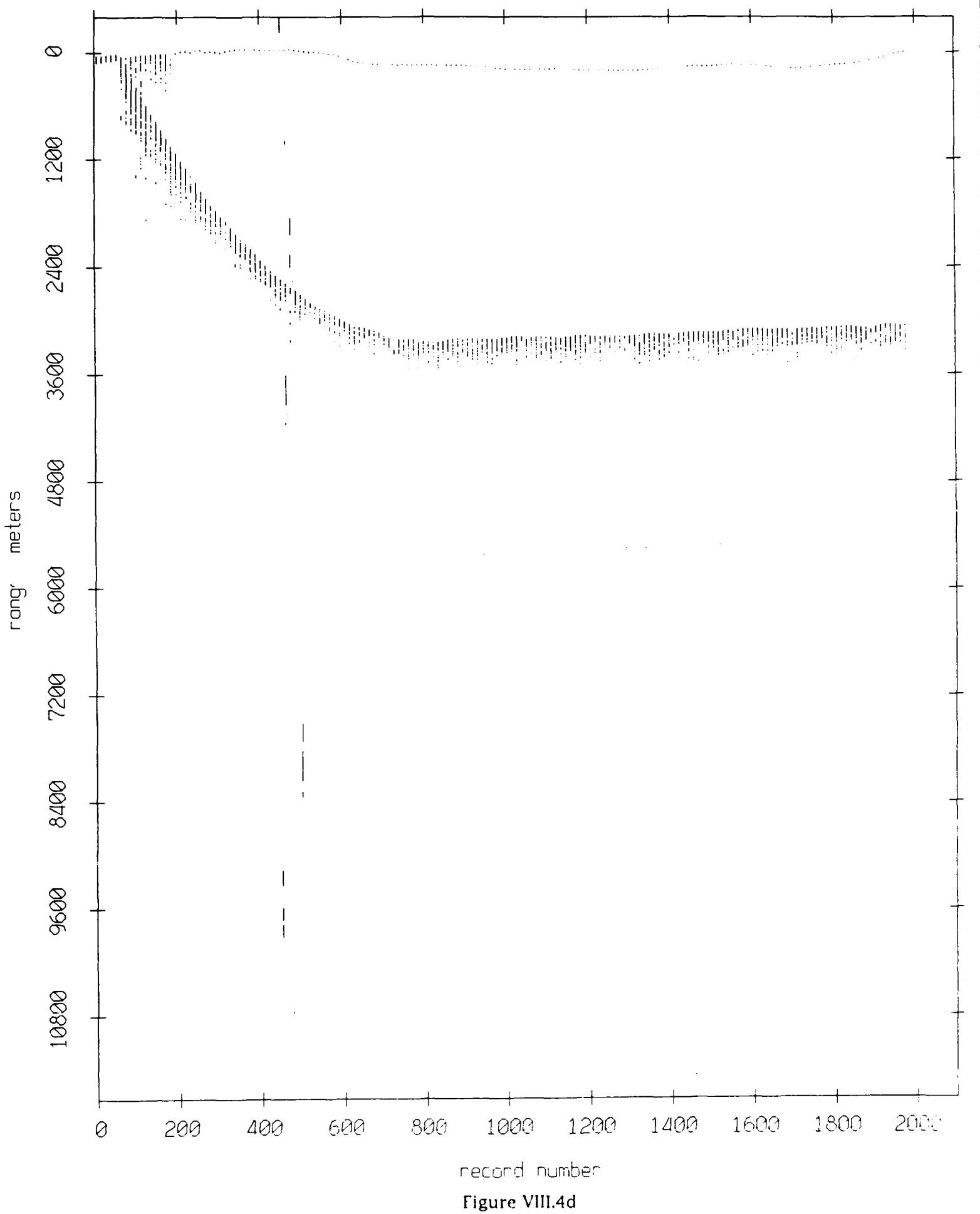


Figure VIII.4d

Float 4, September 1987 Sea Trip: range from float 6

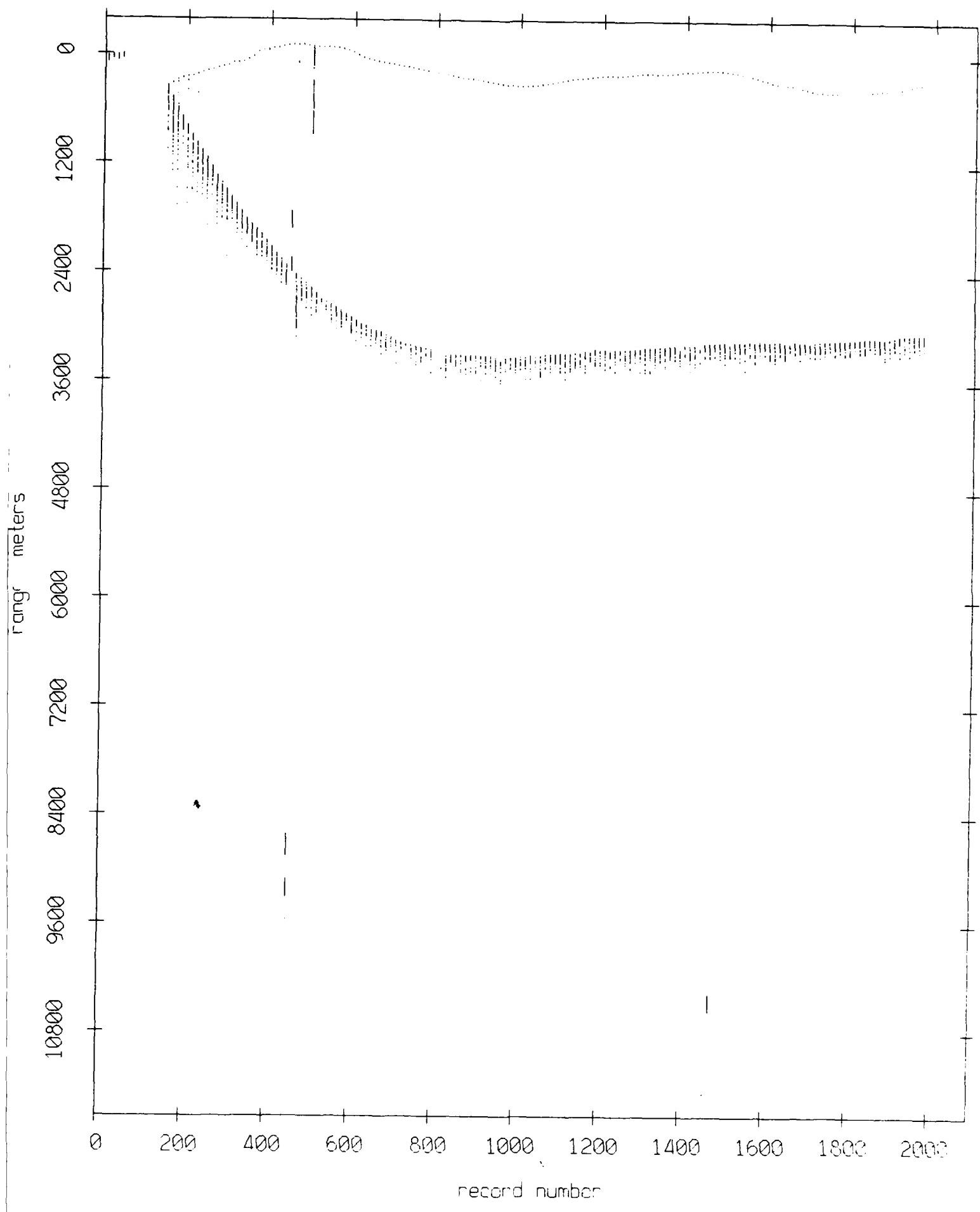


Figure VIII.4e

Float 4, September 1987 Sea Trip: range from float 7

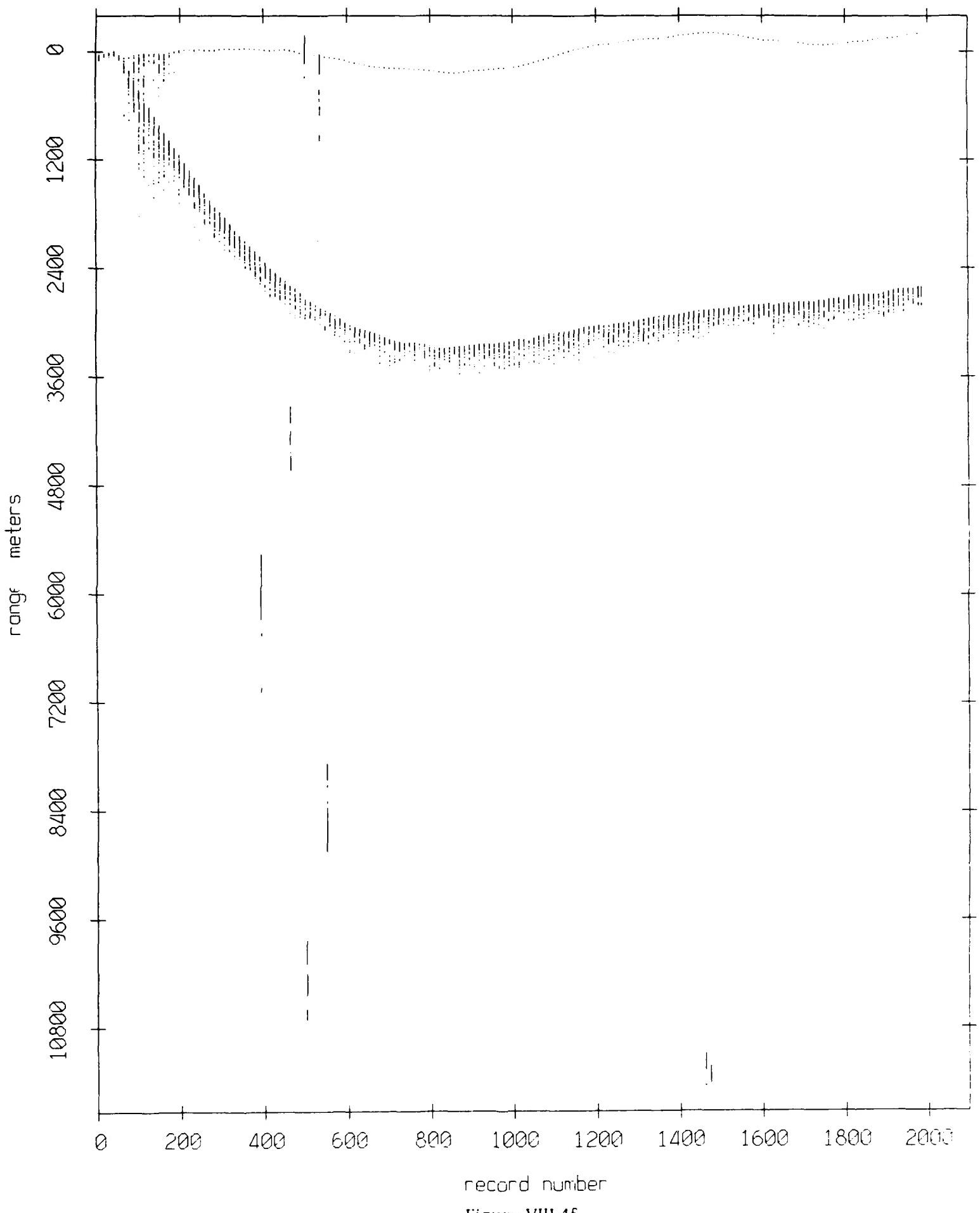


Figure VIII.4f

Float 4, September 1987 Sea Trip: range from float 8

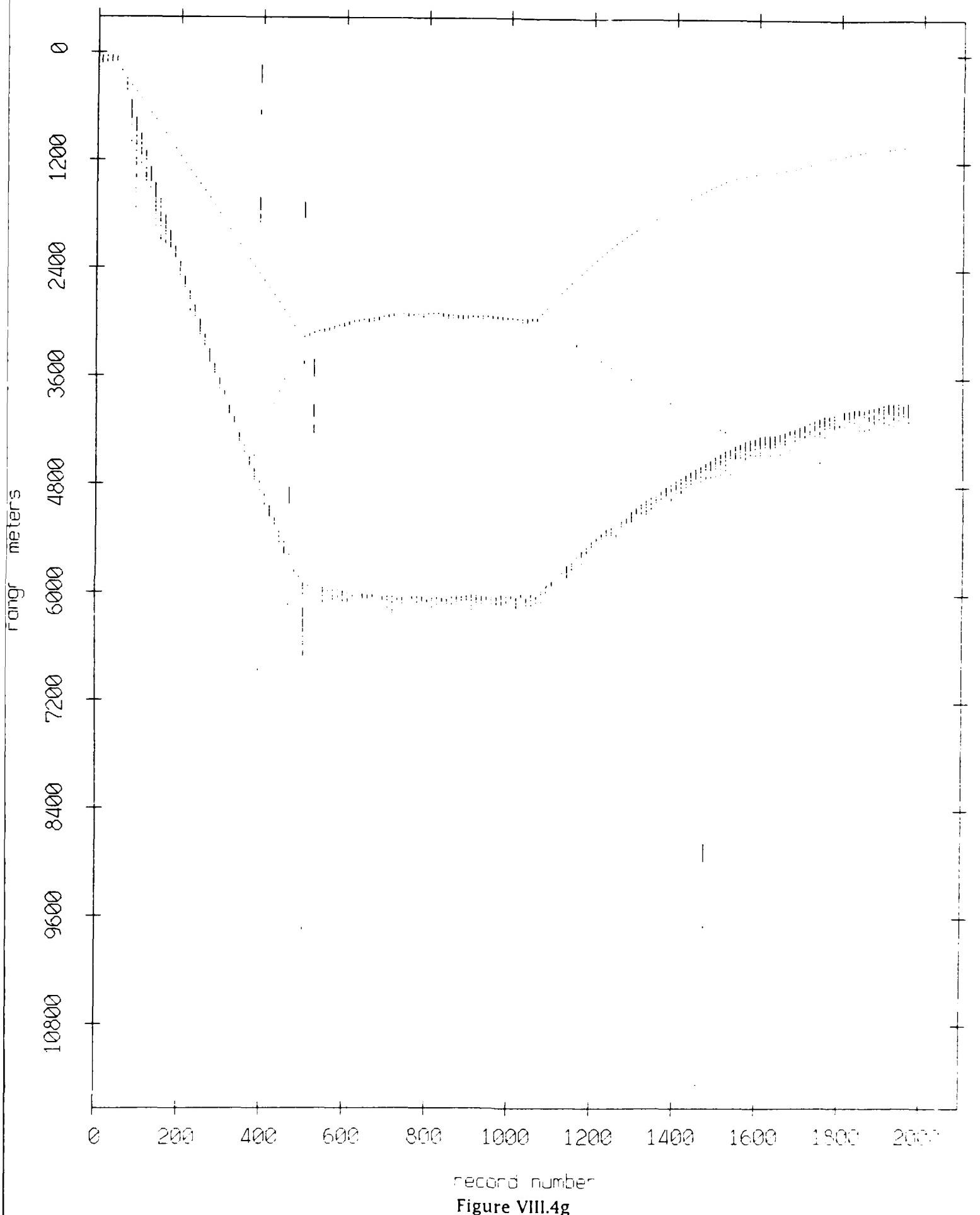


Figure VIII.4g

Float 4, September 1987 Sea Trip: range from float 9

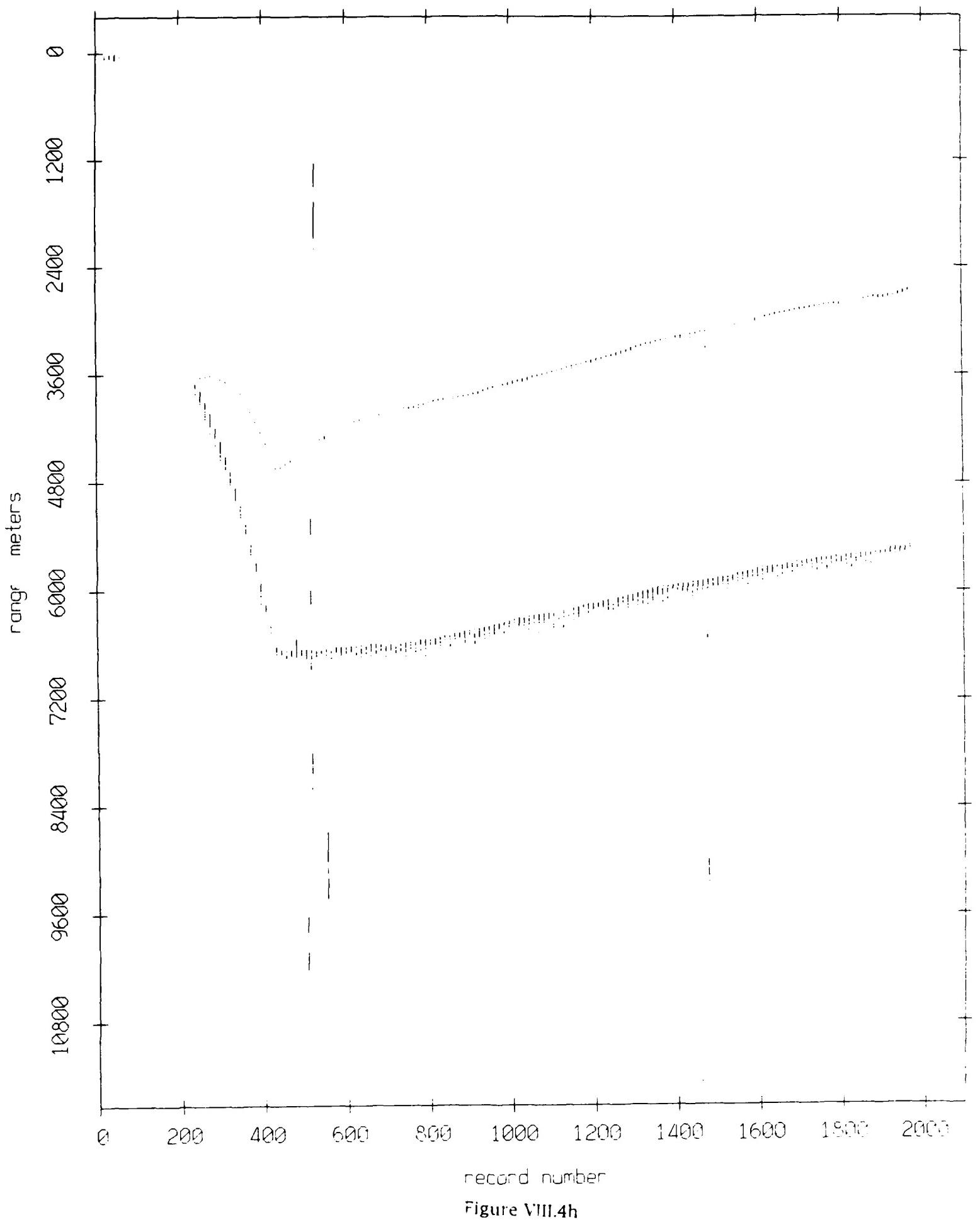


Figure VIII.4h

Float 4, September 1987 Sea Trip: range from float 10

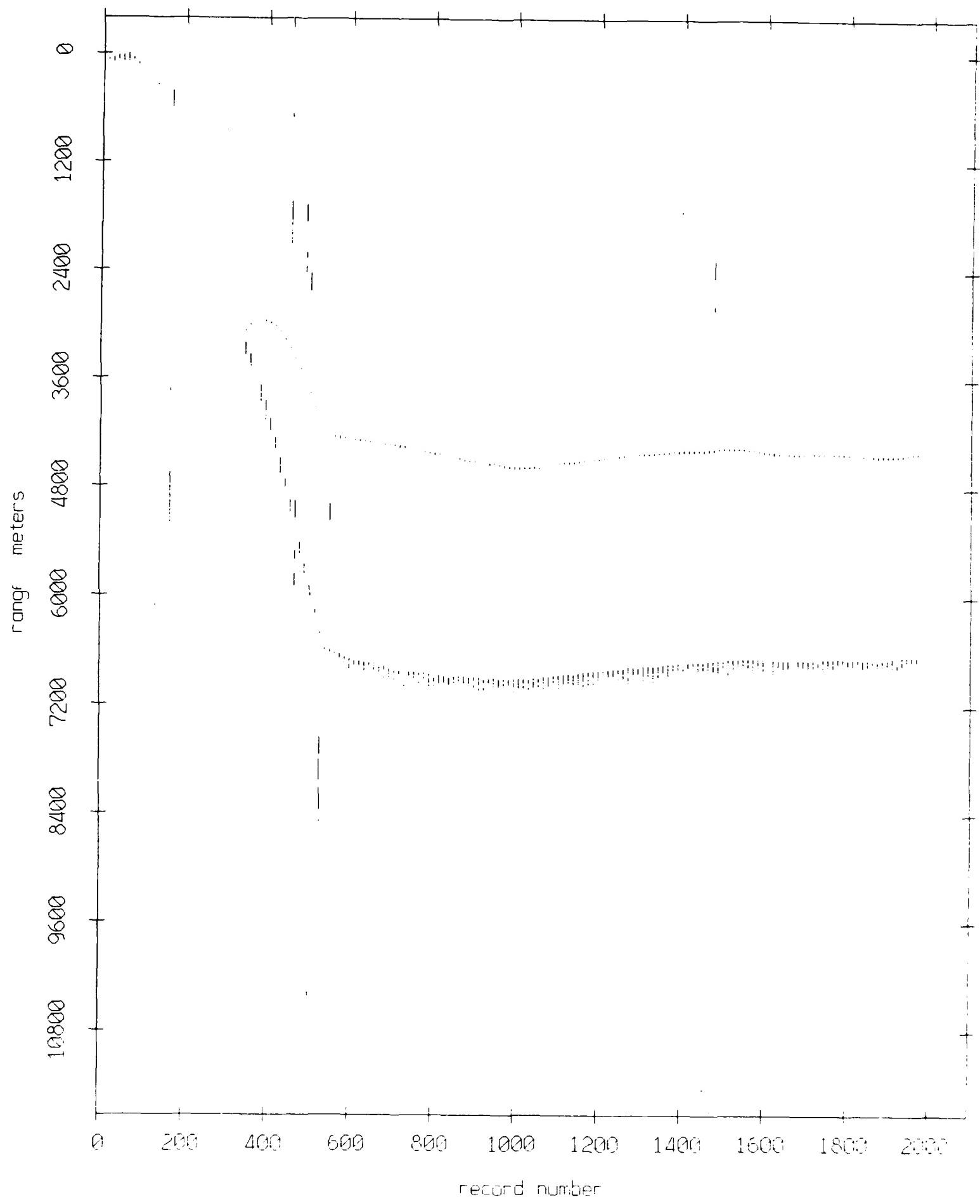
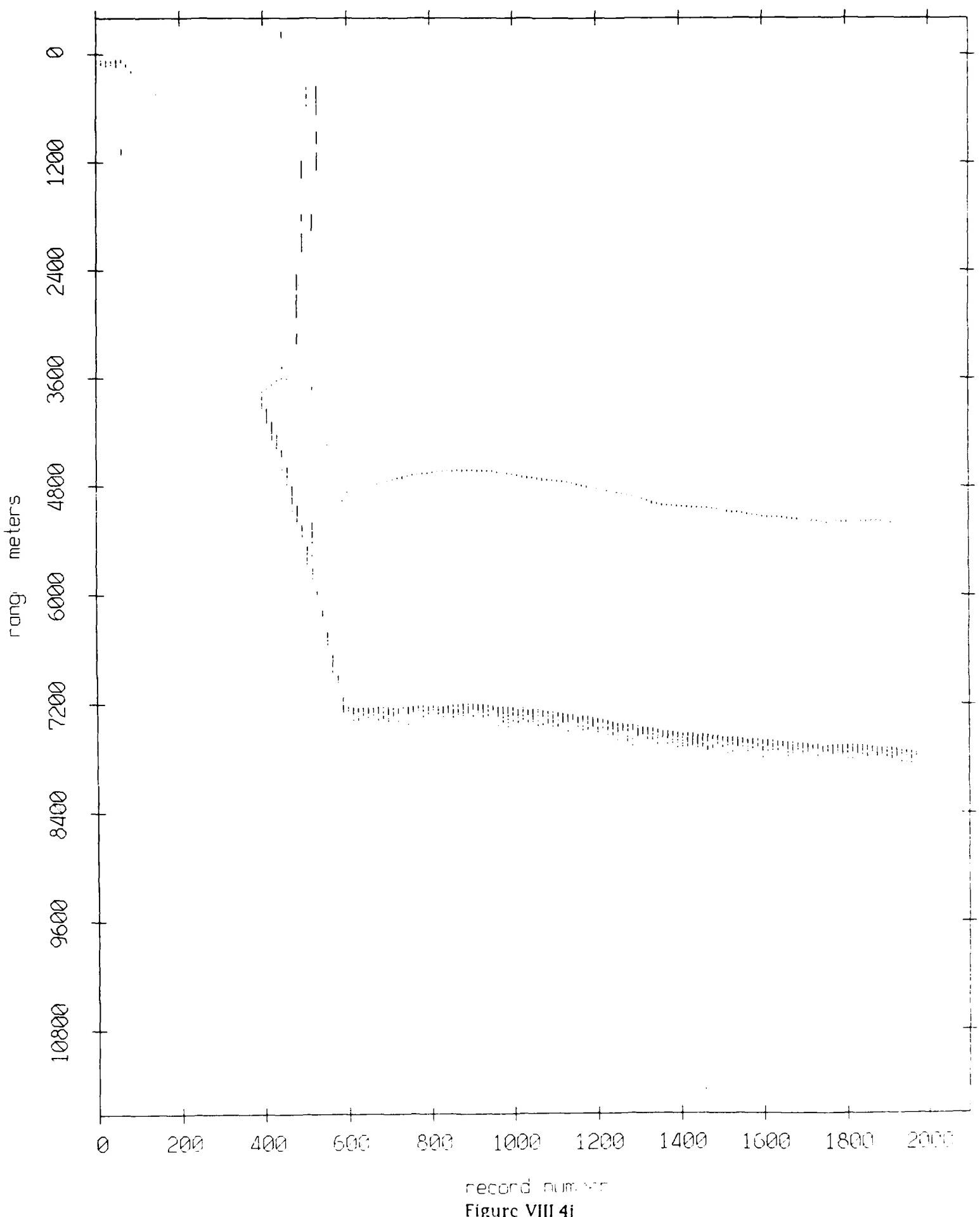


Figure VIII.4i

Float 4, September 1987 Sea Trip: range from float 11



record num 115

Figure VIII 4j

Float 5, September 1987 Sea Trip: range from float 0

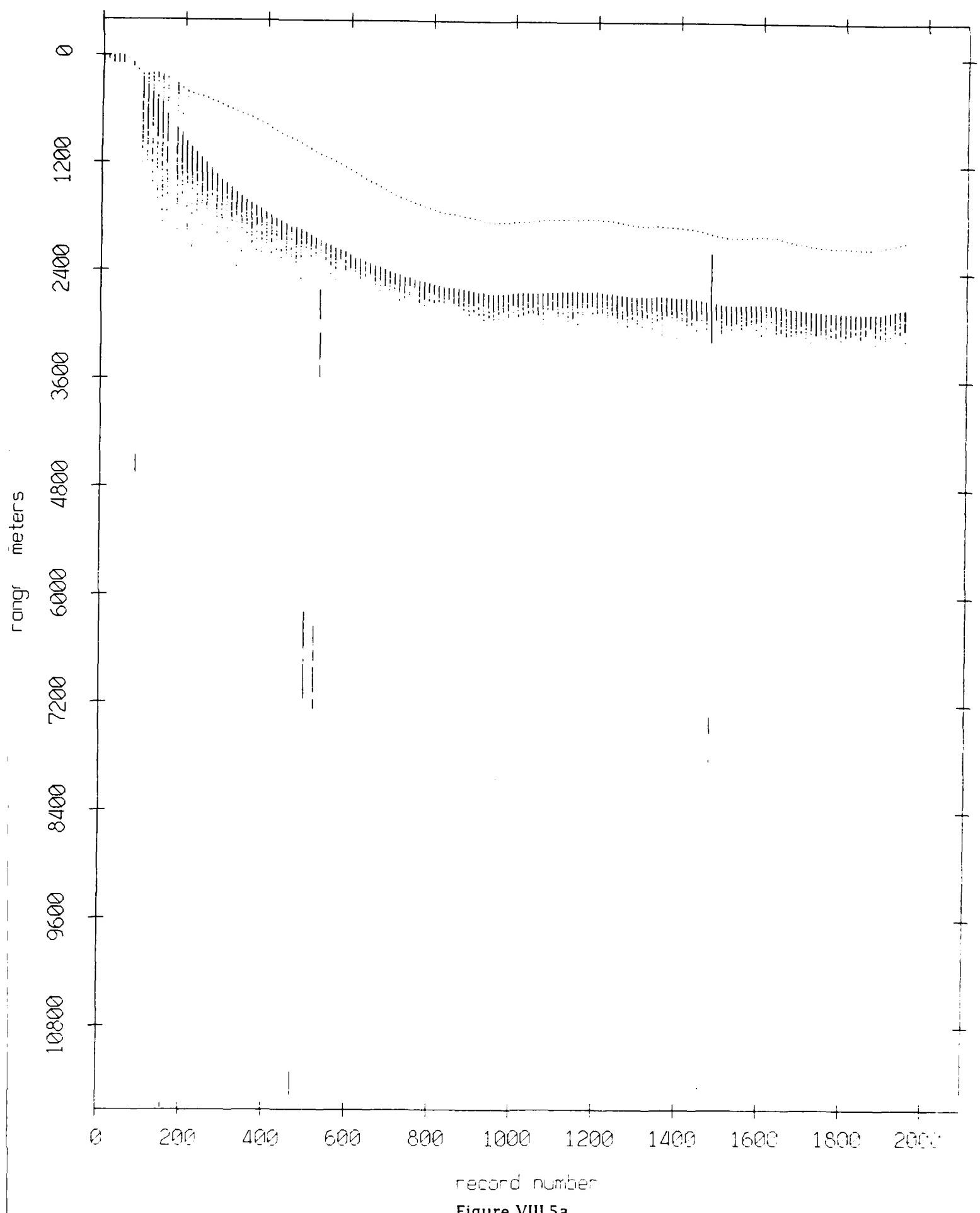
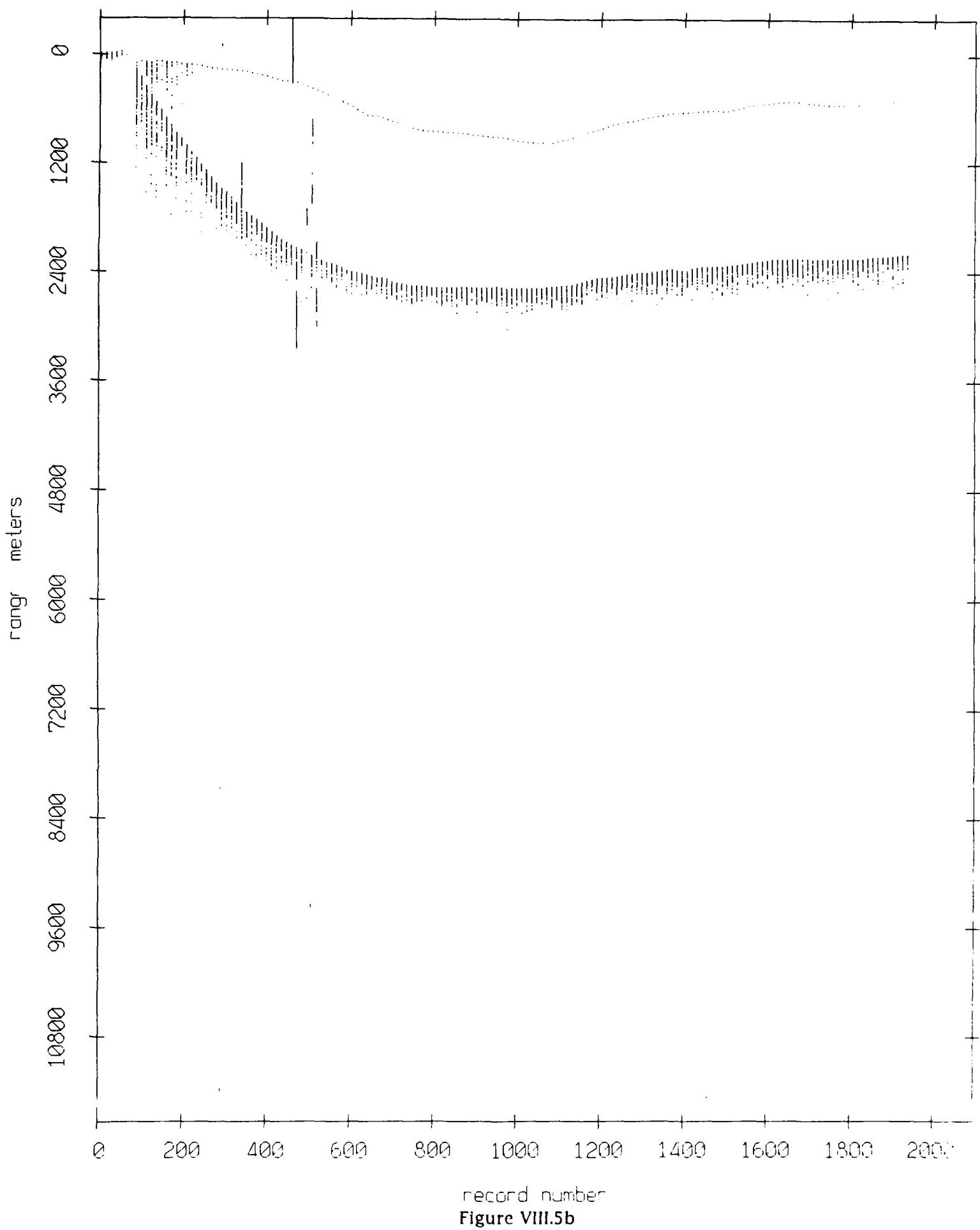


Figure VIII.5a

Float 5, September 1987 Sea Trip: range from float 2



Float 5, September 1987 Sea Trip: range from float 3

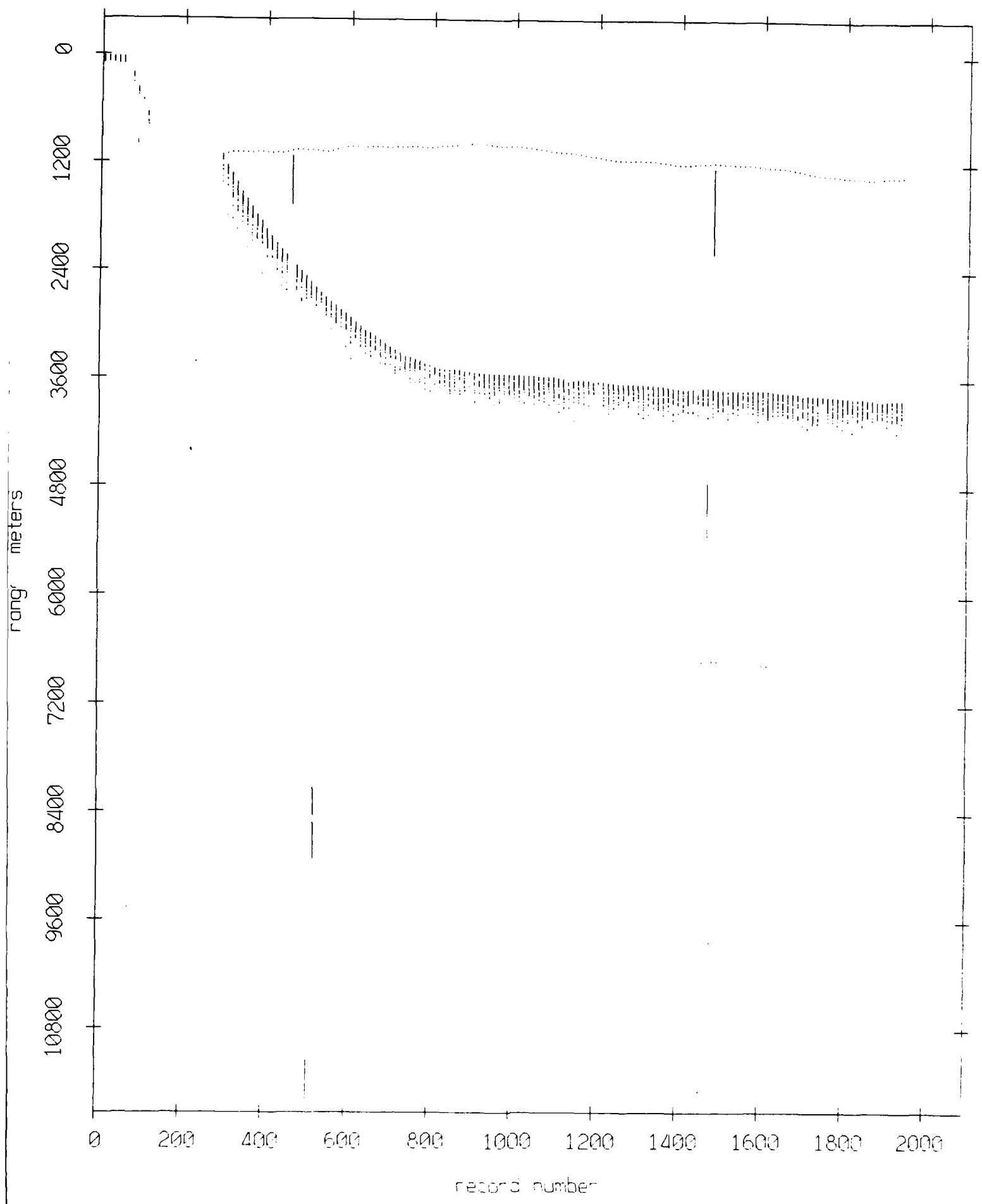


Figure VIII.5c

Float 5, September 1987 Sea Trip: range from float 4

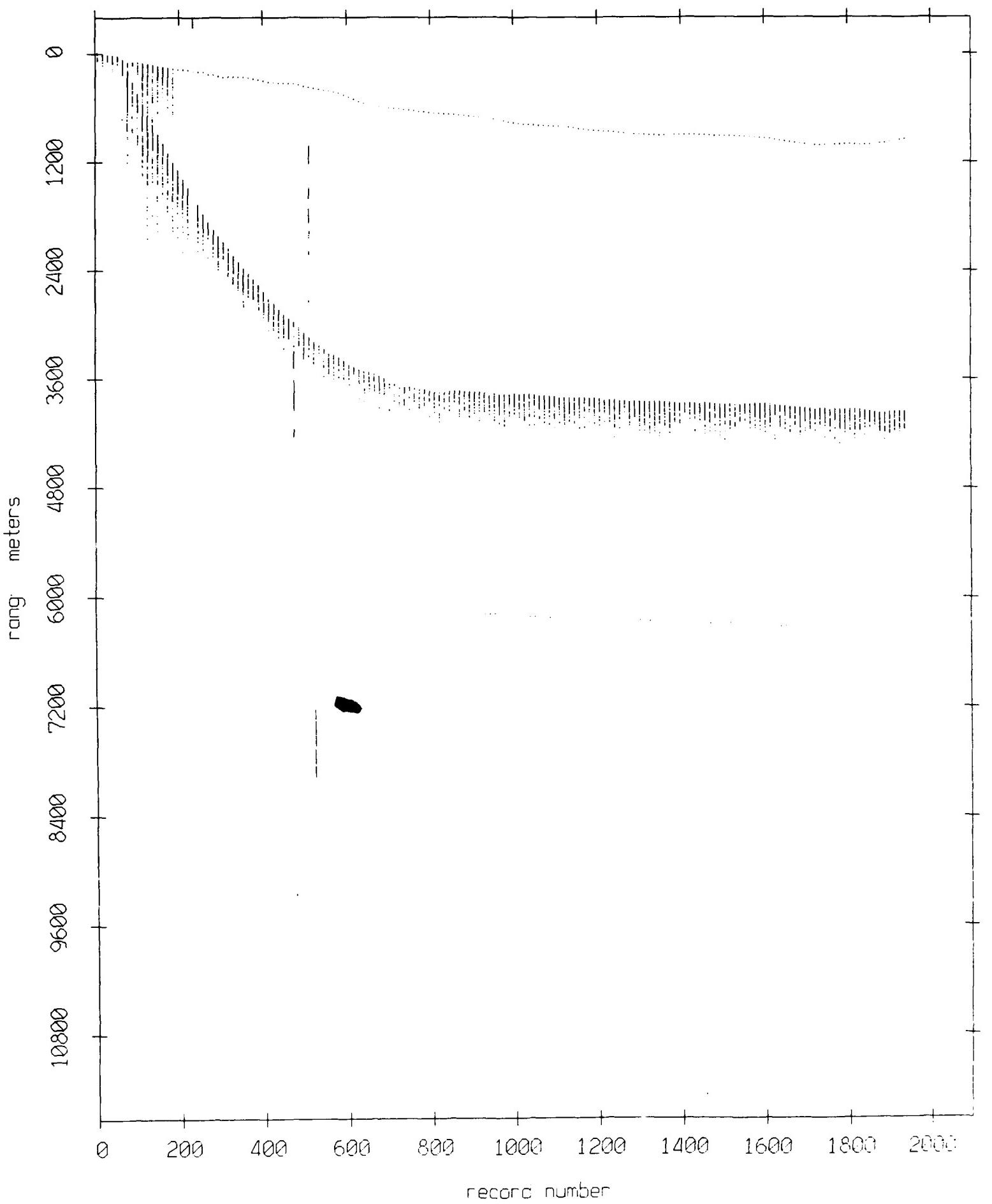


Figure VIII.5d

Float 5, September 1987 Sea Trip: range from float 6

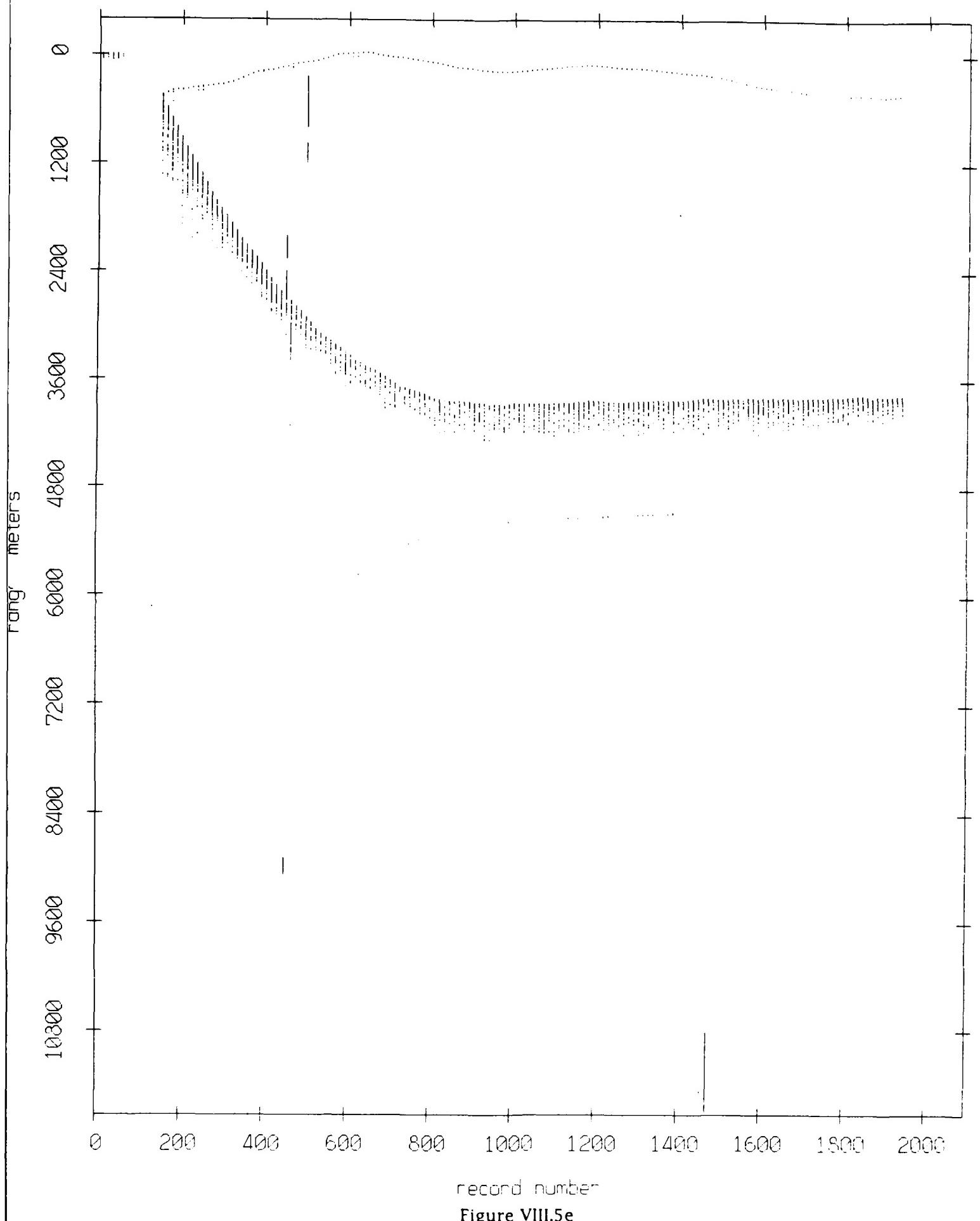
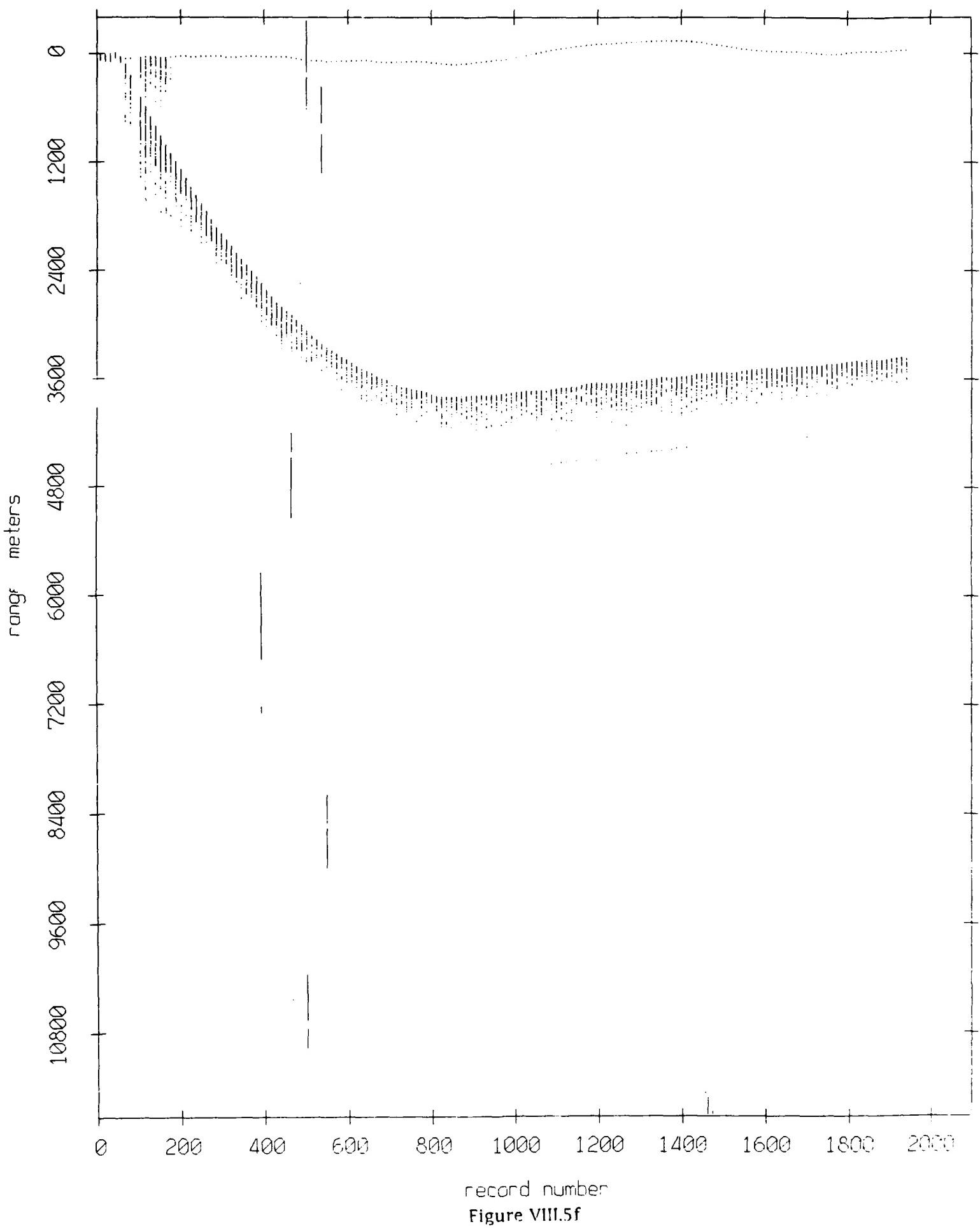


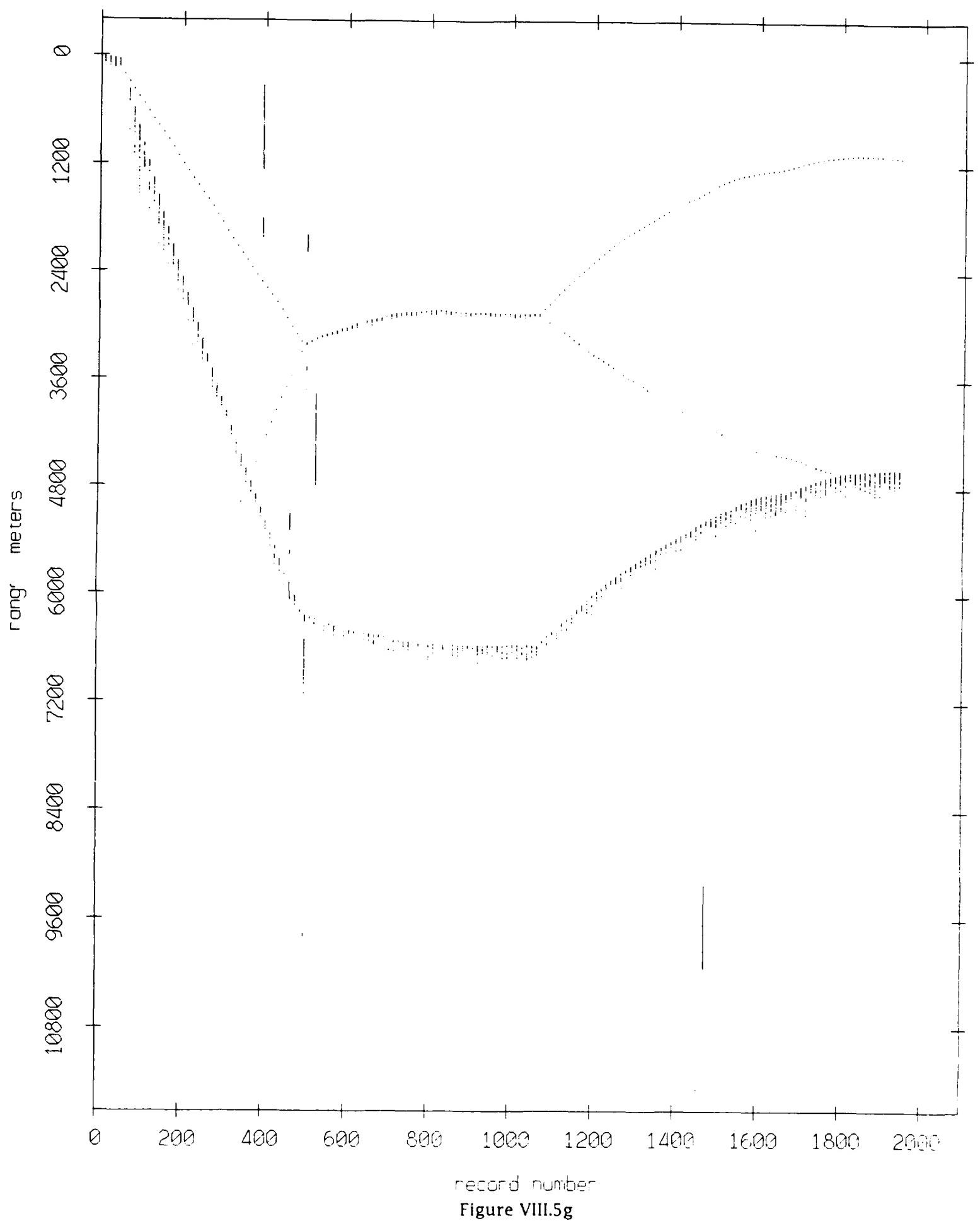
Figure VIII.5e

Float 5, September 1987 Sea Trip: range from float 7



record number
Figure VIII.5f

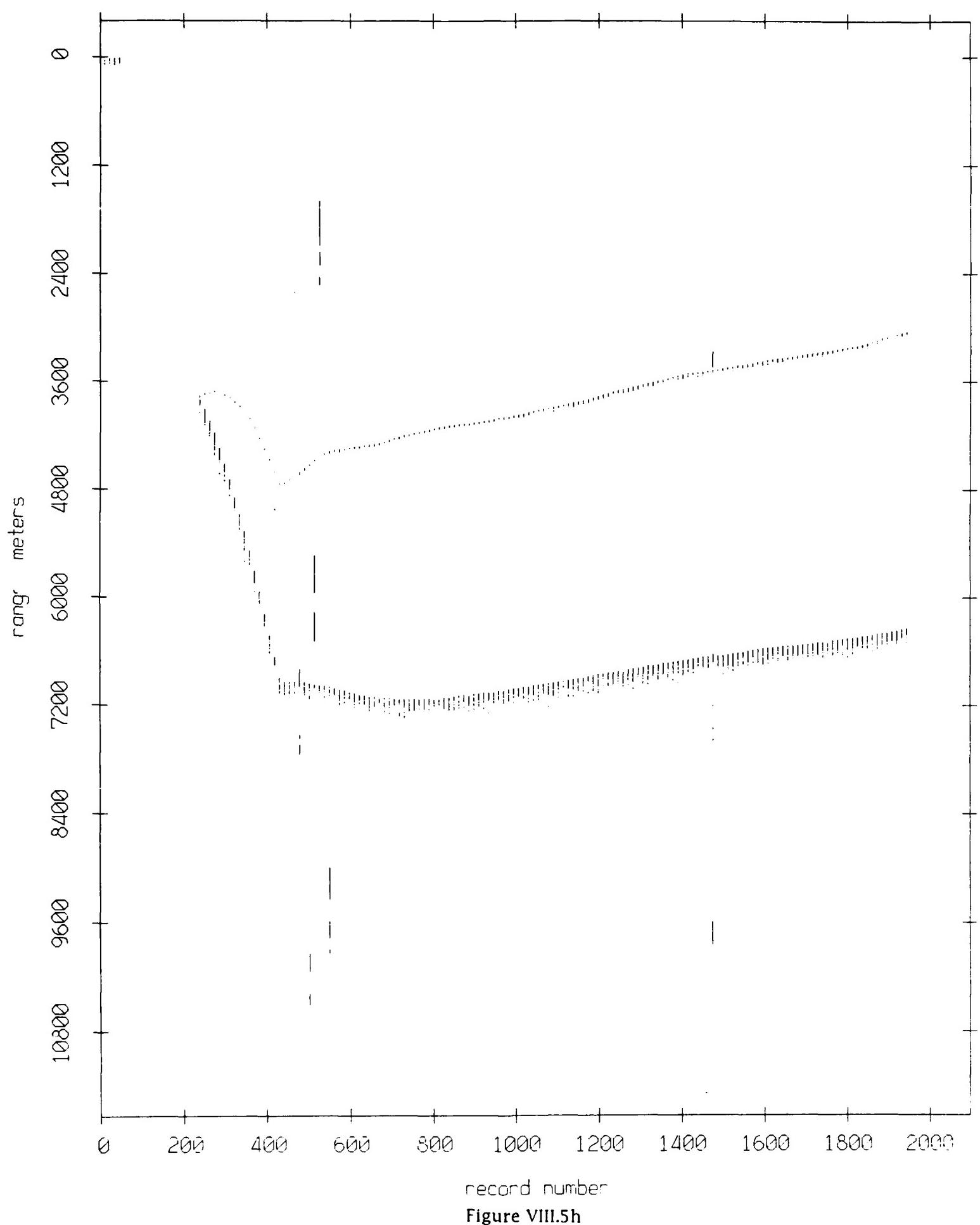
Float 5, September 1987 Sea Trip: range from float 8



record number

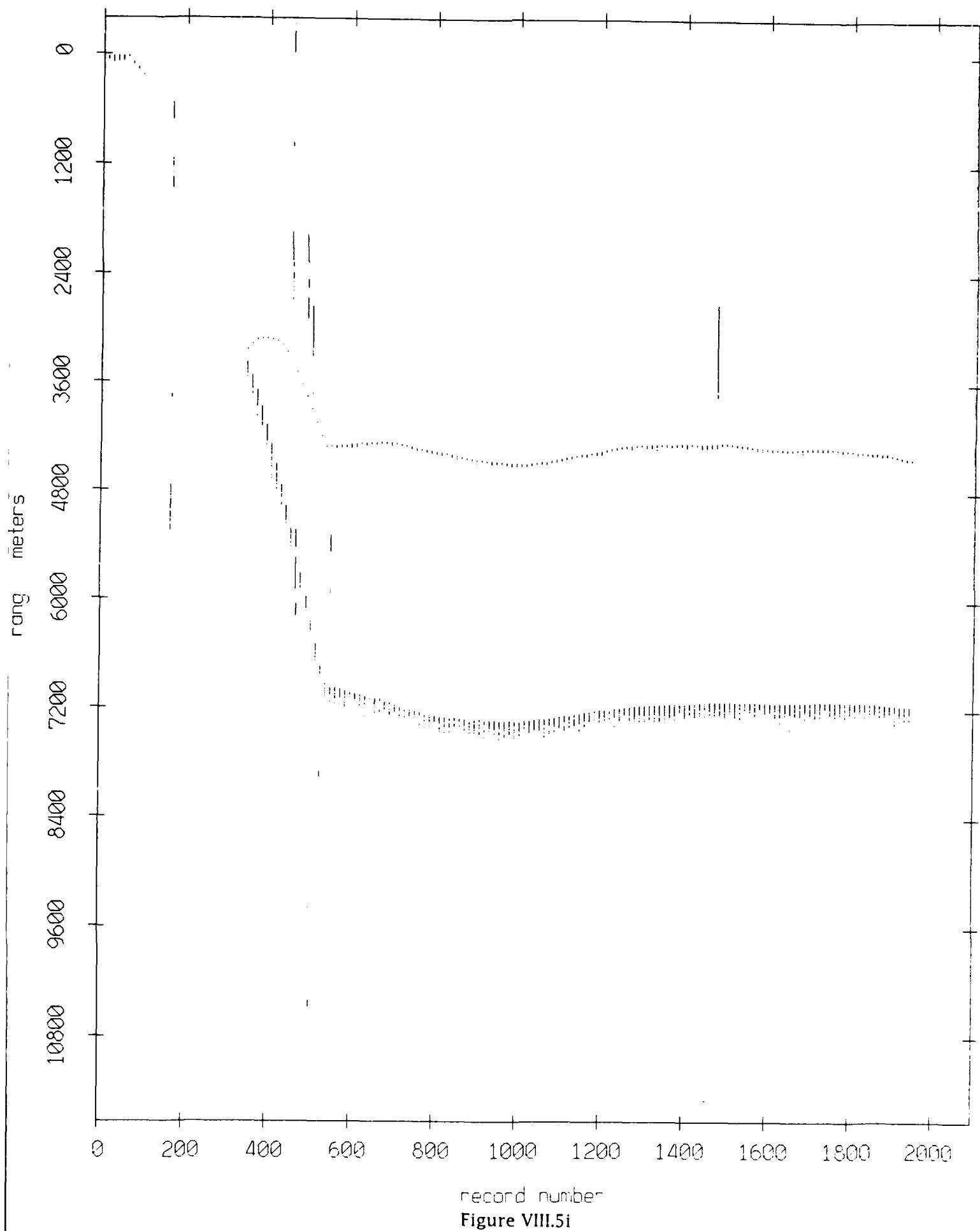
Figure VIII.5g

Float 5, September 1987 Sea Trip: range from float 9

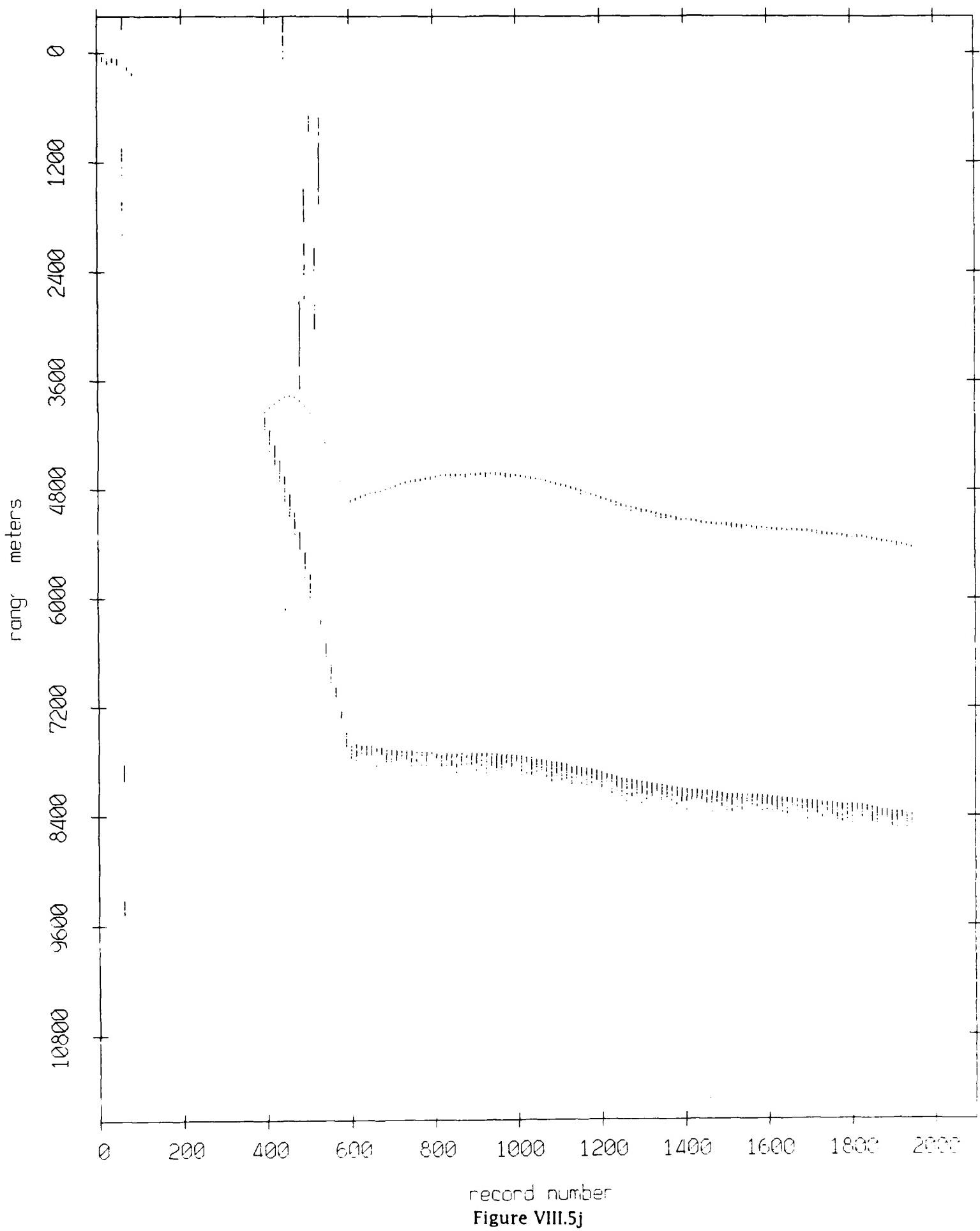


record number
Figure VIII.5h

Float 5, September 1987 Sea Trip: range from float 10



Float 5, September 1987 Sea Trip: range from float 11



record number
Figure VIII.5j

Float 6, September 1987 Sea Trip: range from float 0

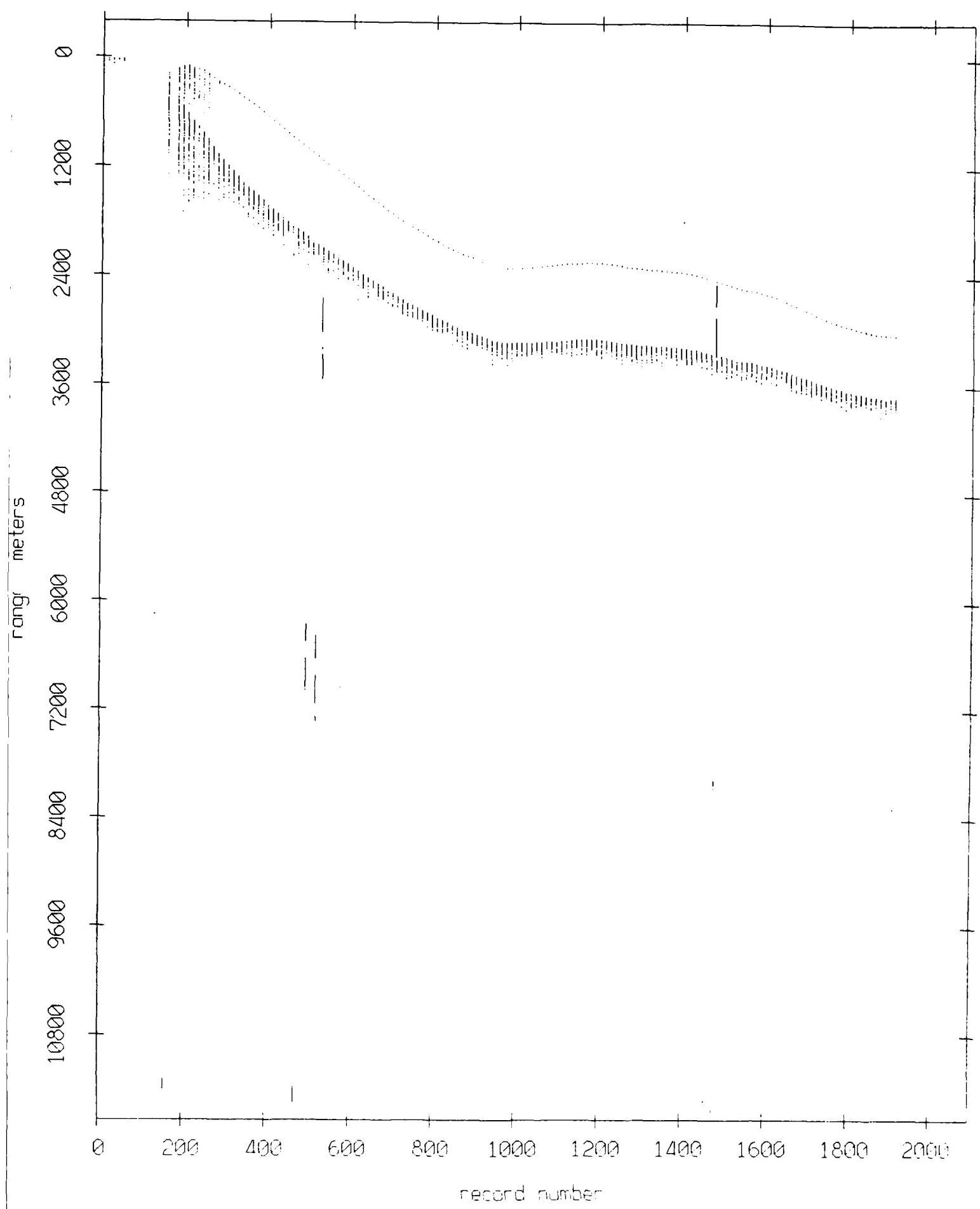


Figure VIII.6a

Float 6, September 1987 Sea Trip: range from float 2

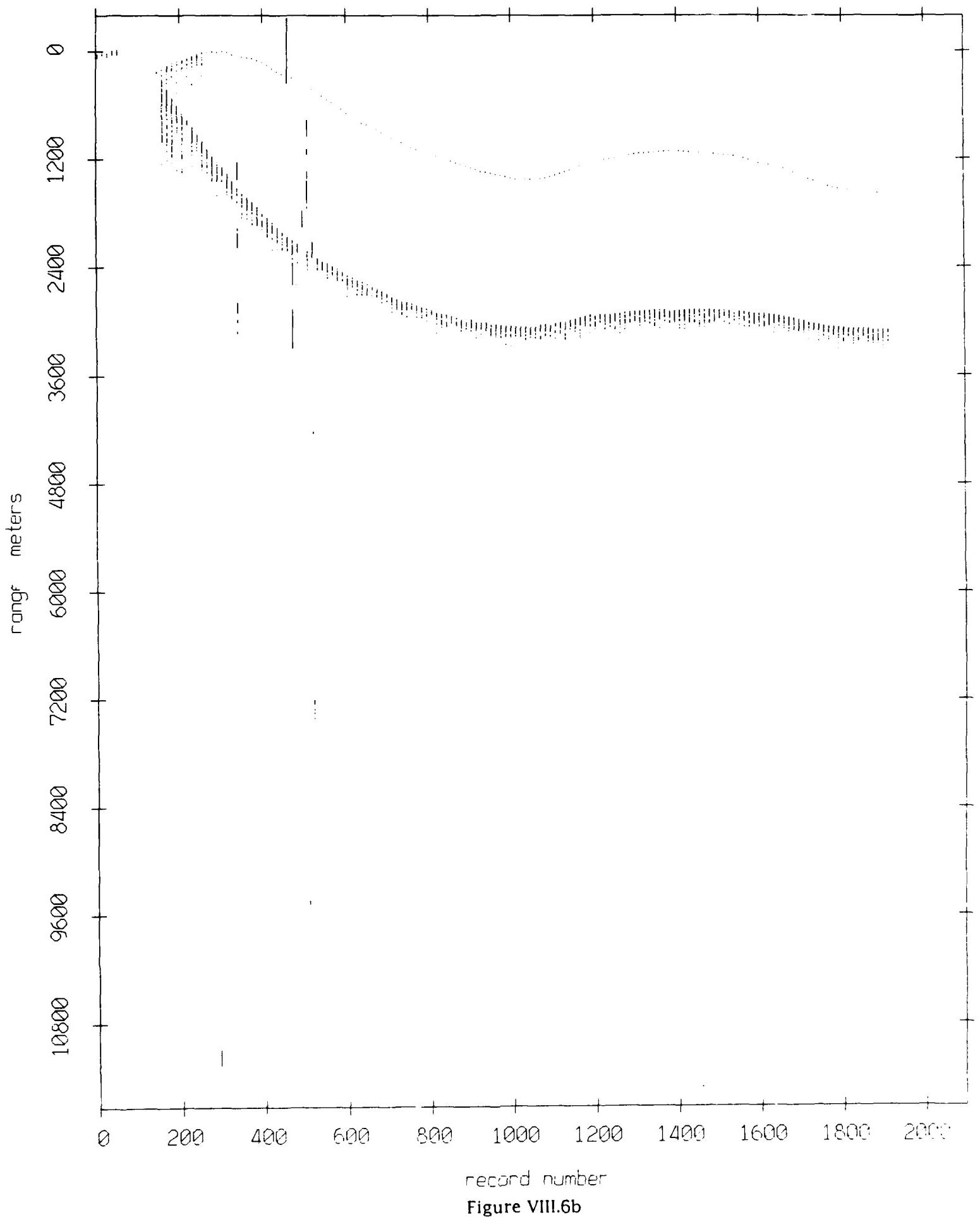


Figure VIII.6b

Float 6, September 1987 Sea Trip: range from float 3

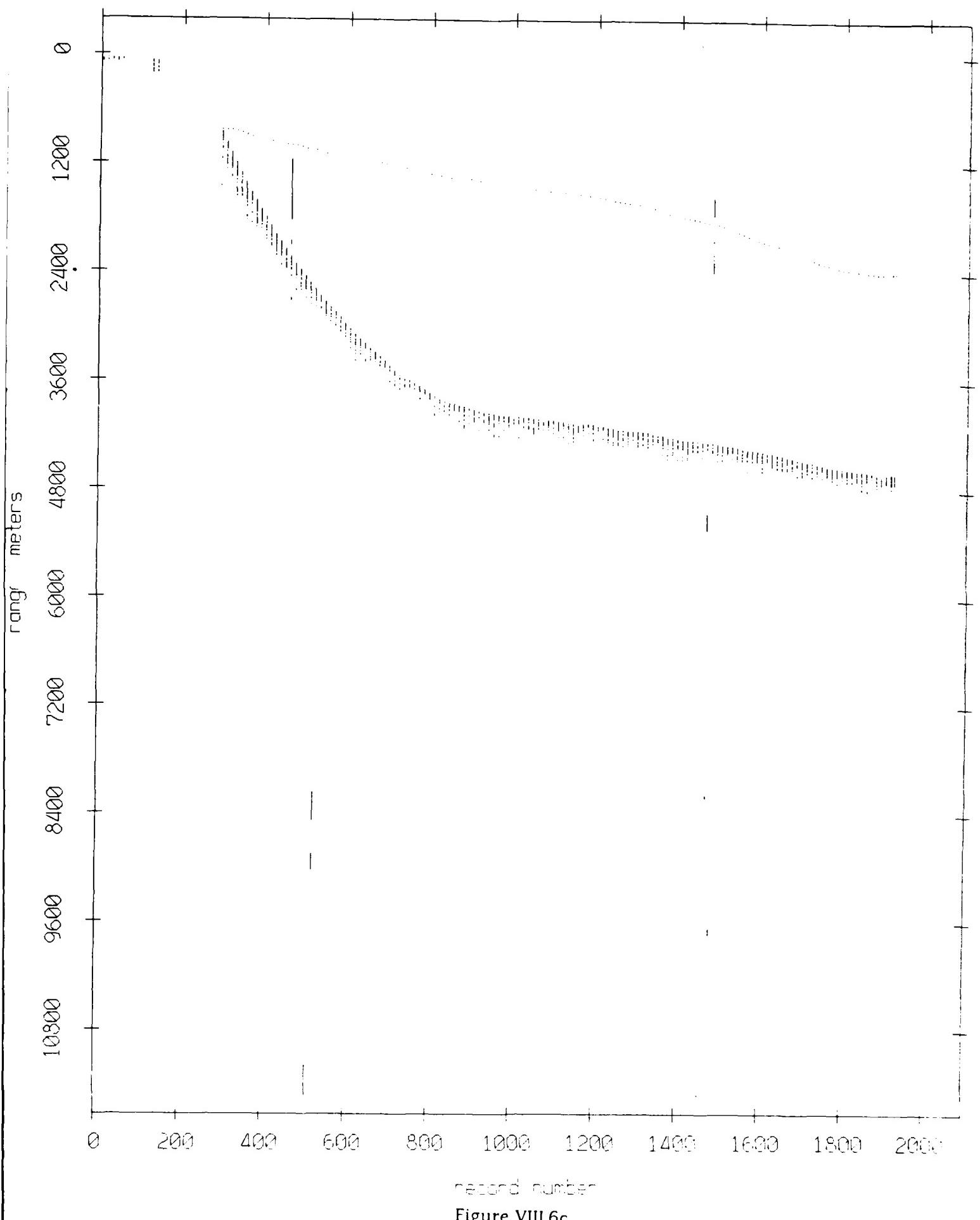


Figure VIII.6c

Float 6, September 1987 Sea Trip: range from float 4

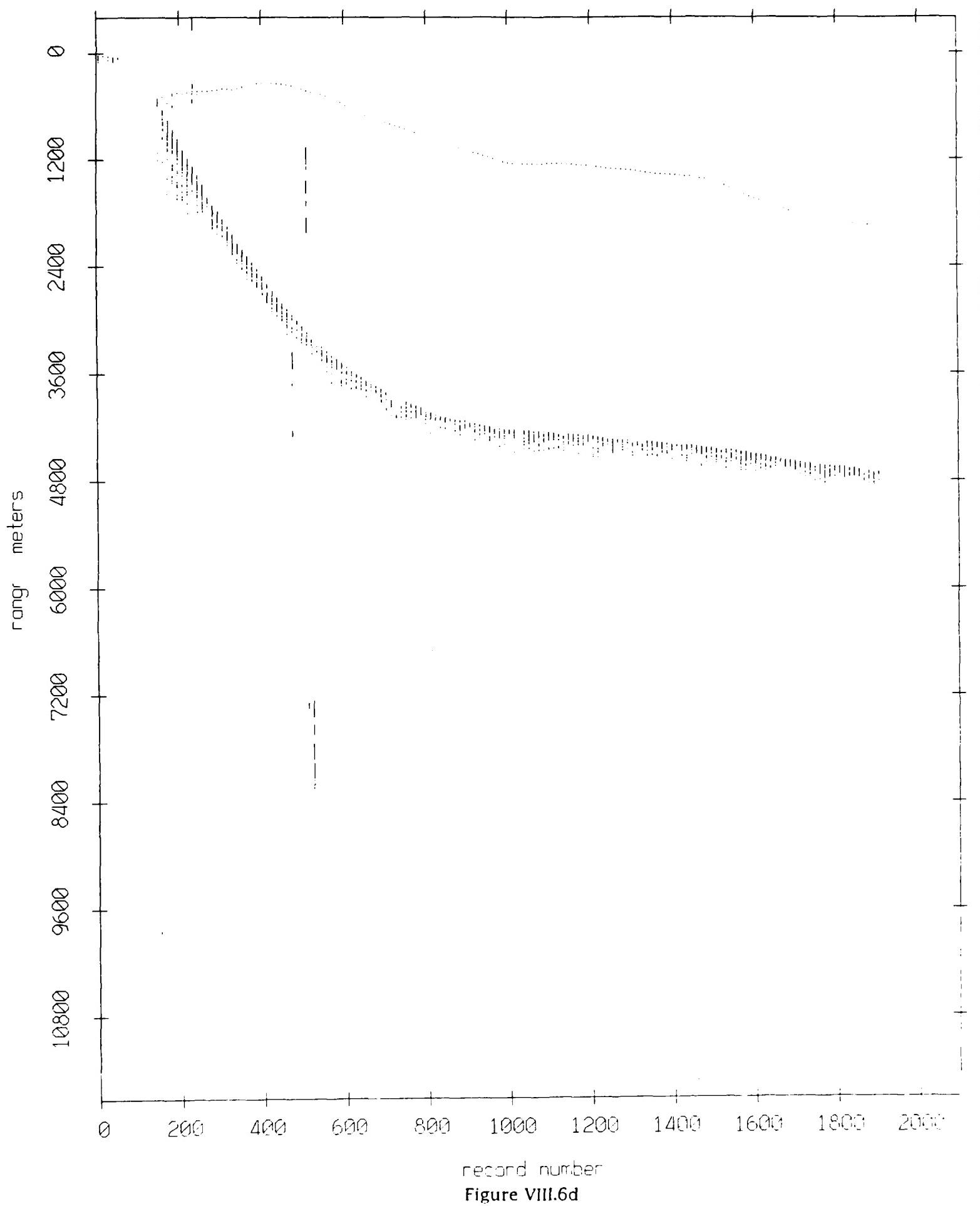


Figure VIII.6d

Float 6, September 1987 Sea Trip: range from float 5

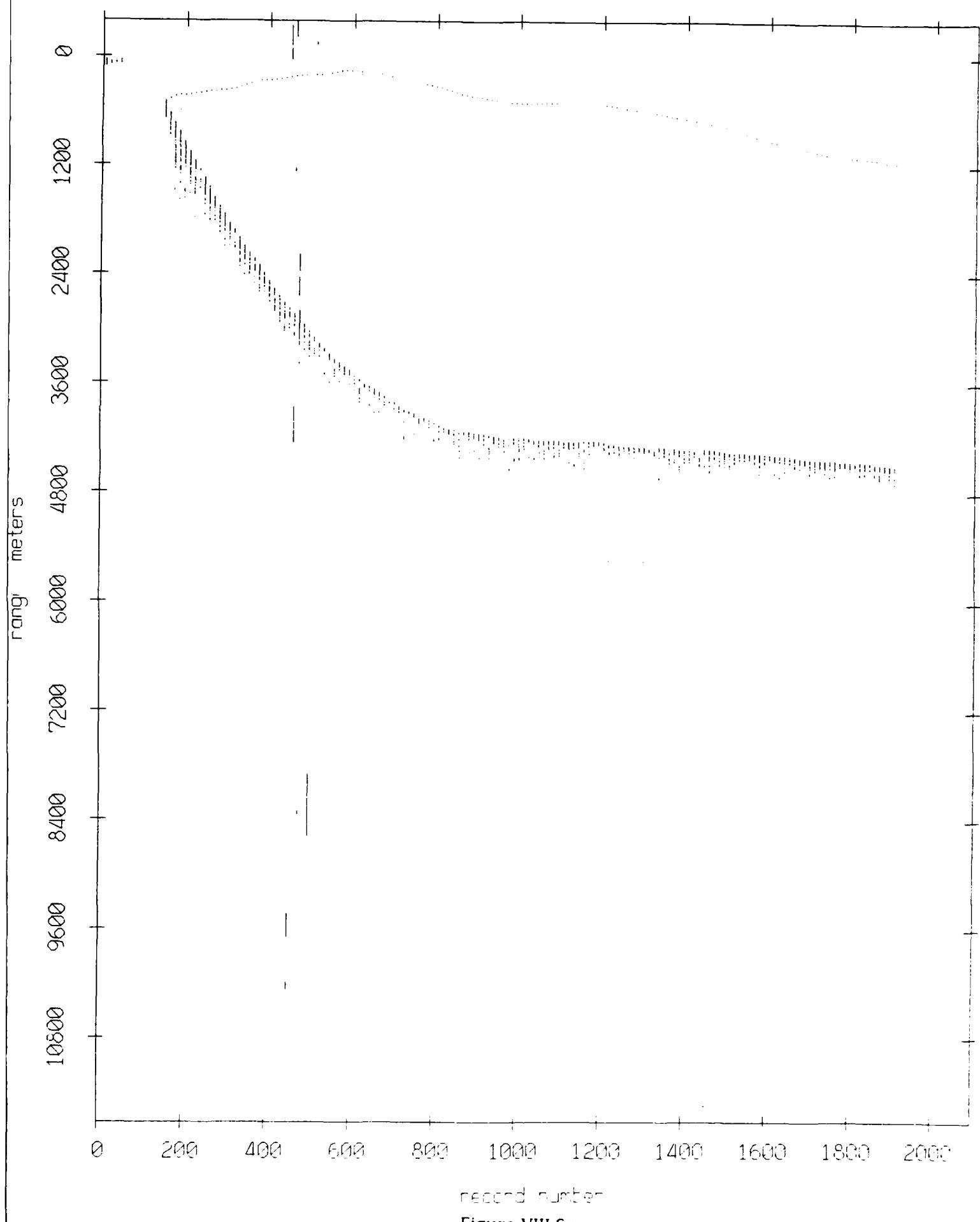


Figure VIII.6e

Float 6, September 1987 Sea Trip: range from float 7

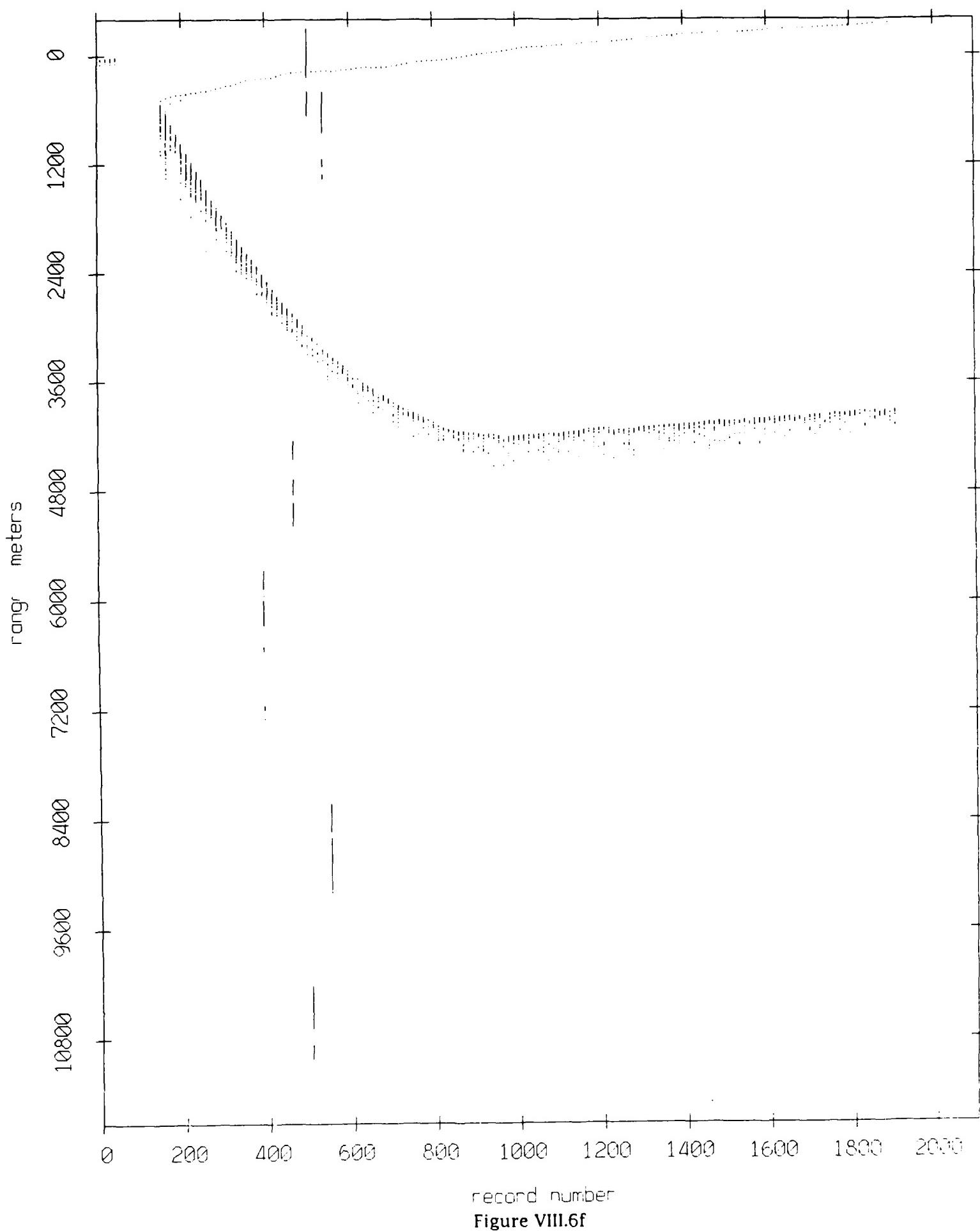


Figure VIII.6f

Float 6, September 1987 Sea Trip: range from float 8

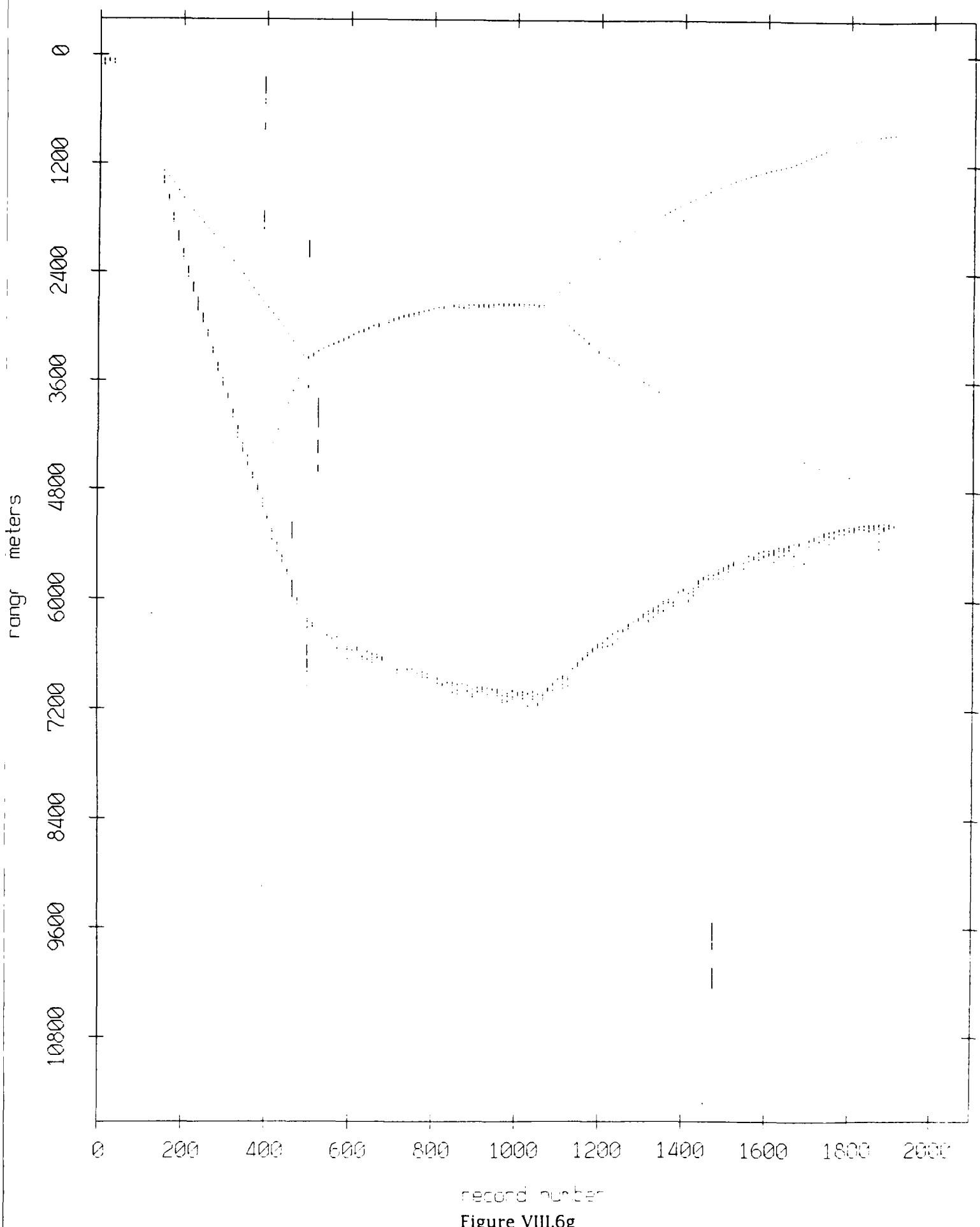
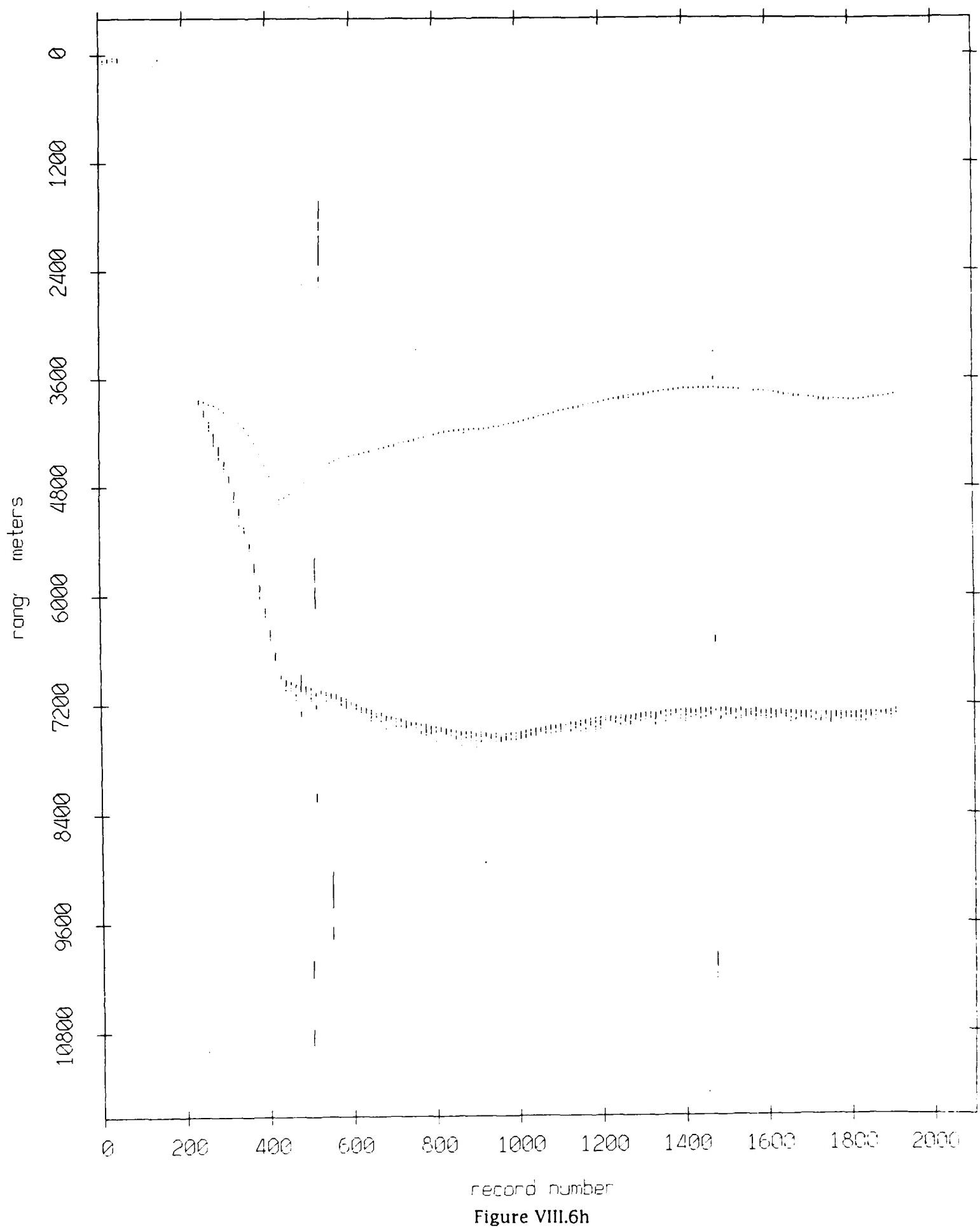


Figure VIII.6g

Float 6, September 1987 Sea Trip: range from float 9



record number

Figure VIII.6h

Float 6, September 1987 Sea Trip: range from float 10

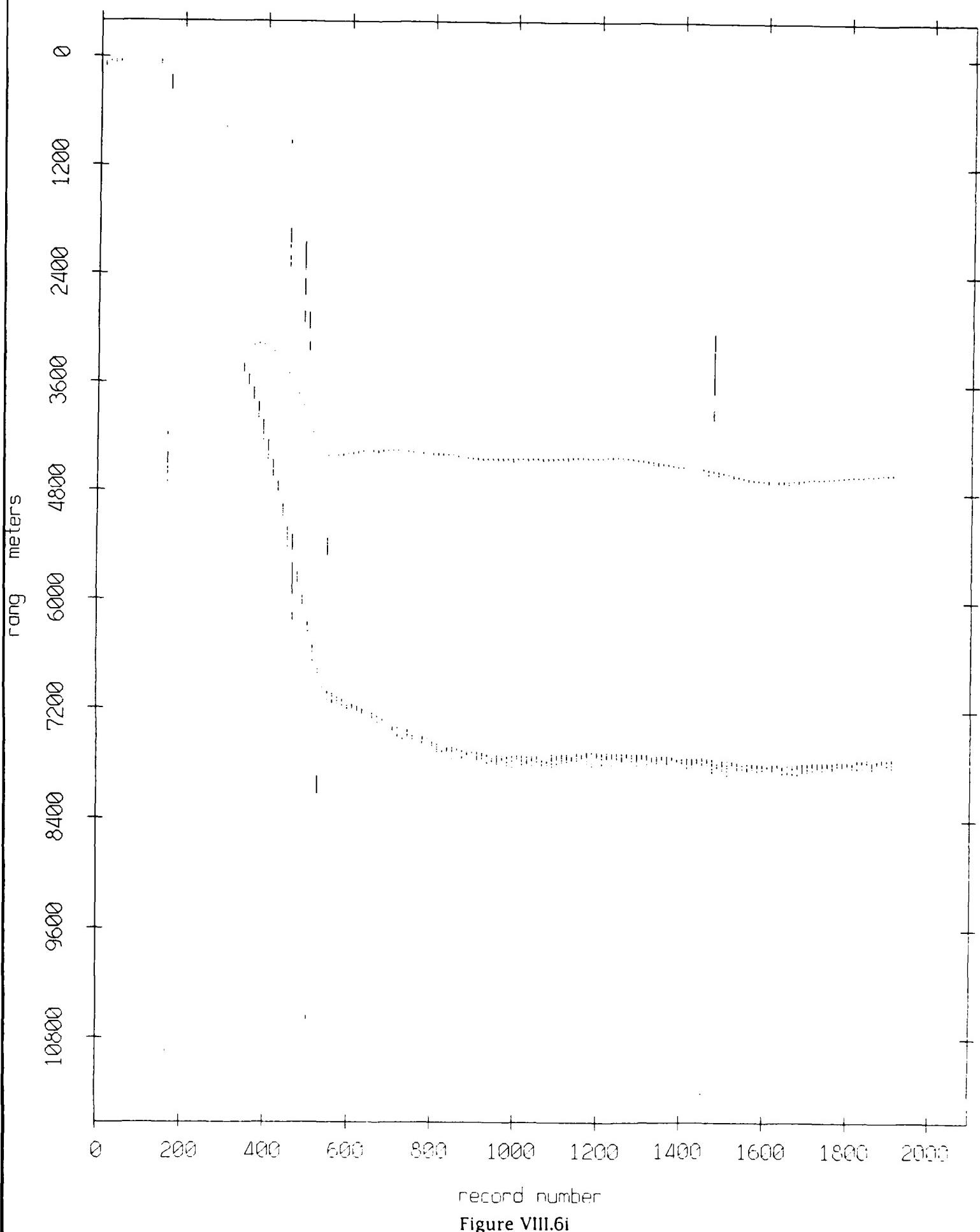


Figure VIII.6i

Float 6, September 1987 Sea Trip: range from float 11

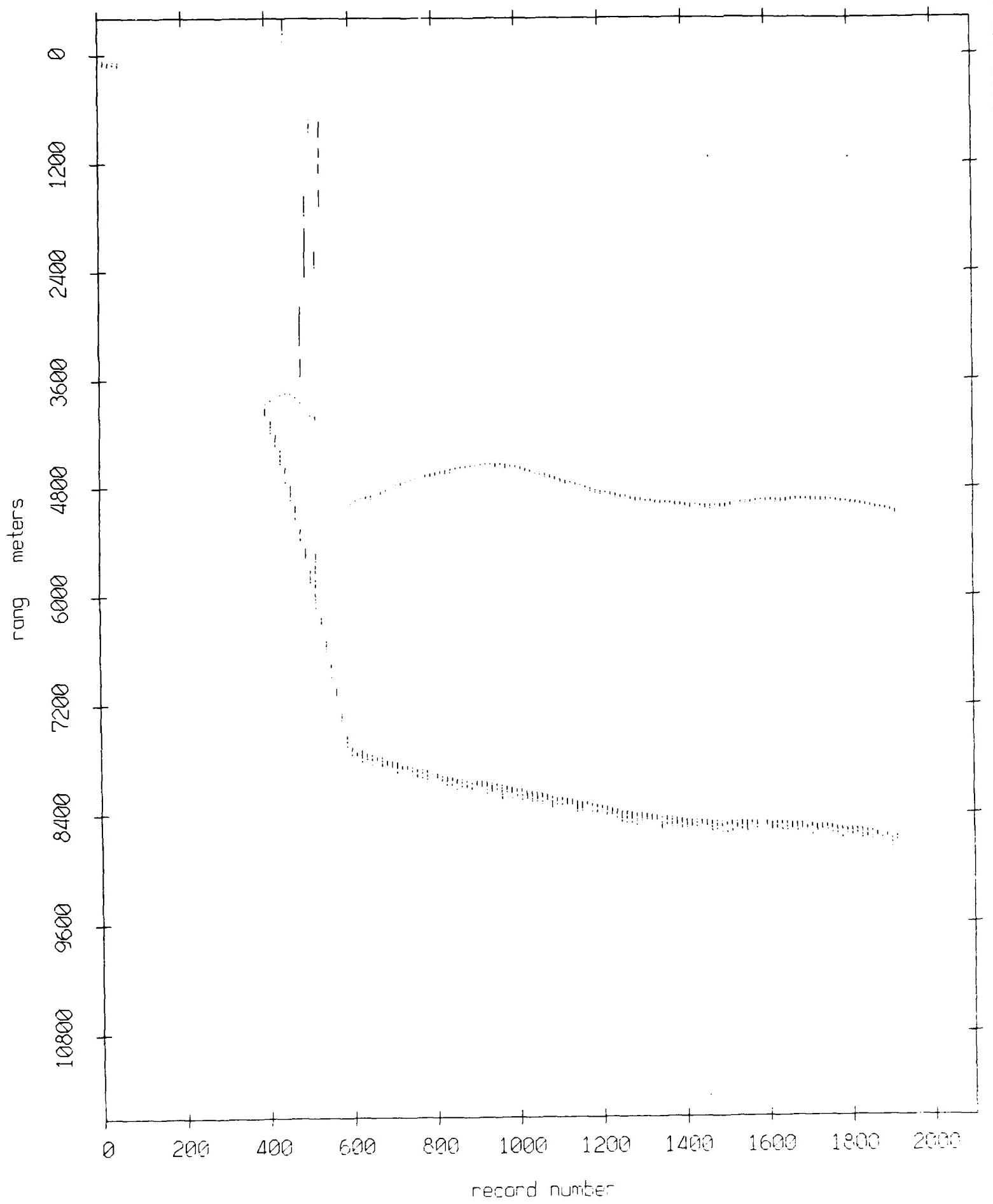


Figure VIII.6j

Float 7, September 1987 Sea Trip: range from float 0

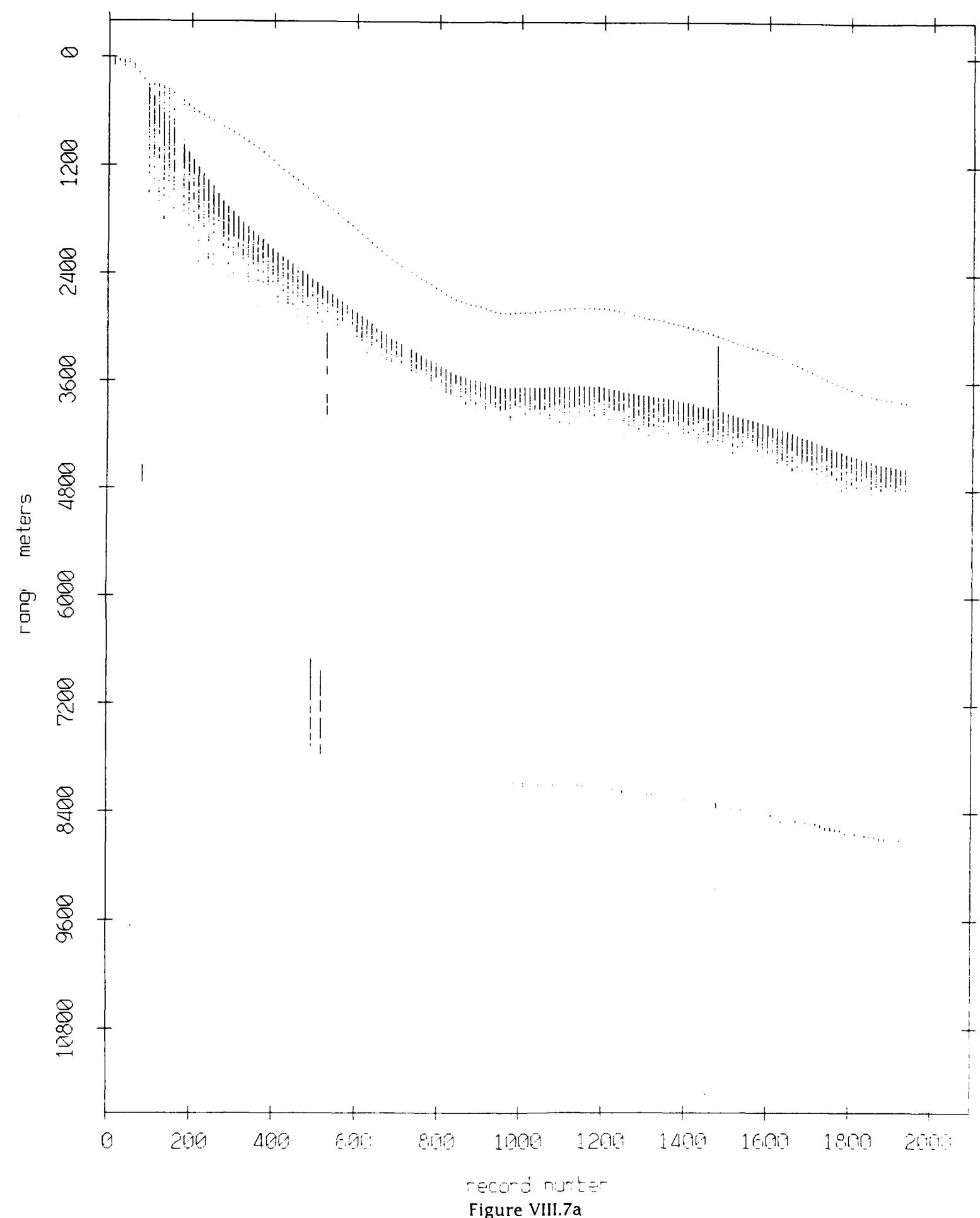


Figure VIII.7a

Float 7, September 1987 Sea Trip: range from float 2

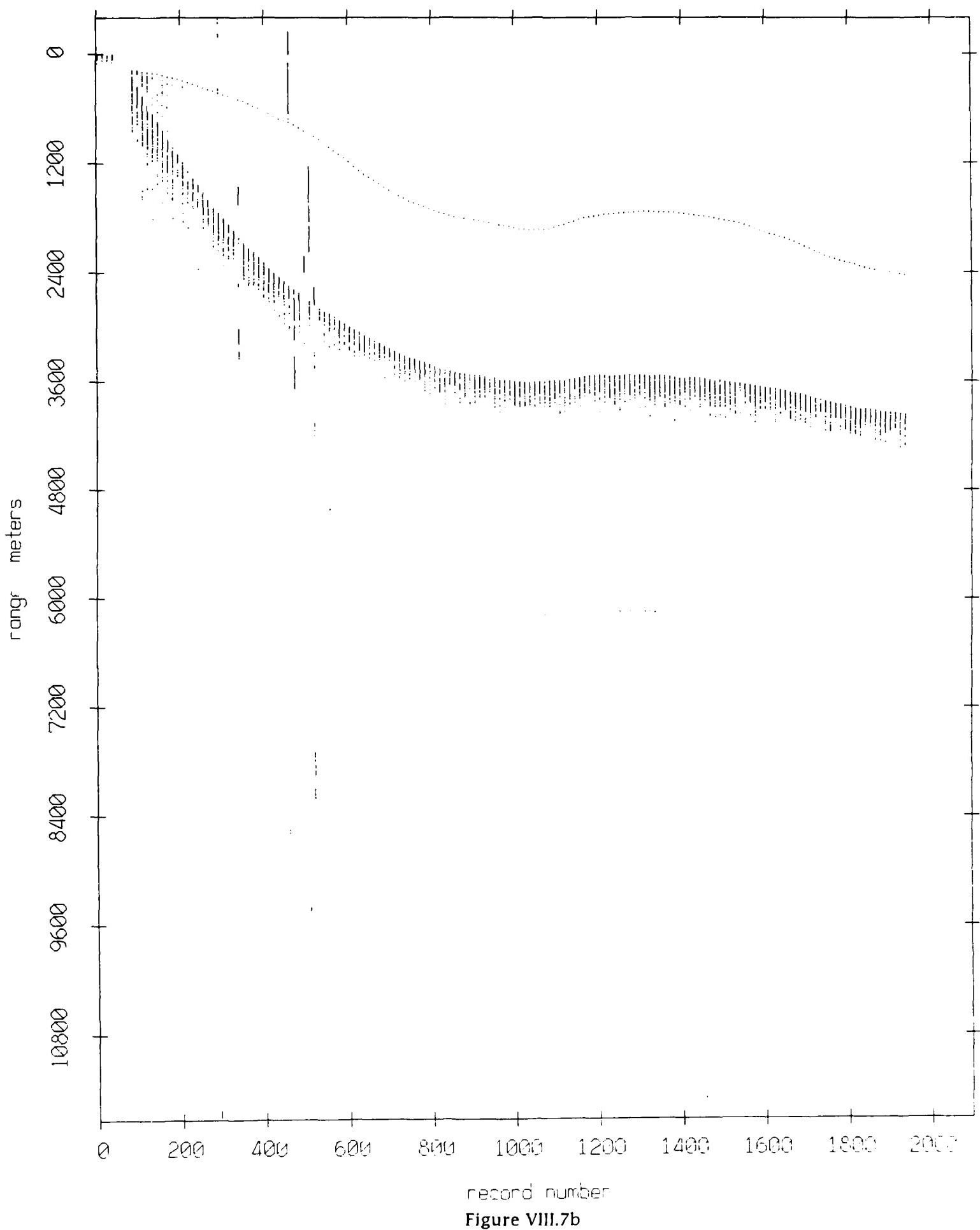


Figure VIII.7b

Float 7, September 1987 Sea Trip: range from float 3

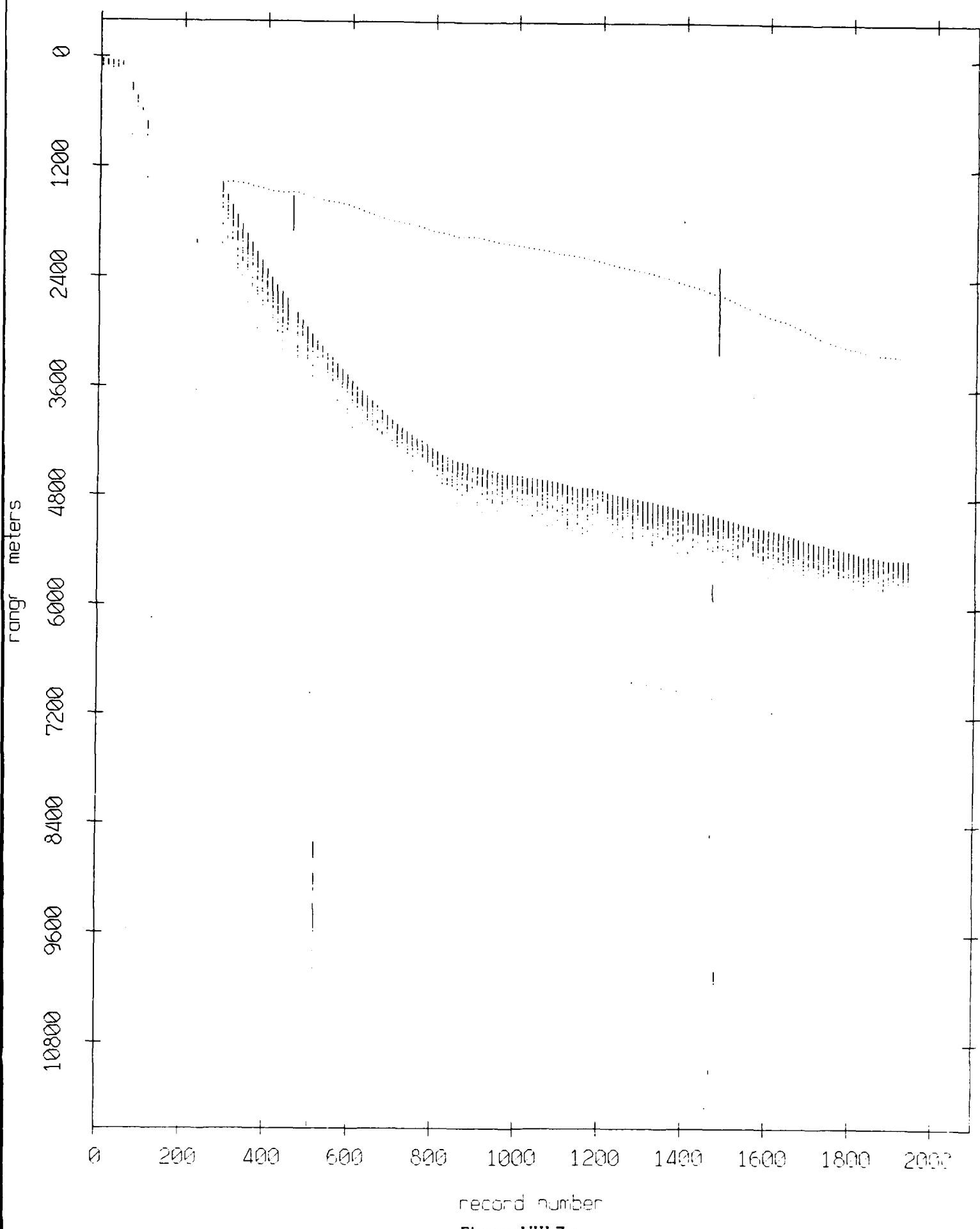


Figure VIII.7c

Float 7, September 1987 Sea Trip: range from float 4

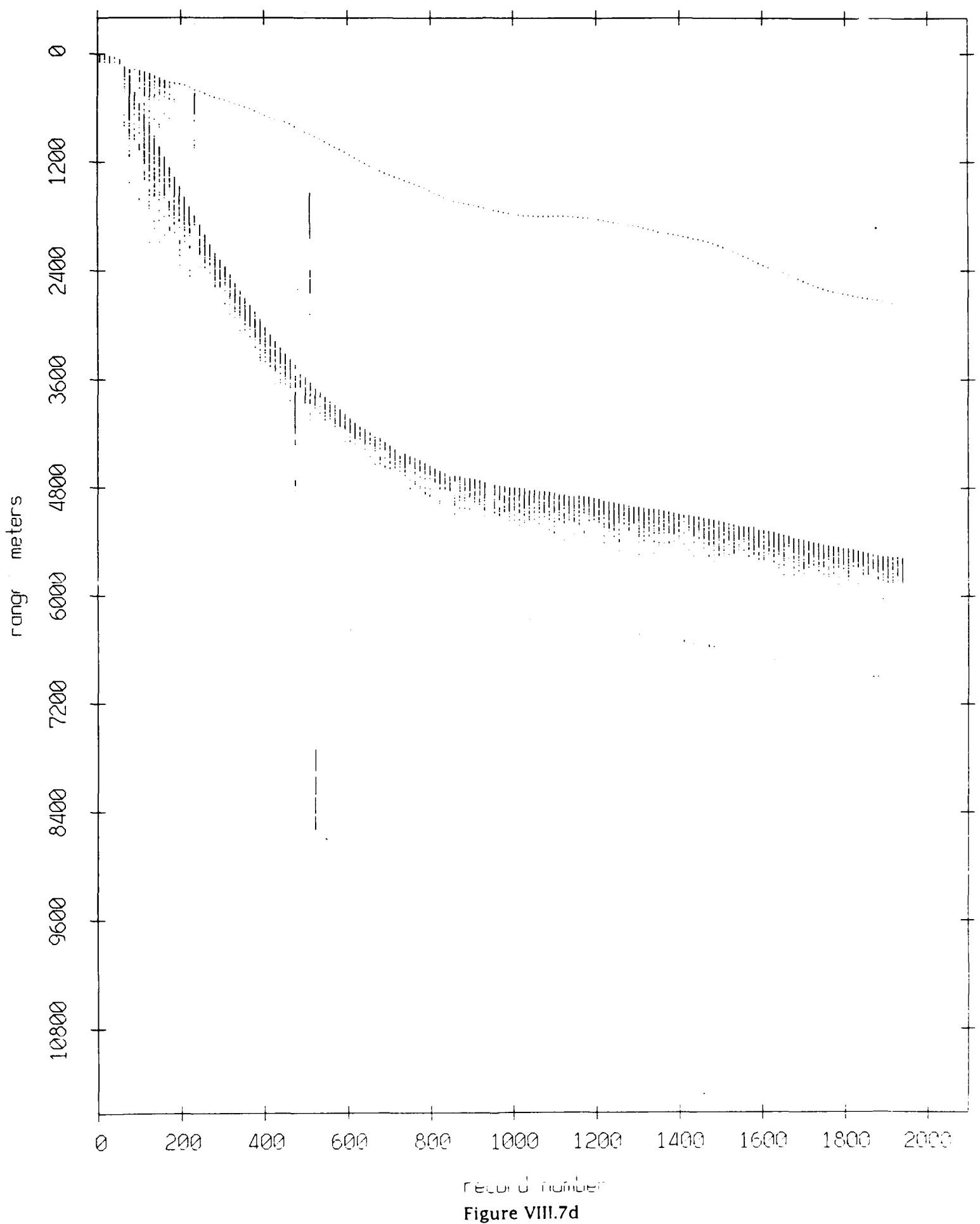


Figure VIII.7d

Float 7, September 1987 Sea Trip: range from float 5

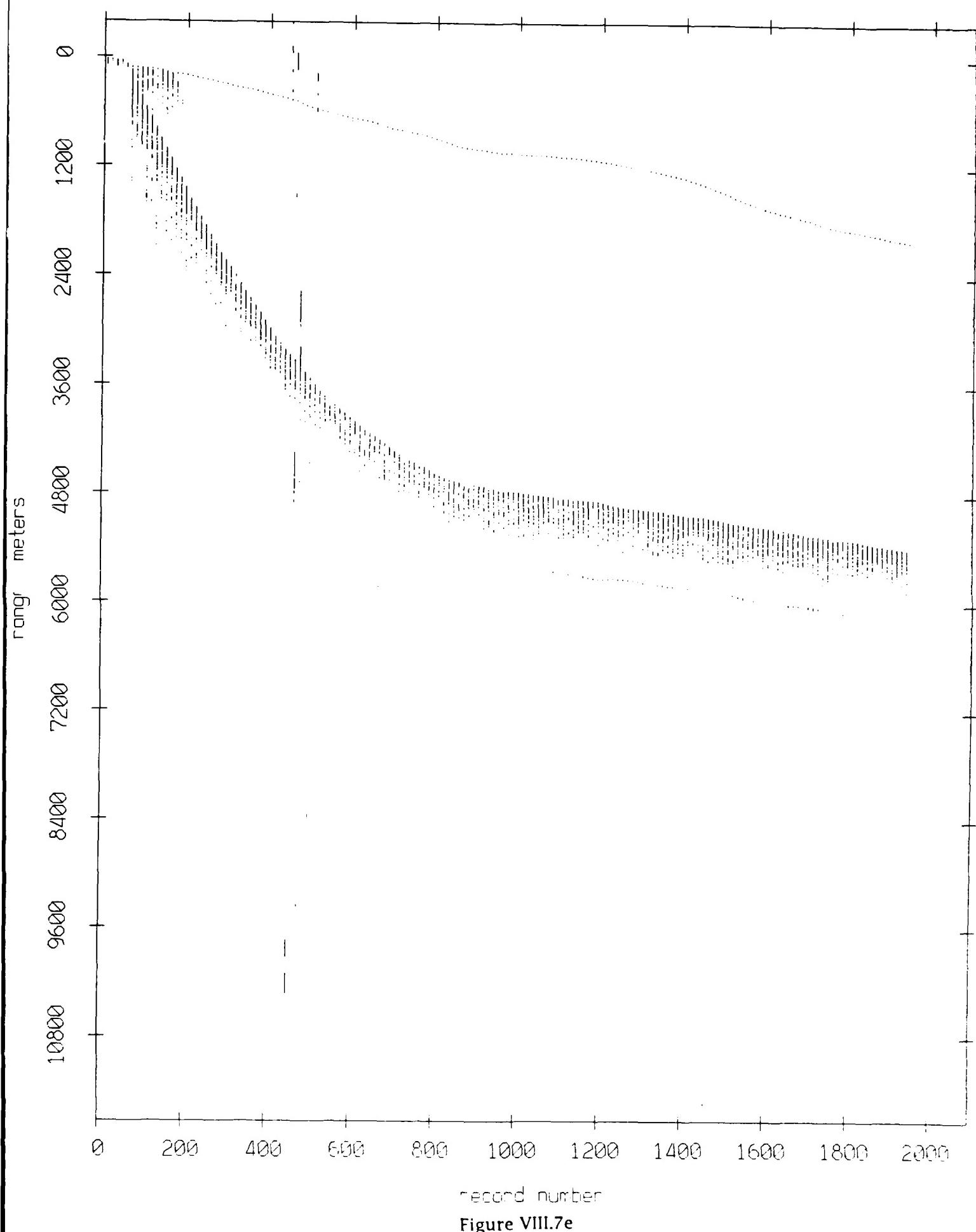


Figure VIII.7e

Float 7, September 1987 Sea Trip: range from float 6

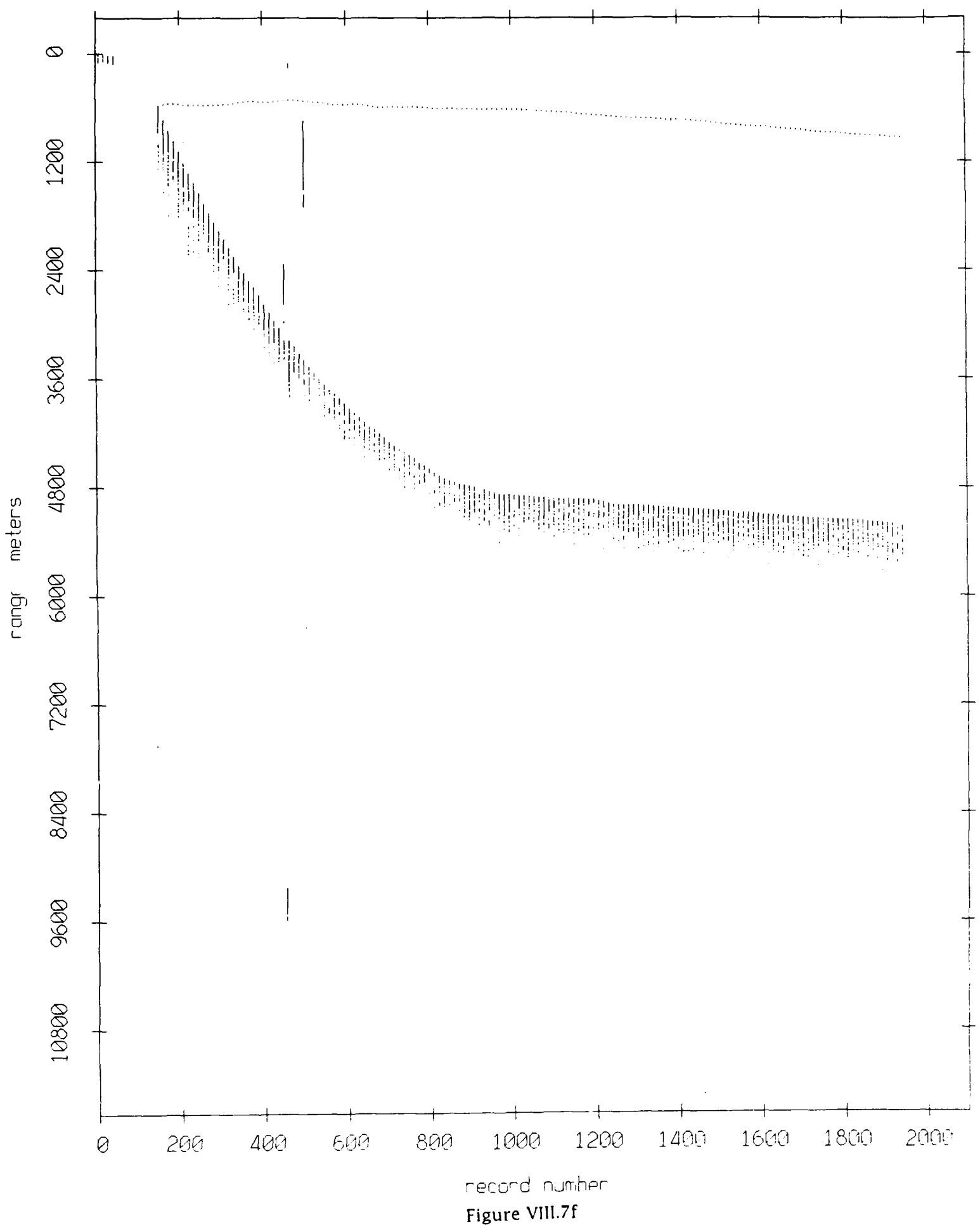


Figure VIII.7f

Float 7, September 1987 Sea Trip: range from float 8

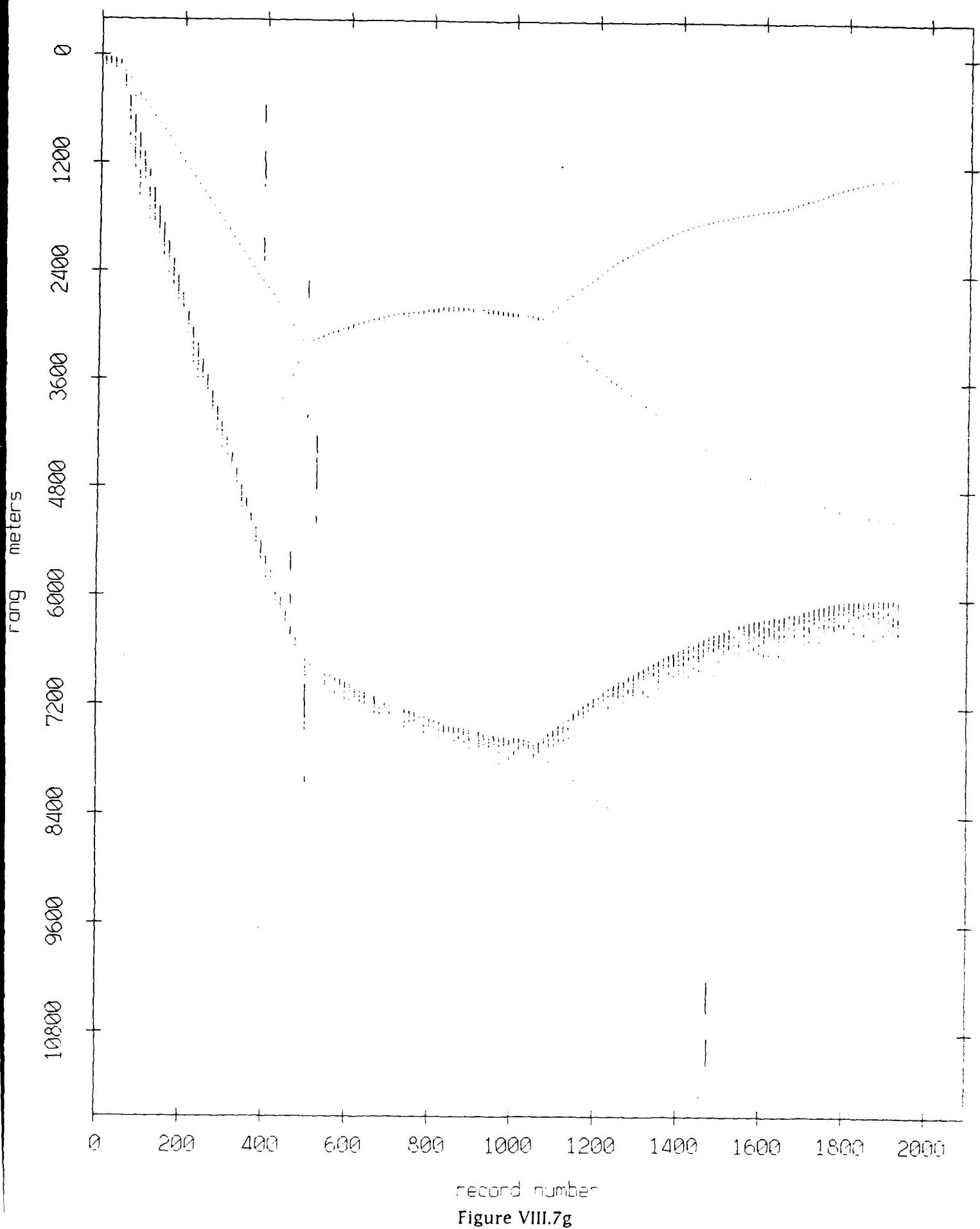
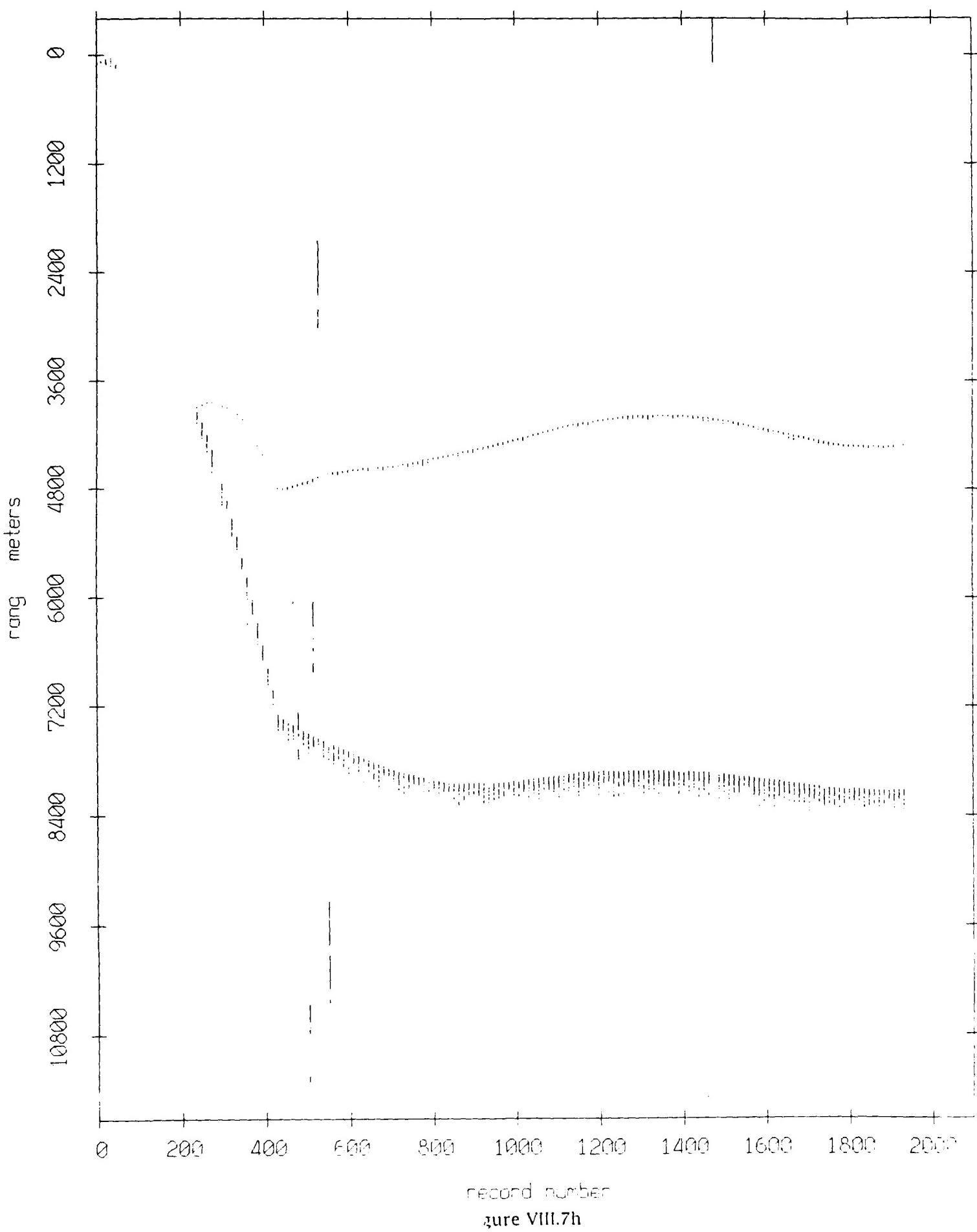


Figure VIII.7g

Float 7, September 1987 Sea Trip: range from float 9



Float 7, September 1987 Sea Trip: range from float 10

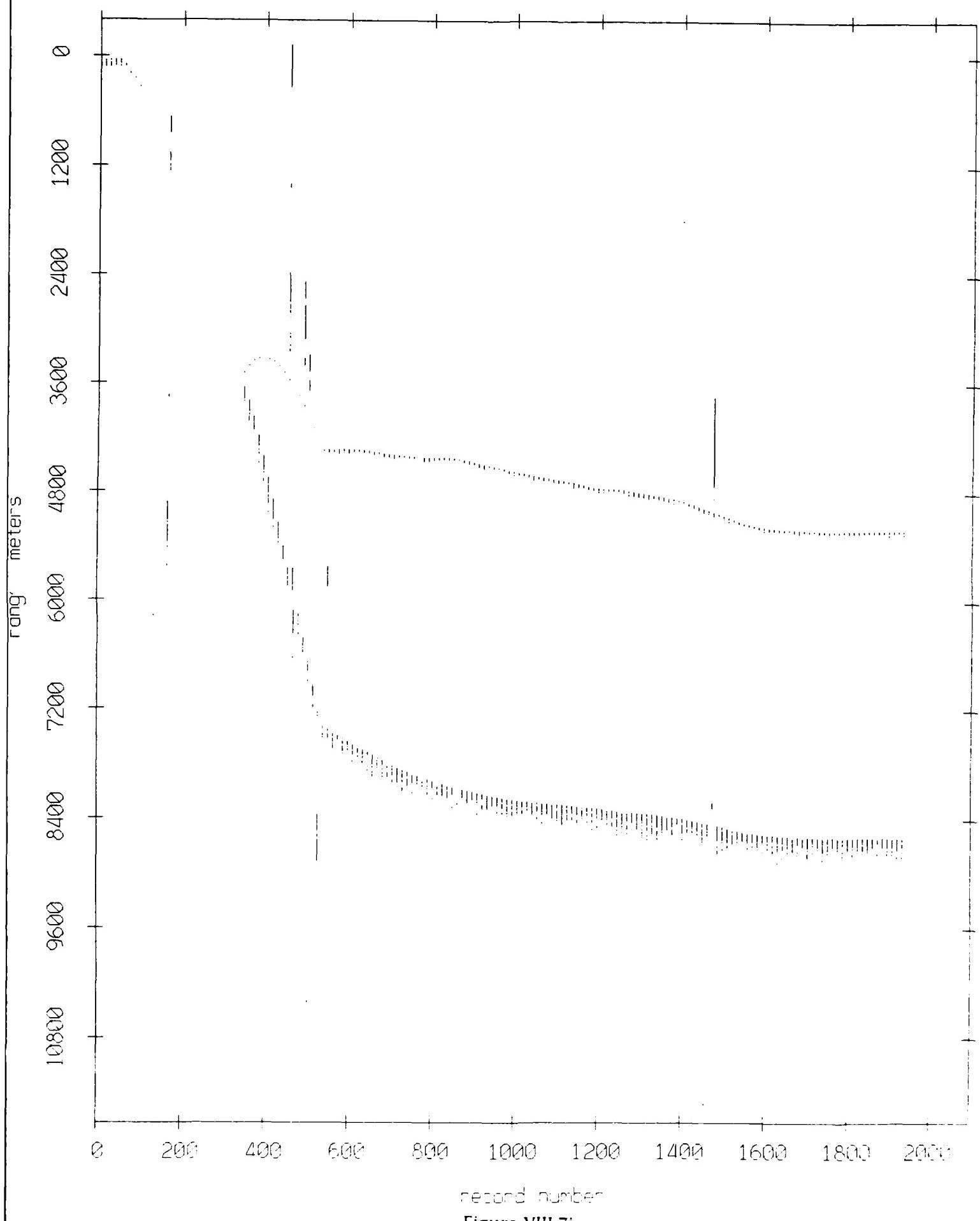
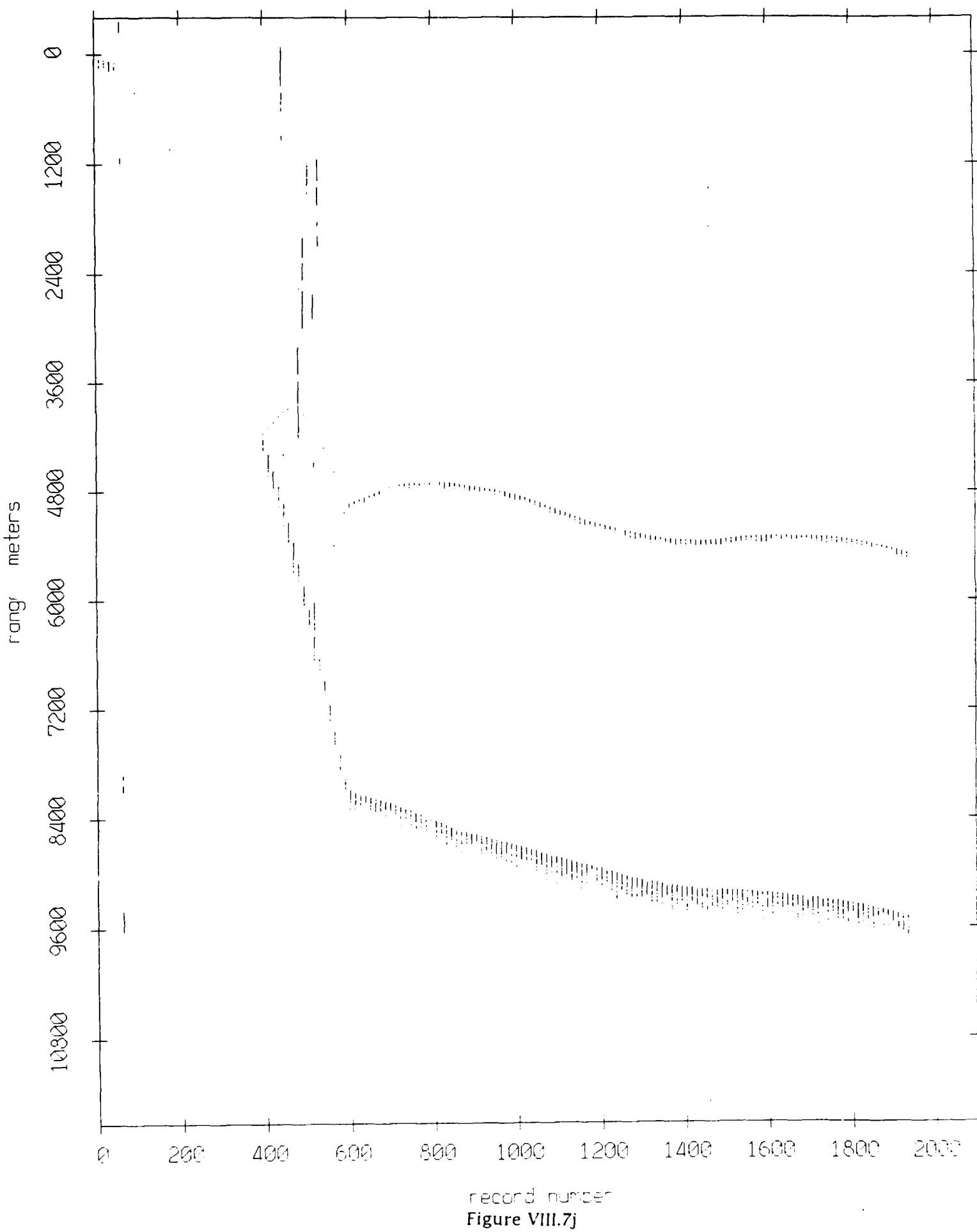


Figure VIII.7i

Float 7, September 1987 Sea Trip: range from float 11



record number
Figure VIII.7j

Float 8, September 1987 Sea Trip: range from float 0

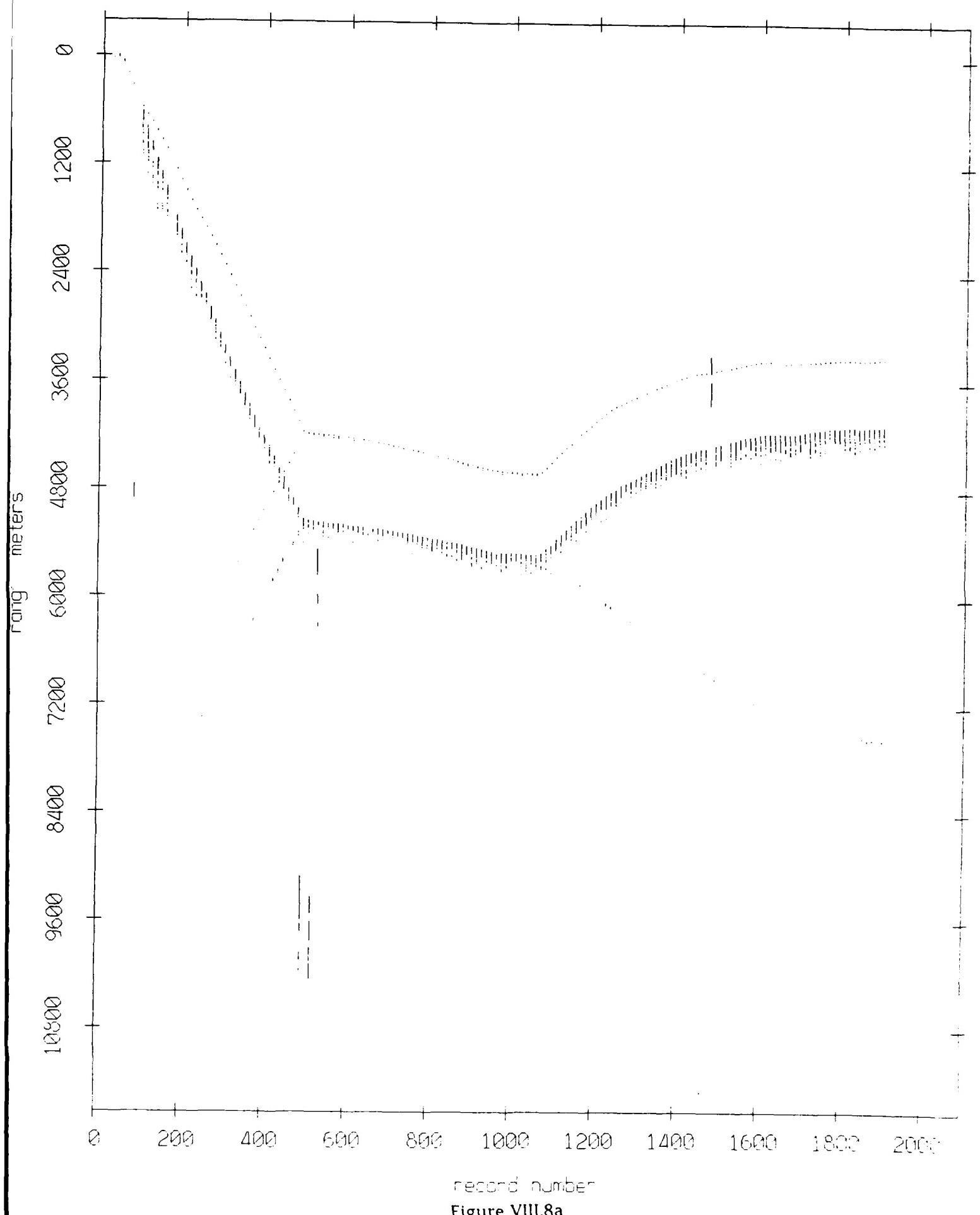
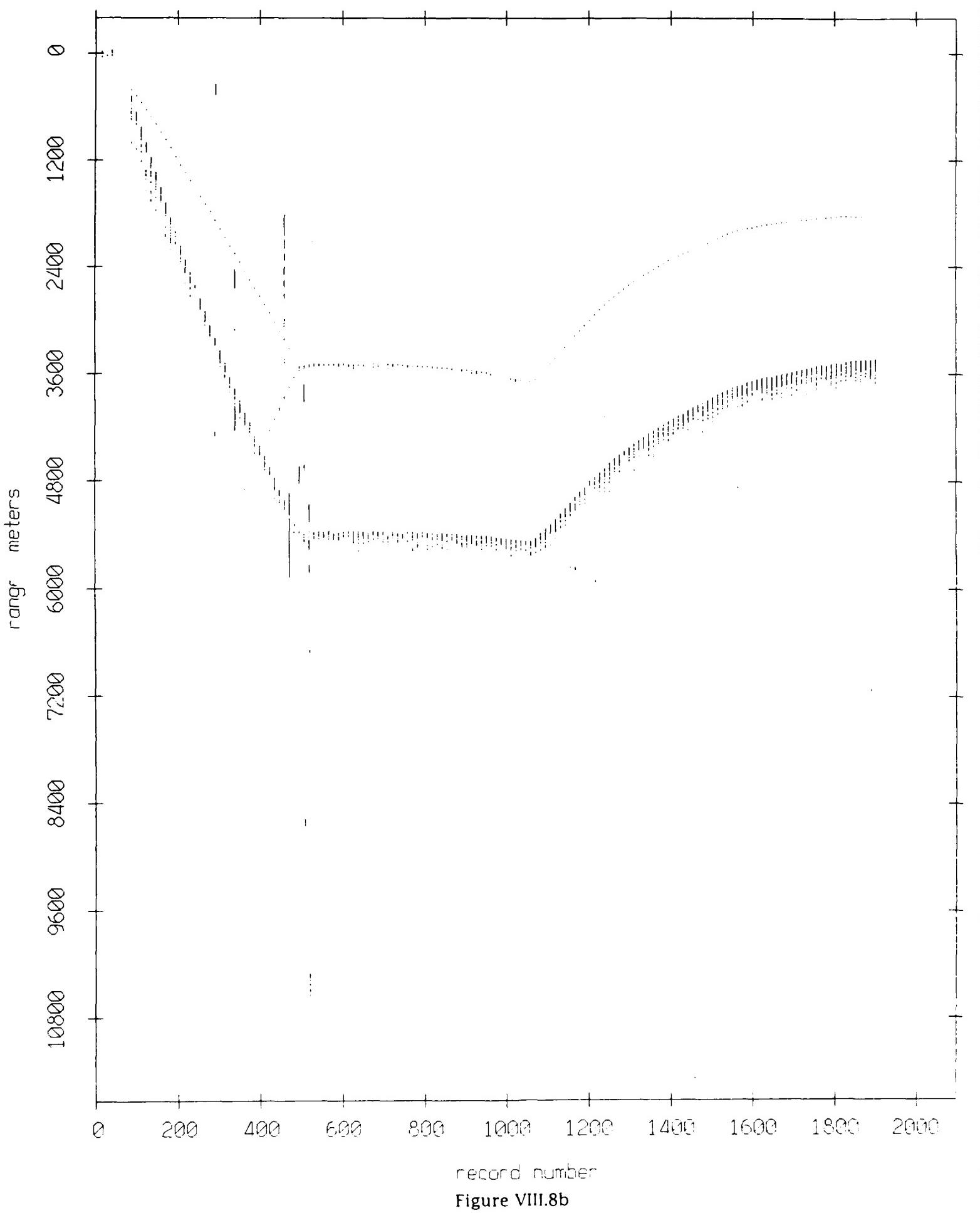


Figure VIII.8a

Float 8, September 1987 Sea Trip: range from float 2



Float 8, September 1987 Sea Trip: range from float 3

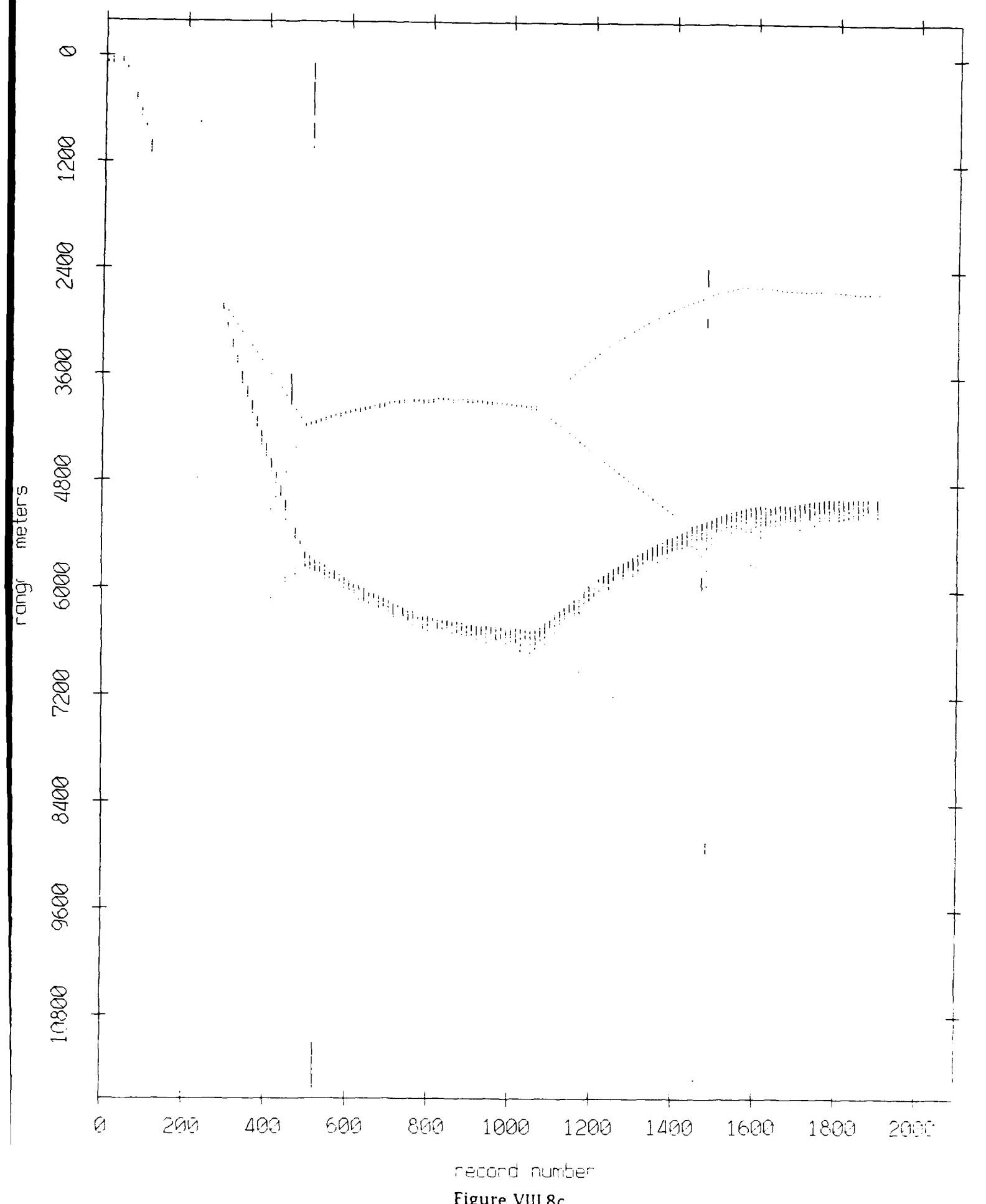


Figure VIII.8c

Float 8, September 1987 Sea Trip: range from float 4

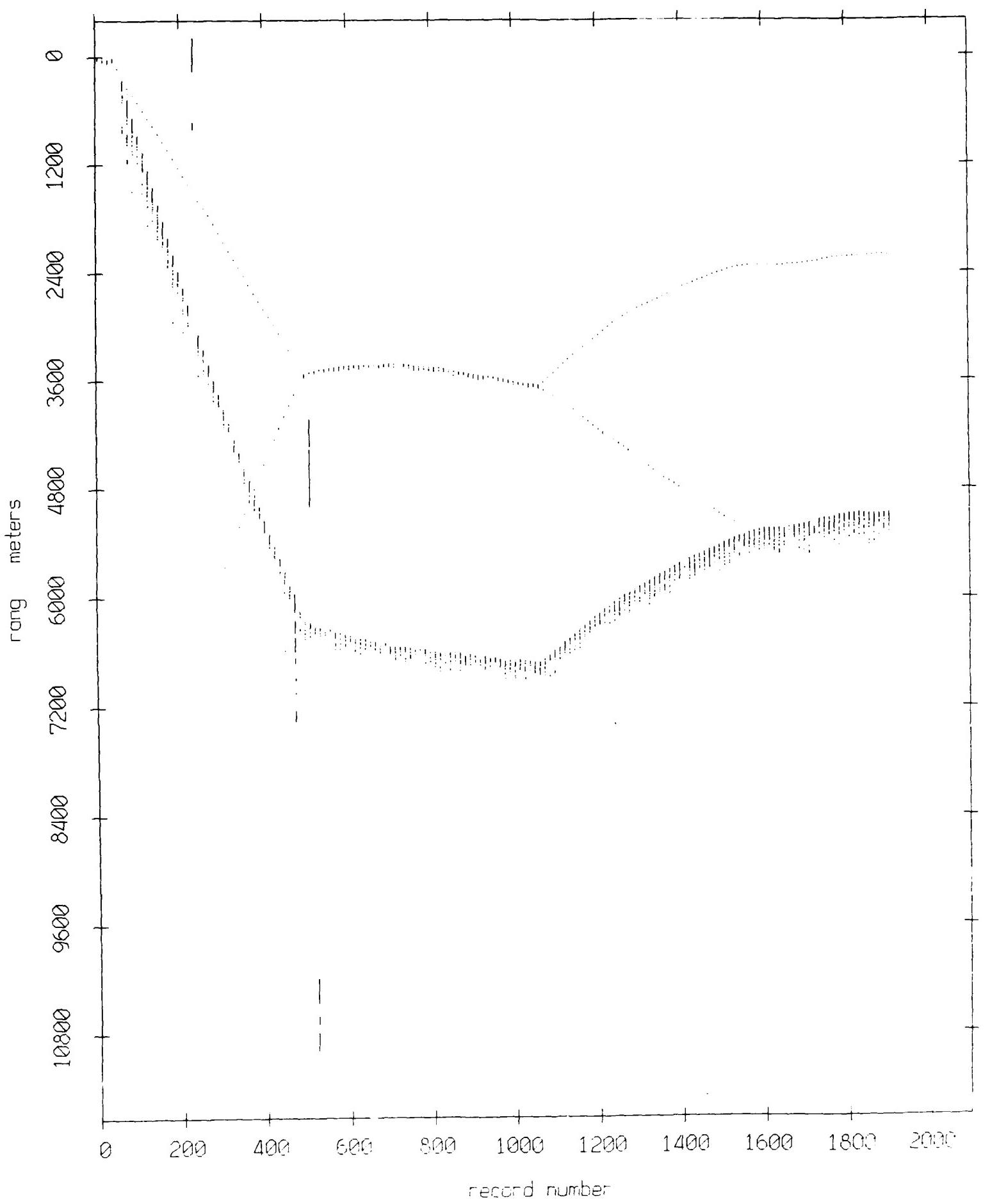


Figure VIII.8d

Float 8, September 1987 Sea Trip: range from float 5

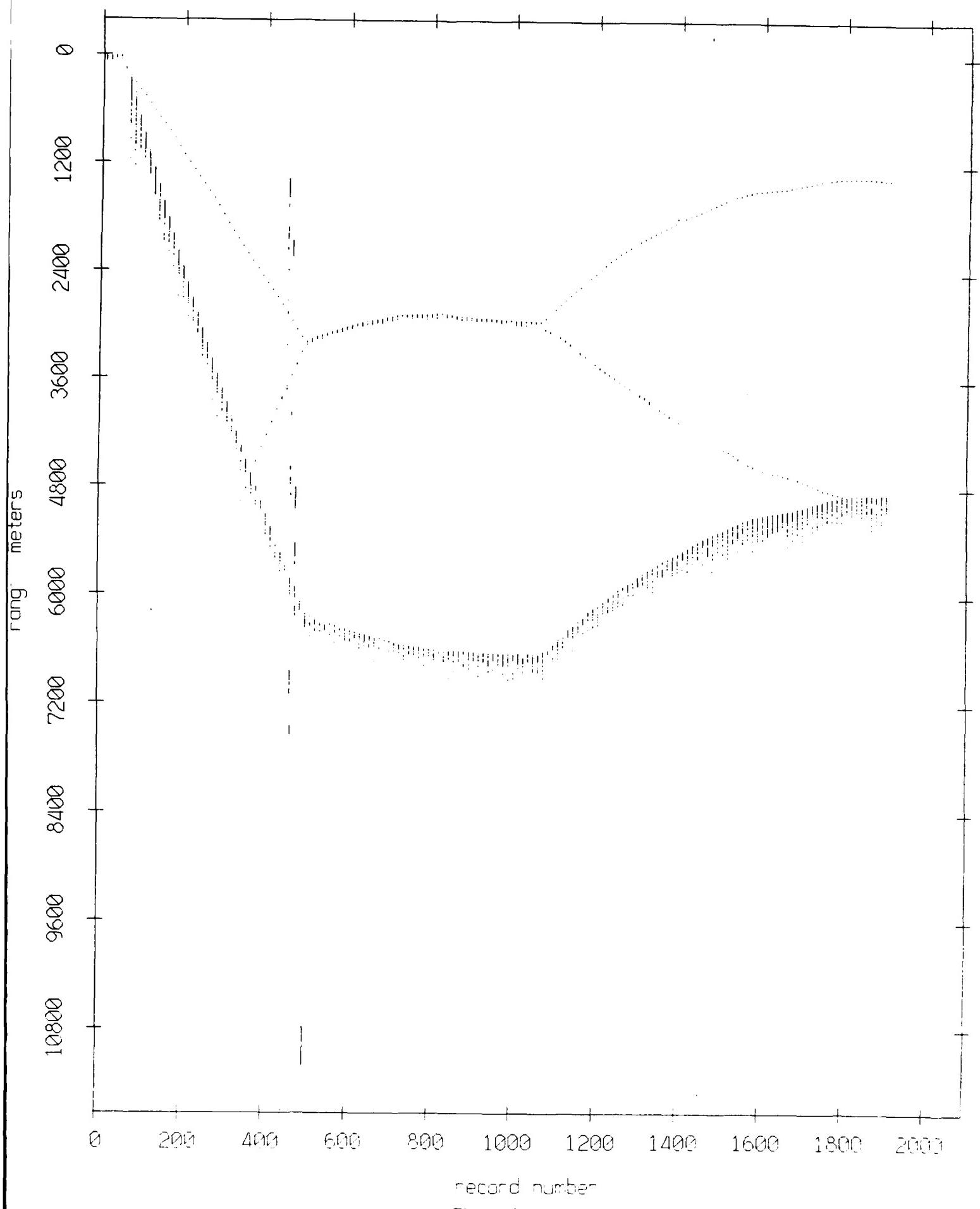


Figure VIII.8e

Float 8, September 1987 Sea Trip: range from float 6

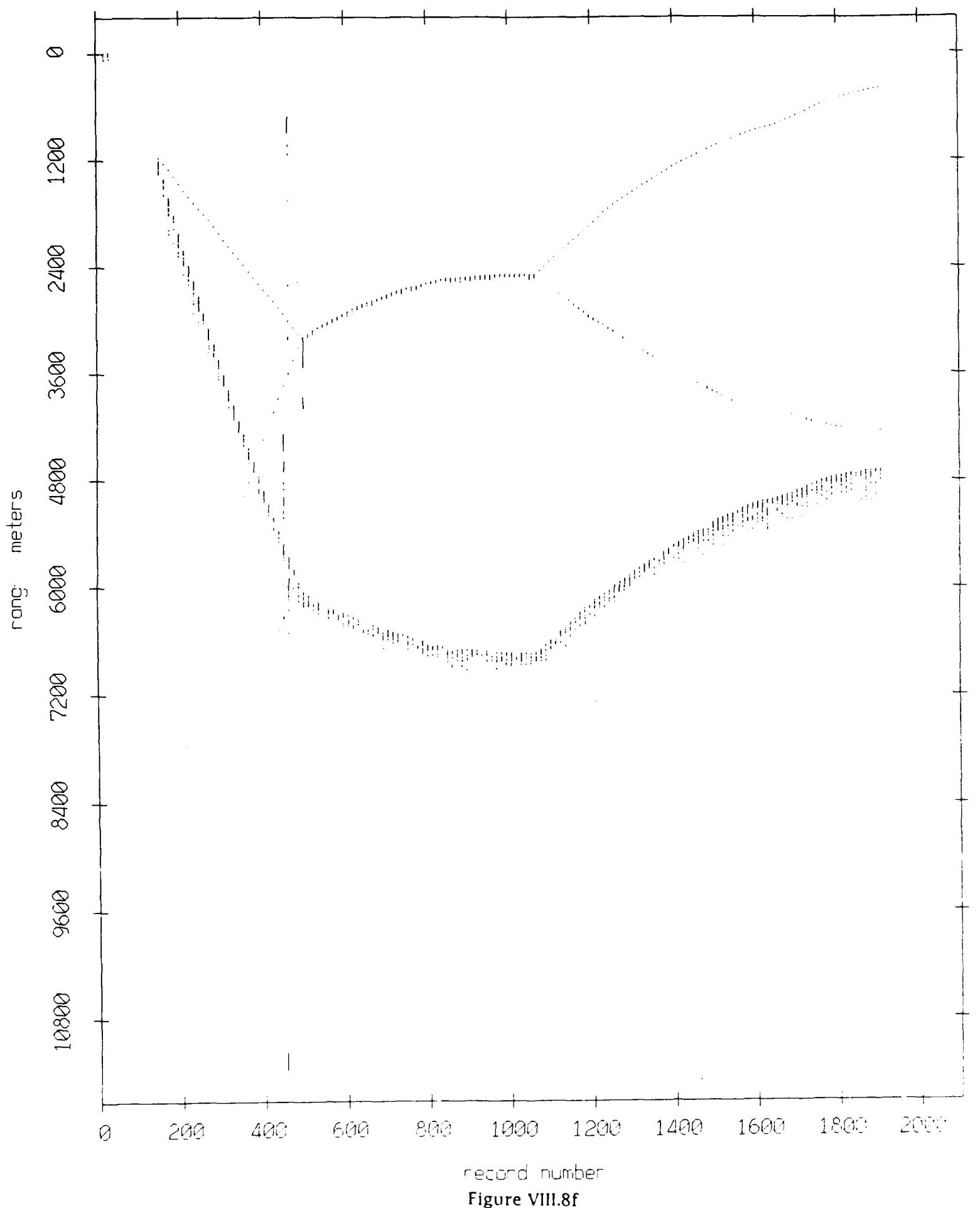


Figure VIII.8f

Float 8, September 1987 Sea Trip: range from float 7

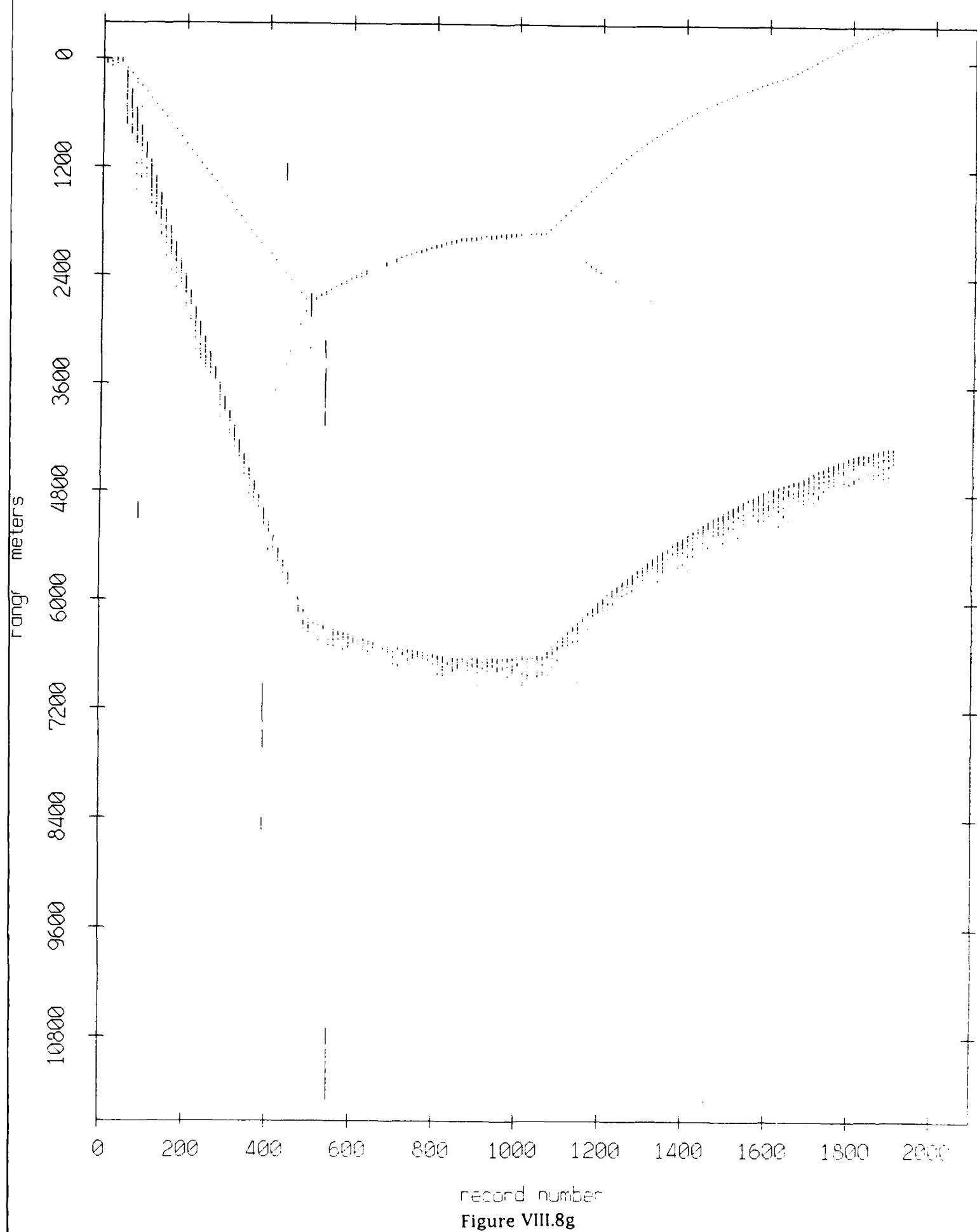
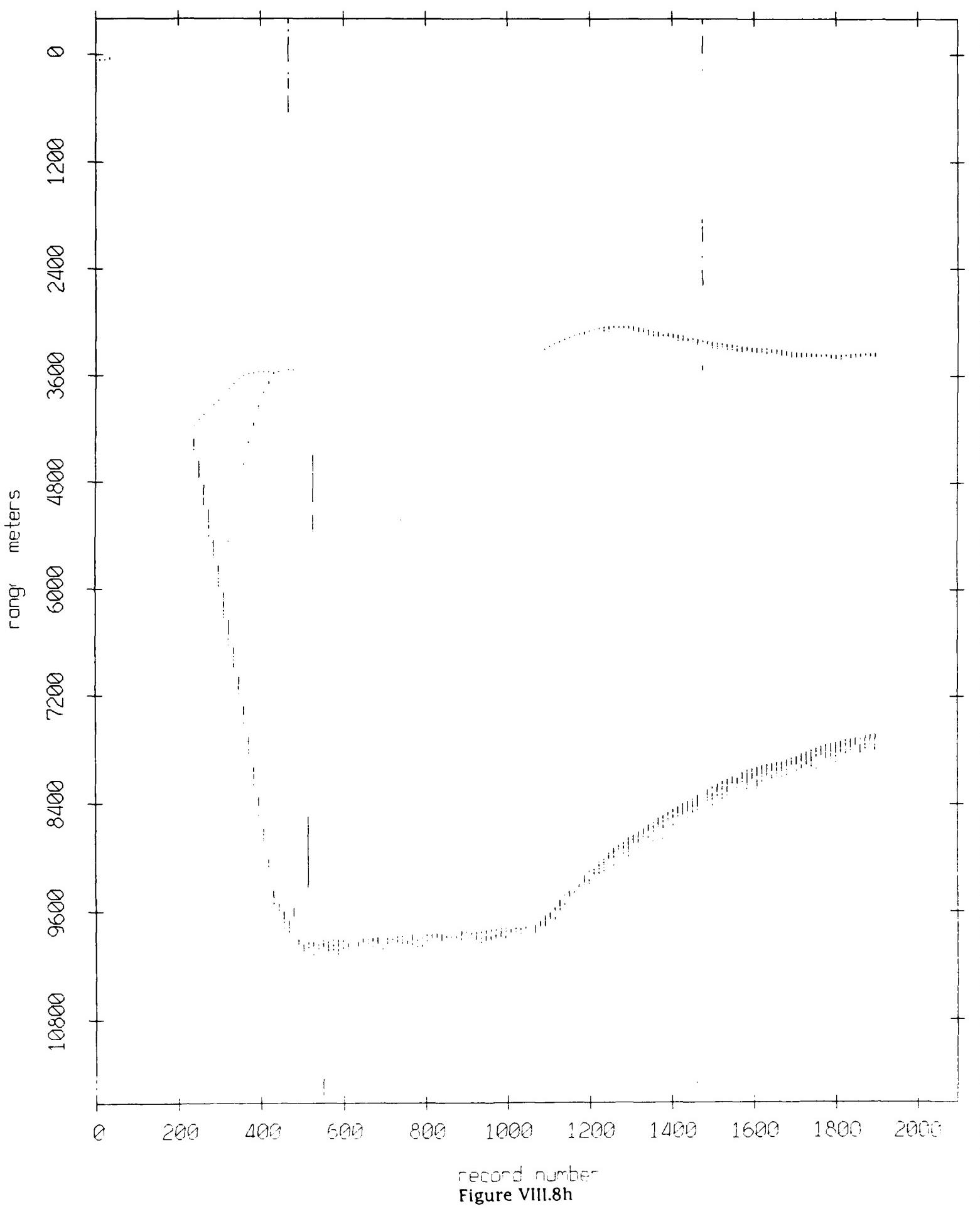
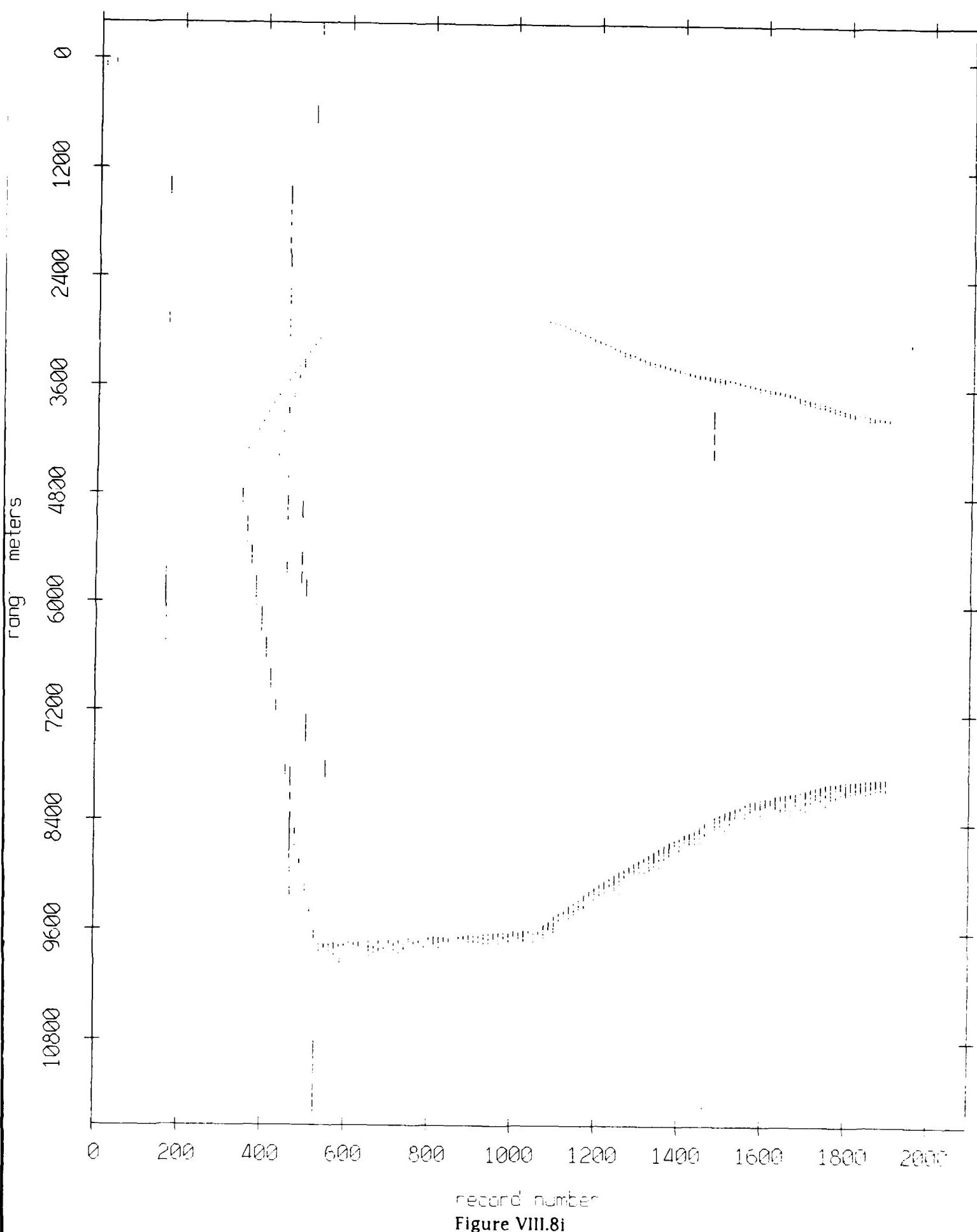


Figure VIII.8g

Float 8, September 1987 Sea Trip: range from float 9



Float 8, September 1987 Sea Trip: range from float 10



record number
Figure VIII.8i

Float 8, September 1987 Sea Trip: range from float 11

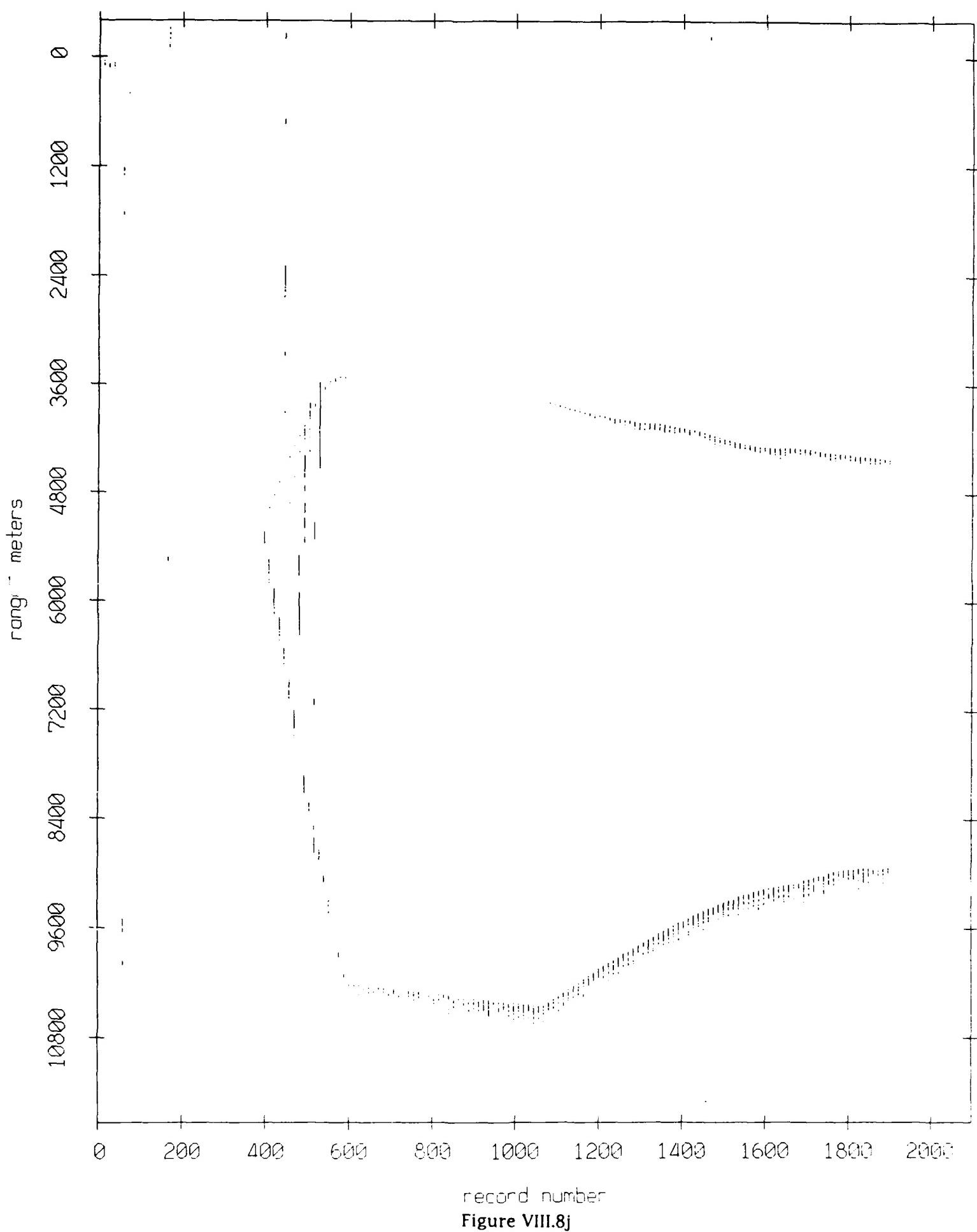


Figure VIII.8j

Float 9, September 1987 Sea Trip: range from float 0

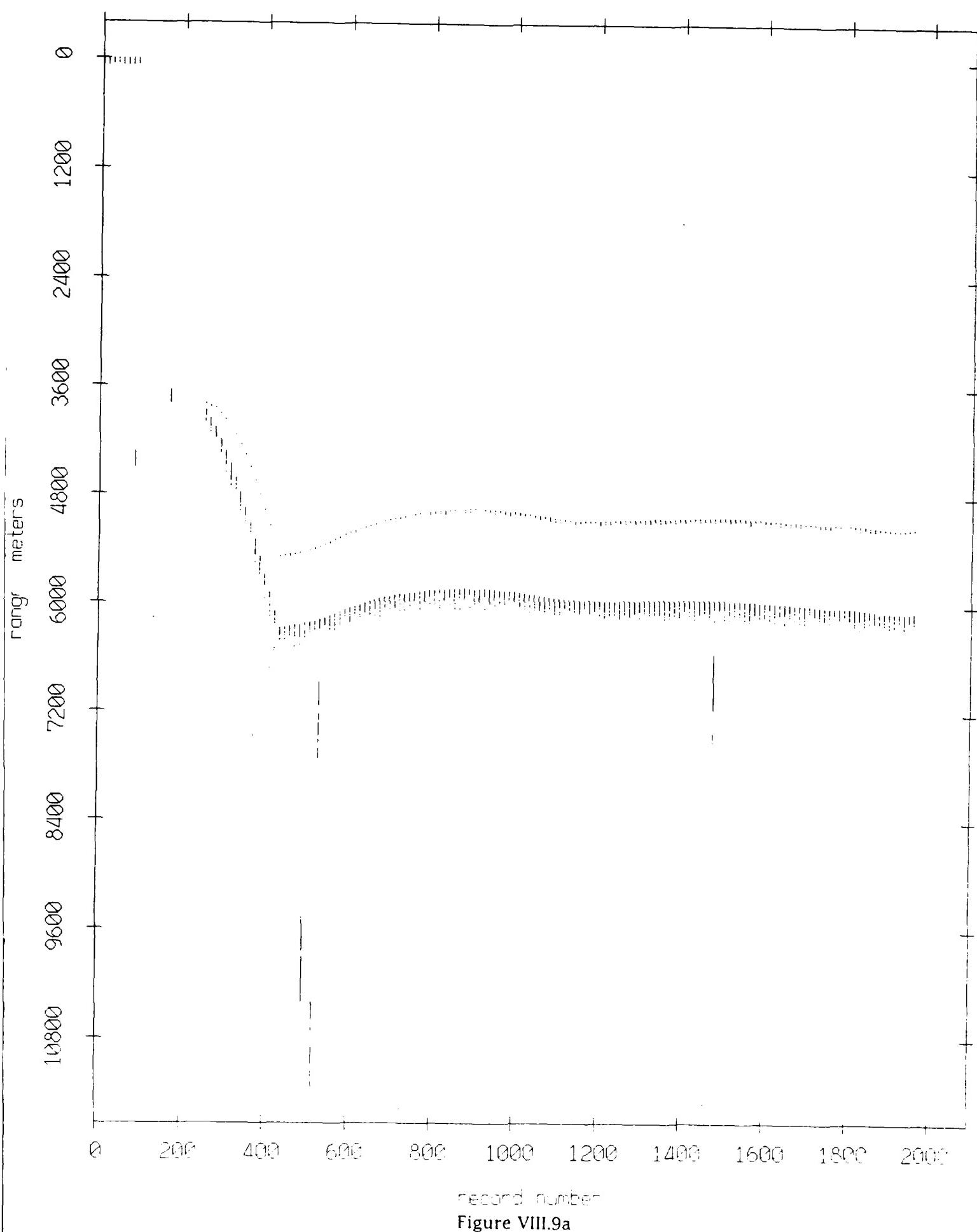


Figure VIII.9a

Float 9, September 1987 Sea Trip: range from float 2

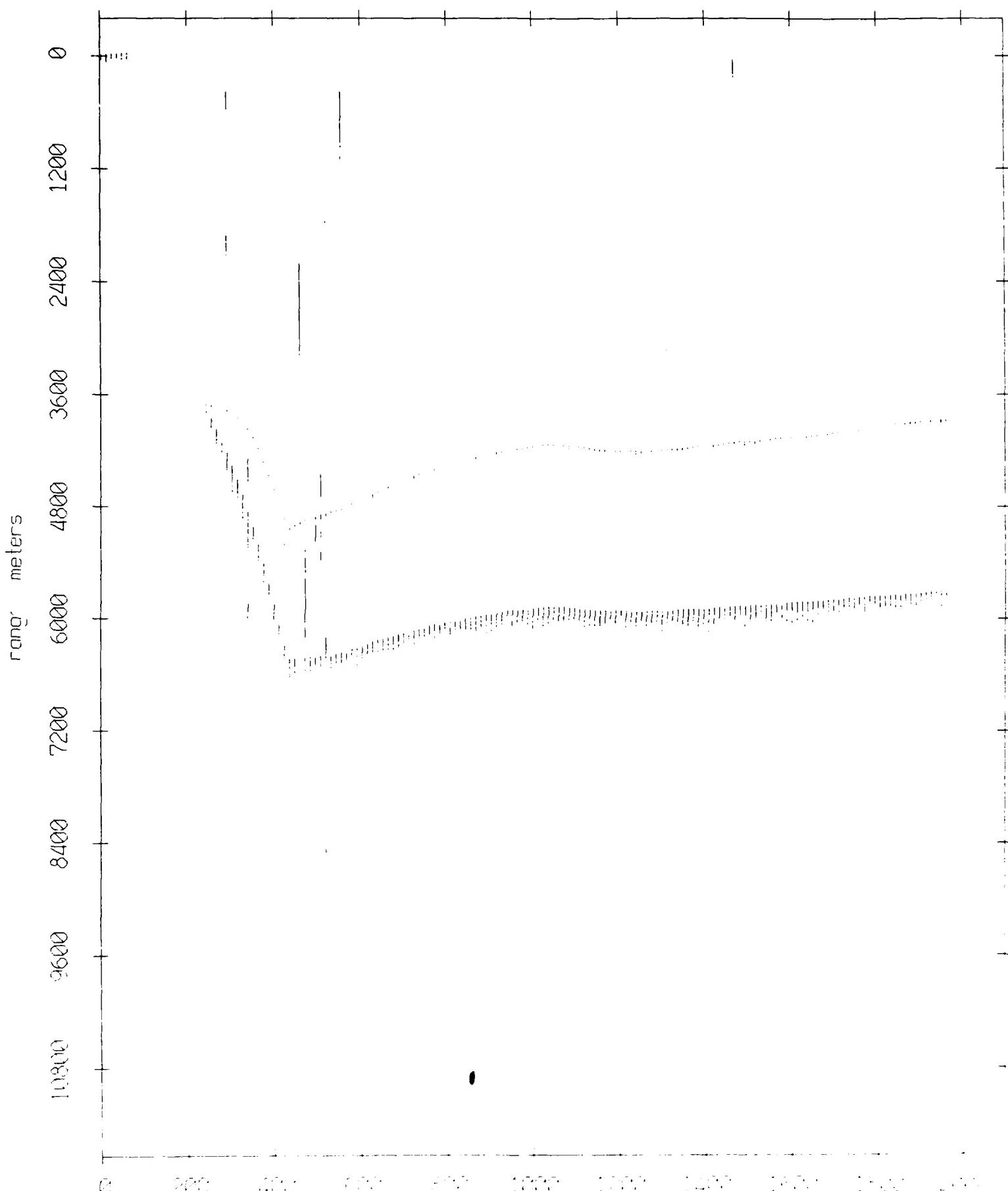


Figure VIII.9b

Float 9, September 1987 Sea Trip: range from float 3

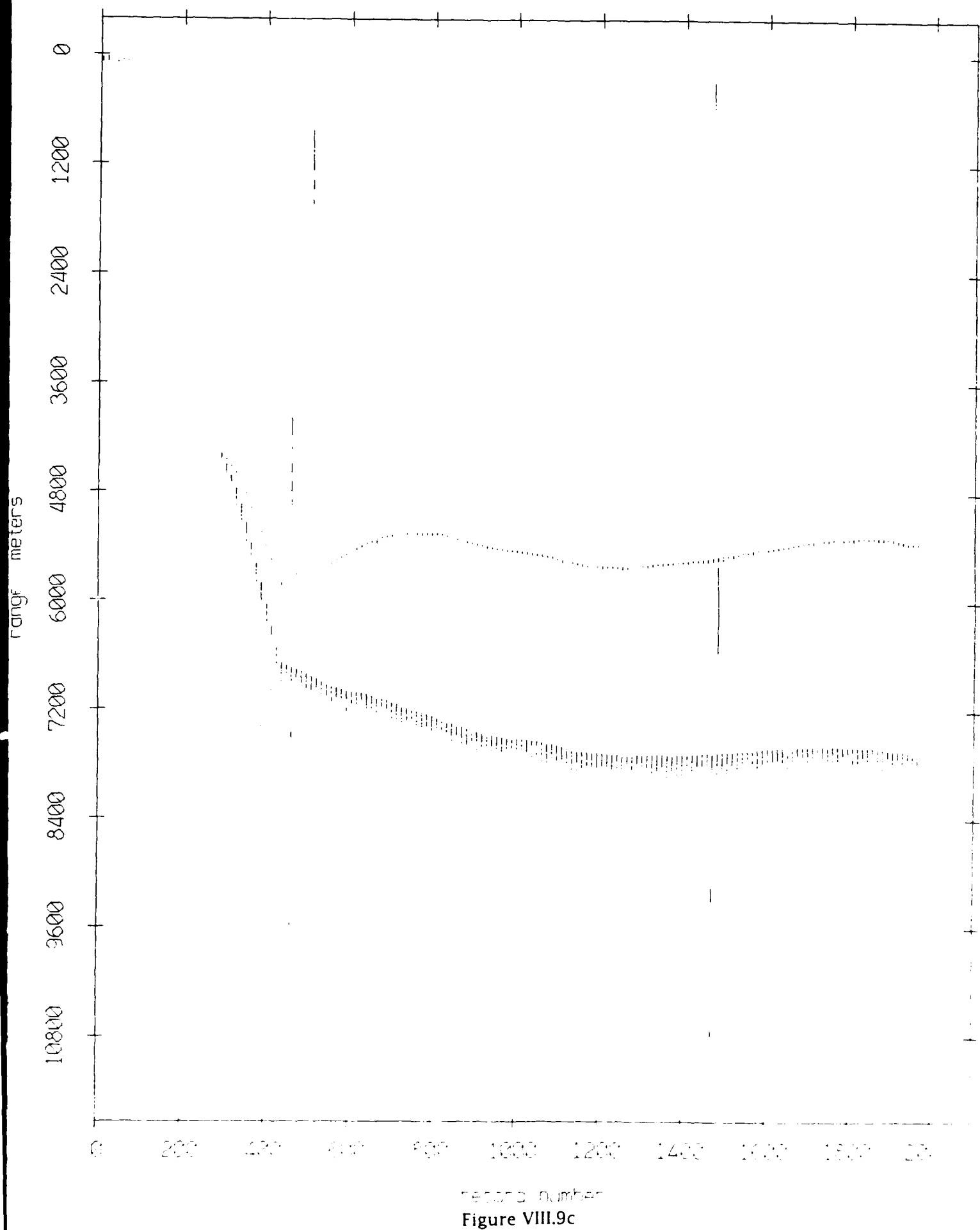
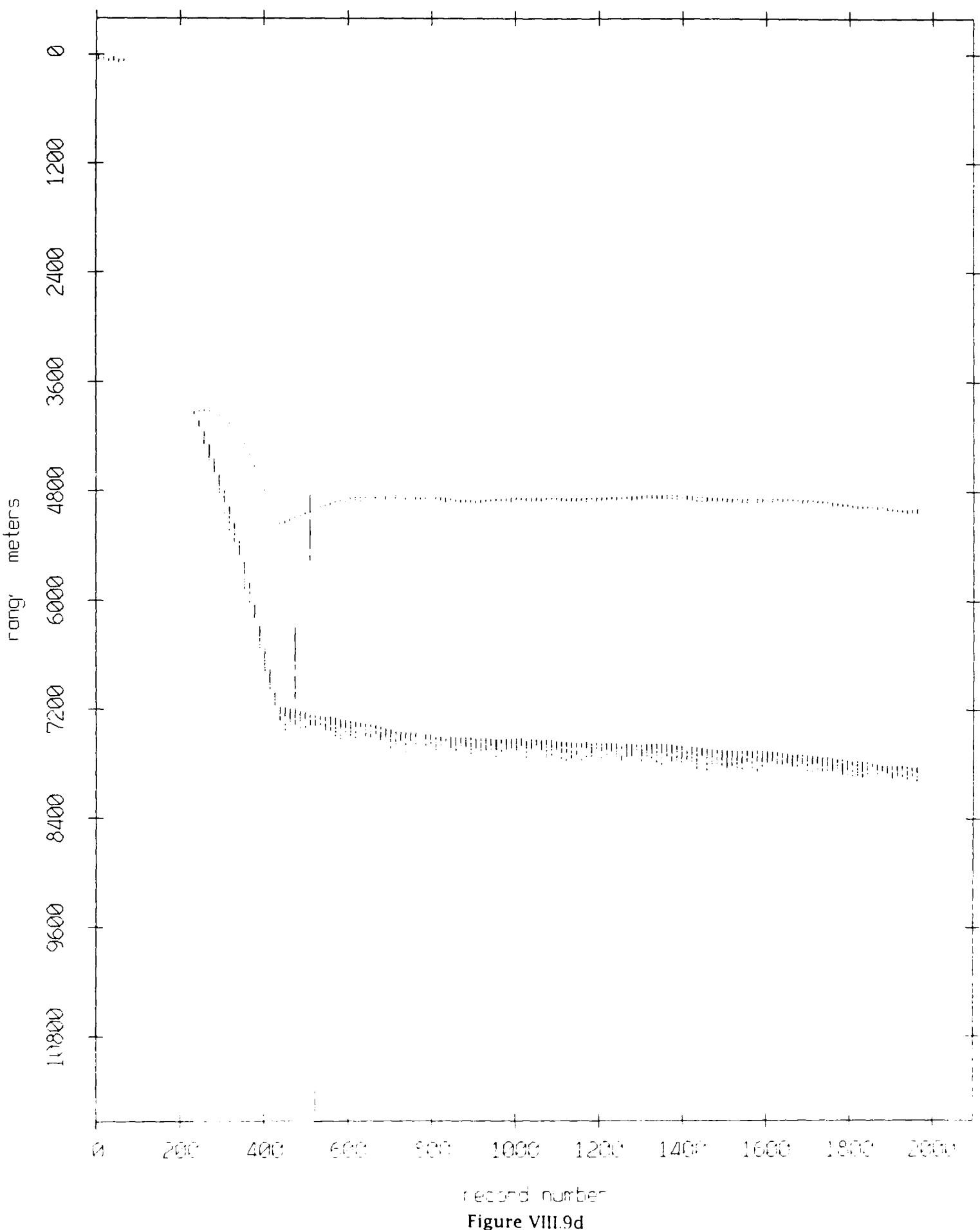


Figure VIII.9c

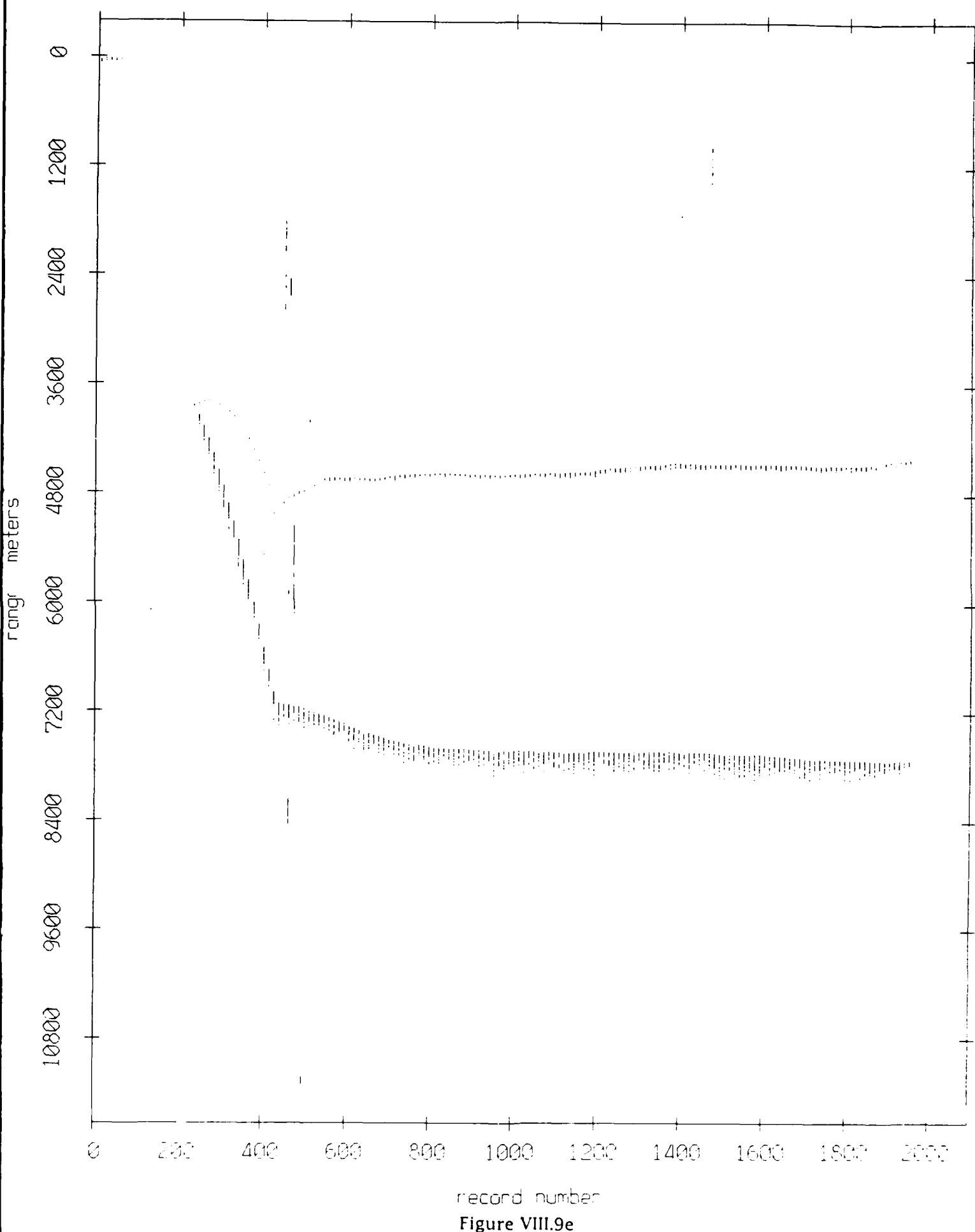
Float 9, September 1987 Sea Trip: range from float 4



record number

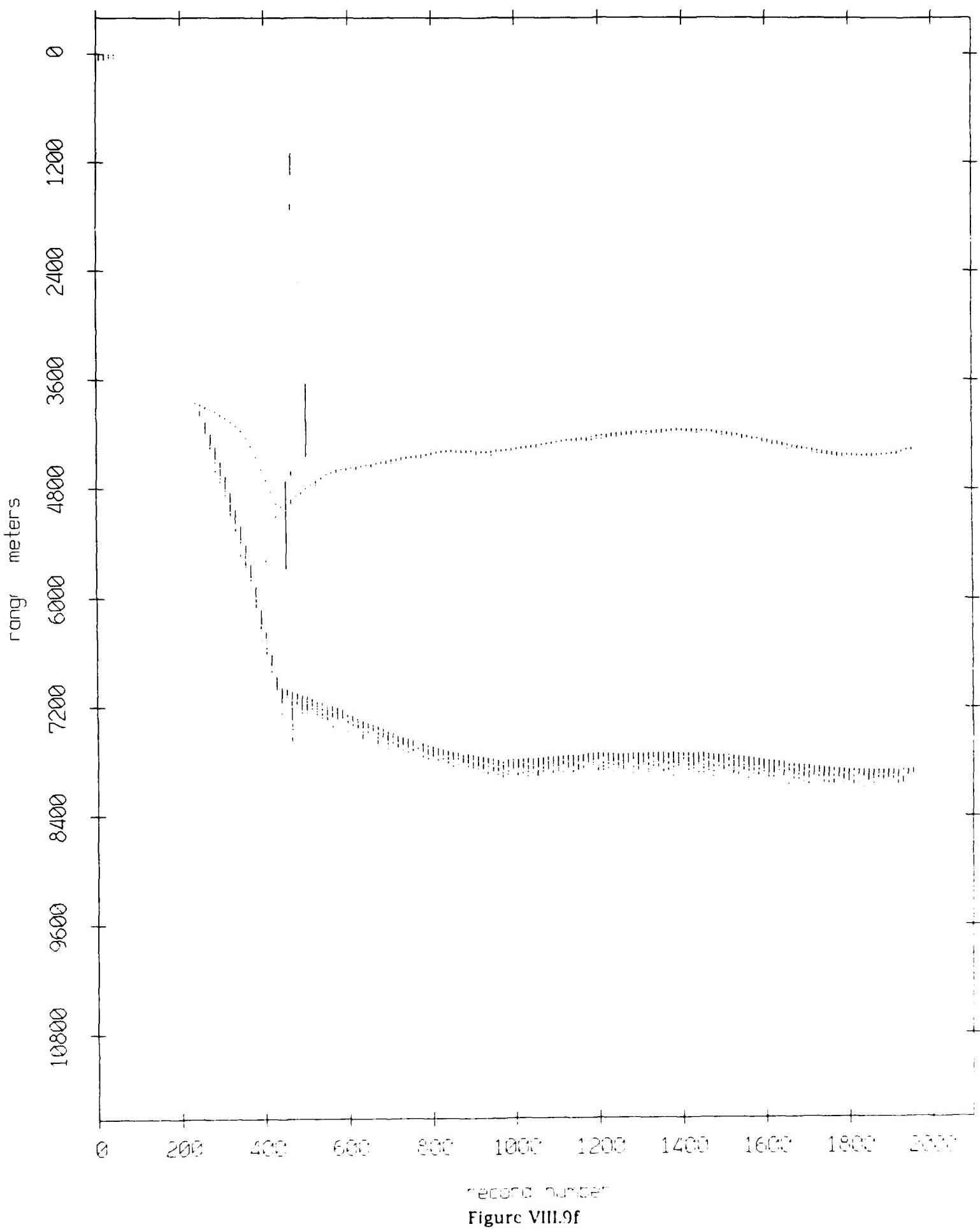
Figure VIII.9d

Float 9, September 1987 Sea Trip: range from float 5



record number
Figure VIII.9e

Float 9, September 1987 Sea Trip: range from float 6



record number

Figure VIII.9f

Float 9, September 1987 Sea Trip: range from float 7

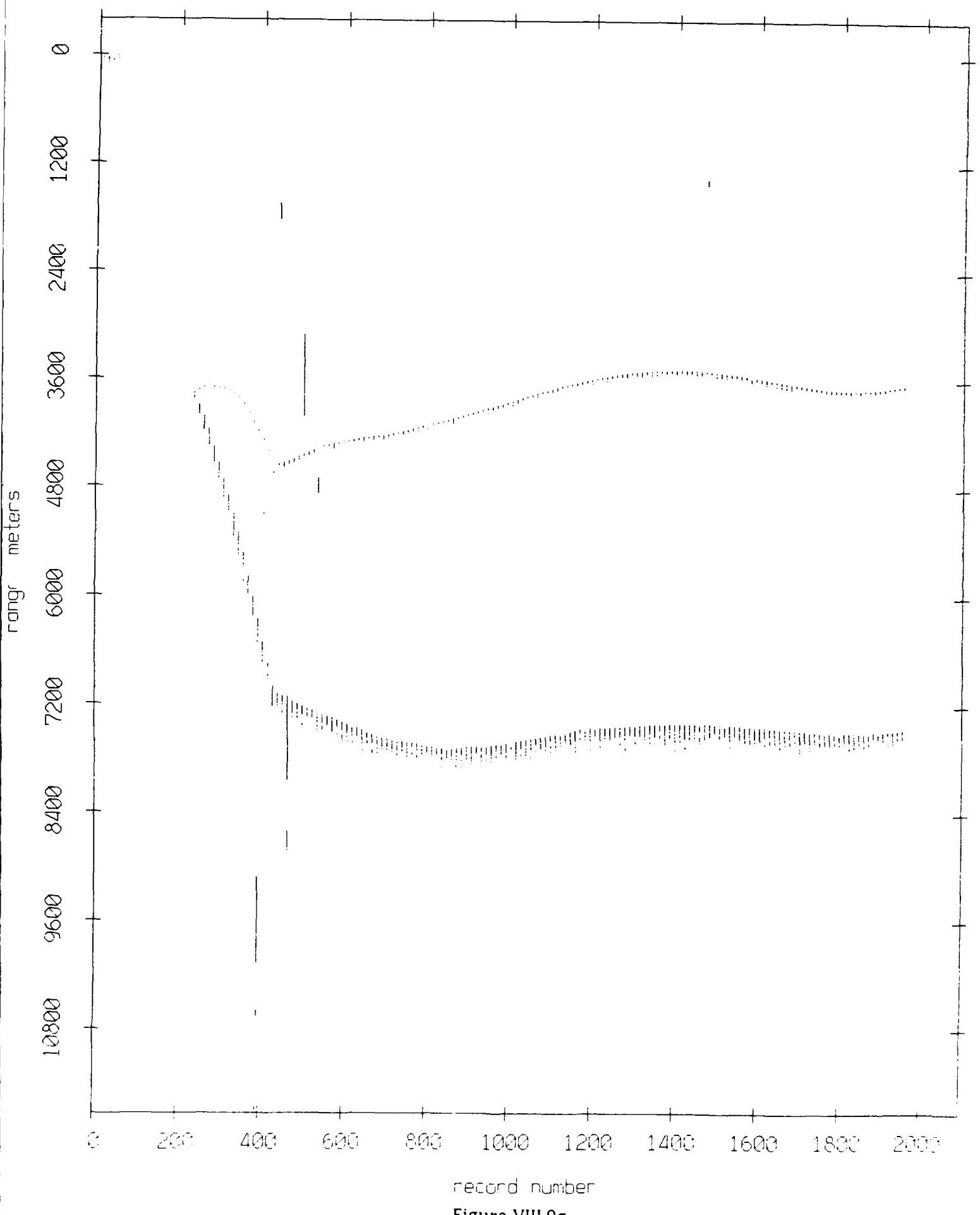


Figure VIII.9g

Float 9, September 1987 Sea Trip: range from float 8

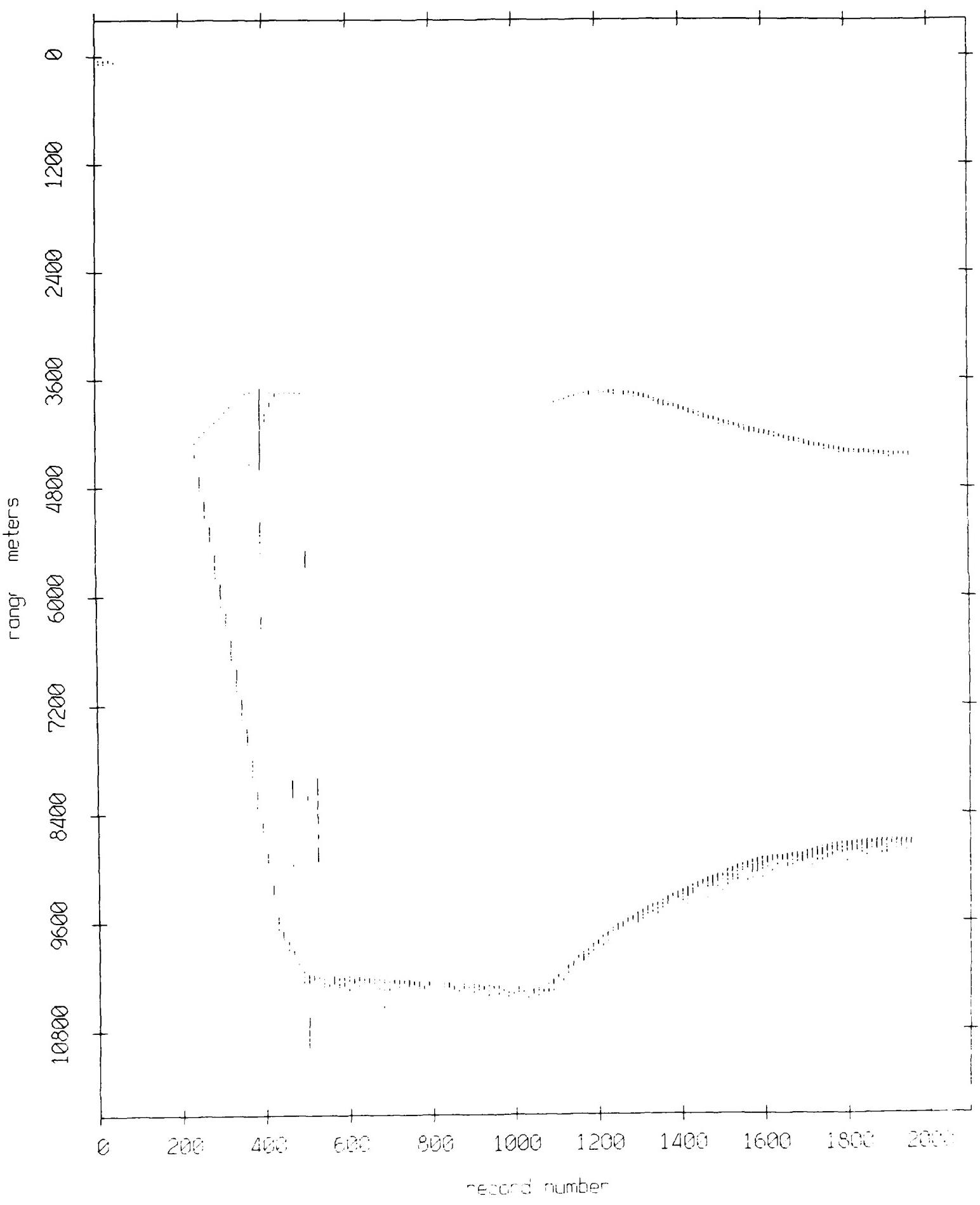


Figure VIII.9h

Float 9, September 1987 Sea Trip: range from float 10

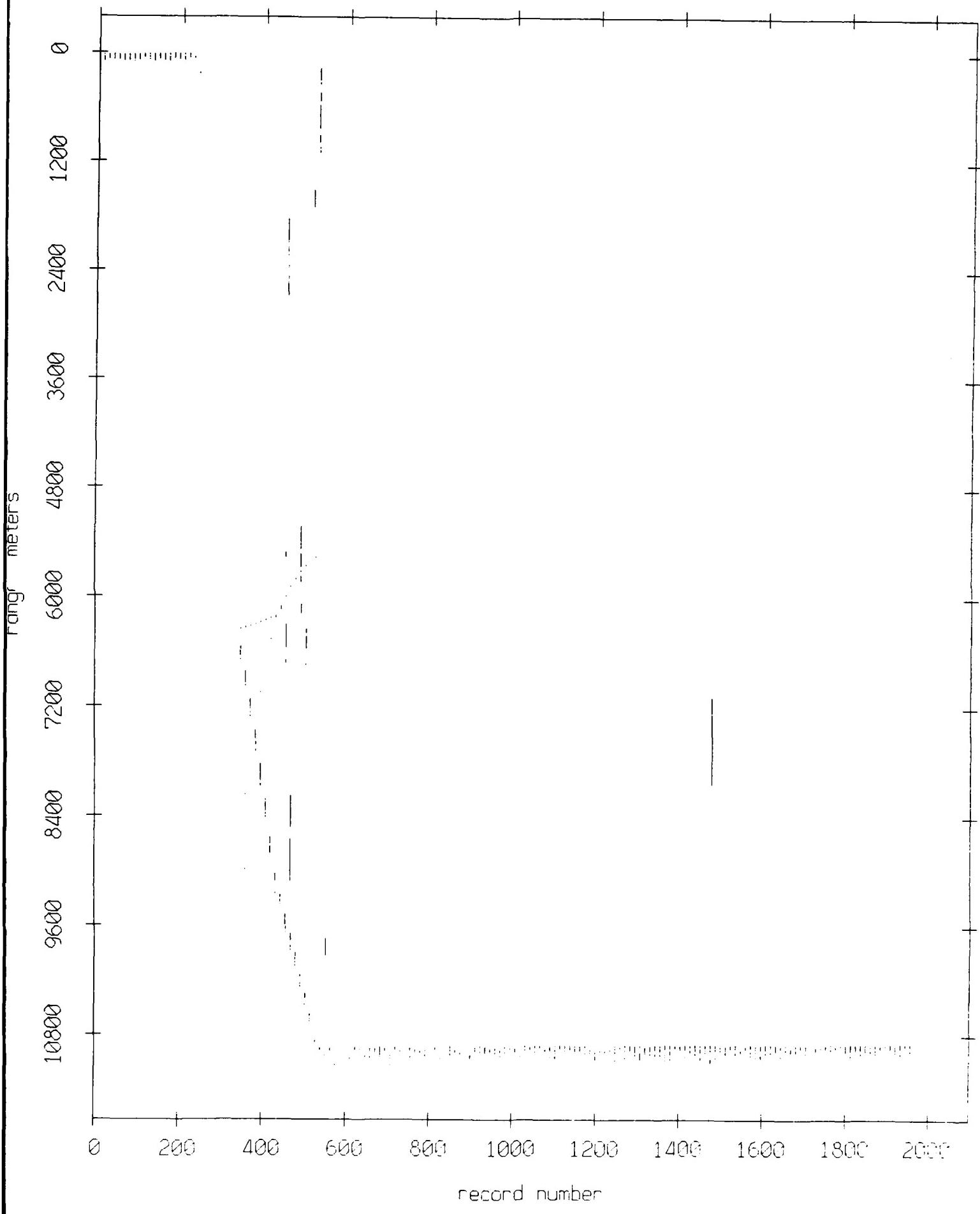


Figure VIII.9i

Float 9, September 1987 Sea Trip: range from float 11

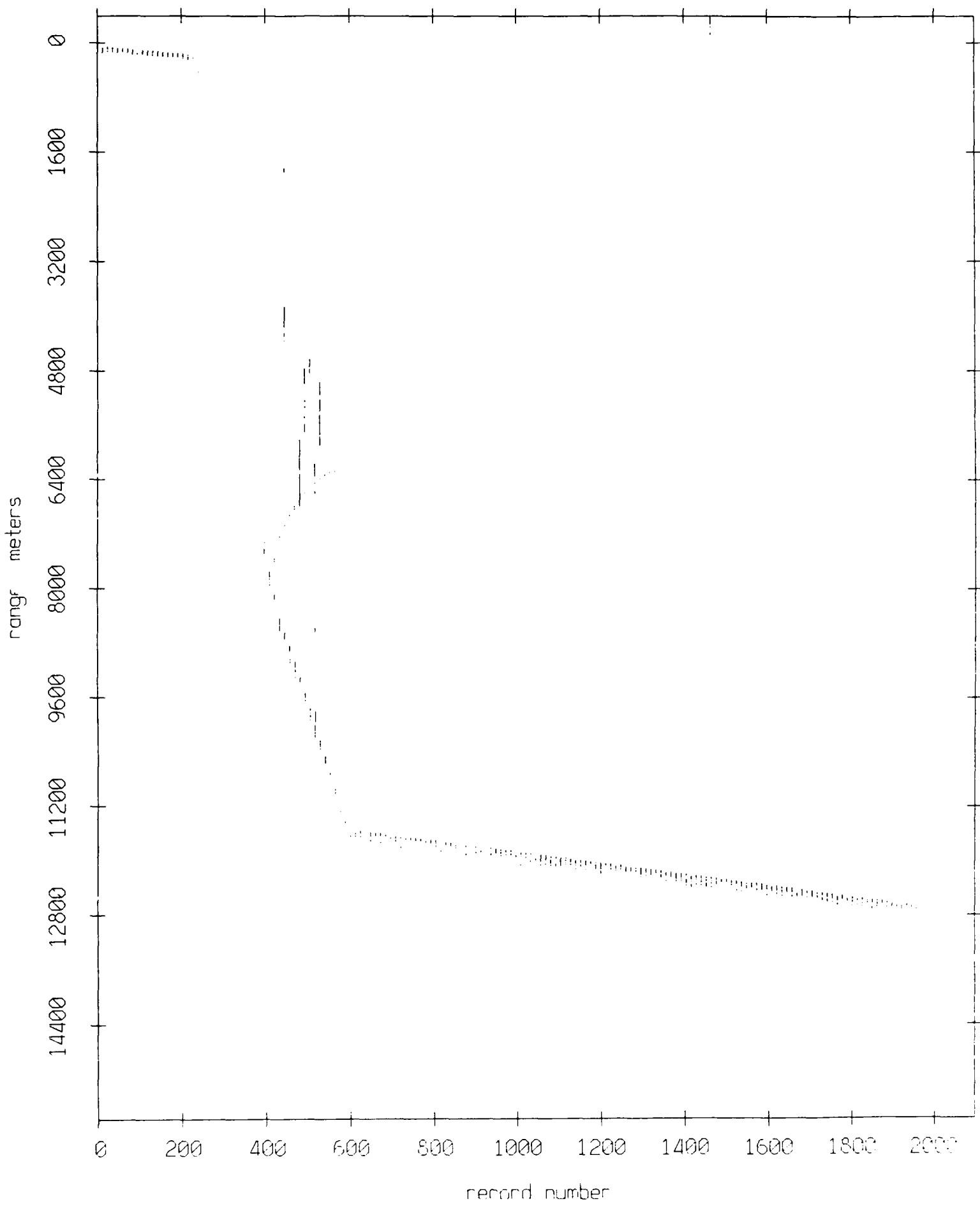


Figure VIII.9j

Float 10, September 1987 Sea Trip: range from float 0

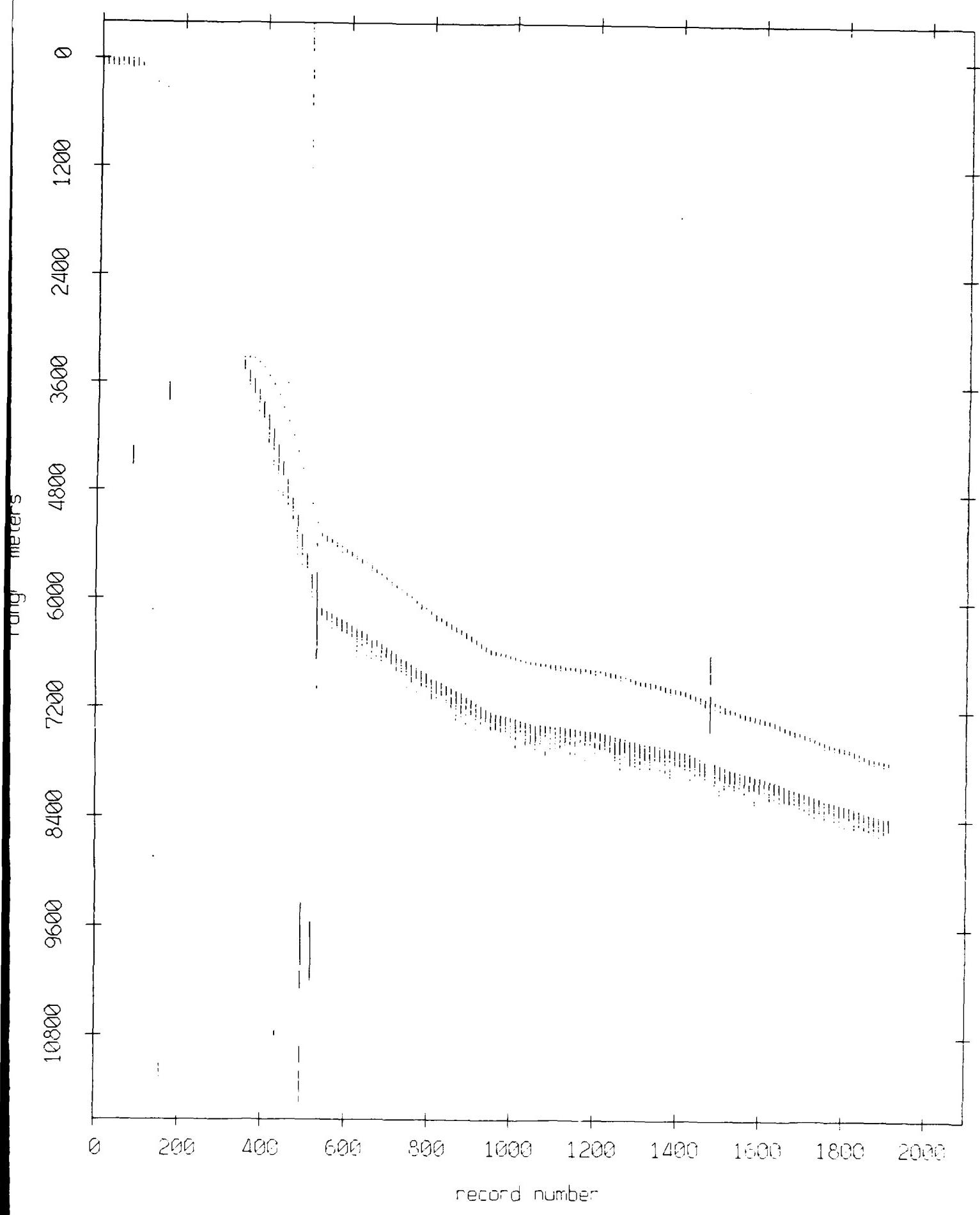


Figure VIII.10a

Float 10, September 1987 Sea Trip: range from float 2

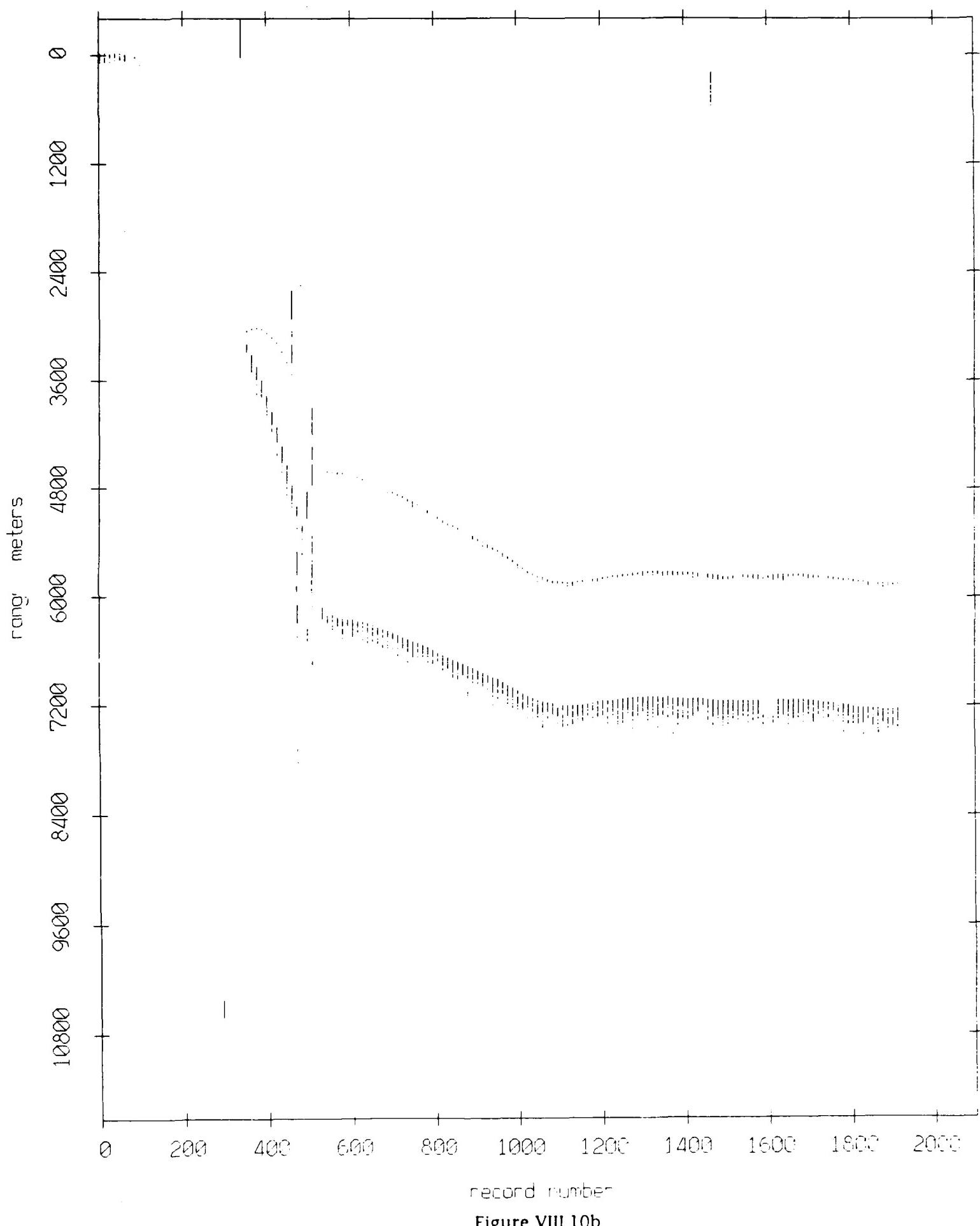


Figure VIII.10b

Float 10, September 1987 Sea Trip: range from float 3

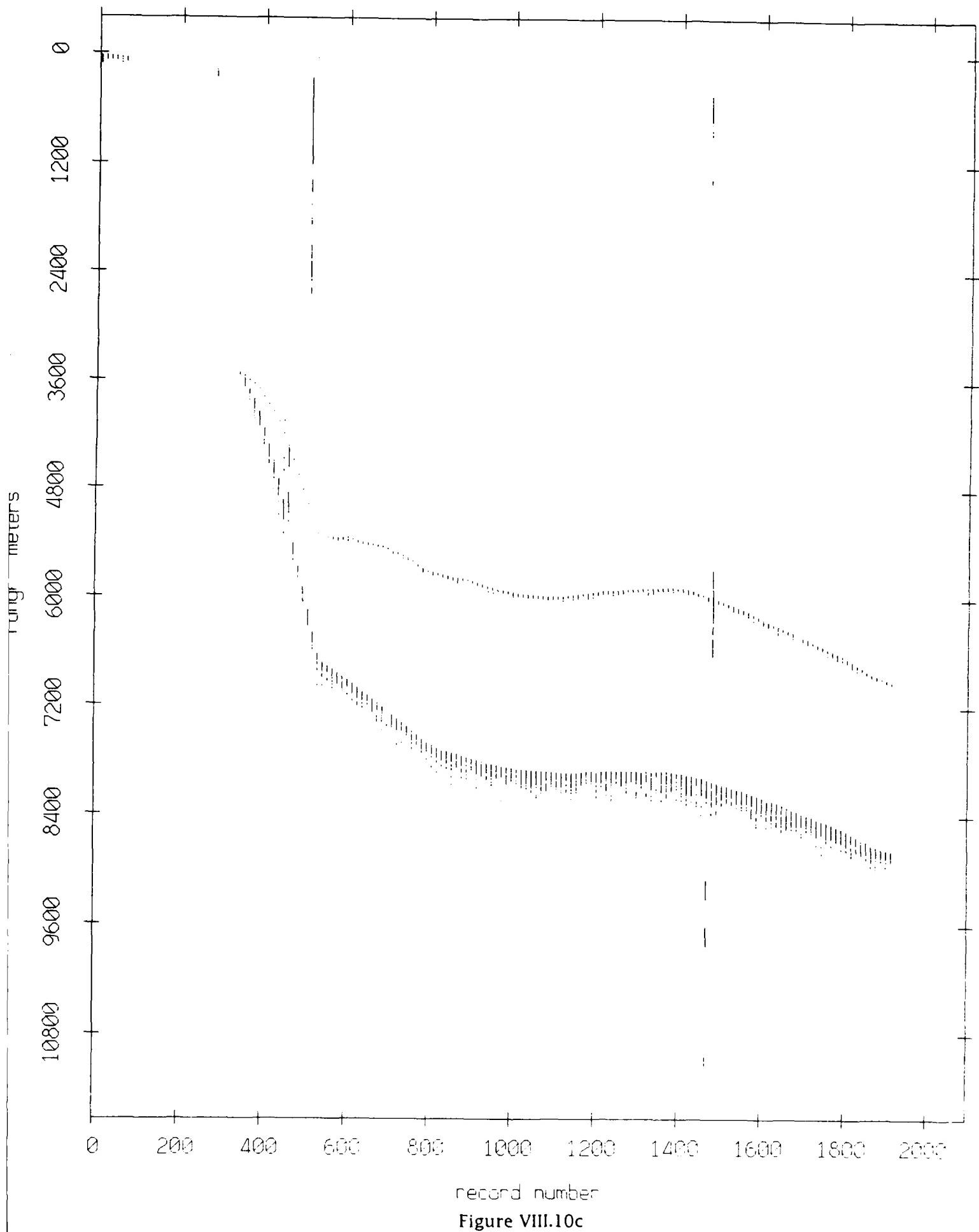


Figure VIII.10c

Float 10, September 1987 Sea Trip: range from float 4

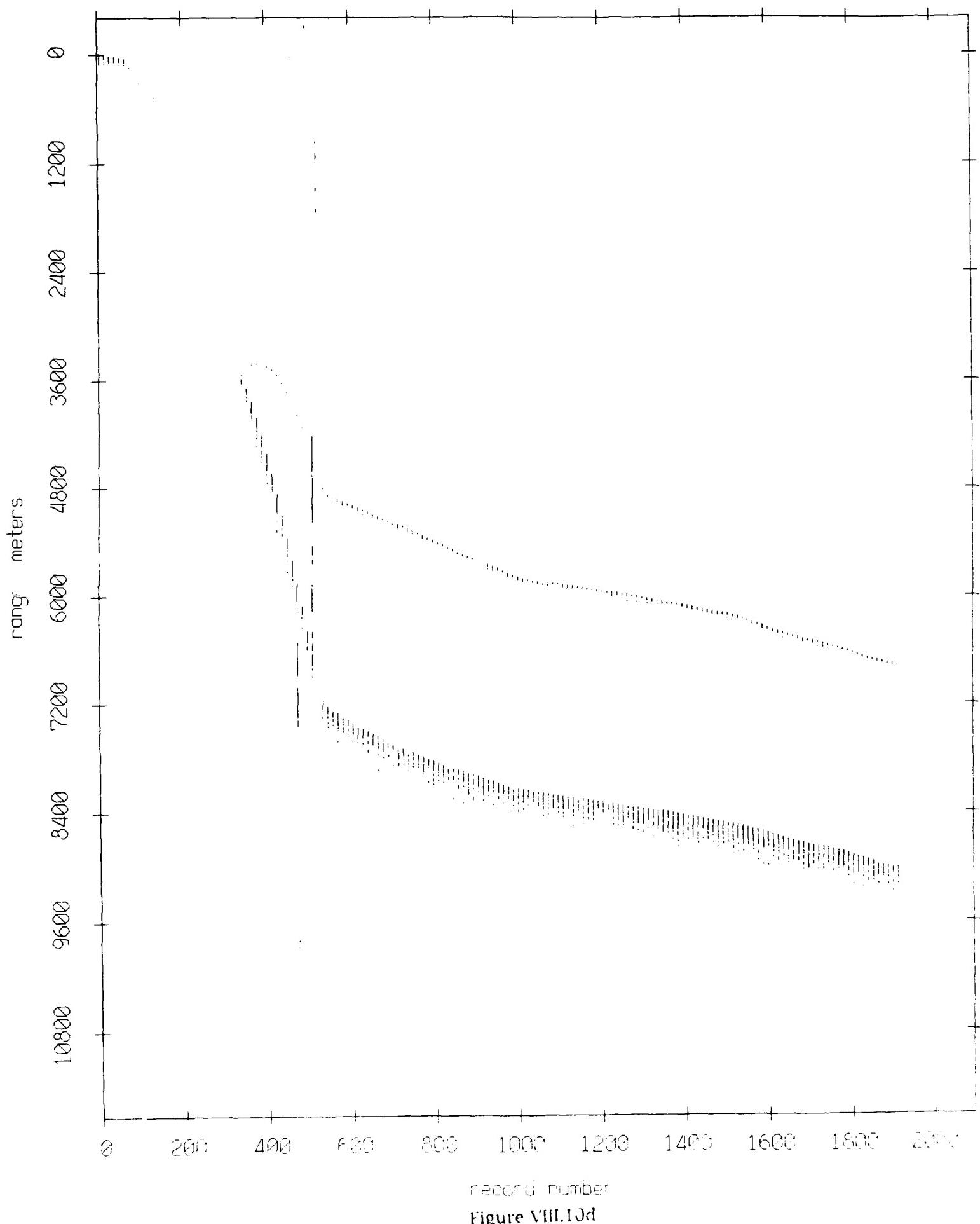
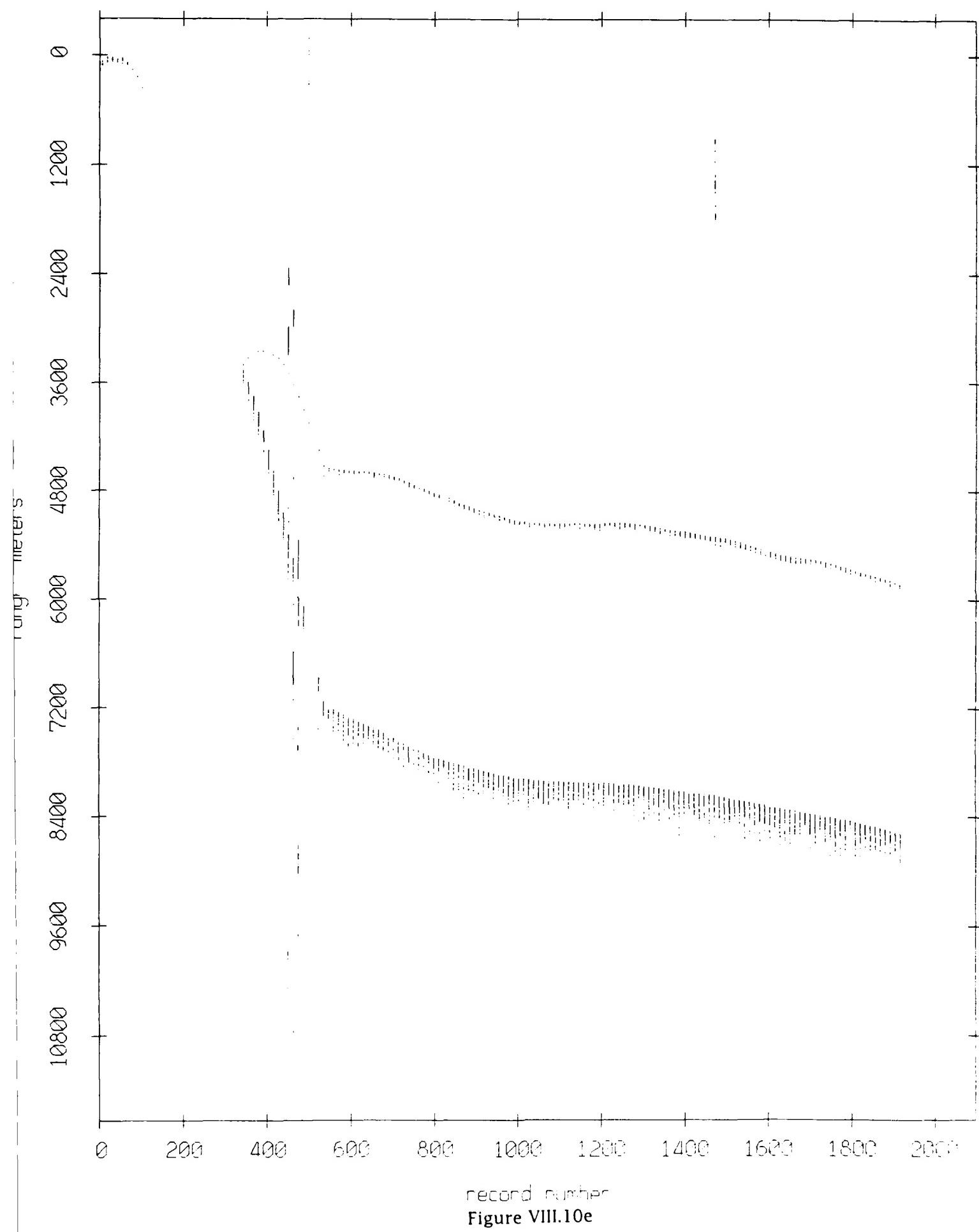
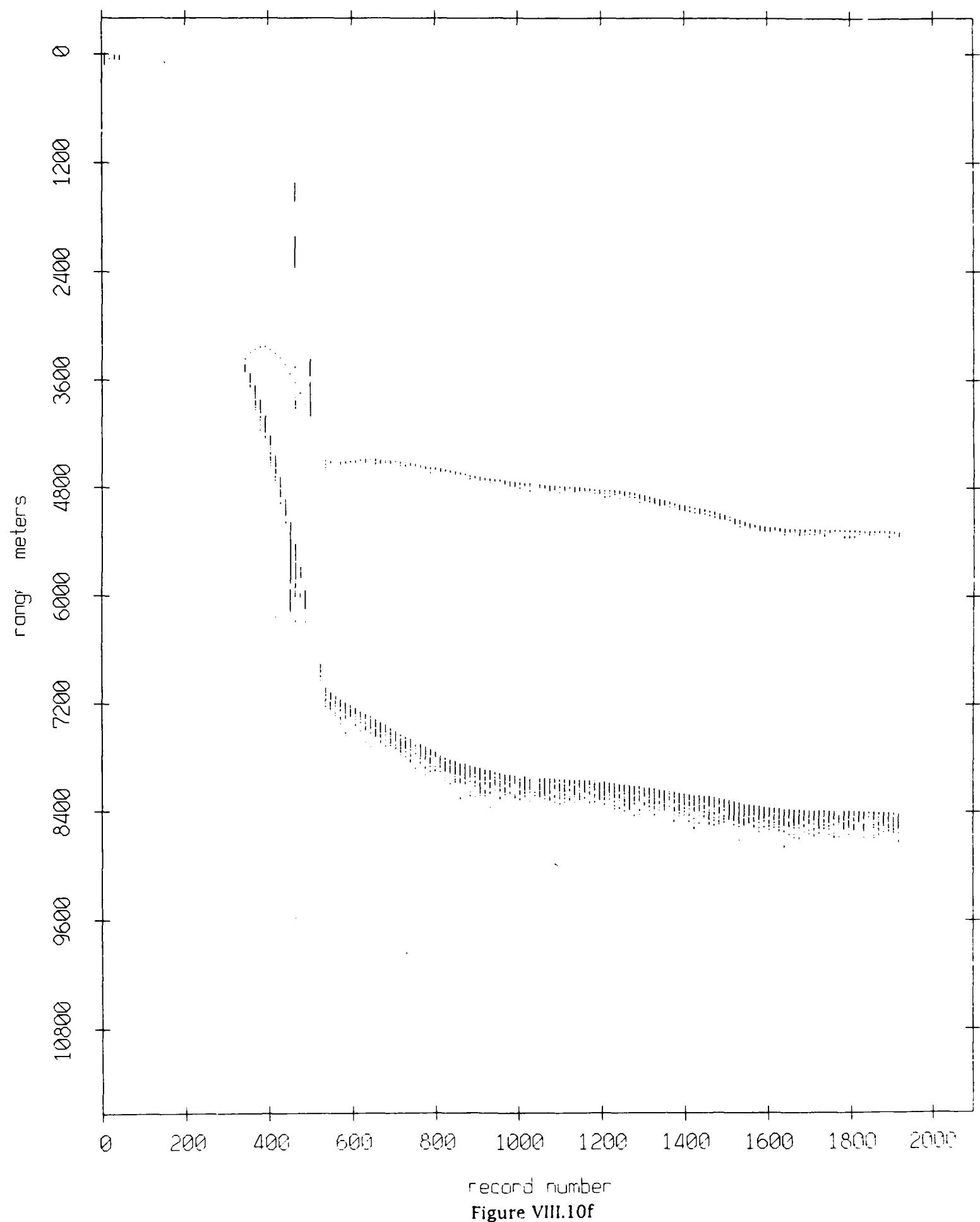


Figure VIII.10d

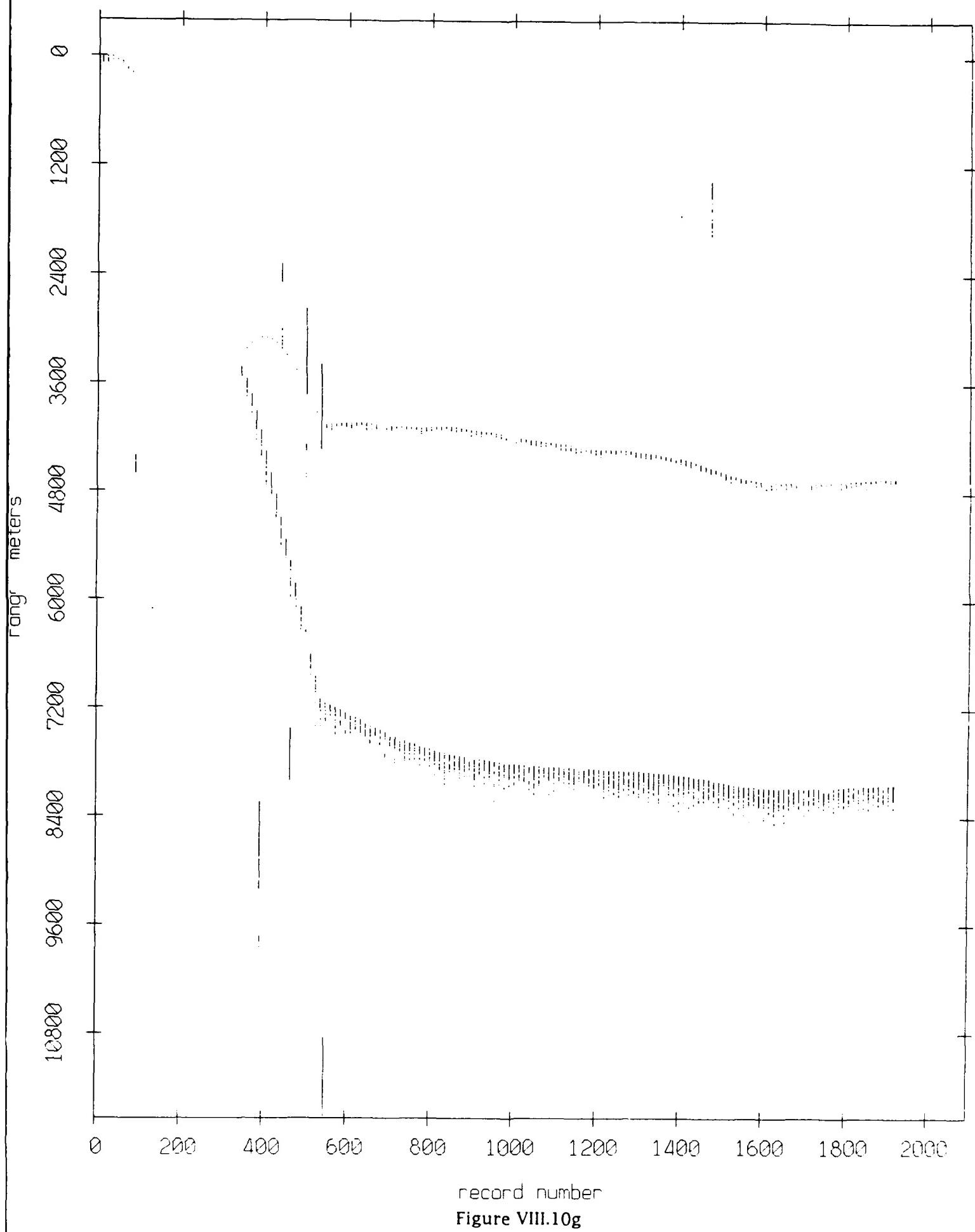
Float 10, September 1987 Sea Trip: range from float 5



Float 10, September 1987 Sea Trip: range from float 6



Float 10, September 1987 Sea Trip: range from float 7



record number
Figure VIII.10g

Float 10, September 1987 Sea Trip: range from float 8

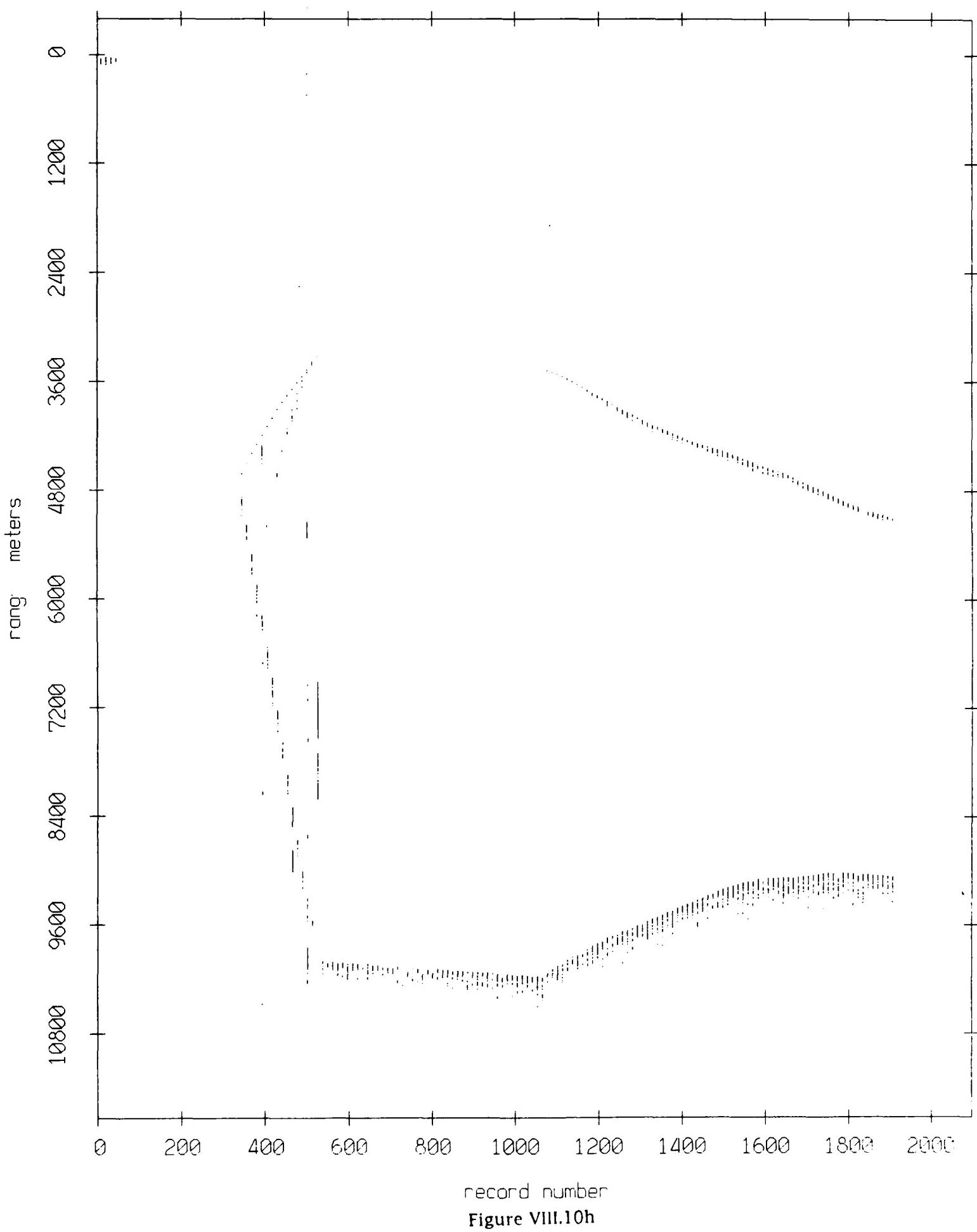
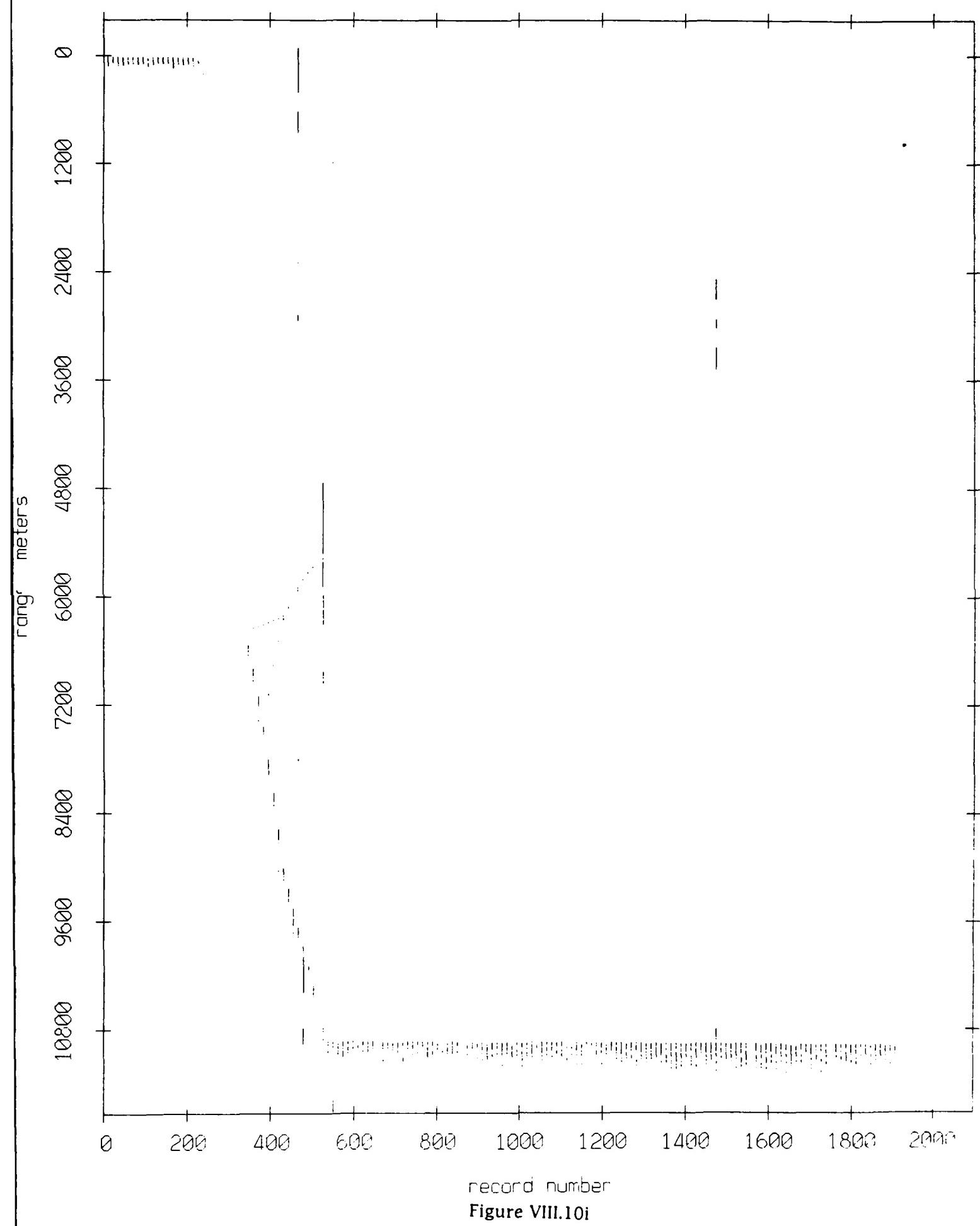
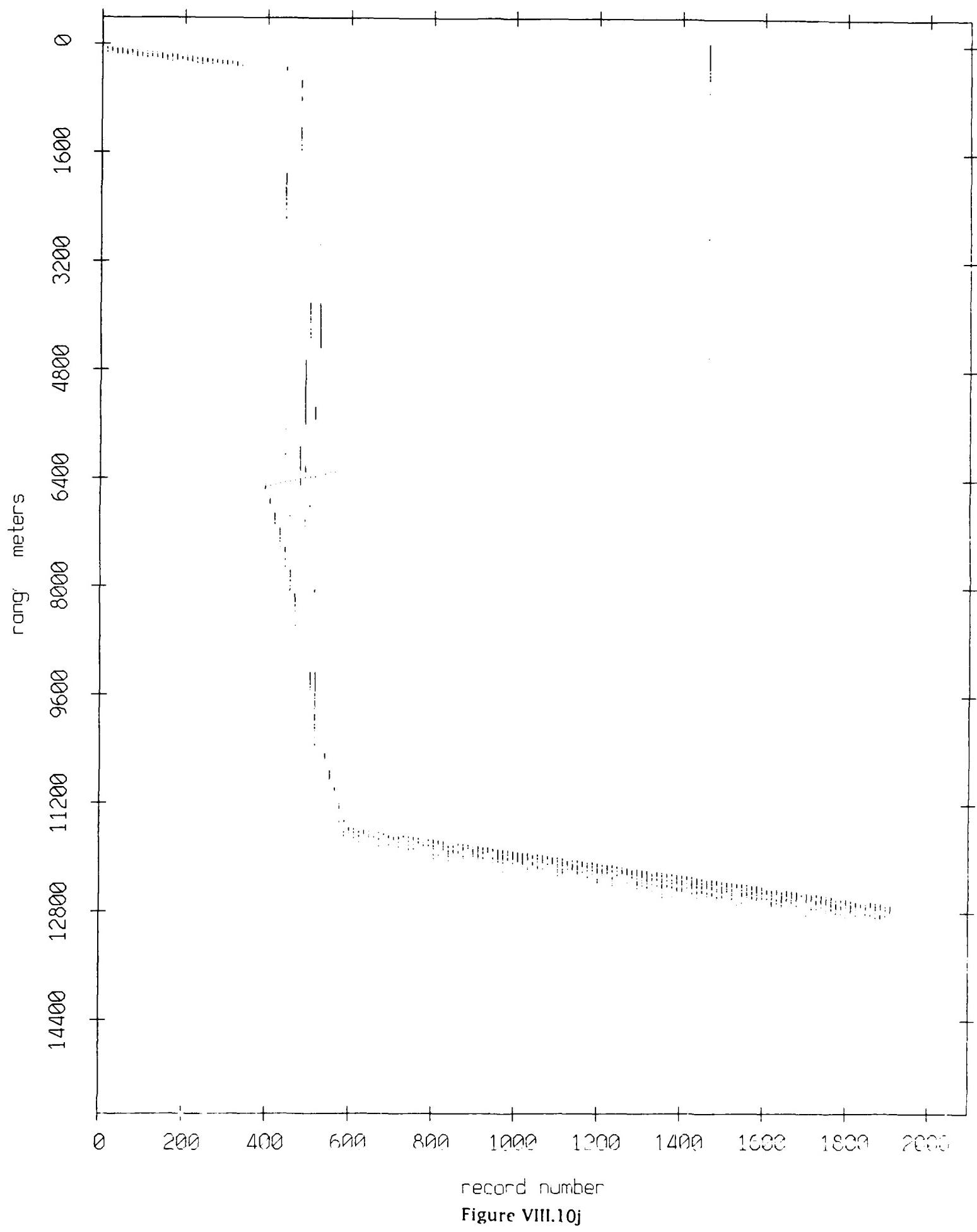


Figure VIII.10h

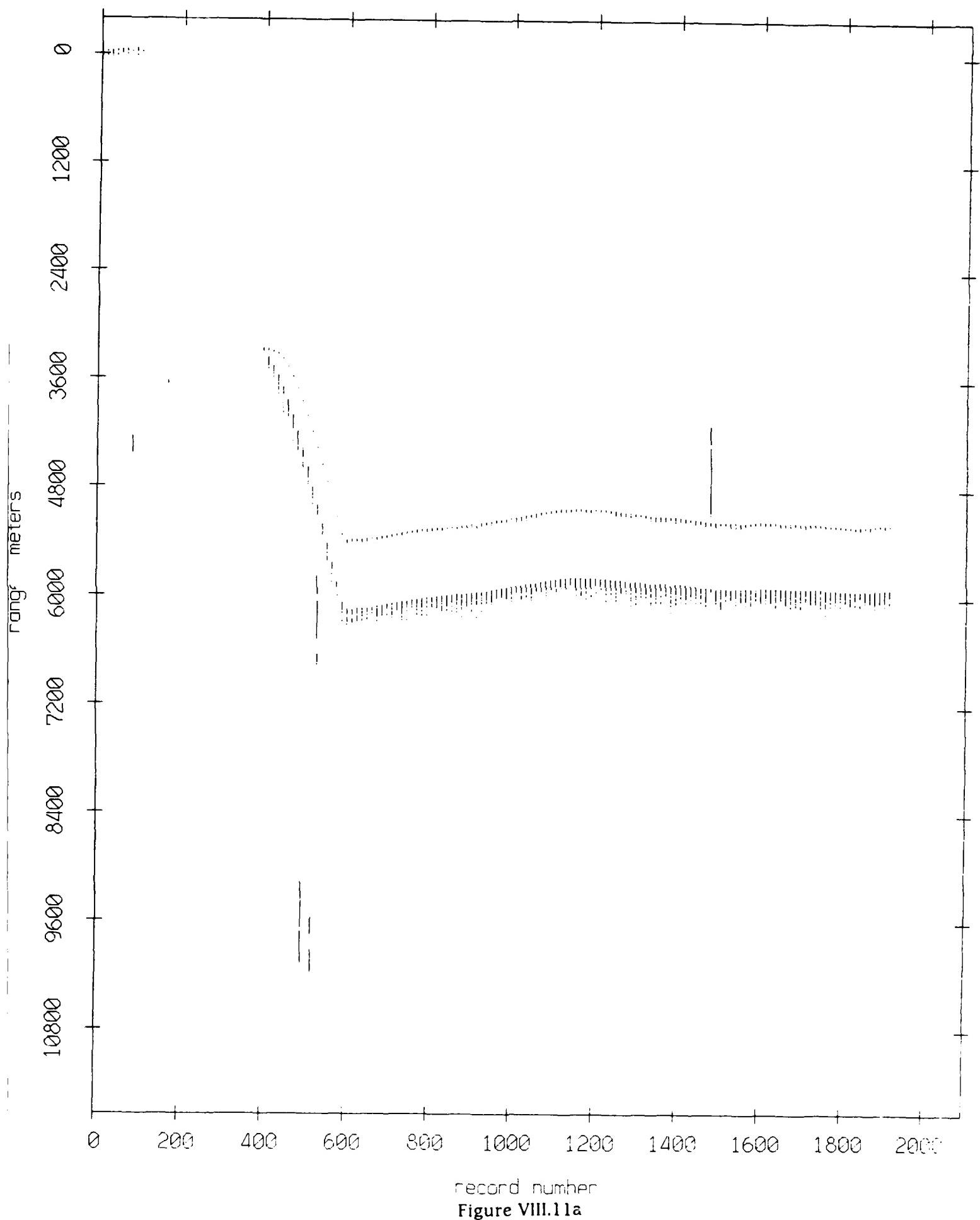
Float 10, September 1987 Sea Trip: range from float 9



Float 10, September 1987 Sea Trip: range from float 11



Float 11, September 1987 Sea Trip: range from float 0



record number
Figure VIII.11a

Float 11, September 1987 Sea Trip: range from float 2

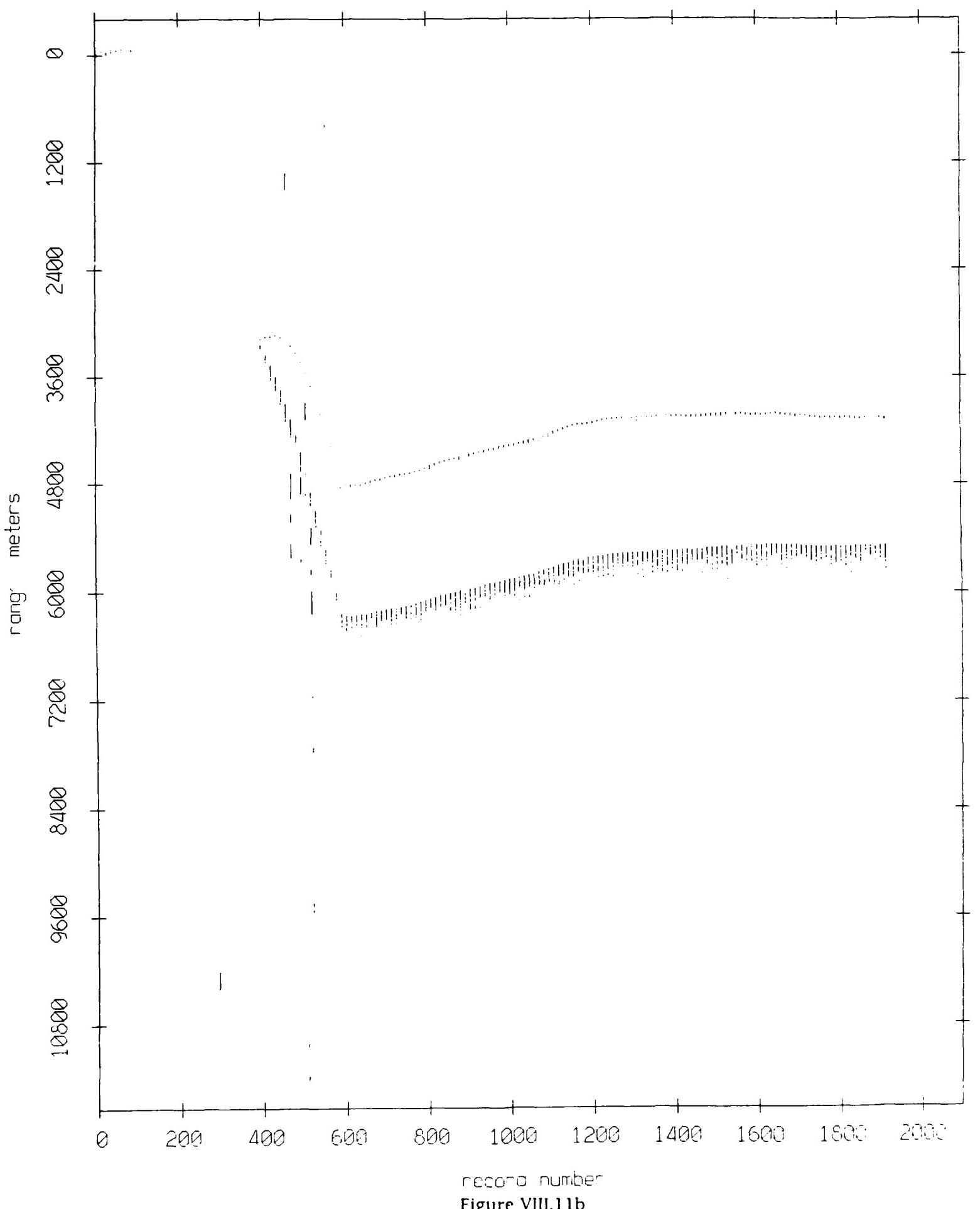
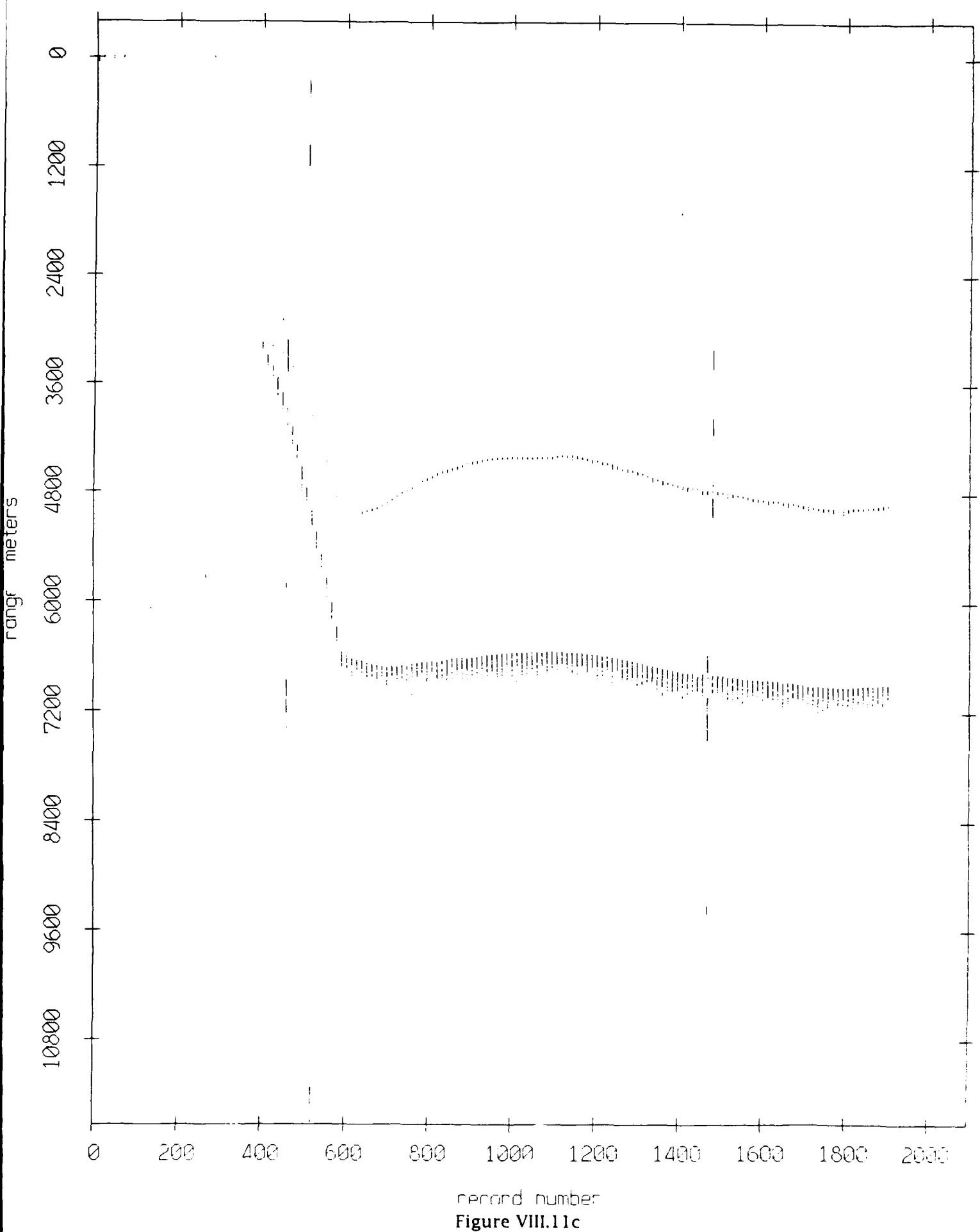


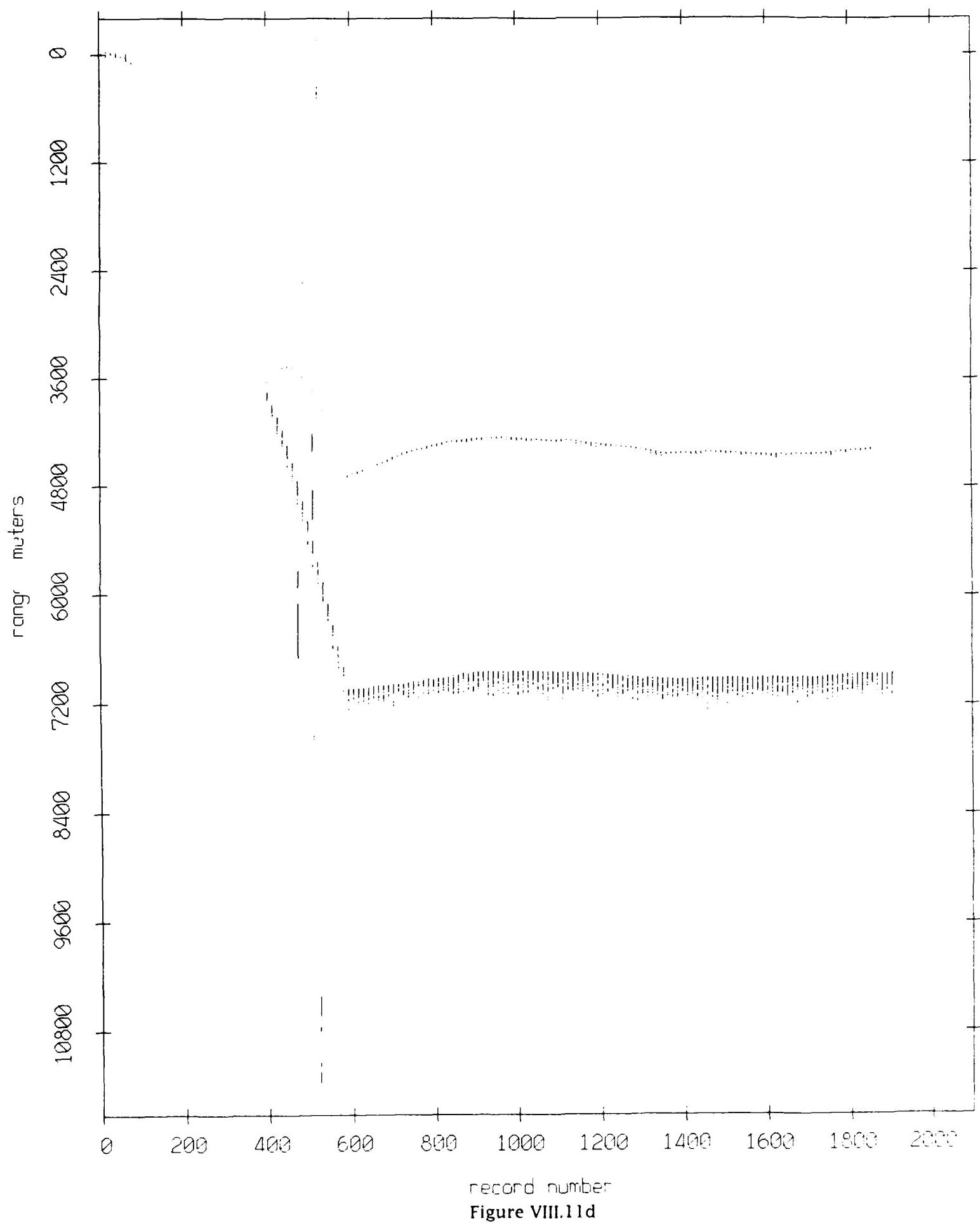
Figure VIII.11b

Float 11, September 1987 Sea Trip: range from float 3

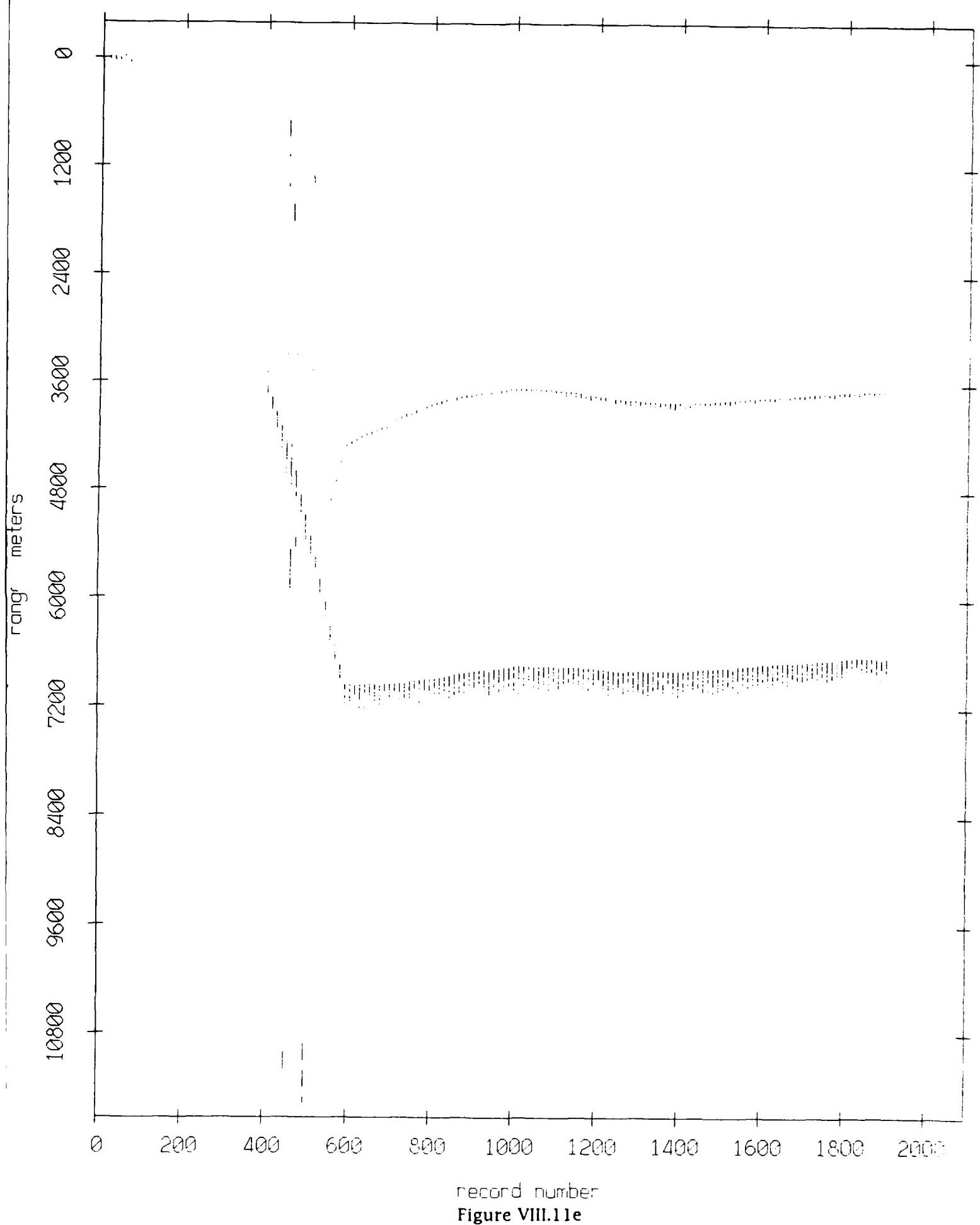


record number
Figure VIII.11c

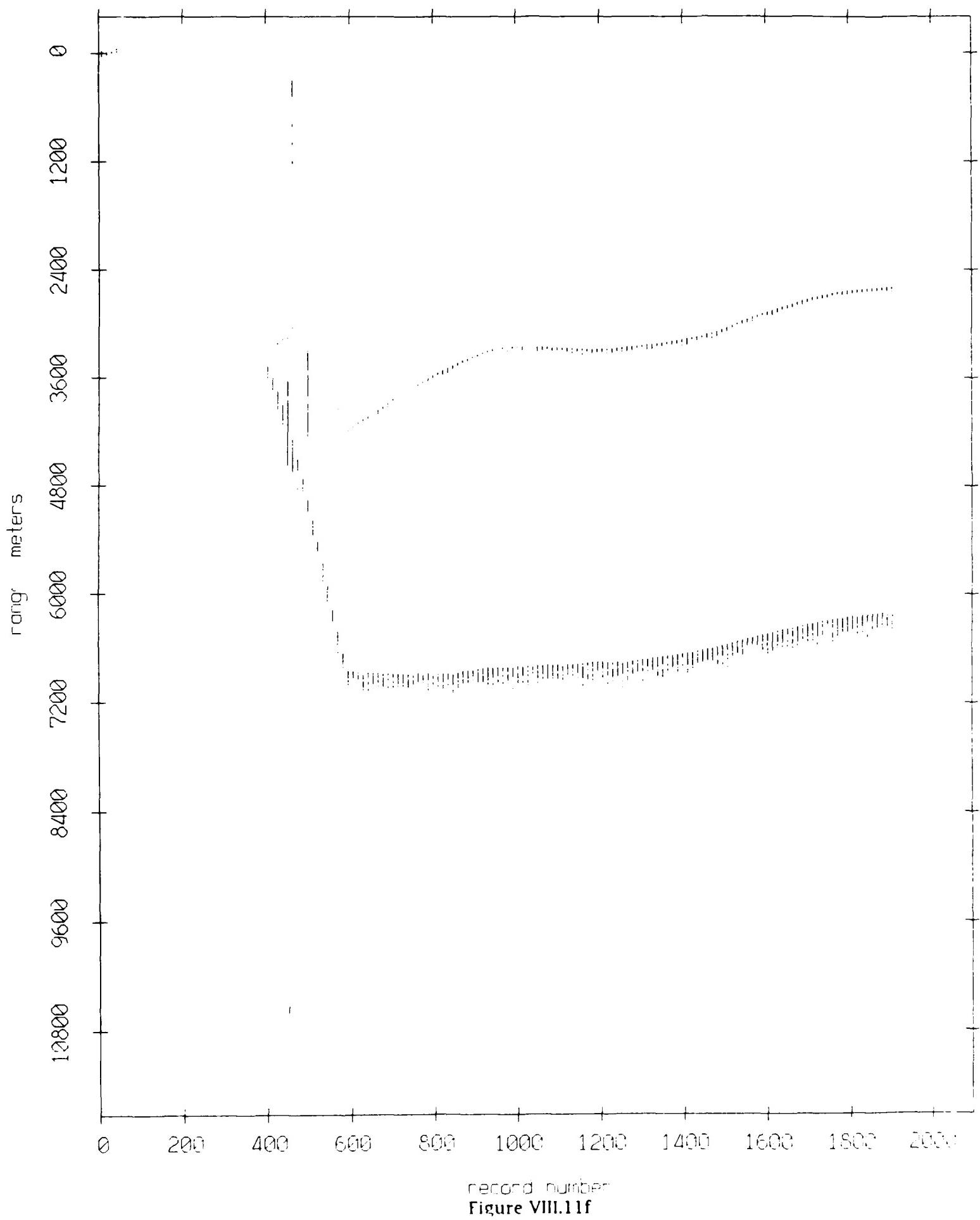
Float 11, September 1987 Sea Trip: range from float 4



Float 11, September 1987 Sea Trip: range from float 5

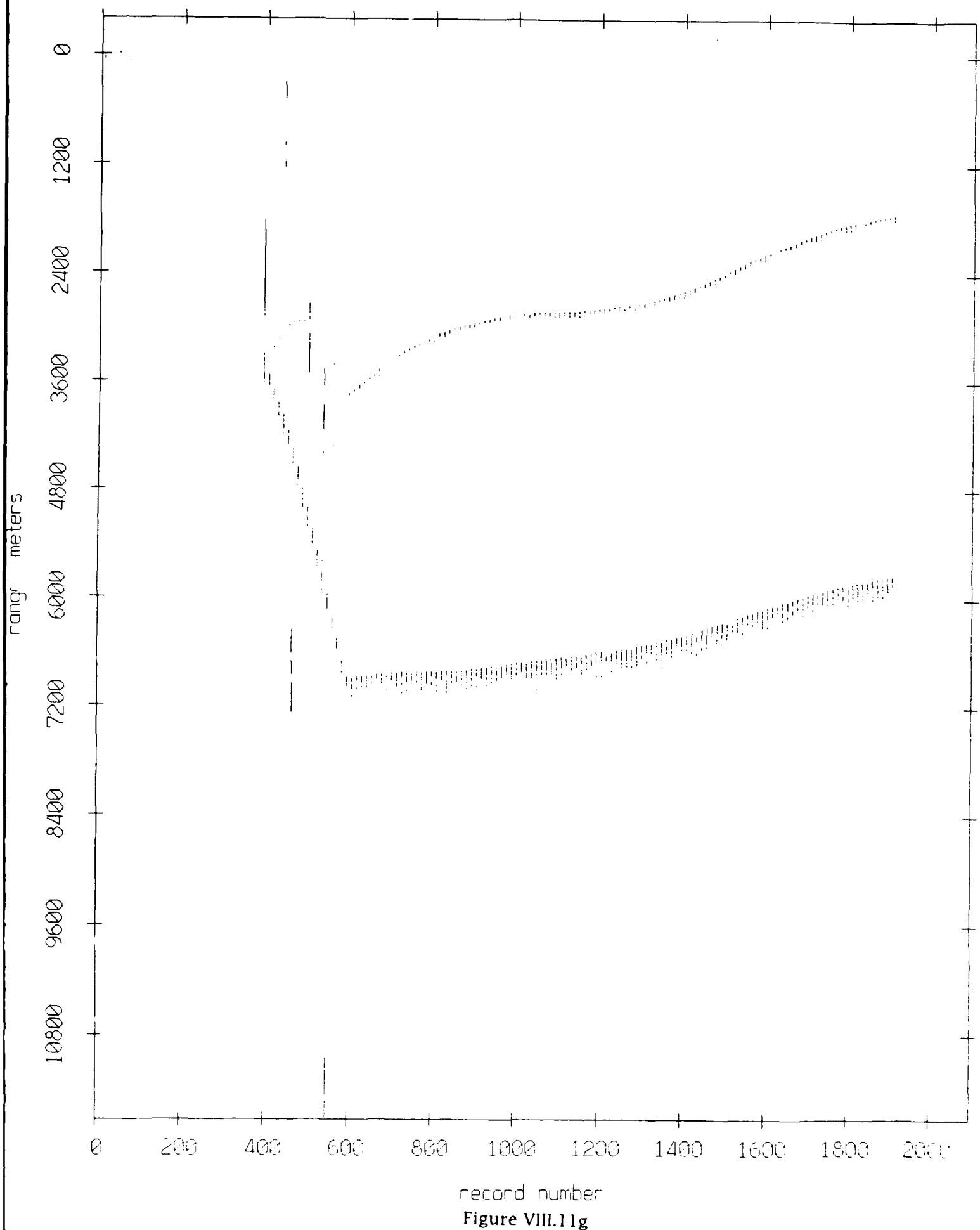


Float 11, September 1987 Sea Trip: range from float 6



record number
Figure VIII.11f

Float 11, September 1987 Sea Trip: range from float 7



record number

Figure VIII.11g

Float 11, September 1987 Sea Trip: range from float 8

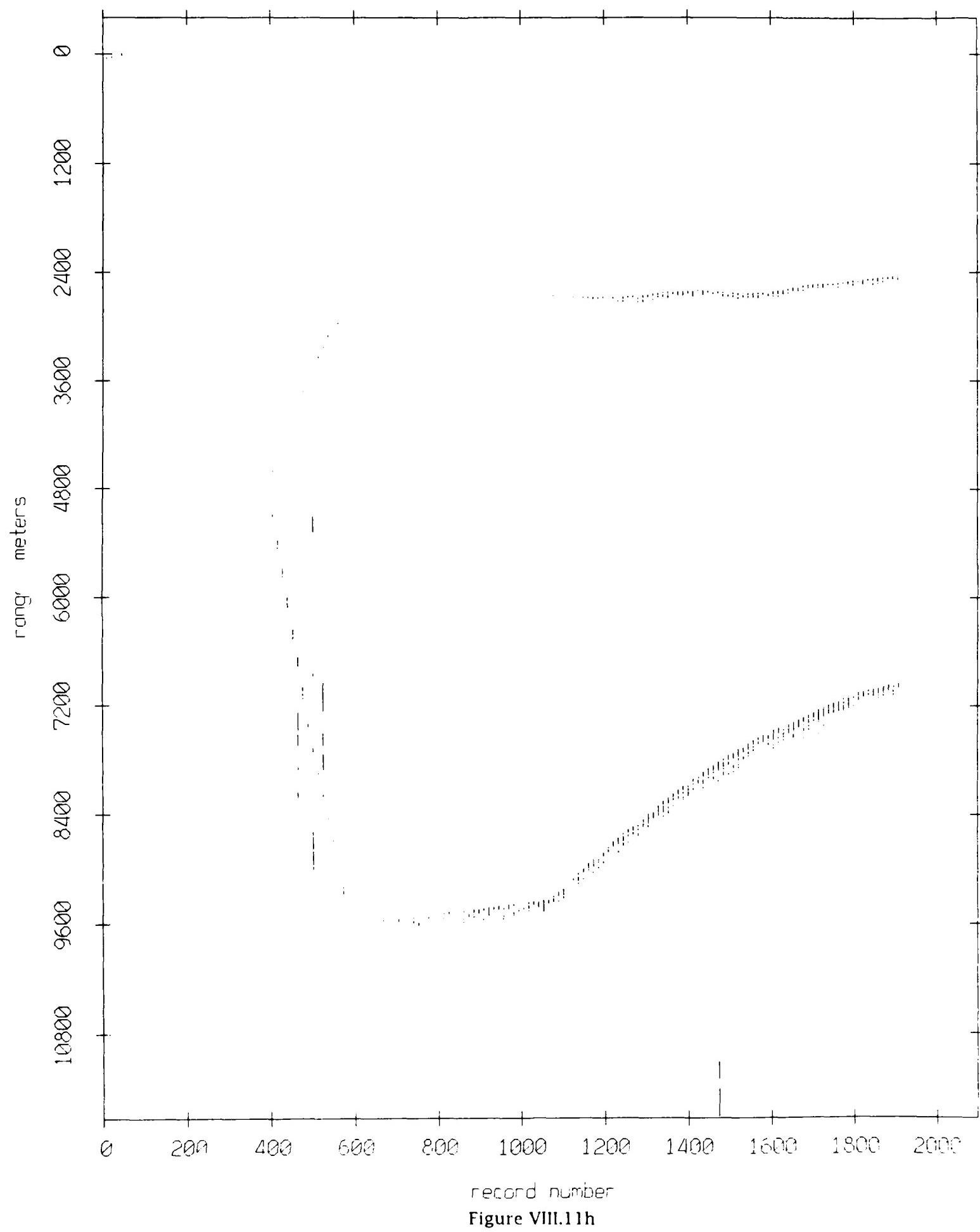
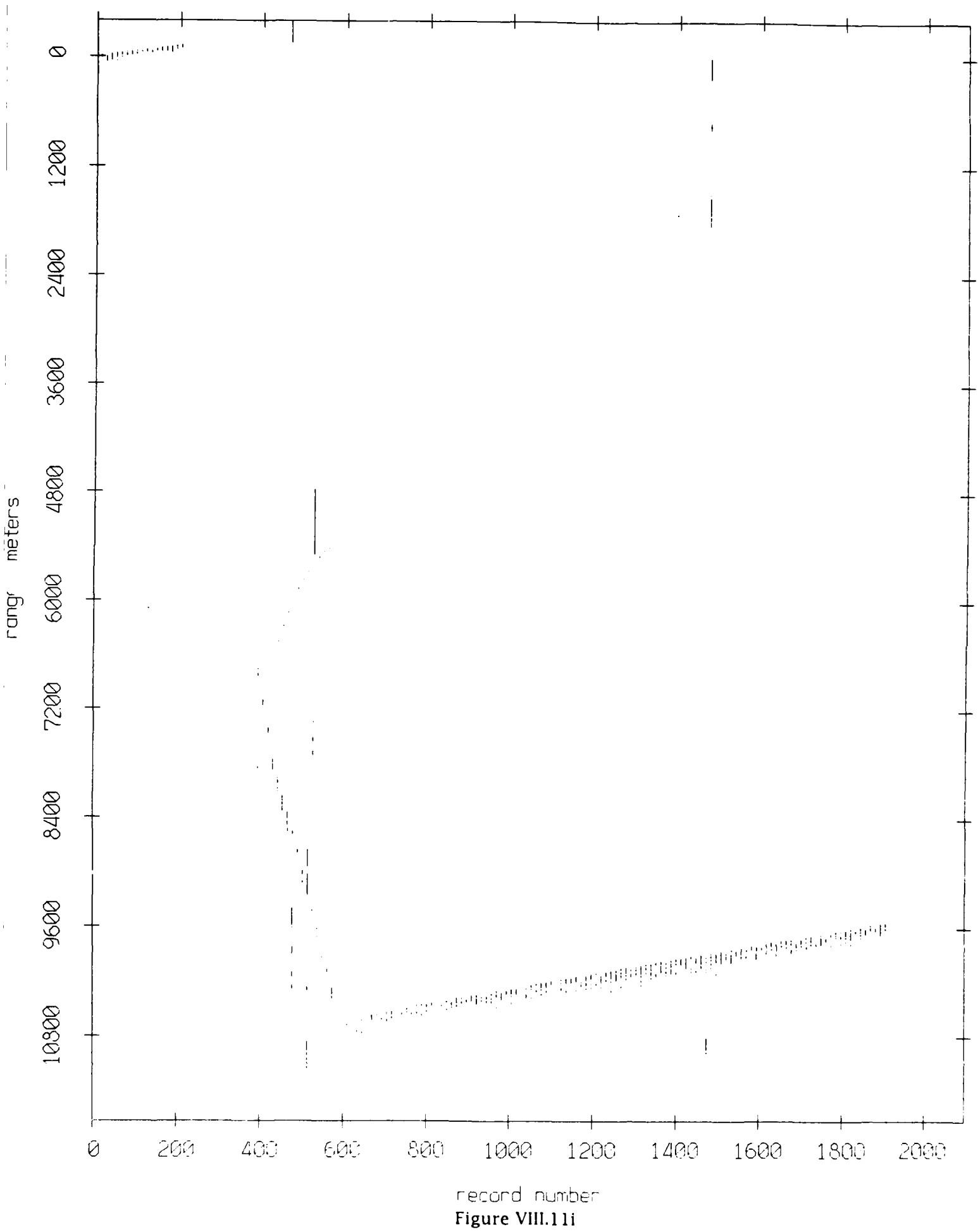


Figure VIII.11h

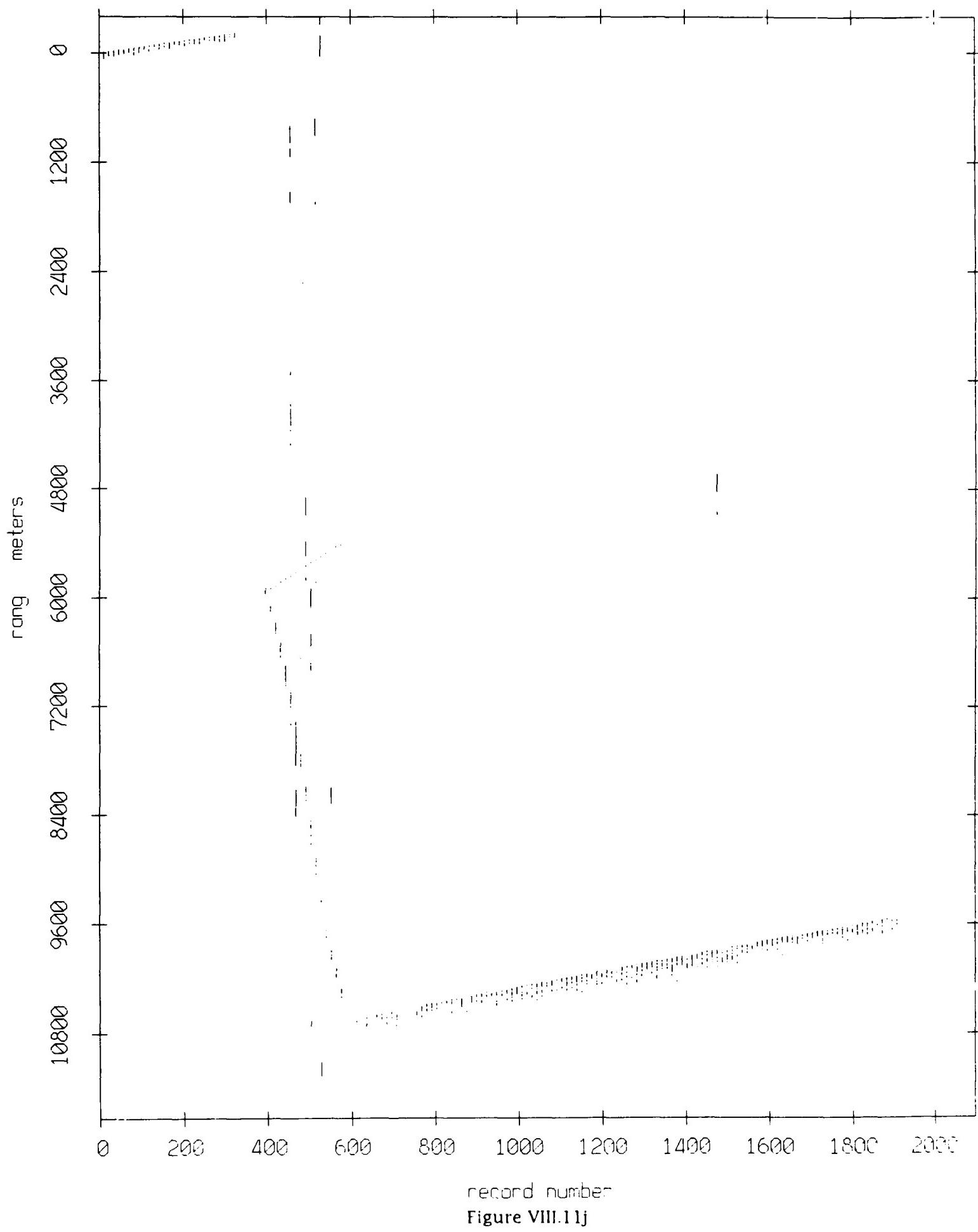
Float 11, September 1987 Sea Trip: range from float 9



record number

Figure VIII.11i

Float 11, September 1987 Sea Trip: range from float 10



record number
Figure VIII.11j

Float 0, September 1987 Sea Trip
overriding period = 5.00 sec.

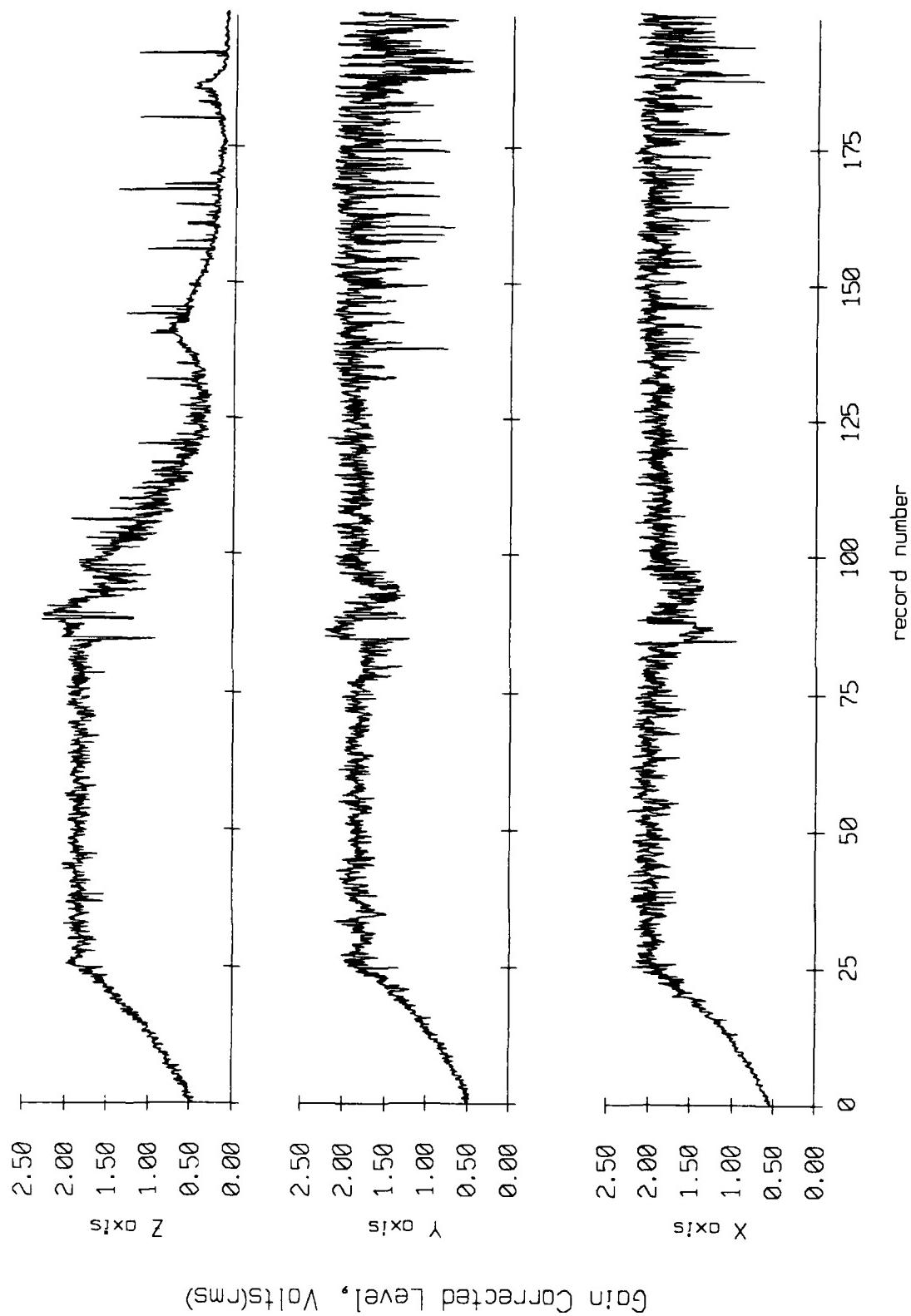


Figure IX.1a

Fleet 0, September 1987 Sea Trip
averaging period = 5.00 sec.

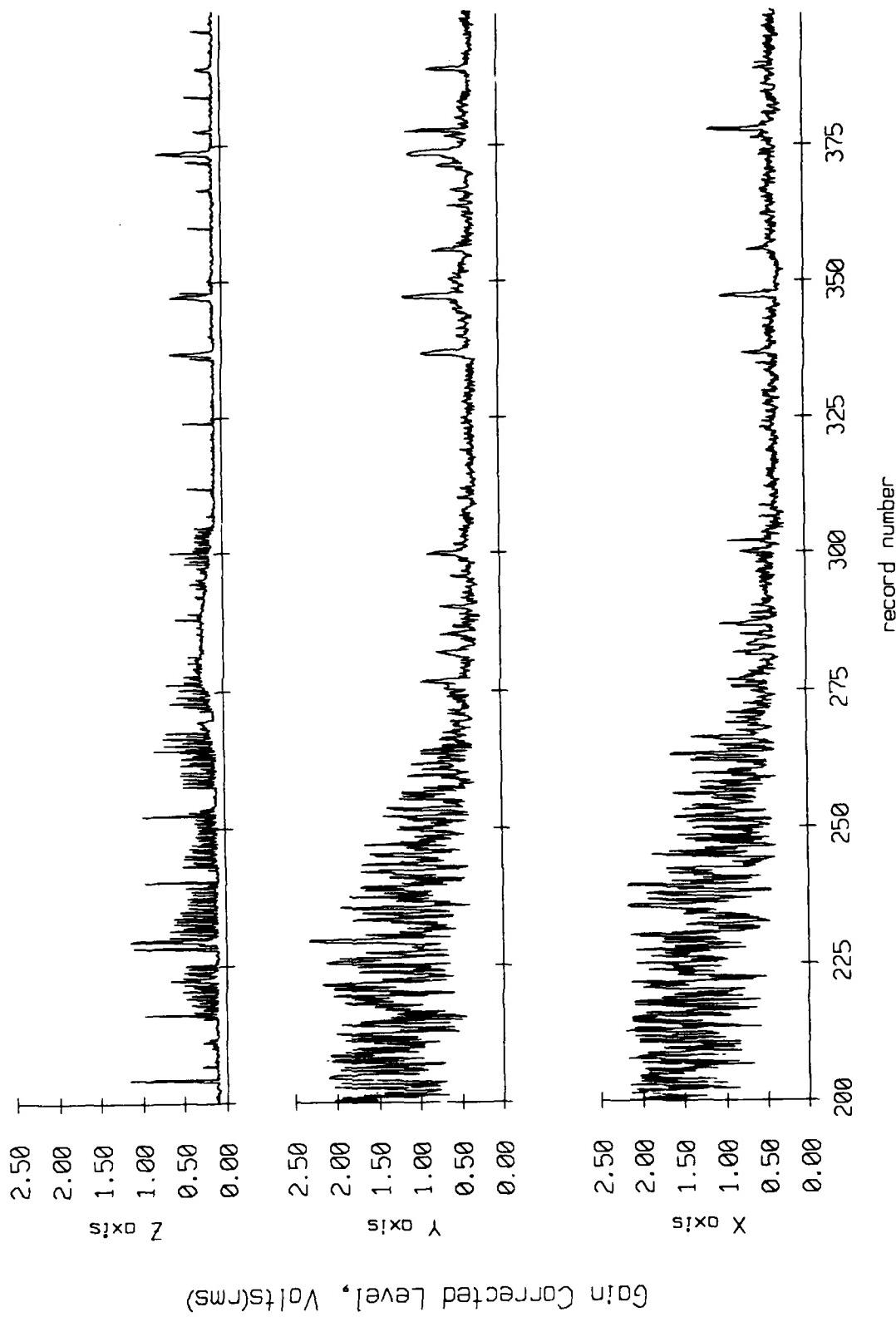


Figure IX.1b

Float 0, September 1987 Sea Trip
averaging period = 5.00 sec.

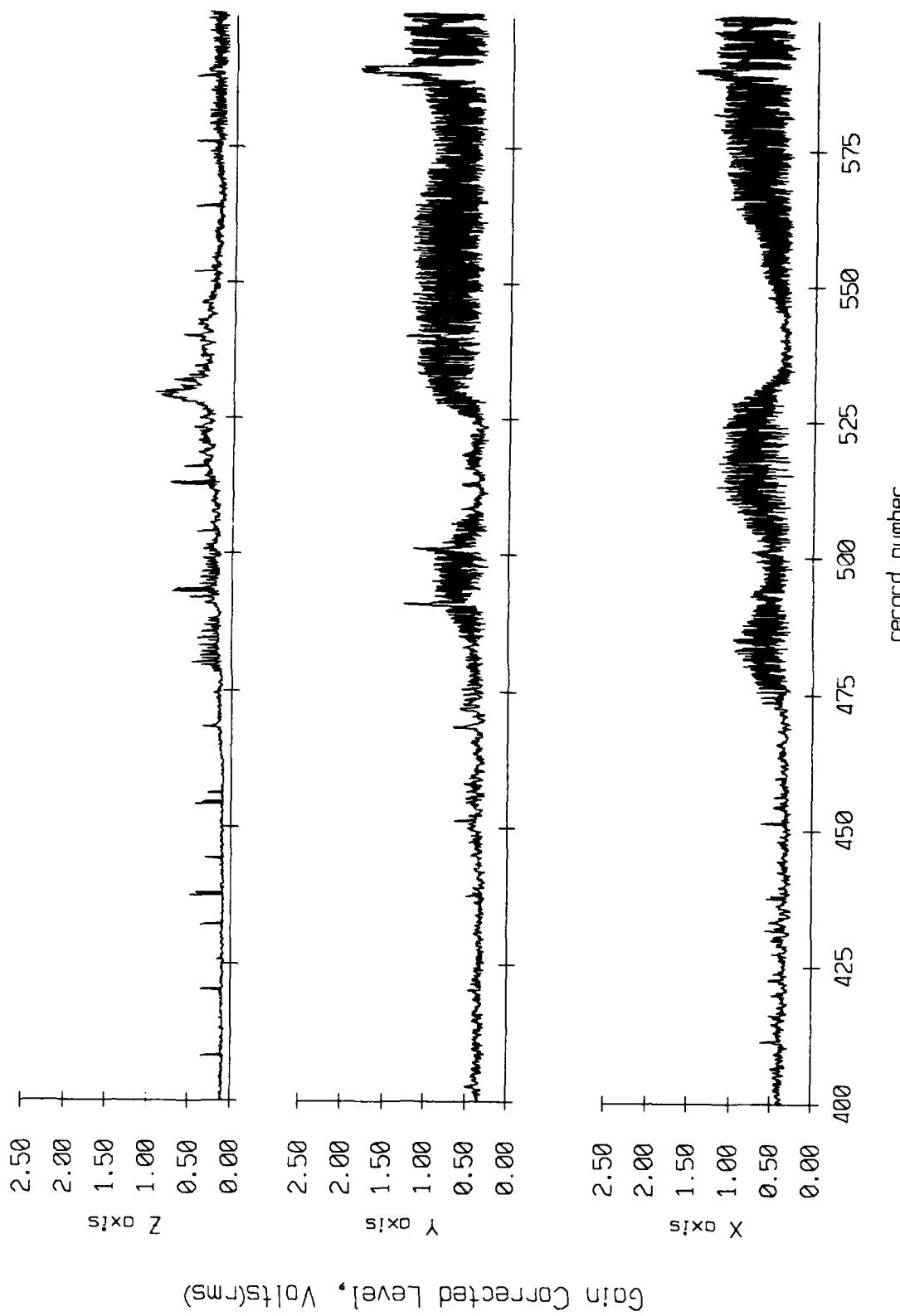


Figure IX.1c

Float 0, September 1987 Sea Trip
averaging period = 5.00 sec.

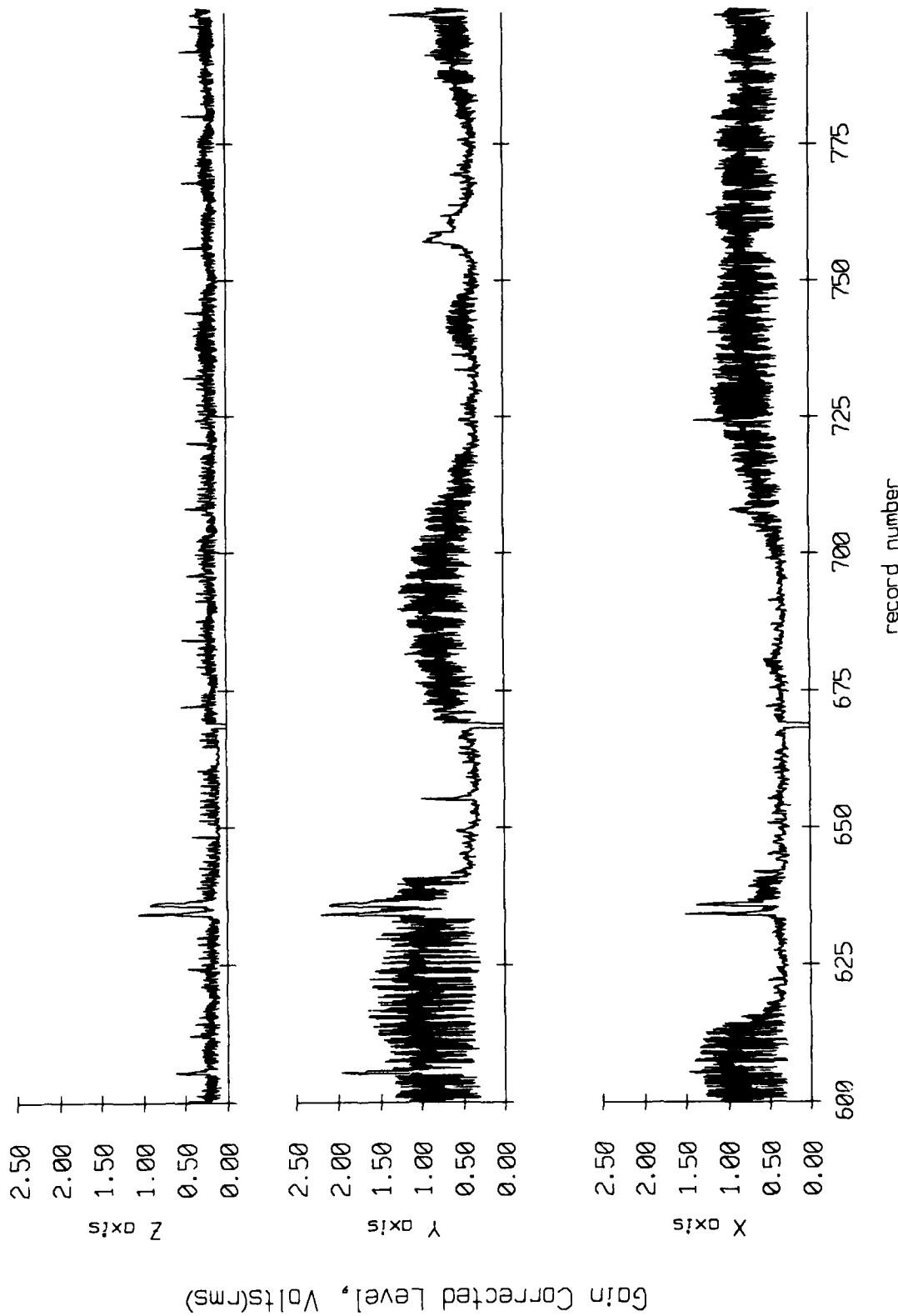


Figure IX.1d

Float 0, September 1987 Sea Trip
averaging period = 5.00 sec.

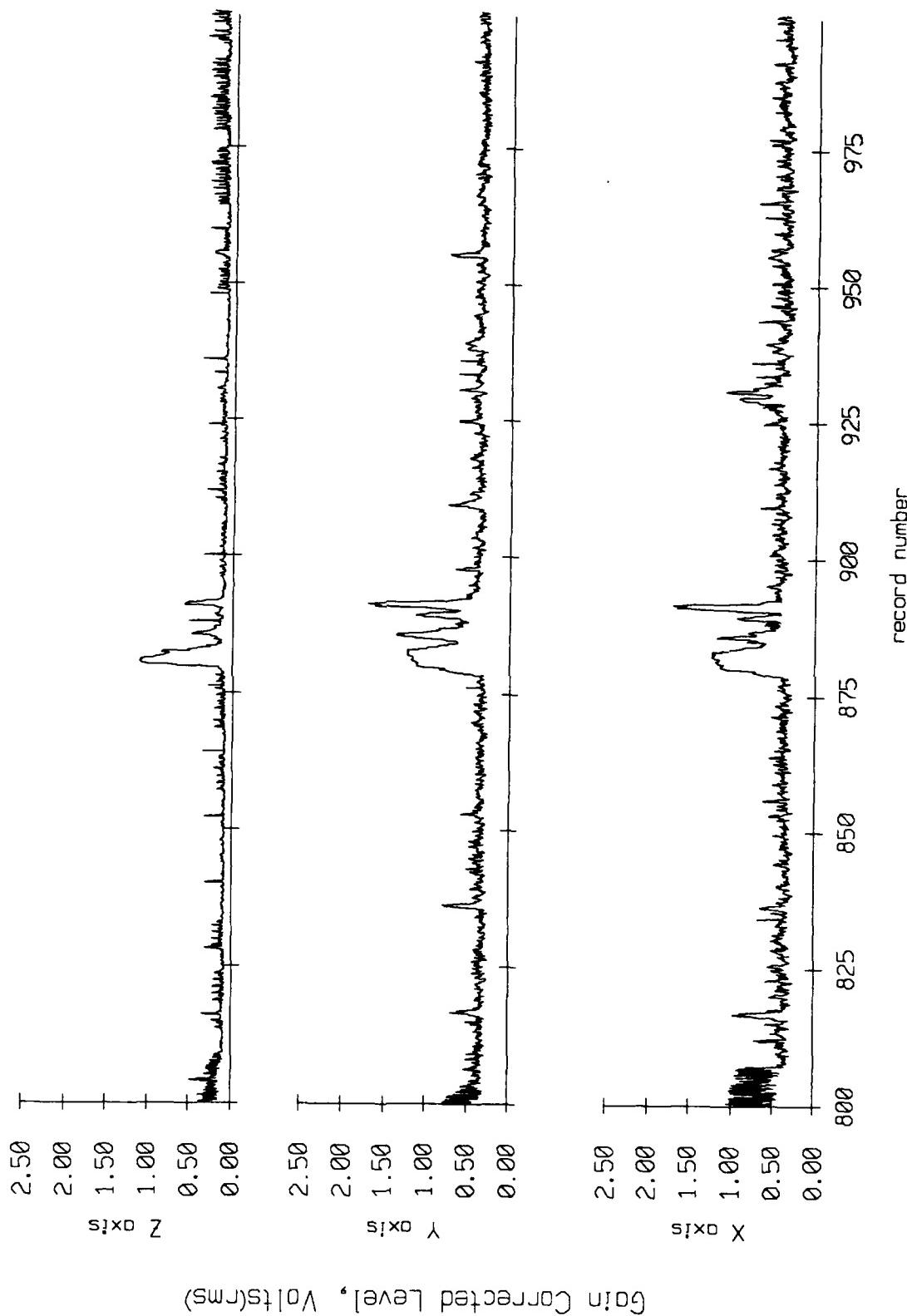
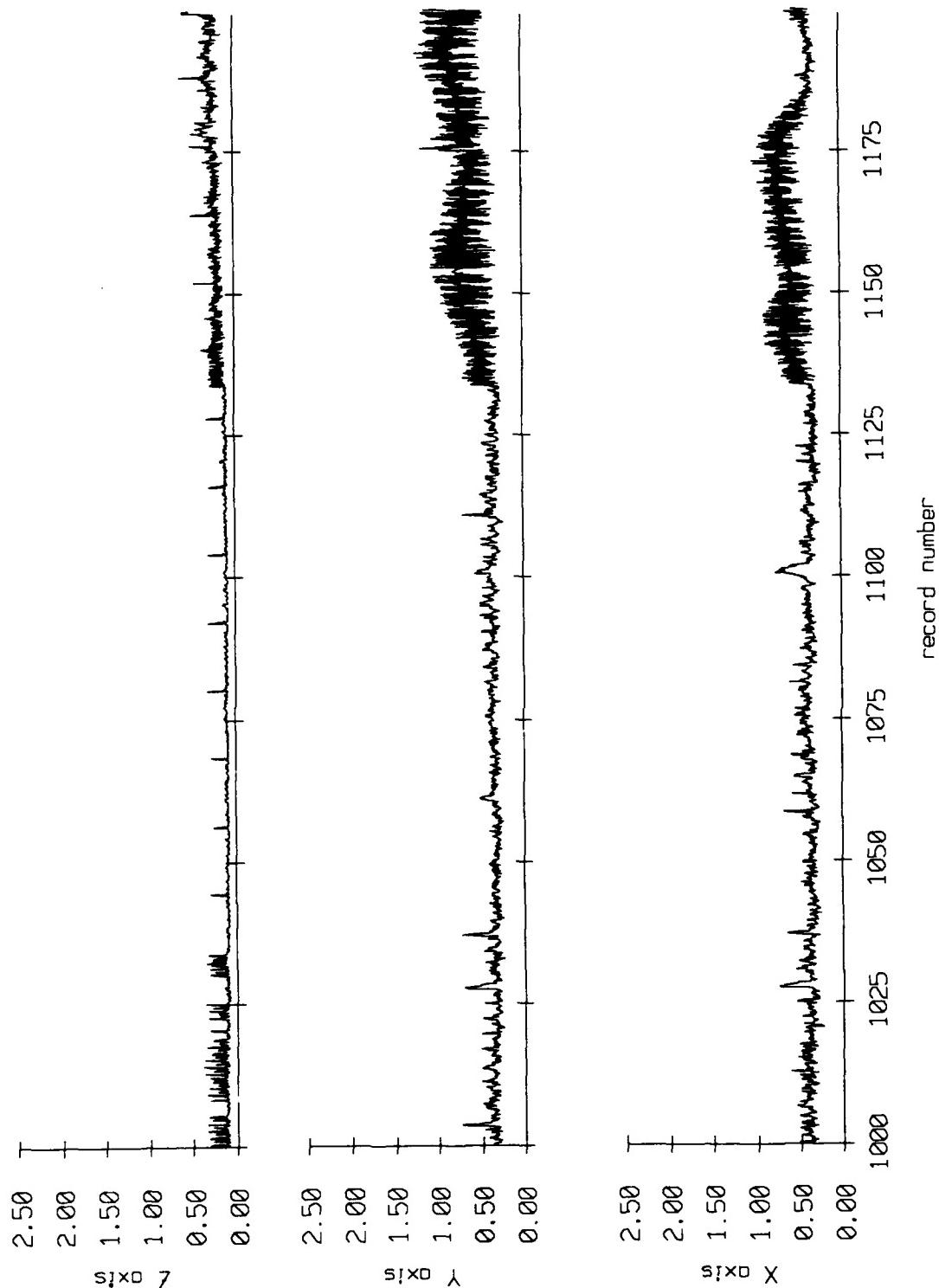


Figure IX.1e

Float 0, September 1987 Sea Trip
overaging period = 5.00 sec.



Gain Corrected Level, Volts(RMS)

Figure IX.1f

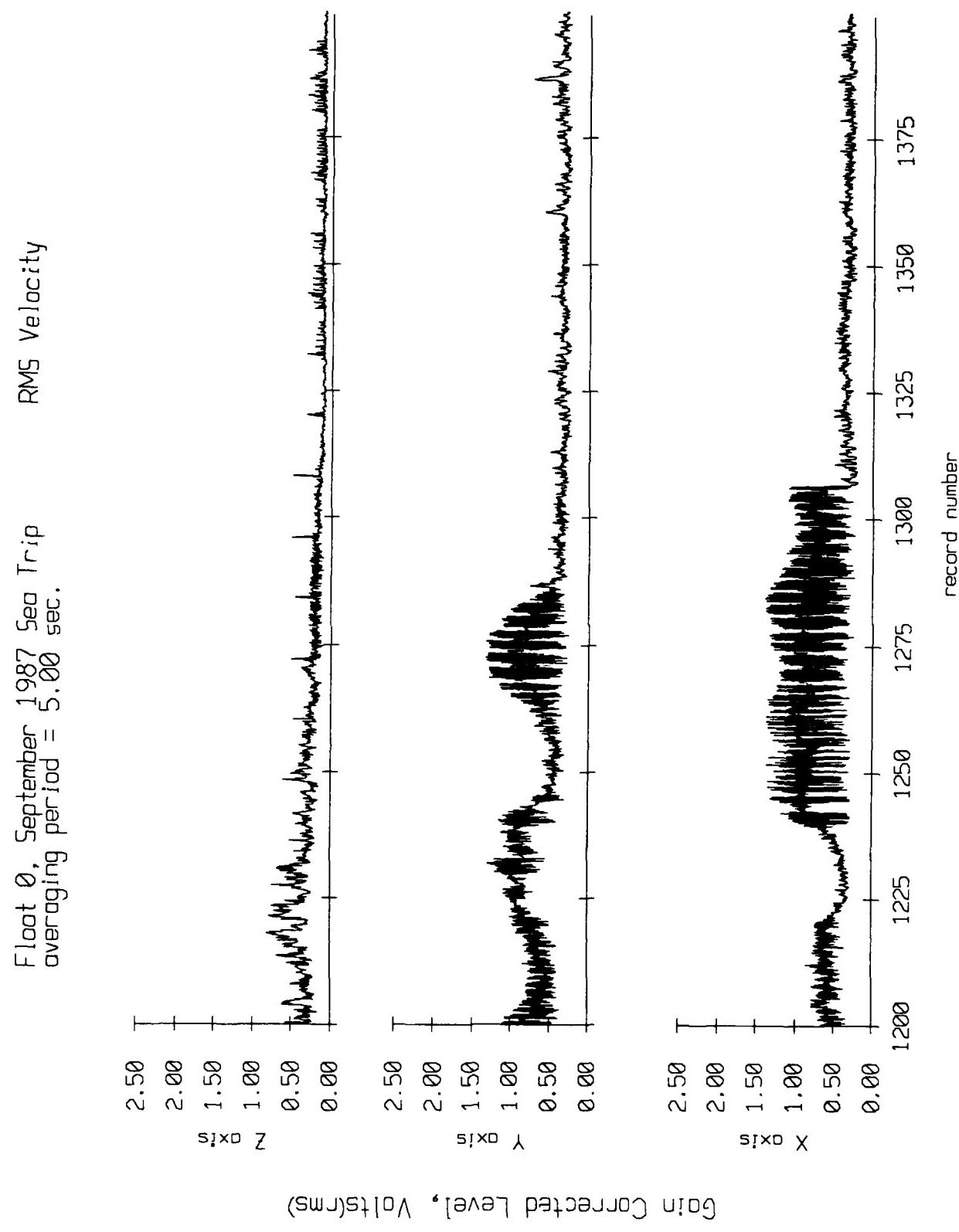
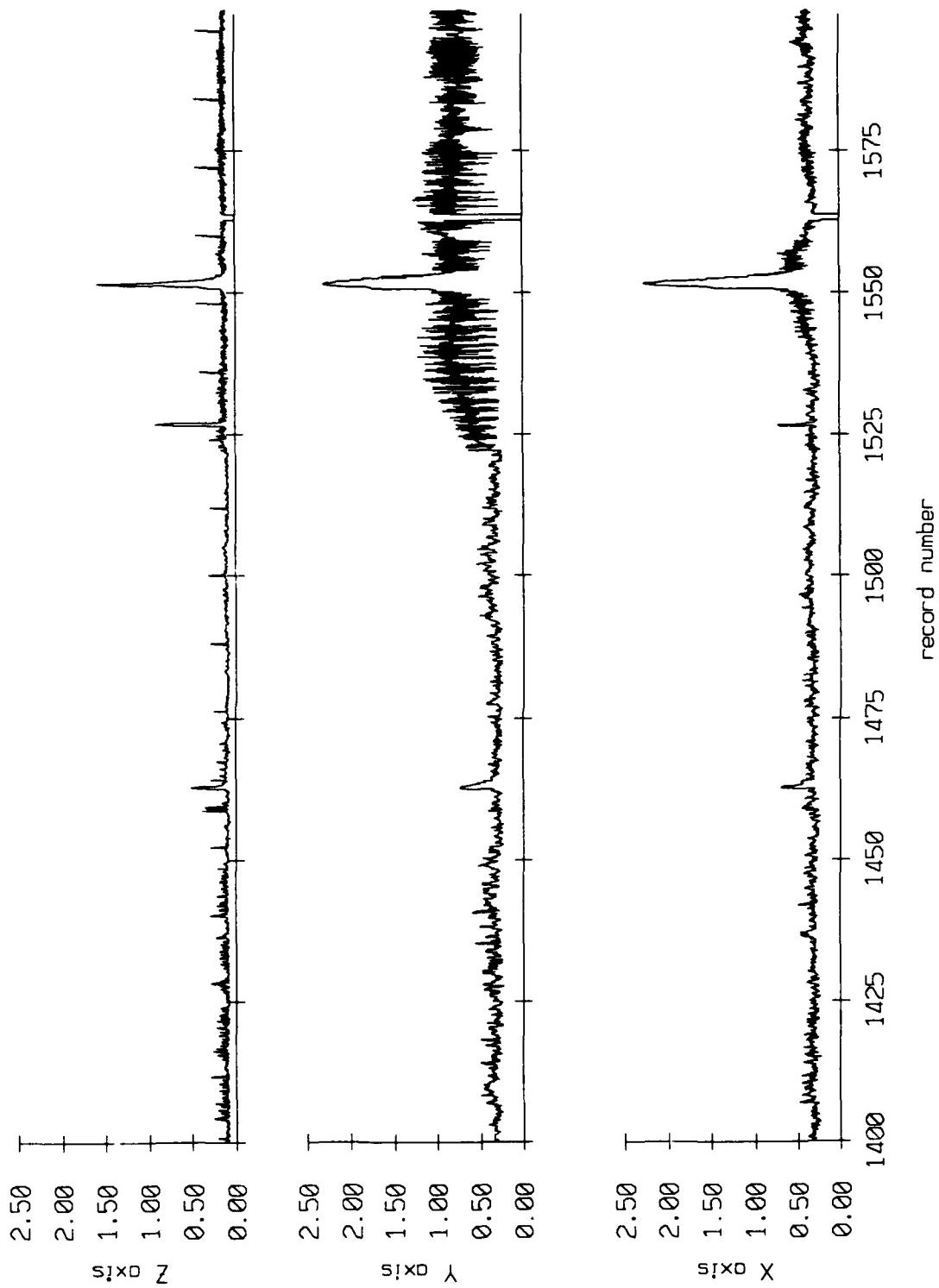


Figure IX.1g

Fleet 0, September 1987 Sea Trip
averaging period = 5.00 sec.



Gain Corrected Level, Volts(rms)

Figure IX.1h

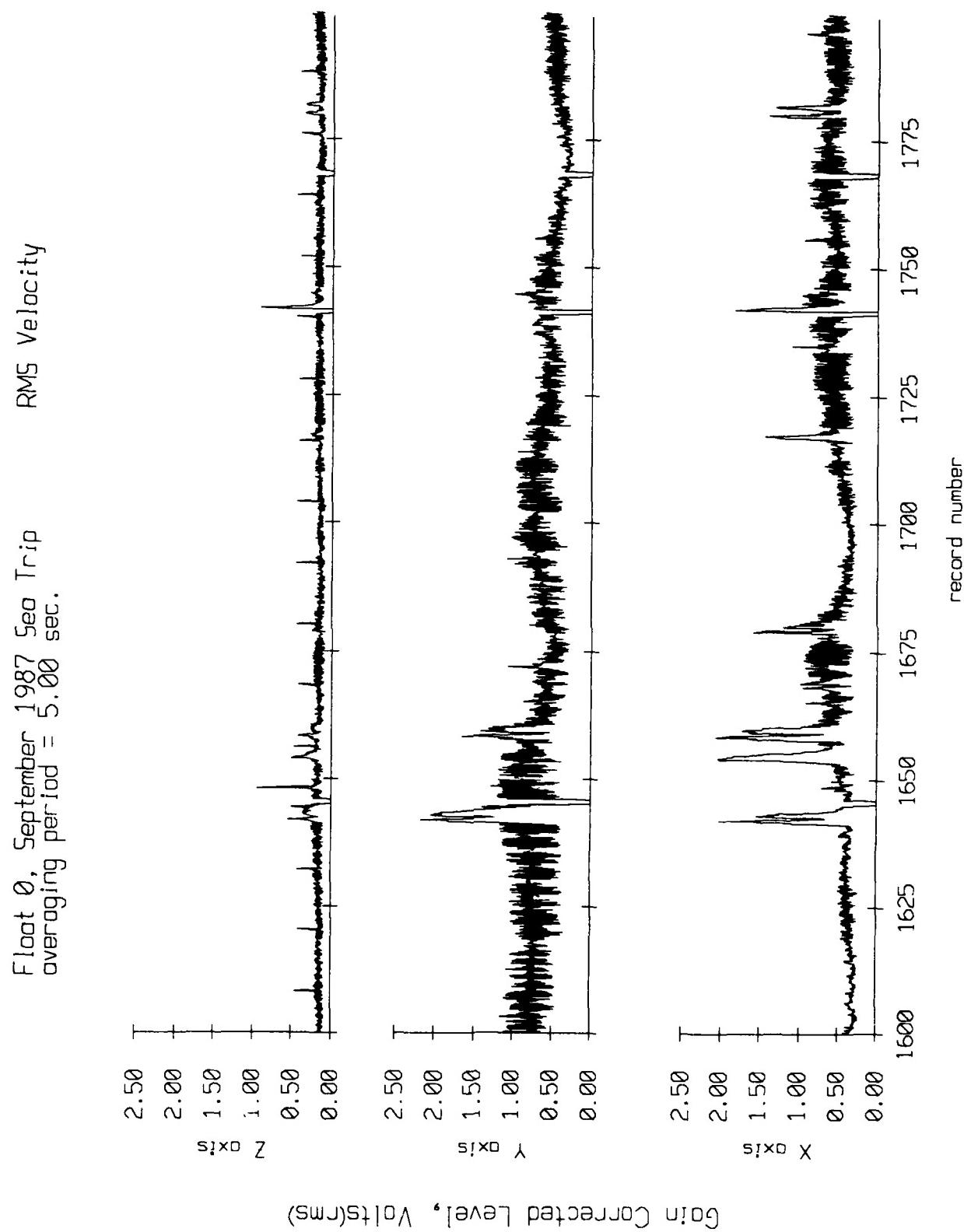


Figure IX.1i

Float 0, September 1987 Sec Trip
averaging period = 5.00 sec.

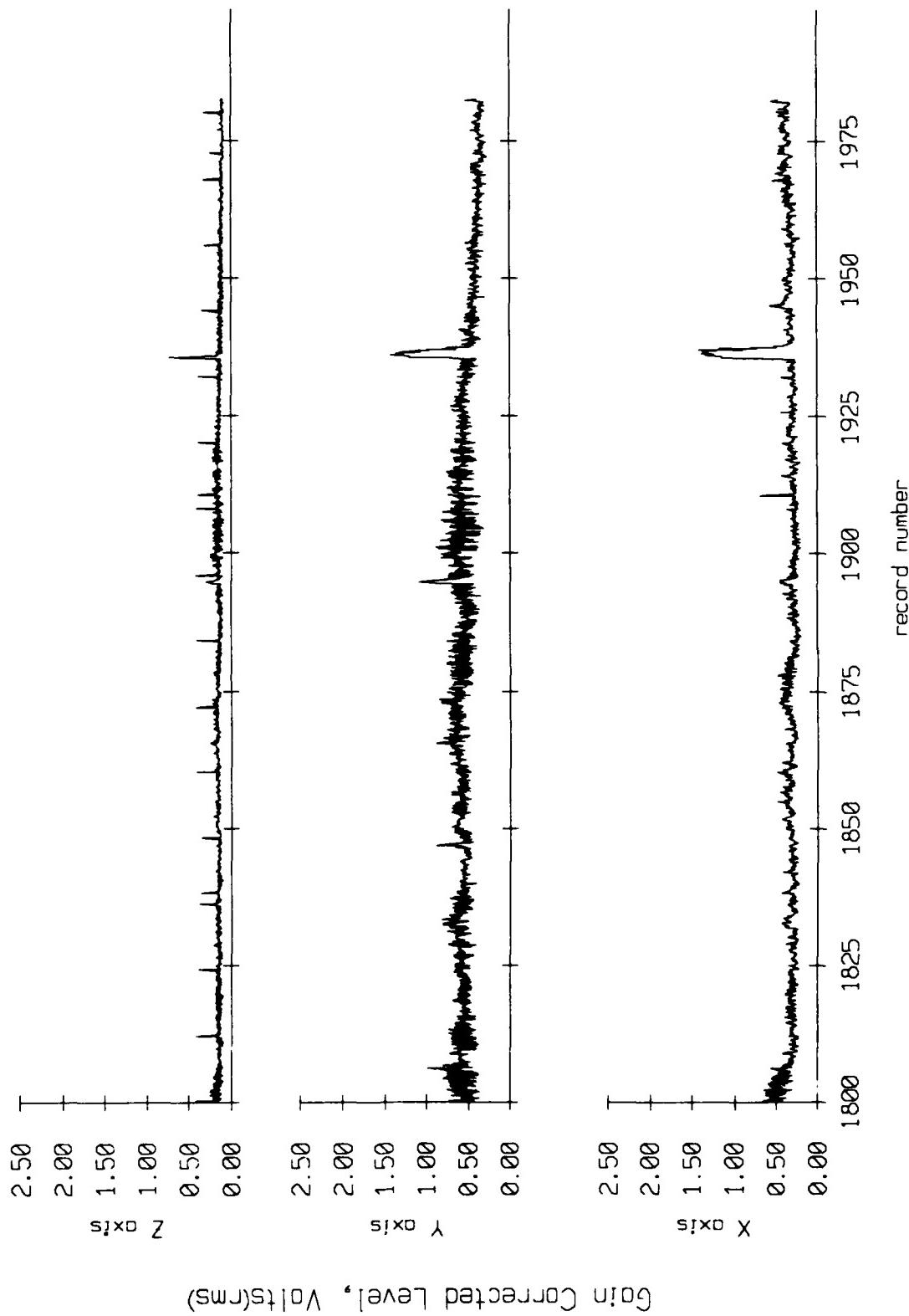
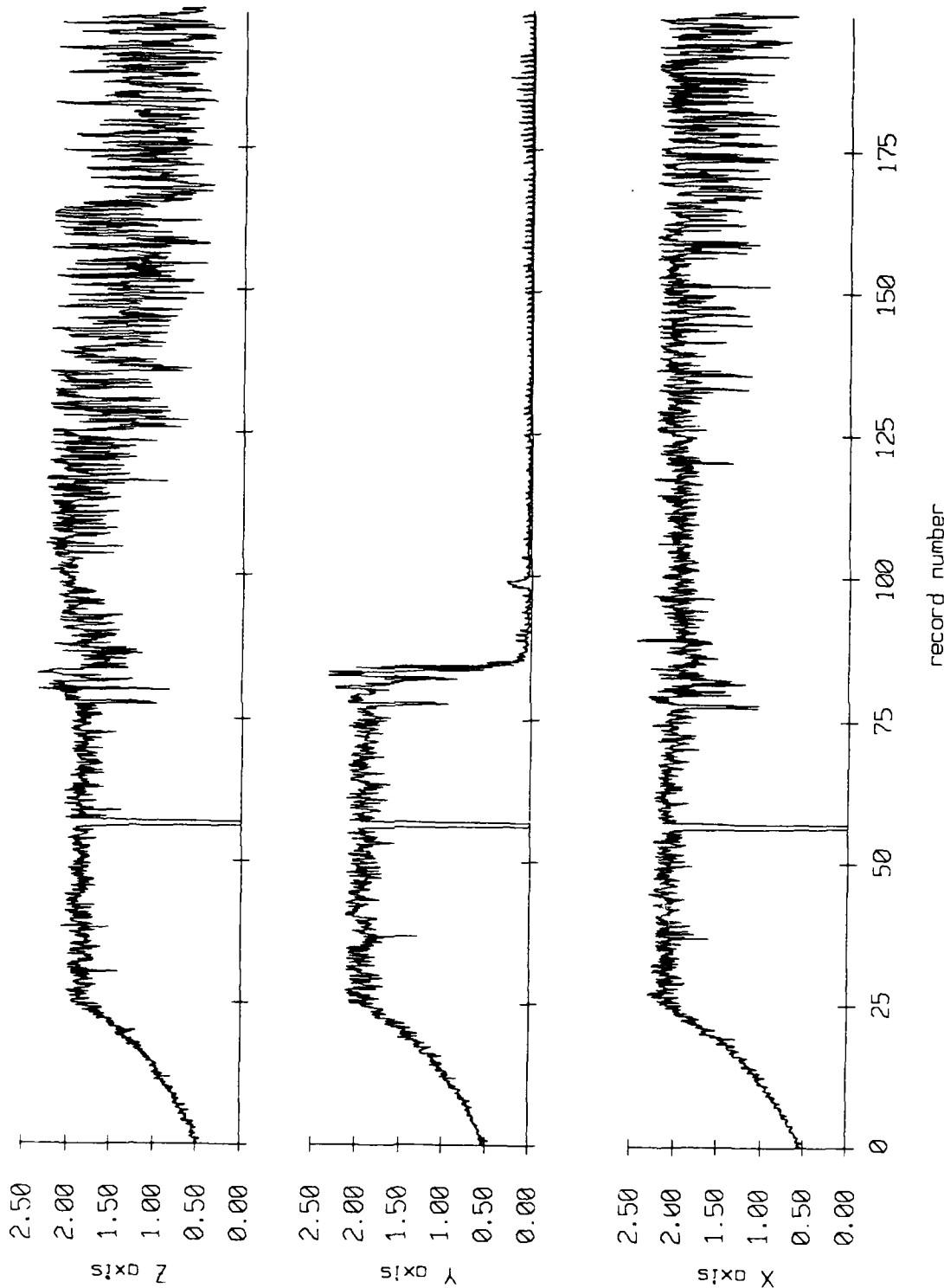


Figure IX.1j

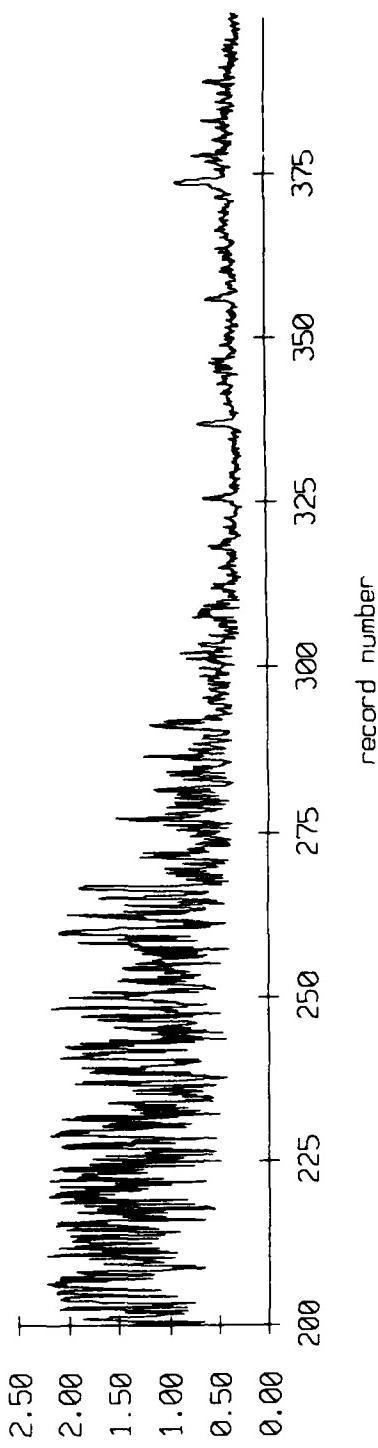
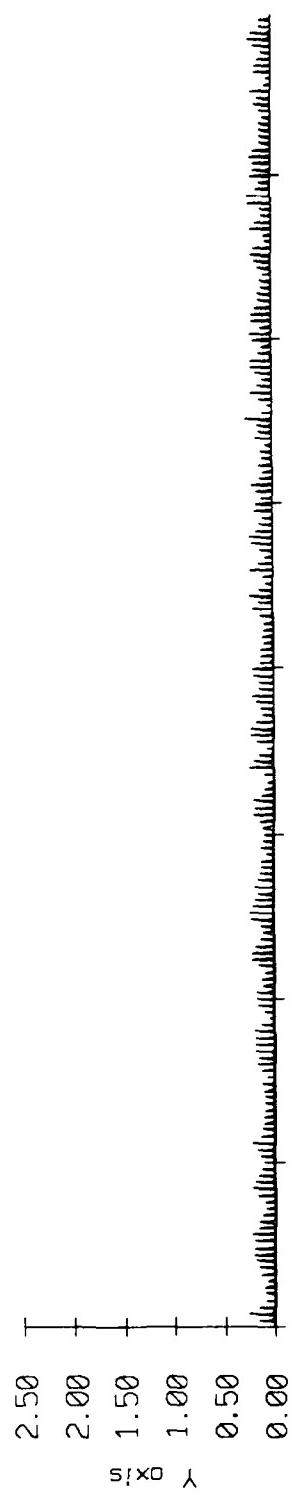
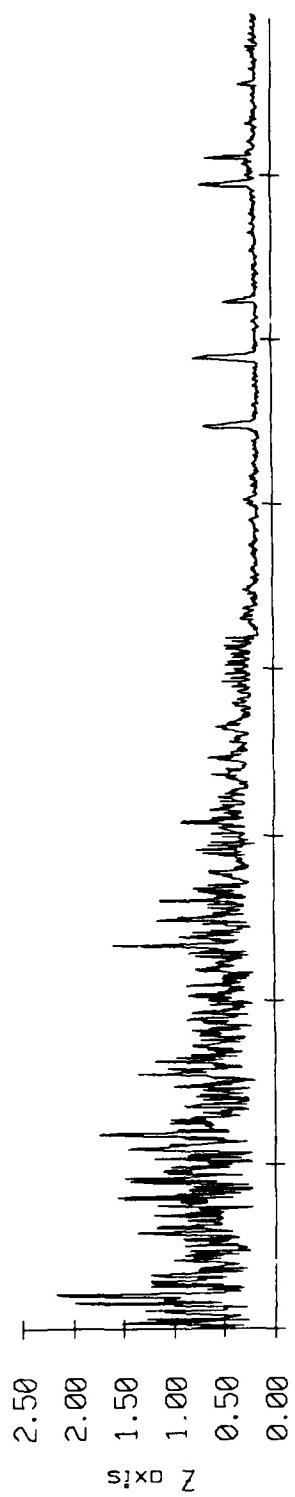
Fleet 1, September 1987 Sea Trip
averaging period = 5.00 sec.



Gain Corrected Level, Volts (RMS)

Figure IX.2a

Float 1, September 1987 Sea Trip
averaging period = 5.00 sec.



Gain Corrected Level, Volts(RMS)

Figure IX.2b

Float 1, September 1987 Sea Trip
averaging period = 5.00 sec.

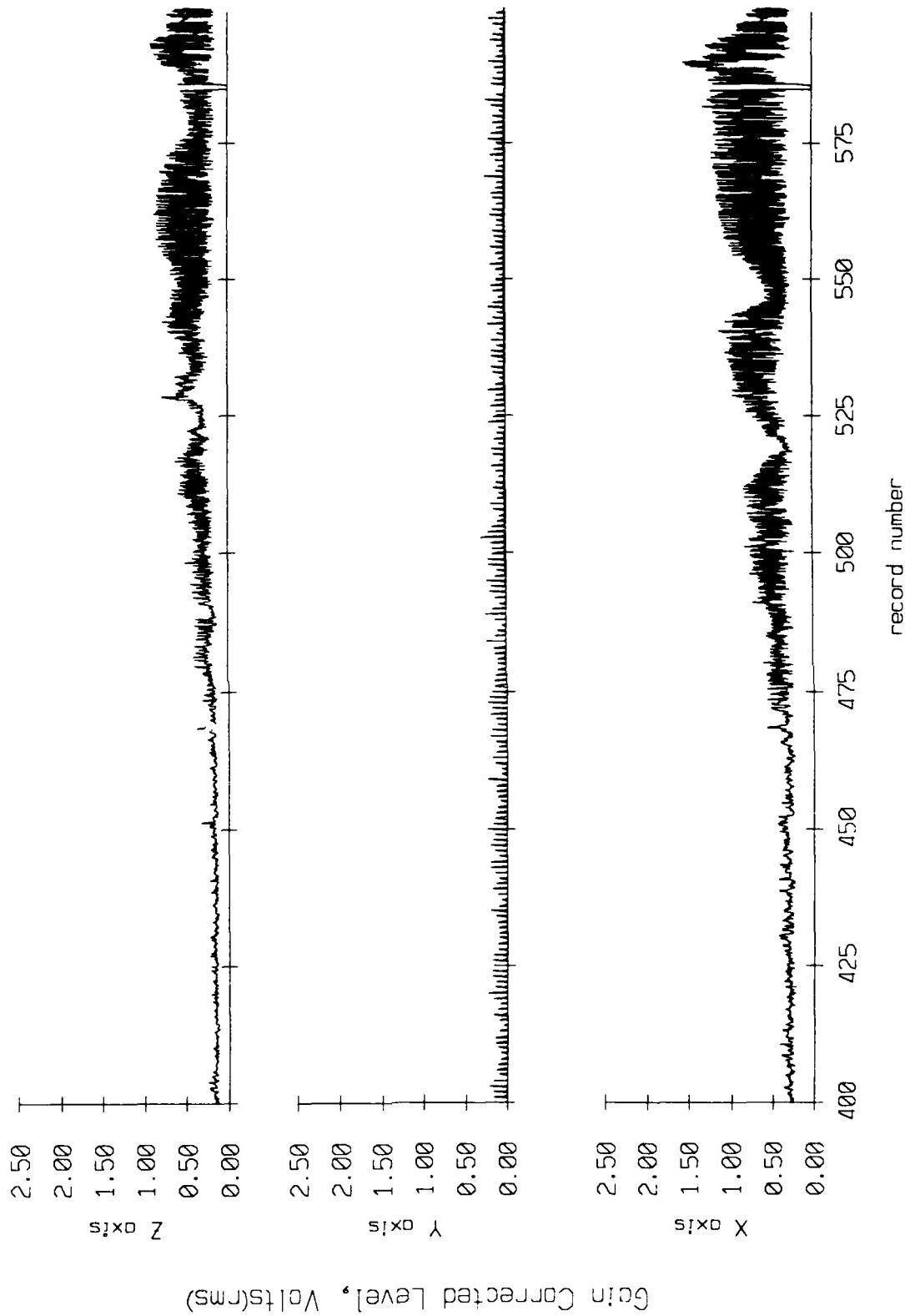
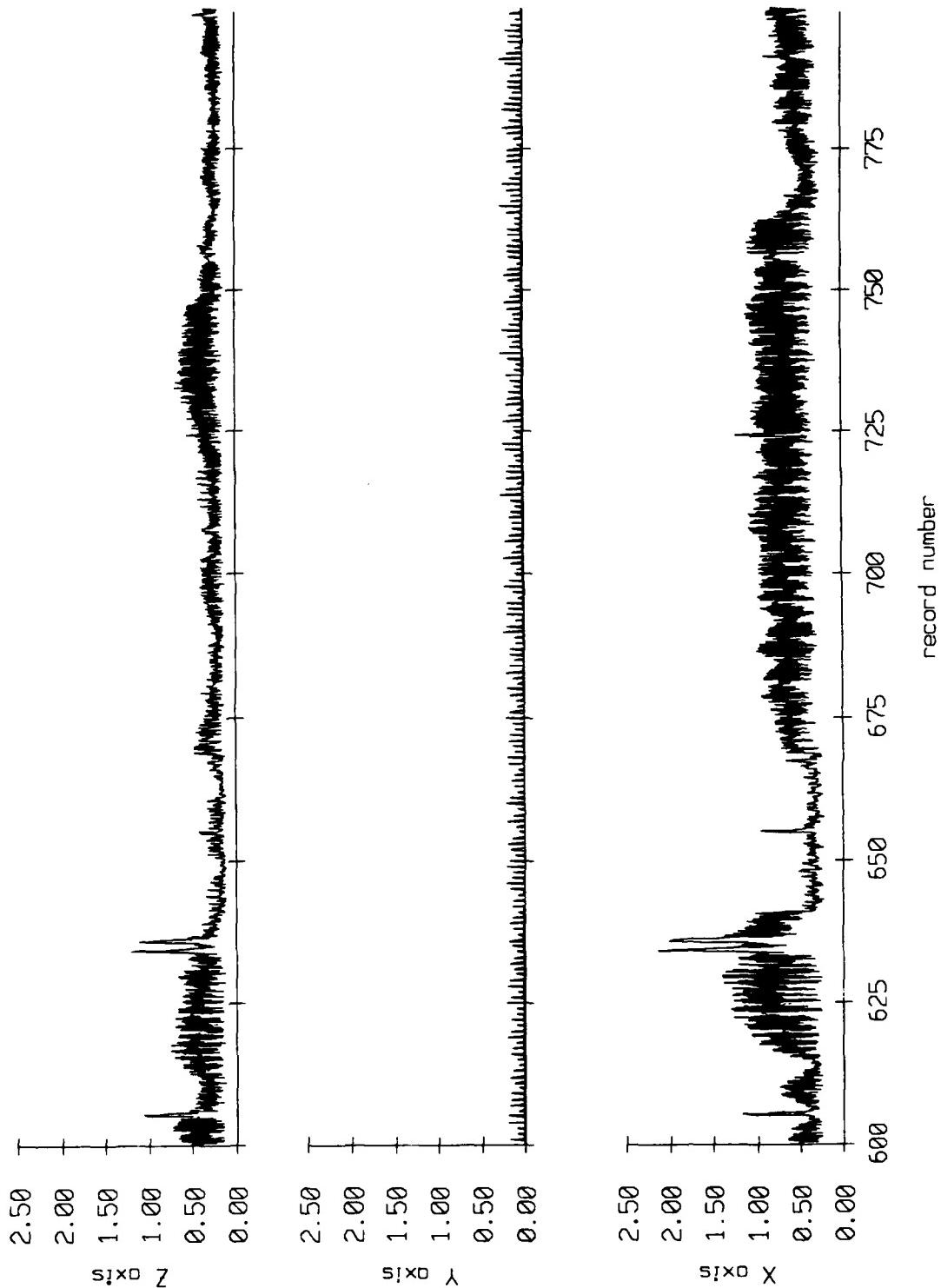


Figure IX.2c

Float 1, September 1987 Sea Trip
averaging period = 5.00 sec.



Gain Corrected Level, Volts(RMS)

Figure IX.2d

Float 1, September 1987 Sea Trip
averaging period = 5.00 sec.

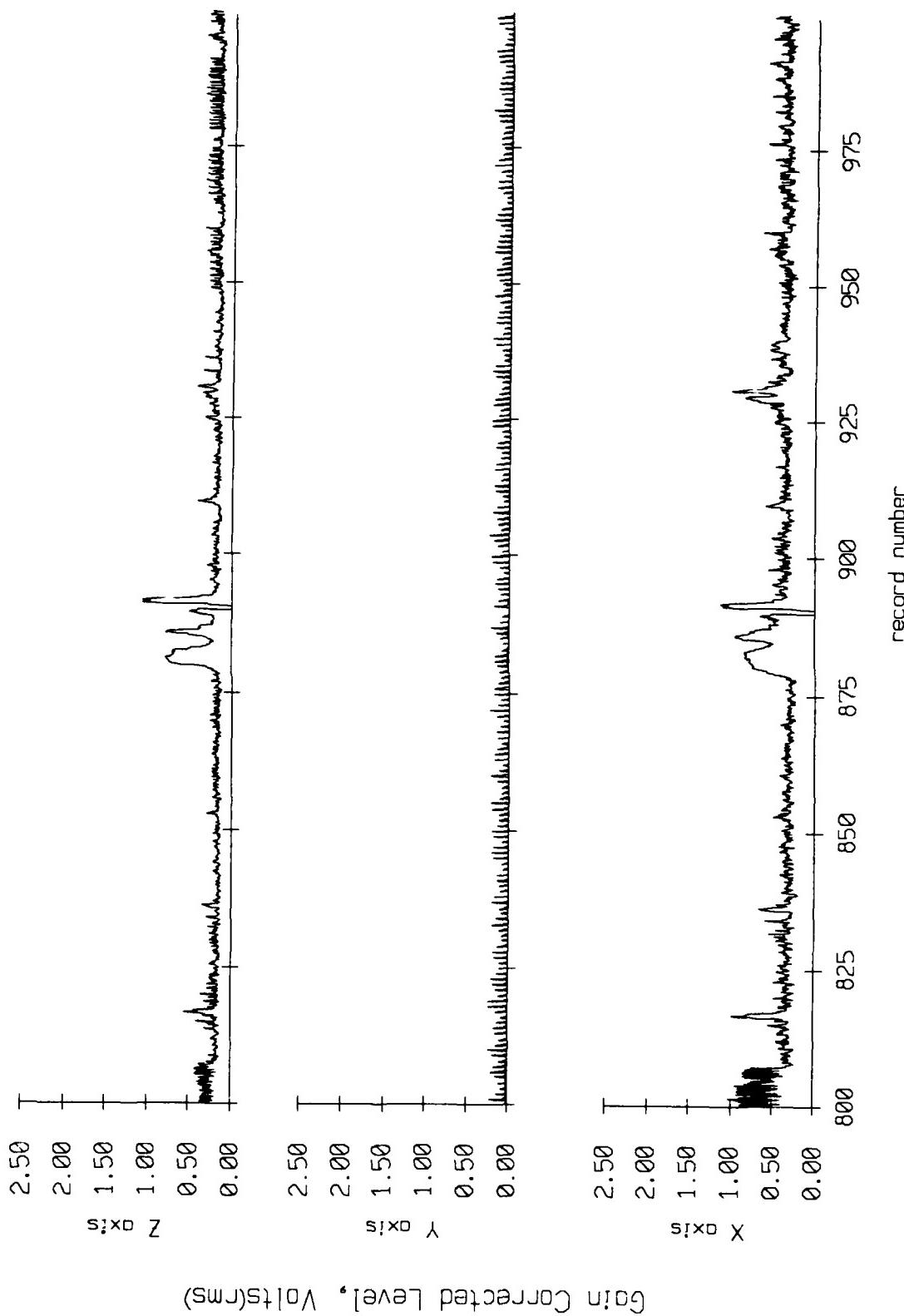


Figure IX.2e

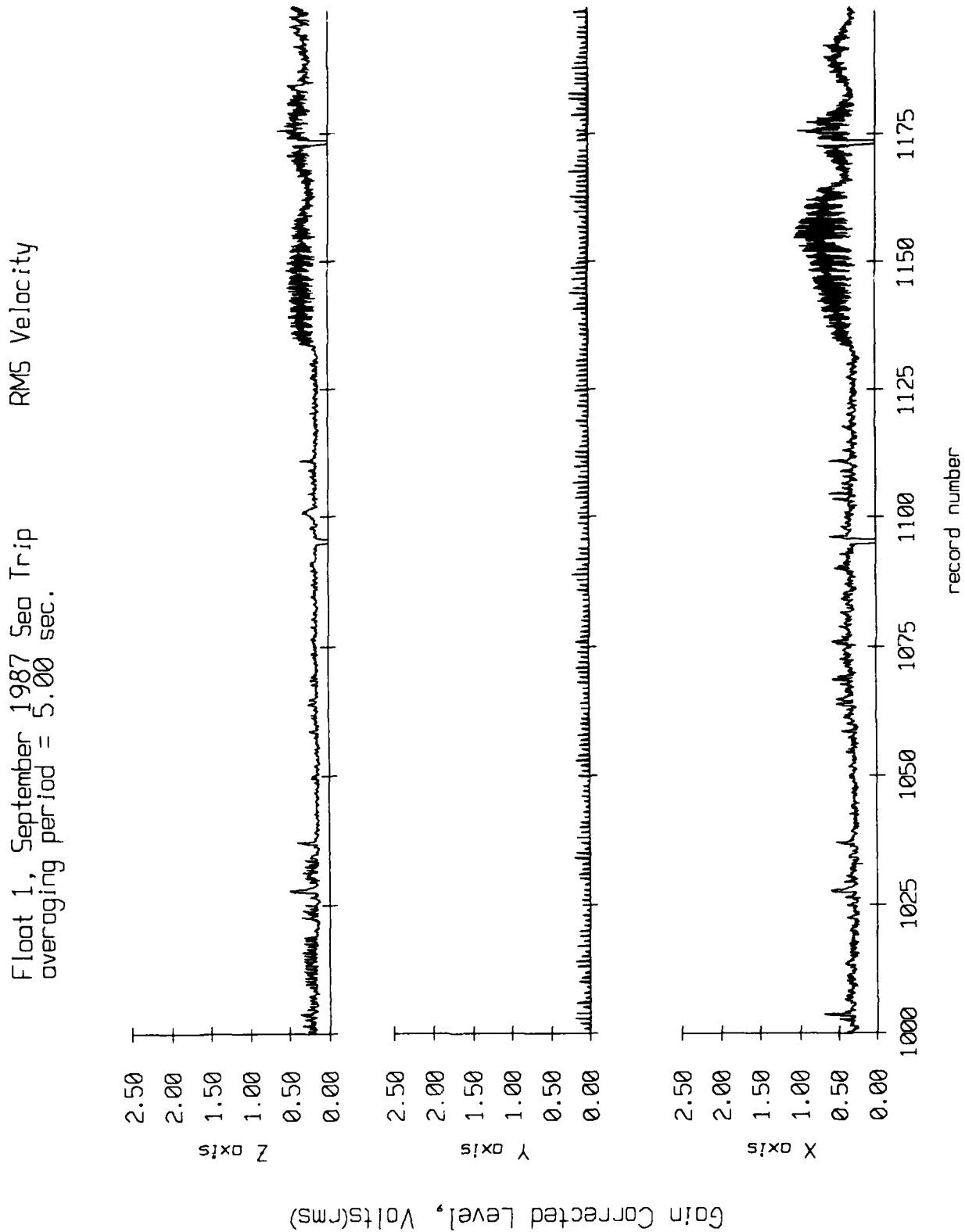


Figure IX.2f

Float 1, September 1987 Sea Trip
averaging period = 5.00 sec.

RMS Velocity

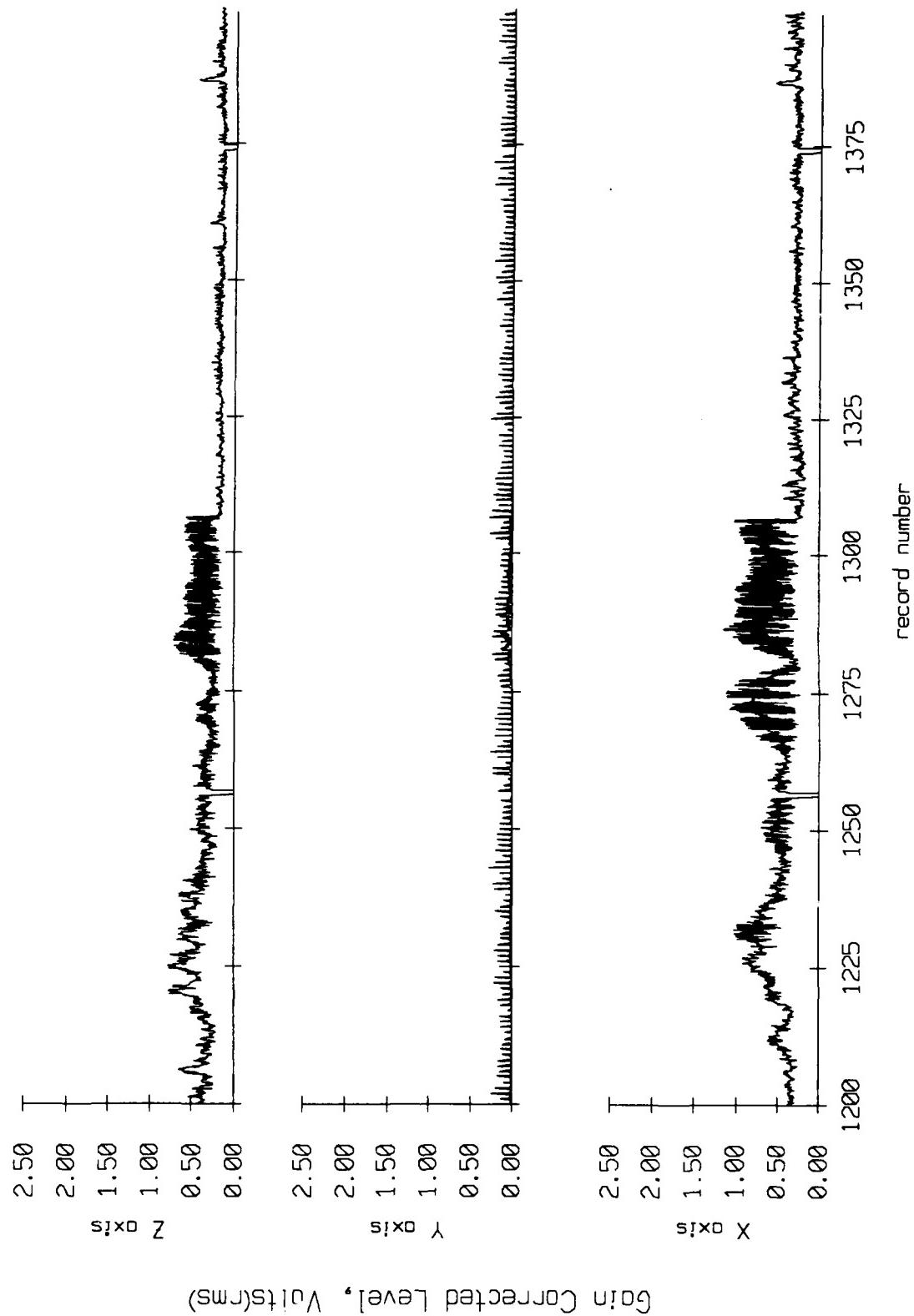


Figure IX.2g

Float 1, September 1987 Sea Trip
averaging period = 5.00 sec.

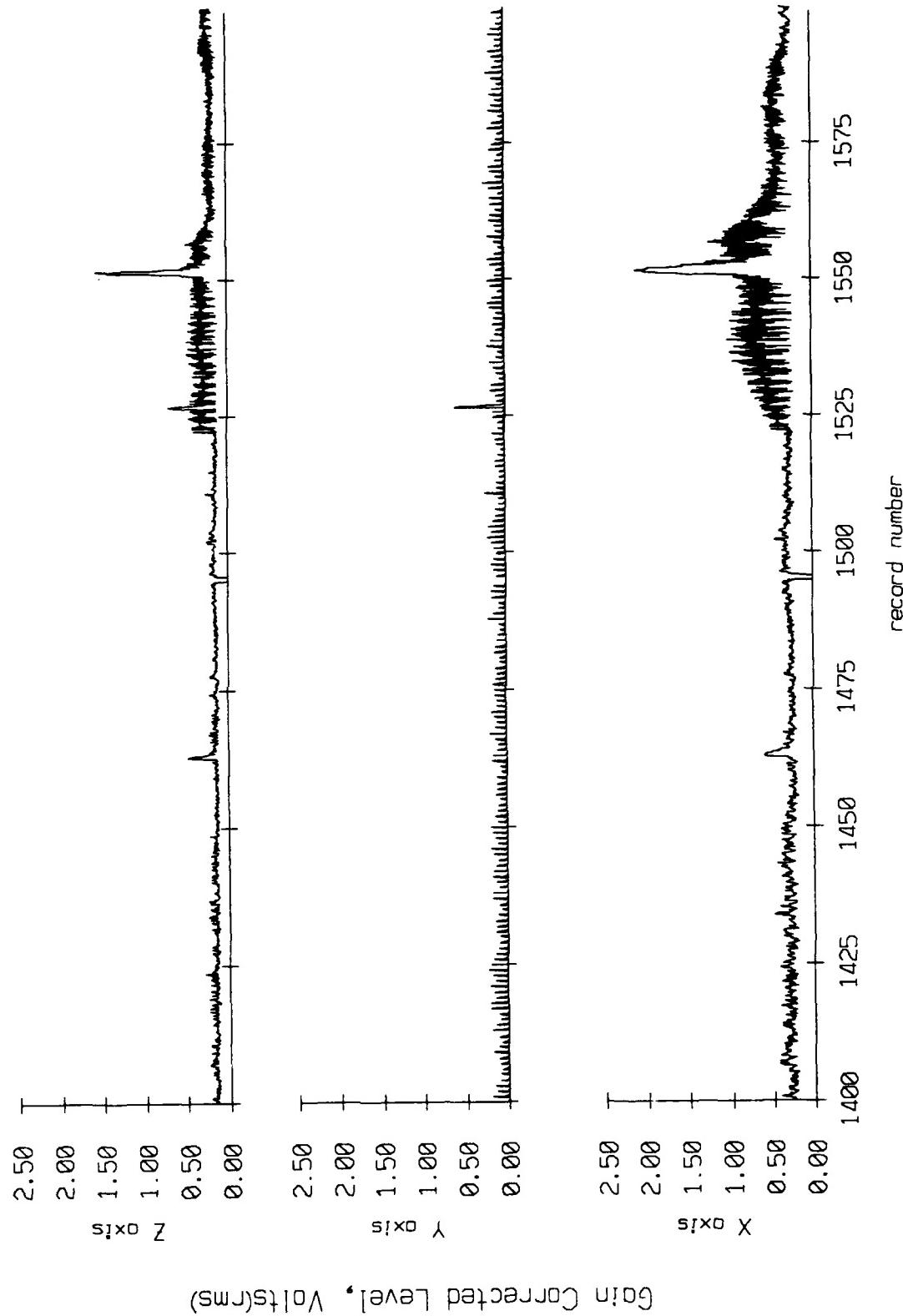


Figure IX.2h

Float 1, September 1987 Sea Trip
overaging period = 5.00 sec.

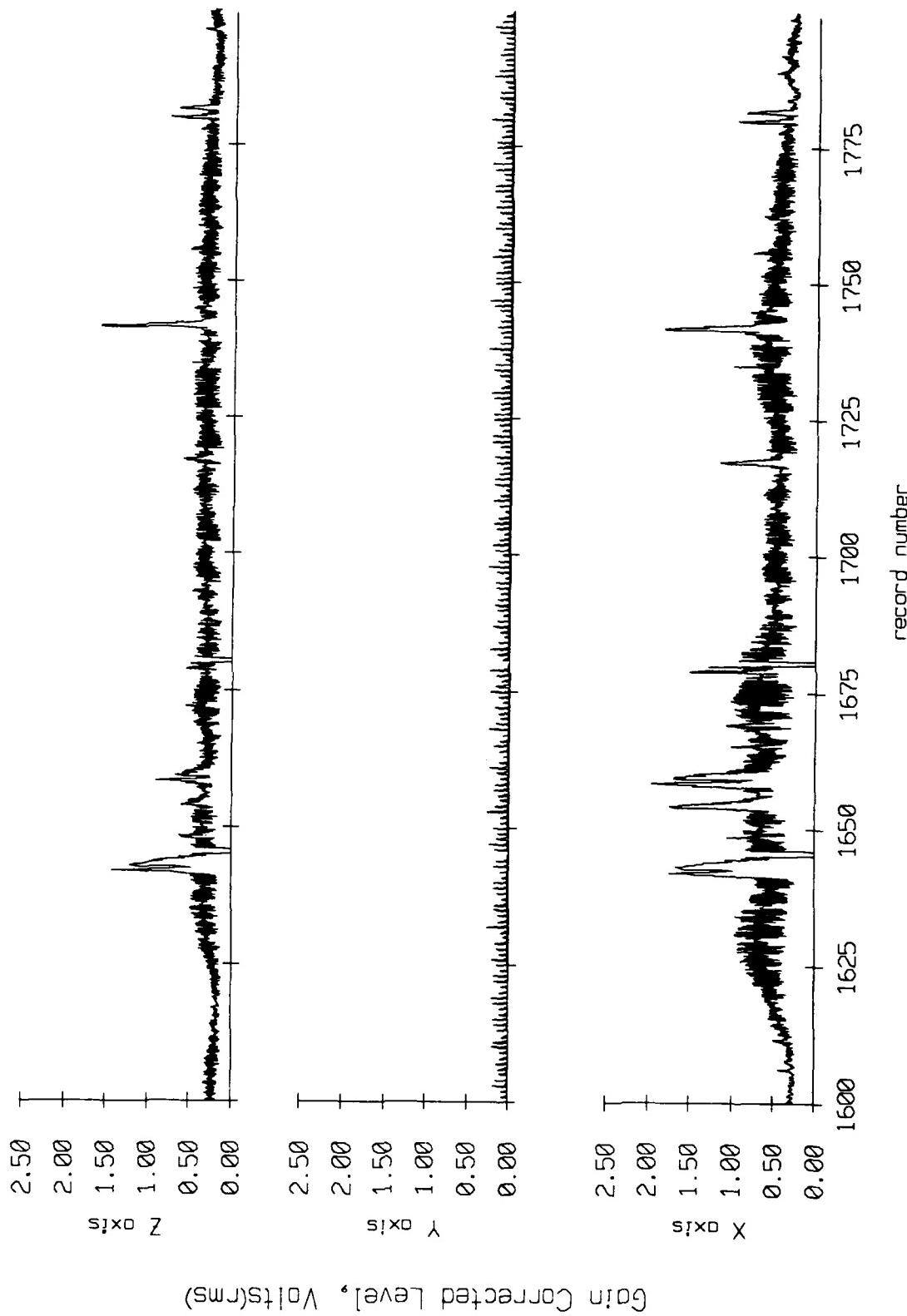


Figure IX.2i

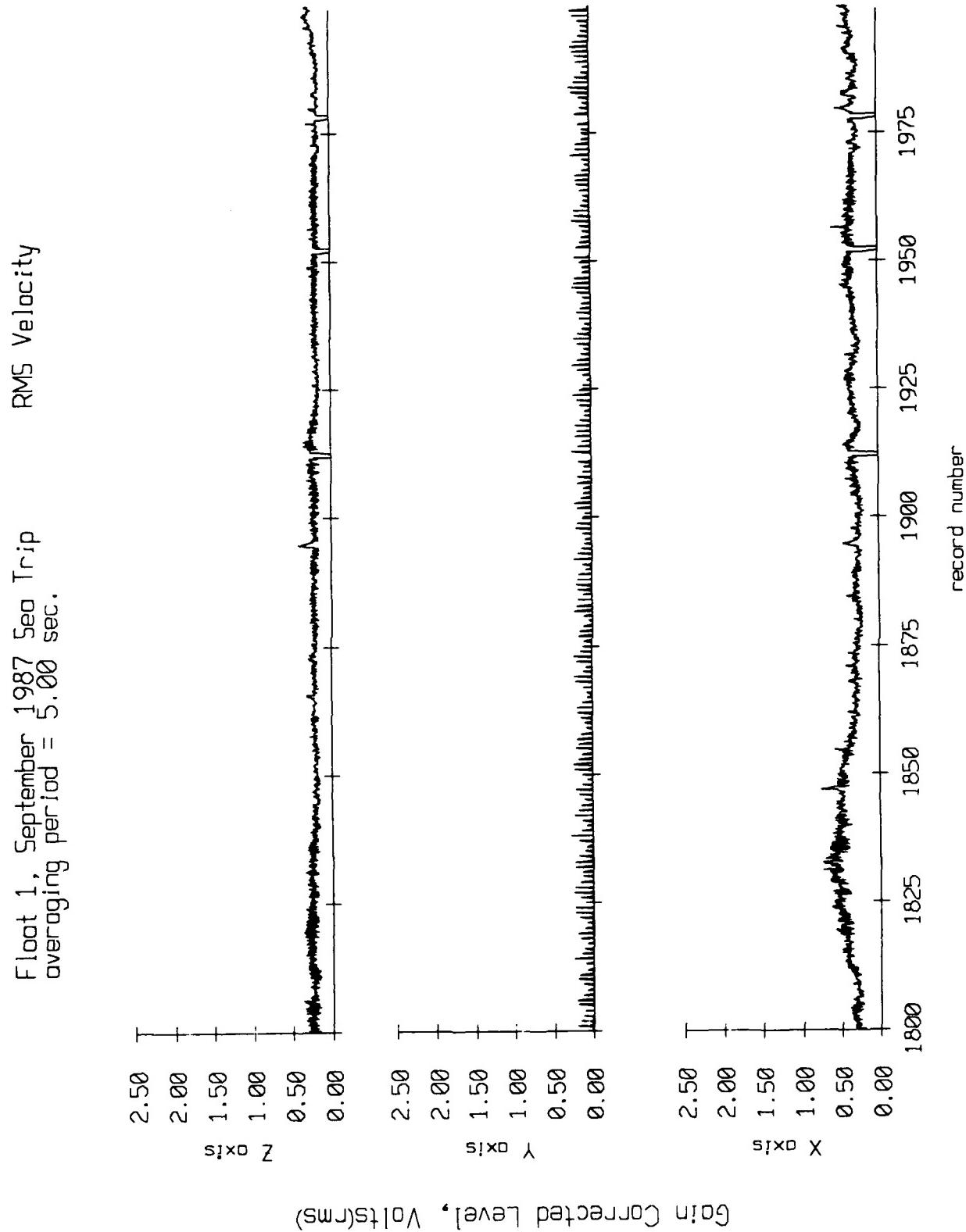


Figure IX.2j

Float 1, September 1987 Sea Trip
averaging period = 5.00 sec.

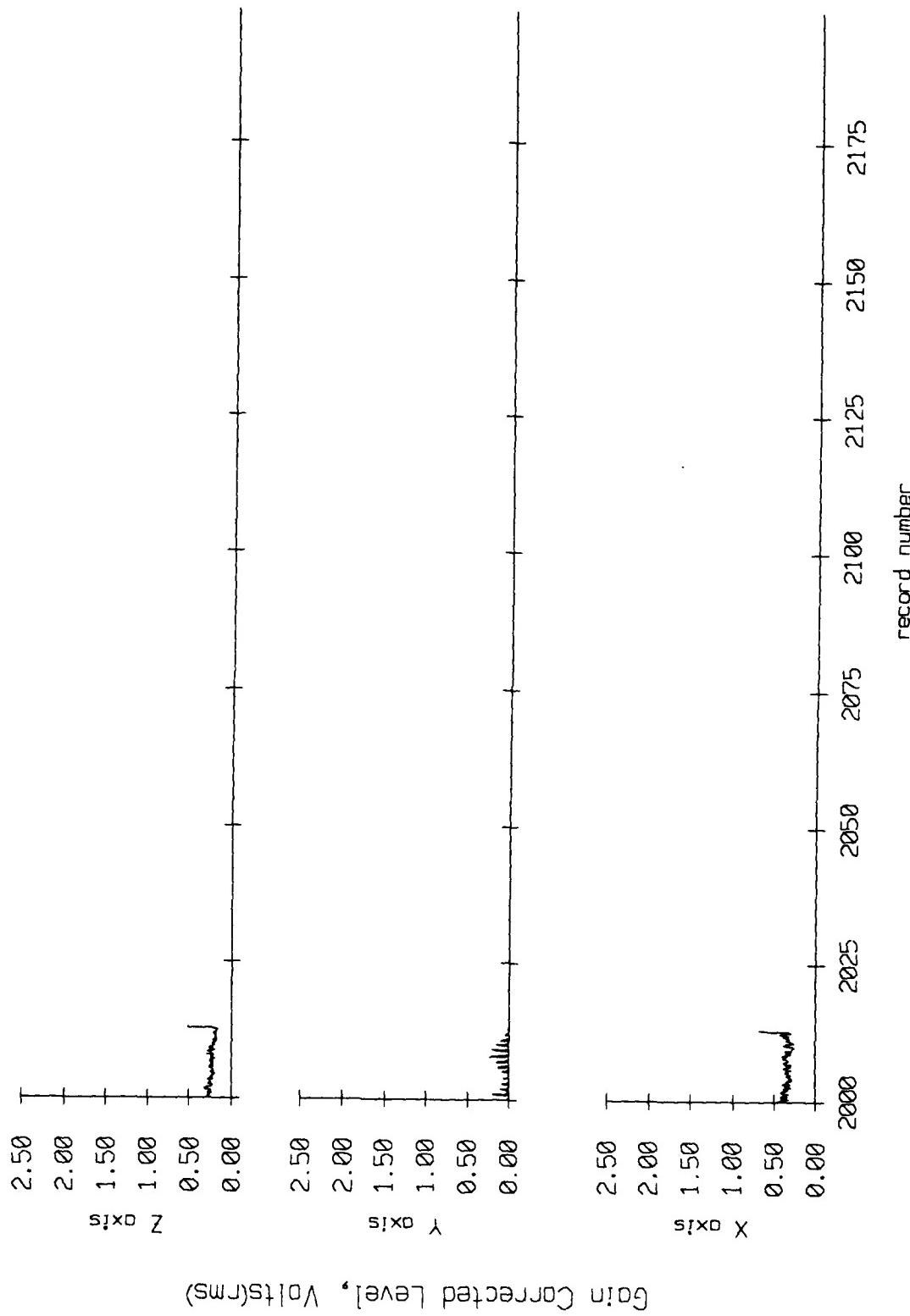


Figure IX.2k

Float 2, September 1987 Sea Trip
averaging period = 5.00 sec.

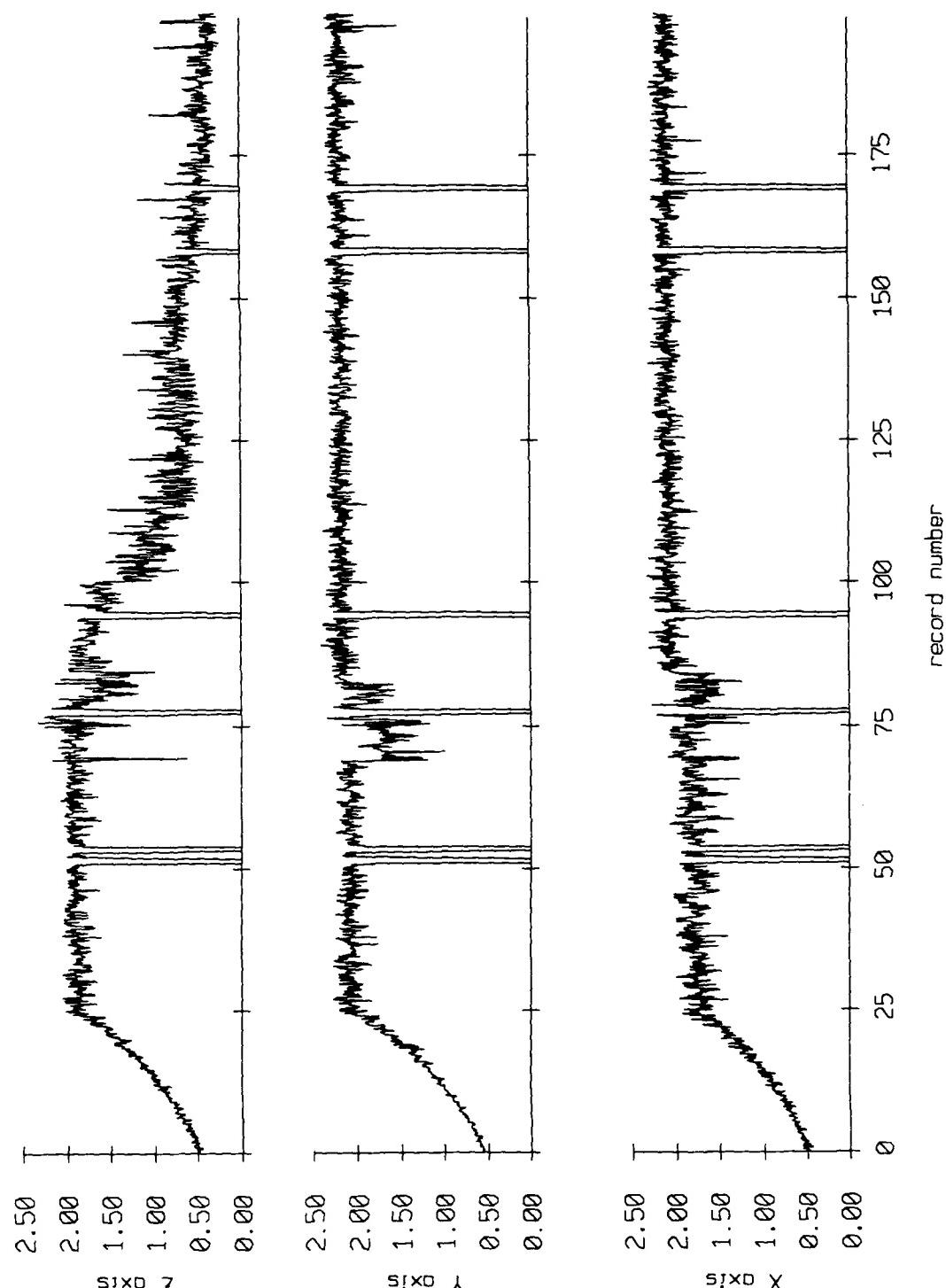
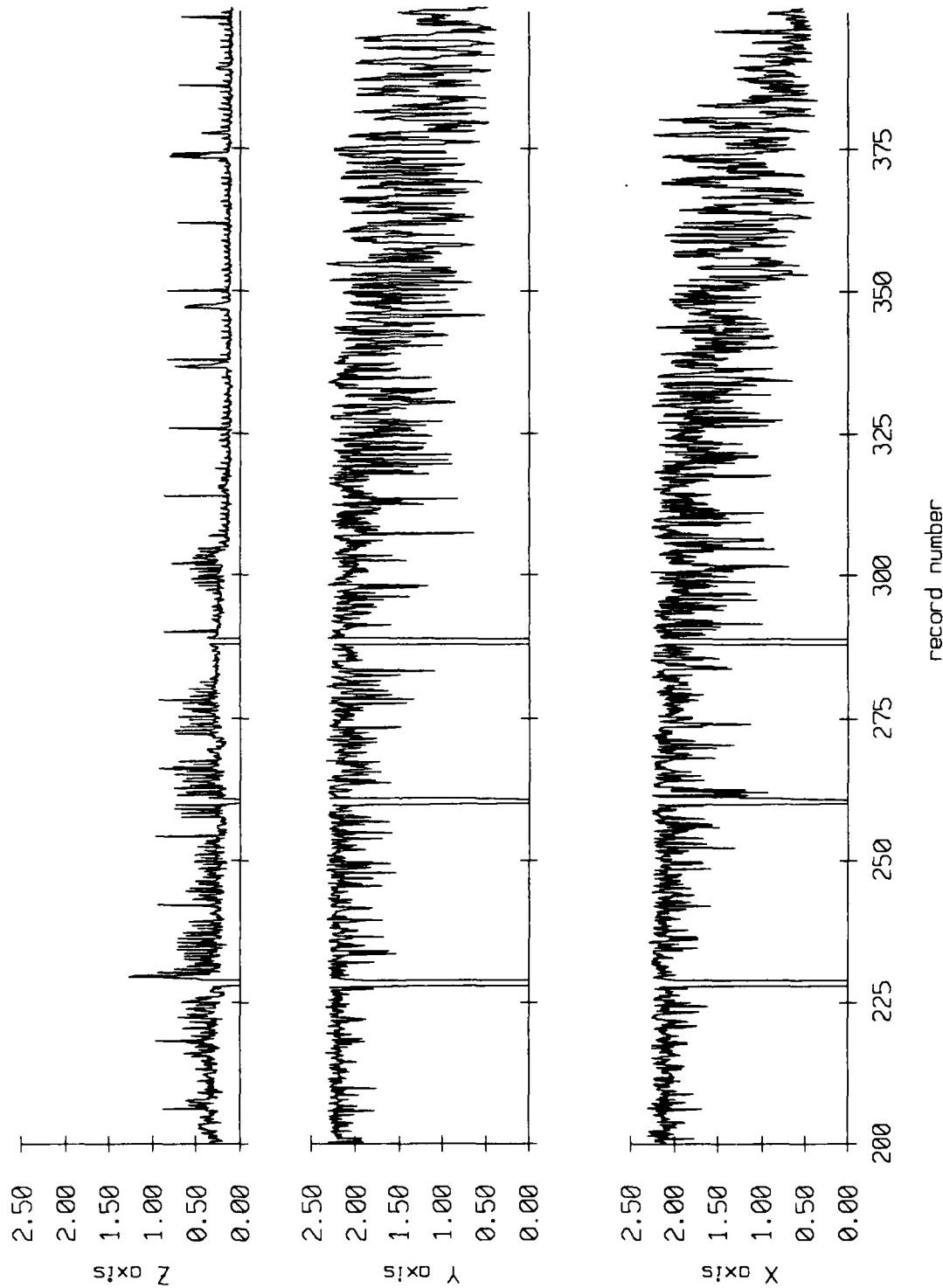


Figure IX.3a

Float 2, September 1987 Sea Trip
averaging period = 5.00 sec.

RMS Velocity



Gain Corrected Level, Volts(rms)

Figure IX.3b

Float 2, September 1987 Sea Trip
overaging period = 5.00 sec.

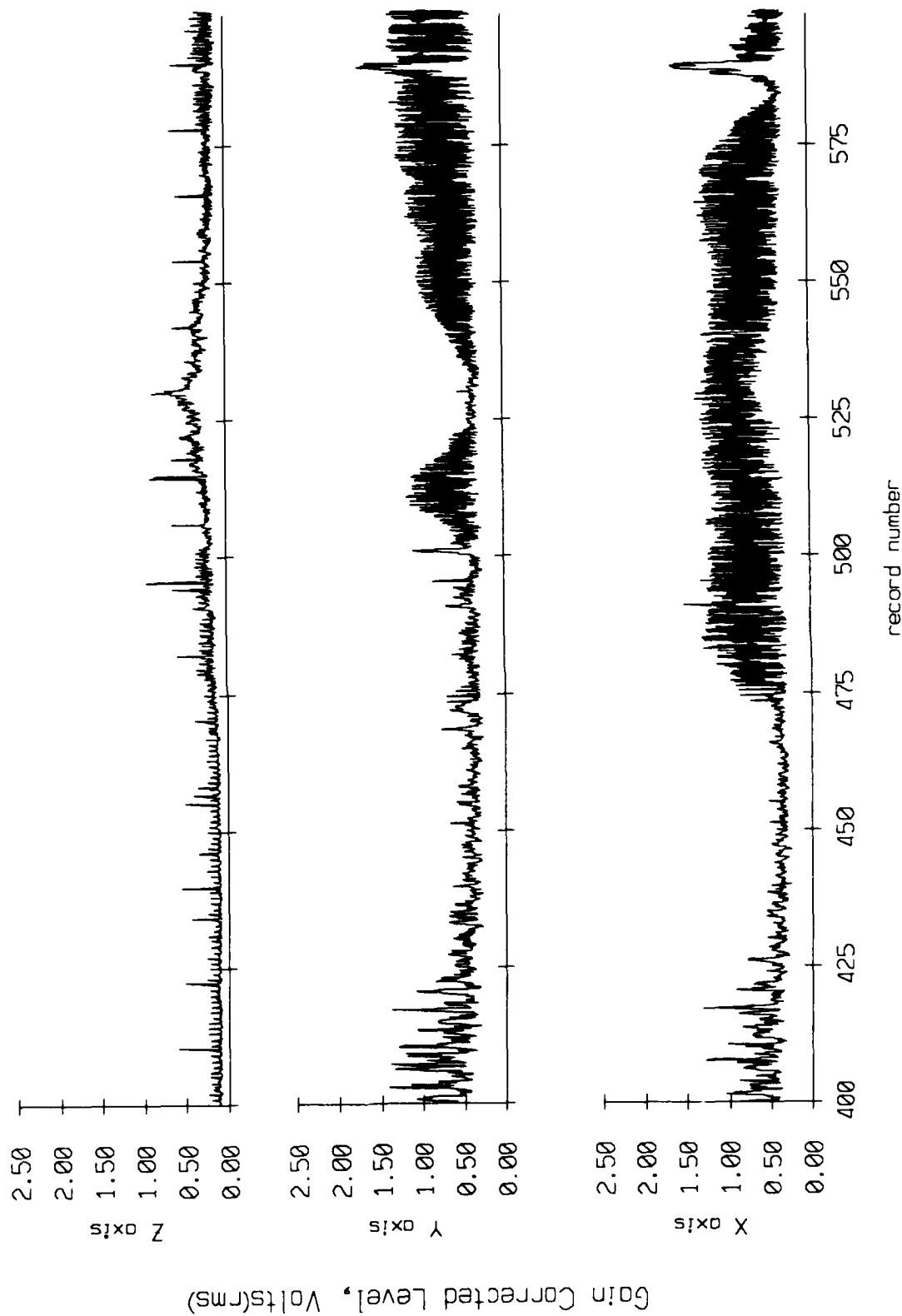


Figure IX.3c

Float 2, September 1987 Sea Trip
averaging period = 5.00 sec.

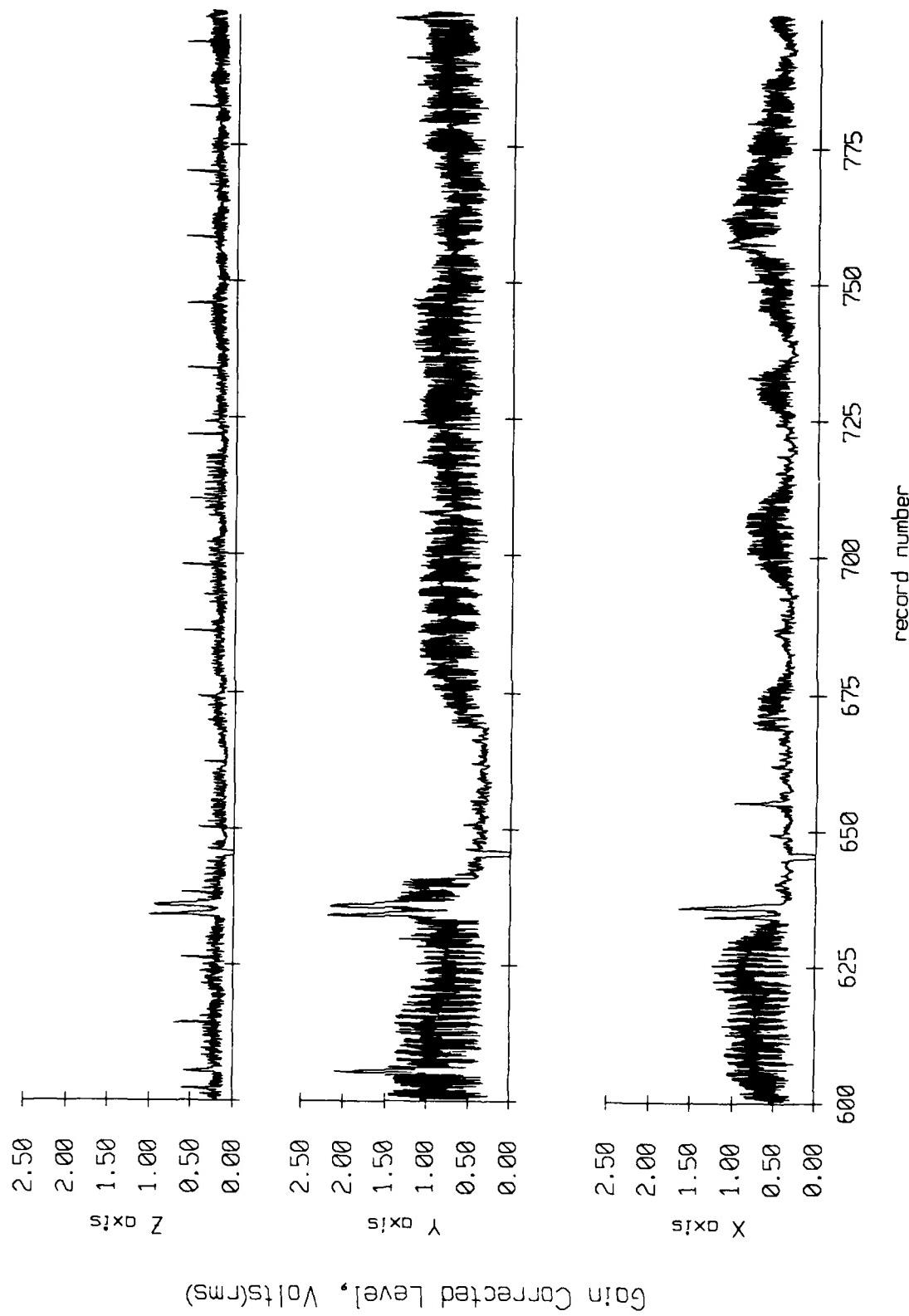


Figure IX.3d

Float 2, September 1987 Sea Trip
averaging period = 5.00 sec.

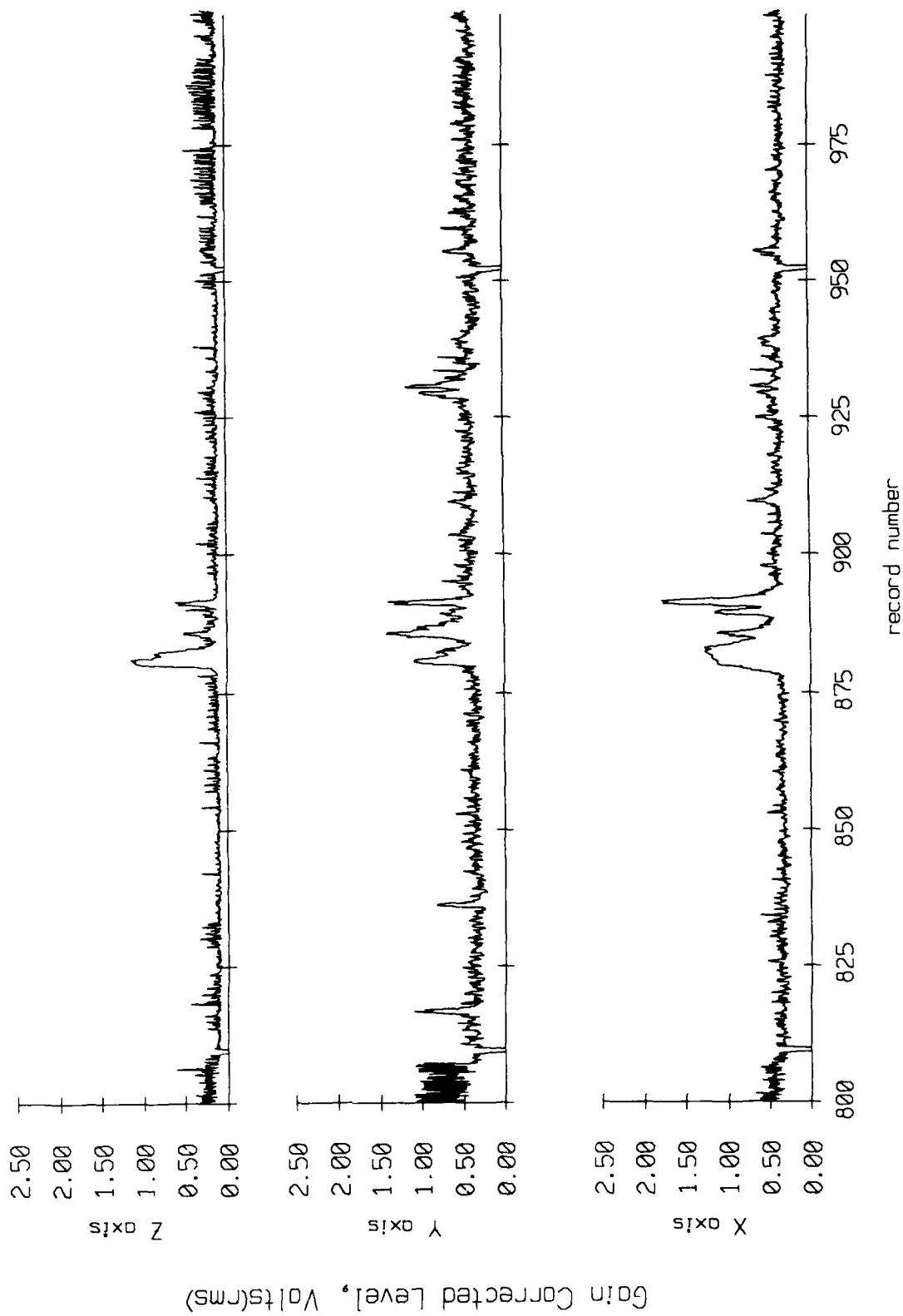


Figure IX.3e

Float 2, September 1987 Sea Trip
averaging period = 5.00 sec.

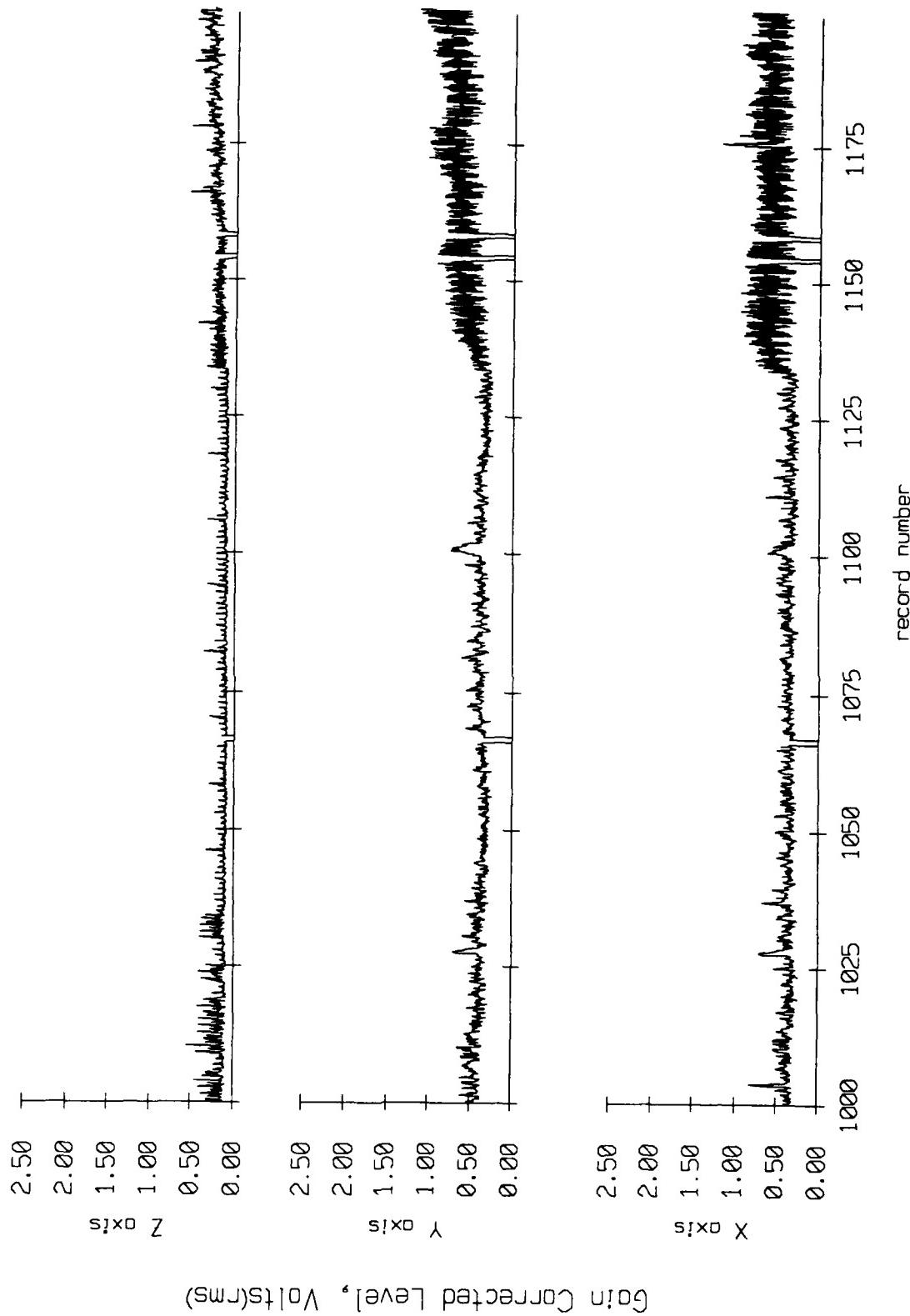


Figure IX.3f

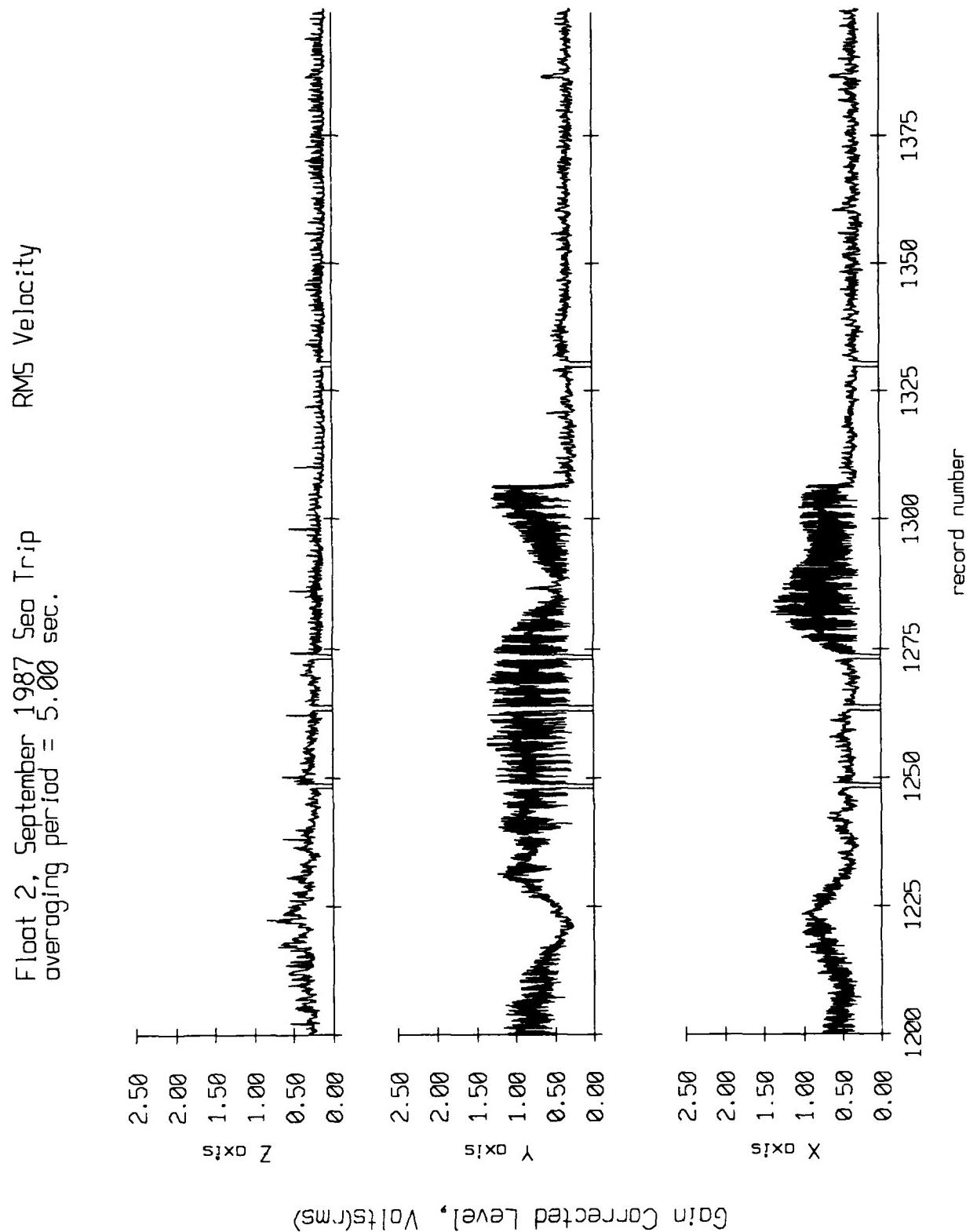


Figure IX.3g

Float 2, September 1987 Sea Trip
averaging period = 5.00 sec.

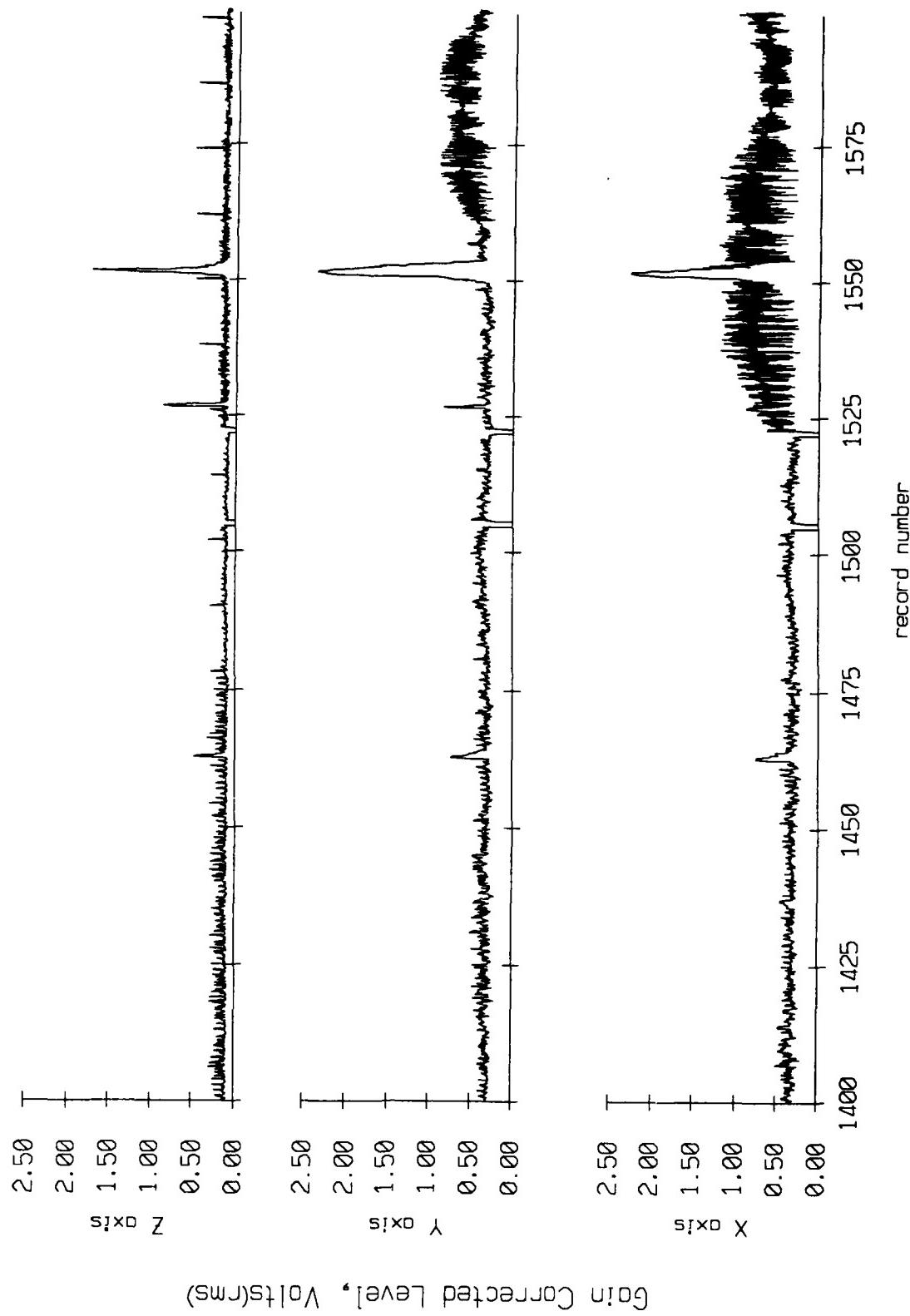


Figure IX.3h

Float 2, September 1987 Sea Trip
overaging period = 5.00 sec.

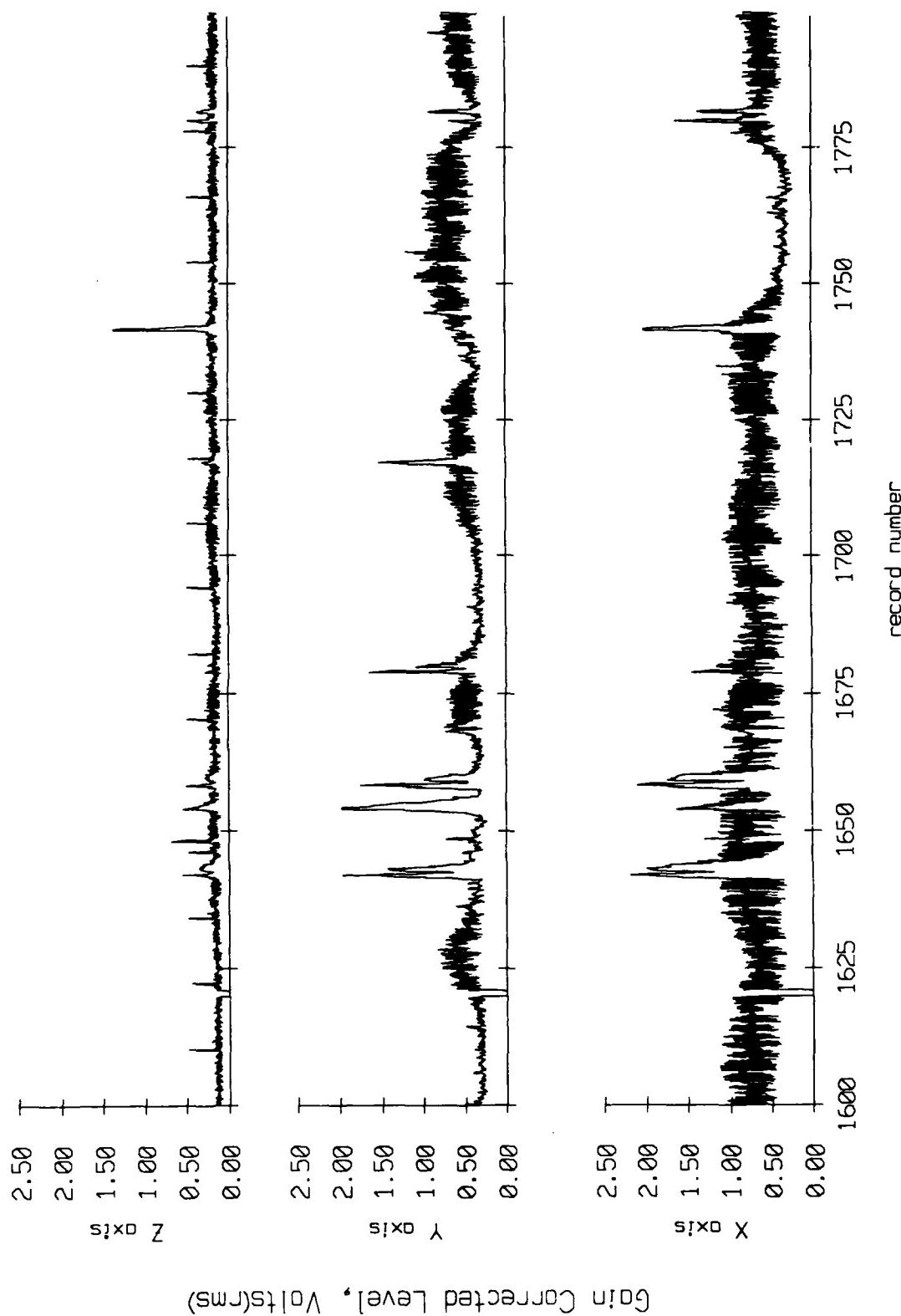


Figure IX.3i

Float 2, September 1987 Sea Trip
averaging period = 5.00 sec.

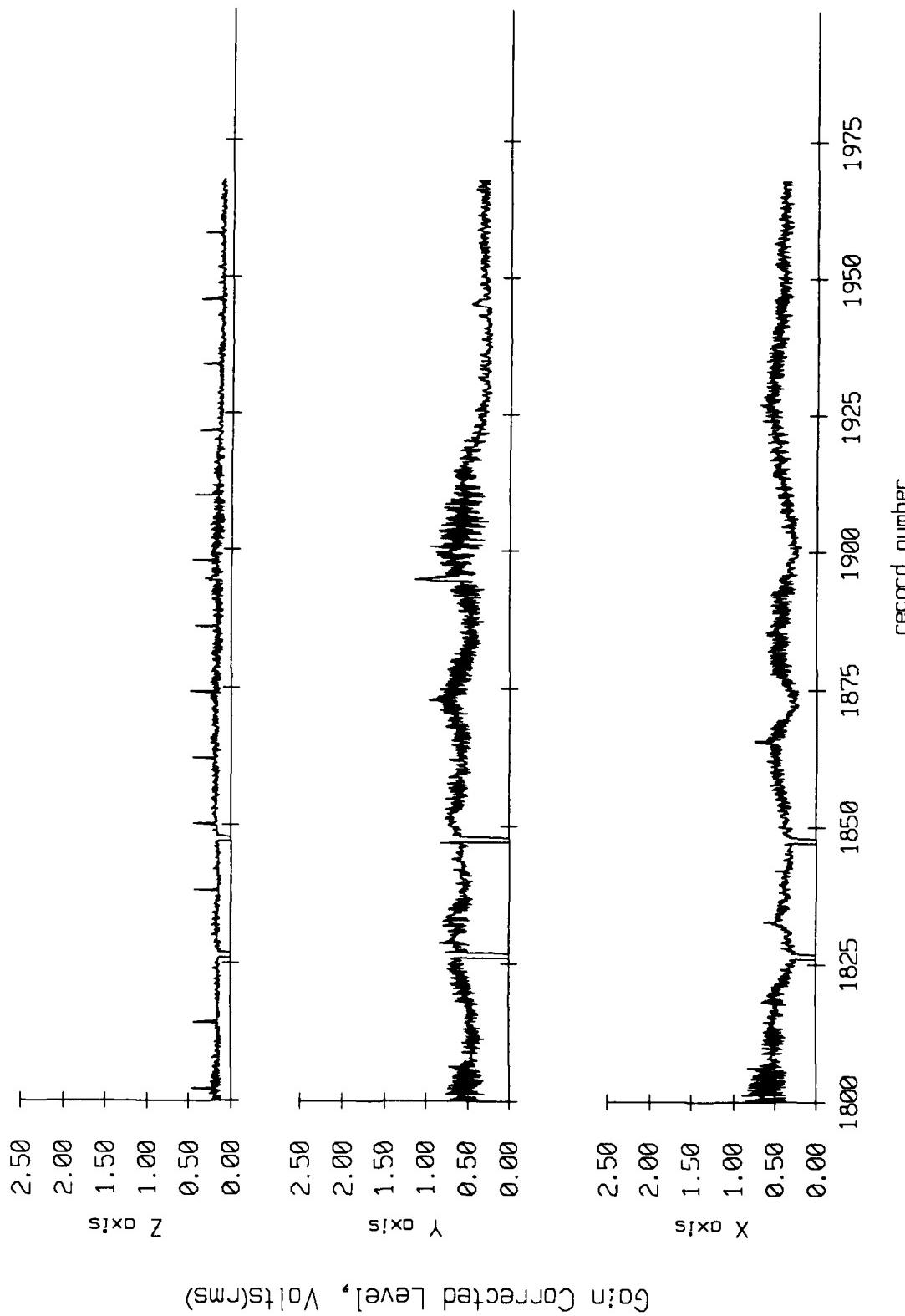
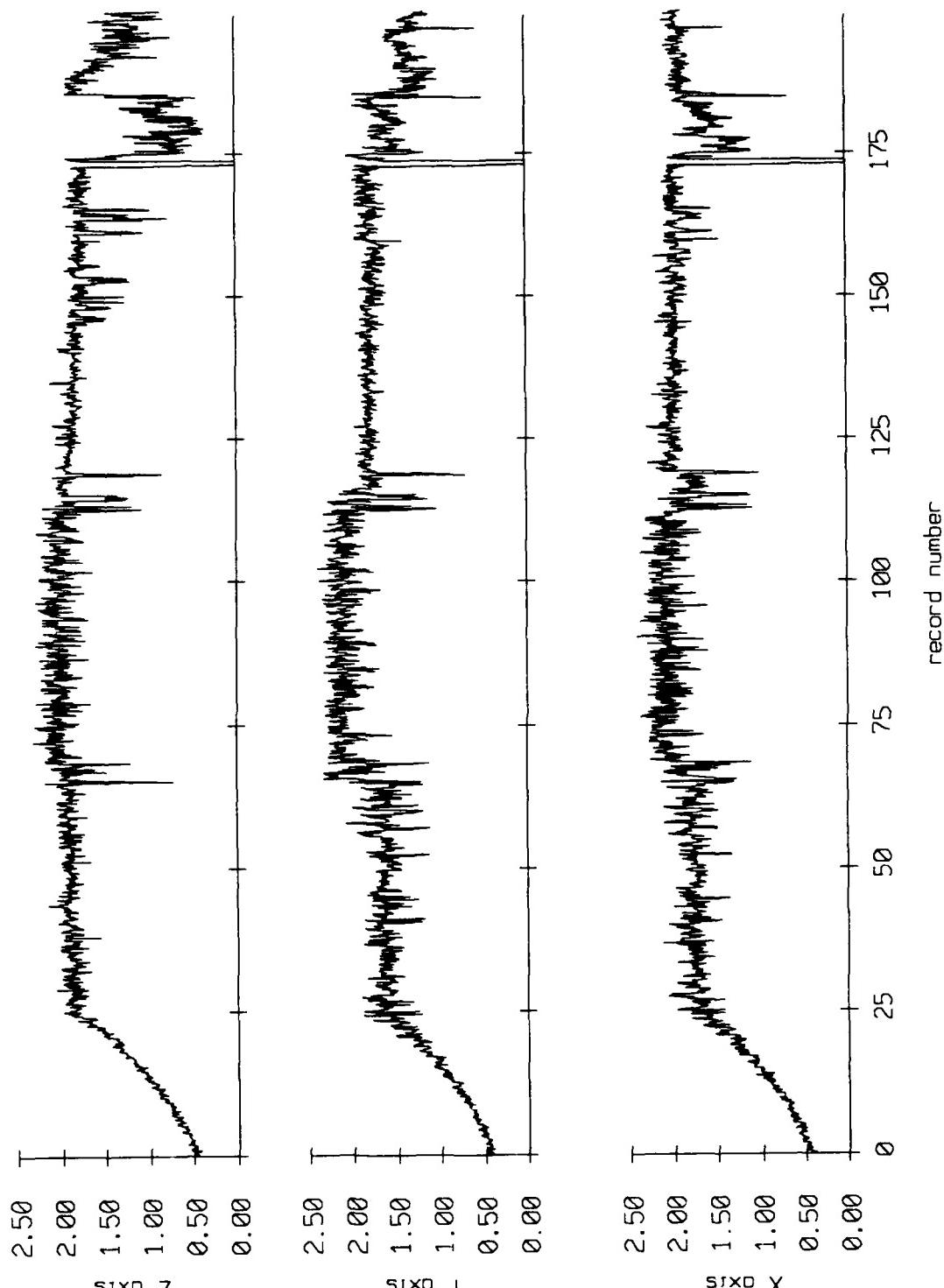


Figure IX.3j

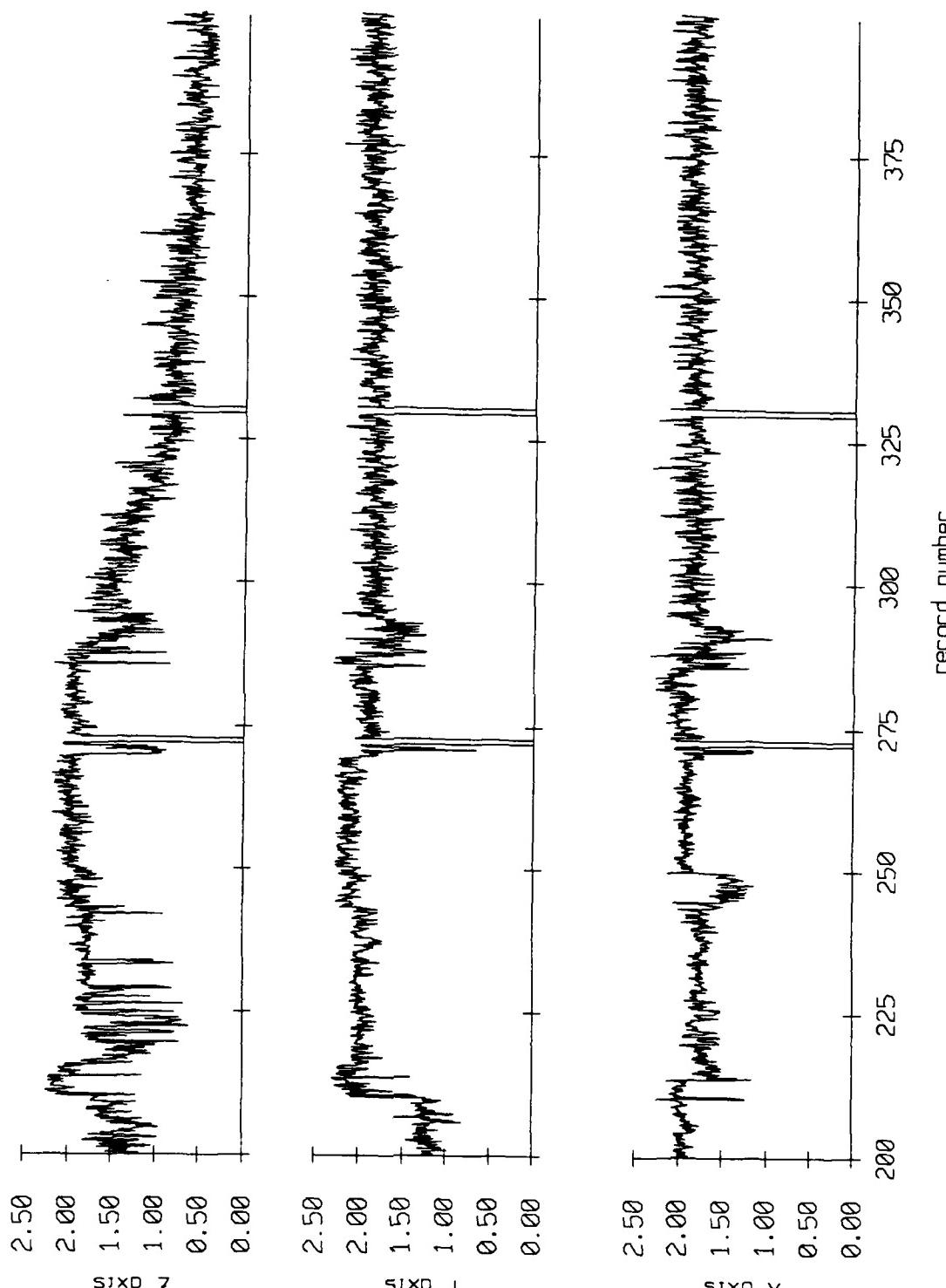
Float 3, September 1987 Sec. Trip
overaging period = 5.00 sec.



Gals Corrected Level, Volts(rms)

Figure IX.4a

Float 3, September 1987 Sea Trip
averaging period = 5.00 sec.



60 in Corrected Level, Volts(RMS)

Figure IX.4b

Float 3, September 1987 Sea Trip
averaging period = 5.00 sec.

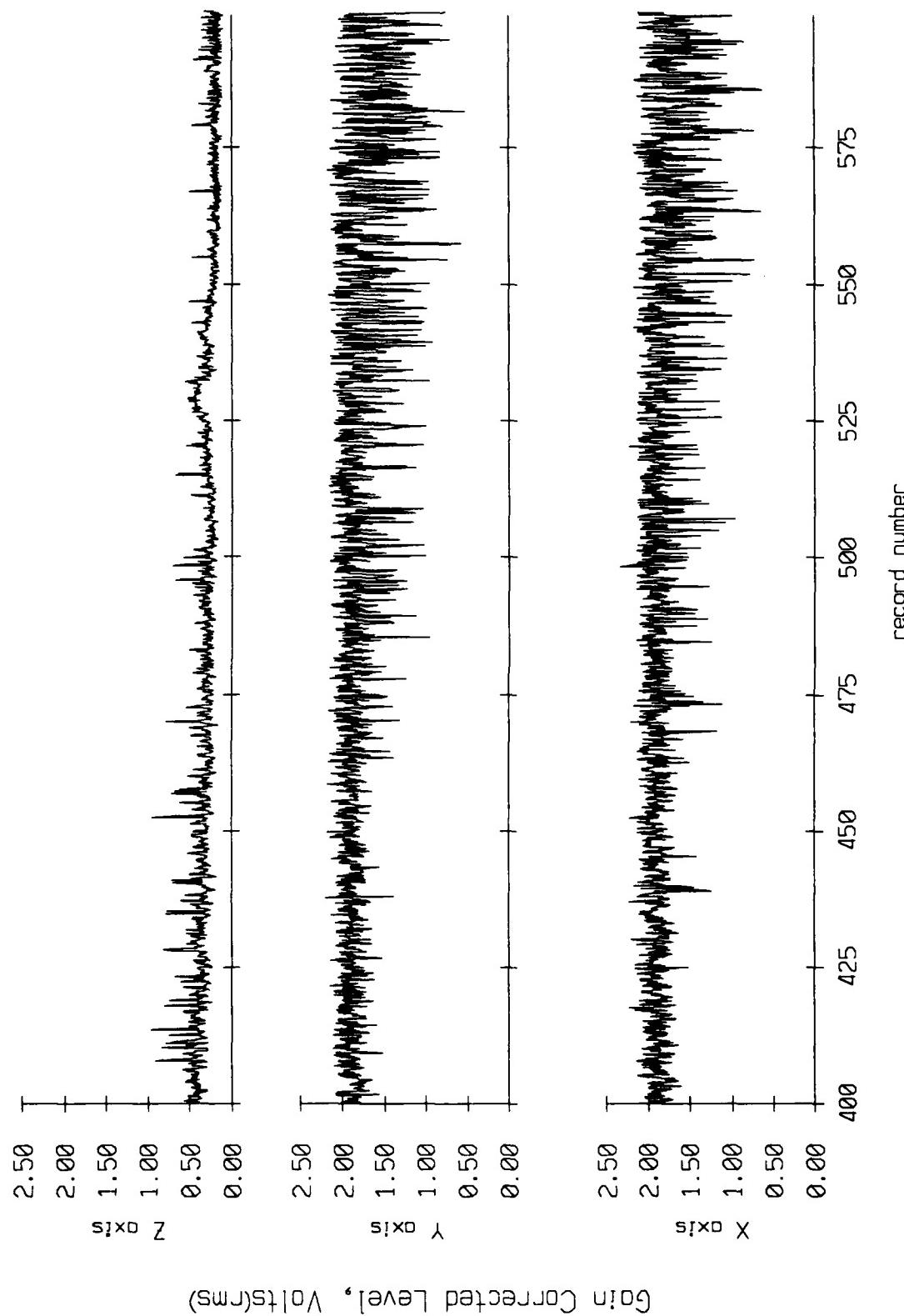


Figure IX.4c

Float 3, September 1987 Sea Trip
overaging period = 5.00 sec.

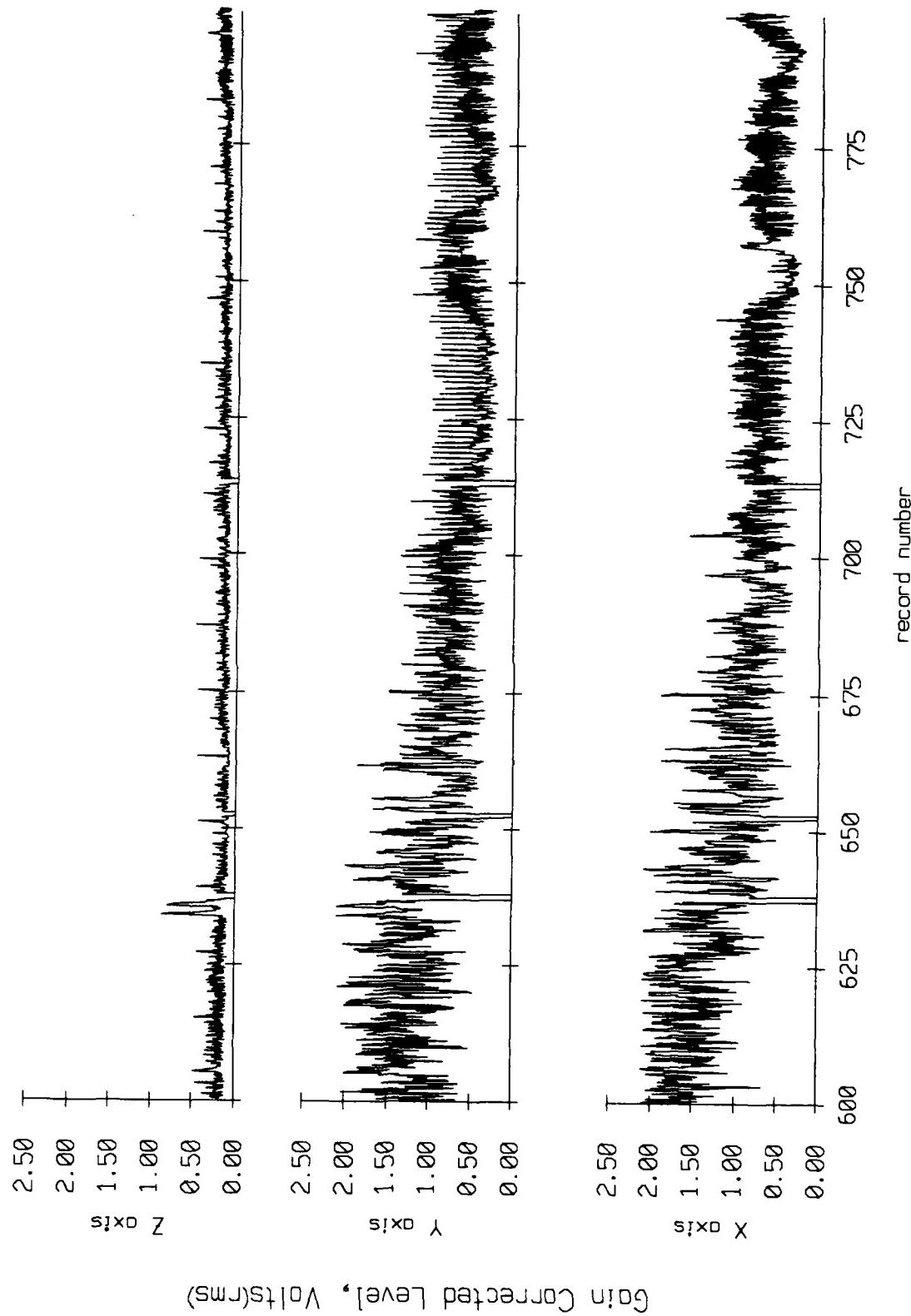
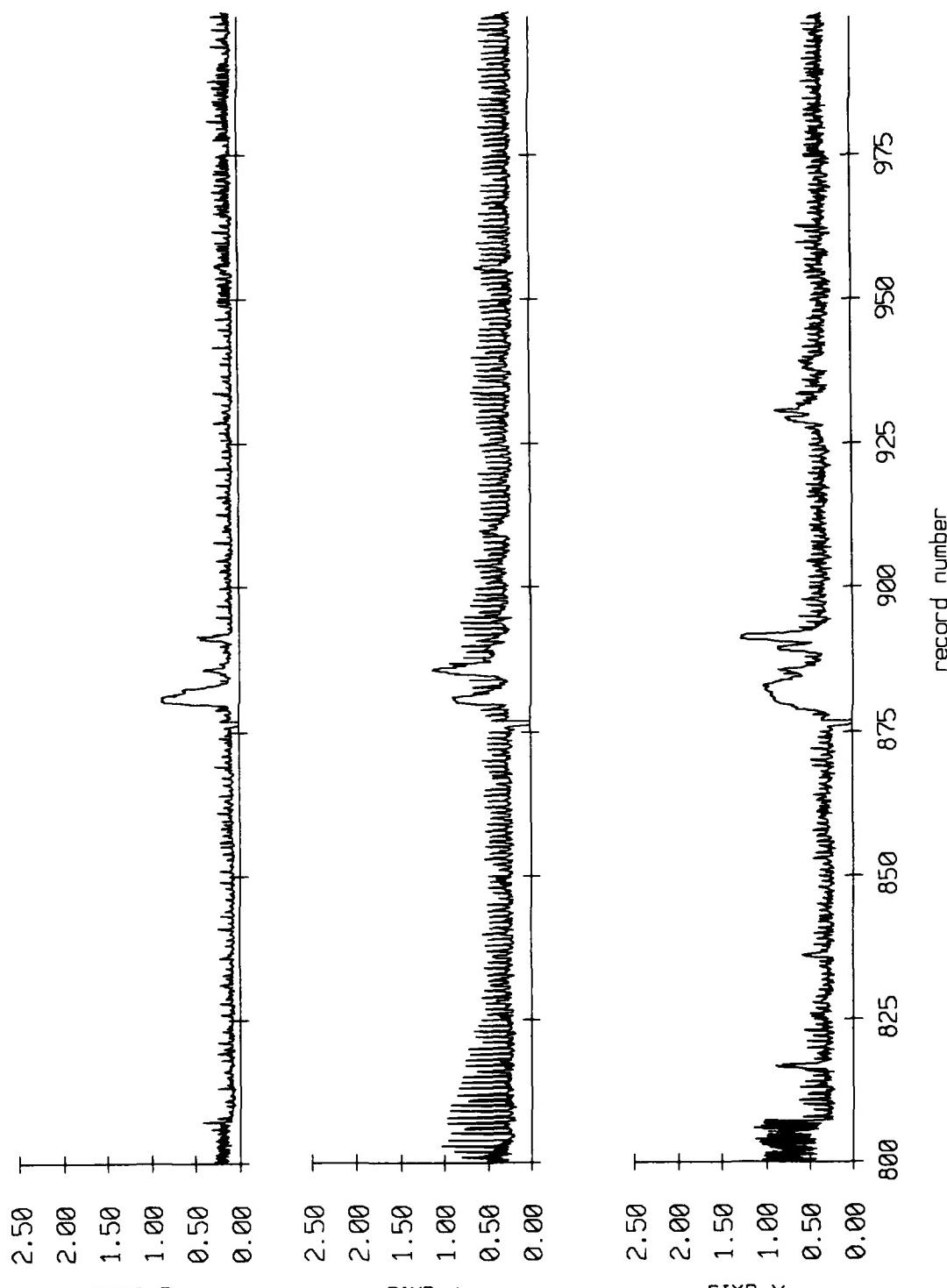


Figure IX.4d

Float 3, September 1987 Sea Trip
averaging period = 5.00 sec.

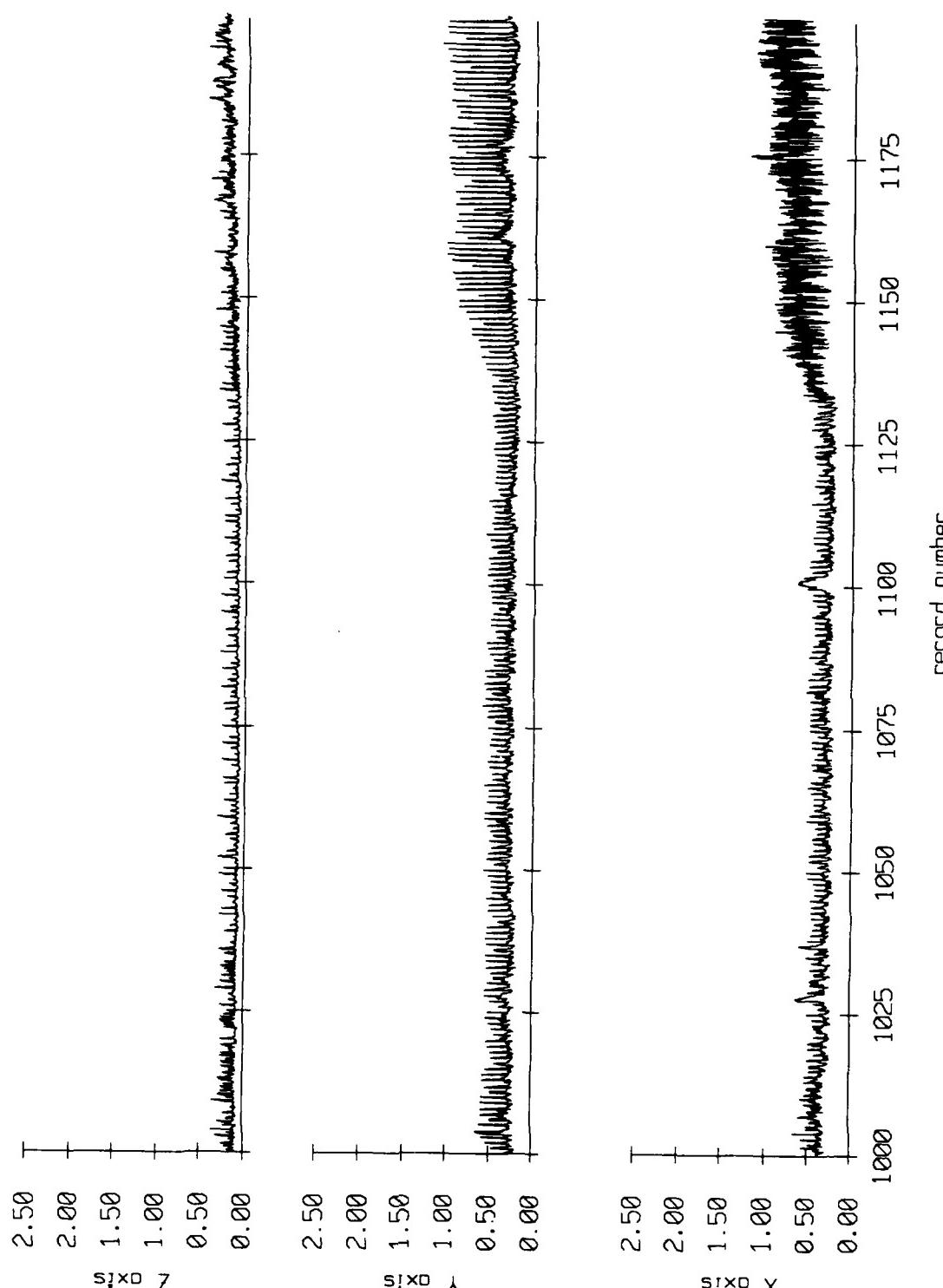
RMS Velocity



GAIN Corrected Level, Volts(RMS)

Figure IX.4e

Float 3, September 1987 Sea Trip
averaging period = 5.00 sec.

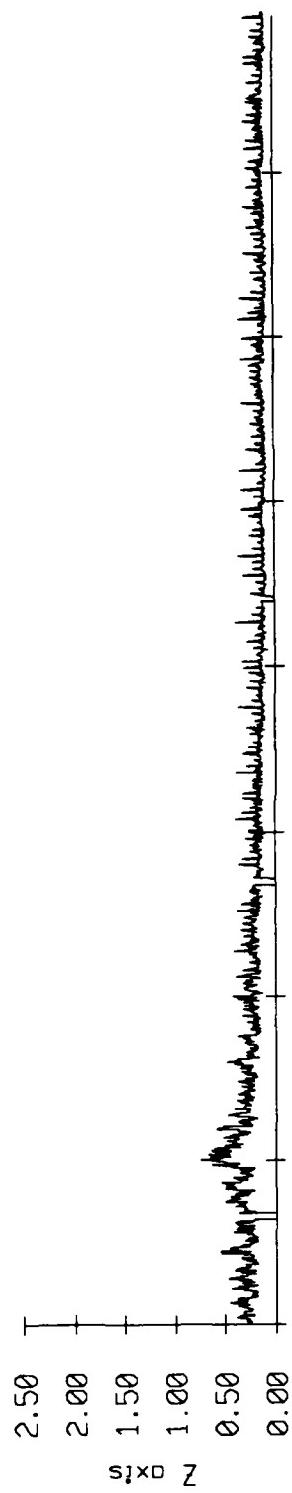


Gain Corrected Level, Volts(rms)

Figure IX.4f

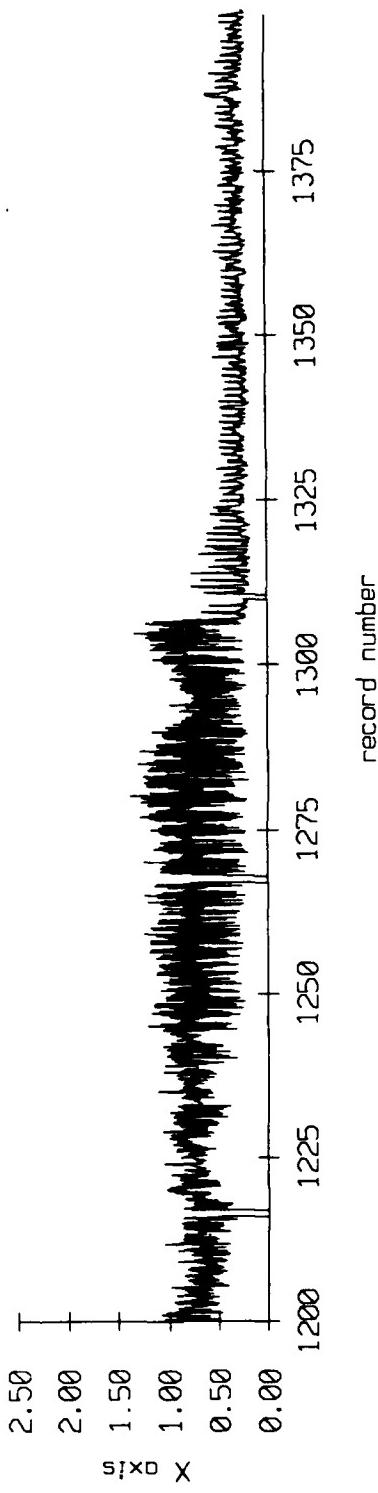
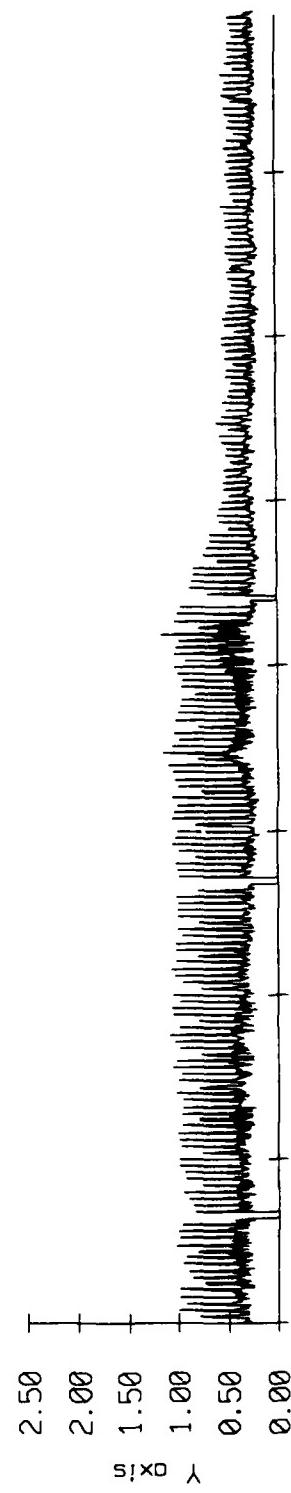
Float 3, September 1987 Sea Trip
averaging period = 5.00 sec.

RMS Velocity



60 in Corrected Level, Volts(RMS)

Figure IX.4g



record number

Float 3, September 1987 Sea Trip
overaging period = 5.00 sec.

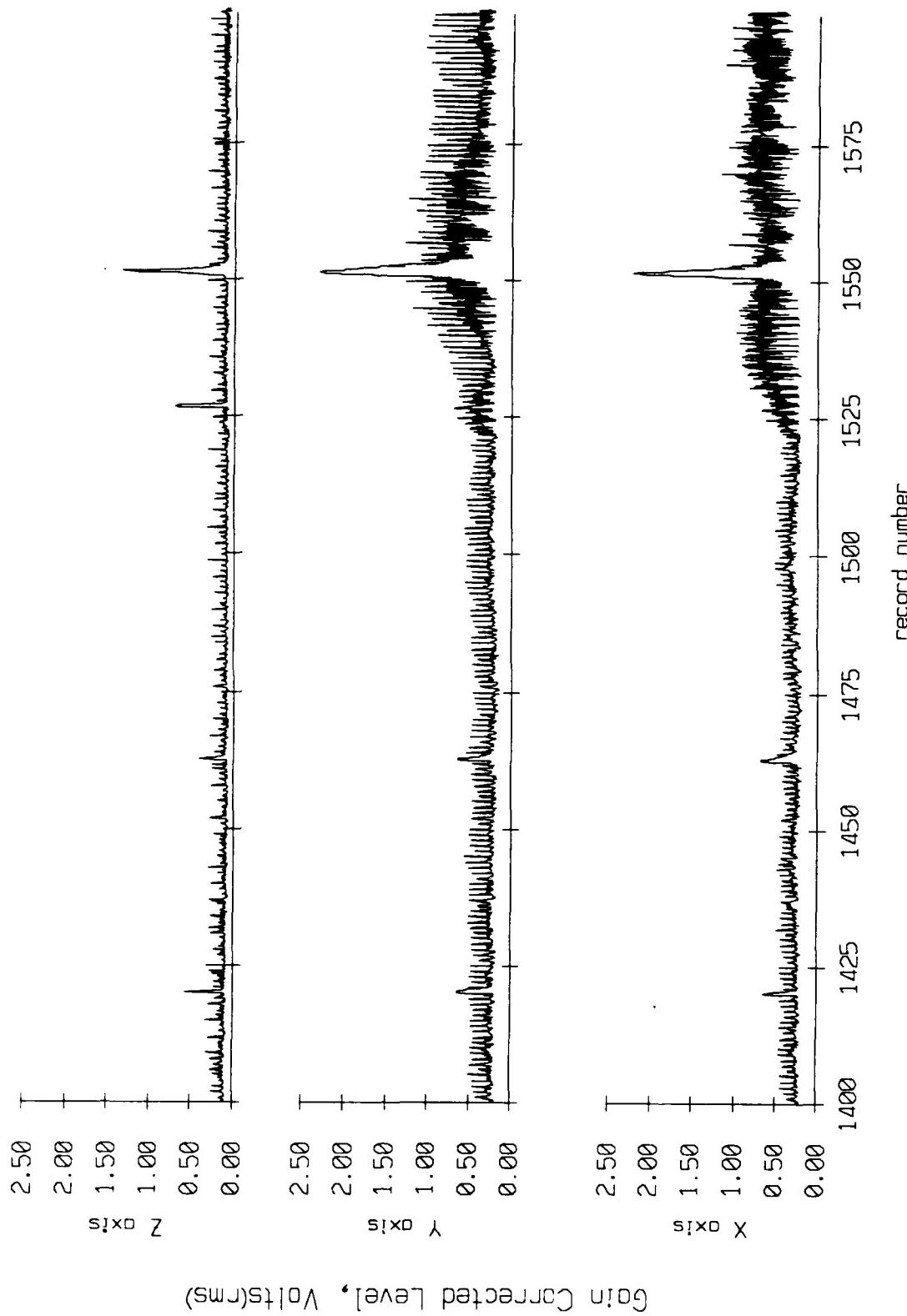
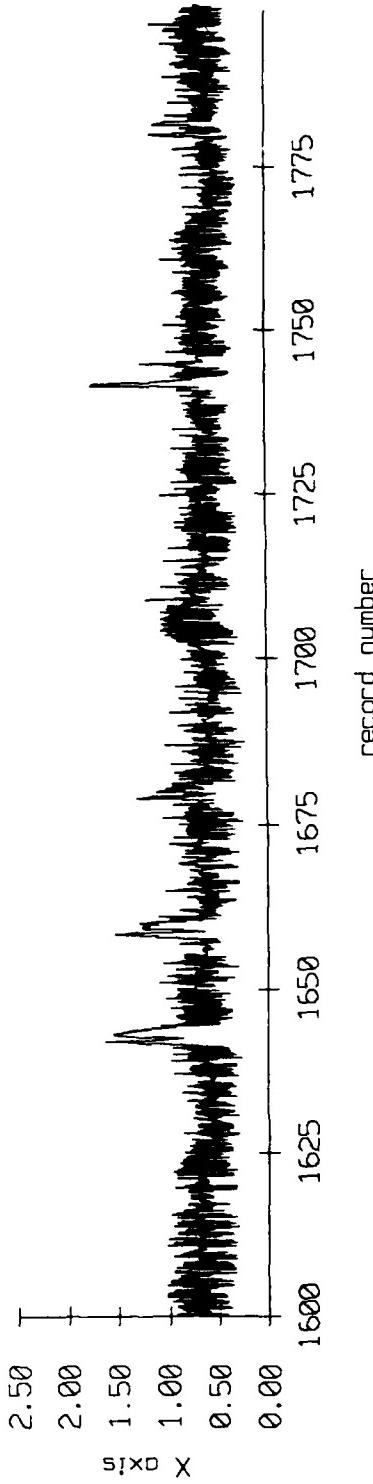
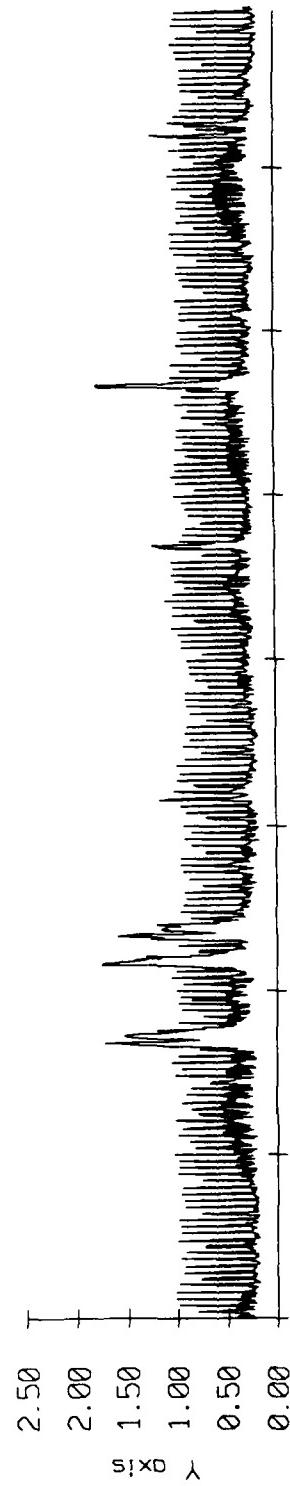
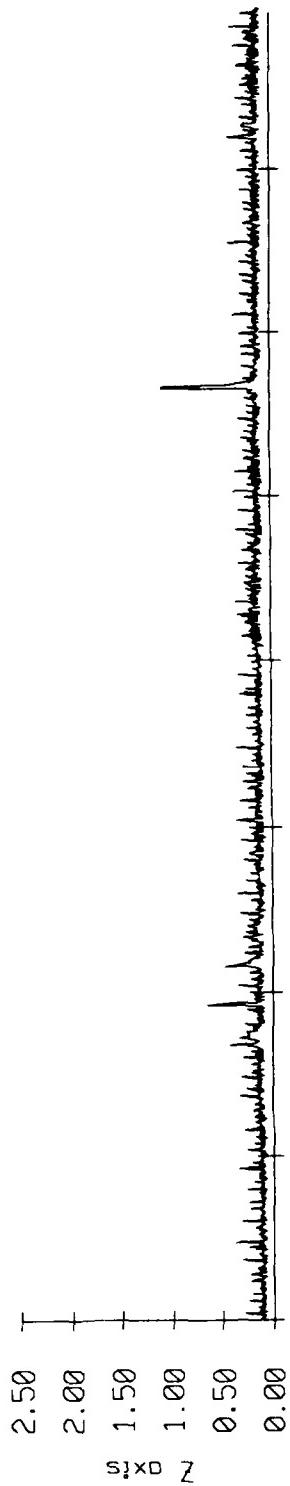


Figure IX.4h

Float 3, September 1987 Sea Trip RM
averaging period = 5.00 sec.



Gain Corrected Level, Volts(rms)

Figure IX.4i

Floot 3, September 1987 Sea Trip
averaging period = 5.00 sec.

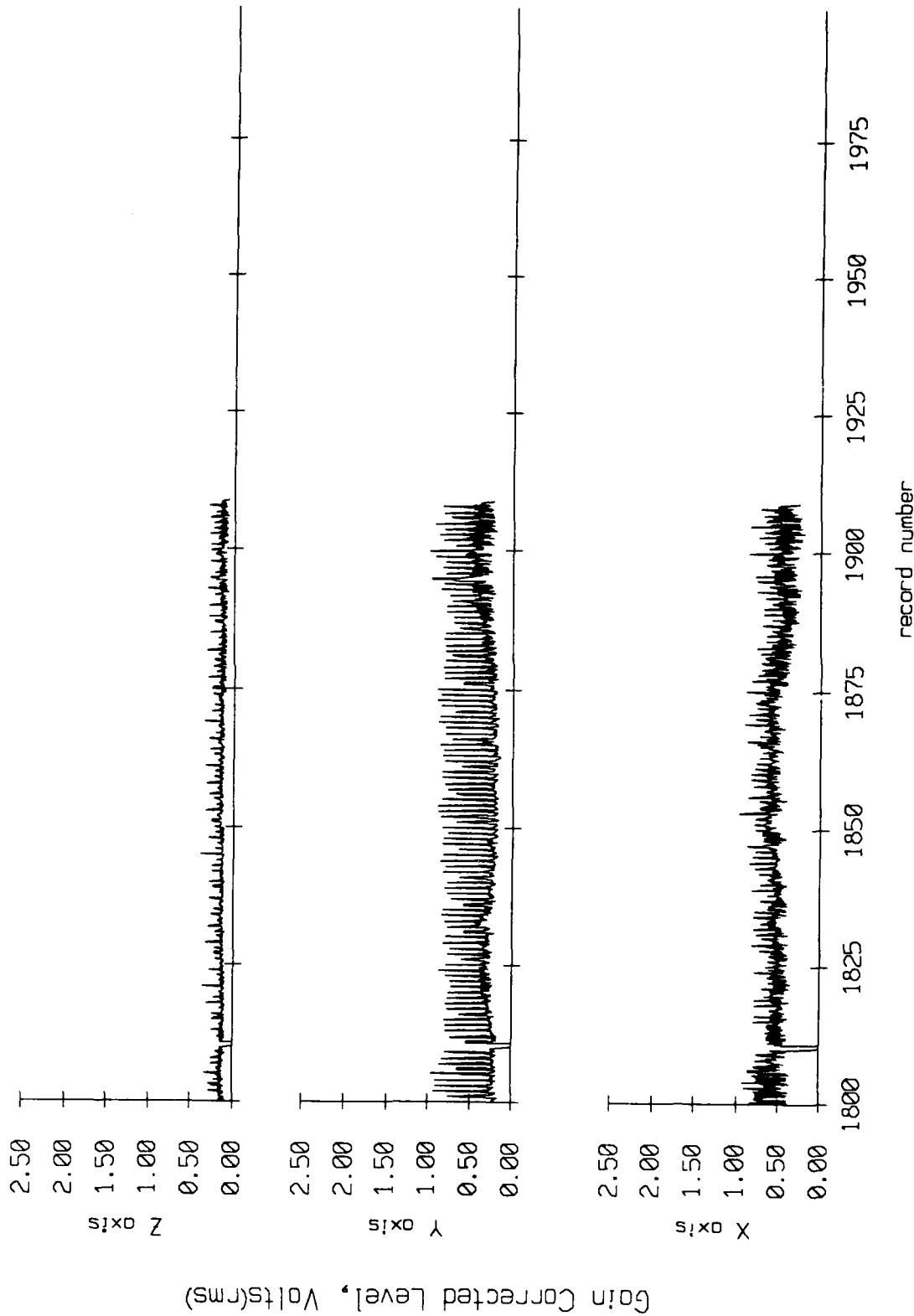


Figure IX.4j

Float 4, September 1987 Sea Trip
overaging period = 5.00 sec.

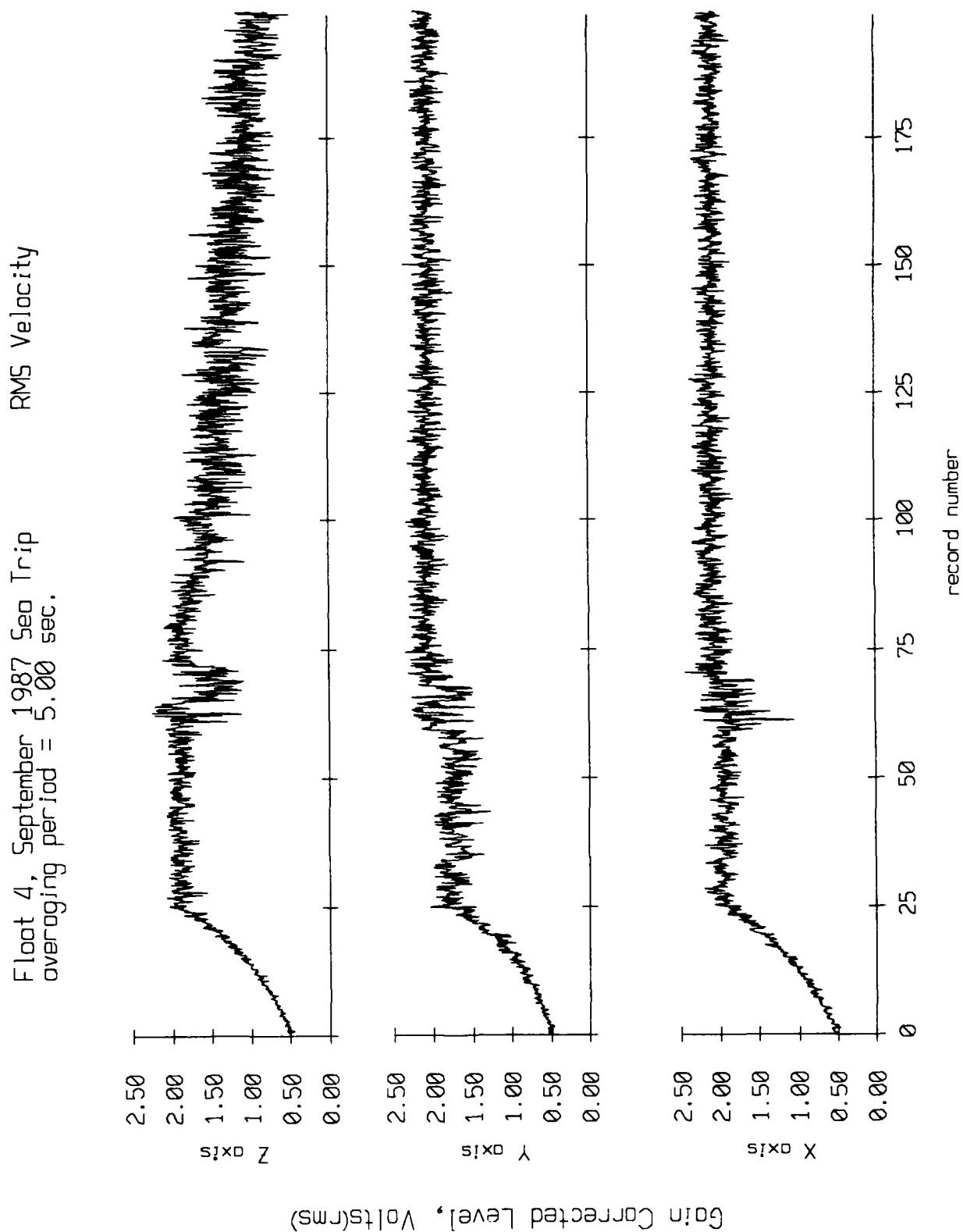


Figure IX.5a

Float 4, September 1987 Sea Trip
averaging period = 5.00 sec.

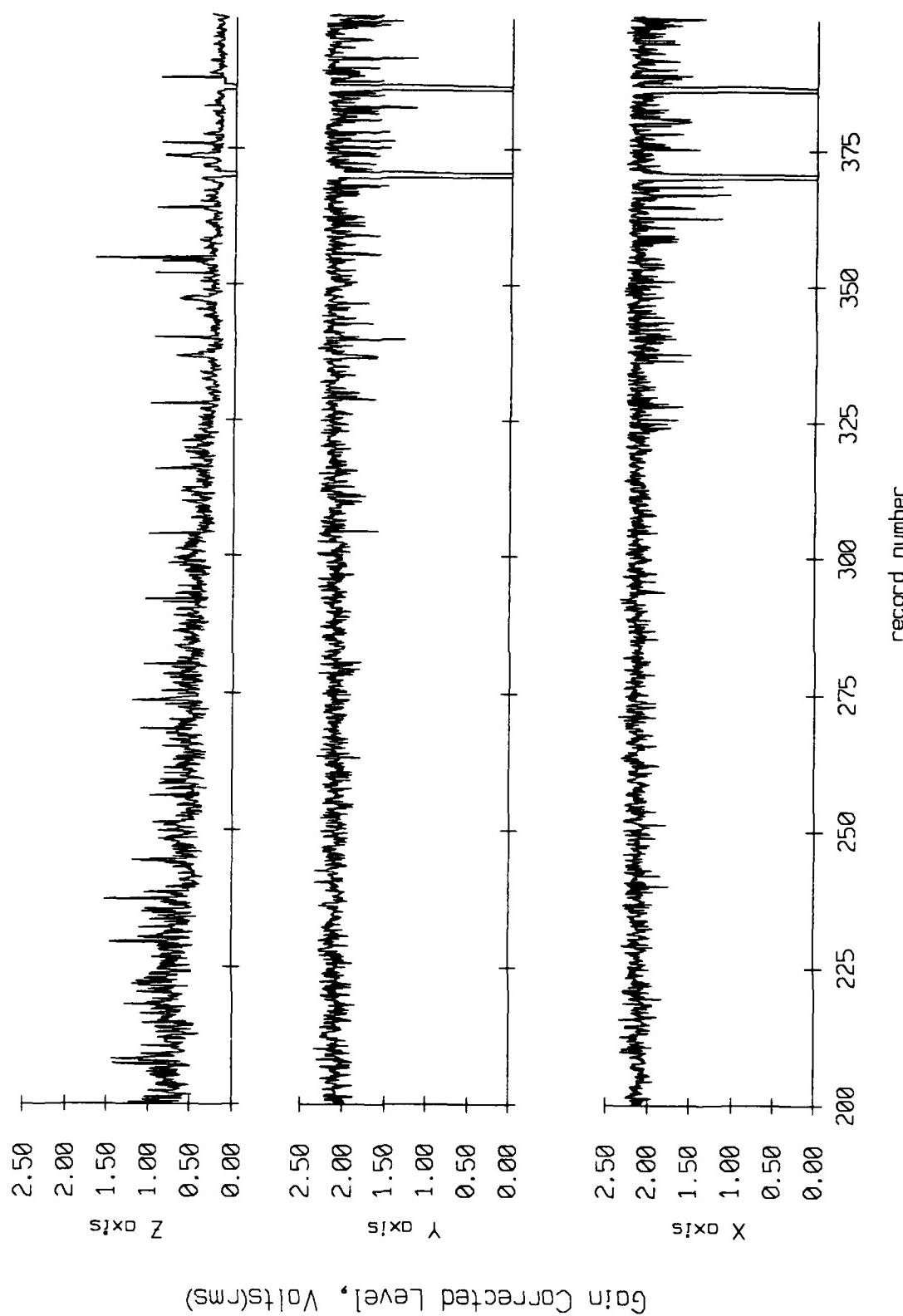


Figure IX.5b

Float 4, September 1987 Sea Trip
overaging period = 5.00 sec.

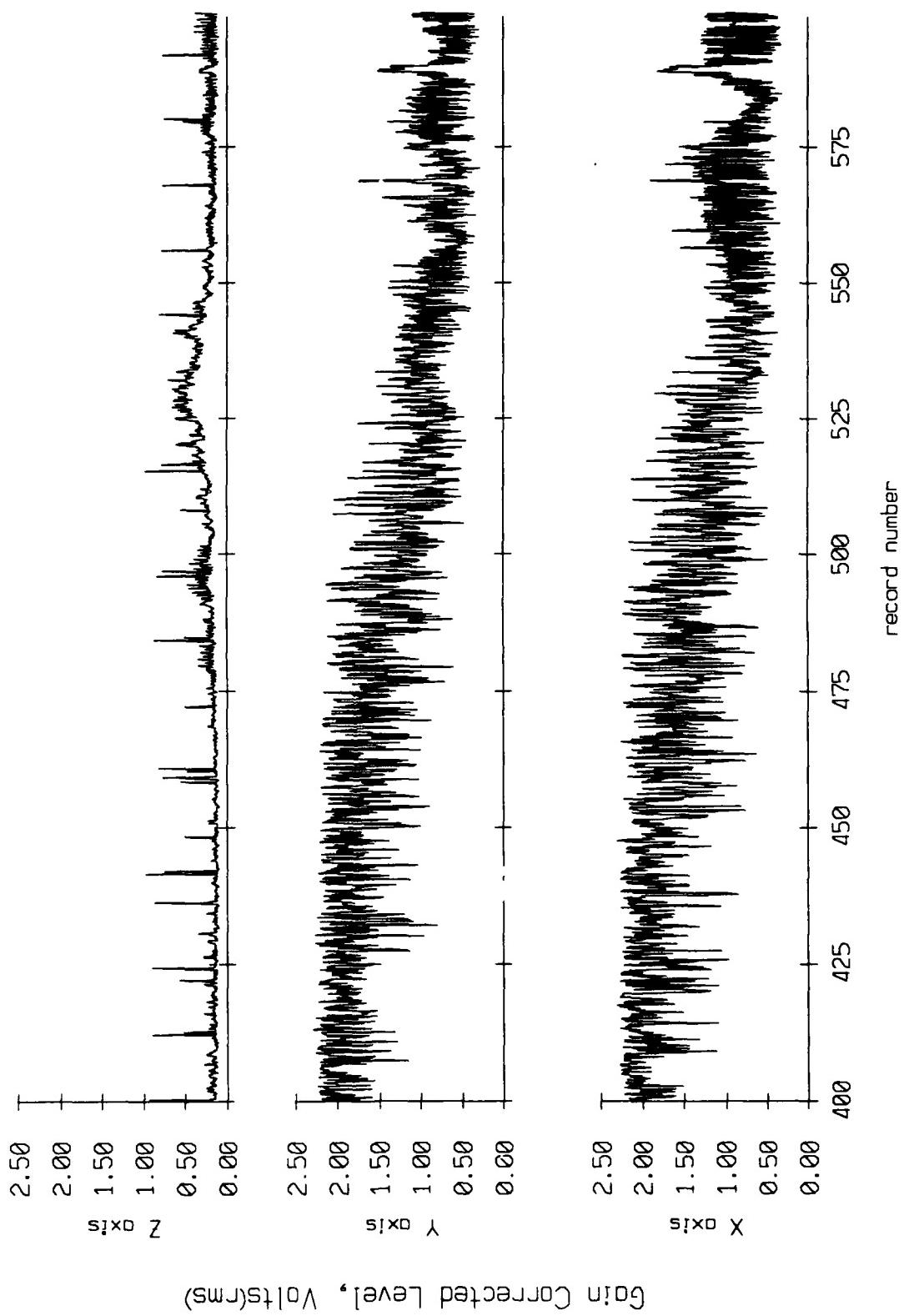


Figure IX.5c

Float 4, September 1987 Sea Trip
averaging period = 5.00 sec.

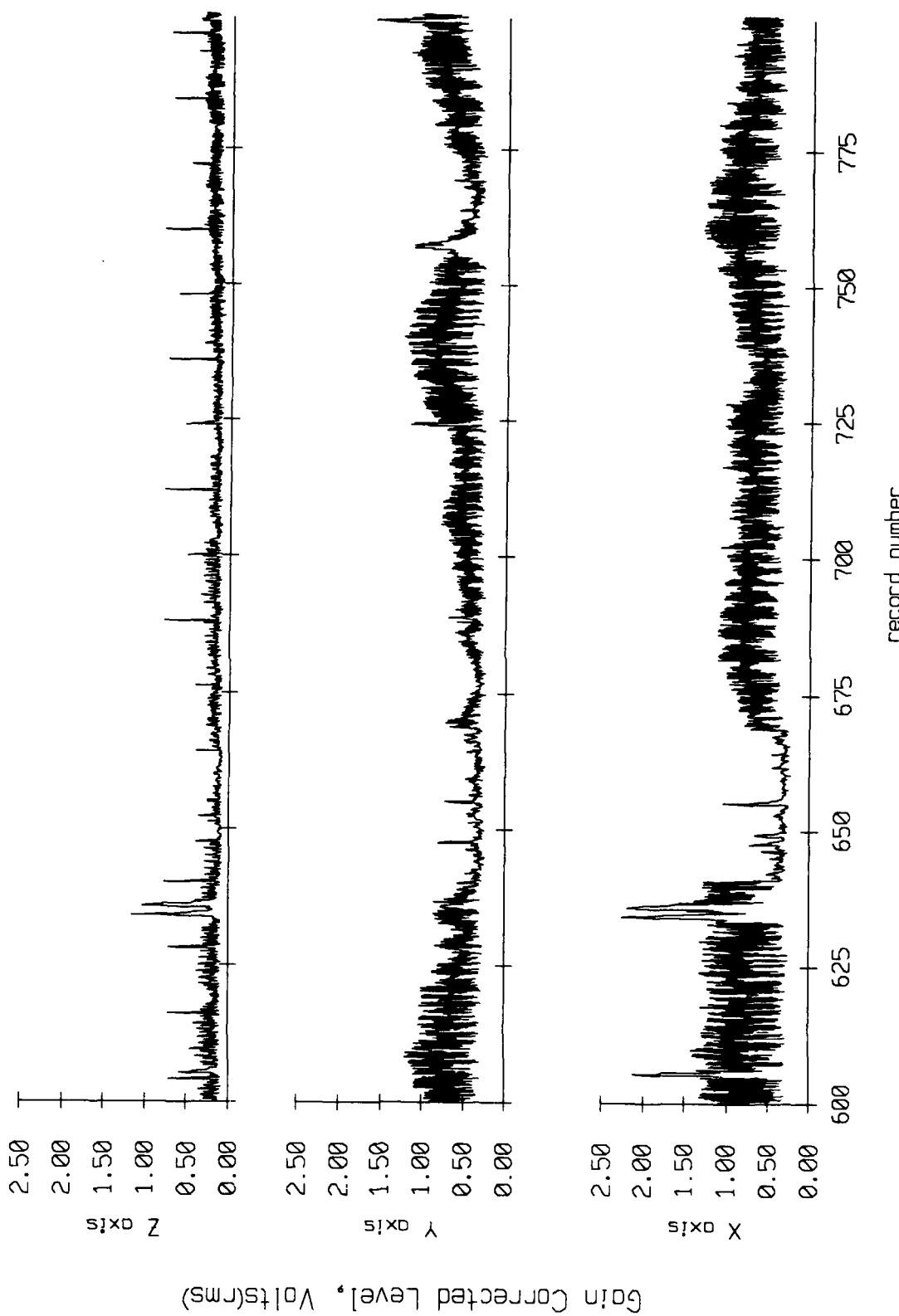


Figure IX.5d

Float 4, September 1987 Sea Trip
averaging period = 5.00 sec.

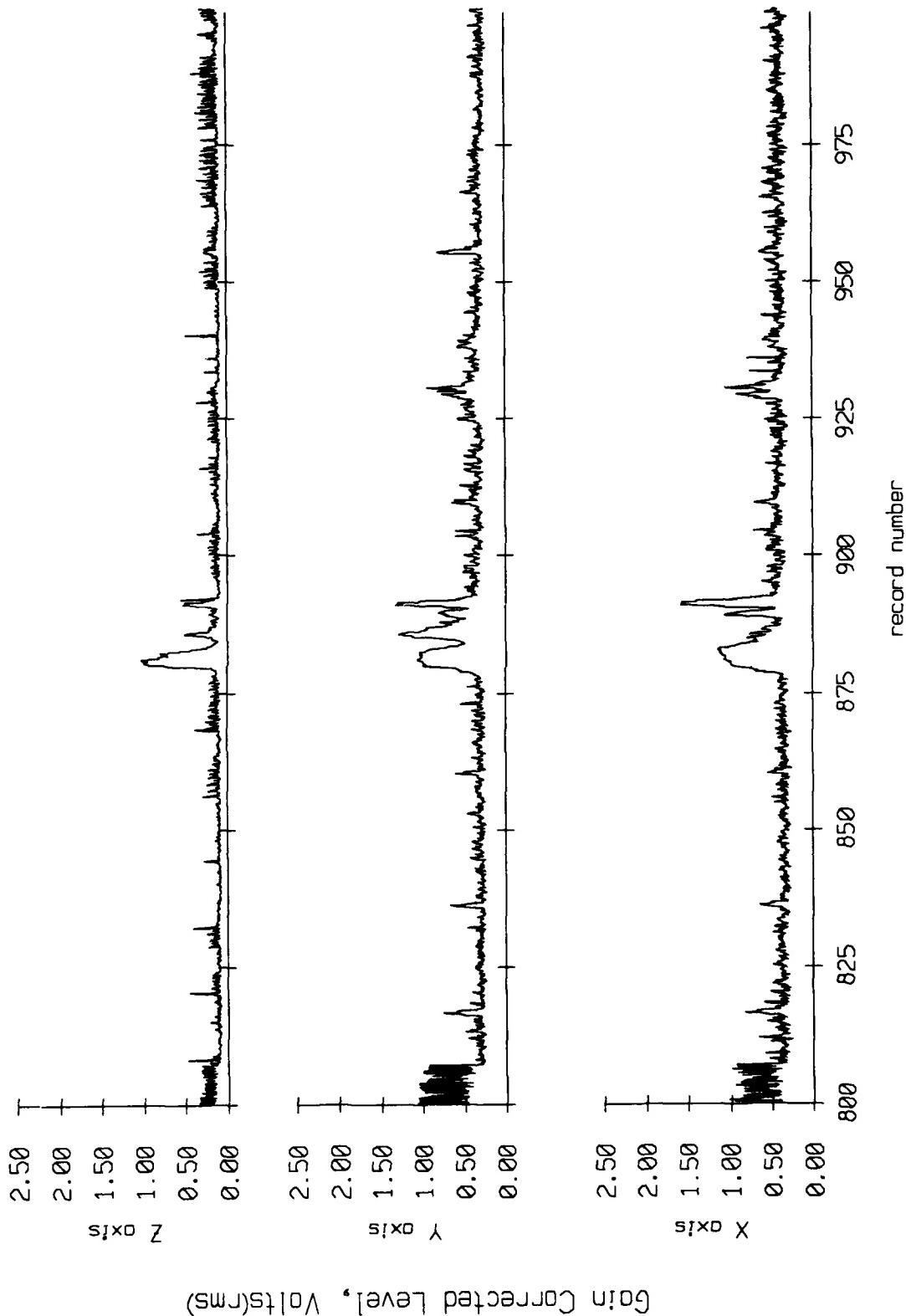


Figure IX.5e

Float 4, September 1987 Sea Trip
averaging period = 5.00 sec.

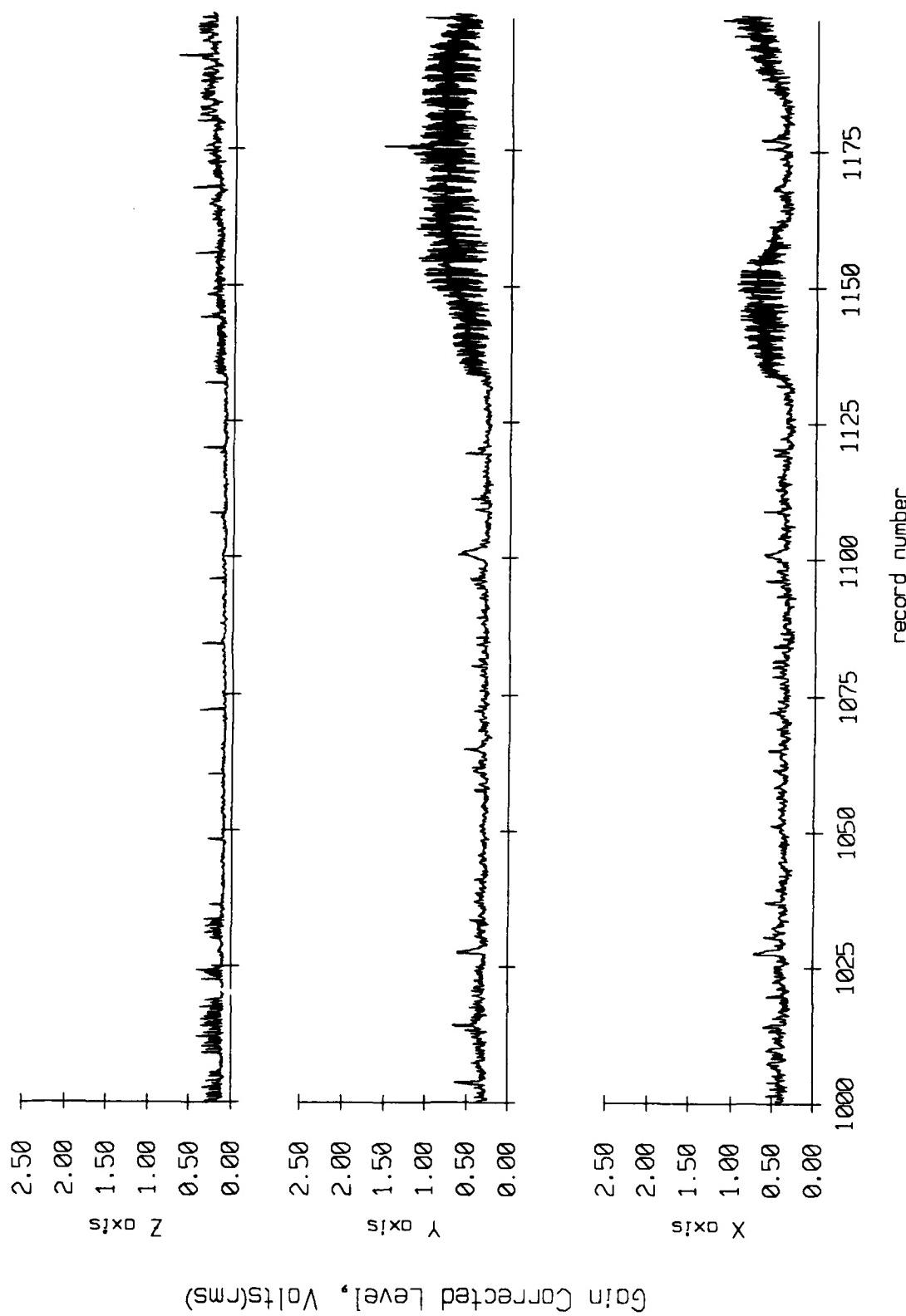


Figure IX.5f

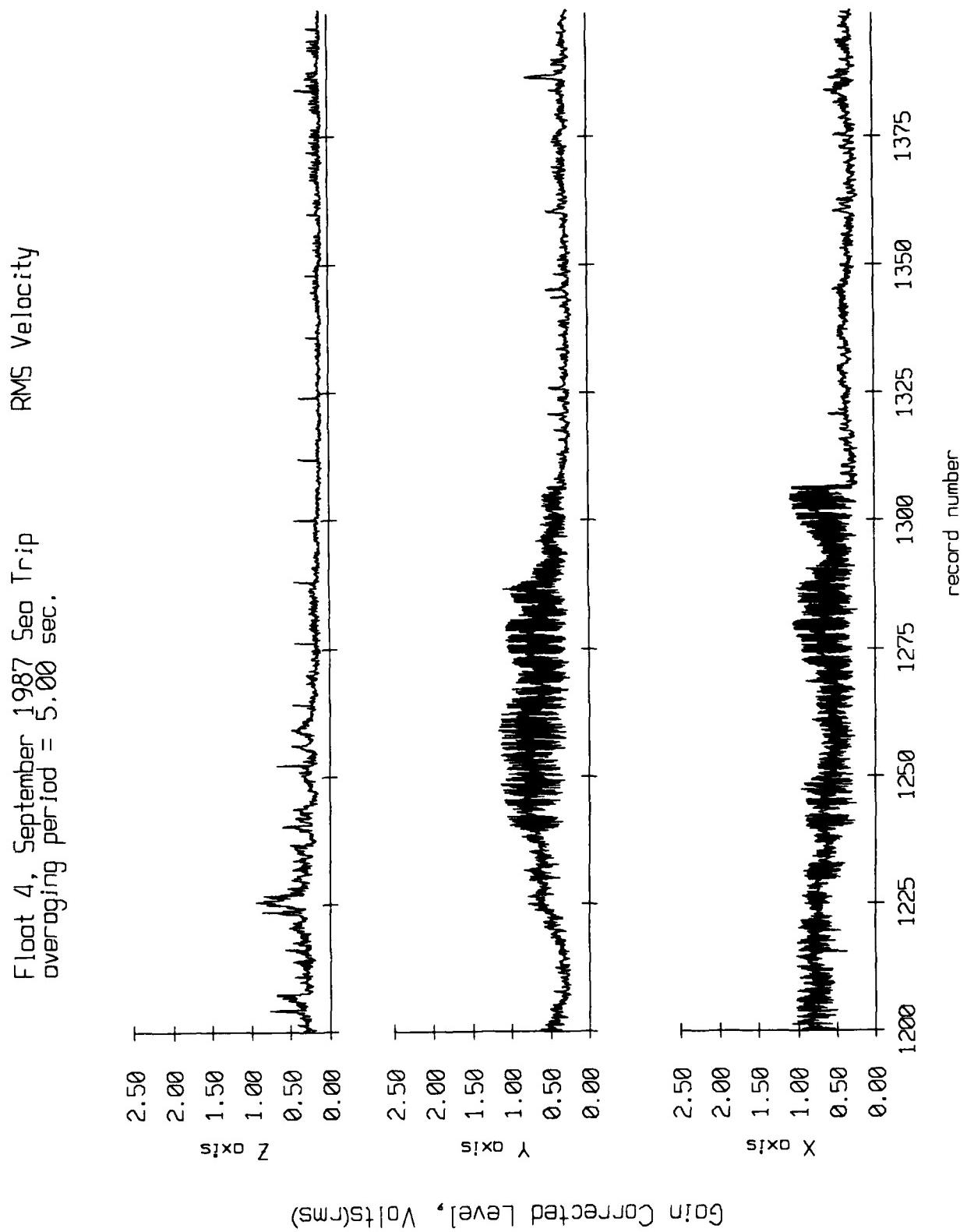


Figure IX.5g

Float 4, September 1987 Sec. Trip
overaging period = 5.00 sec.

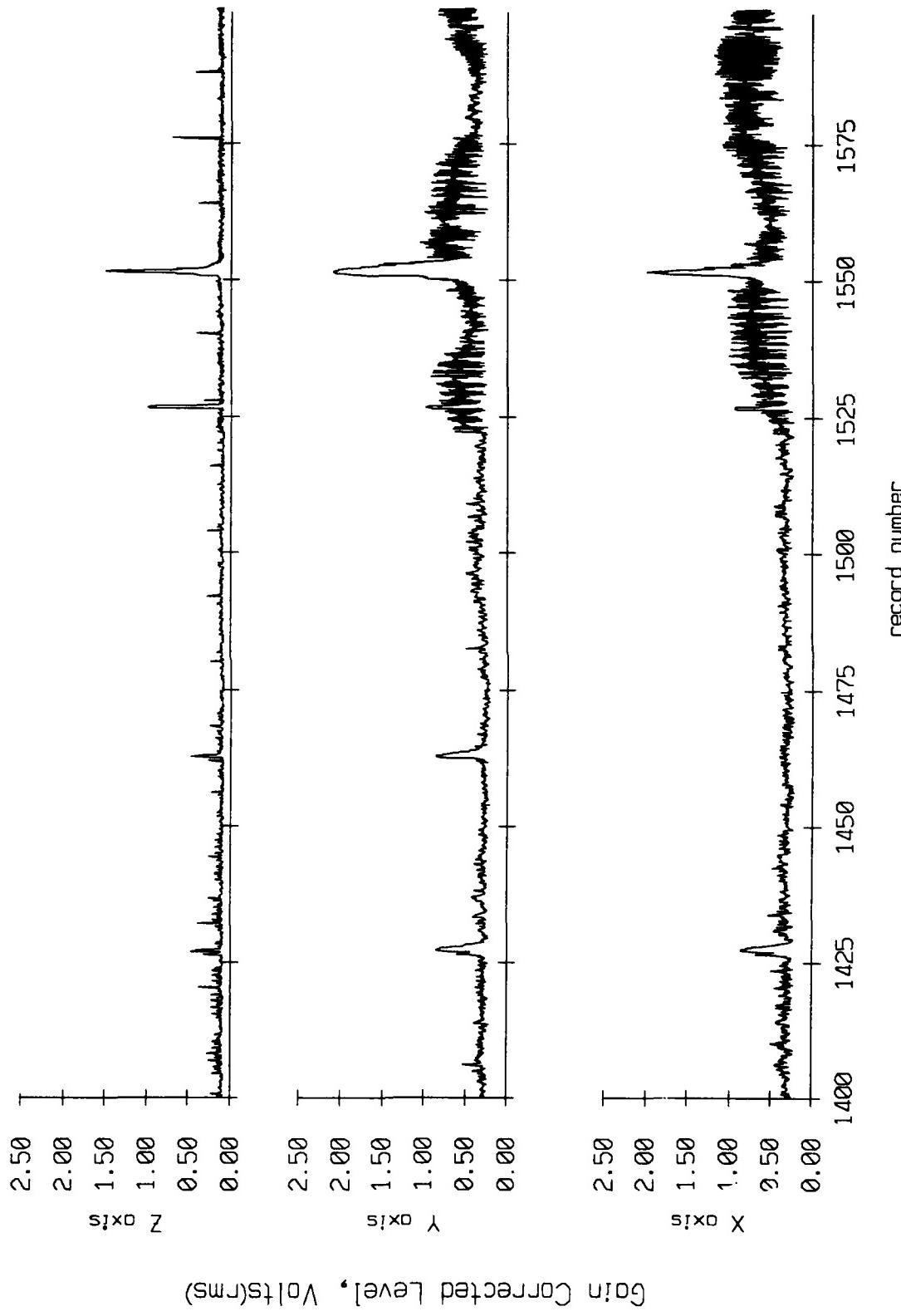
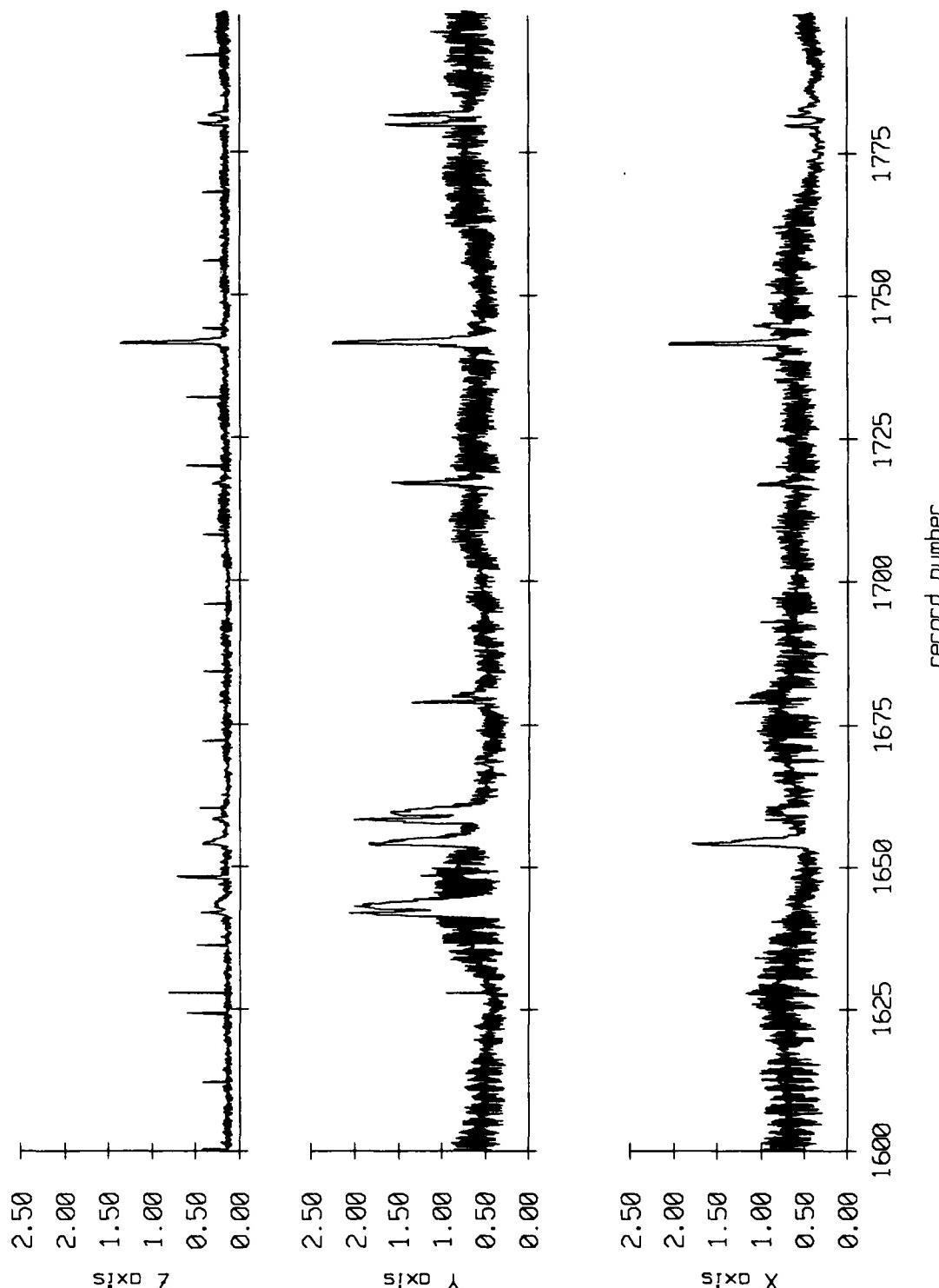


Figure IX.5h

Float 4, September 1987 Sea Trip
averaging period = 5.00 sec.

RMS Velocity



Gain Corrected Level, Volts(RMS)

Figure IX.5i

Float 4, September 1987 Sea Trip
averaging period = 5.00 sec.

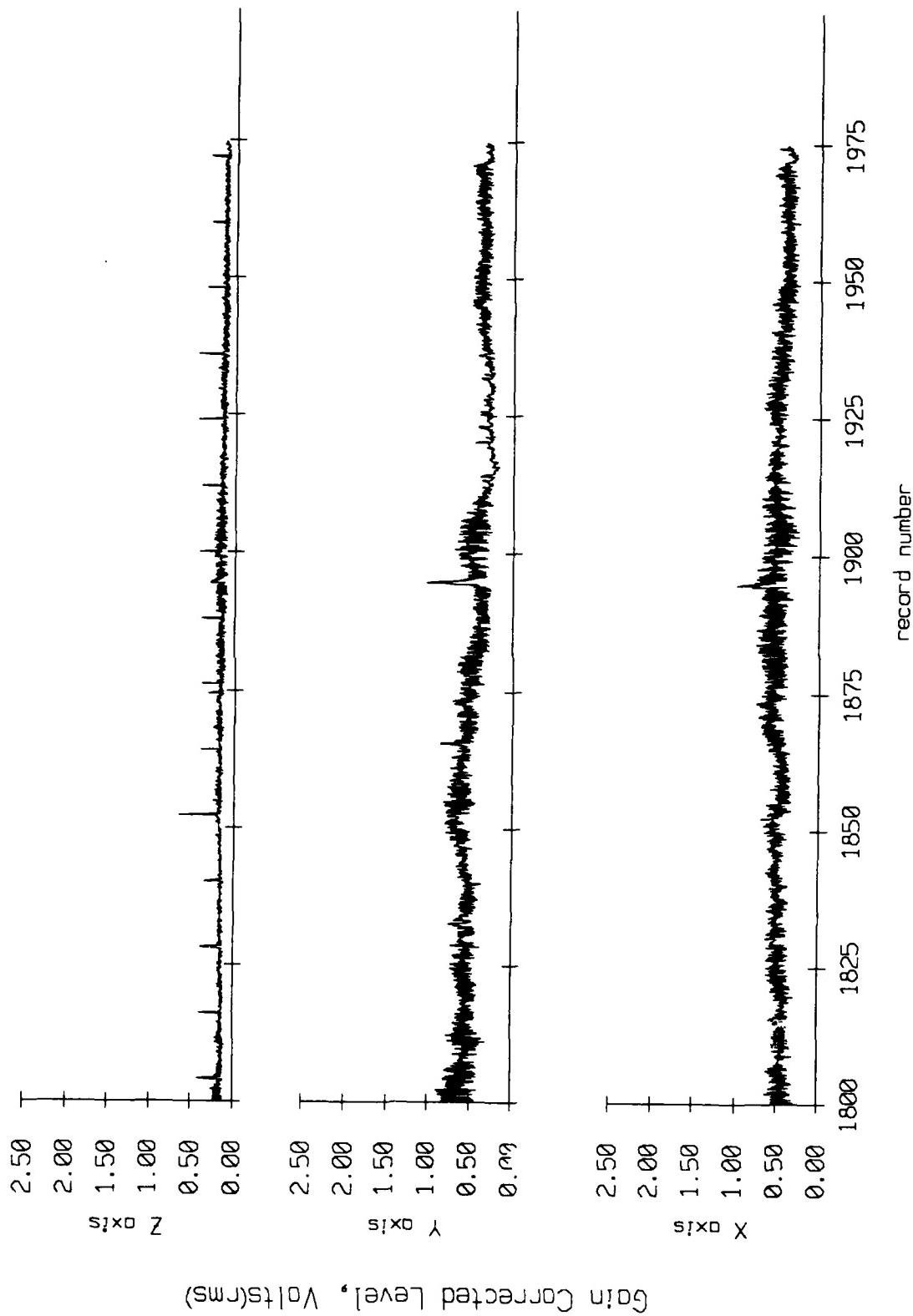
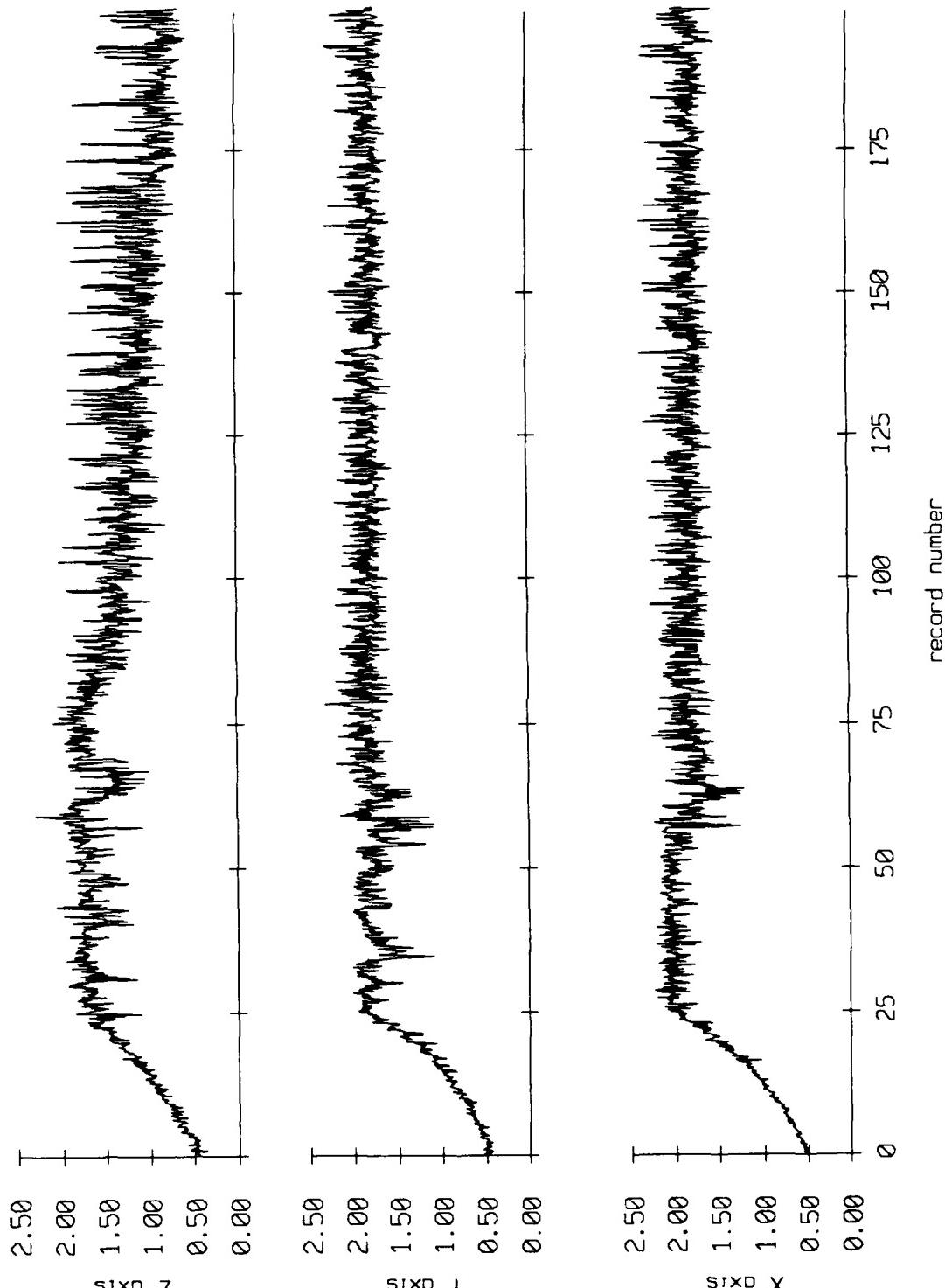


Figure IX.5j

Float 5, September 1987 Sea Trip
averaging period = 5.00 sec.



Go in Corrected Level, Volts(RMS)

Figure IX.6a

Float 5, September 1987 Sea Trip
averaging period = 5.00 sec.

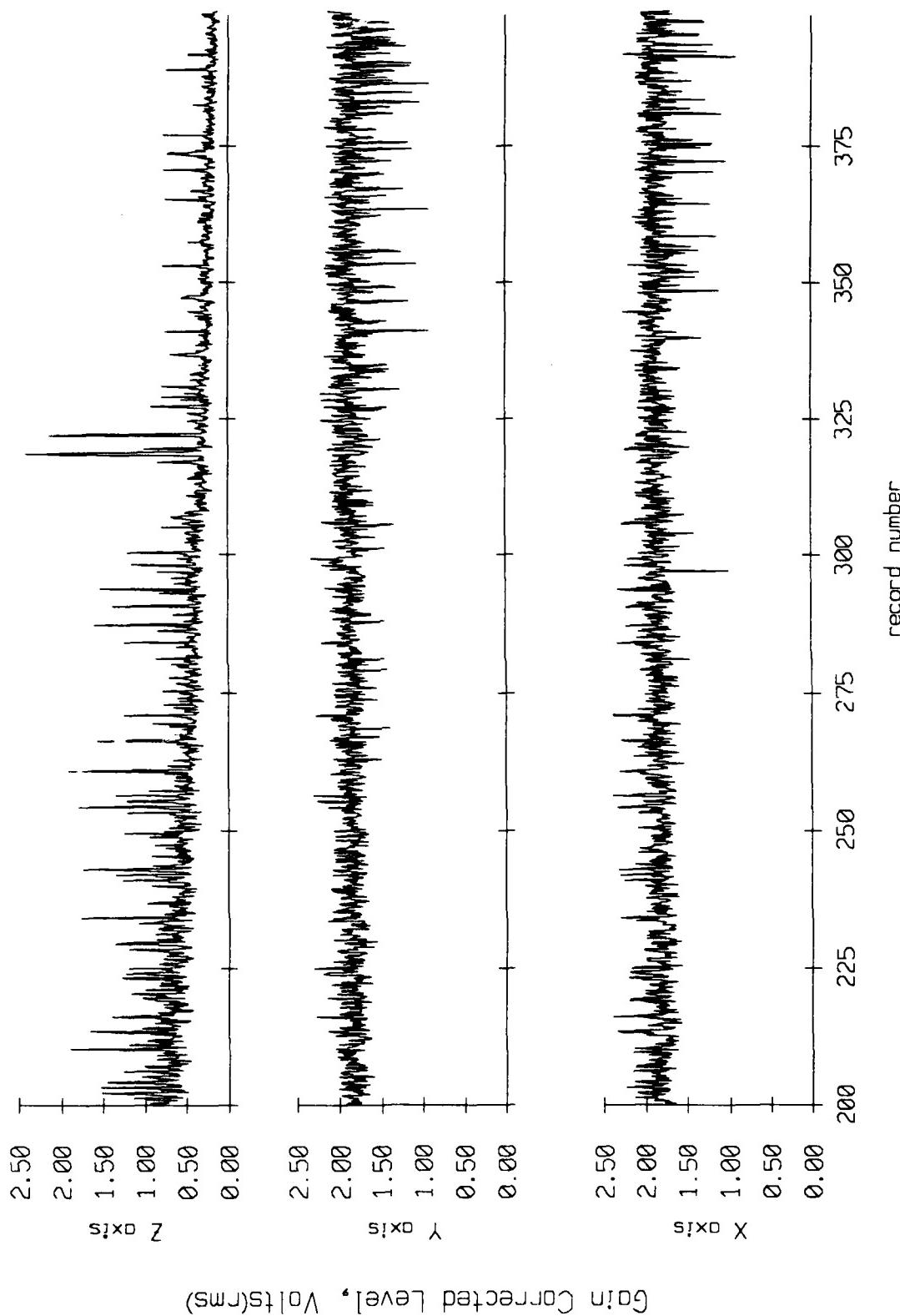


Figure IX.6b

Float 5, September 1987 Sea Trip
averaging period = 5.00 sec.

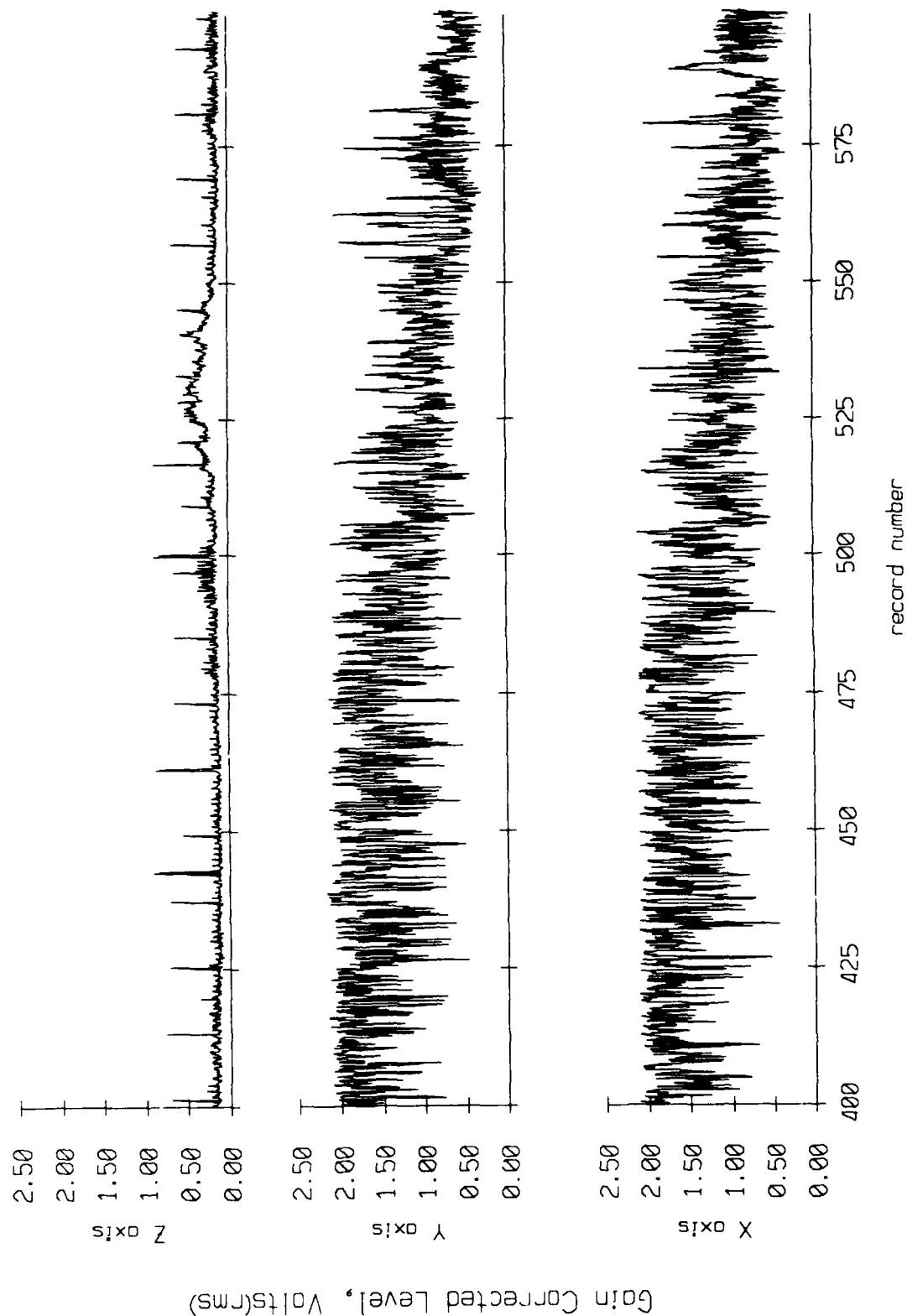


Figure IX.6c

Float 5, September 1987 Sea Trip
averaging period = 5.00 sec.

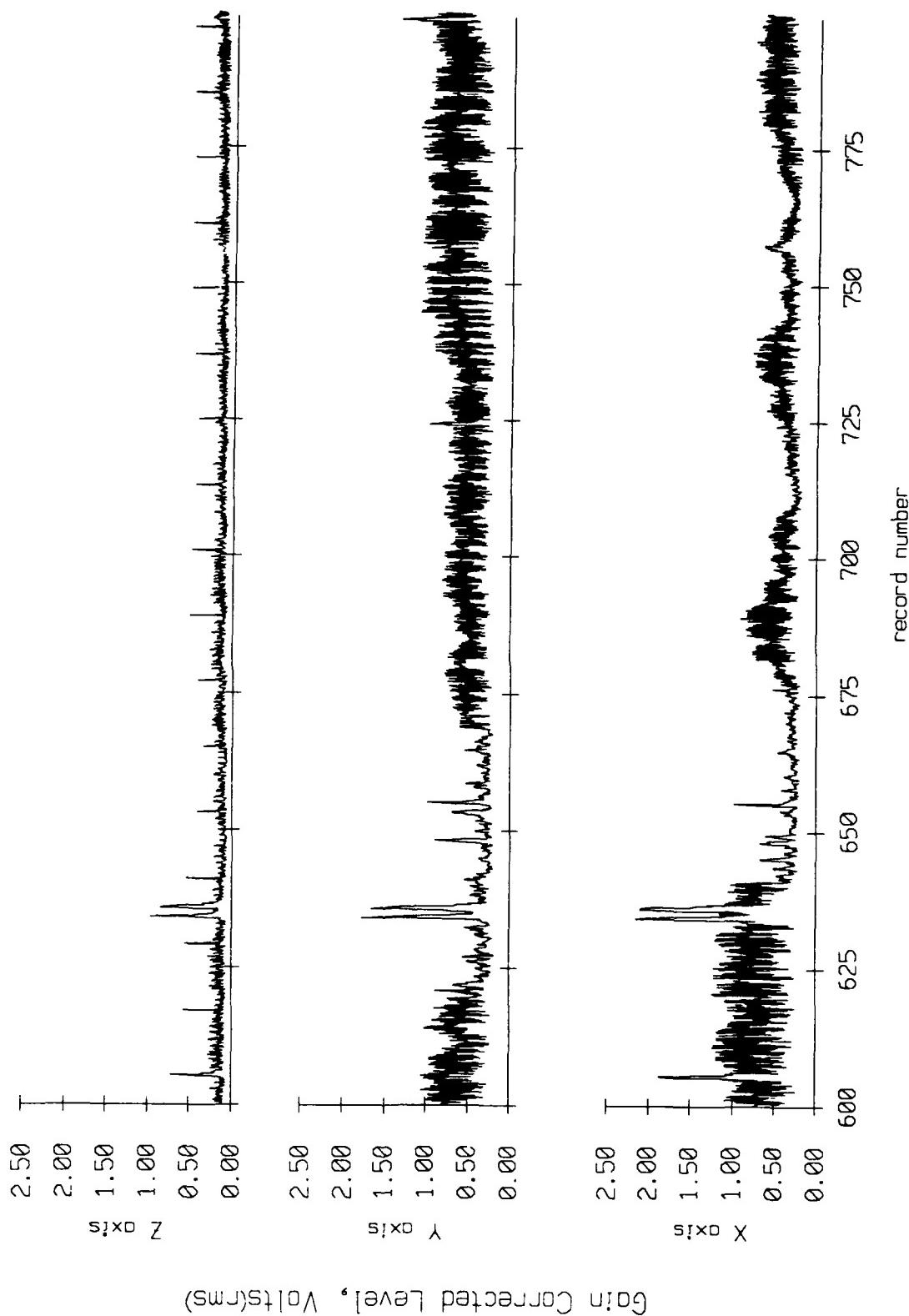
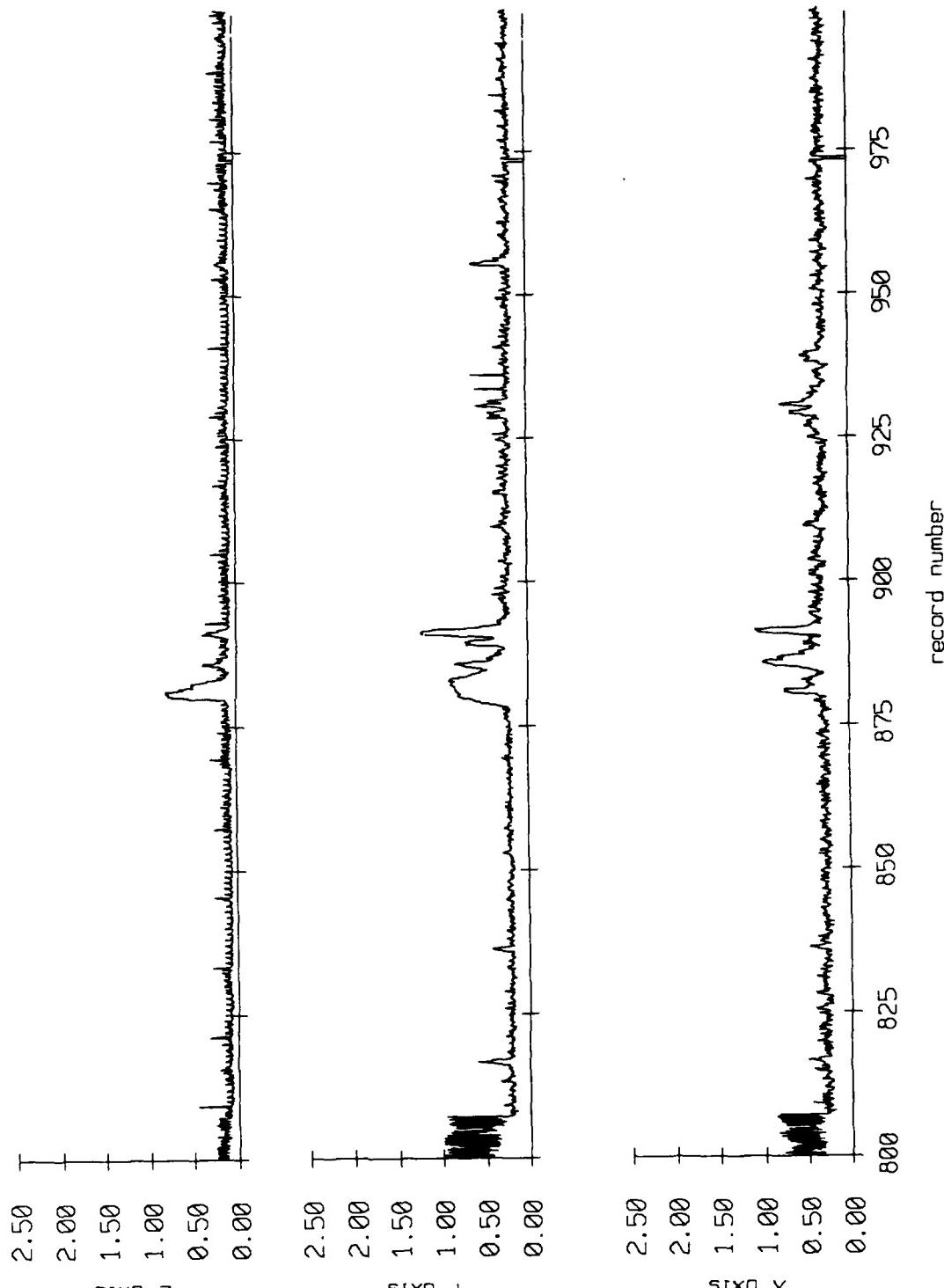


Figure IX.6d

Float 5, September 1987 Sea Trip
averaging period = 5.00 sec.

RMS Velocity



Gain Corrected Level, Volts(rms)

Figure IX.6e

Float 5, September 1987 Sec Trip
averaging period = 5.00 sec.

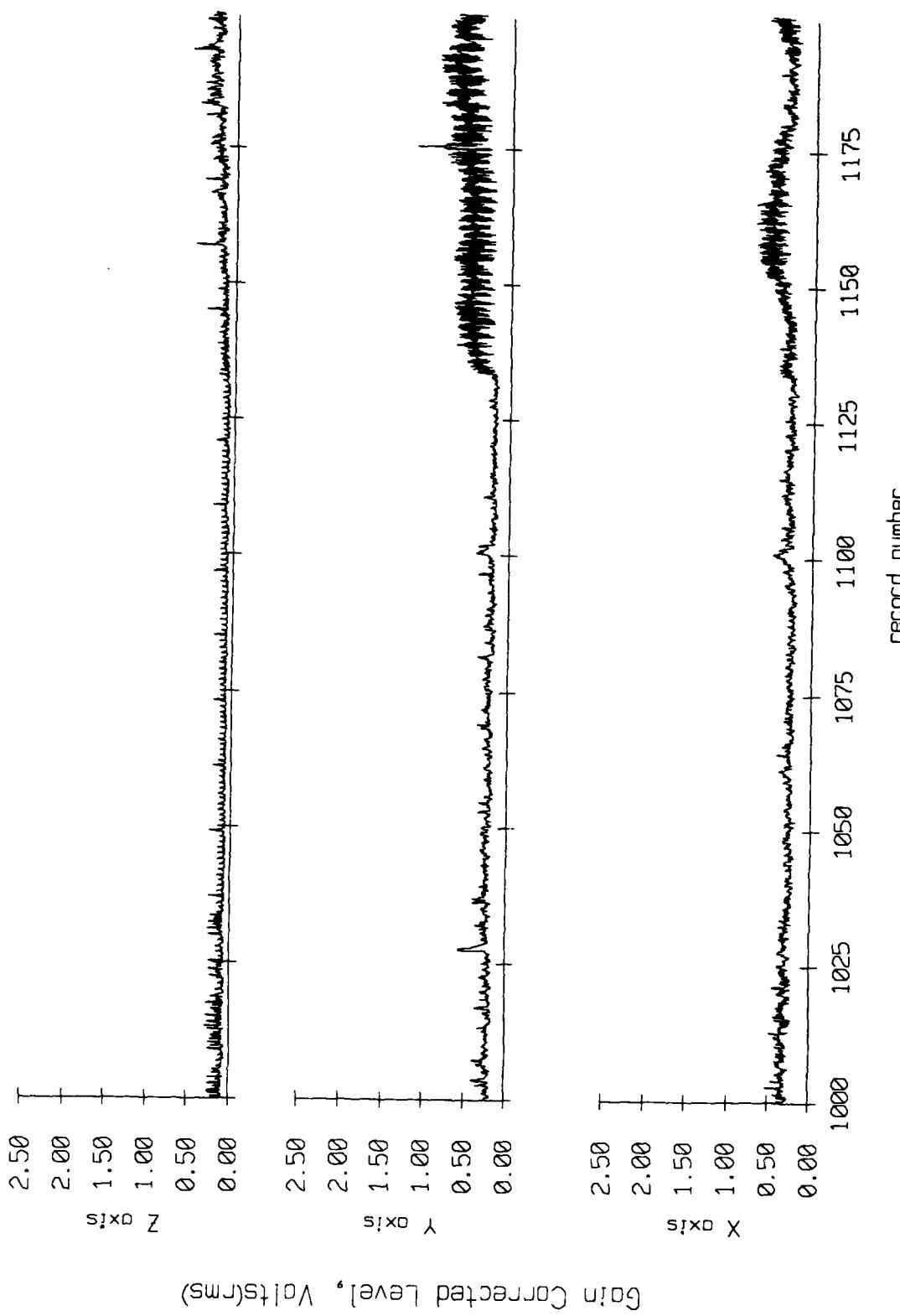


Figure IX.6f

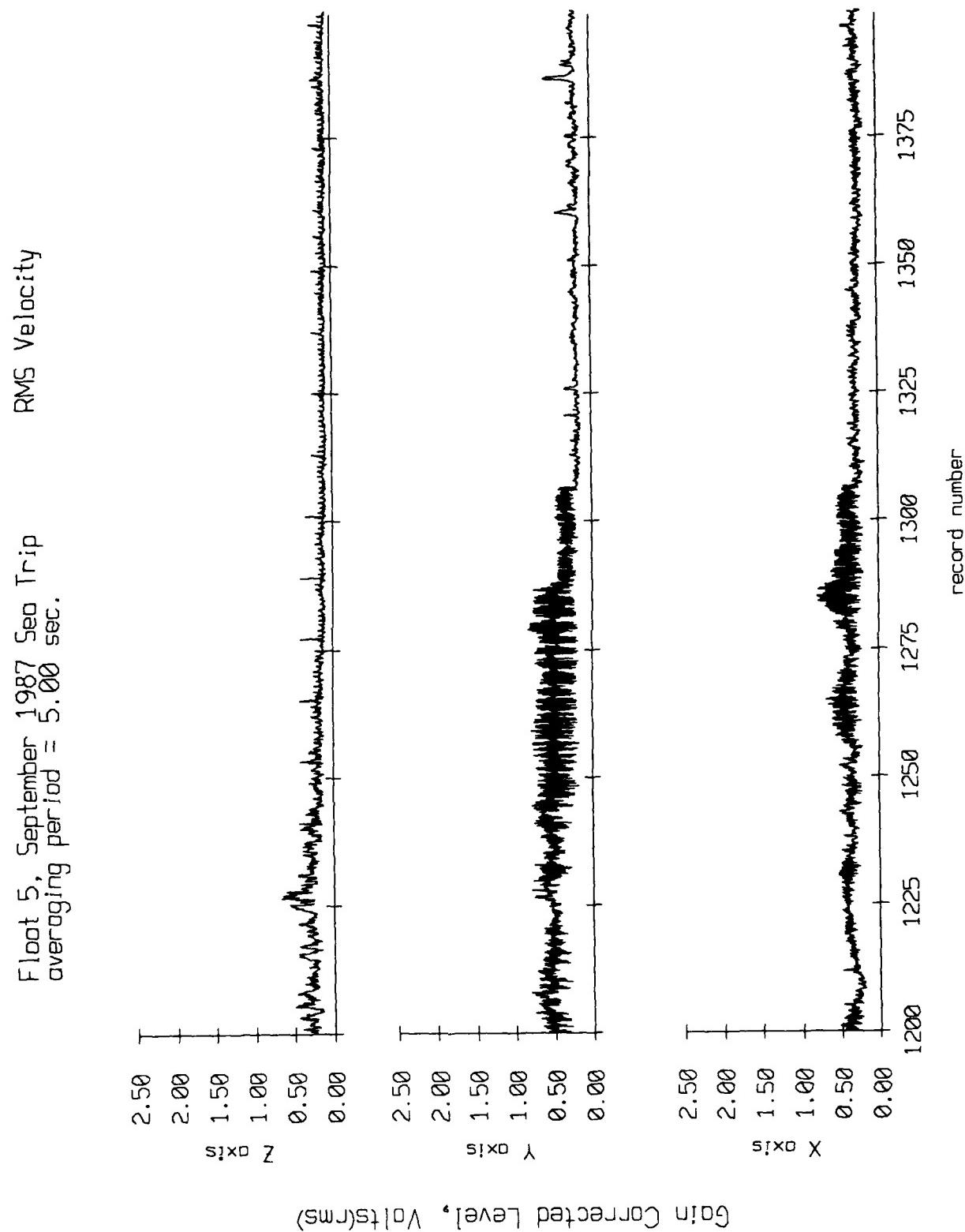


Figure IX.6g

Float 5, September 1987 Sea Trip
averaging period = 5.00 sec.

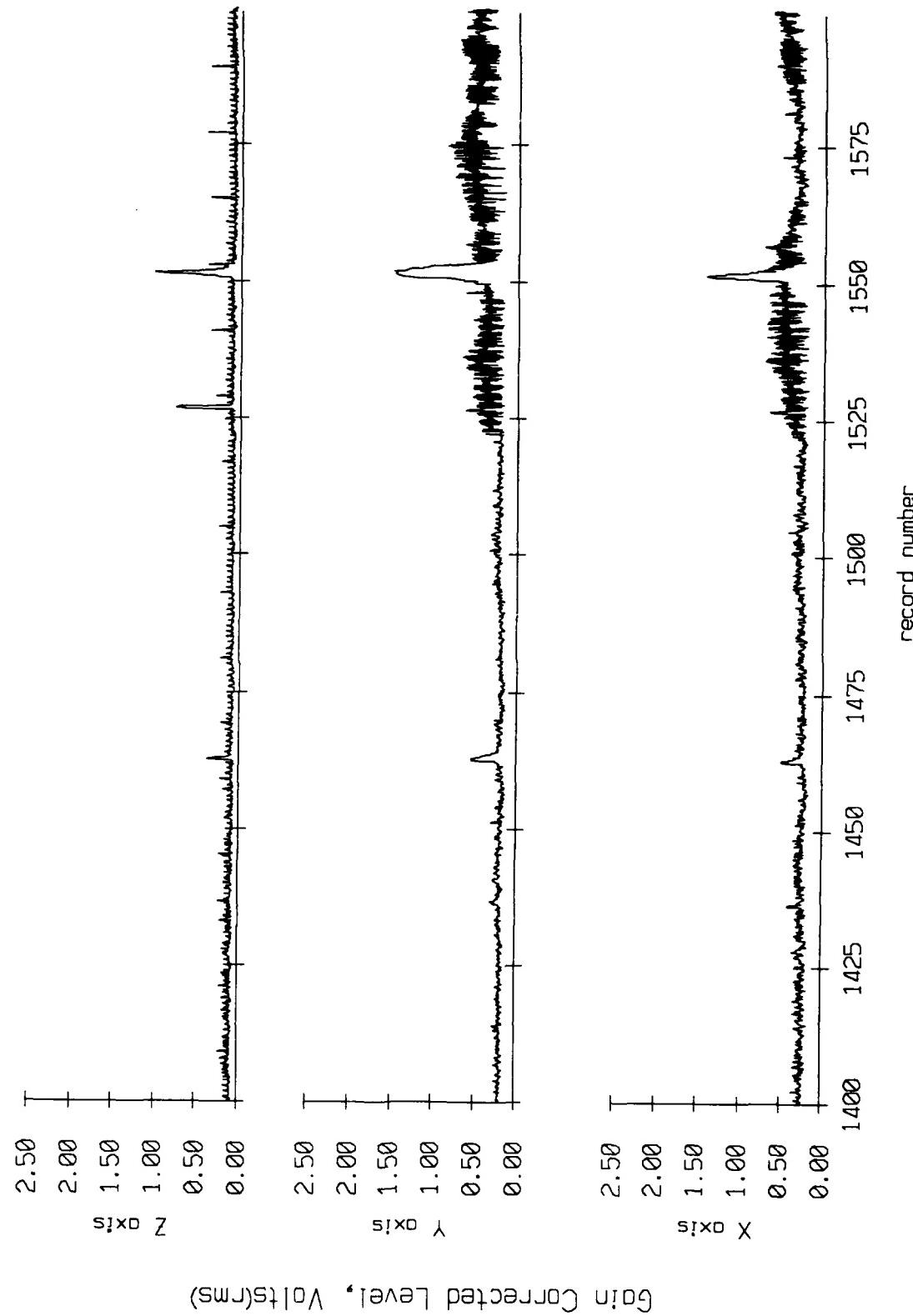


Figure IX.6h

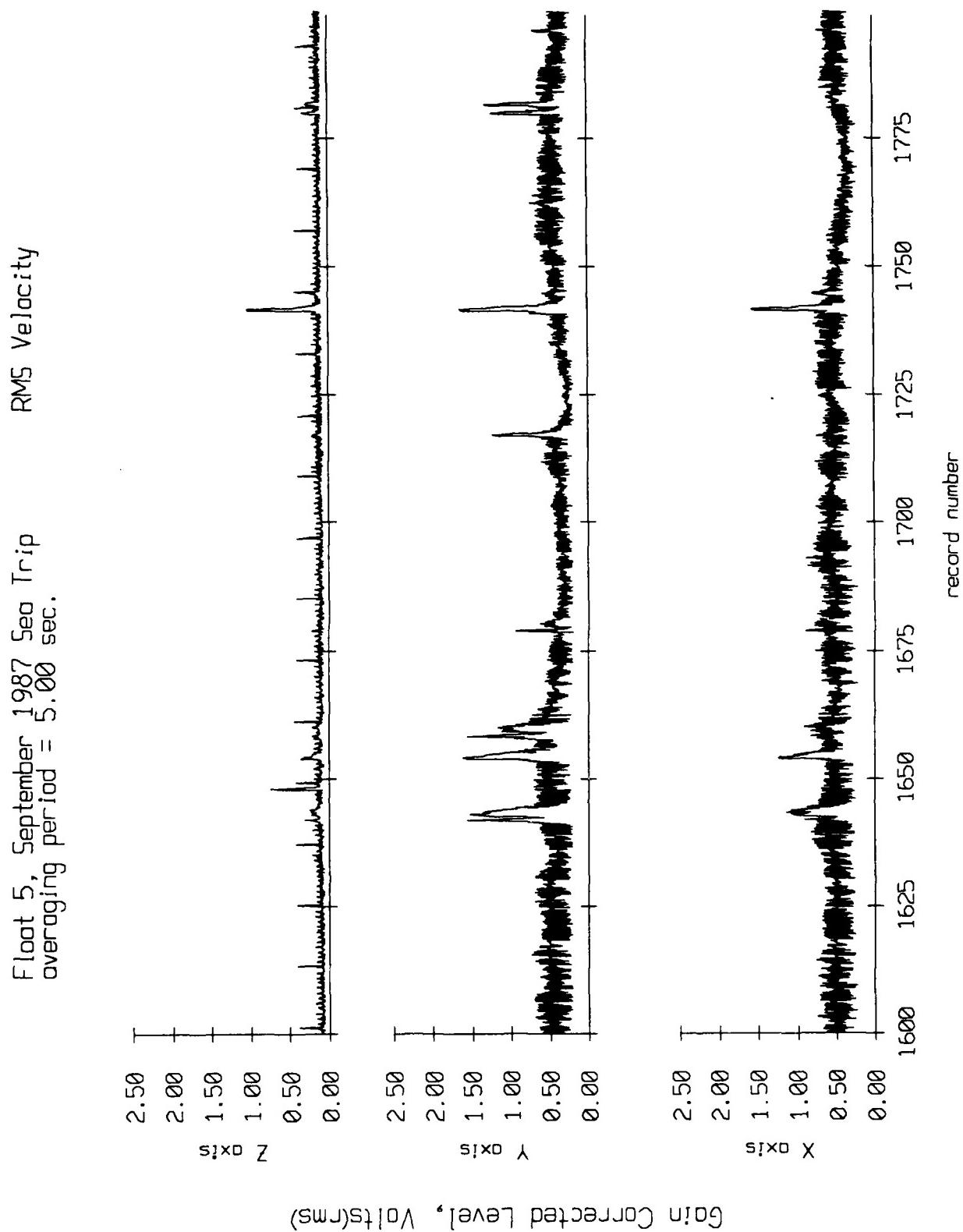


Figure IX.6i

Float 5, September 1987 Sea Trip
overaging period = 5.00 sec.

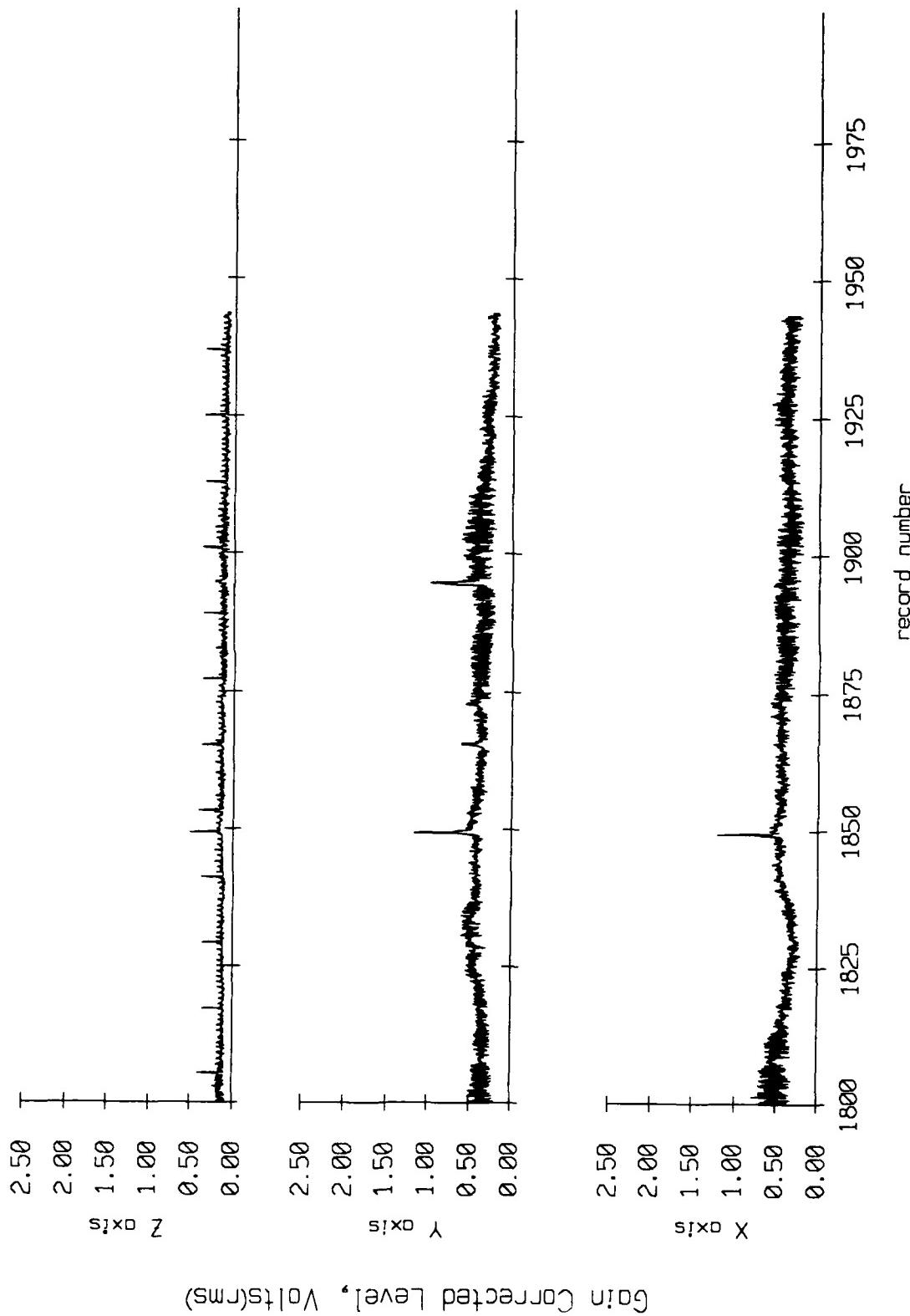
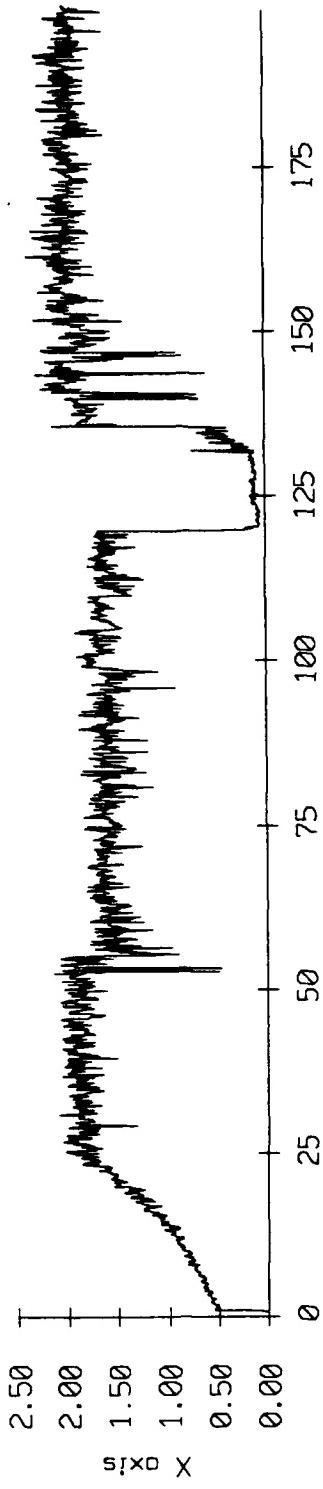
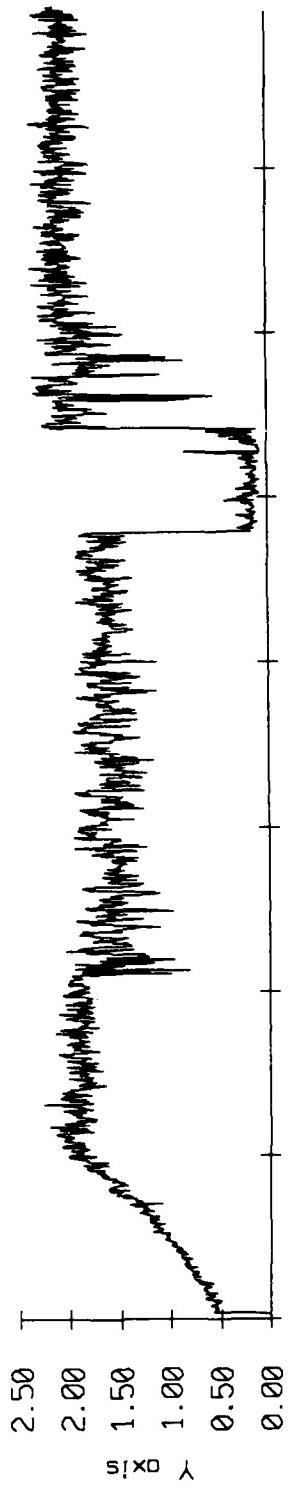
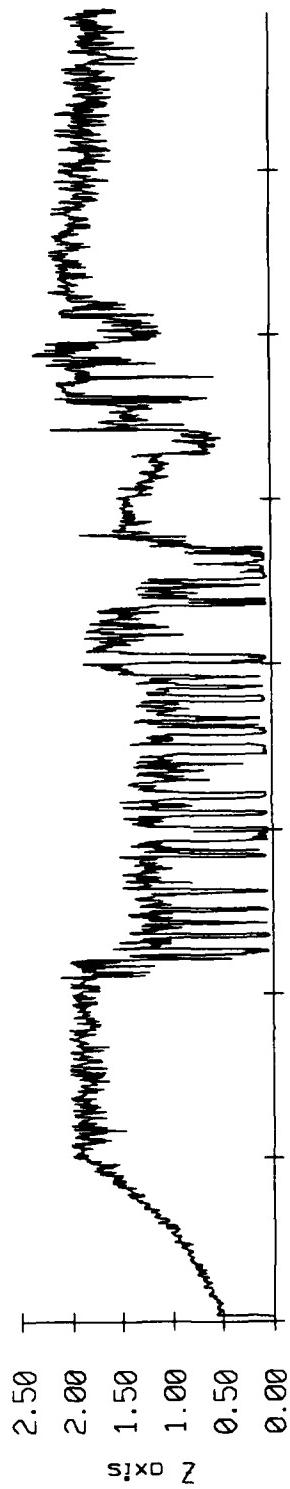


Figure IX.6j

Float 6, September 1987 Sea Trip
averaging period = 5.00 sec.

RMS Velocity



Gain Corrected Level, Volts(RMS)

Figure IX.7a

Float 6, September 1987 Sea Trip
averaging period = 5.00 sec.

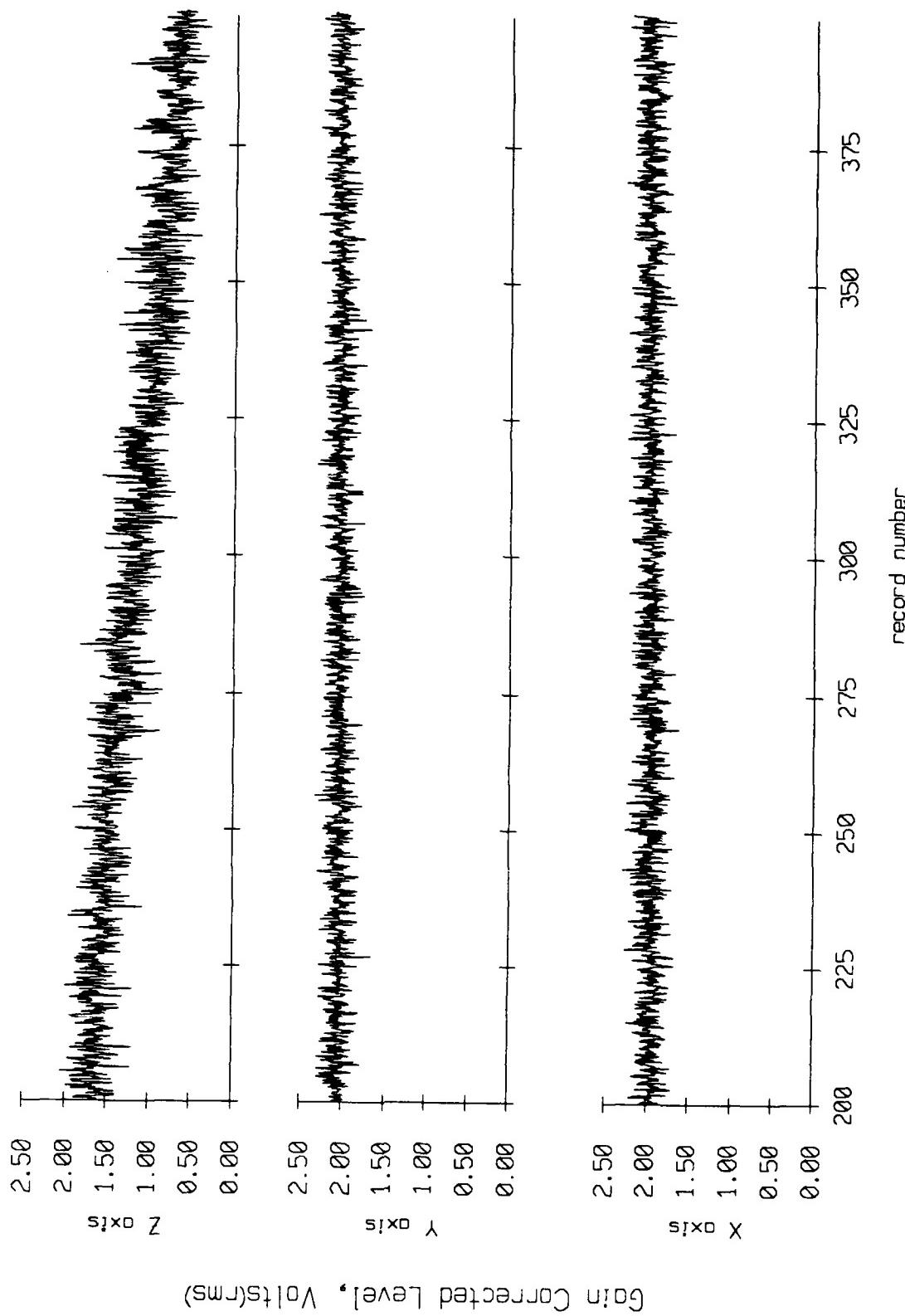


Figure IX.7b

Float 6, September 1987 Sea Trip
overaging period = 5.00 sec.

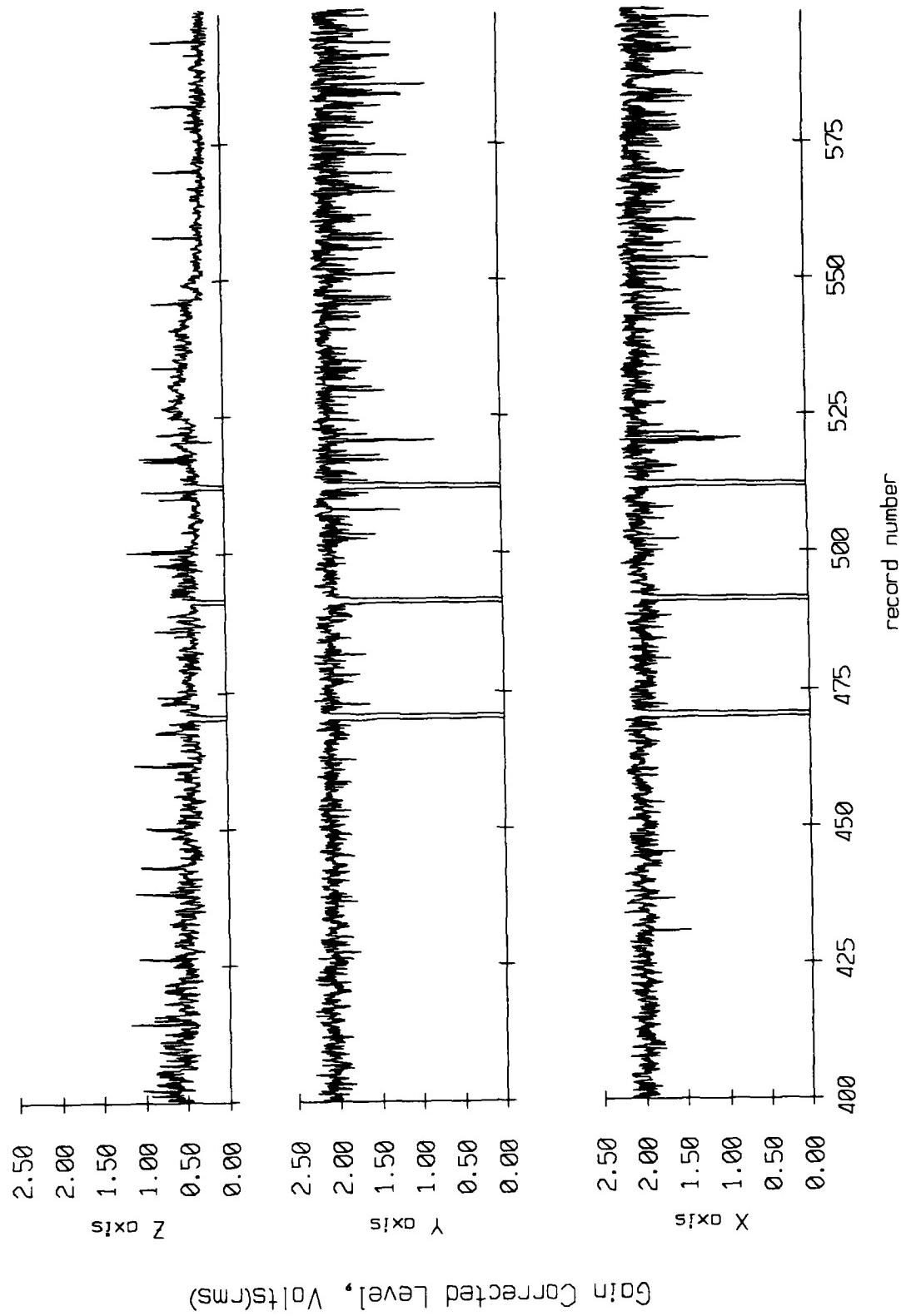


Figure IX.7c

Float 6, September 1987 Sea Trip
averaging period = 5.00 sec.

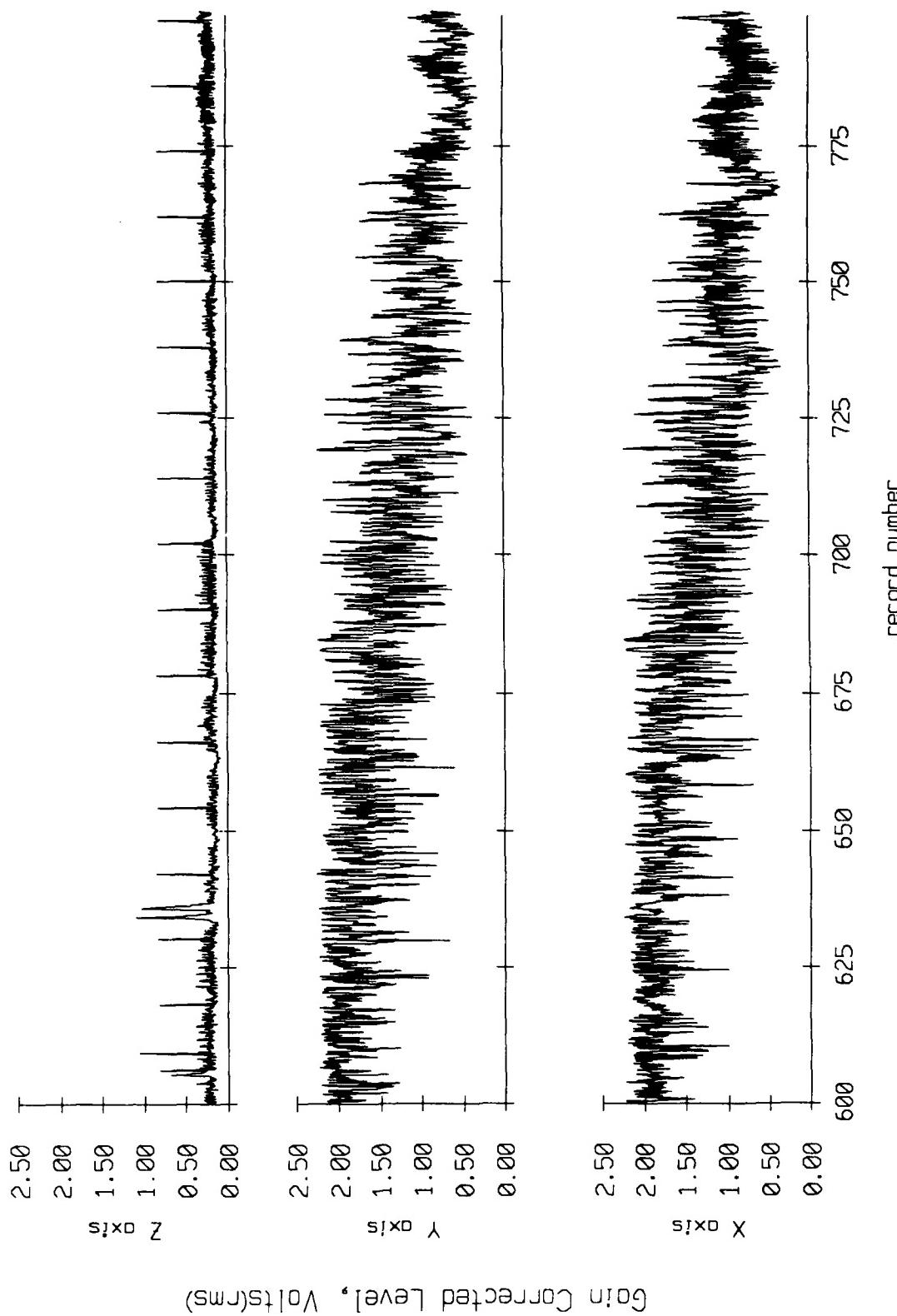


Figure IX.7d

Float 6, September 1987 Sec. Trip
averaging period = 5.00 sec.

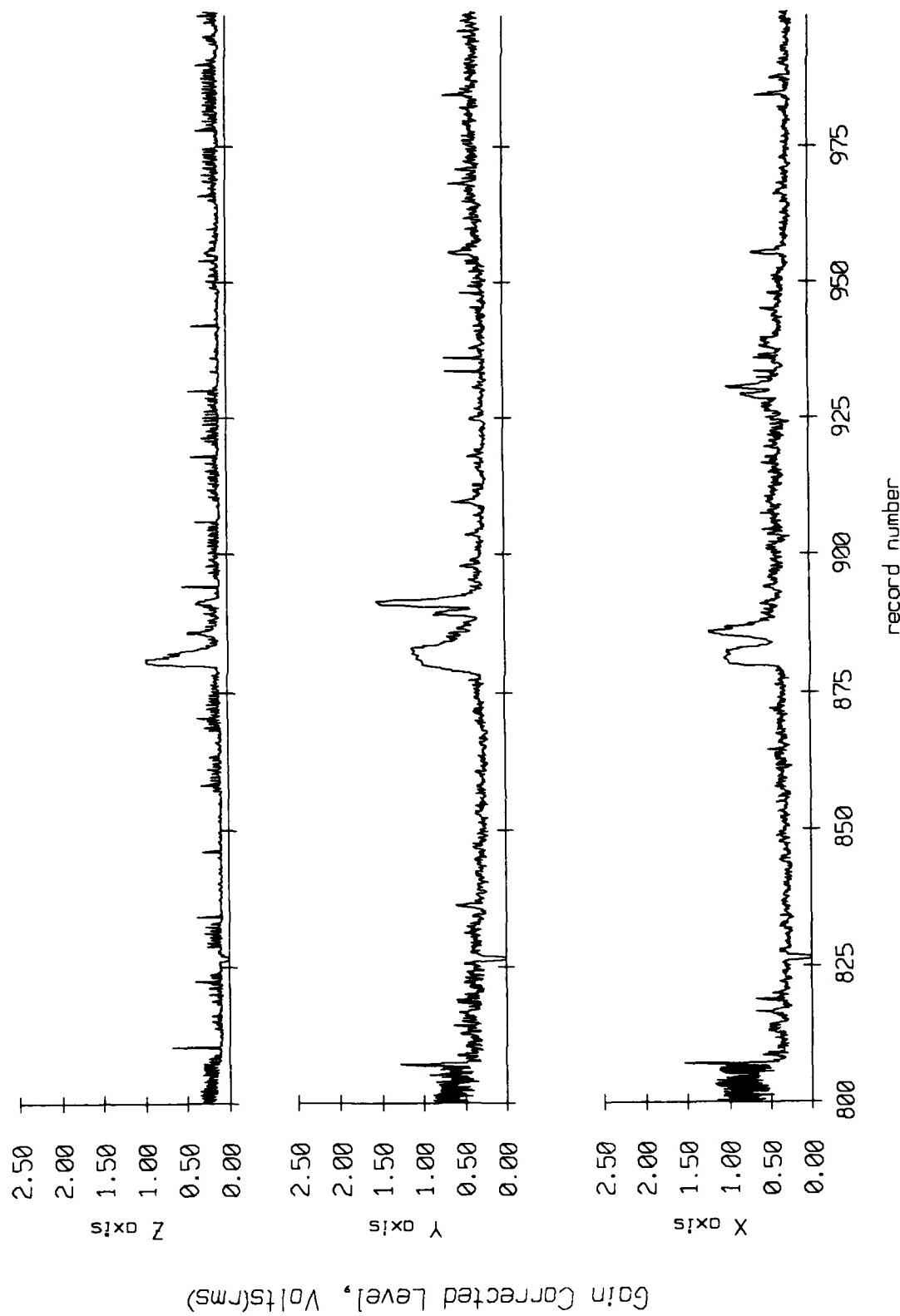
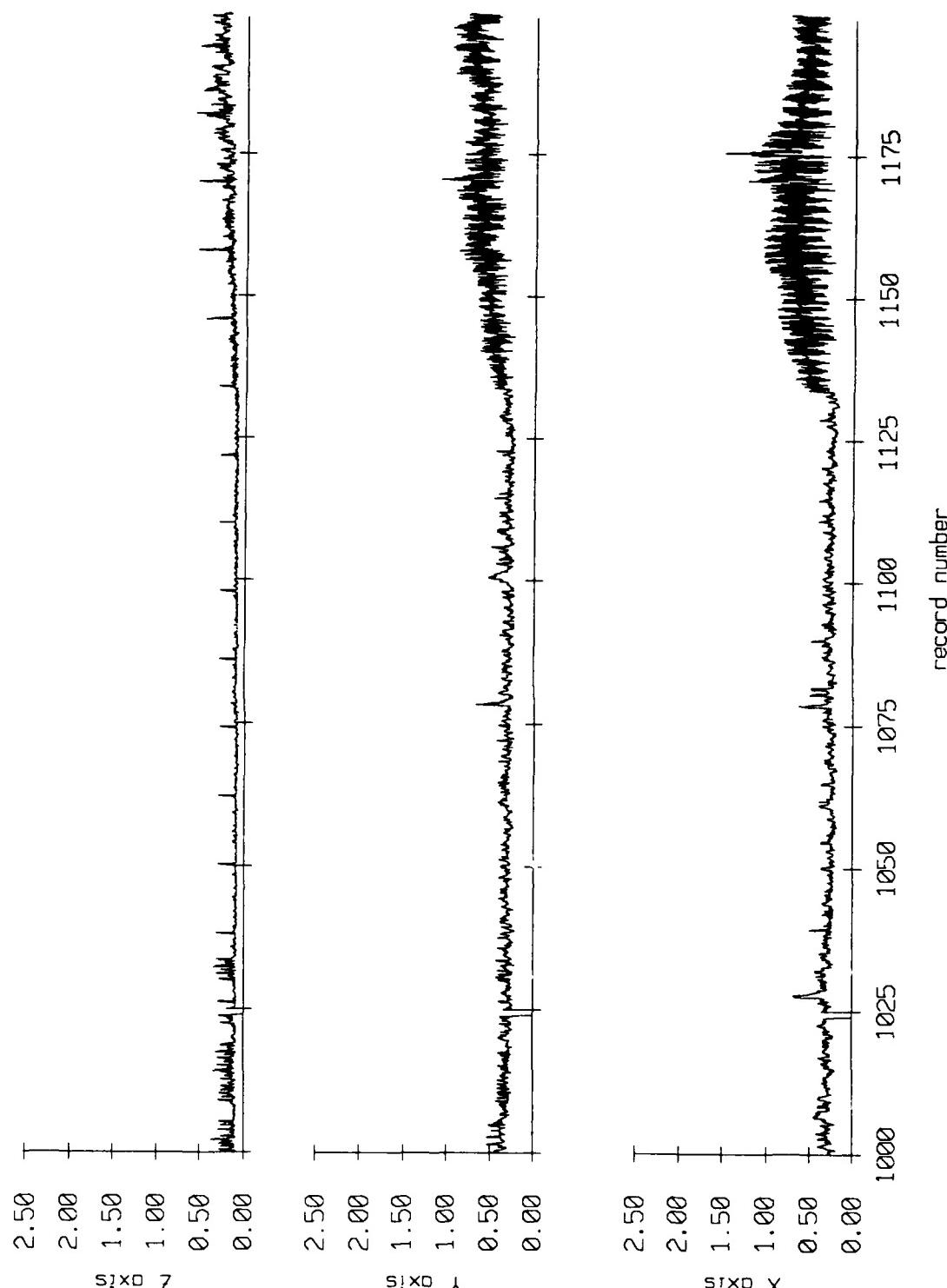


Figure IX.7e

Float 6, September 1987 Sea Trip
overaging period = 5.00 sec.



Gain Corrected Level, Volts(rms)

Figure IX.7f

Float 6, September 1987 Sea Trip
overaging period = 5.00 sec.

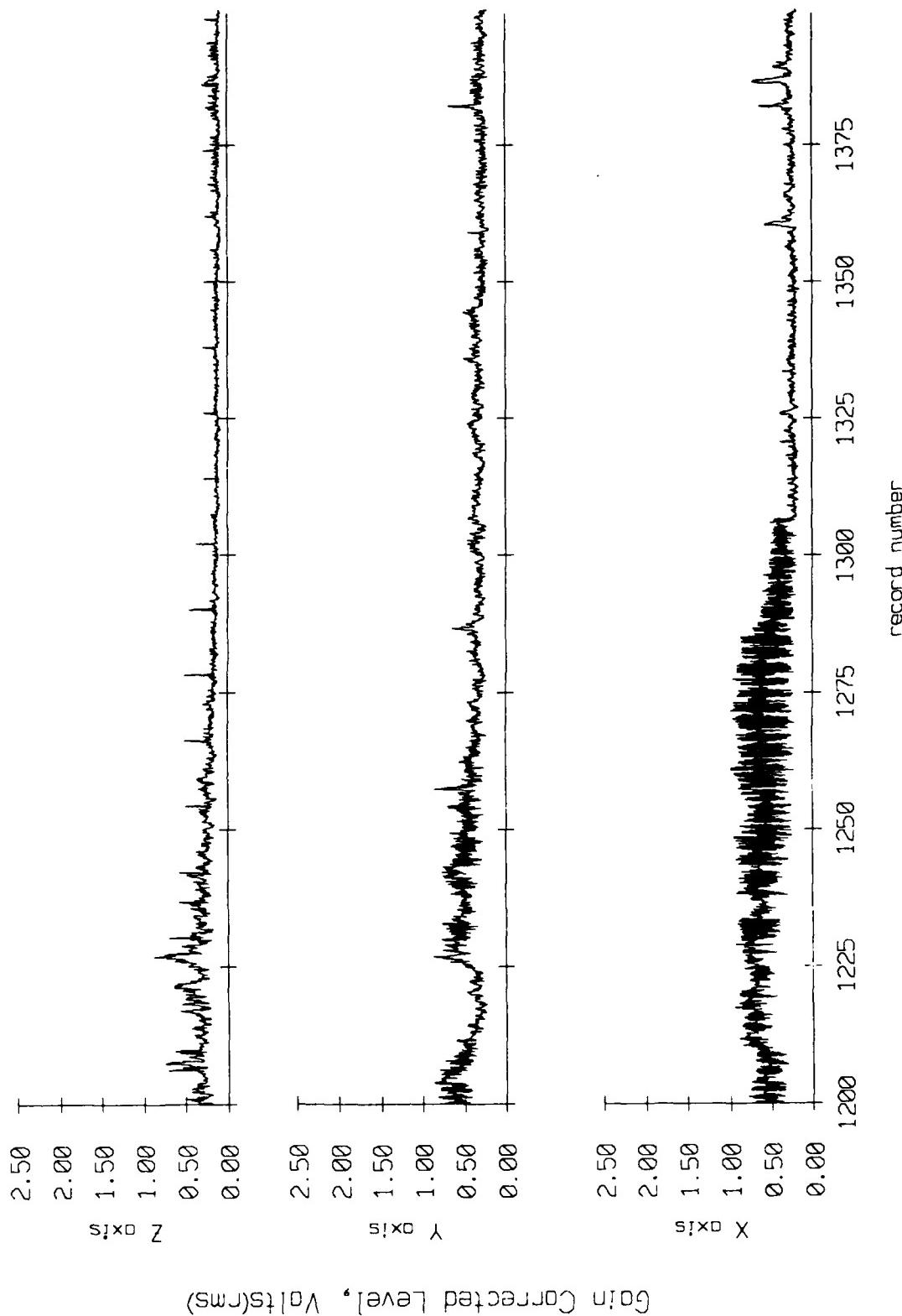


Figure IX.7g

Float 6, September 1987 Sea Trip
averaging period = 5.00 sec.

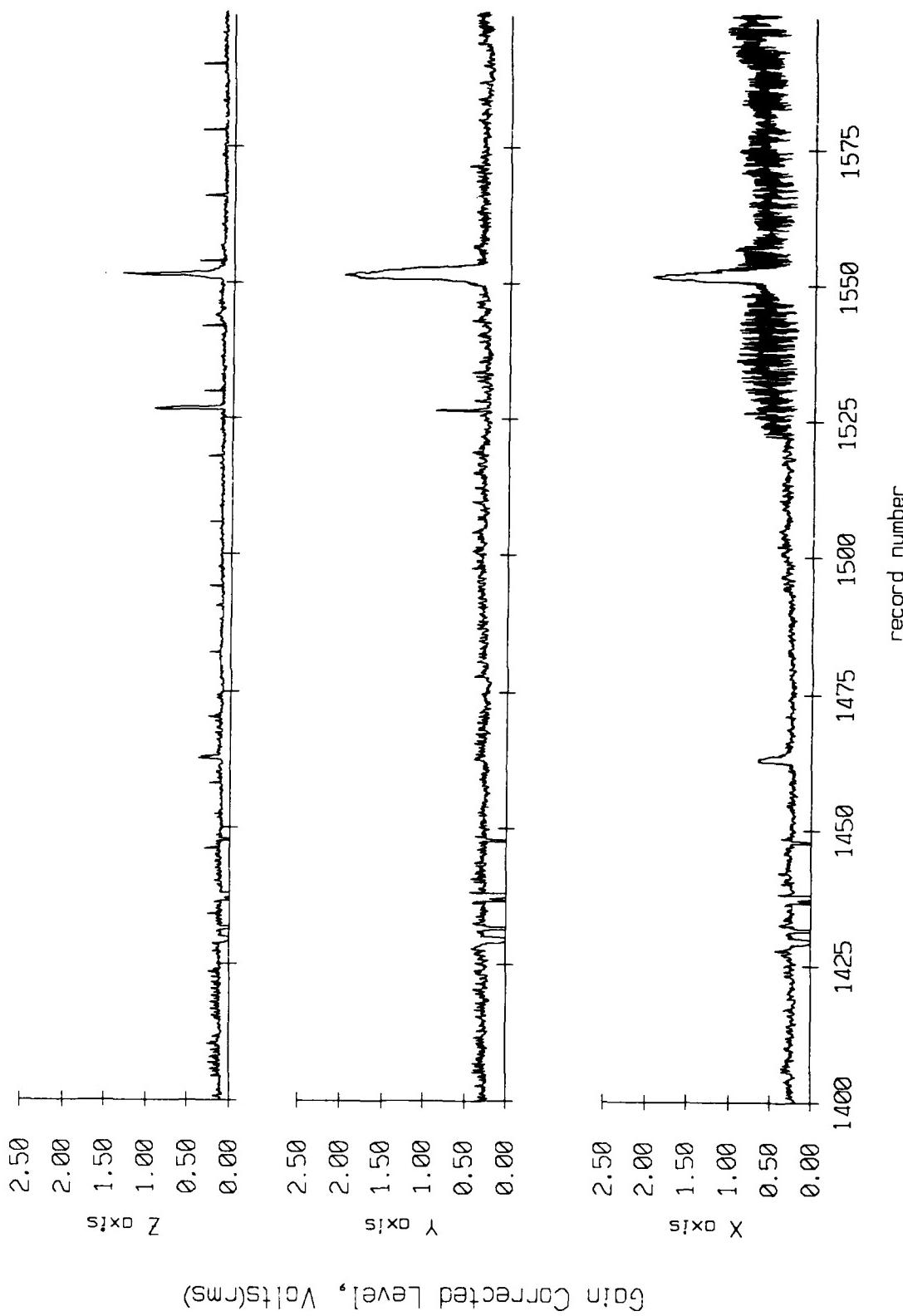


Figure IX.7h

Float 6, September 1987 Sea Trip
averaging period = 5.00 sec.

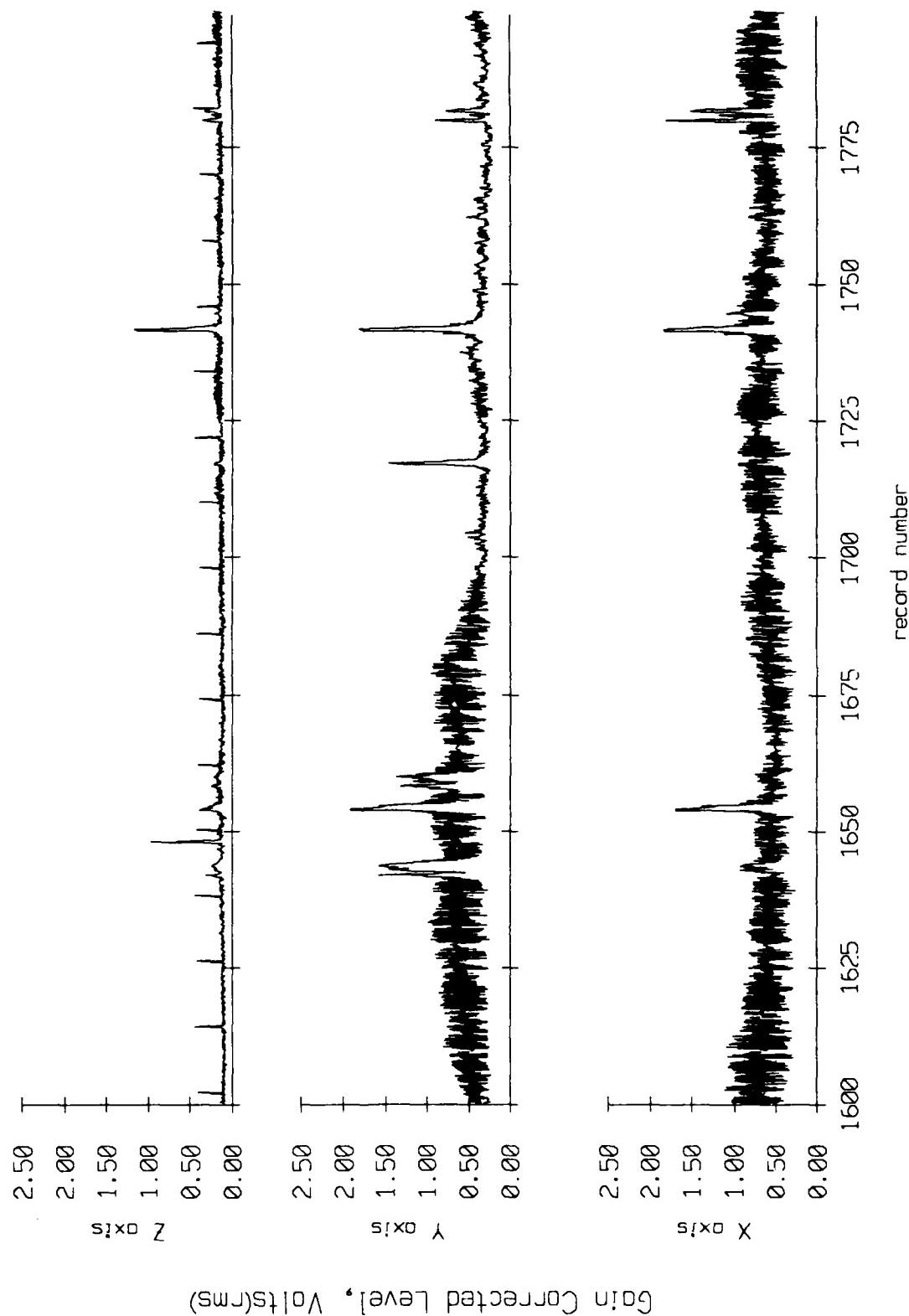
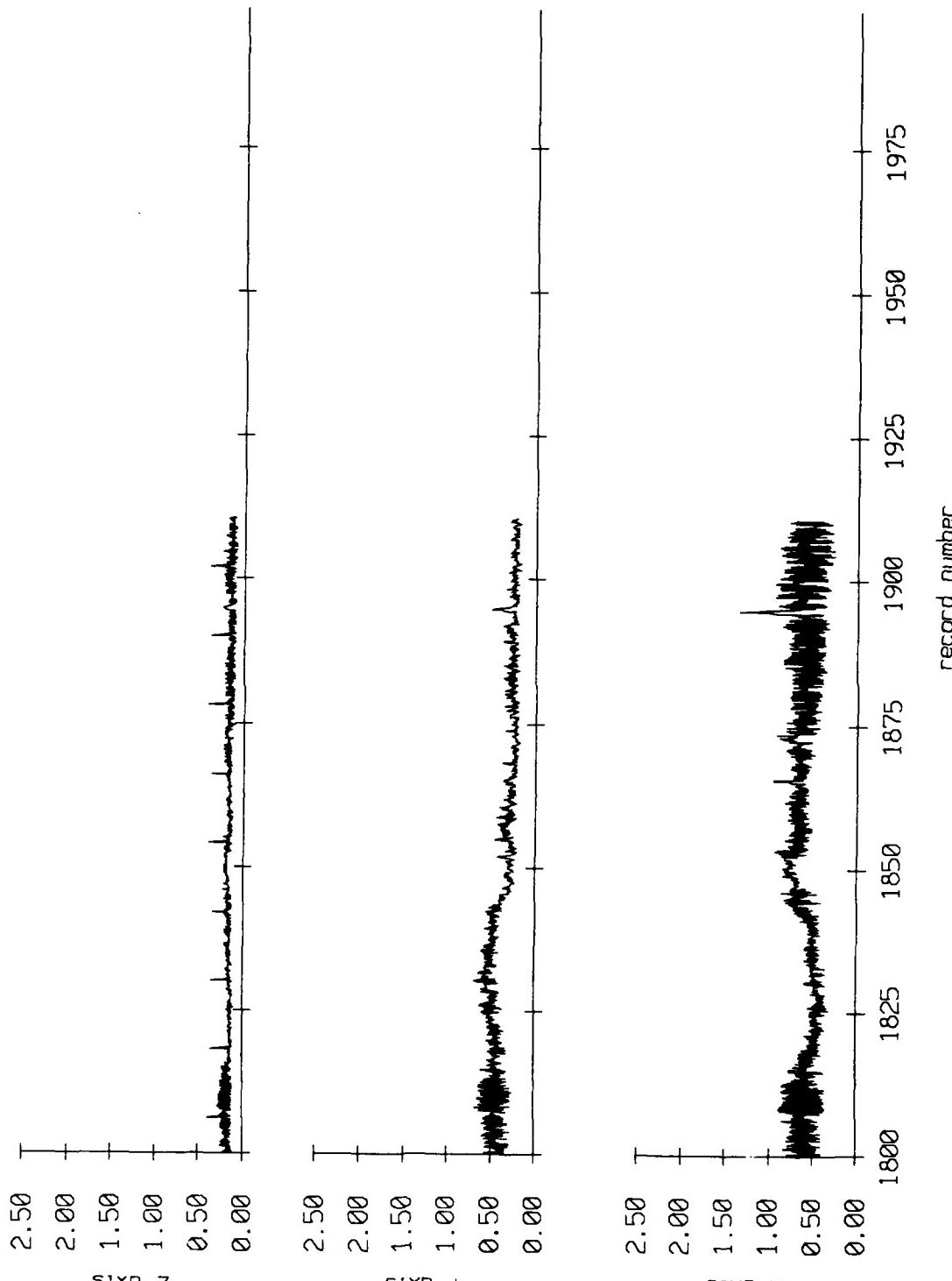


Figure IX.7i

Float 6, September 1987 Sea Trip
averaging period = 5.00 sec.



Gain Corrected Level, Volts(rms)

Figure IX.7j

Float 7, September 1987 Sea Trip
averaging period = 5.00 sec.

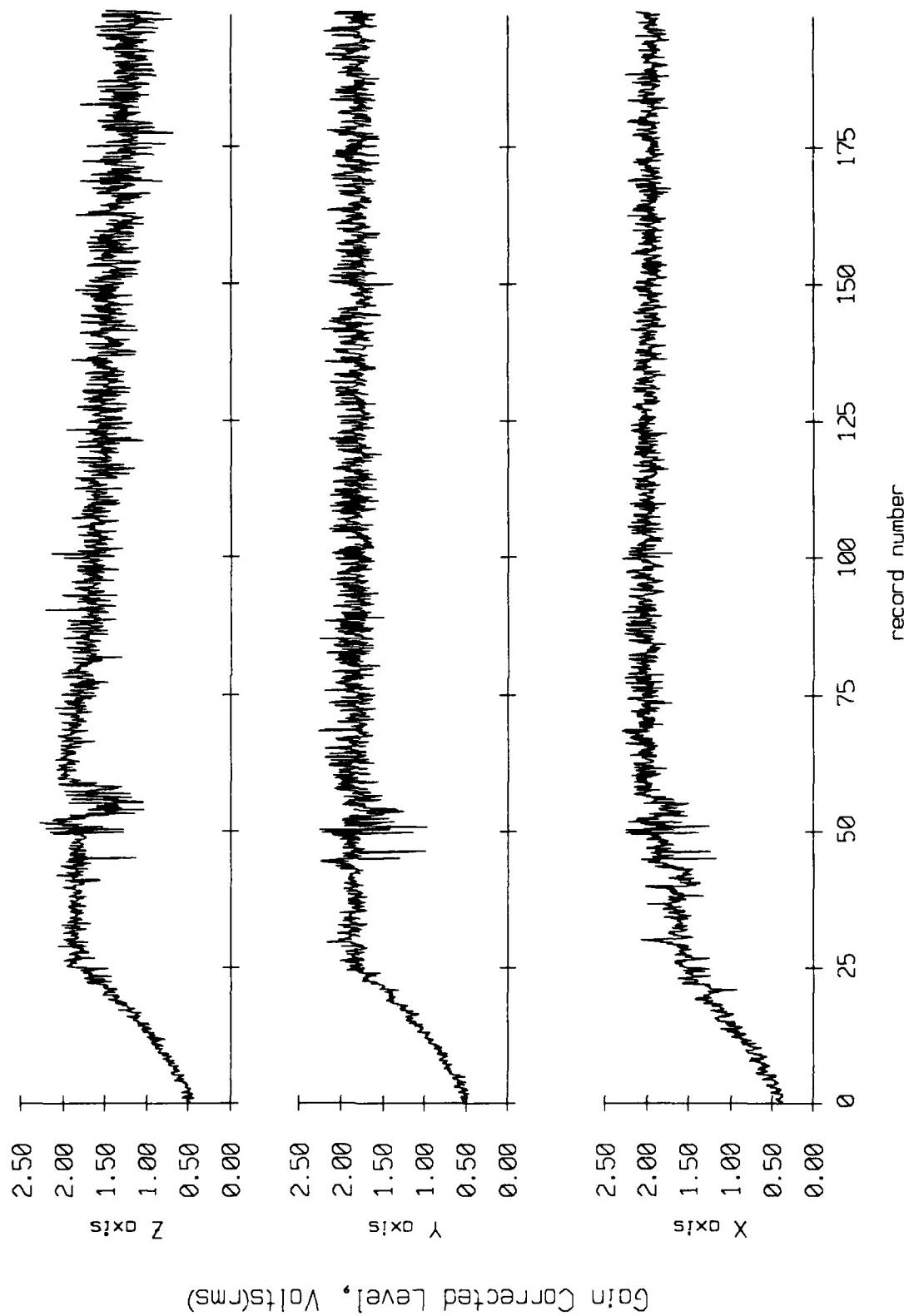


Figure IX.8a

Float 7, September 1987 Sea Trip
averaging period = 5.00 sec.

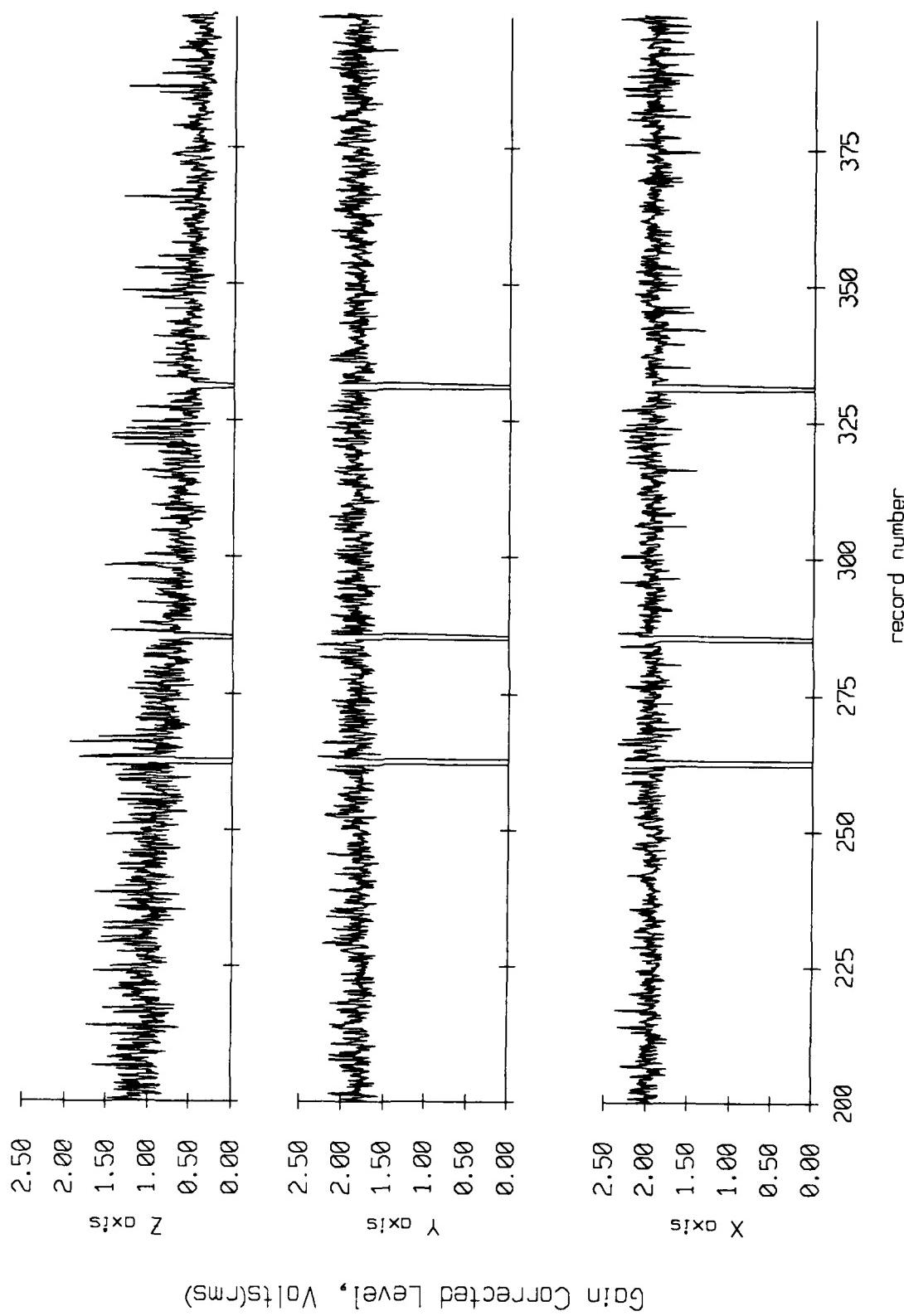


Figure IX.8b

Float 7, September 1987 Sea Trip
averaging period = 5.00 sec.

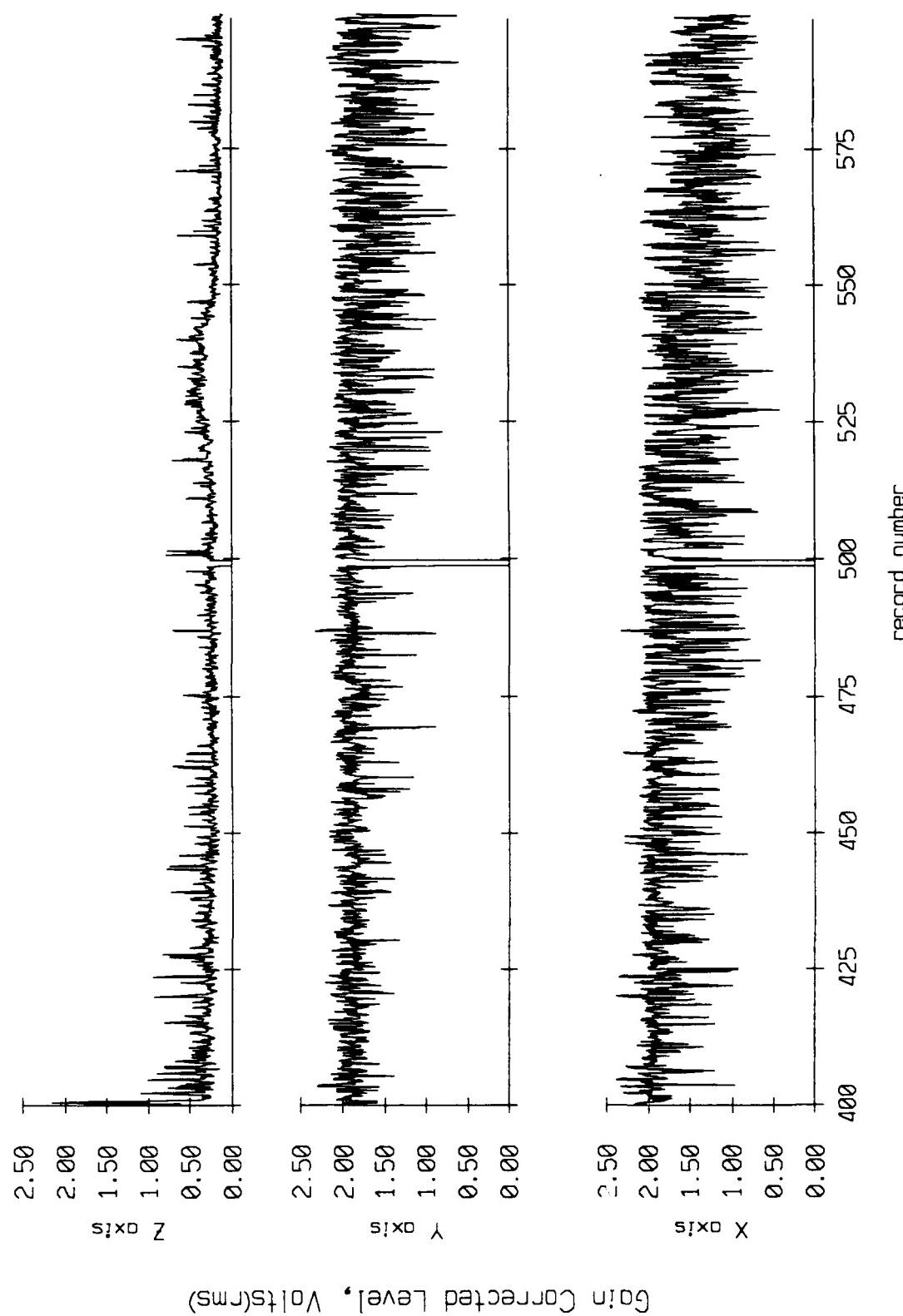


Figure IX.8c

Float 7, September 1987 Sea Trip
overriding period = 5.00 sec.

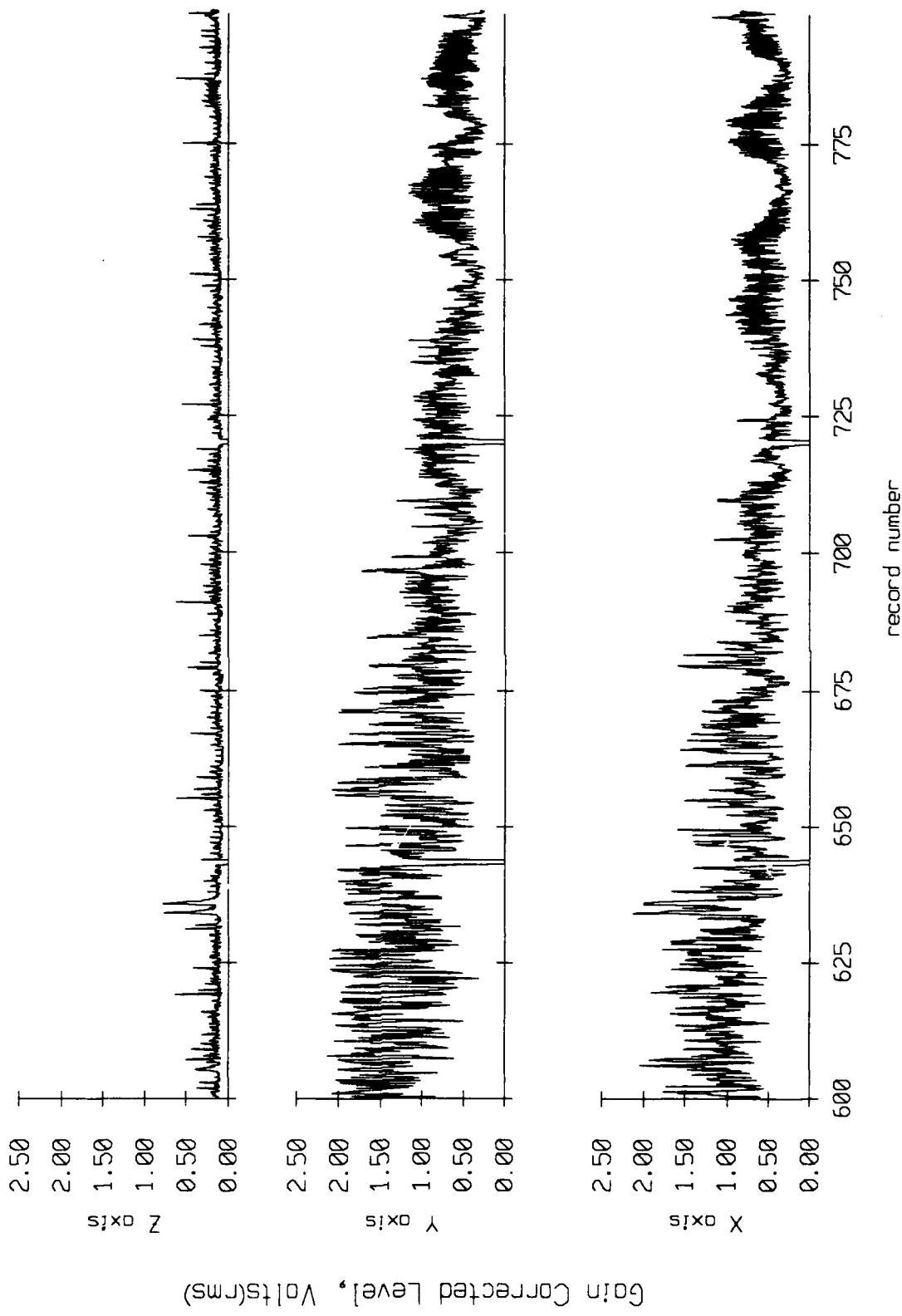


Figure IX.8d

Float 7, September 1987 Sea Trip
averaging period = 5.00 sec.

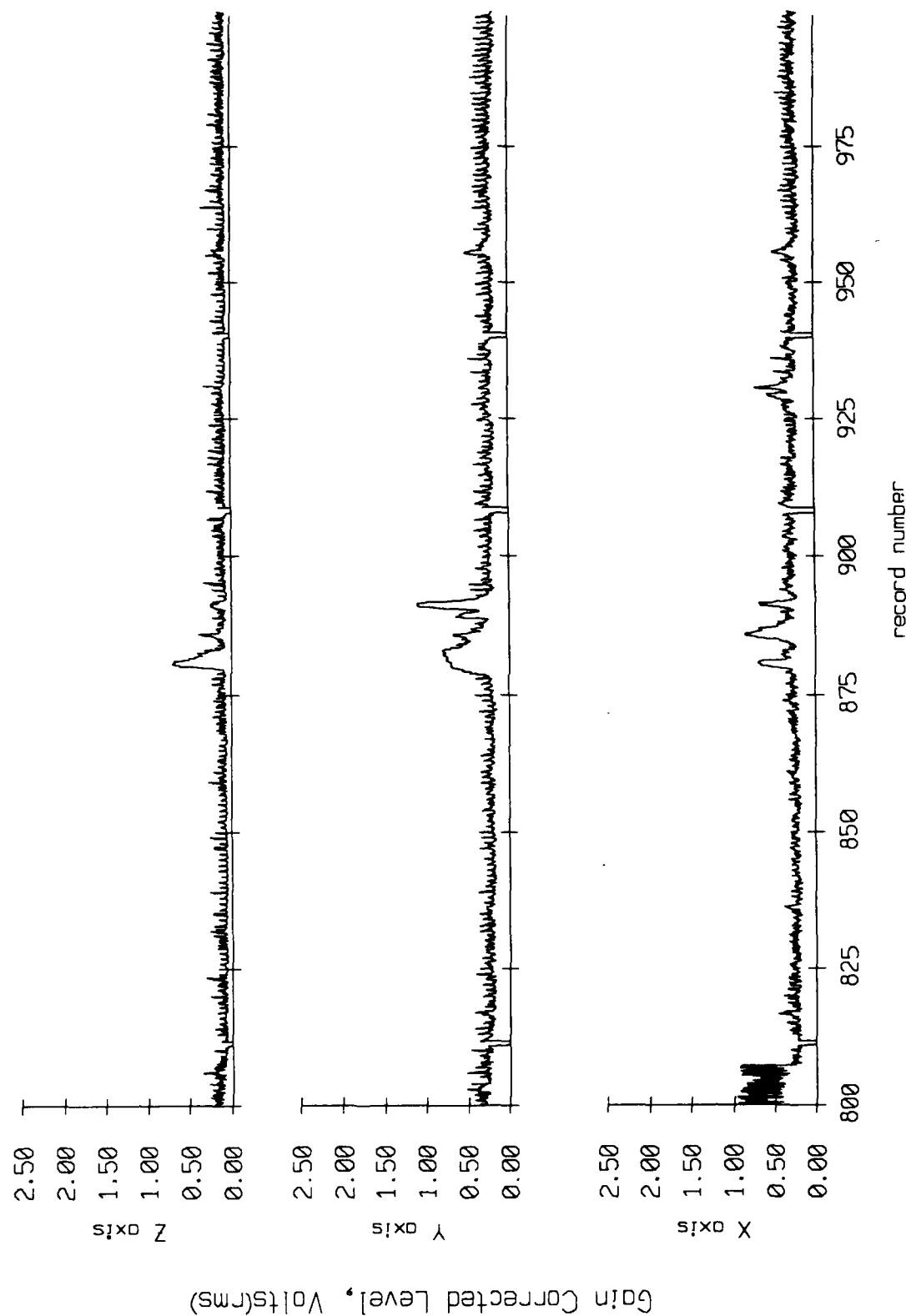


Figure IX.8e

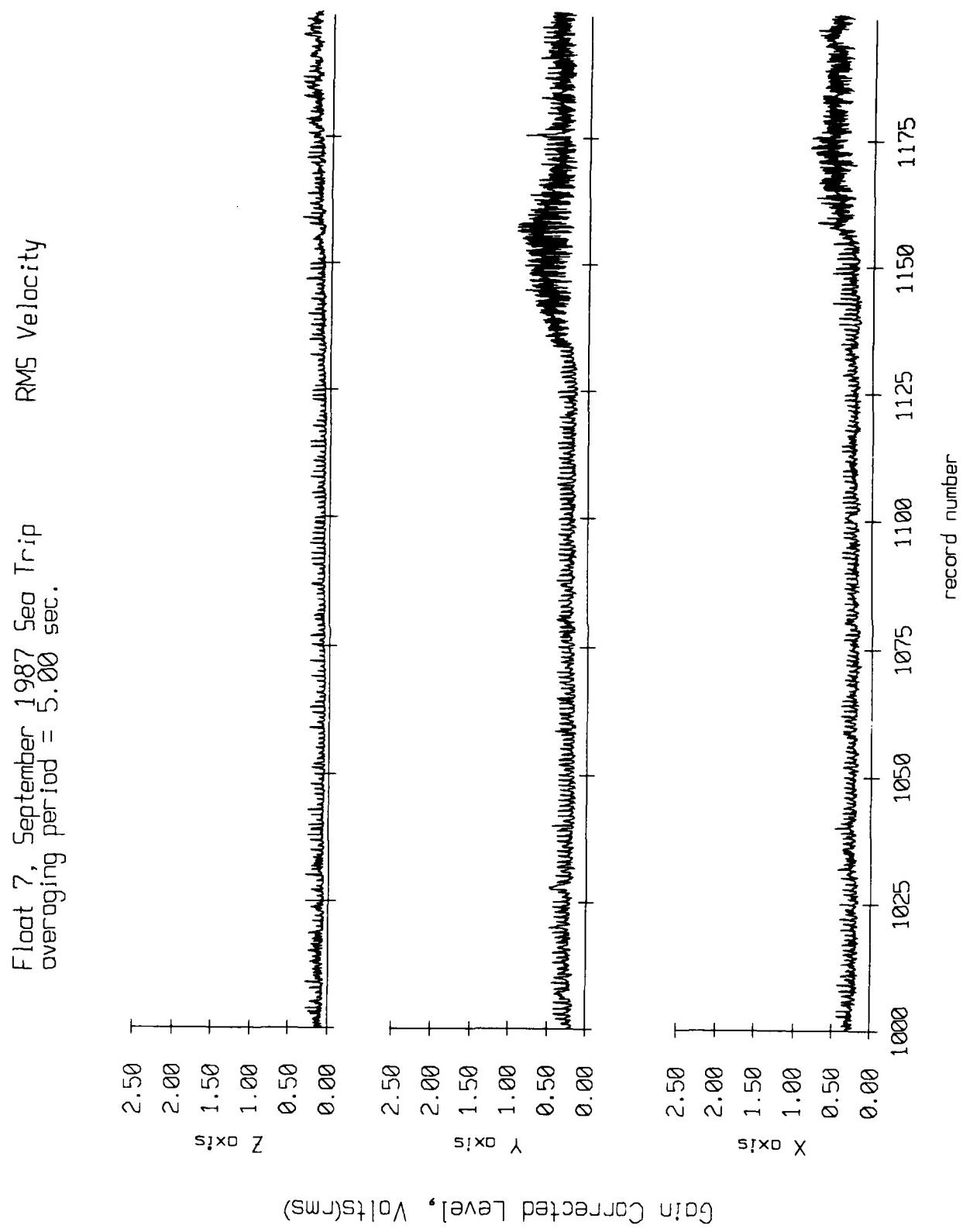


Figure IX.8f

Float 7, September 1987 Sea Trip
averaging period = 5.00 sec.

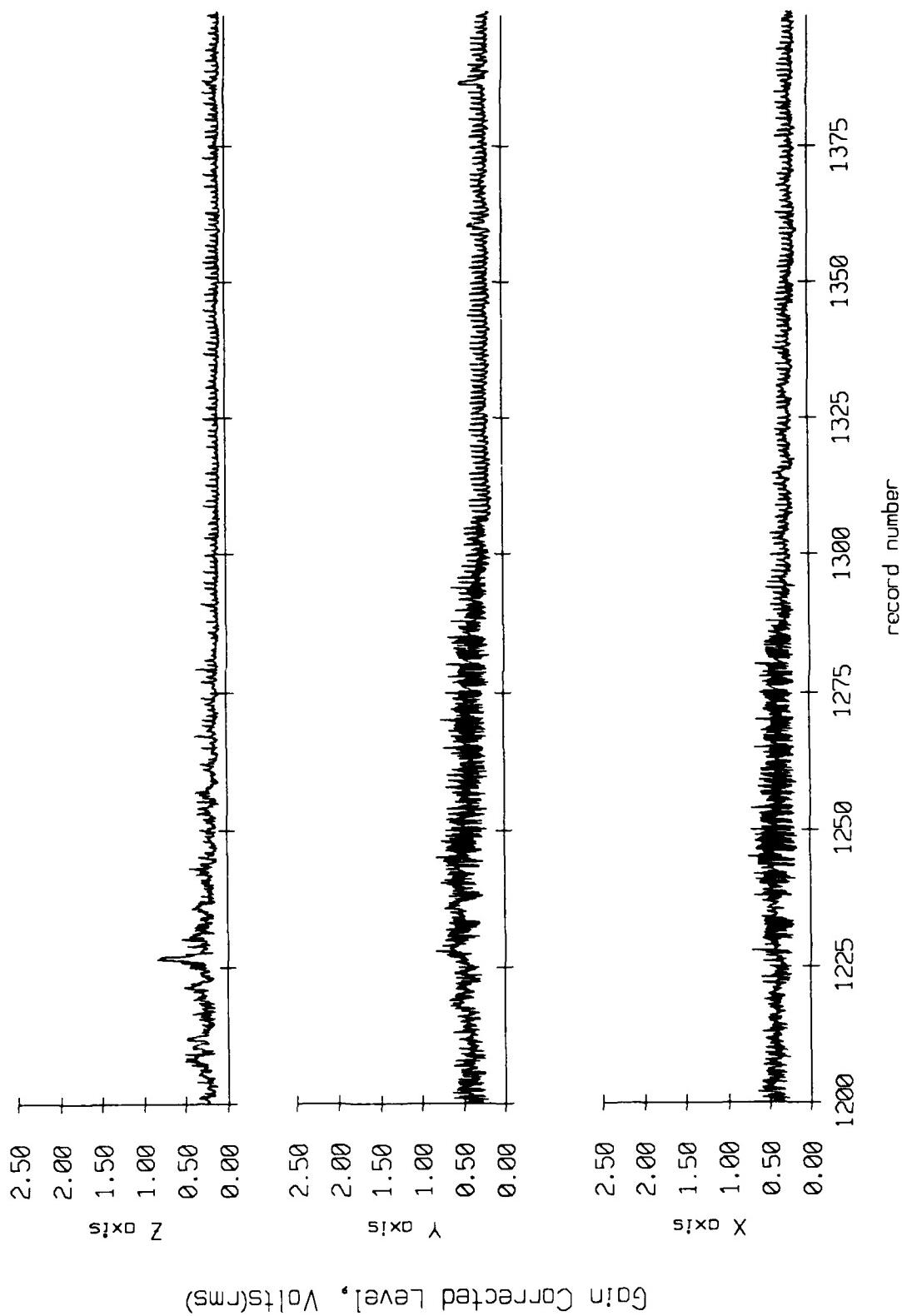


Figure IX.8g

Float 7, September 1987 Sea Trip
overaging period = 5.00 sec.

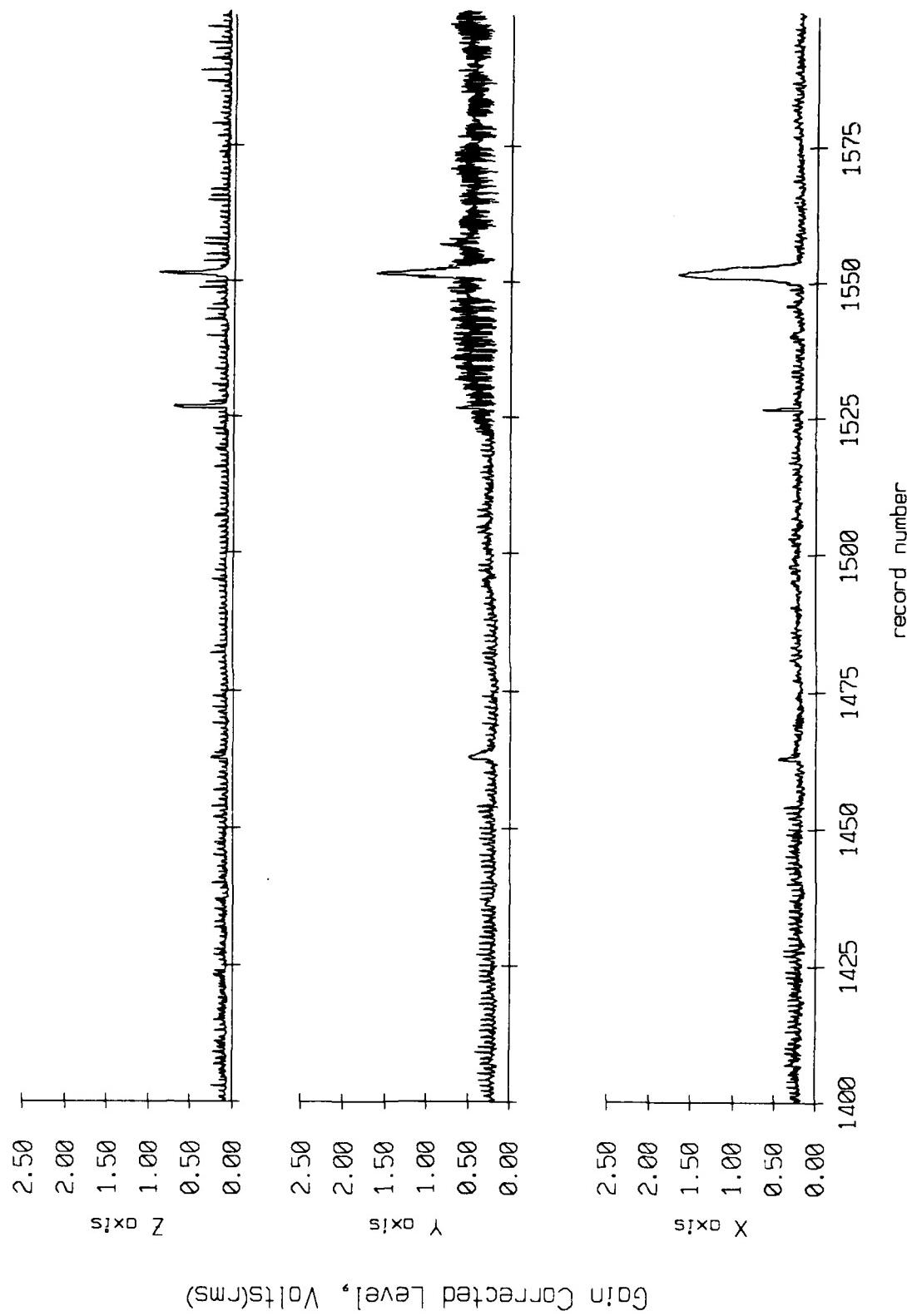


Figure IX.8h

Float 7, September 1987 Sea Trip
averaging period = 5.00 sec.

RMS Velocity

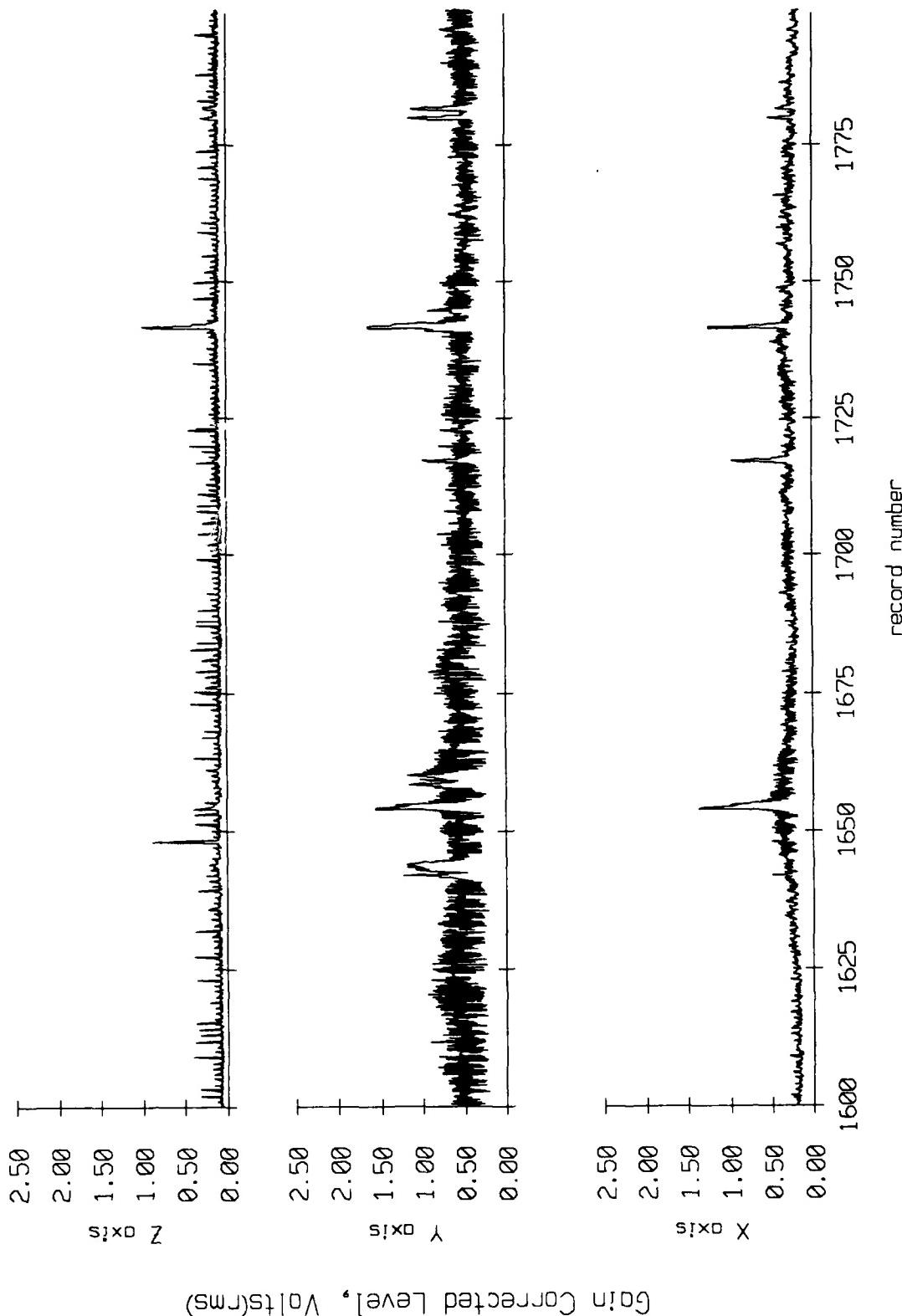


Figure IX.8i

Float 7, September 1987 Sea Trip
averaging period = 5.00 sec.

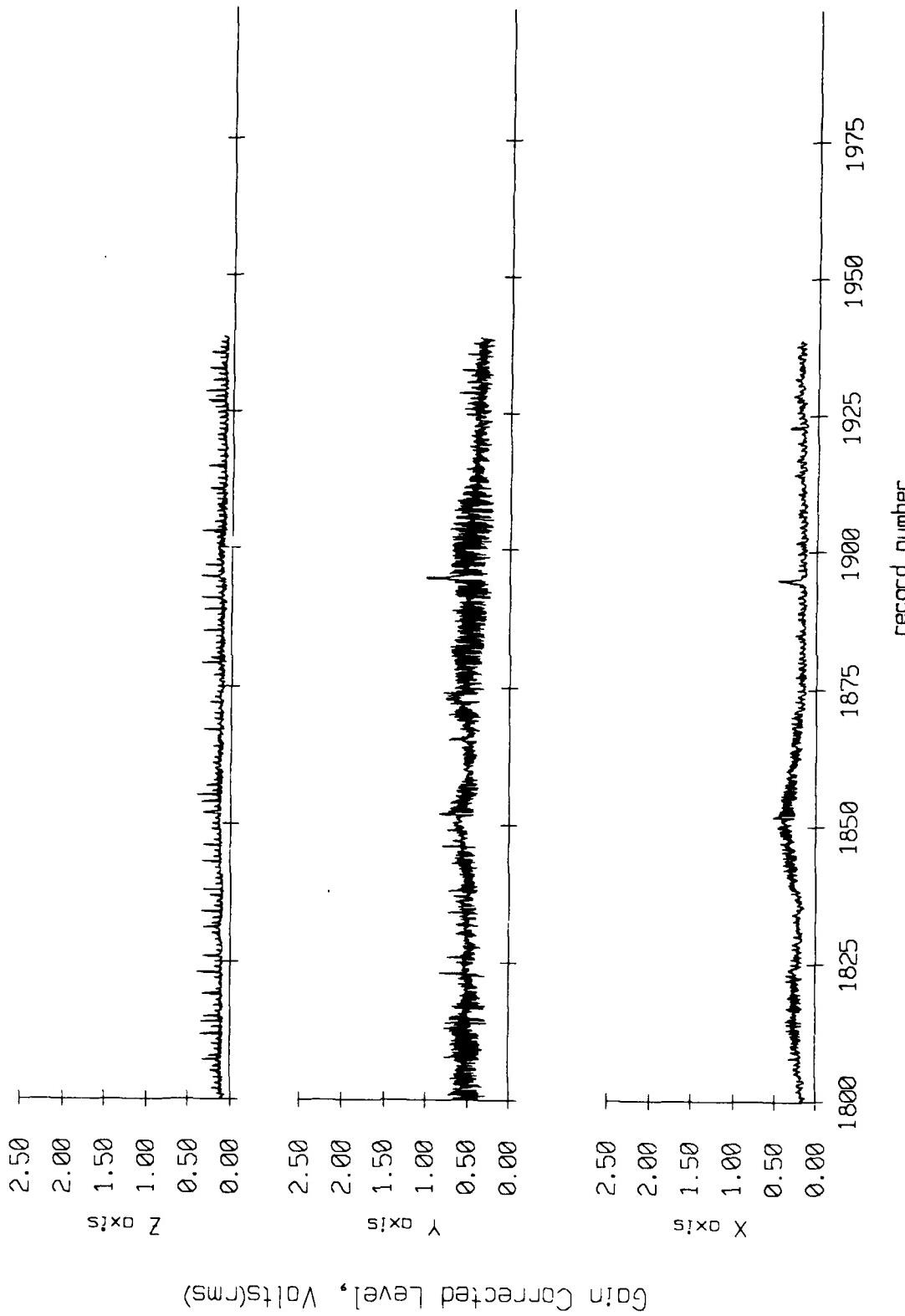
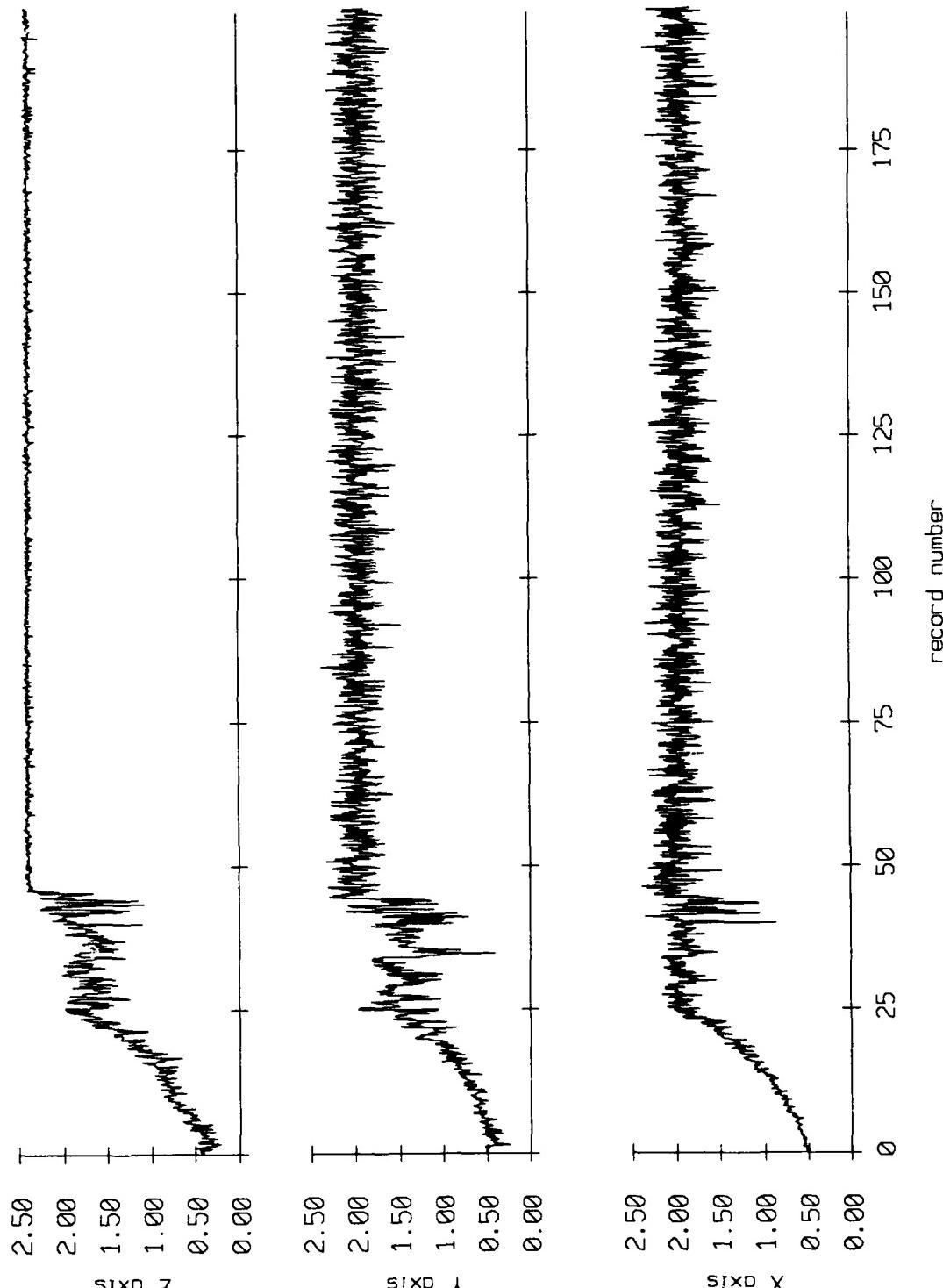


Figure IX.8j

Float 8, September 1987 Sea Trip
averaging period = 5.00 sec.

RMS Velocity



Gain Corrected Level, Volts(RMS)

Figure IX.9a

Float 8, September 1987 Sea Trip
averaging period = 5.00 sec.

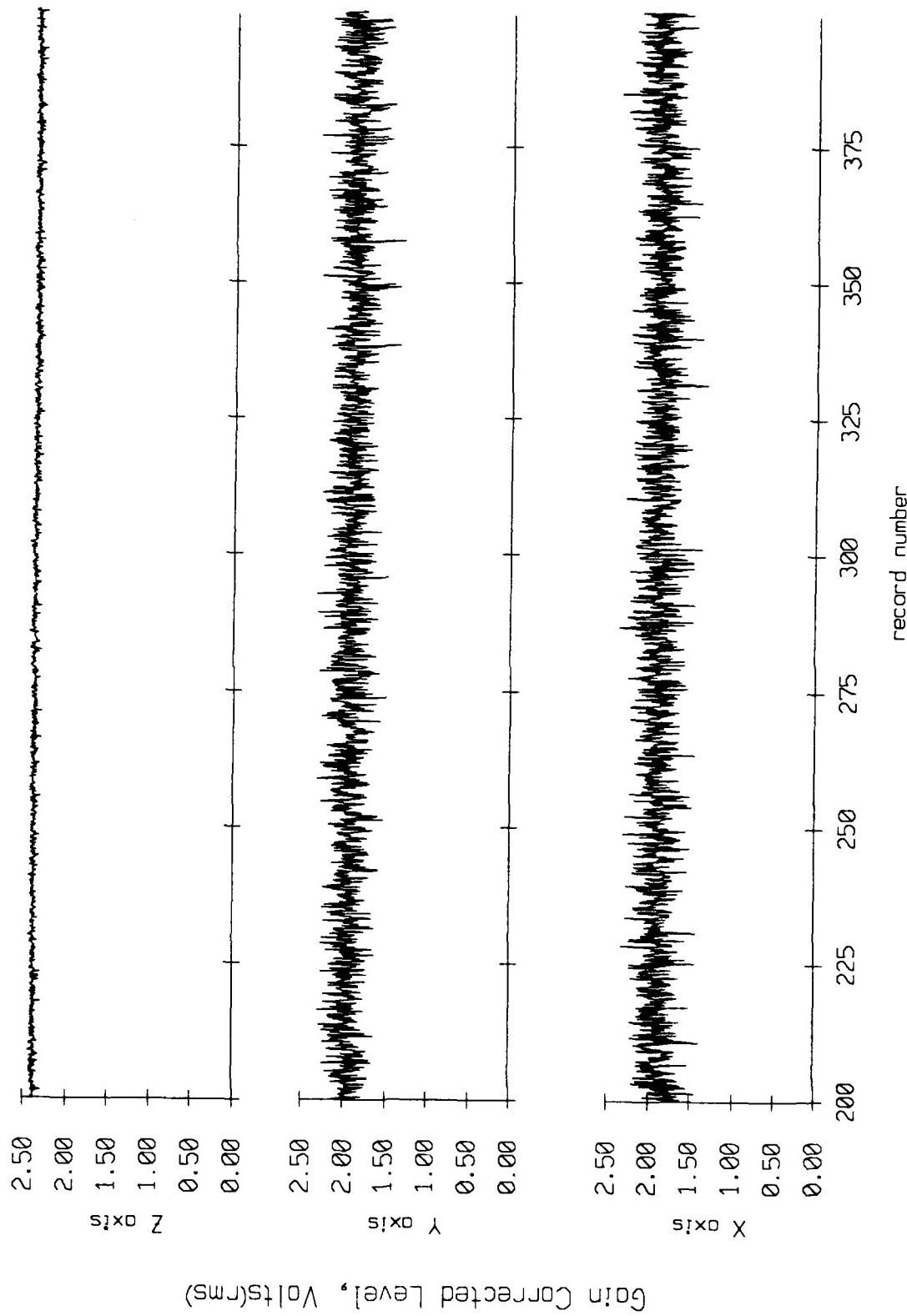
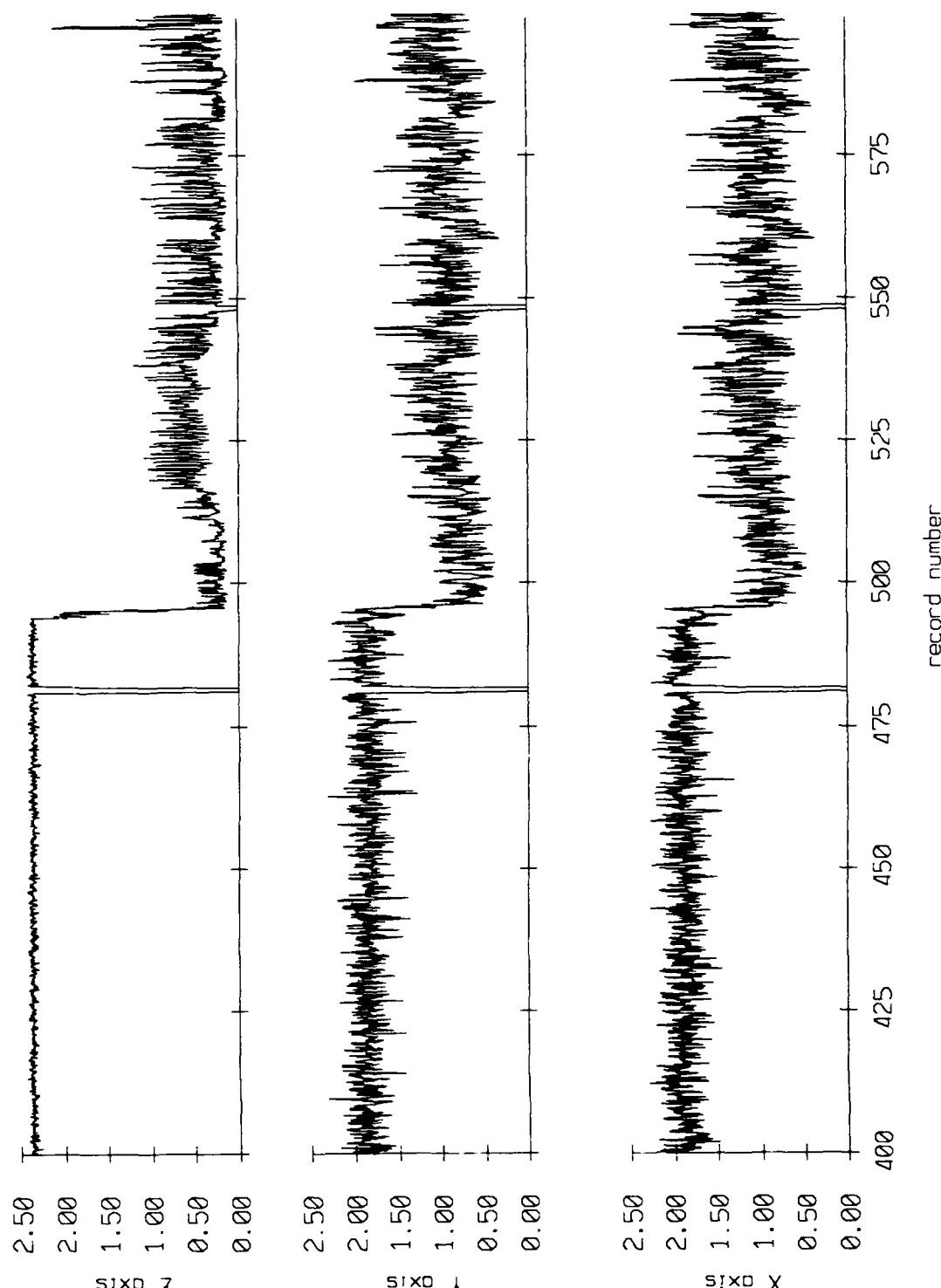


Figure IX.9b

Float 8, September 1987 Sea Trip
averaging period = 5.00 sec.



Gain Corrected Level, Volts(RMS)

Figure IX.9c

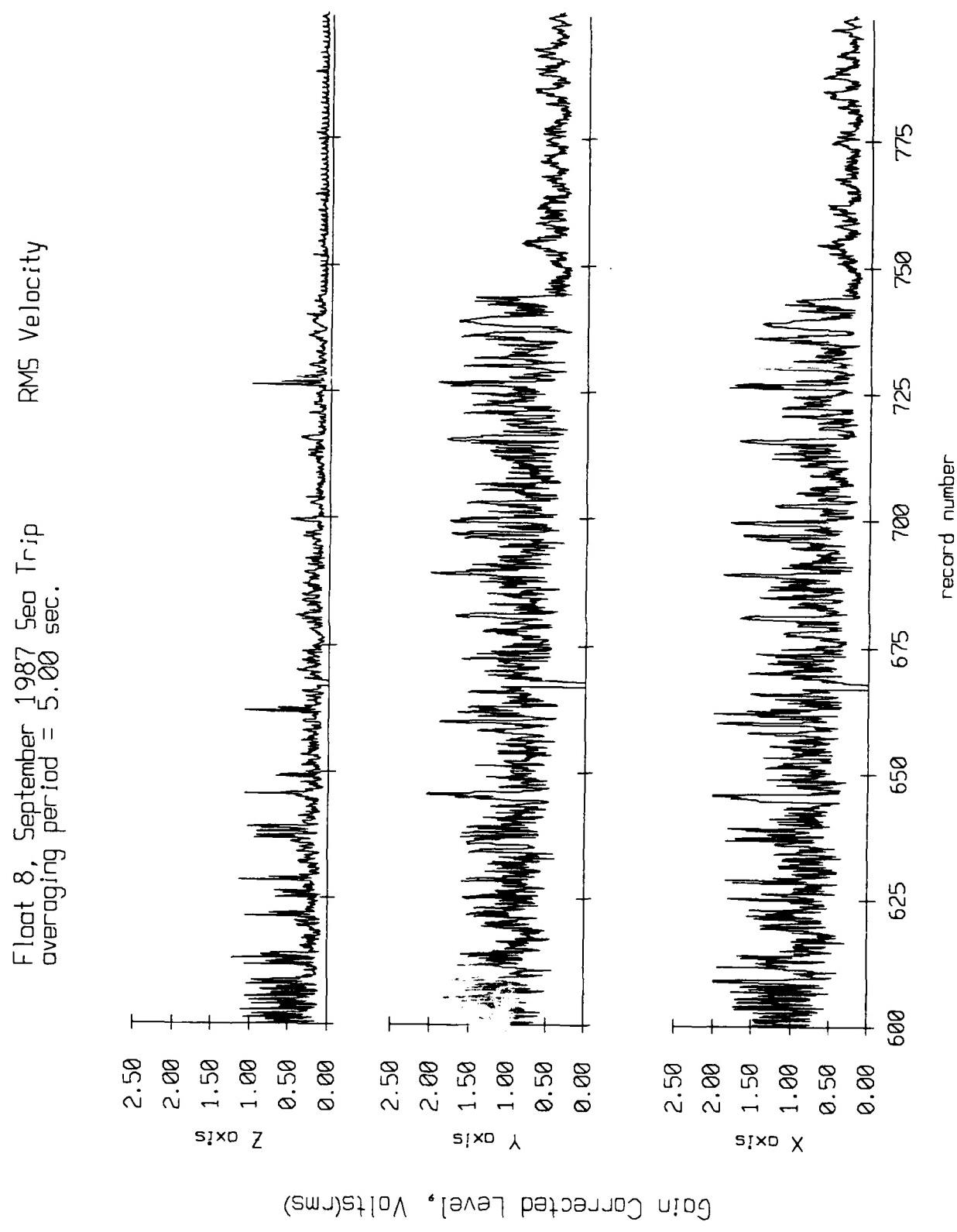


Figure IX.9d

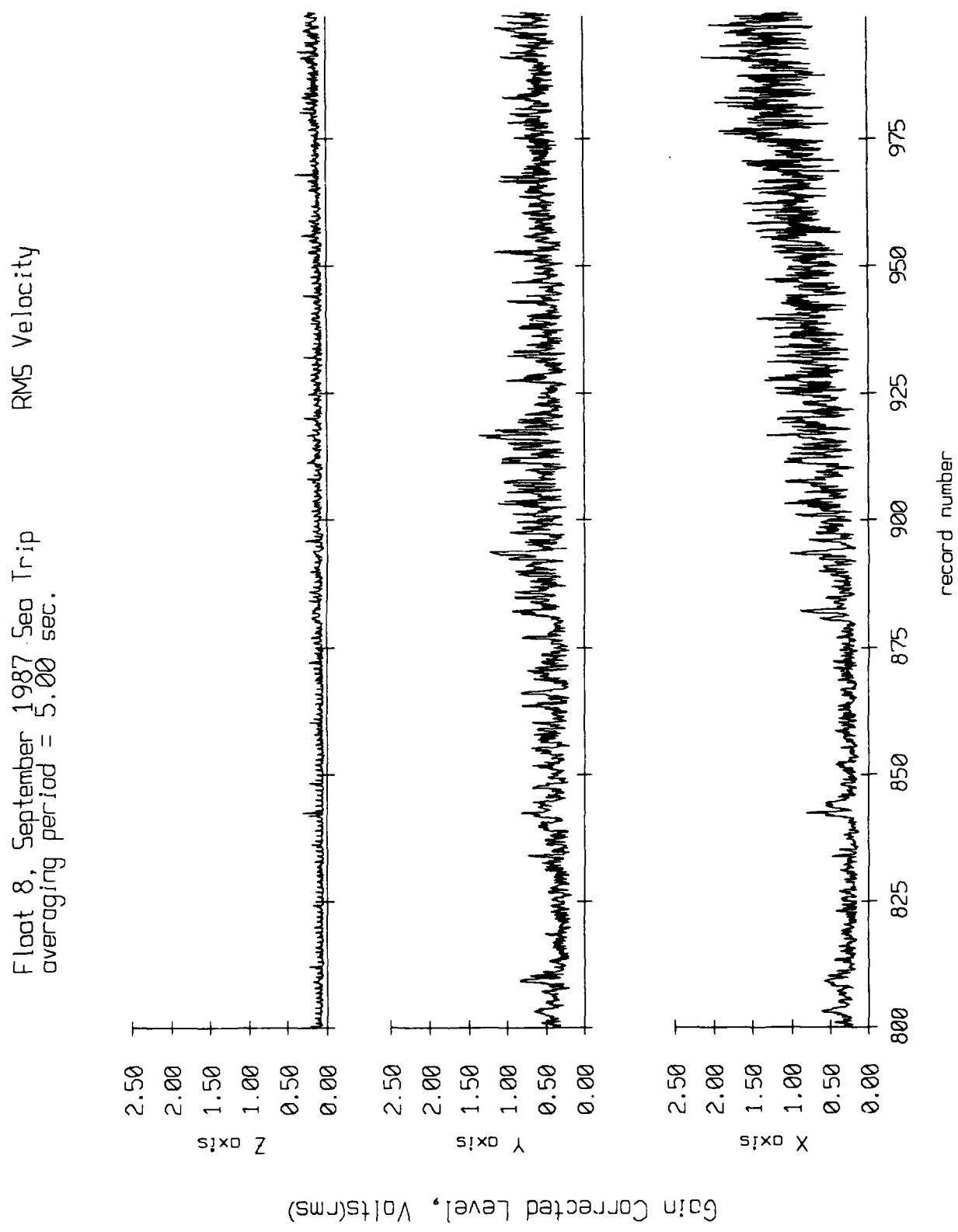


Figure IX.9e

Float 8, September 1987 Sea Trip
averaging period = 5.00 sec.

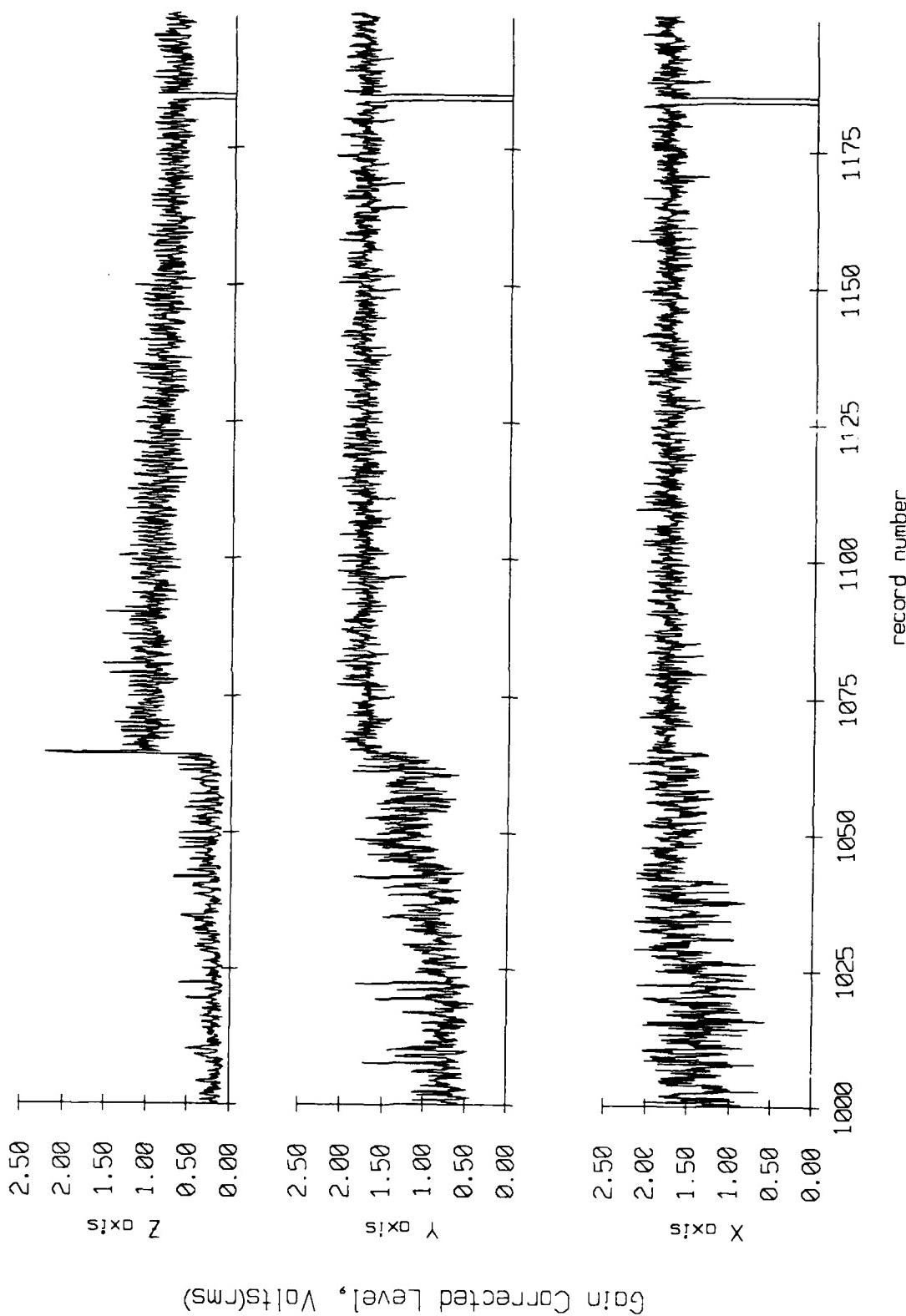


Figure IX.9f

Float 8, September 1987 Sec Trip
averaging period = 5.00 sec.

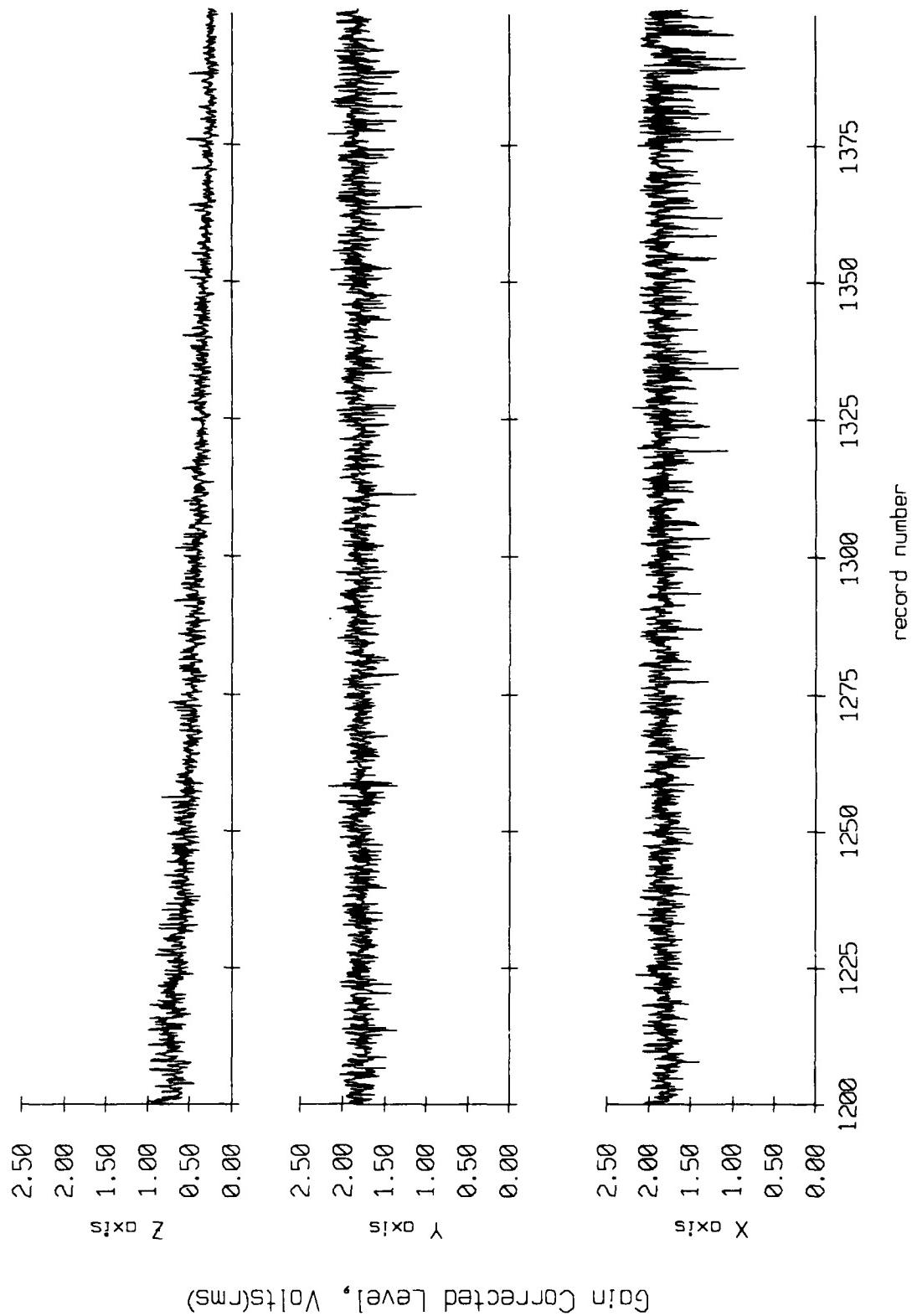


Figure IX.9g

Float 8, September 1987 Sea Trip
overgaging period = 5.00 sec.

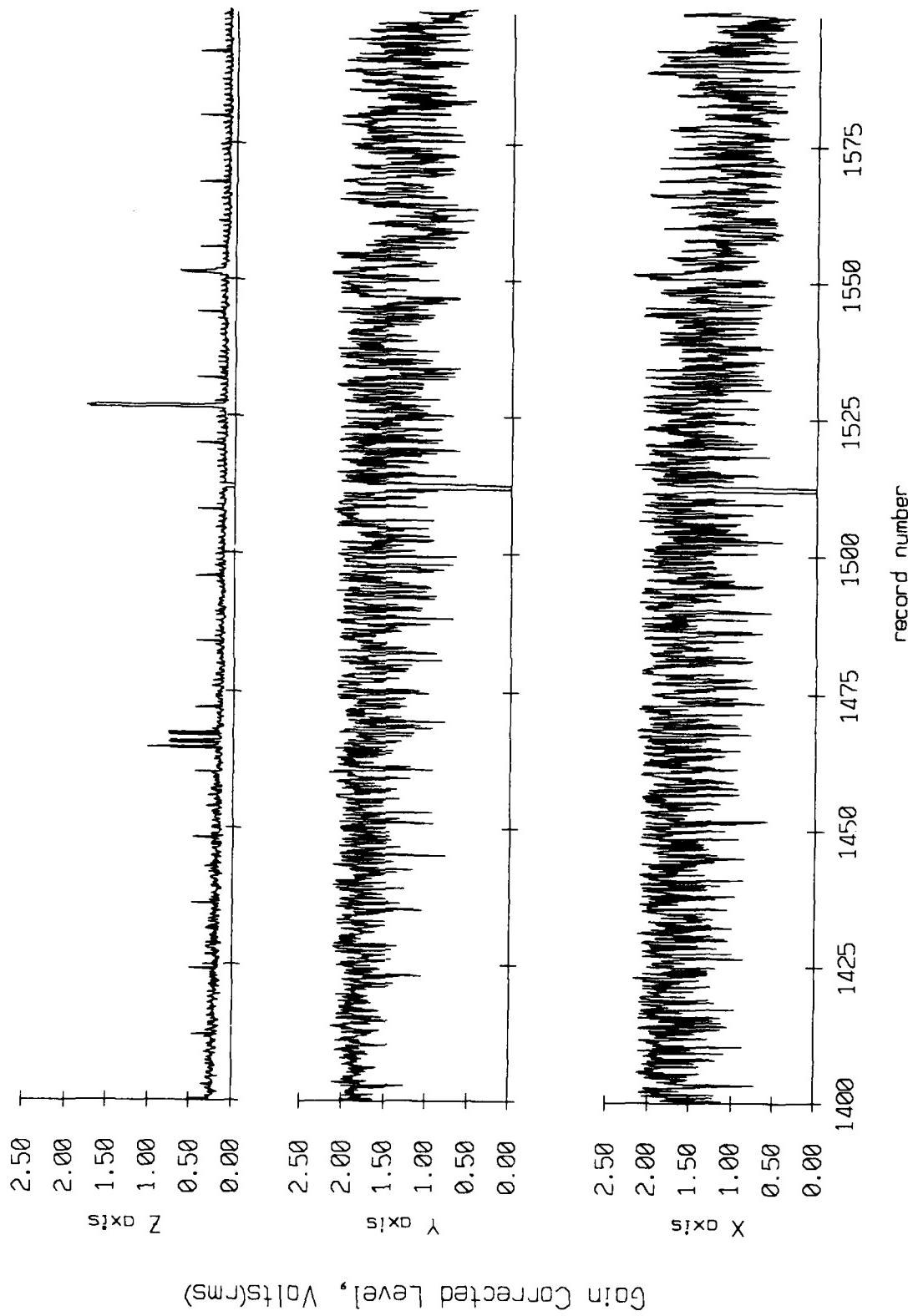


Figure IX.9h

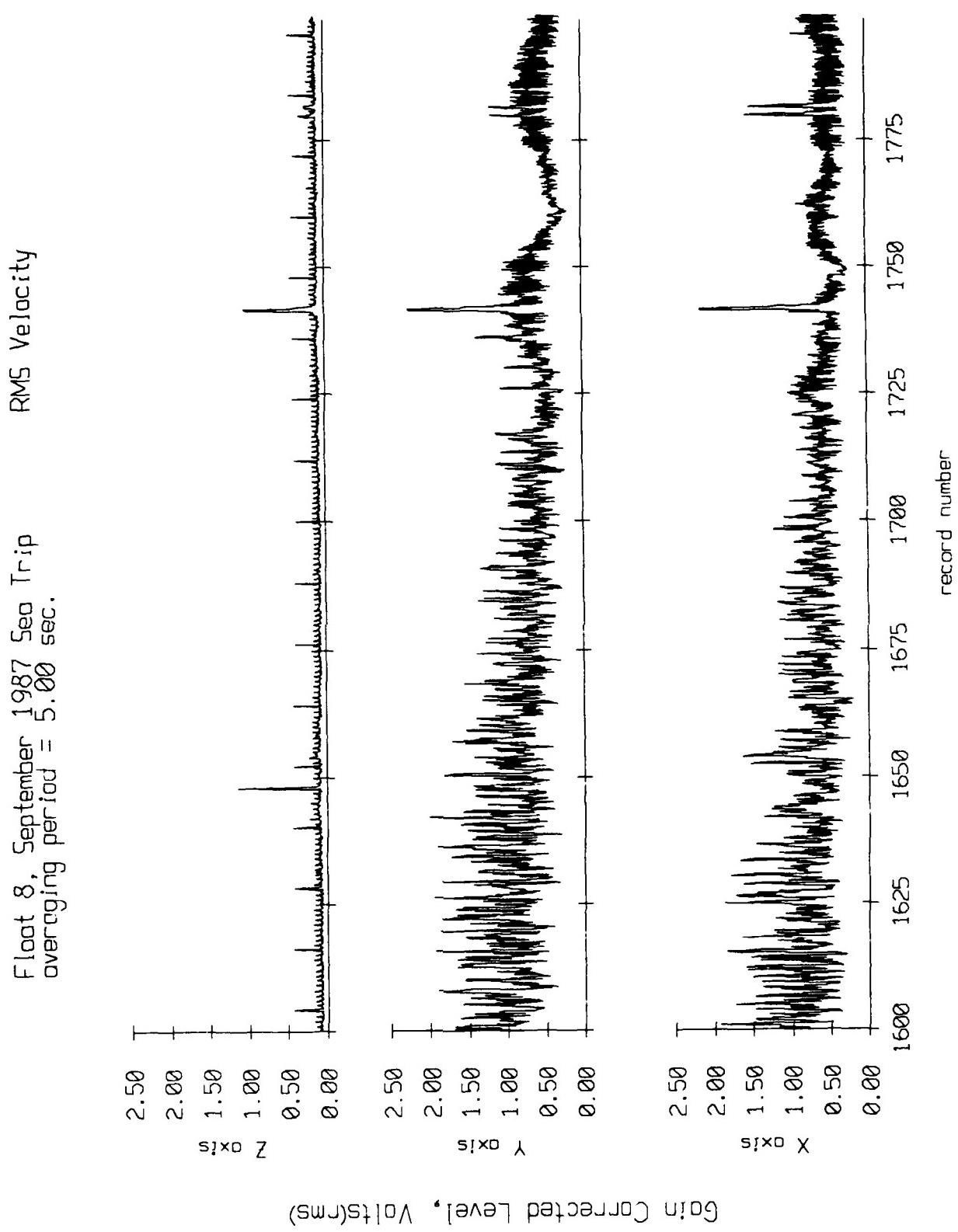


Figure IX.9i

Float 8, September 1987 Sea Trip
averaging period = 5.00 sec.

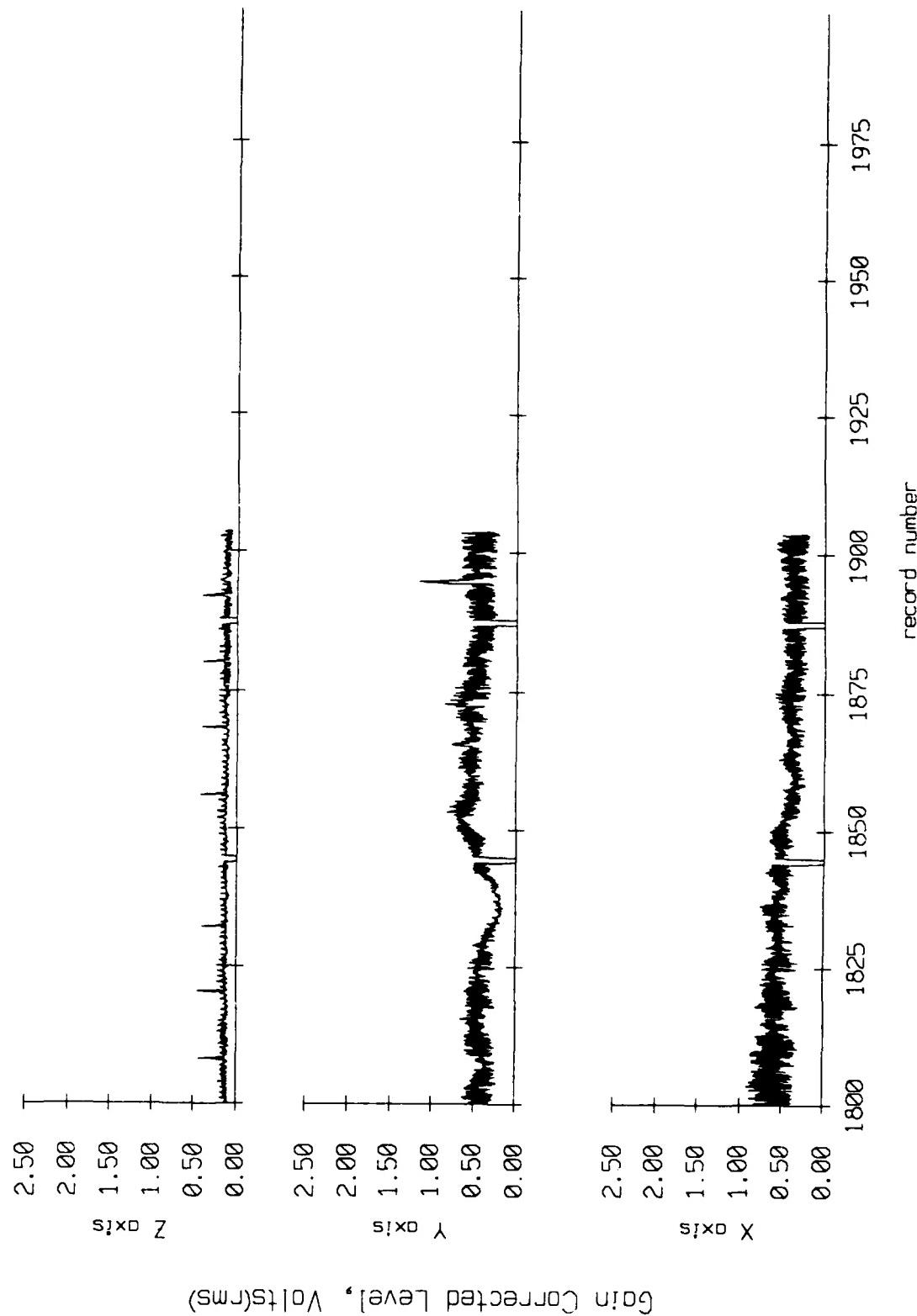
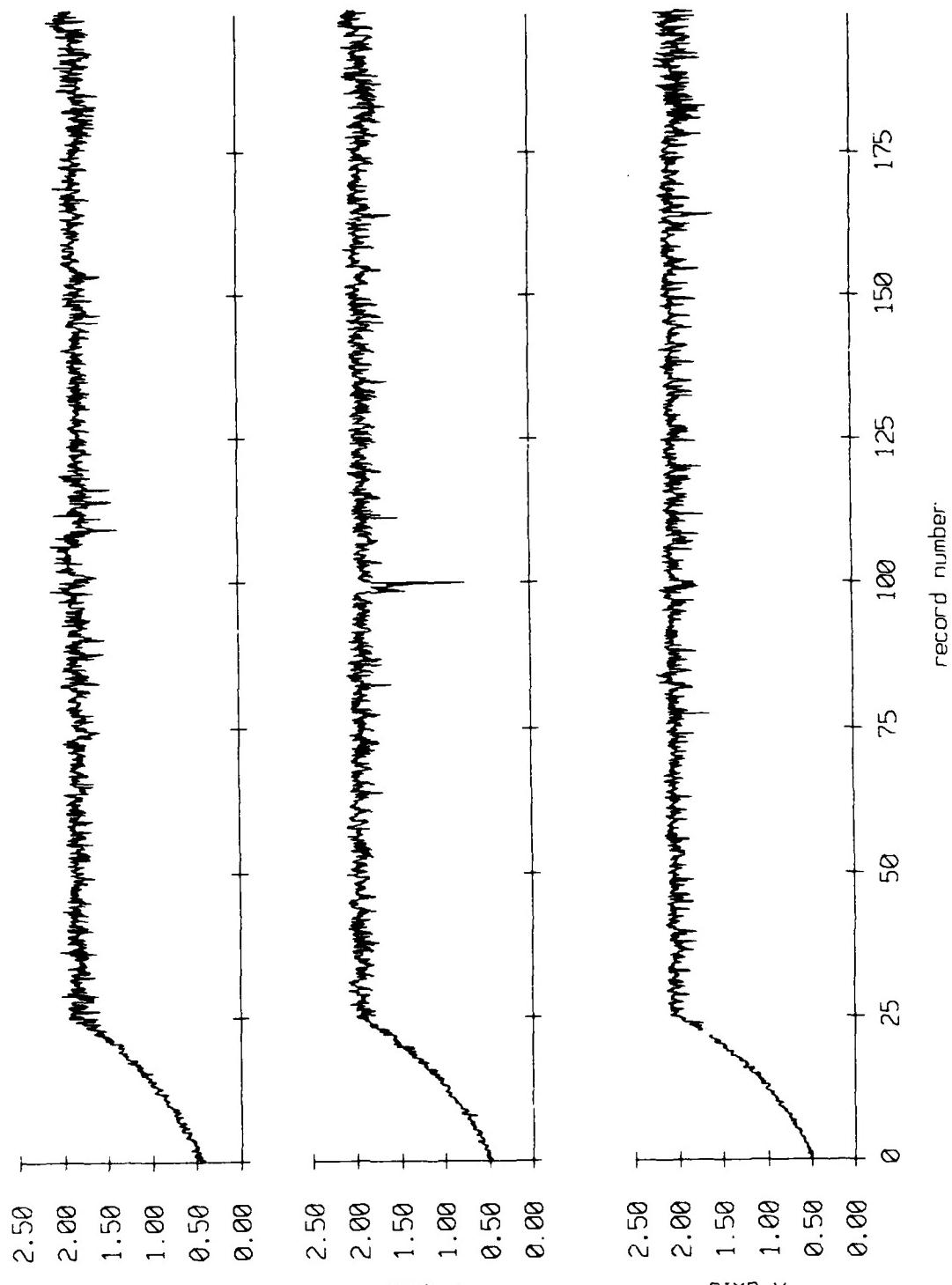


Figure IX.9j

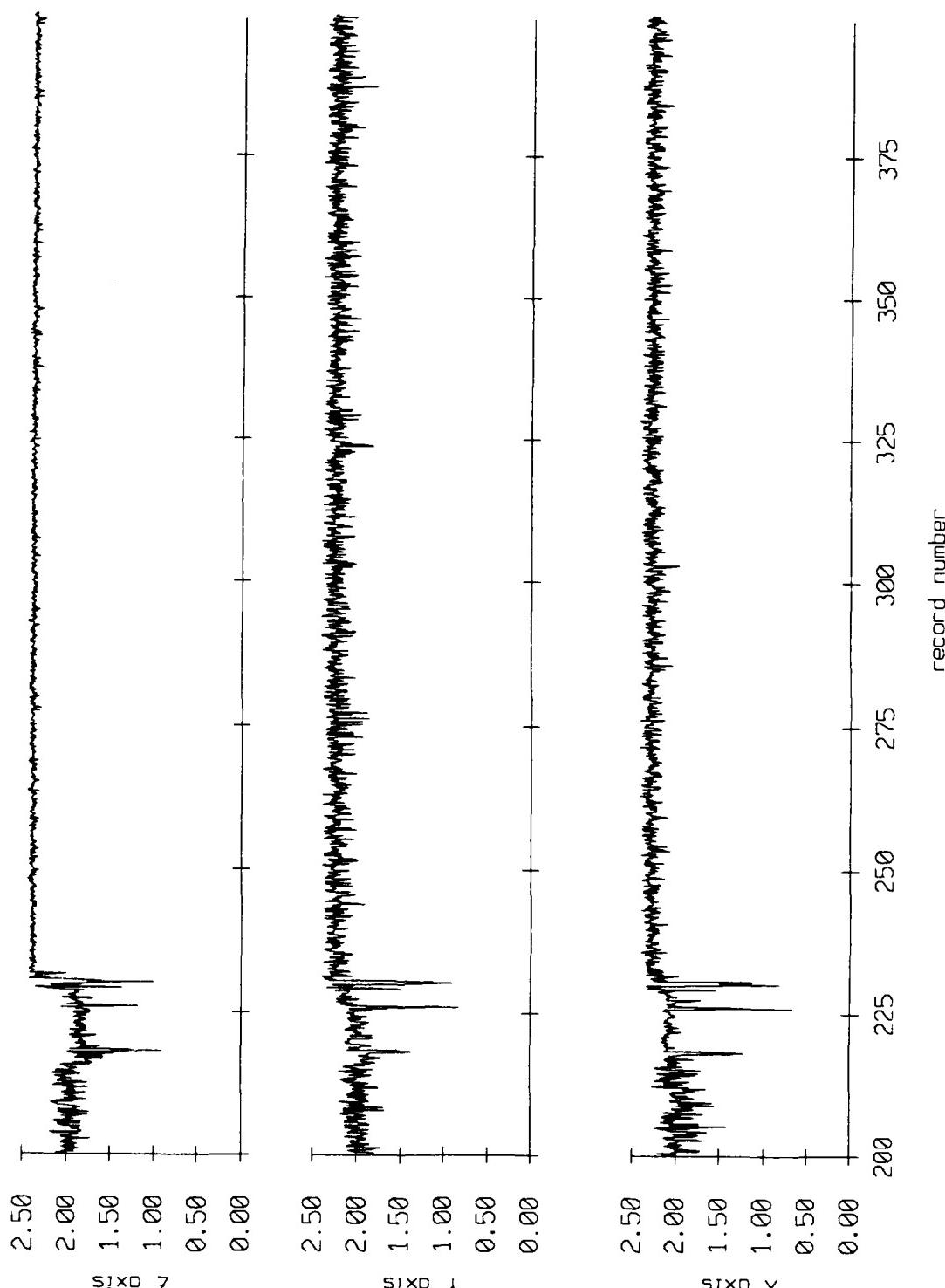
Float 9, September 1987 Sea Trip
averaging period = 5.00 sec.



Gain Corrected Level, Volts(rms)

Figure IX.10a

Float 9, September 1987 Sea Trip
averaging period = 5.00 sec.



Gain Corrected Level, Volts(RMS)

Figure IX.10b

Float 9, September 1987
overranging period = 5.00 sec.

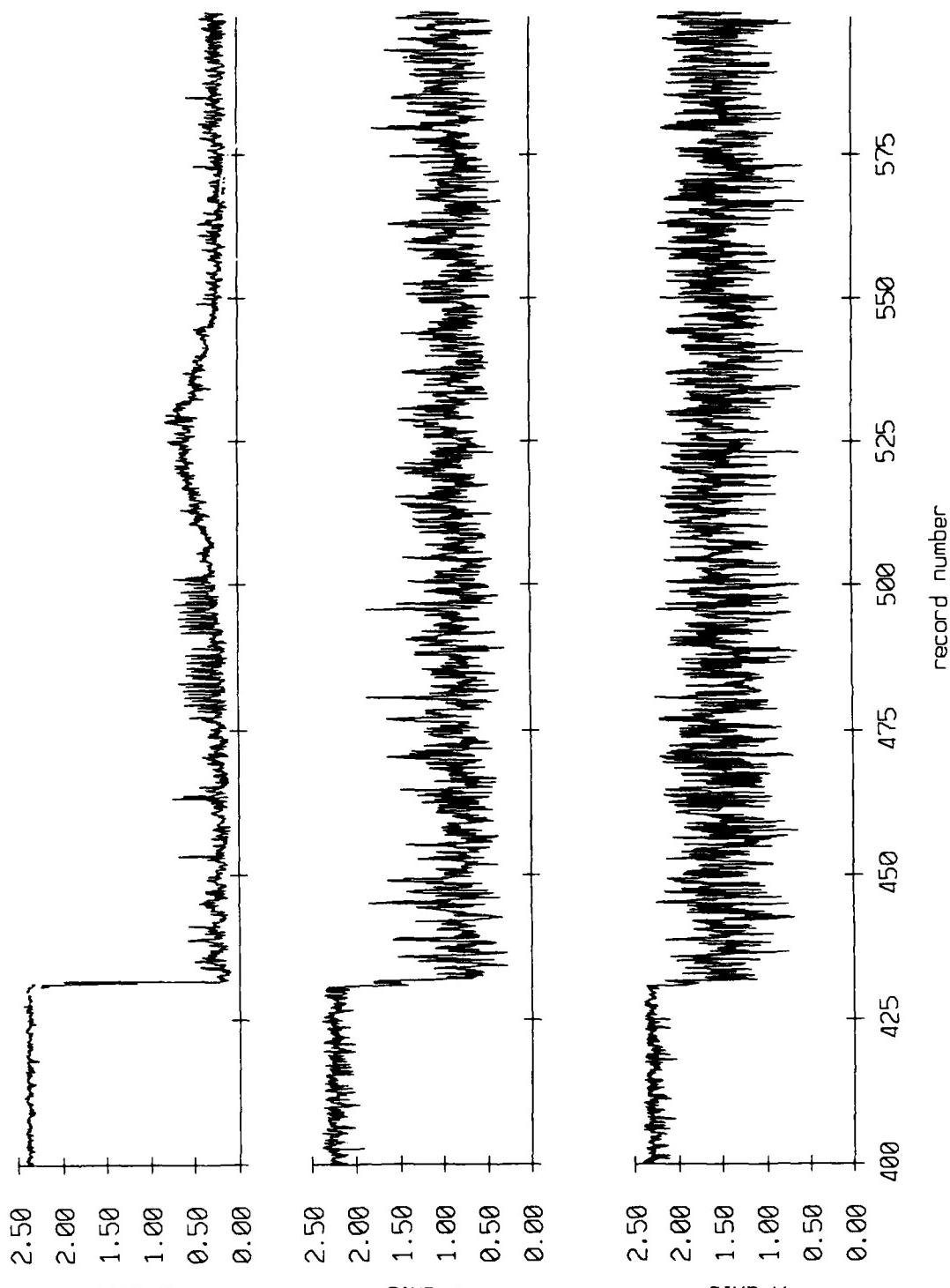


Figure IX.10c

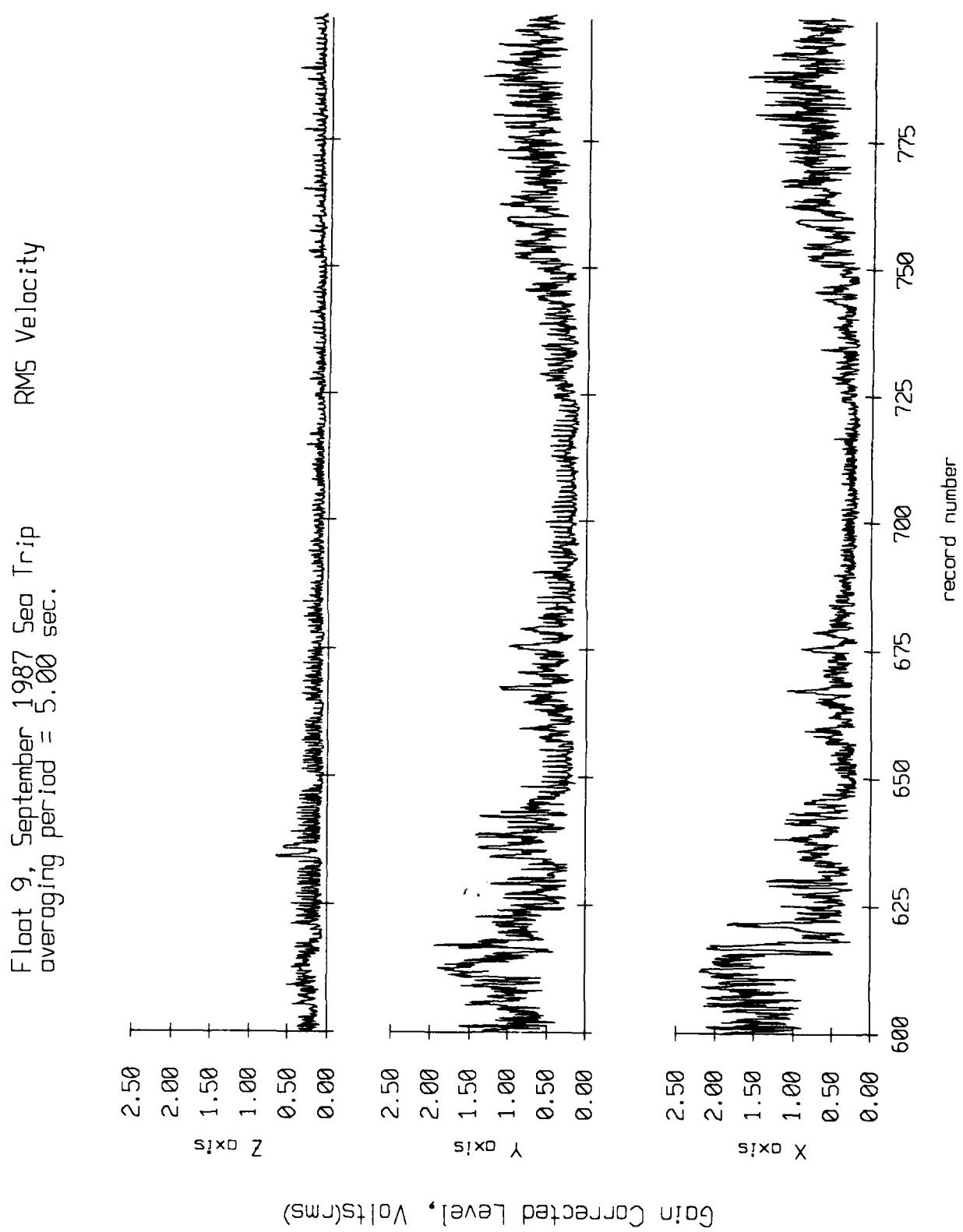


Figure IX.10d

Float 9, September 1987 Sea Trip
overaging period = 5.00 sec.

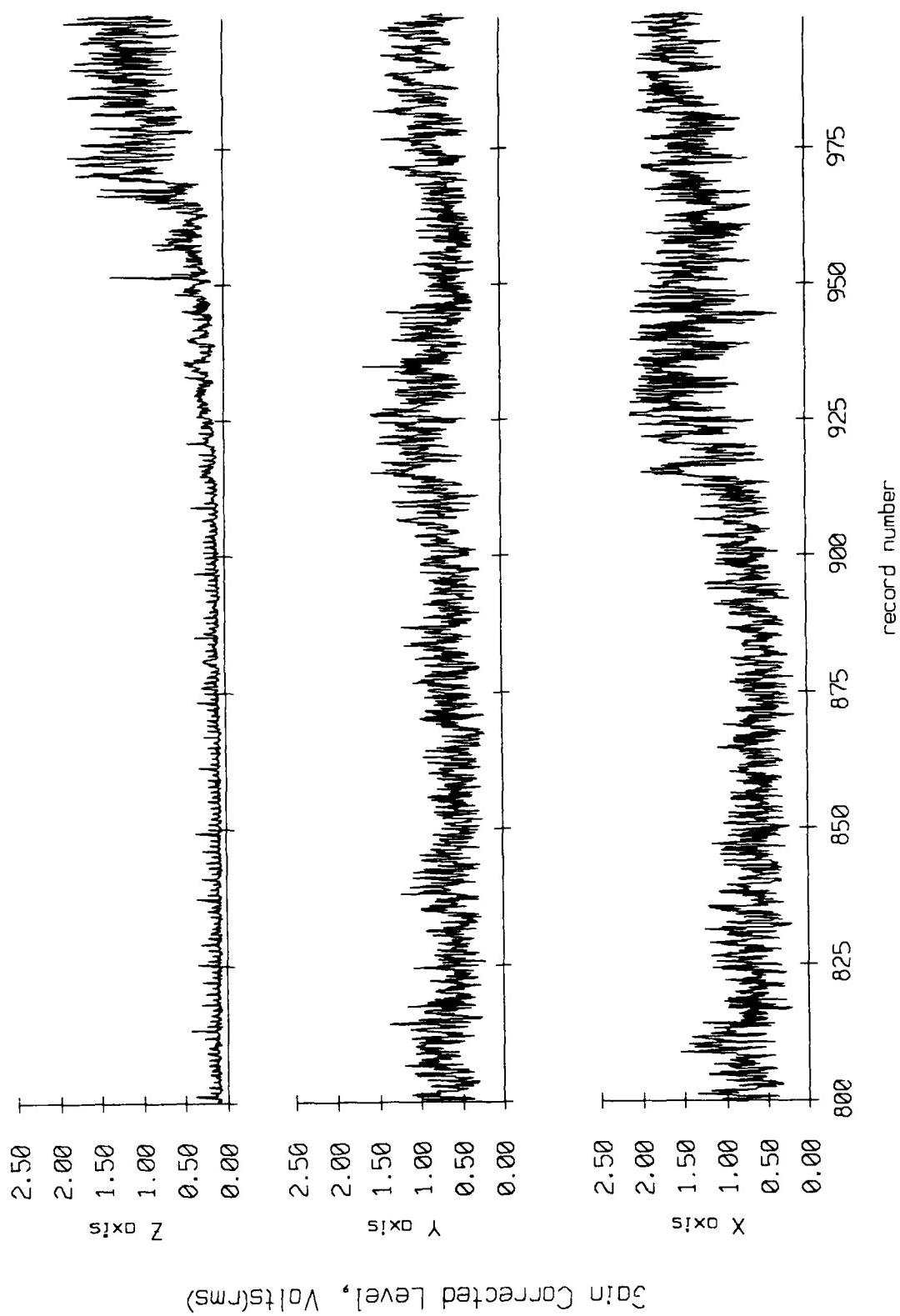


Figure IX.10e

Float 9, September 1987 Sea Trip
averaging period = 5.00 sec.

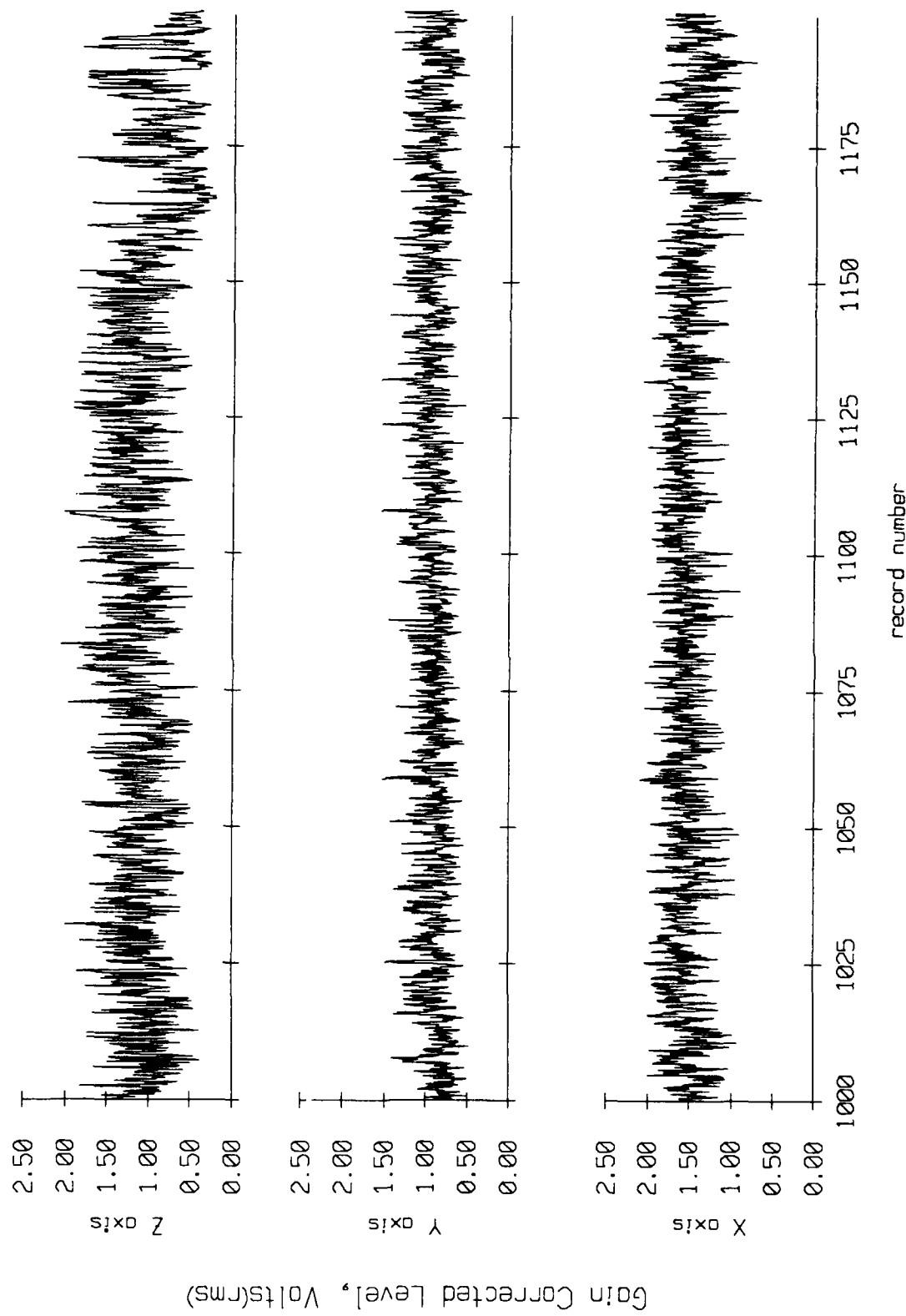


Figure IX.10f

Float 9, September 1987 Sea Trip
overaging period = 5.00 sec.

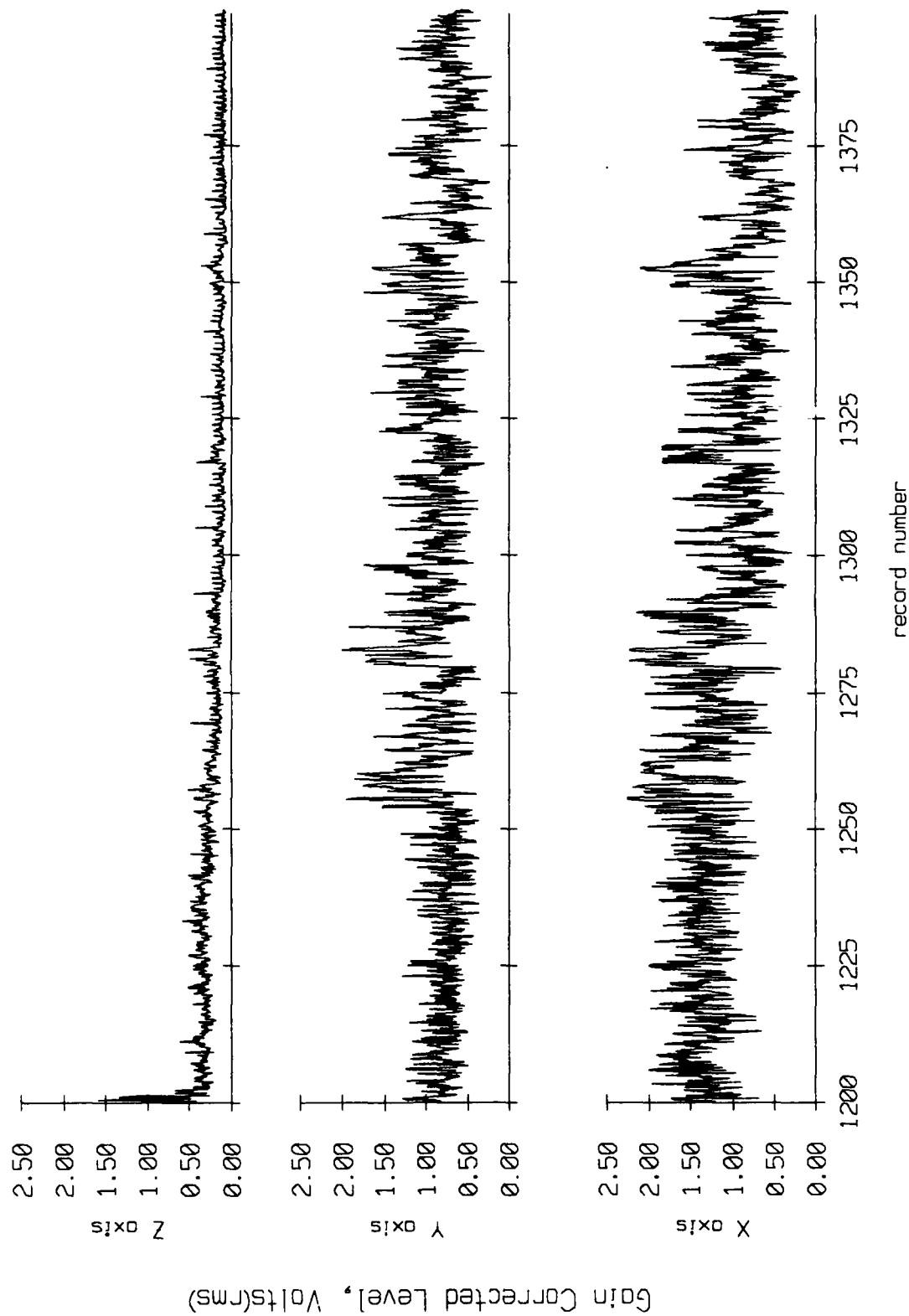


Figure IX.10g

Fleet 9, September 1987 Sea Trip
averaging period = 5.00 sec.

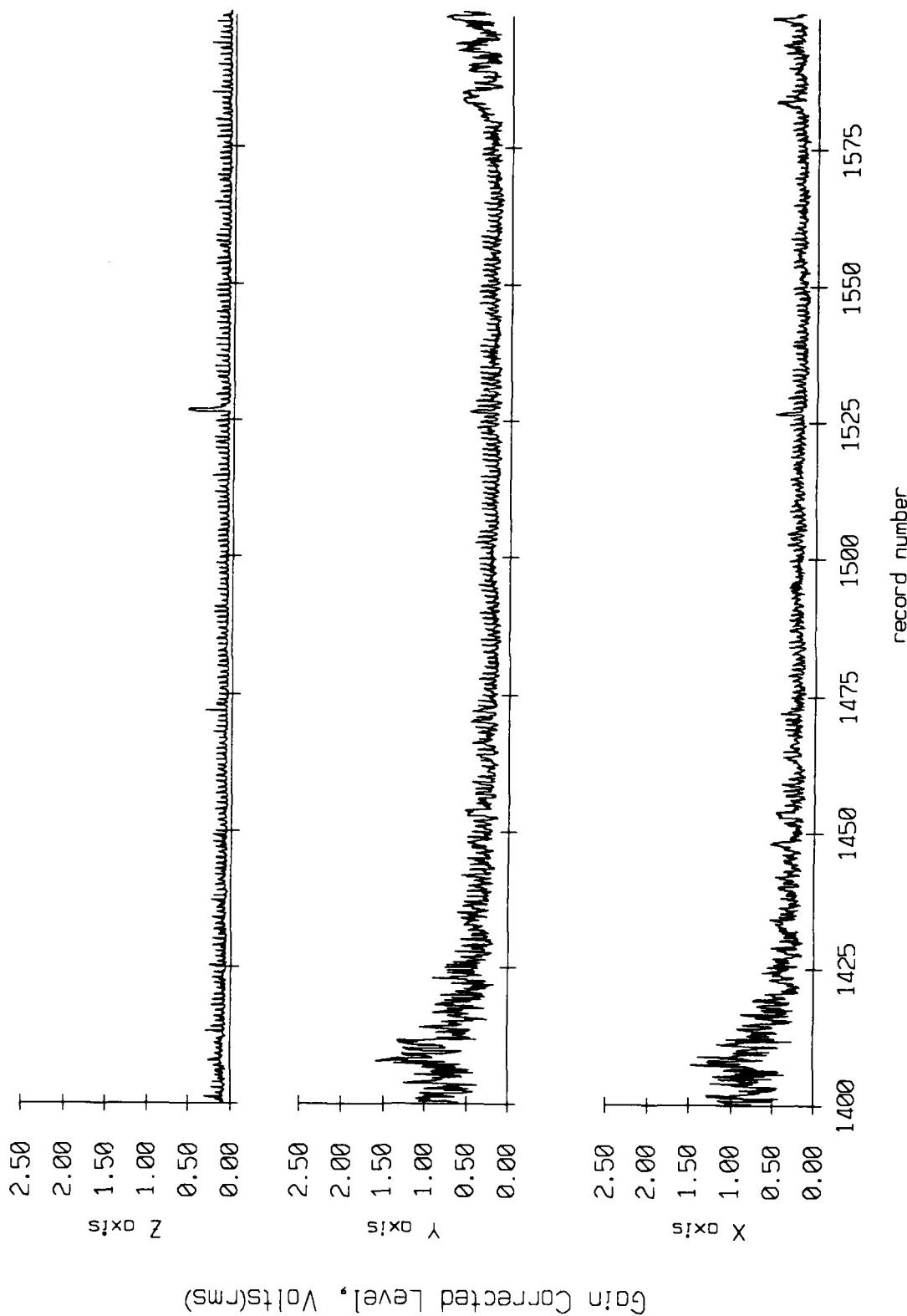


Figure IX.10h

Float 9, September 1987 Sea Trip
averaging period = 5.00 sec.

RMS Velocity

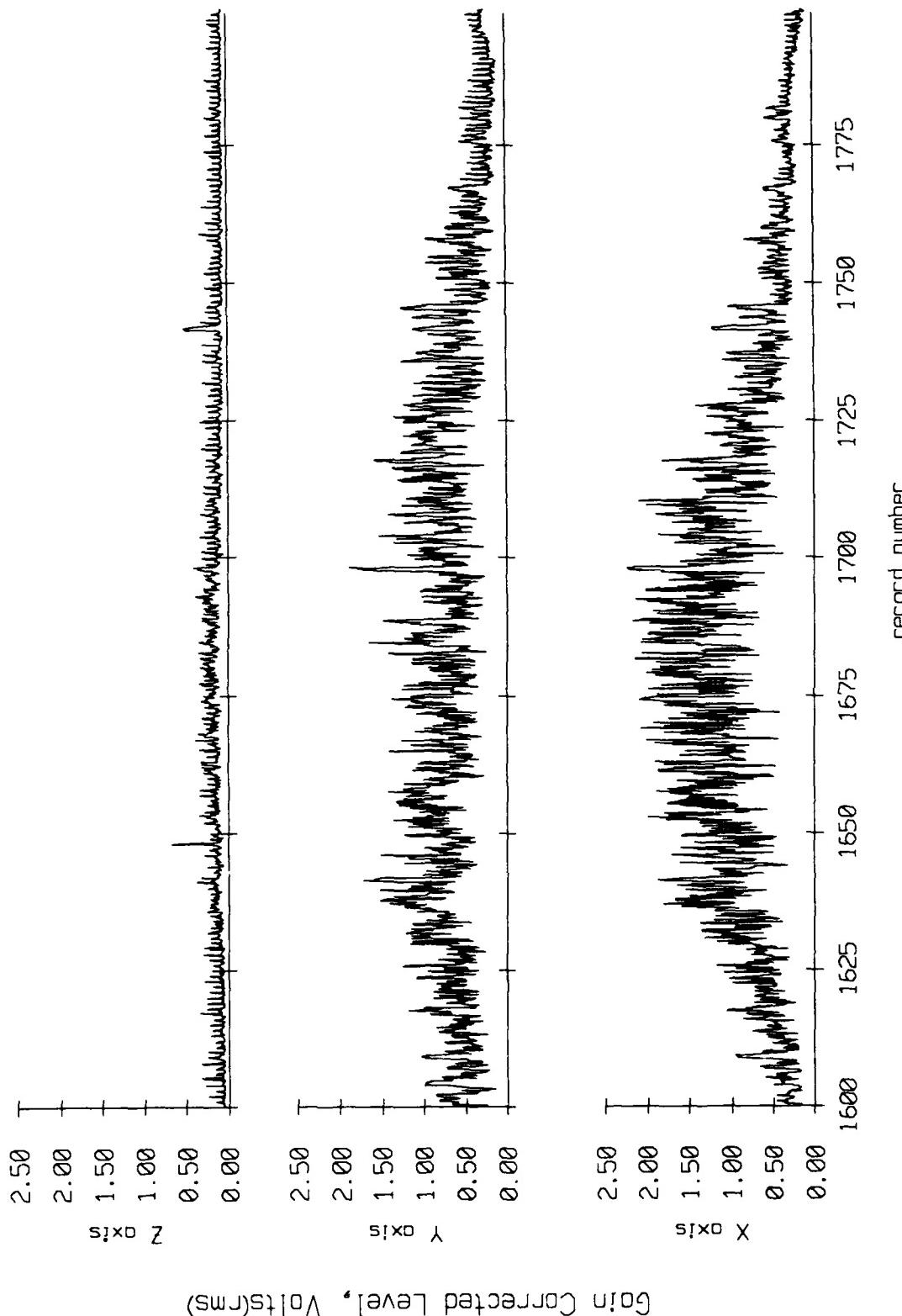


Figure IX.10i

Fleet 9, September 1987 Sea Trip
overgaging period = 5.00 sec.

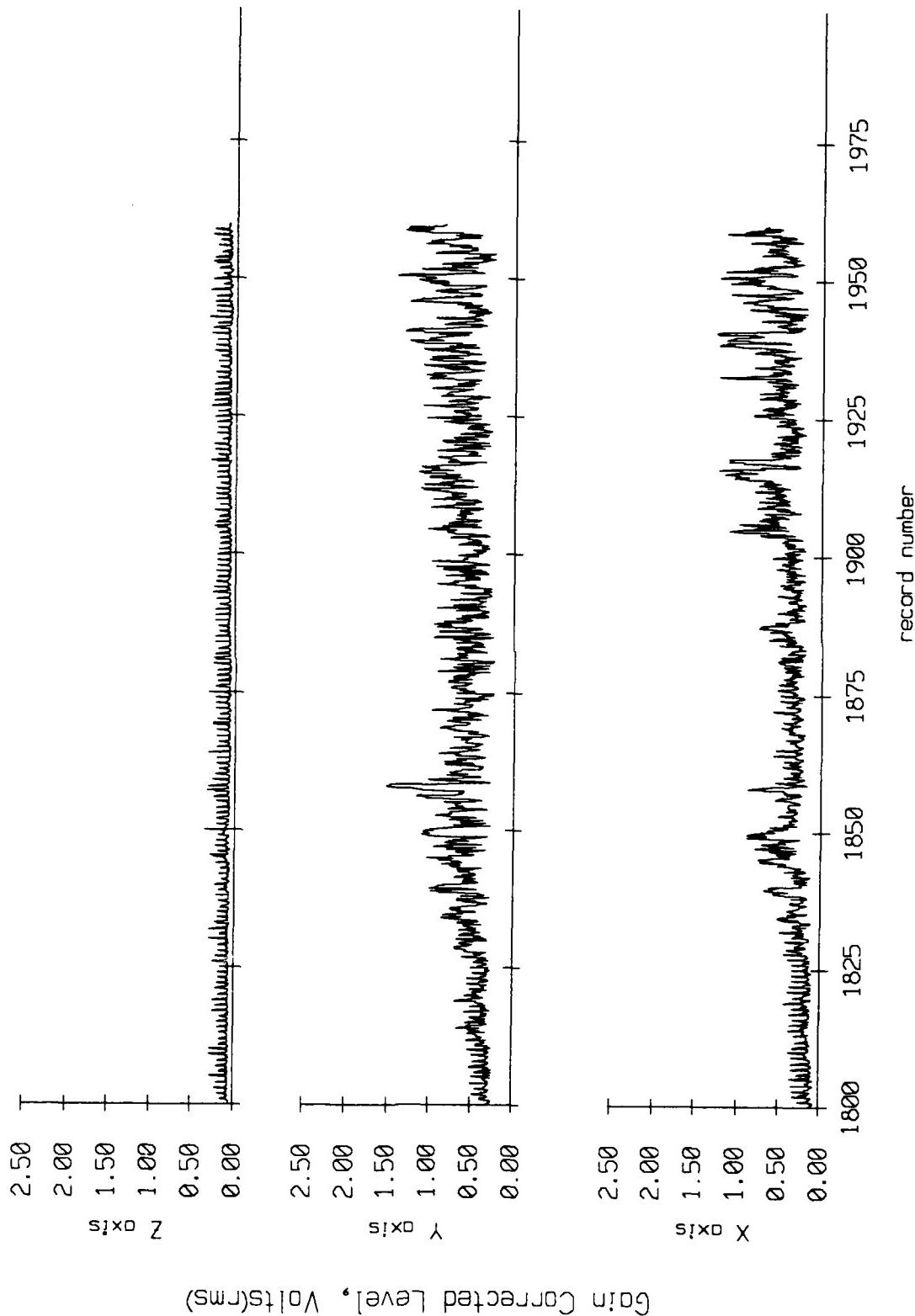
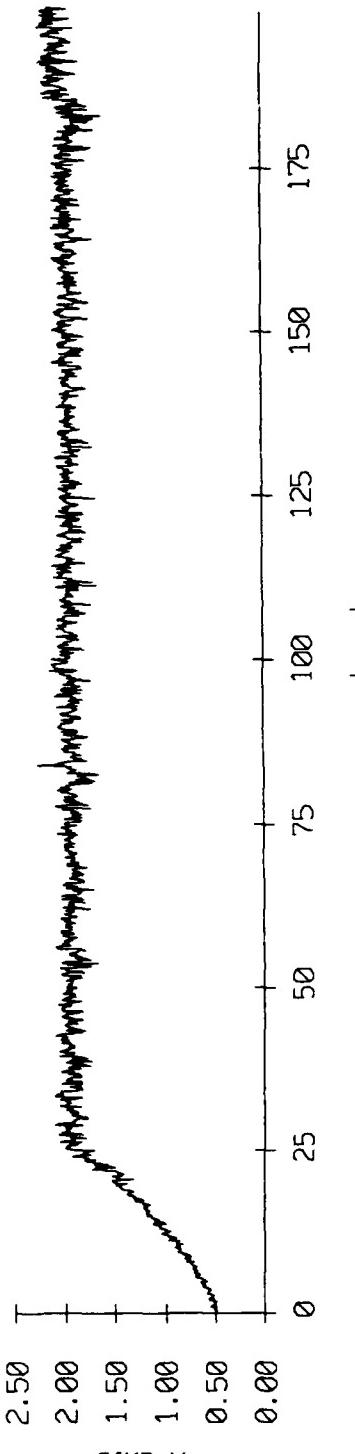
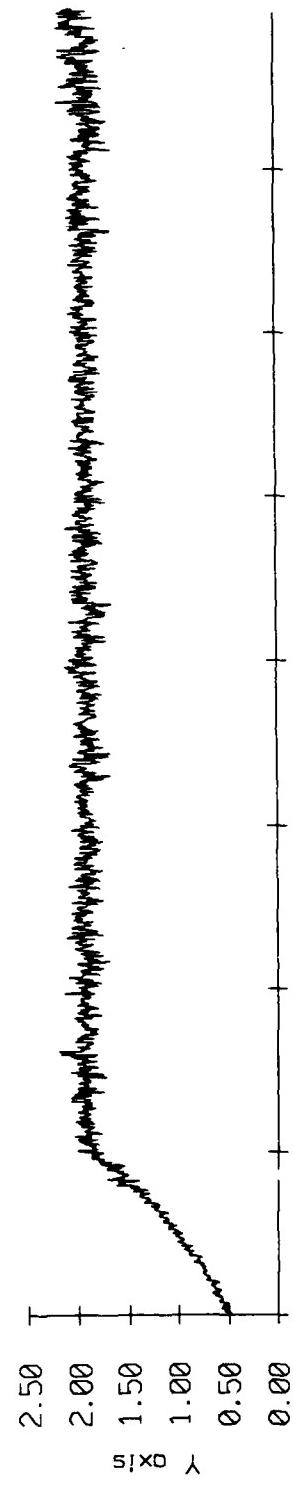
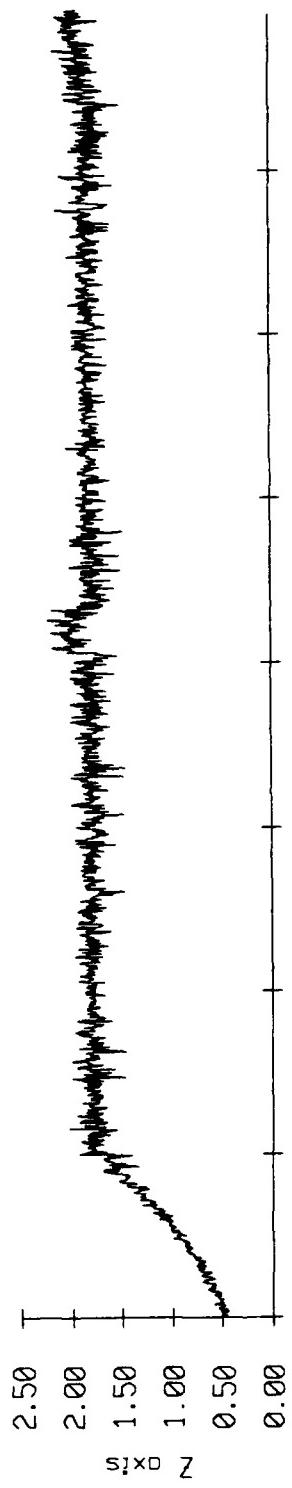


Figure IX.10j

Float 10, September 1987 Sea Trip
averaging period = 5.00 sec.

RMS Velocity



Gain Corrected Level, Volts (rms)

Figure IX.11a

Float 10, September 1987 Sea Trip
averaging period = 5.00 sec.

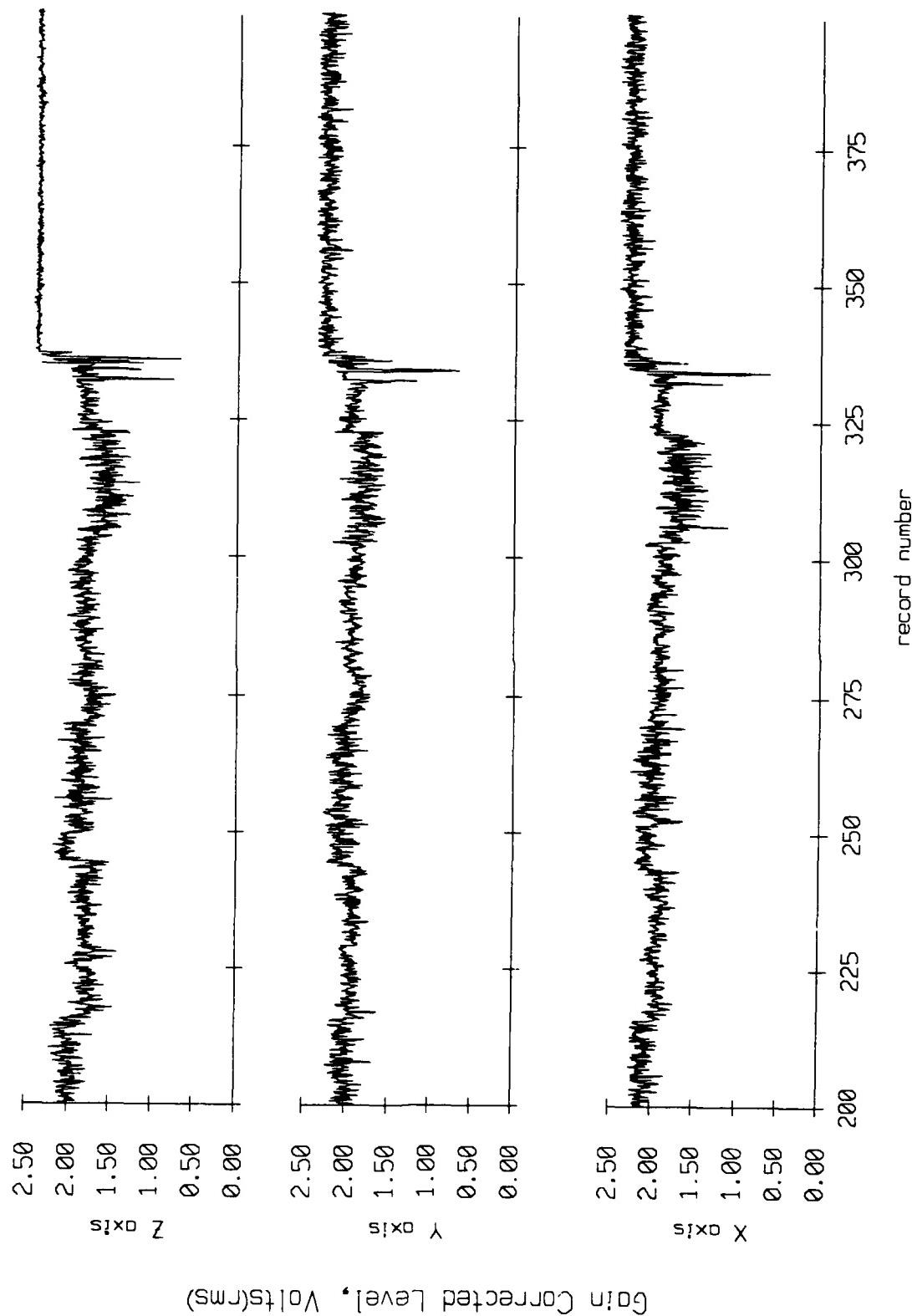
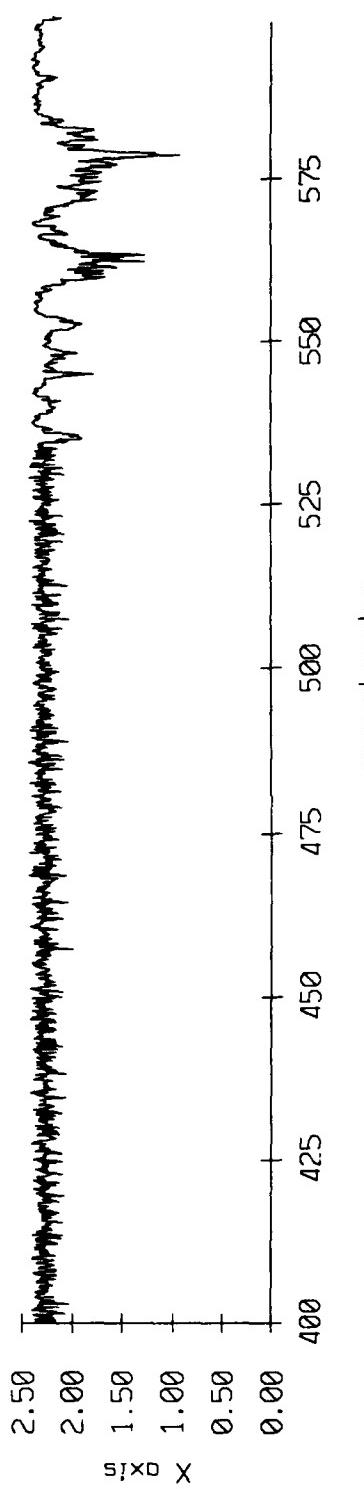
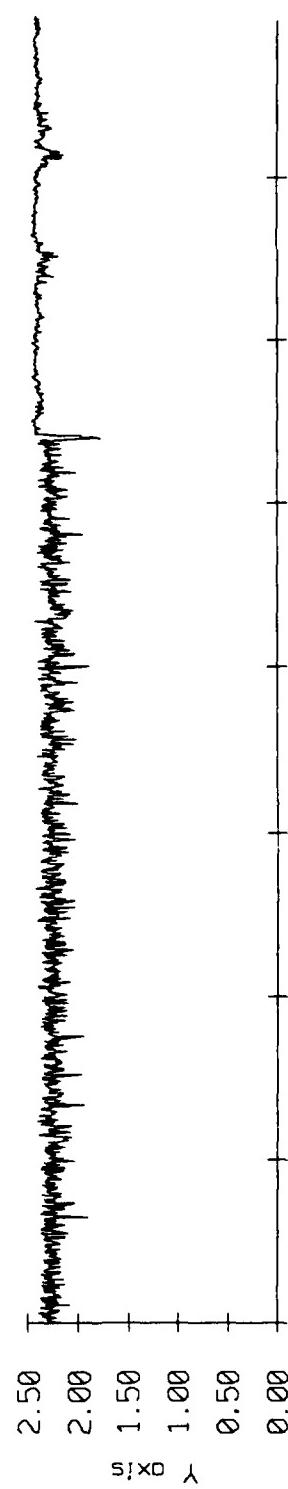
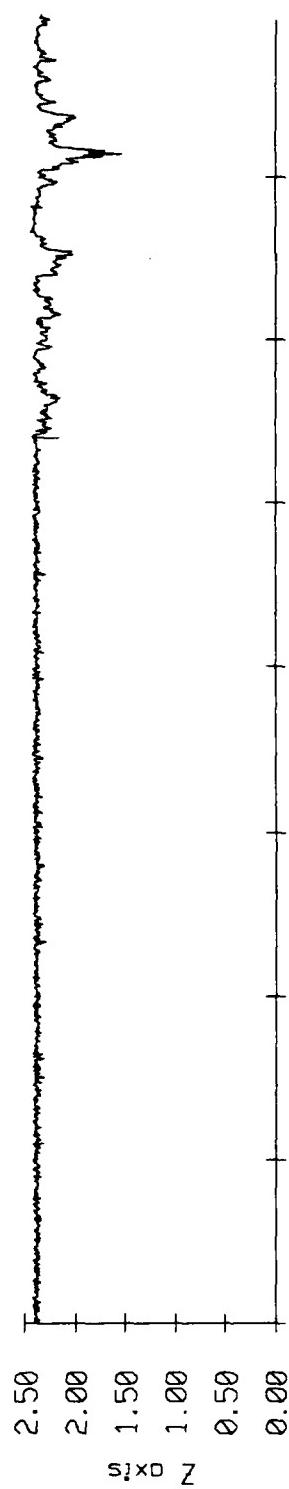


Figure IX.11b

Fleet 10, September 1987 Sea Trip
overaging period = 5.00 sec.

RMS Velocity



Gain Corrected Level, Volts(RMS)

Figure IX.11c

Fleet 10, September 1987 Sea Trip
overaging period = 5.00 sec.

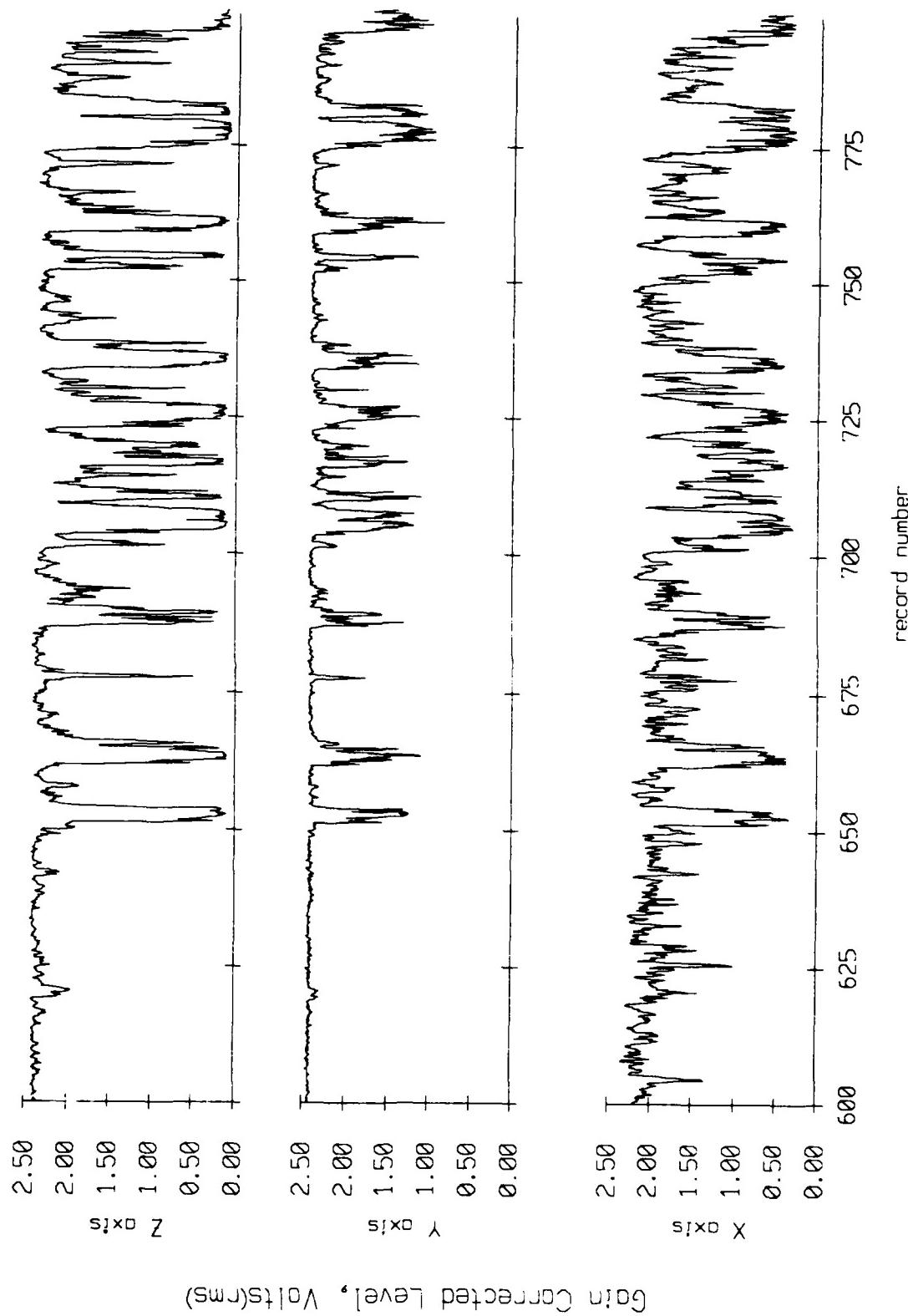


Figure IX.11d

Float 10, September 1987 Sec Trip
overaging period = 5.00 sec.

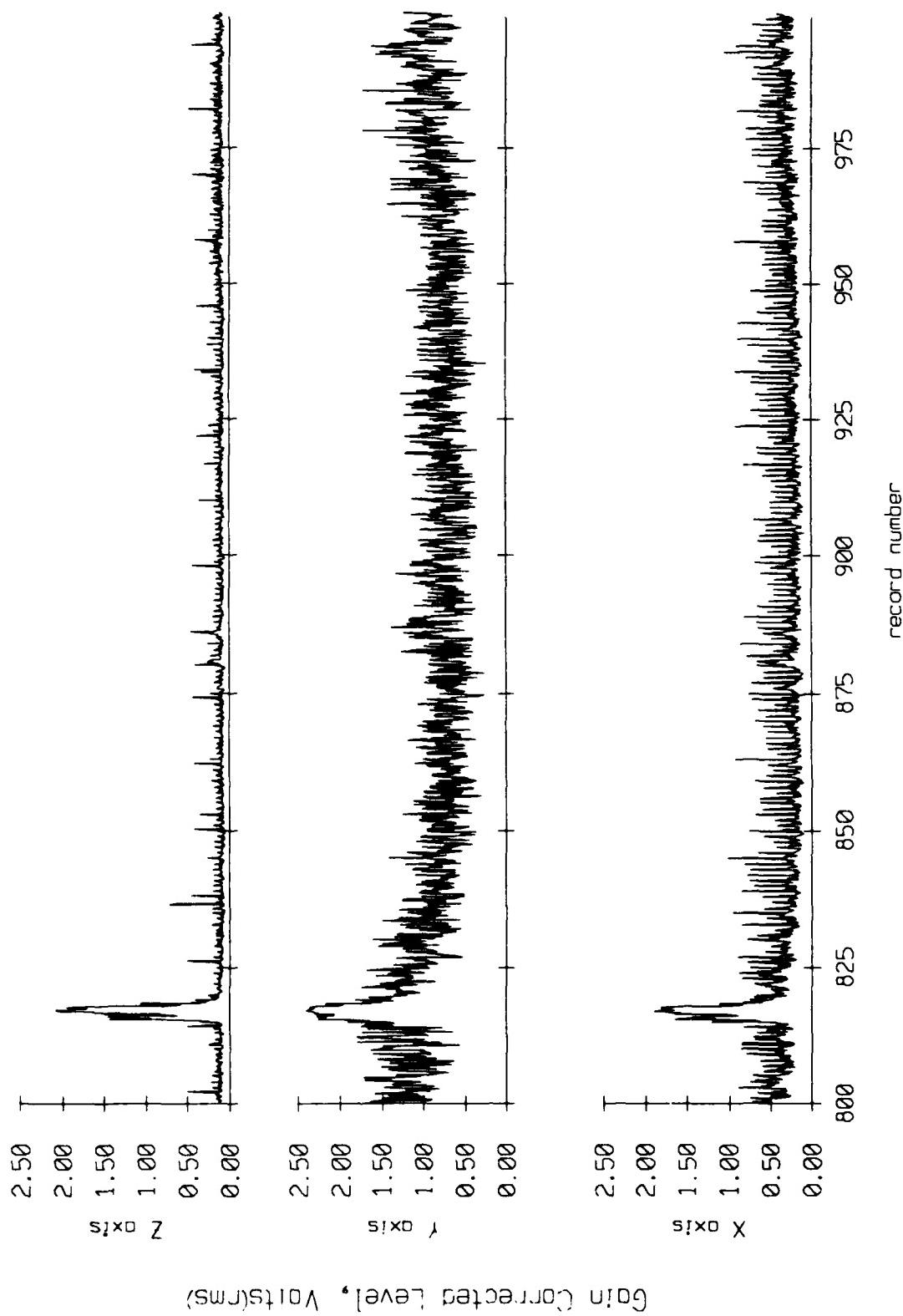
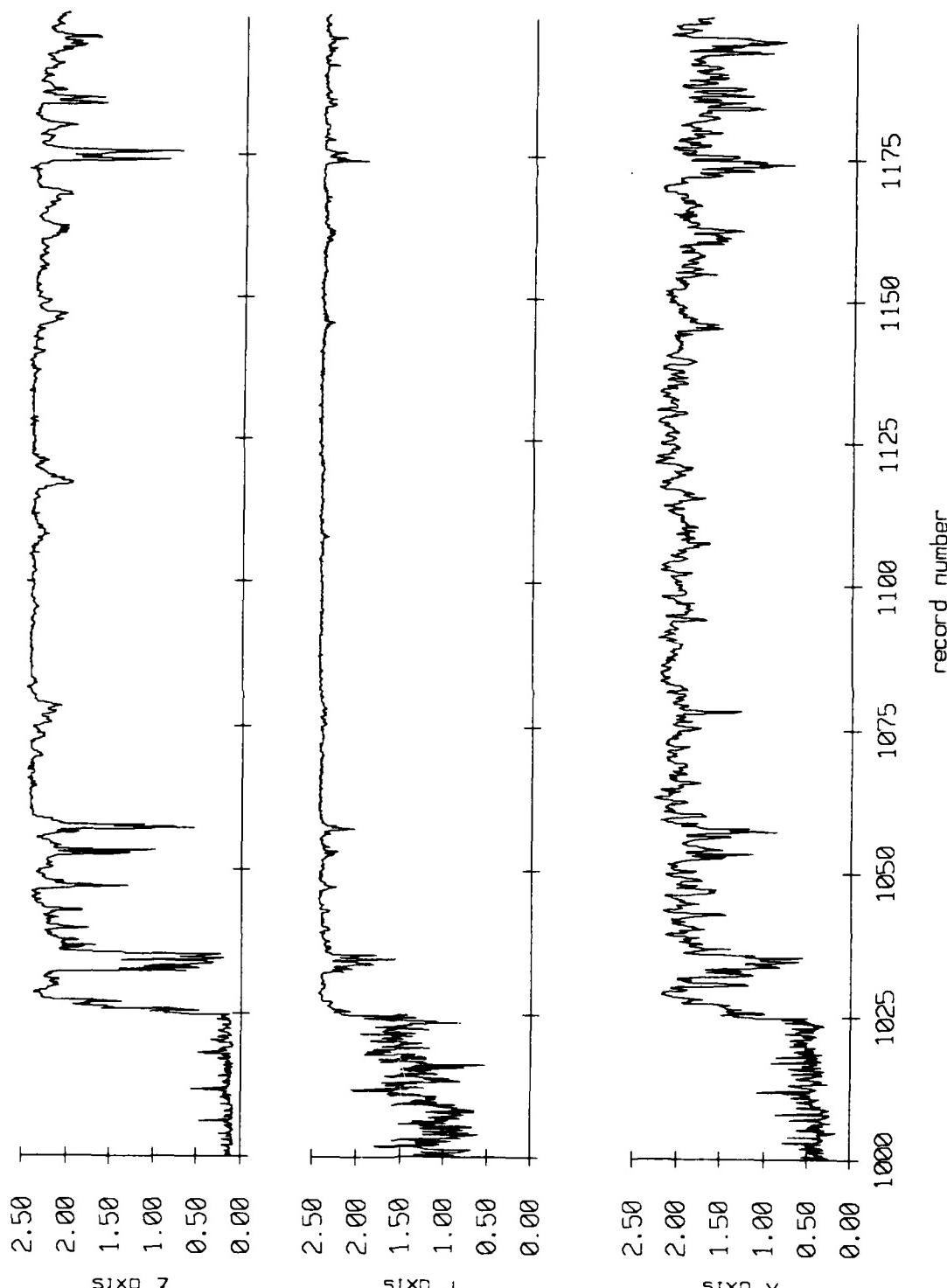


Figure IX.11e

Float 10, September 1987 Sea Trip
averaging period = 5.00 sec.

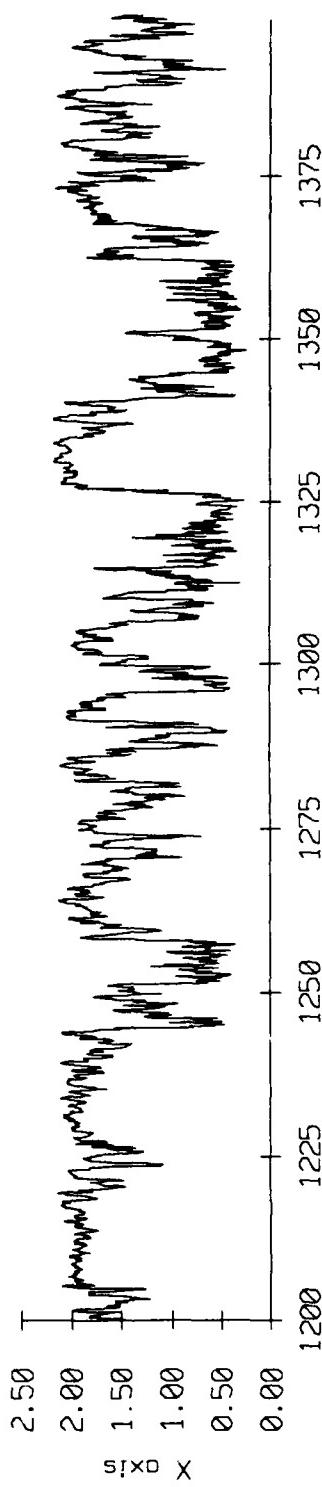
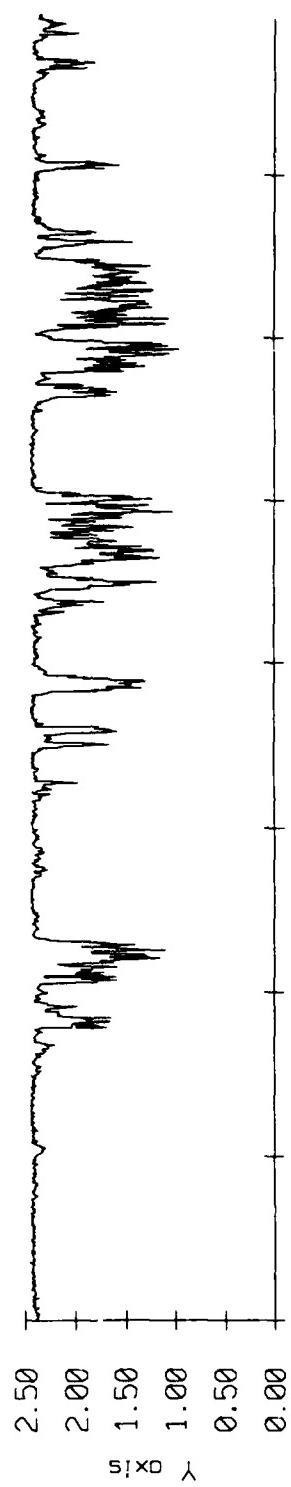
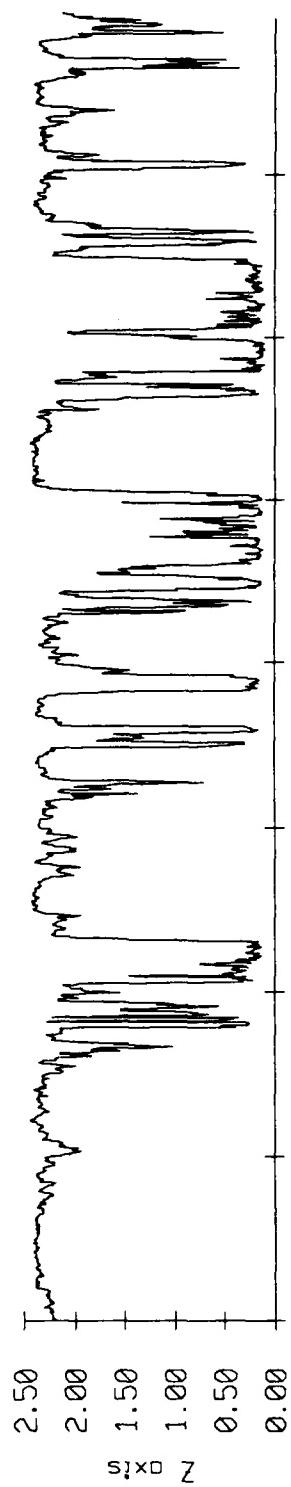


Gain Corrected Level, Volts(RMS)

Figure IX.11f

Fleet 10, September 1987 Sea Trip
overaging period = 5.00 sec.

RMS Velocity



Gain Corrected Level, Volts(RMS)

Figure IX.11g

Float 10, September 1987 Sea Trip
averaging period = 5.00 sec.

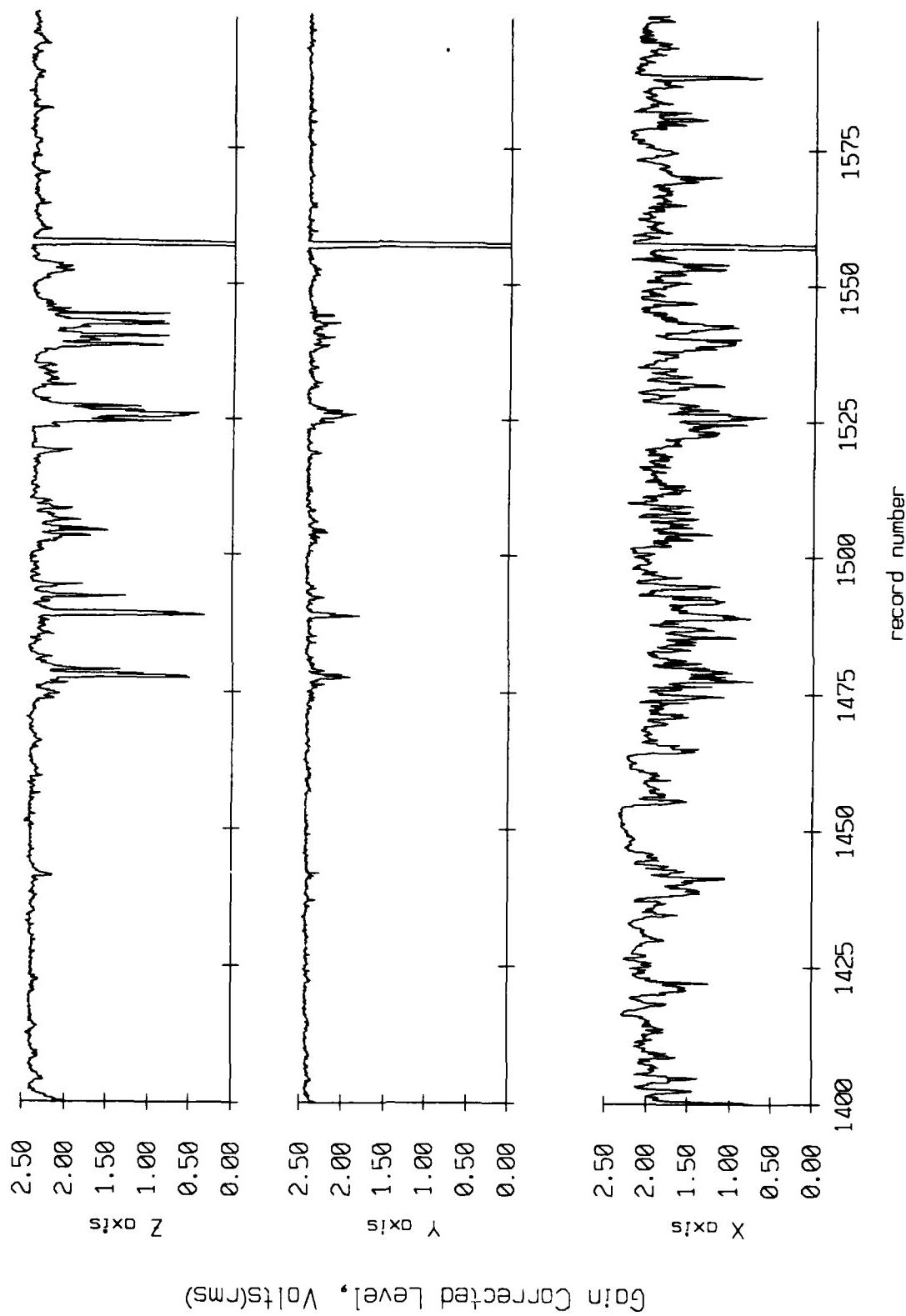
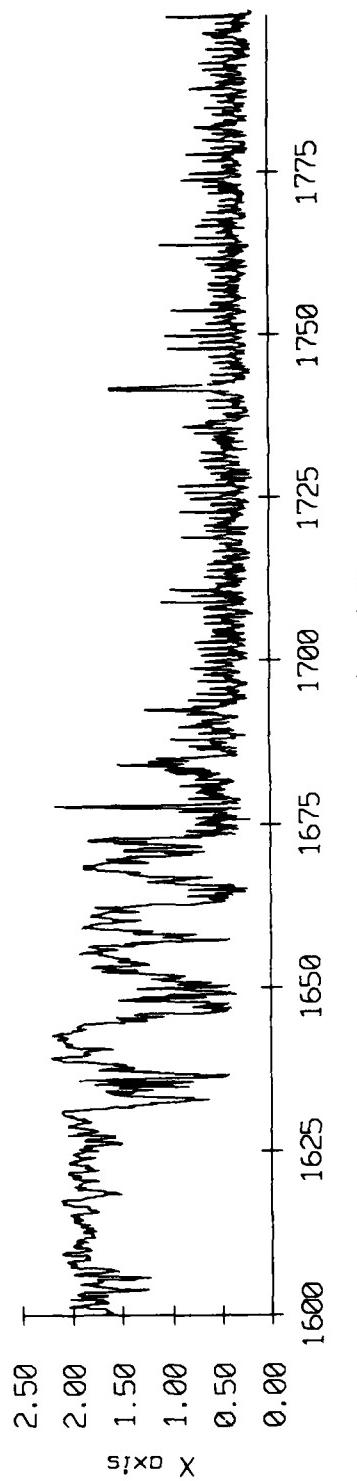
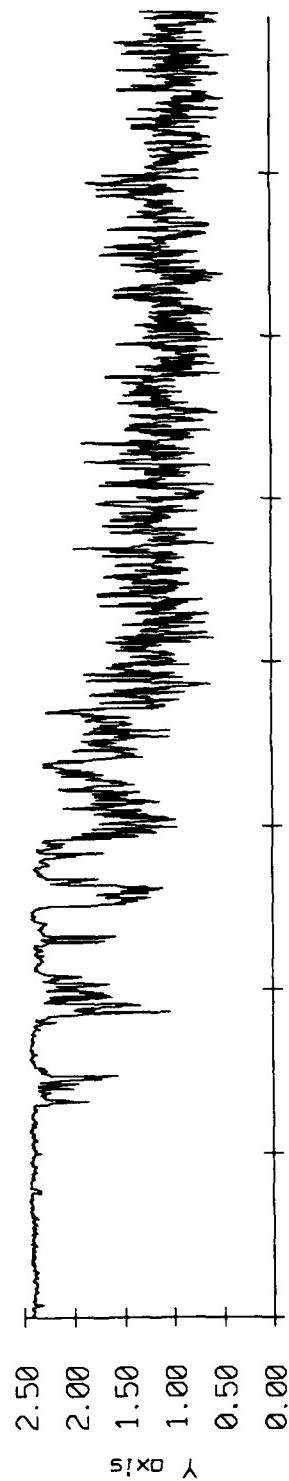
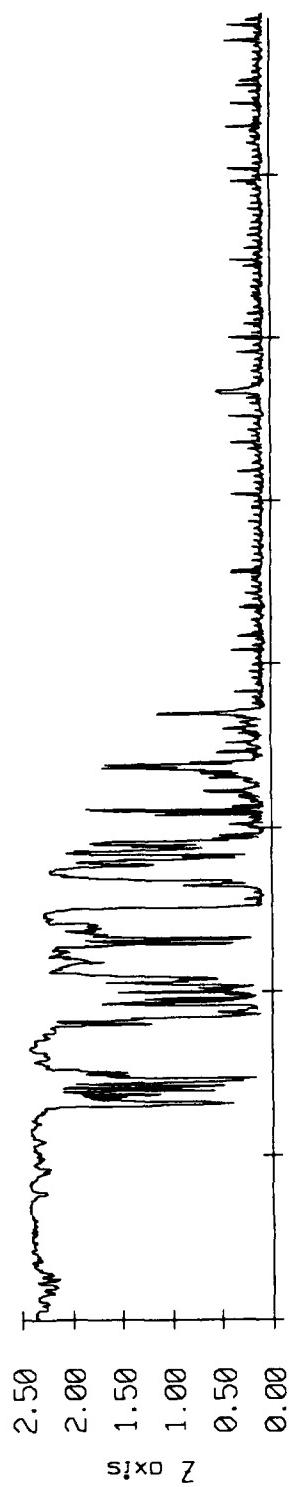


Figure IX.11h

Float 10, September 1987 Sea Trip
overaging period = 5.00 sec.

RMS Velocity



Gain Corrected Level, Volts(rms)

Figure IX.11i

Float 10, September 1987 Sea Trip
averaging period = 5.00 sec.

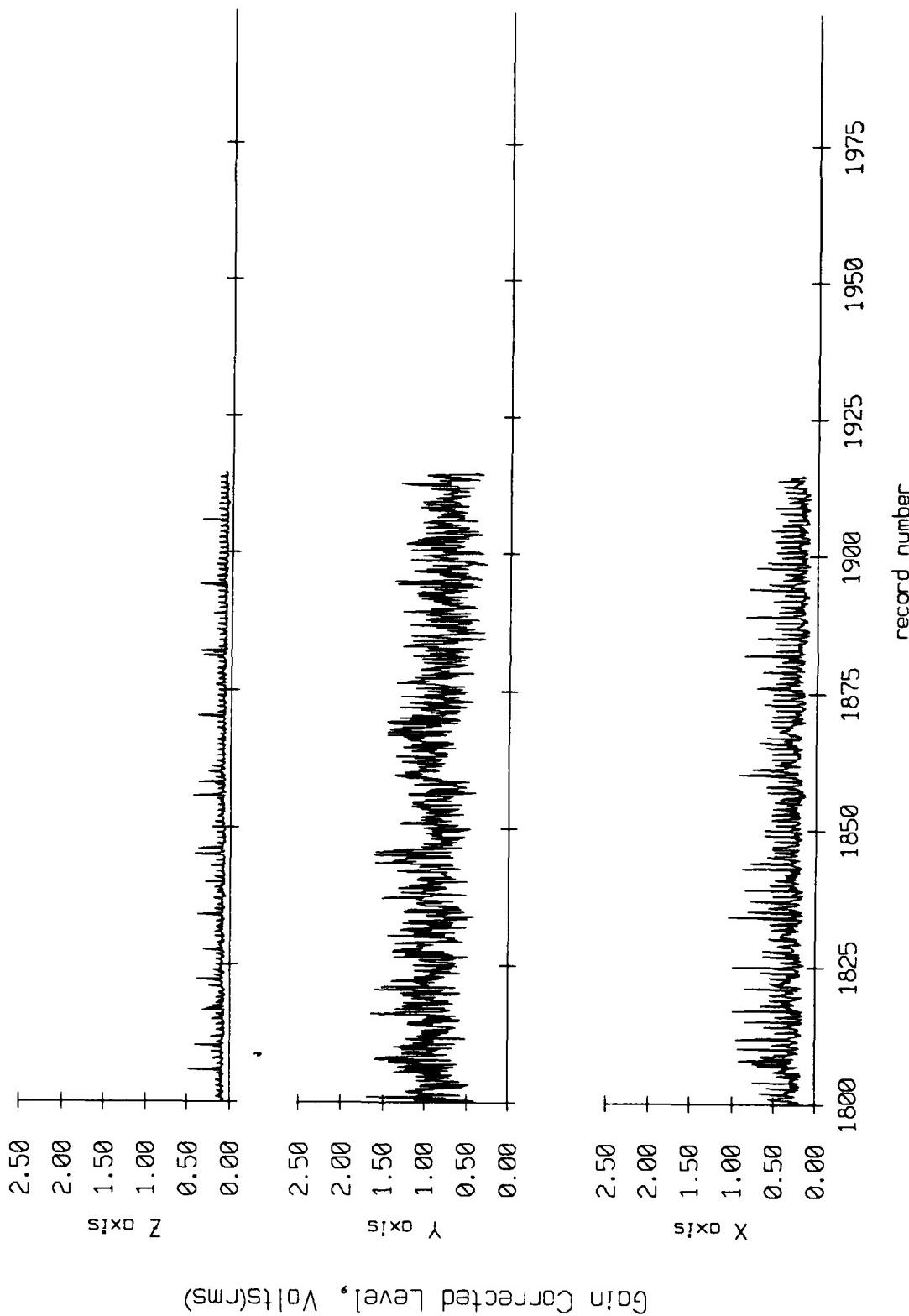


Figure IX.11j

Float 11, September 1987 Sea Trip
averaging period = 5.00 sec.

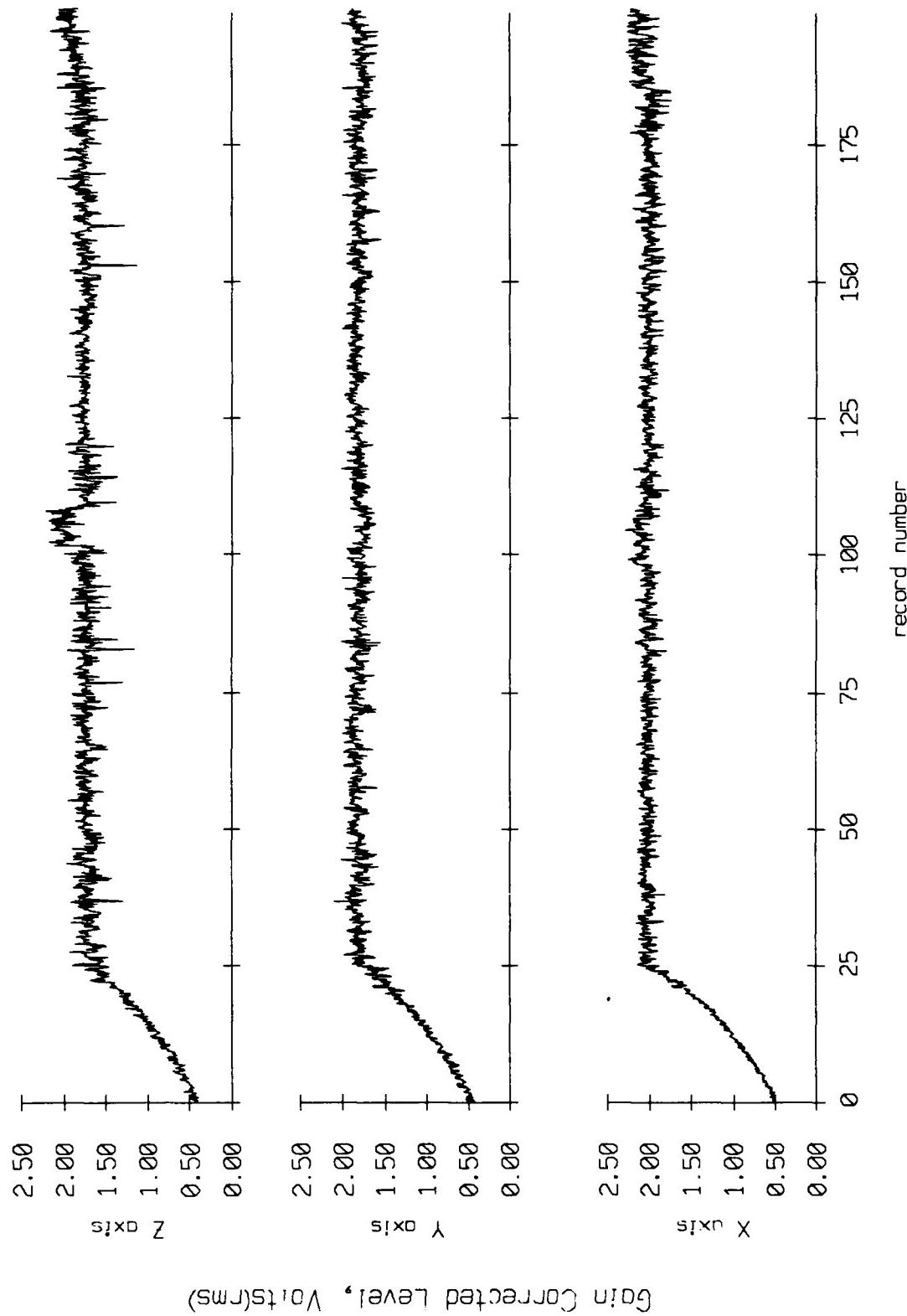


Figure IX.12a

Flood 11, September 1987 Sea Trip
averaging period = 5.00 sec.

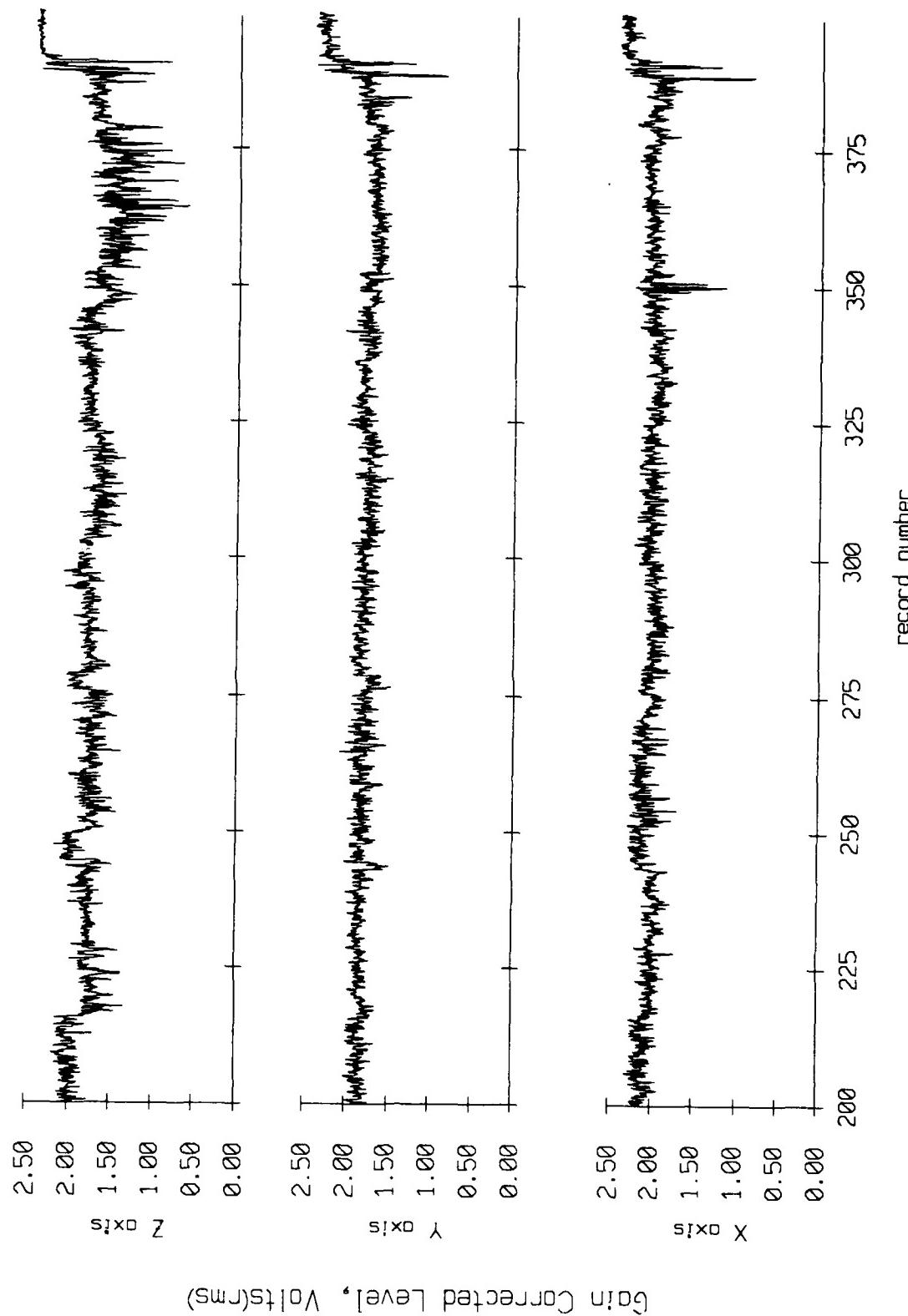


Figure IX.12b

Float 11, September 1987 Sea Trip
averaging period = 5.00 sec.

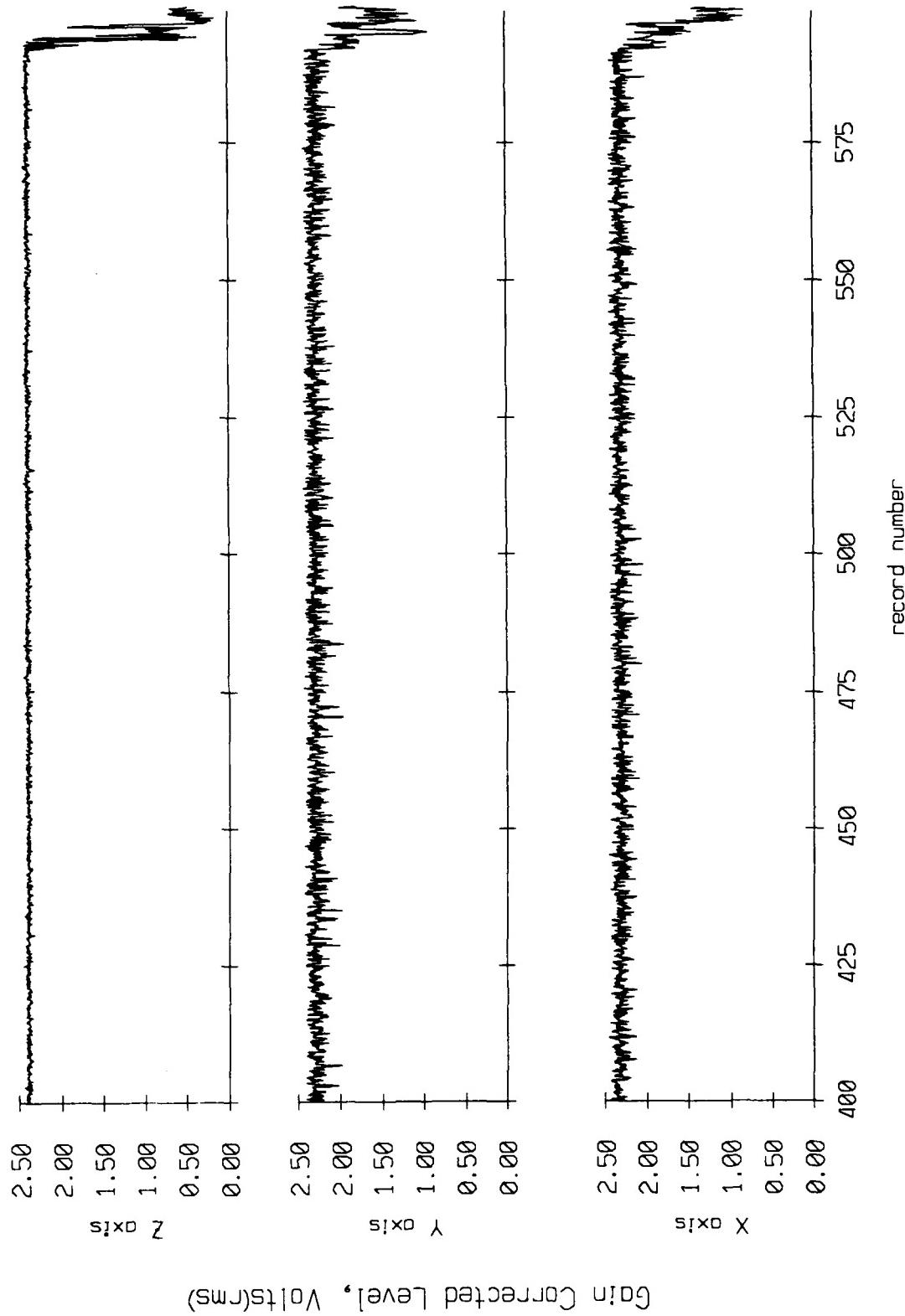


Figure IX.12c

Fleet 11, September 1987 Sea Trip
overaging period = 5.00 sec.

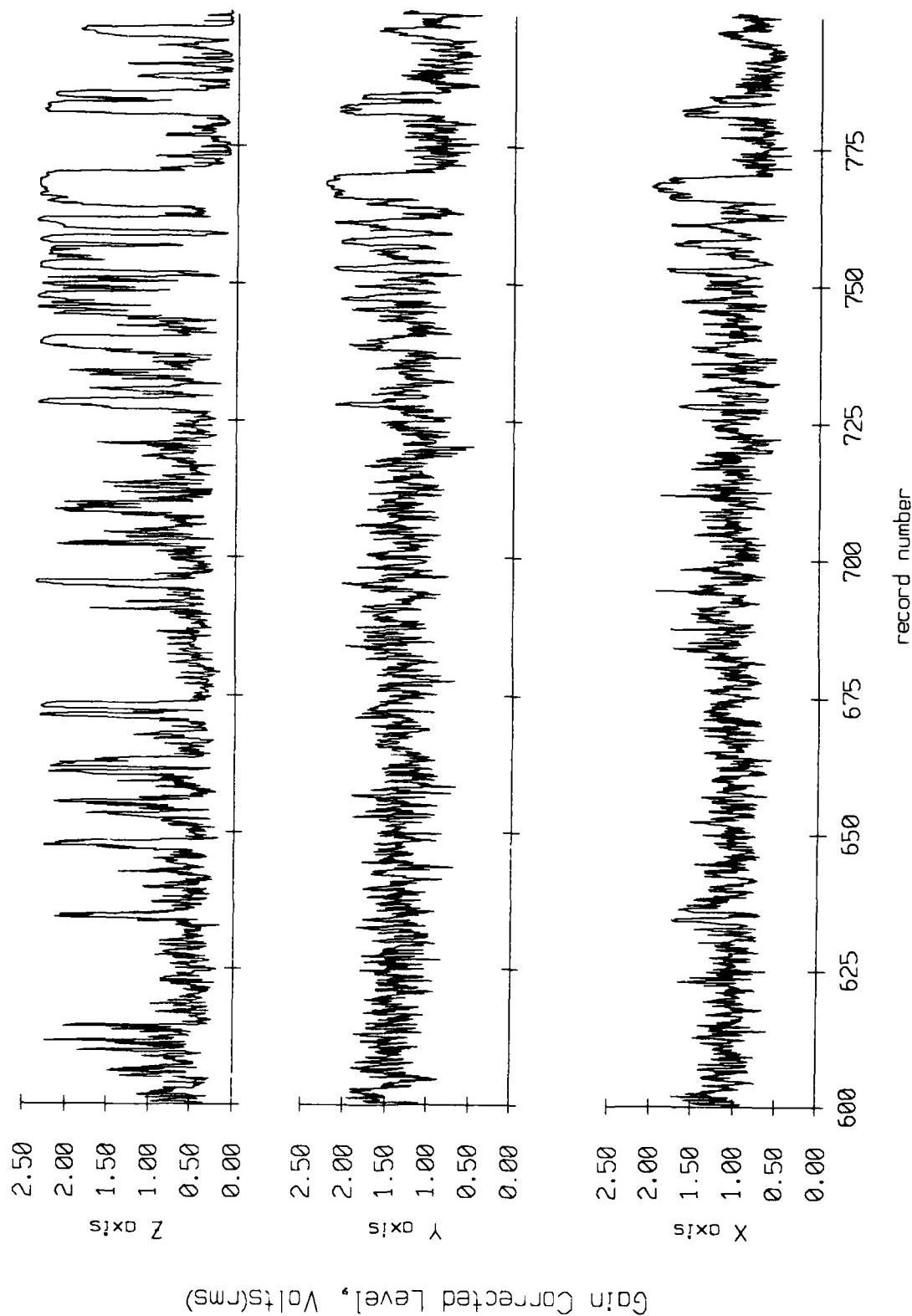


Figure IX.12d

Float 11, September 1987 Sea Trip
averaging period = 5.00 sec.

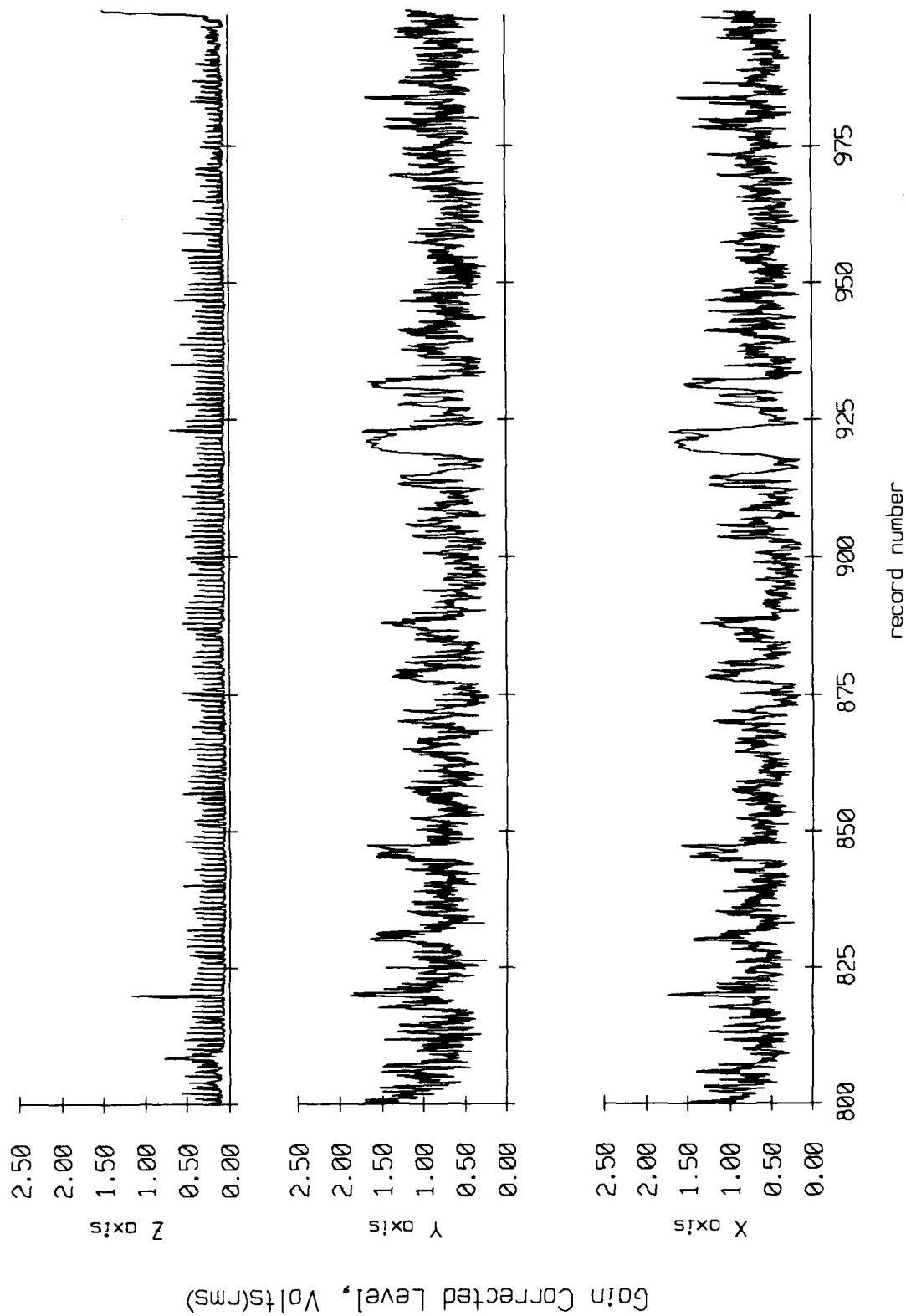


Figure IX.12e

Float 11, September 1987 Sea Trip
overaging period = 5.00 sec.

RMS Velocity

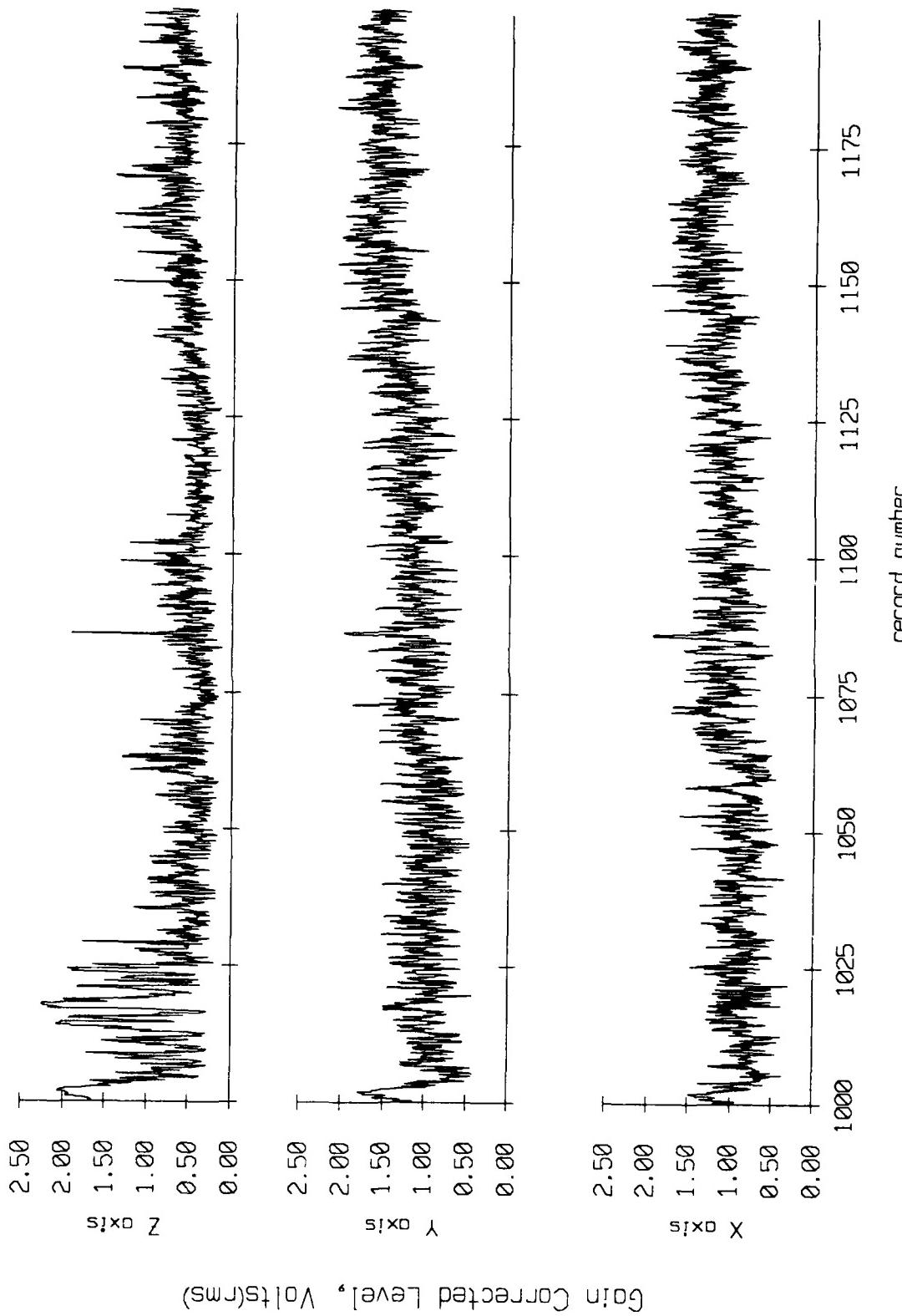
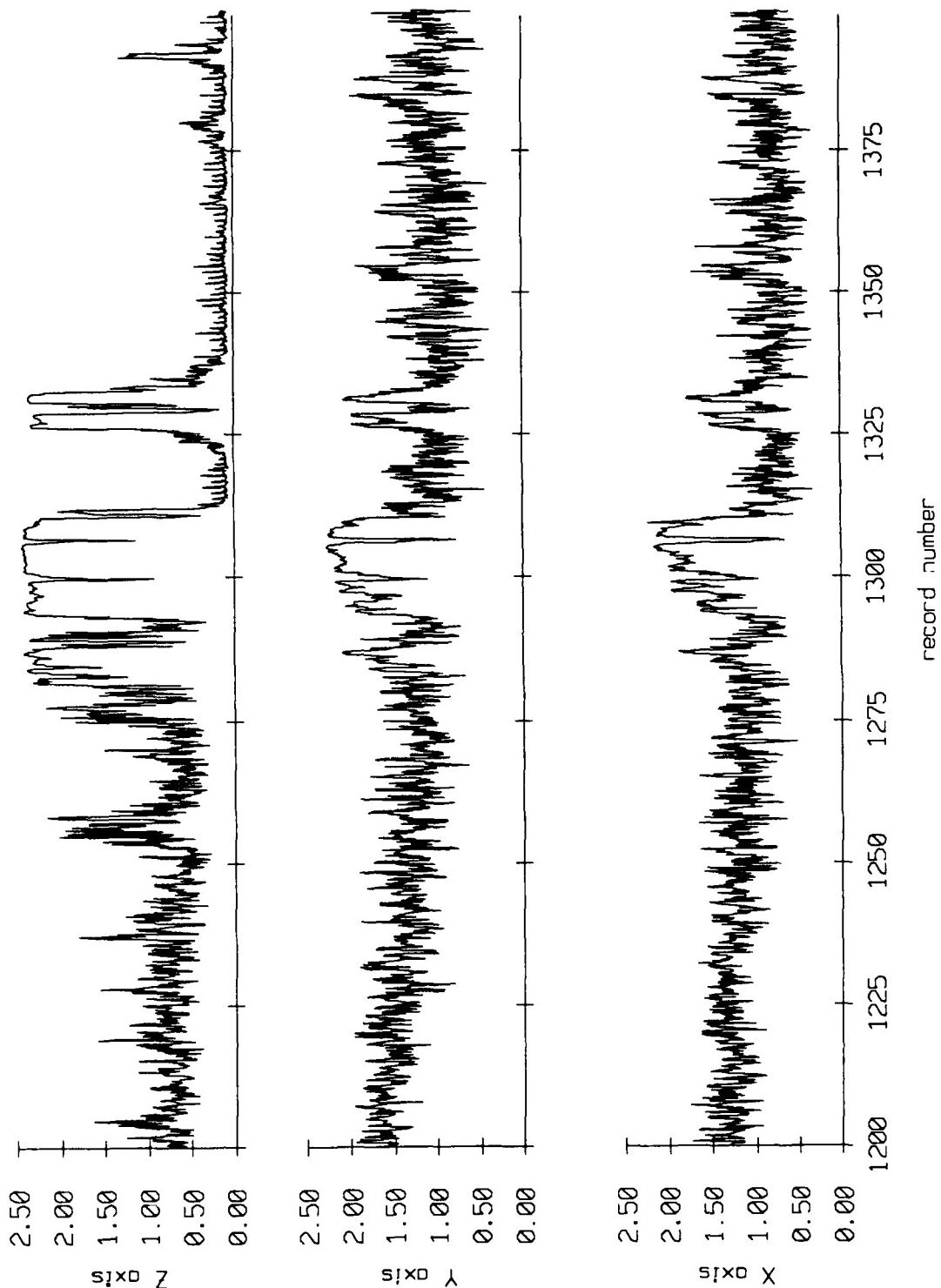


Figure IX.12f

Float 11, September 1987 Sea Trip
averaging period = 5.00 sec.



Gain Corrected Level, Volts(rms)

Figure IX.12g

Float 11, September 1987 Sea Trip
overaging period = 5.00 sec.

RMS Velocity

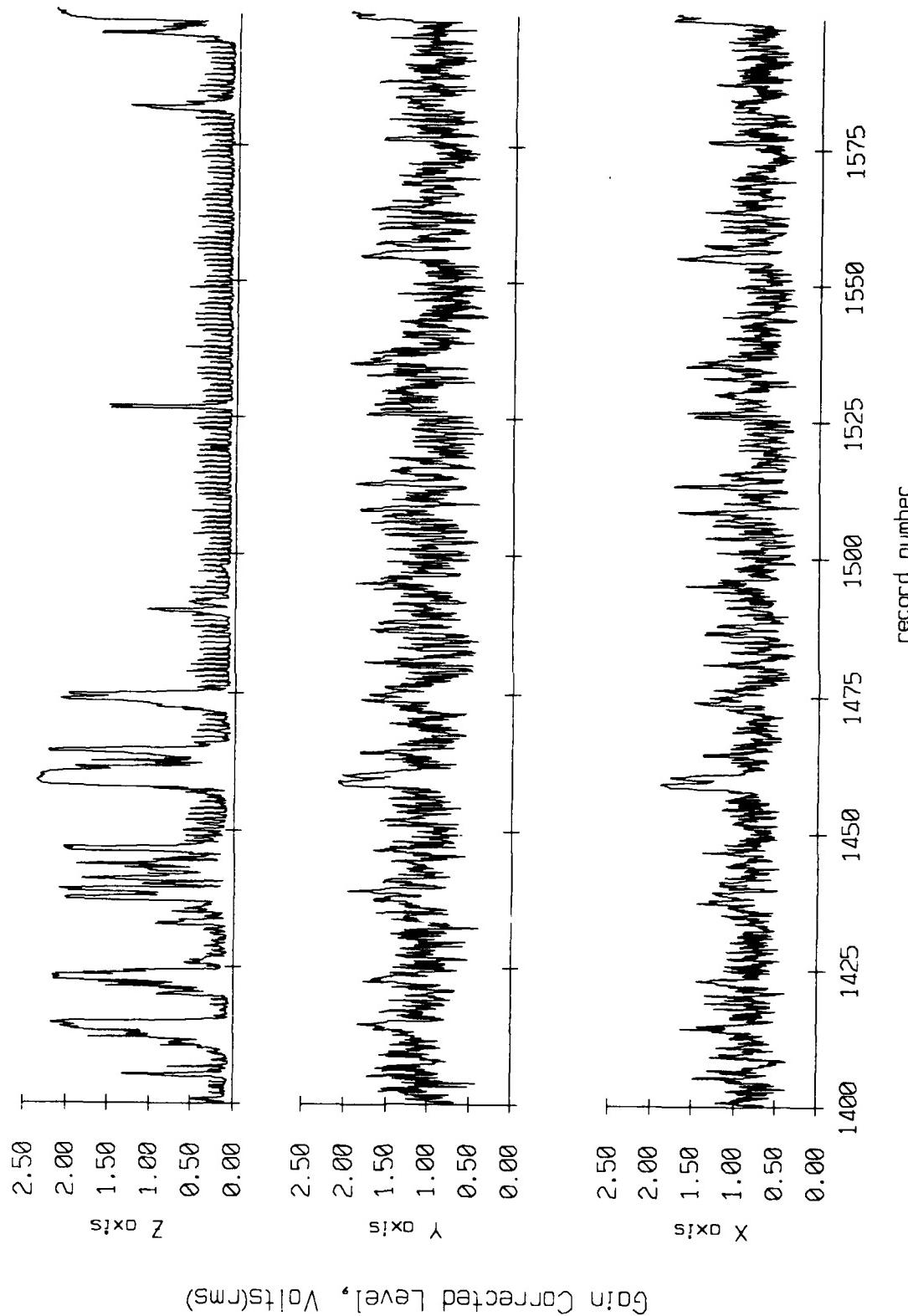
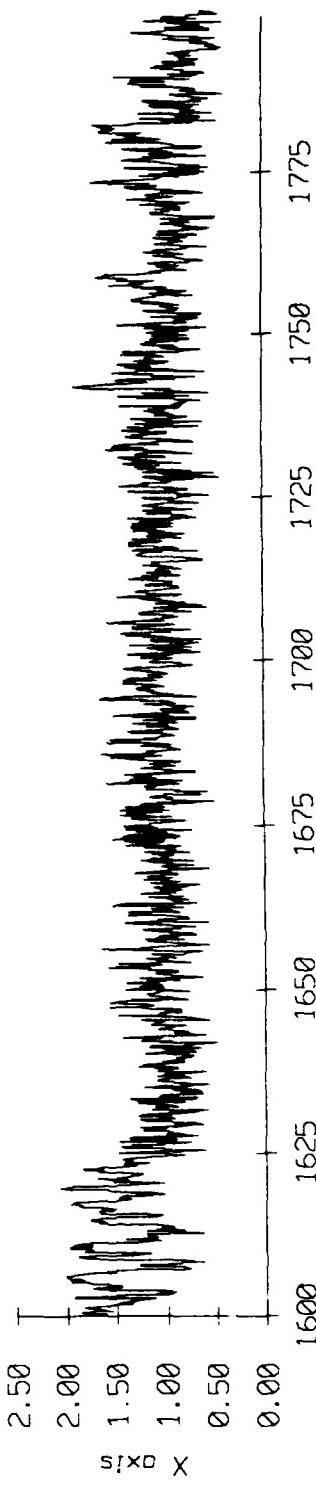
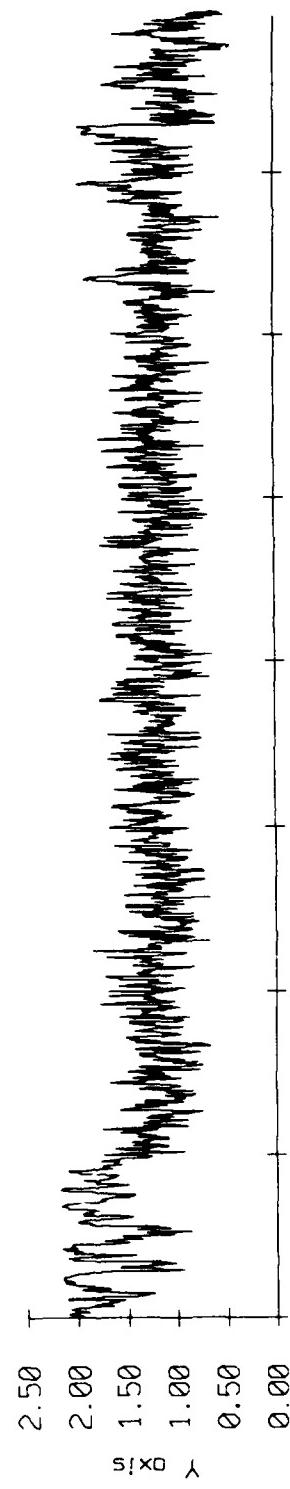
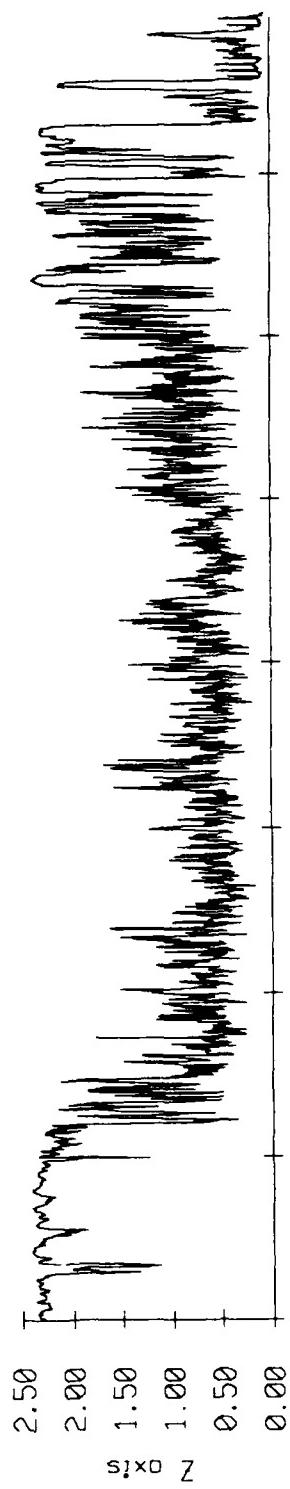


Figure IX.12h

Float 11, September 1987 Sea Trip
averaging period = 5.00 sec.

RMS Velocity



Gain Corrected Level, Volts(RMS)

Figure IX.121

Float 11, September 1987 Sea Trip
averaging period = 5.00 sec.

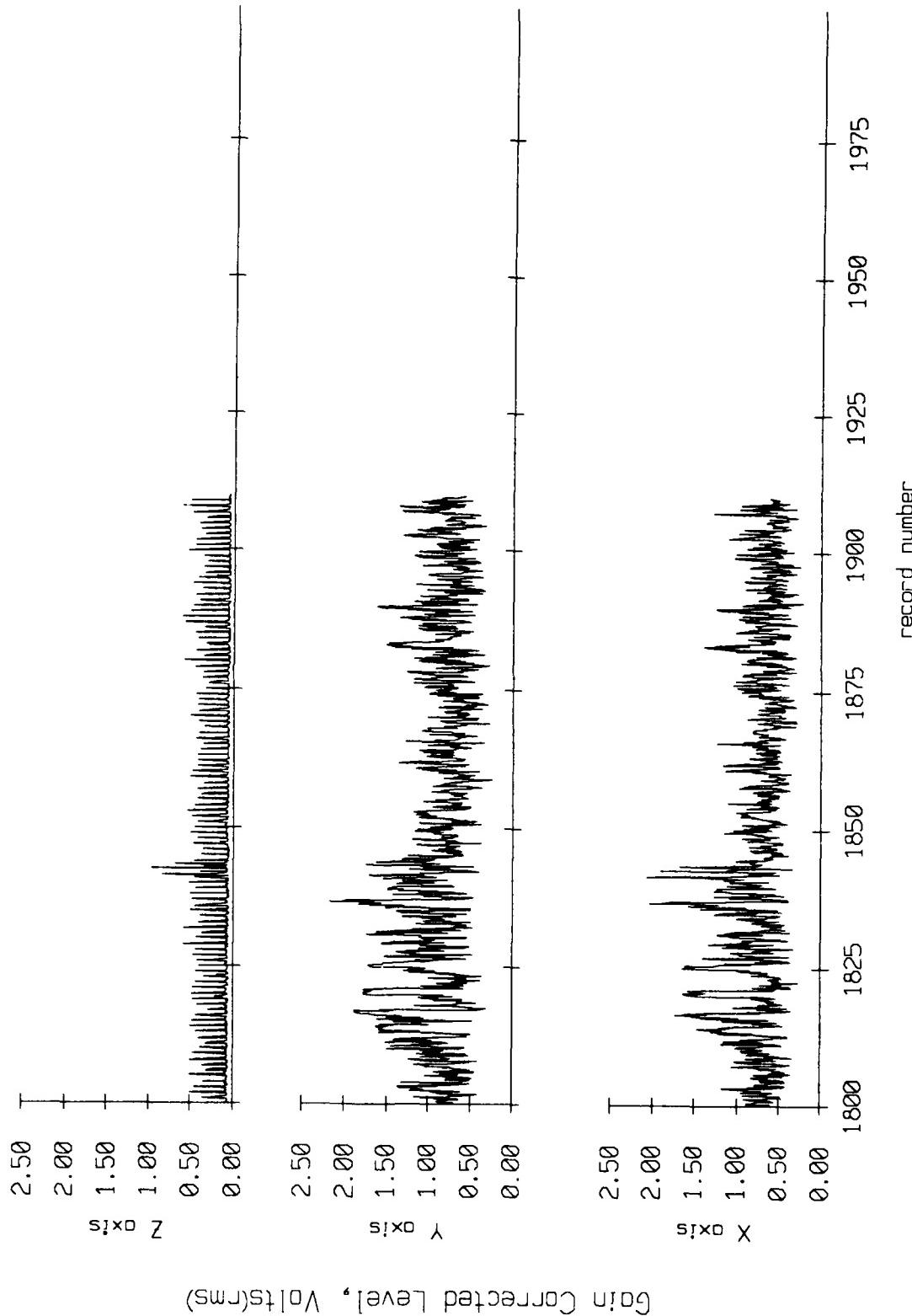


Figure IX.12j

Float 0, Sept, 1987 Trip - records 875-886 (x-axis)
vertical axis scale is approx. -1.5 to 1.5 volts

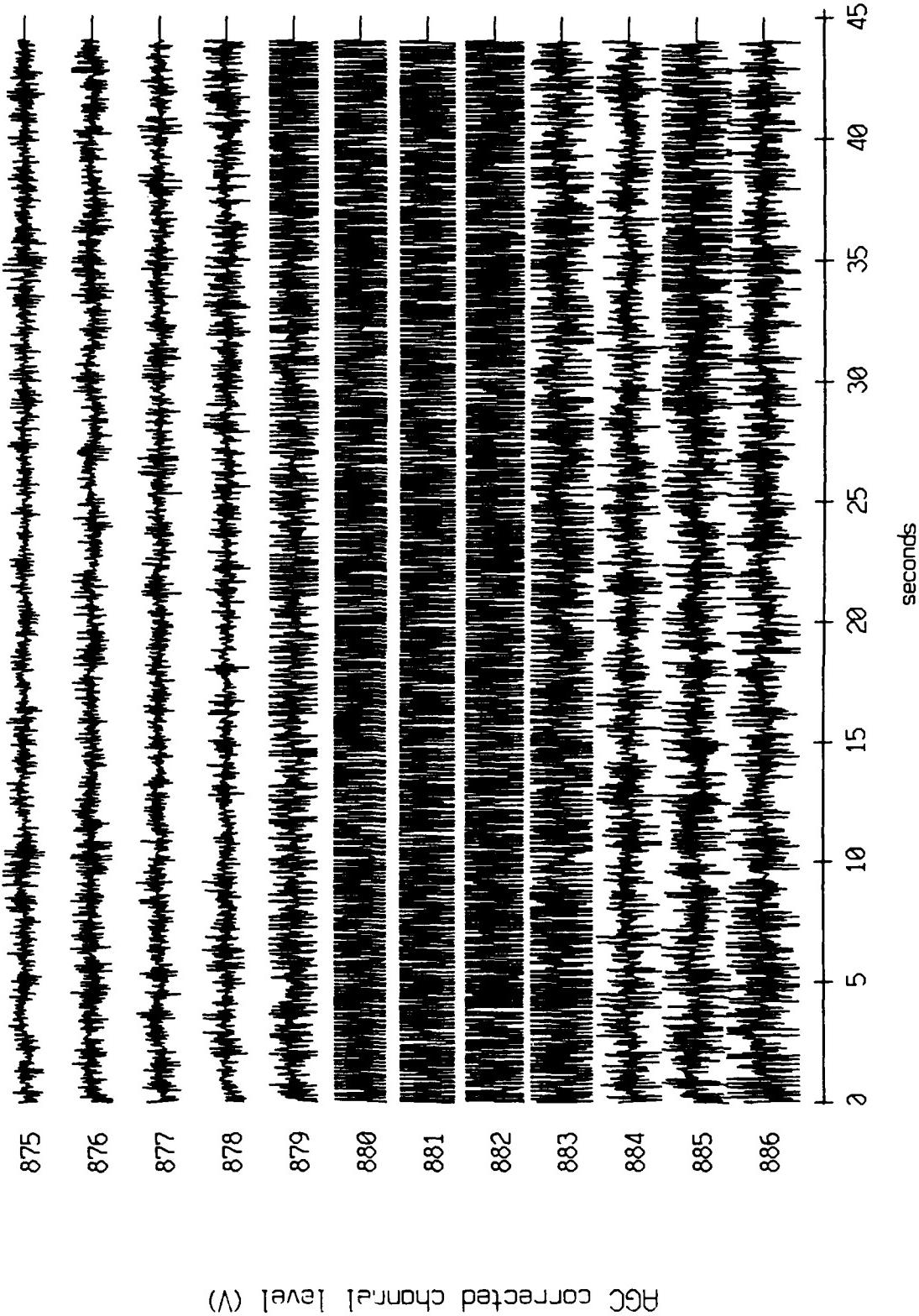


Figure X.I.1a

Float 0, Sept, 1987 Trip - records 875-886 (y-axis vertical axis is approx. -1.5 to 1.5 volts)

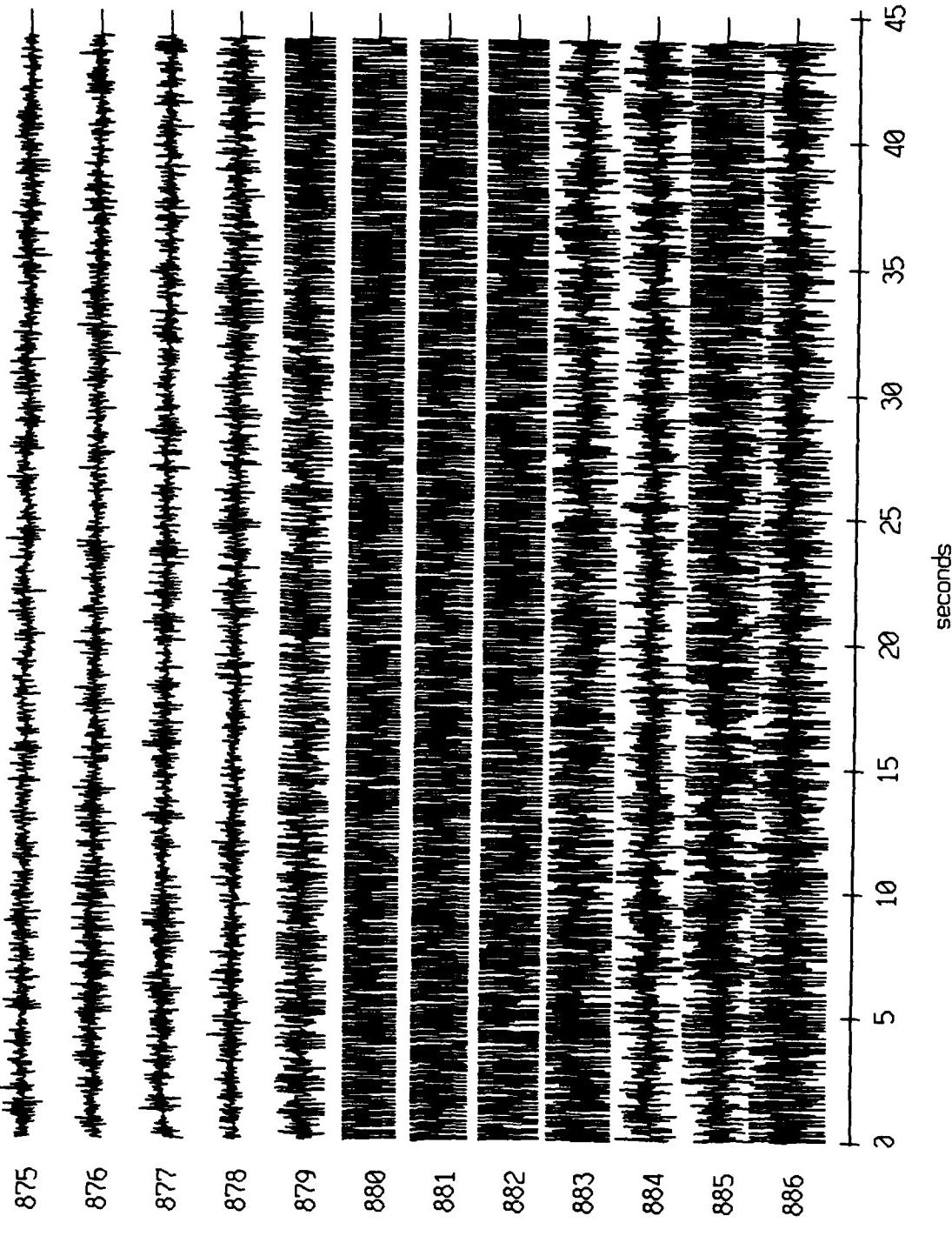


Figure X.1.1b

Float 0, Sept, 1987 Trip - records 875-886 (z-axis)
vertical axis scale is approx. -1.5 to 1.5 volts

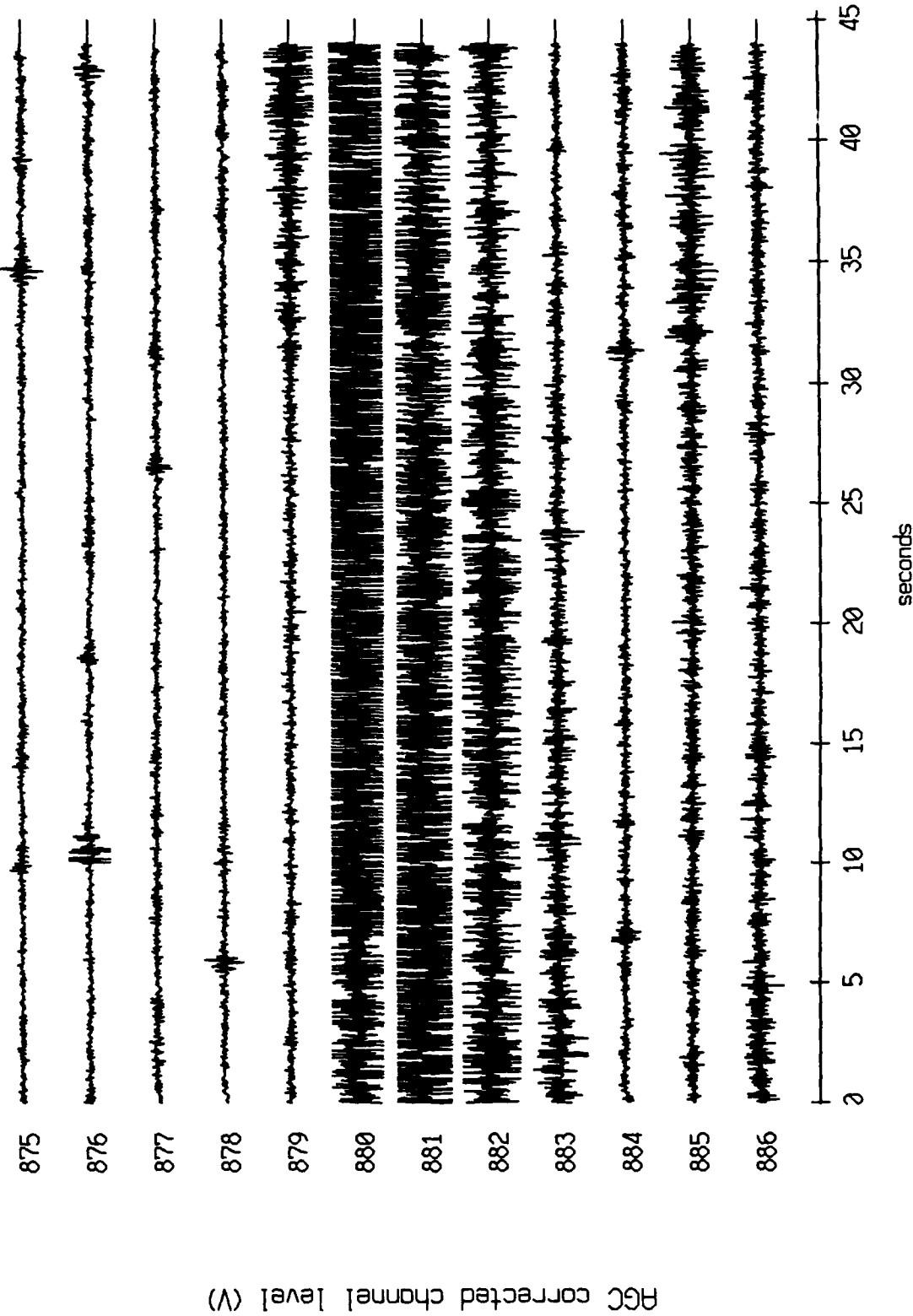


Figure X.1.1c

Float 0, September 1987 Sea Trip - records 1100-1111 (x-axis)
vertical axis scale is approx. -1.0 to 1.0 volts

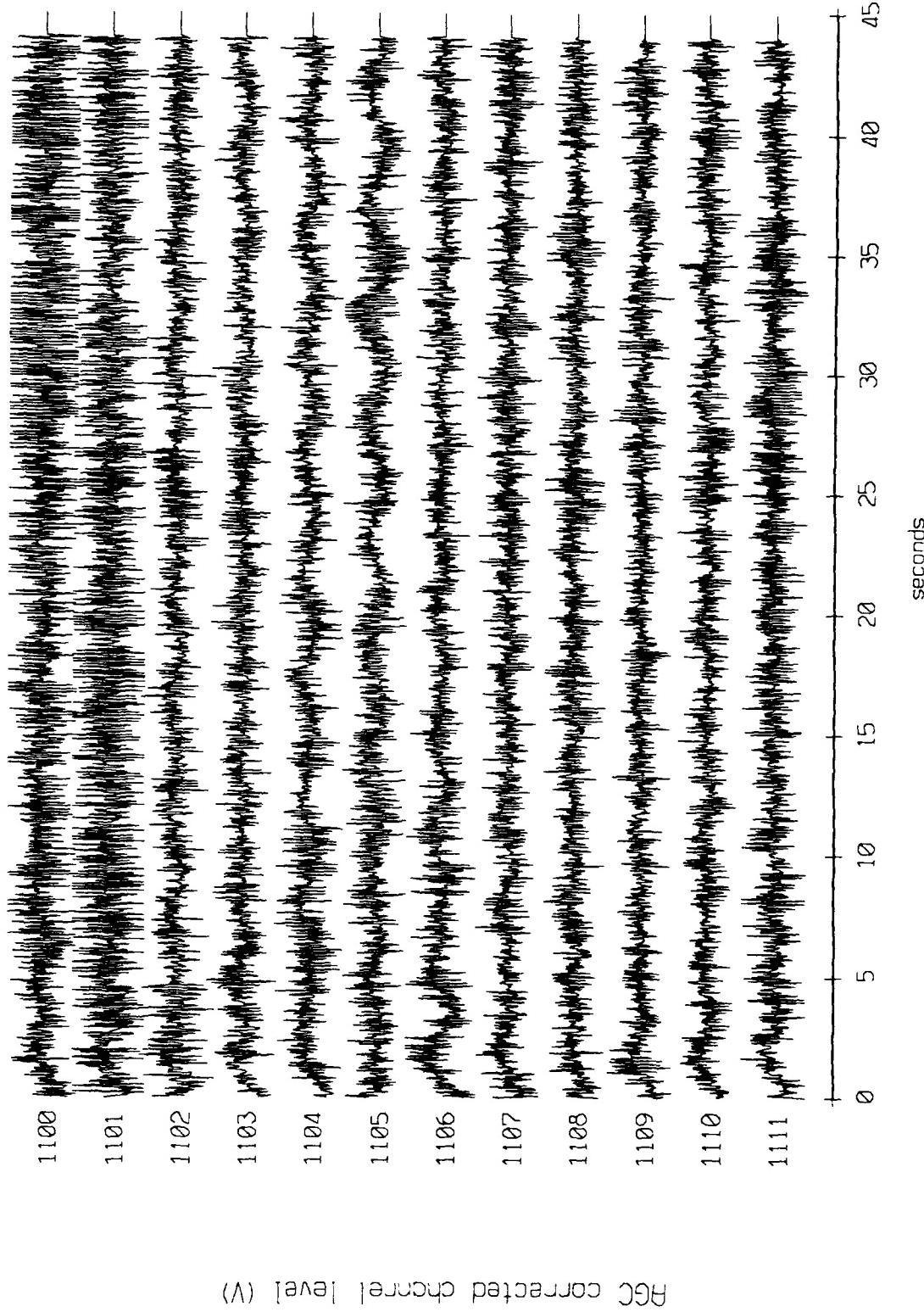


Figure X.2.1a

Float 0, September 1987 Sea Trip - records 1100-1111 (y-axis)
vertical axis scale is approx. -1.0 to 1.0 volts

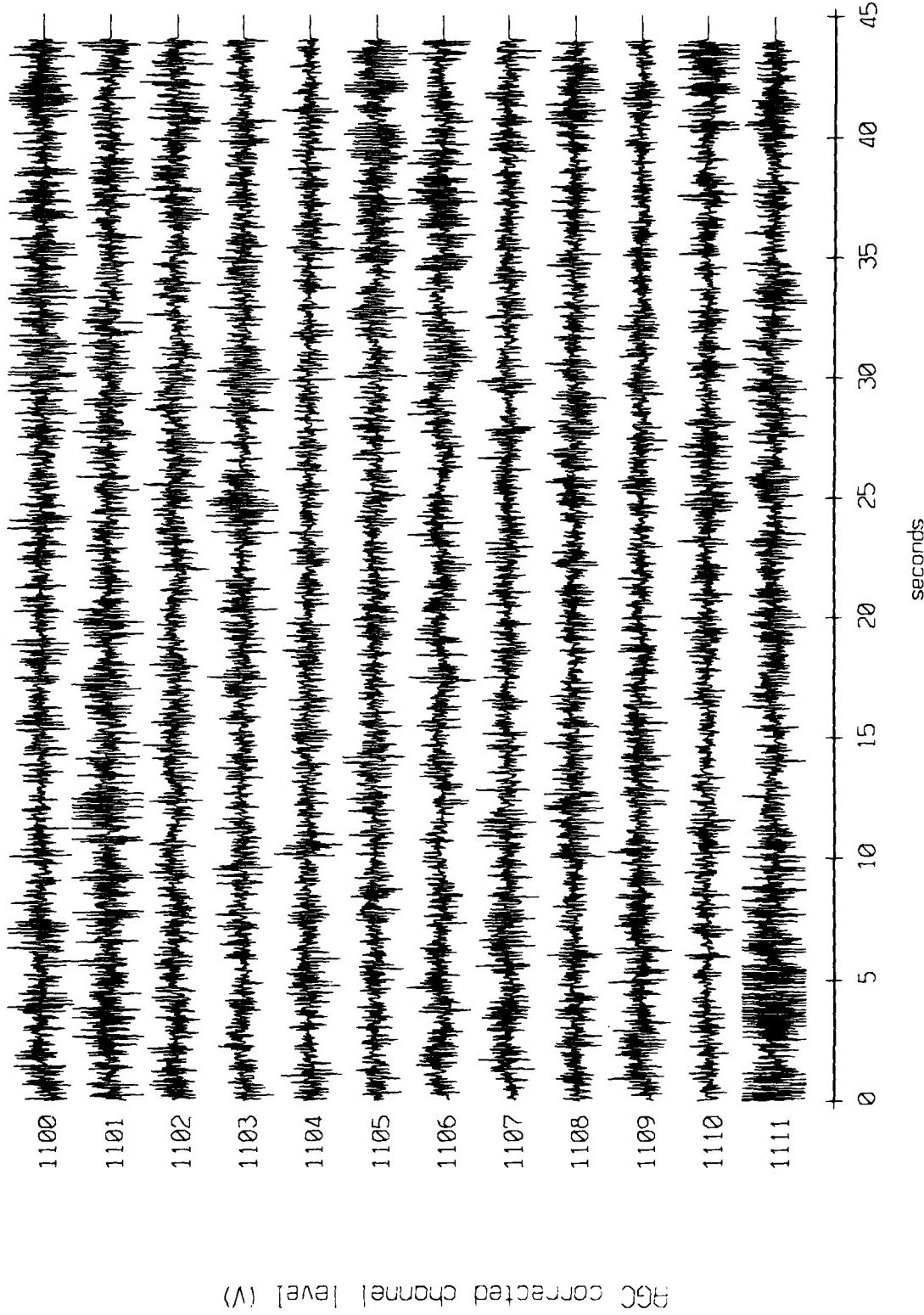
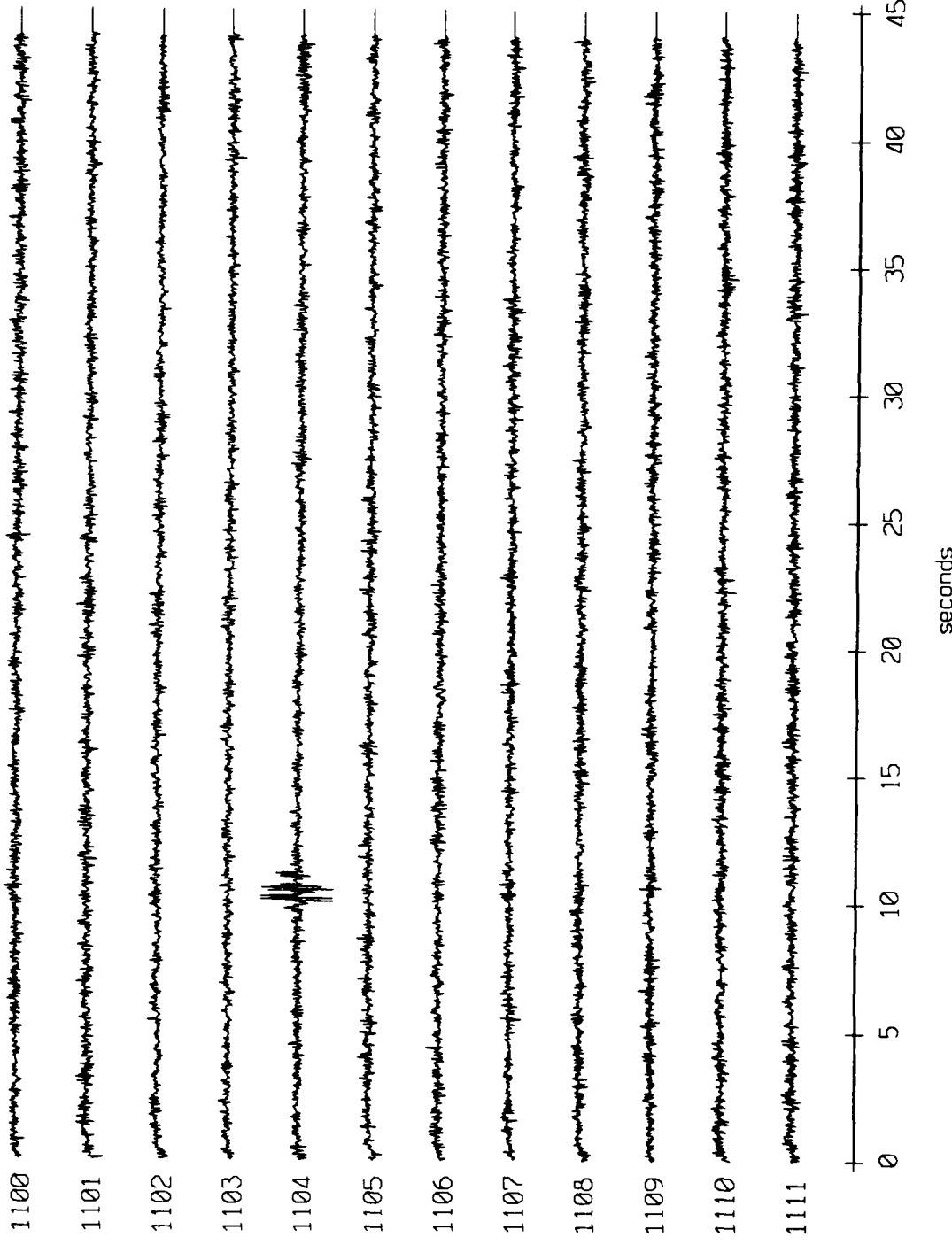


Figure X.2.1b

Flight 0, September 1987 Sea Trip - records 1100-1111 (z-axis)
vertical axis scale is approx. 1.0 volt_s



AGC corrected channel level (V)

Figure X.2.1c

Float 1, September 1987 Sea Trip - records 1100-1111 (x-axis
vertical axis scale is approx. 1.0 volts)

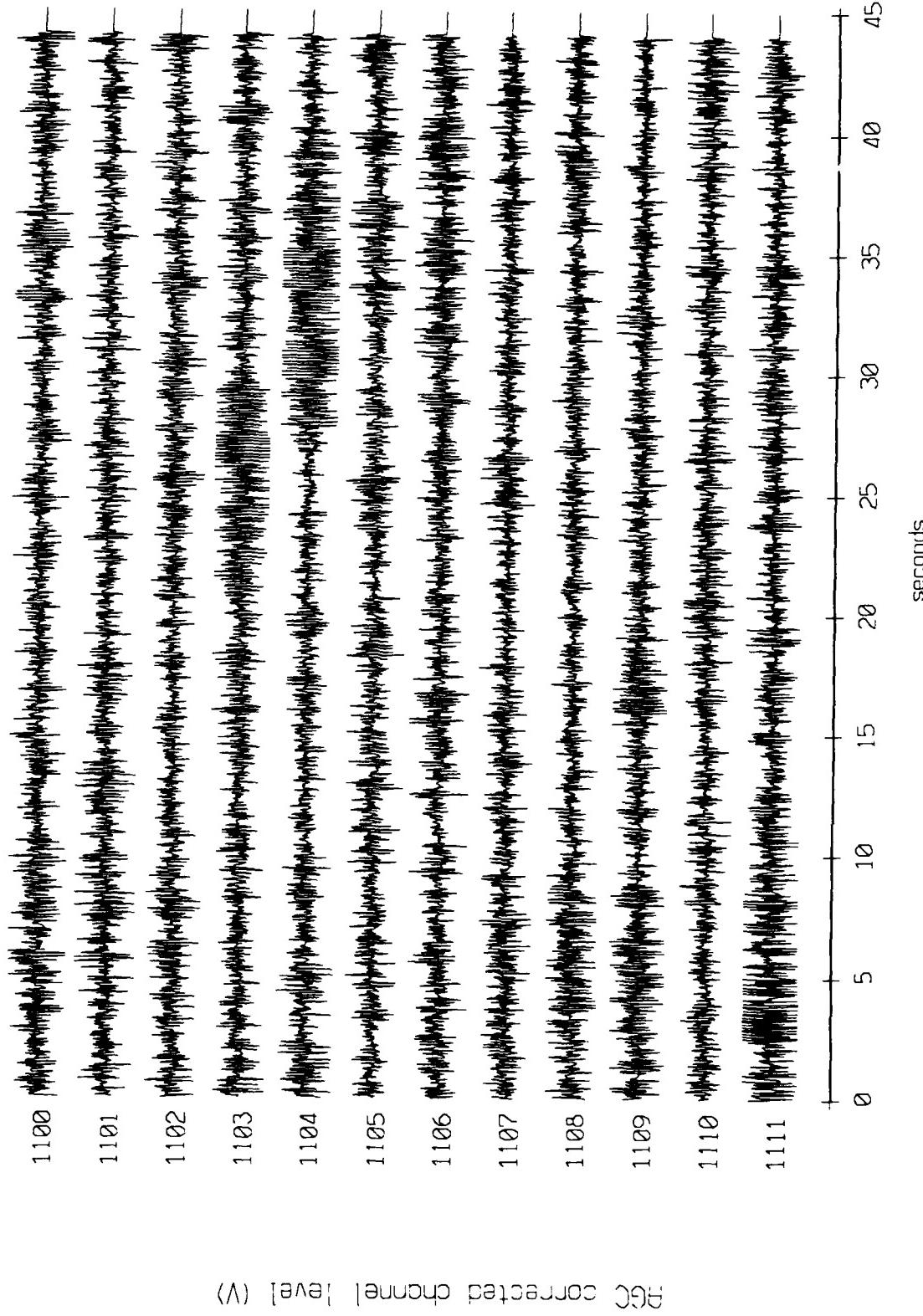


Figure X.2.2a

Flight 1, September 1987 Sea Trip - records 1100-1111 (y-axis
vertical axis scale is approx. 1.0 to 1.0 volts)

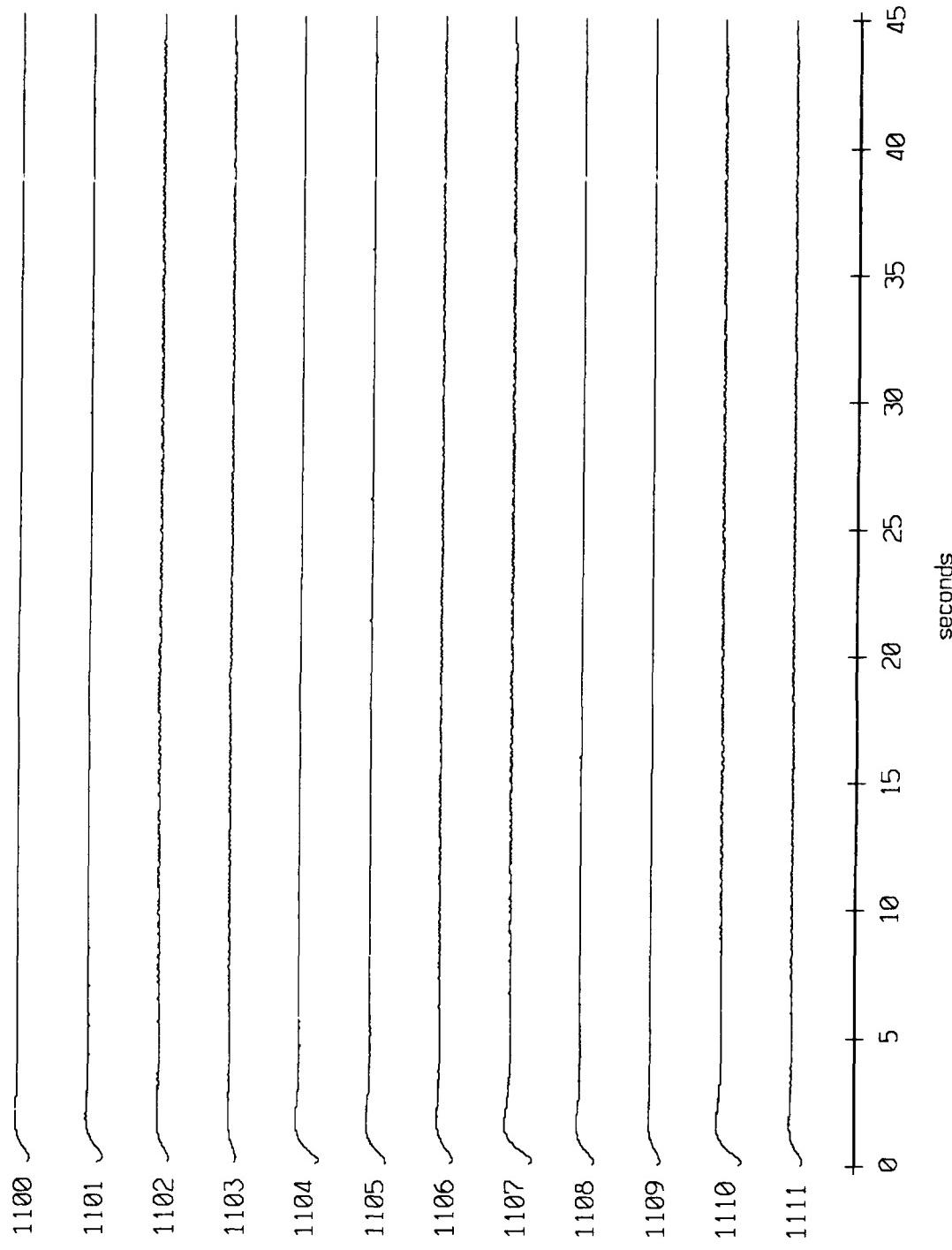


Figure X.2.2b

Flood 1, September 1987 Sea Trip - records 1100-1111 (z-axis)
vertical axis scale is approx. -1.0 to 1.0 volts

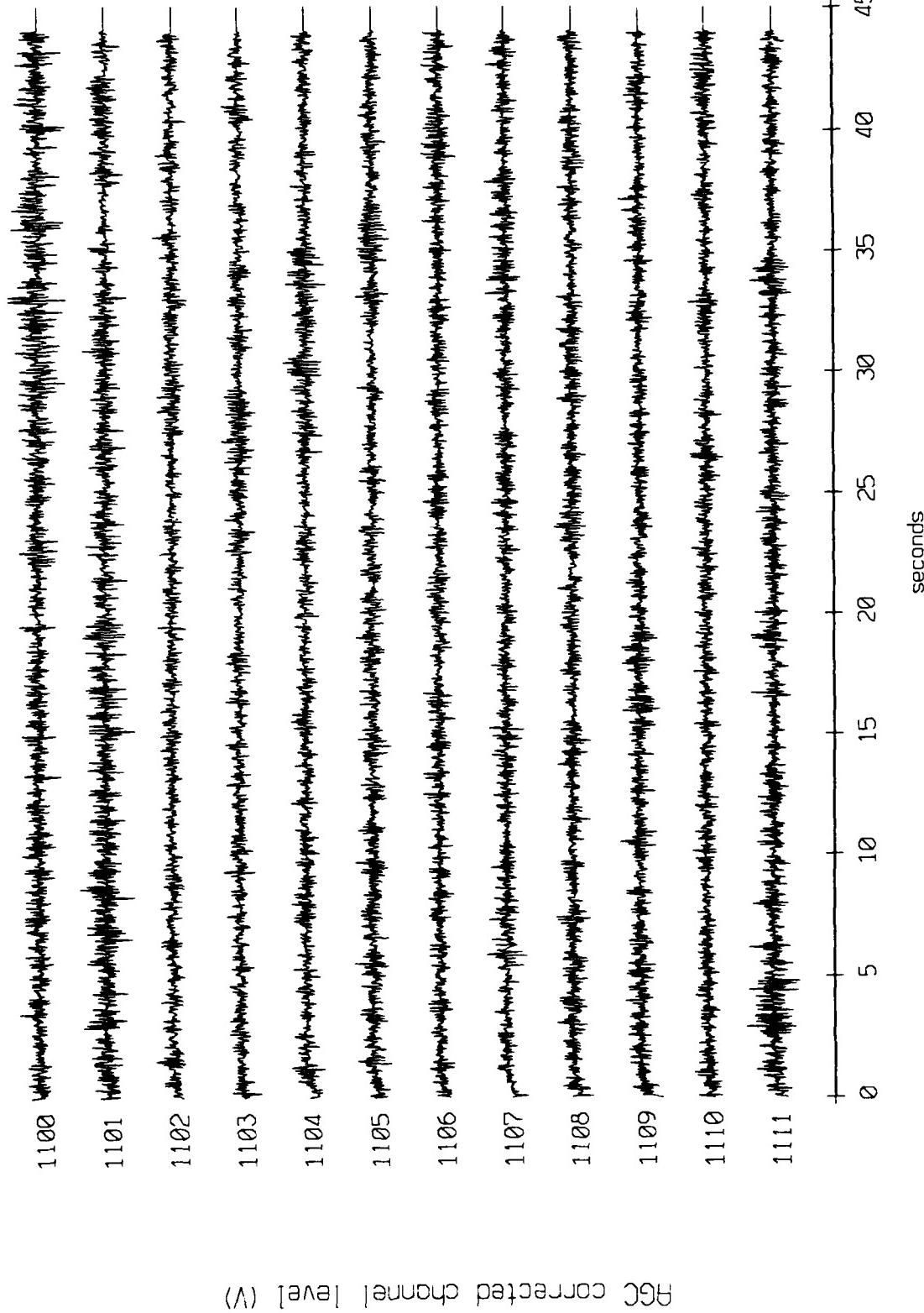
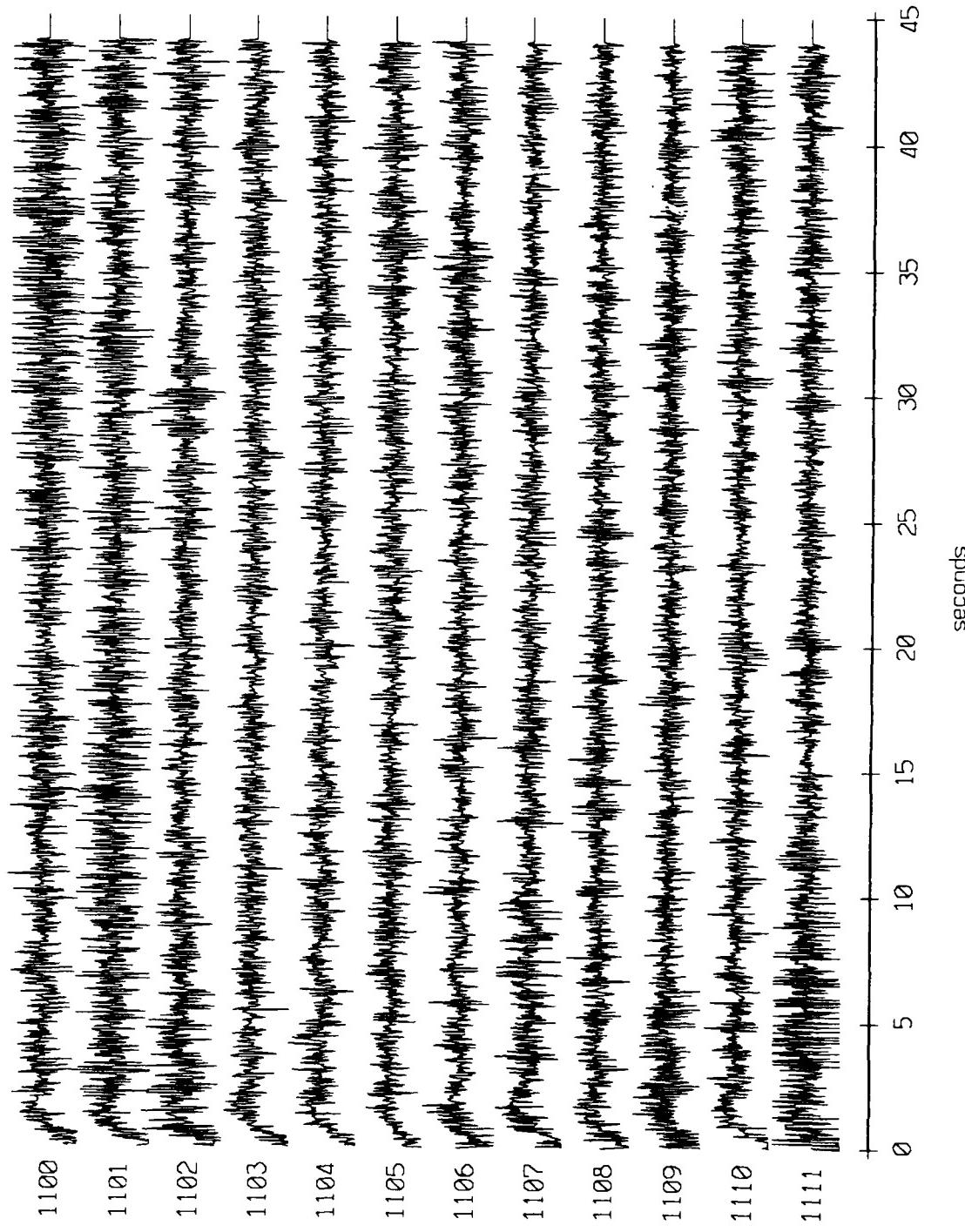


Figure X.2.2c

Flight 2, September 1987 Sea Trip - records 1100-1111 (x-axis is vertical axis scale is approx. 1.0 volt)



AGC corrected channel level (V)

Figure X.2.3a

Float 2, September 1987 Sea Trip - records 1100-1111 (y-axis)
vertical axis scale is approx. -1.0 to 1.0 volts

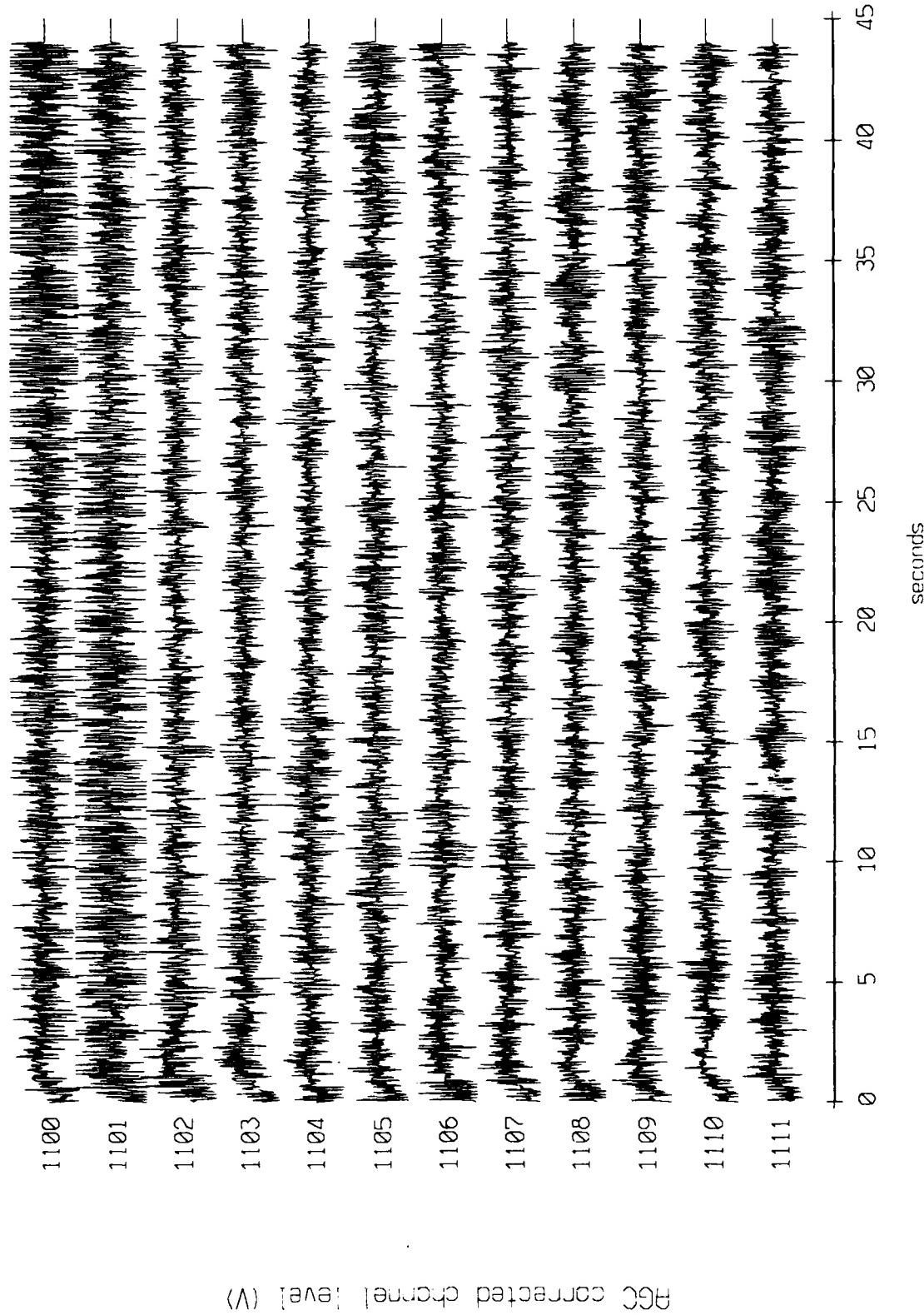


Figure X.2.3b

Float 2, September 1987 Sea Trip - records 1100-1111 (z-axis)
vertical axis scale is approx. -1.0 to 1.0 volts

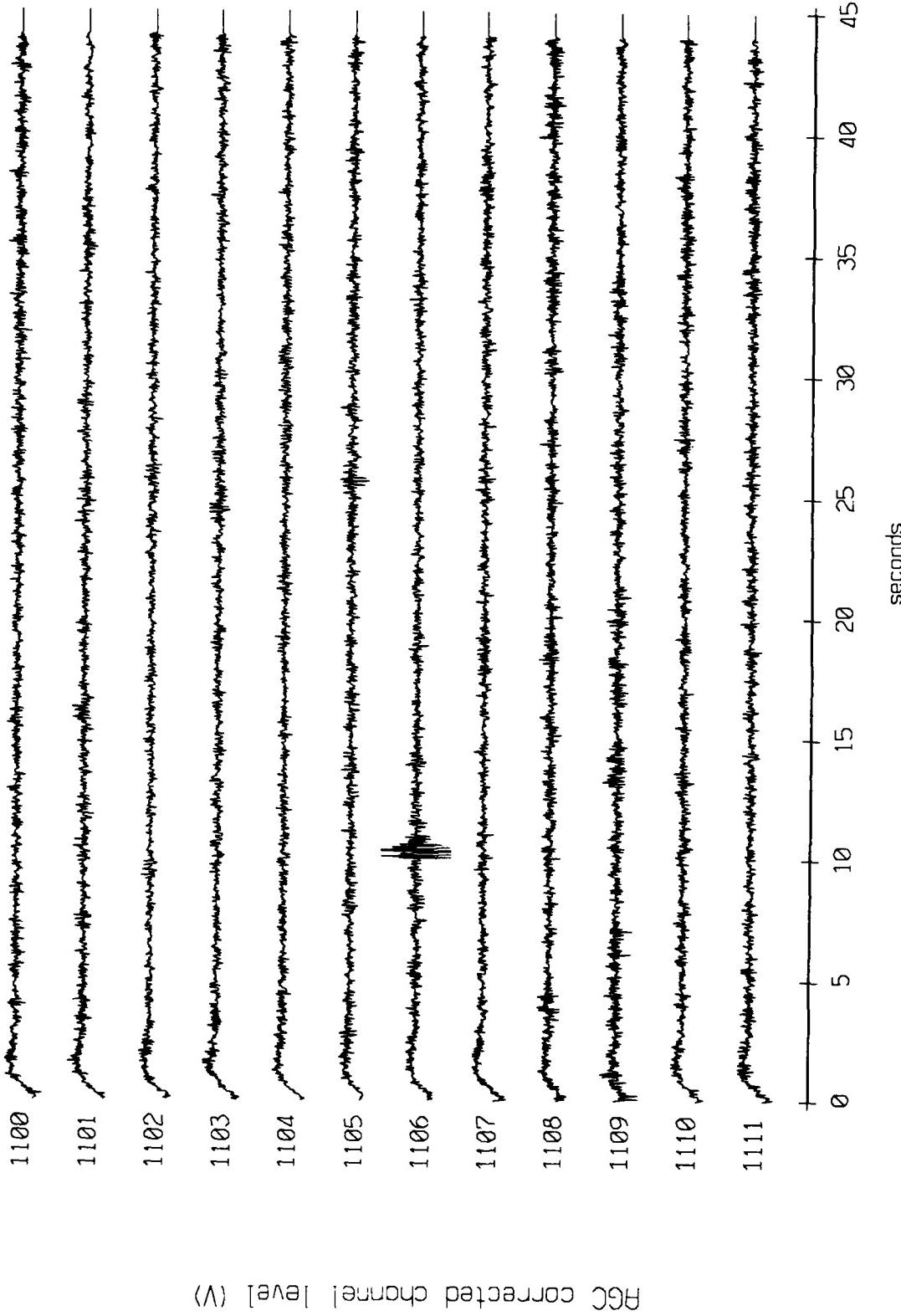


Figure X.2.3c

Float 3, September 1987 Sea Trip - records 1100-1111 (x-axis)
vertical axis scale is approx. -1.0 to 1.0 volts

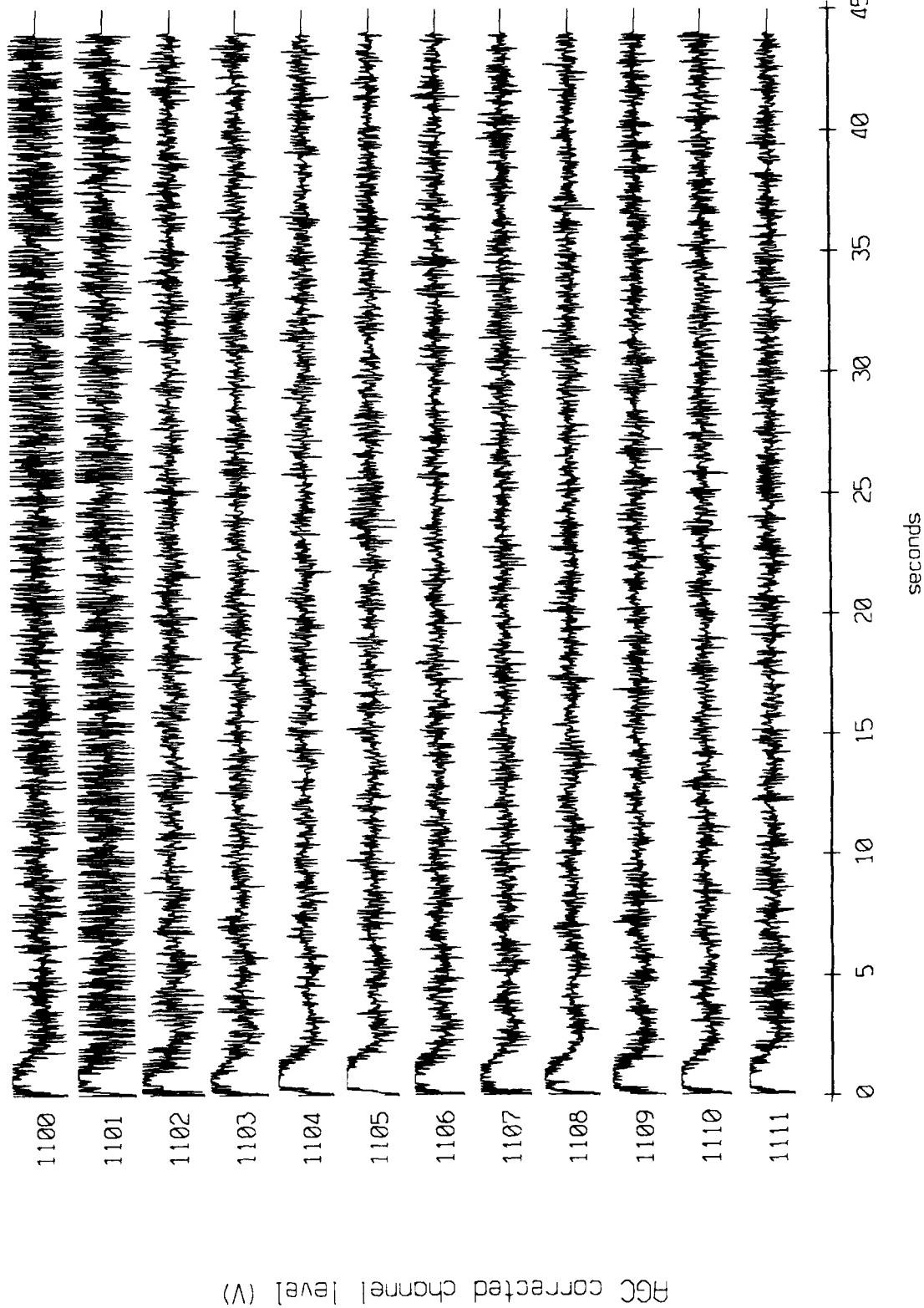


Figure X.2.4a

Float 3, September 1987 Sea Trip - records 1100-1111 (y-axis
vertical axis scale is approx. -1.0 to 1.0 volts

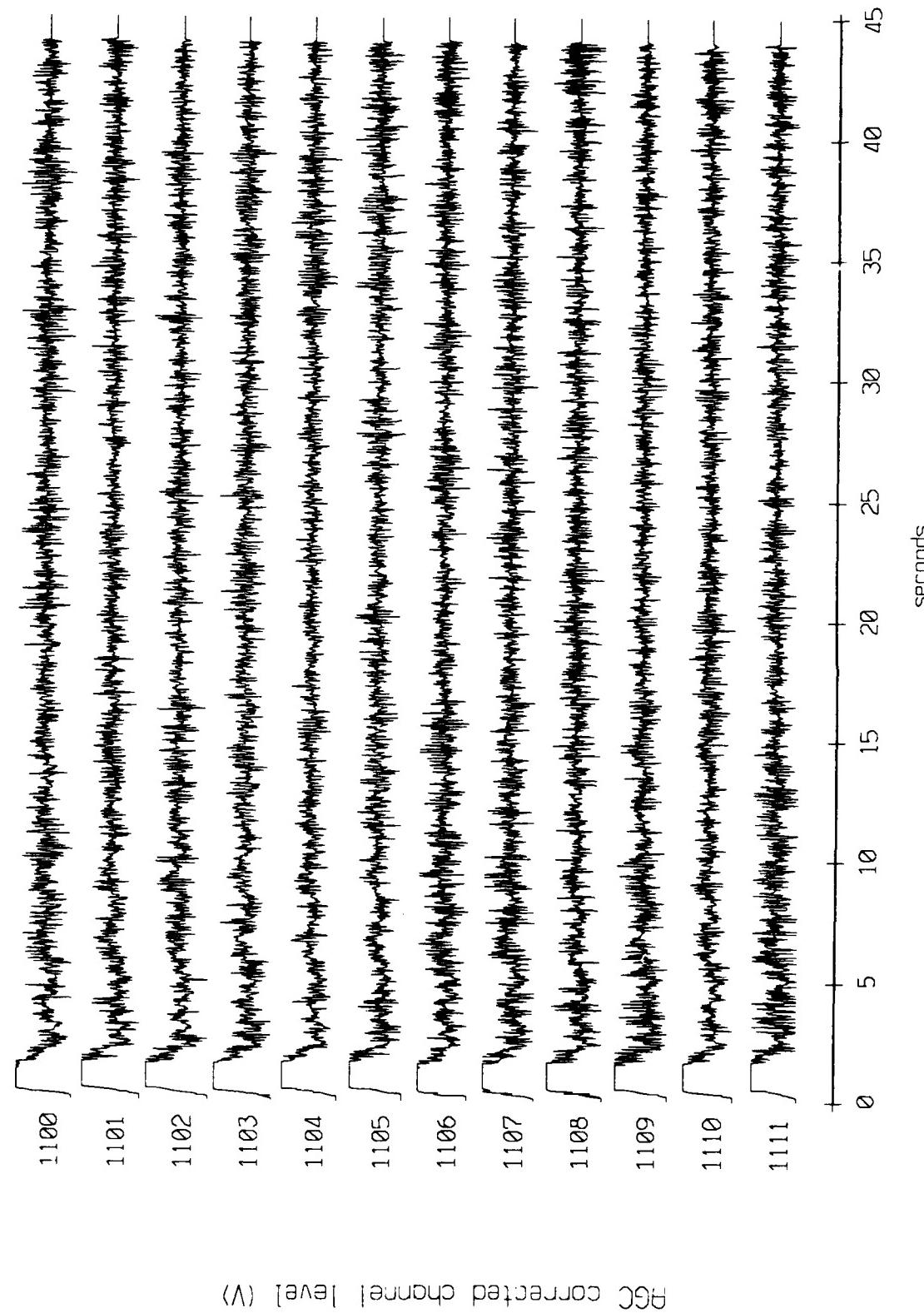


Figure X.2.4b

Flight 3, September 1987 Sea Trip - records 11000-11111 (z-axis)
vertical axis scale is approx. -1.0 to 1.0 volts

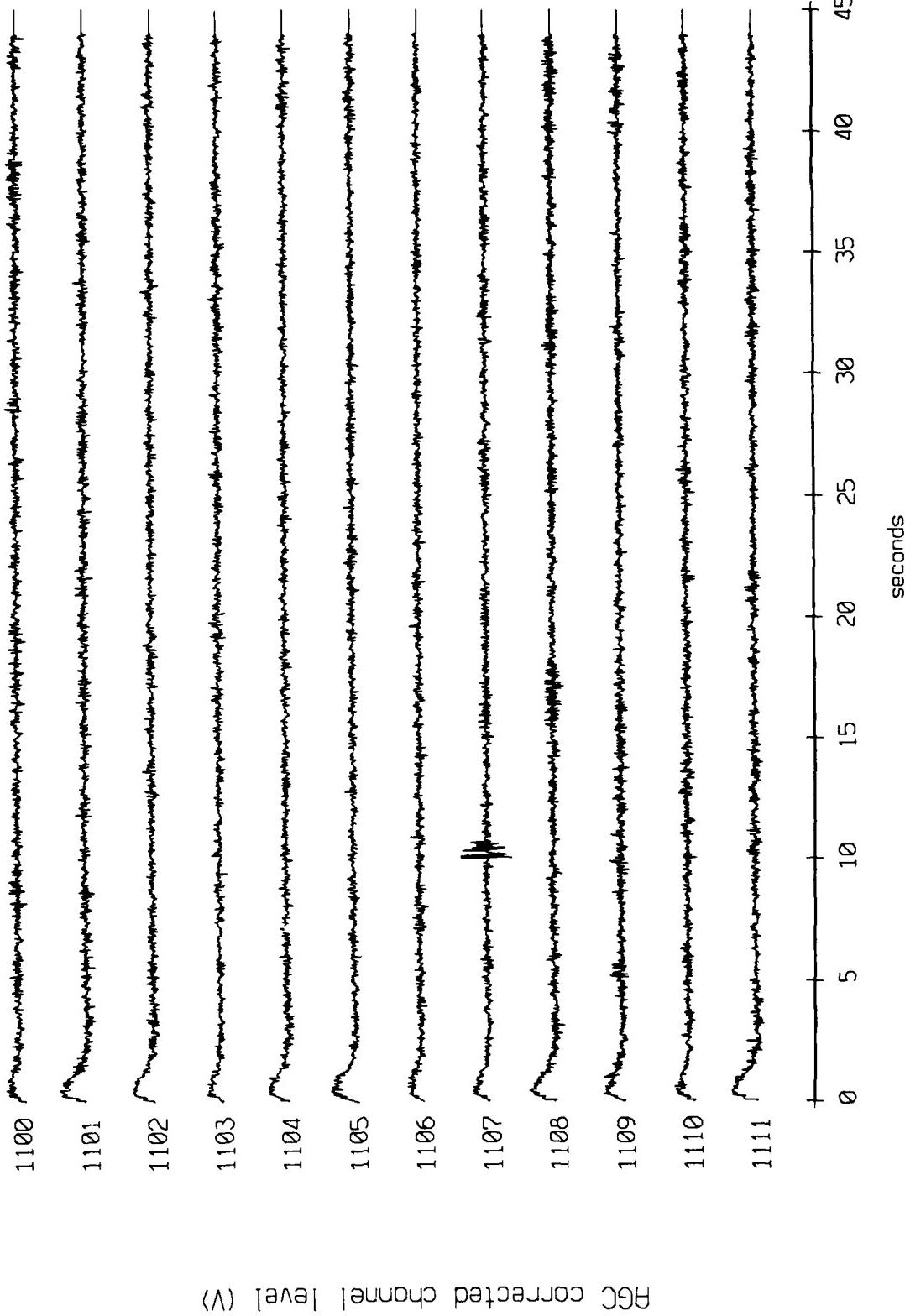


Figure X.2.4c

Float 4, September 1987 Sea Trip - records 1100-1111 (x-axis)
vertical axis scale is approx. -1.0 to 1.0 volts

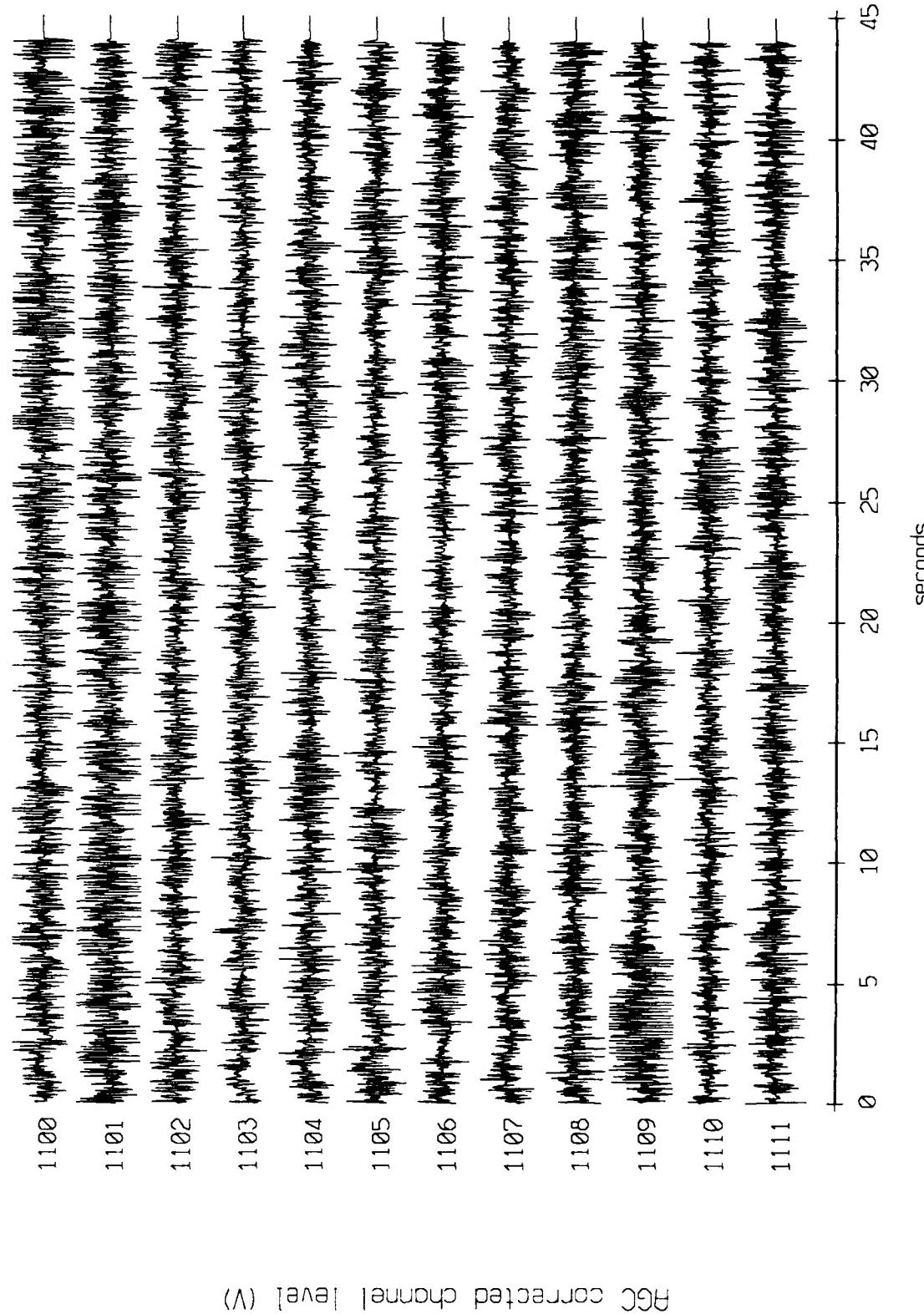


Figure X.2.5a

Float 4, September 1987 Sea Trip - records 1100-1111 (y-axis)
vertical axis scale is approx. -1.0 to 1.0 volts

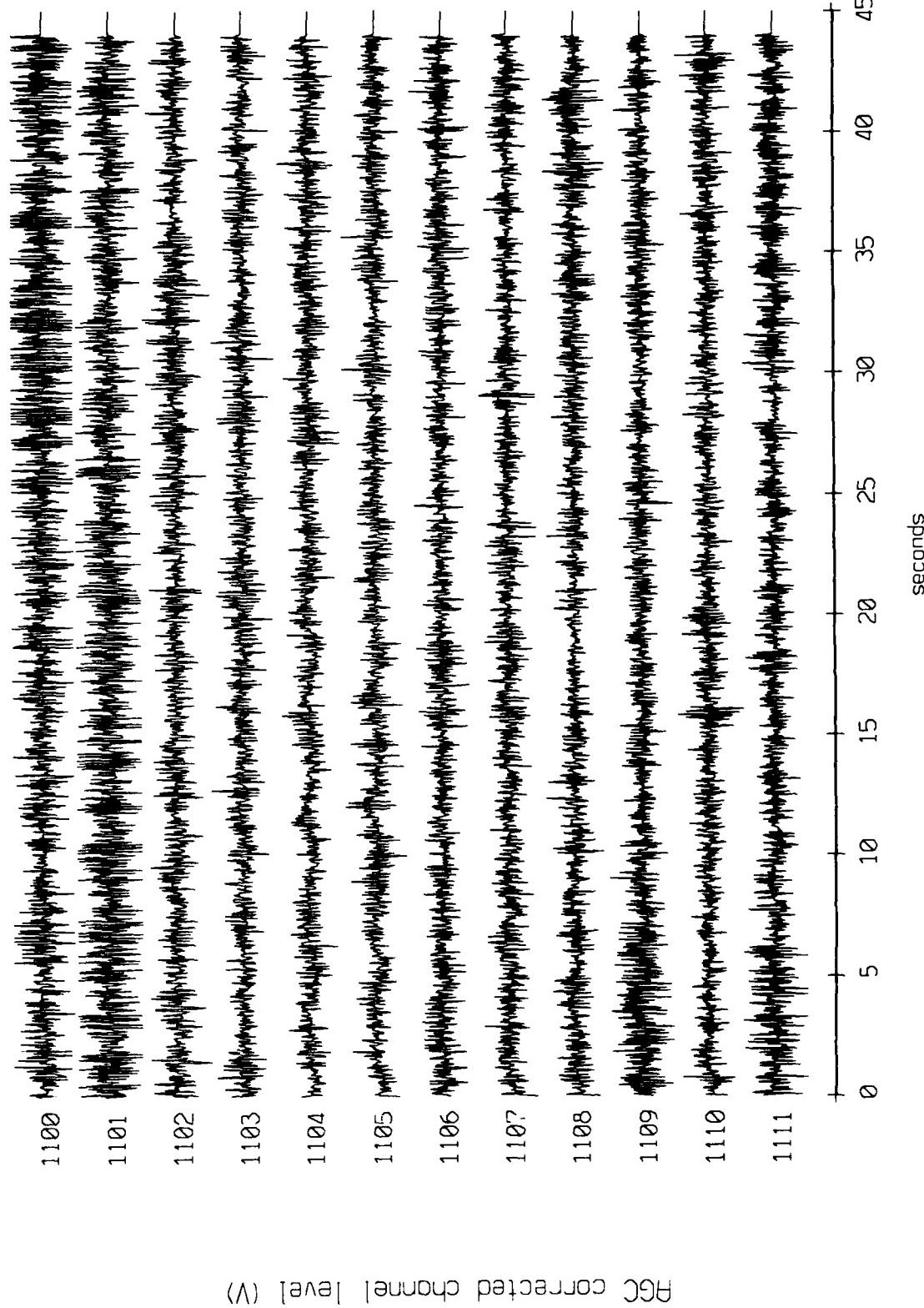


Figure X.2.5b

Flight 4, September 1987 Sea Trip - records 1100-1111 (z-axis)
vertical axis scale is approx. -1.0 to 1.0 volts

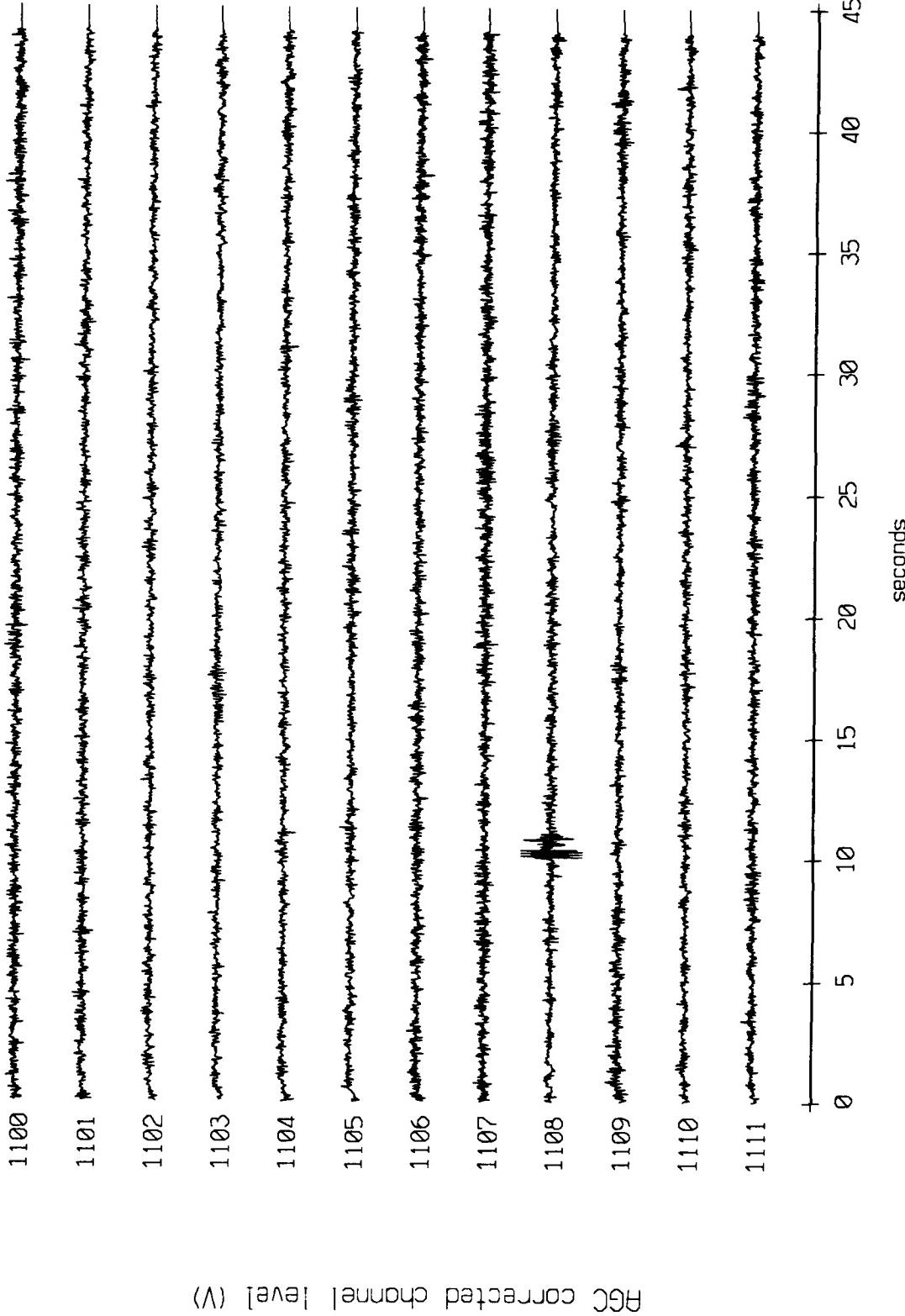


Figure X.2.5c

Float 5, September 1987 Trip - records 1100-1111 (x-axis)
vertical axis scale is approx. -1.0 to 1.0 volts

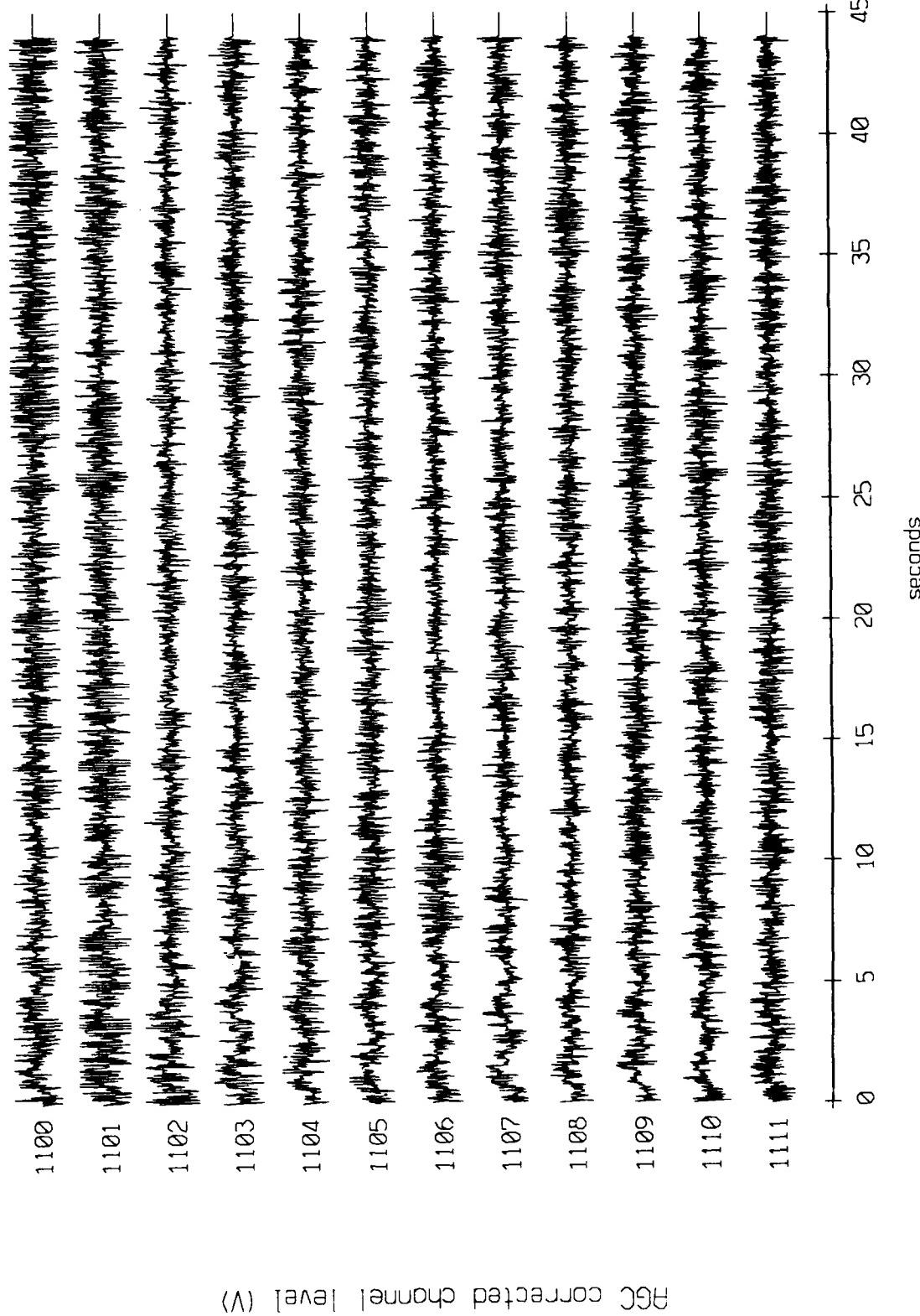


Figure X.2.6a

Float 5, September 1987 Trip - records 1100-1111 (y-axis
vertical axis scale is approx. -1.0 to 1.0 volts

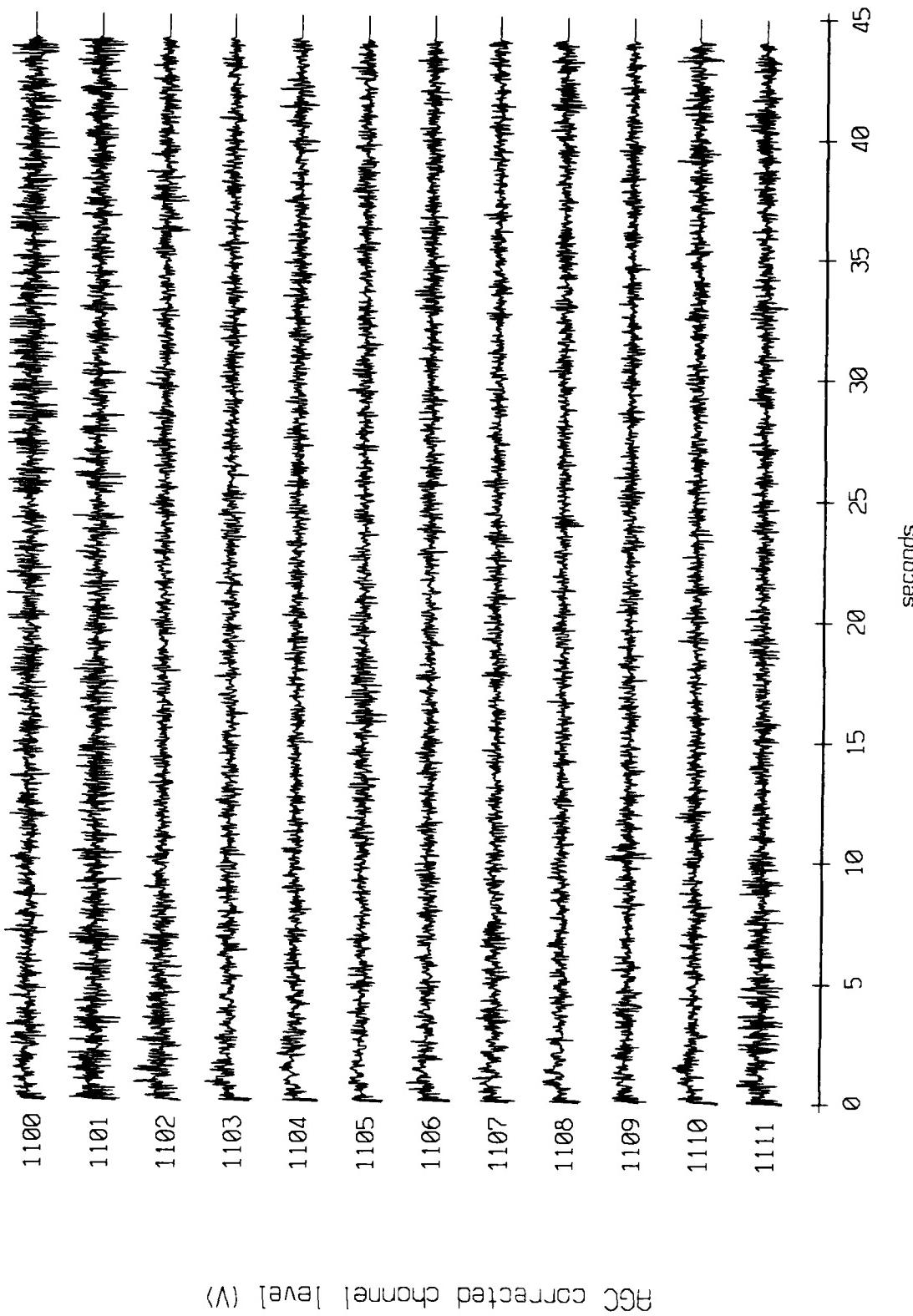


Figure X.2.6b

Flight 5, September 1987 Trip - records 1100-1111 (z-axis
vertical axis scale is approx. -1.0 to 1.0 volts

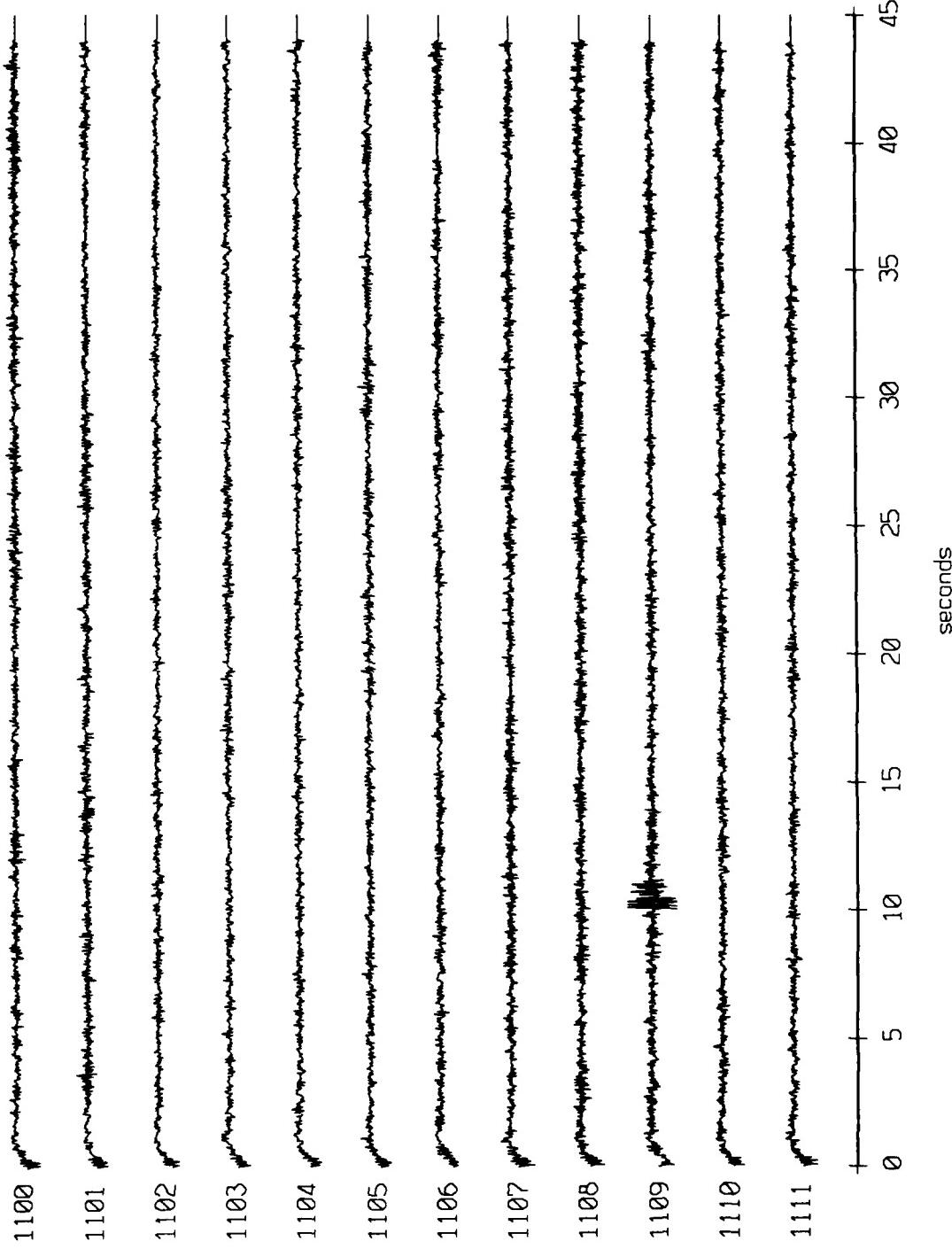


Figure X.2.6c

Float 6, September 1987 Trip - records 1100-1111 (x-axis)
vertical axis scale is approx. -1.0 to 1.0 volts

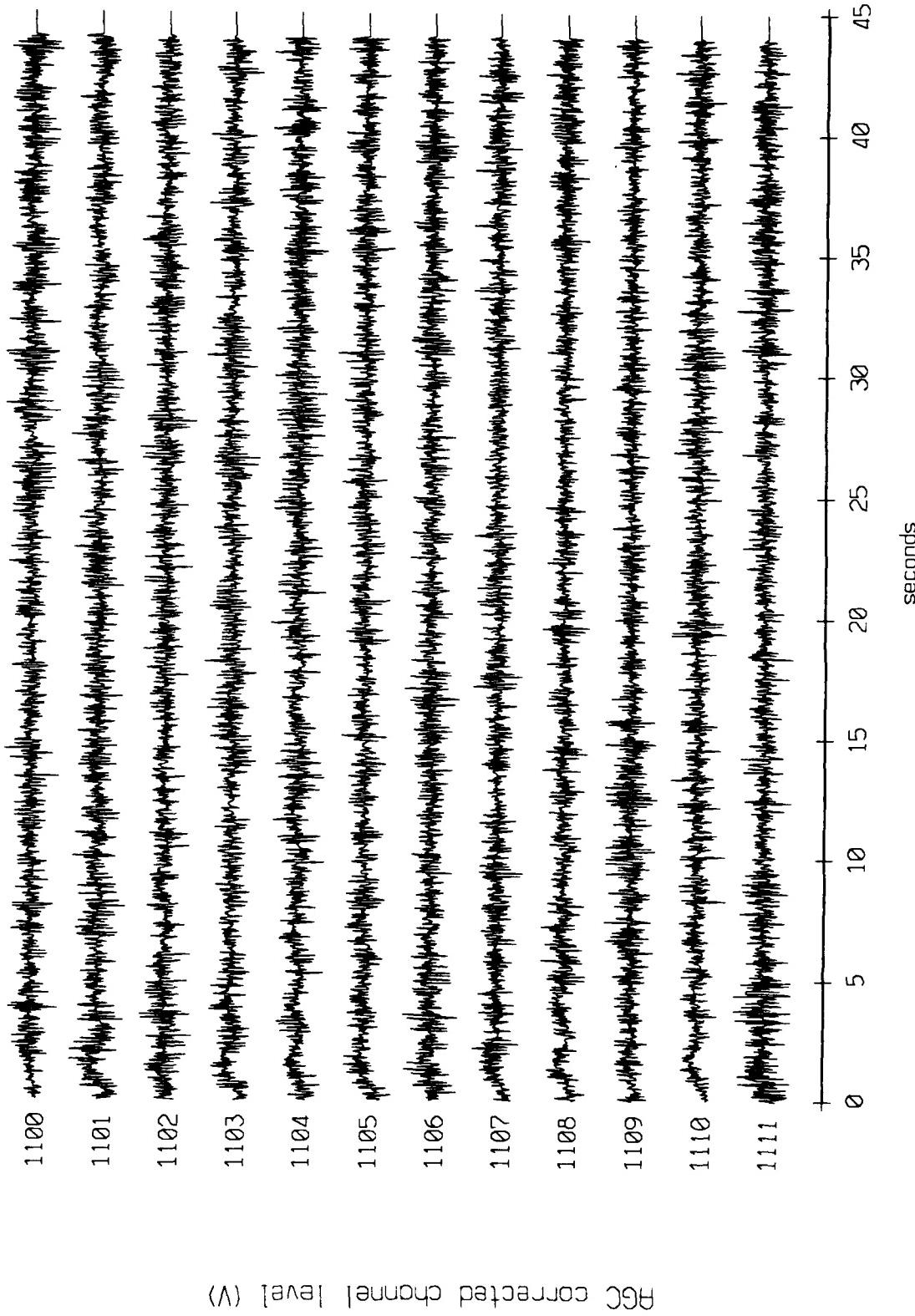


Figure X.2.7a

Float 6, September 1987 Trip - records 1100-1111 (y-axis
vertical axis scale is approx. -1.0 to 1.0 volts

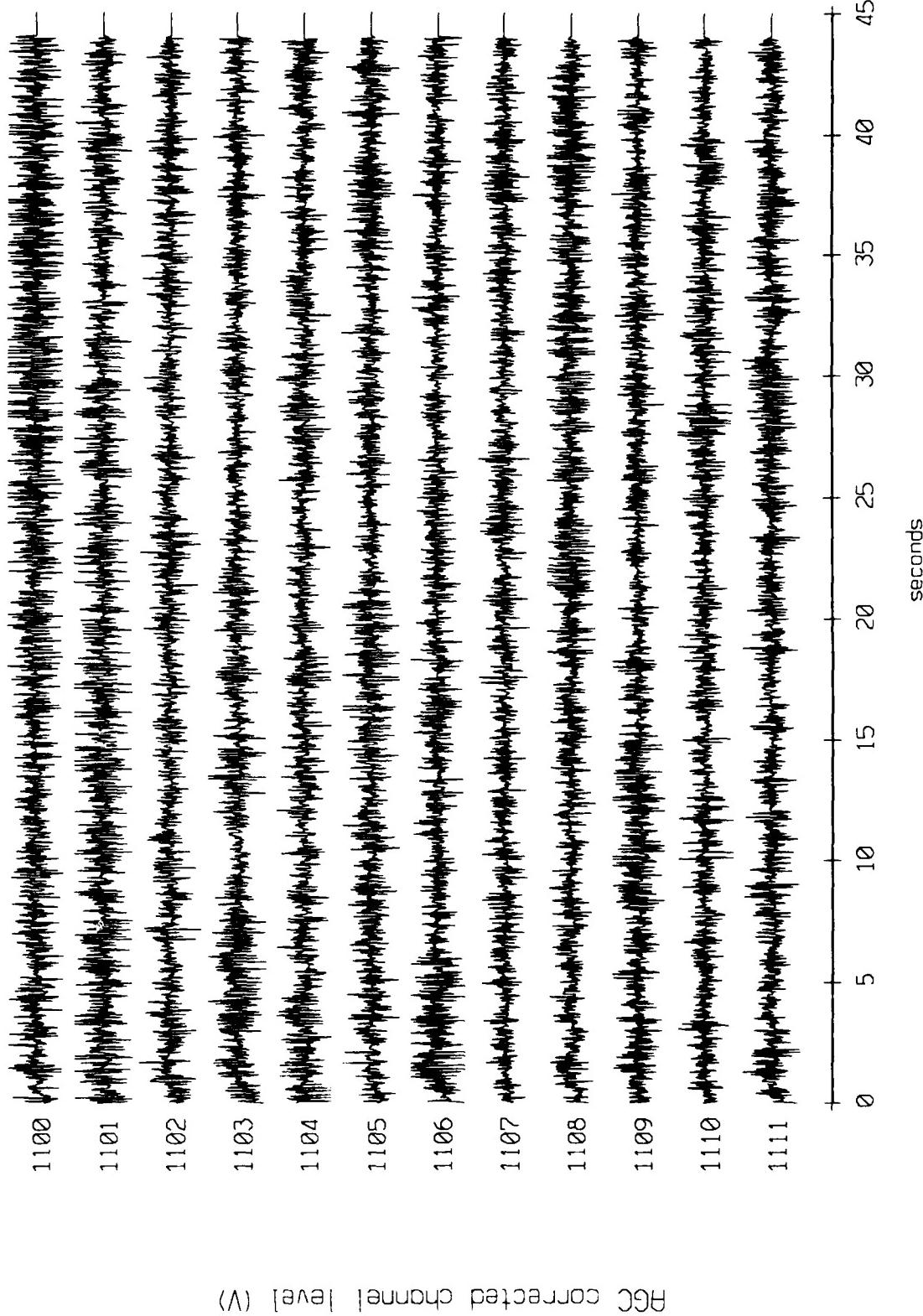


Figure X.2.7b

Flight 6, September 1987 Trip - records 1100-1111 (z-axis)
vertical axis scale is approx. -1.0 to 1.0 volts

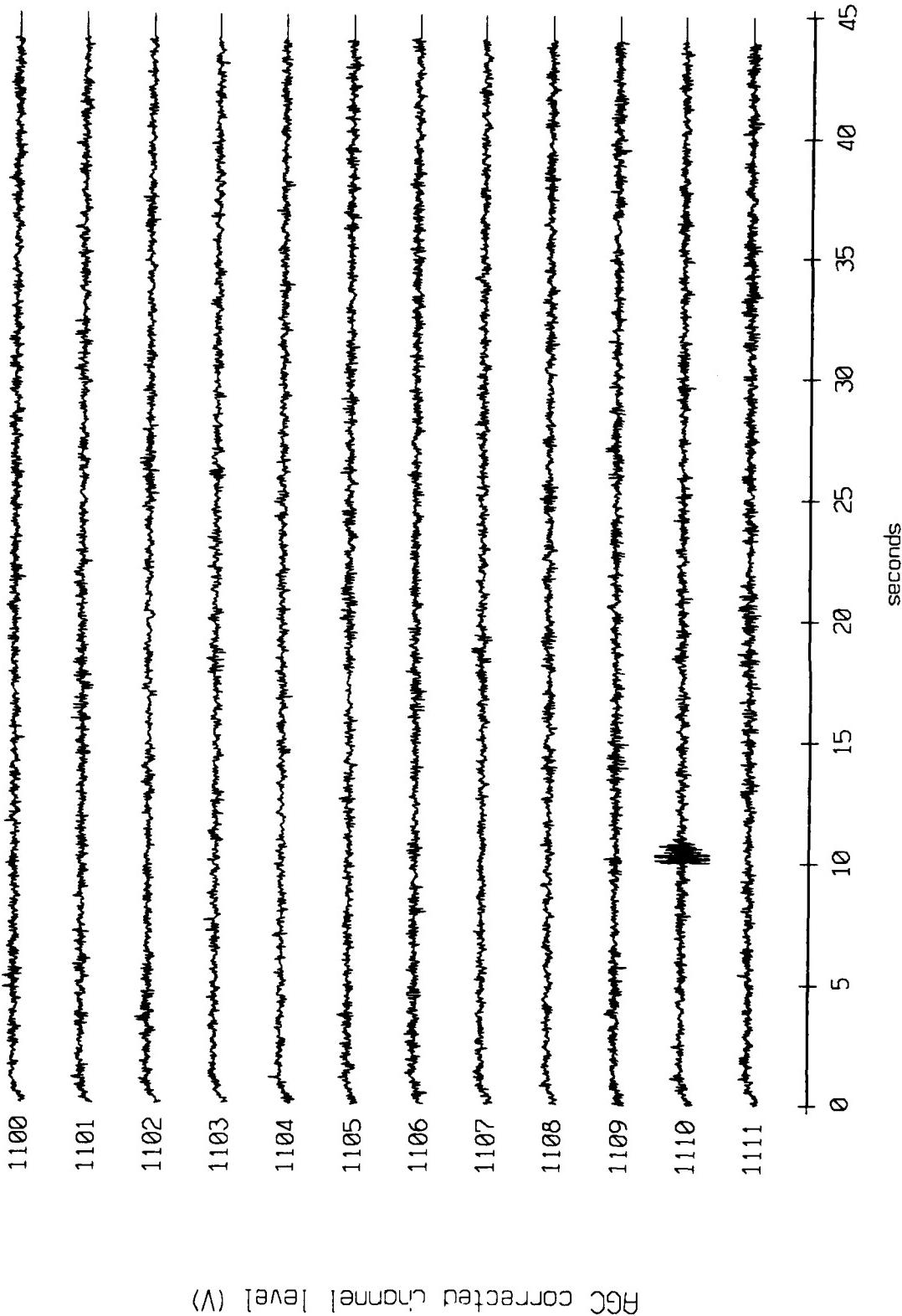


Figure X.2.7c

Float 7, September 1987 Trip - records 1100-1111 (x-axis)
vertical axis scale is approx. -1.0 to 1.0 volts

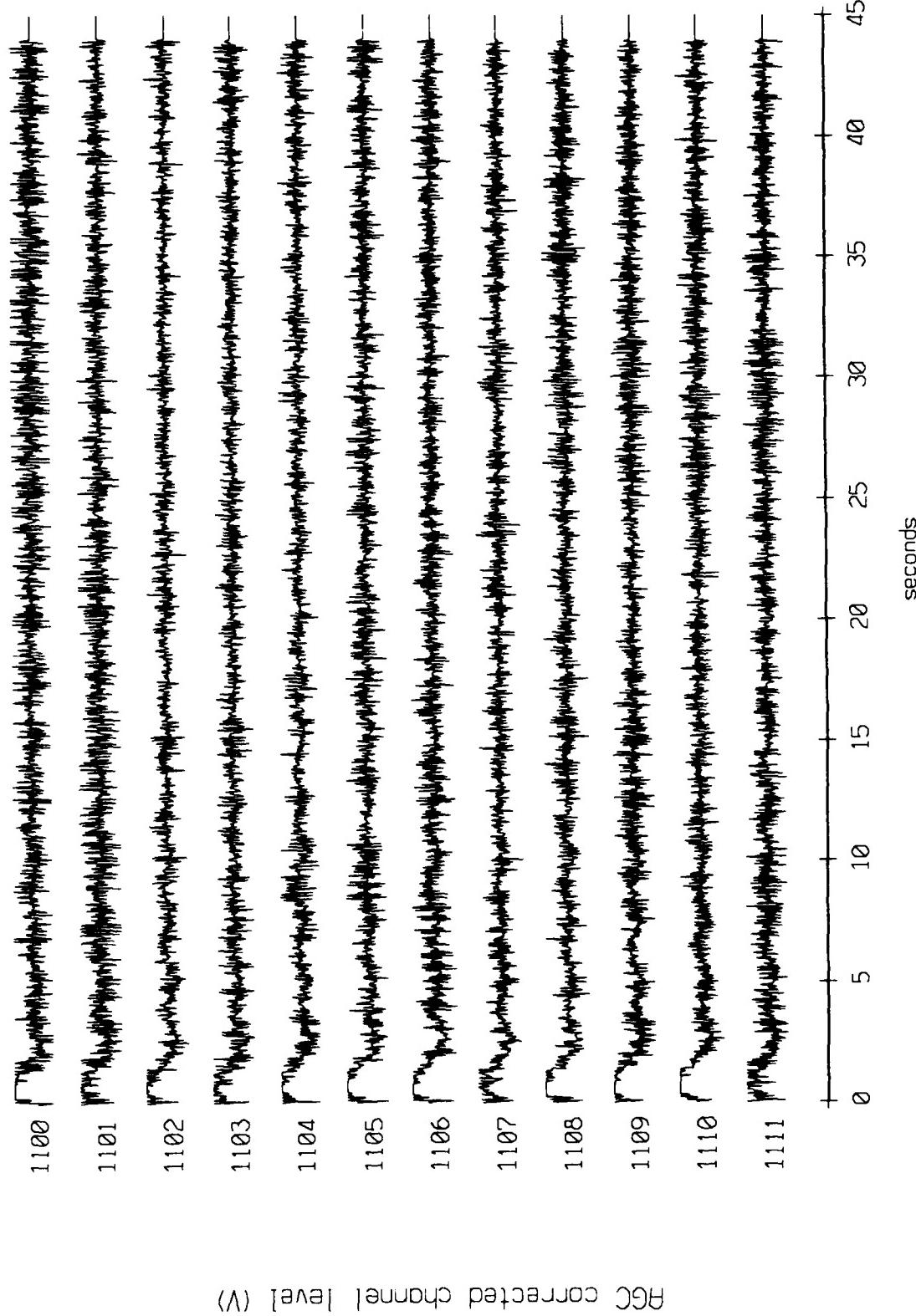


Figure λ.2.8a

Float 7, September 1987 Trip - records 1100-1111 (y-axis)
vertical axis scale is approx. -1.0 to 1.0 volts

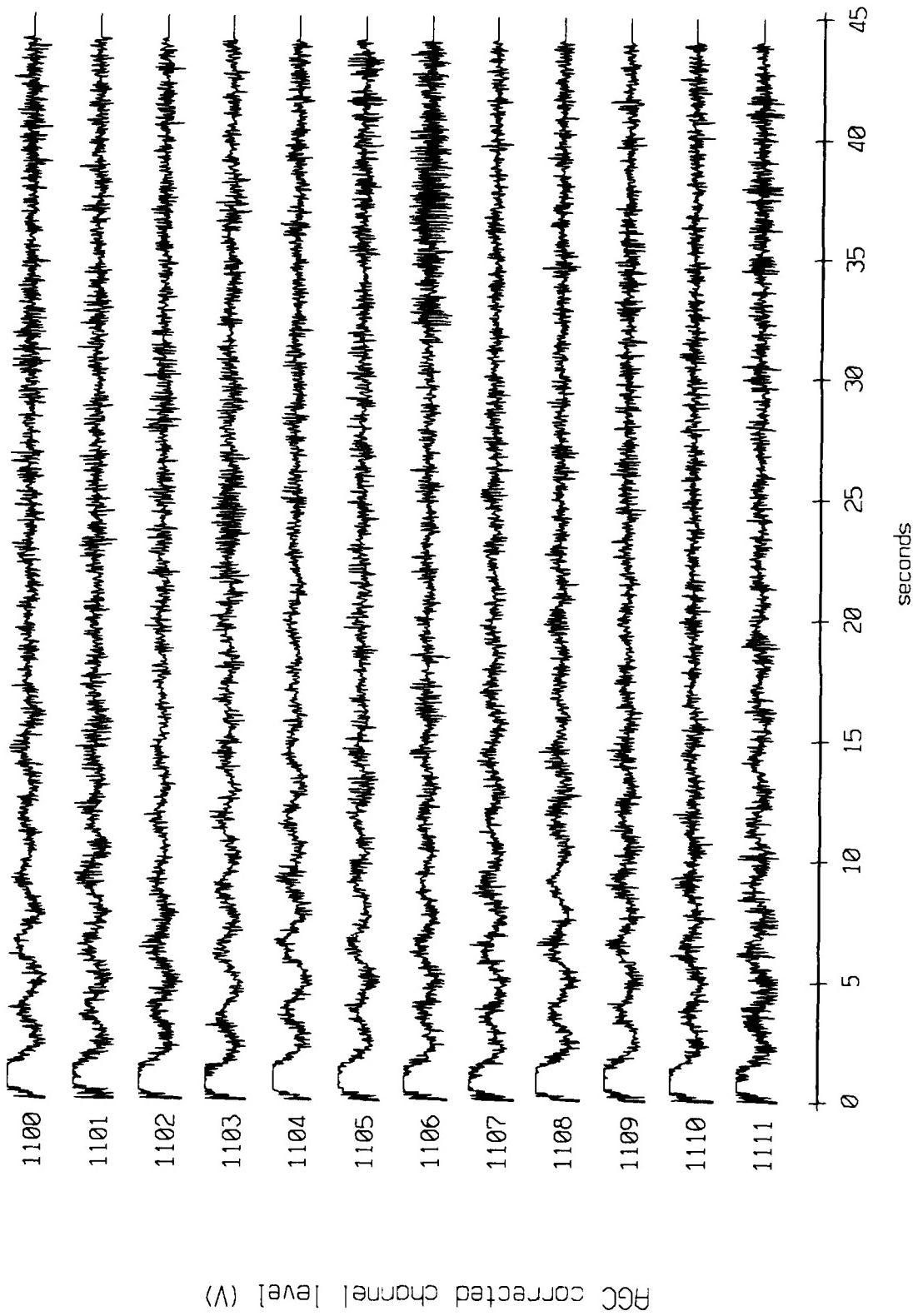


Figure X.2.8b

Flight 7, September 1987 Trip - records 1100-1111 (z-axis)
vertical axis scale is approx. -1.0 to 1.0 volts

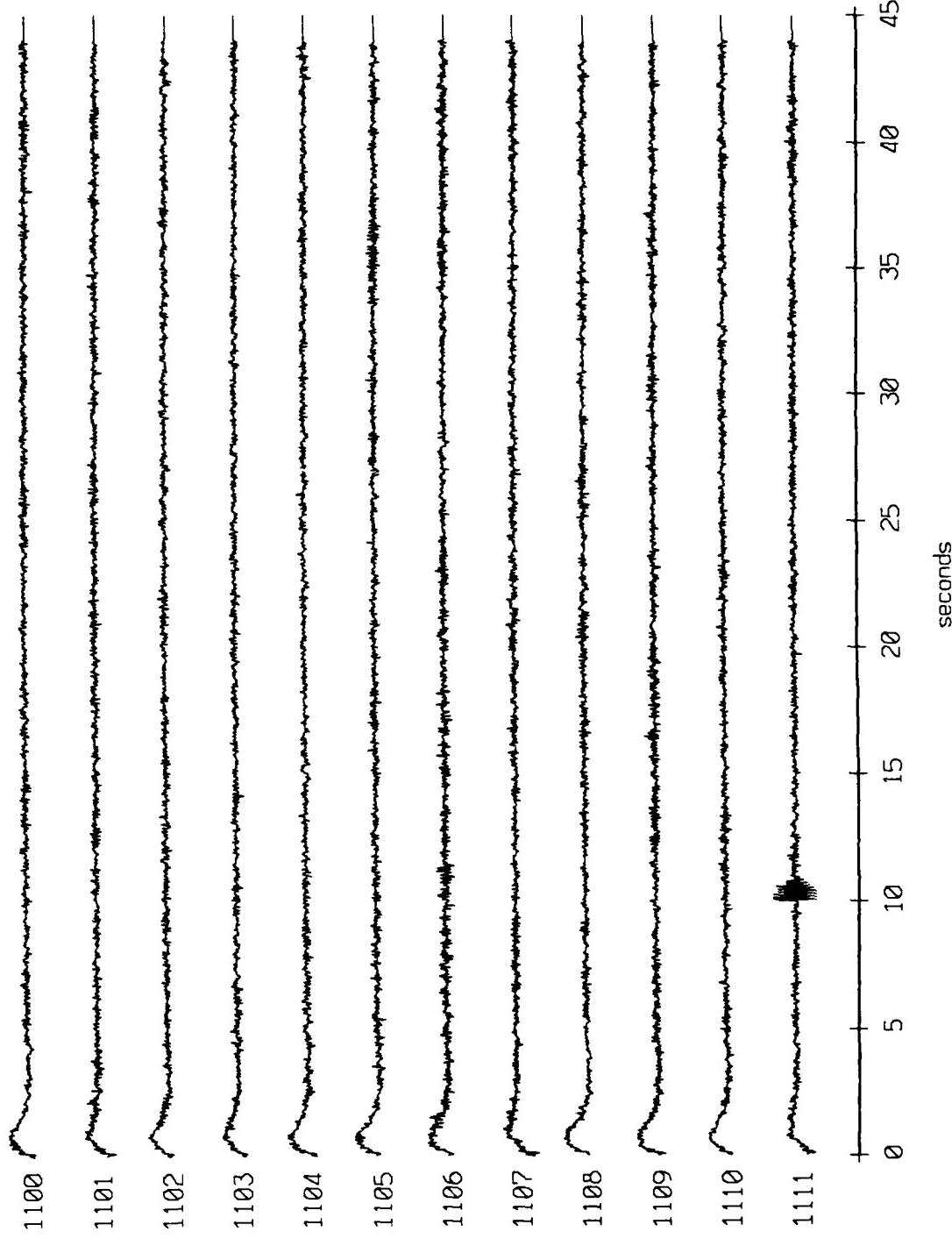


Figure X.2.8c

Float 0, September 1987 Sea Trip - records 1380-1391 (x-axis
vertical axis scale is approx. -1.0 to 1.0 volts)

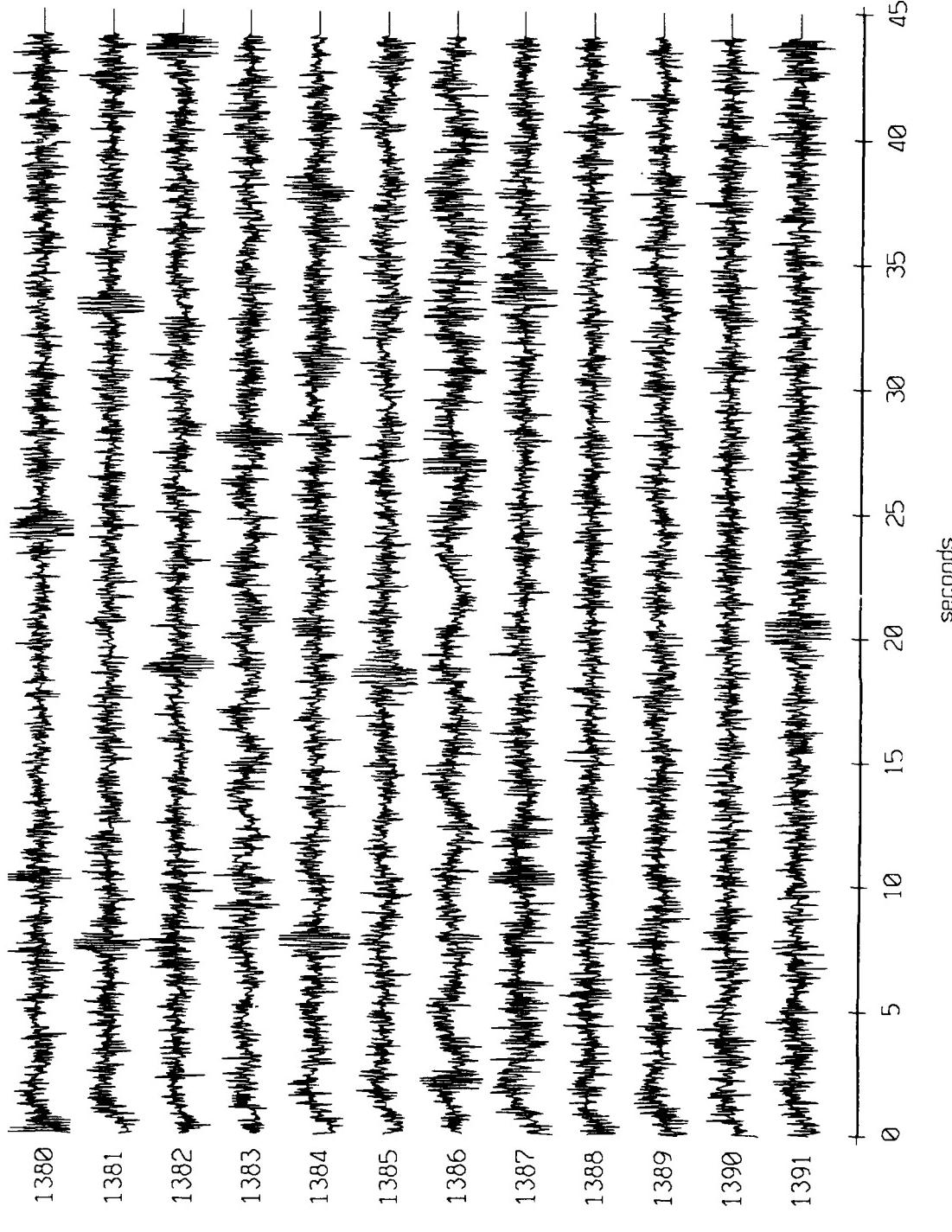


Figure X.3.1a

Float 0, September 1987 Sea Trip - records 1380-1391 (y-axis vertical, axis scale is approx. -1.0 to 1.0 volts)

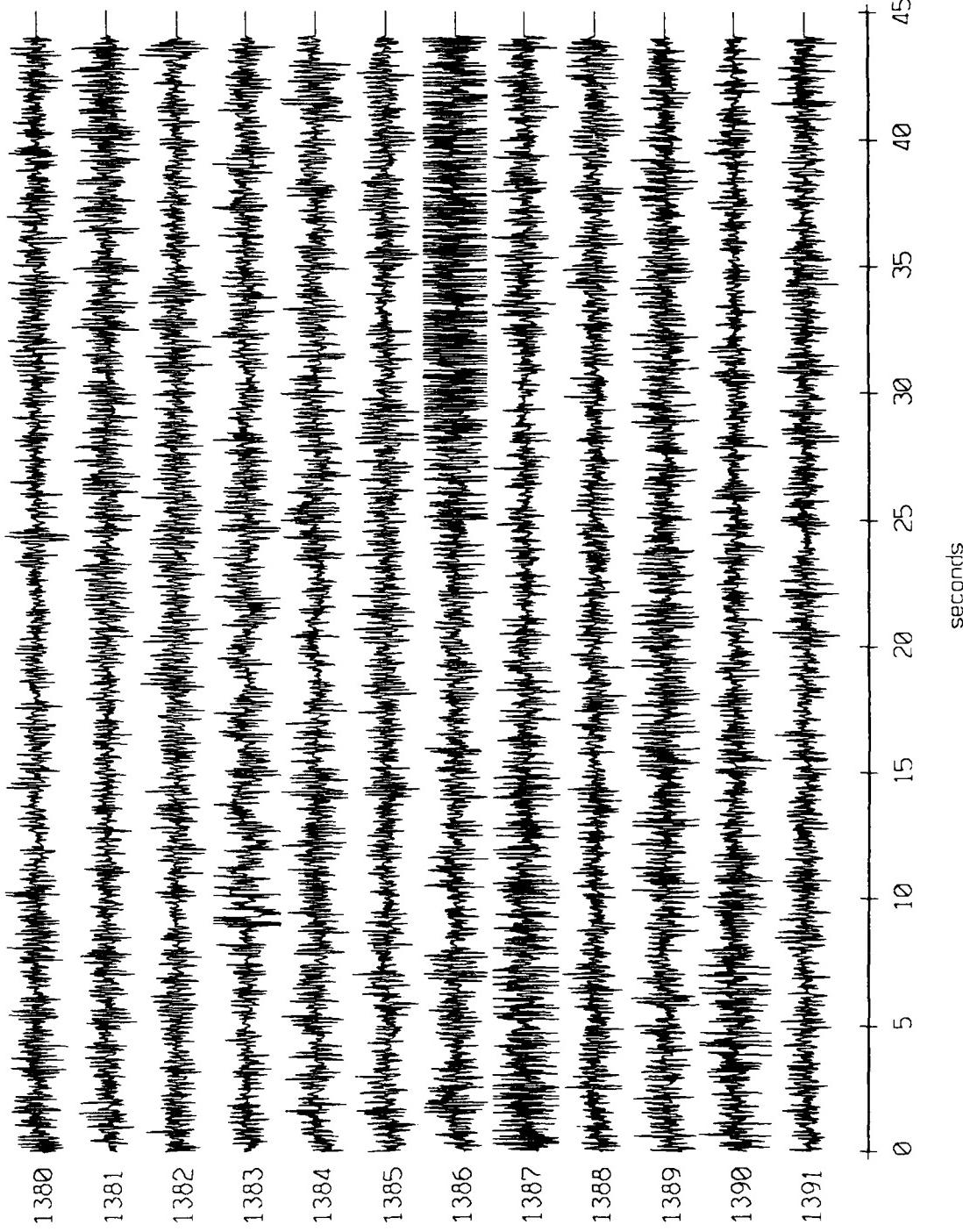


Figure X.3.1b

Flight 0, September 1987 Sea Trip - records 1380-1391 (z-axis vertical axis scale is approx. 1.0 volts)

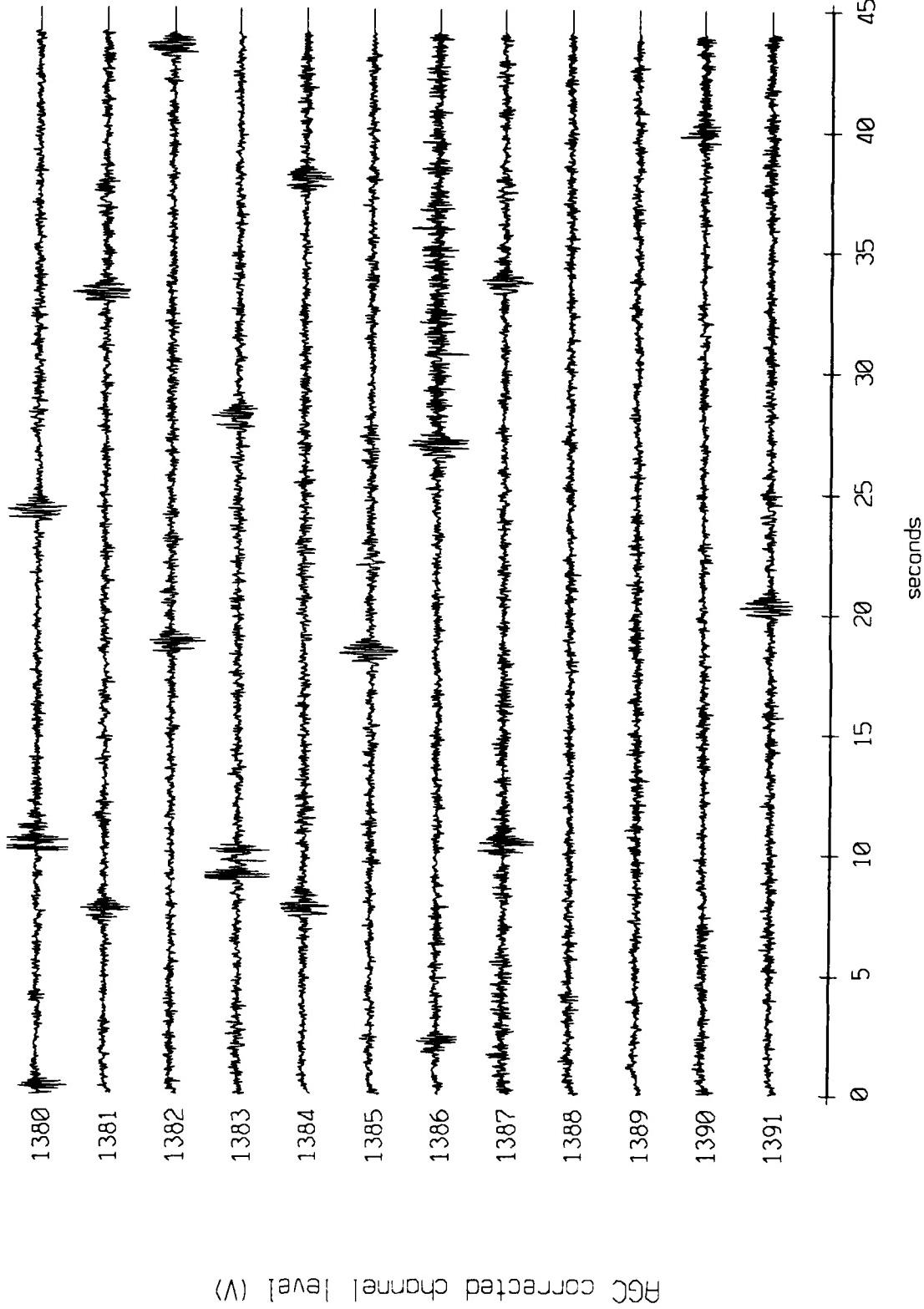


Figure X.3.1c

Flight 1, September 1987 Sea Trip - records 1380-1391 (x-axis
vertical axis scale is approx. -1.0 to 1.0 volts

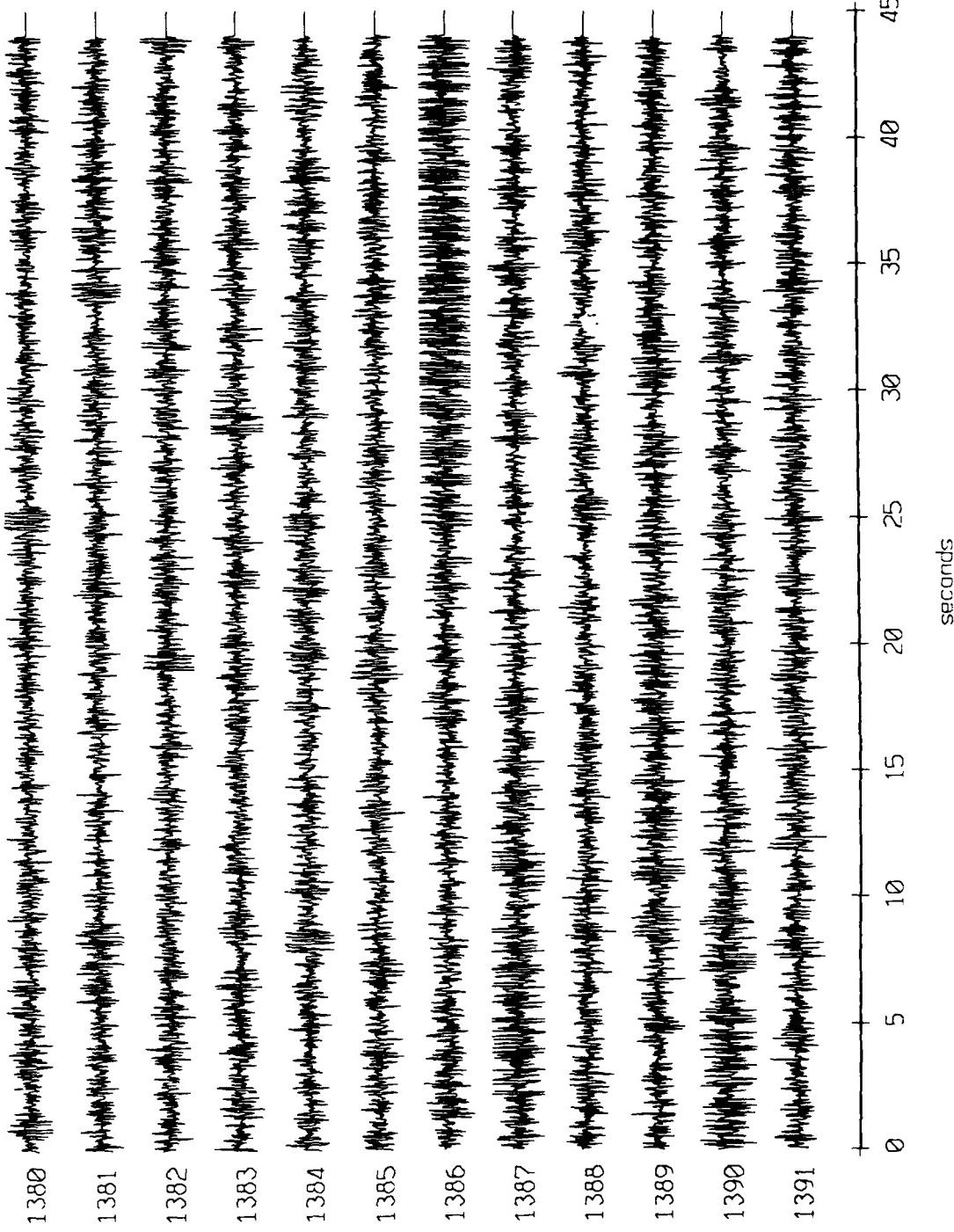


Figure X.3.2a

Float 1, September 1987 Sea Trip - records 1380-1391 (y-axis)
vertical axis scale is approx. -1.0 to 1.0 volts

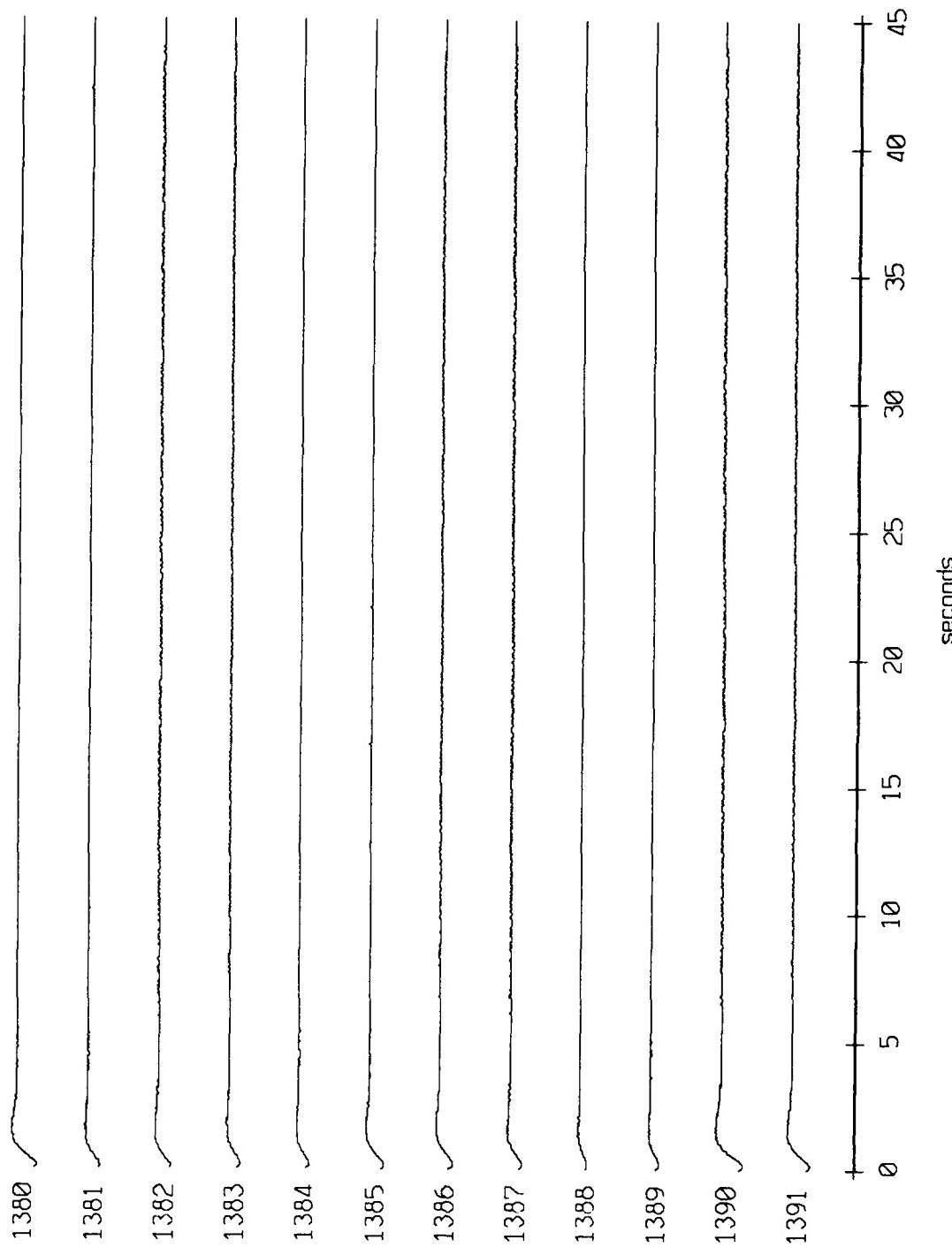


Figure X.3.2b

Float 1, September 1987 Sea Trip - records 1380-1391 (z-axis)
vertical axis scale is approx. -1.0 to 1.0 volts

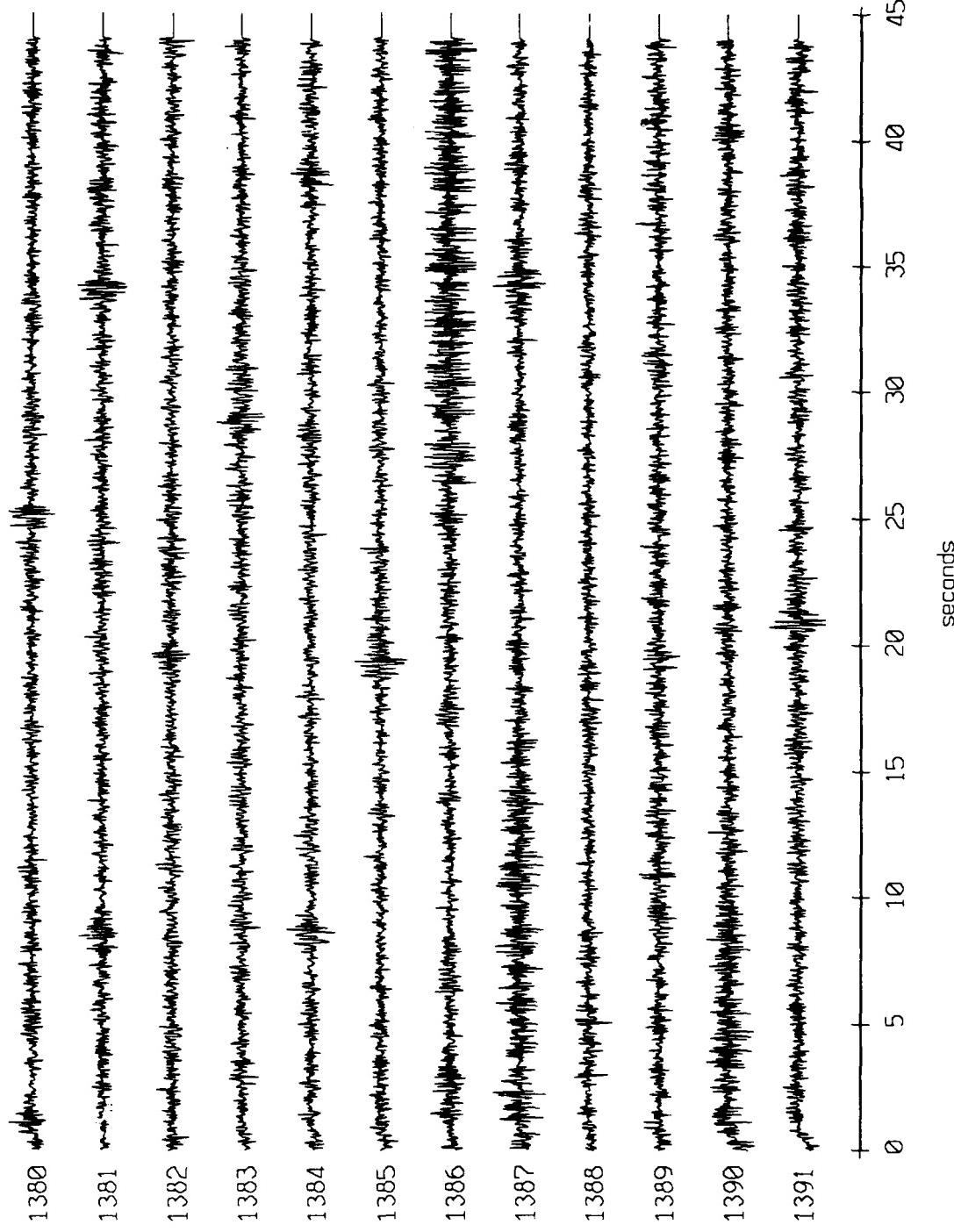


Figure X.3.2c

Float 2, September 1987 Sea Trip - records 1380-1391 (x-axis)
vertical axis scale is approx. -1.0 to 1.0 volts

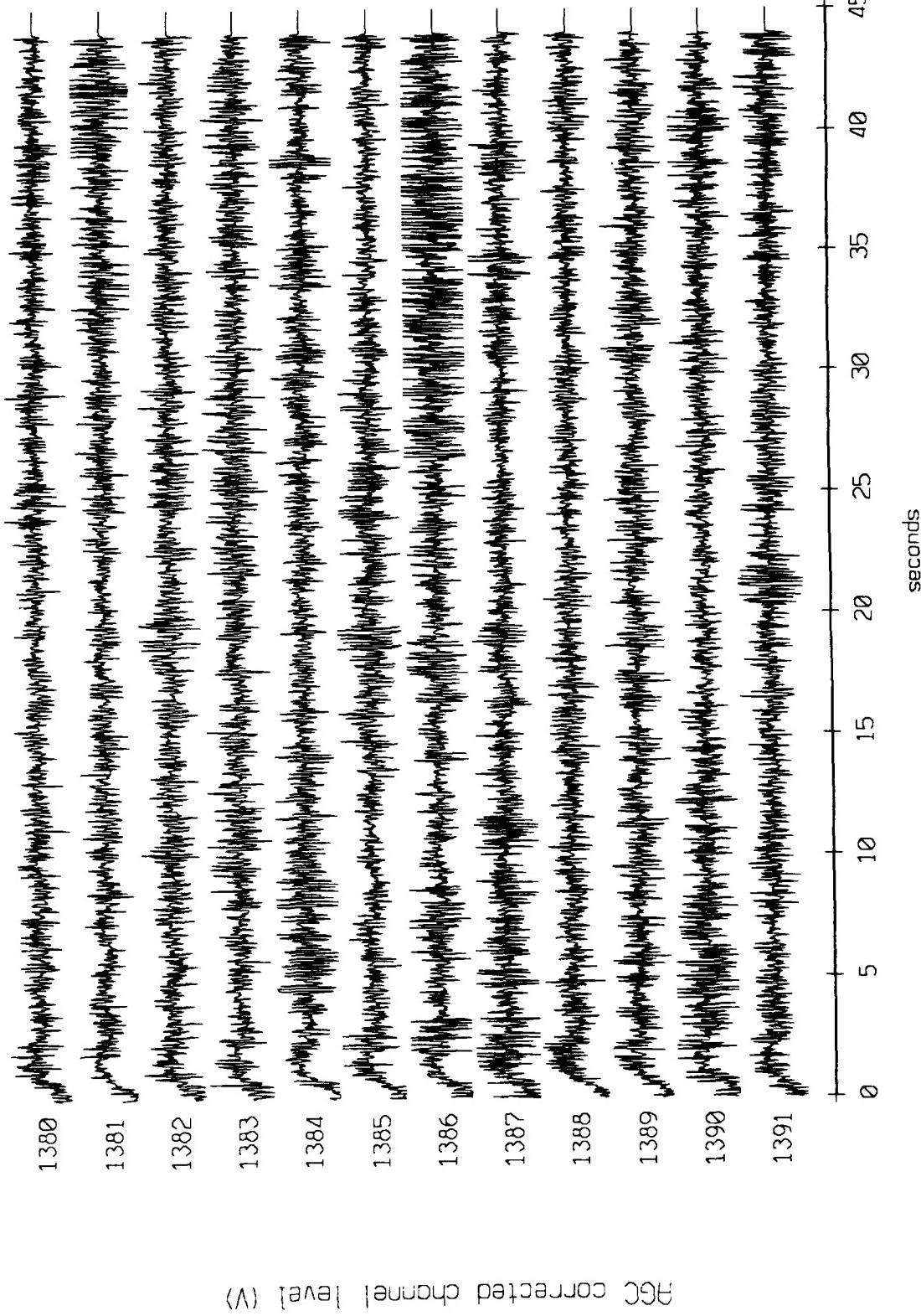


Figure X.3.3a

Float 2, September 1987 Sea Trip - records 1380-1391 (y-axis)
vertical axis scale is approx. -1.0 to 1.0 volts

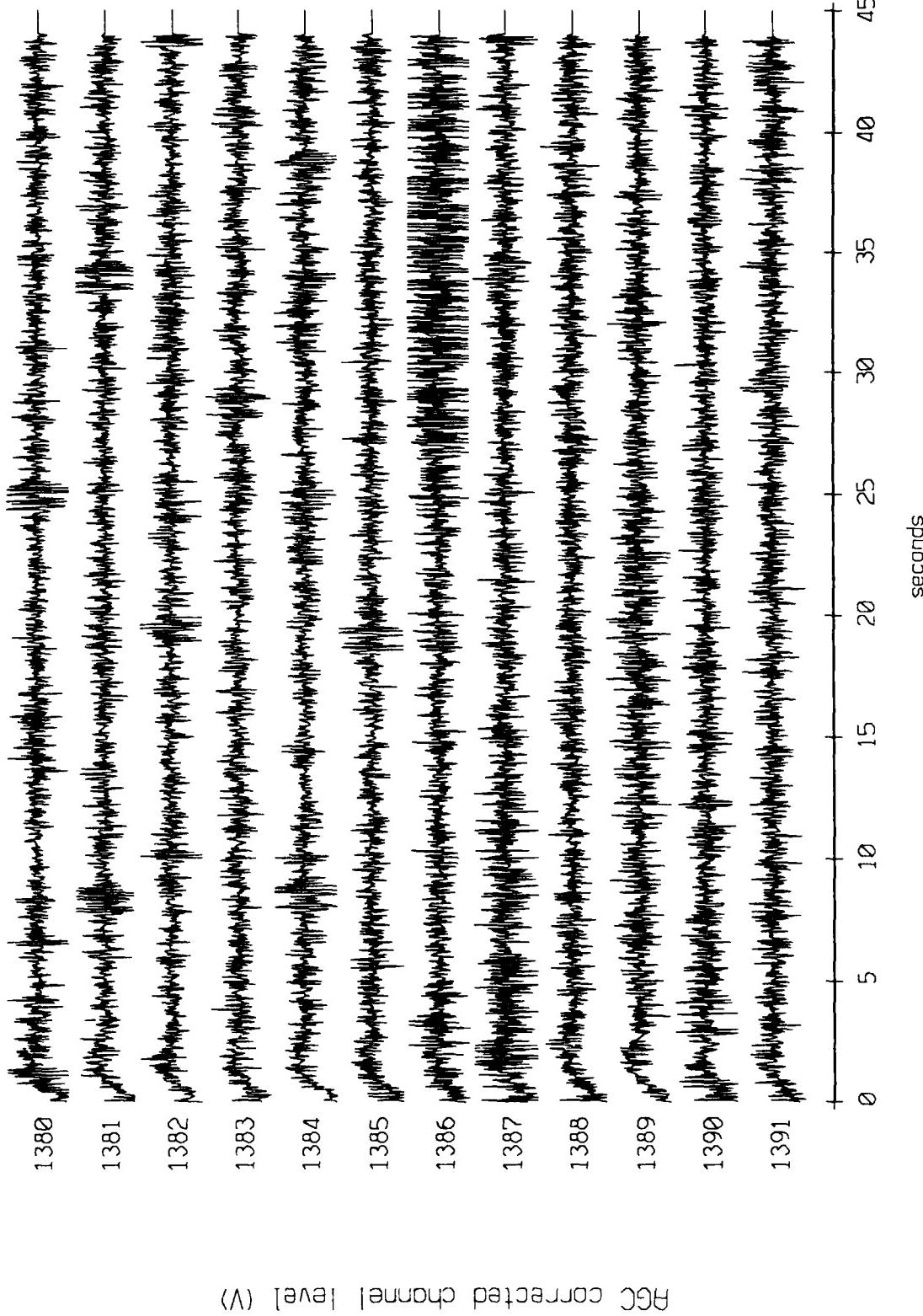


Figure X.3.3b

Flood 2, September 1987 Sea Trip - records 1380-1391 (z-axis)
vertical axis scale is approx. -1.0 to 1.0 volts

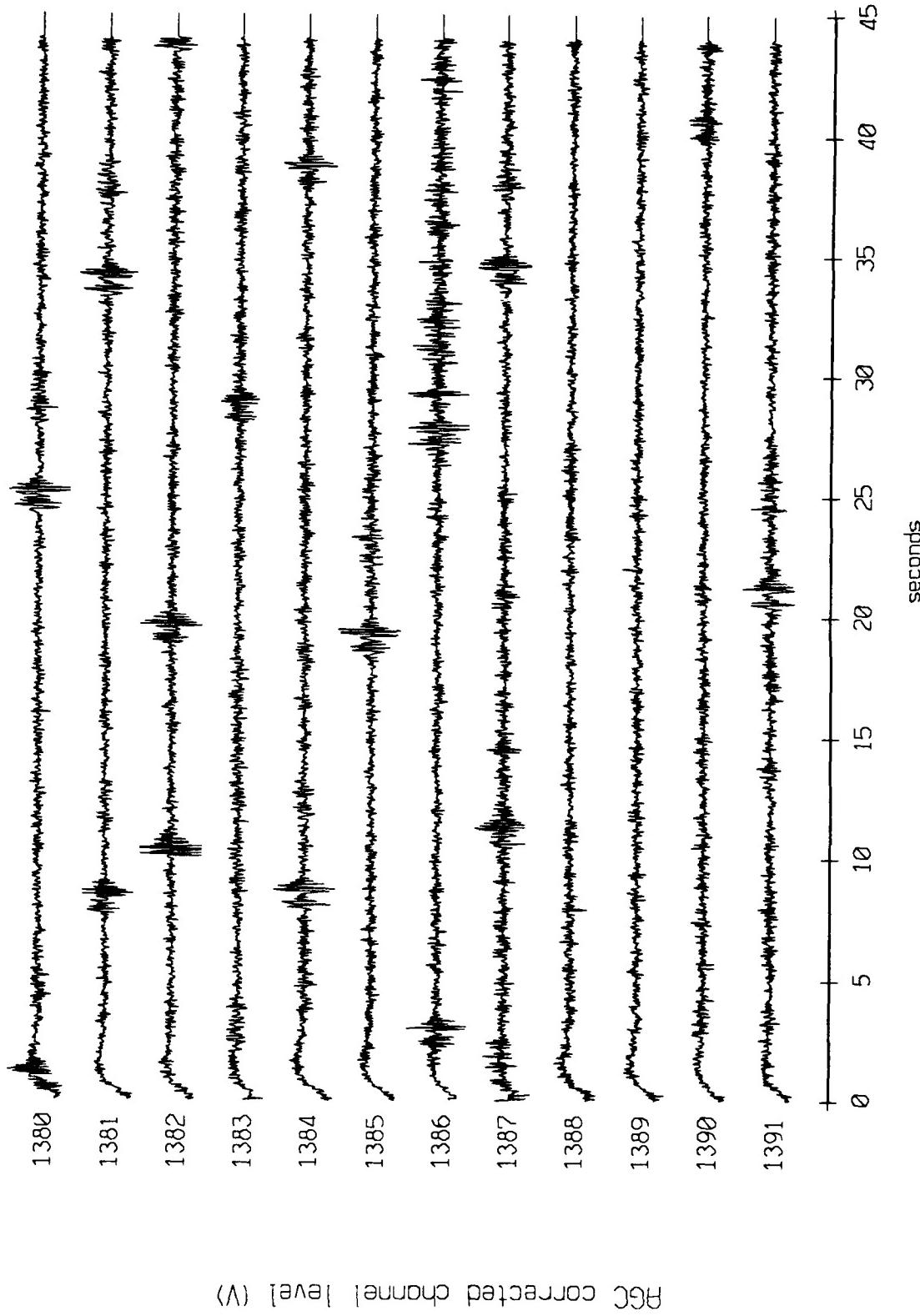


Figure X.3.3c

Flood 3, September 1987 Sea Trip - records 1380-1391 (x-axis is vertical axis scale is approx. -1.0 to 1.0 volts)

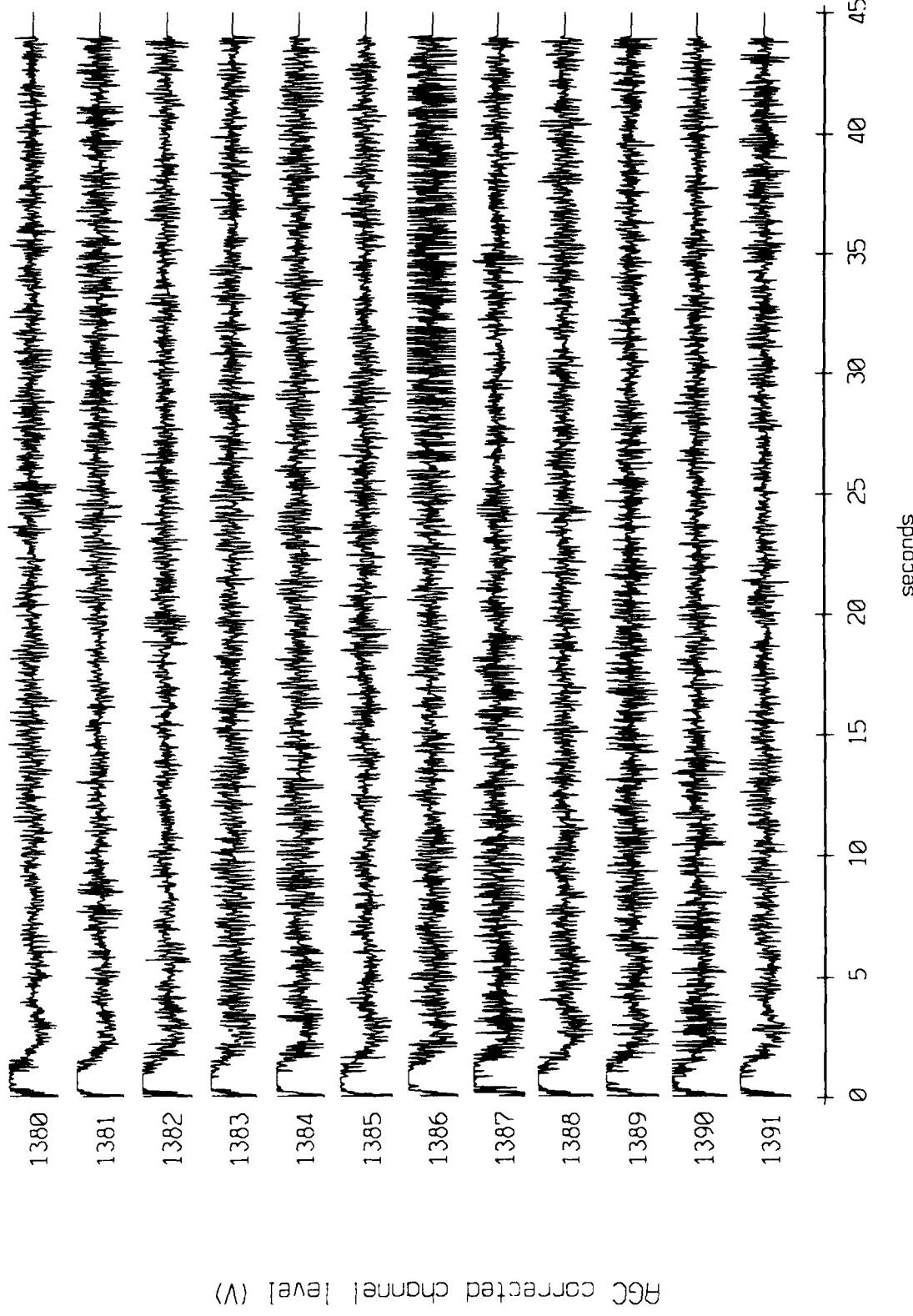


Figure X.3.4a

Float 3, September 1987 Sea Trip records 1380-1391 (y-axis vertical axis scale is approx. 1.0 to 1.0 volts)

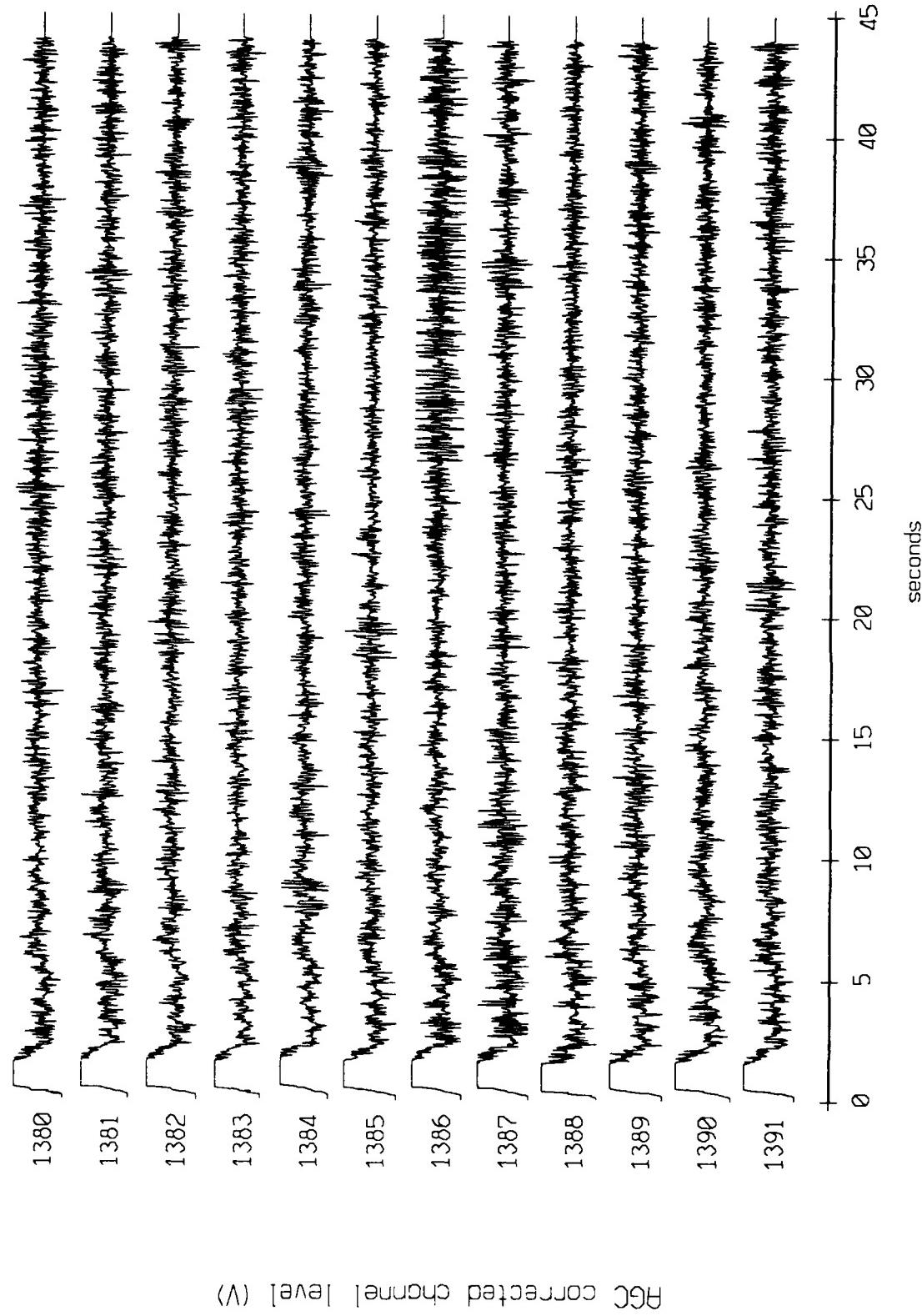


Figure X.3.4b

Float 3, September 1987 Sea Trip - records 1380-1391 (z-axis)
vertical axis scale is approx. -1.0 to 1.0 volts

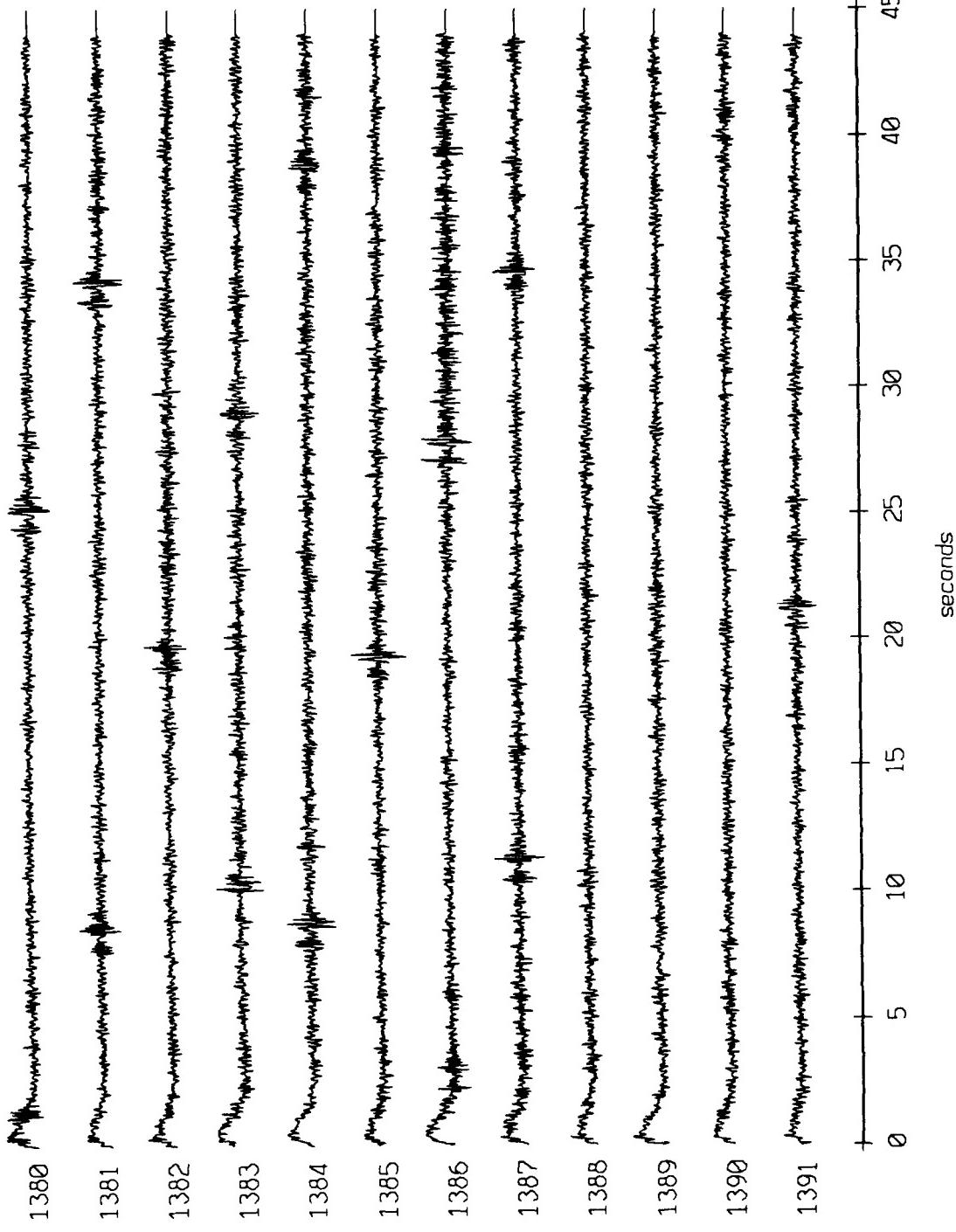


Figure X.3.4c

Float 4, September 1987 Sea Trip - records 1380-1391 (x-axis
vertical axis scale is approx. 1.0 to 1.0 volts)

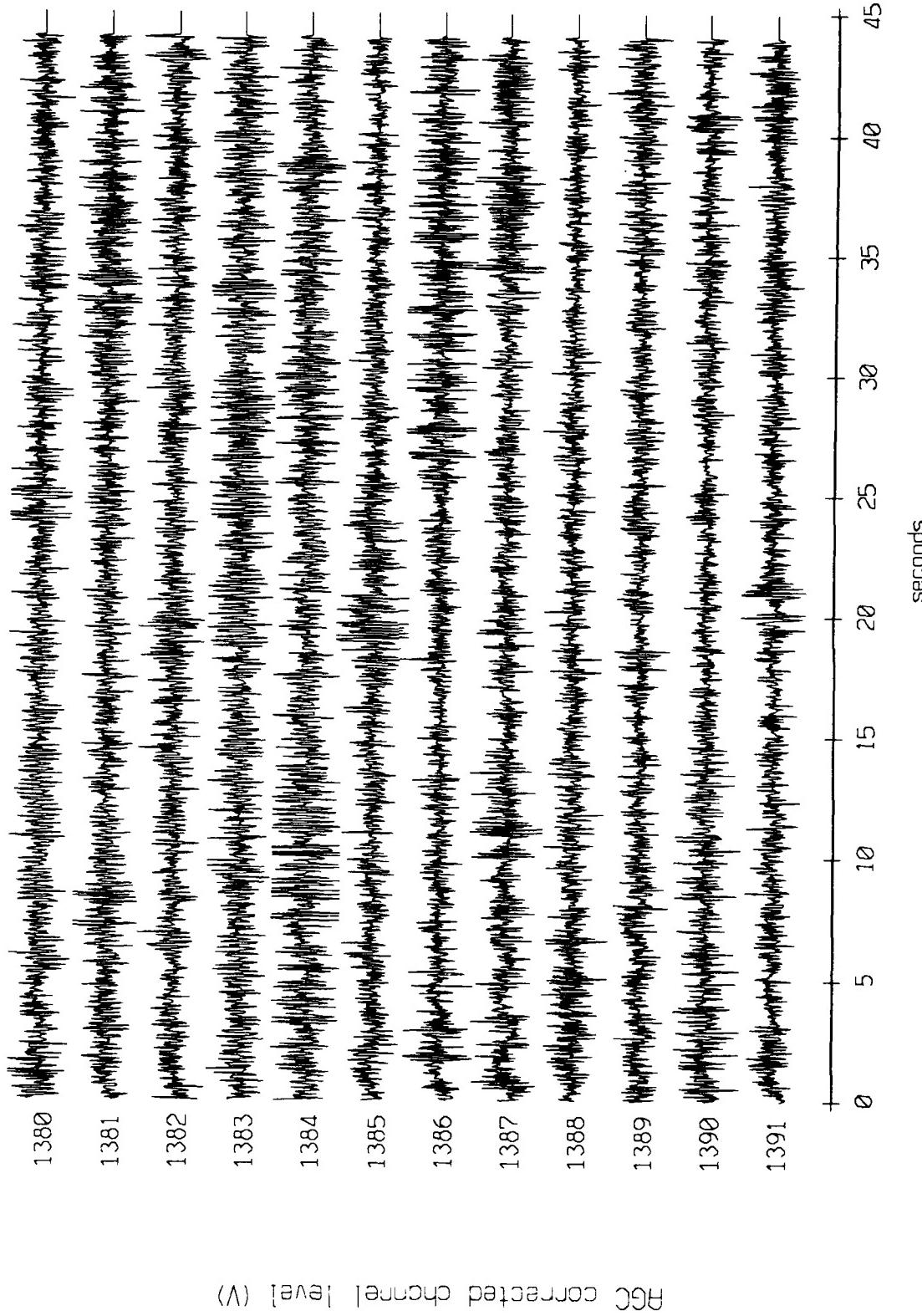


Figure X.3.5a

Float 4, September 1987 Sea Trip - records 1380-1391 (y-axis)
vertical axis scale is approx. -1.0 to 1.0 volts

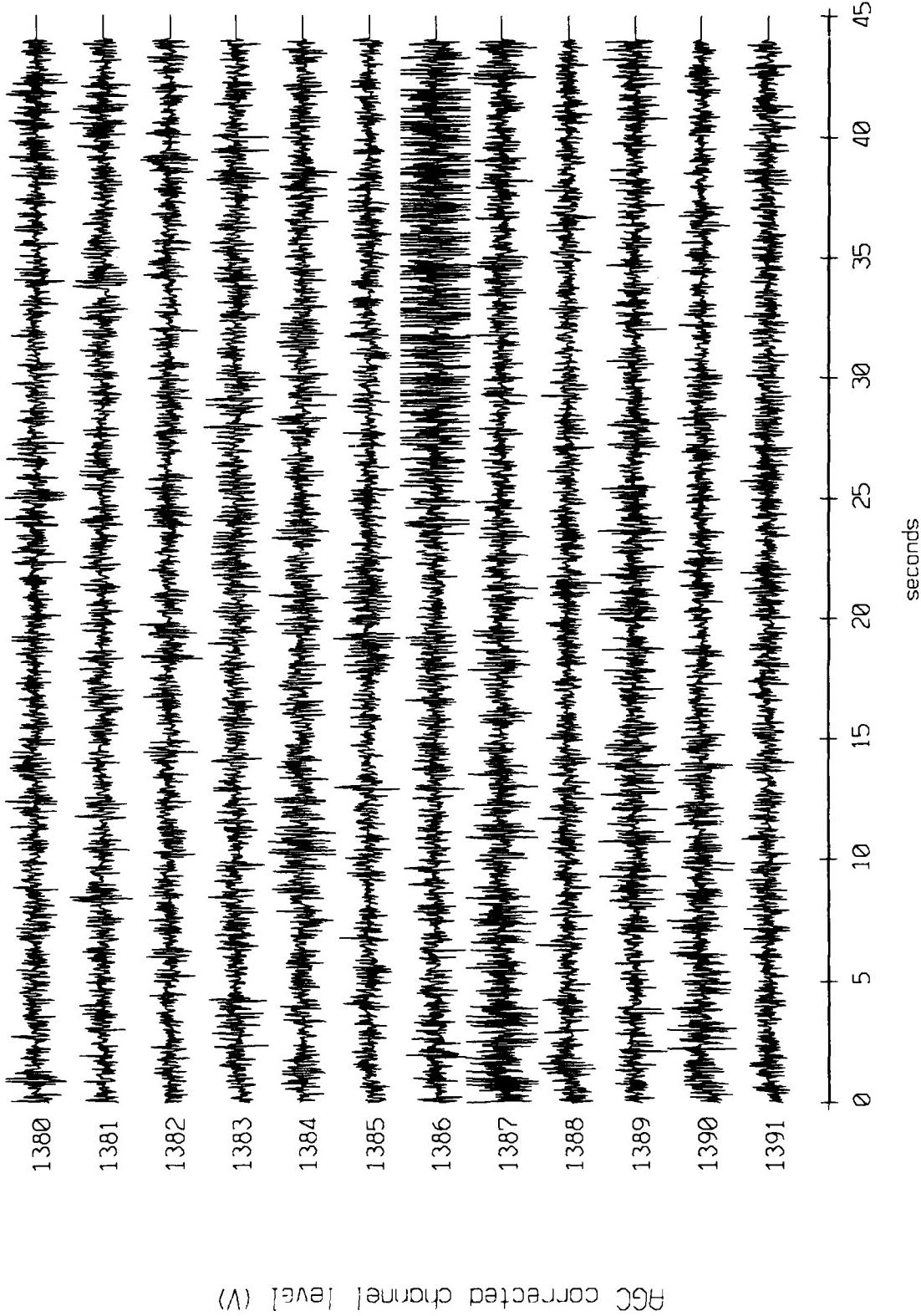


Figure X.3.5b

Float 4, September 1987 Sea Trip - records 1380-1391 (z-axis)
vertical axis scale is approx. -1.0 to 1.0 volts

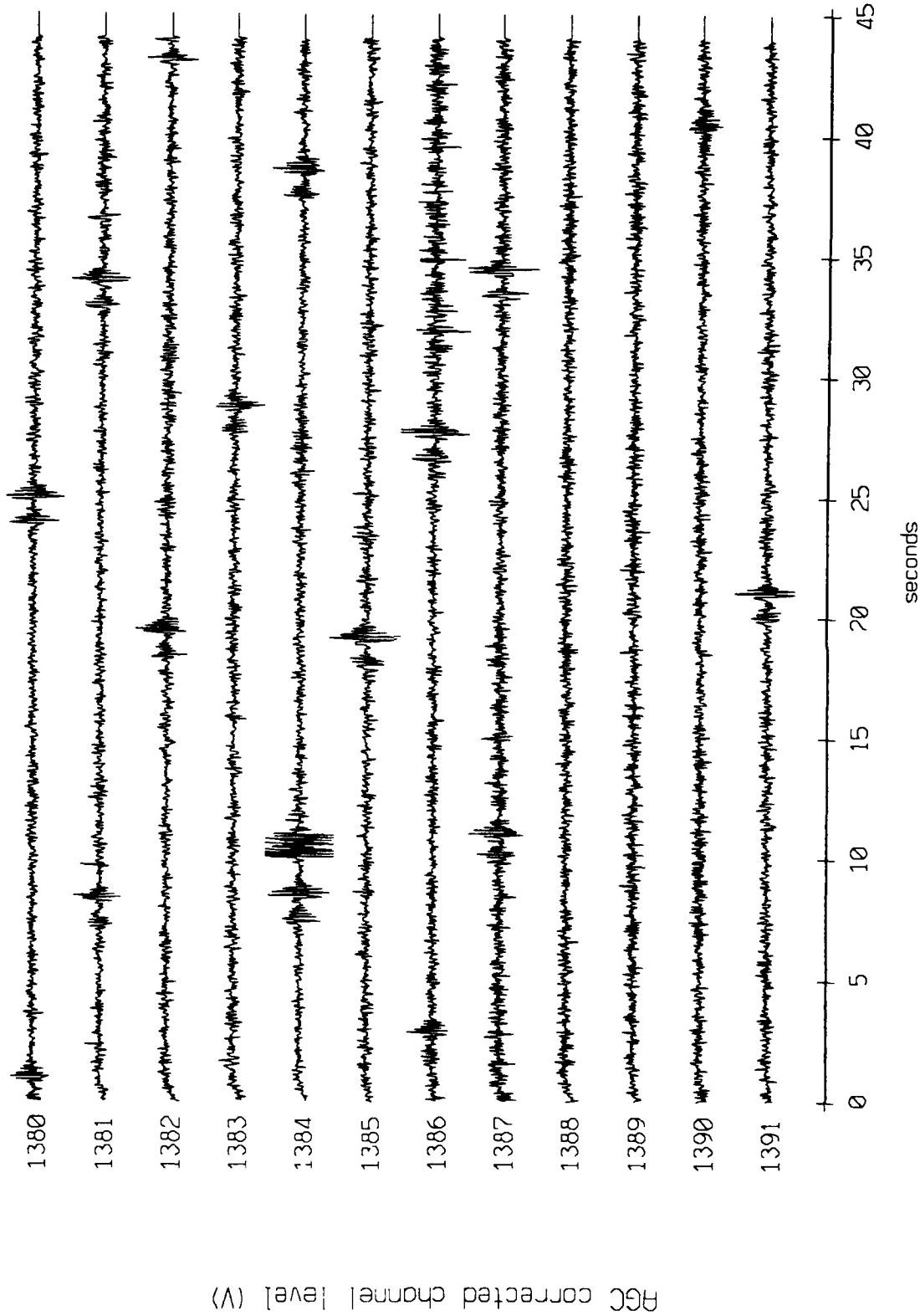


Figure X.3.5c

Flight 5, September 1987 Trip - records 1380-1391 (x-axis)
vertical axis scale is approx. -1.0 to 1.0 volts

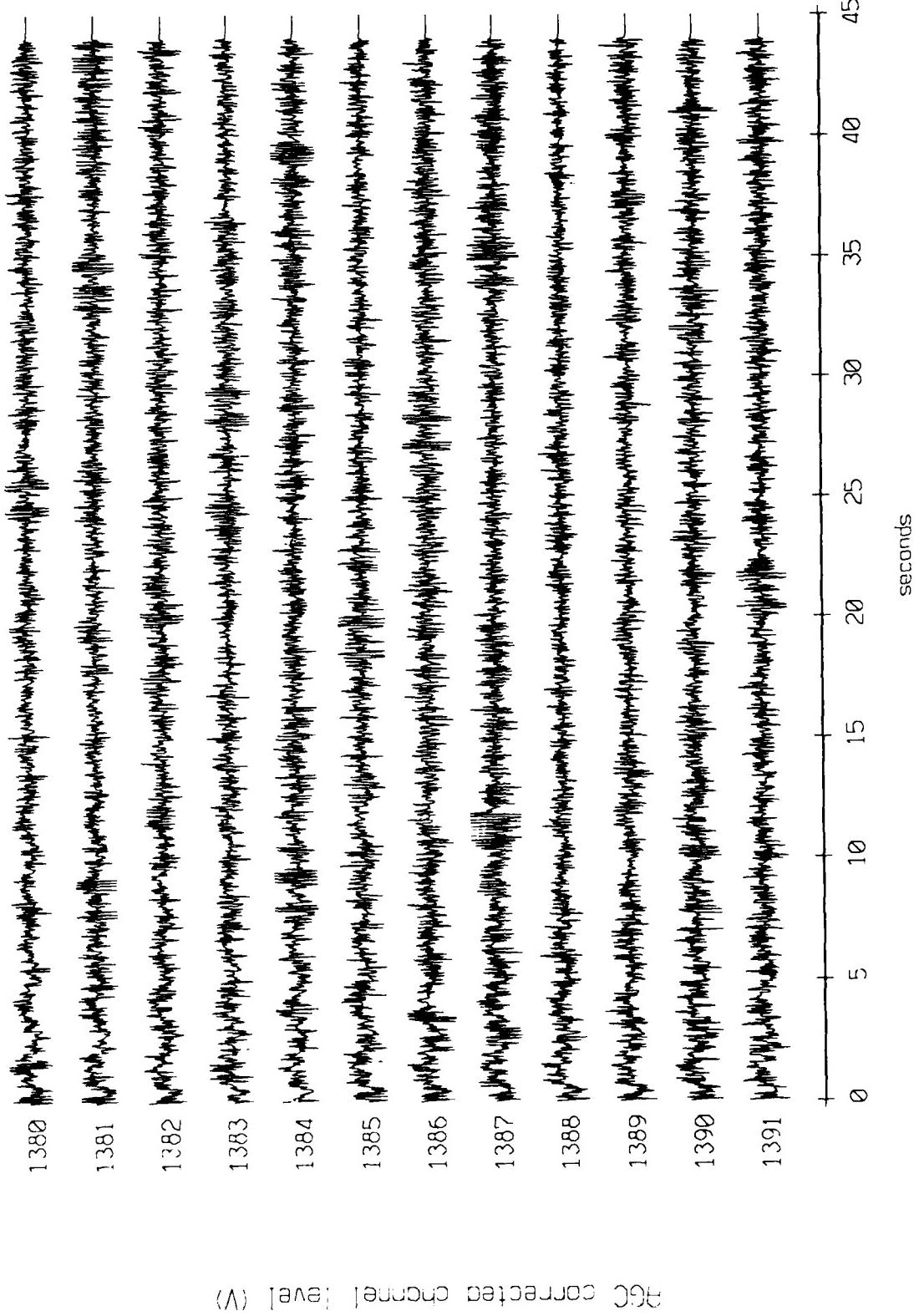


Figure X.3.6a

Float 5, September 1987 Trip - records 1380-1391 (y-axis)
vertical axis scale is approx. -1.0 to 1.0 volts

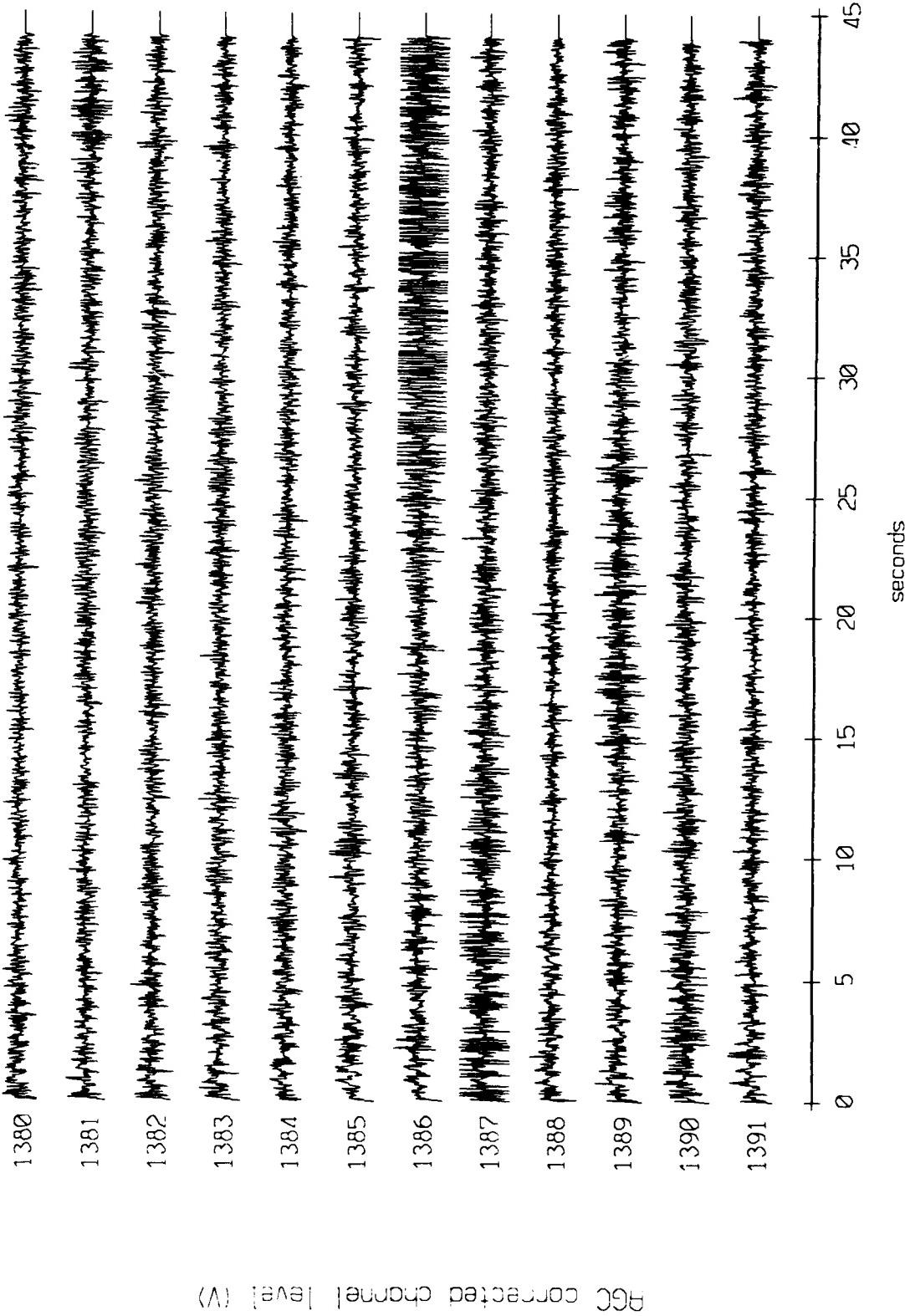


Figure X.3.6b

Flight 5, September 1987 Trip - records 1380-1391 (z-axis)
vertical axis scale is approx. -1.0 to 1.0 volts

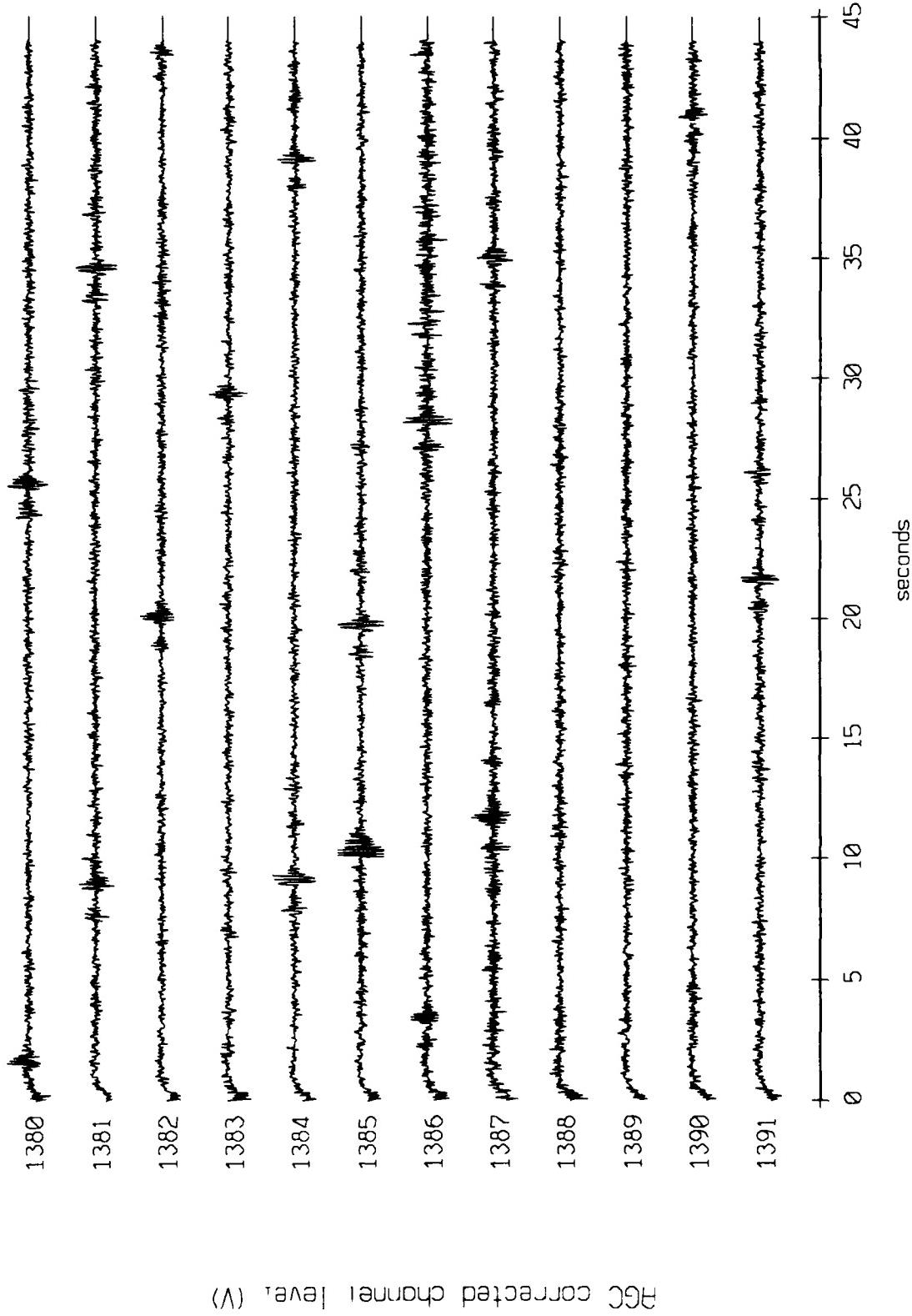


Figure X.3.6c

Float 6, September 1987 Trip - records 1380-1391 (x-axis)
vertical axis scale is approx. -1.0 to 1.0 volts

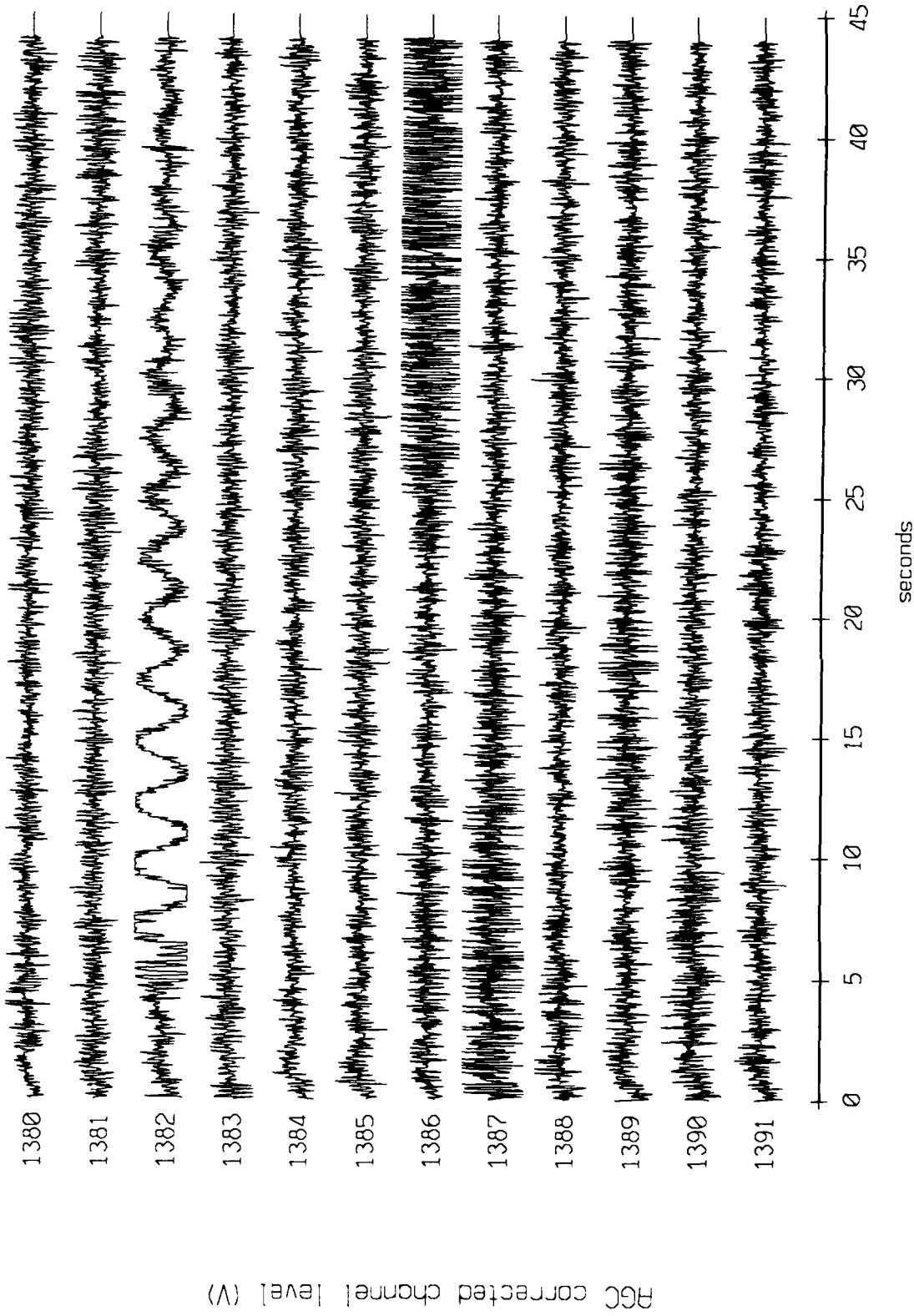


Figure X.3.7a

Float 6, September 1987 Trip - records 1380-1391 (y-axis
vertical axis scale is approx. -1.0 to 1.0 volts

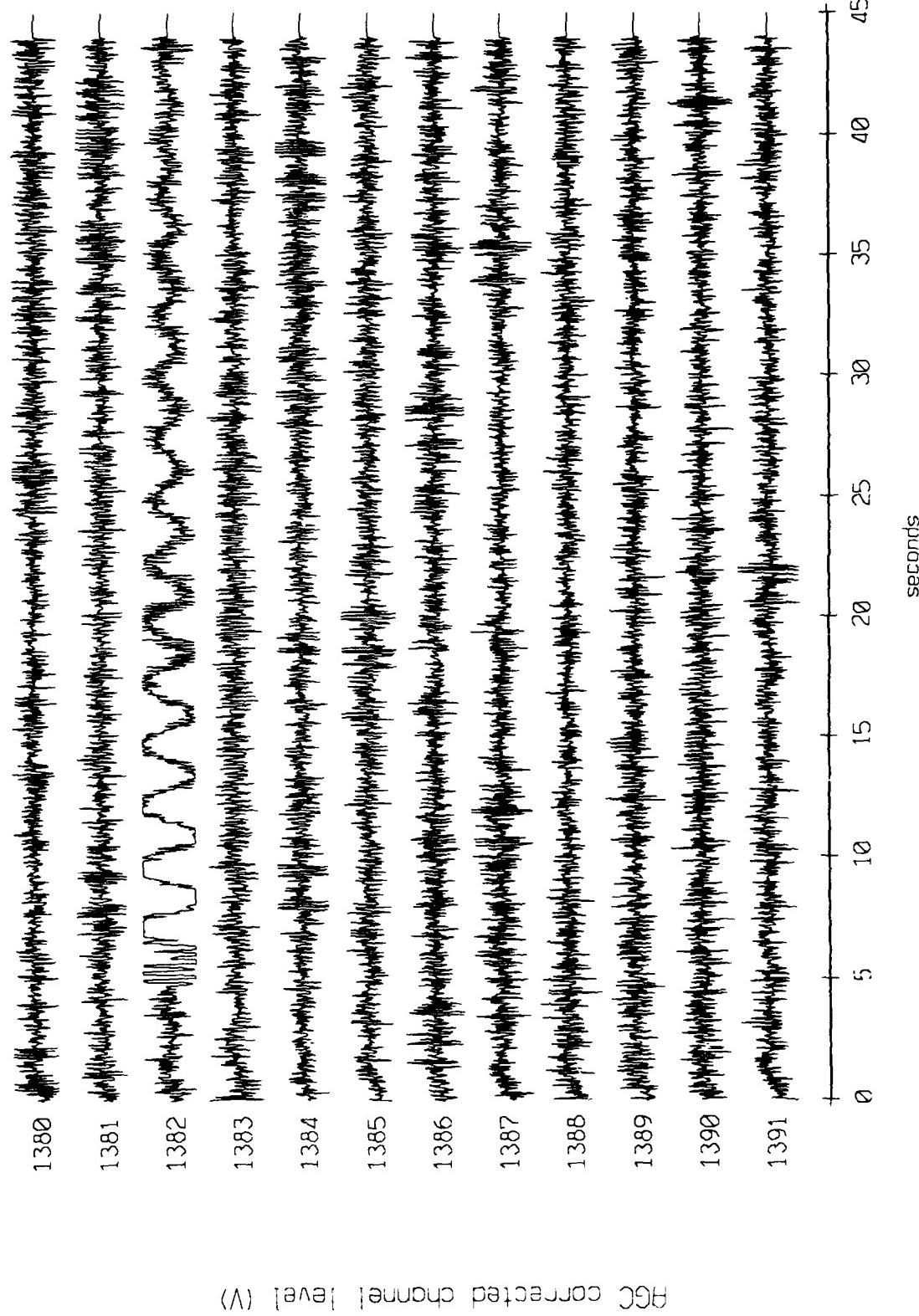


Figure X.3.7b

Flight 6, September 1987 Trip - records 1380-1391 (z-axis)
vertical axis scale is approx. -1.0 to 1.0 volts

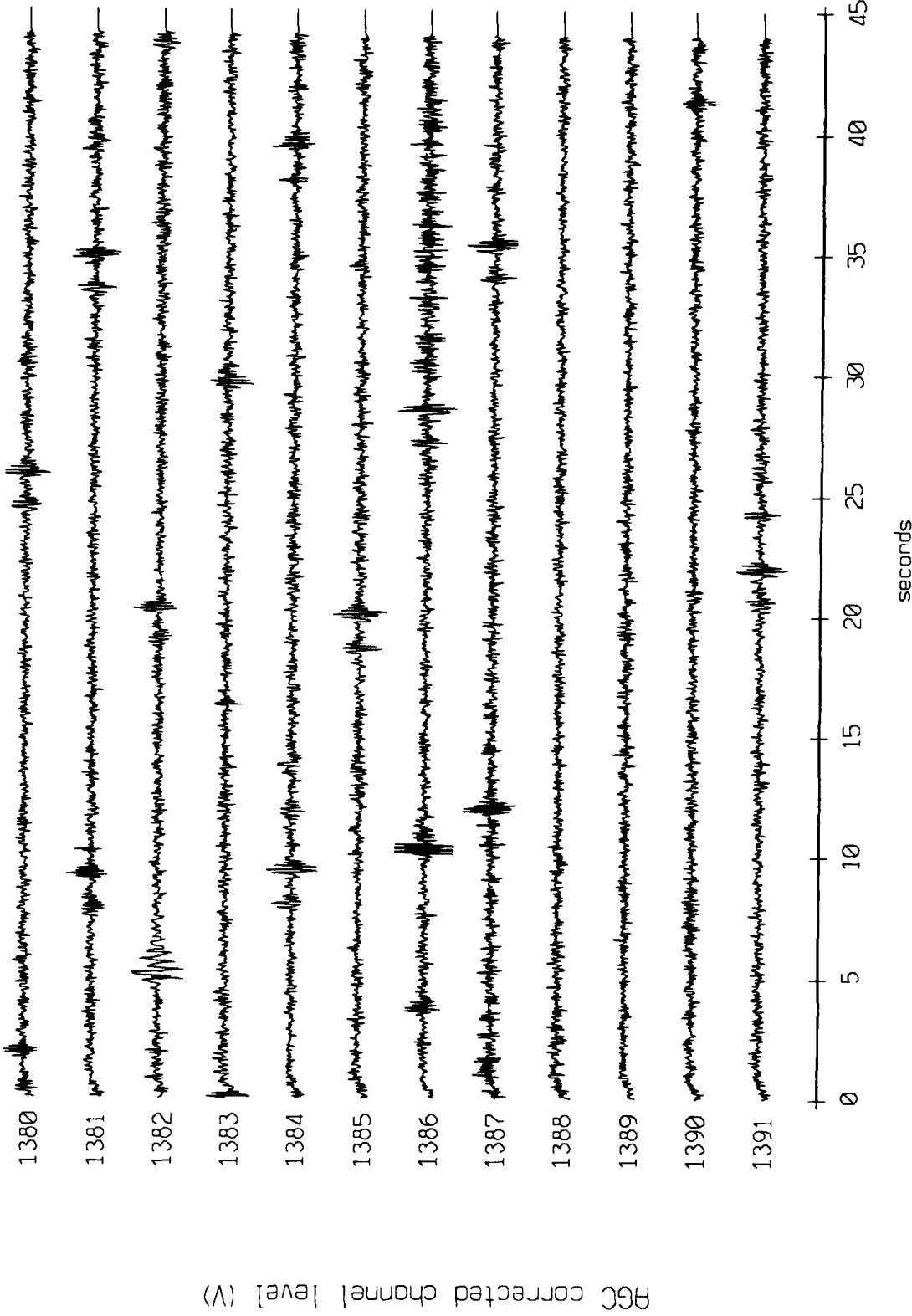


Figure X.3.7c

Flood 7, September 1987 Trip - records 1380-1391 (x-axis)
vertical axis scale is approx. -1.0 to 1.0 volts

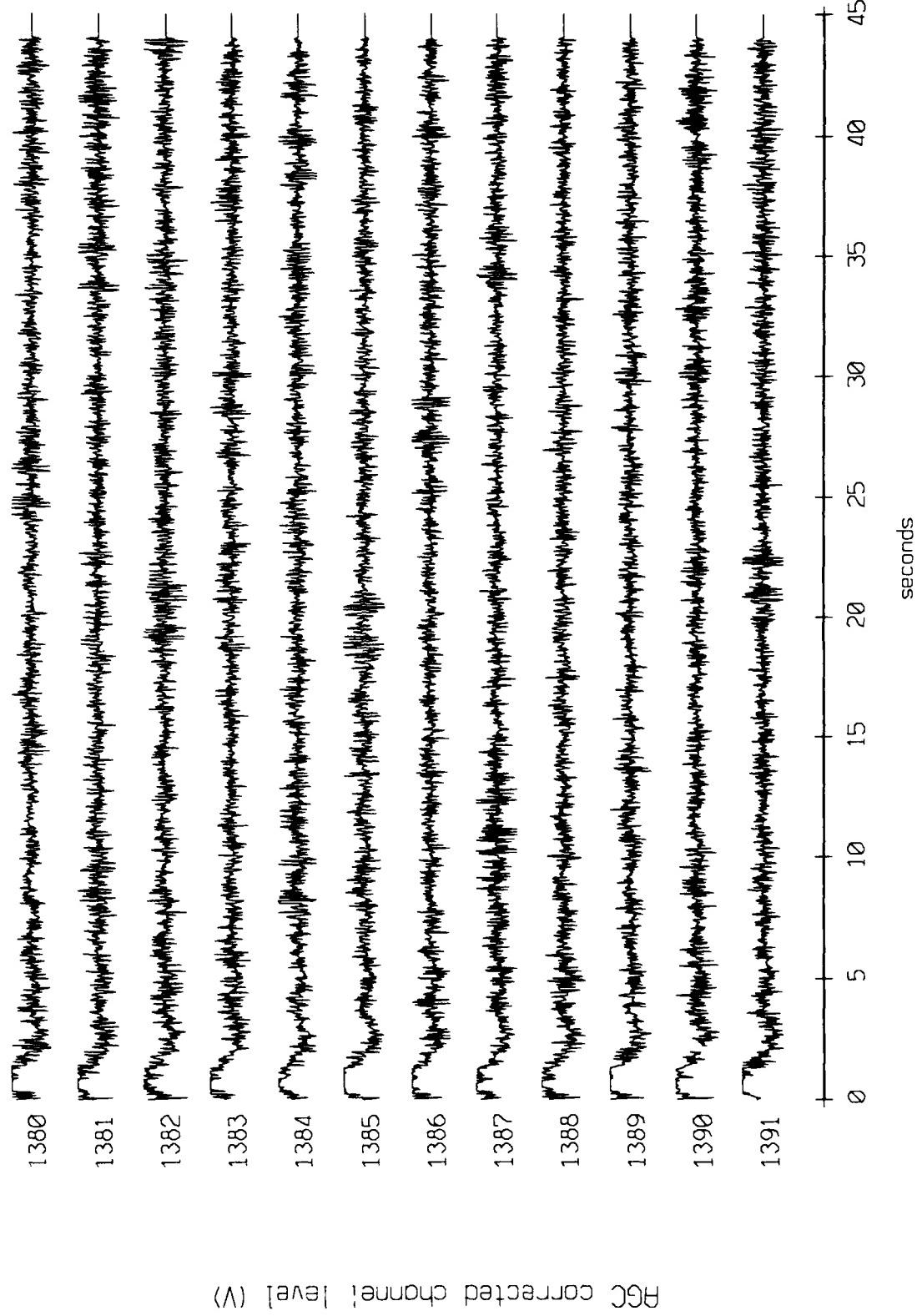
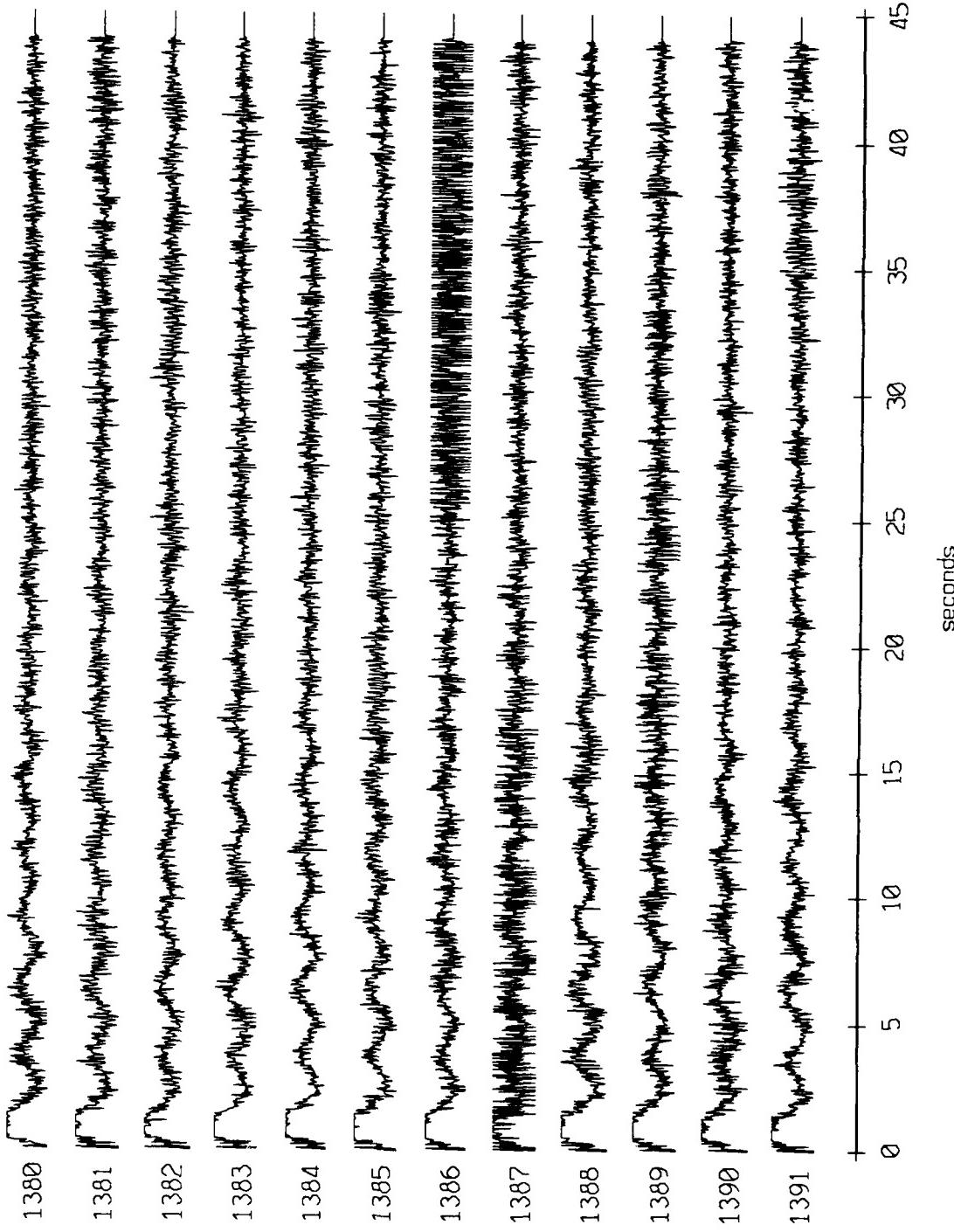


Figure X.3.8a

Float 7, September 1987 Trip - records 1380-1391 (y-axis)
vertical axis scale is approx. -1.0 to 1.0 volts



AGC corrected channel level (V)

Figure X.3.8b

Flight 7, September 1987 Trip - records 1380-1391 (z-axis)
vertical axis scale is approx. -1.0 to 1.0 volts

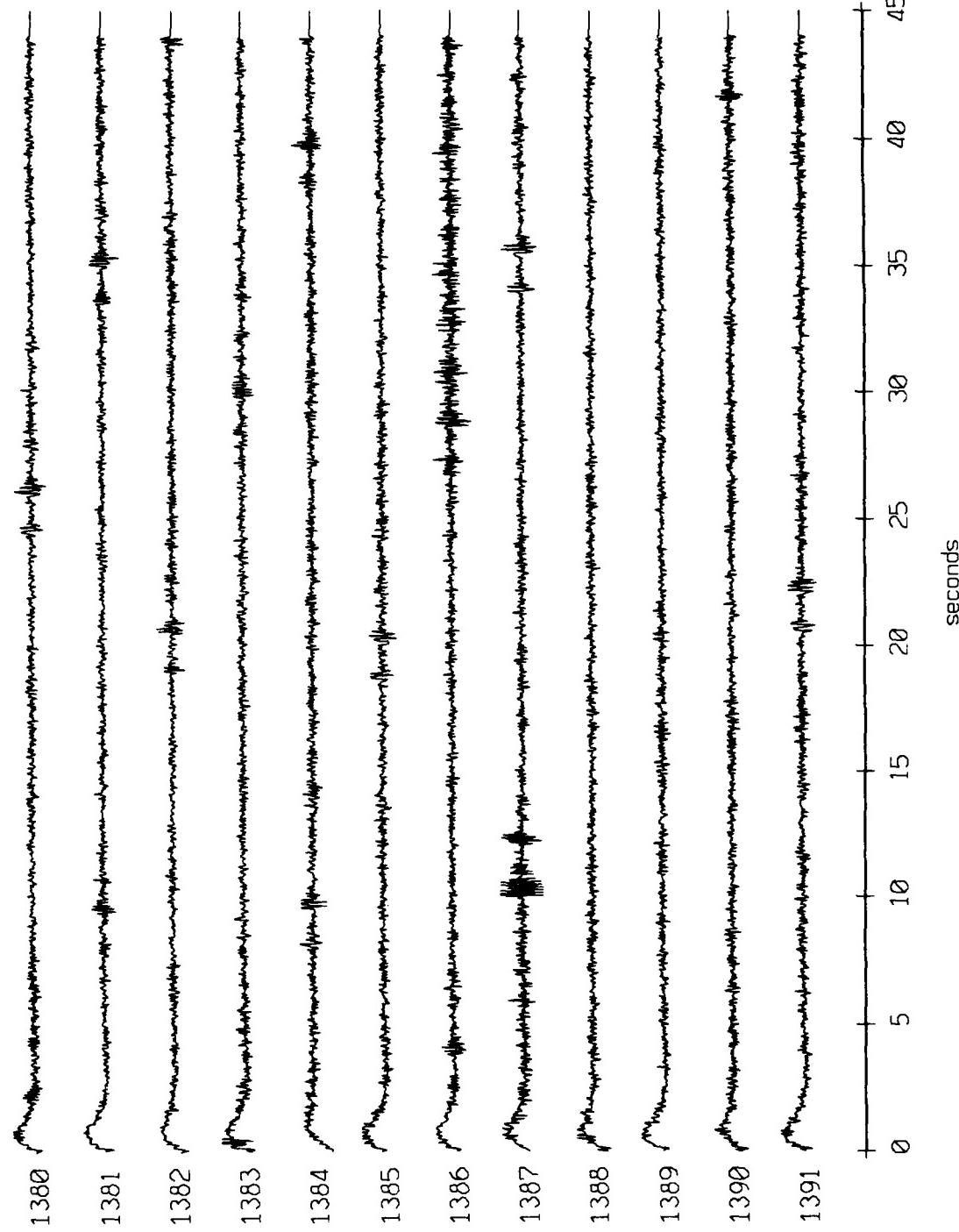


Figure X.3.8c

Flight 9, September 1987 Sea Trip records 1380-1391 (x-axis
vertical axis scale is approx. 1.0 volt)

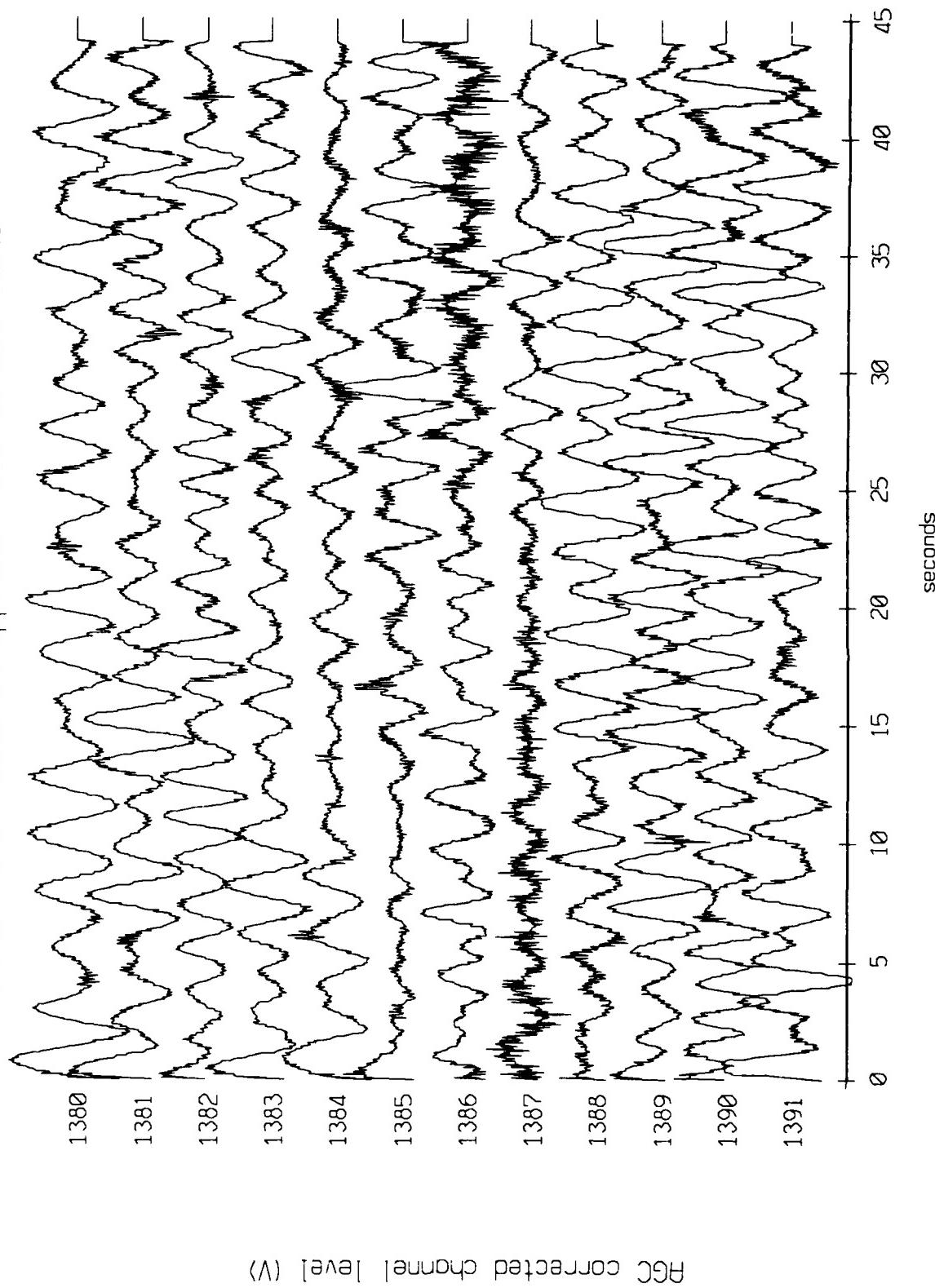


Figure X.3.9a

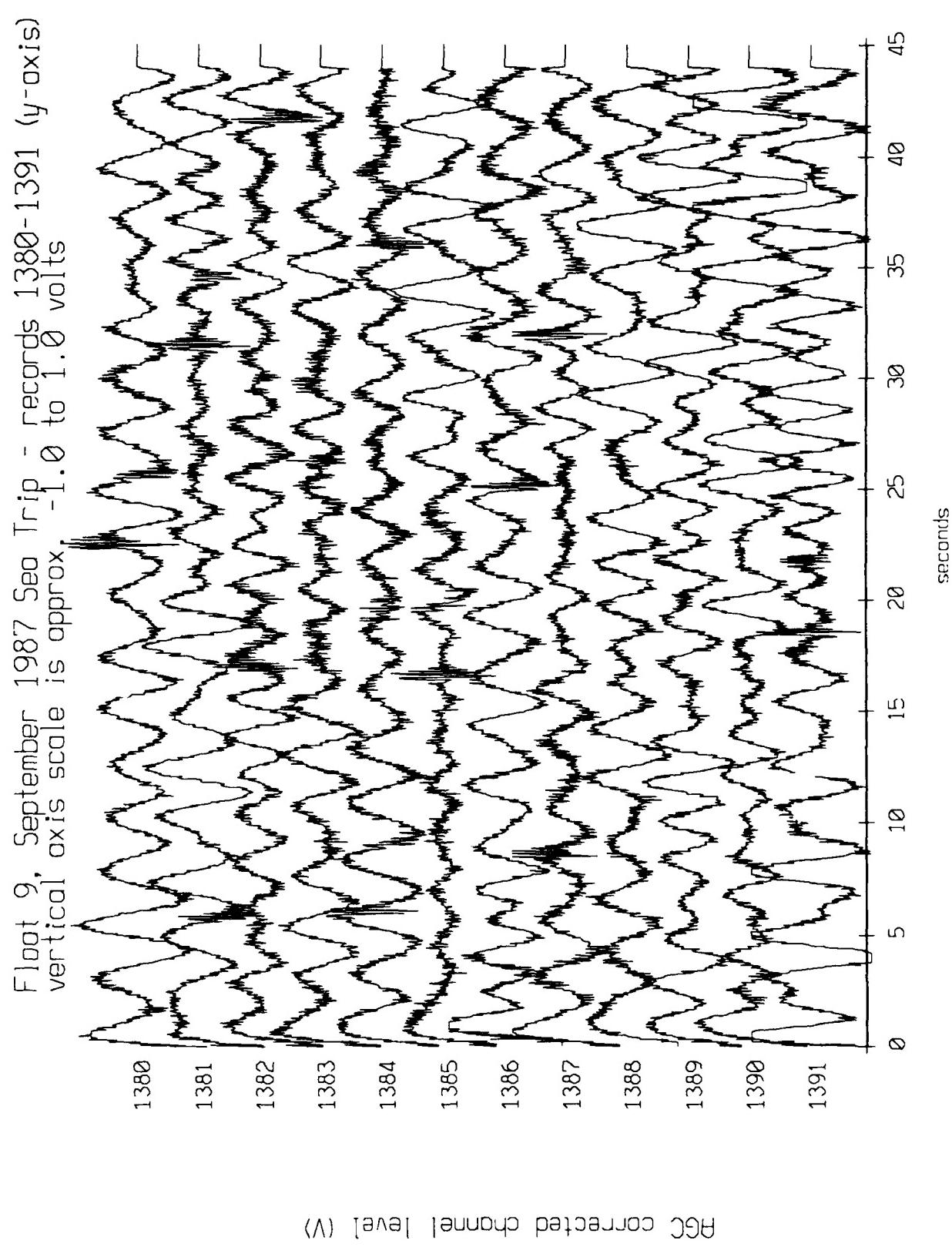


Figure X.3.9b

Float 9, September 1987 Sea Trip - records 1380-1391 (z-axis)
vertical axis scale is approx. -1.0 to 1.0 volts

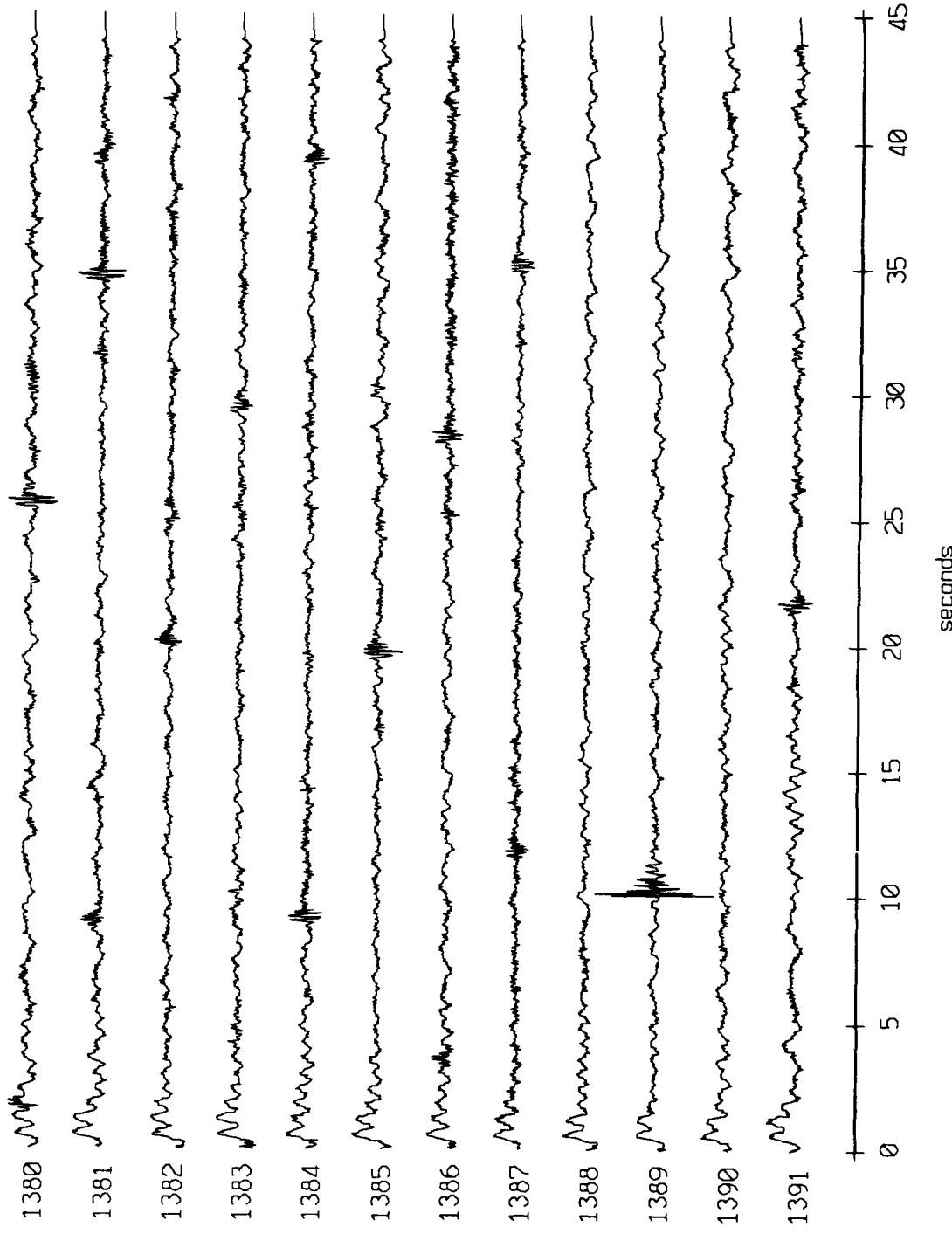


Figure X.3.9c

Float 0, September 1987 Sea Trip - records 1450-1461 (x-axis
vertical axis scale is approx. -1.0 to 1.0 volts

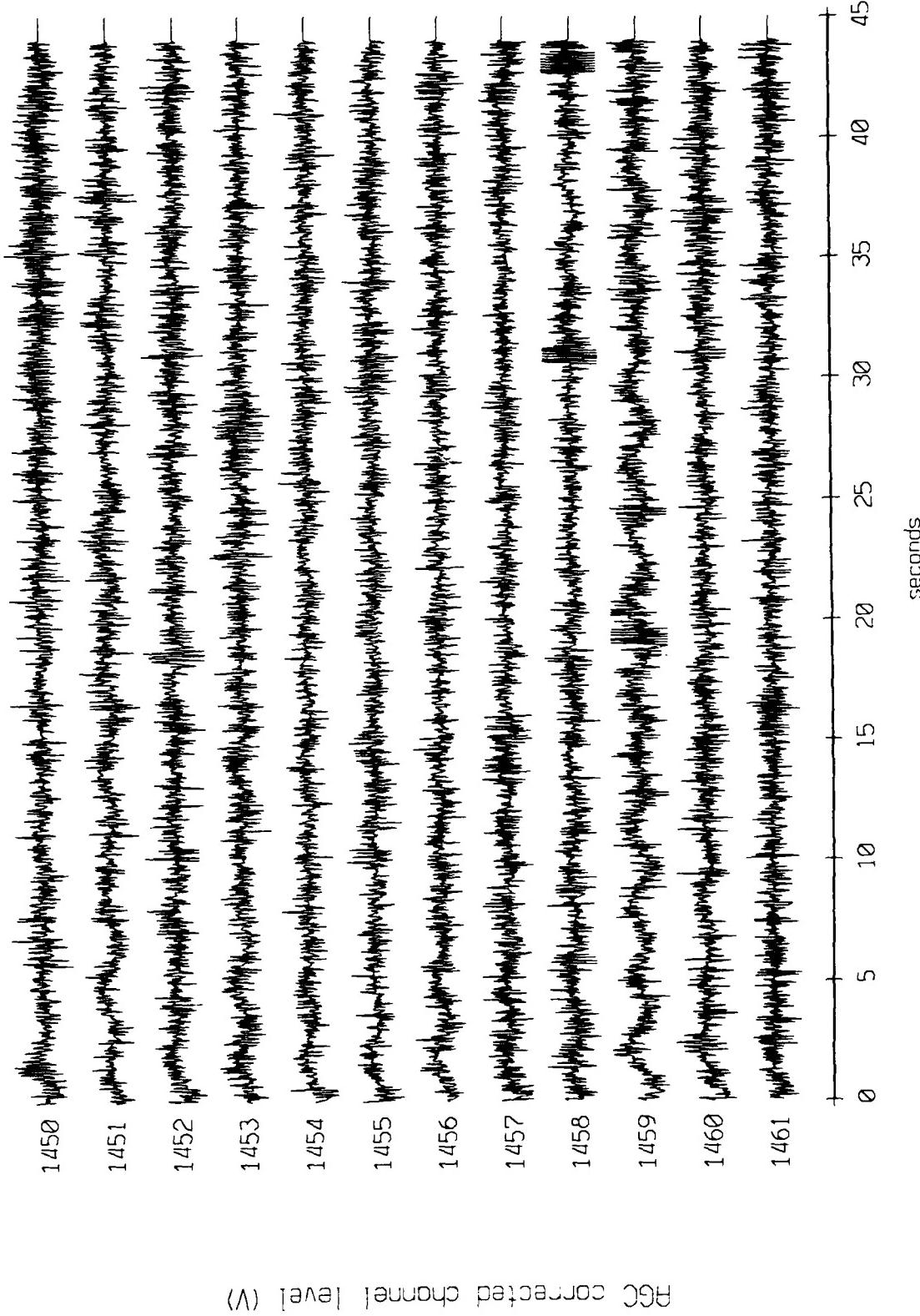


Figure X.4.1a

Float 0, September 1987 Sea Trip - records 1450-1461 (y-axis)
vertical axis scale is approx. 1.0 to 1.0 volts

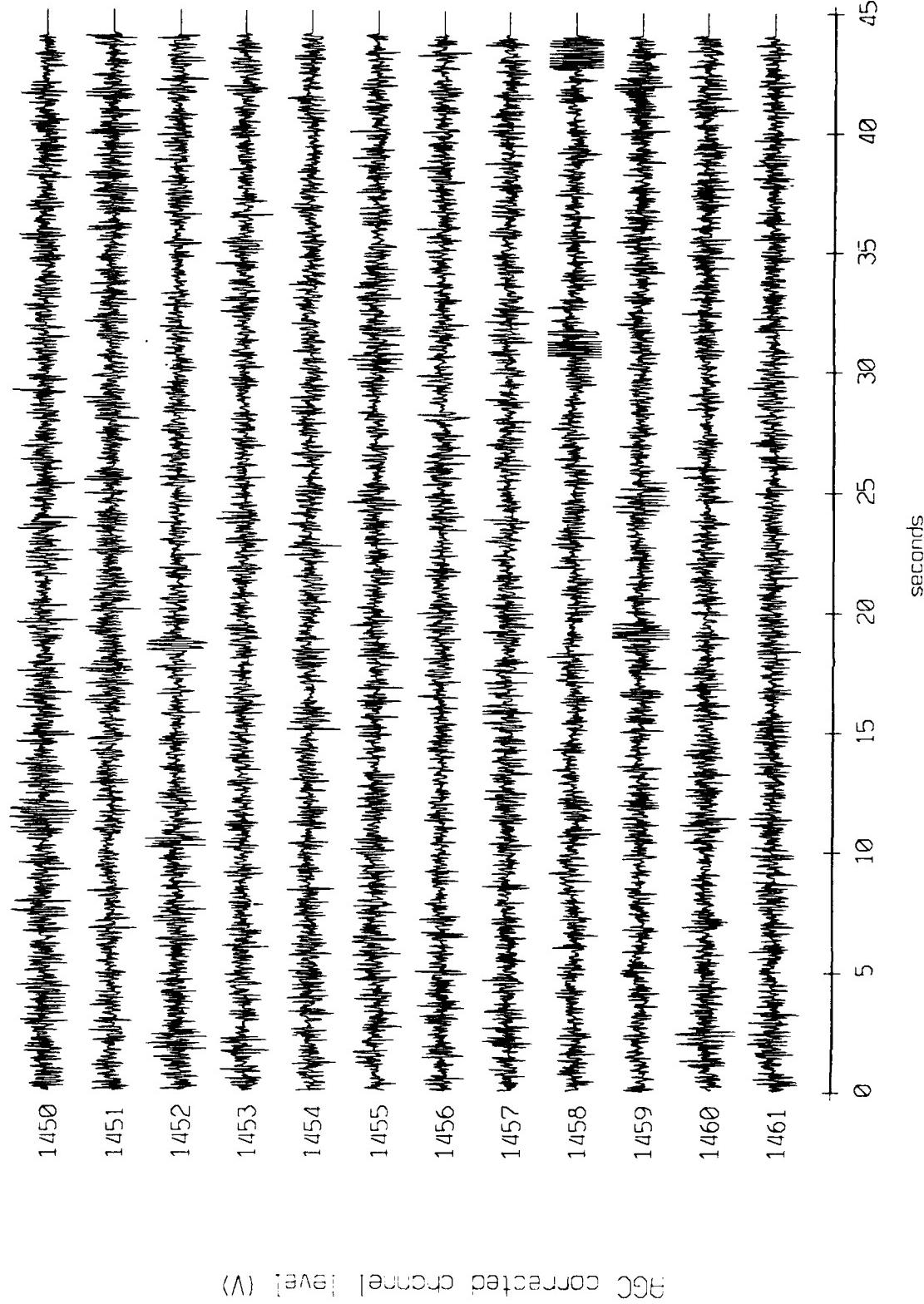


Figure X.4.1b

Float 0, September 1987 Sea Trip - records 1450-1461 (z-axis)
vertical axis scale is approx. -1.0 to 1.0 volts

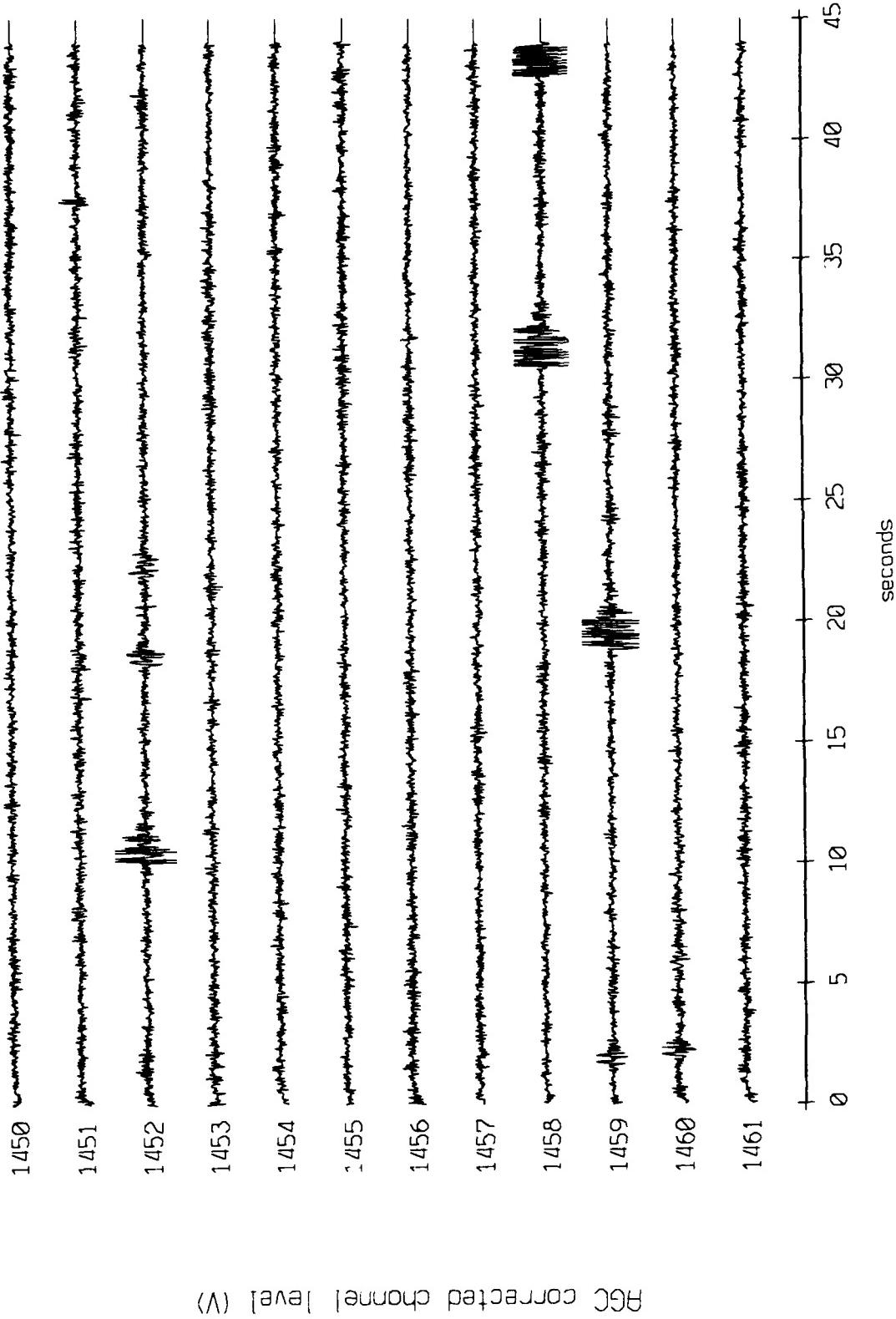


Figure X.4.1c

F10ot 1, September 1987 Sea Trip - records 1450-1461 (x-axis)
vertical axis scale is approx. -1.0 to 1.0 volts

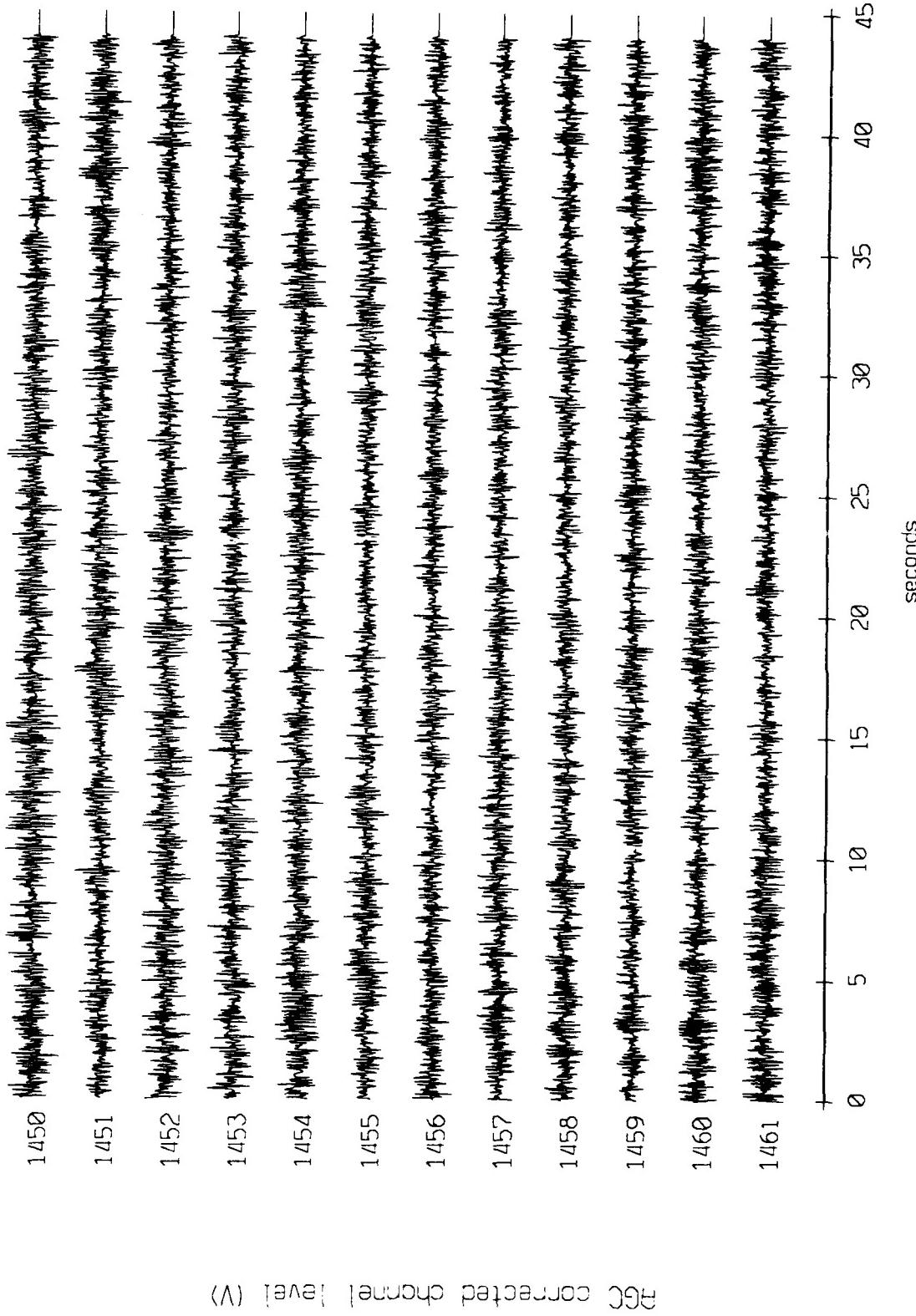


Figure X.4.2a

Flight 1, September 1987 Sea Trip - records 1450-1461 (y-axis)
vertical axis scale is approx. -1.0 to 1.0 volts

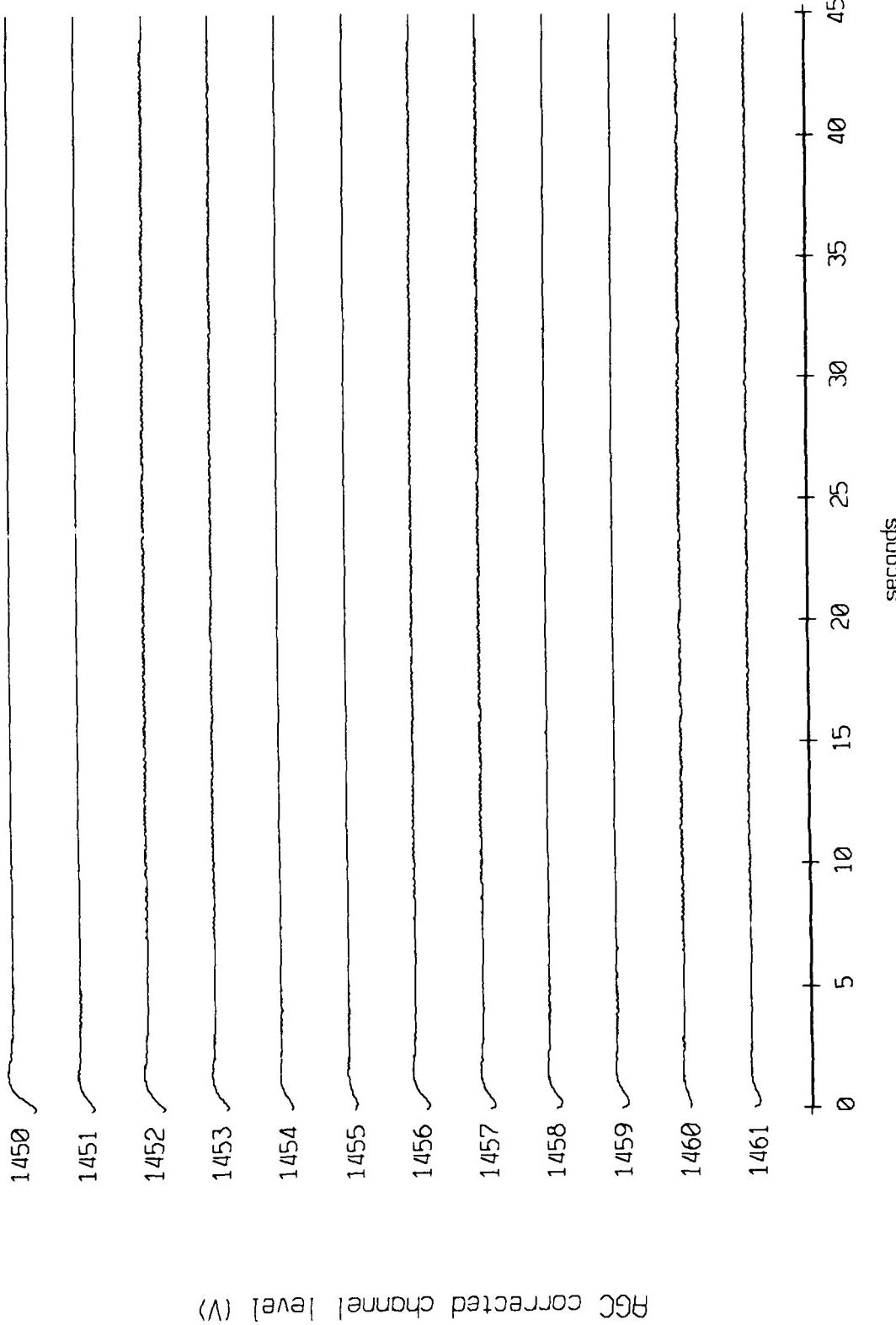


Figure X.4.2b

Flight 1, September 1987 Sea Trip - records 1450-1461 (z-axis)
vertical axis scale is approx. -1.0 to 1.0 volts

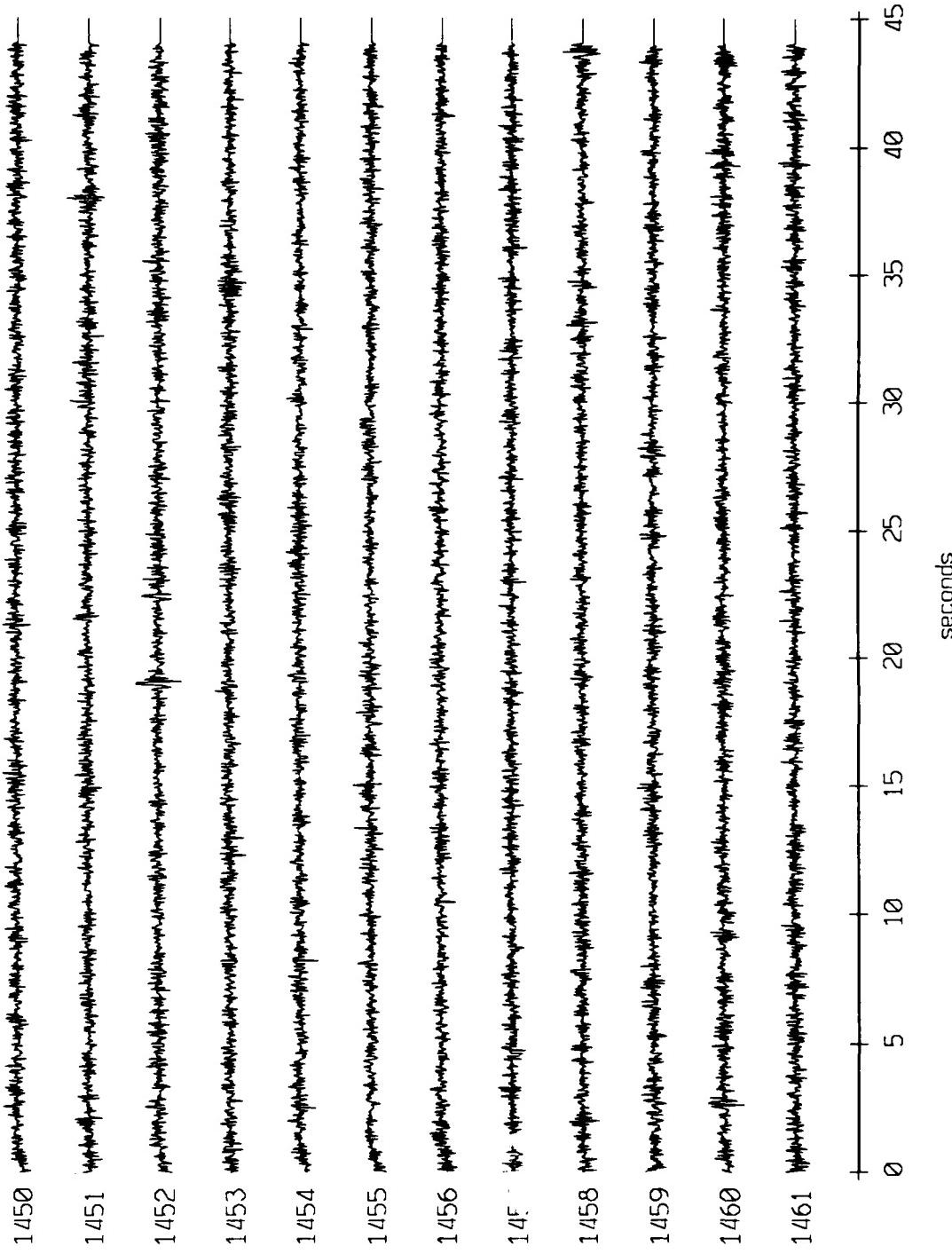
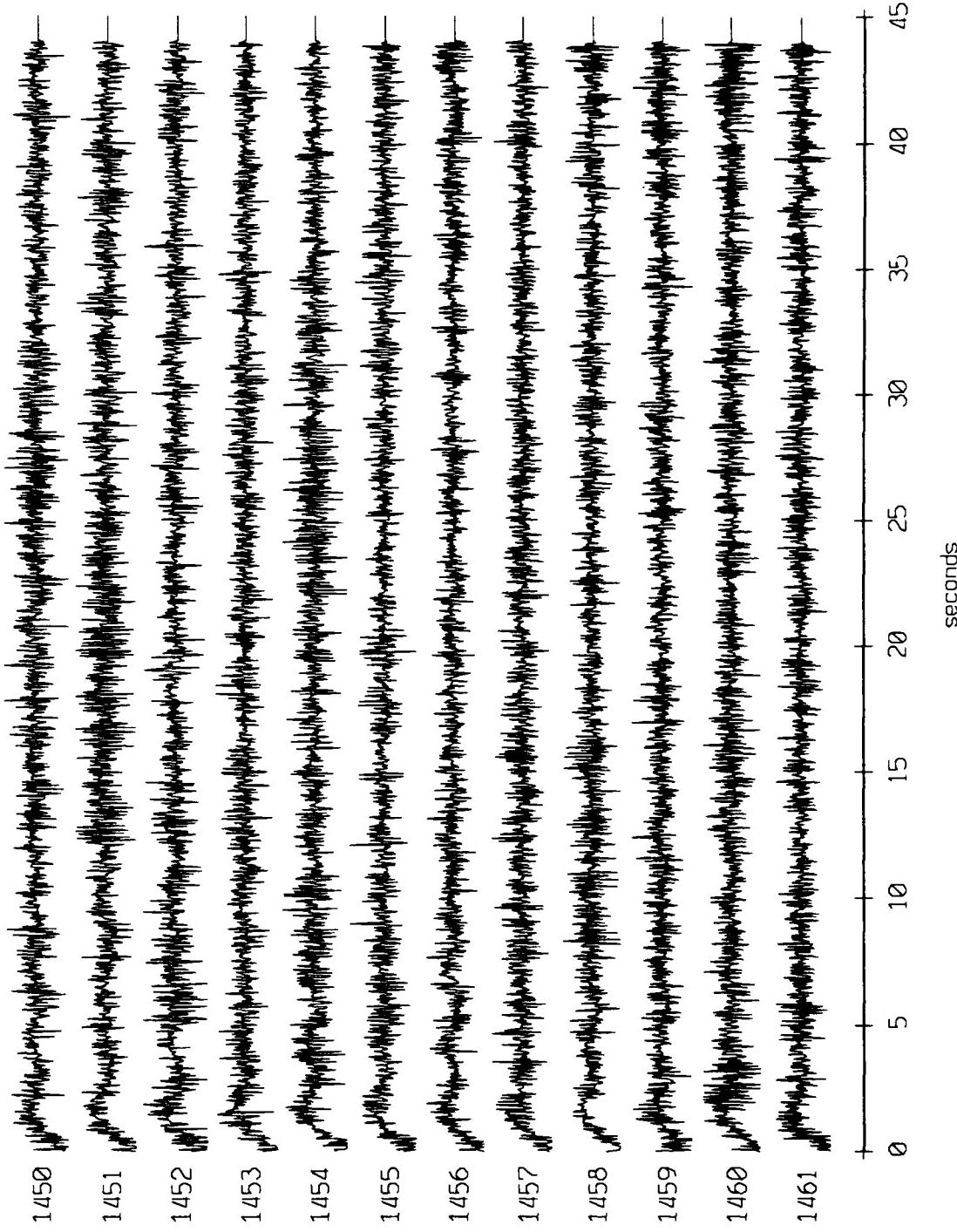


Figure X.4.2c

Float 2, September 1987 Sea Trip - records 1450-1461 (x-axis)
vertical axis scale is approx. -1.0 to 1.0 volts



RGC corrected channel level (V)

Figure X.4.3a

Float 2, September 1987 Sea Trip - records 1450-1461 (y-axis vertical axis scale is approx. -1.0 to 1.0 volts)

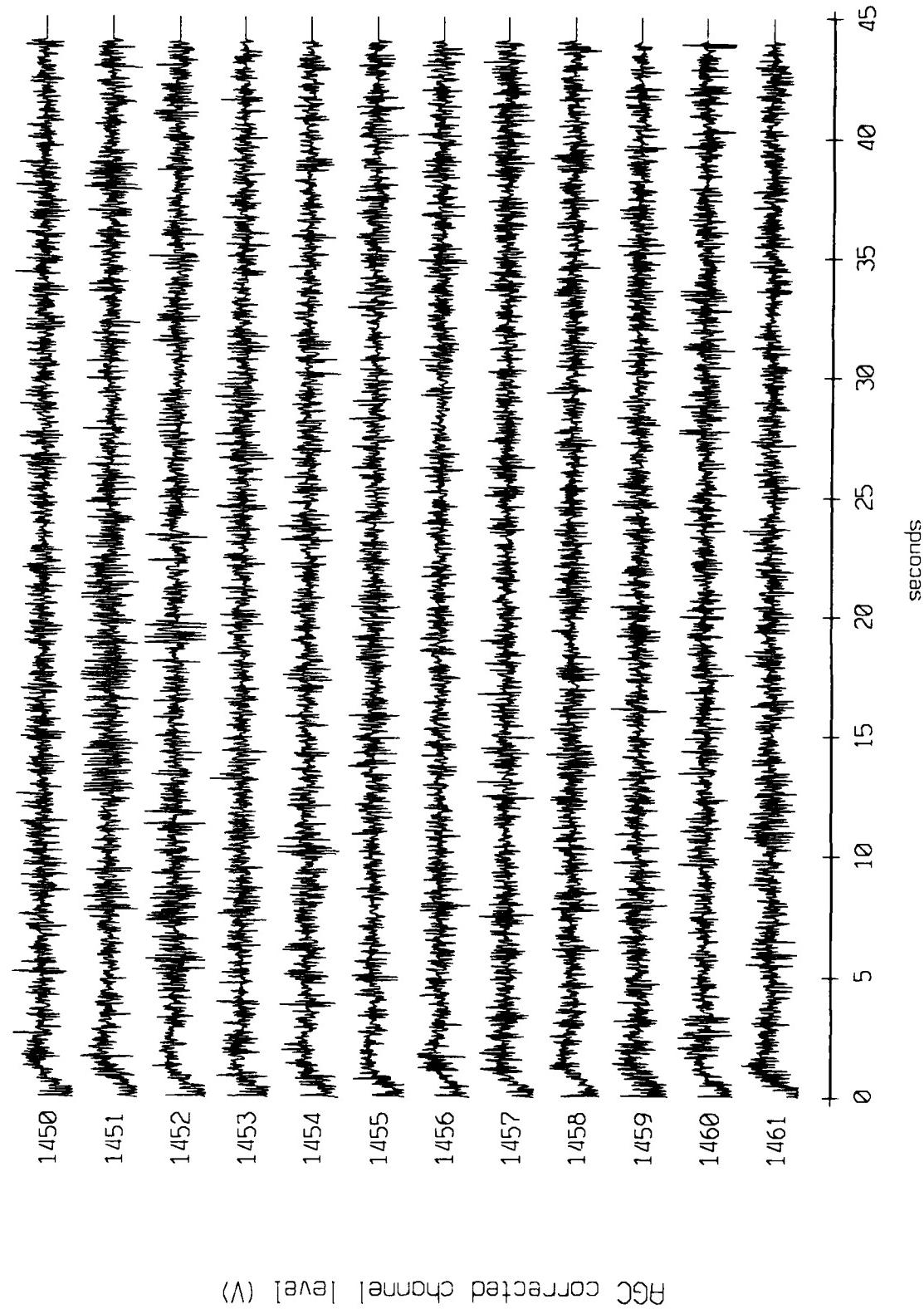


Figure X.4.3b

Flight 2, September 1987 Sea Trip - records 1450-1461 (z-axis)
vertical axis scale is approx. -1.0 to 1.0 volts

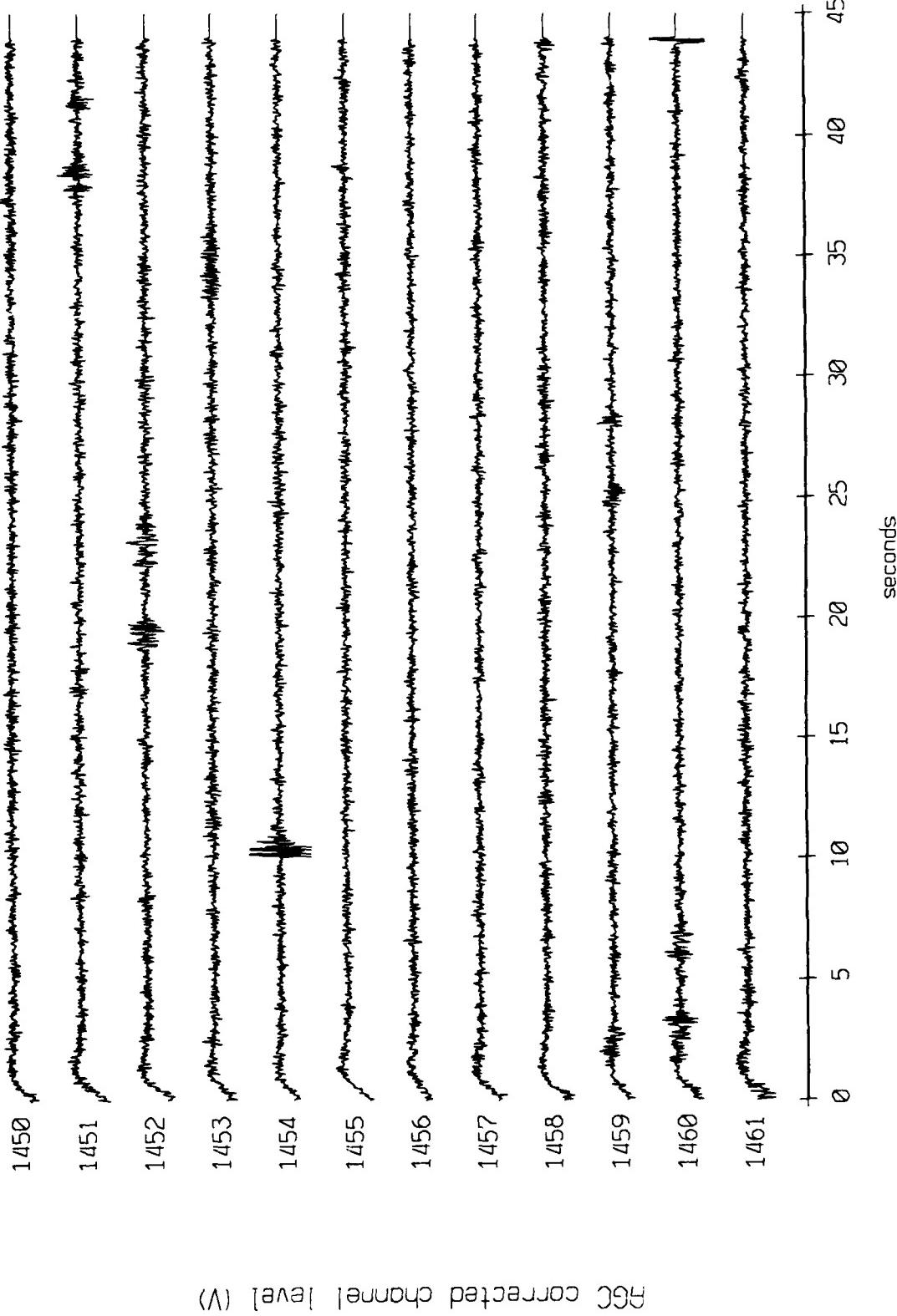


Figure X.4.3c

Float 3, September 1987 Sea Trip - records 1450-1461 (x-axis)
vertical axis scale is approx. -1.0 to 1.0 volts

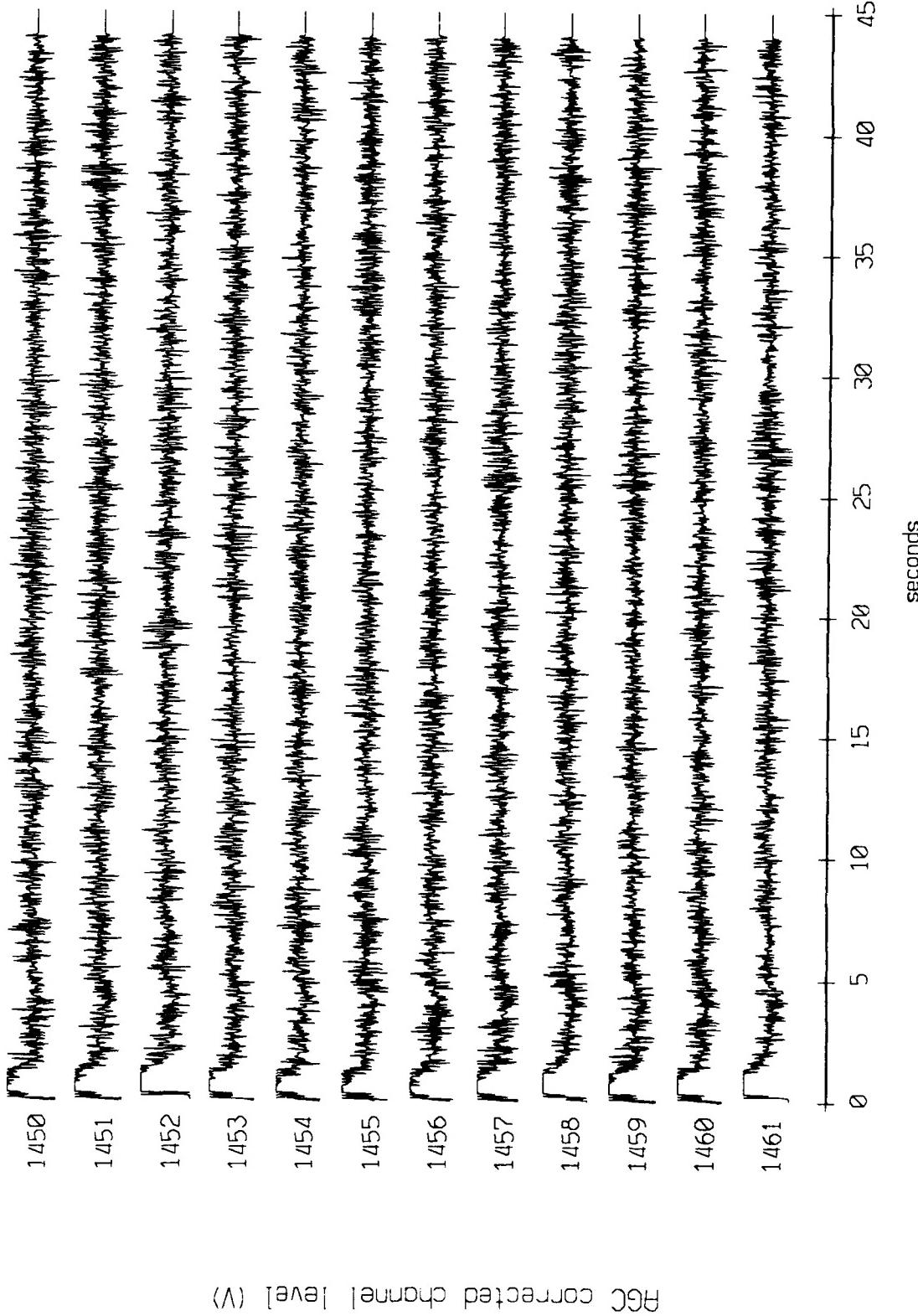


Figure X.4.4a

Flood 3, September 1987 Sea Trip - records 1450-1461 (y-axis vertical axis scale is approx. 1.0 to 1.0 volts)

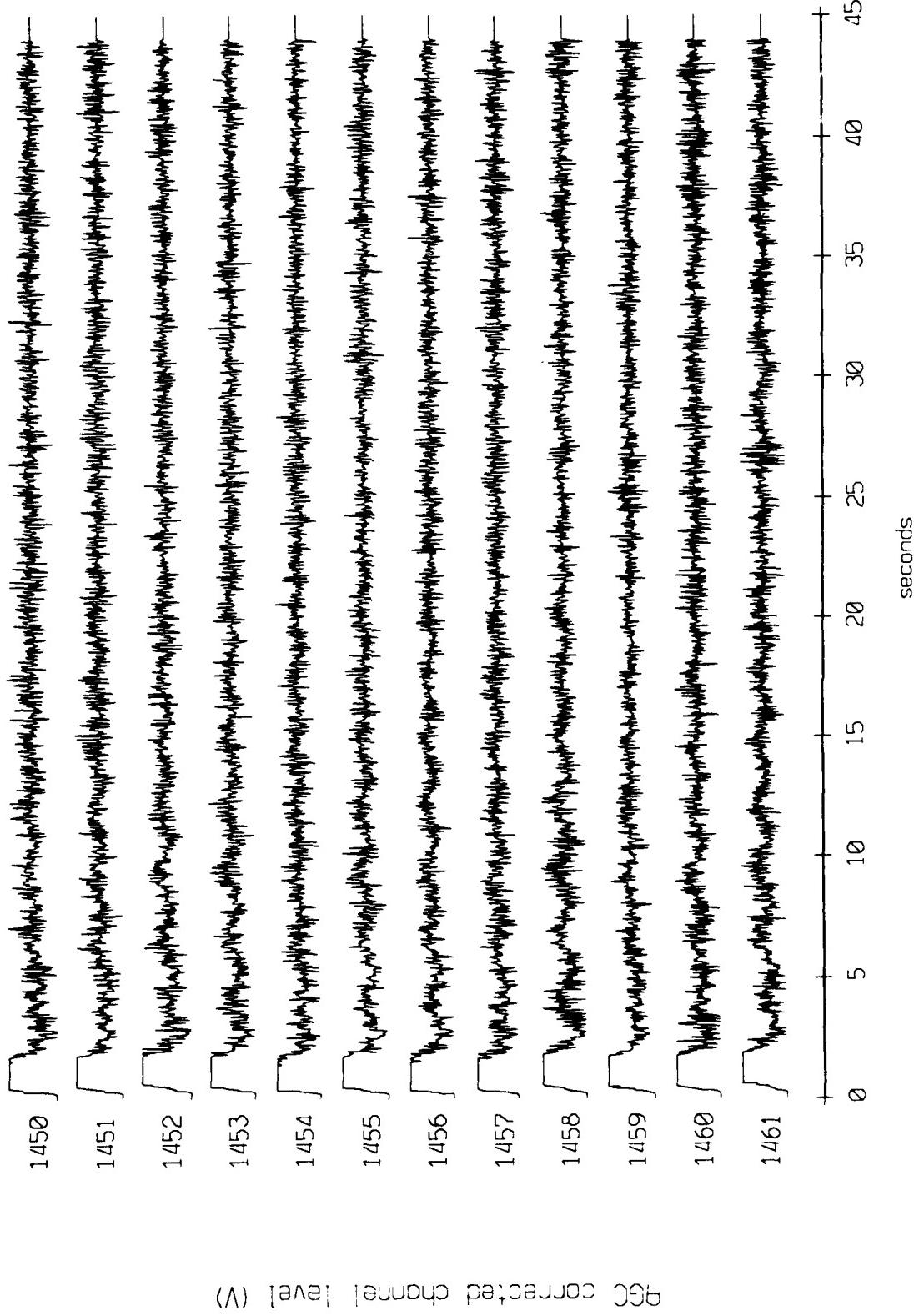
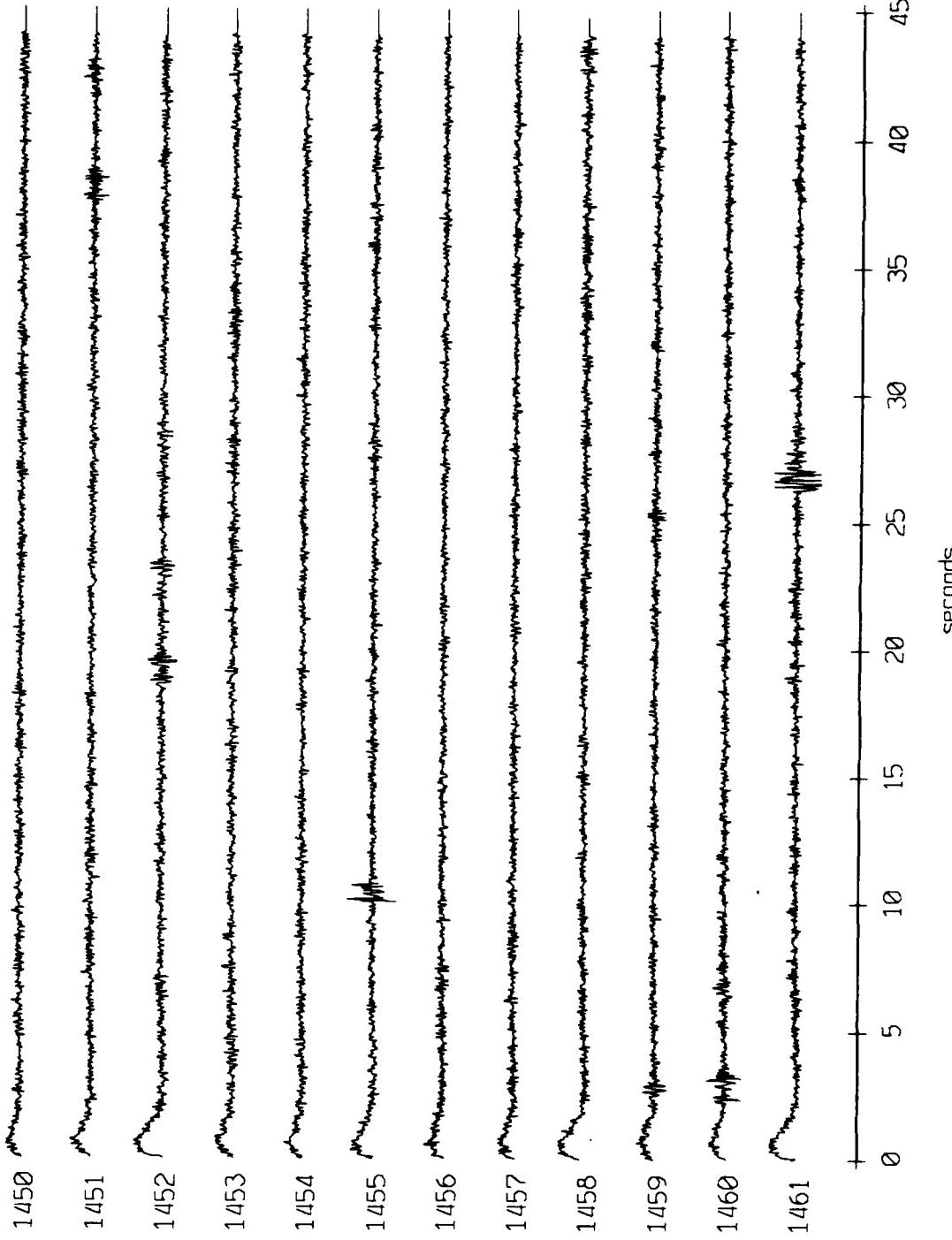


Figure X.4.4b

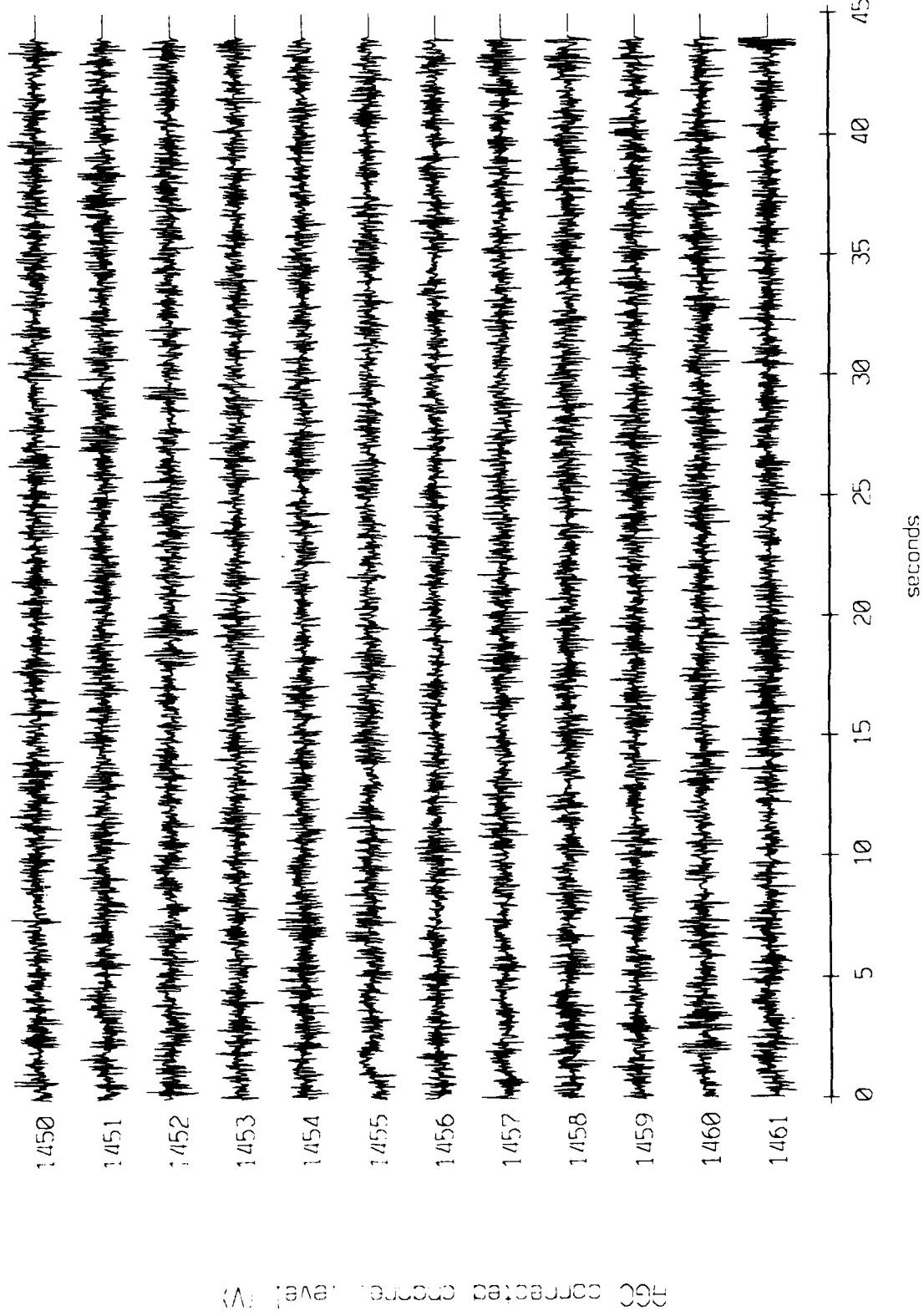
Floot 3, September 1987 Sea Trip - records 1450-1461 (z-axis)
vertical axis scale is approx. -1.0 to 1.0 volts



AGC CORRECTED CHANNEL LEVEL (V)

Figure X.4.4c

Float 4, September 1987 Trip - records 1450-1461 (x-axis)
vertical axis scale is approx. -1.0 to 1.0 volts



DGC corrected corrected level (V)

Figure X.4.5a

Figure 4, September 1987 Trip - records 1450-1461 (y-axis)
vertical axis scale is approx. -1.0 to 1.0 volts

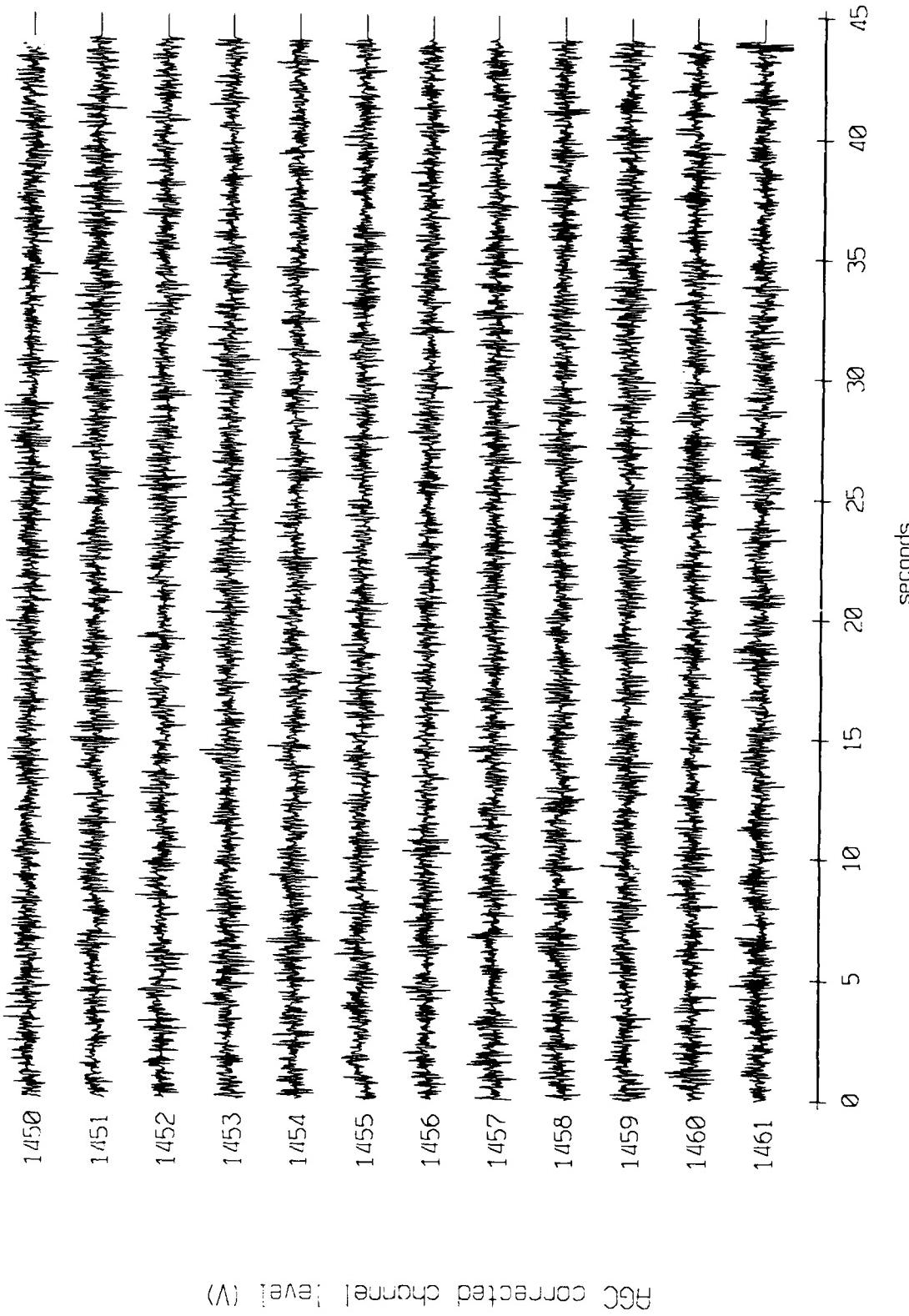


Figure X.4.5b

Flight 4, September 1987 Trip - records 1450-1461 (z-axis)
vertical axis scale is approx. -1.0 to 1.0 volts

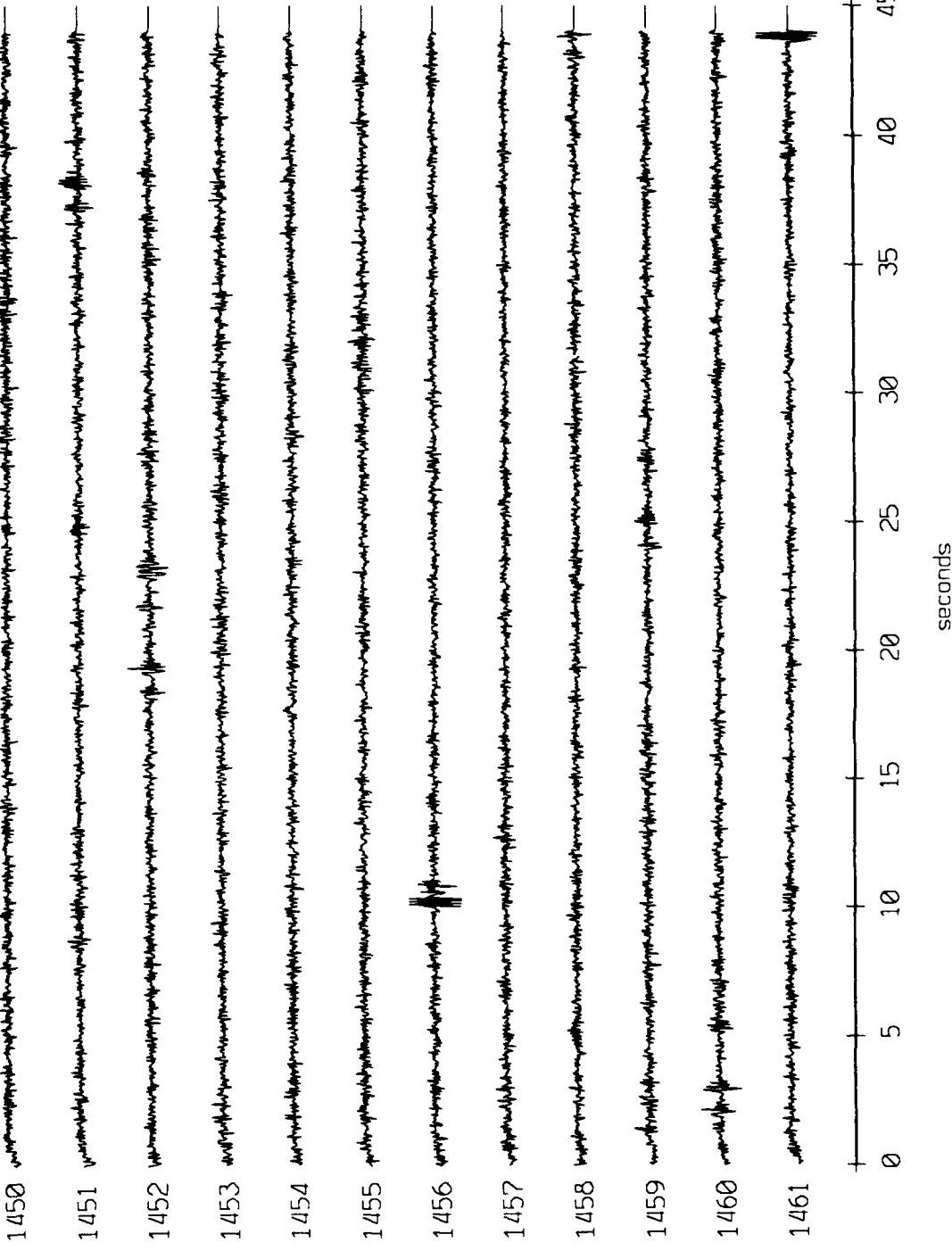


Figure X.4.5c

Float 5, September 1987 Trip - records 1450-1461 (x-axis)
vertical axis scale is approx. -1.0 to 1.0 volts

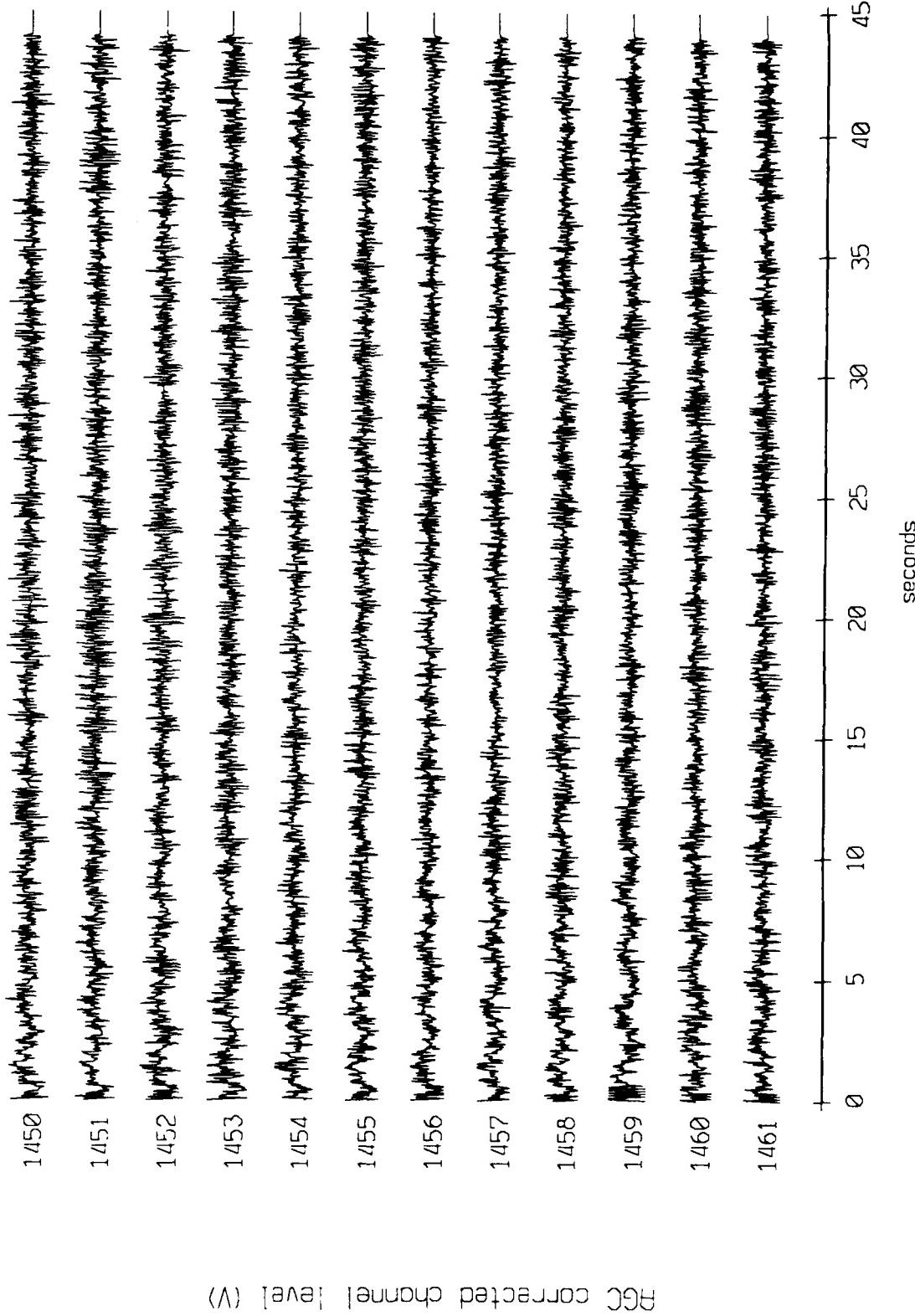


Figure X.4.6a

Float 5, September 1987 Trip - records 1450-1461 (y-axis)
vertical axis scale is approx. -1.0 to 1.0 volts

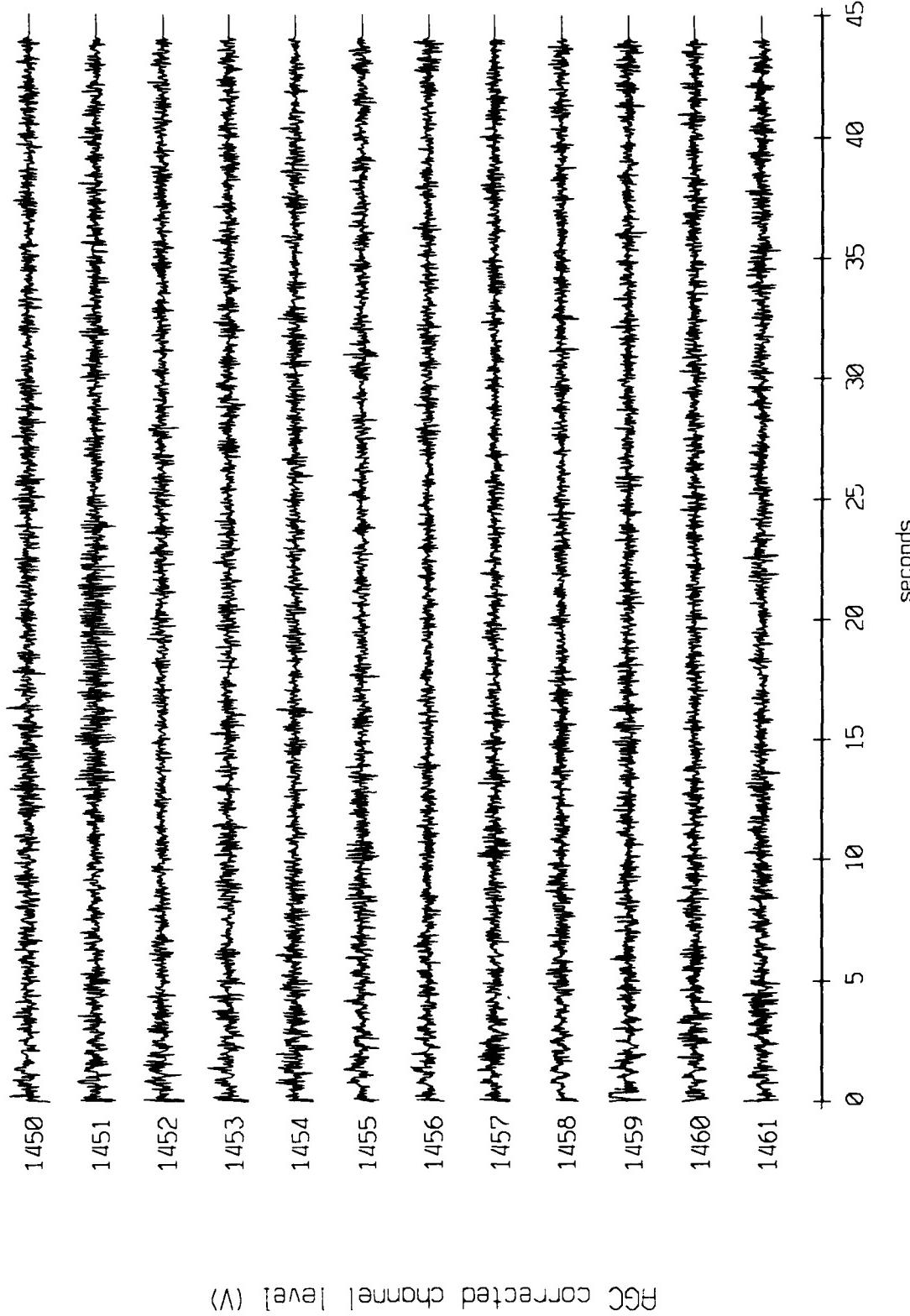


Figure X.4.6b

Float 5, September 1987 Trip - records 1450-1461 (z-axis)
vertical axis scale is approx. -1.0 to 1.0 volts

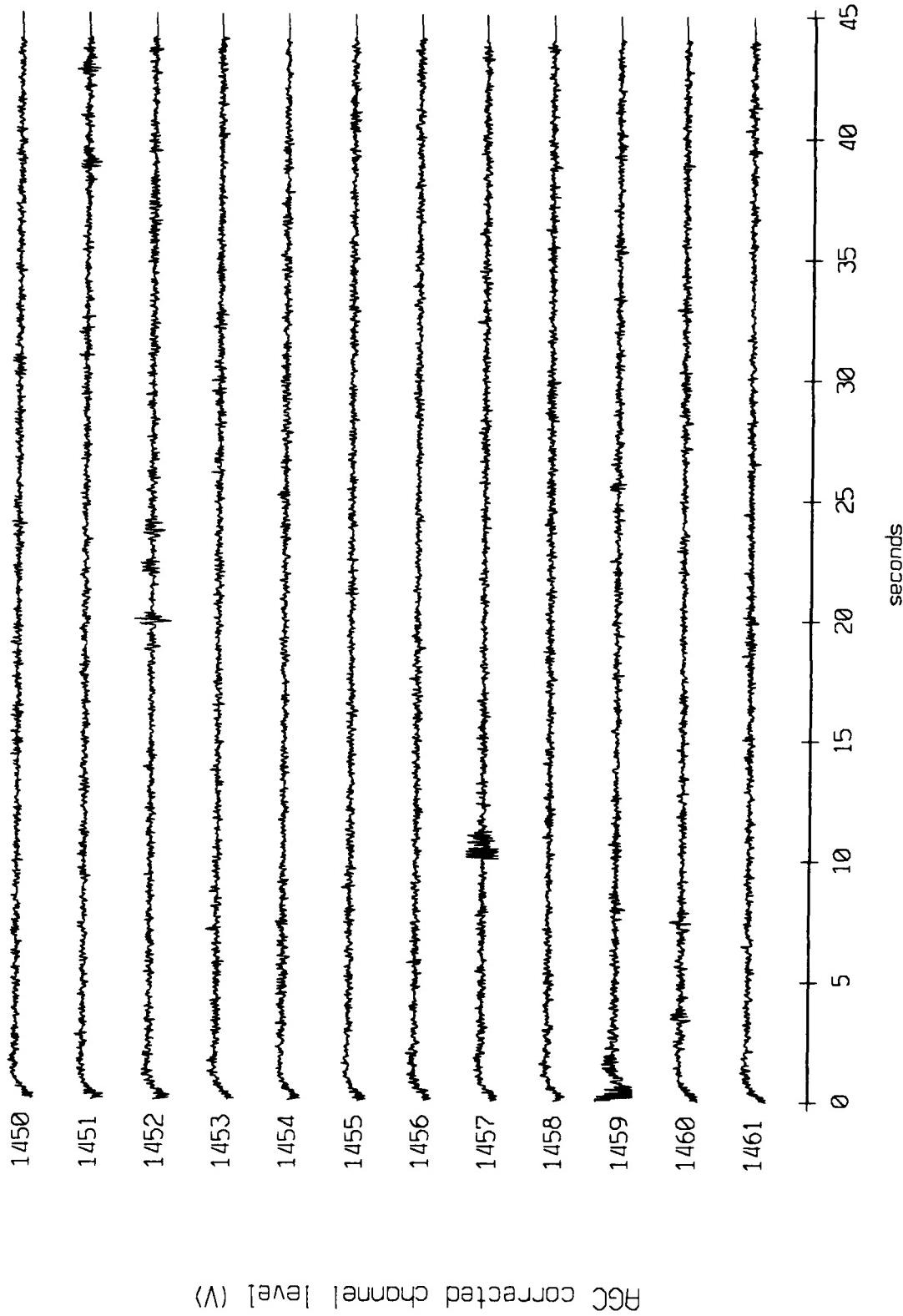


Figure X.4.6c

Float 6, September 1987 Trip - records 1450-1461 (x-axis)
vertical axis scale is approx. -1.0 to 1.0 volts

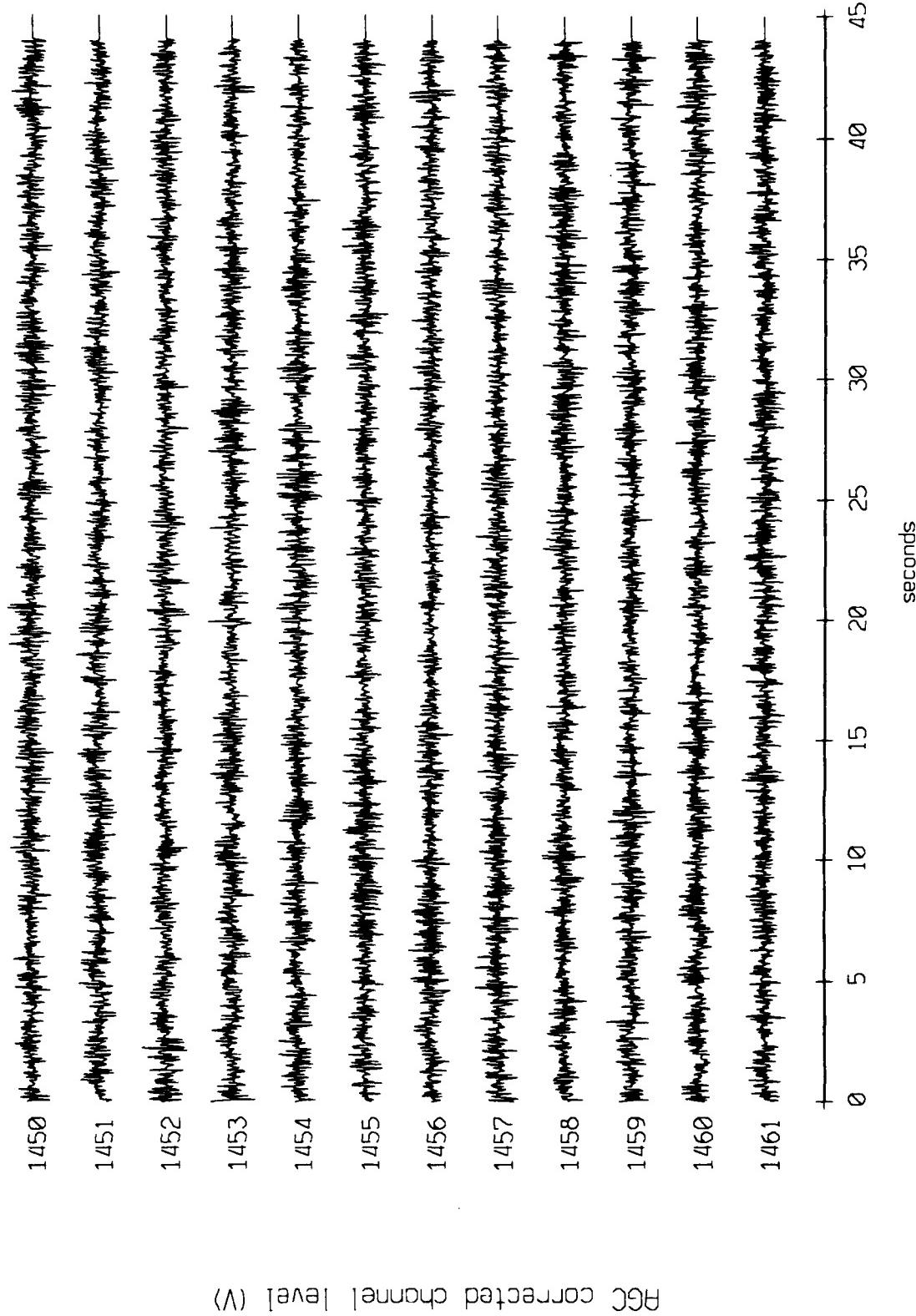


Figure X.4.7a

Float 6, September 1987 Trip - Records 1450-1461 (y-axis)
vertical axis scale is approx. -1.0 to 1.0 volts

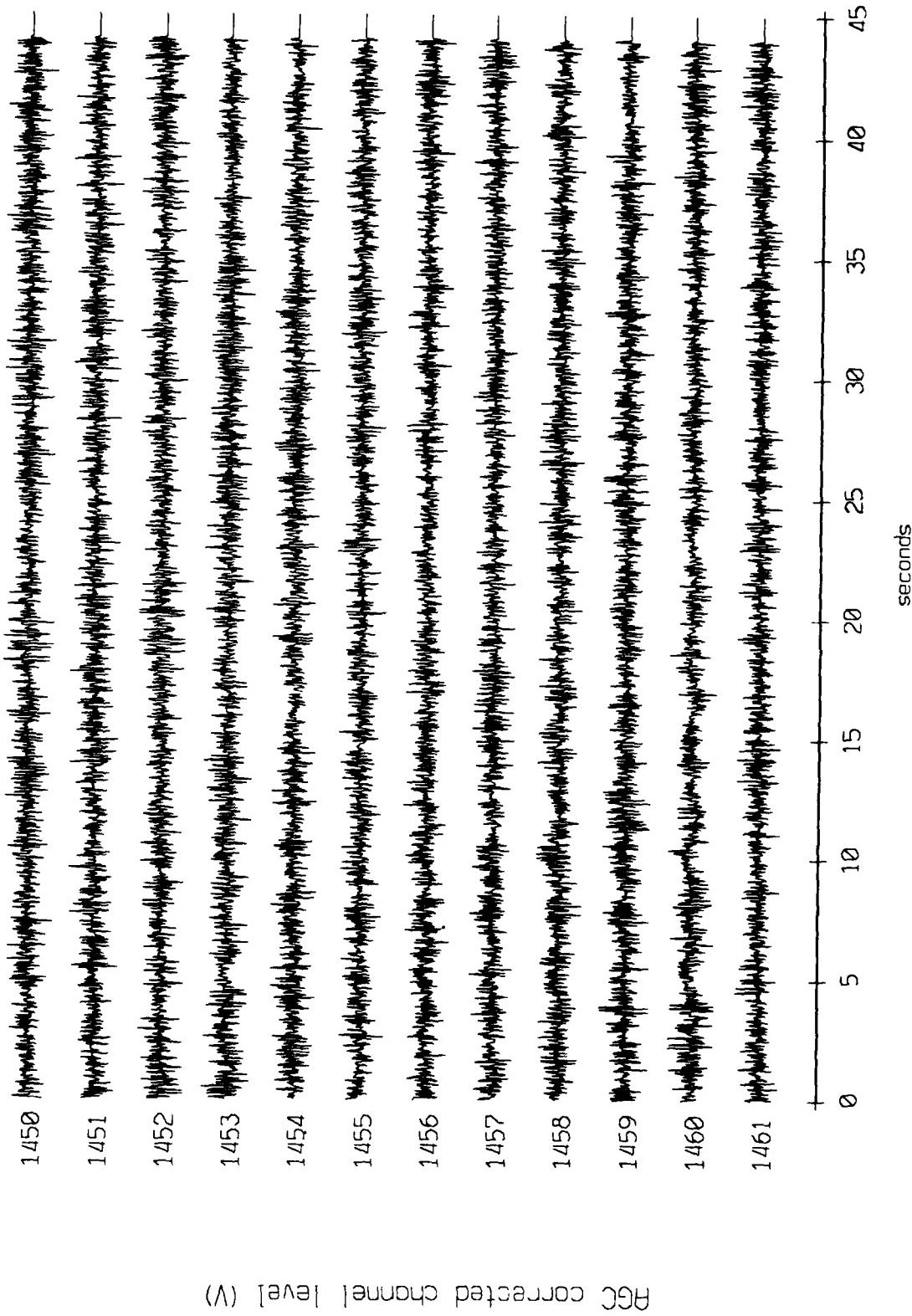
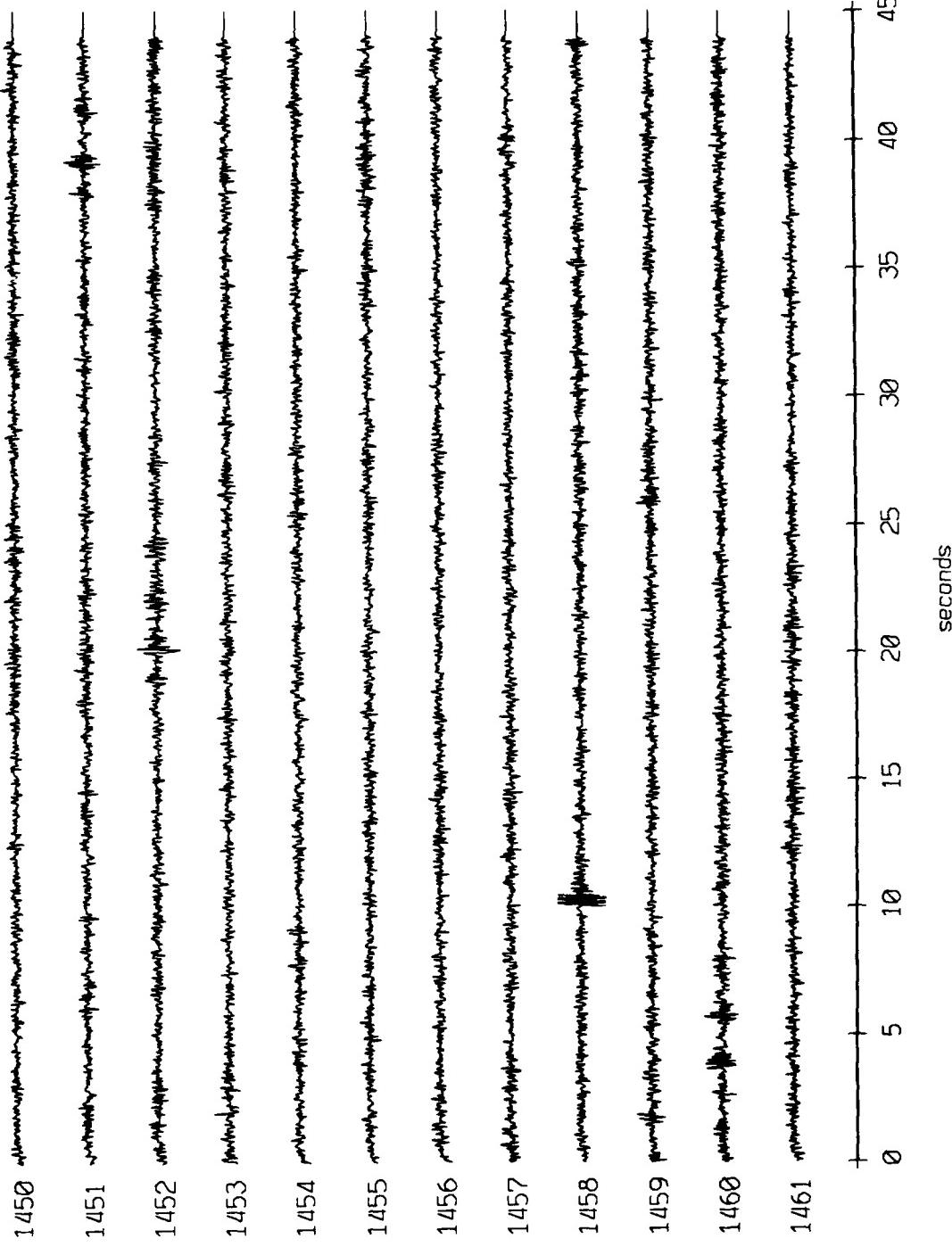


Figure X.4.7b

Floor 6, September 1987 Trip - records 1450-1461 (z-axis)
vertical axis scale is approx. -1.0 to 1.0 volts



AGC corrected channel level (V)

Figure X.4.7c

Flight 7, September 1987 Trip - records 1450-1461 (x-axis)
vertical axis scale is approx. -1.0 to 1.0 volts

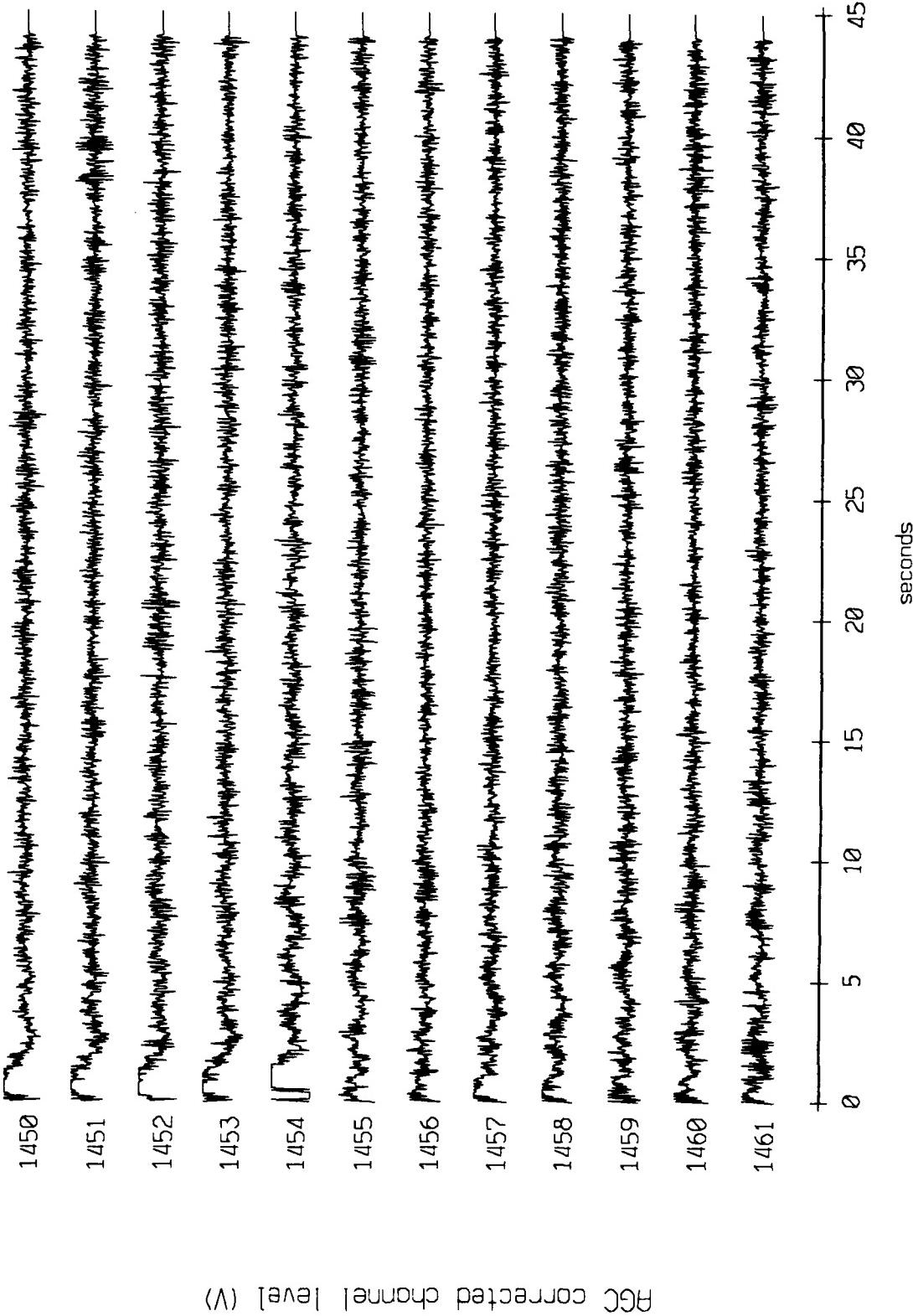


Figure X.4.8a

Float 7, September 1987 Trip - records 1450-1461 (y-axis)
vertical axis scale is approx. -1.0 to 1.0 volts

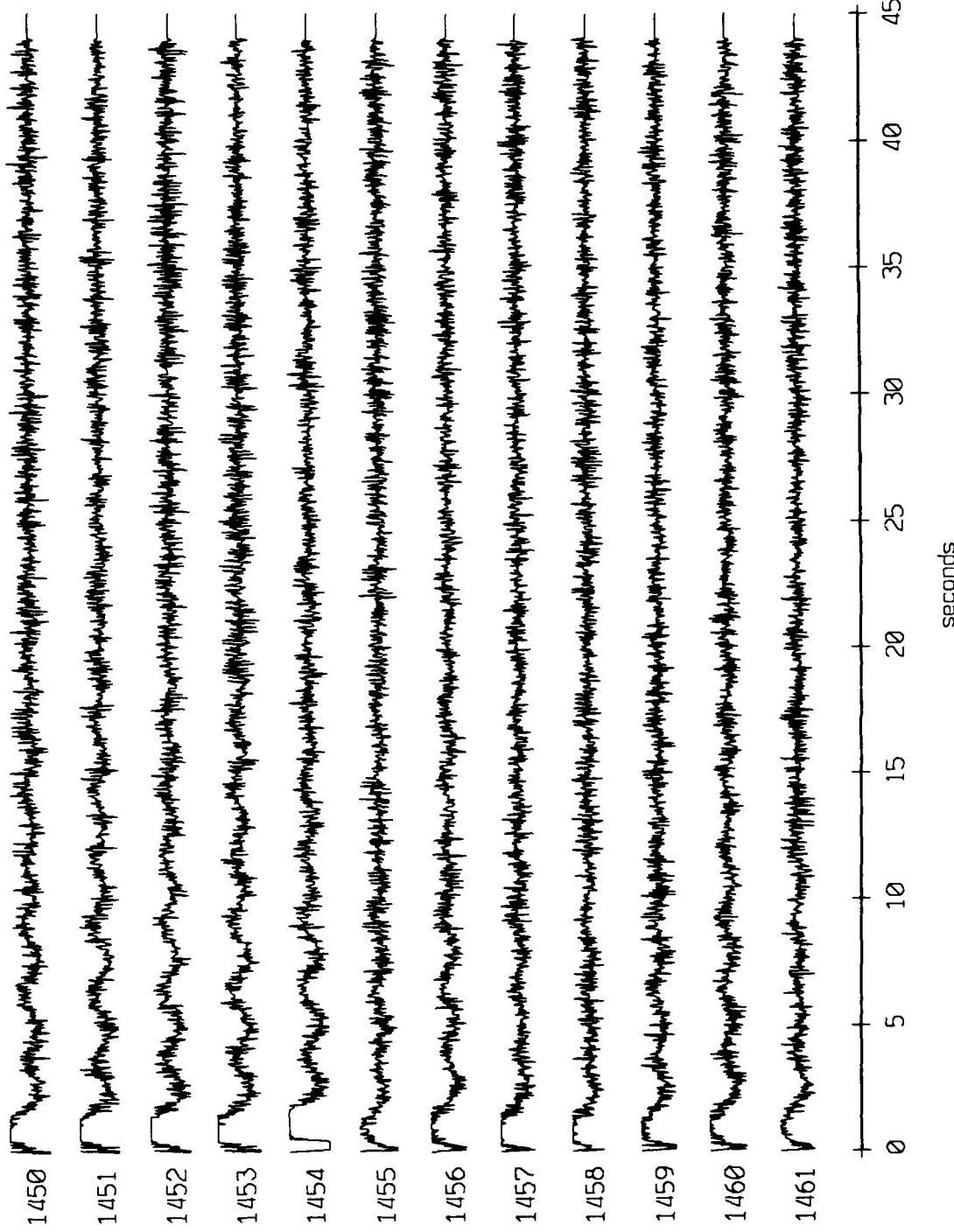


Figure X.4.8b

Flight 7, September 1987 Trip - records 1450-1461 (z-axis)
vertical axis scale is approx. -1.0 to 1.0 volts

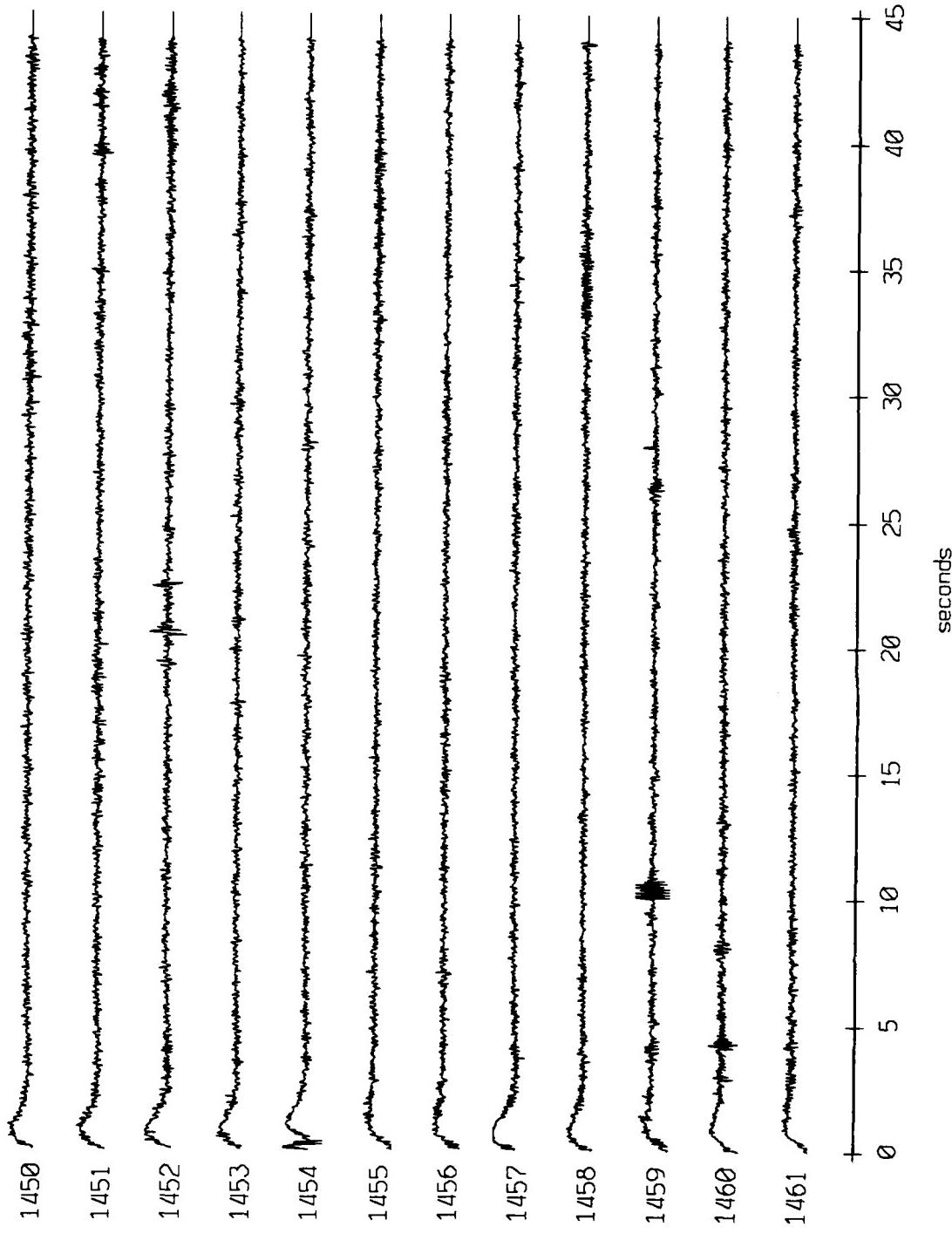


Figure X.4.8c

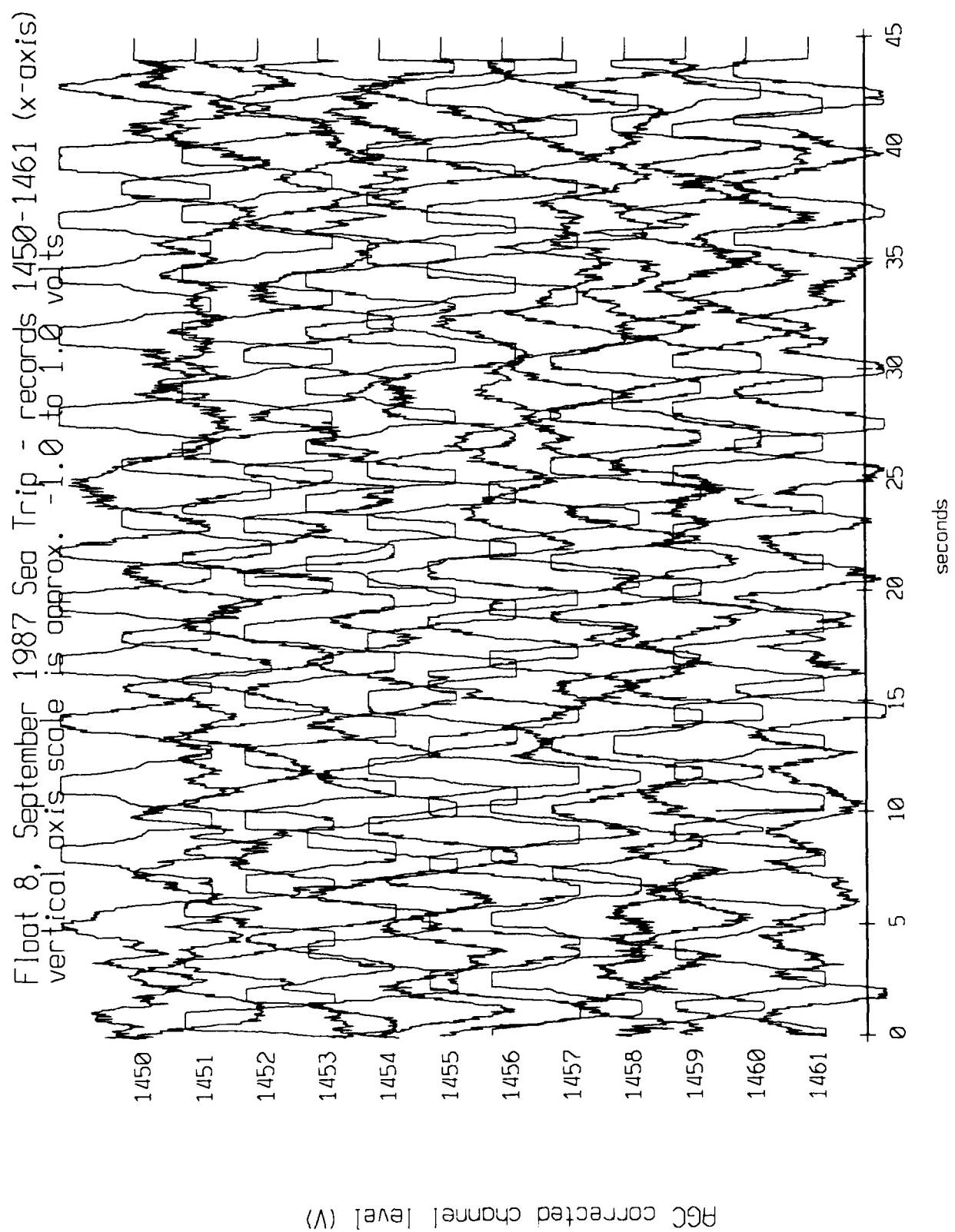


Figure X.4.9a

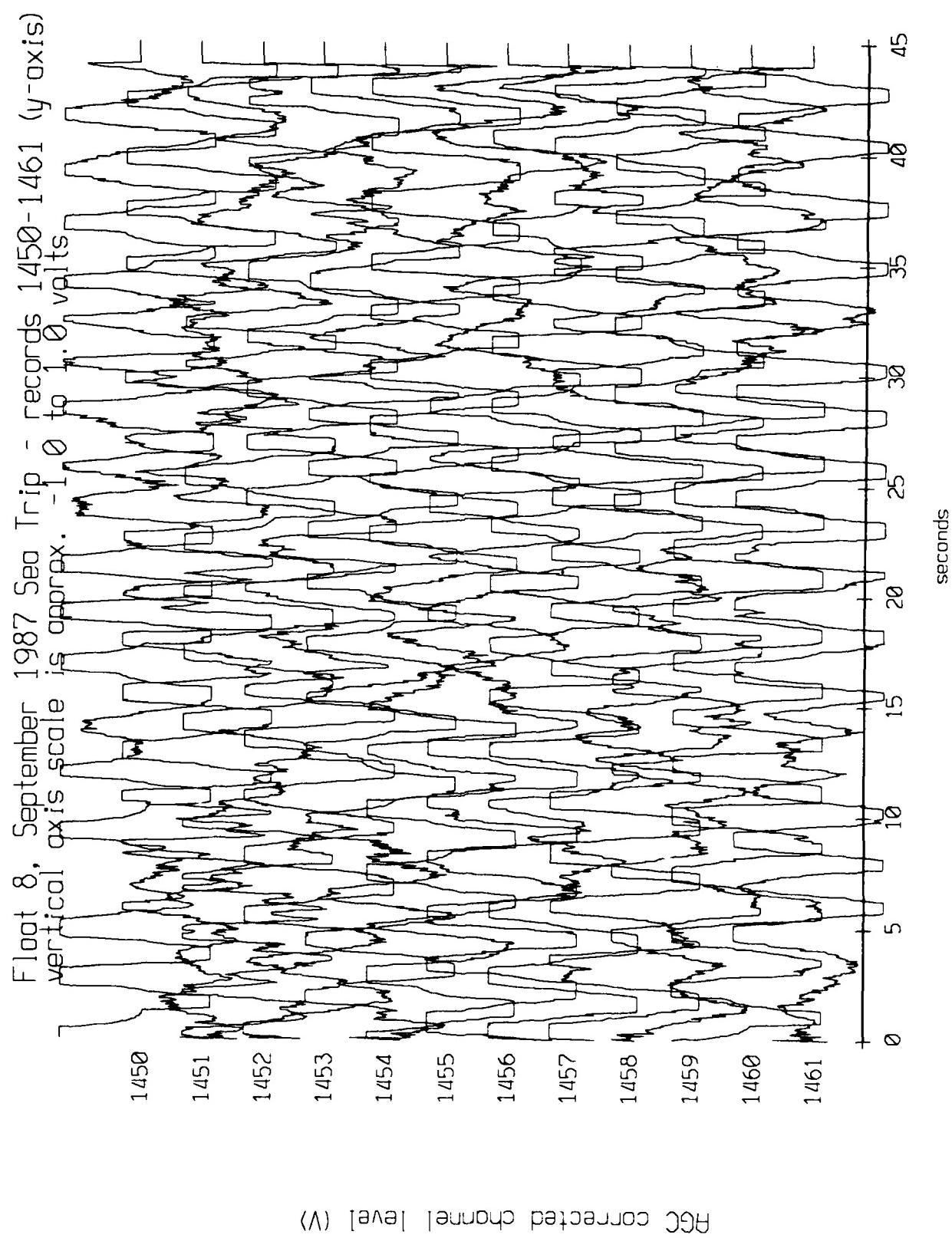


Figure X.4.9b

Float 8, September 1987 Sea Trip - records 1450-1461 (z-axis)
vertical axis scale is approx. -1.0 to 1.0 volts

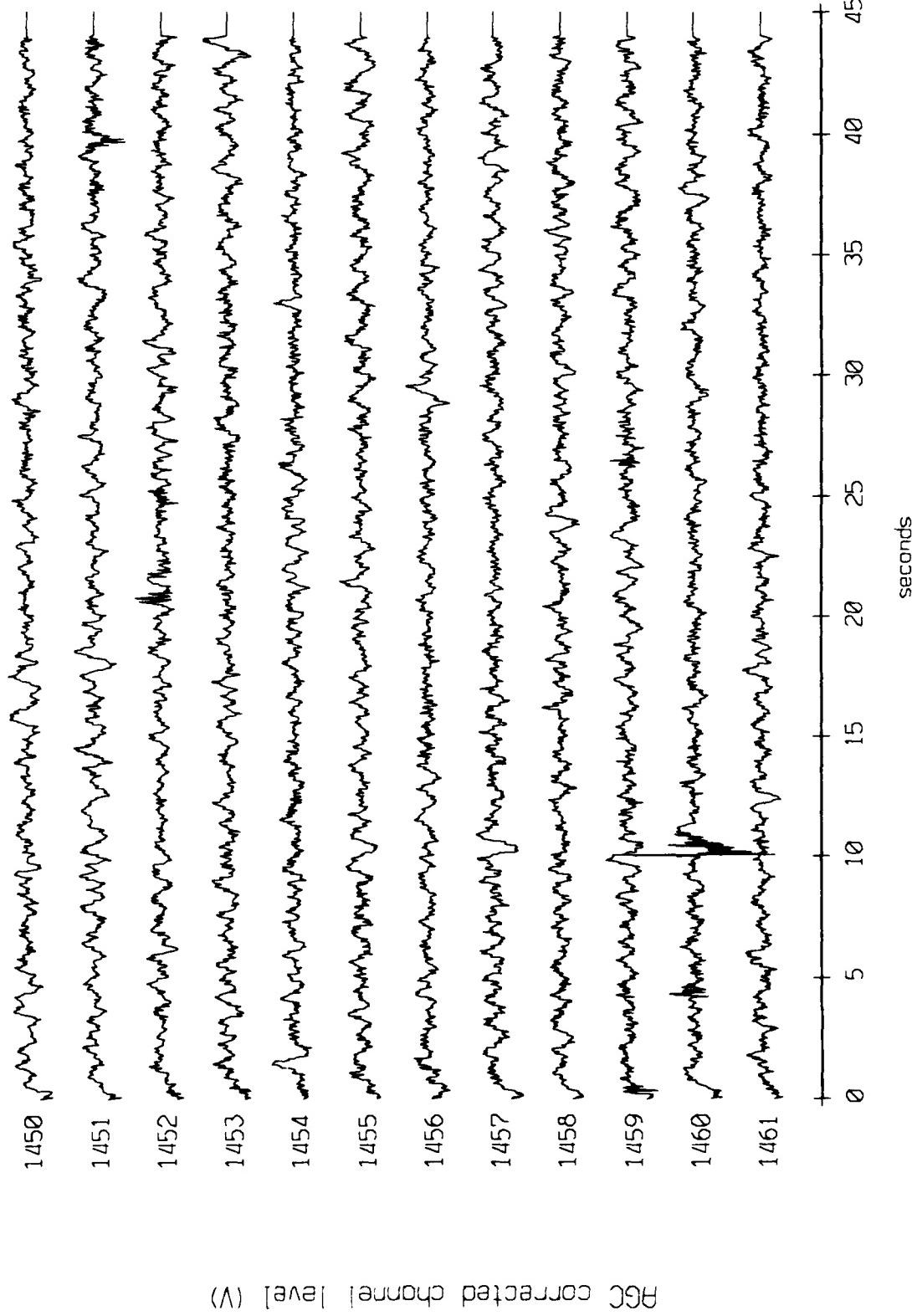


Figure X.4.9c

Float 9, September 1987 Sea Trip - records 1450-1461 (x-axis
vertical axis scale is approx. -1.0 to 1.0 volts)

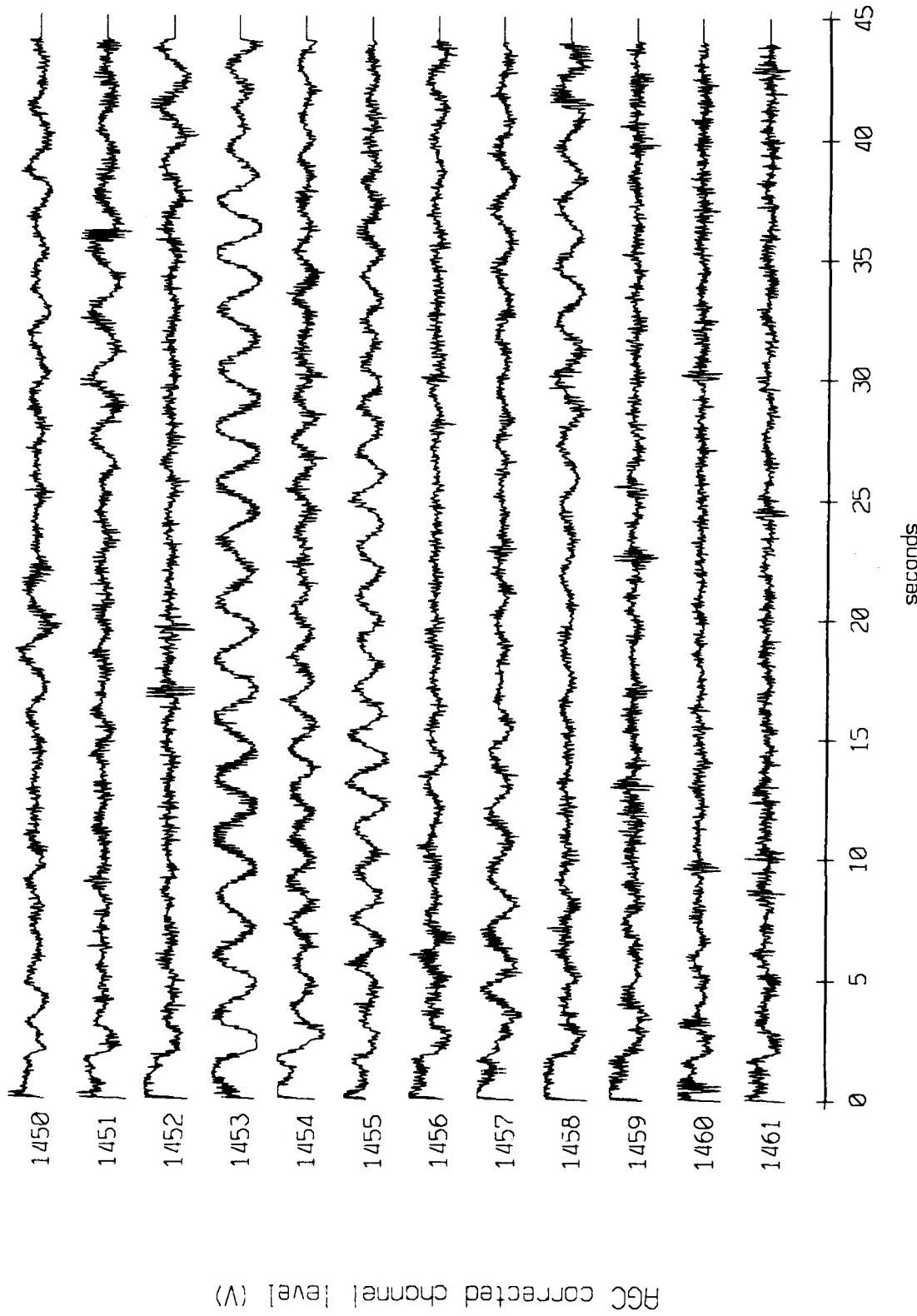


Figure X.4.10a

Float 9, September 1987 Sea Trip - records 1450-1461 (y-axis)
vertical axis scale is approx. -1.0 to 1.0 volts

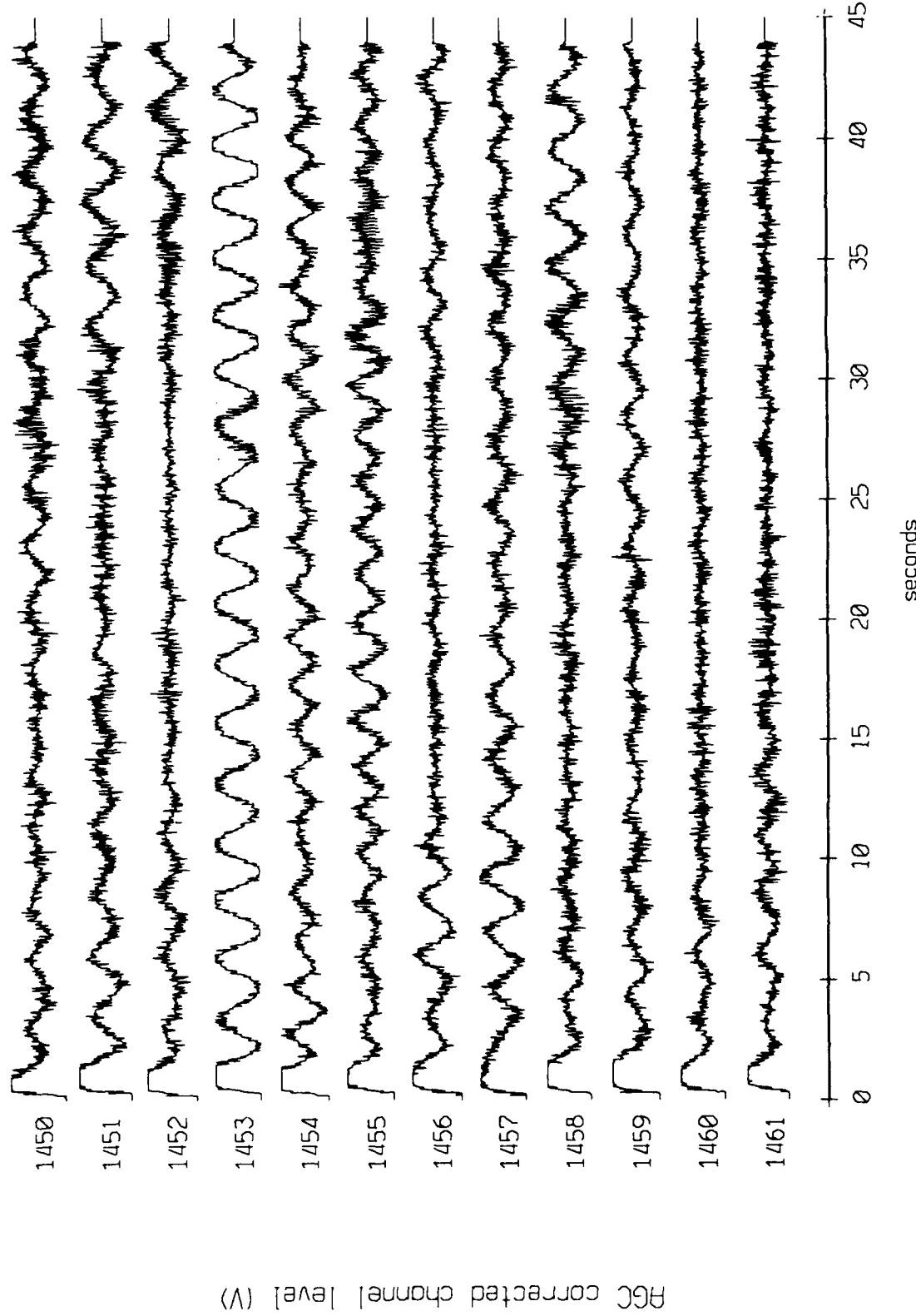


Figure X.4.10b

Flight 9, September 1987 Sea Trip - records 1450-1461 (z-axis)
vertical axis scale is approx. -1.0 to 1.0 volts

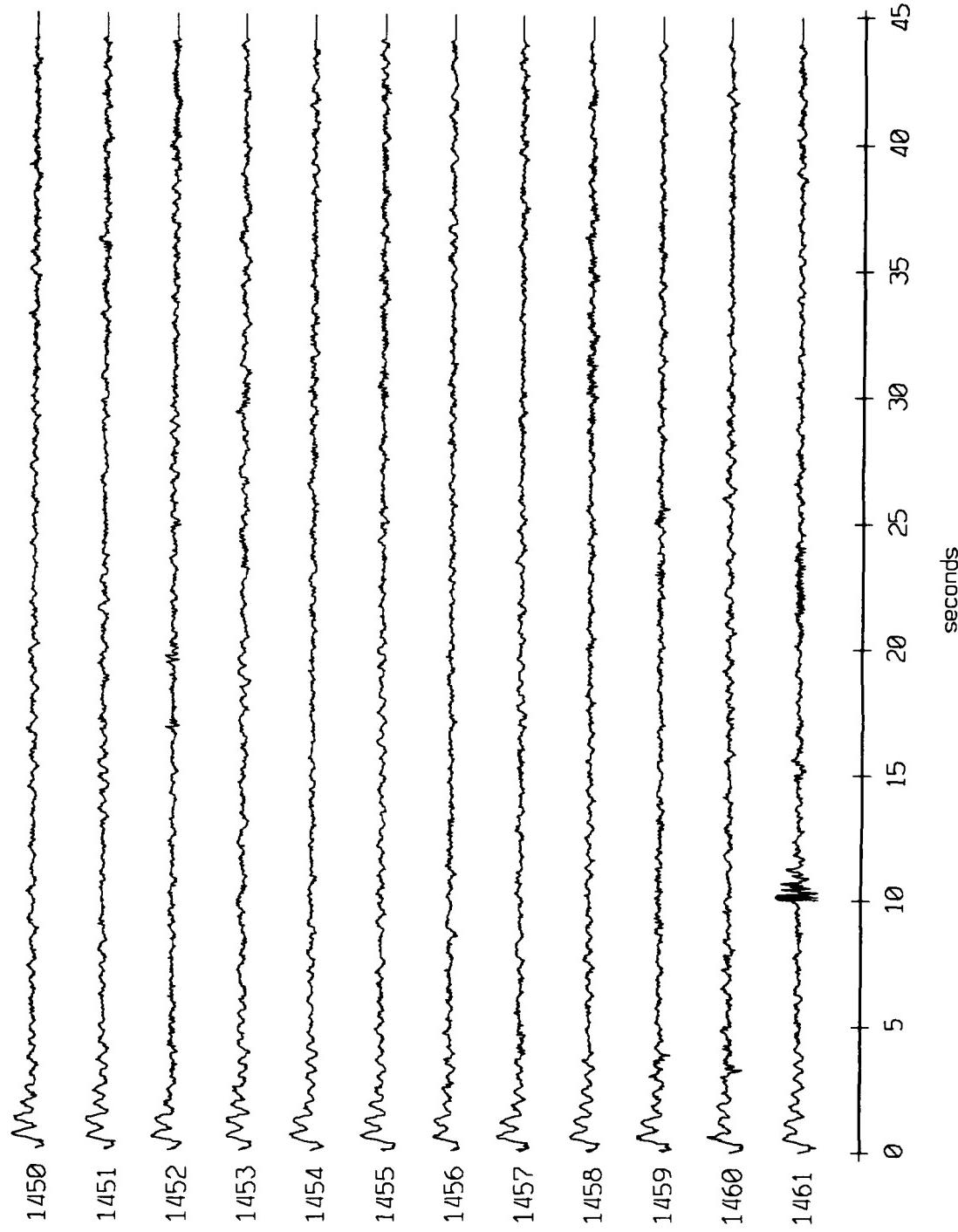


Figure X.4.10c

1st Pop, September 1987 Trip - records 1526-1527 (x-axis)
vertical axis scale is -1.0 to 1.0 volts

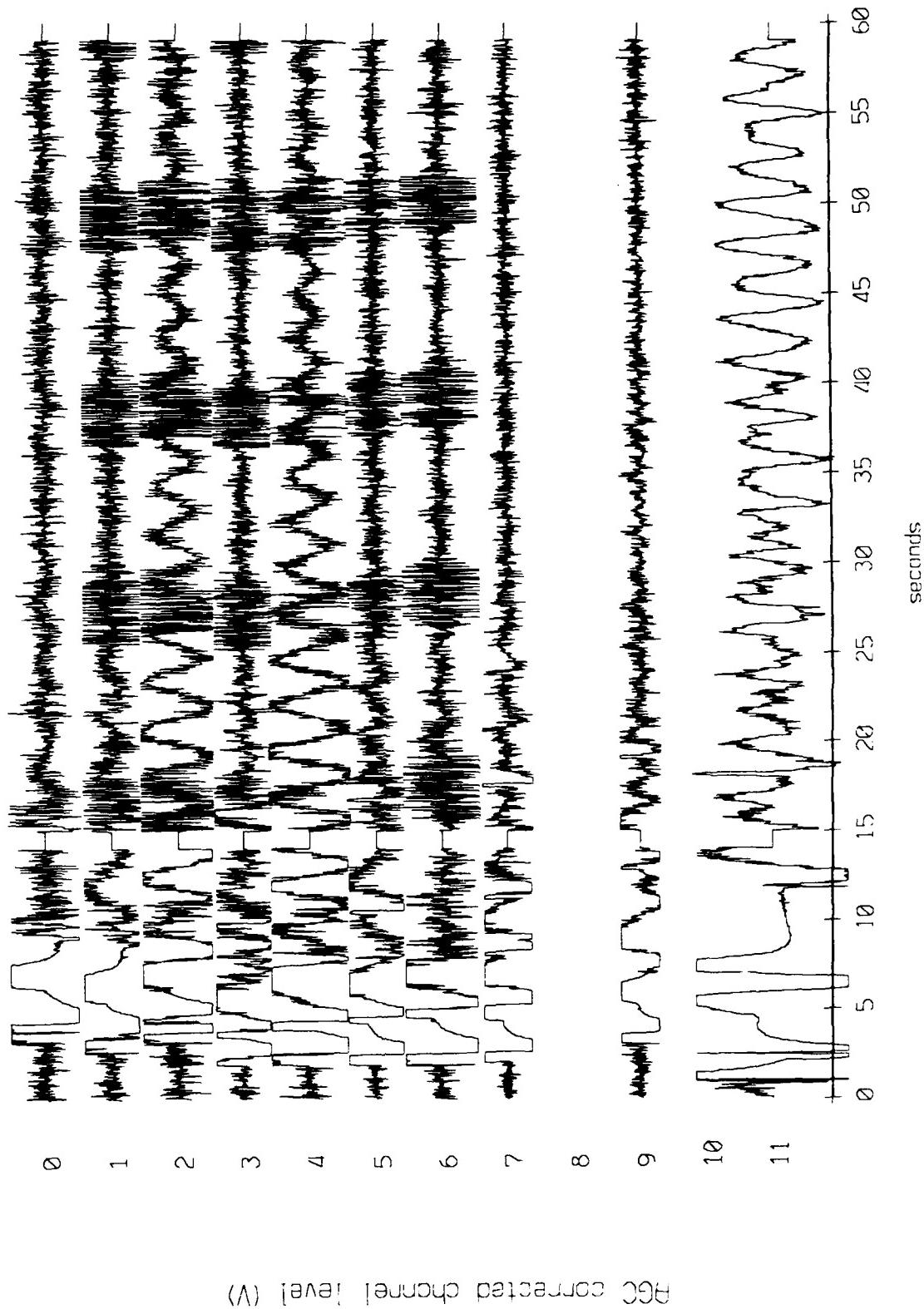
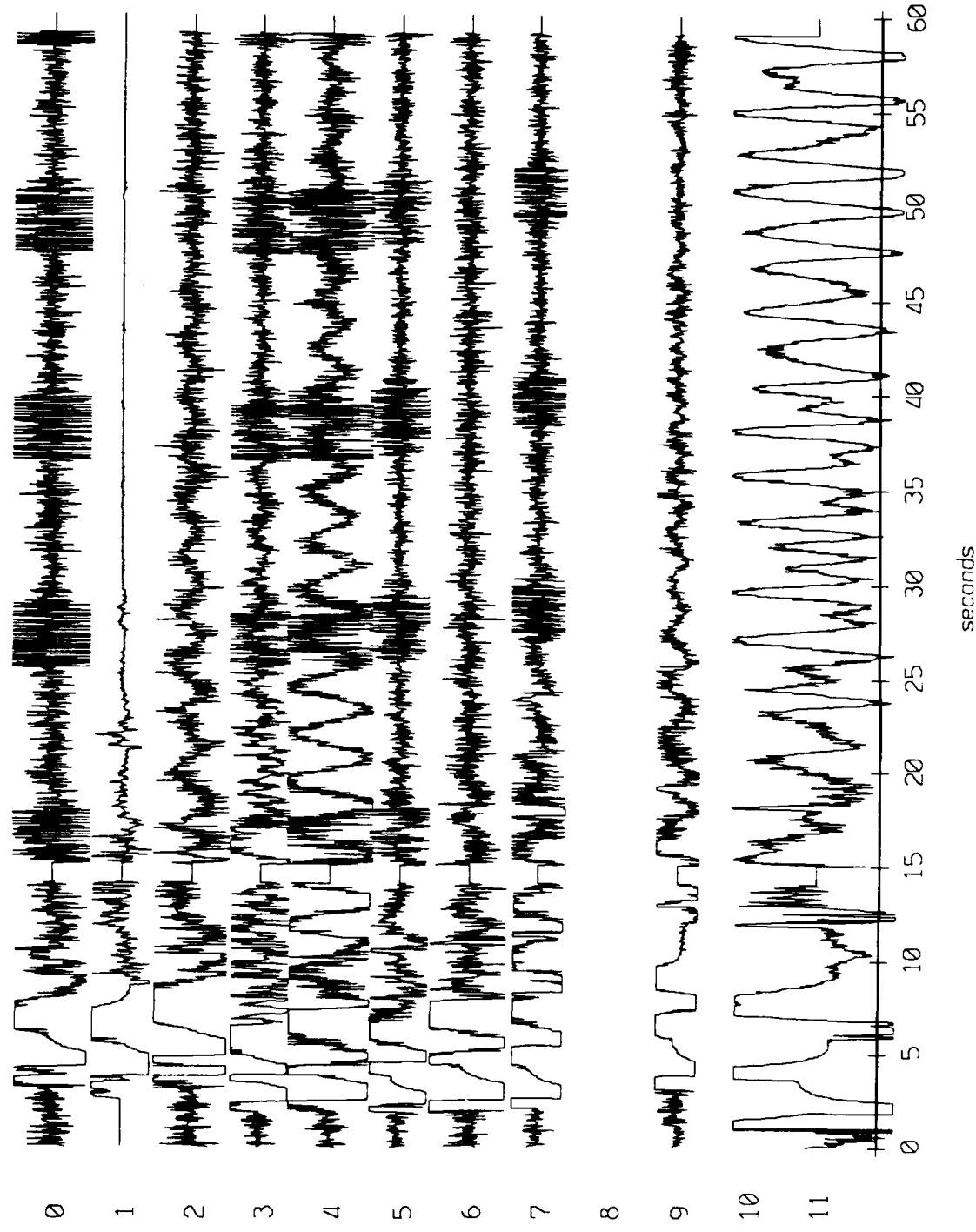


Figure X.5.1a

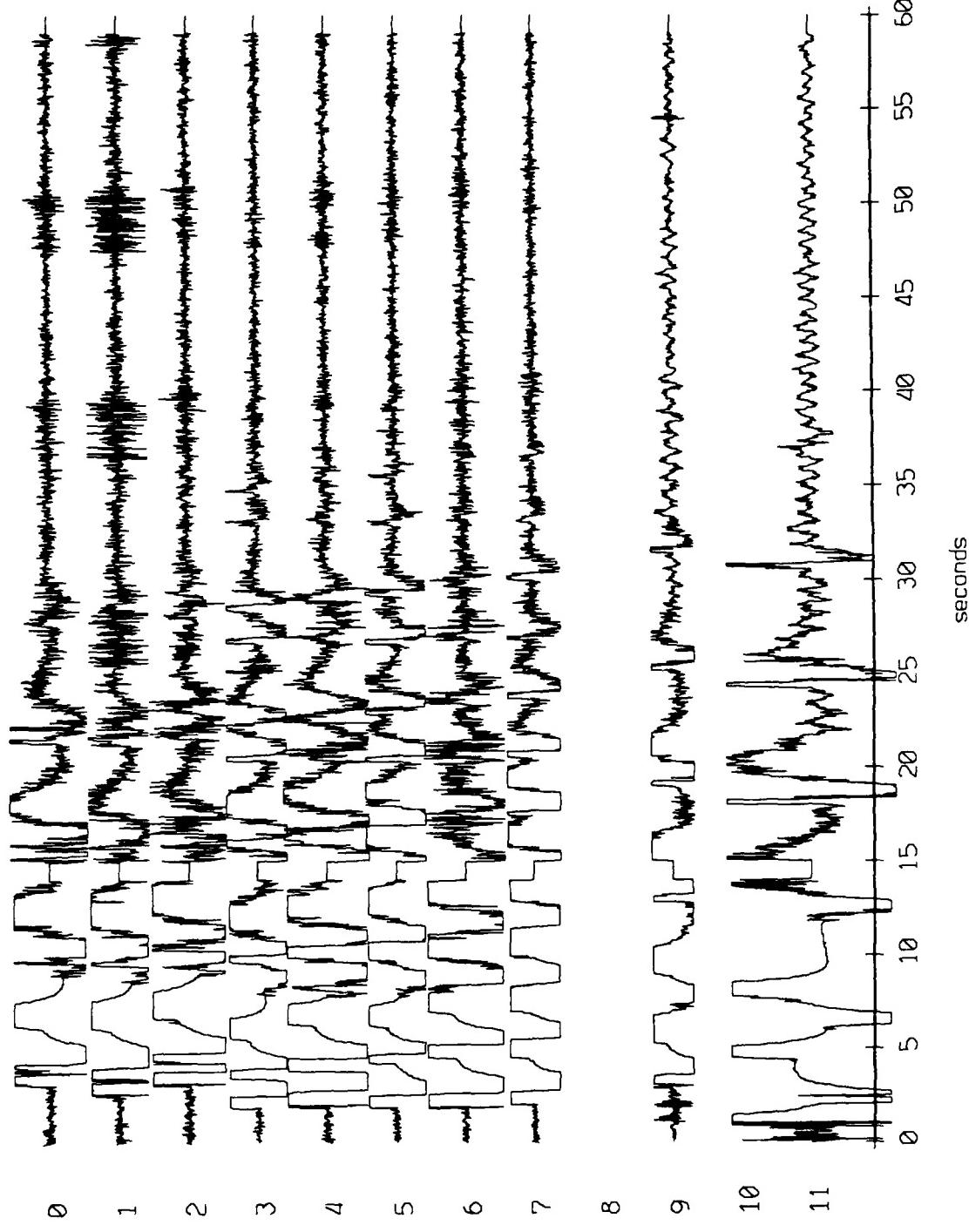
1st Pop, September 1987 Trip - records 1526-1527 (y-axis)
vertical axis scale is 1.0 to 1.0 volts



AGC corrected channel level (V)

Figure X.5.1b

1st Pop, September 1987 Trip - records 1526-1527 (z-axis)
vertical axis scale is -1.0 to 1.0 volts



AGC corrected channel level (V)

Figure X.5.1c

Float 9, September 1987 Sea Trip - records 1523-1534 (z-axis)
vertical axis scale is approx. -1.0 to 1.0 volts

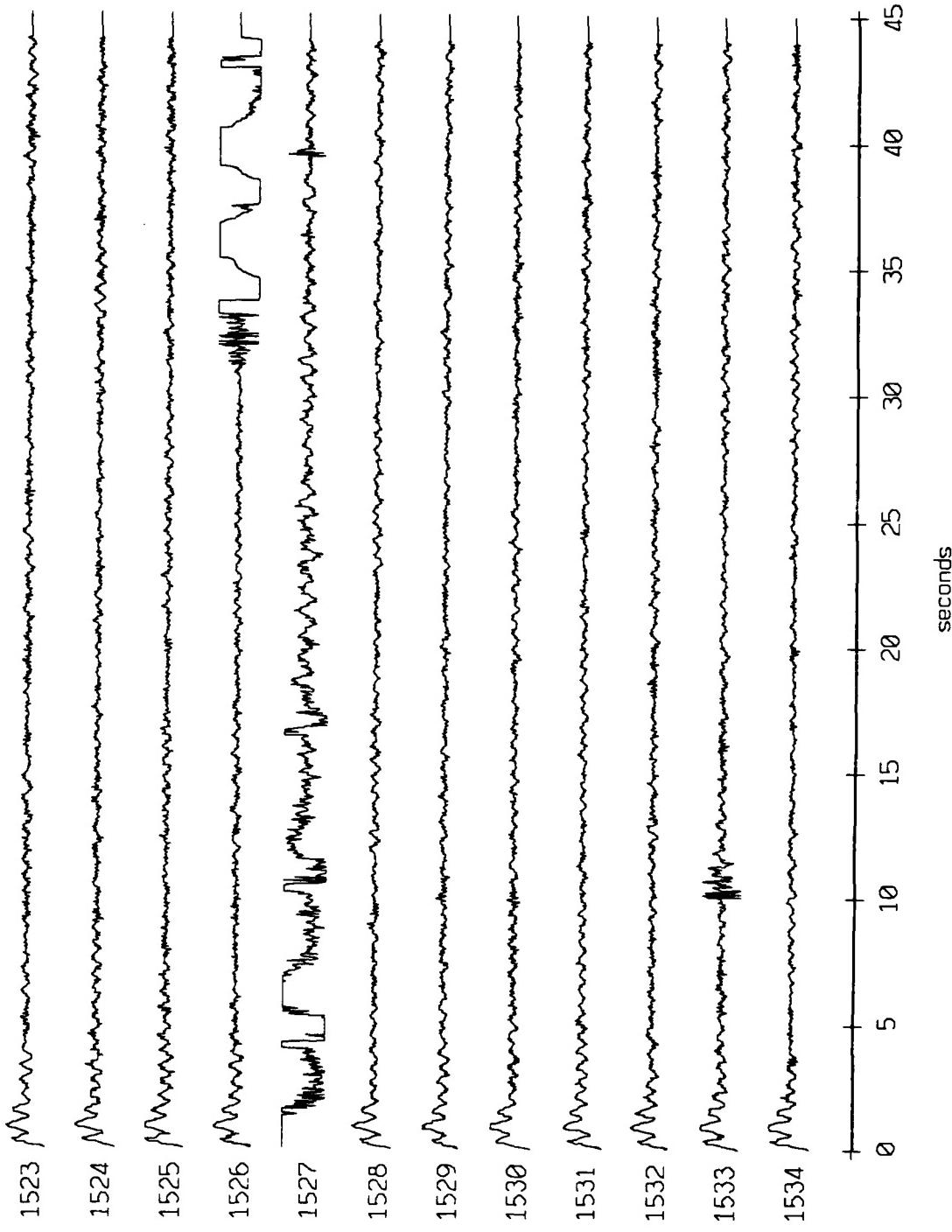


Figure X.5.2a

Float 11, September 1987 Trip - records 1523-1534 (z-axis)
vertical axis scale is approx. -1.0 to 1.0 volts

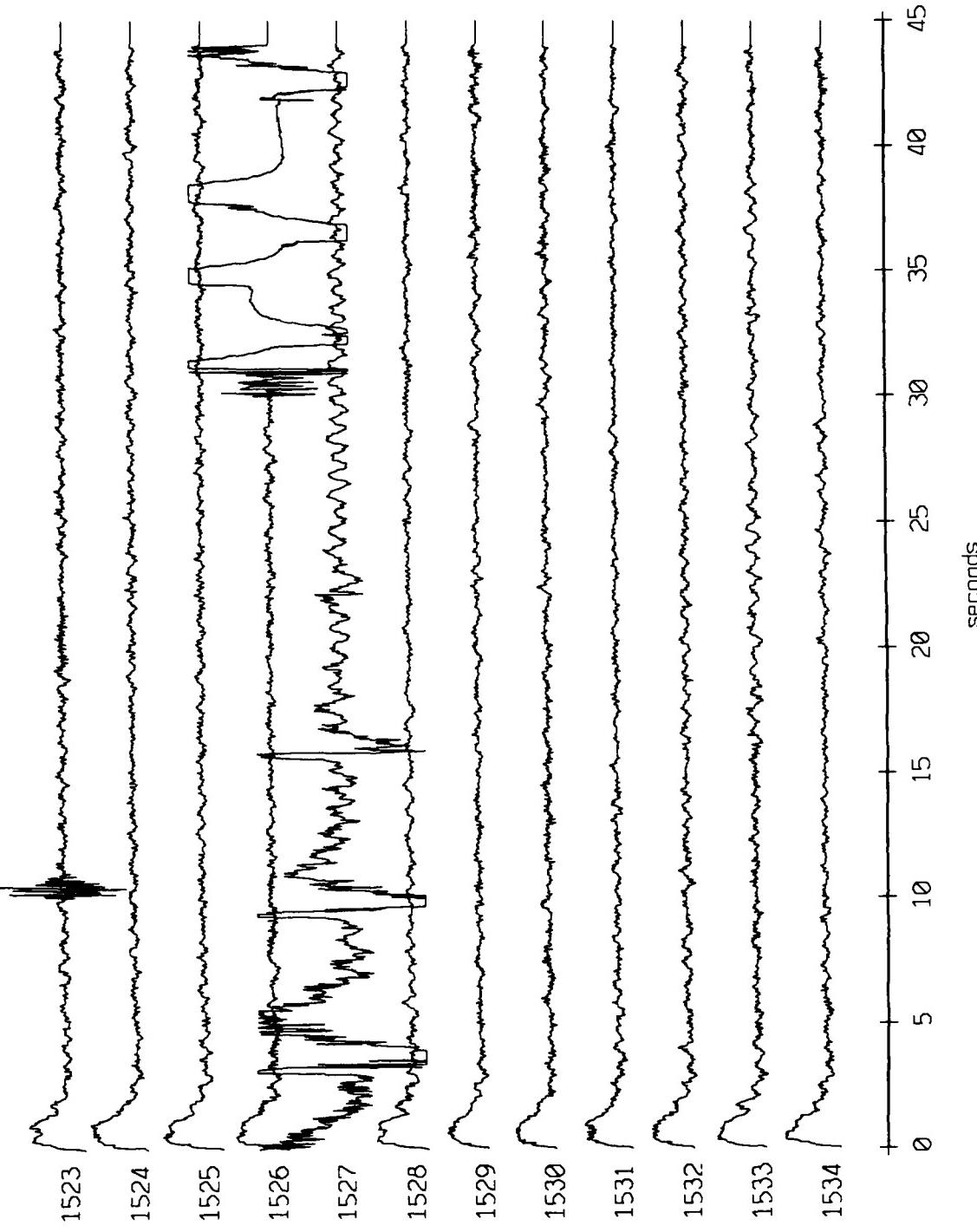


Figure X.5.2b

Float 0, September 1987 Trip - records 1543-1554 (x-axis)
vertical axis scale is approx. -1.0 to 1.0 volts

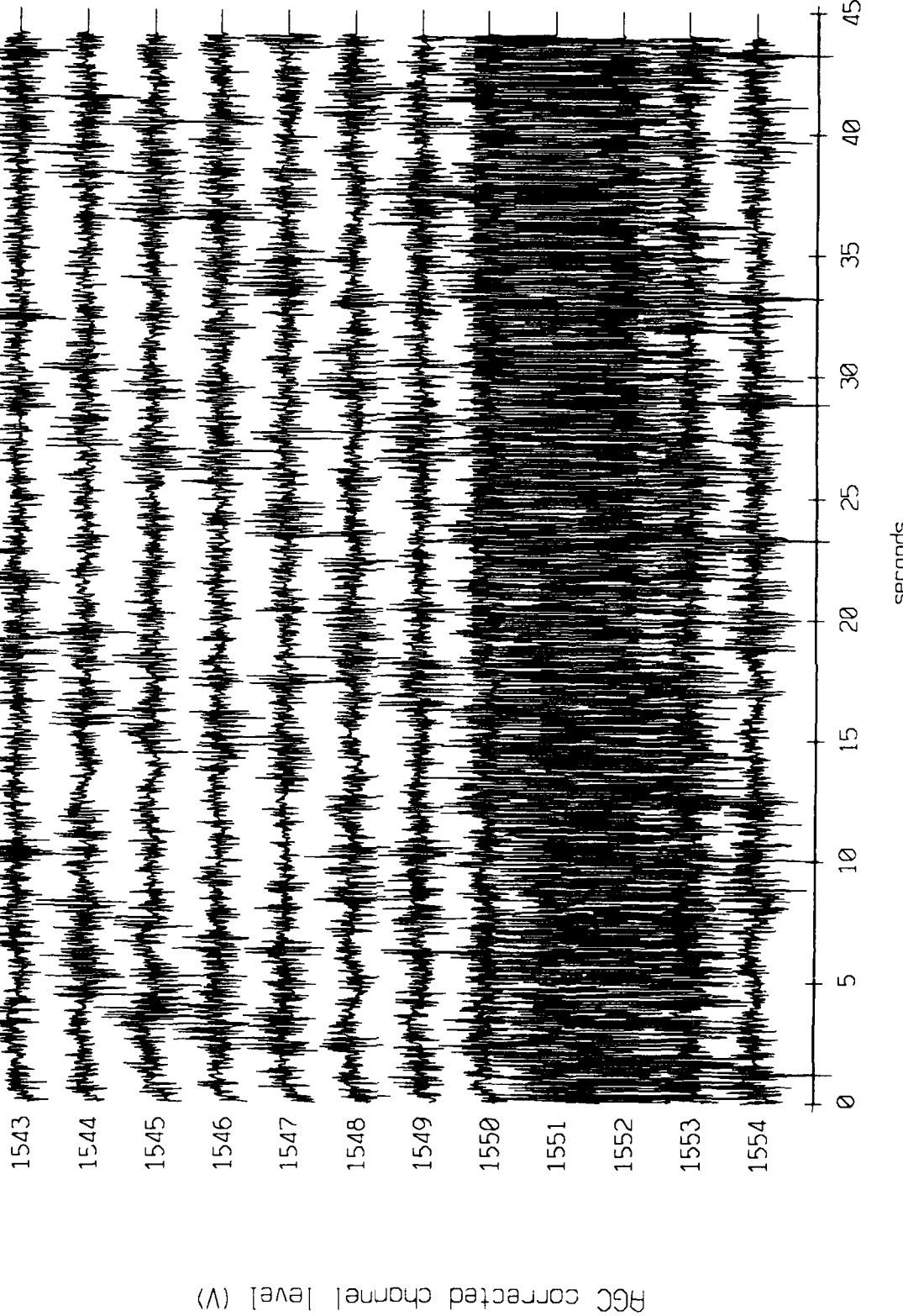


Figure X.6.1a

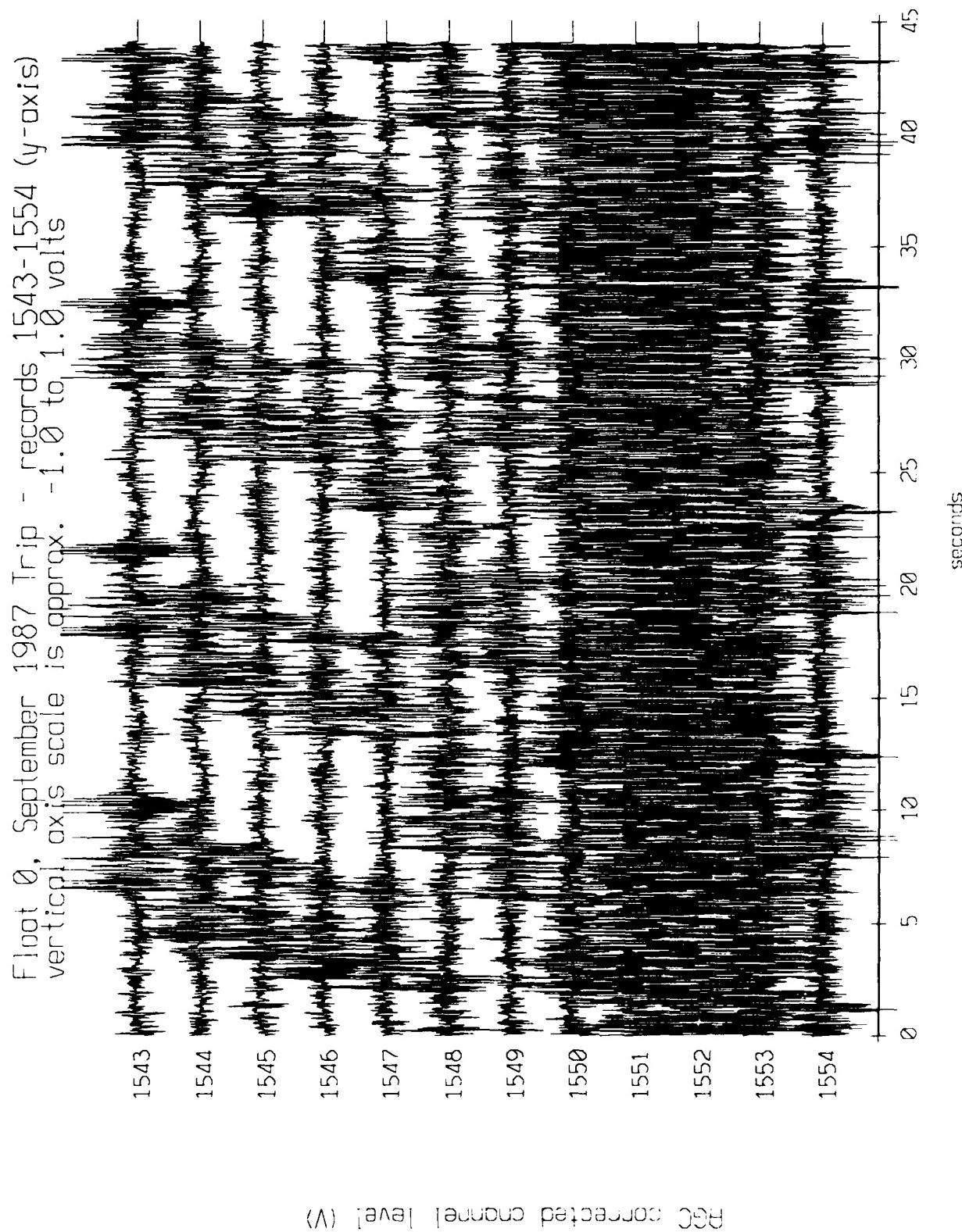


Figure X.6.1b

Flight 0, September 1987 Trip - records 1543-1554 (z-axis)
vertical axis scale is approx. -1.0 to 1.0 volts

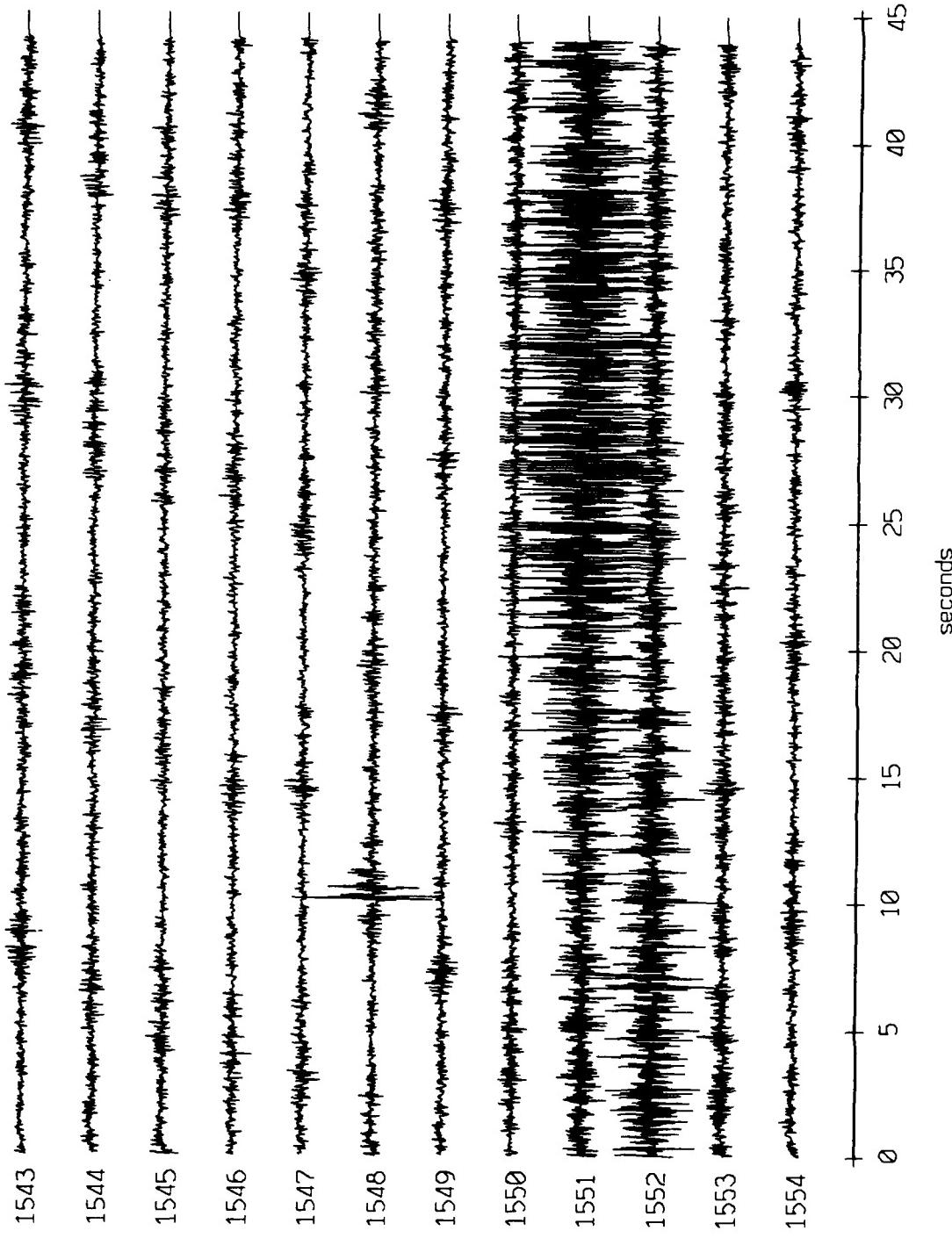


Figure X.6.1c

Float 2, September 1987 Trip - records 1640-1651 (x-axis
vertical axis scale is approx. -1.0 to 1.0 Volts

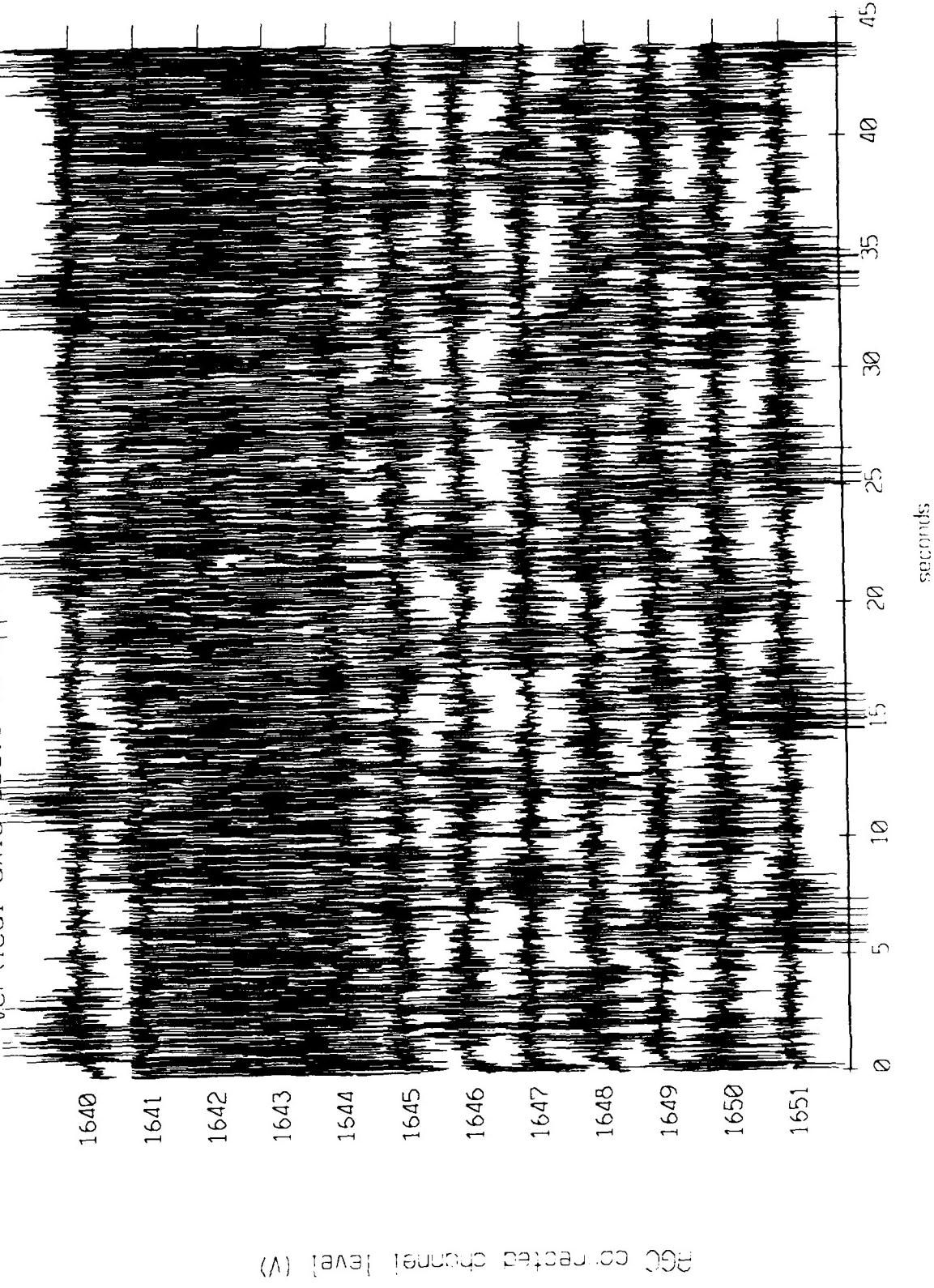


Figure X.7.1a

Float 2, September 1987 Trip - records 1640-1651 (y-axis)
vertical axis scale is approx. -1.0 to 1.0 volts

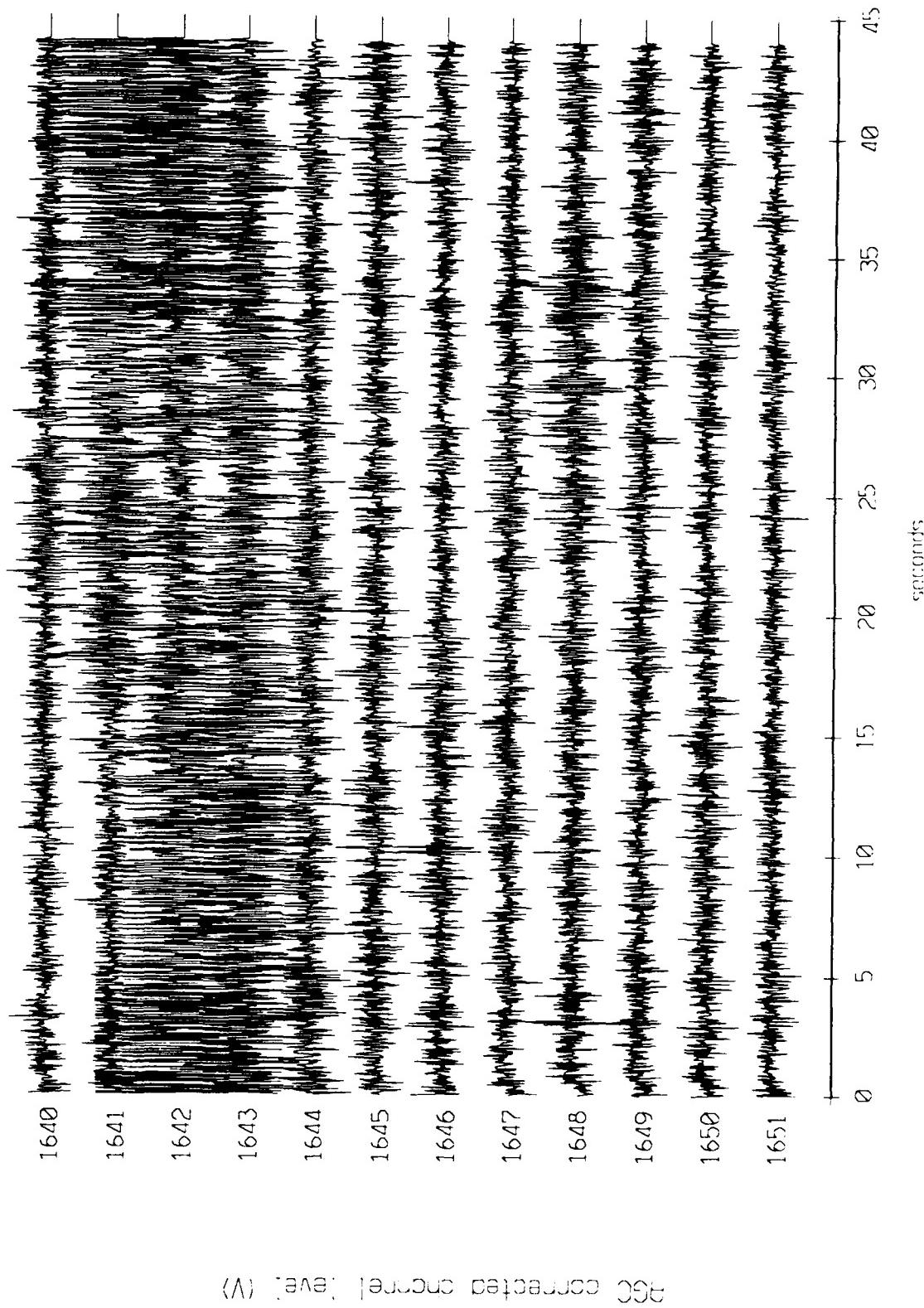


Figure X.7.1b

Float 2, September 1987 Trip - records 1640-1651 (z-axis)
vertical axis scale is approx. -1.0 to 1.0 volts

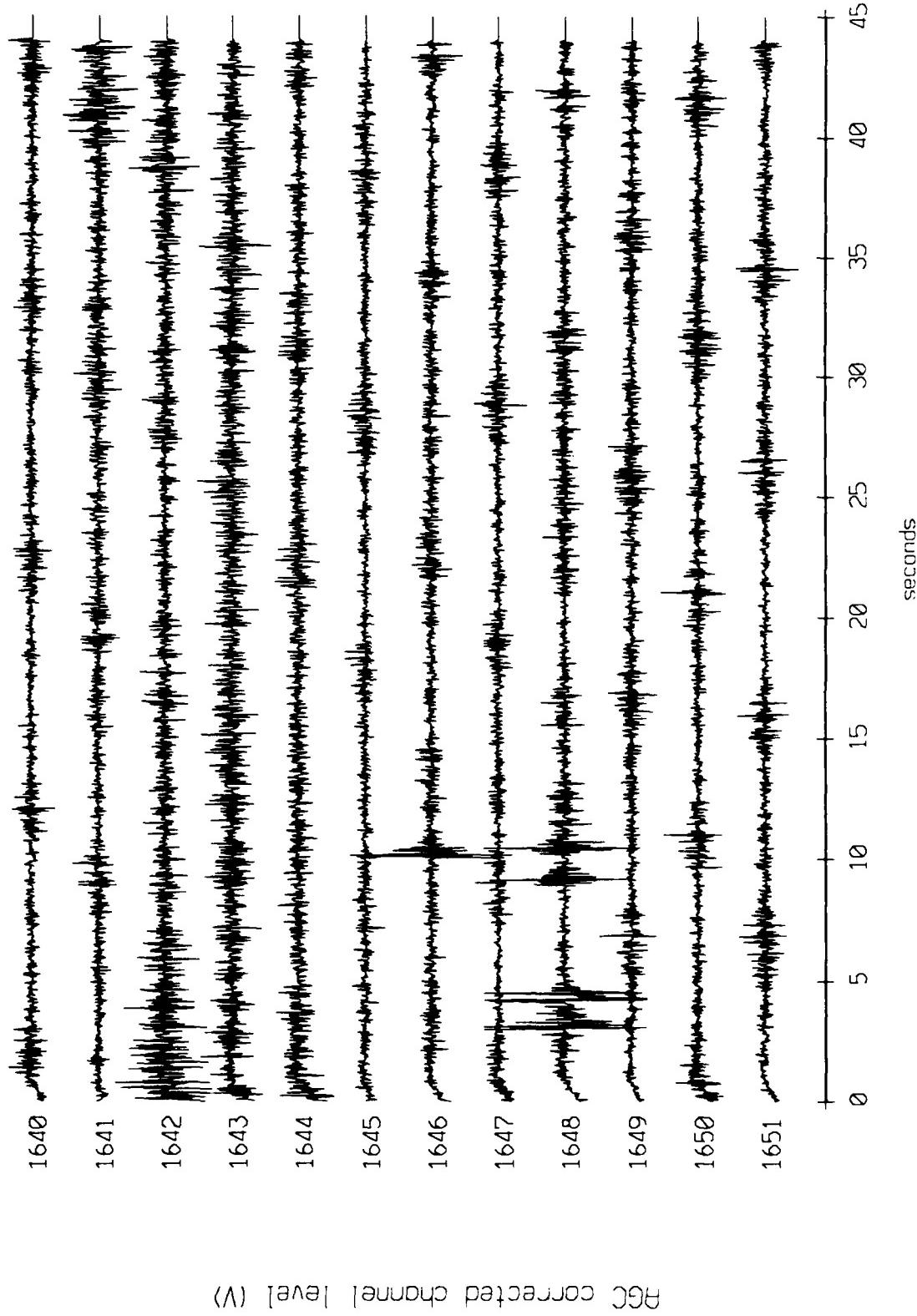


Figure X.7.1c

Float 2, September 1987 Trip - records 1648-1659 (x-axis)
Vertical axis scale is approx -1.0 to 1.0 volts

1648

1649

1650

1651

1652

1653

1654

1655

1656

1657

1658

1659

HGC corrected channel (wave) (V)

seconds

45
40
35
30
25
20
15
10
5
0

Figure X.7.2a

Float 2, September 1987 Trip - records 1648-1659 (y-axis)
vertical axis scale is approx. -1.0 to 1.0 volts

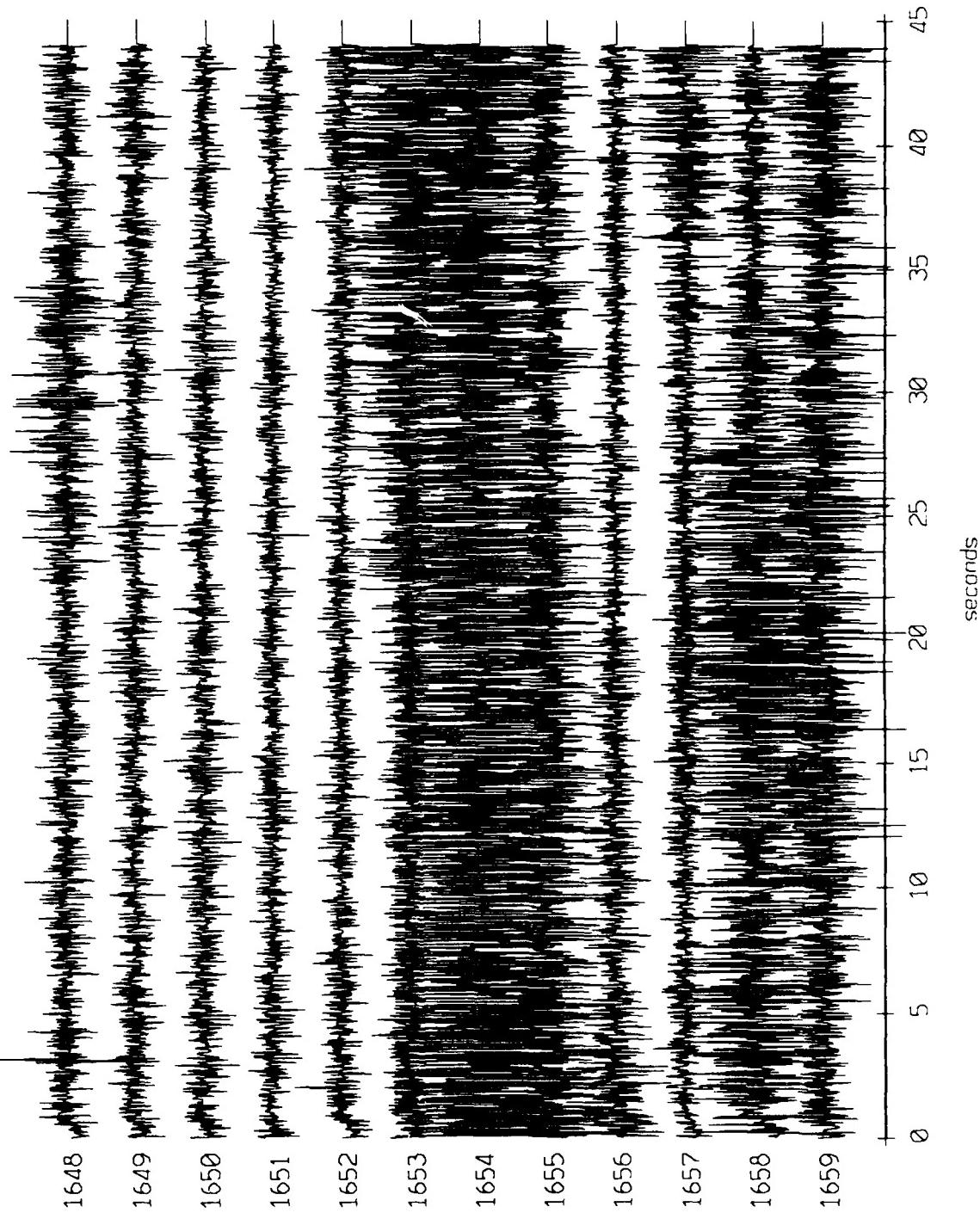


Figure X.7.2b

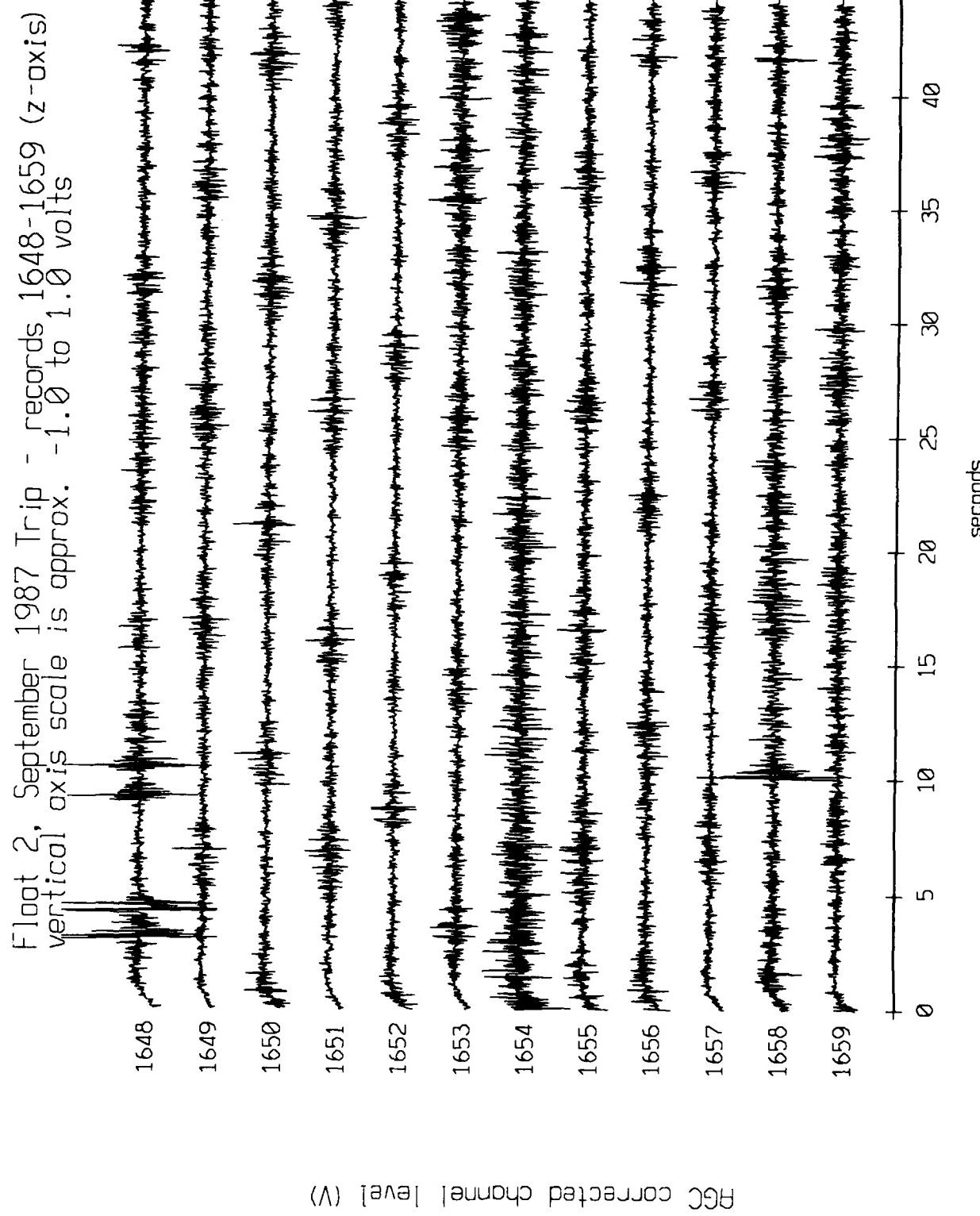


Figure X.7.2c

Float 0, Sept, 1987 Trip - records 1800-1811 (x-axis)
vertical axis scale is approx. -1.0 to 1.0 volts

1800

1801

1802

1803

1804

1805

1806

1807

1808

1809

1810

1811

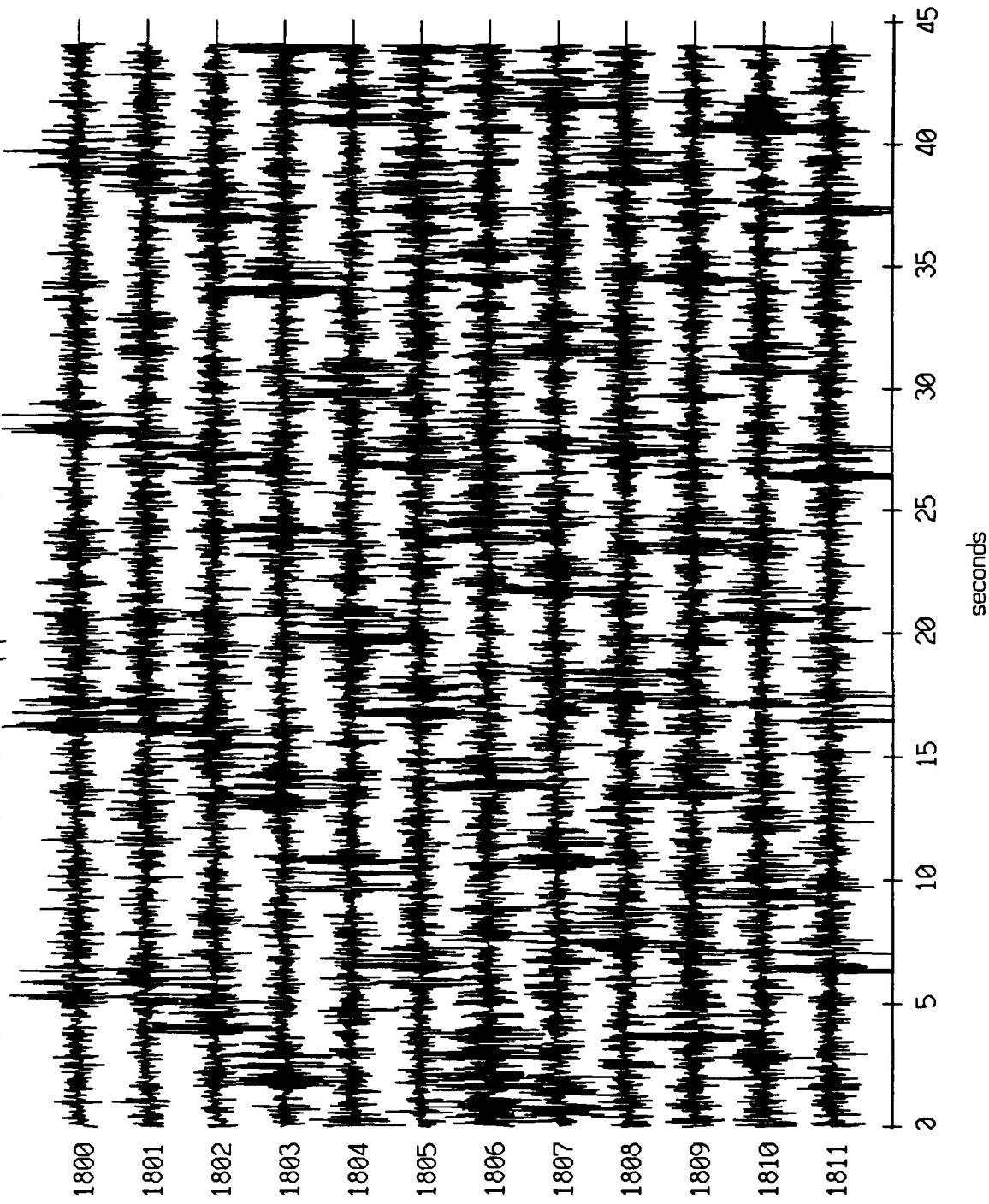
AGC corrected channel level (V)

seconds

0 5 10 15 20 25 30 35 40 45

Figure X.8.1a

Float 0, Sept, 1987 Trip - records 1800-1811 (y-axis)
vertical axis scale is approx. -1.0 to 1.0 volts



RGC corrected channel level (V)

Figure X.8.1b

Float 0, Sept, 1987 Trip - records 1800-1811 (z-axis)
vertical axis scale is approx. -1.0 to 1.0 volts

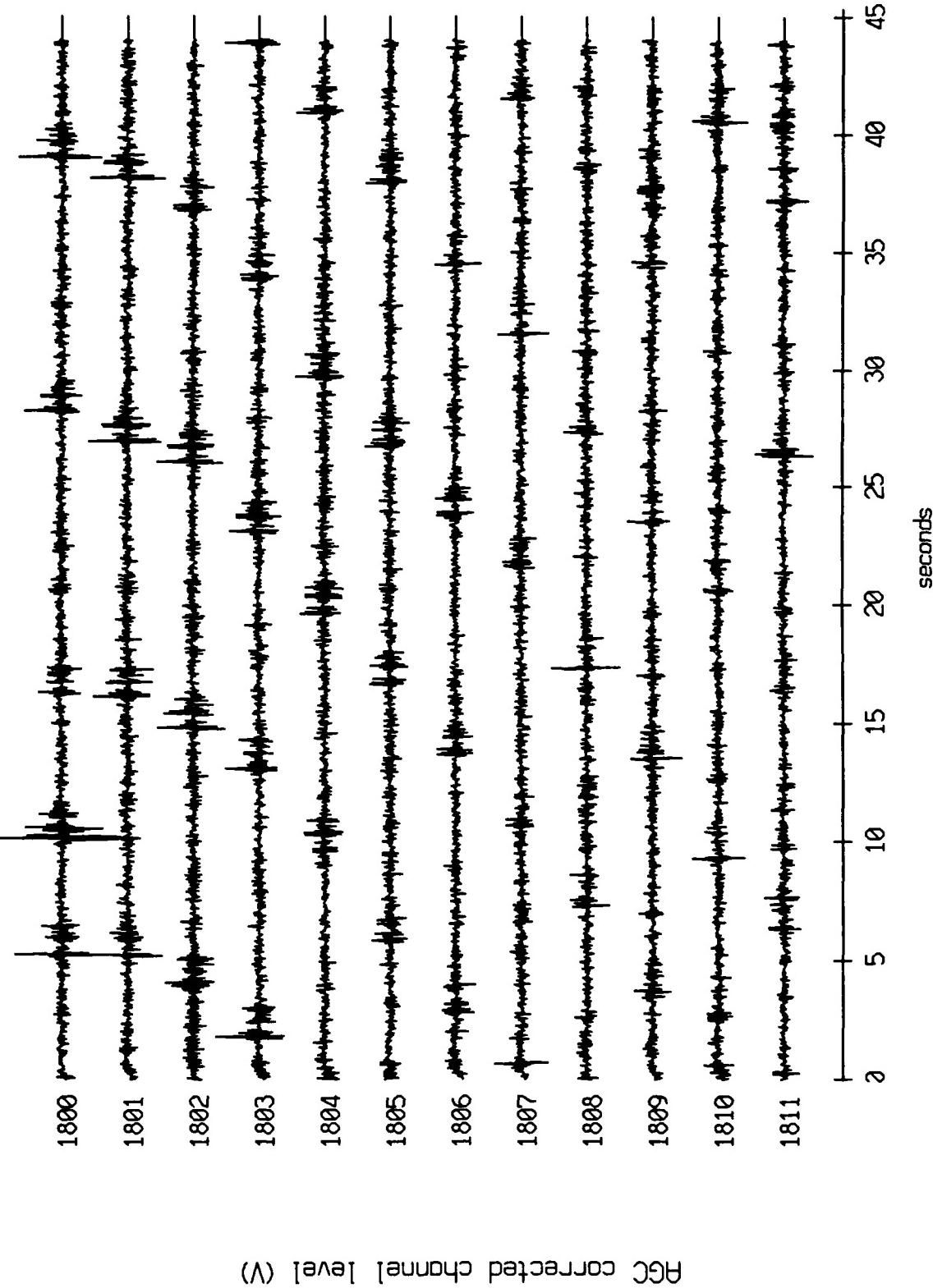


Figure X.8.1c

OBS 08, Sept, 1987 TriP - events 901 and 902 (x_axis)
max gain-corrected amplitude is 6. 491421 counts

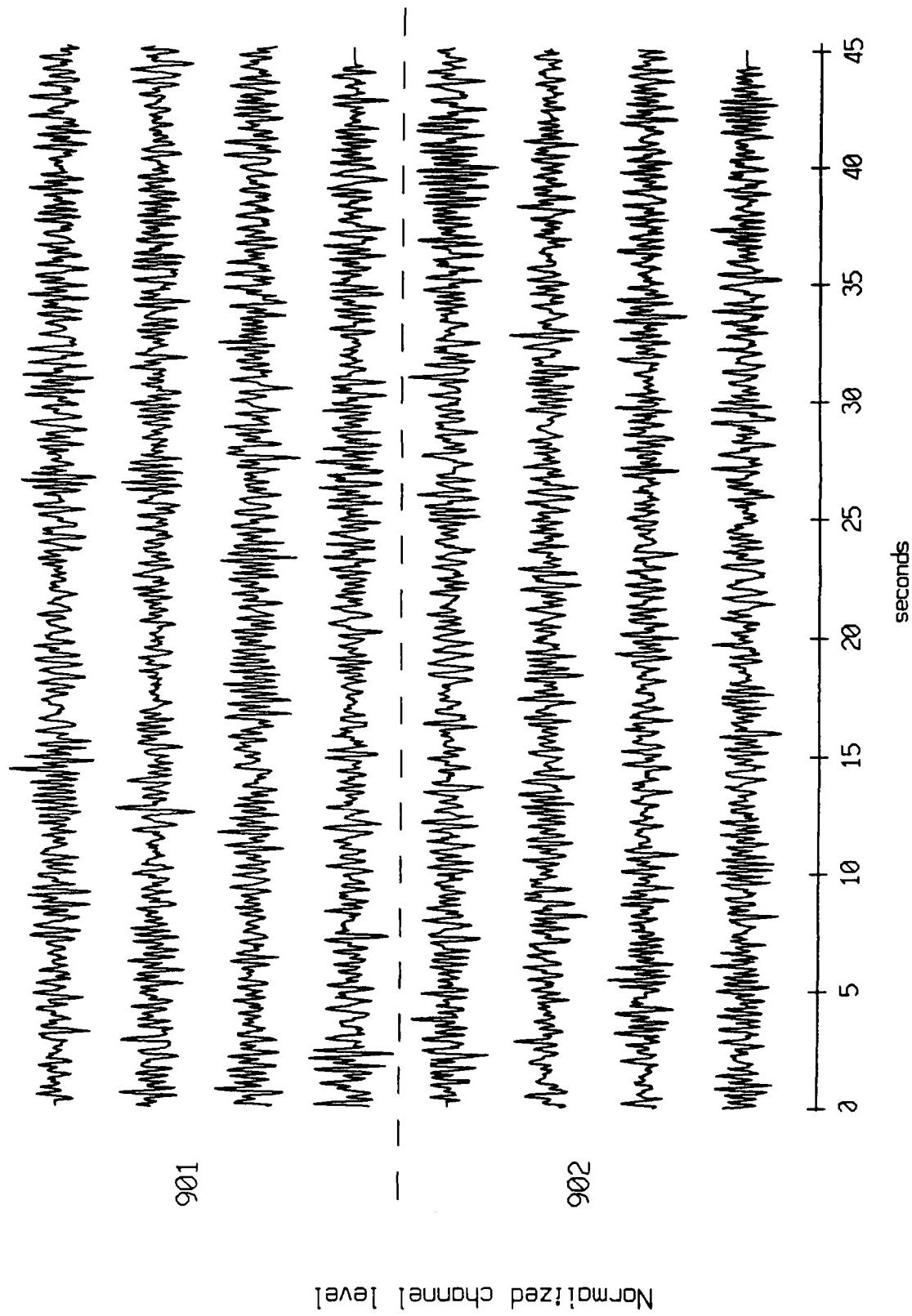


Figure X.9.1a

OBS 08, Sept, 1987 Trip - events 901 and 902 (y-axis)
max gain-corrected amplitude is 7.986419 counts

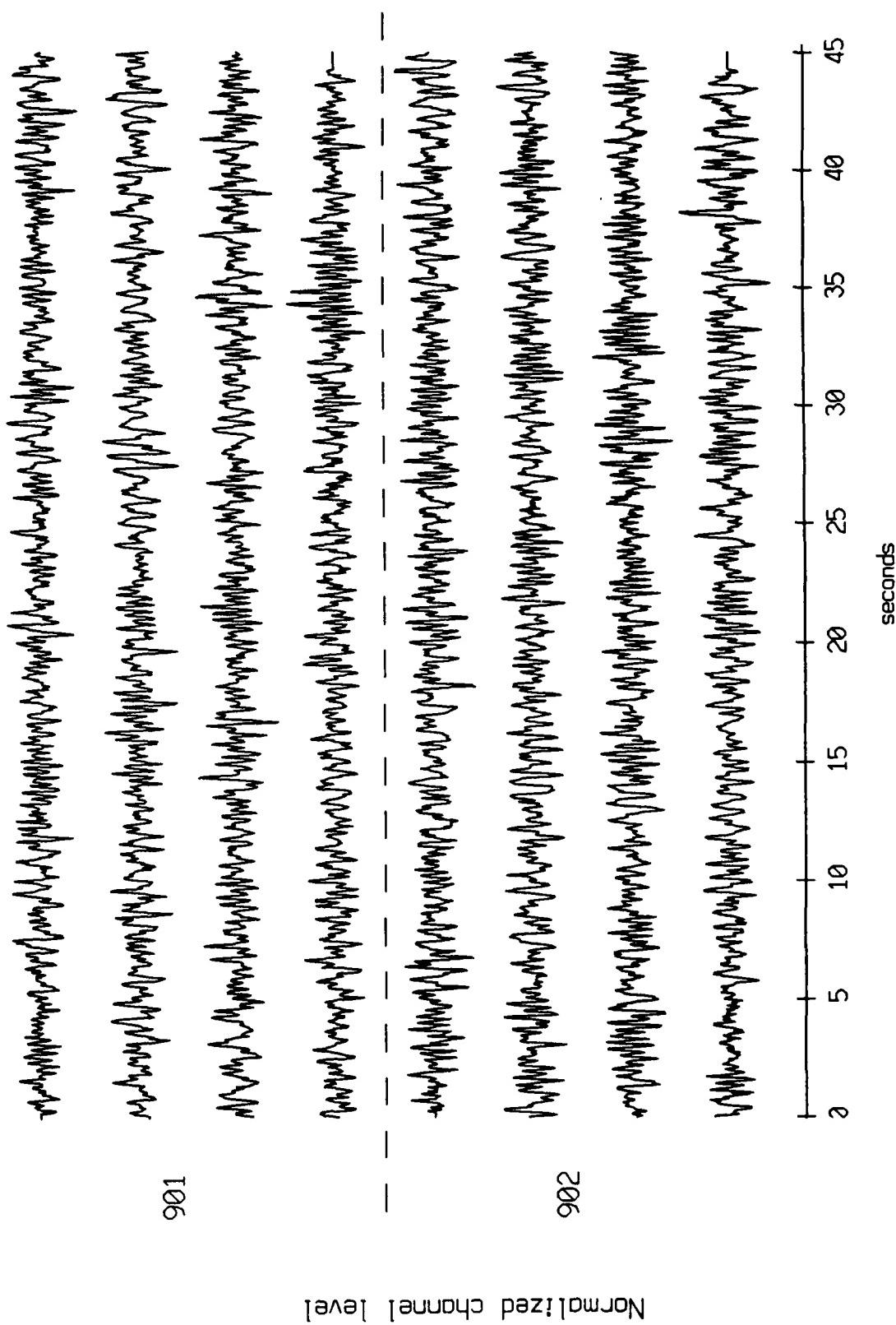


Figure X.9.1b

OBS 08, Sept, 1987 Trip - events 901 and 902 (z-axis)
max gain-corrected amplitude is 1.209673 counts

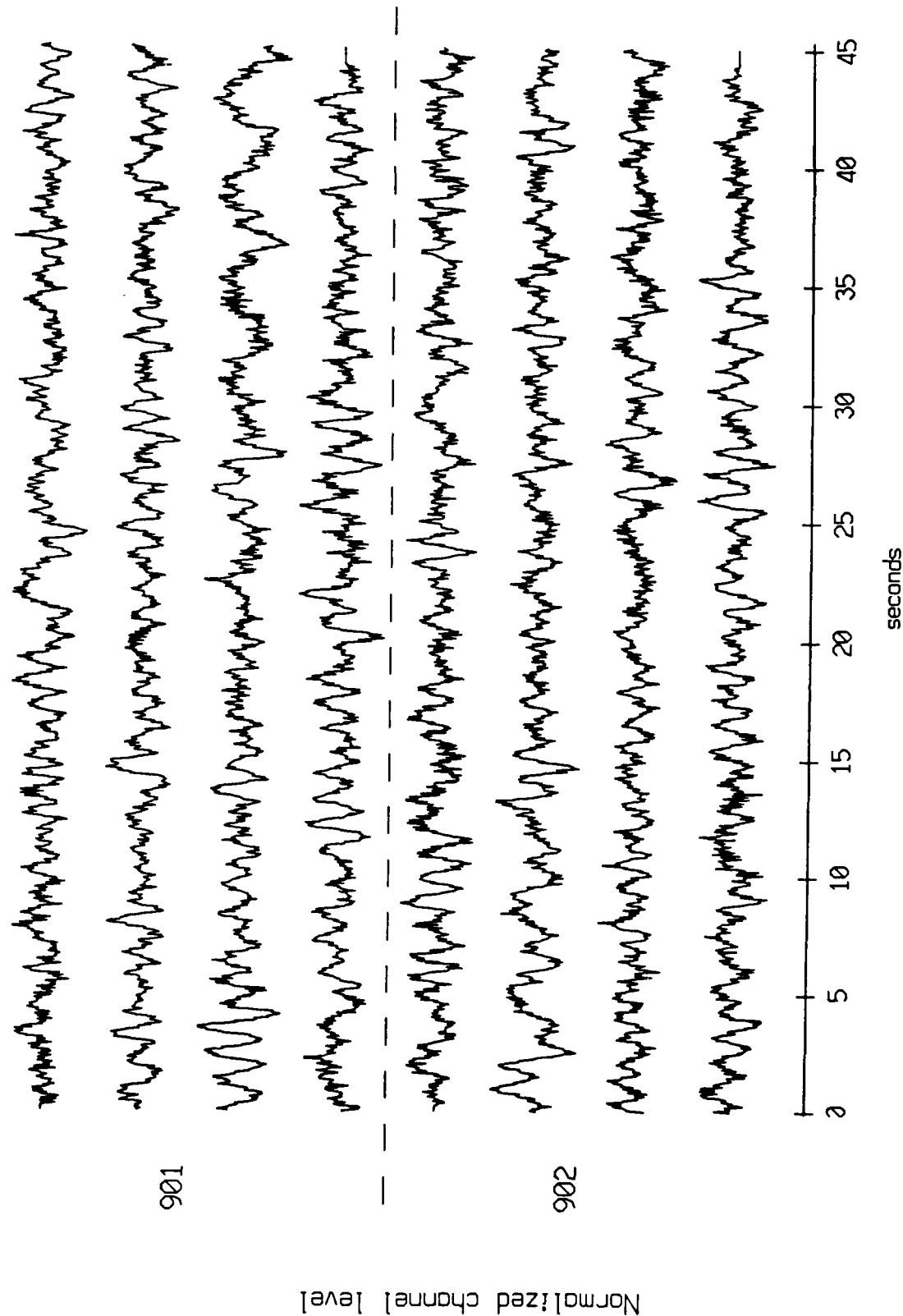


Figure X.9.1c

OBS 08, Sept, 1987 Trip - events 901 and 902 (pressure)
max gain-corrected amplitude is 2.609913 counts

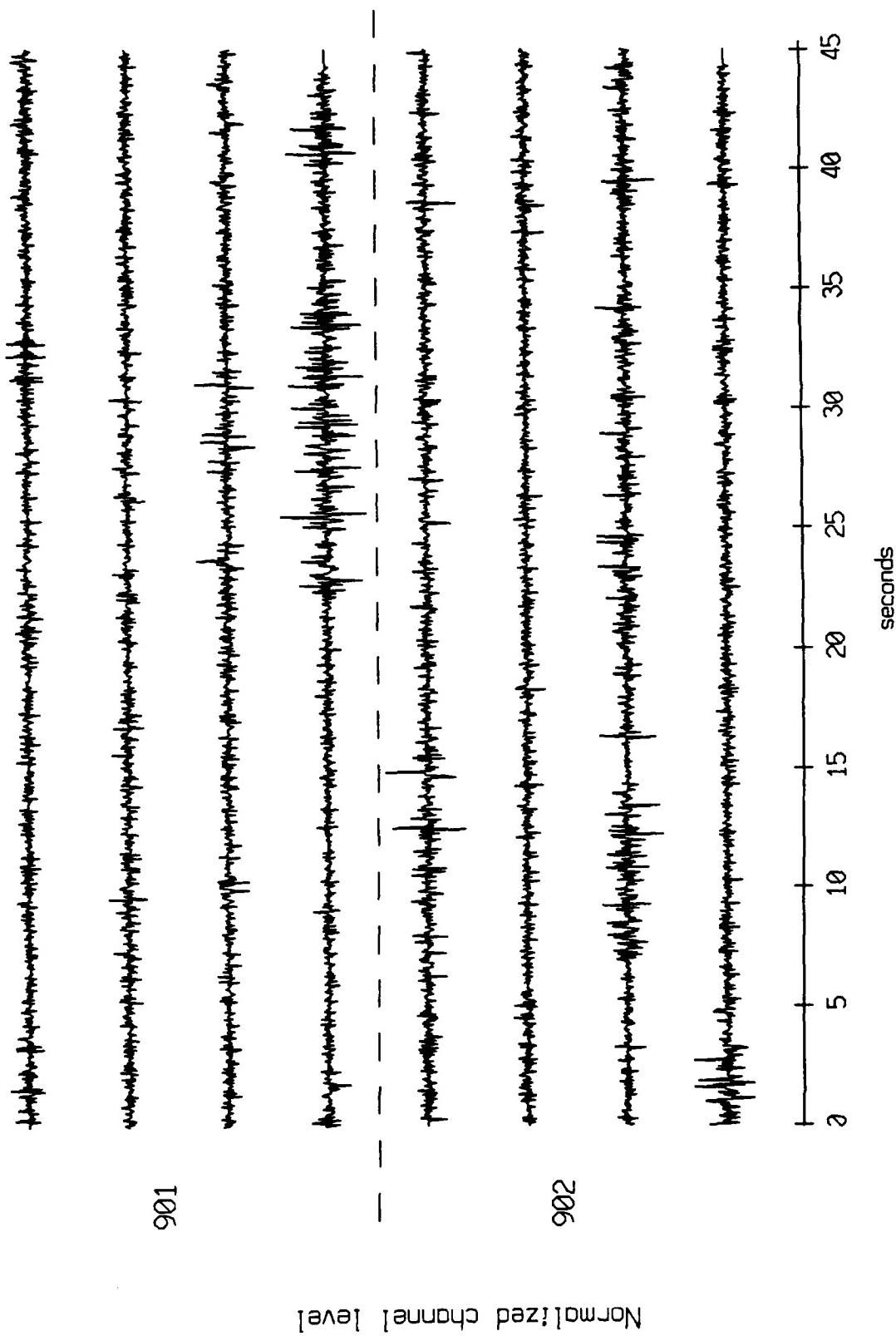


Figure X.9.1d

OBS 08, Sept, 1987 Tri β - events 903 and 904 (x-axis)
max gain-corrected amplitude is 7.875313 counts

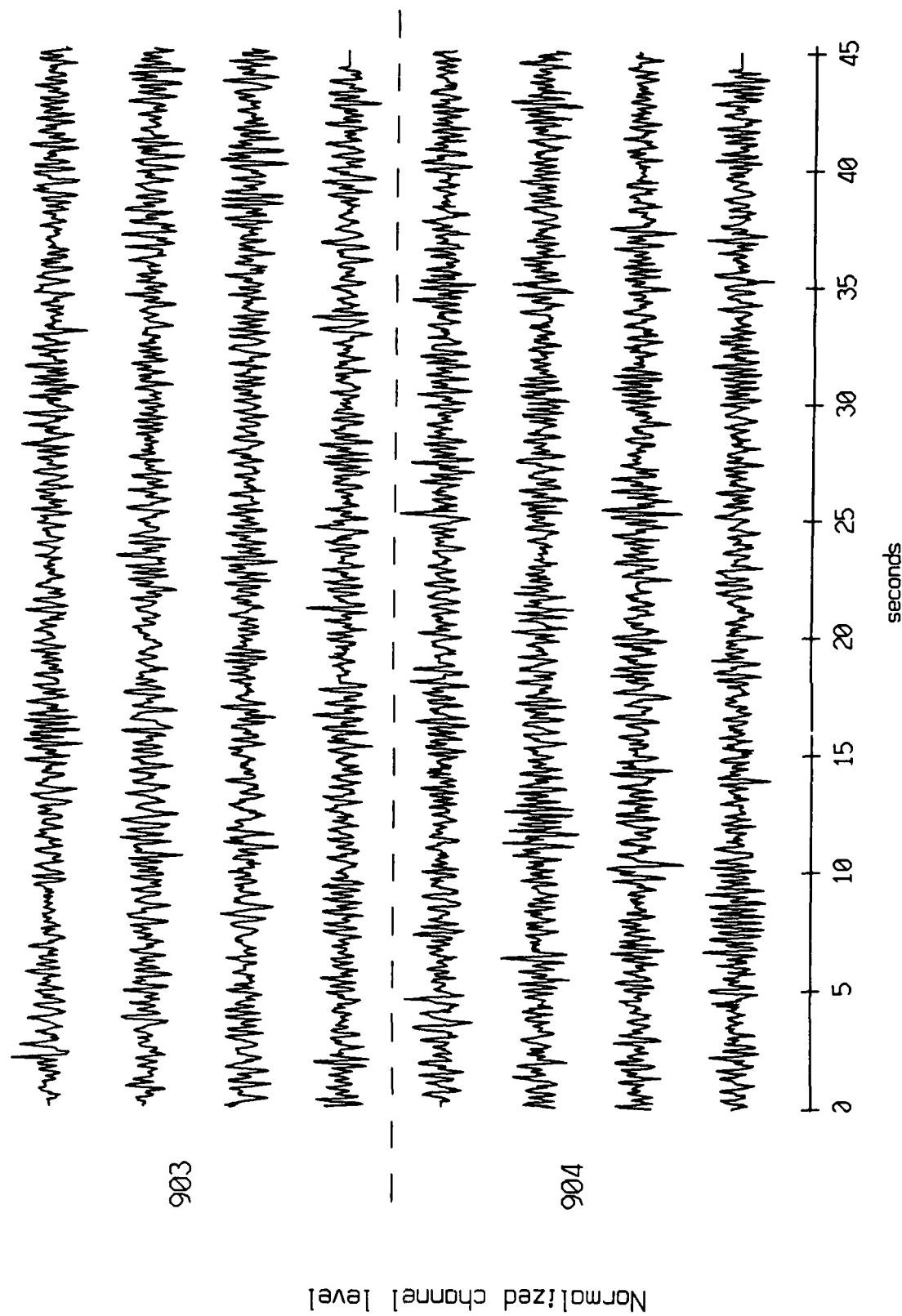


Figure X.10.1a

OBS 08, Sept, 1987 Trip - events 903 and 904 (y-axis)
max gain-corrected amplitude is 8.533936 counts

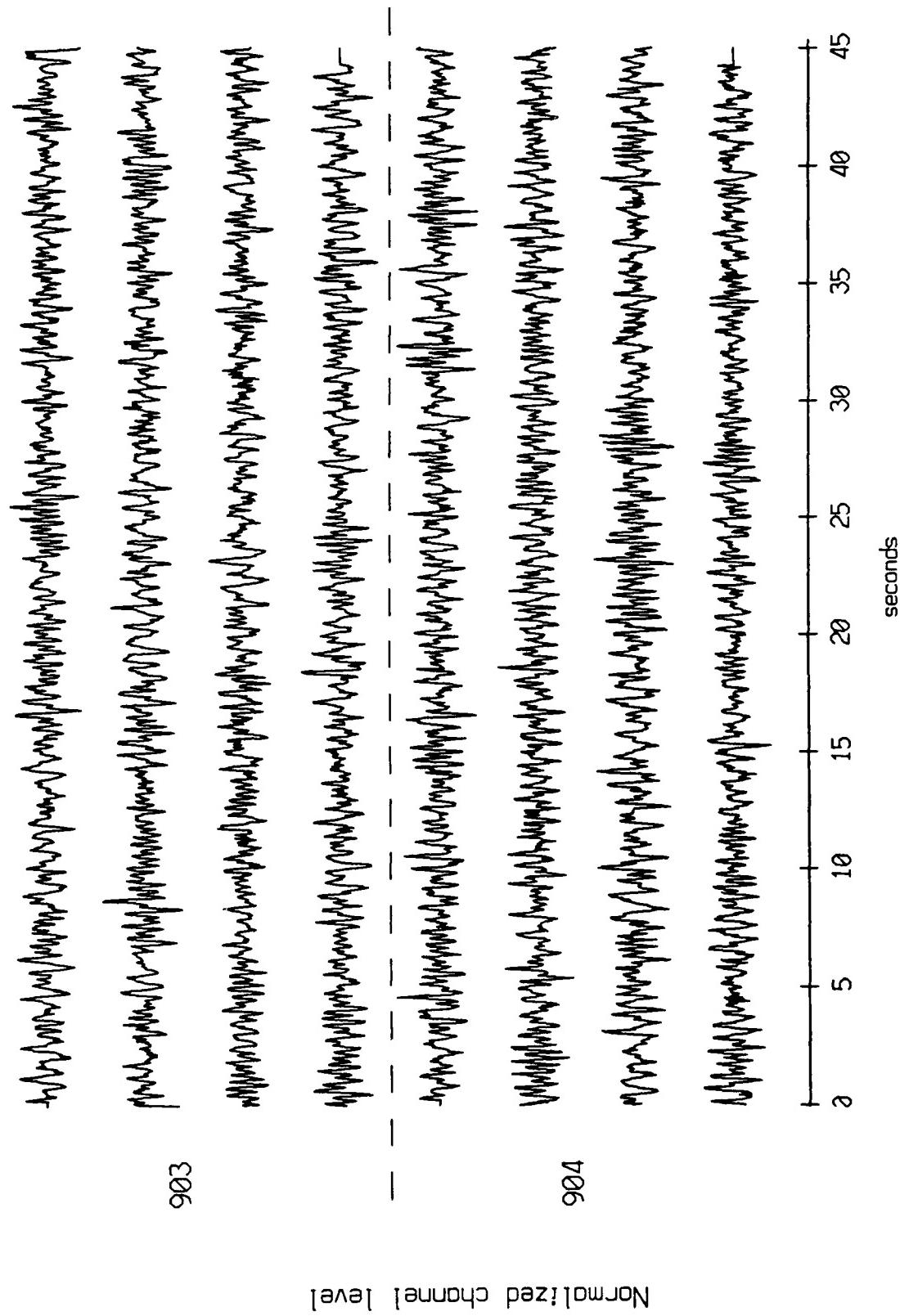
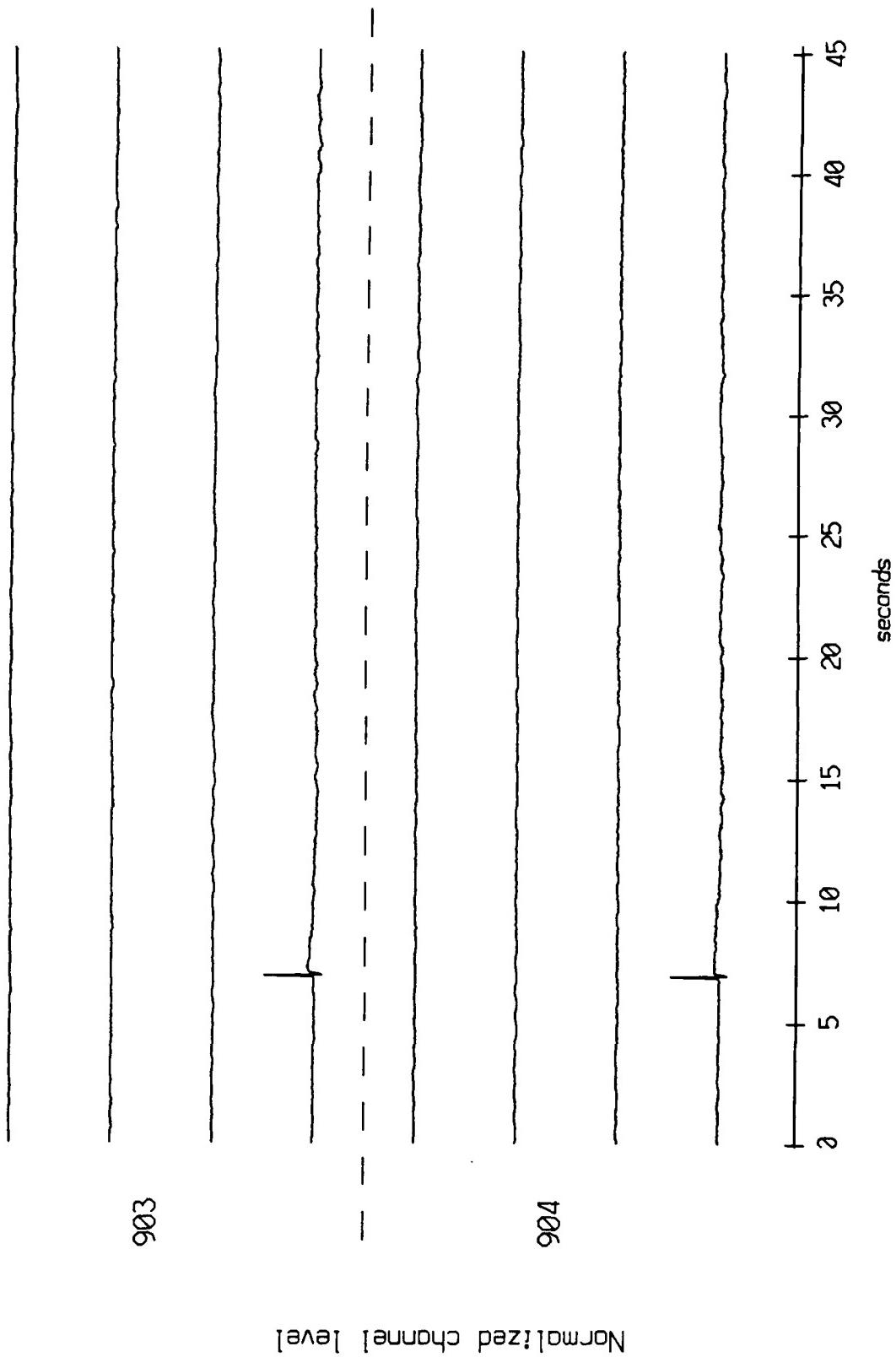


Figure X.10.1b

OBS 08, Sept, 1987 Trip - events 903 and 904 (z_axis)
max gain-corrected amplitude is 42.21020 counts



Normalized channel level

Figure X.10.1c.i

OBS 08, Sept, 1987 Trip - events 903 and 904 (z_axis)
max gain-corrected amplitude is 3.438658 counts

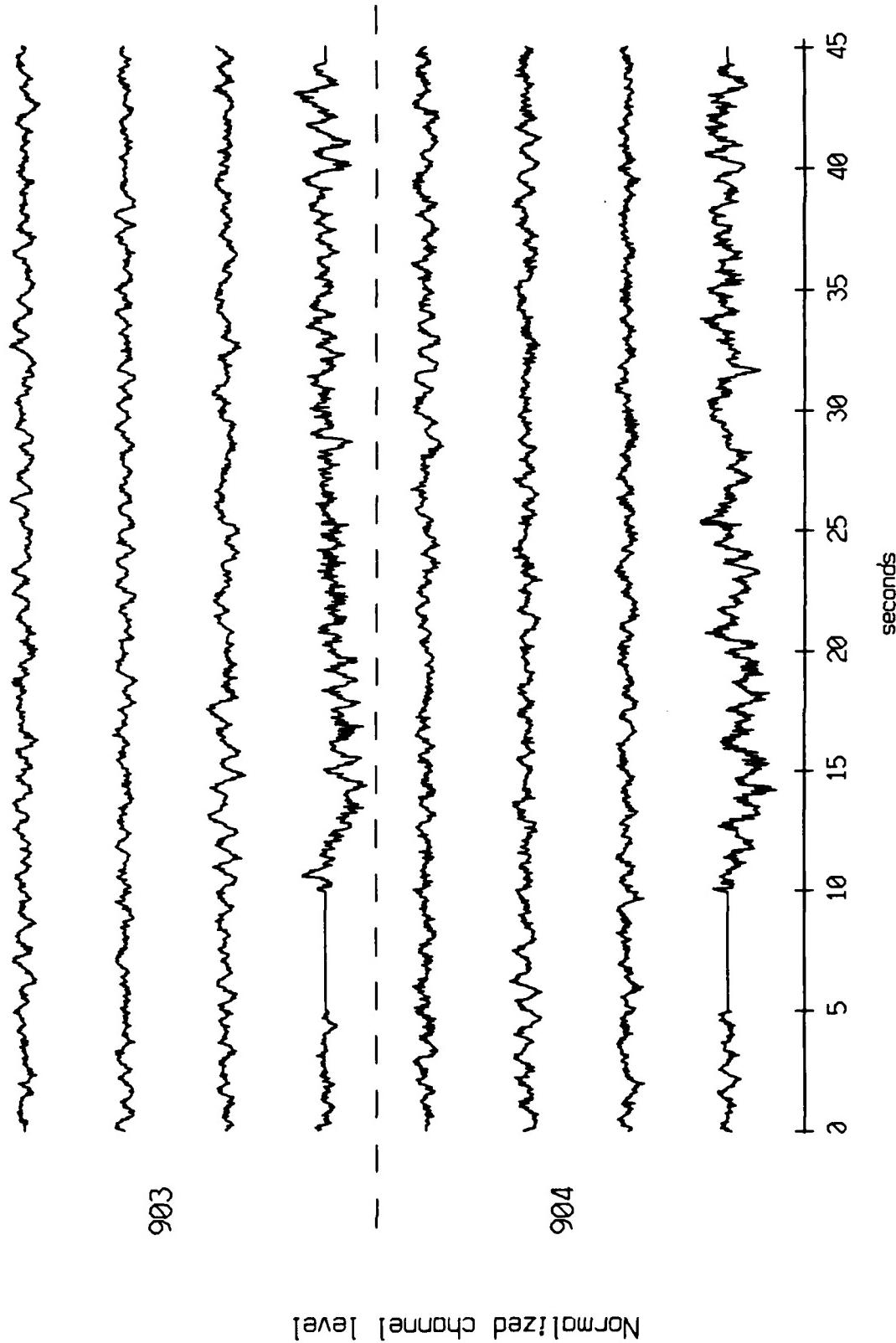


Figure X.10.1c.ii

OBS 08, Sept., 1987 Trip - events 903 and 904 (pressure)
max gain-corrected amplitude is 2.072845 counts

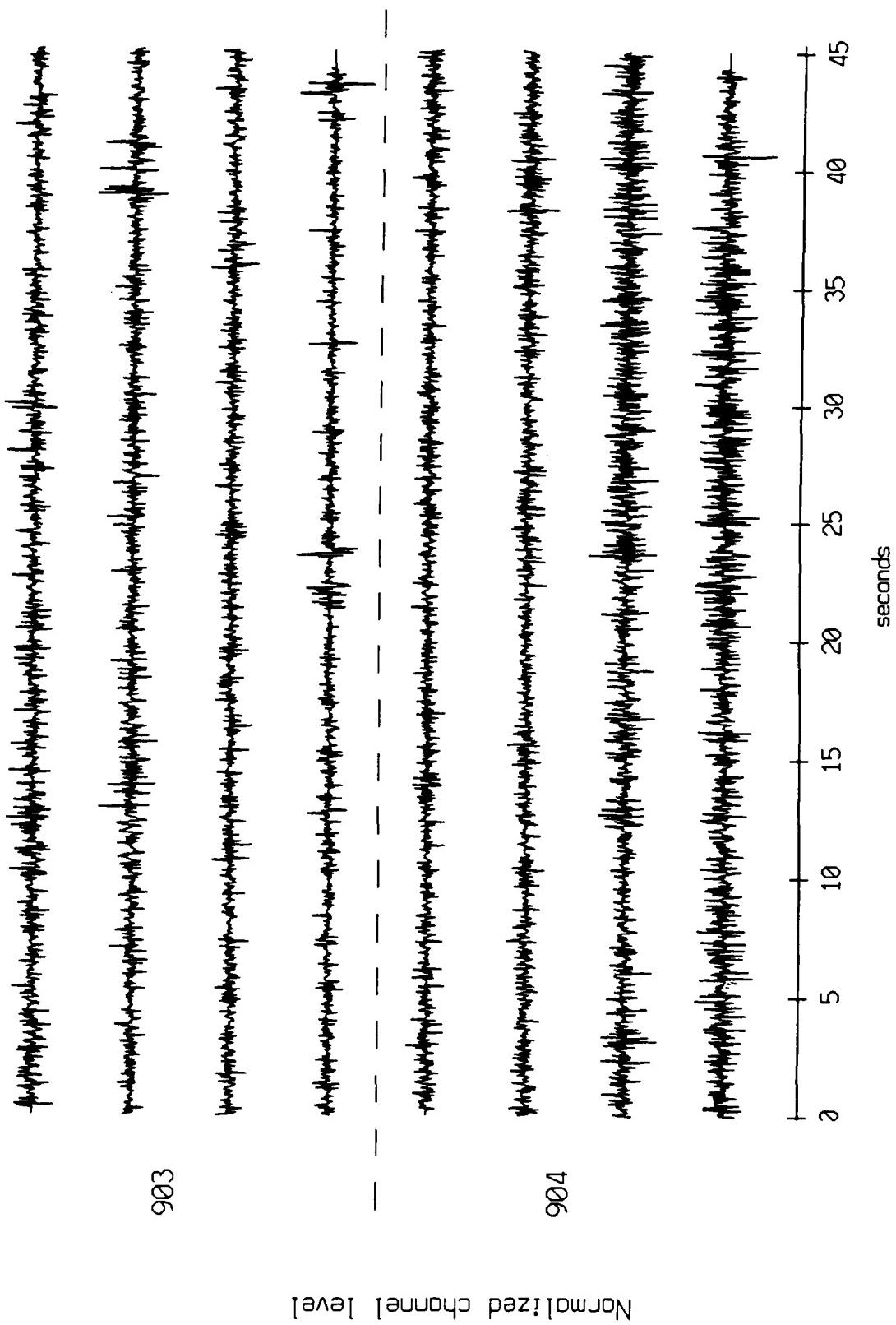


Figure X.10.1d

OBS 08, Sept, 1987 Trip - events 905 and 906 (x_axis)
max gain-corrected amplitude is 7.158109 counts

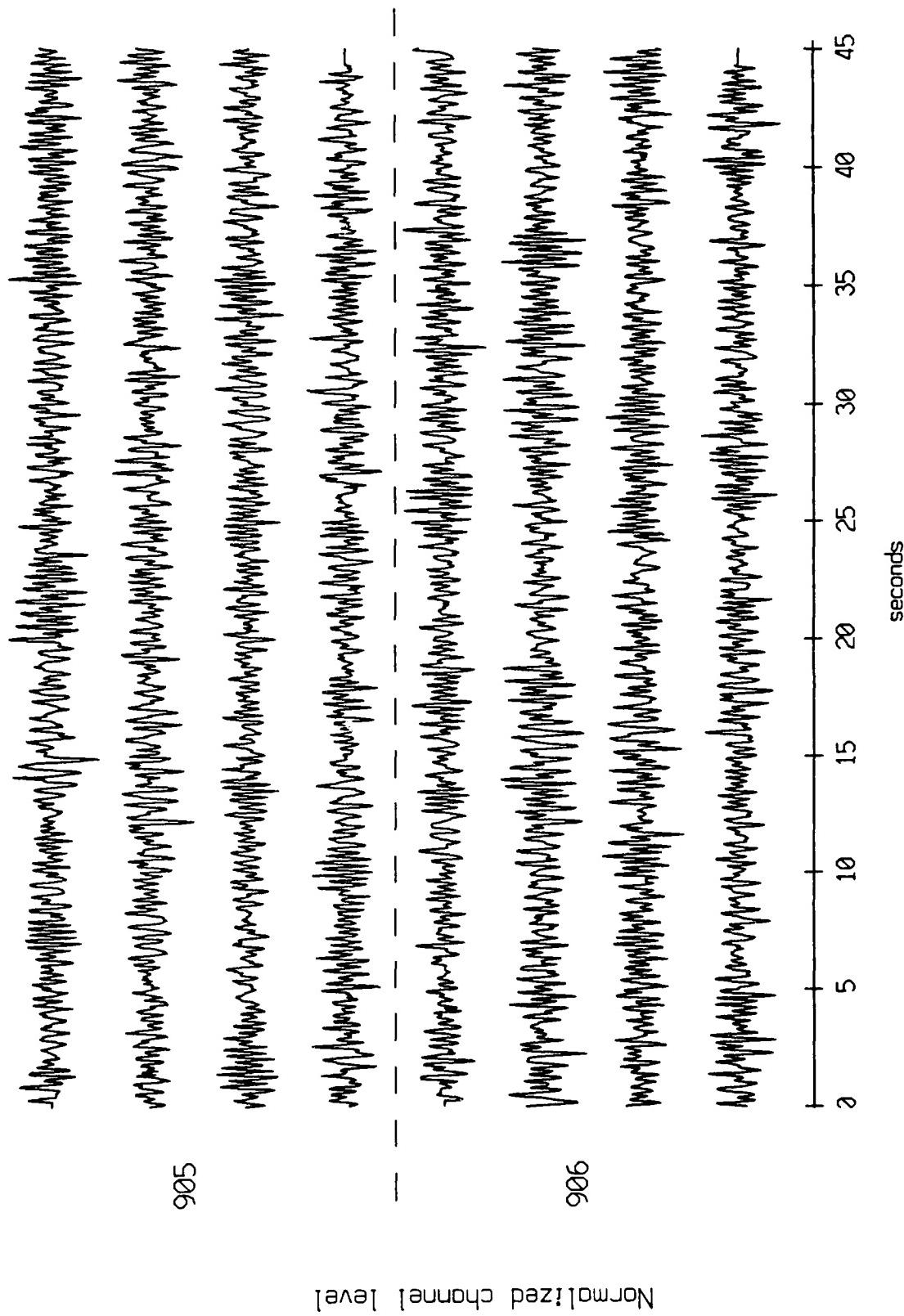


Figure X.11.1a

OBS 08, Sept, 1987 Trip - events 905 and 906 (y-axis)
max gain-corrected amplitude is 8.522415 counts

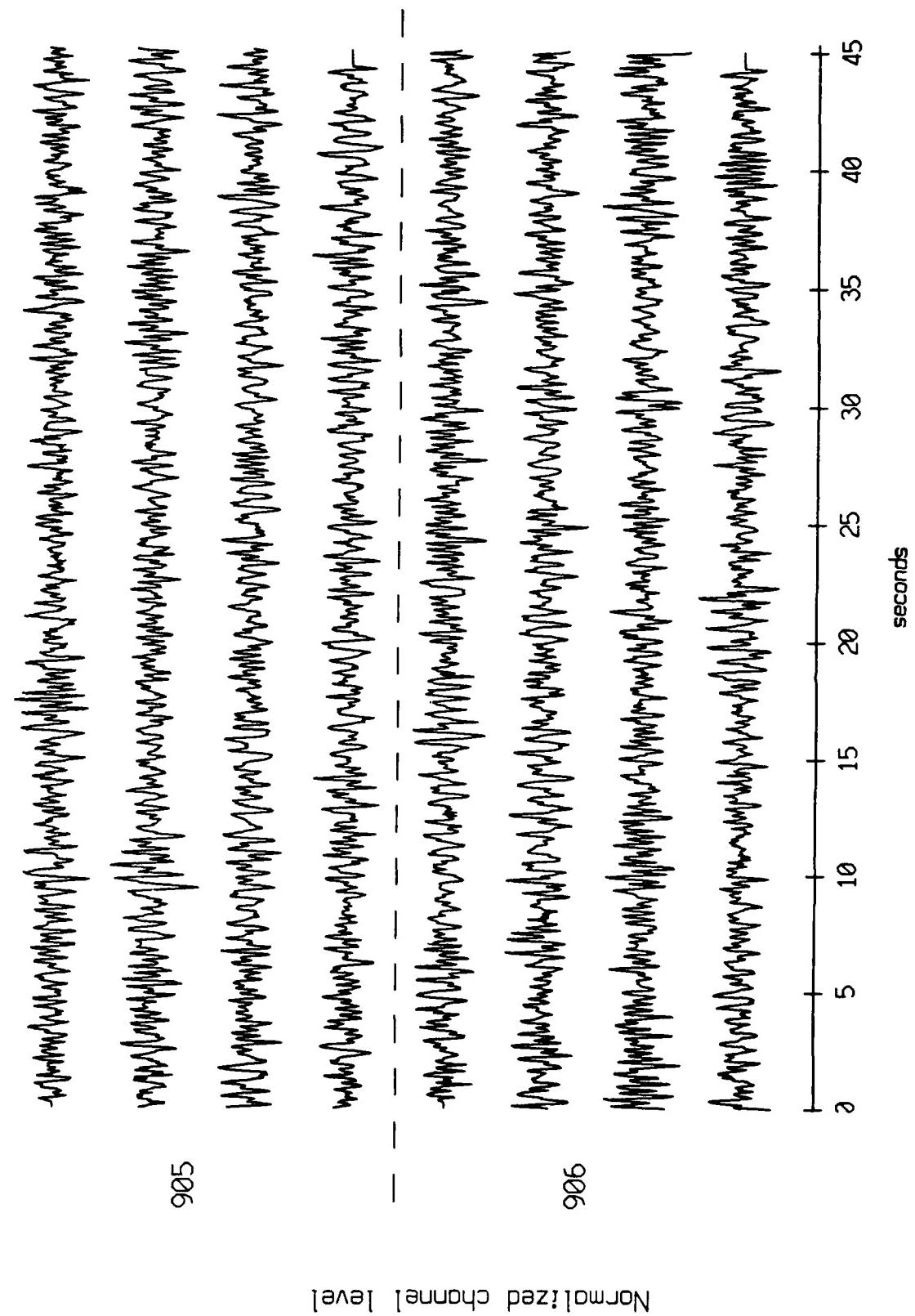
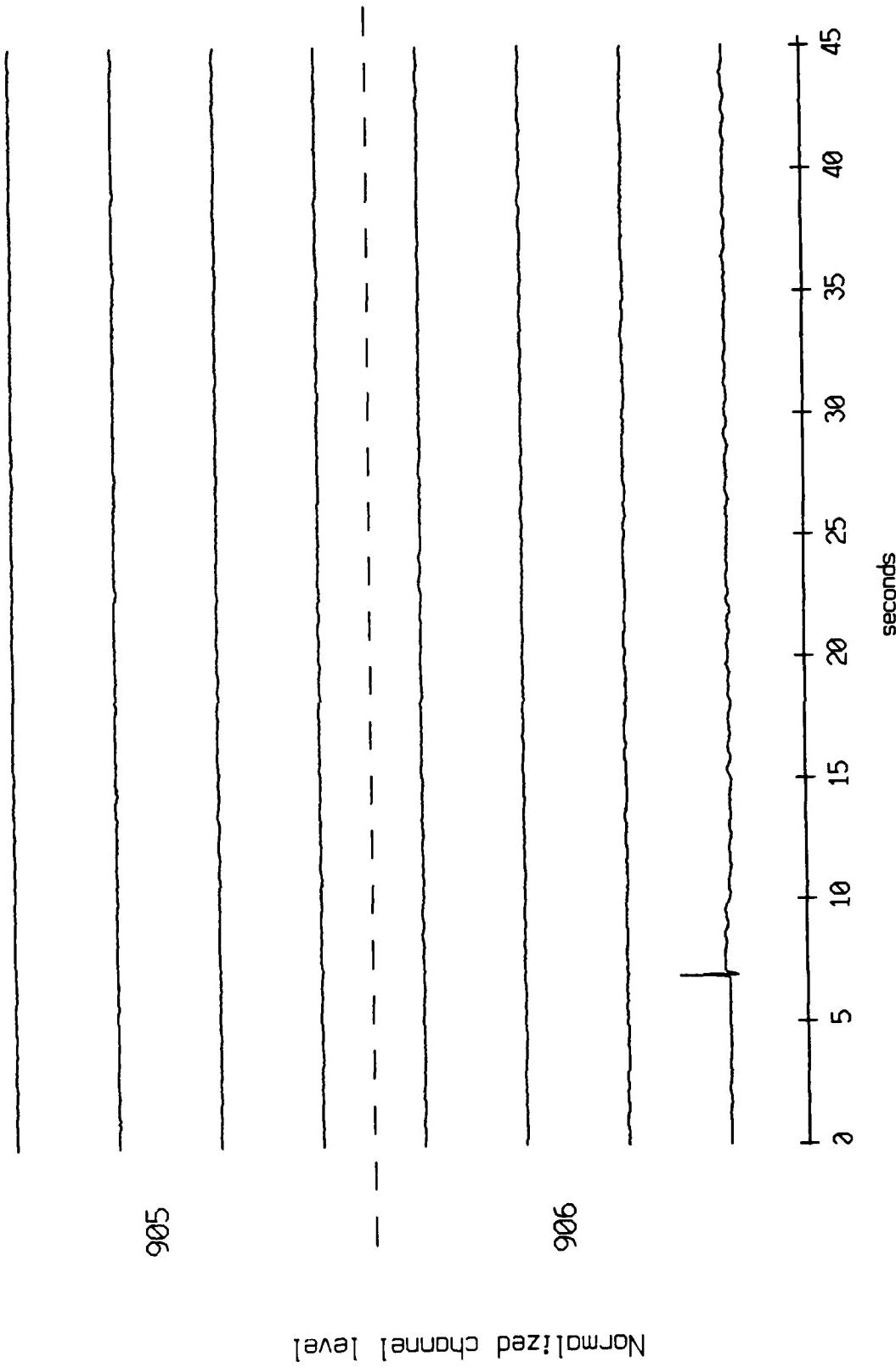


Figure X.11.1b

OBS 08, Sept, 1987 Trip - events 905 and 906 (z_axis)
max gain-corrected amplitude is 42.80397 counts



Normalized channel level

Figure X.11.1c

OBS 08, Sept, 1987 Trip - events 905 and 906 (pressure)
max gain-corrected amplitude is 2.606013 counts

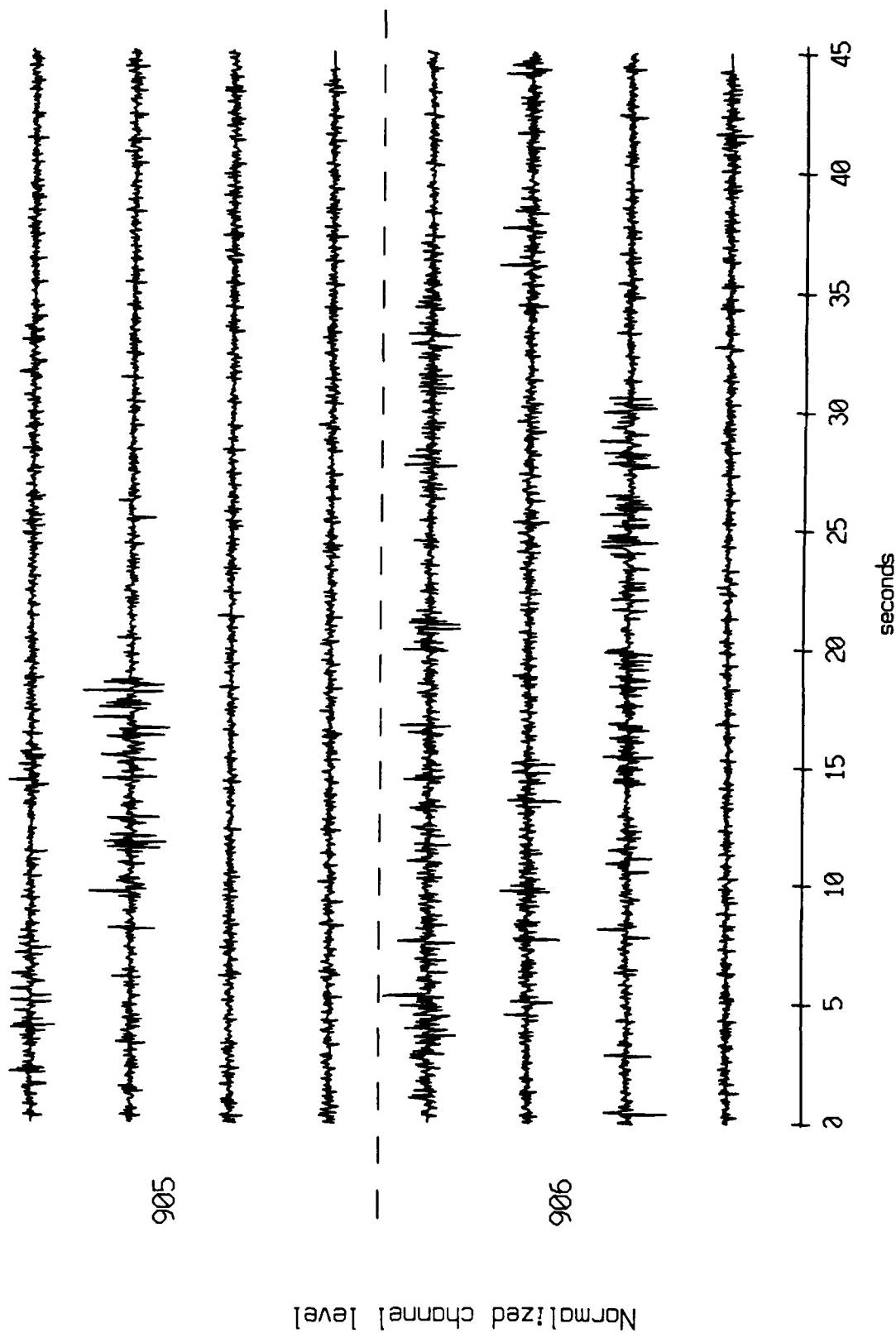


Figure X.11.1d

data file: /USR/SPOOL/UUCP/LIC/MP-8-1.ROSE
corrections: NONE
scaling: AUTO
no filter

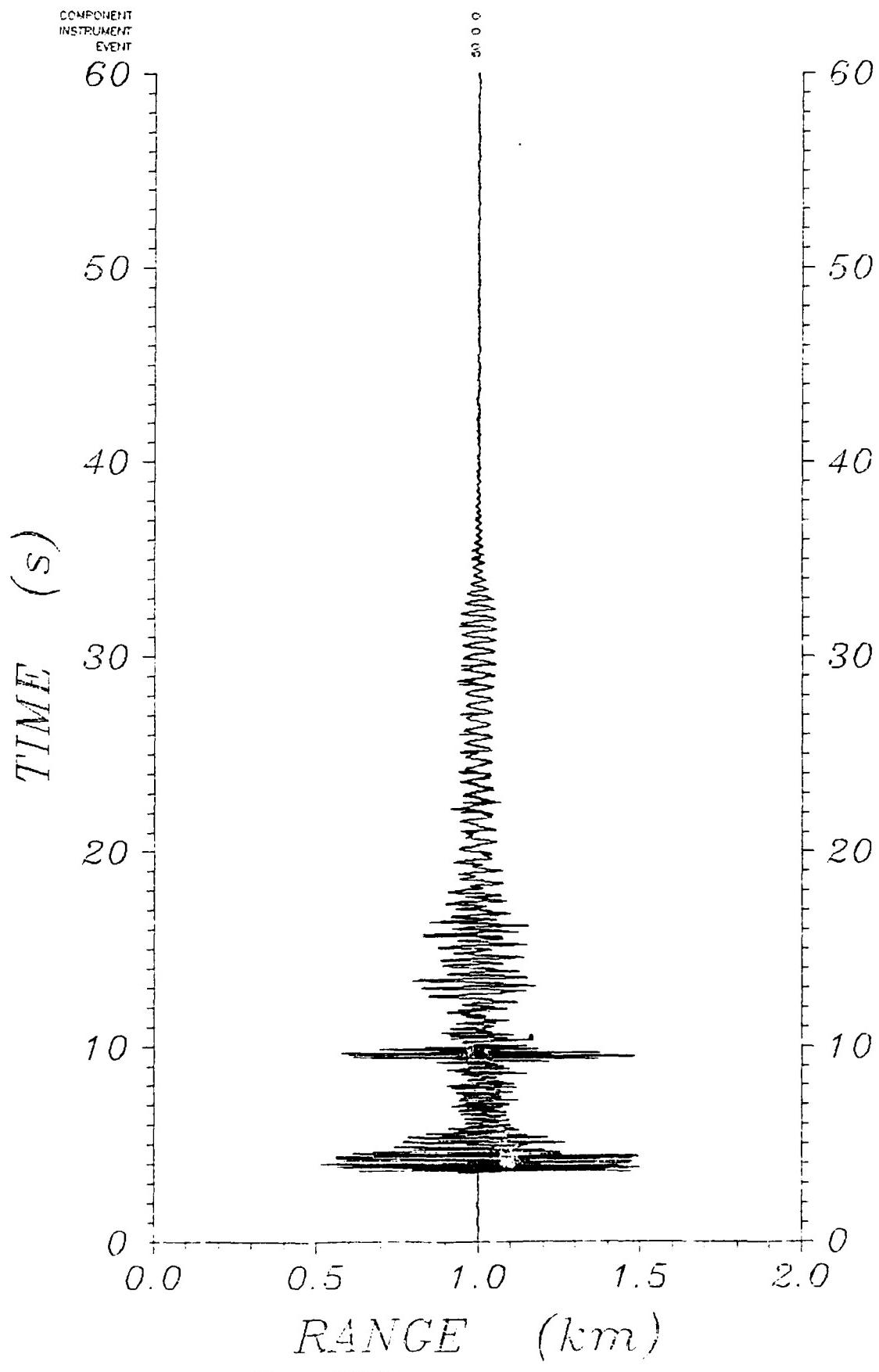


Figure X.12.1a

VLA Tape 433, Sept., 1987 Trip - Time 07:45:15 fs = 50 Hz
vertical axis scale is approx. -2000 to 2000 counts

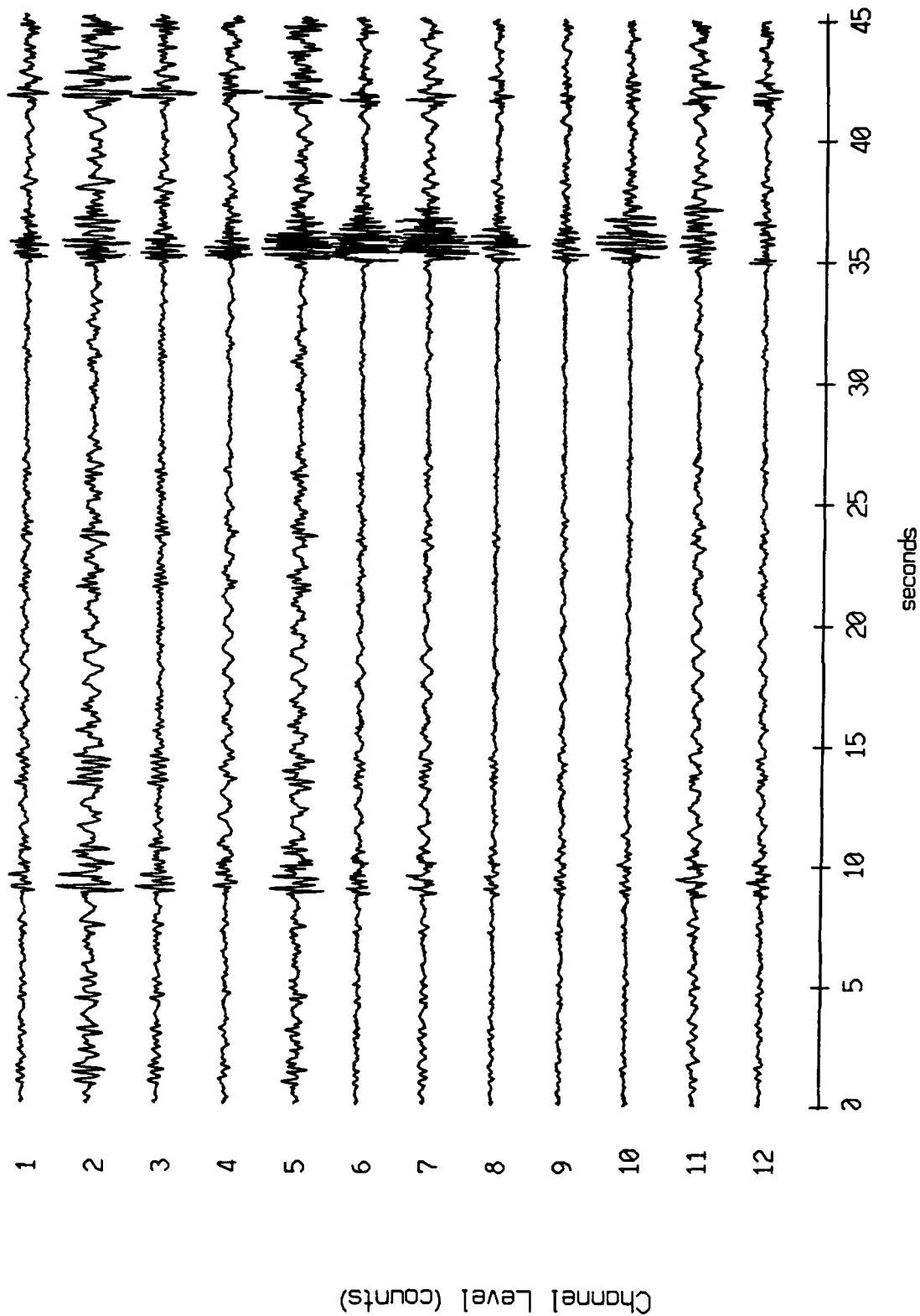


Figure X.13.1a

VLA Tape 433, Sept, 1987 Trip - Time 07:45:15 fs = 50 Hz
vertical axis scale is approx. -2000 to 2000 counts

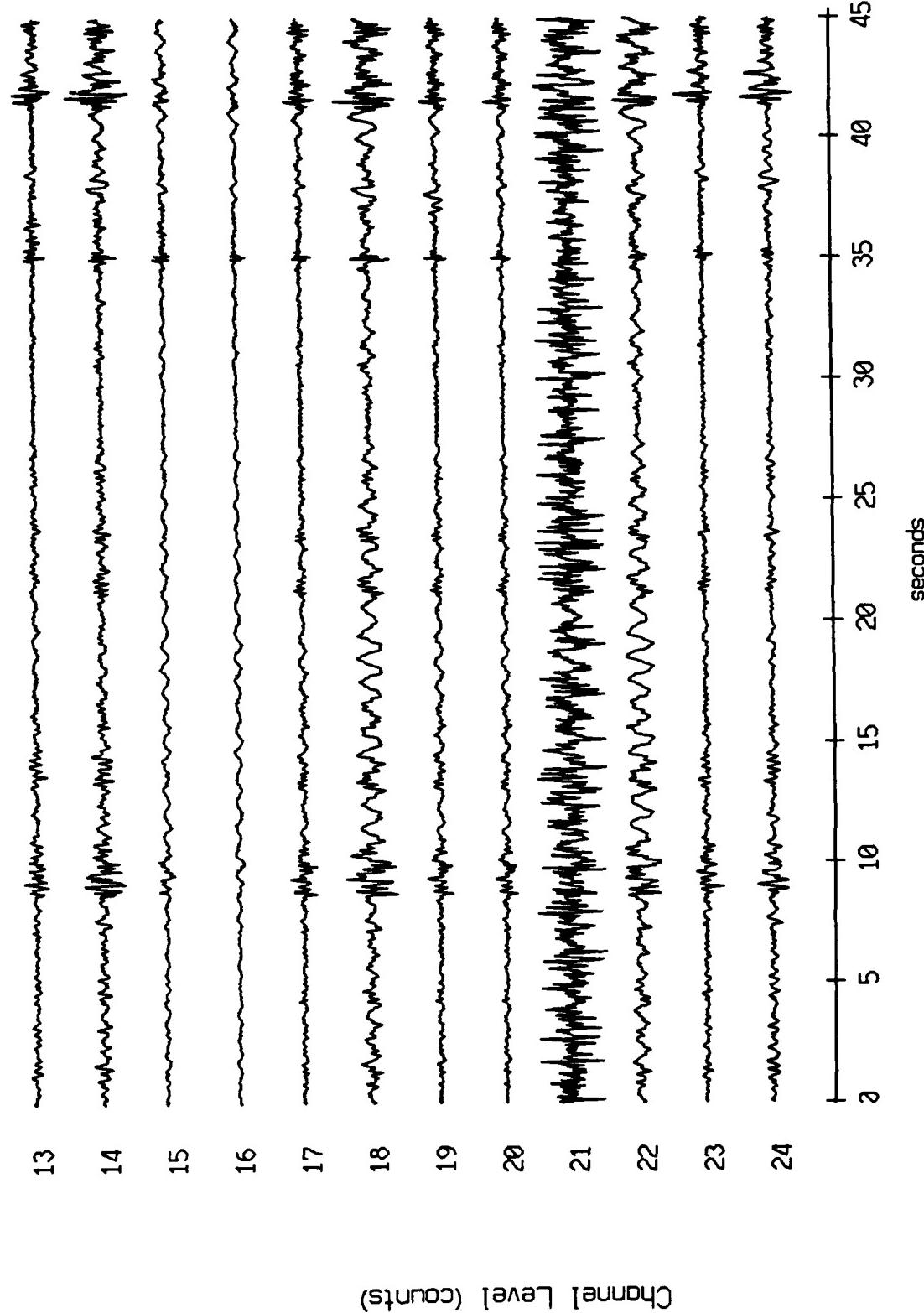


Figure X.13.1b

VLA Tape 433, Sept, 1987 Trip - Time 07:45:15 fs = 50 Hz
vertical axis scale is approx. -2000 to 2000 counts

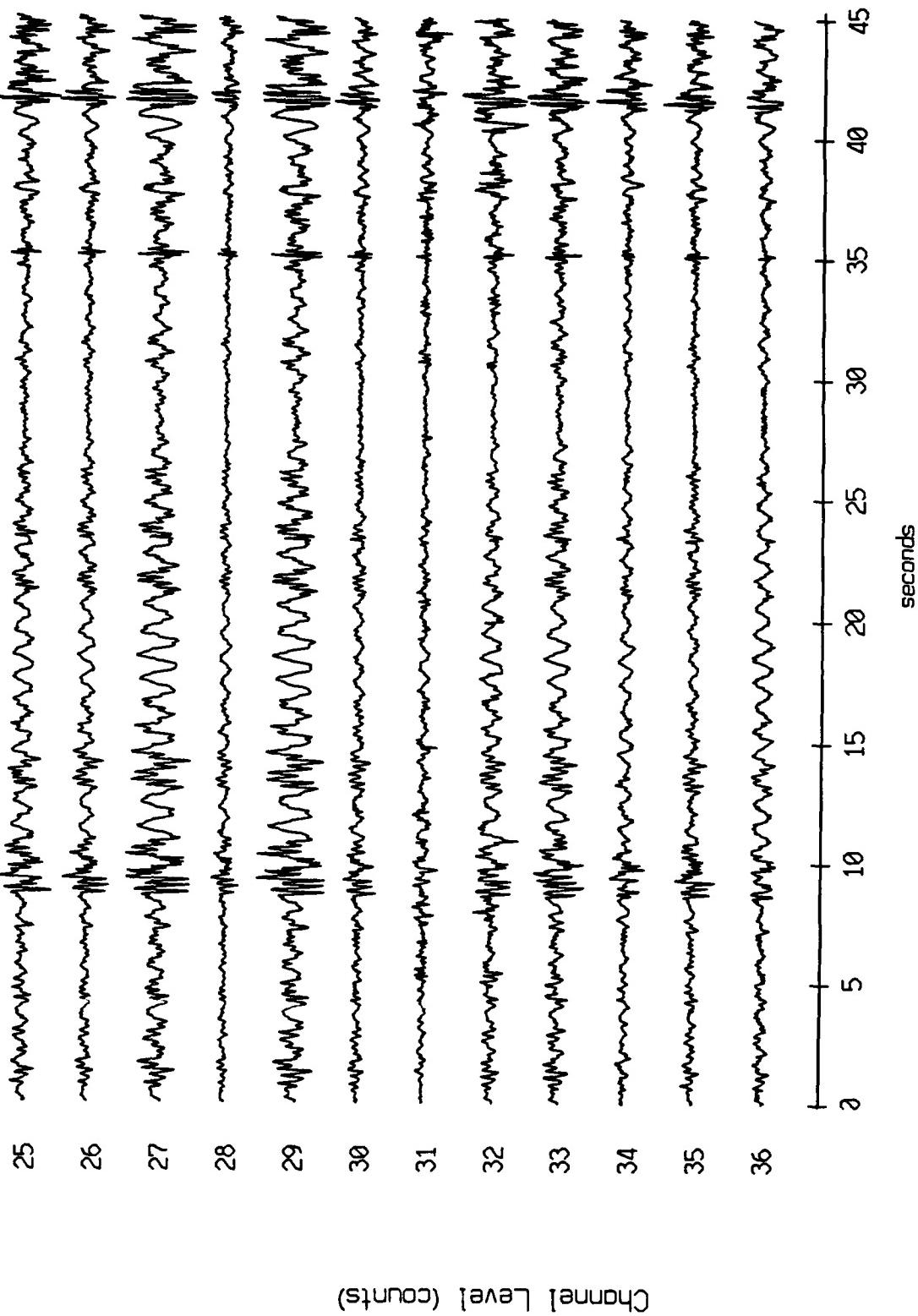
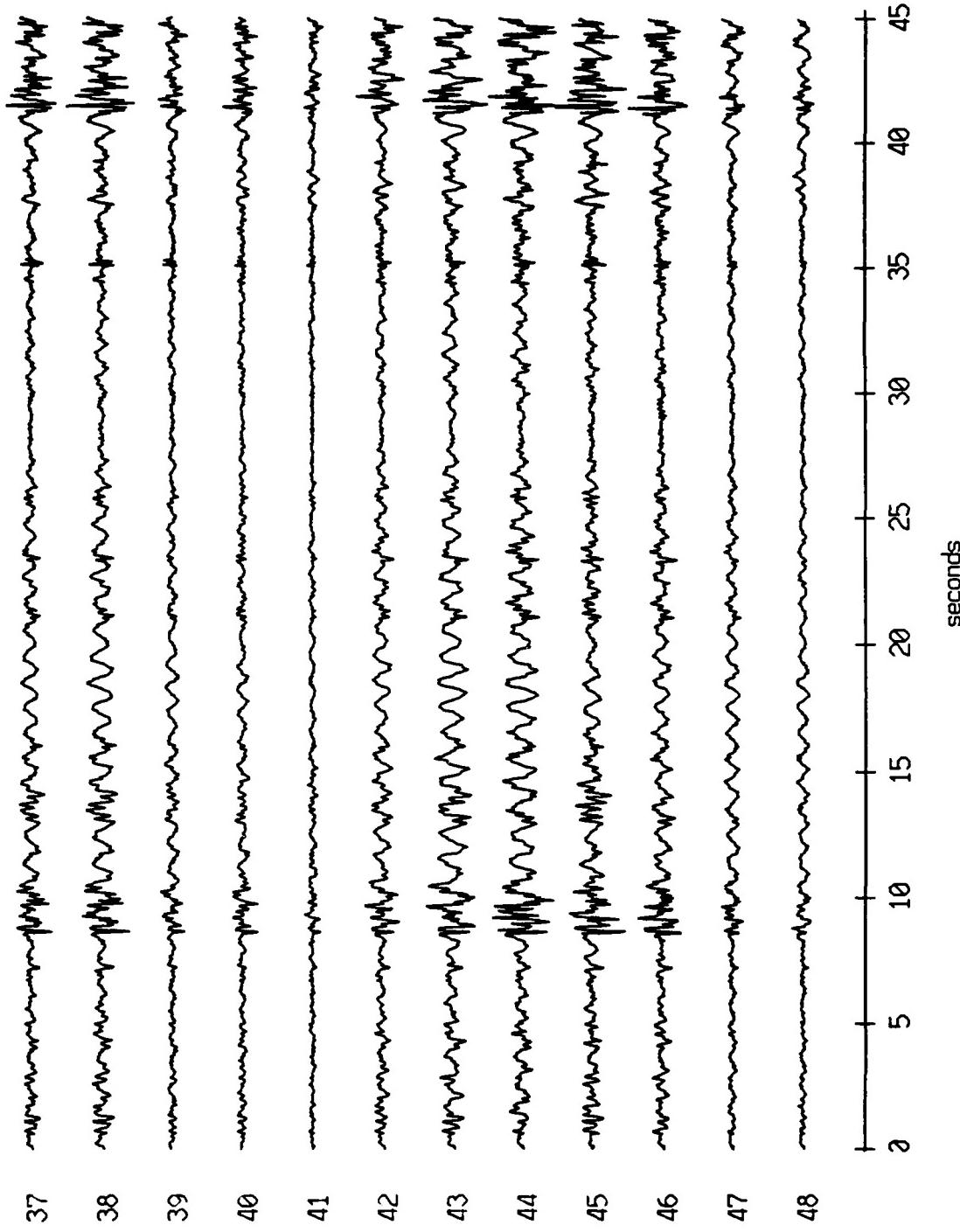


Figure X.13.1c

VLA Tape 433, Sept, 1987 Trip - Time 07:45:15 fs = 50 Hz
vertical axis scale is approx. -2000 to 2000 counts



Channel Level (counts)

Figure X.13.1d

VLA Tape 433, Sept, 1987 Trip - Time 07:45:15 fs = 50 Hz
vertical axis scale is approx. -2000 to 2000 counts

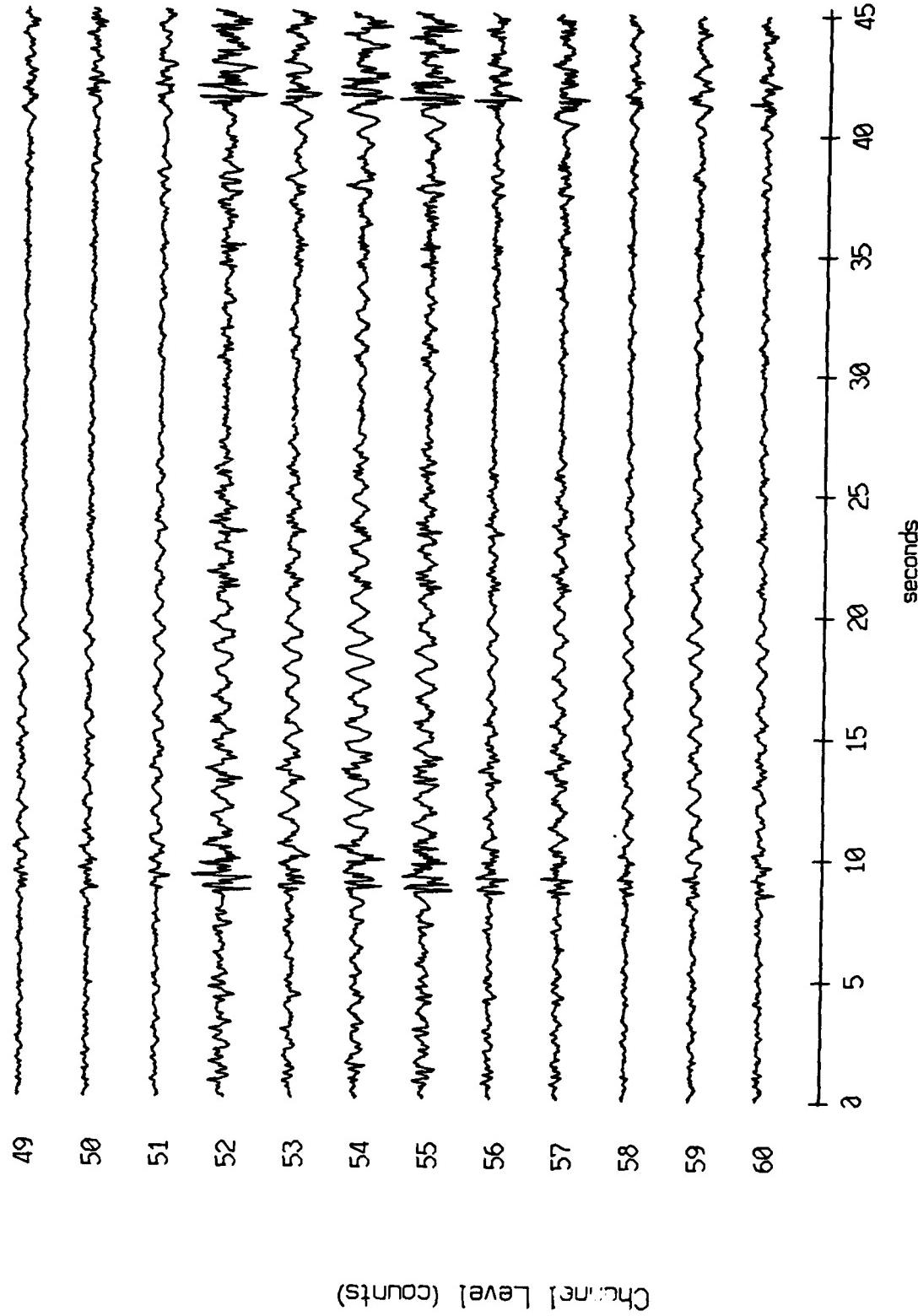


Figure X.13.1e

VLA Tape 433, Sept, 1987 Trip - Time 07:45:15 fs = 50 Hz
vertical axis scale is approx. -2000 to 2000 counts

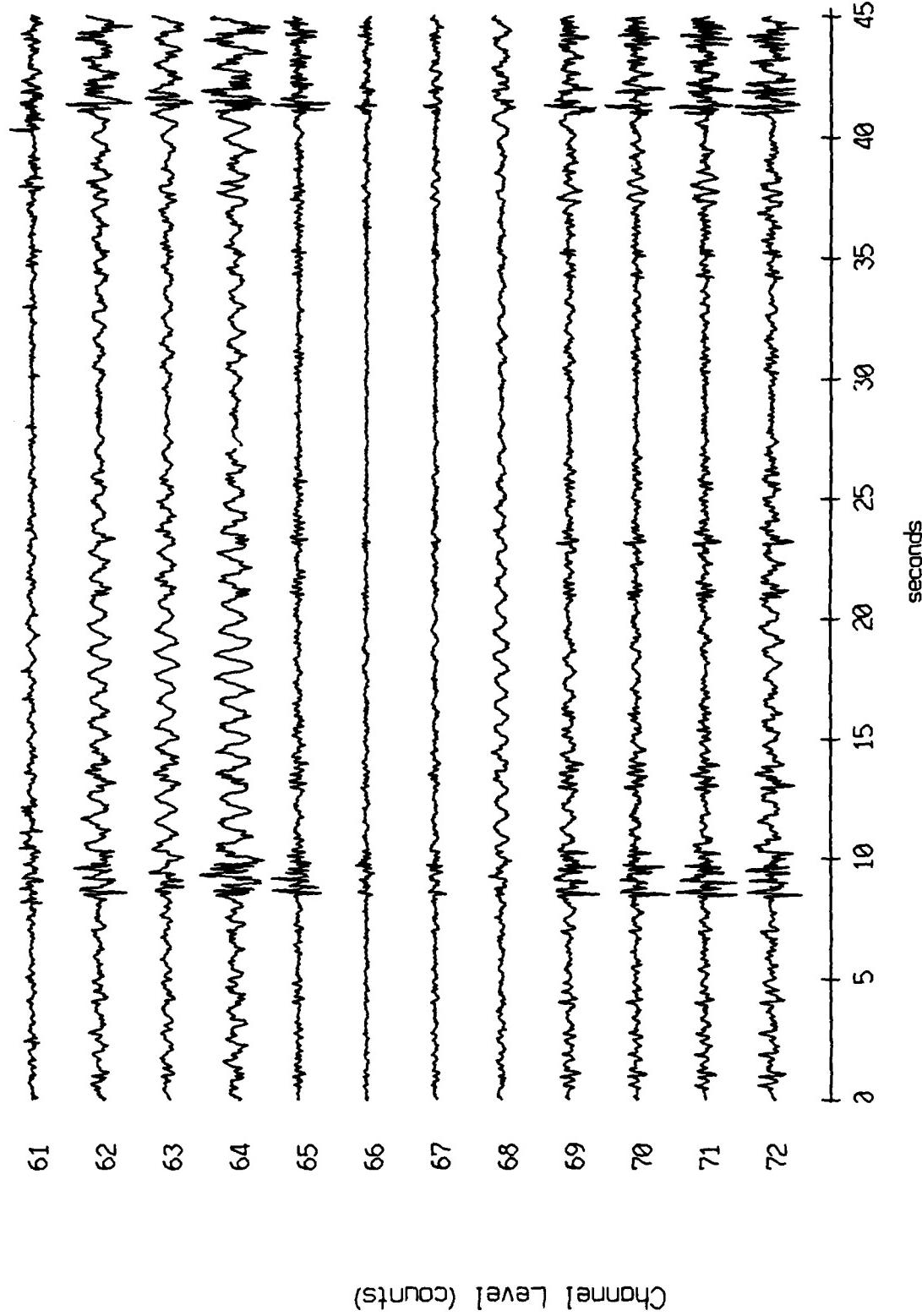


Figure X.13.1f

VLA Tape 433, Sept., 1987 Trip - Time 07:45:15 fs = 50 Hz
vertical axis scale is approx. -2000 to 2000 counts

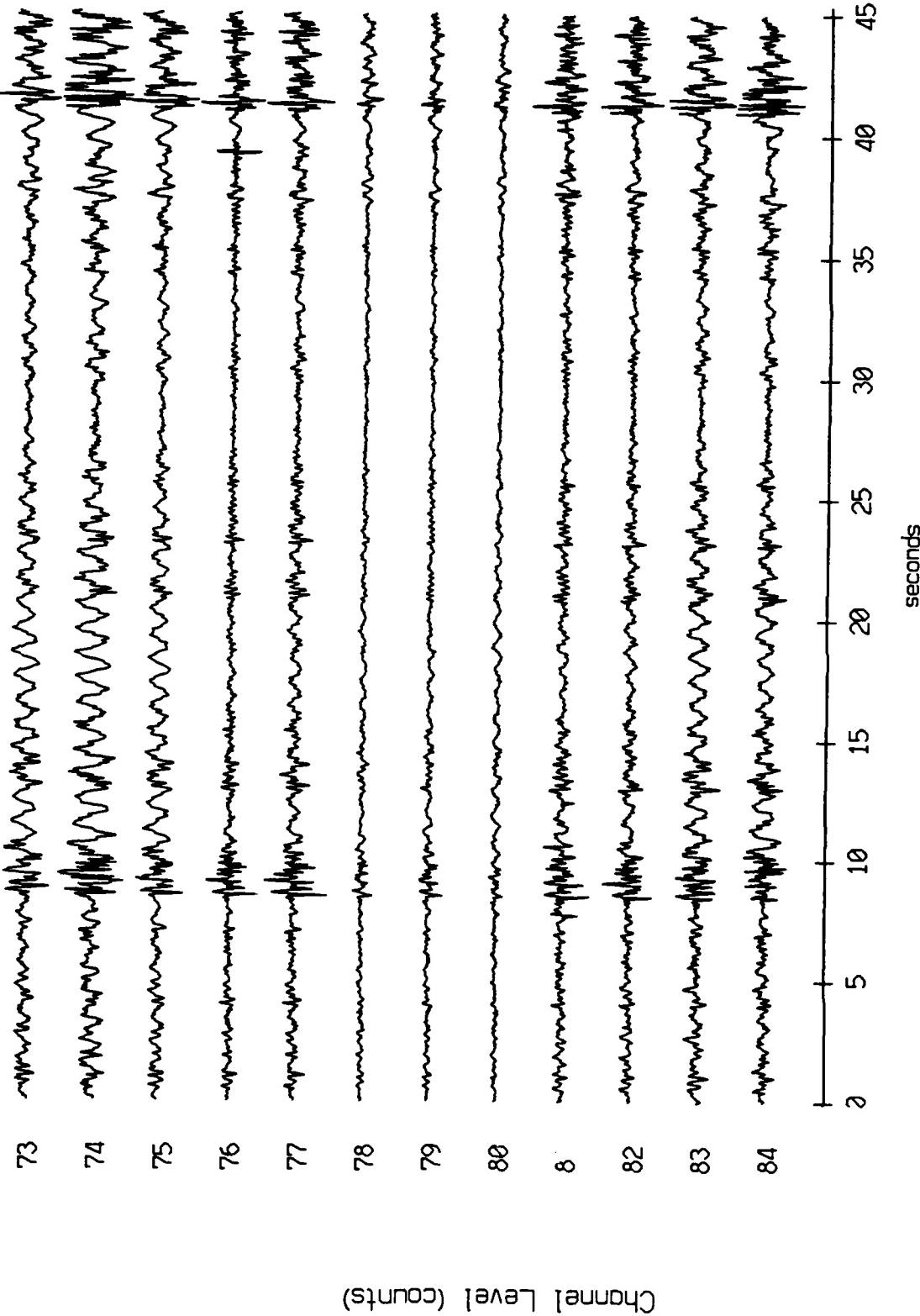


Figure X.13.1g

VLA Tape 433, Sept., 1987 Trip - Time 07:45:15 fs = 50 Hz
vertical axis scale is approx. -2000 to 2000 counts

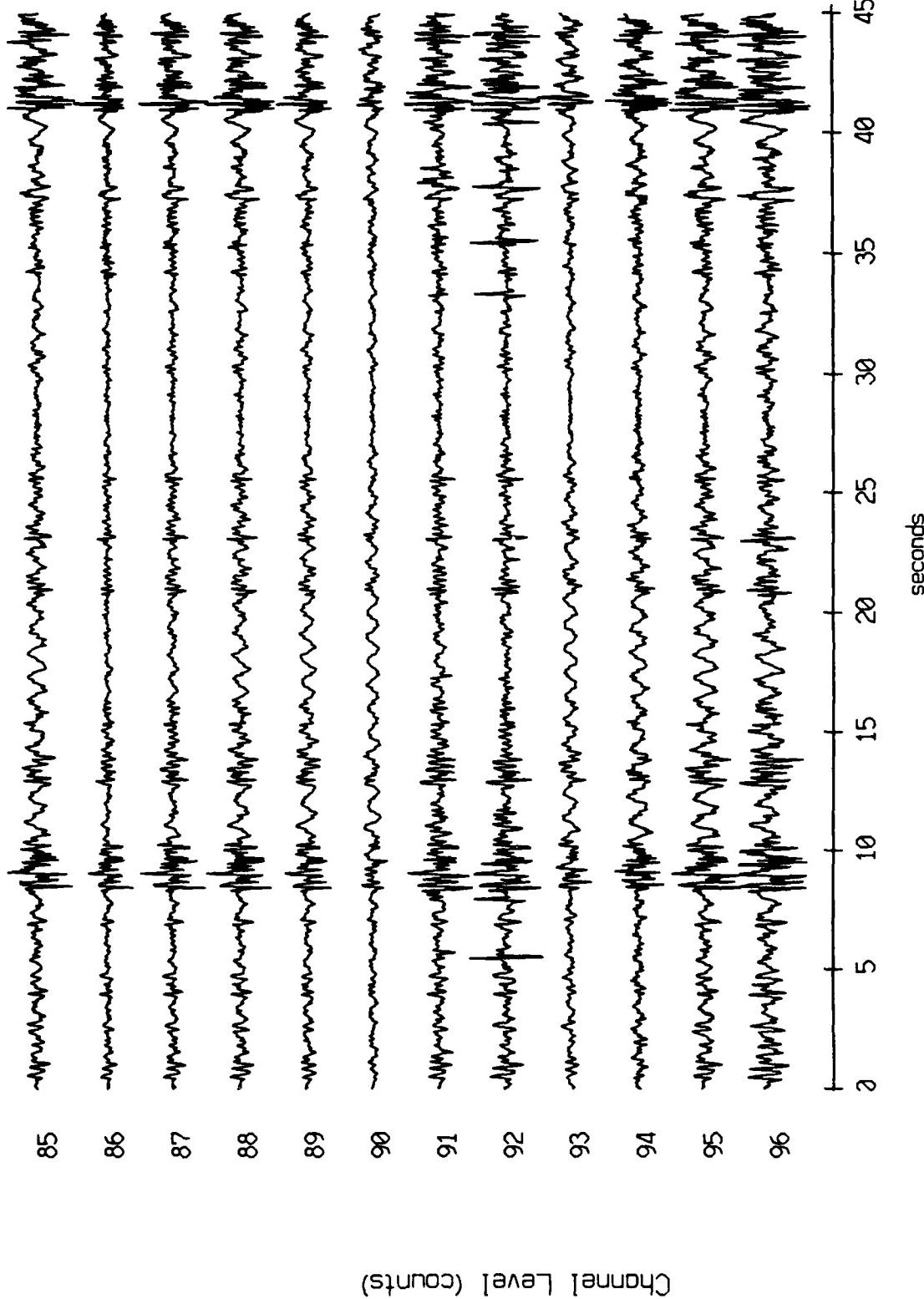


Figure X.13.1h

VLA Tape 433, Sept., 1987 Trip - Time 07:45:15 fs = 50 Hz
vertical axis scale is approx. -2000 to 2000 counts

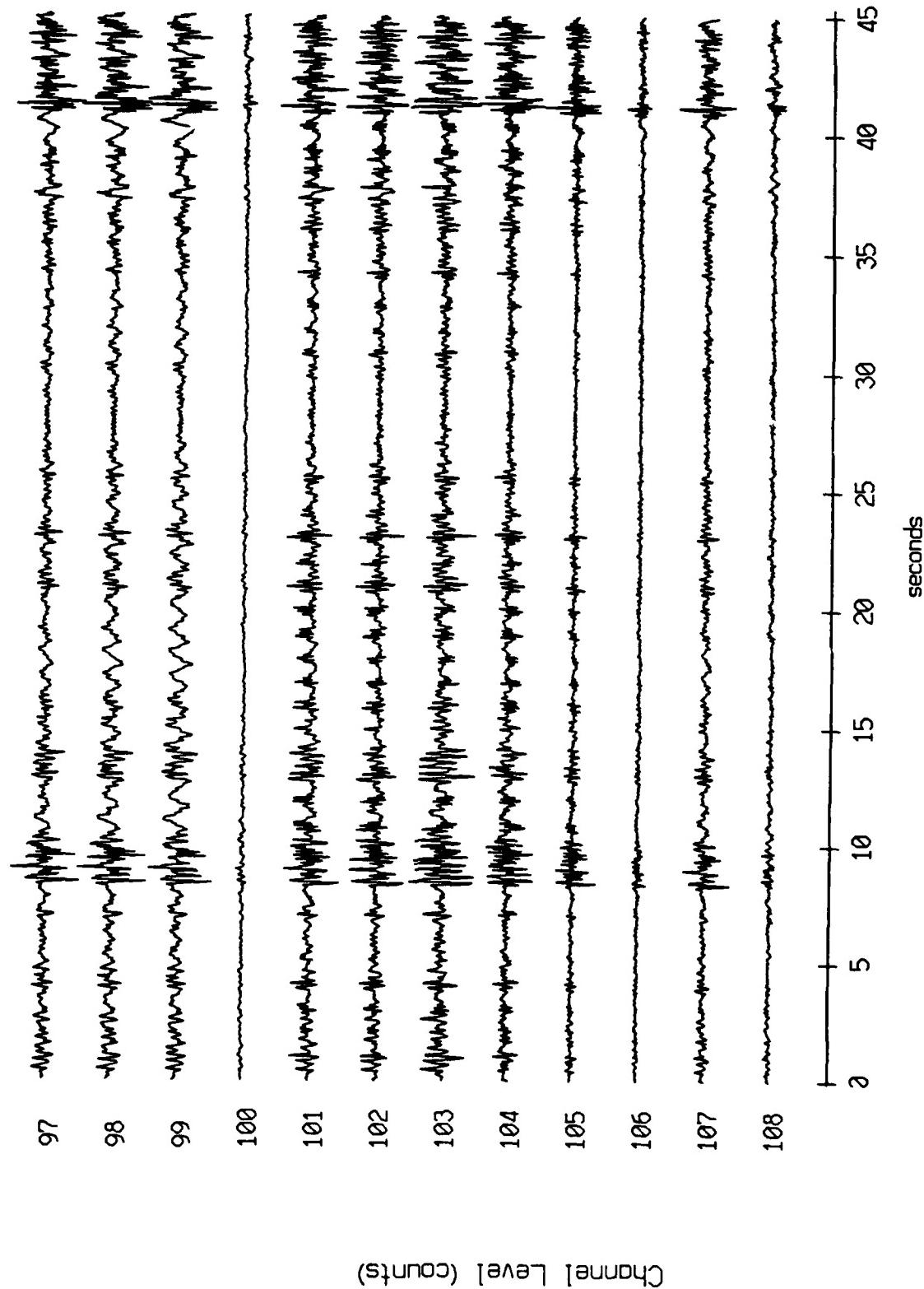


Figure X.13.11

VLA Tape 433, Sept, 1987 Trip - Time 07:45:15 fs = 50 Hz
vertical axis scale is approx. -2000 to 2000 counts

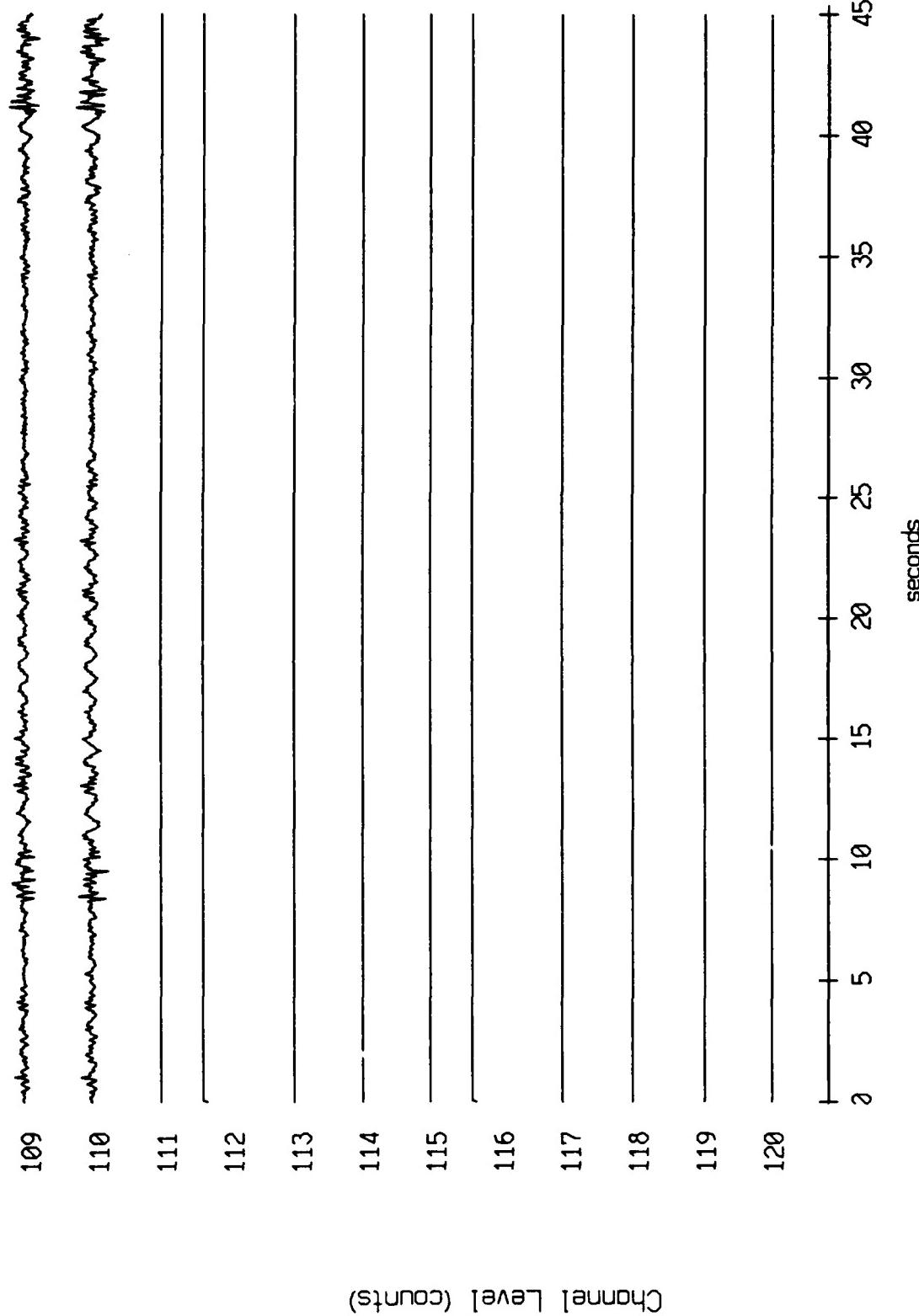


Figure X.13.1j

VLA Tape 440, Sept, 1987 Trip - Time 10:49:00.000 $f_s = 50$ Hz
vertical axis scale is approx. -2000 to 2000 counts

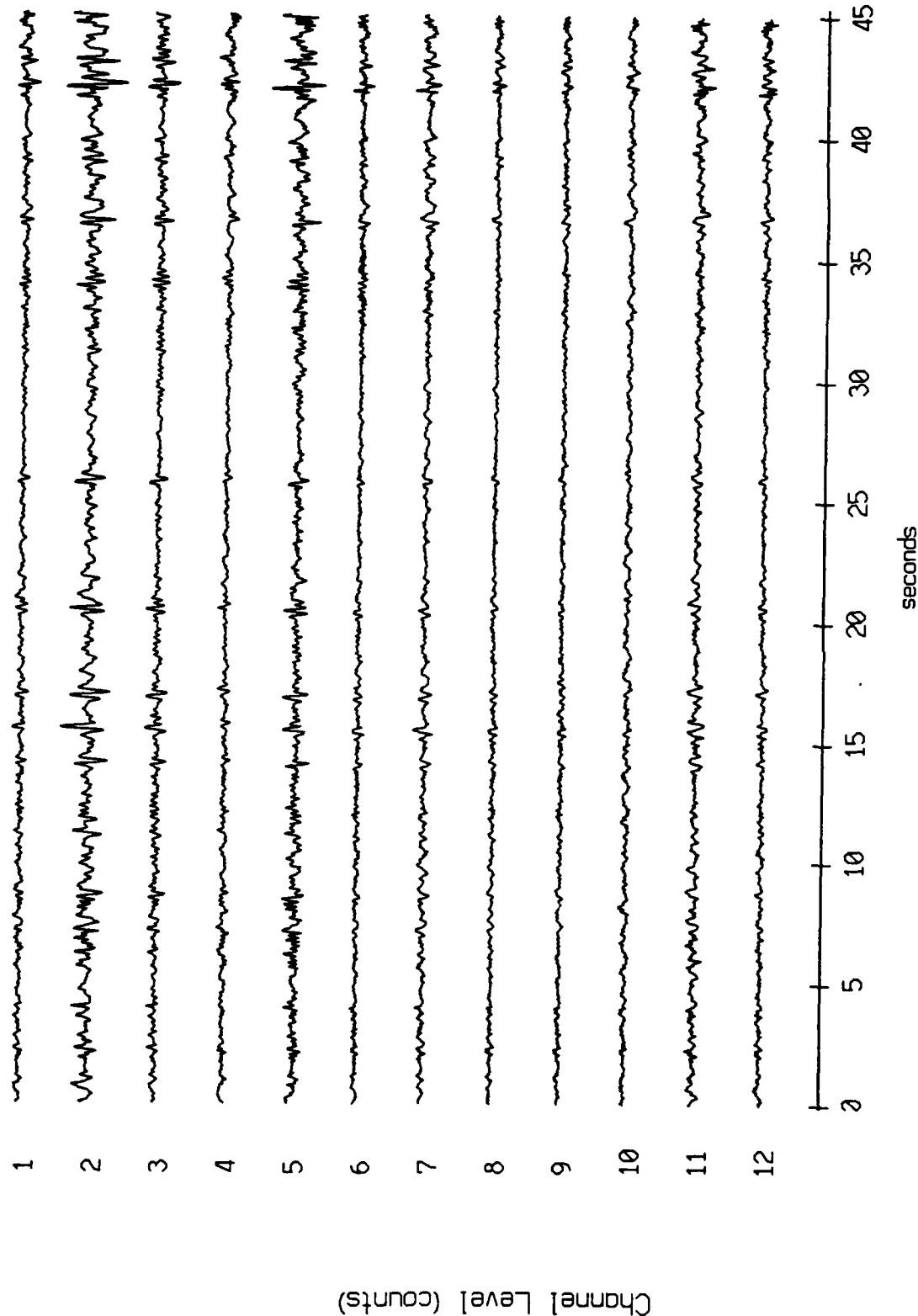


Figure X.14.1a

VLA Tape 440, Sept, 1987 Trip - Time 10:49:00.000 $f_s = 50$ Hz
vertical axis scale is approx. -2000 to 2000 counts

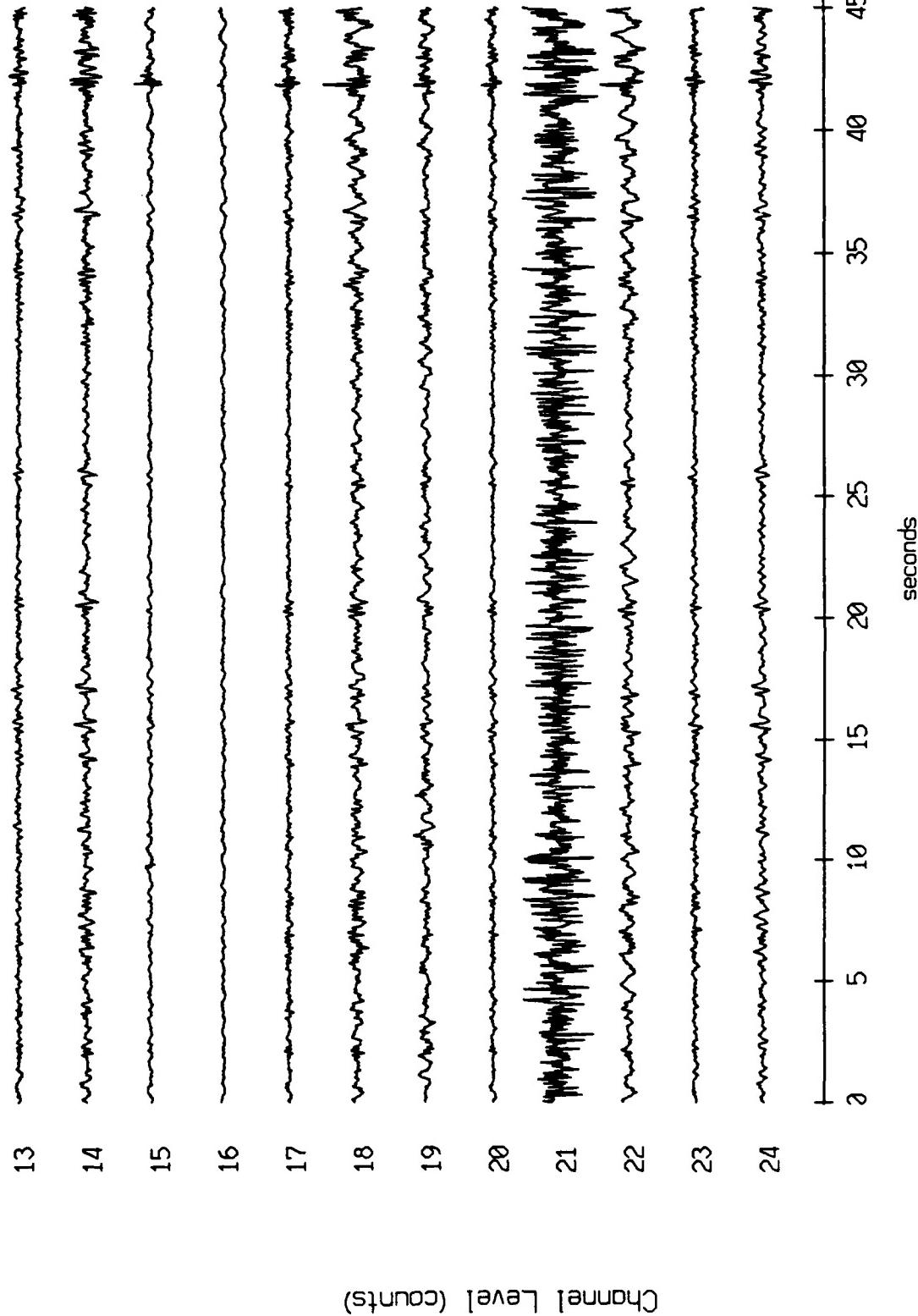


Figure X.14.1b

VLA Tape 440, Sept, 1987 Trip - Time 10:49:00.000 $f_s = 50$ Hz
vertical axis scale is approx. -2000 to 2000 counts

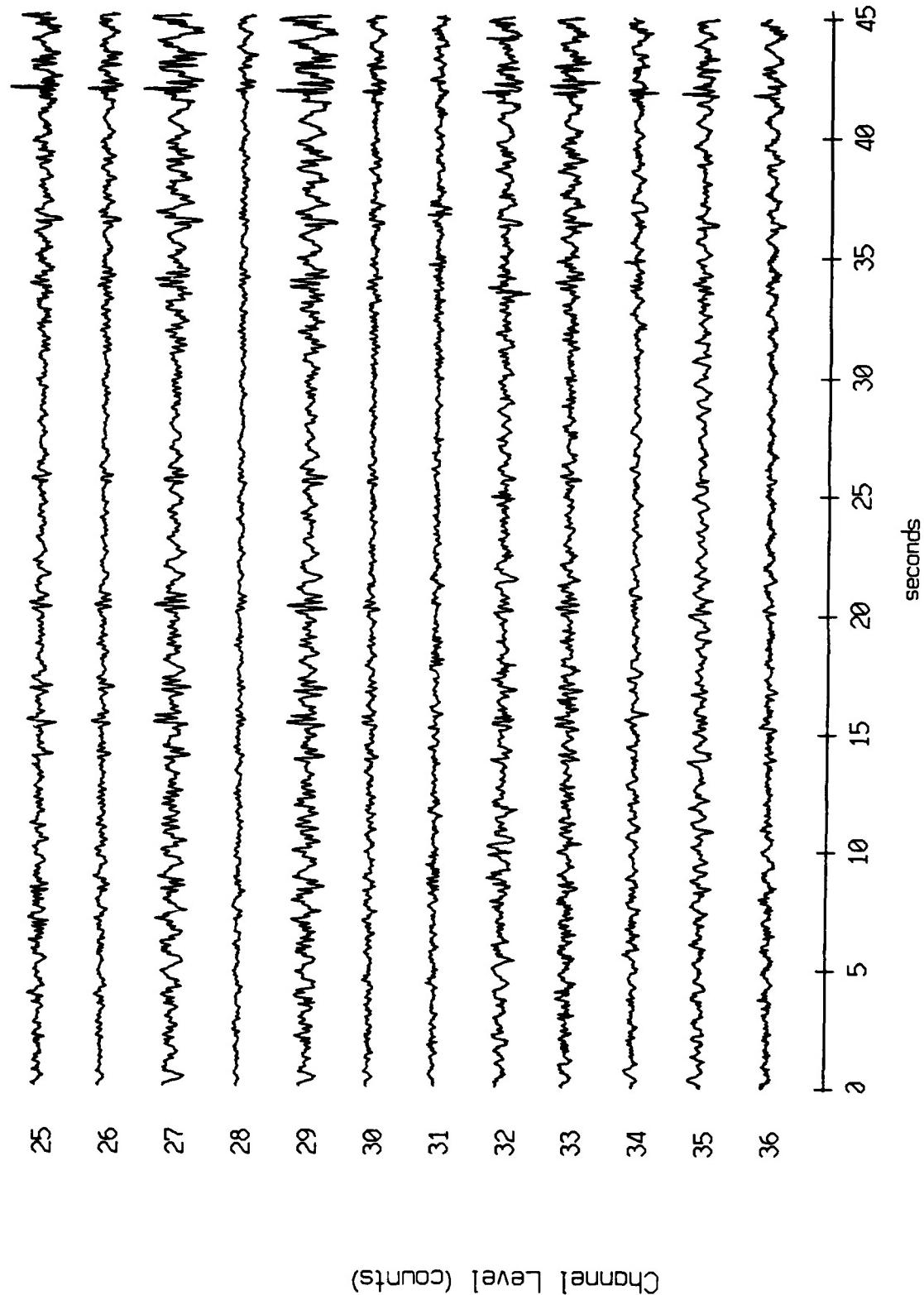


Figure X.14.1c

VLA Tape 440, Sept, 1987 Trip - Time 10:49:00.000 $f_s = 50$ Hz
vertical axis scale is approx. -2000 to 2000 counts

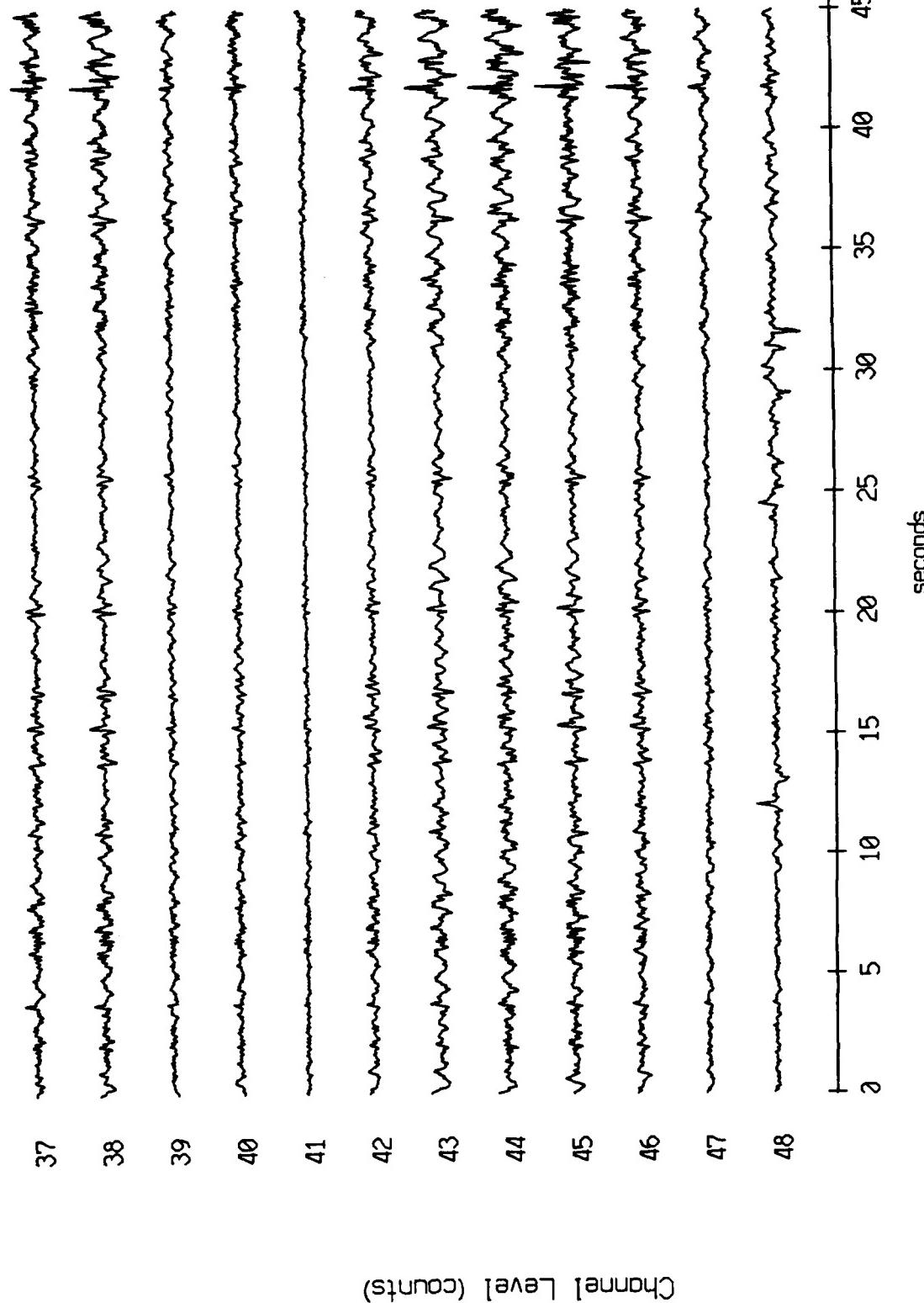


Figure X.14.1d

V' 3 Tape 440, Sept, 1987 Trip - Time 10:49:00.000 fs = 50 Hz
vertical axis scale is approx. -2000 to 2000 counts

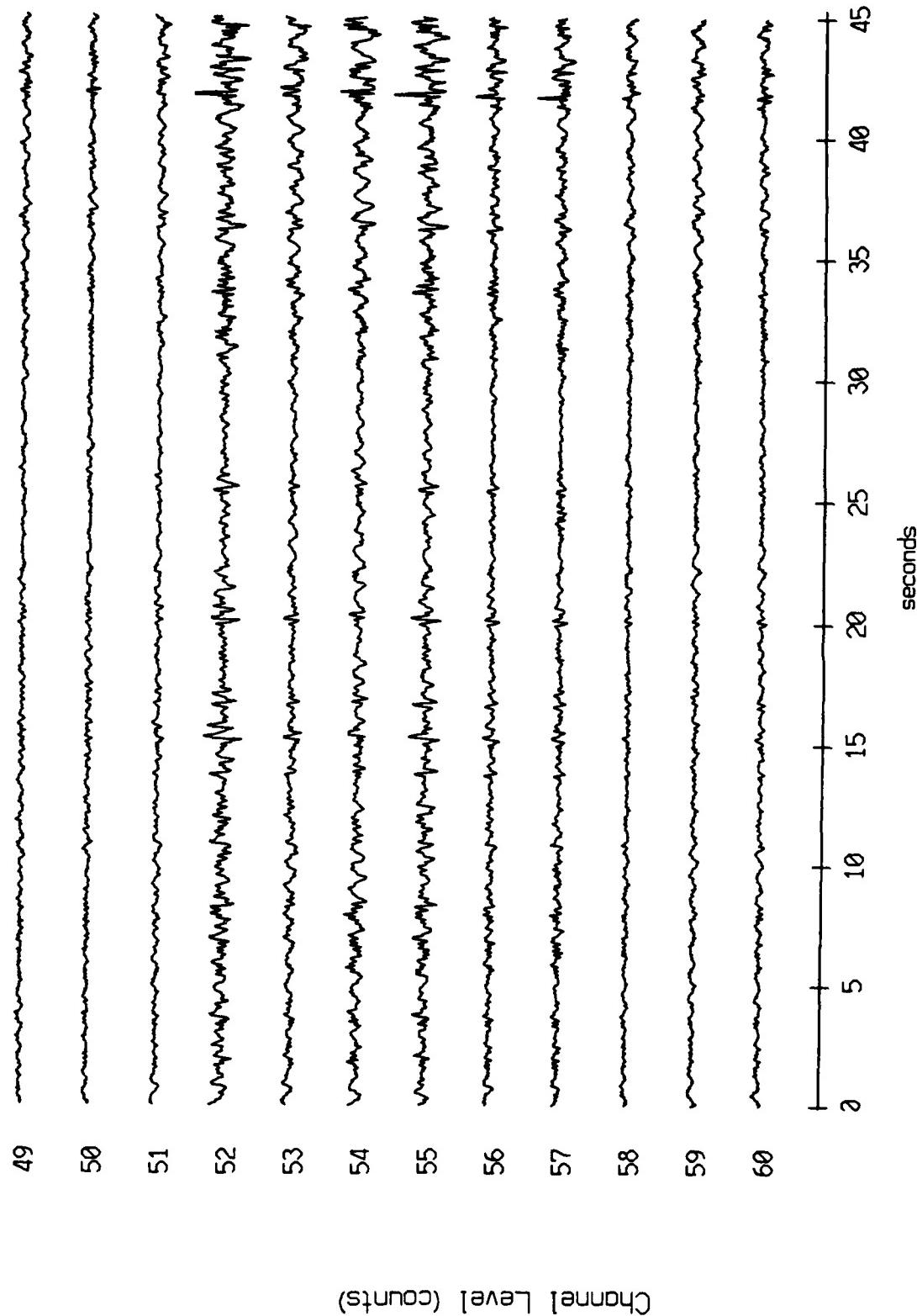


Figure X.14.1e

VLA Tape 440, Sept, 1987 Trip - Time 10:49:00.000 $f_s = 50$ Hz
vertical axis scale is approx. -2000 to 2000 counts

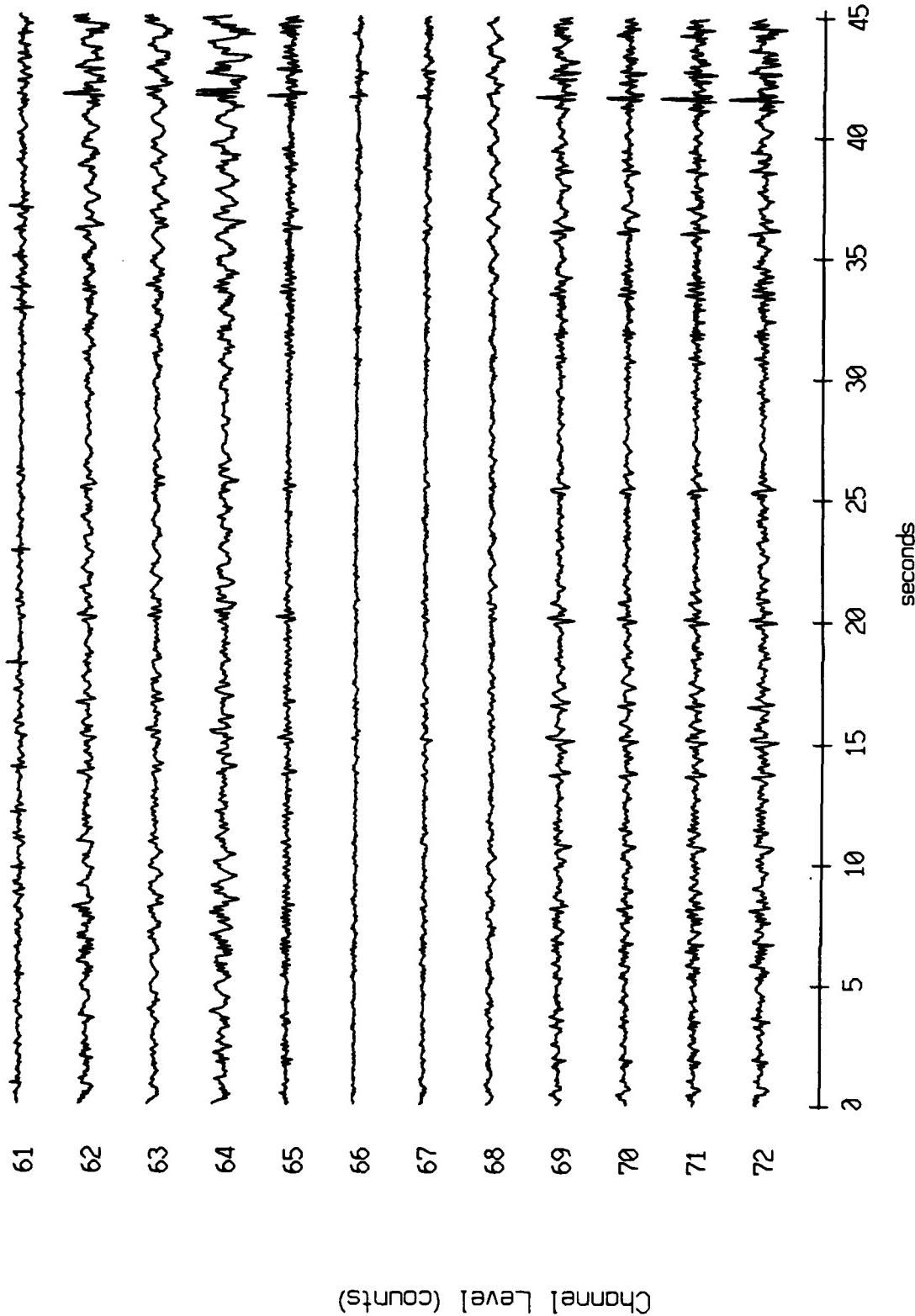


Figure X.14.1f

VLA Tape 440, Sept., 1987 Trip - Time 10:49:00.000 fs = 50 Hz
vertical axis scale is approx. -2000 to 2000 counts

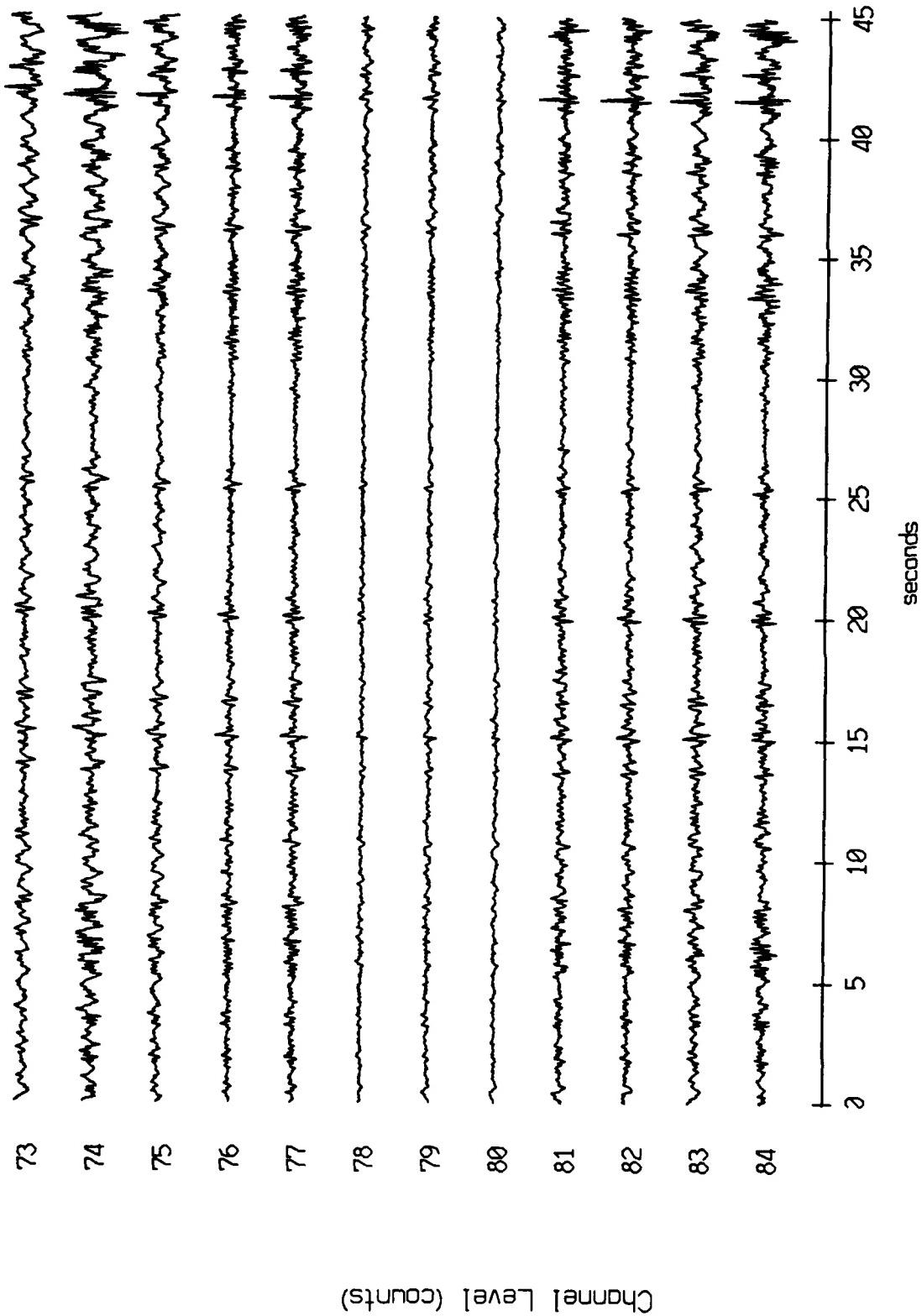


Figure X.14.1g

VLA Tape 440, Sept., 1987 Trip - Time 10:49:00.000 $f_s = 50$ Hz
vertical axis scale is approx. -2000 to 2000 counts

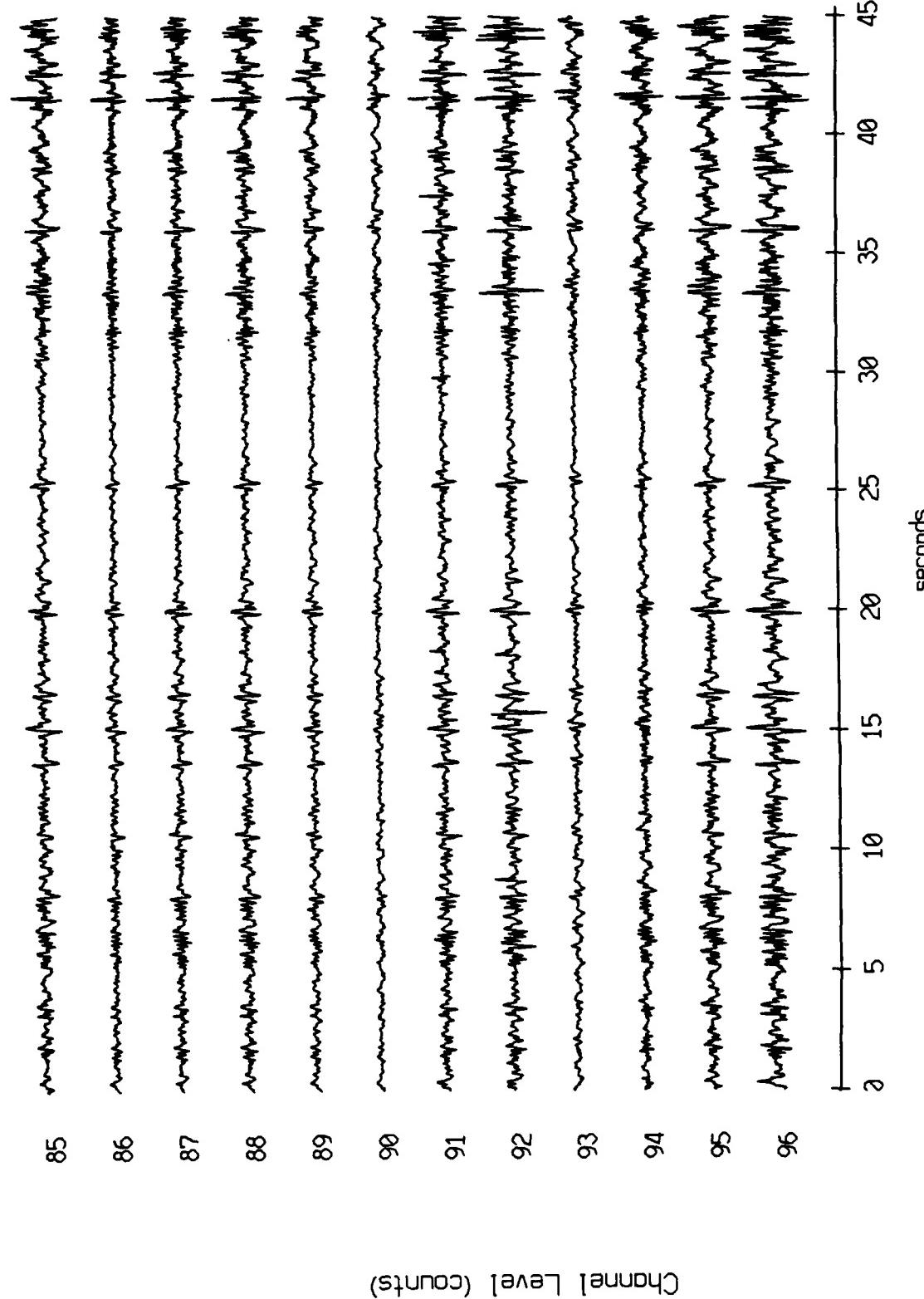


Figure X.14.1h

VLA Tape 440, Sept, 1987 Trip - Time 10:49:00.000 f_s = 50 Hz
vertical axis scale is approx. -2000 to 2000 counts

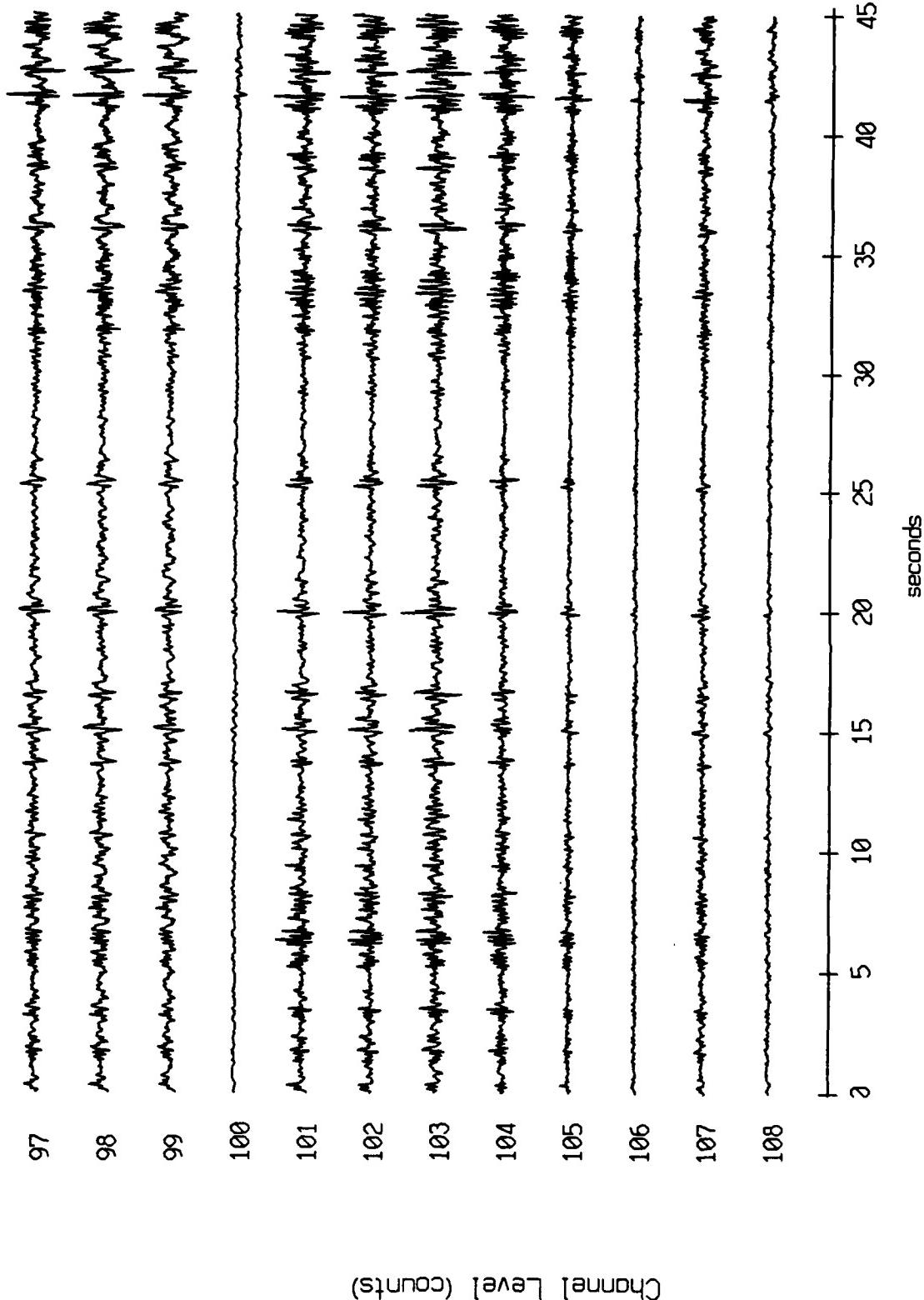


Figure X.14.11

VLA Tape 440, Sept, 1987 Trip - Time 10:49:00.000 fs = 50 Hz
vertical axis scale is approx. -2000 to 2000 counts

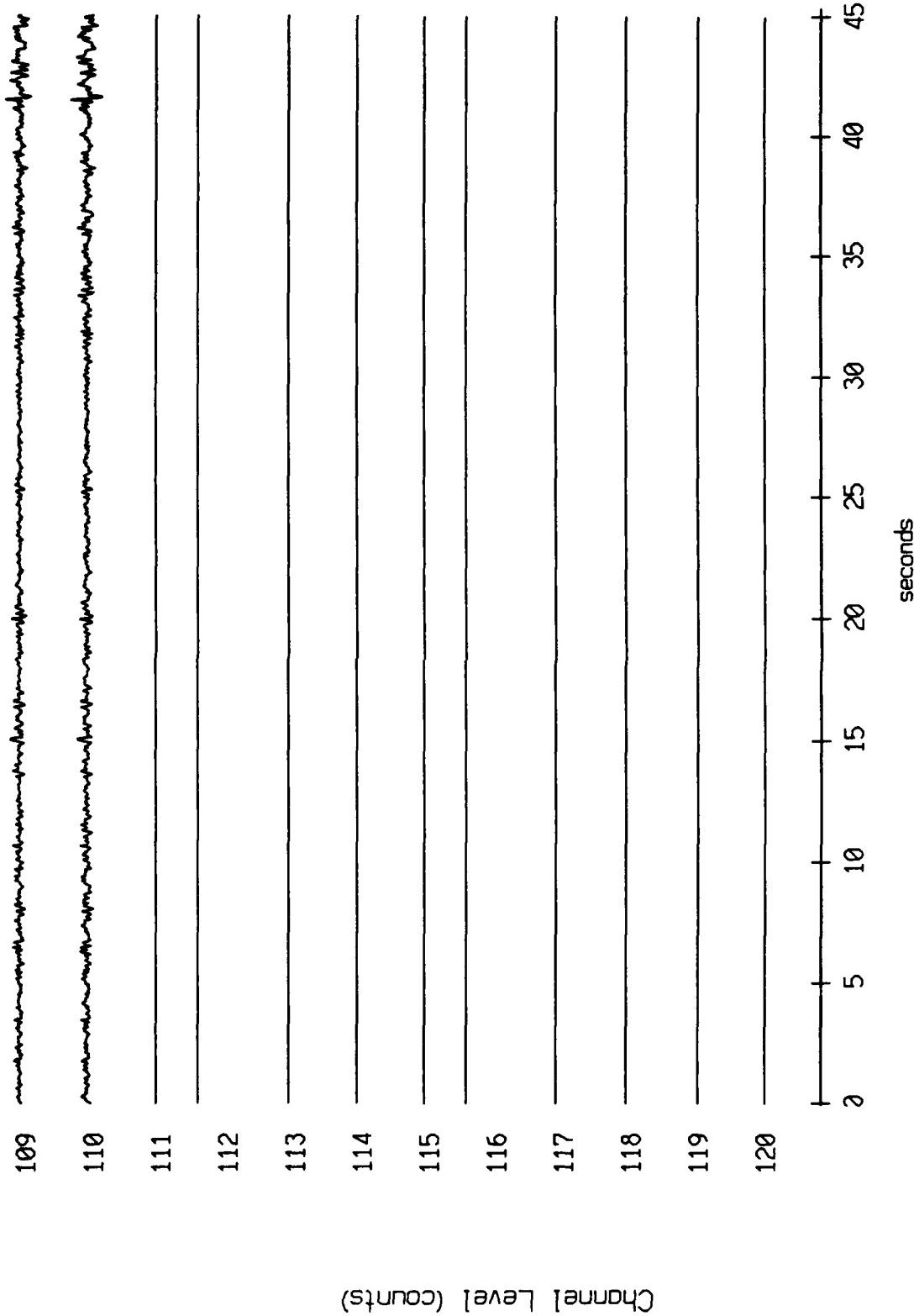


Figure X.14.1j

VLA Tape 442, Sept, 1987 Trip - Time 12:02:00.000 $f_s = 50$ Hz
vertical axis scale is approx. -2000 to 2000 counts

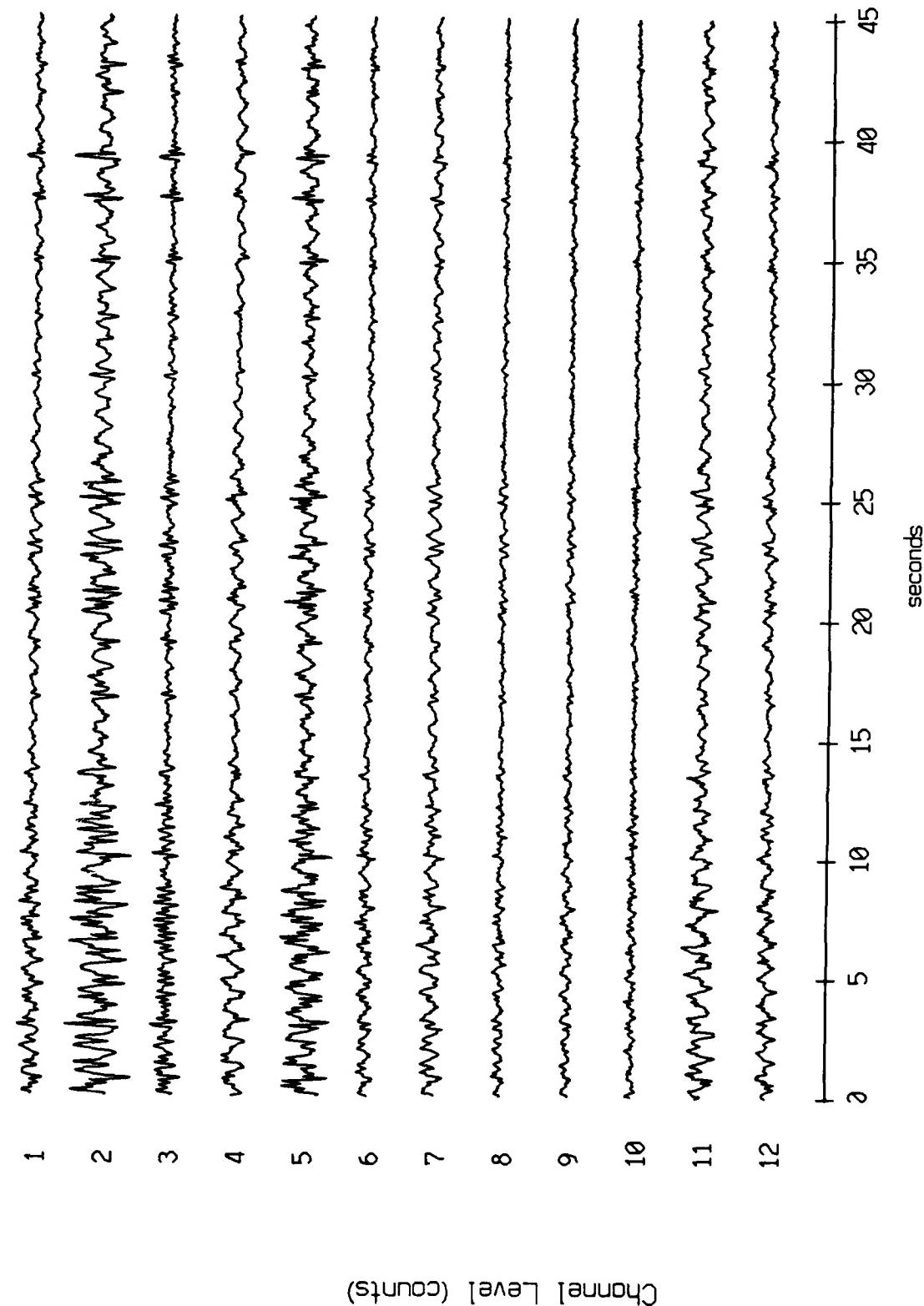


Figure X.15.1a

VLA Tape 442, Sept, 1987 Trip - Time 12:02:00.000 fs = 50 Hz
vertical axis scale is approx. -2000 to 2000 counts

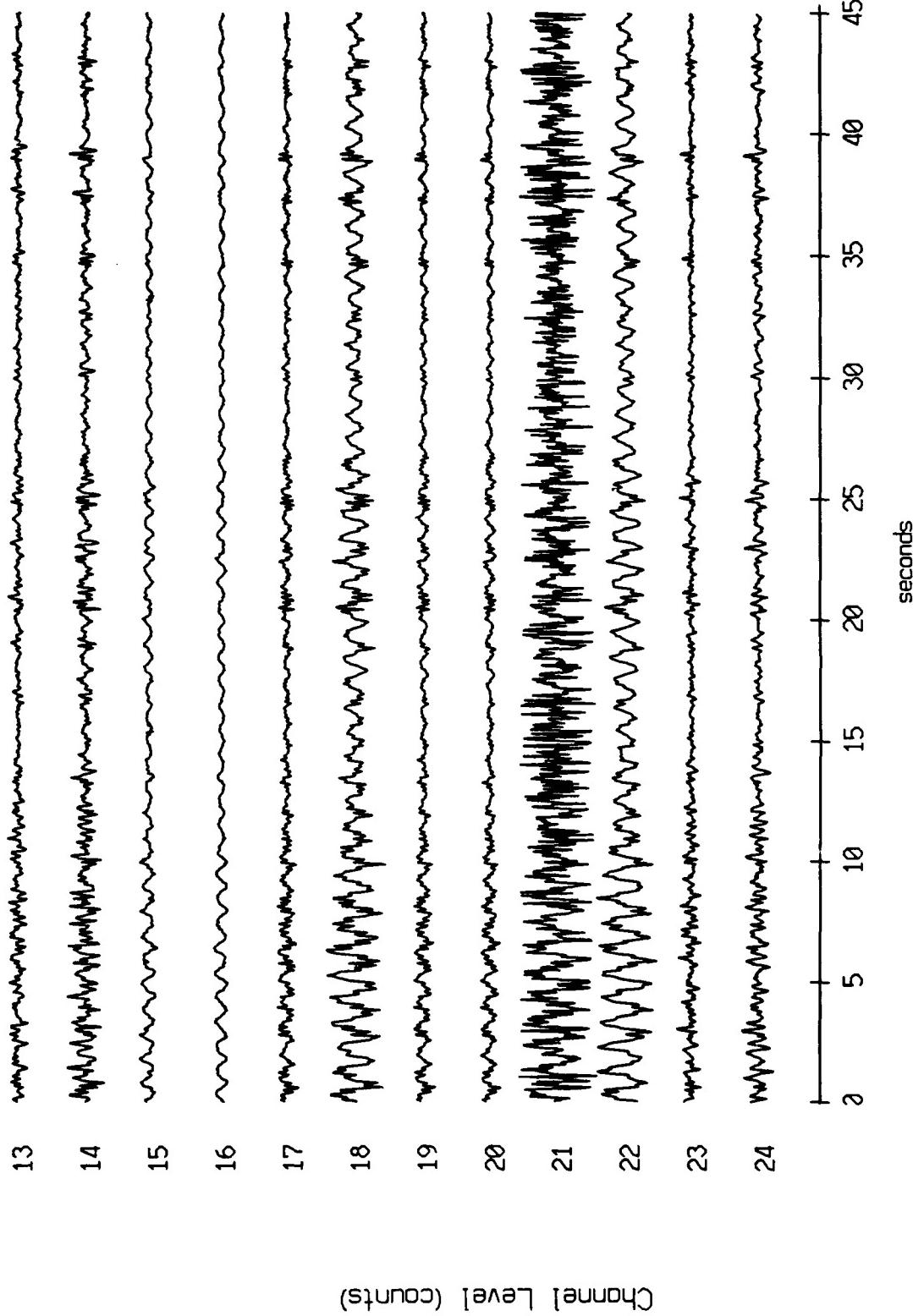


Figure X.15.1b

VLA Tape 442, Sept, 1987 Trip - Time 12:02:00.000 $f_s = 50$ Hz
vertical axis scale is approx. -2000 to 2000 counts

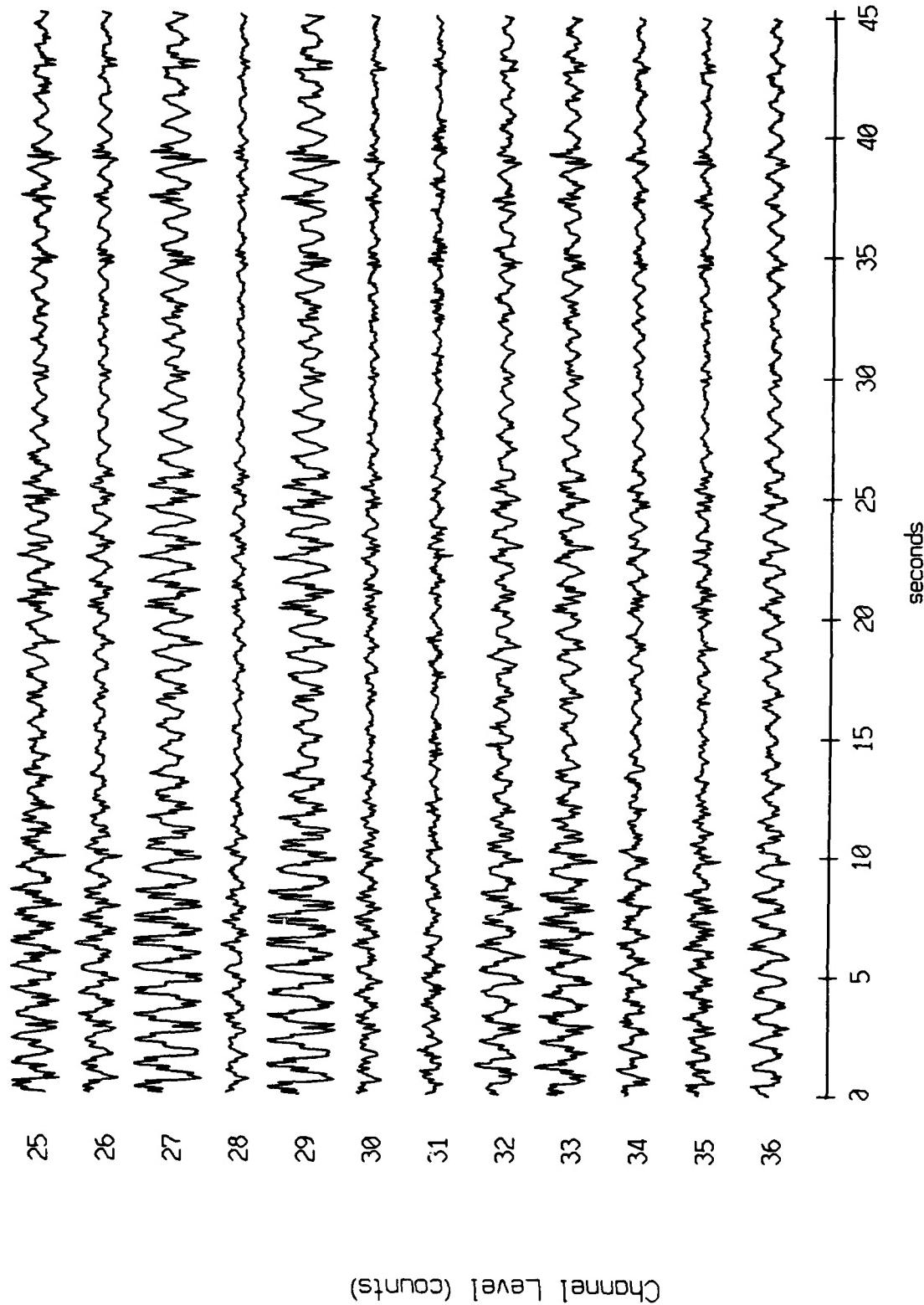


Figure X.15.1c

VLA Tape 442, Sept, 1987 Trip - Time 12:02:00.000 fs = 50 Hz
vertical axis scale is approx. -2000 to 2000 counts

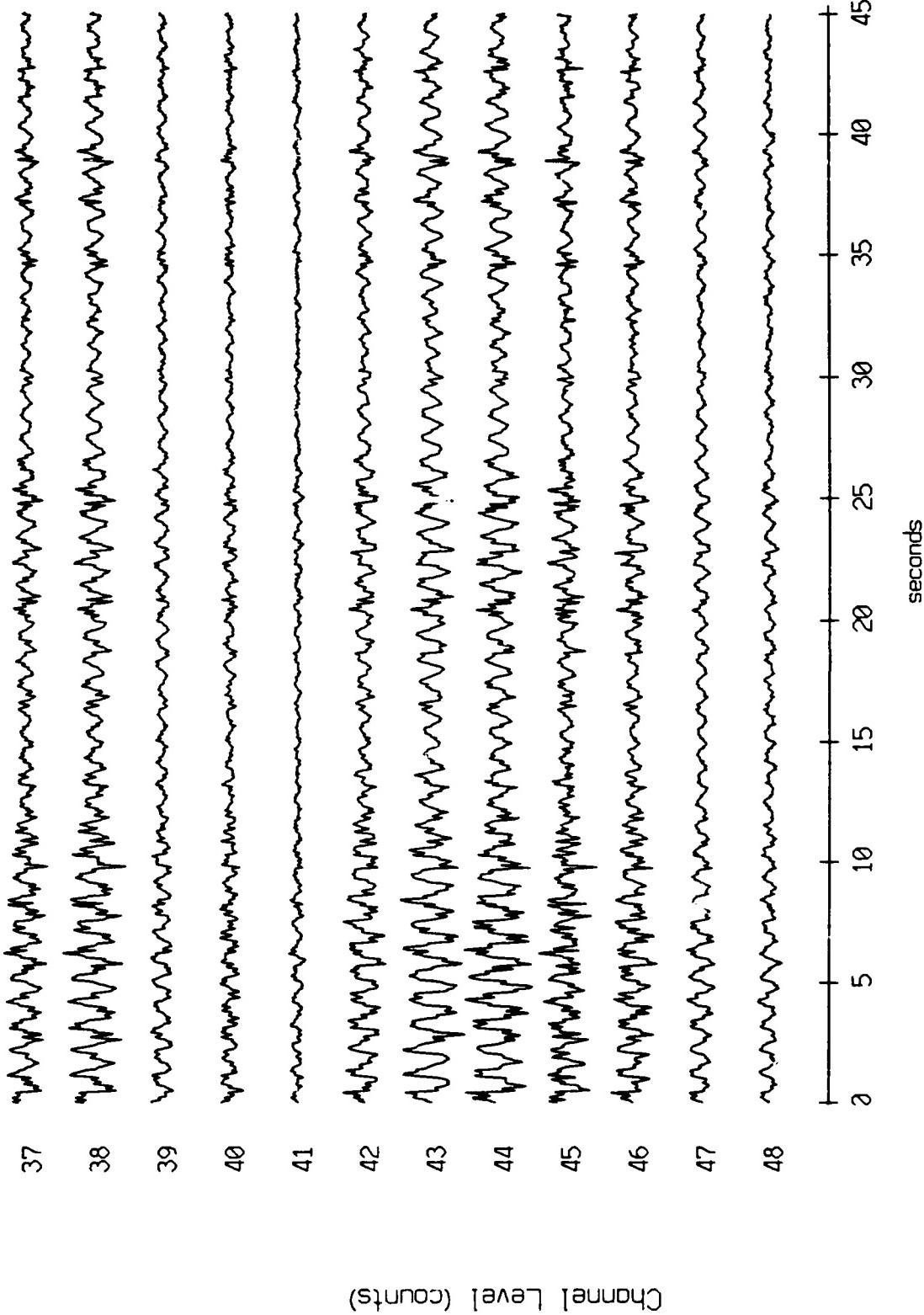


Figure X.15.1d

VLA Tape 442, Sept, 1987 Trip - Time 12:02:00.000 $f_s = 50$ Hz
vertical axis scale is approx. -2000 to 2000 counts

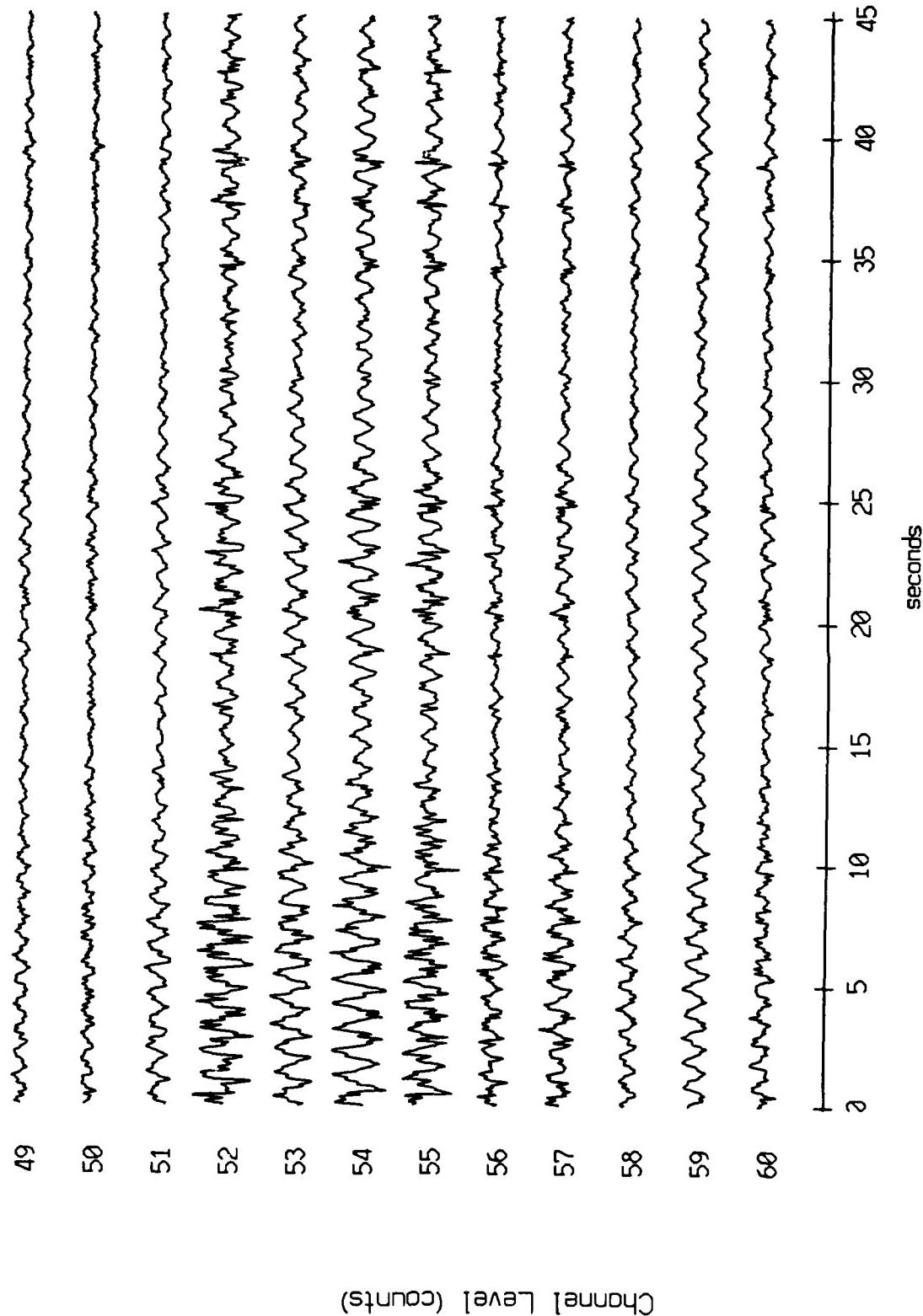


Figure X.15.1e

VLA Tape 442, Sept, 1987 Trip - Time 12:02:00.000 fs = 50 Hz
vertical axis scale is approx. -2000 to 2000 counts

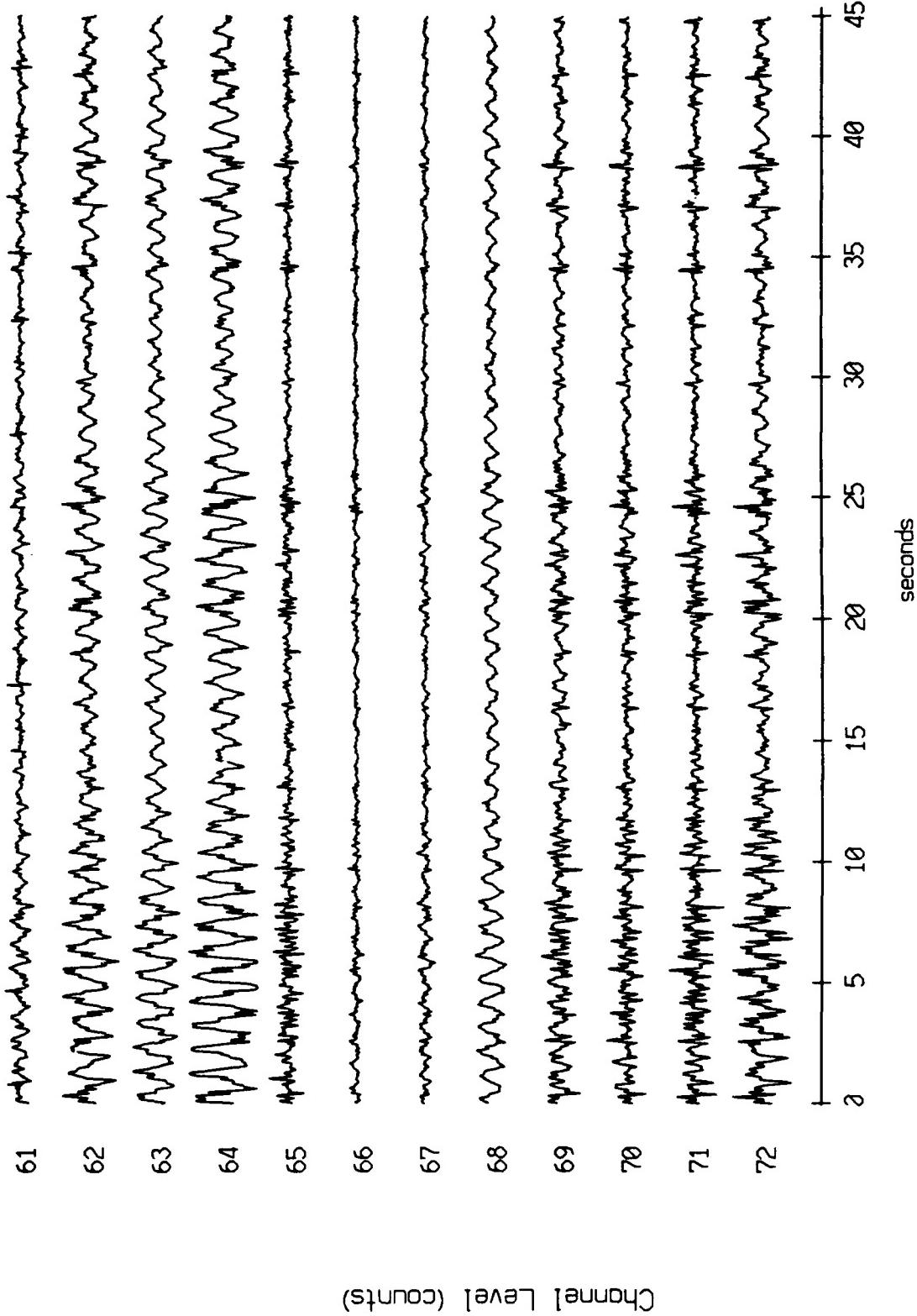


Figure X.15.1f

VLA Tape 442, Sept., 1987 Trip - Time 12:02:00.000 $f_s = 50$ Hz
vertical axis scale is approx. 2000 to 2000 counts

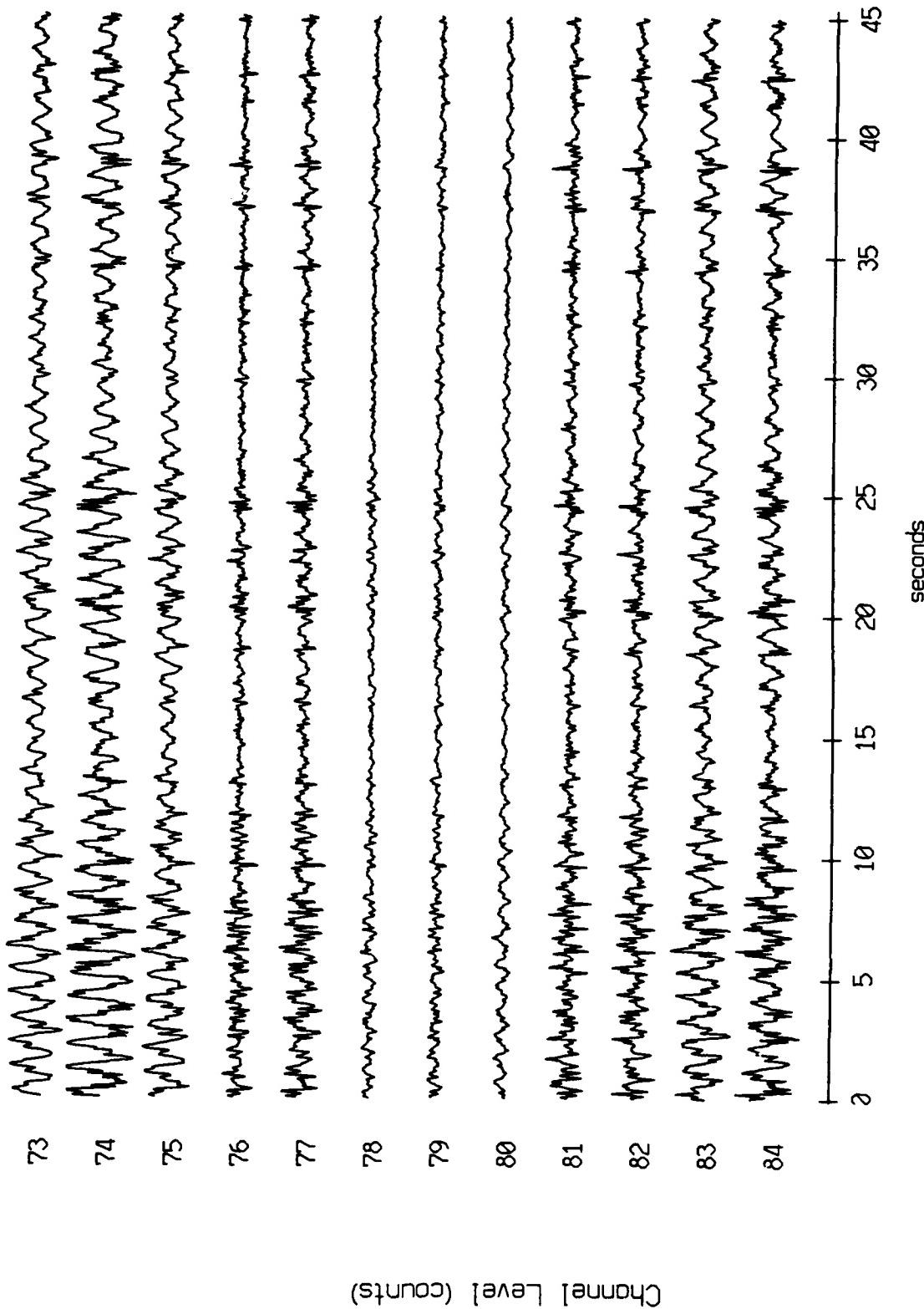


Figure X.15.1g

VLA Tape 442, Sept., 1987 Trip - Time 12:02:00.000 $f_s = 50$ Hz
vertical axis scale is approx. -2000 to 2000 counts

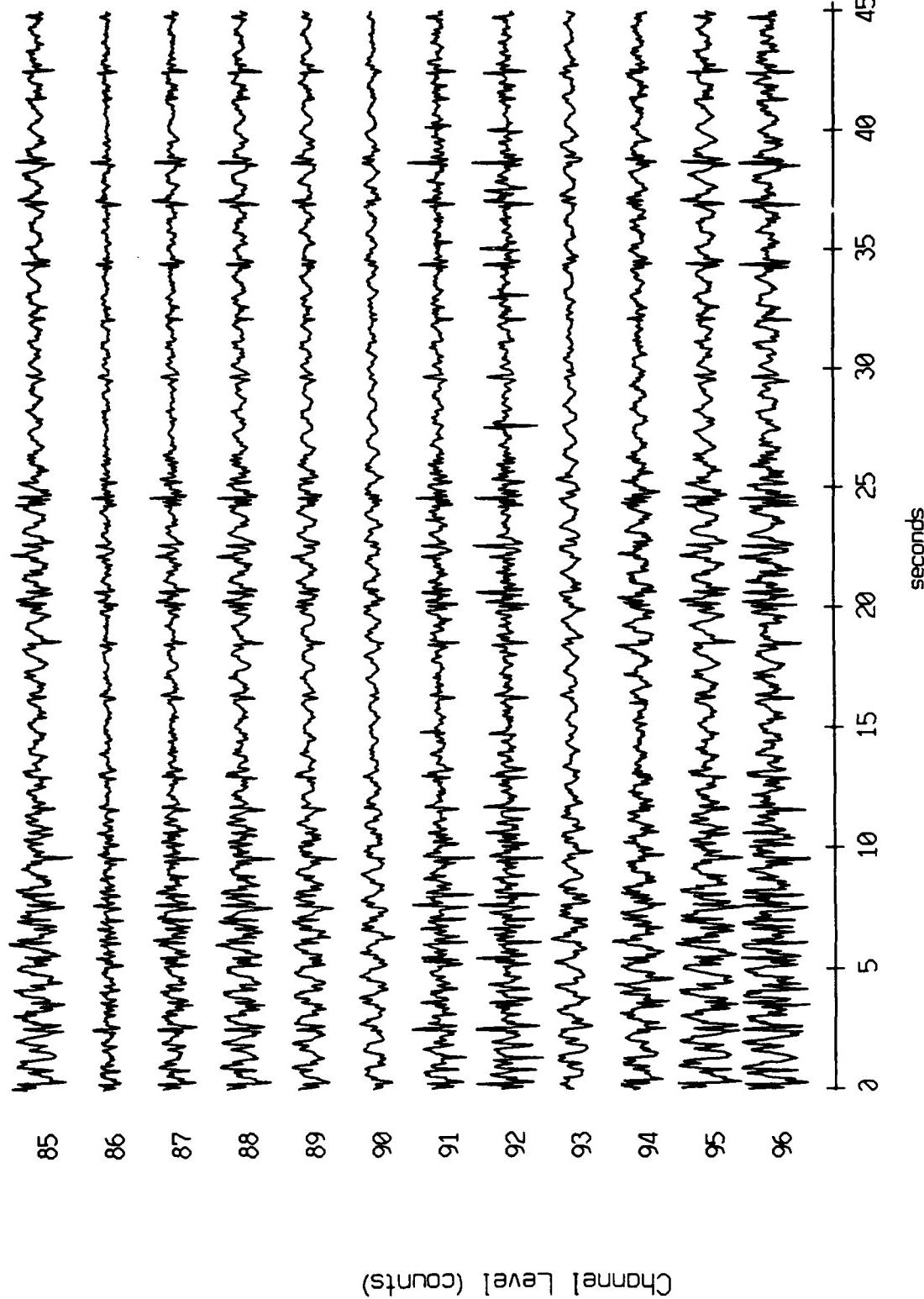


Figure X.15.1h

VLA Tape 442, Sept, 1987 Trip - Time 12:02:00.000 $f_s = 50$ Hz
vertical axis scale is approx. -2000 to 2000 counts

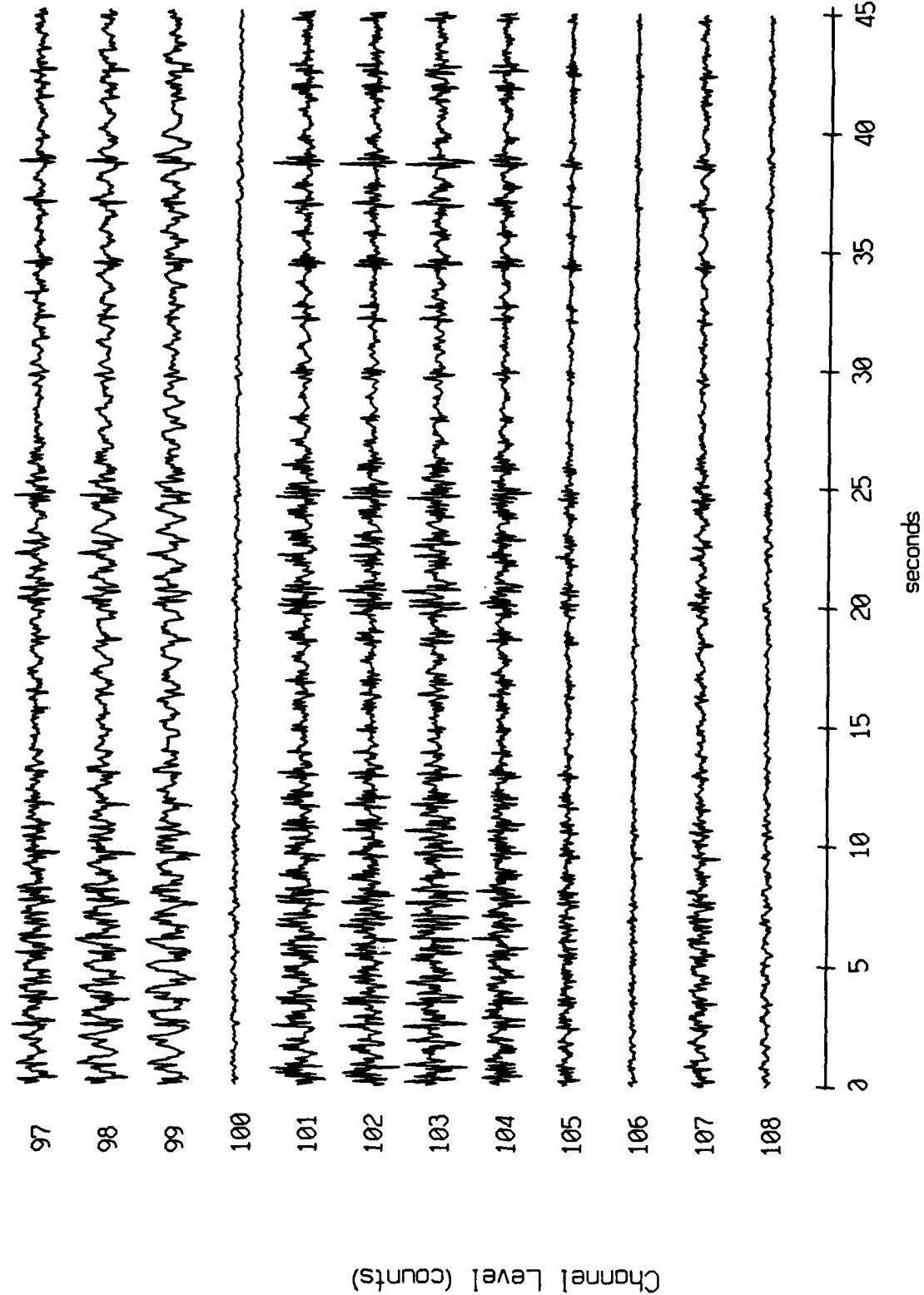
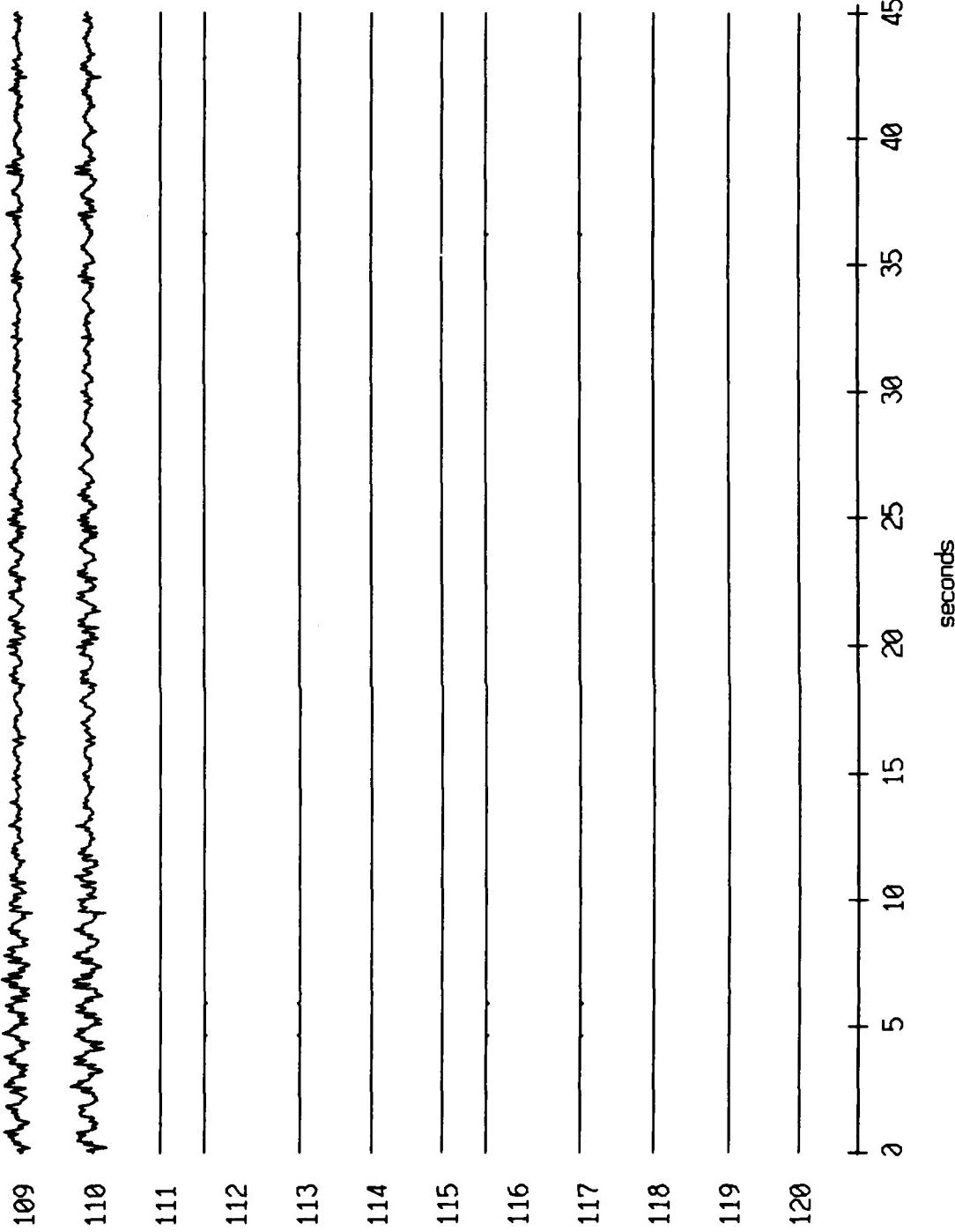


Figure X.15.1i

VLA Tape 442, Sept, 1987 Trip - Time 12:02:00.000 $f_s = 50$ Hz
vertical axis scale is approx. -2000 to 2000 counts



Channel Level (counts)

Figure X.15.1j

VLA Tape 447, Sept, 1987 Trip - Time 13:52:00.000 $f_s = 50$ Hz
vertical axis scale is approx. -2000 to 2000 counts

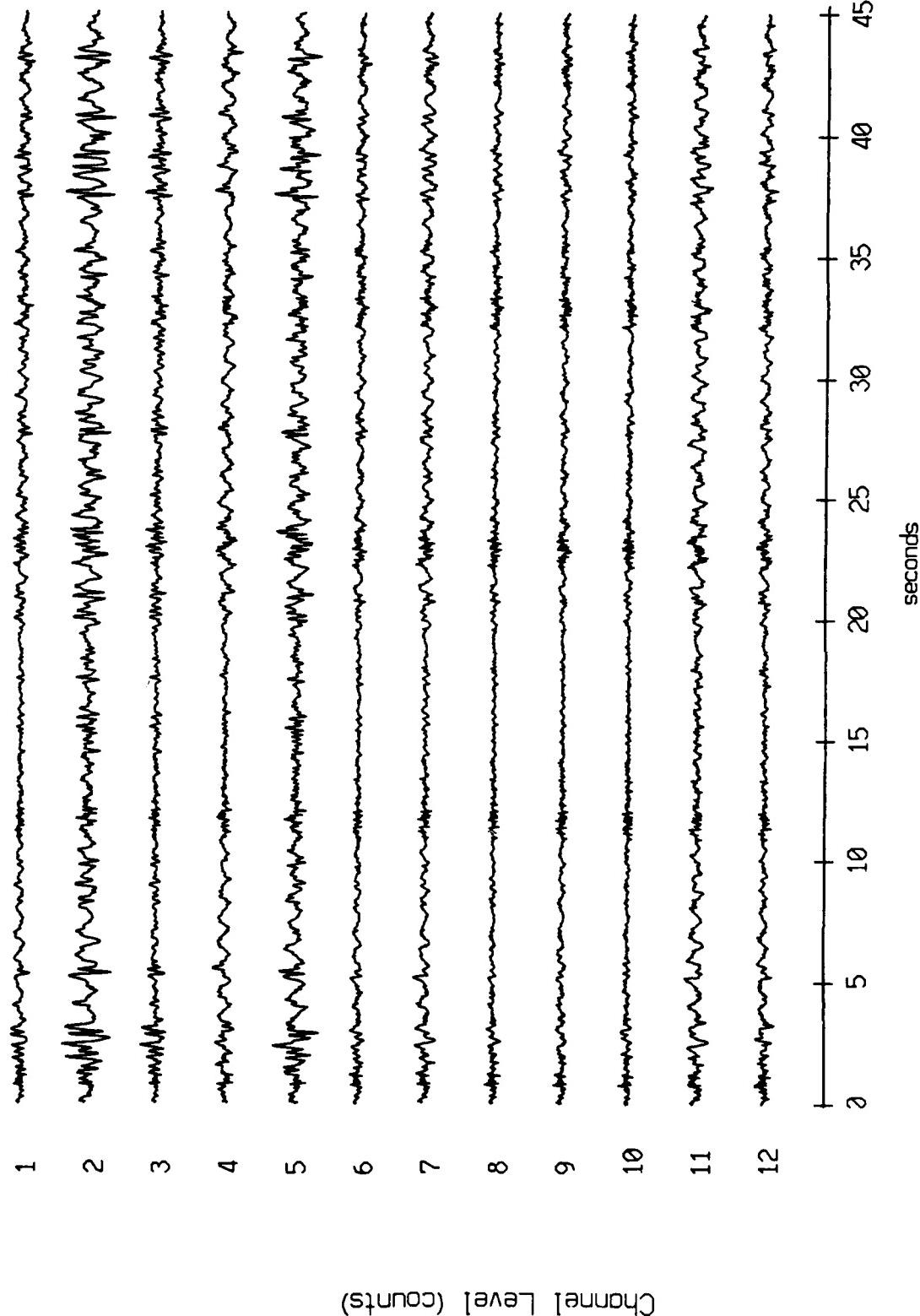


Figure X.16.1a

VLA Tape 447, Sept., 1987 Trip - Time 13:52:00.000 $f_s = 50$ Hz
vertical axis scale is approx. -2000 to 2000 counts

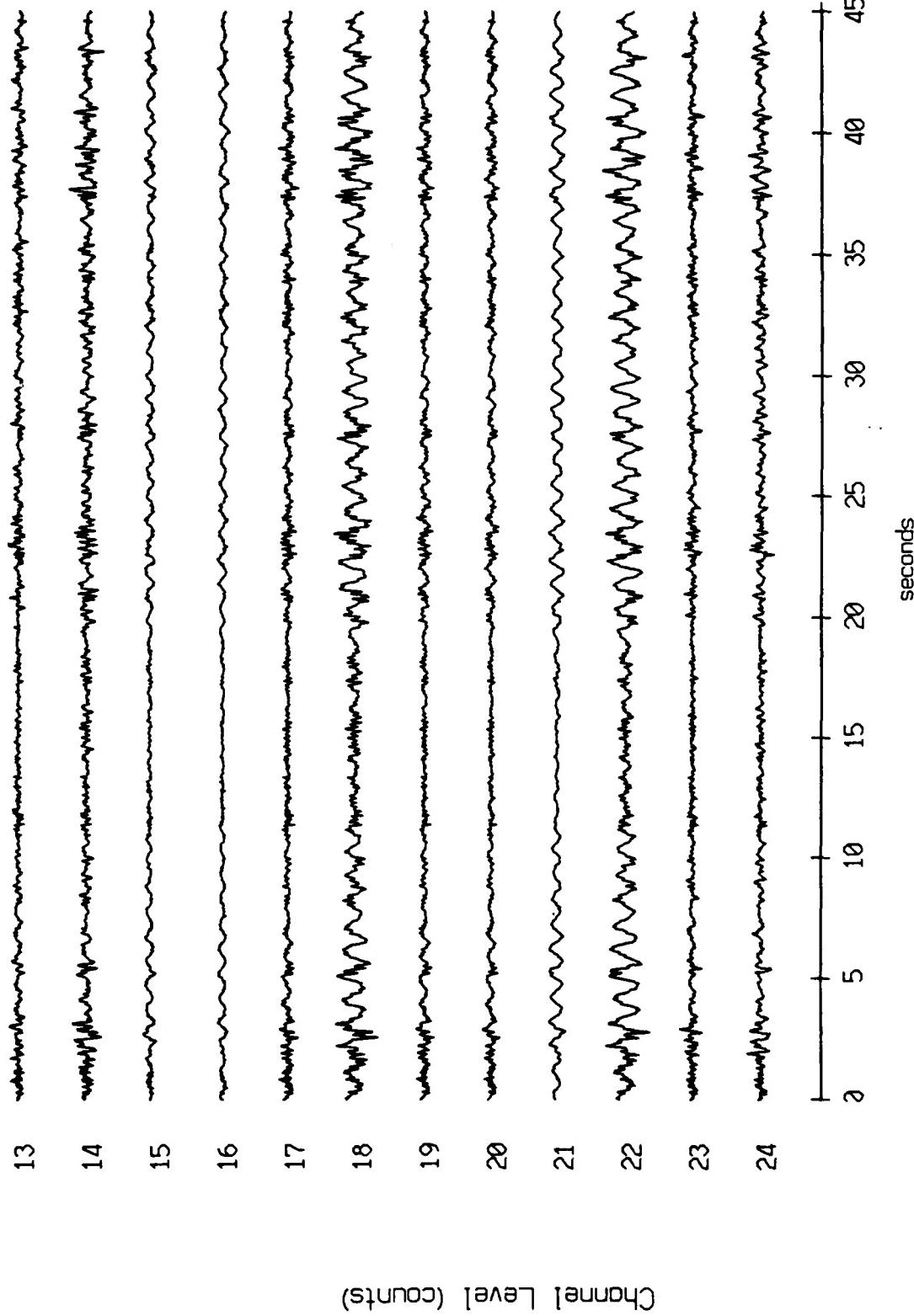


Figure X.16.1b

VLA Tape 447, Sept, 1987 Trip - Time 13:52:00.000 $f_s = 50$ Hz
vertical axis scale is approx. -2000 to 2000 counts

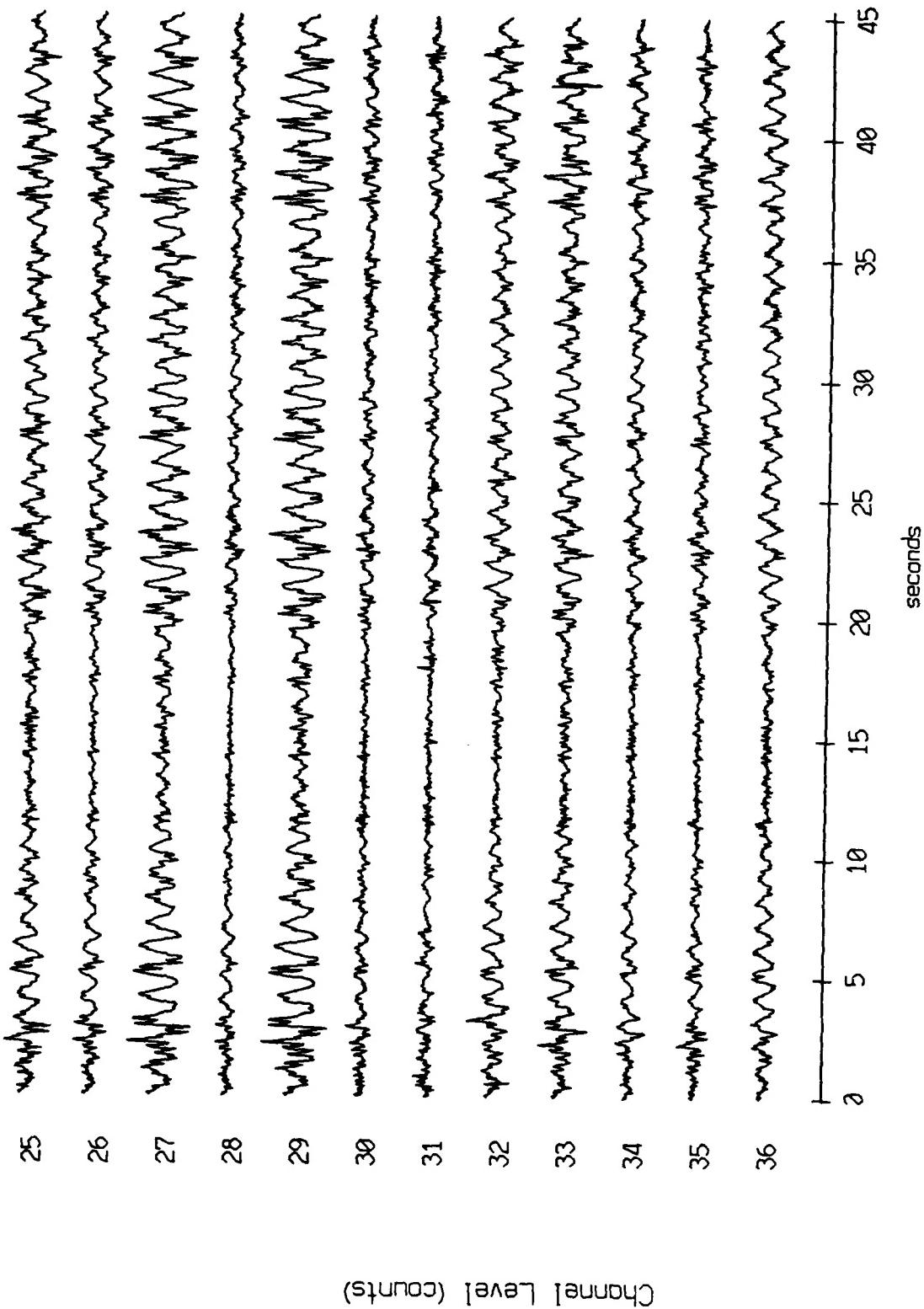


Figure X.16.1c

VLA Tape 447, Sept, 1987 Trip - Time 13:52:00.000 $f_s = 50$ Hz
vertical axis scale is approx. -2000 to 2000 counts

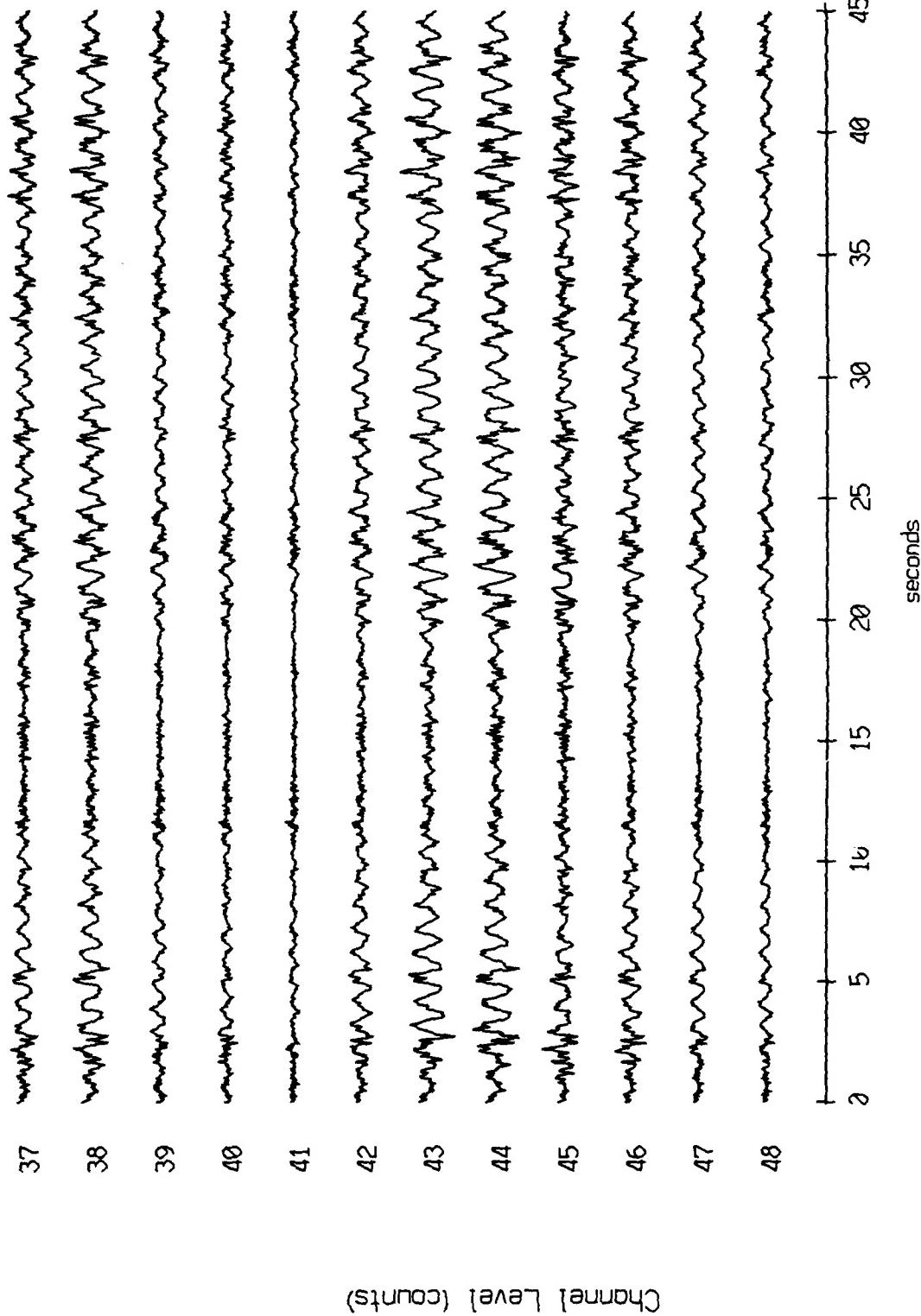


Figure X.16.1d

VLA Tape 447, Sept, 1987 Trip - Time 13:52:00.000 $f_s = 50$ Hz
vertical axis scale is approx. -2000 to 2000 counts

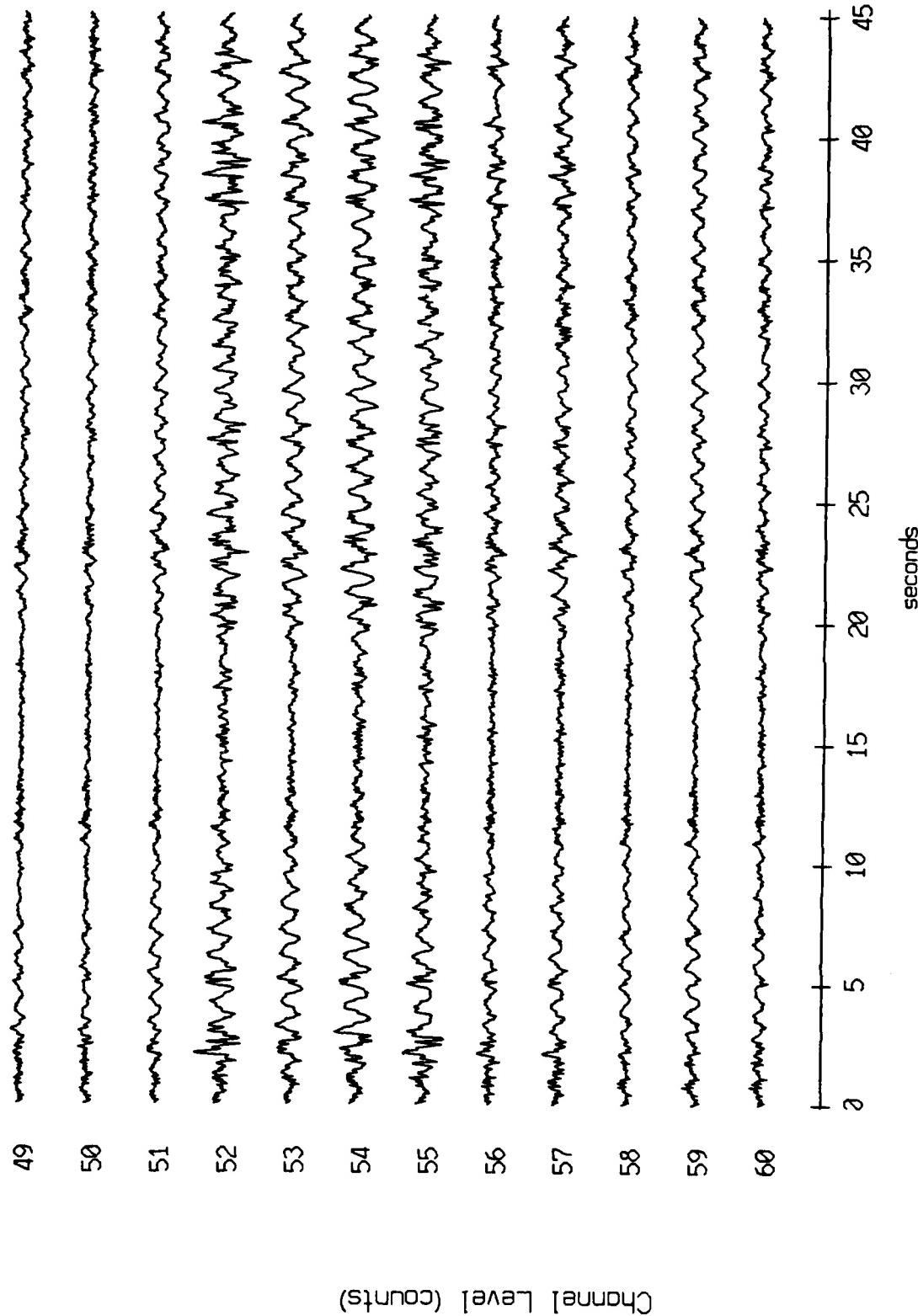


Figure X.16.1e

VLA Tape 447, Sept, 1987 Trip - Time 13:52:00.000 fs = 50 Hz
vertical axis scale is approx. -2000 to 2000 counts

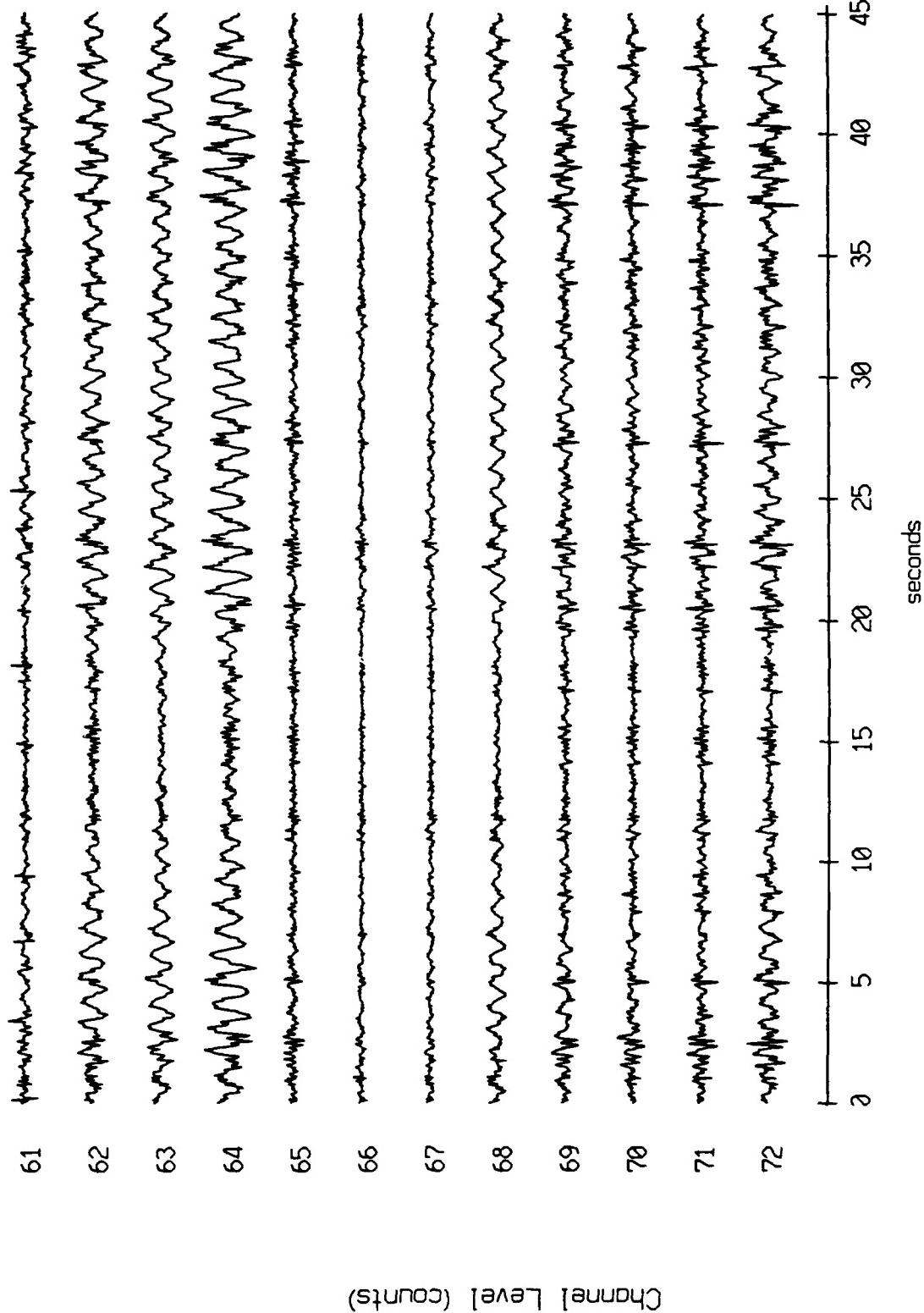


Figure X.16.1f

VLA Tape 447, Sept, 1987 Trip - Time 13:52:00.000 fs = 50 Hz
vertical axis scale is approx. -2000 to 2000 counts

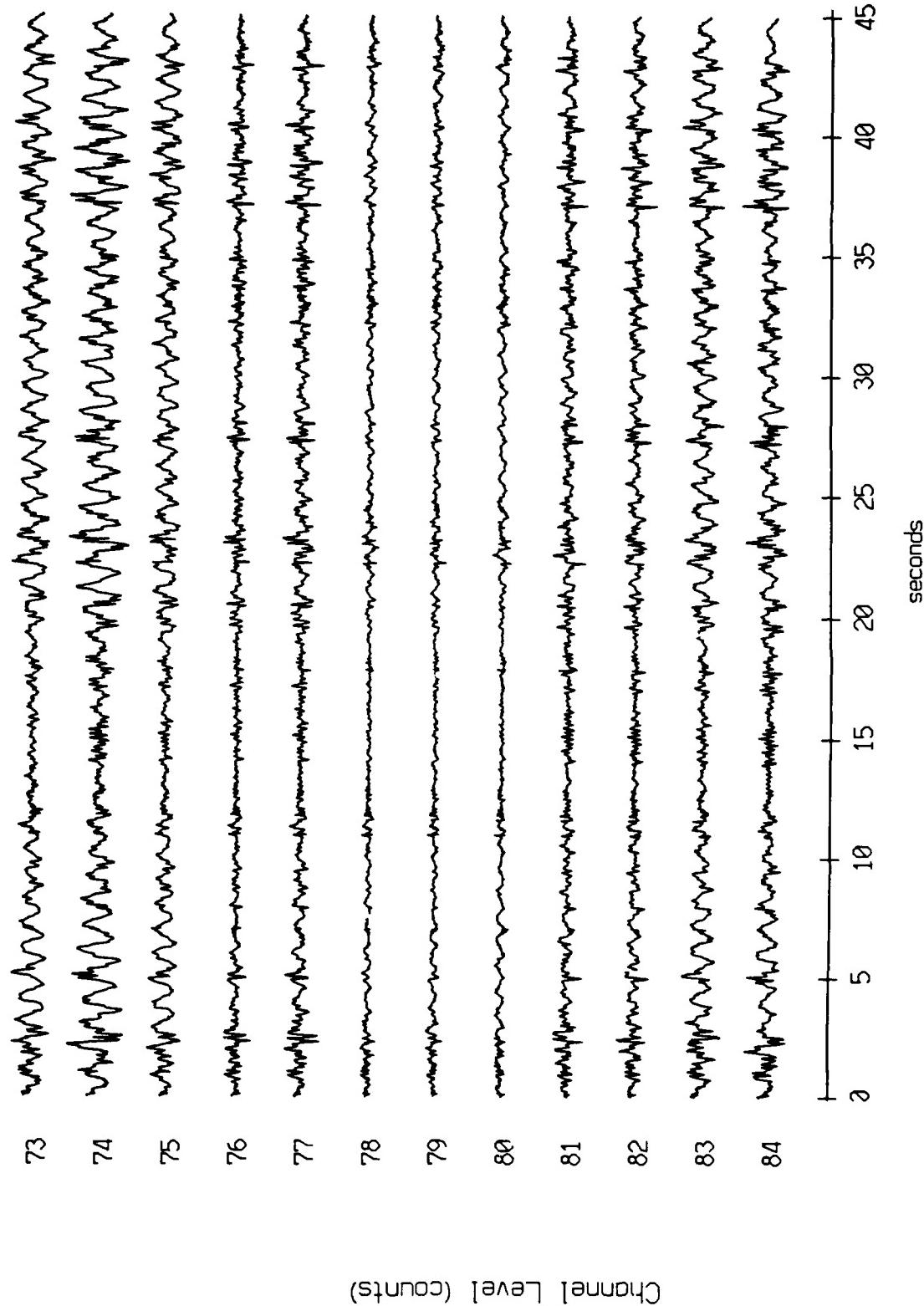


Figure X.16.1g

VLA Tape 447, Sept, 1987 Trip - Time 13:52:00.000 fs = 50 Hz
vertical axis is approx. -2000 to 2000 counts

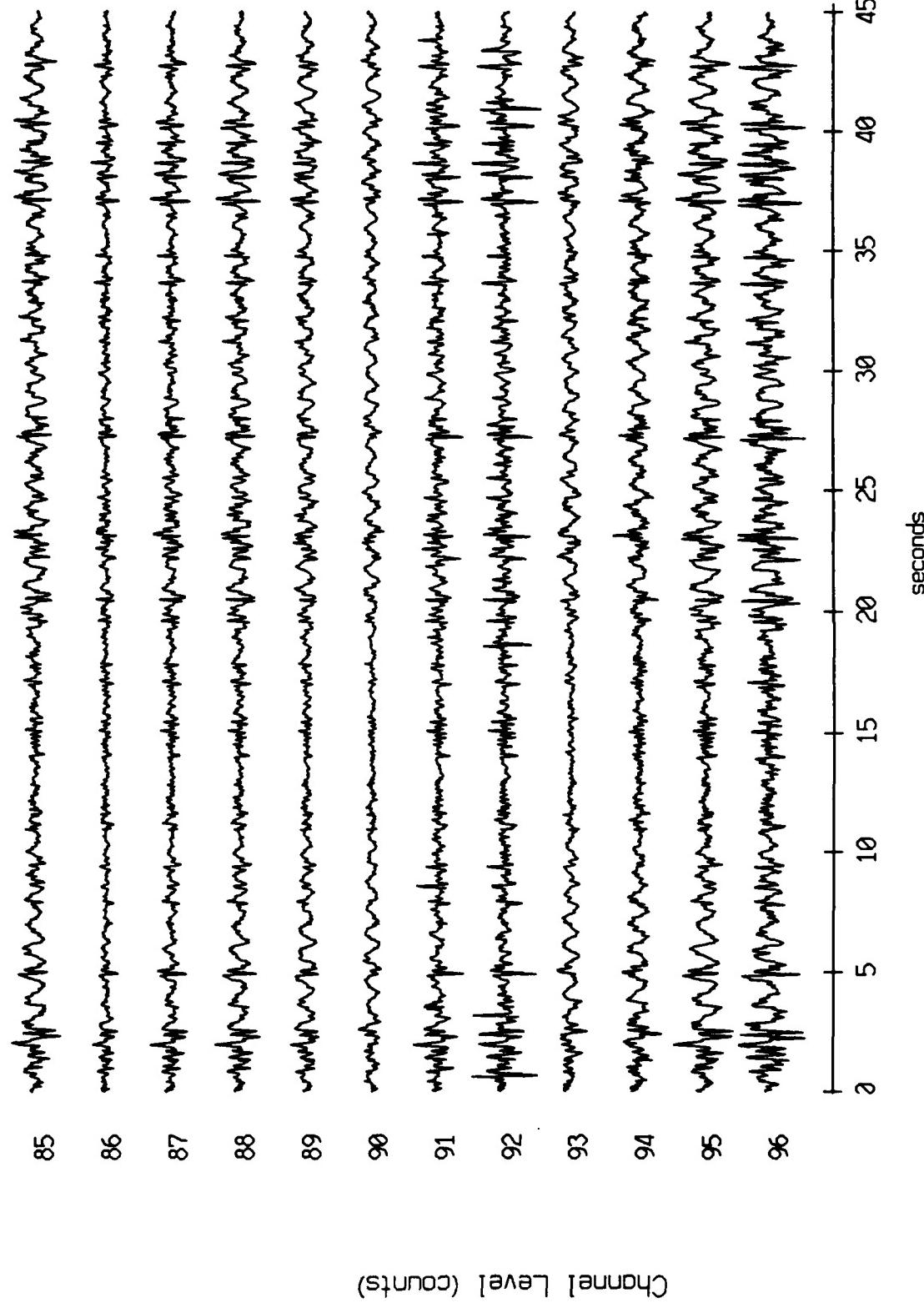


Figure X.16.1h

VLA Tape 447, Sept, 1987 Trip - Time 13:52:00.000 fs = 50 Hz
vertical axis scale is approx. -2000 to 2000 counts

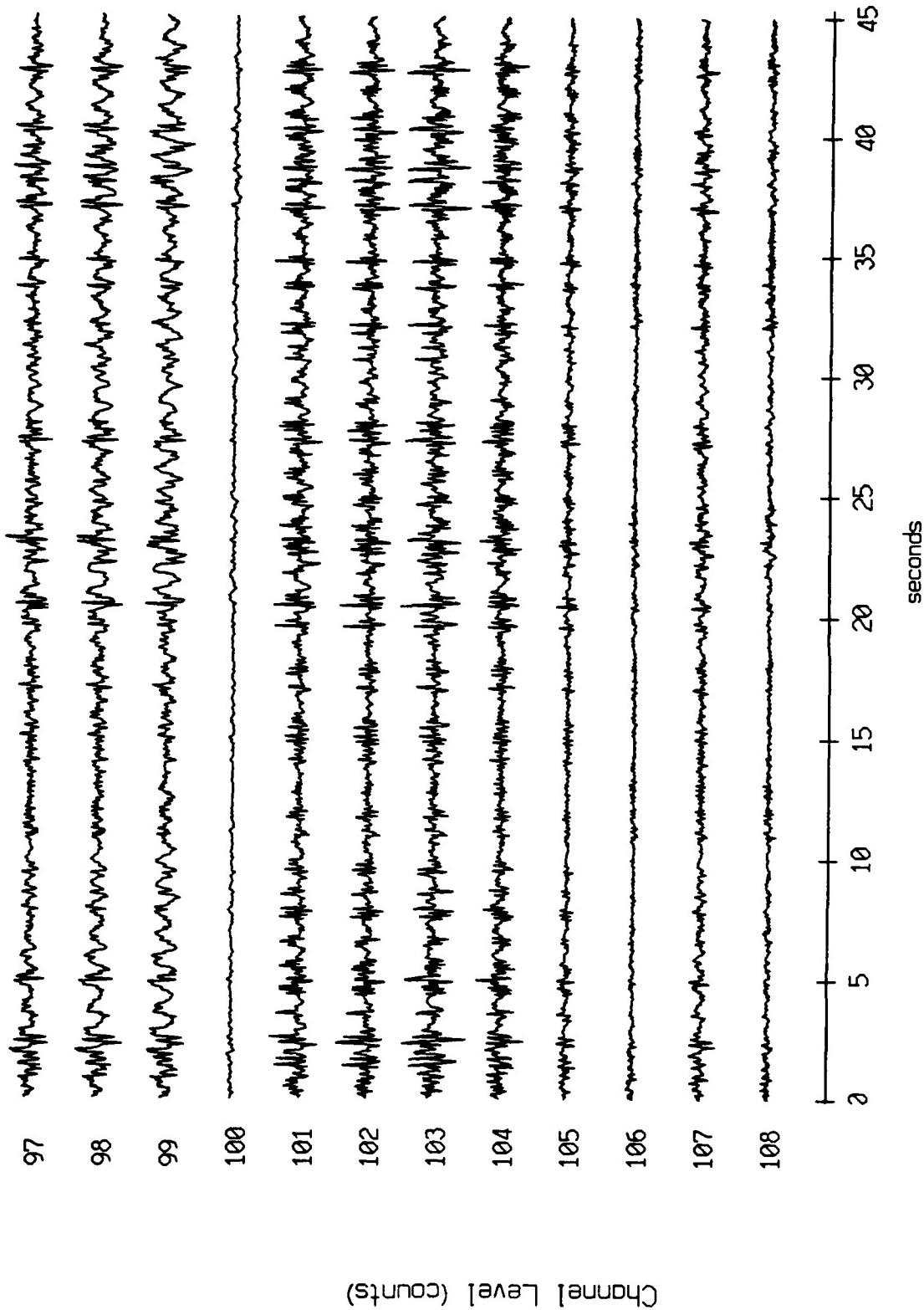


Figure X.16.11

VLA Tape 447, Sept, 1987 Trip - Time 13:52:00.000 $f_s = 50$ Hz
vertical axis scale is approx. -2000 to 2000 counts

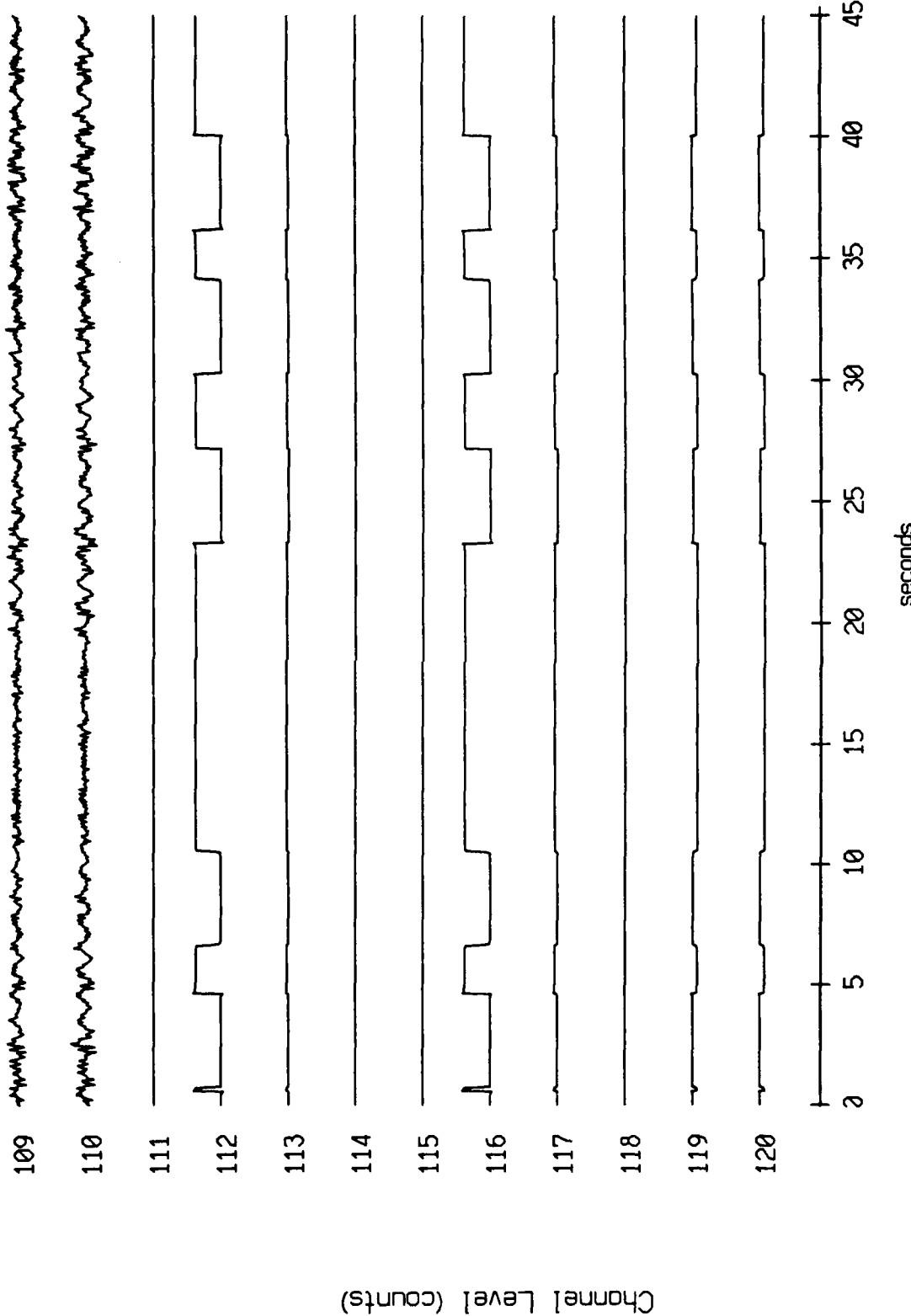


Figure X.16.1j

VLA Tape 453, Sept. 1987 Trip - Time 16:30:00.000 $f_s = 50$ Hz
vertical axis scale is approx. -2000 to 2000 counts

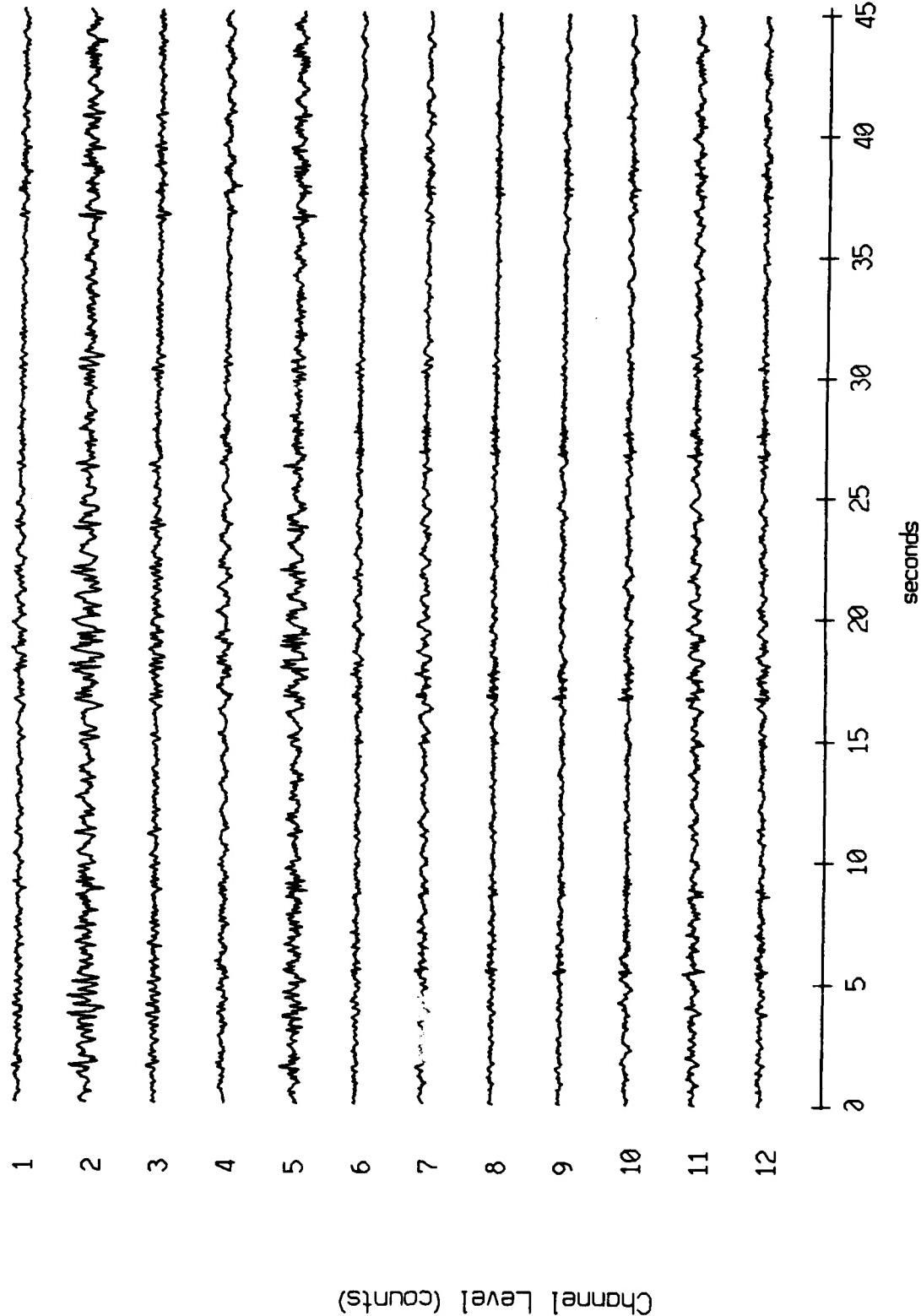


Figure X.17.1a

VLA Tape 453, Sept, 1987 Trip - Time 16:30:00.000 fs = 50 Hz
vertical axis scale is approx. -2000 to 2000 counts

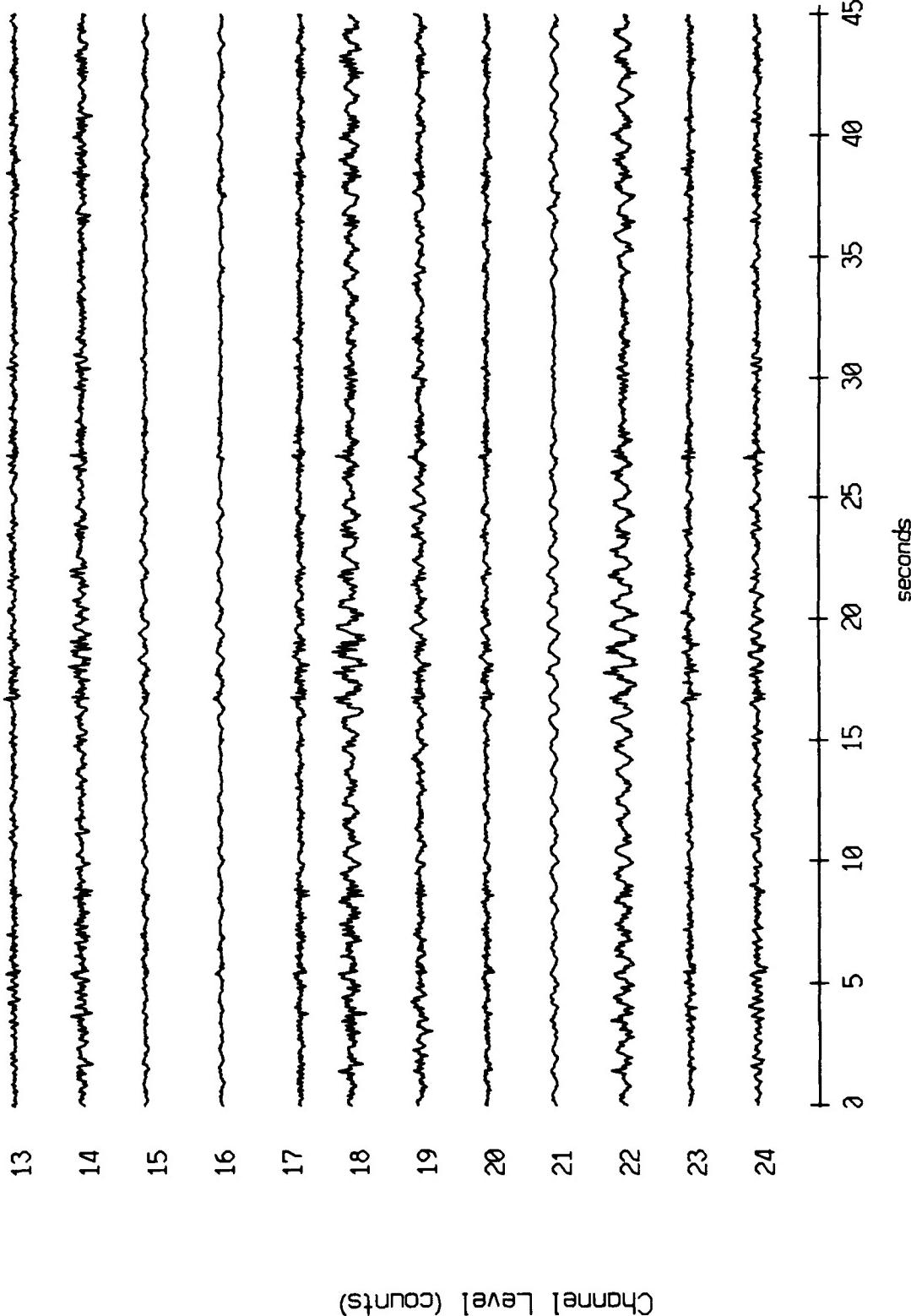


Figure X.17.1b

VLA Tape 453, Sept, 1987 Trip - Time 16:30:00.000 fs = 50 Hz
vertical axis scale is approx. -2000 to 2000 counts

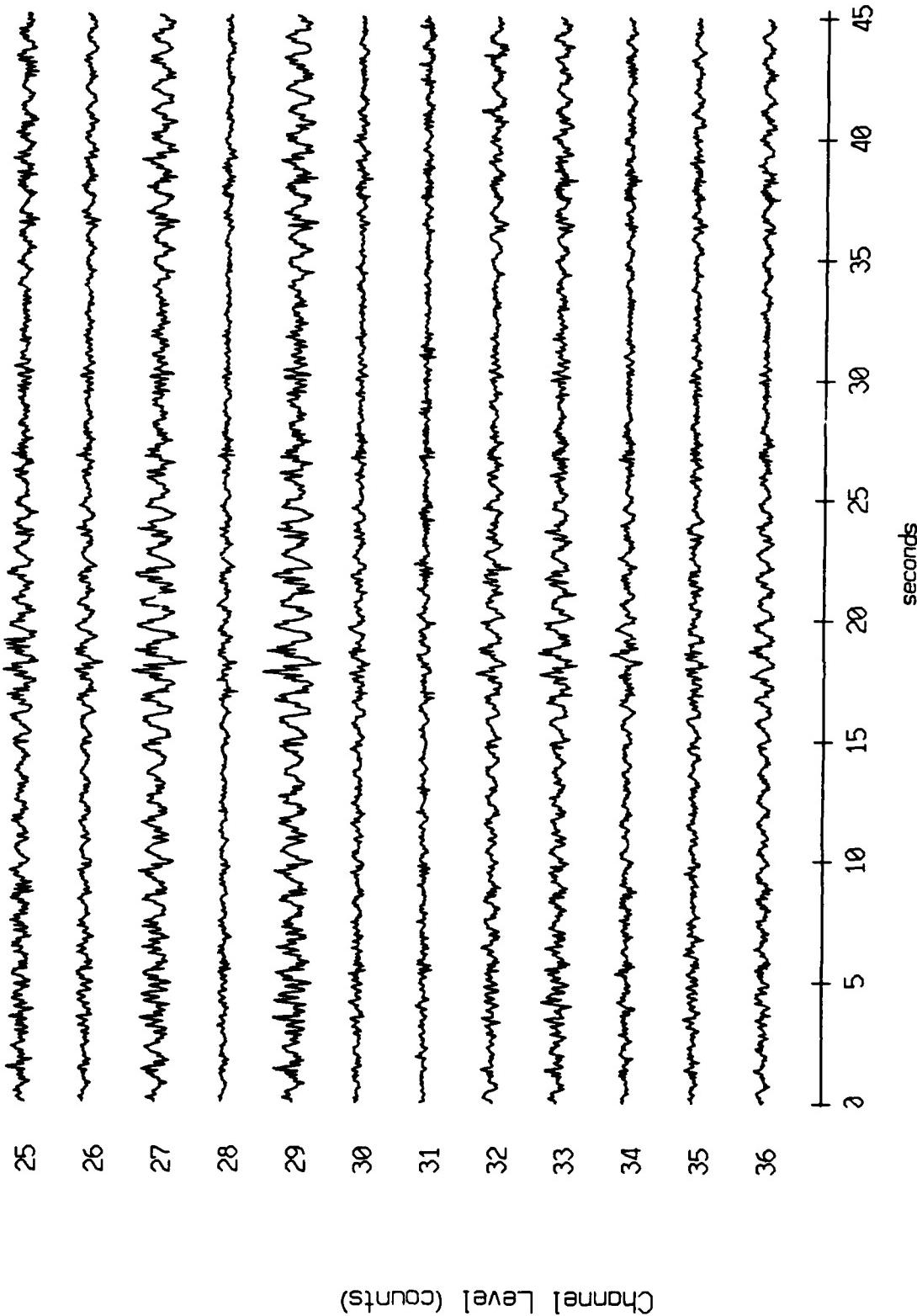


Figure X.17.1c

VLA Tape 453, Sept, 1987 Trip - Time 16:30:00.000 fs = 50 Hz
vertical axis scale is approx. -2000 to 2000 counts

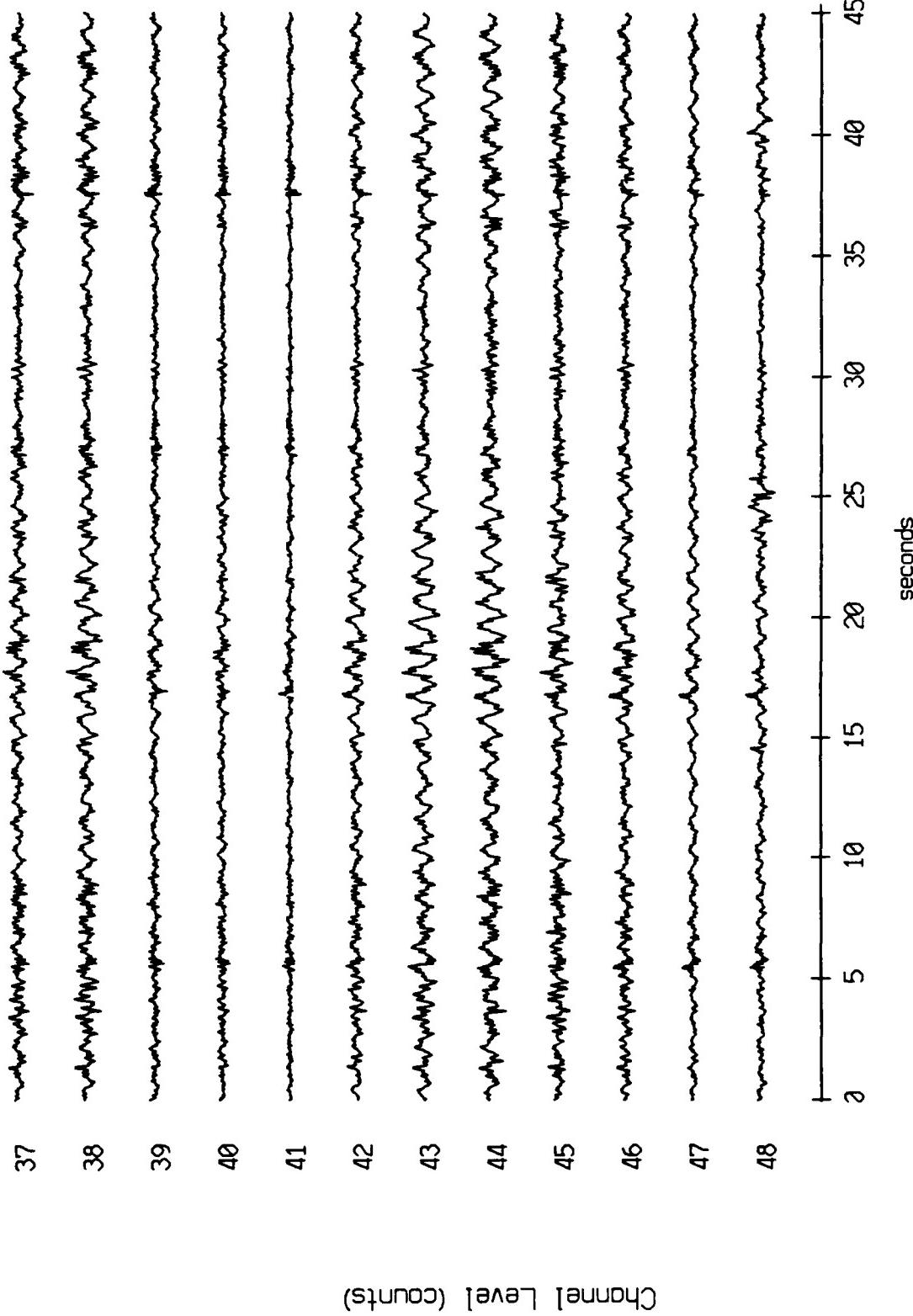


Figure X.17.1d

VLA Tape 453, Sept, 1987 Trip - Time 16:30:00.000 $f_s = 50$ Hz
vertical axis scale is approx. -2000 to 2000 counts

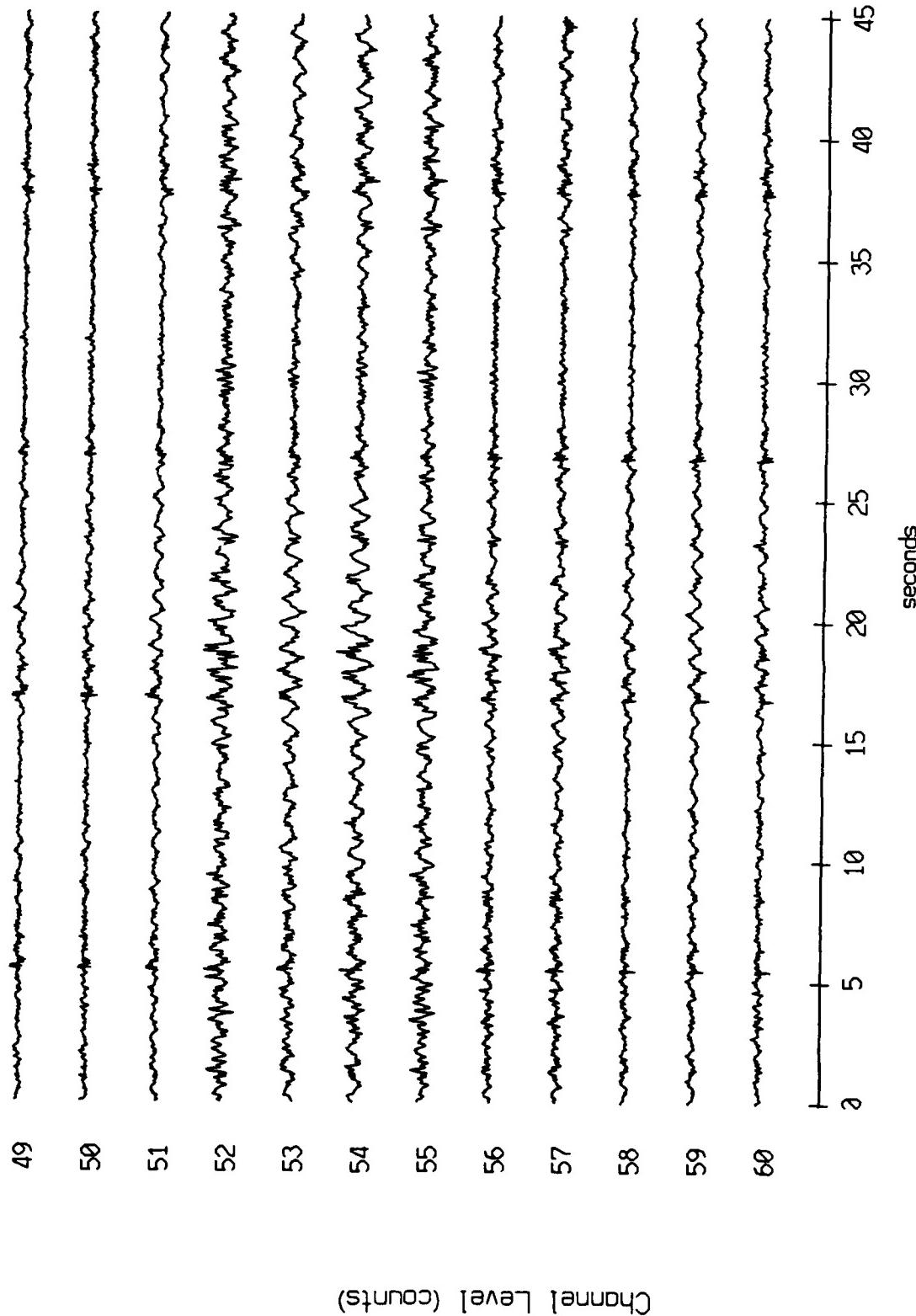


Figure X.17.1e

VLA Tape 453, Sept, 1987 Trip - Time 16:30:00.000 fs = 50 Hz
vertical axis scale is approx. -2000 to 2000 counts

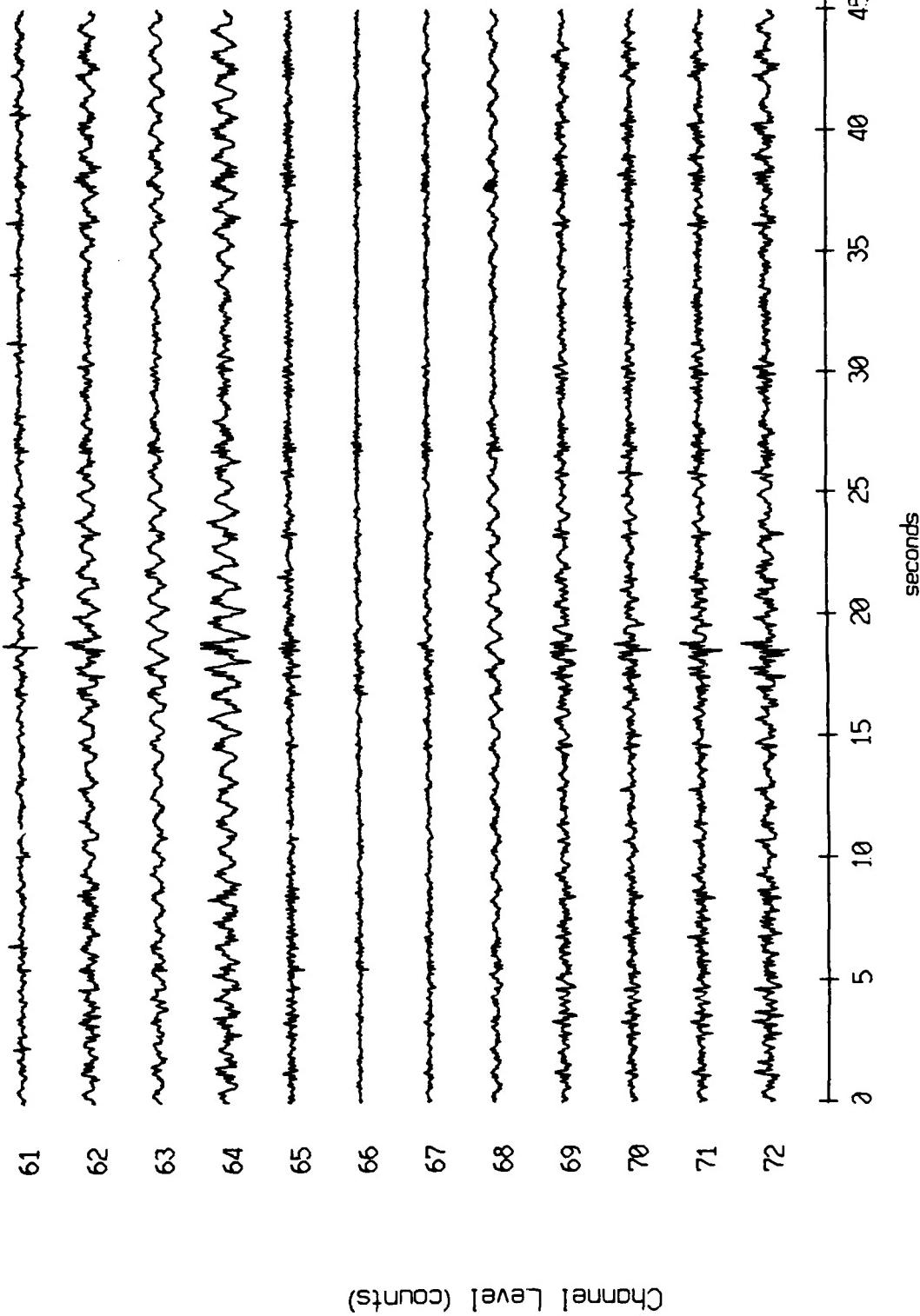


Figure X.17.1f

VLA Tape 453, Sept., 1987 Trip - Time 16:30:00.000 fs = 50 Hz
vertical axis scale is approx. -2000 to 2000 counts

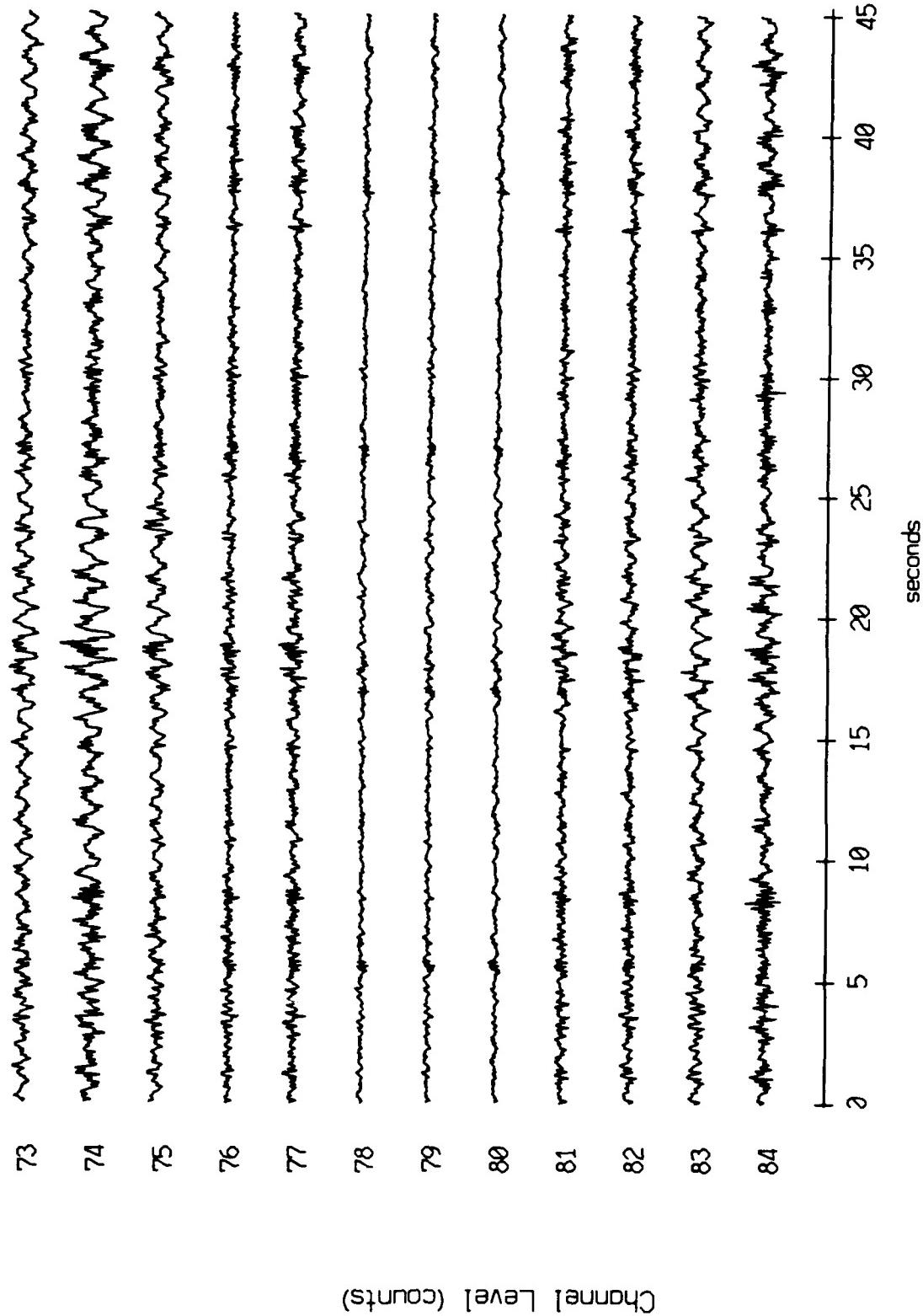


Figure X.17.1g

VLA Tape 453, Sept, 1987 Trip - Time 16:30:00.000 fs = 50 Hz
vertical axis scale is approx. -2000 to 2000 counts

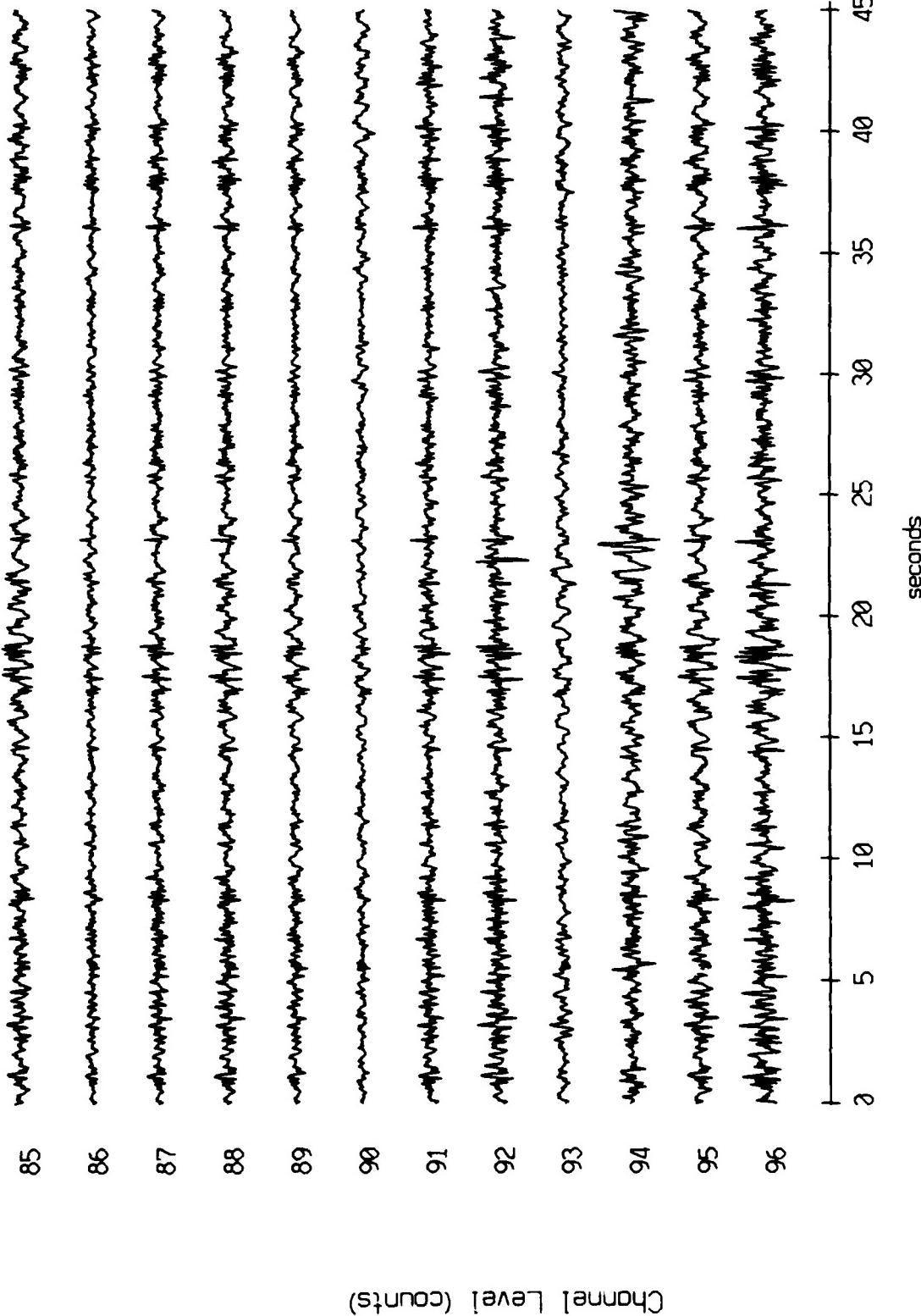


Figure X.17.1h

VLA Tape 453, Sept, 1987 Trip - Time 16:30:00.000 $f_s = 50$ Hz
vertical axis scale is approx. -2000 to 2000 counts

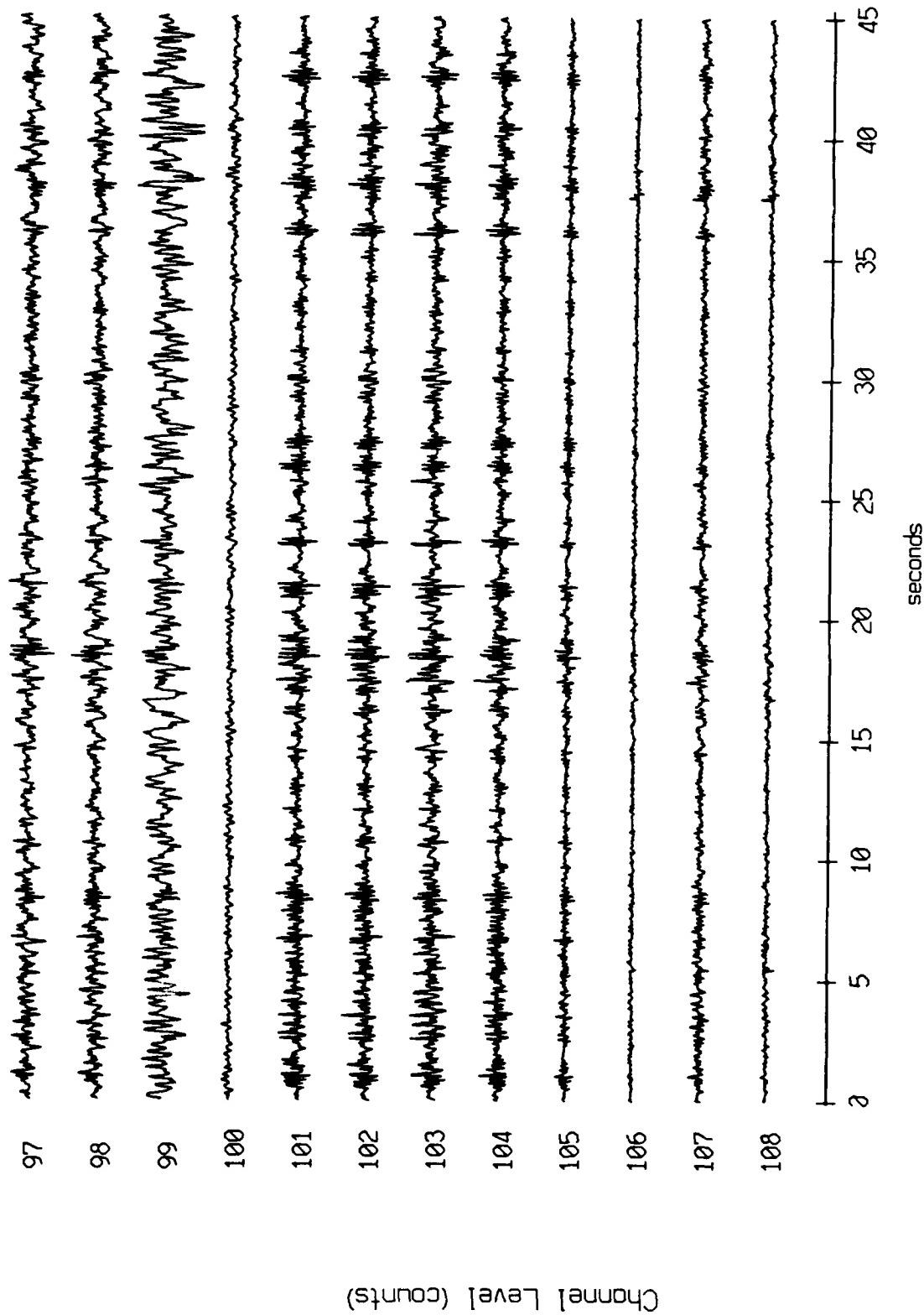


Figure X.17.1i

VLA Tape 453, Sept, 1987 Trip - Time 16:30:00.000 $f_s = 50$ Hz
vertical axis scale is approx. -2000 to 2000 counts

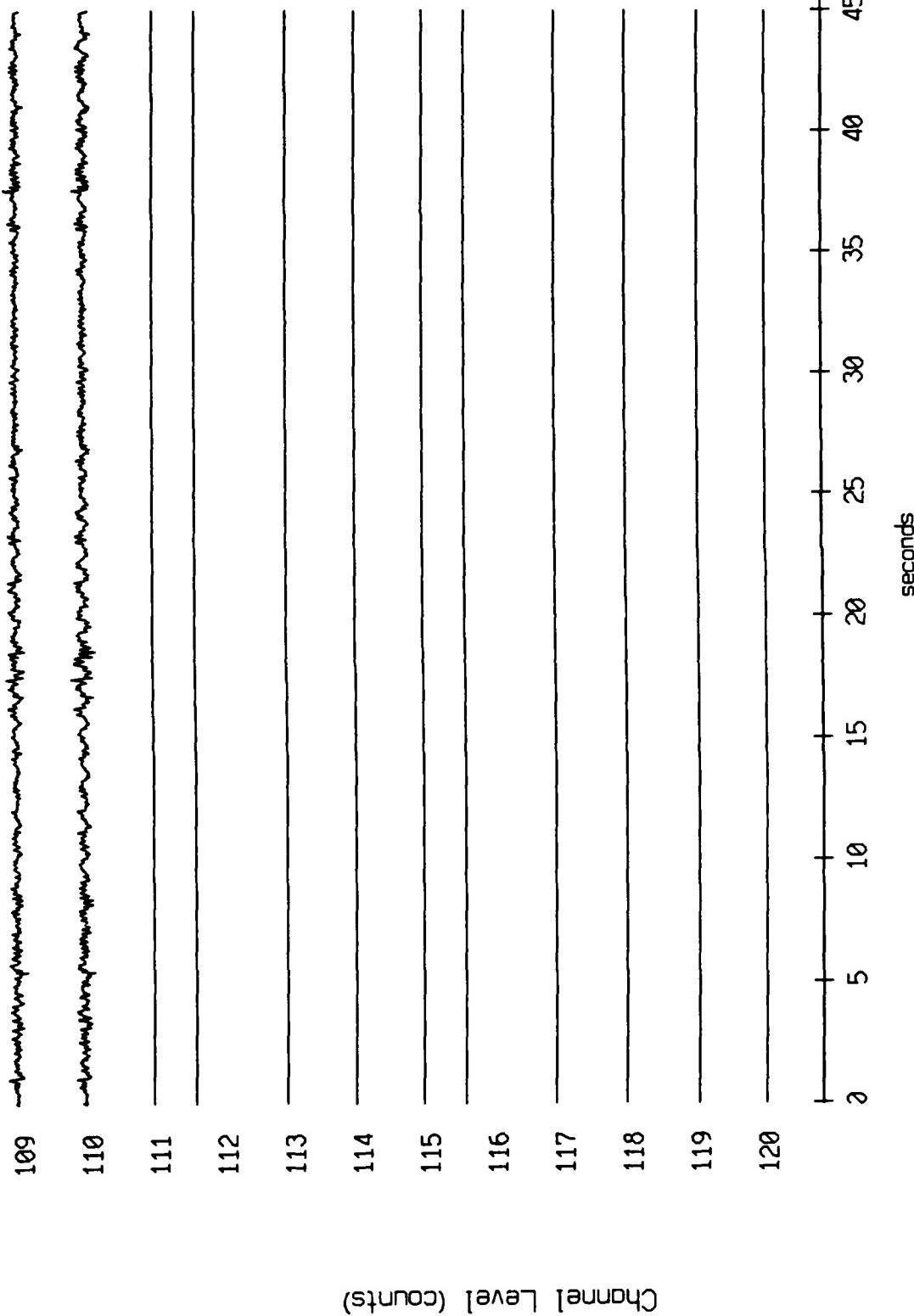


Figure X.17.1j

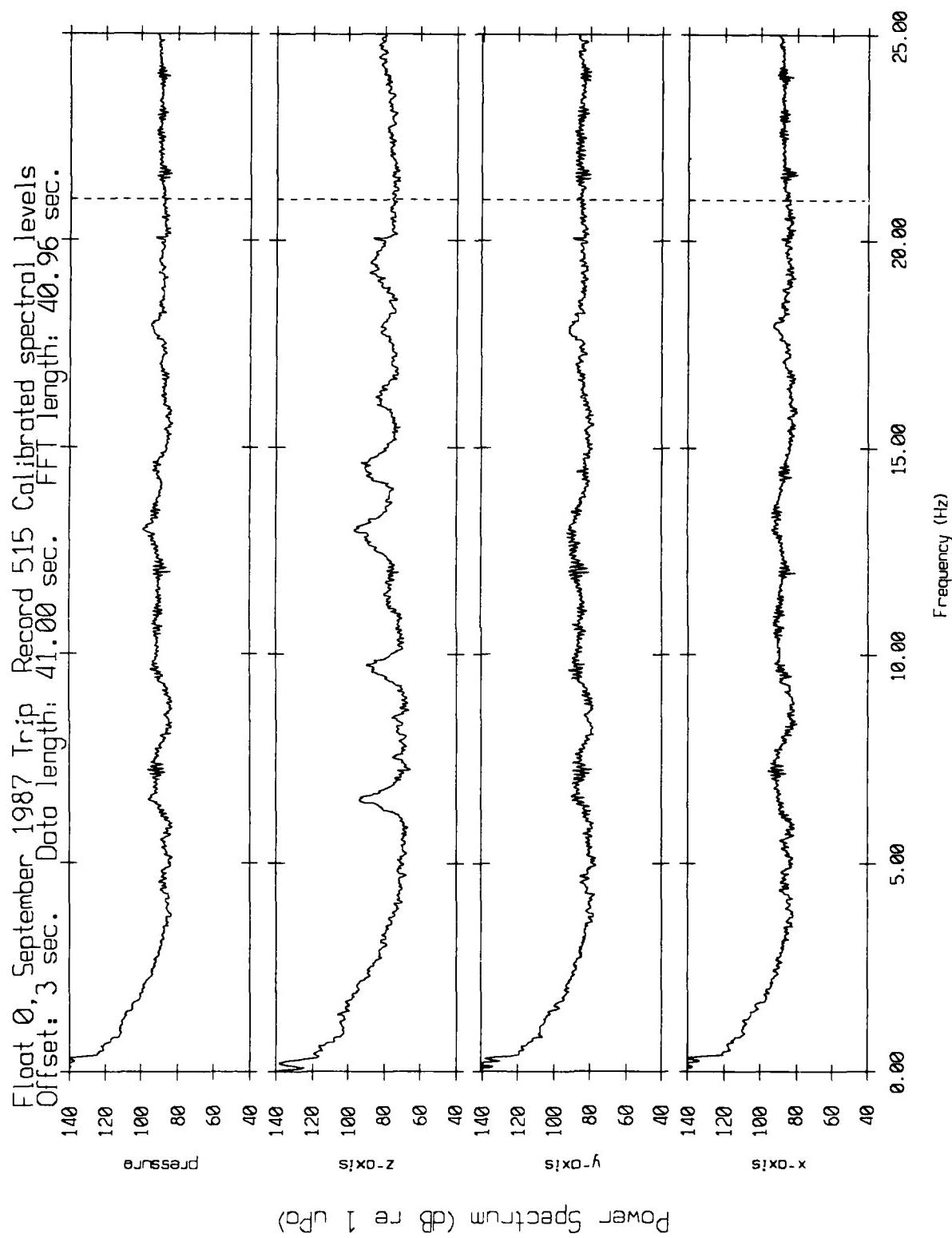


Figure XI.1a

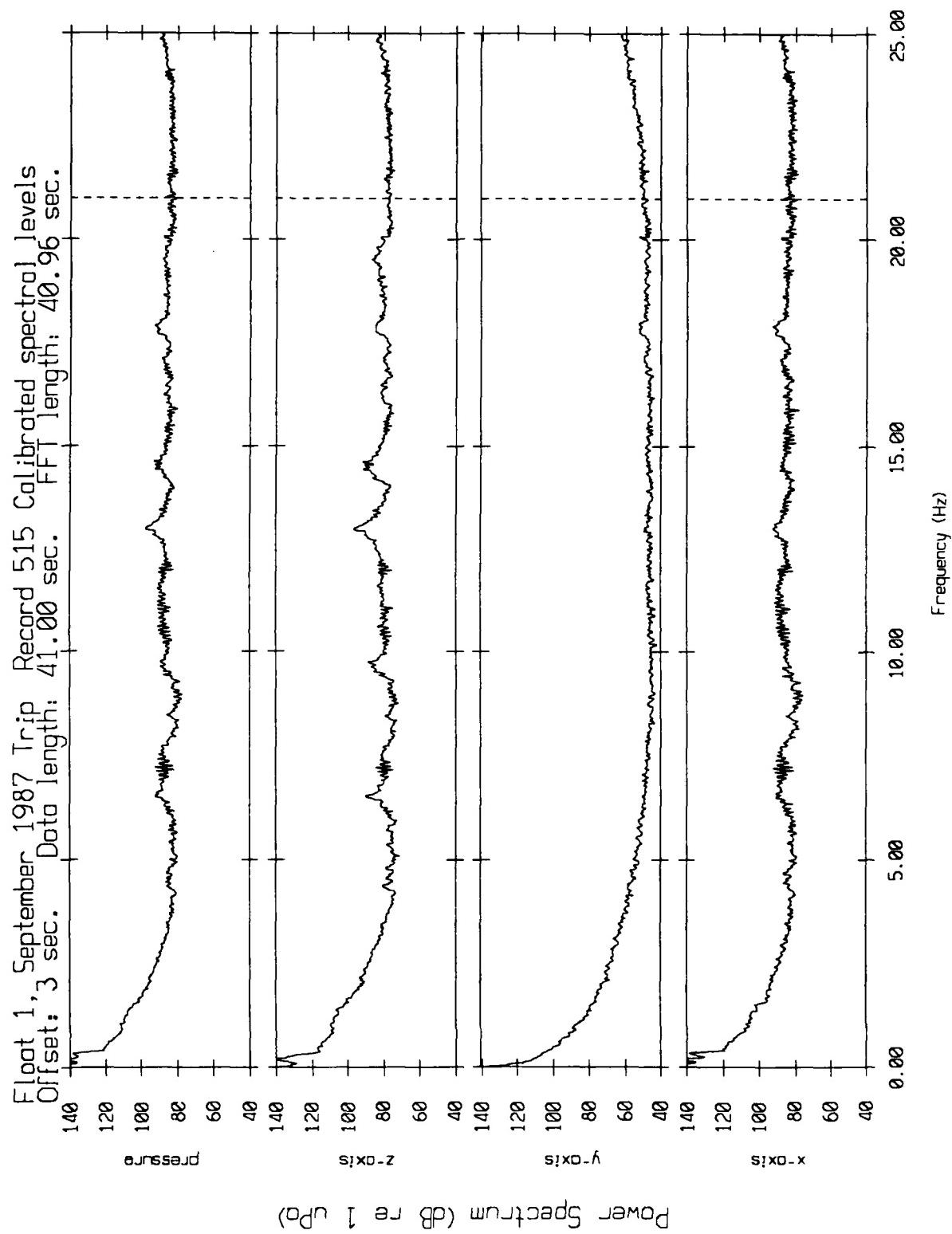


Figure XI.1b

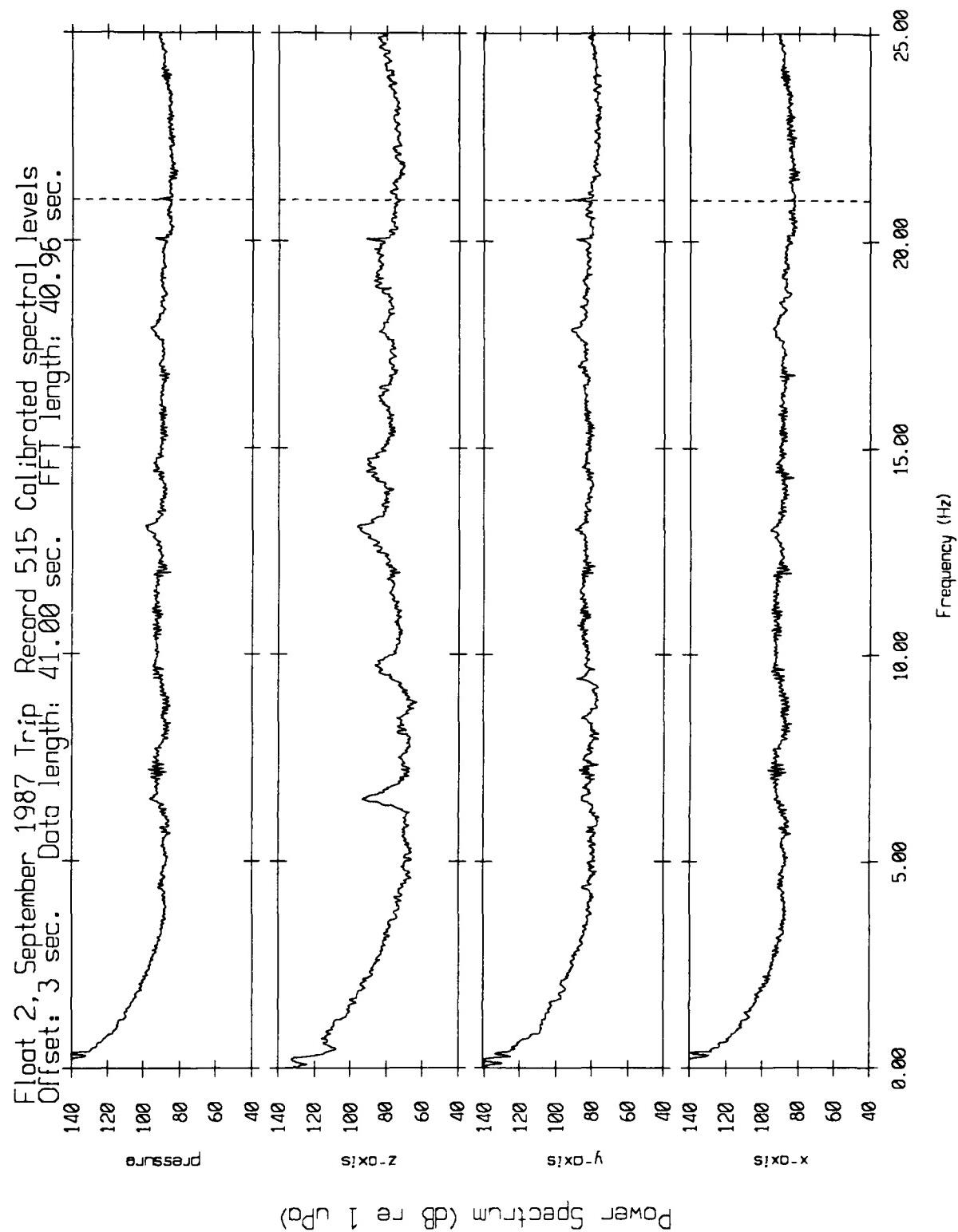


Figure XI.1c

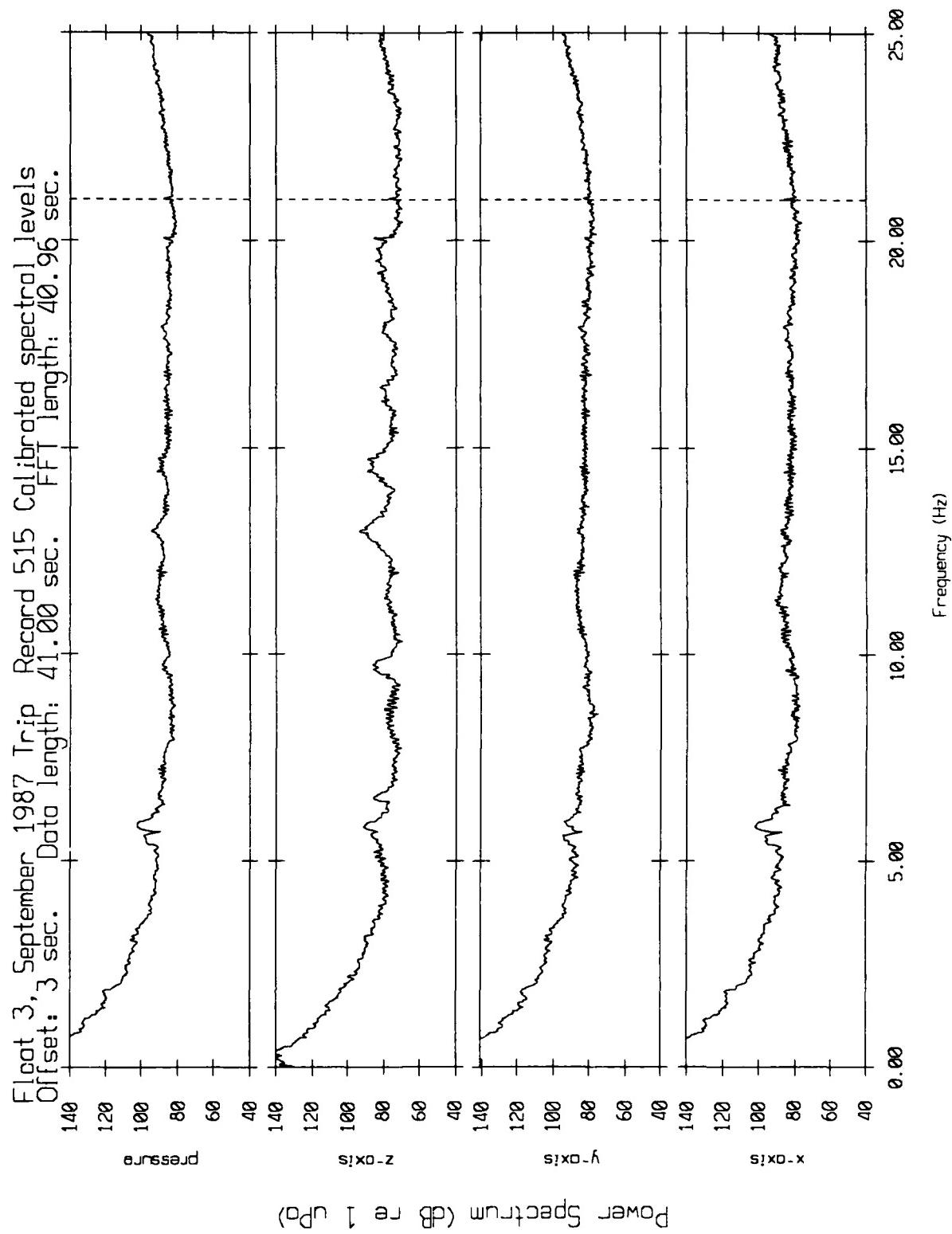


Figure XI.1d

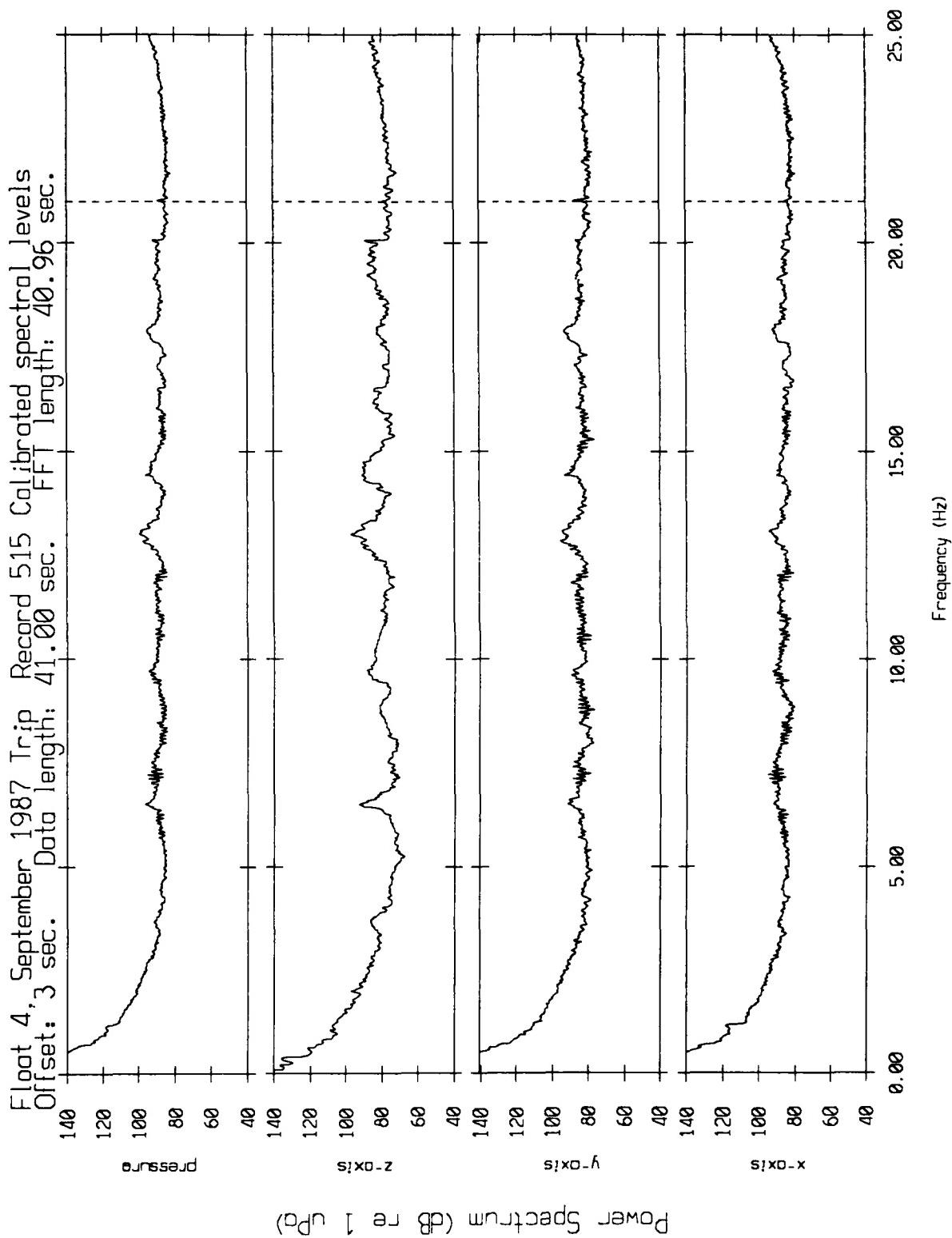


Figure XI.1e

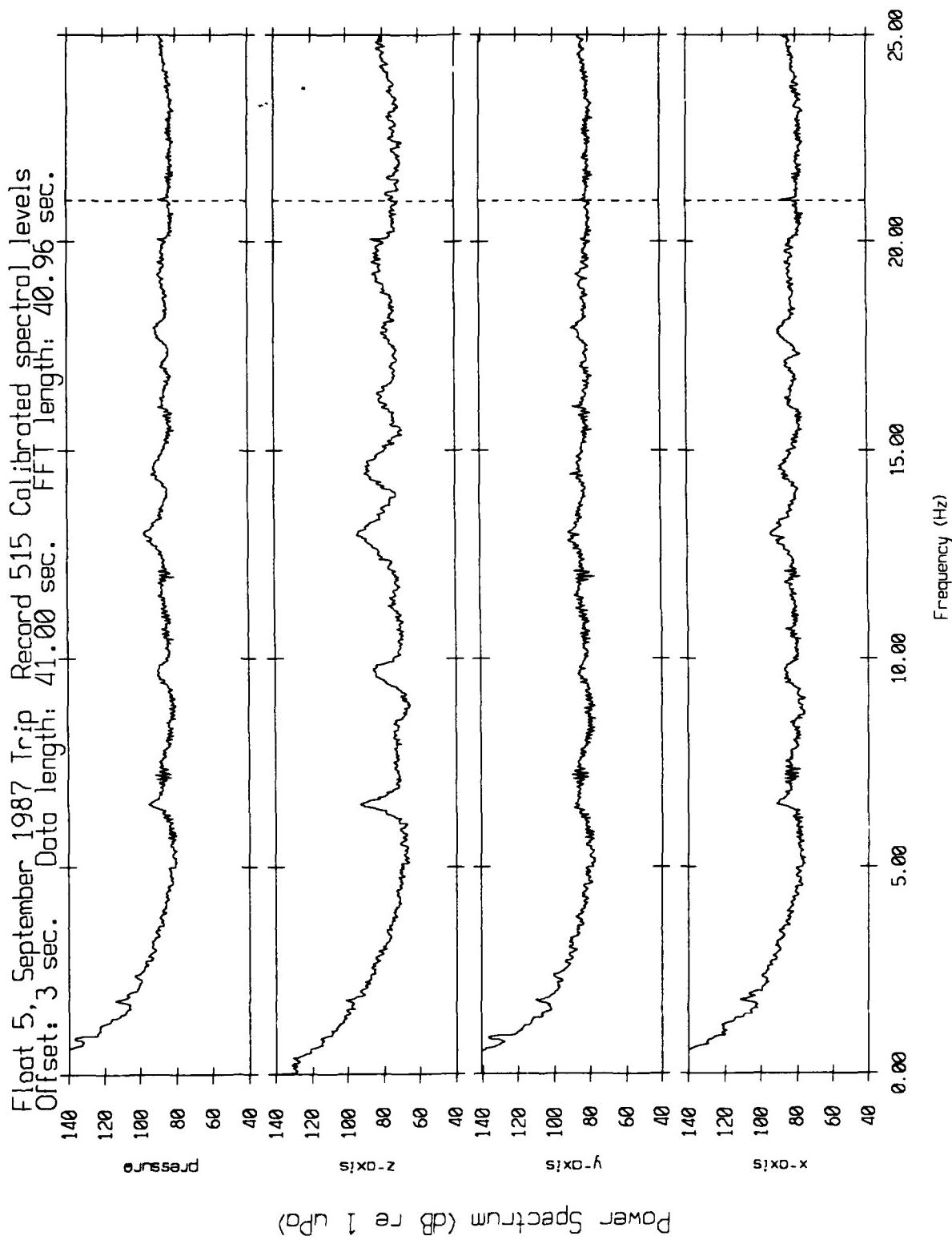


Figure XI.1f

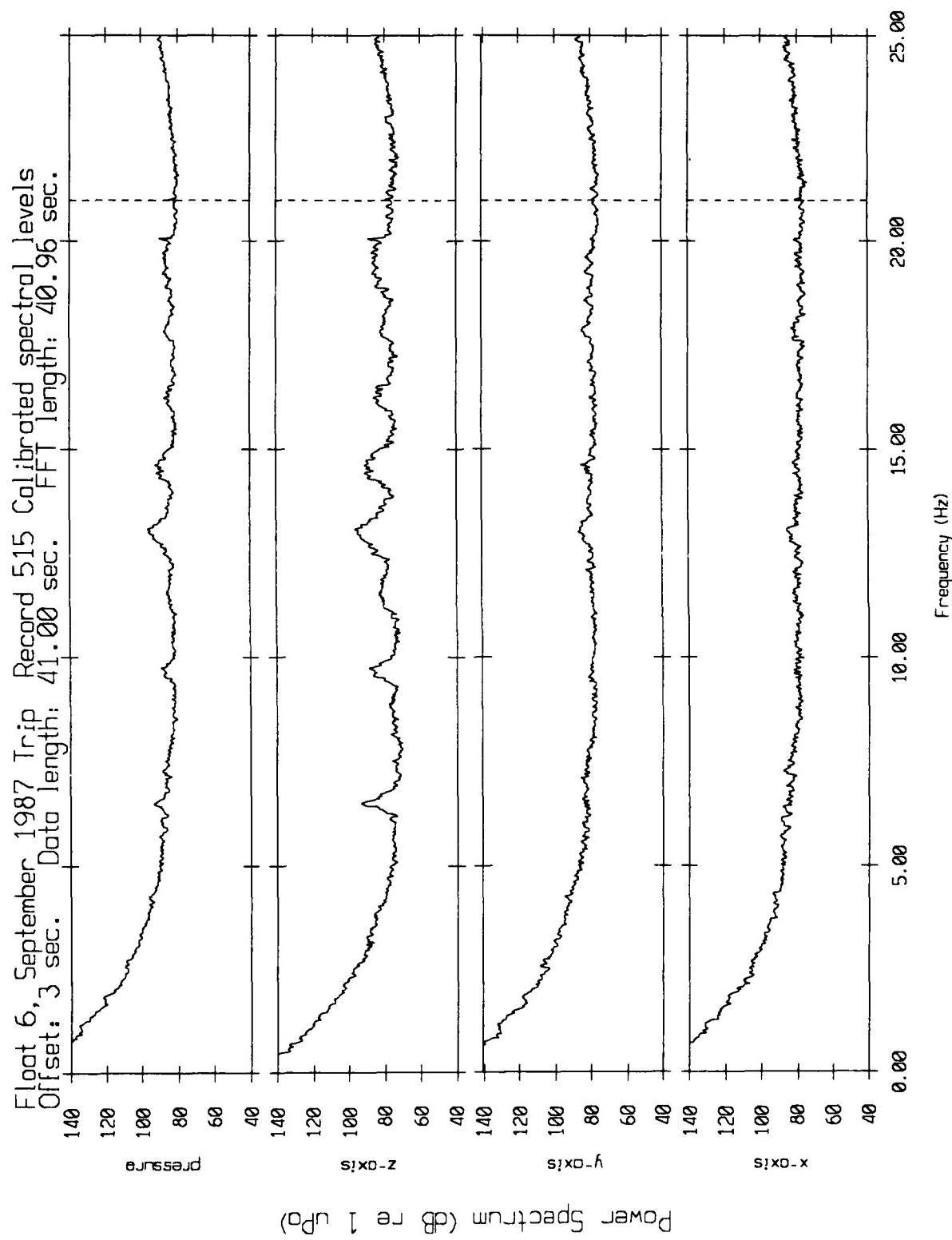


Figure XI.1g

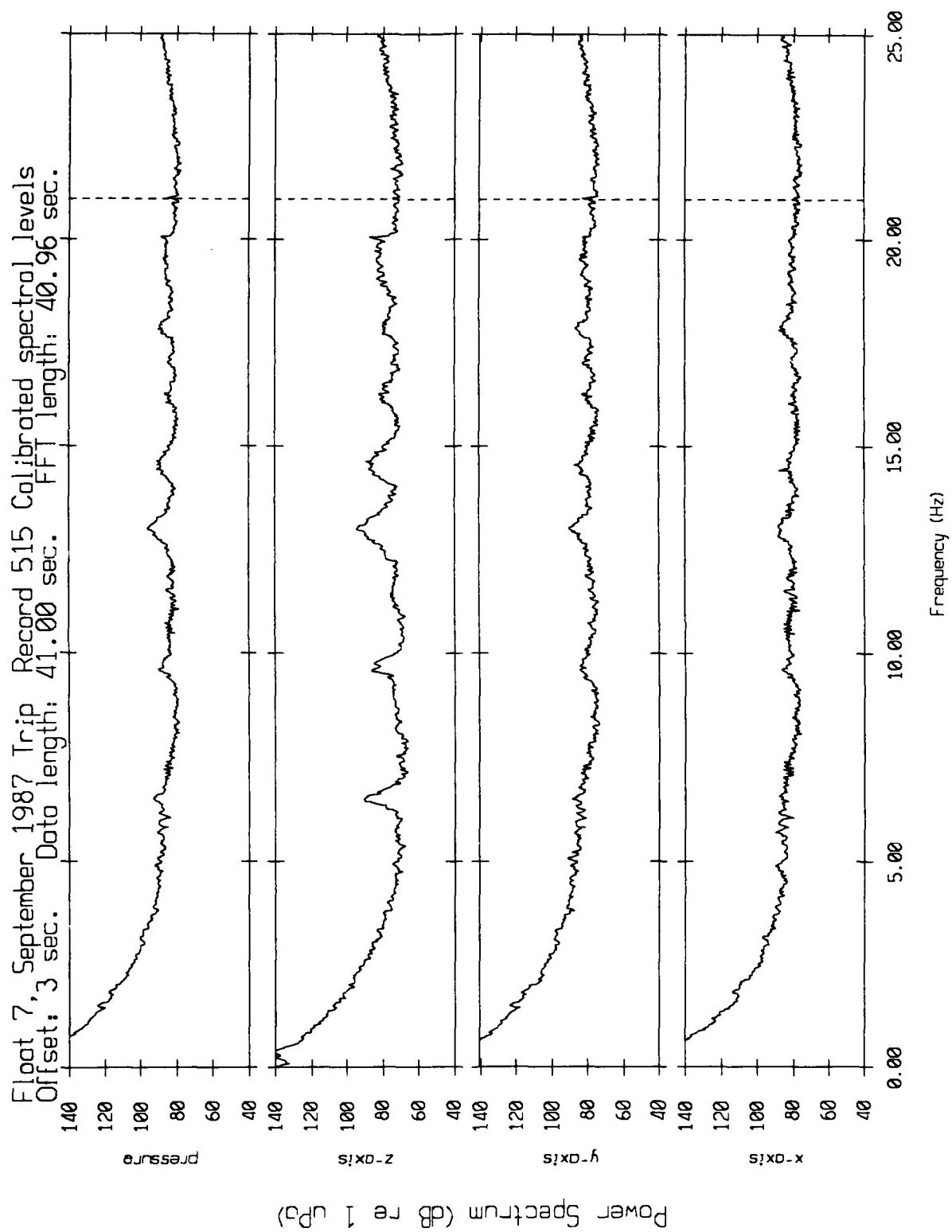


Figure XI.1h

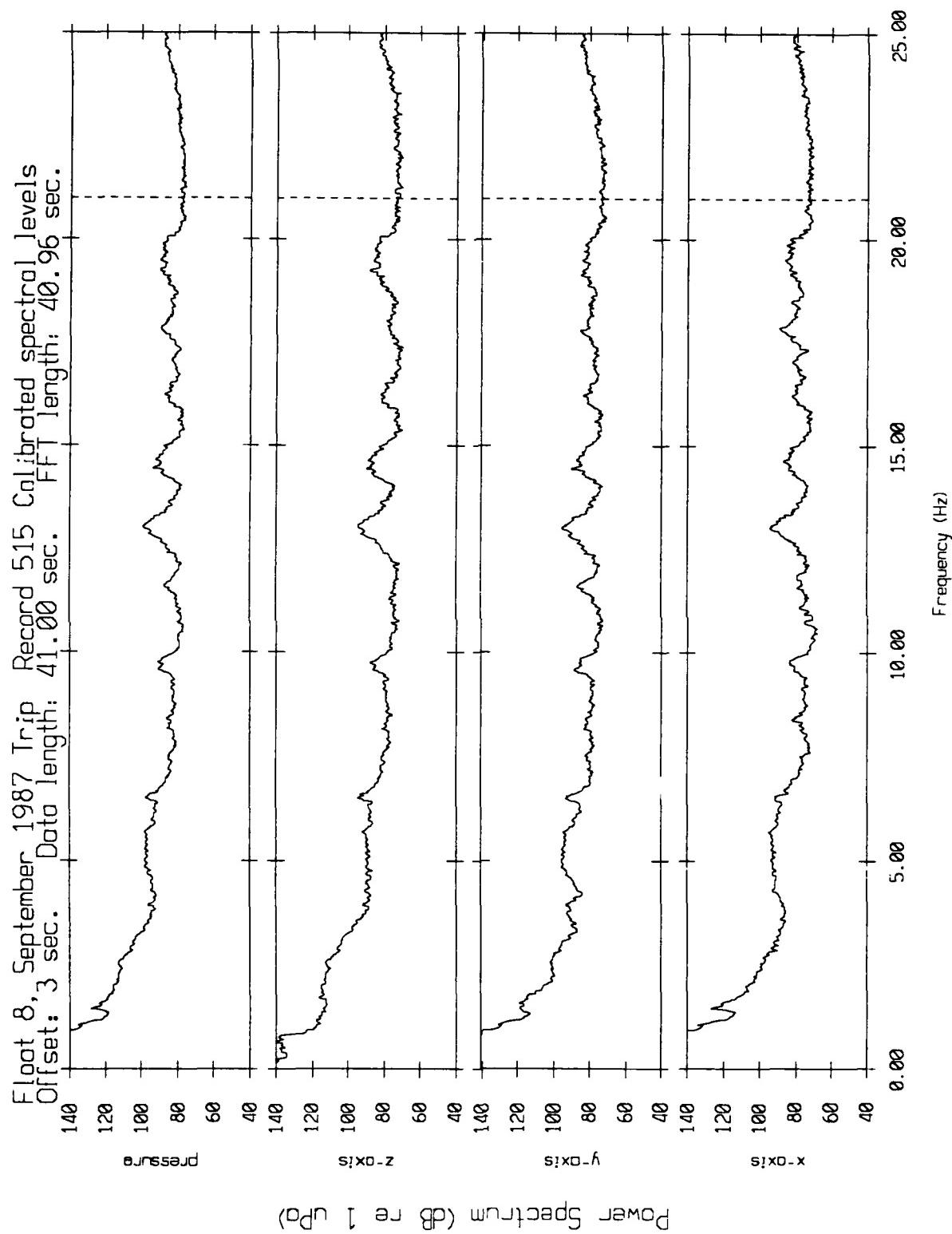


Figure XI.1i

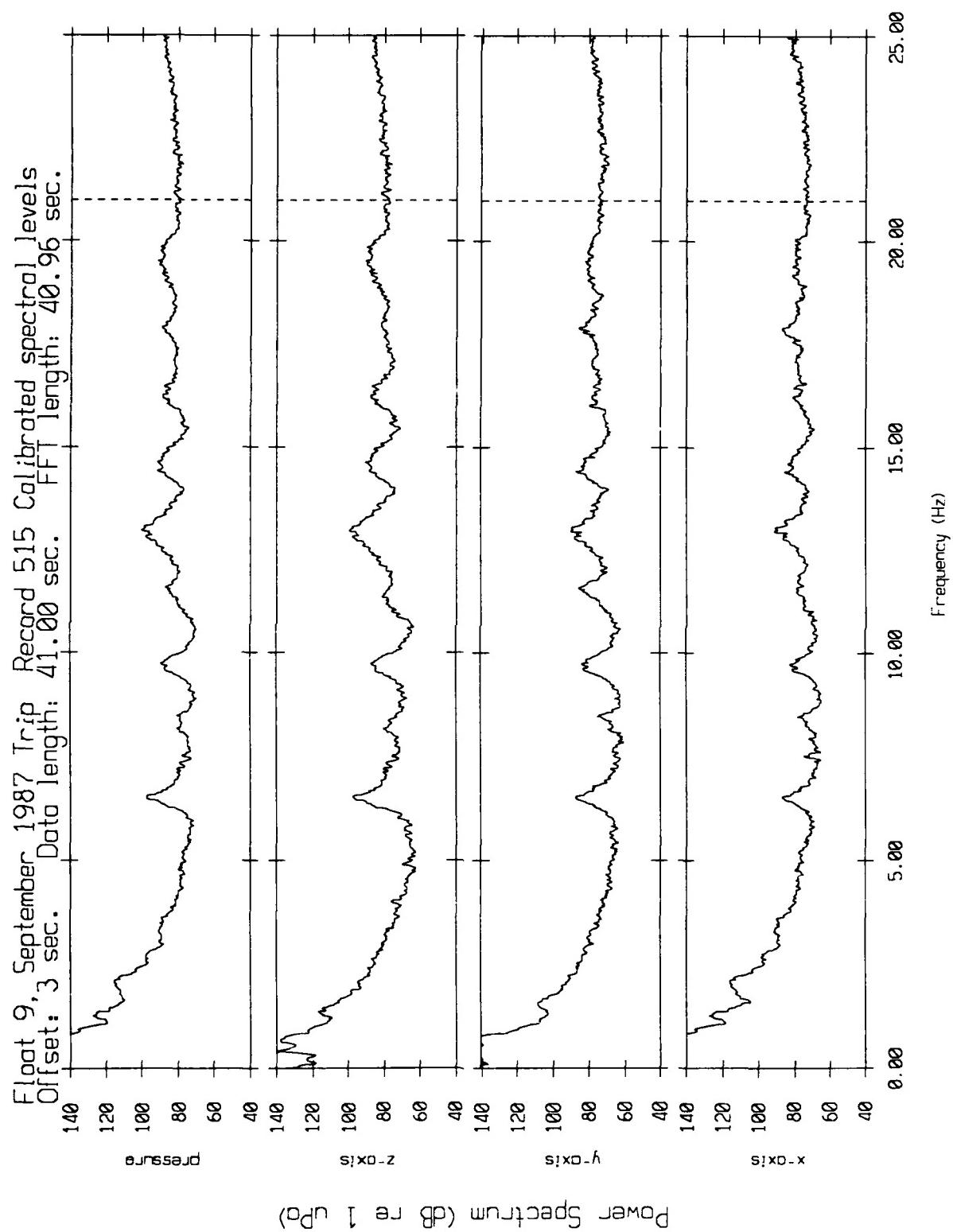


Figure XI.1j

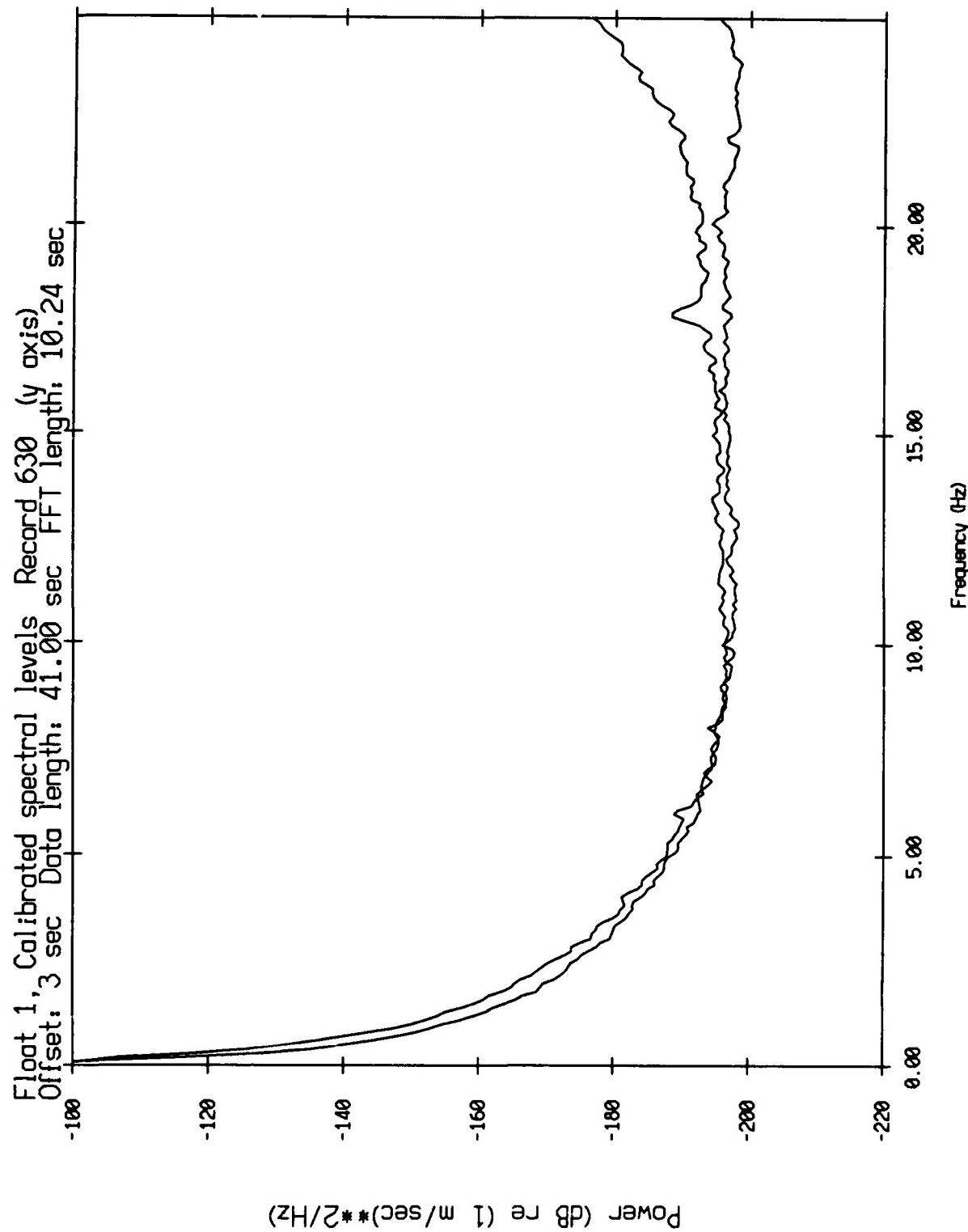


Figure XI.2

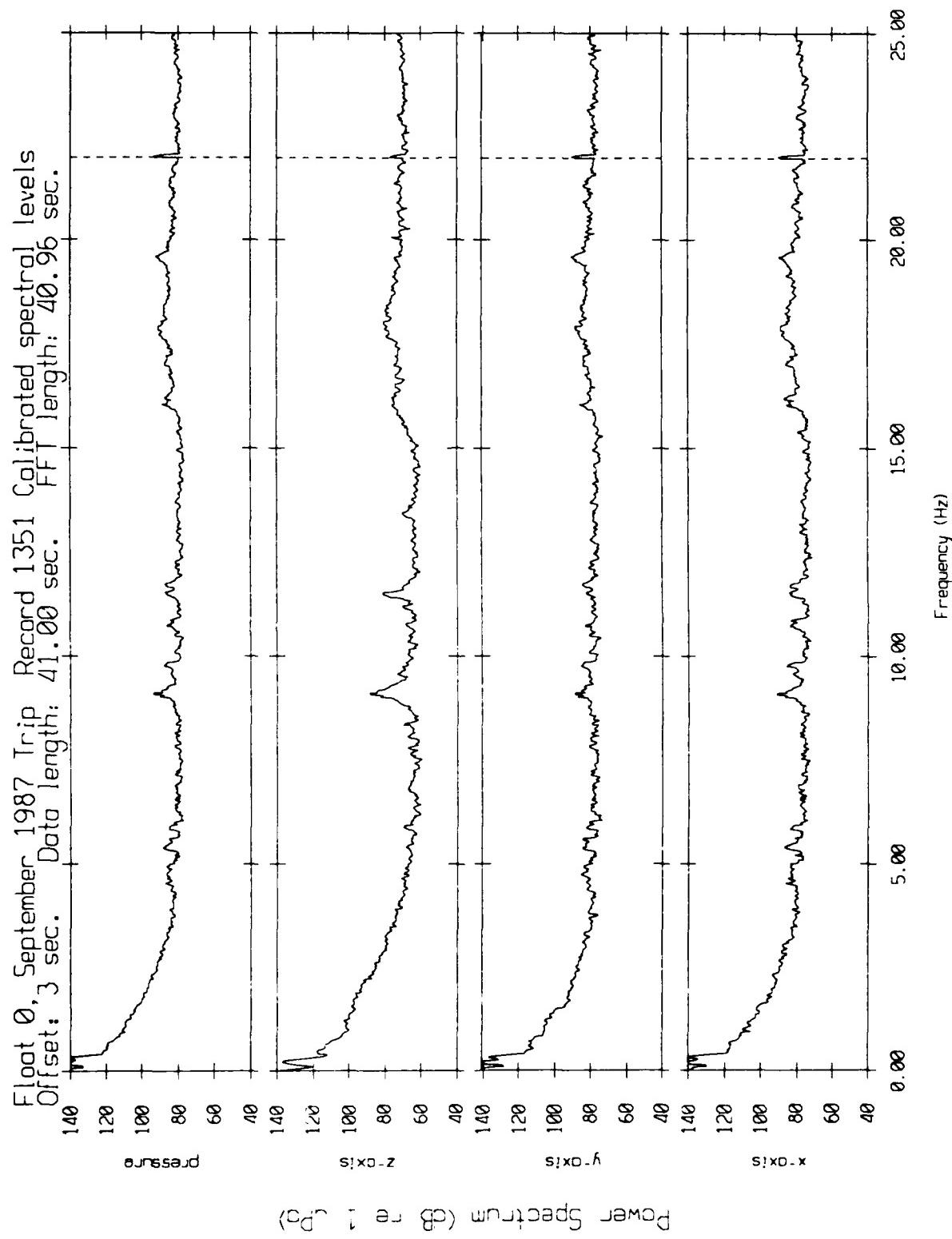


Figure XI.3a

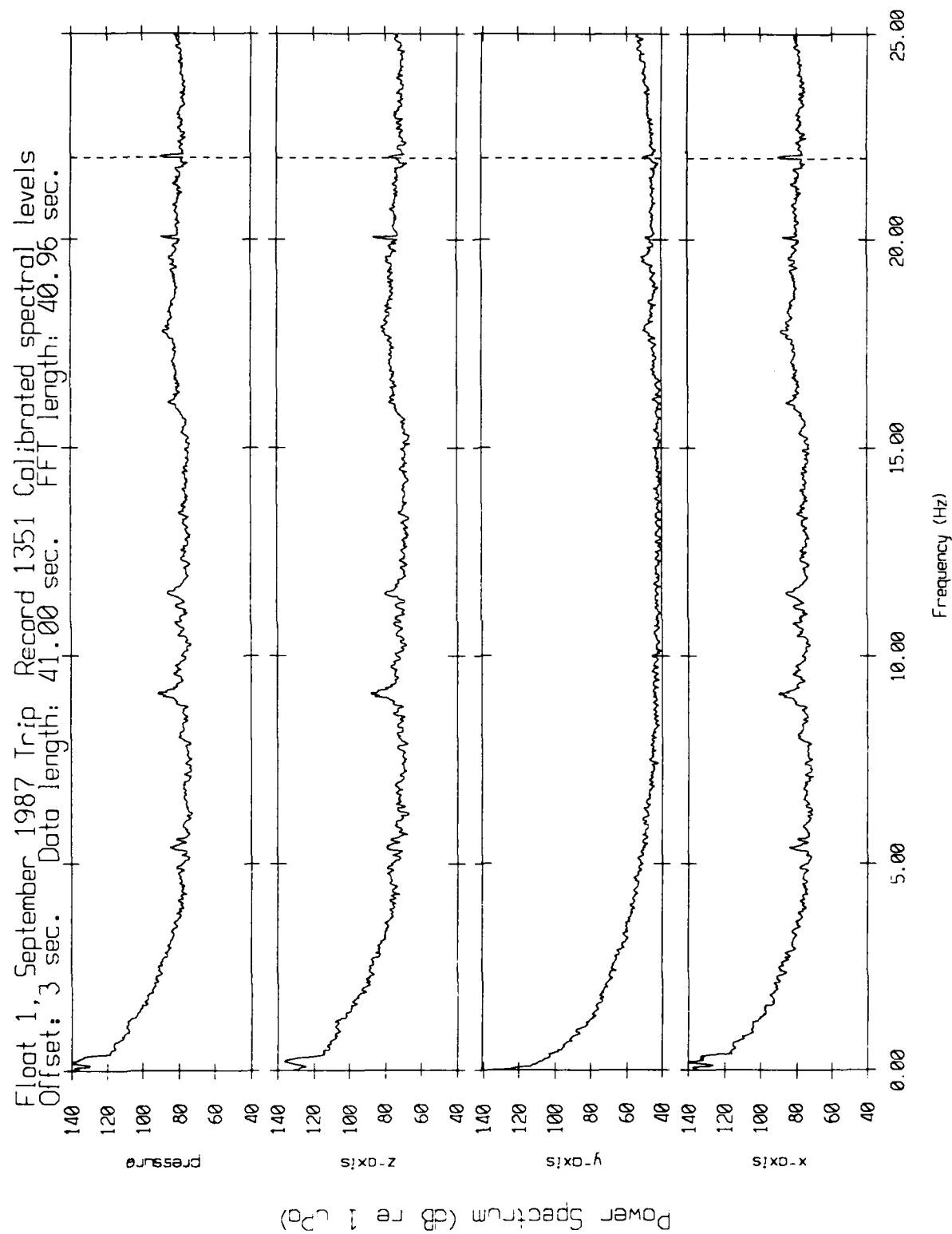


Figure XI.3b

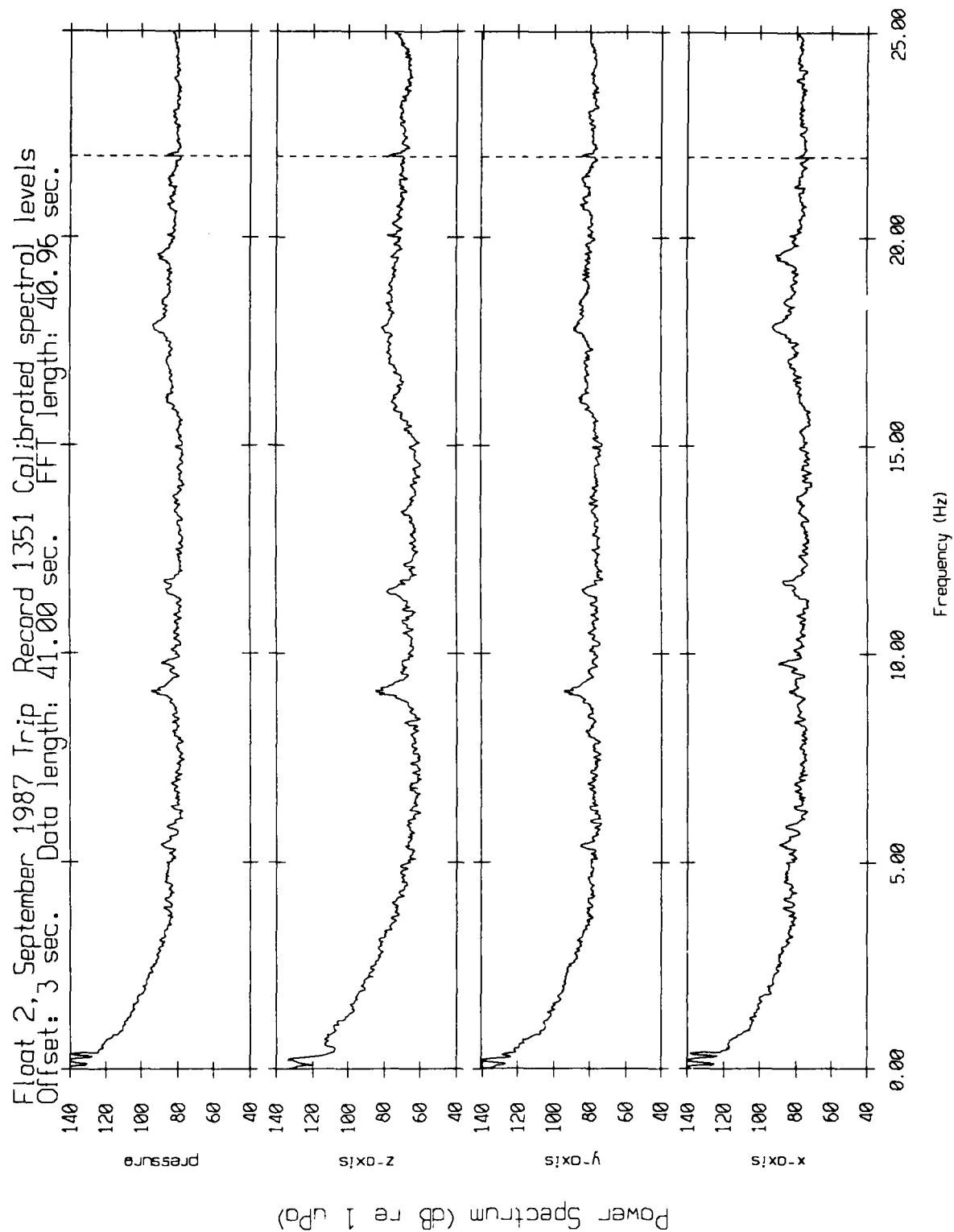


Figure XI.3c

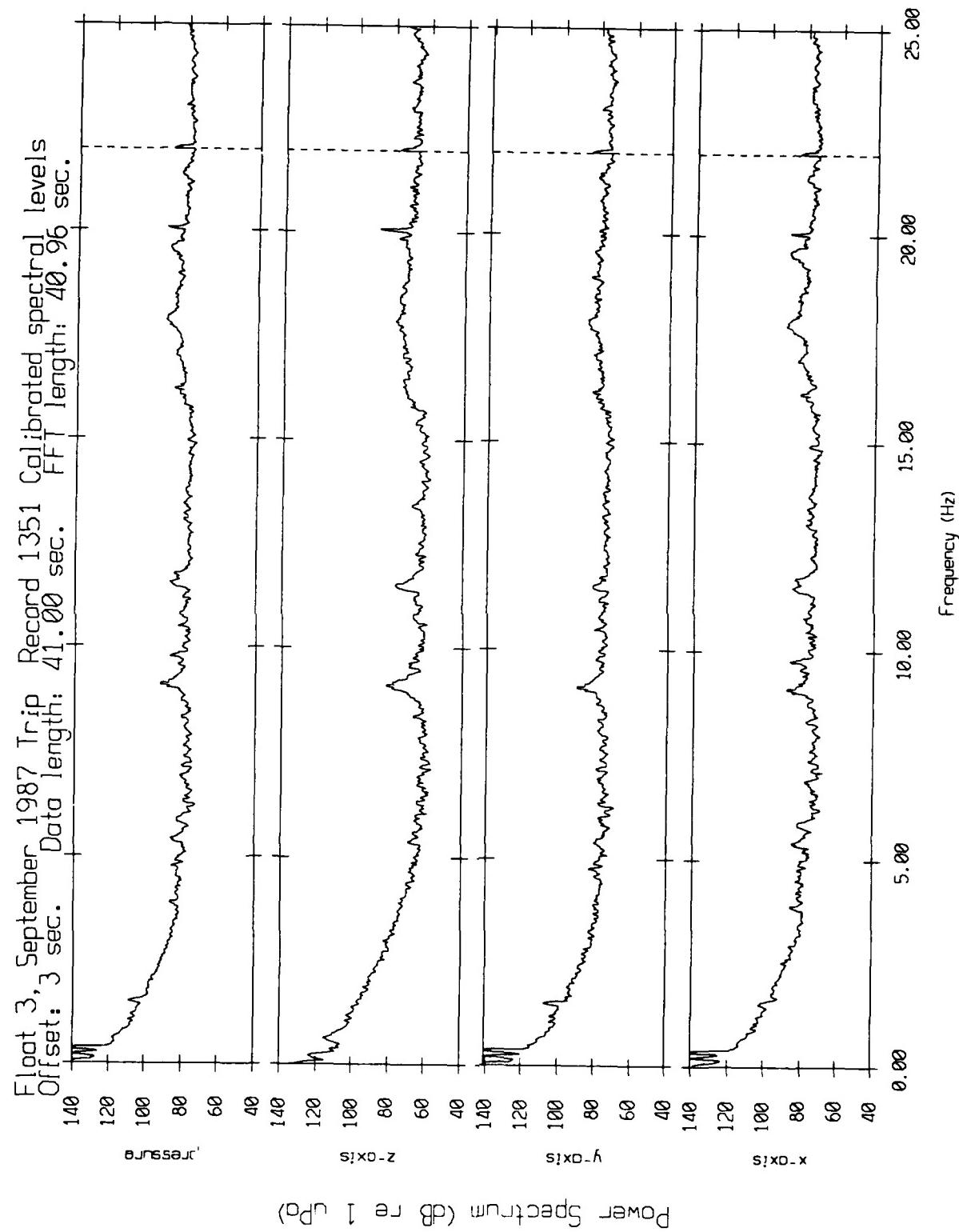


Figure XI.3d

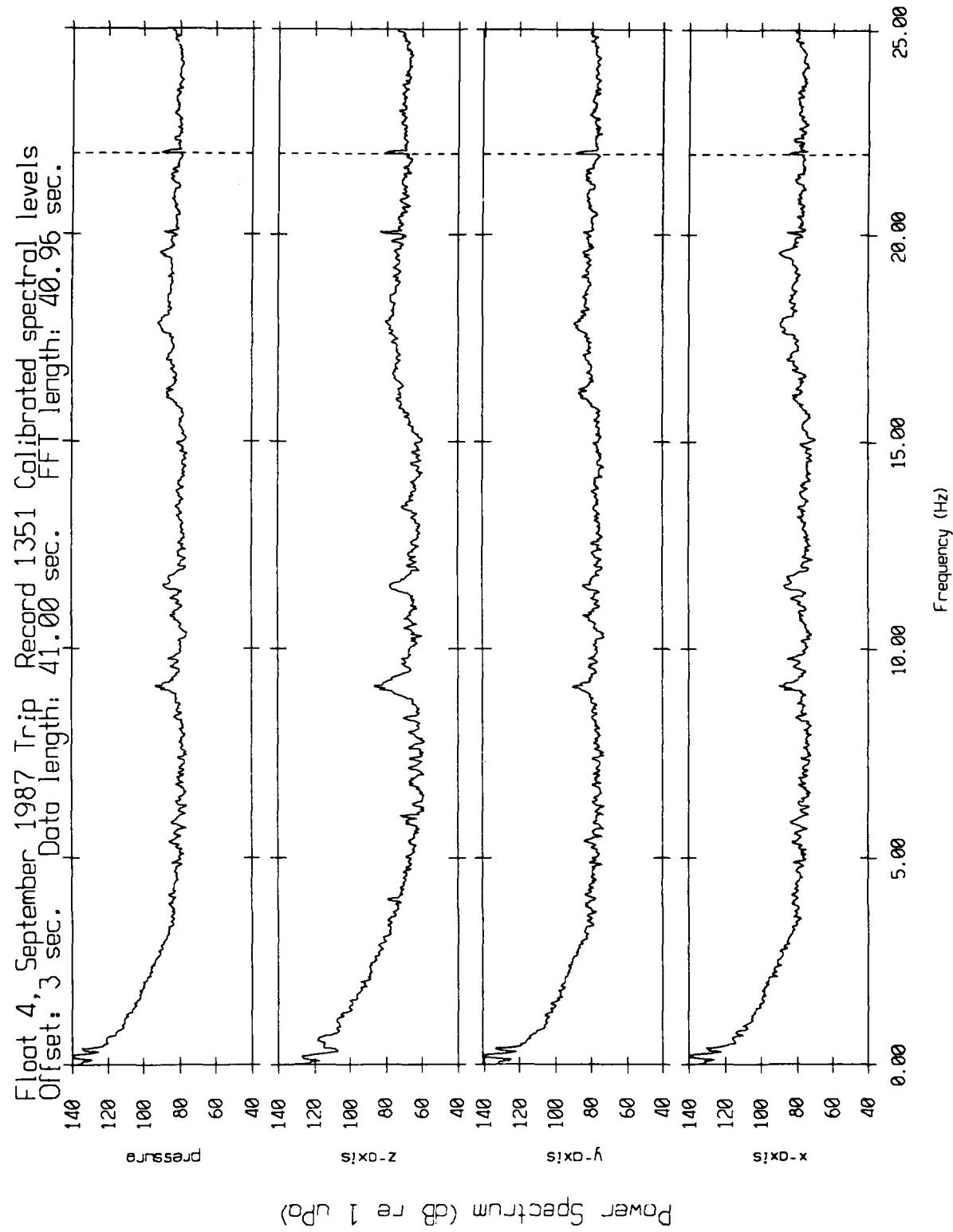


Figure XI.3e

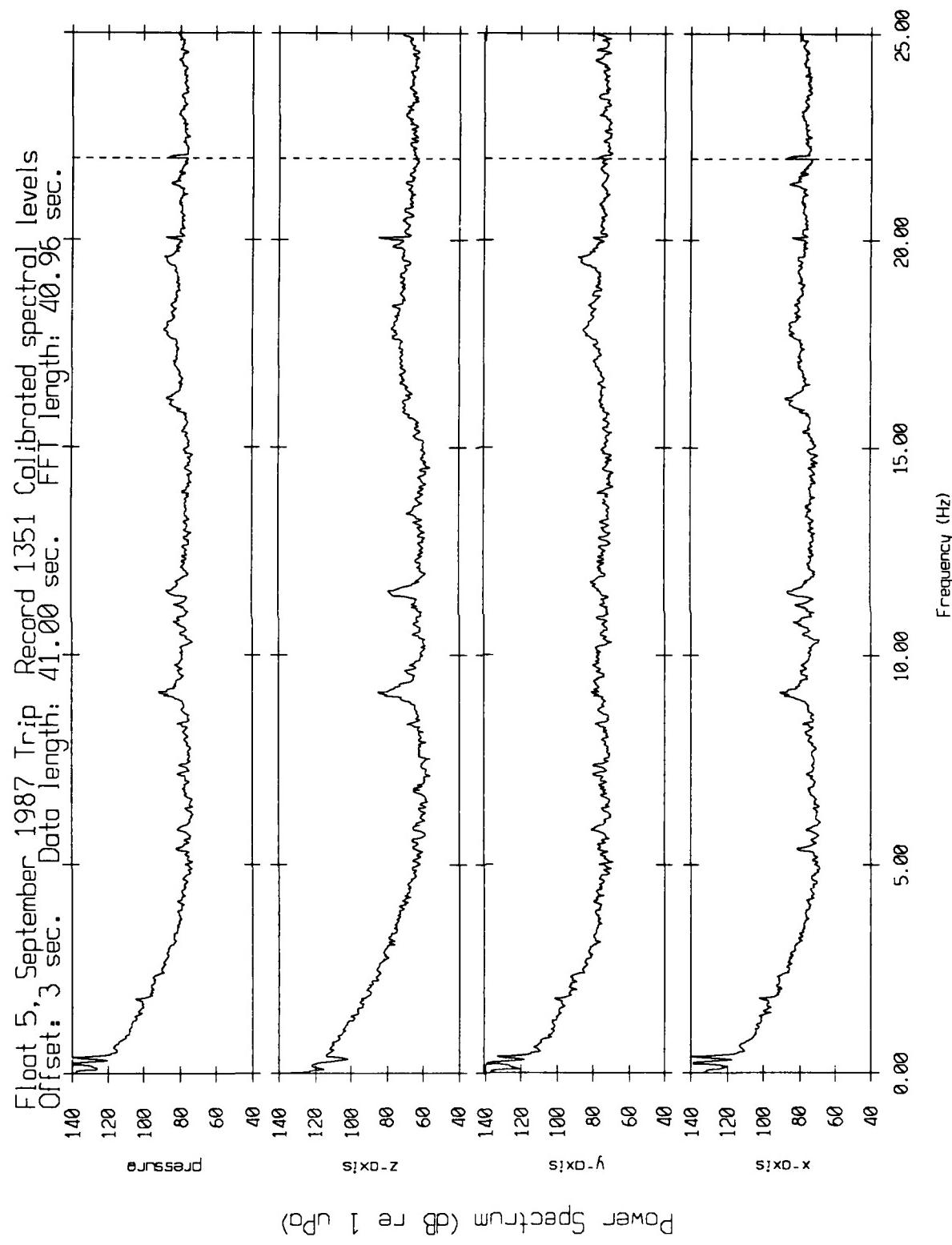


Figure XI.3f

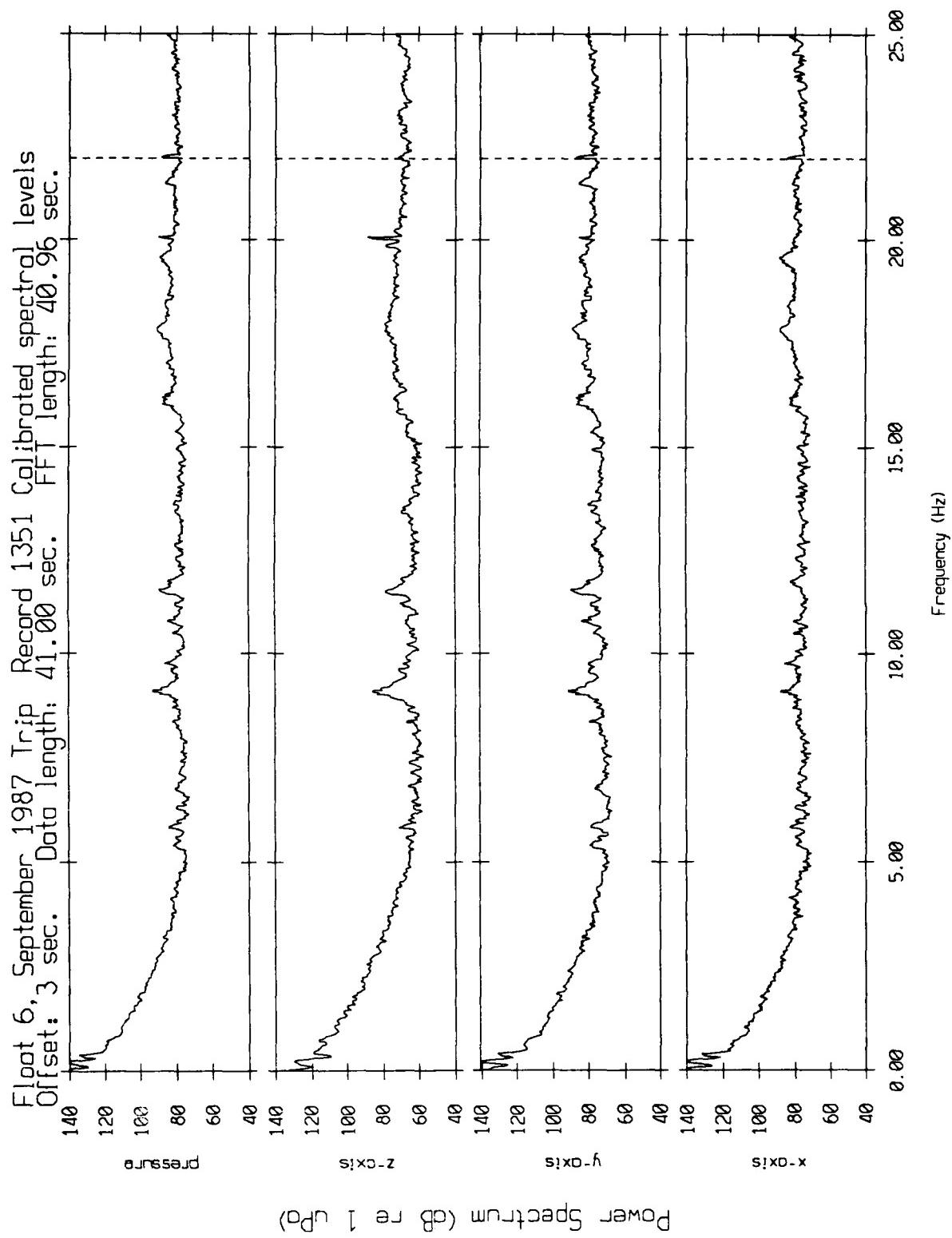


Figure XI.3g

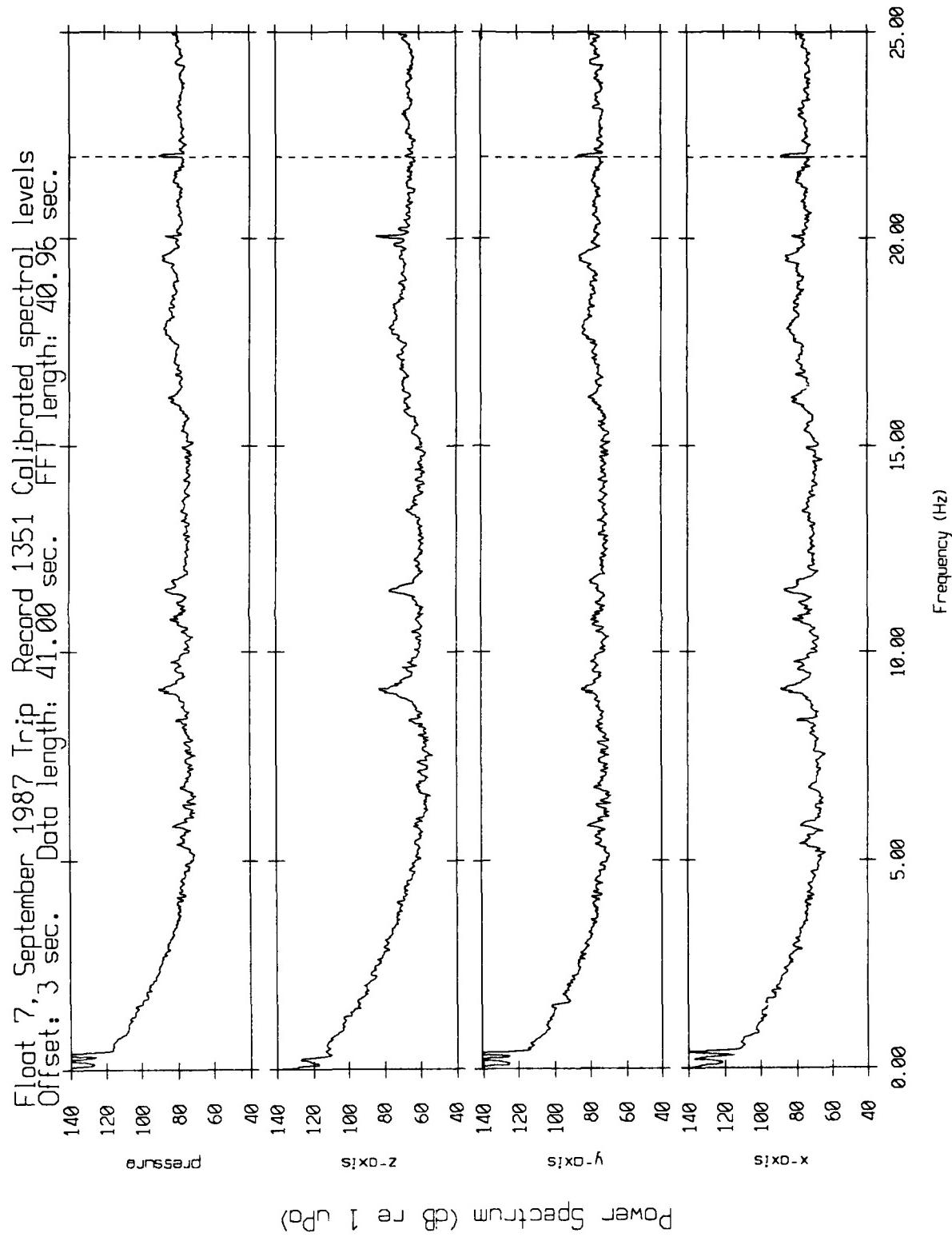


Figure XI.3h

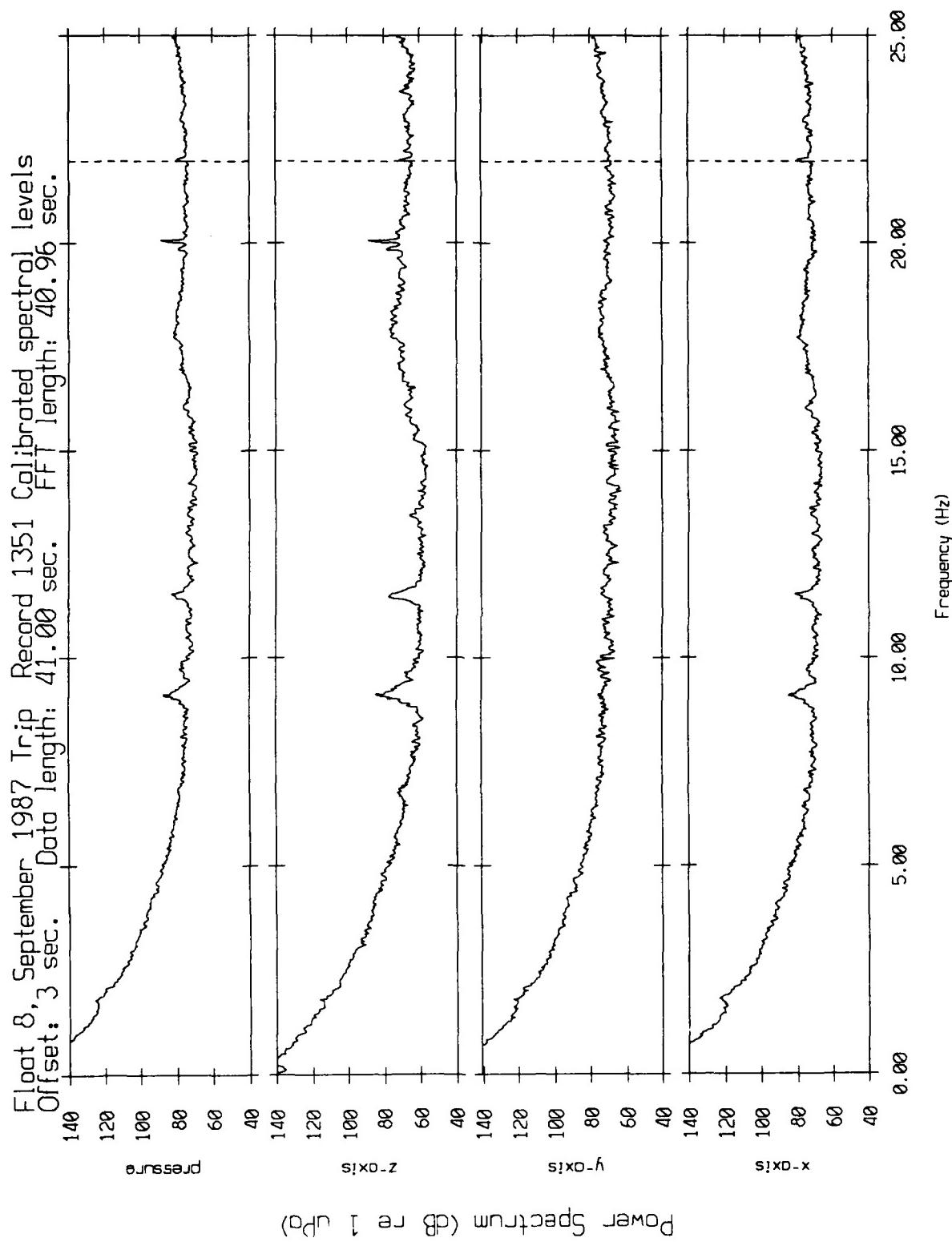


Figure XI.3i

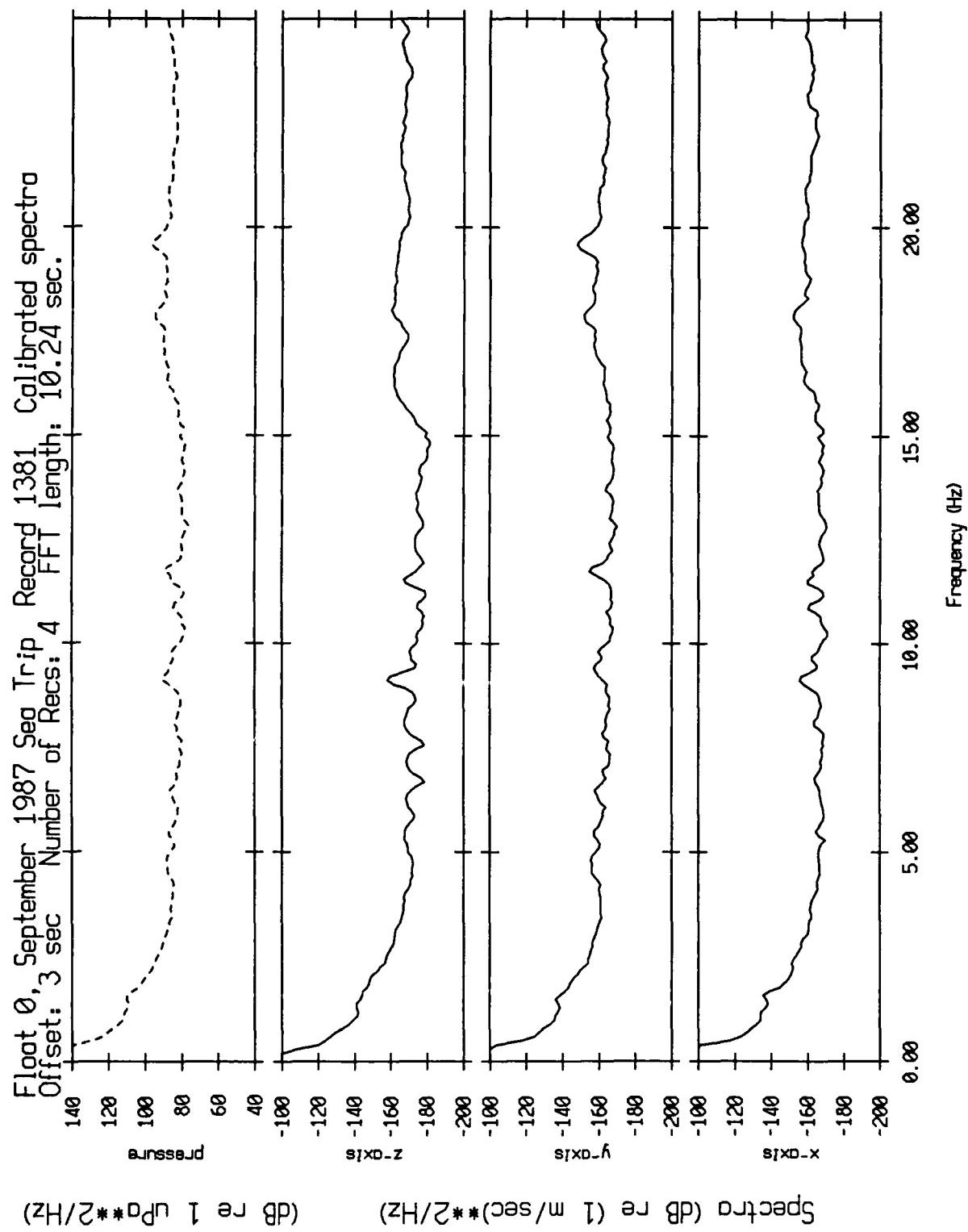


Figure XI.4a

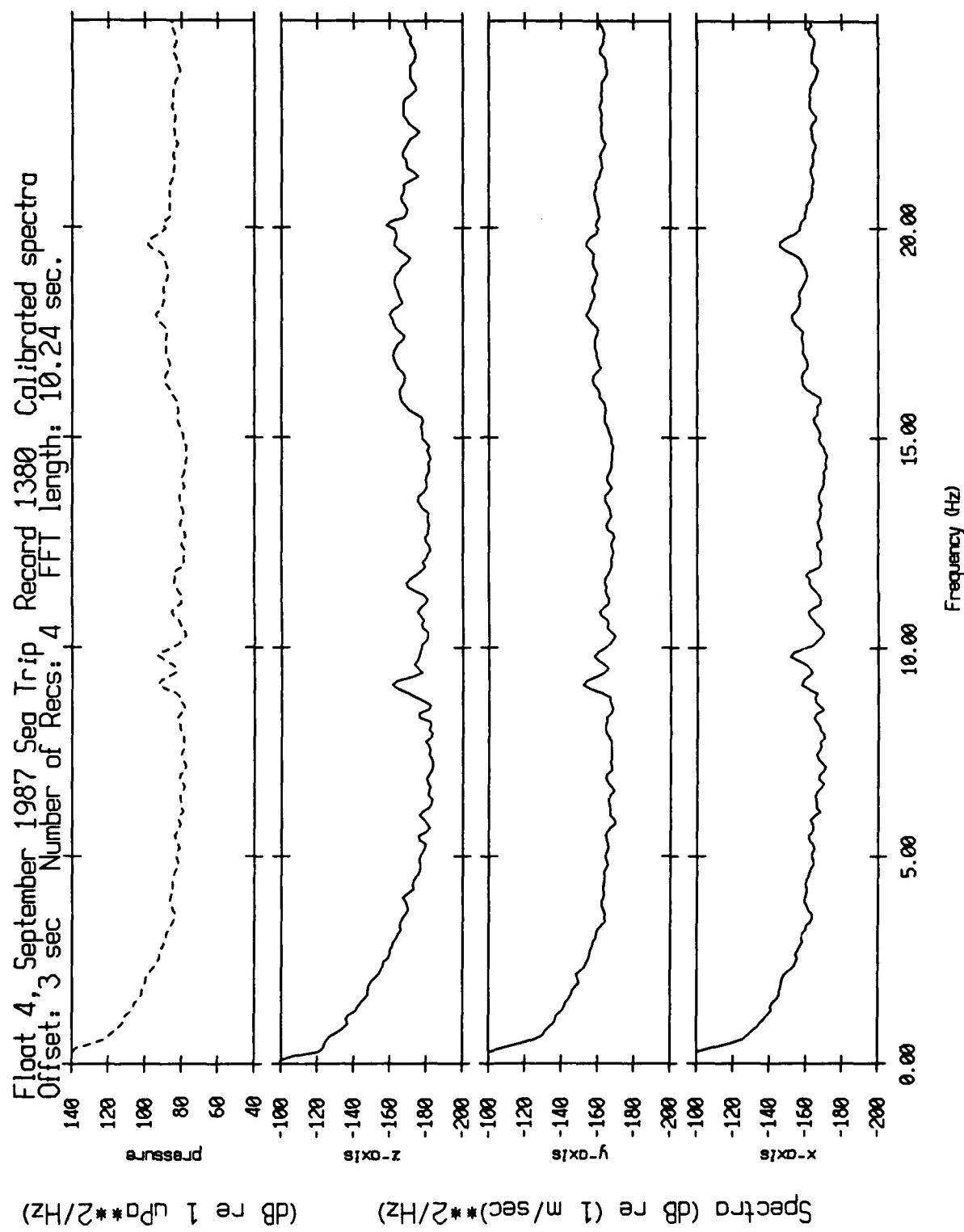


Figure XI.4b

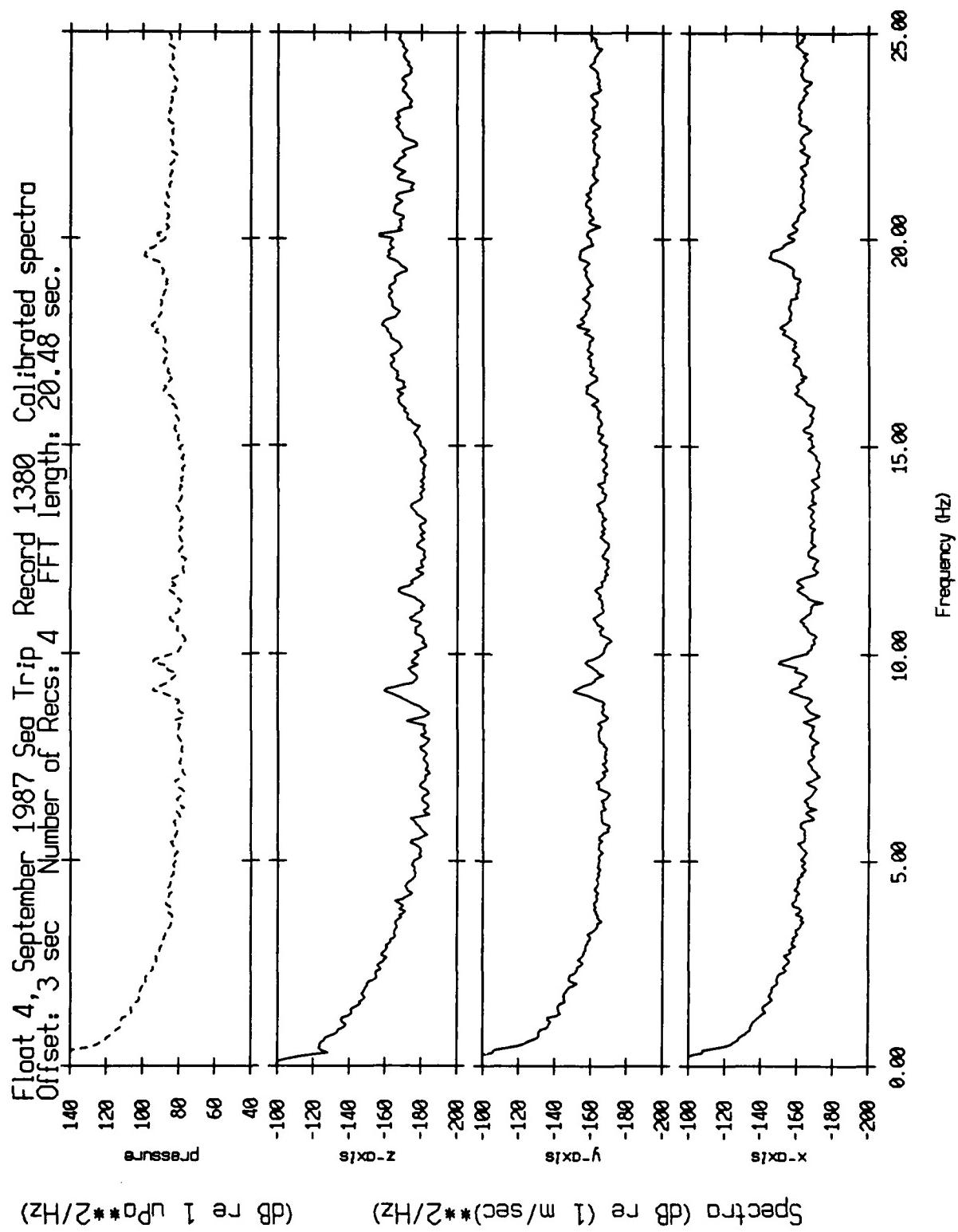


Figure XI.4c

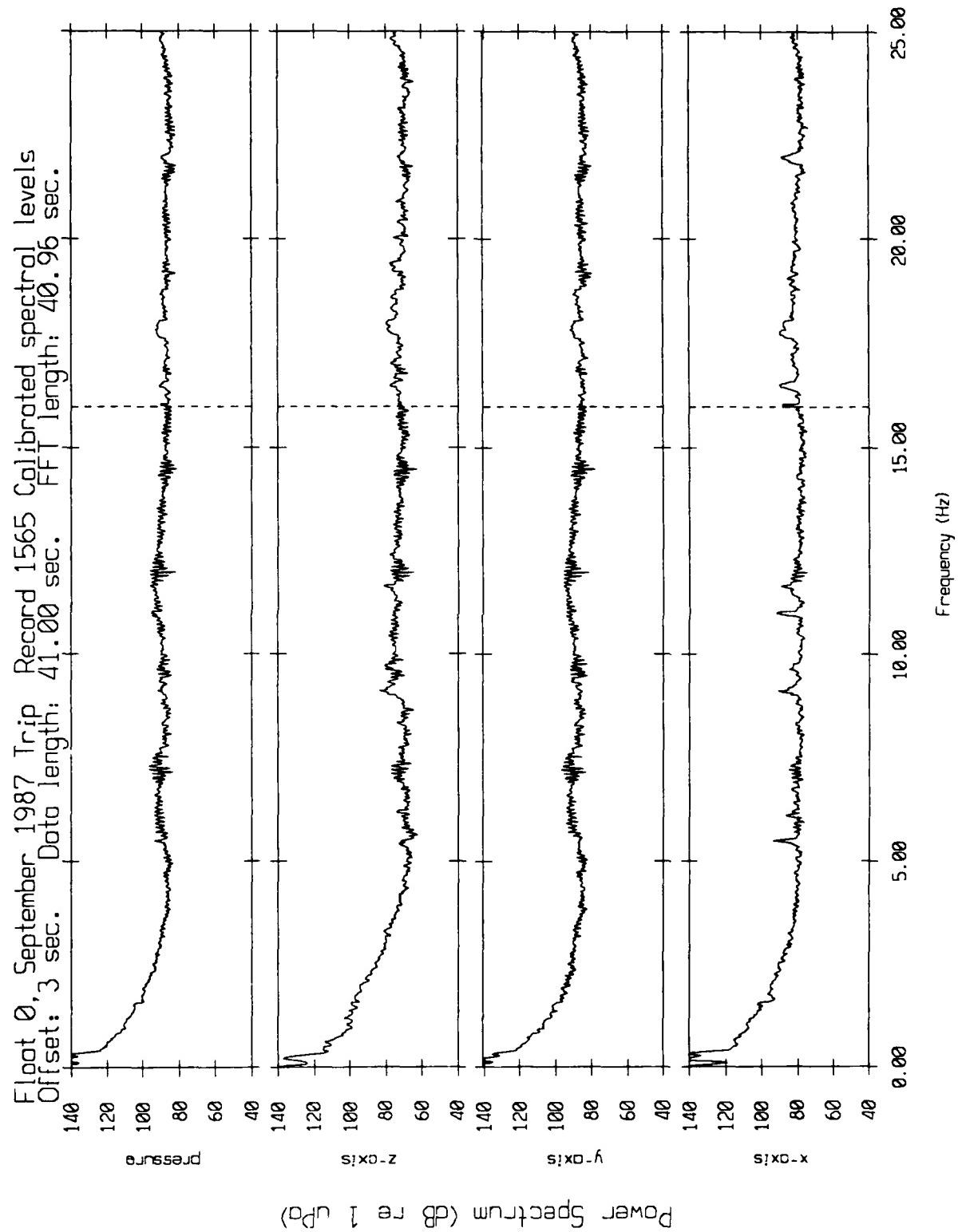


Figure XI.5a

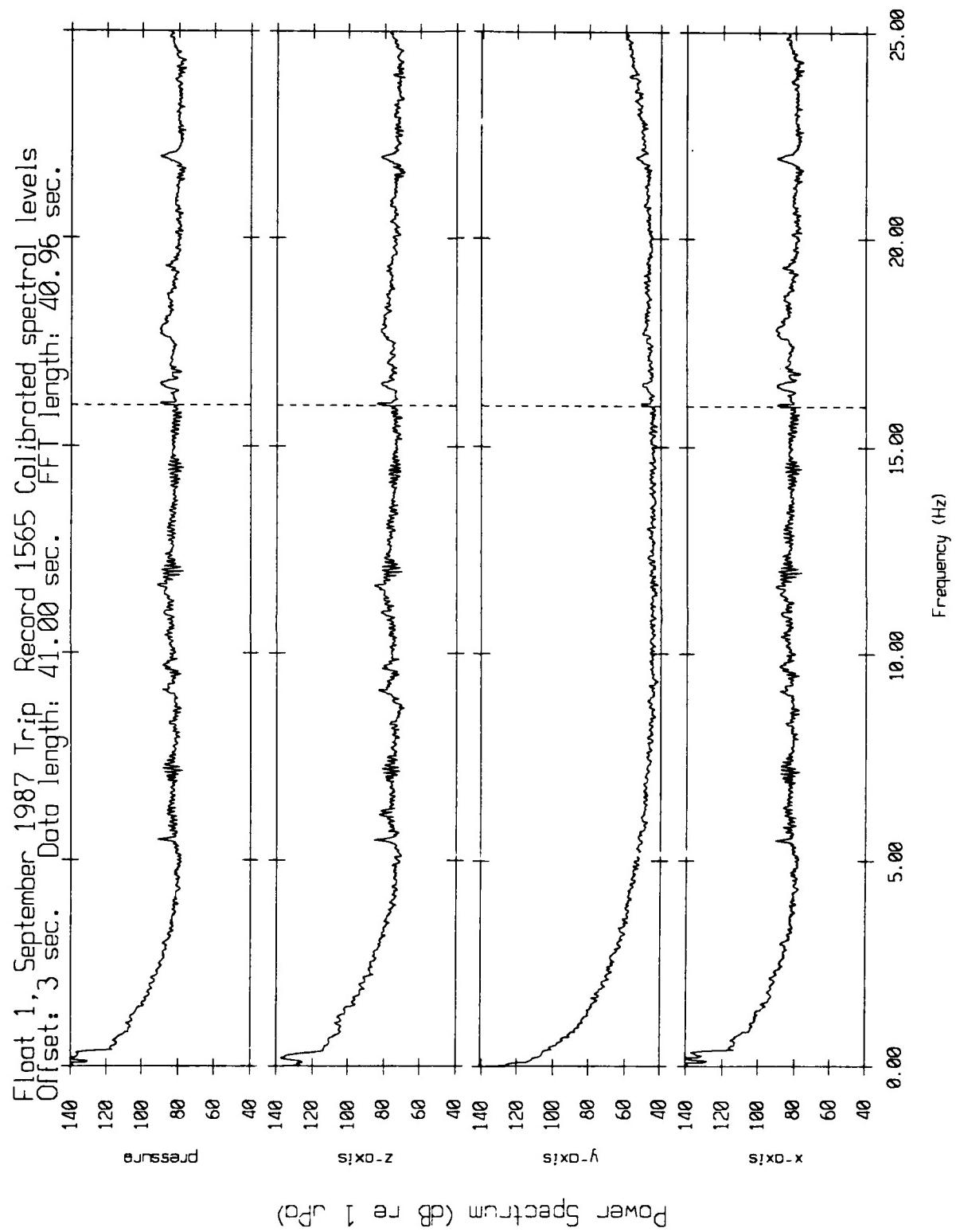


Figure XI.5b

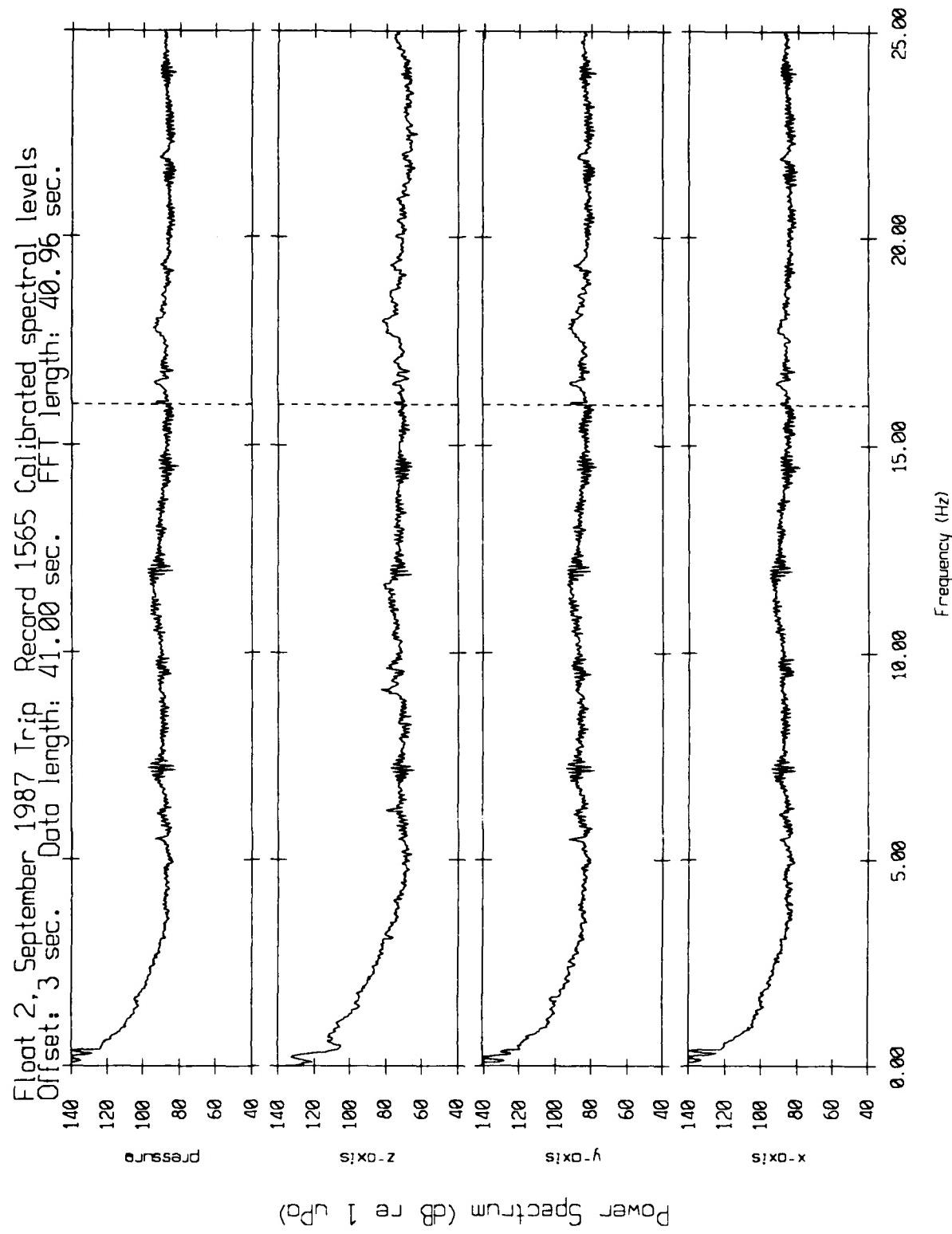


Figure XI.5c

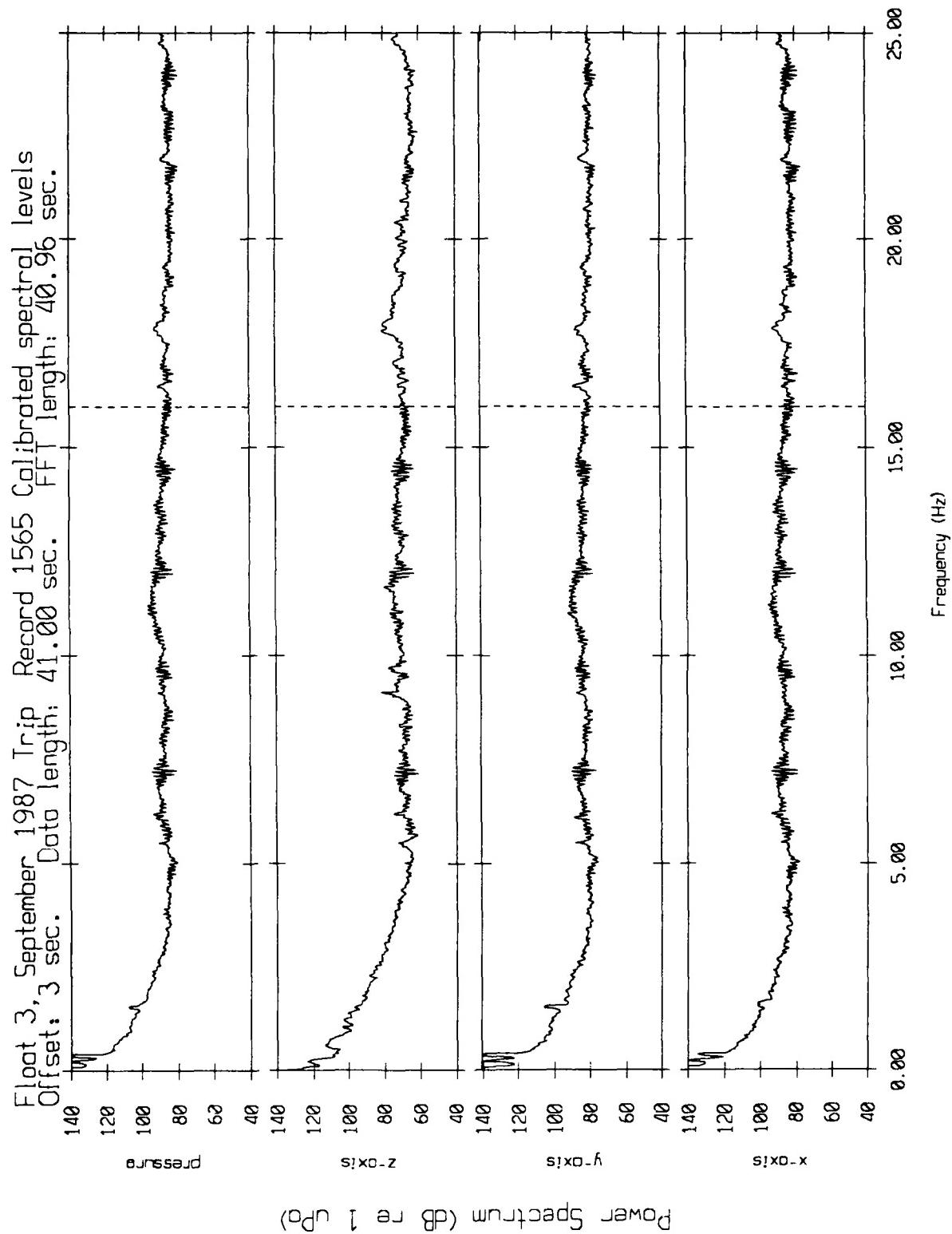


Figure XI.5d

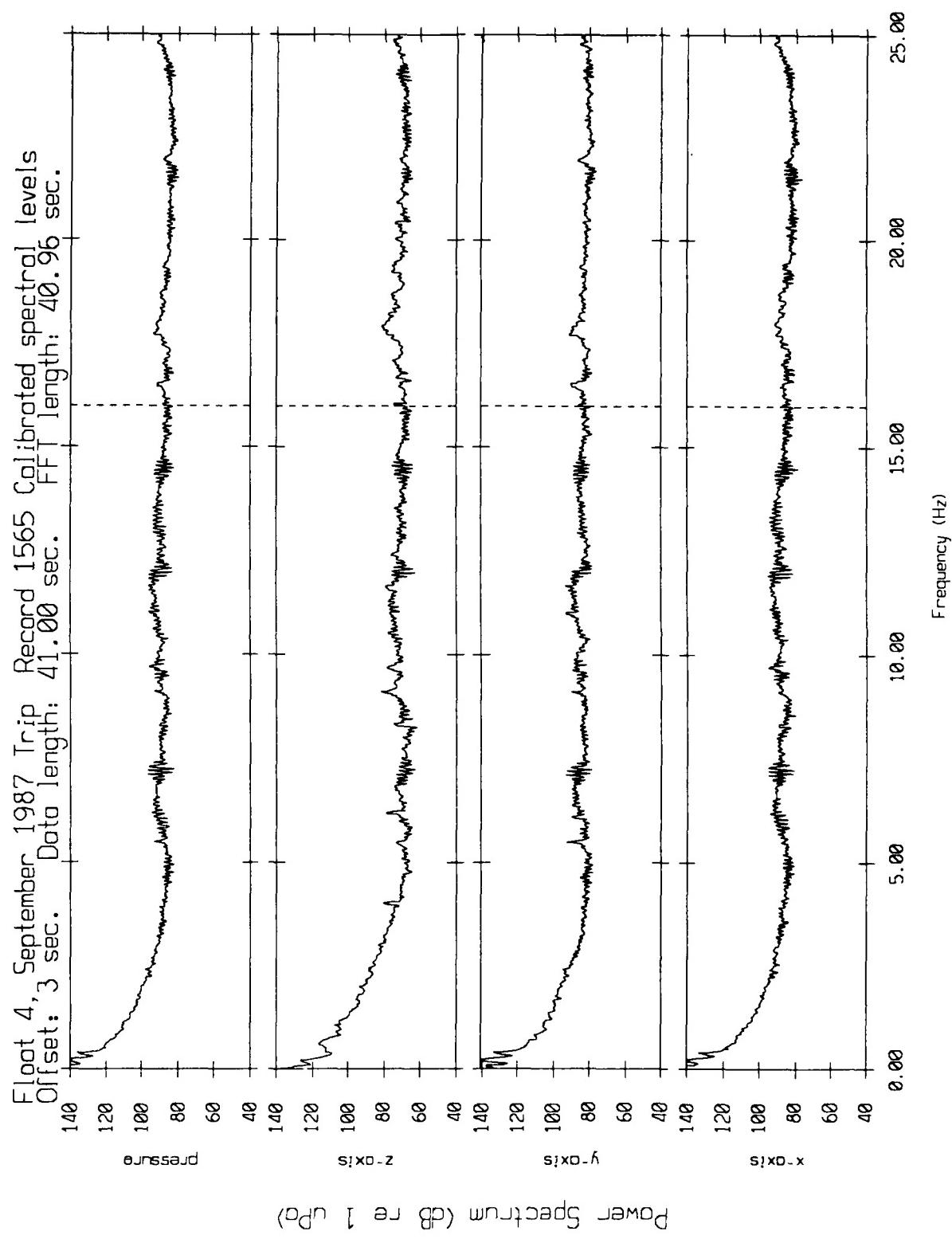


Figure XI.5e

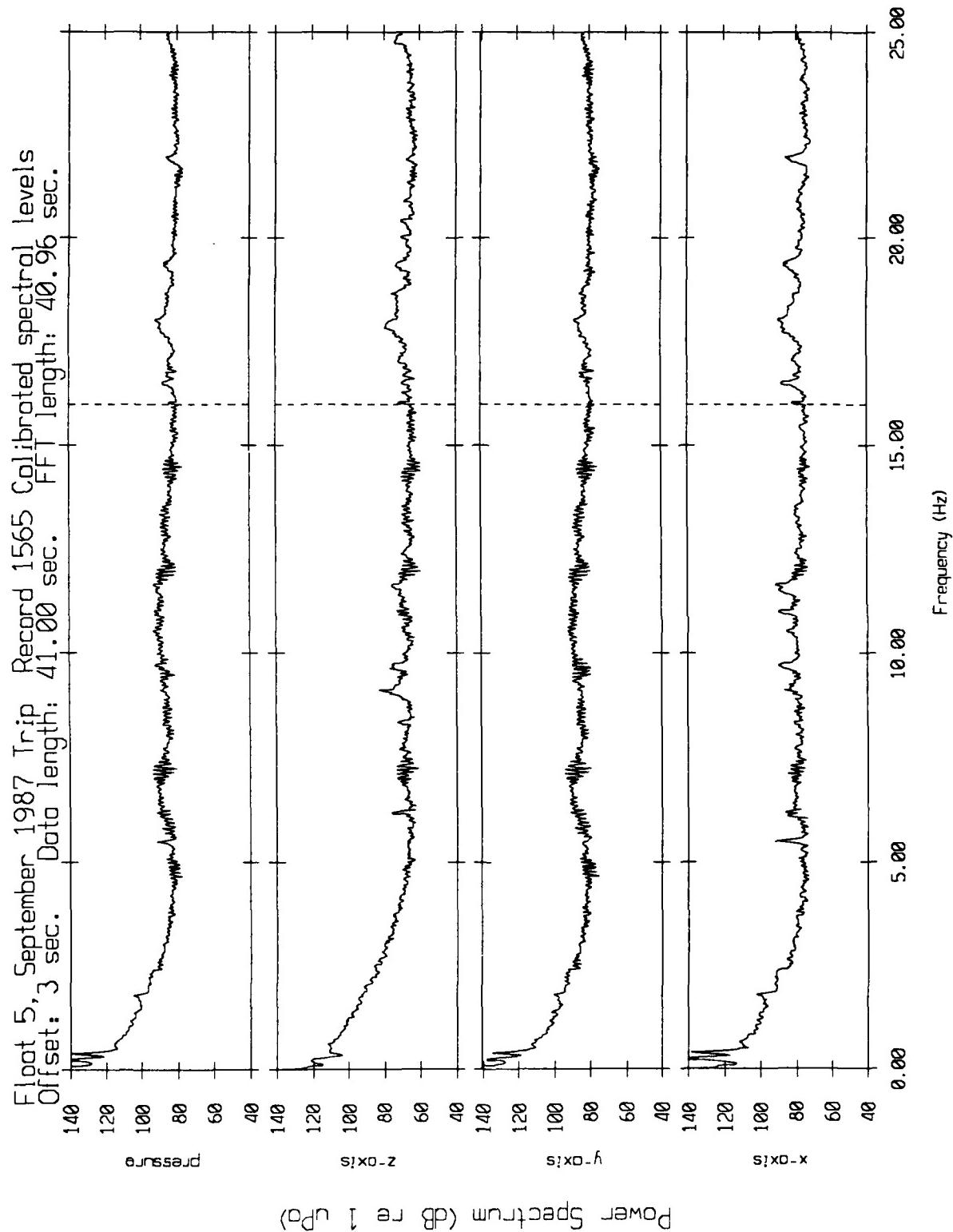


Figure XI.5f

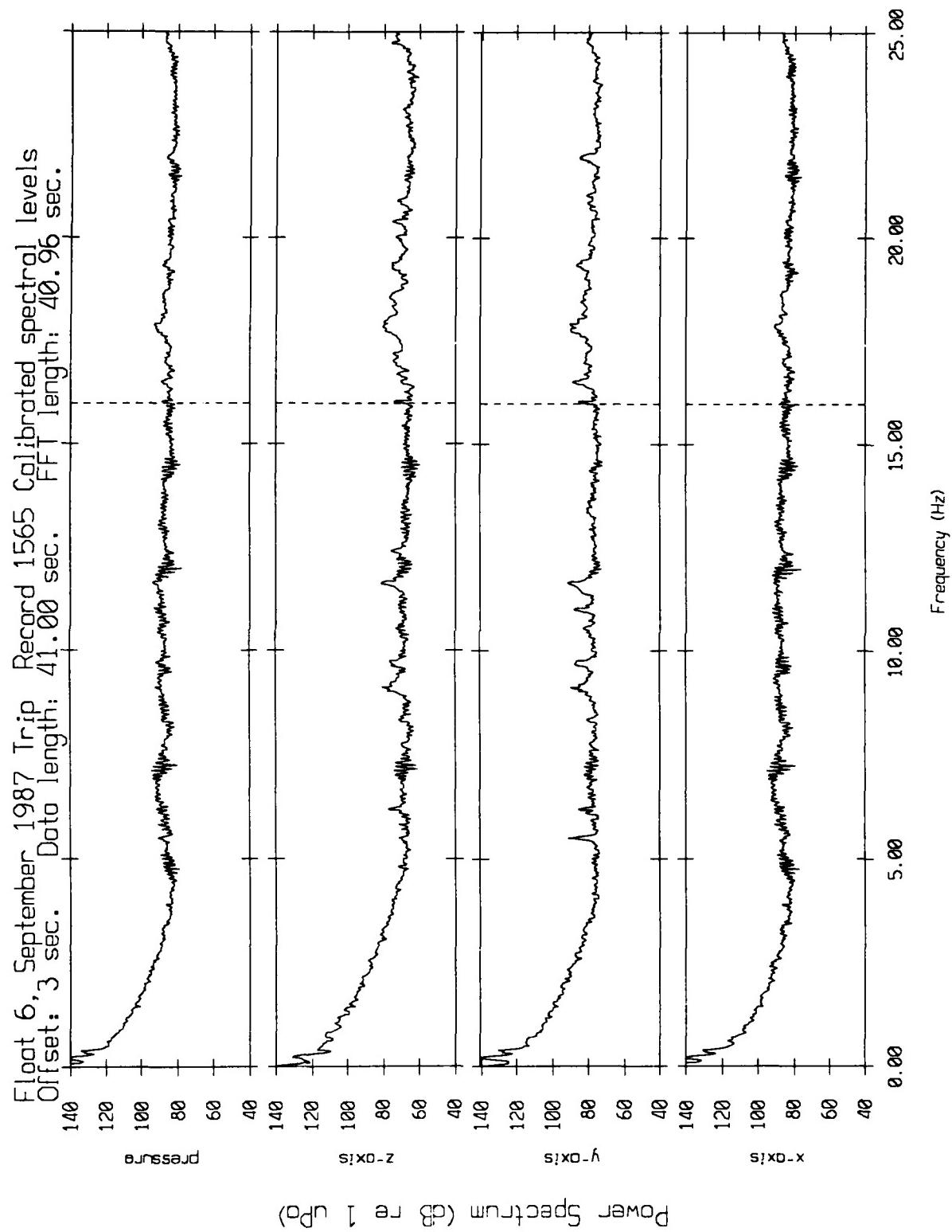


Figure XI.5g

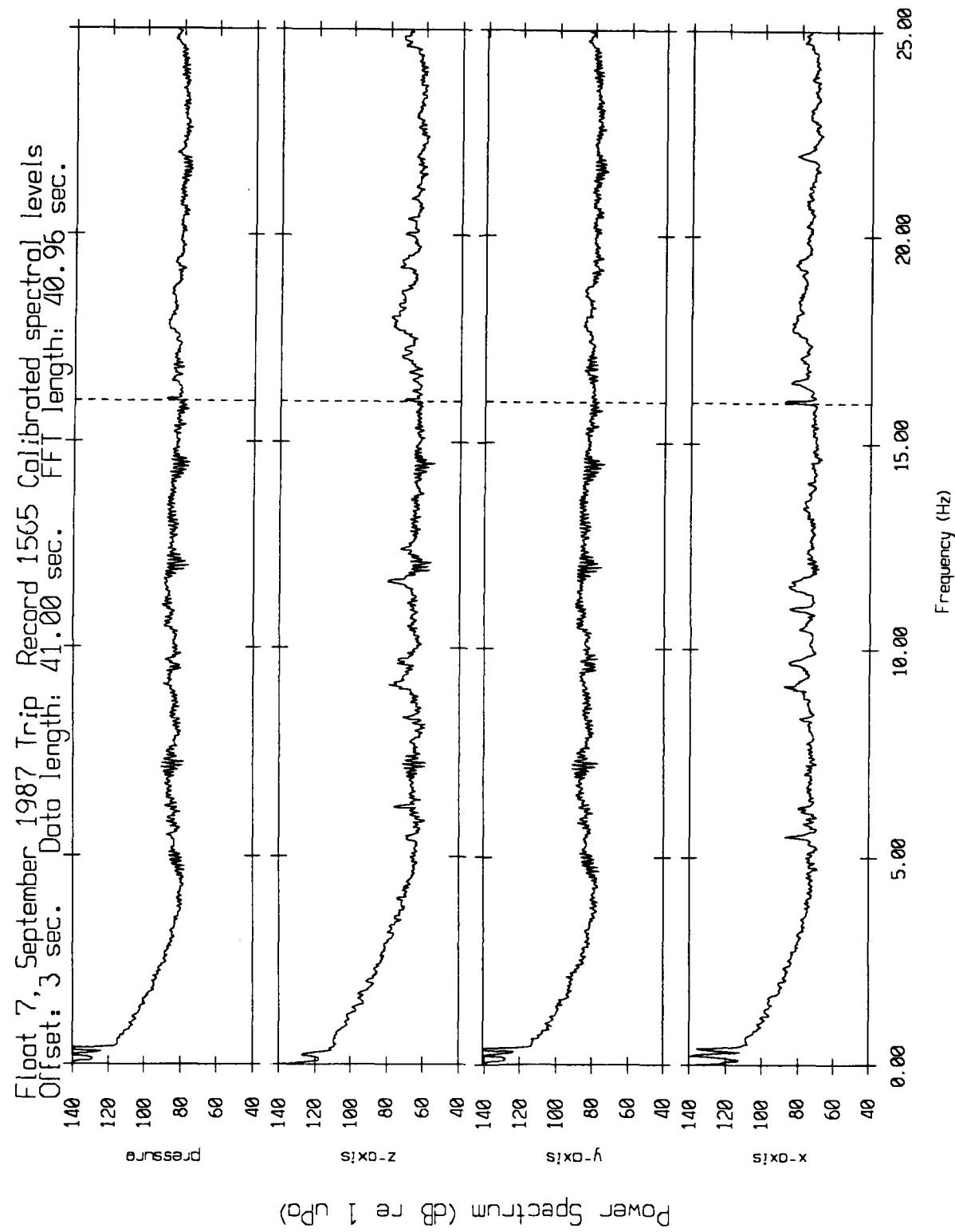


Figure XI.5h

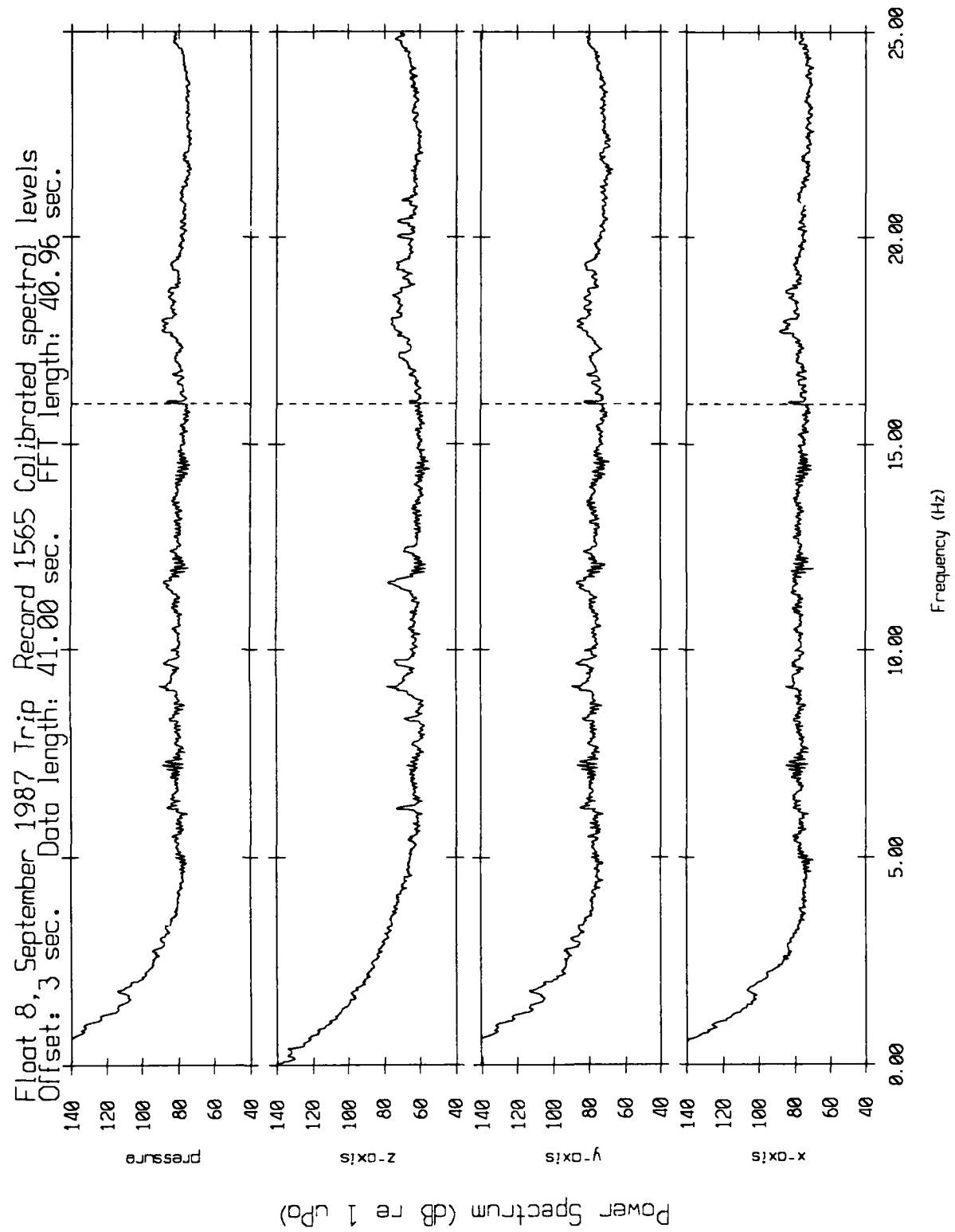


Figure XI.5i

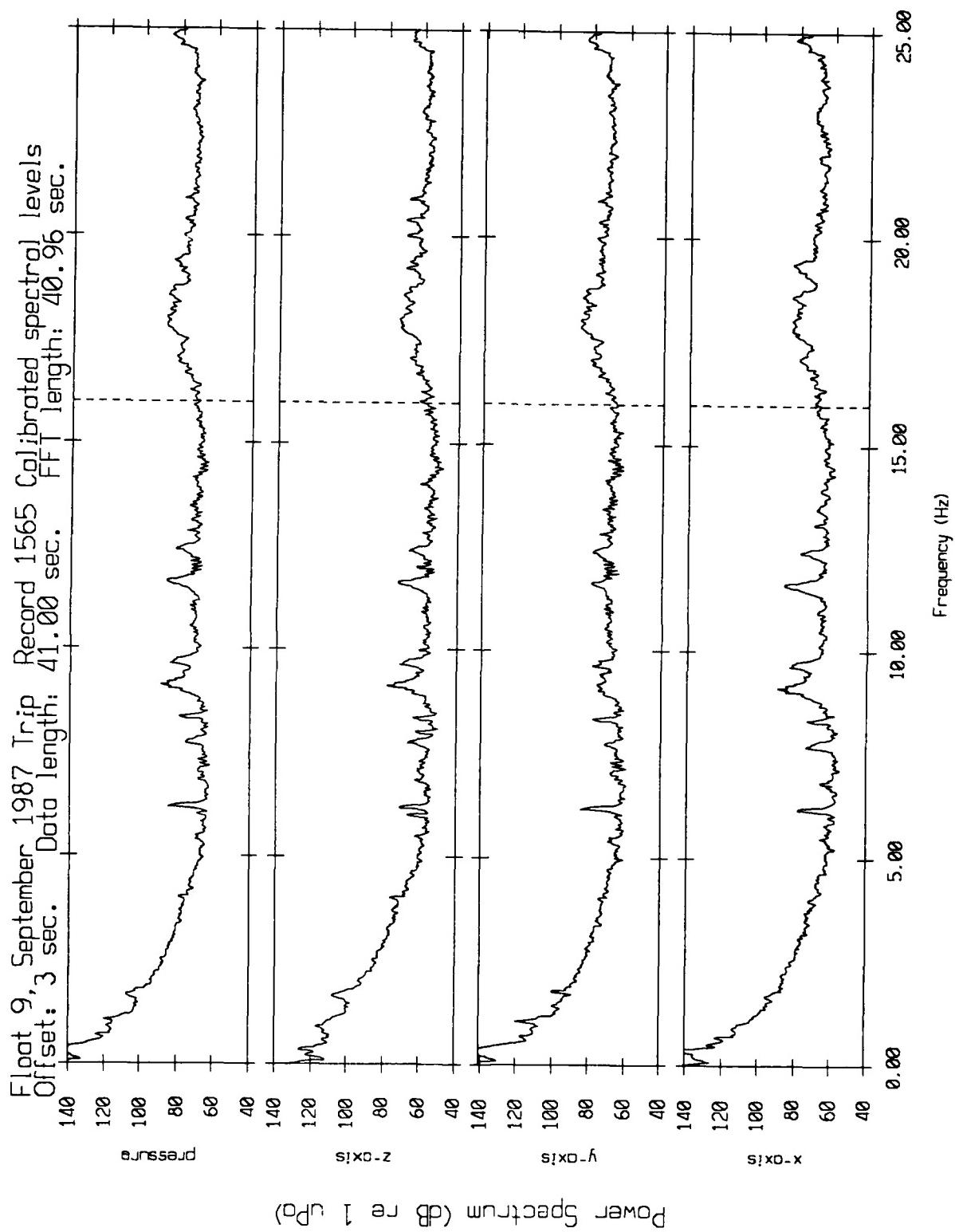


Figure XI.5j

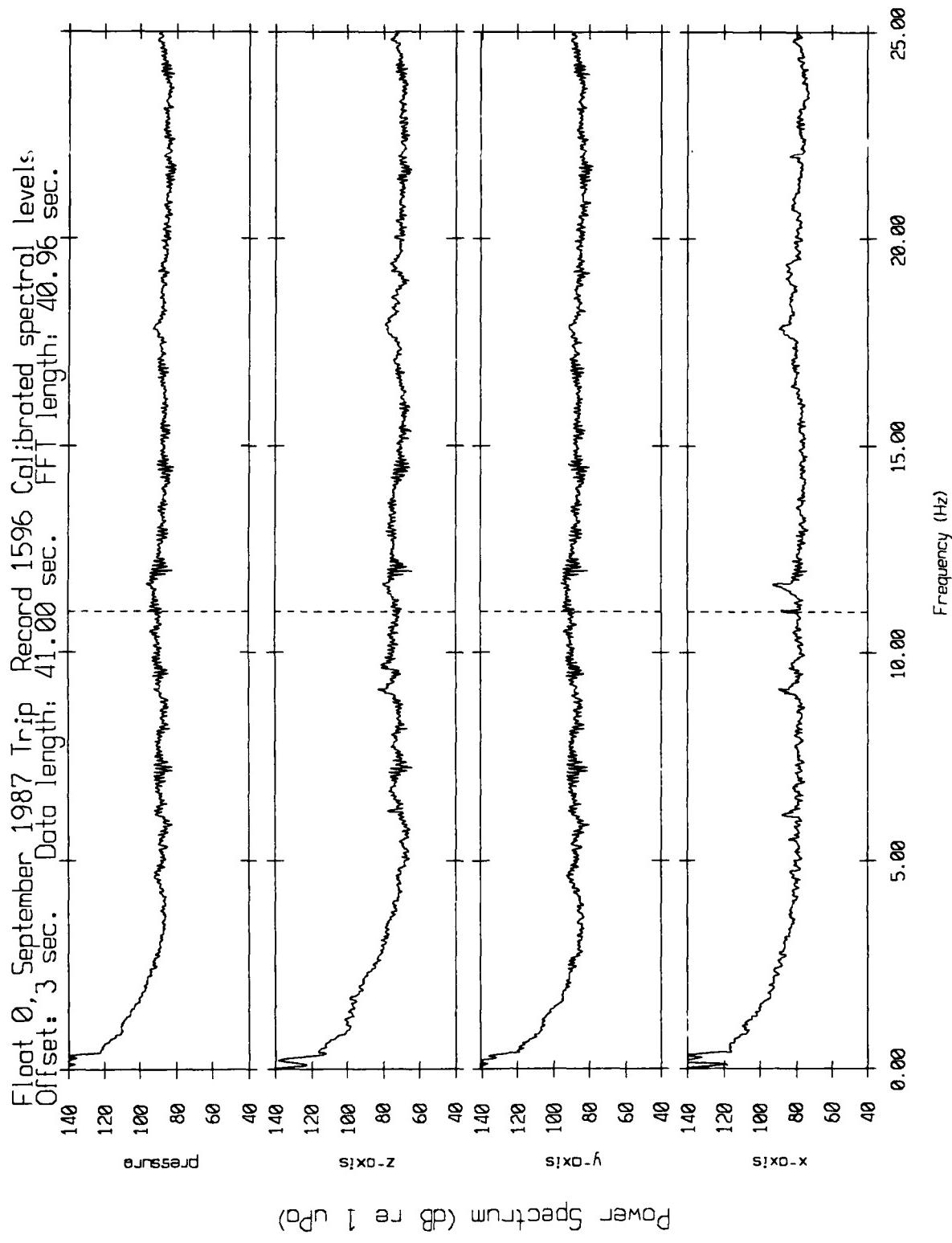


Figure XI.6a

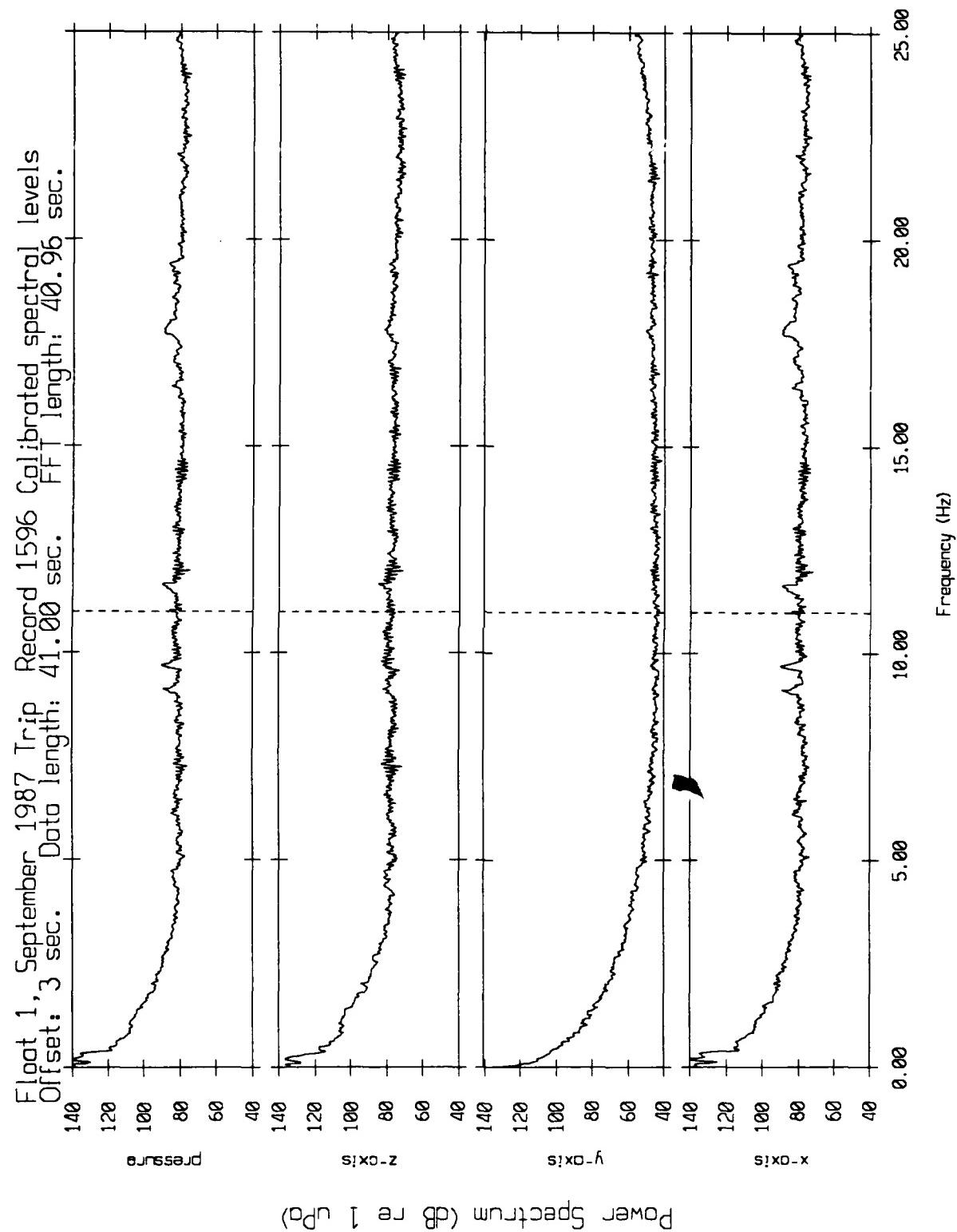


Figure XI.6b

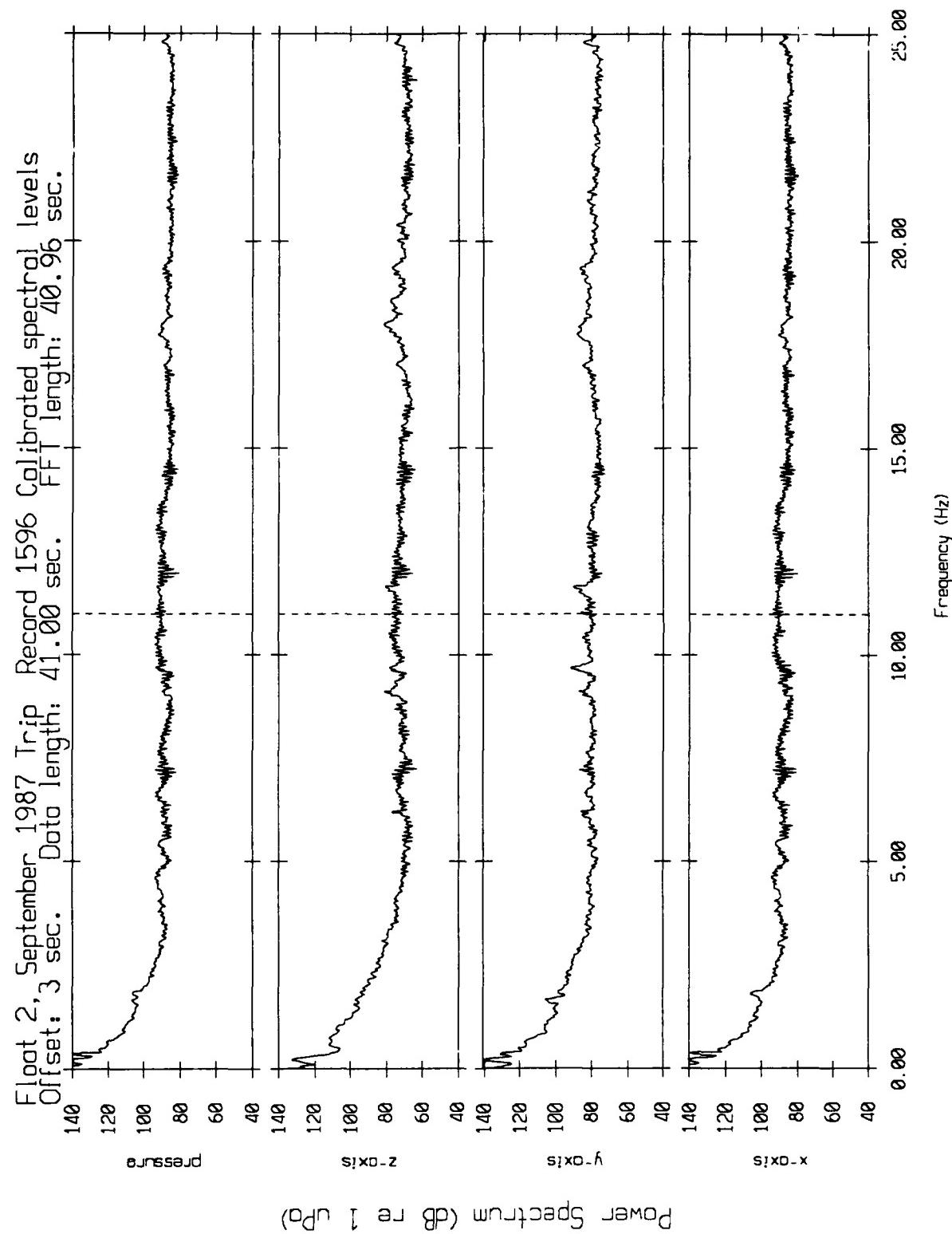


Figure XI.6c

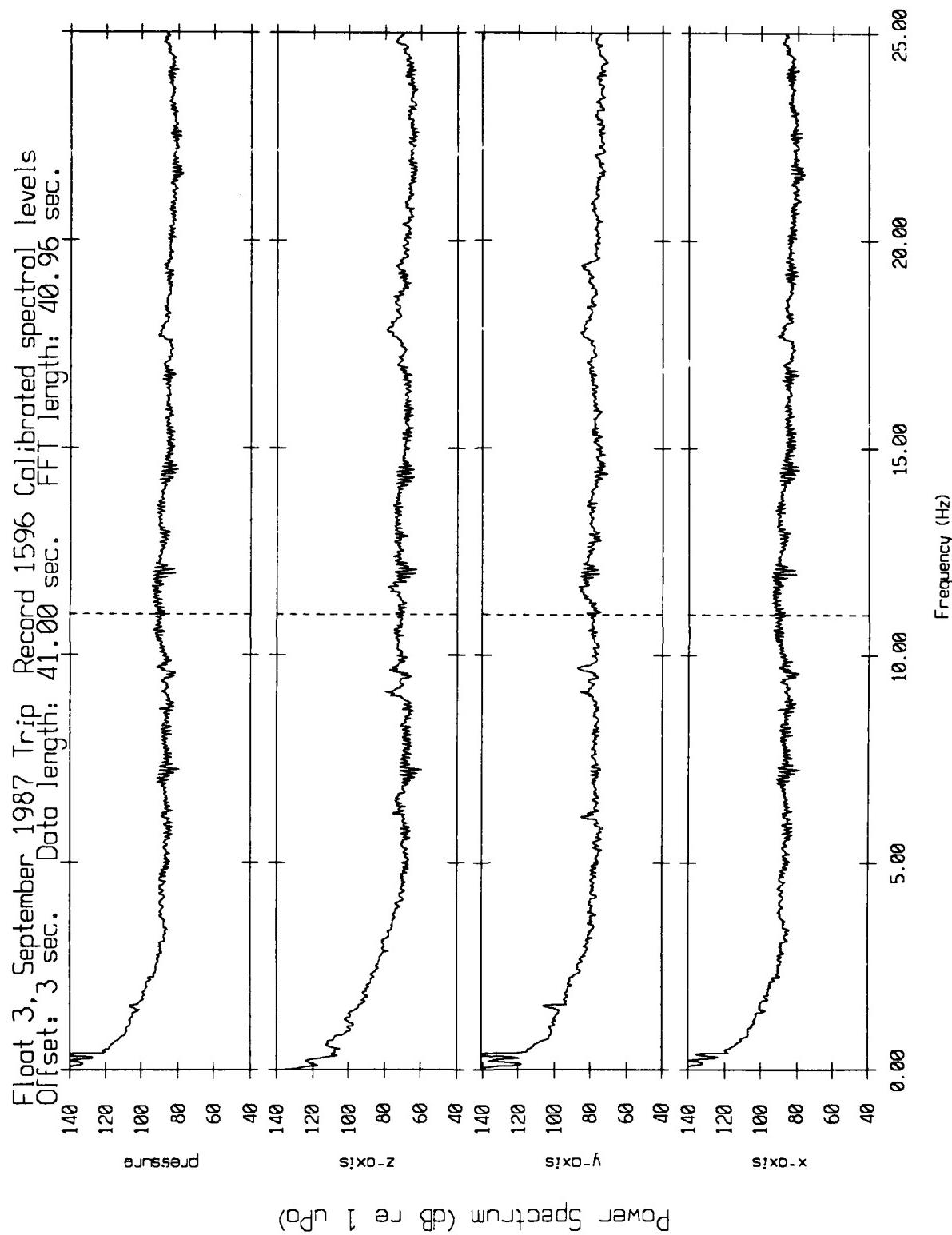


Figure XI.6d

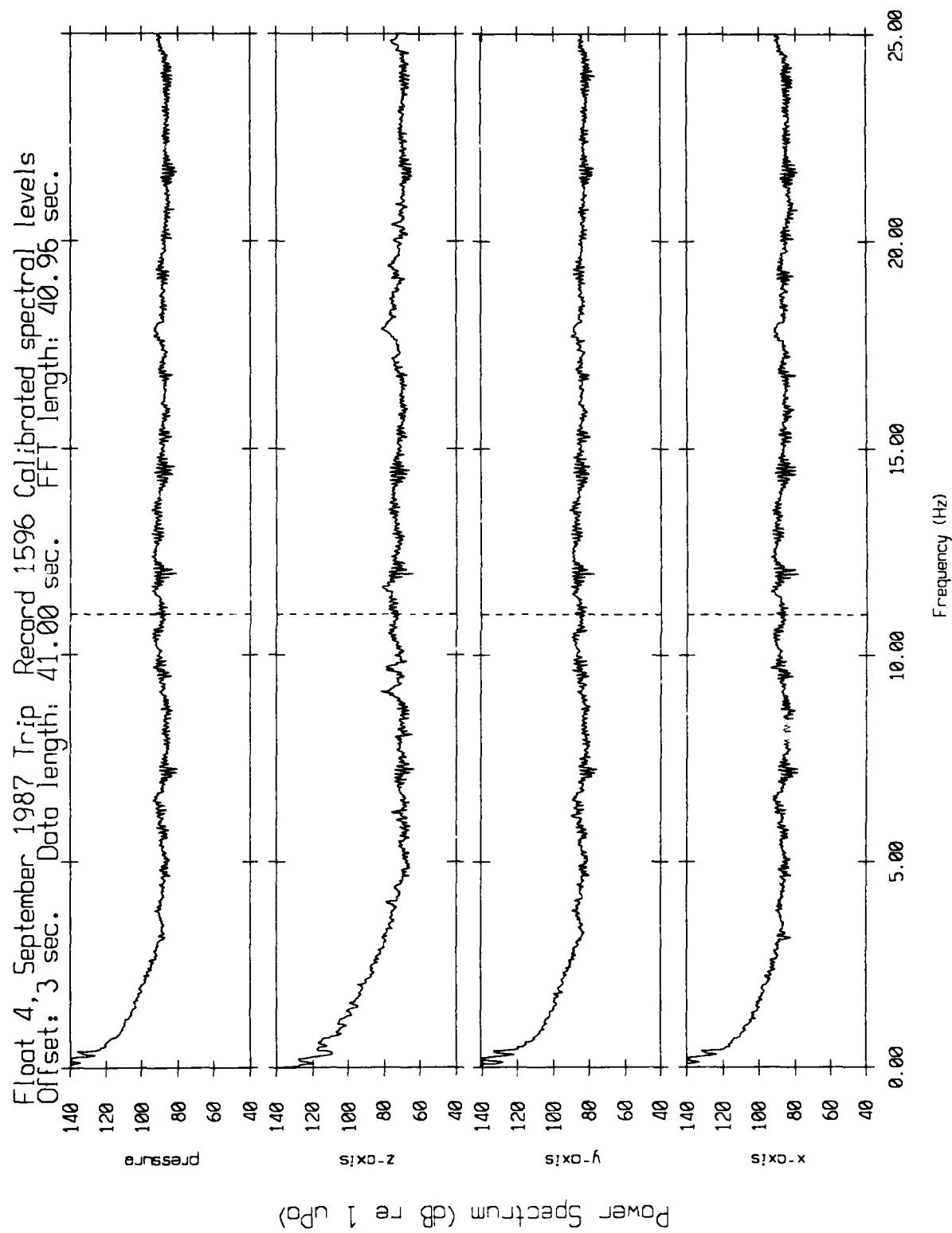


Figure XI.6e

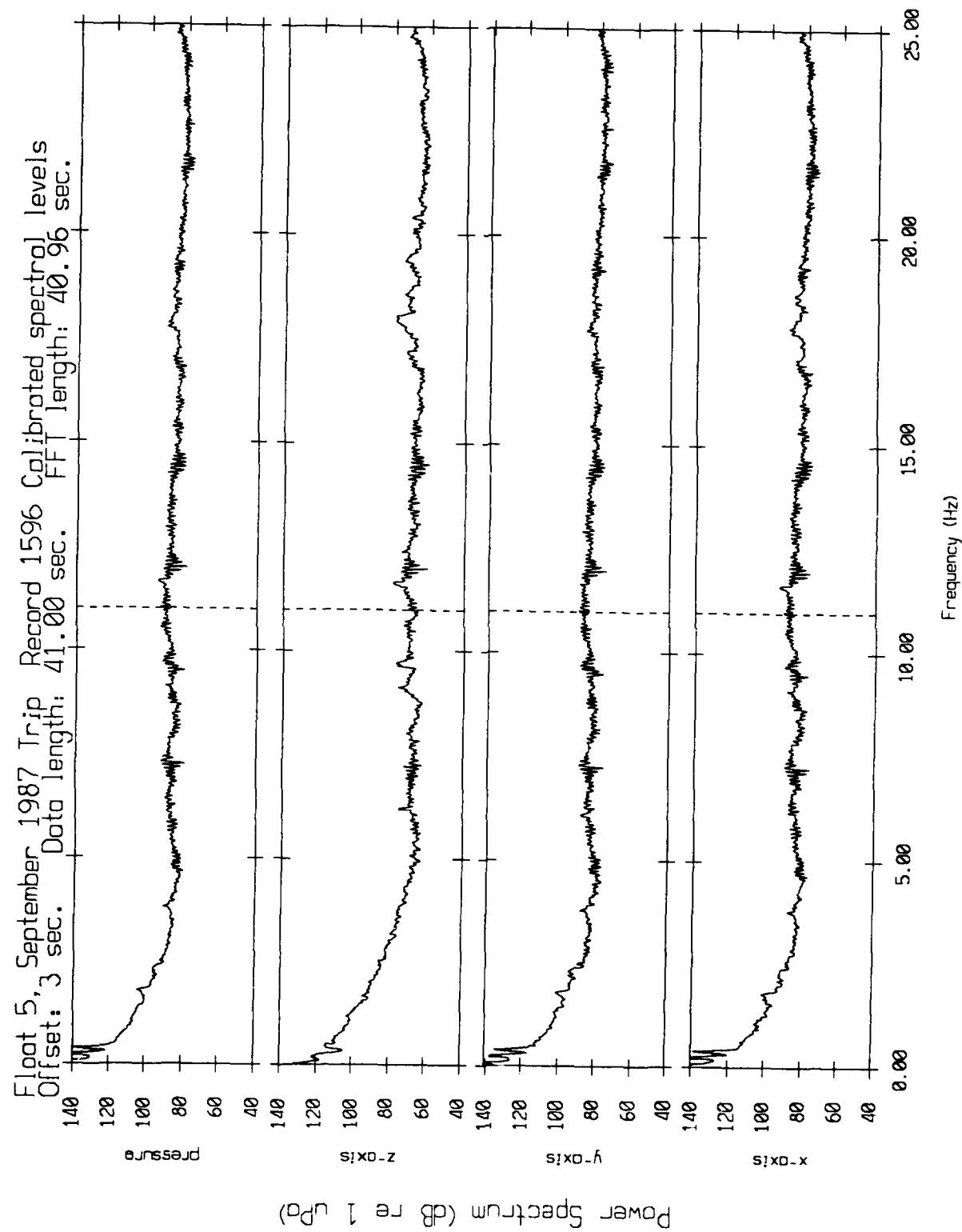
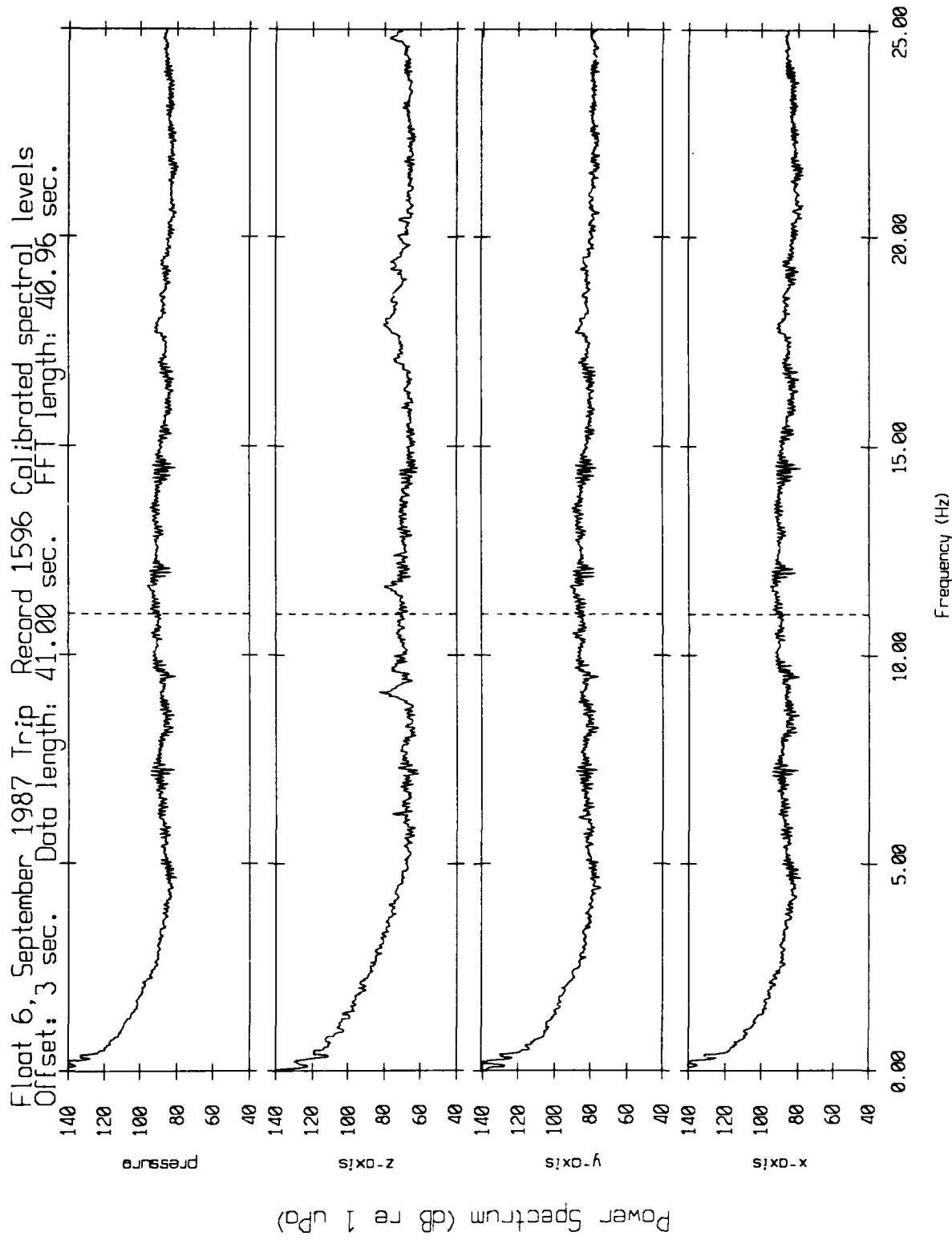


Figure XI.6f



Power Spectrum (dB re 1 UPa)

Figure XI.6g

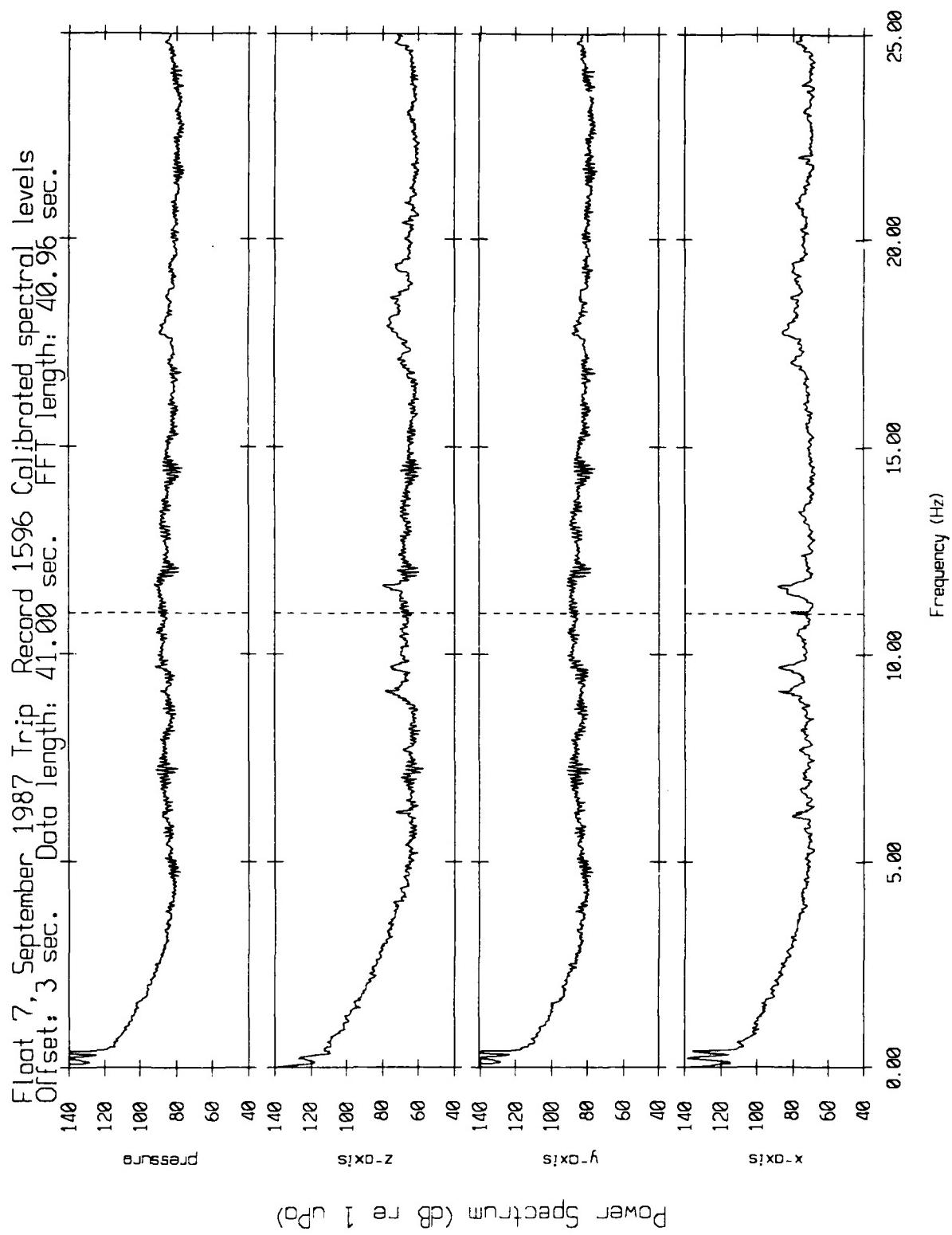


Figure XI.6h

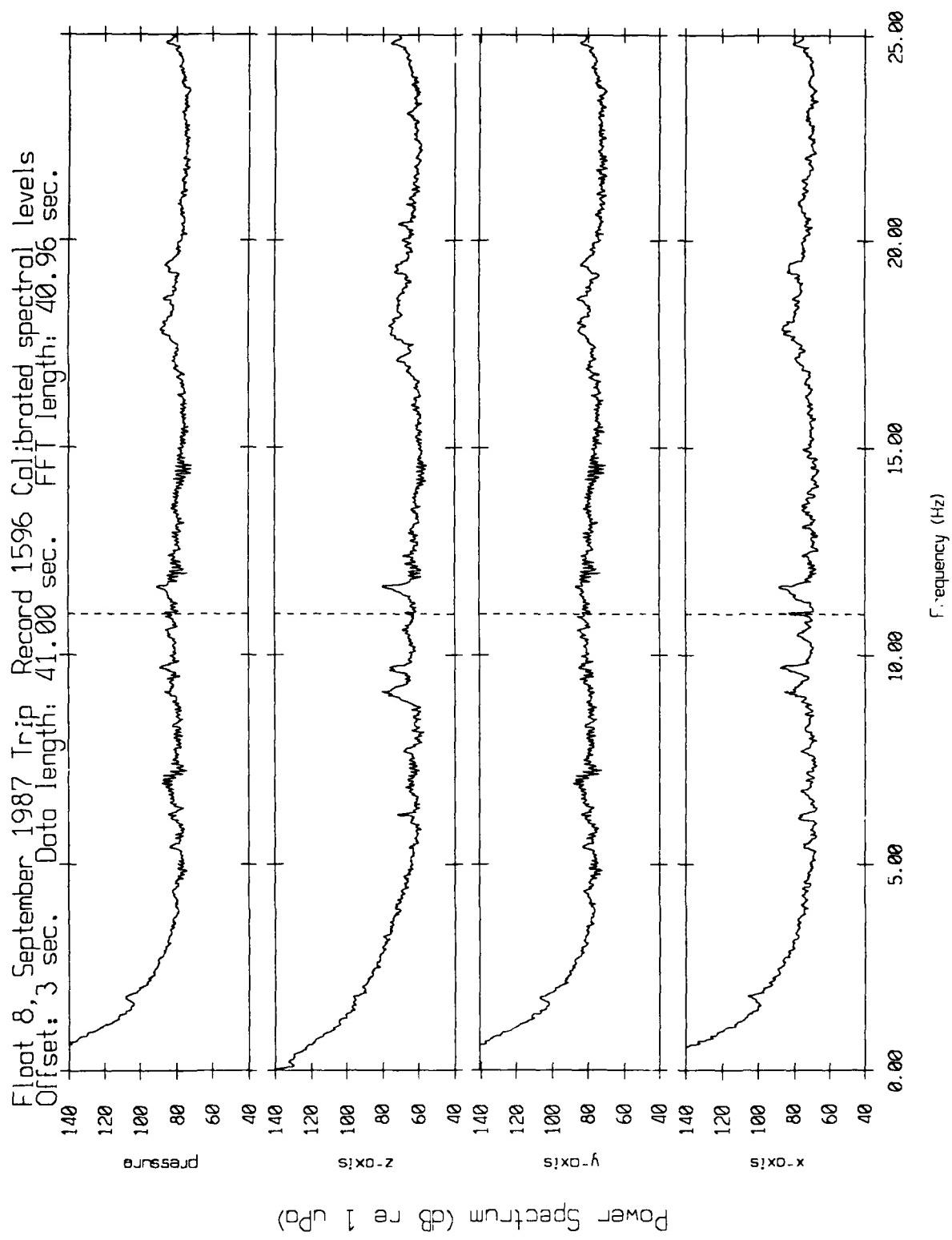


Figure XI.6i

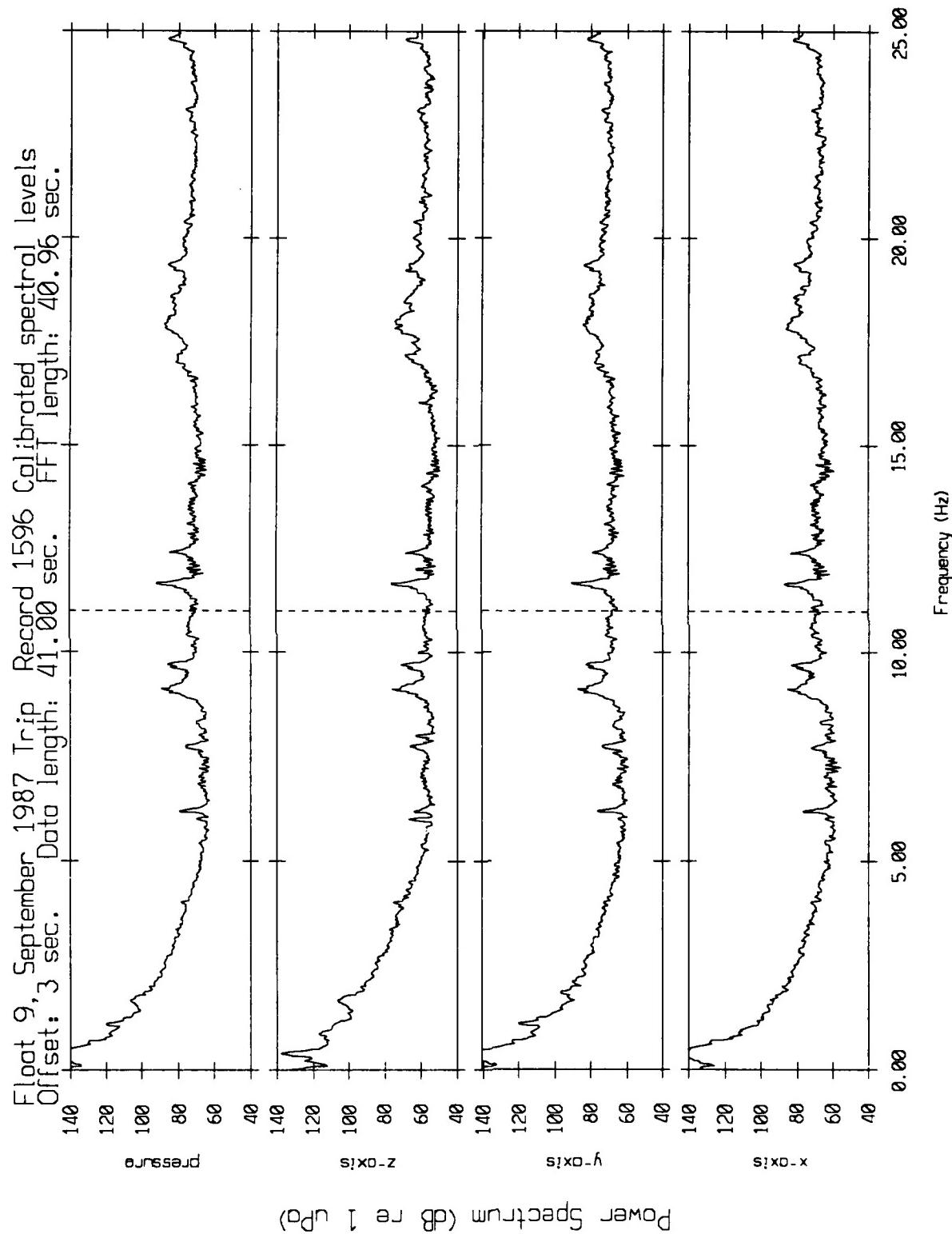


Figure XI.6j

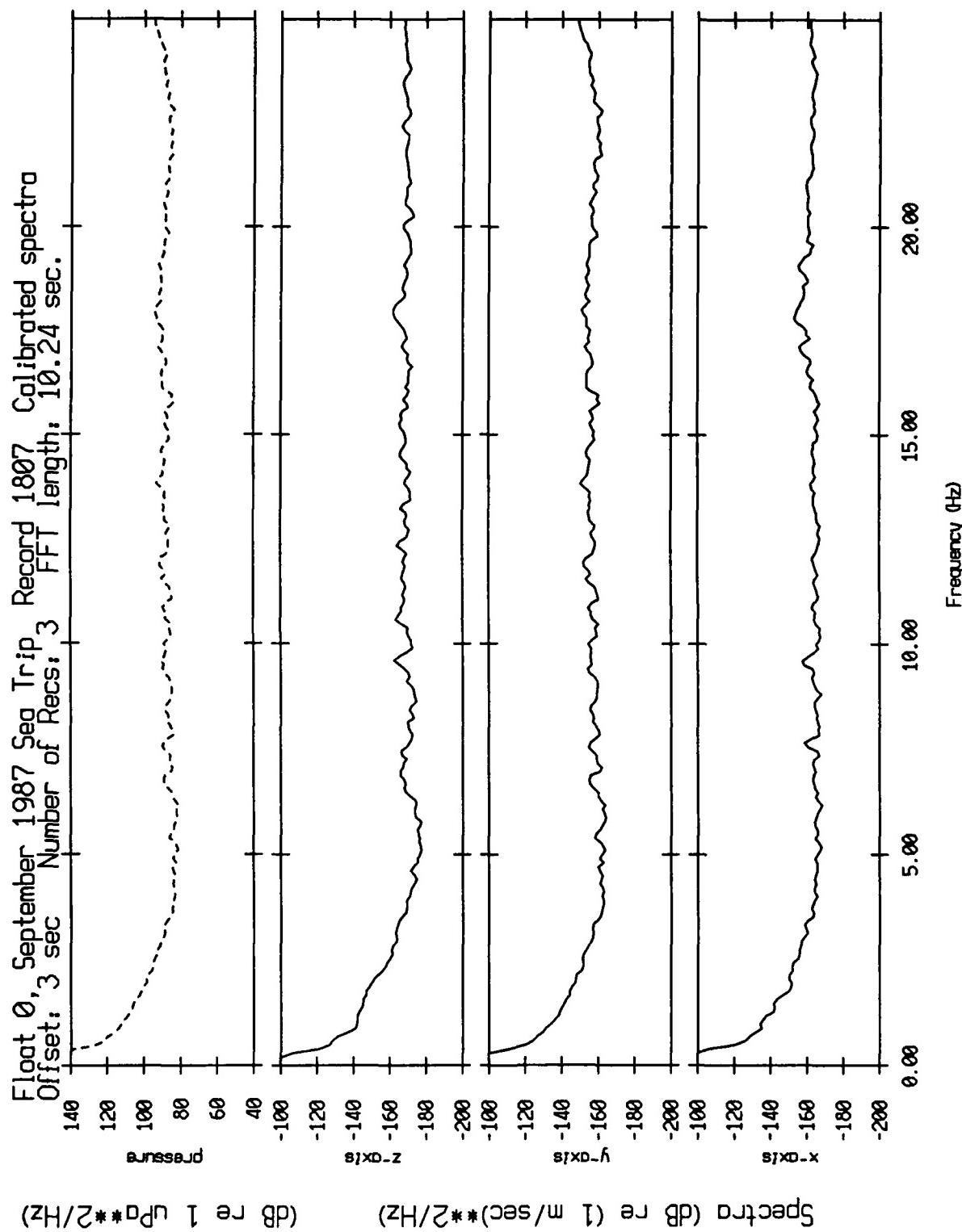


Figure XI.7a

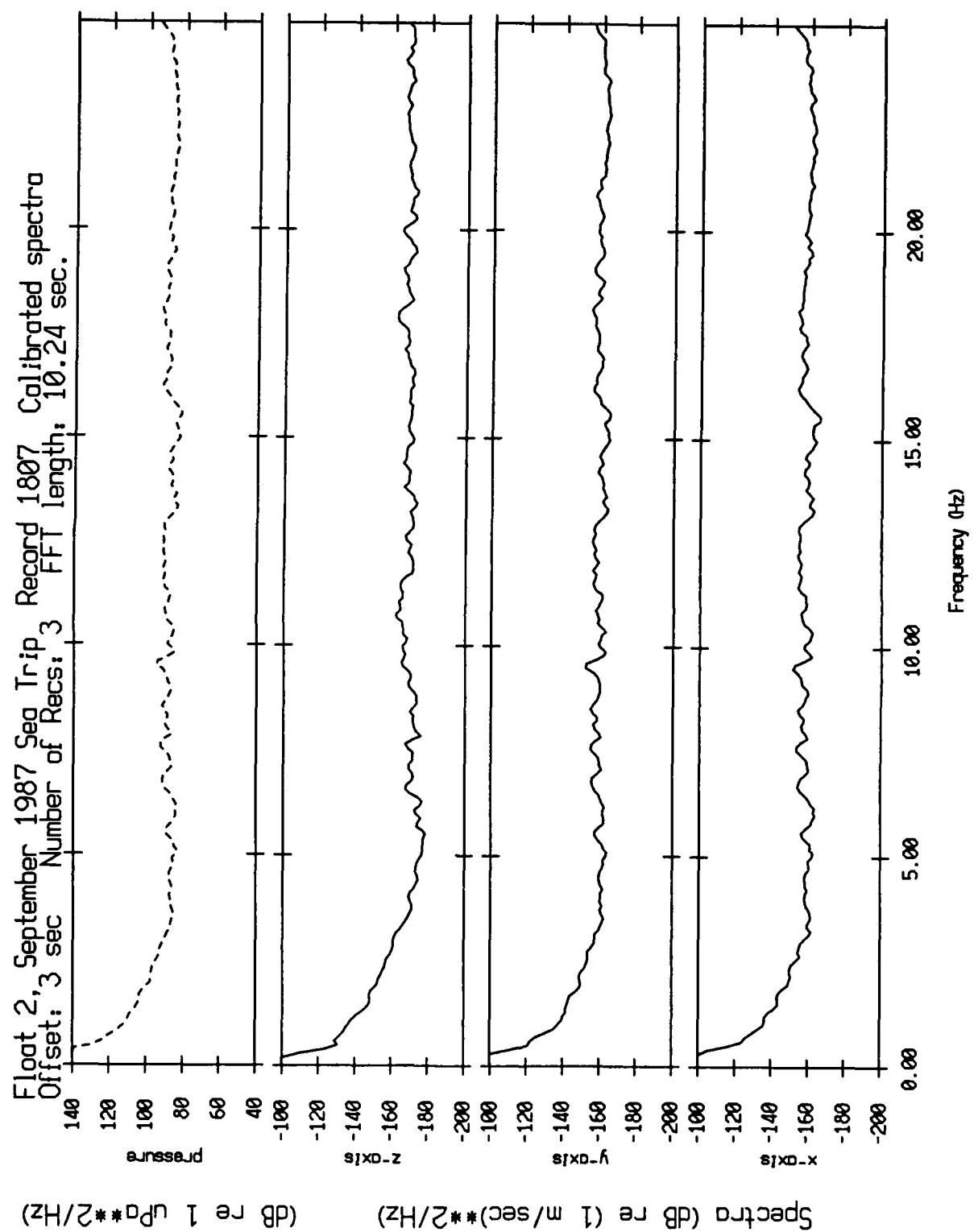


Figure XI.7b

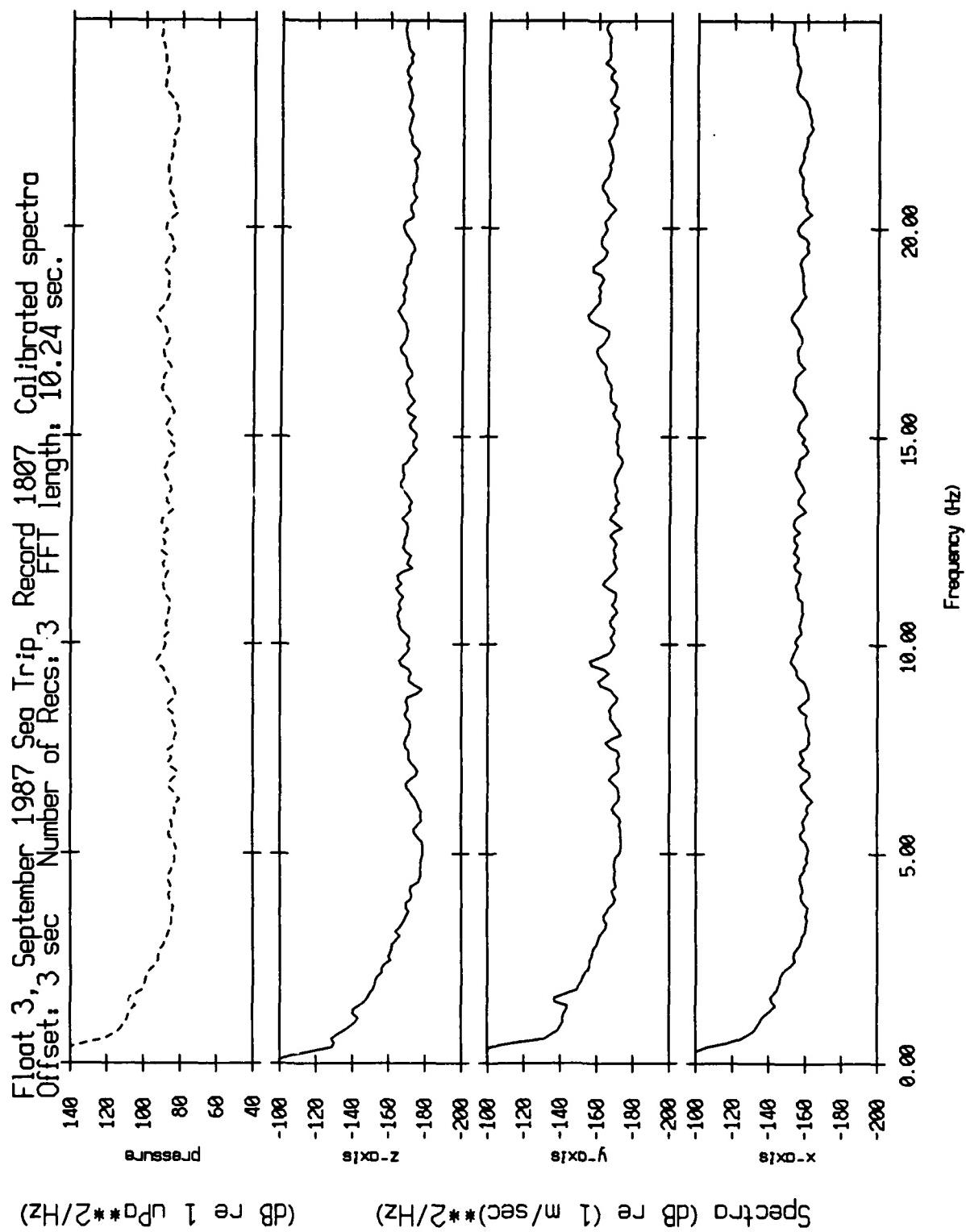


Figure XI.7c

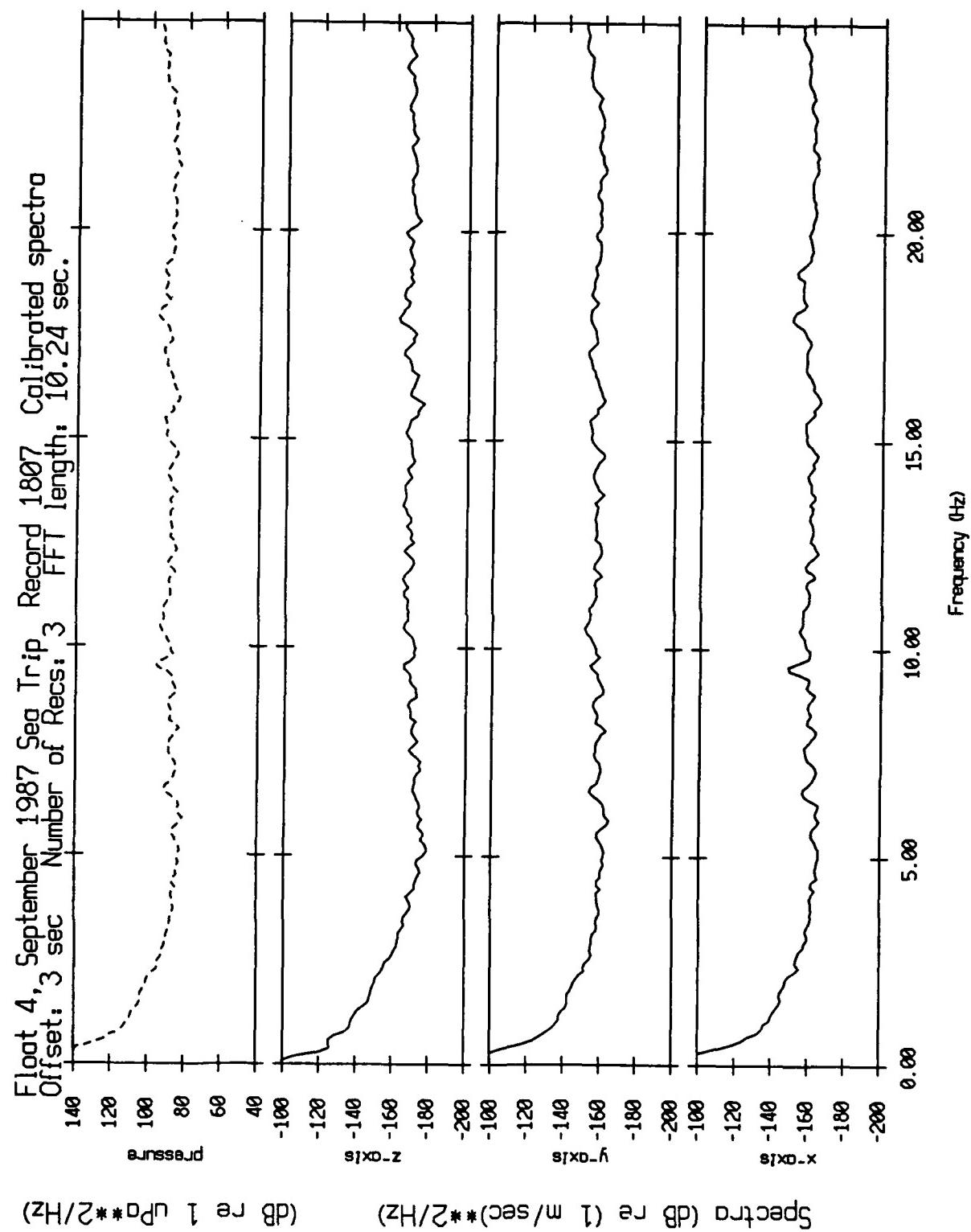


Figure XI.7d

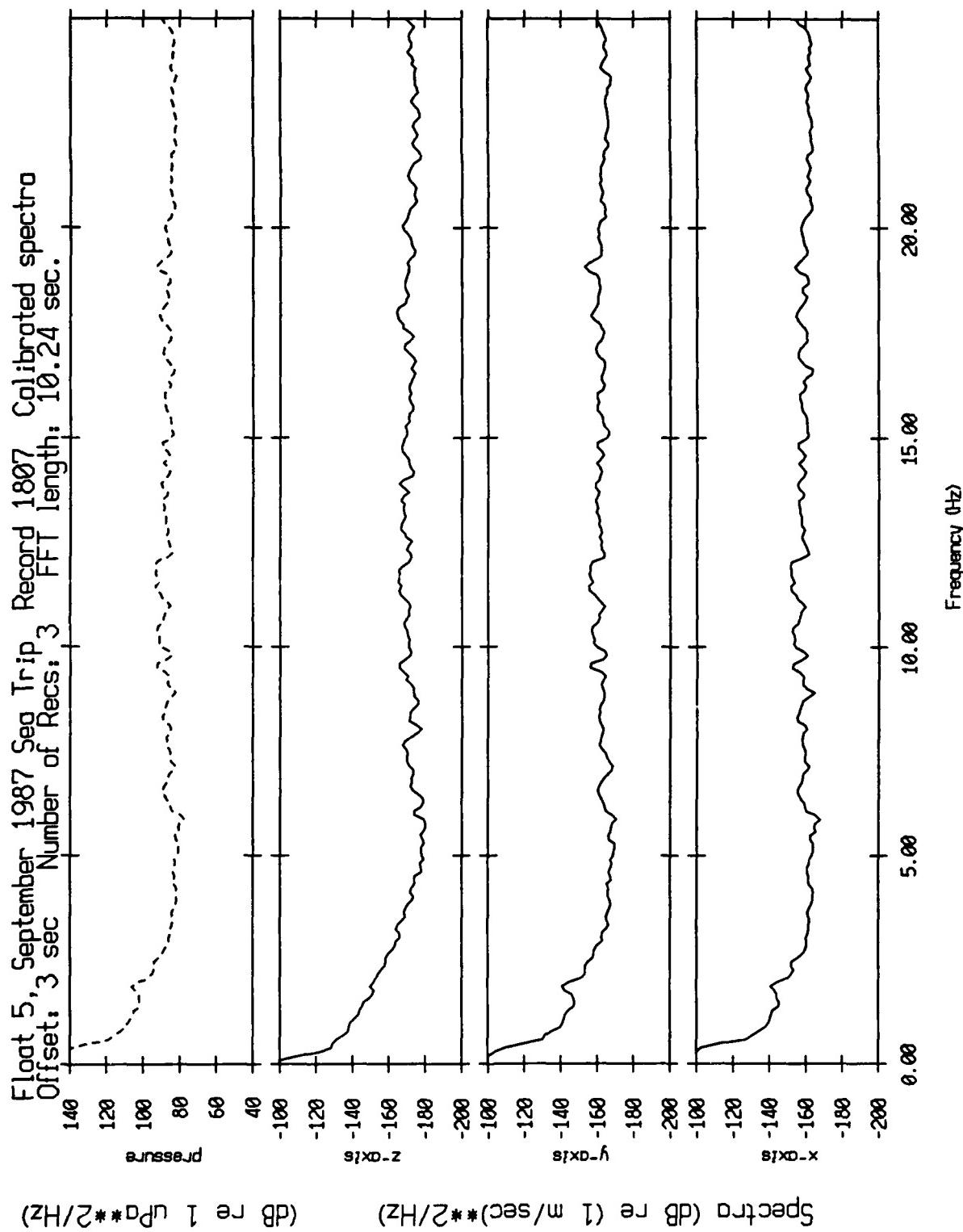


Figure XI.7e

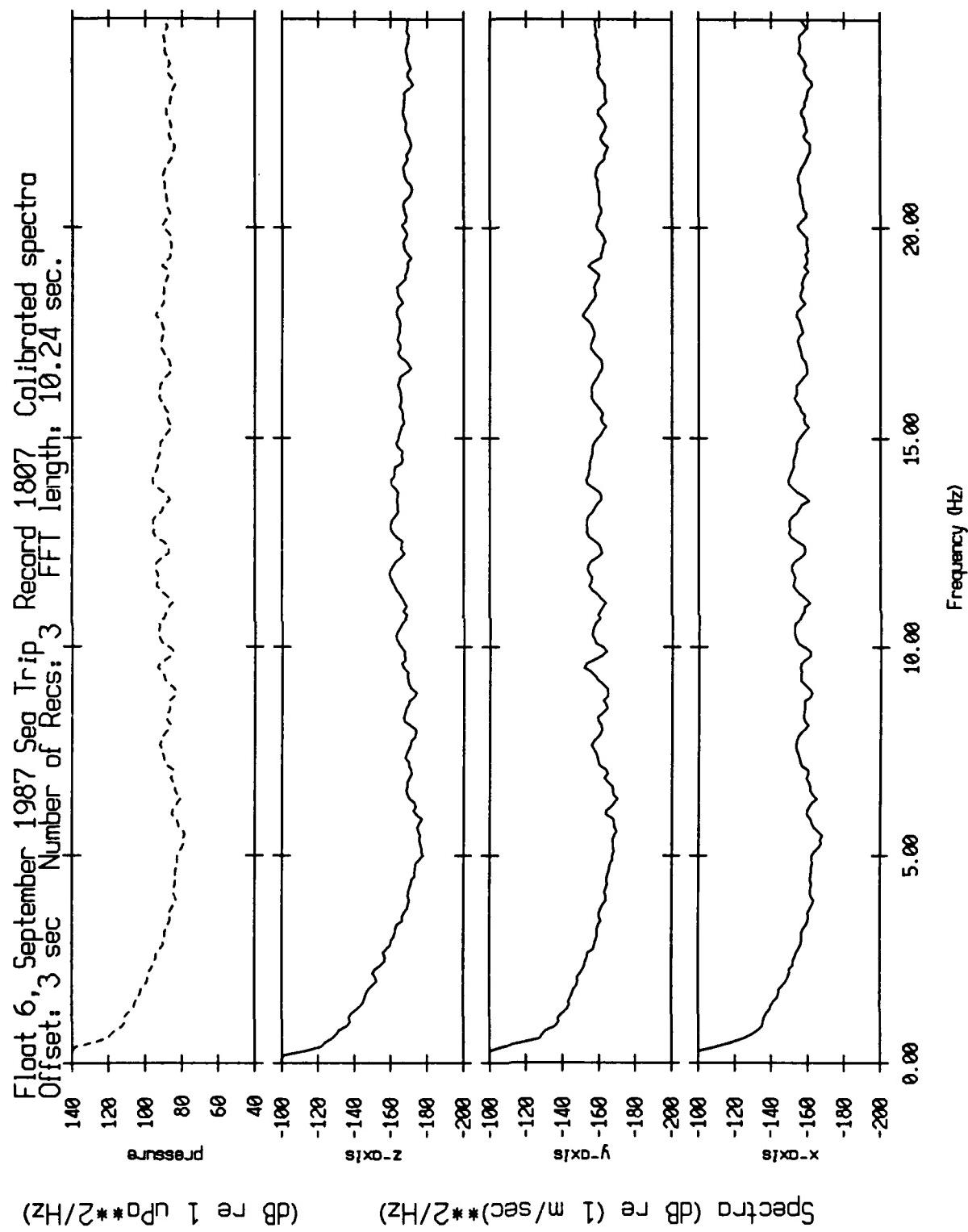


Figure XI.7f

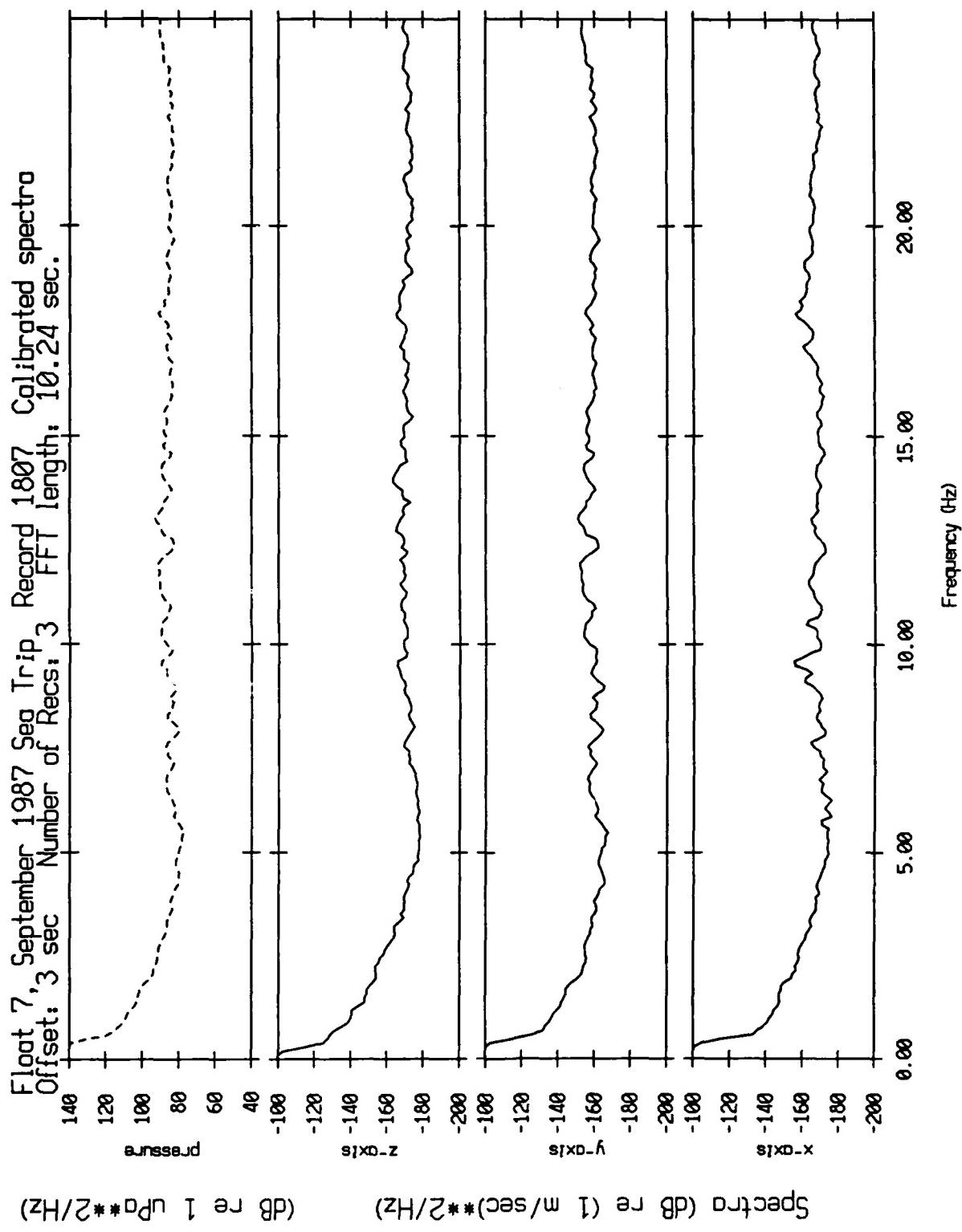


Figure XI.7g

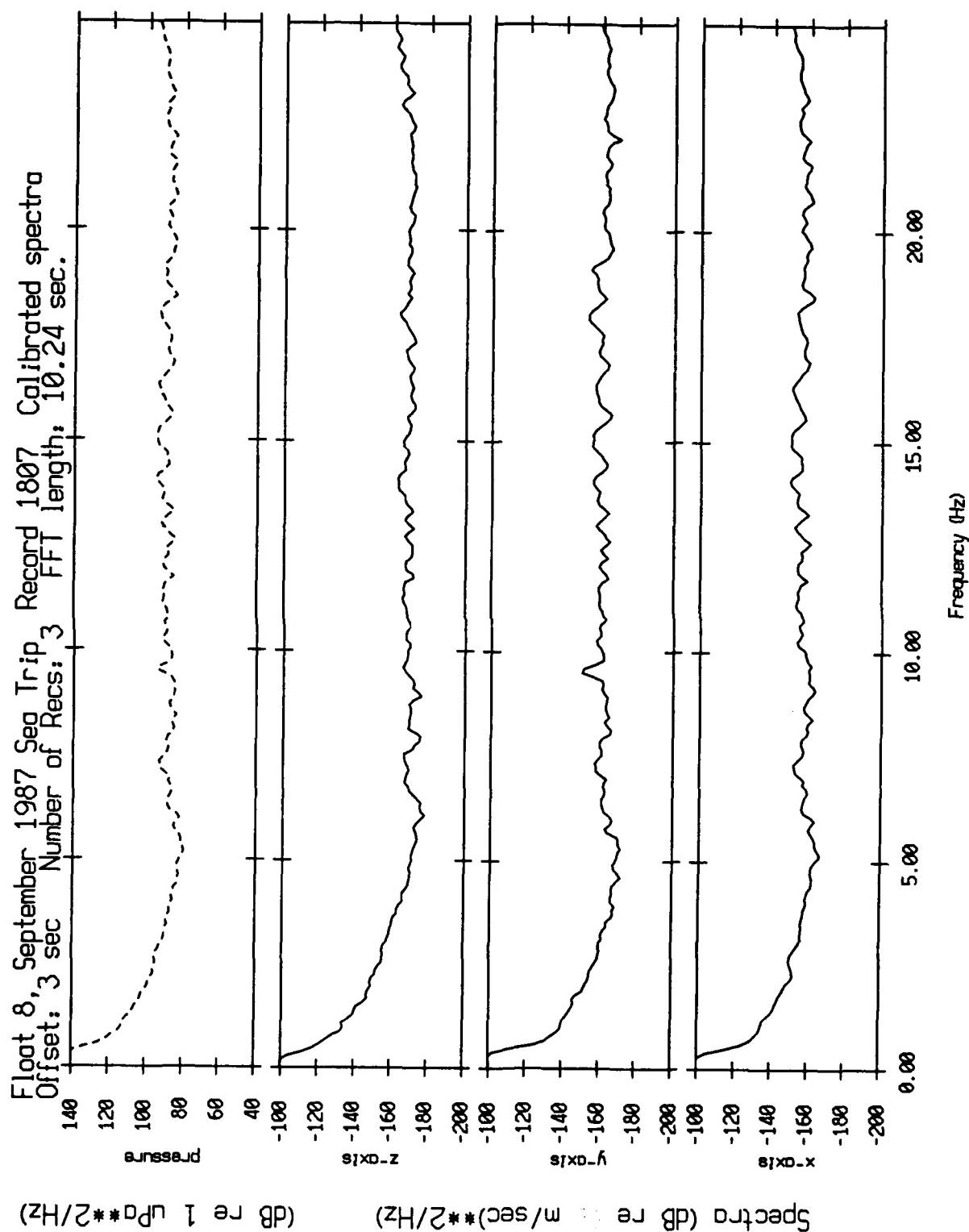


Figure XI.7h

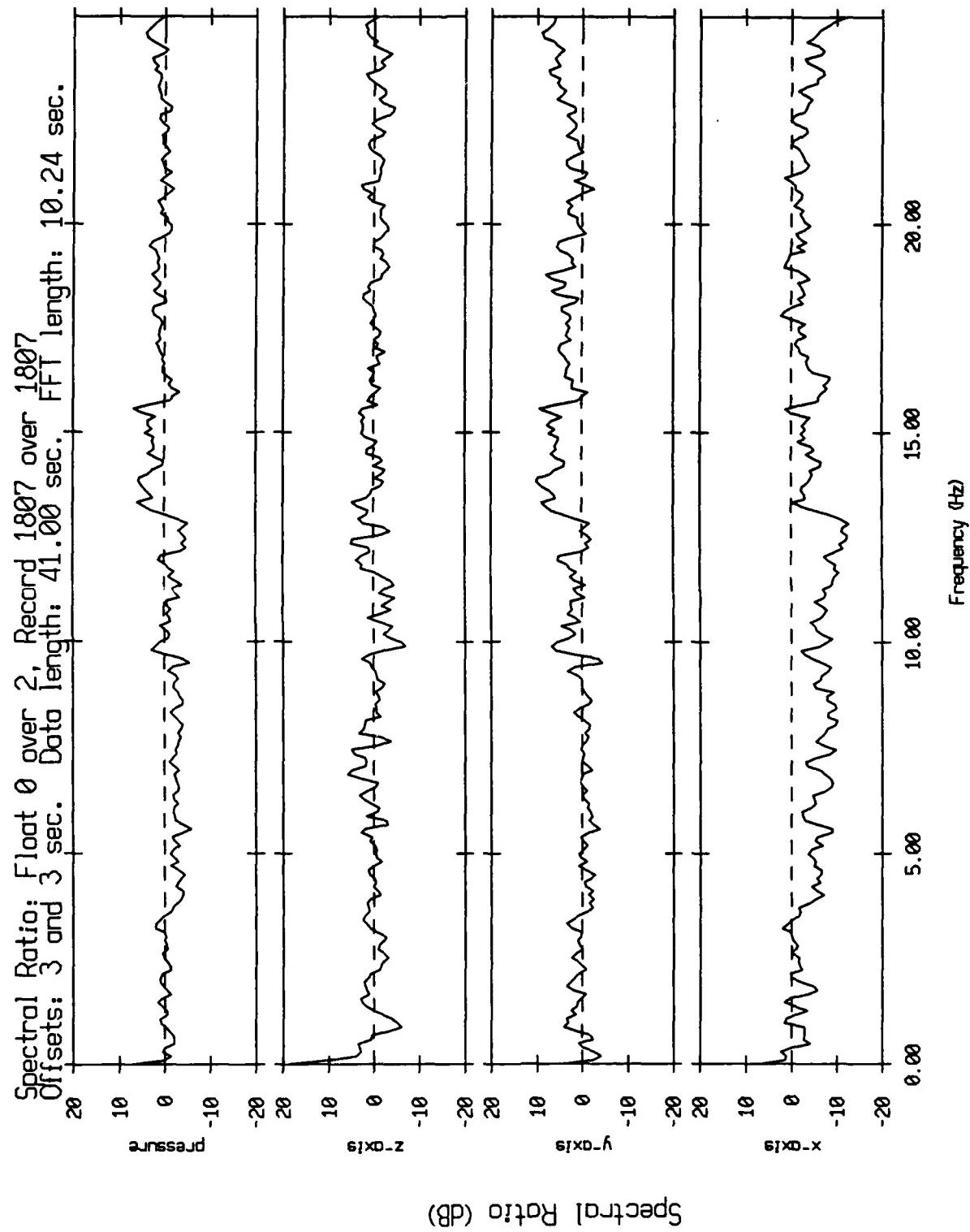


Figure XI.8a

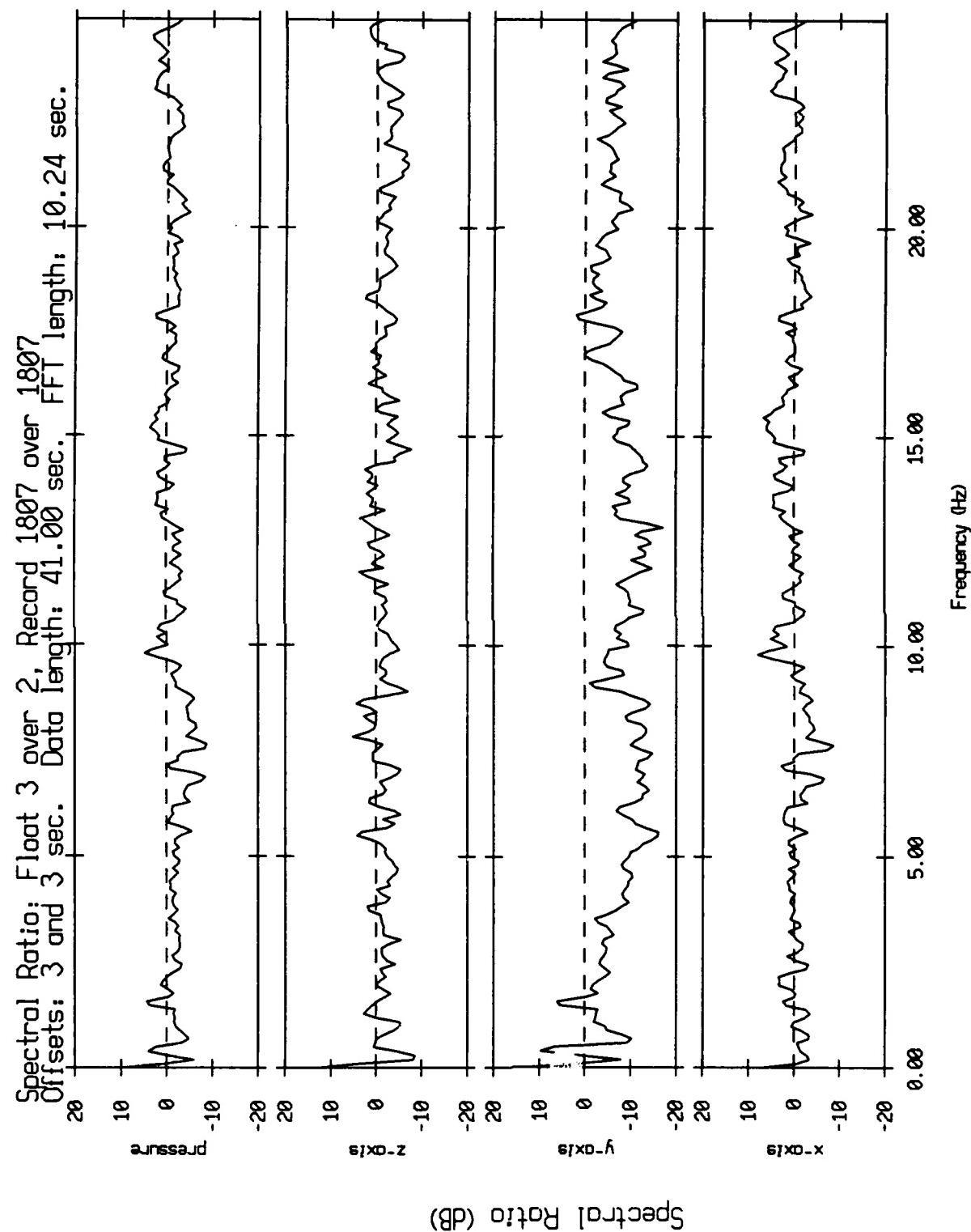


Figure XI.8b

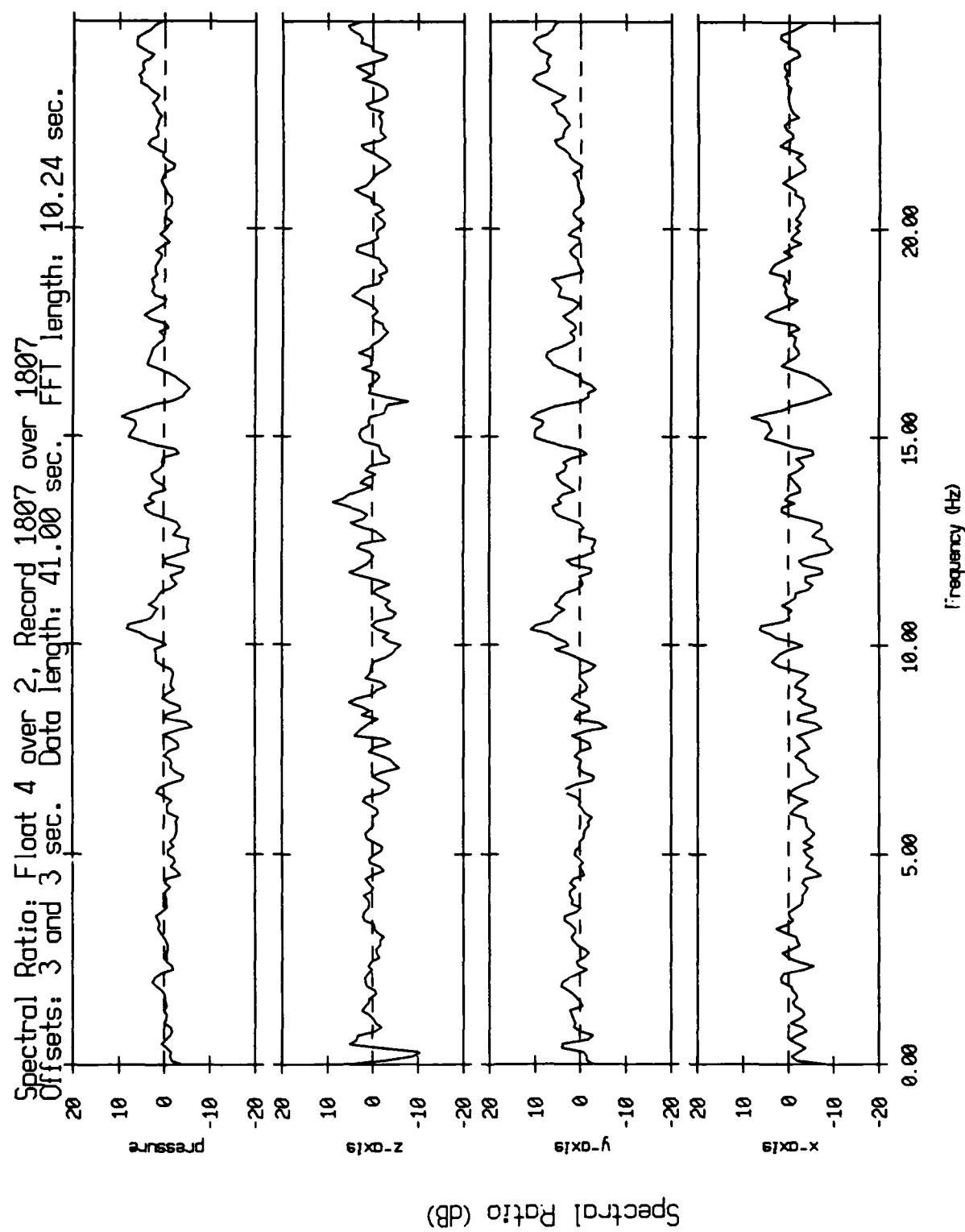


Figure XI.8c

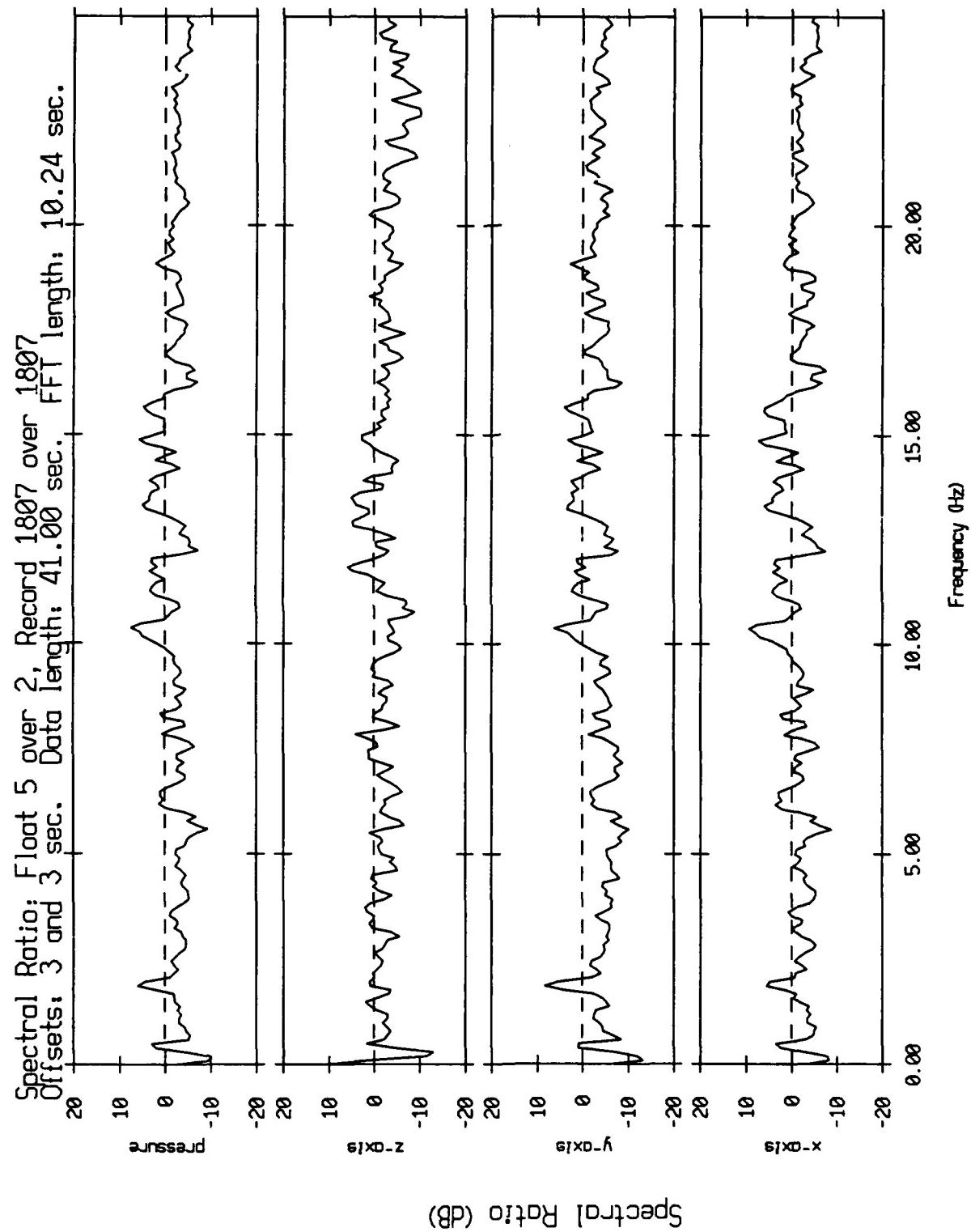


Figure XI.8d

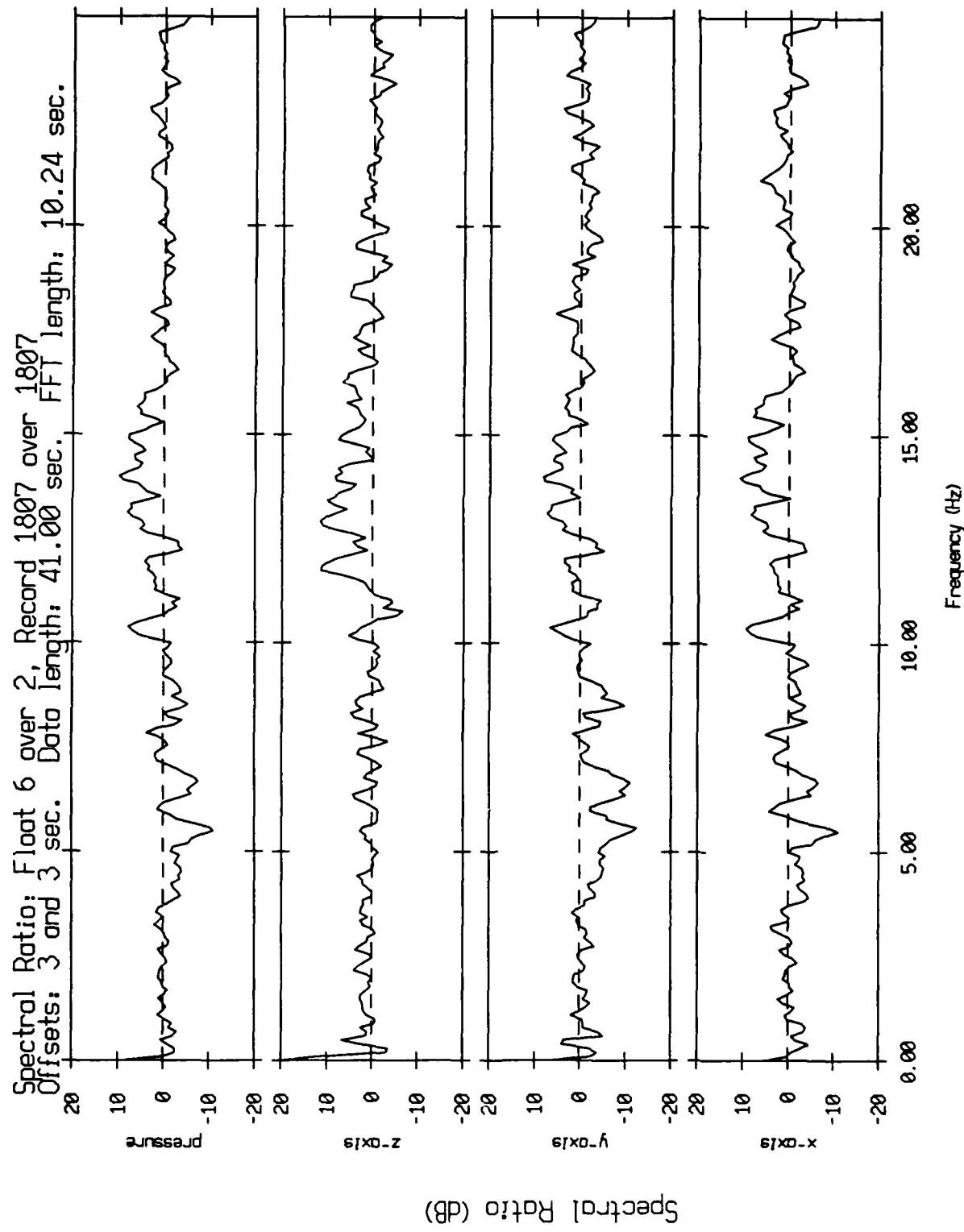


Figure XI.2a

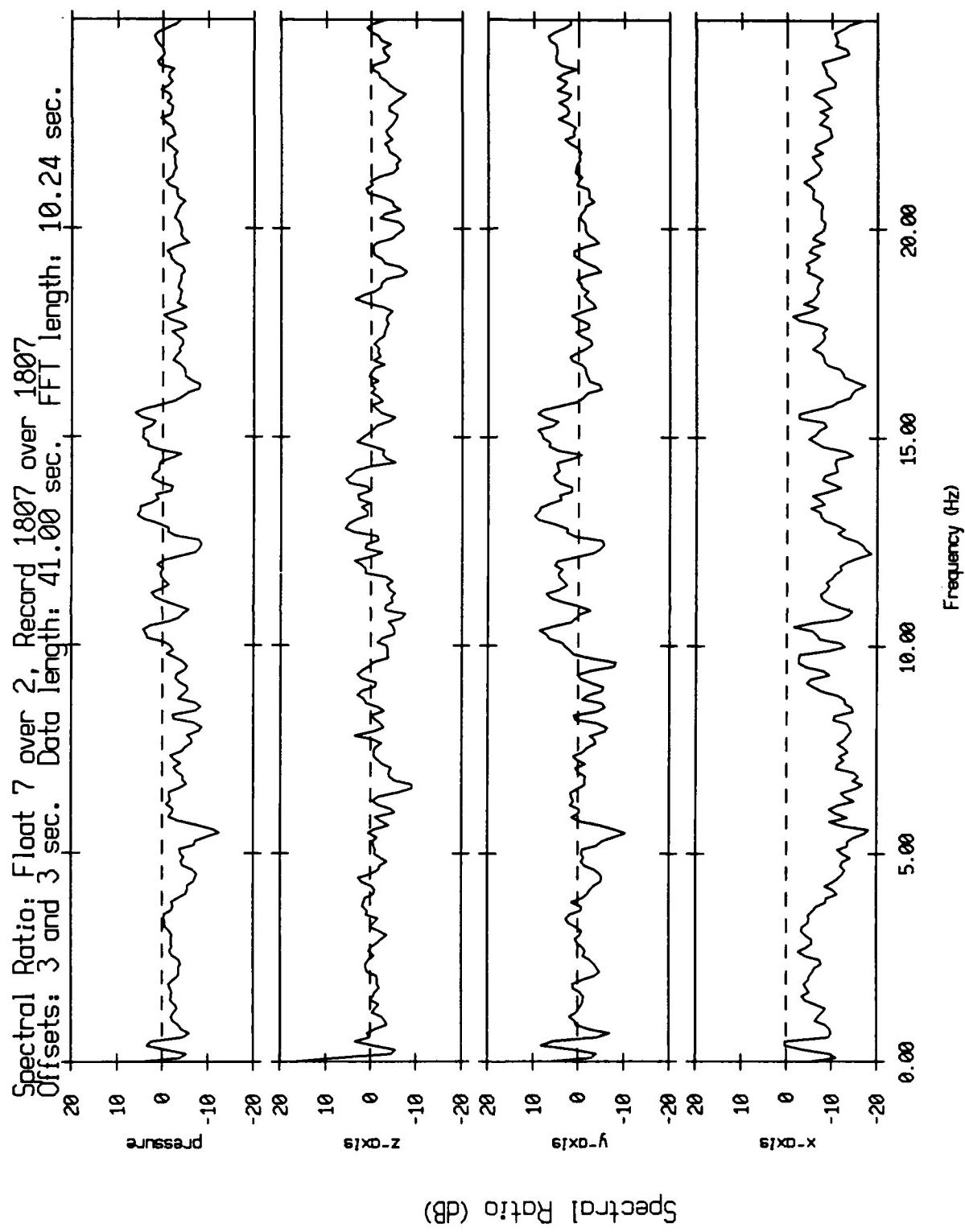


Figure XI.8f

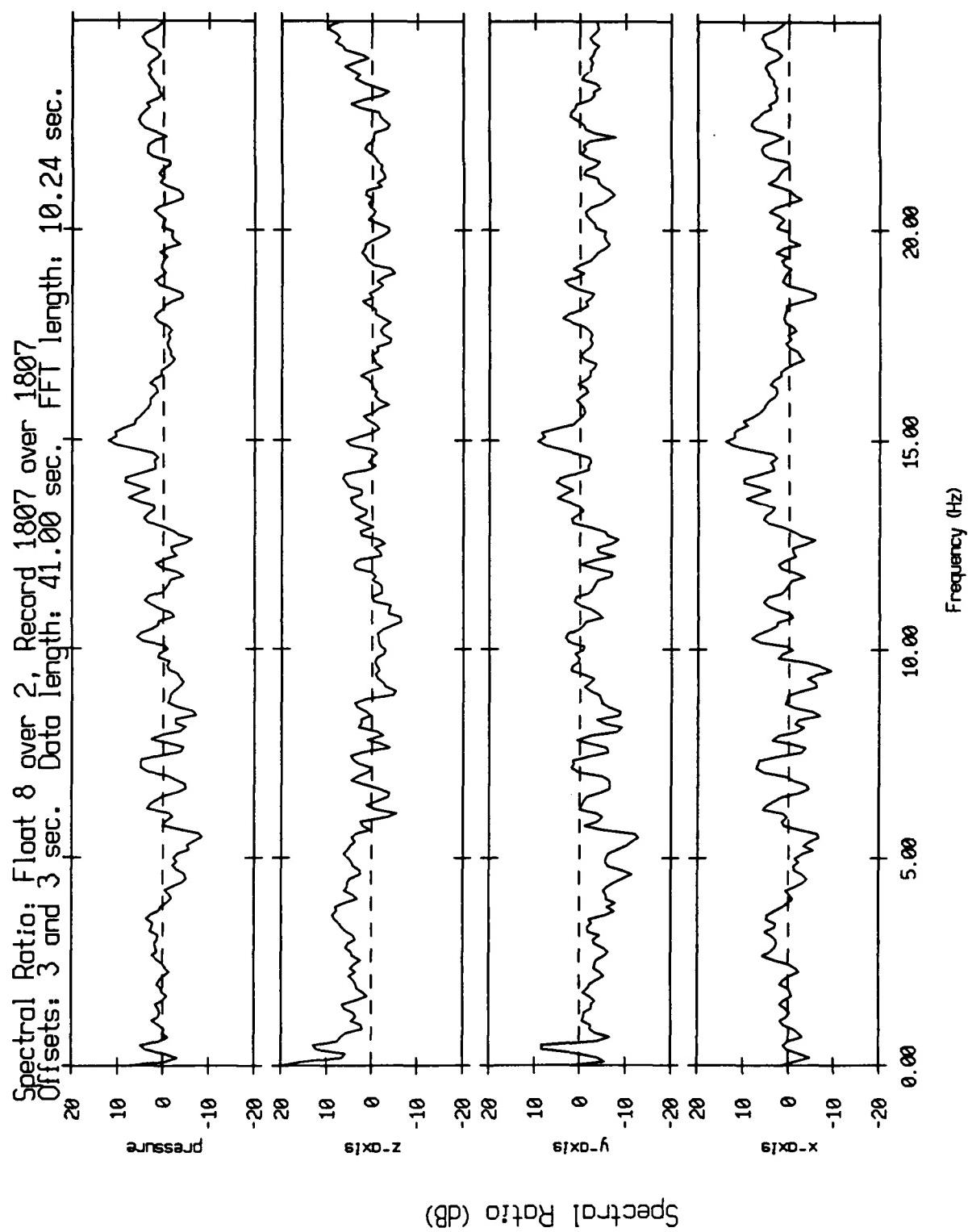


Figure XI.8g

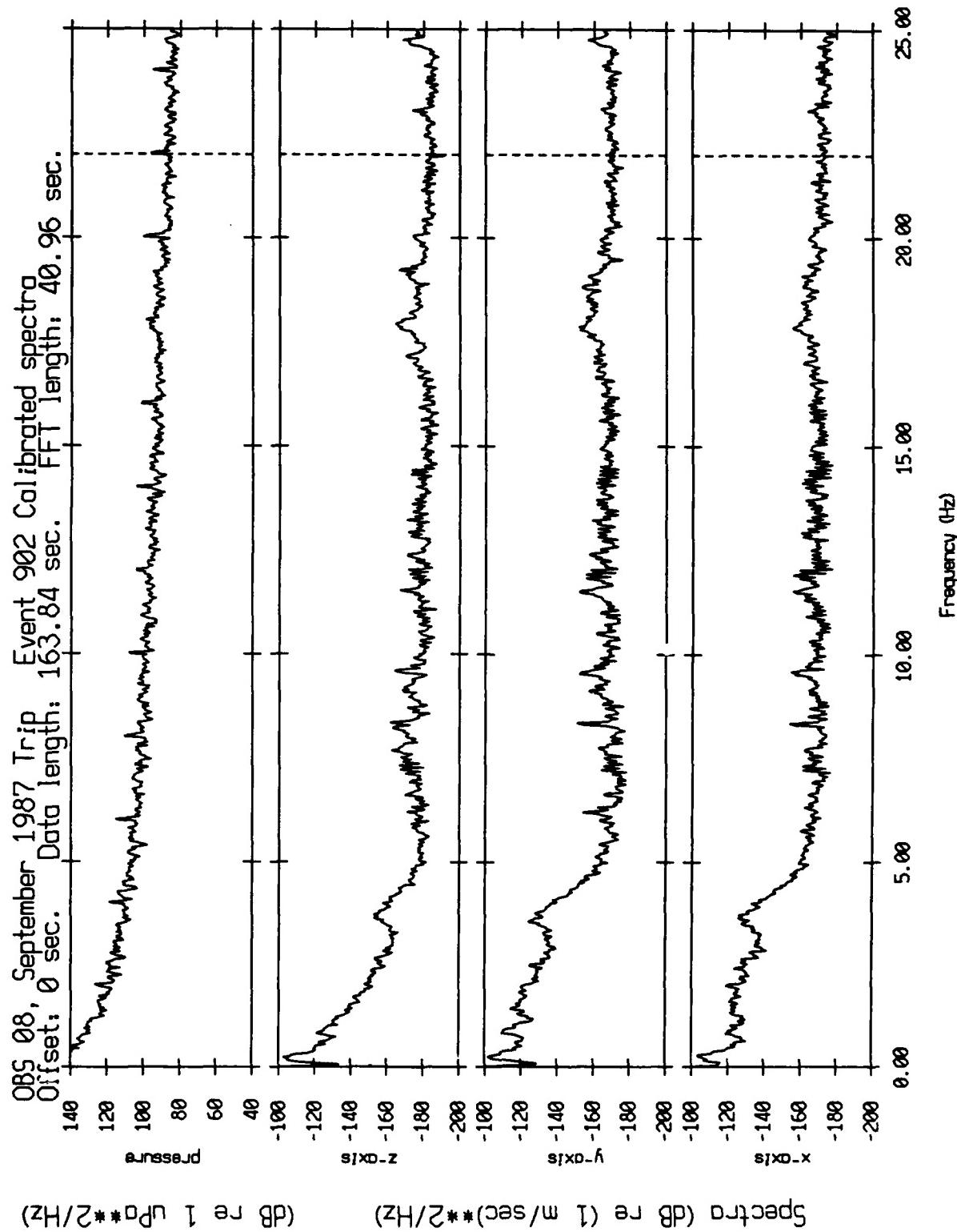


Figure XI.9

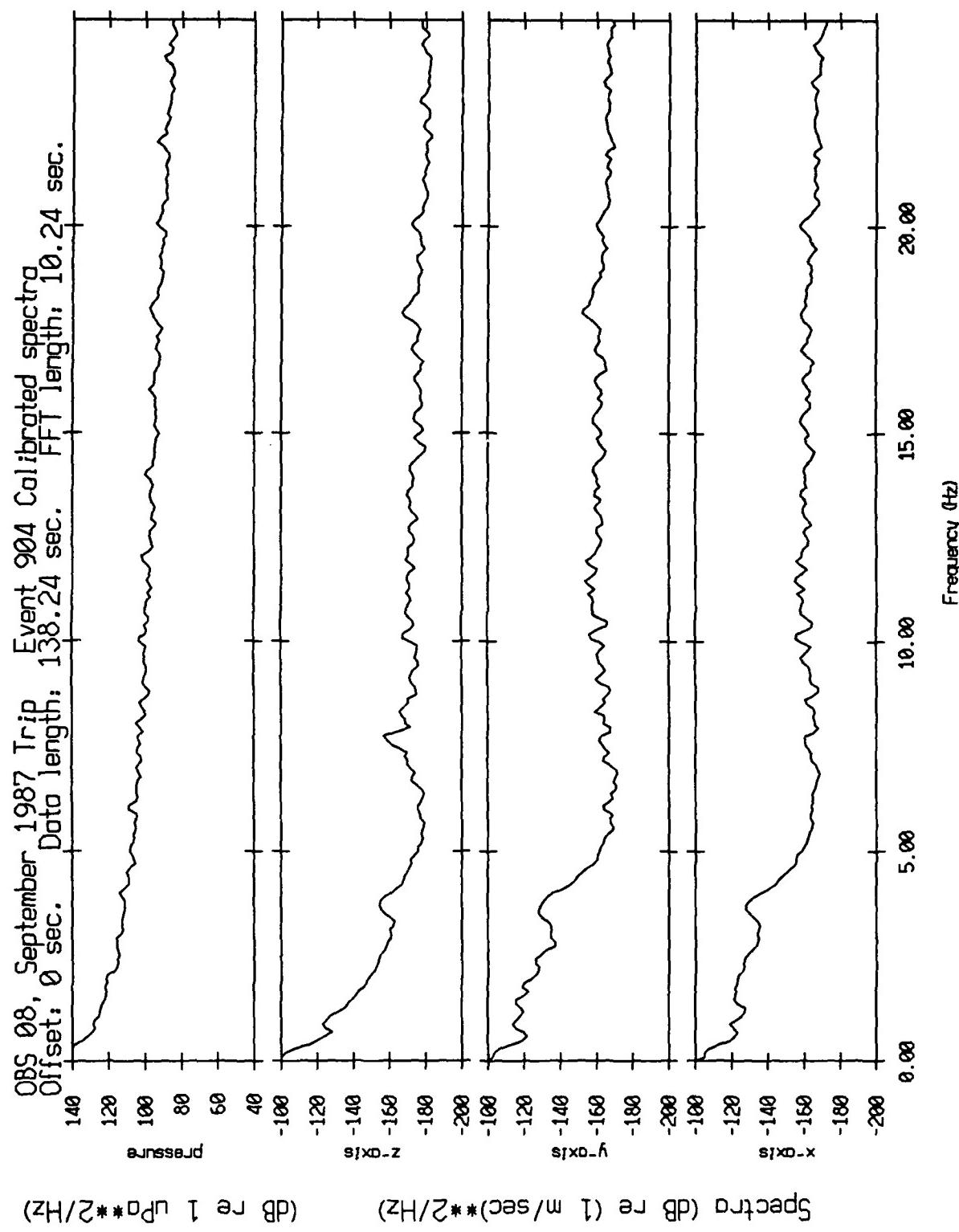


Figure XI.10

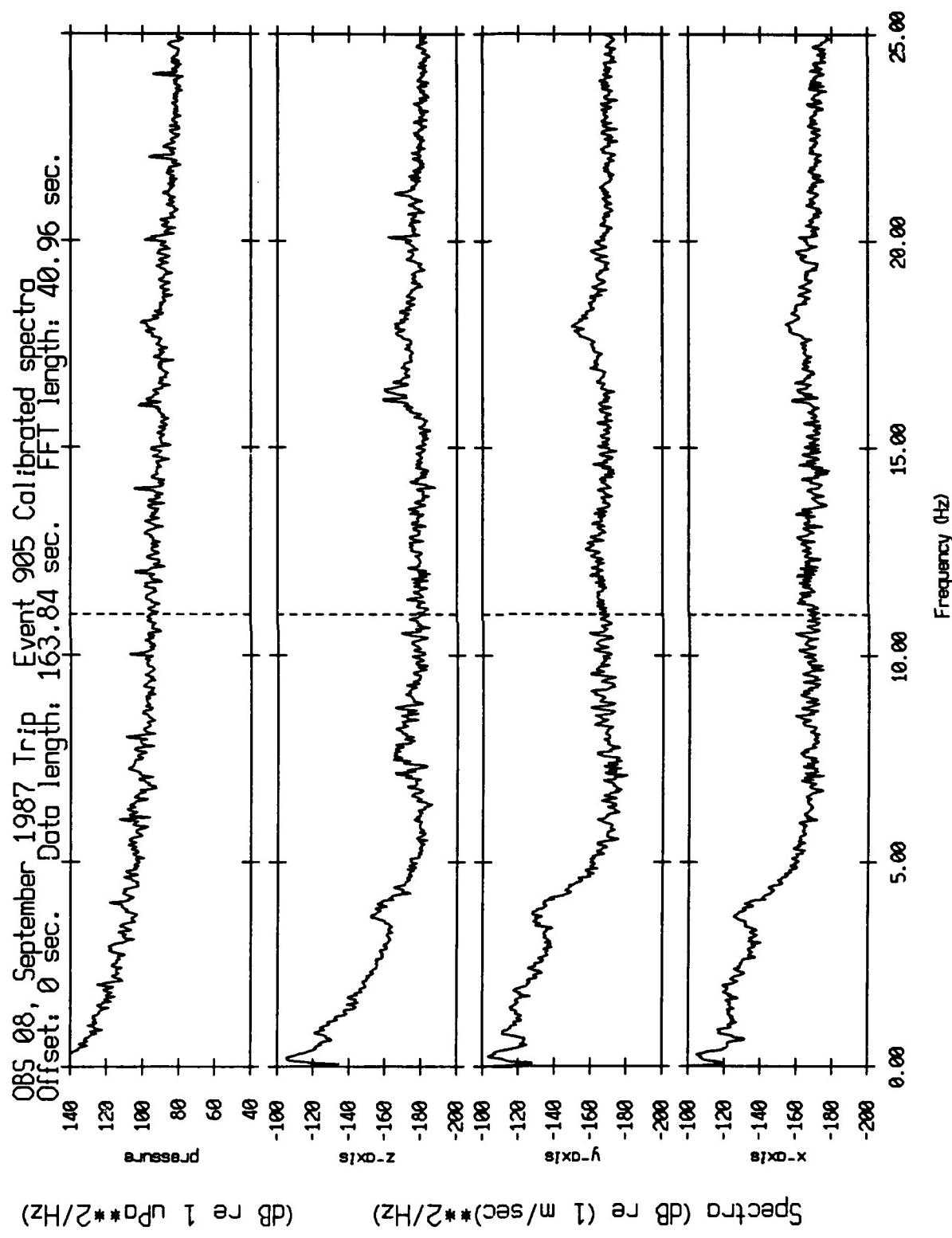


Figure XI.11

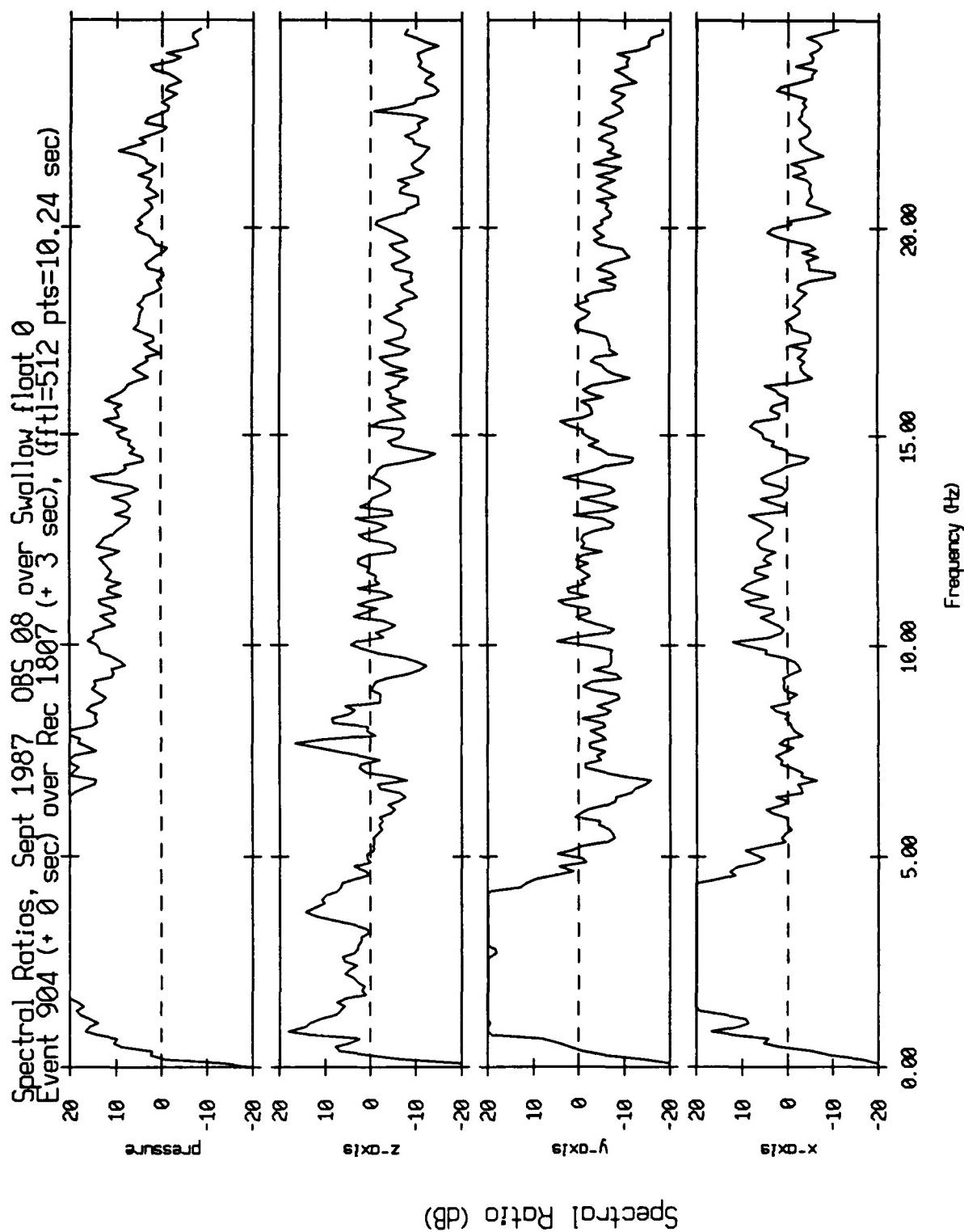


Figure XI.12a

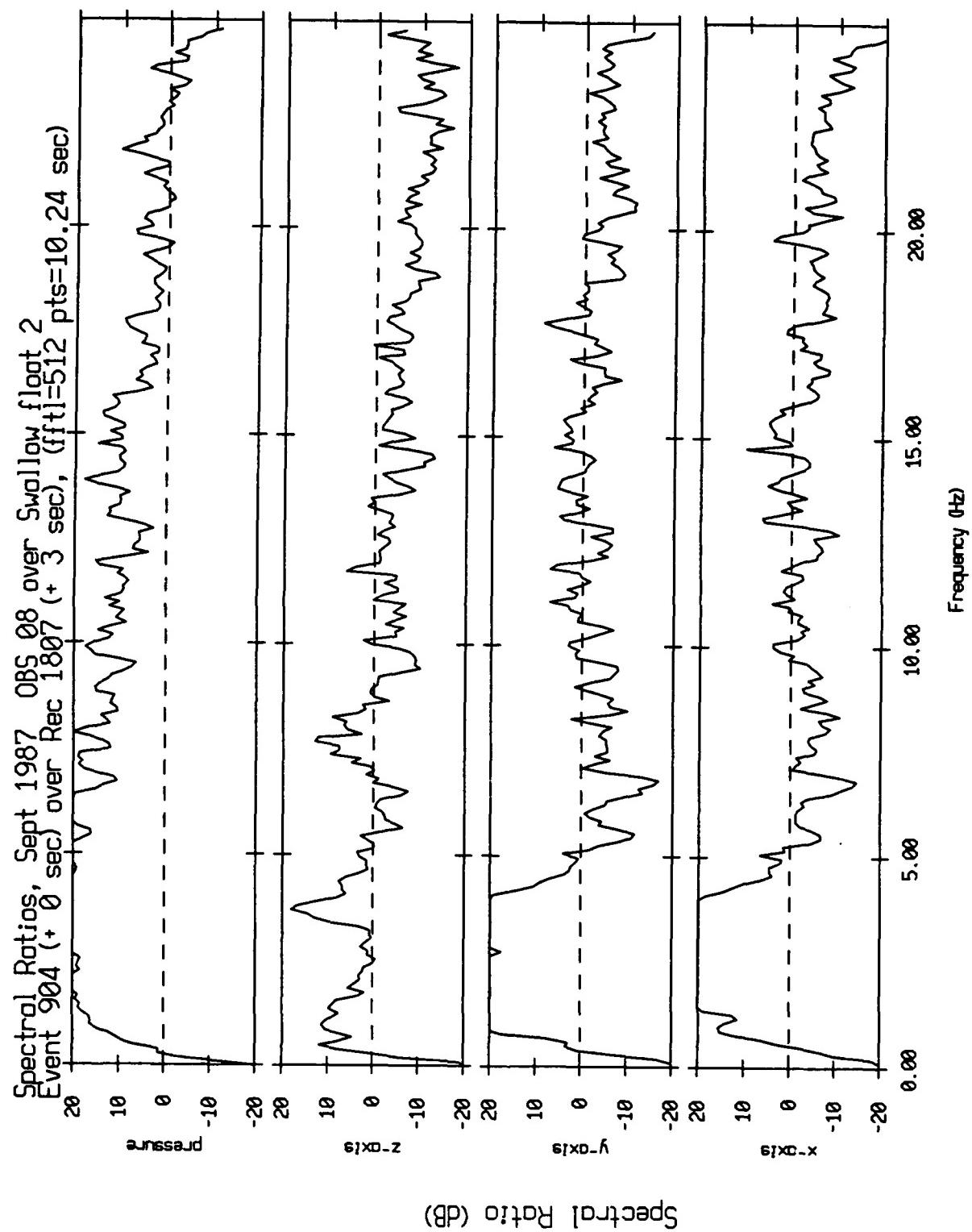


Figure XI.12b

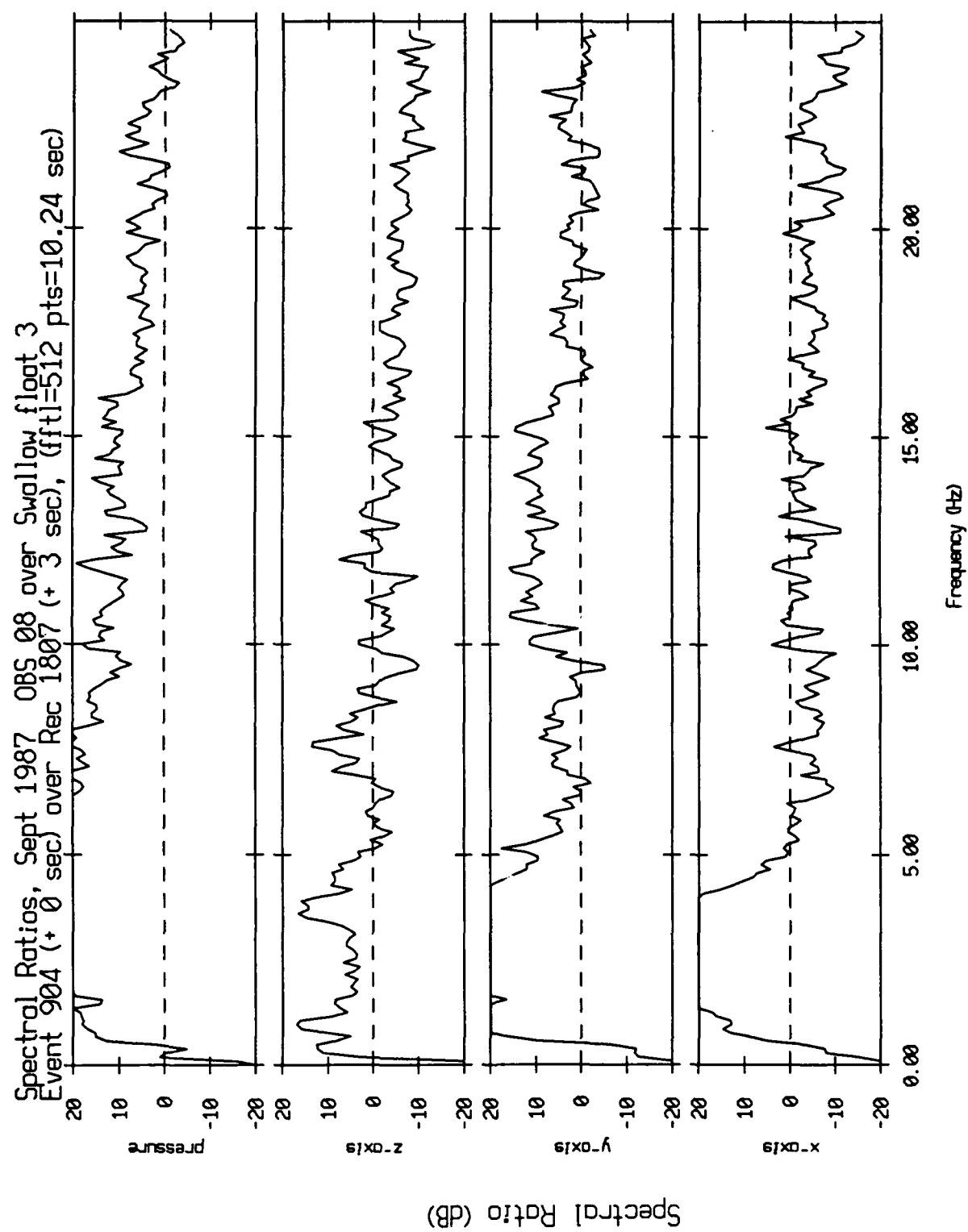


Figure XI.12c

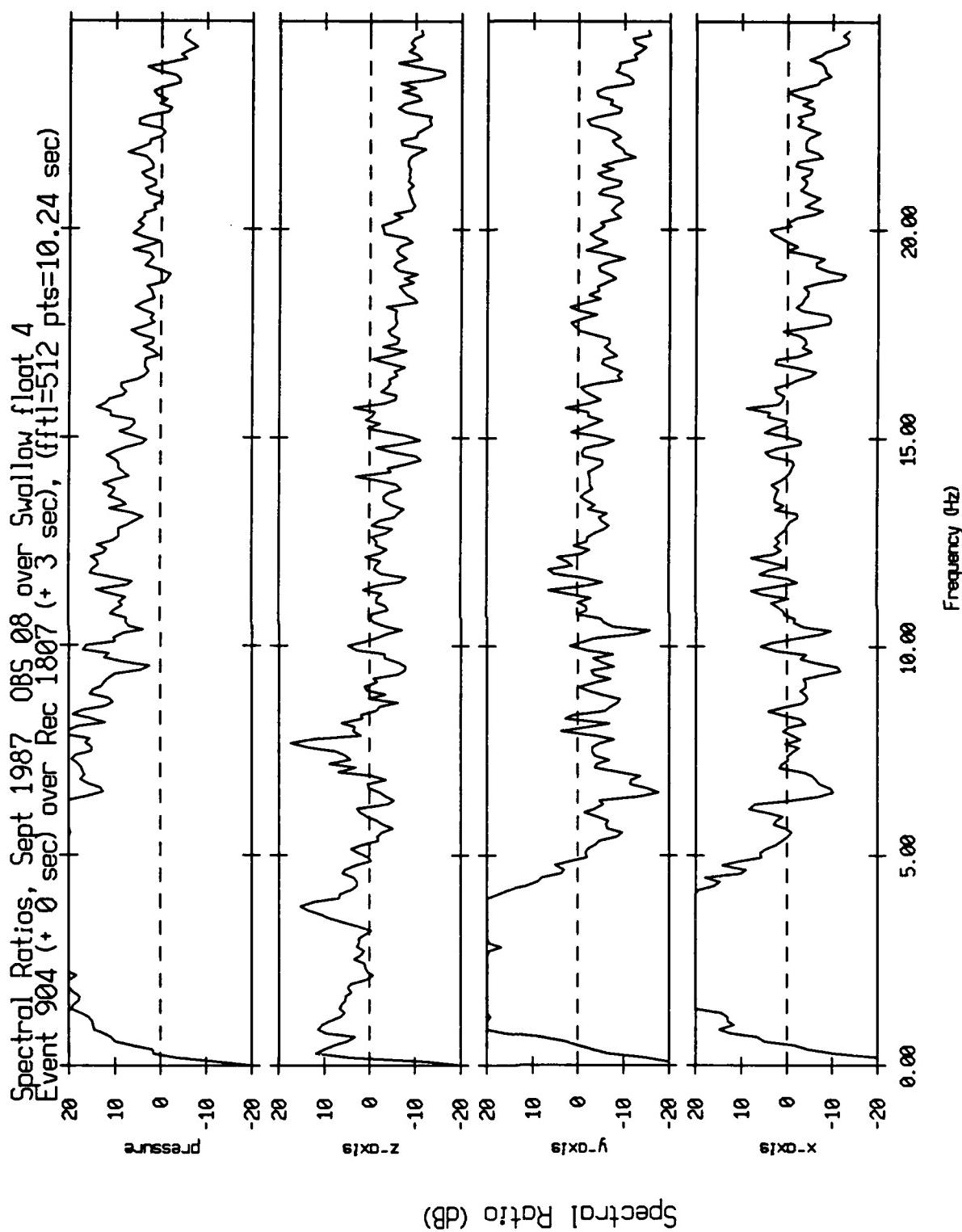


Figure XI.12d

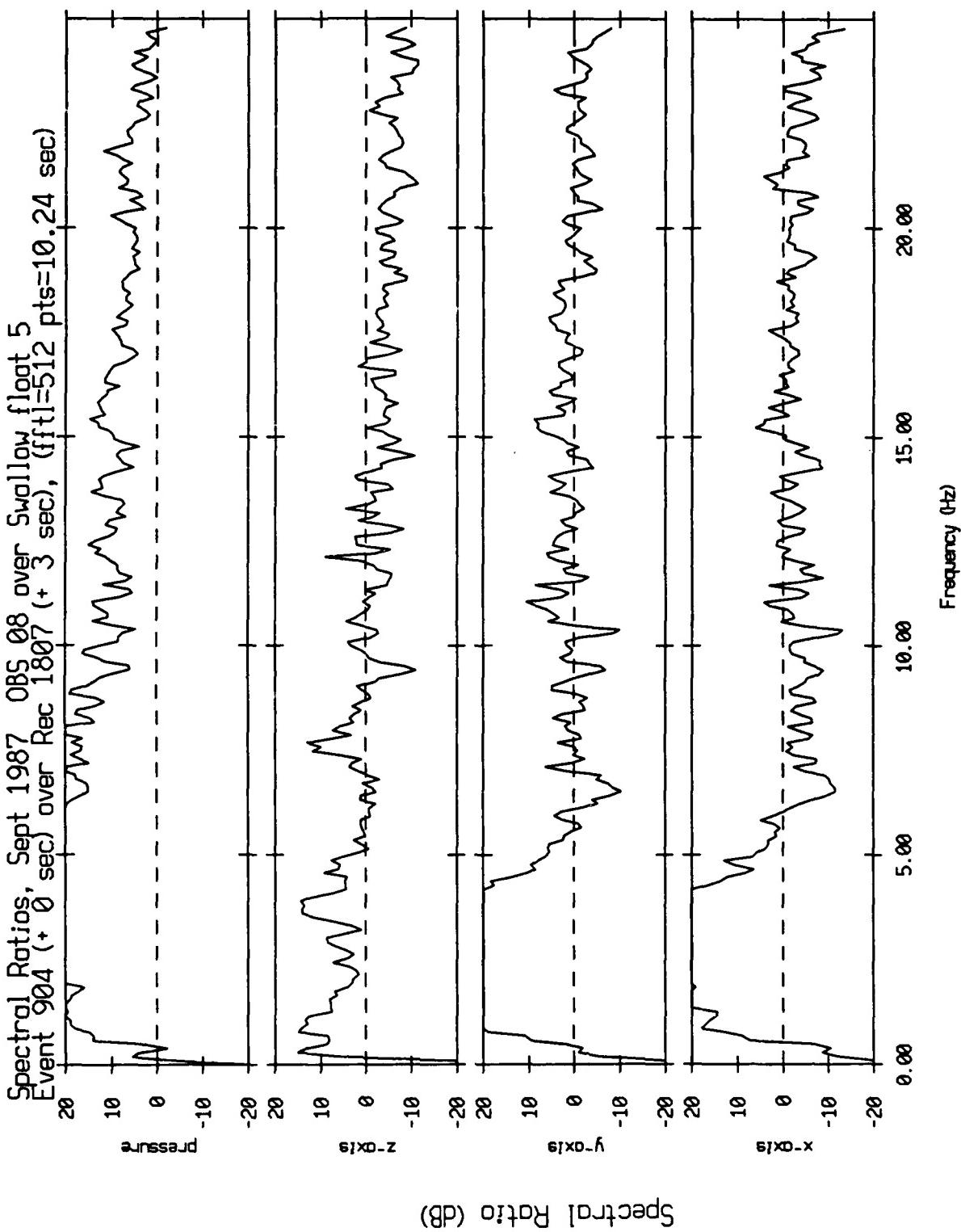


Figure XI.12e

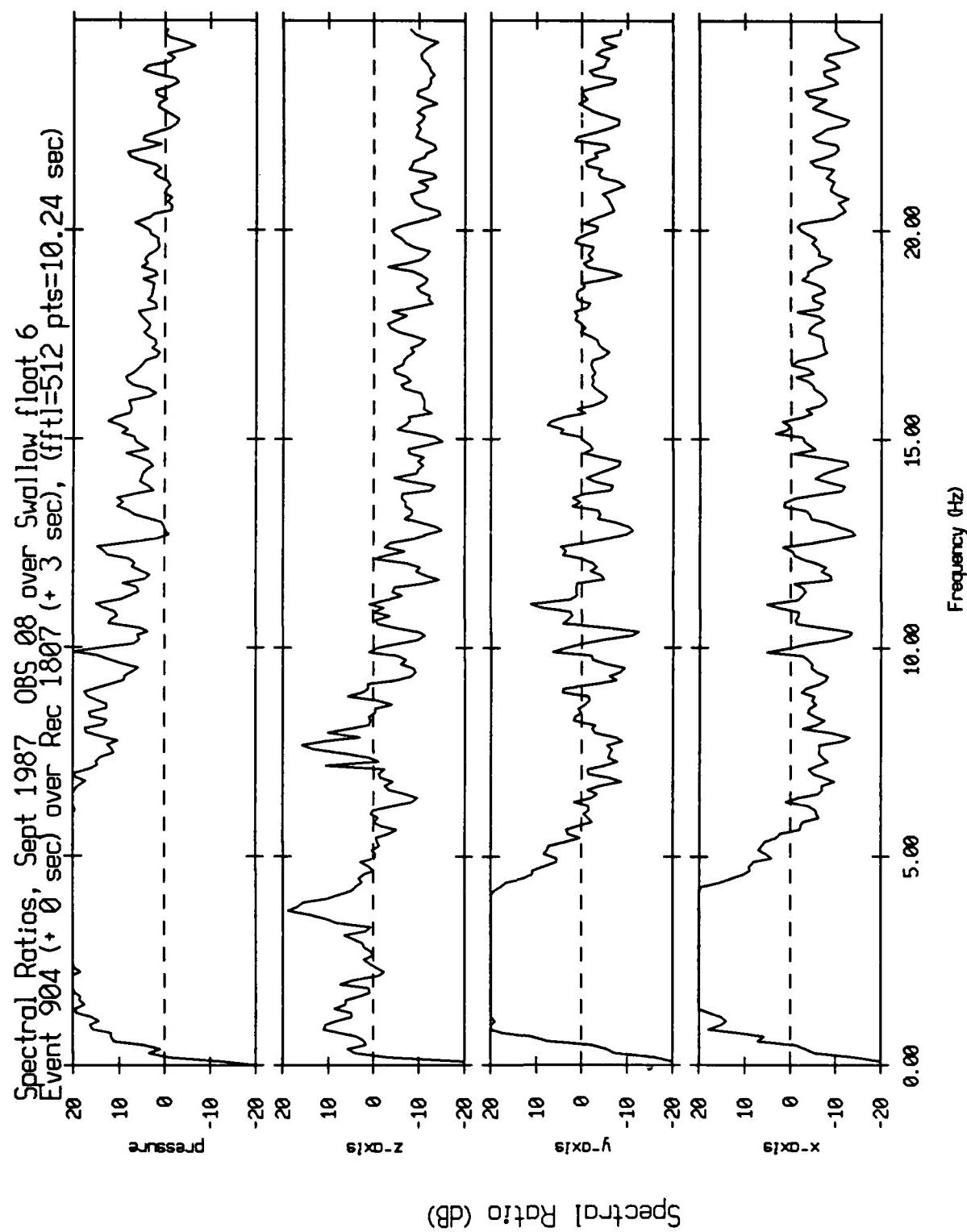


Figure XI.12f

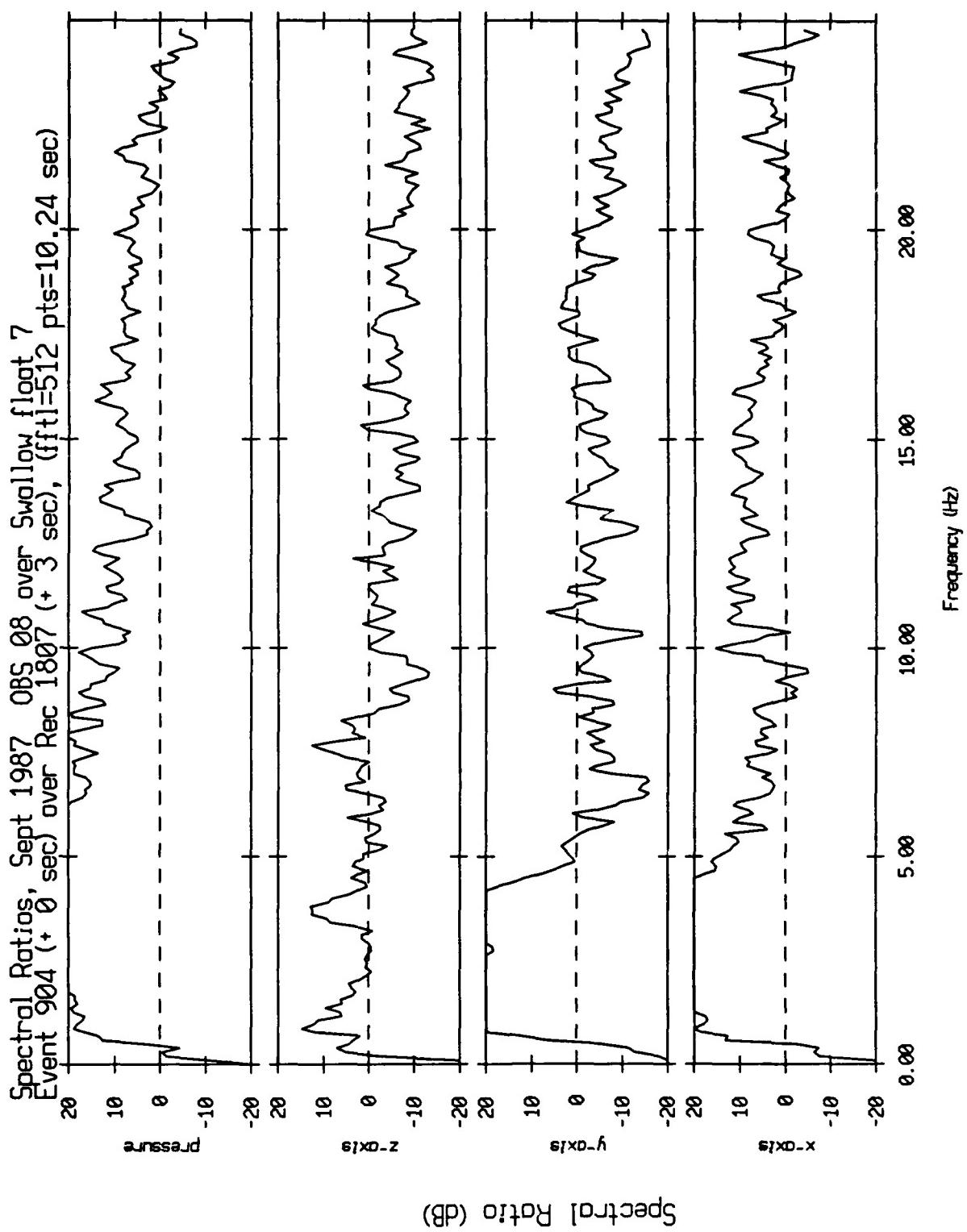


Figure XI.12g

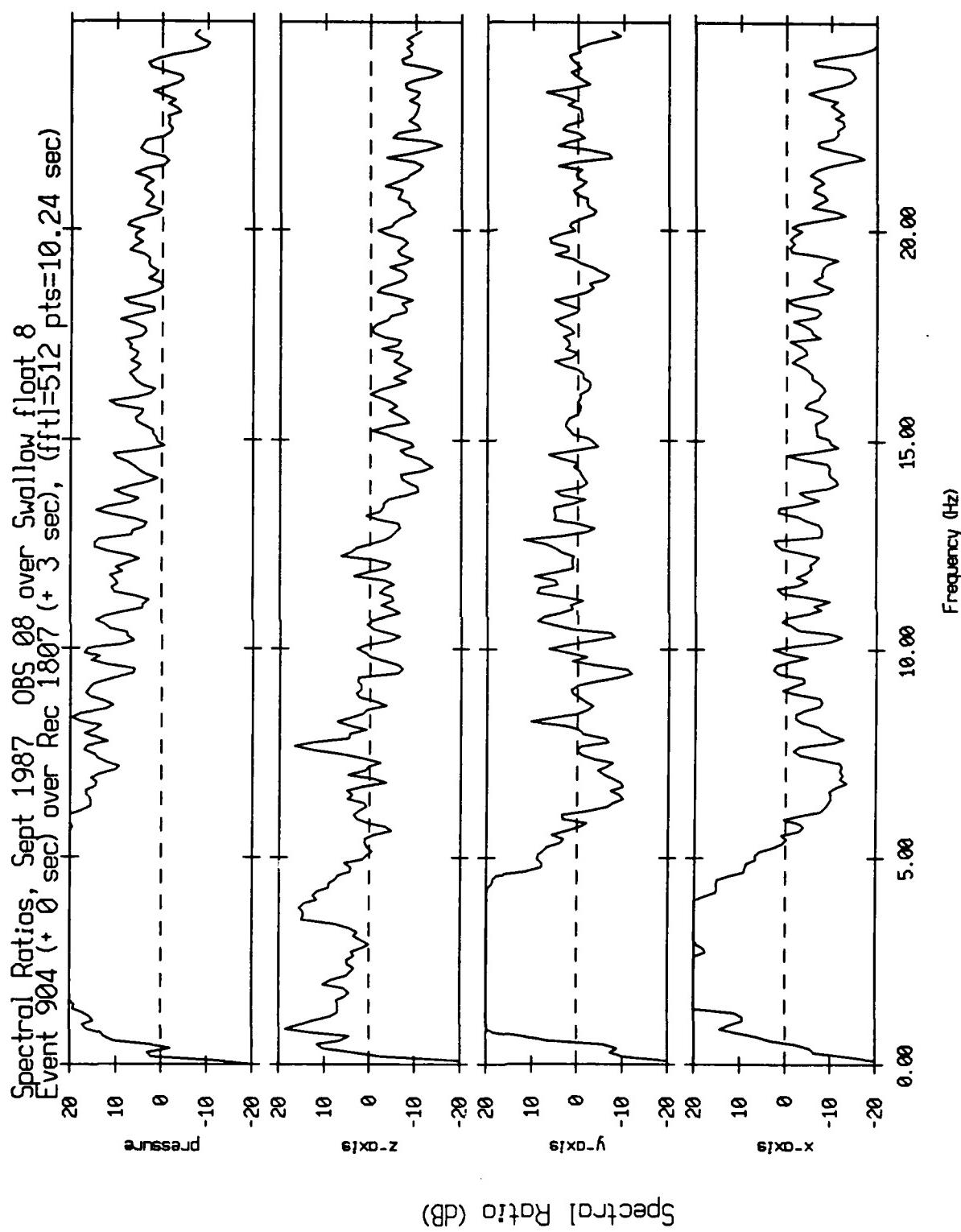


Figure XI.12h

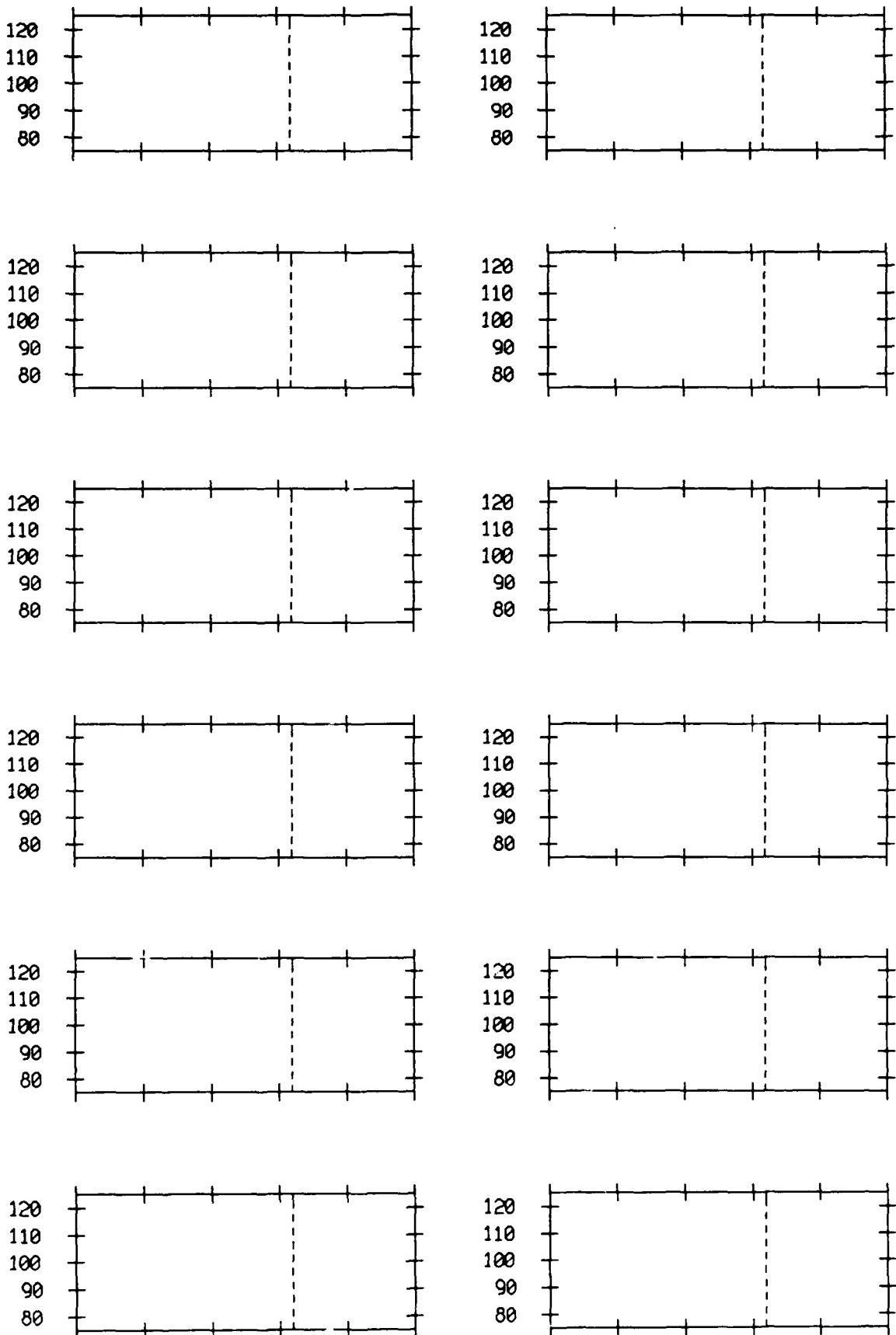


Figure XI.13a

VLA Tape 433, Sept, 1987 - Time 07:45:15 Cal. Pressure Spectra
Data dur.: 532.48 sec. FFT Length: 40.96 sec. Samp Freq: 50 Hz

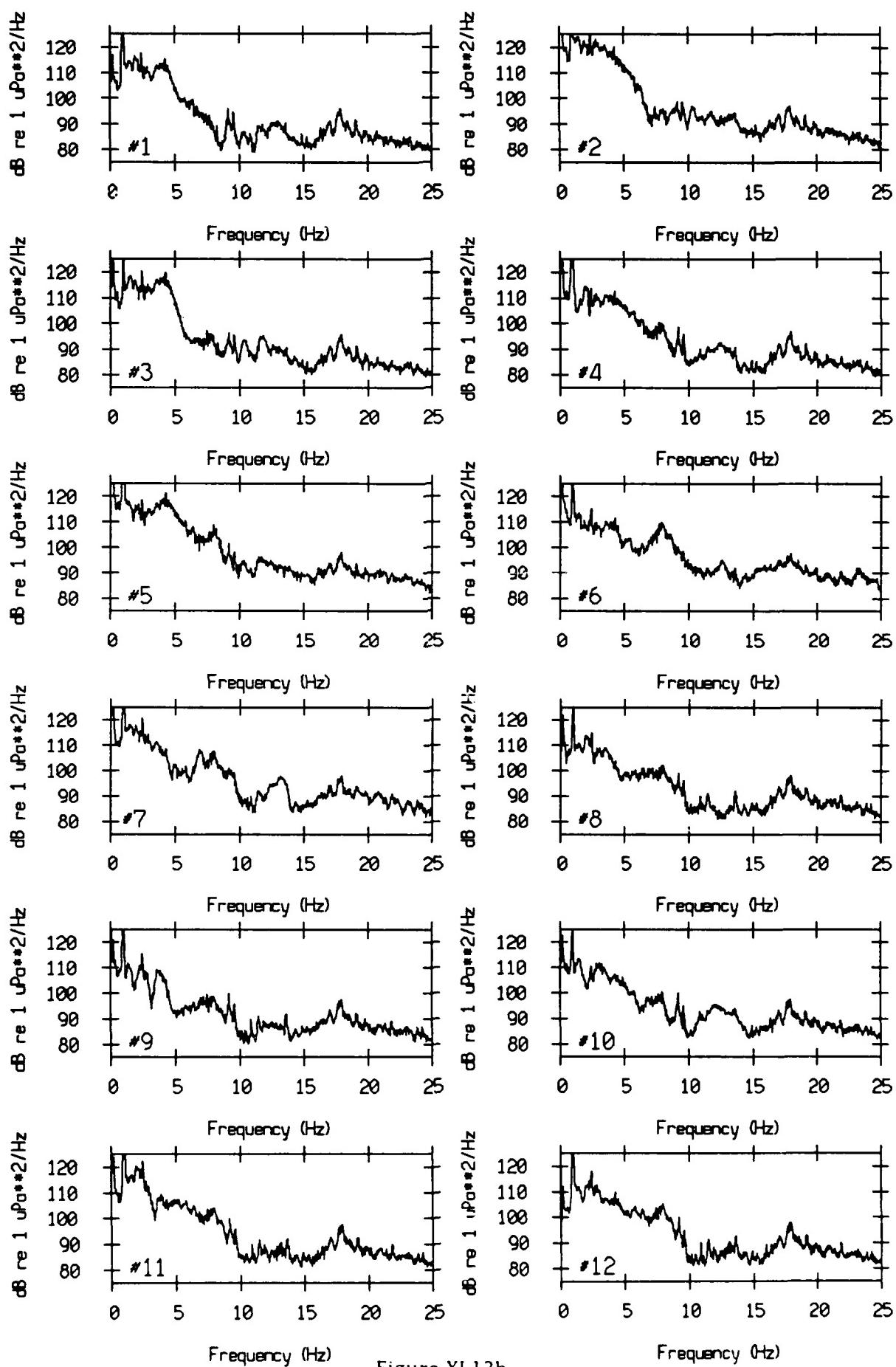


Figure XI.13b

VLA Tape 433, Sept, 1987 - Time 07:45:15 Cal. Pressure Spectra
Data dur.: 532.48 sec. FFT Length: 40.96 sec. Samp Freq: 50 Hz

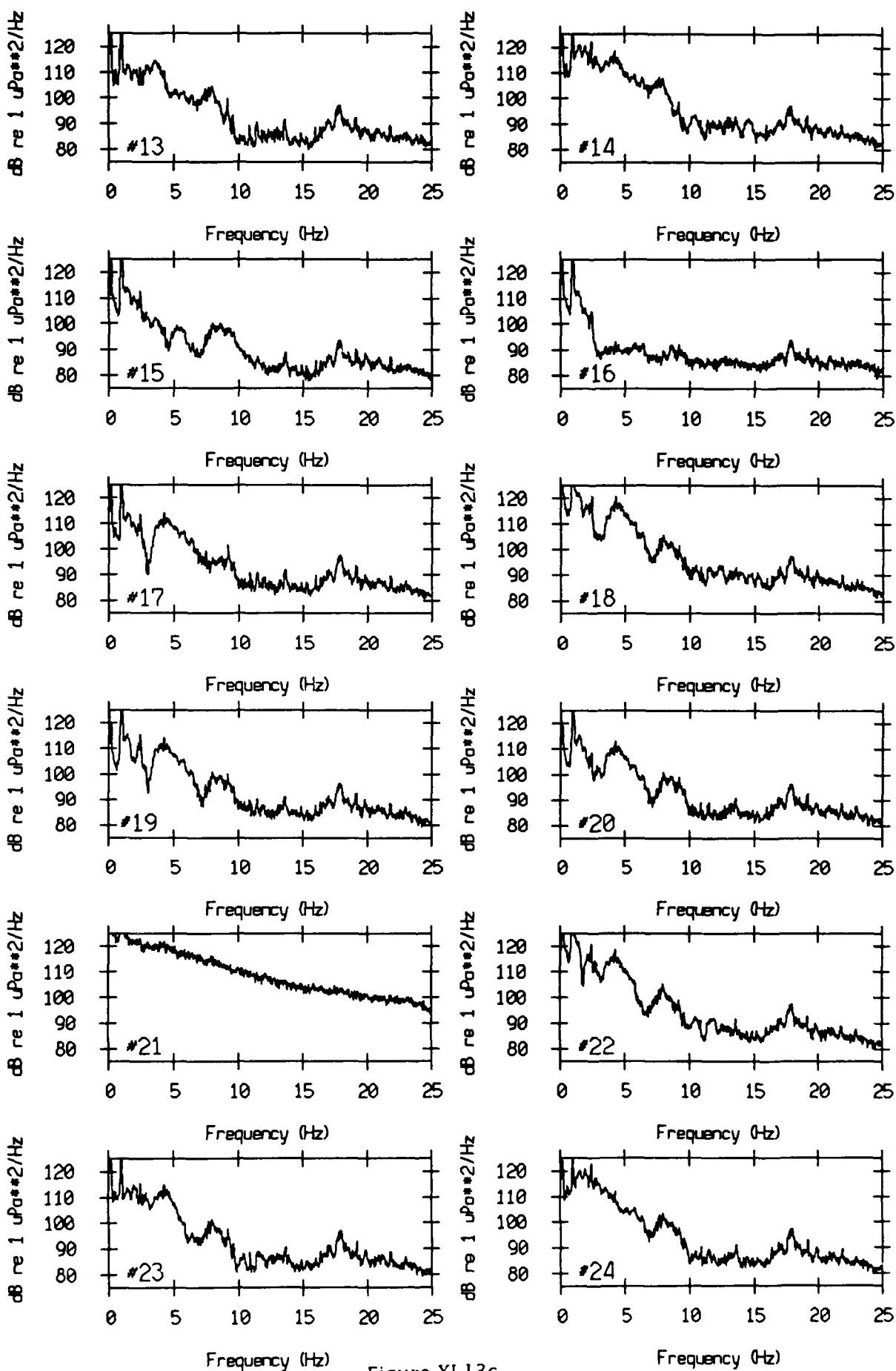


Figure XI.13c

VLA Tape 433, Sept, 1987 - Time 07:45:15 Cal. Pressure Spectra
Data dur.: 532.48 sec. FFT Length: 40.96 sec. Samp Freq: 50 Hz

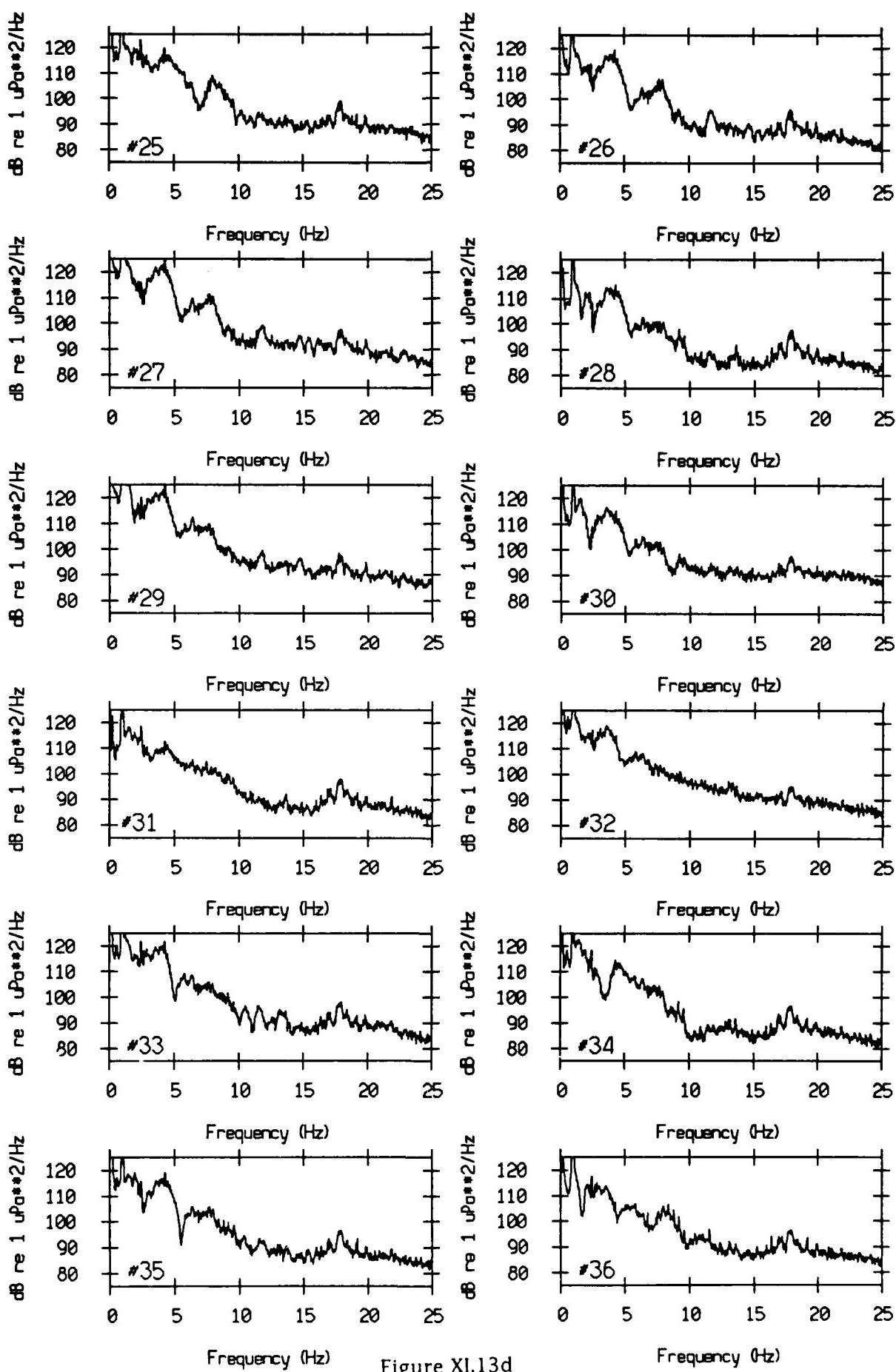


Figure XI.13d

VLA Tape 433, Sept, 1987 - Time 07:45:15 Cal. Pressure Spectro
Data dur.: 532.48 sec. FFT Length: 40.96 sec. Samp Freq: 50 Hz

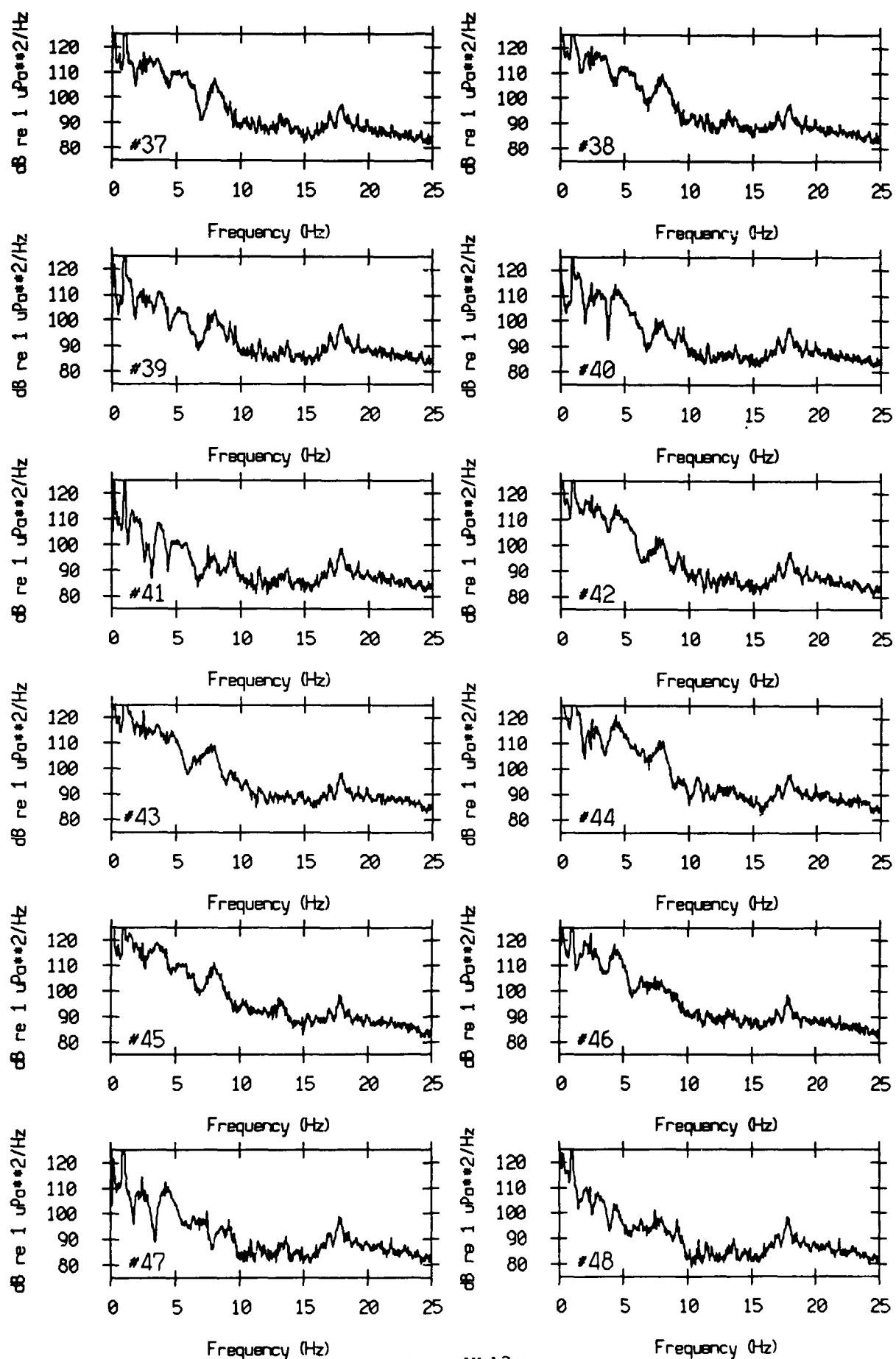


Figure XI.13e

VLA Tape 433, Sept, 1987 - Time 07:45:15 Cal. Pressure Spectra
Data dur.: 532.48 sec. FFT Length: 40.96 sec. Samp Freq: 50 Hz

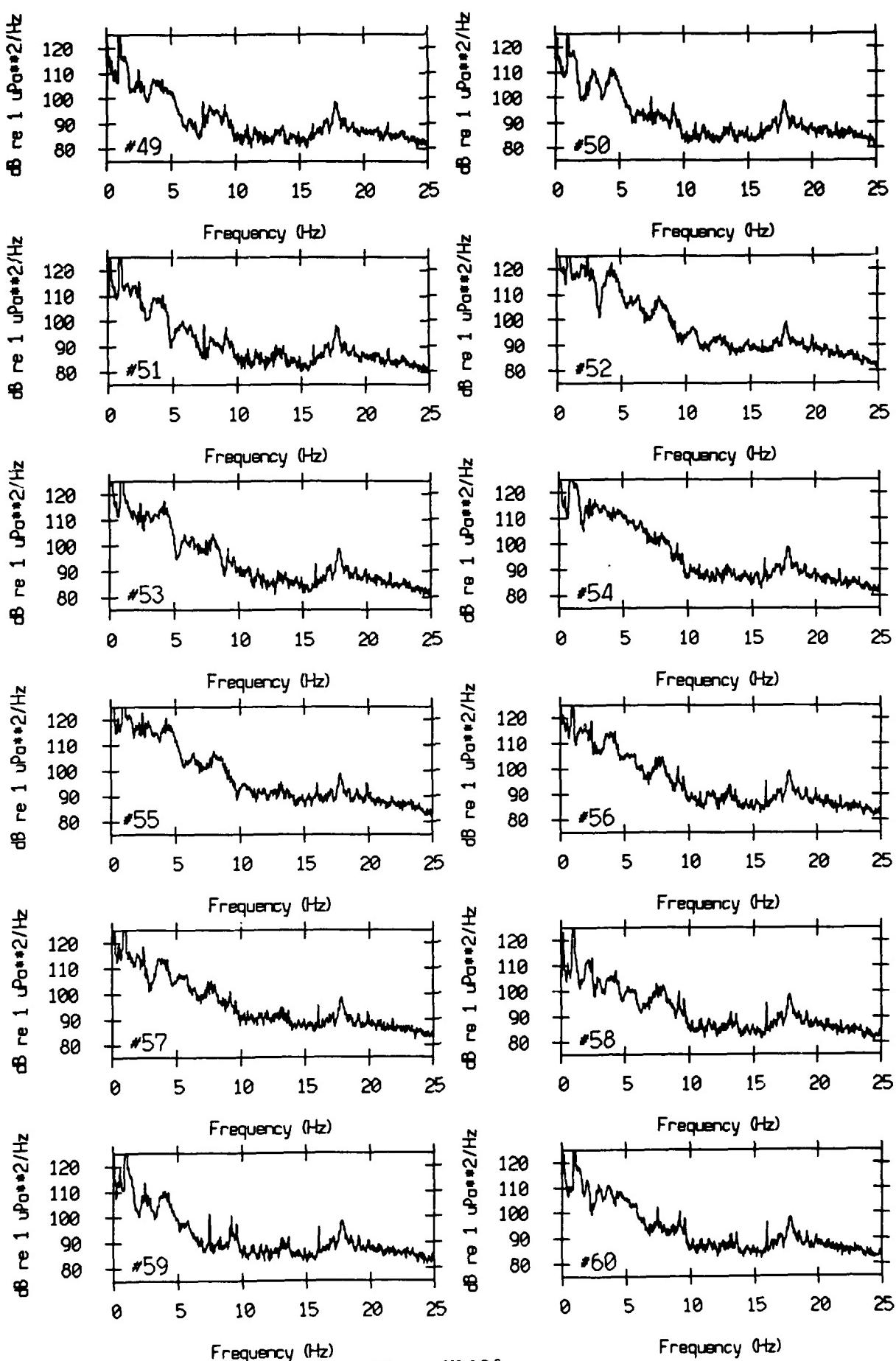


Figure XI.13f

VLA Tape 433, Sept, 1987 - Time 07:45:15 Cal. Pressure Spectro
Data dur.: 532.48 sec. FFT Length: 40.96 sec. Samp Freq: 50 Hz

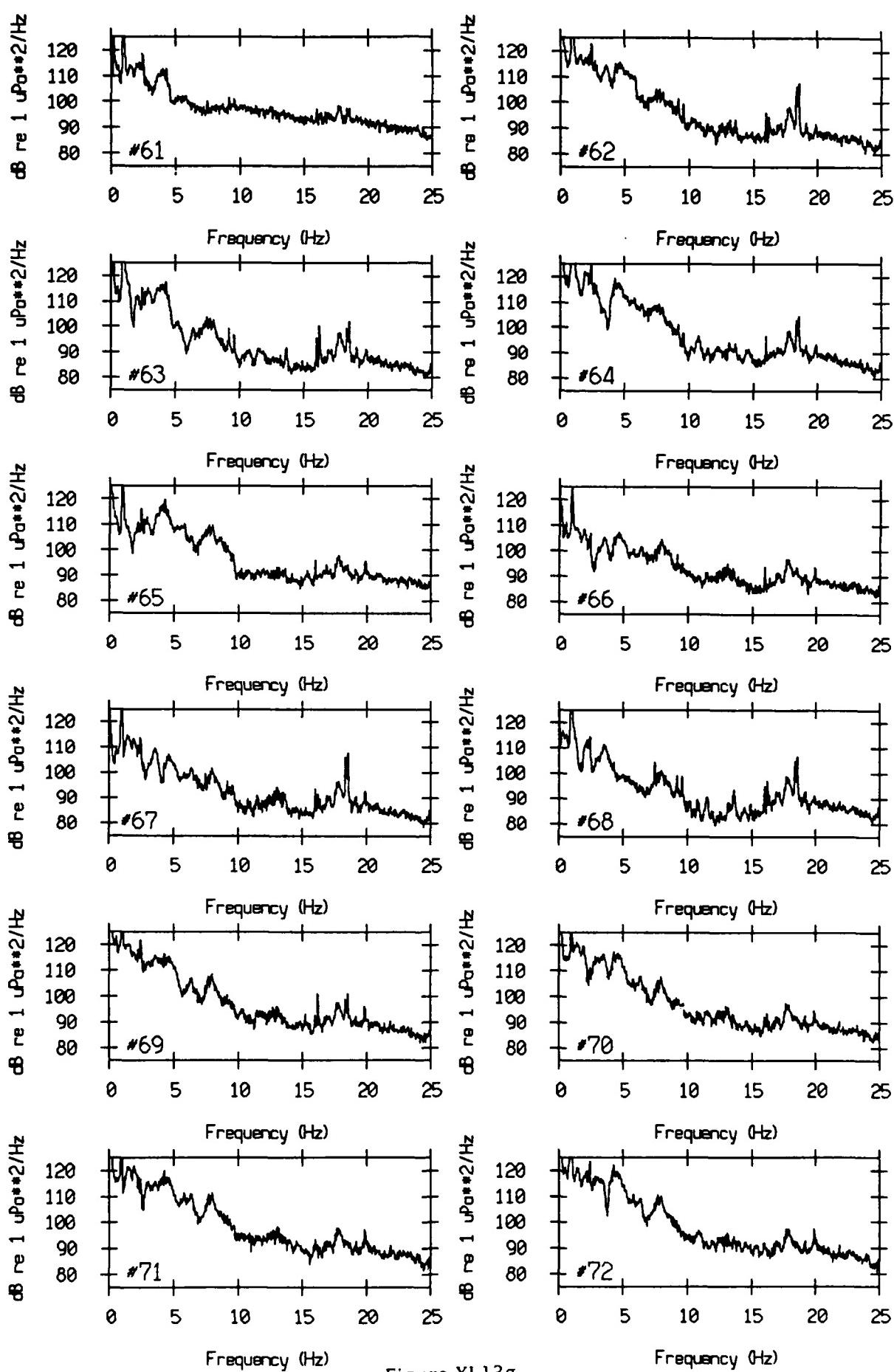


Figure XI.13g

VLA Tape 433, Sept, 1987 - Time 07:45:15 Cal. Pressure Spectra
Data dur.: 532.48 sec. FFT Length: 40.96 sec. Samp Freq: 50 Hz

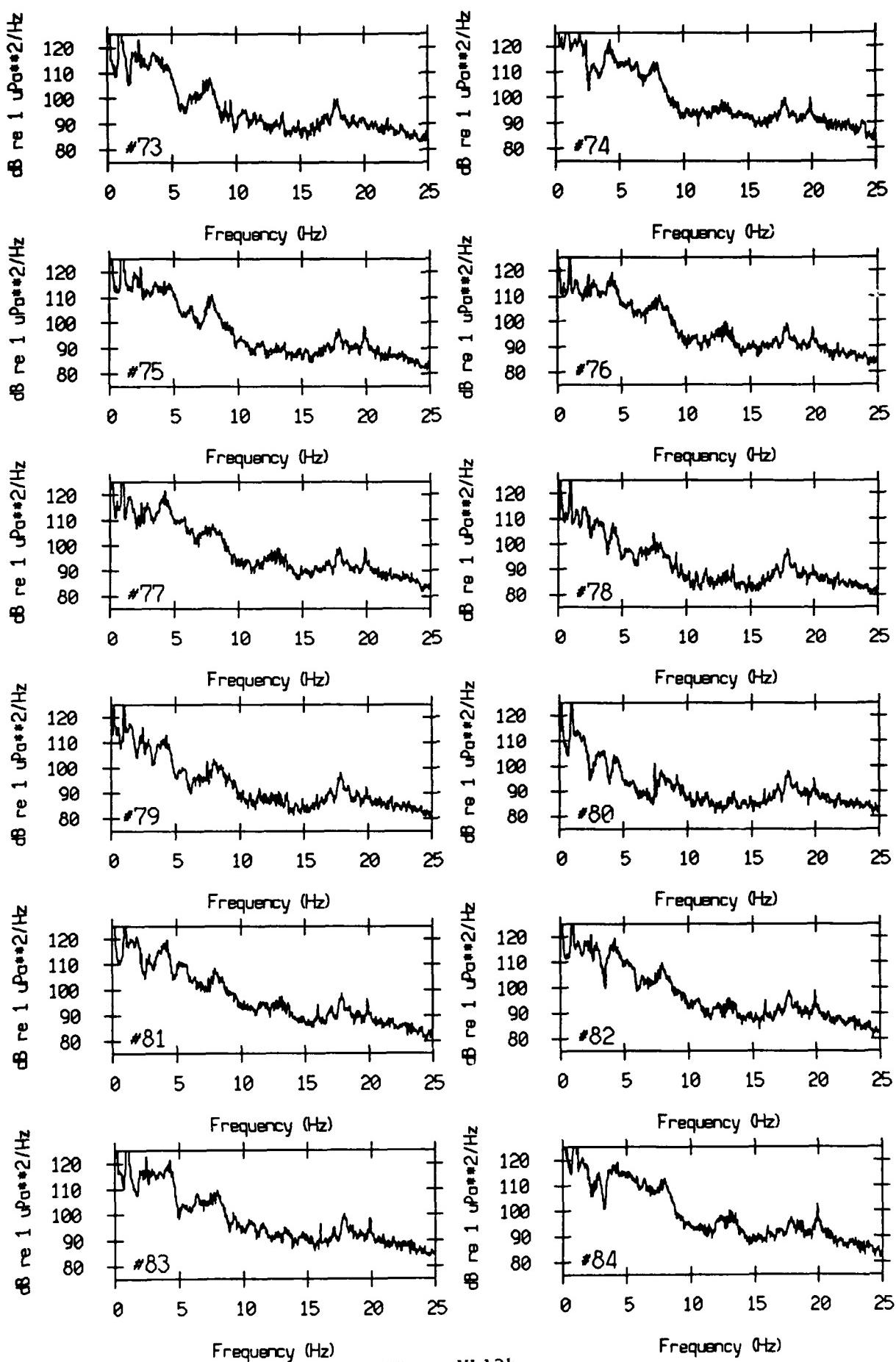


Figure XI.13h

VLA Tape 433, Sept, 1987 - Time 07:45:15 Cal. Pressure Spectra
Data dur.: 532.48 sec. FFT Length: 40.96 sec. Samp Freq: 50 Hz

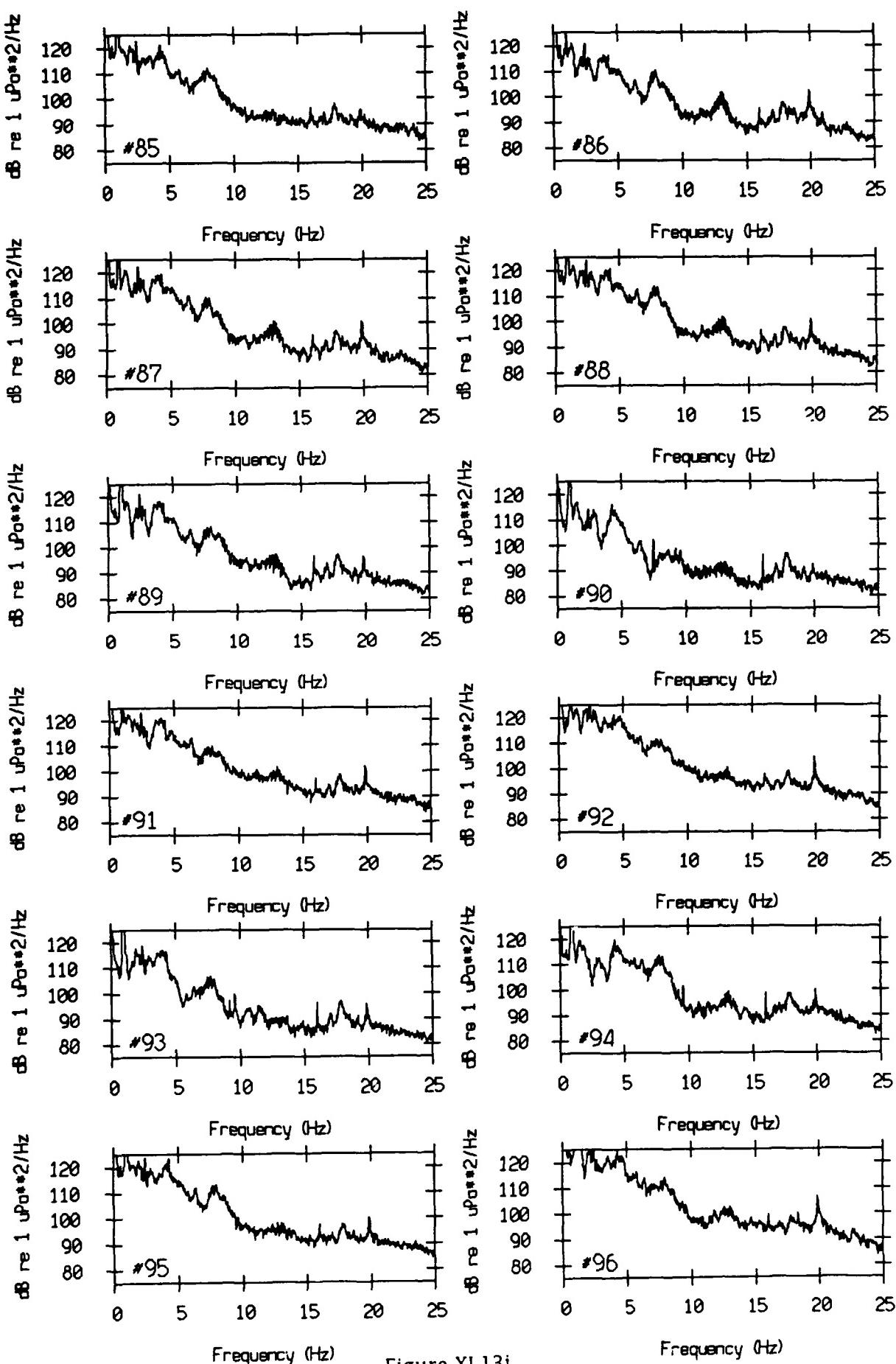


Figure XI.13i

VLA Tape 433, Sept, 1987 - Time 07:45:15 Cal. Pressure Spectro
Data dur.: 532.48 sec. FFT Length: 40.96 sec. Samp Freq: 50 Hz

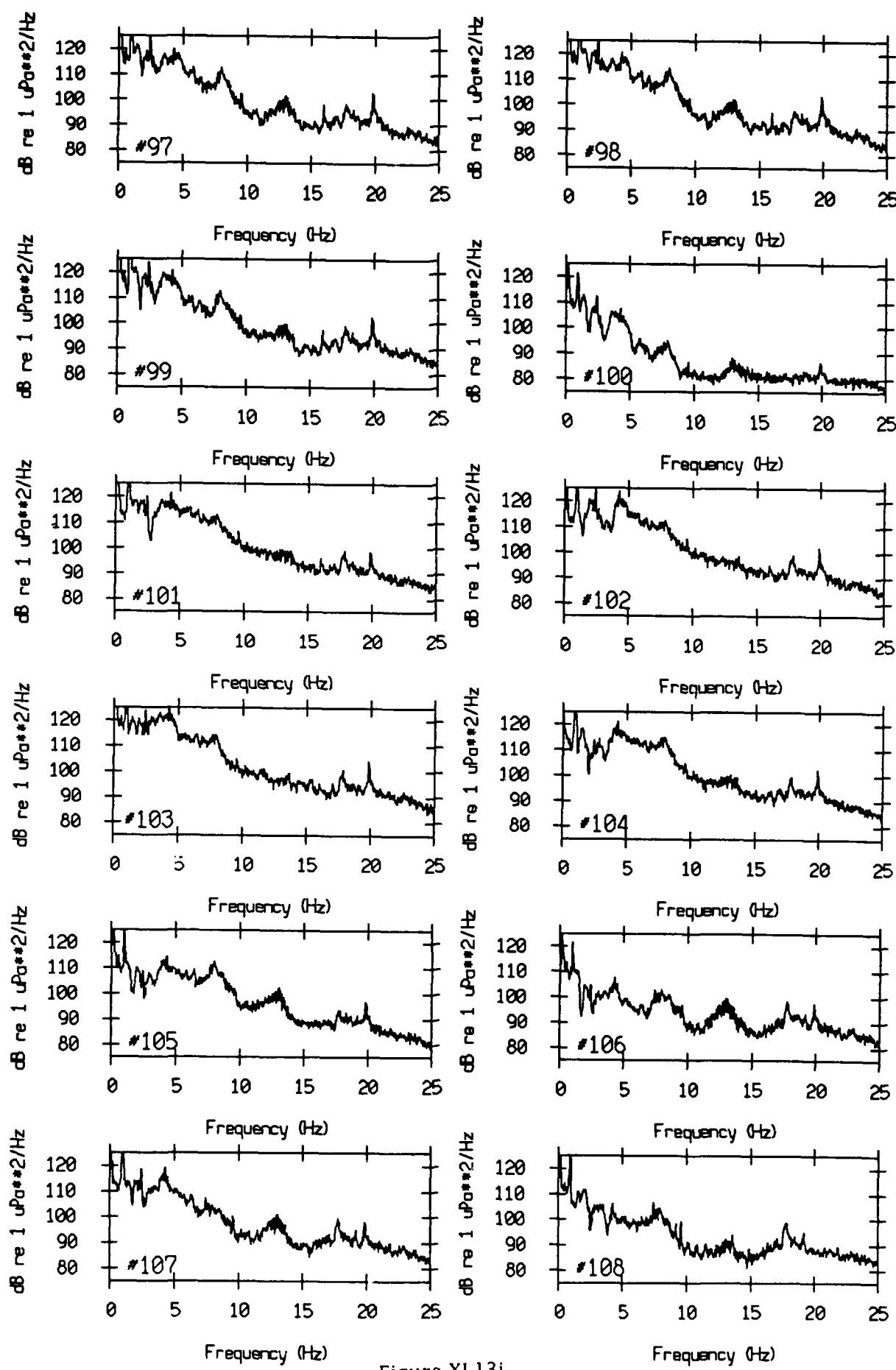


Figure XI.13j

VLA Tape 433, Sept, 1987 - Time 07:45:15 Cal. Pressure Spectra
Data dur.: 532.48 sec. FFT Length: 40.96 sec. Samp Freq: 50 Hz

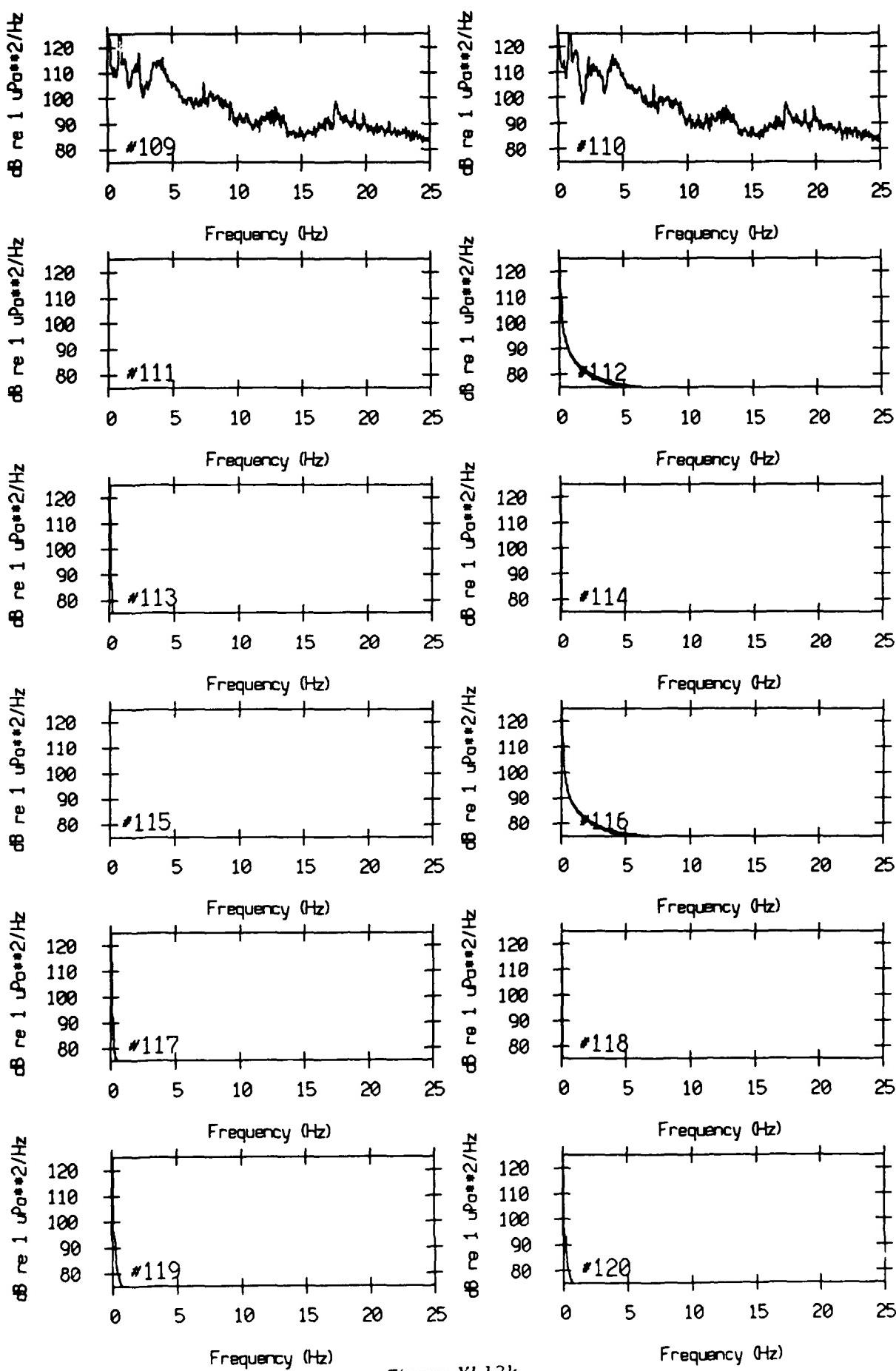


Figure XI.13k

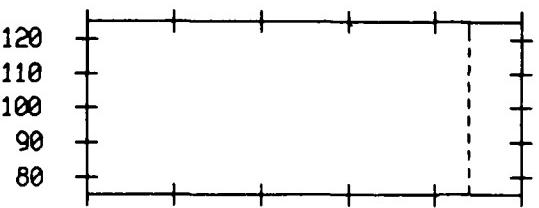
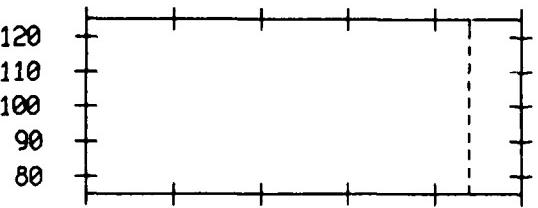
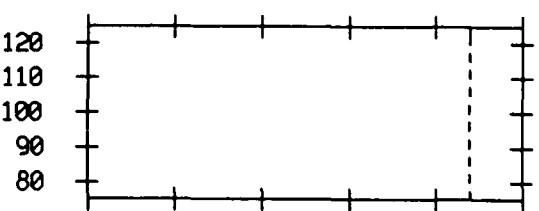
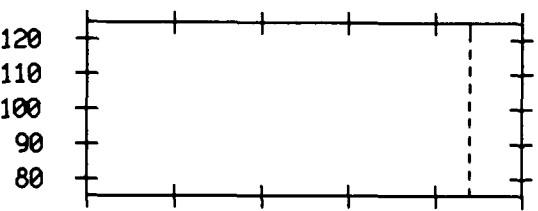
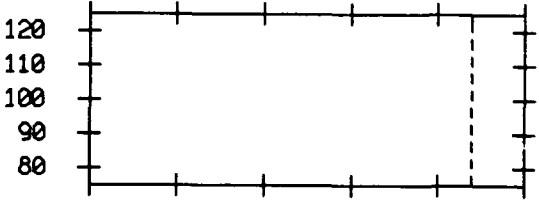
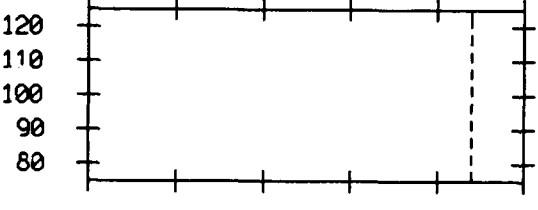
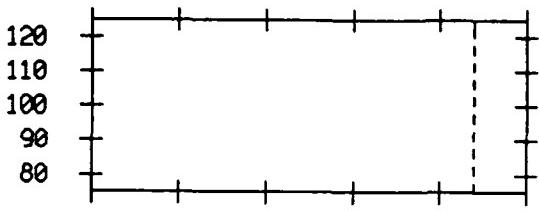
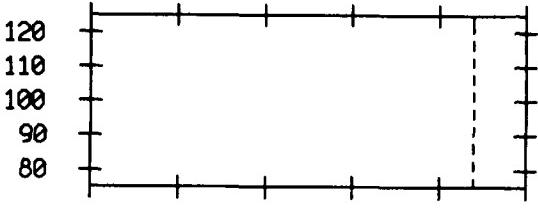
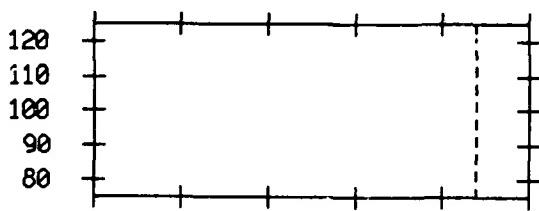
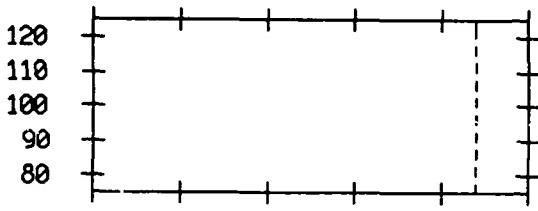
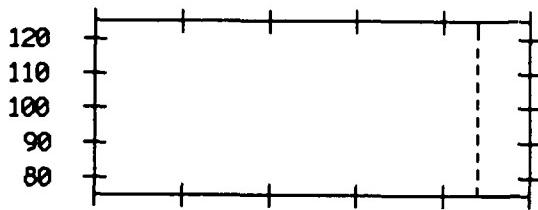


Figure XI.14a

VLA Tape 440, Sept, 1987 - Time 10:49:00.000 Cal. Pressure Spectra
Data dur.: 163.84 sec. FFT Length: 40.96 sec. Samp Freq: 50 Hz

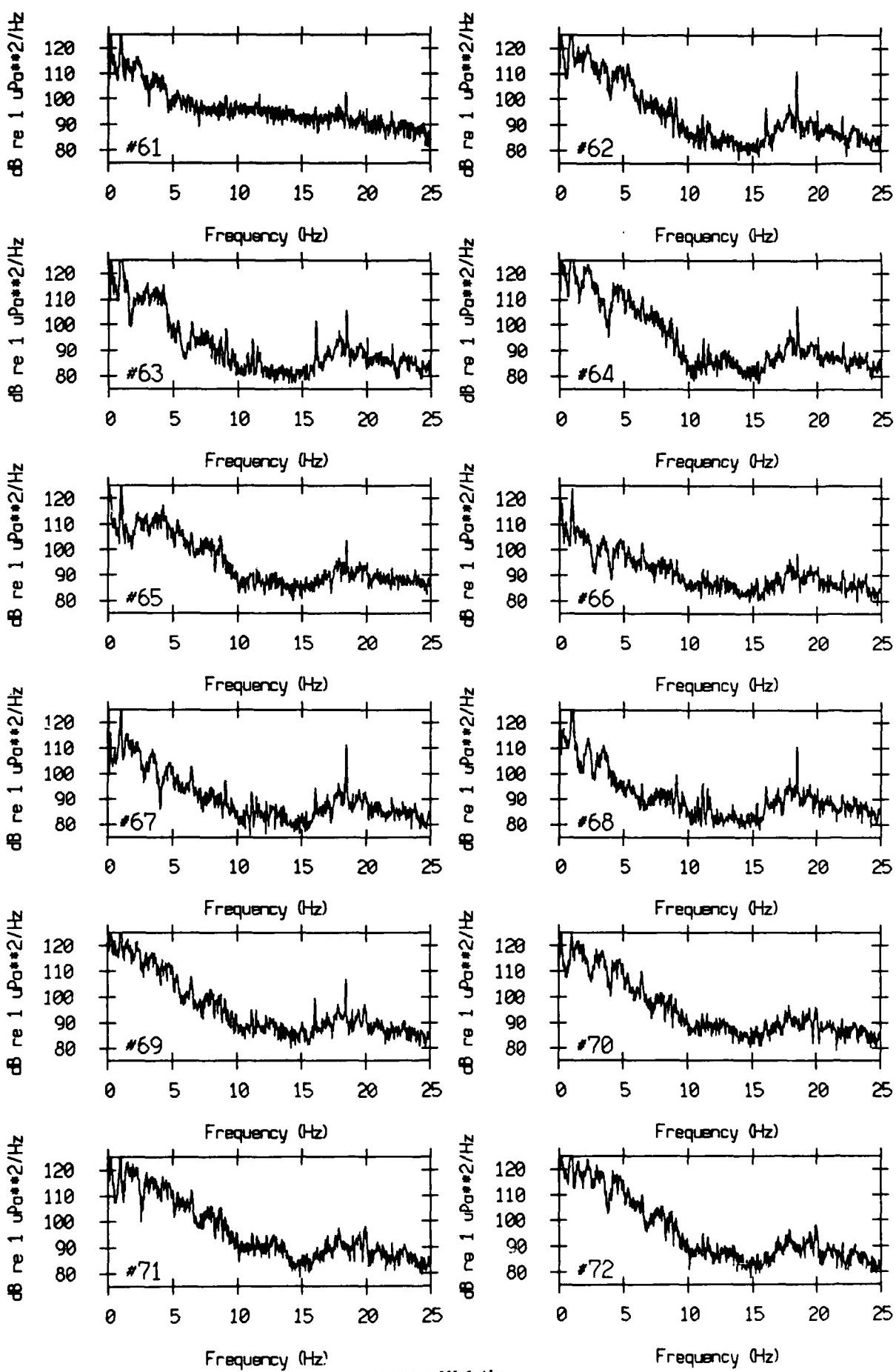


Figure XI.14b

VLA Tape 440, Sept, 1987 - Time 10:49:00.000 Cal. Pressure Spectra
Data dur.: 163.84 sec. FFT Length: 40.96 sec. Samp Freq: 50 Hz

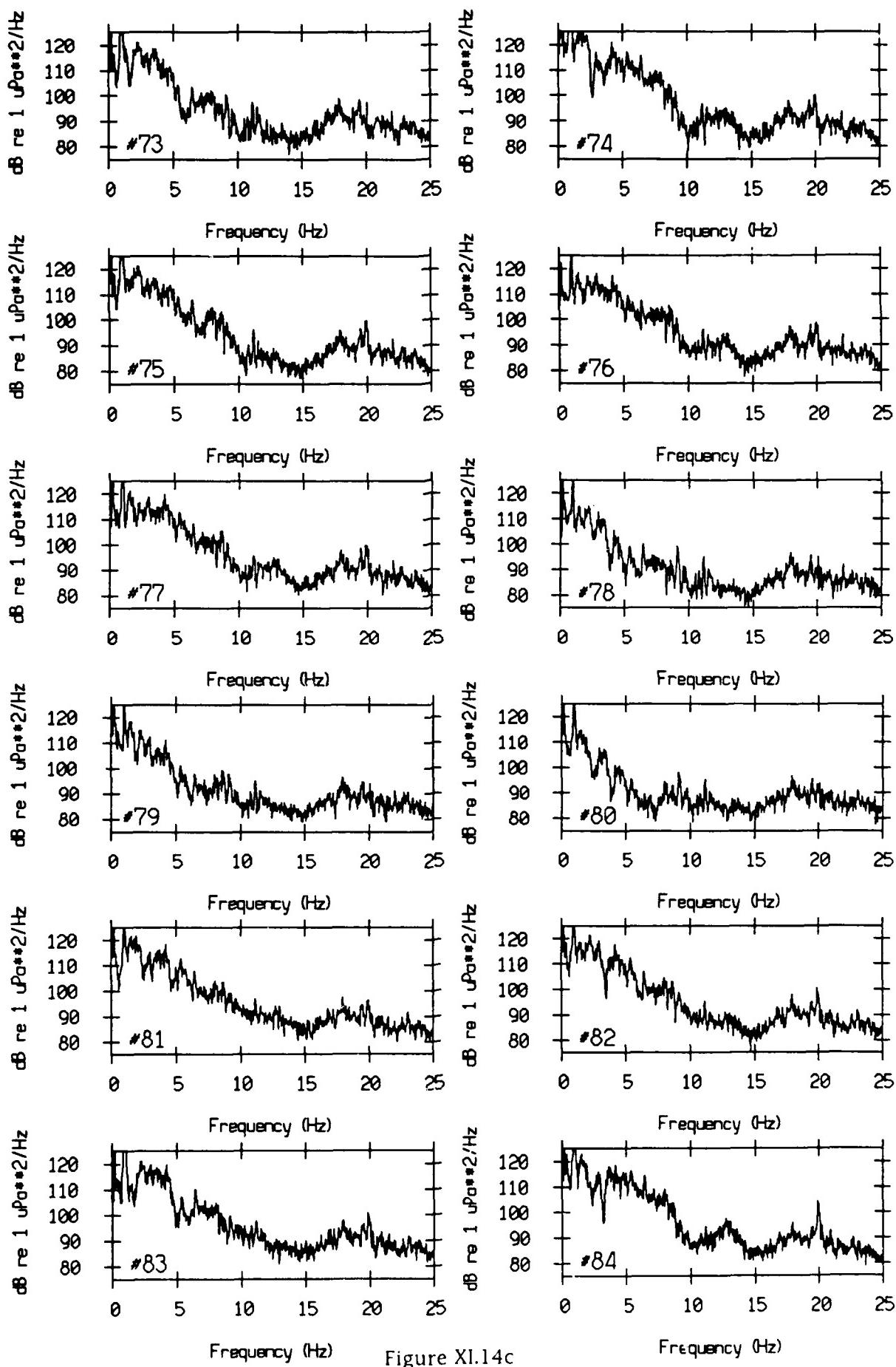


Figure XI.14c

VLA Tape 440, Sept, 1987 - Time 10:49:00.000 Cal. Pressure Spectra
Data dur.: 163.84 sec. FFT Length: 40.96 sec. Samp Freq: 50 Hz

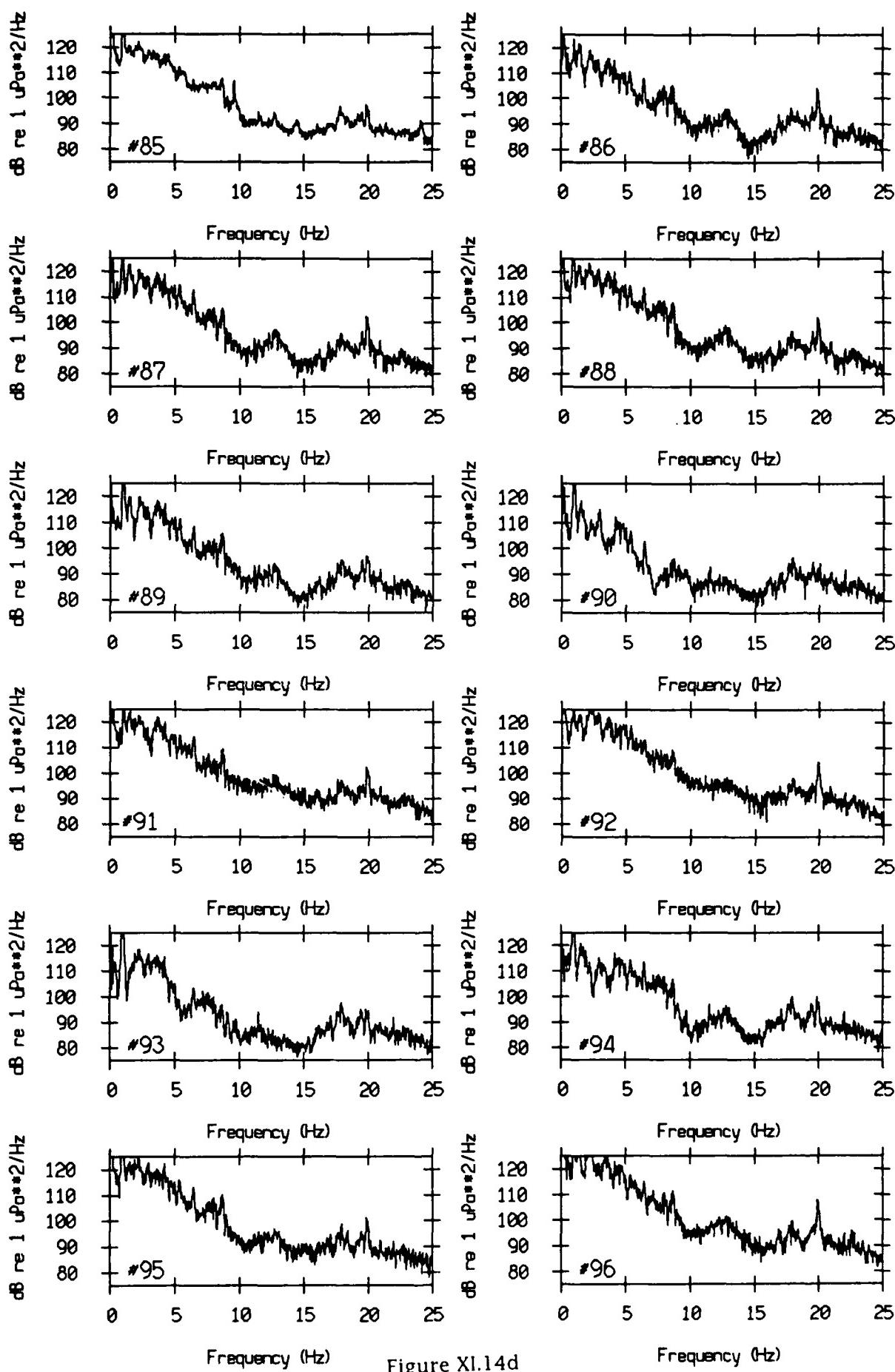


Figure XI.14d

VLA Tape 440, Sept, 1987 - Time 10:49:00.000 Cal. Pressure Spectra
Data dur.: 163.84 sec. FFT Length: 40.96 sec. Samp Freq: 50 Hz

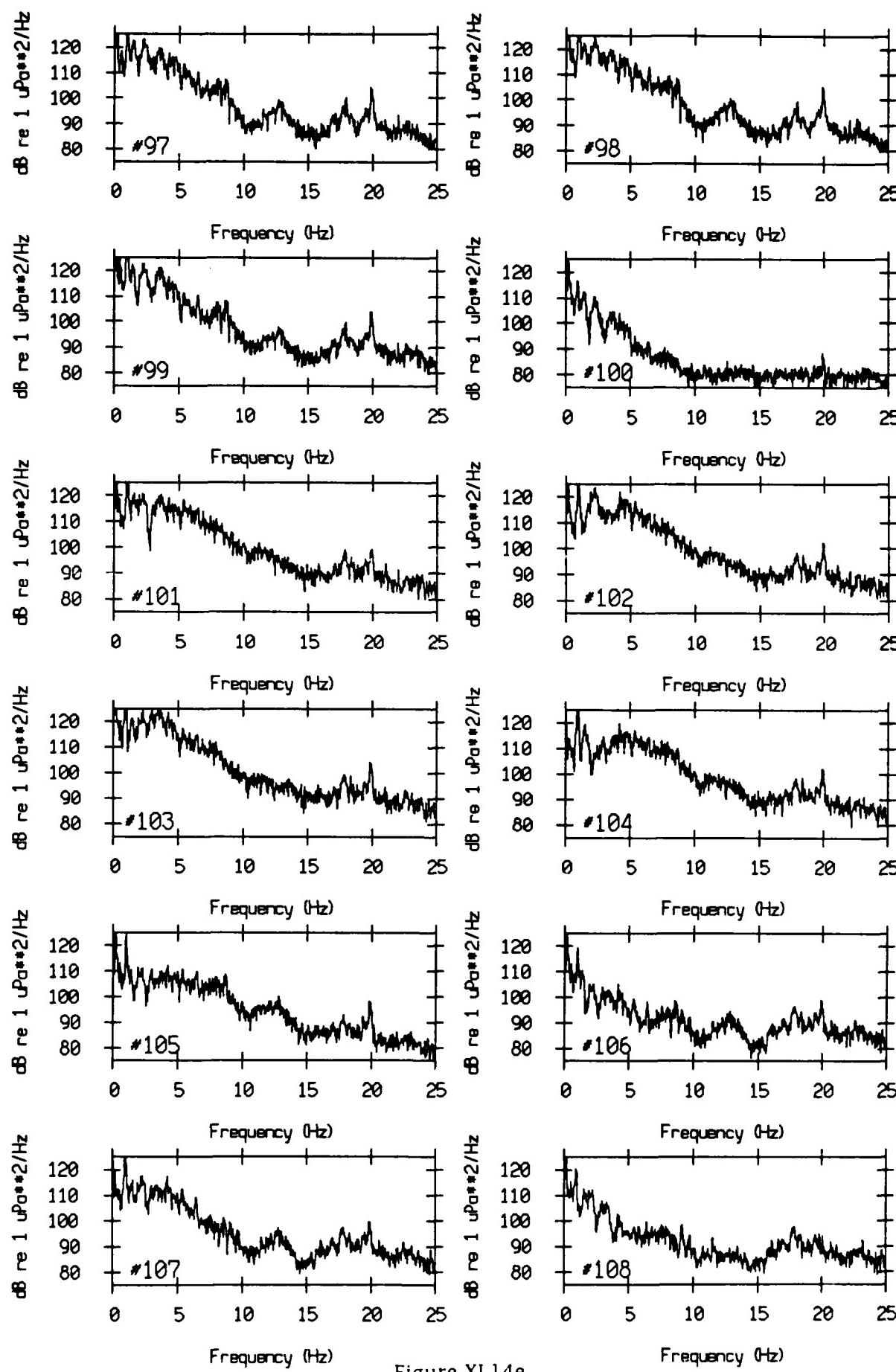


Figure XI.14e

VLA Tape 440, Sept, 1987 - Time 10:49:00.000 Cal. Pressure Spectra
Data dur.: 163.84 sec. FFT Length: 40.96 sec. Samp Freq: 50 Hz

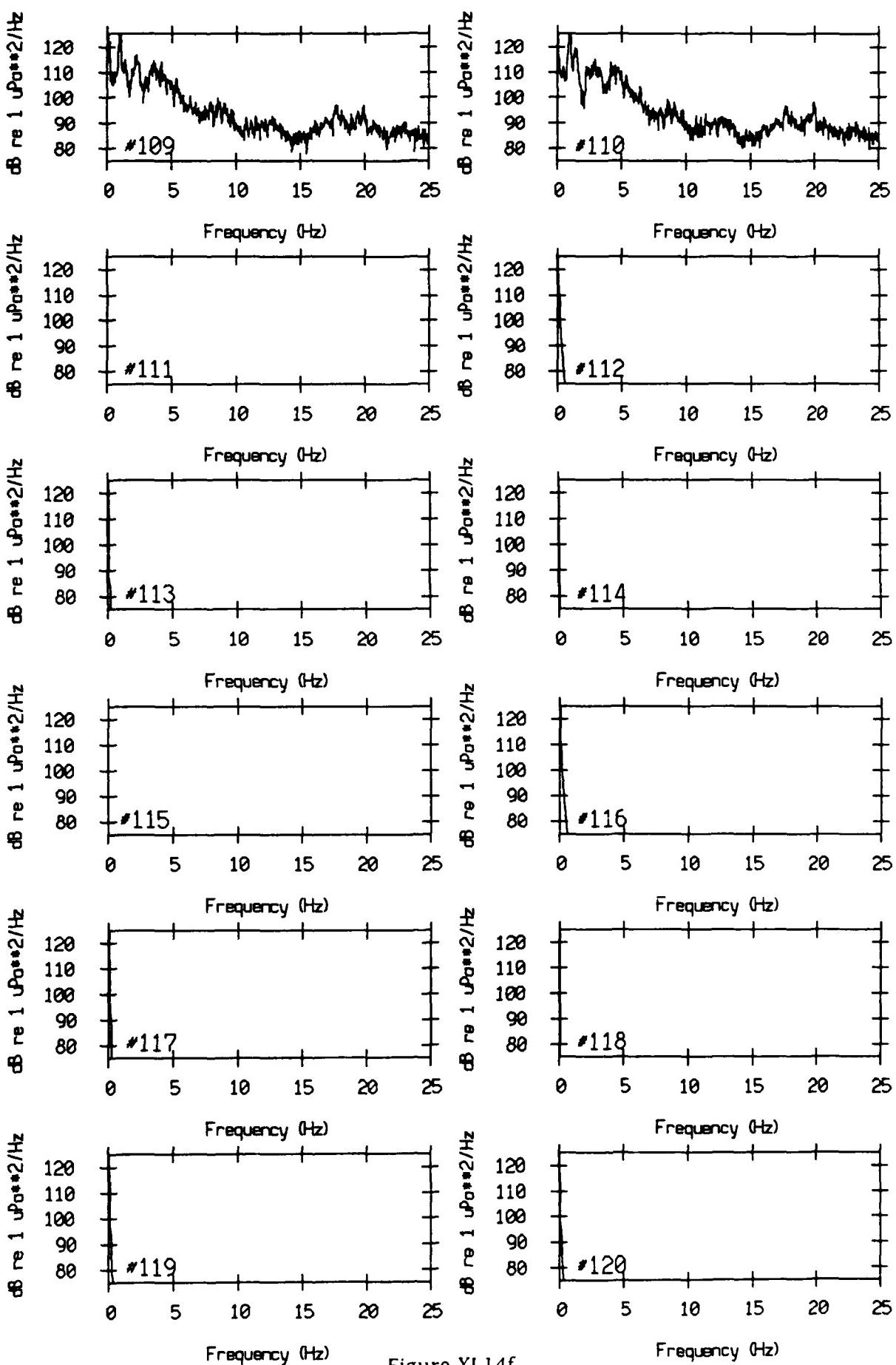


Figure XI.14f

VLA Tape 442, Sept, 1987 - Time 12:01:00.000 Col. Pressure Spectra
Data dur.: 163.84 sec. FFT Length: 10.24 sec. Samp Freq: 50 Hz

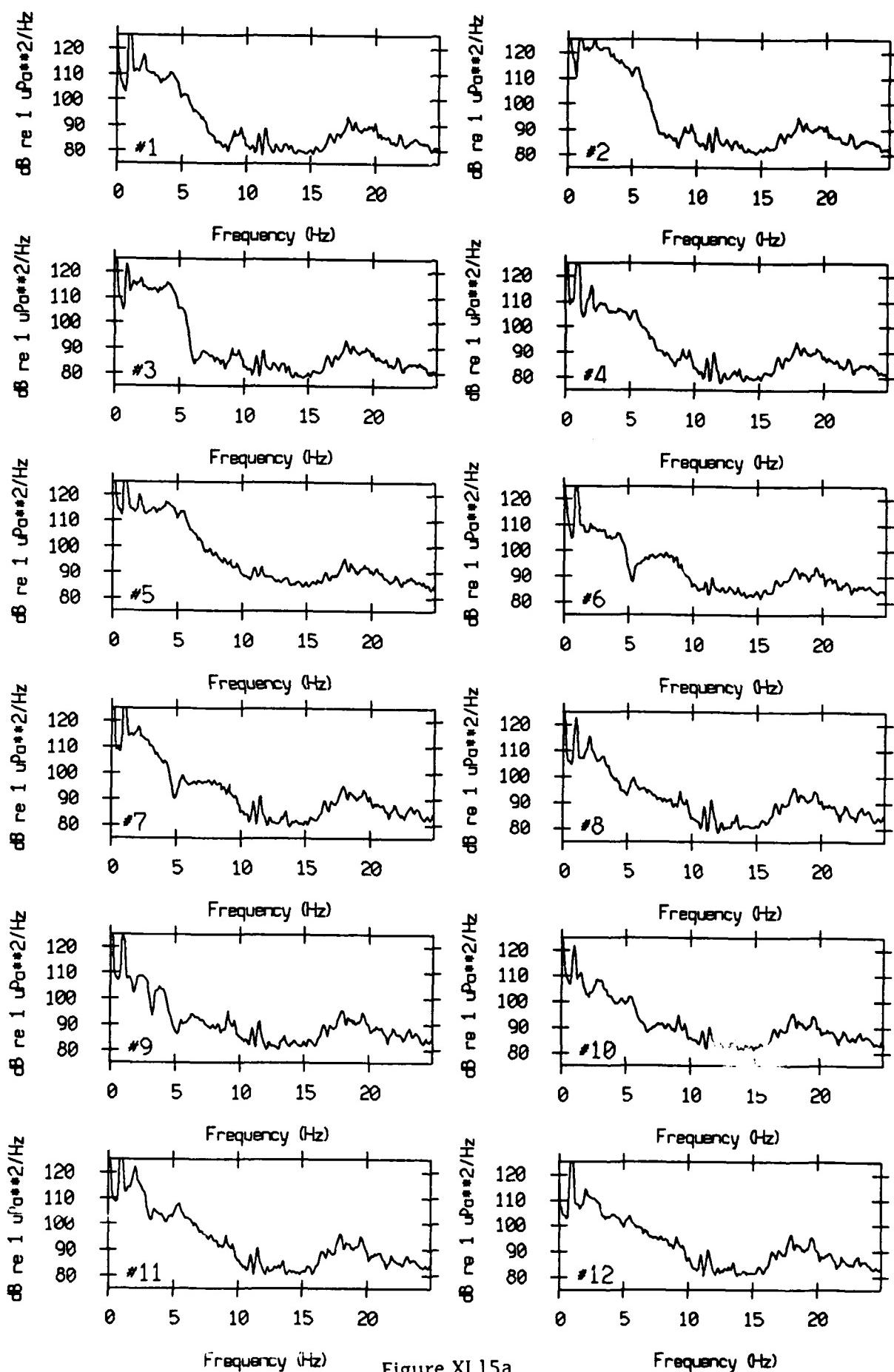


Figure XI.15a

VLA Tape 442, Sept, 1987 - Time 12:01:00.000 Cal. Pressure Spectra
Data dur.: 163.84 sec. FFT Length: 10.24 sec. Samp Freq: 50 Hz

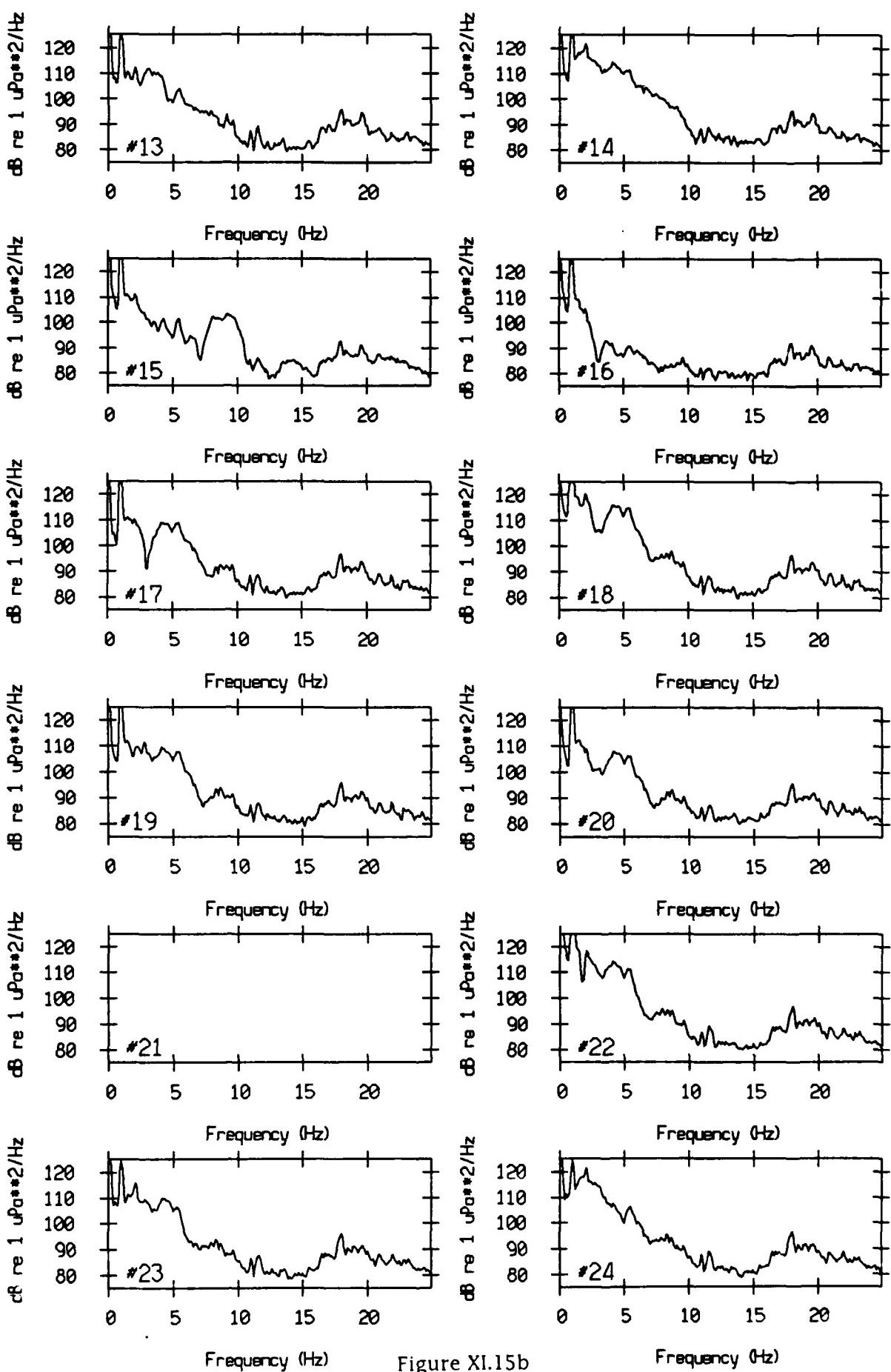


Figure XI.15b

VLA Tape 442, Sept, 1987 - Time 12:01:00.000 Cal. Pressure Spectra
Data dur.: 163.84 sec. FFT Length: 10.24 sec. Samp Freq: 50 Hz

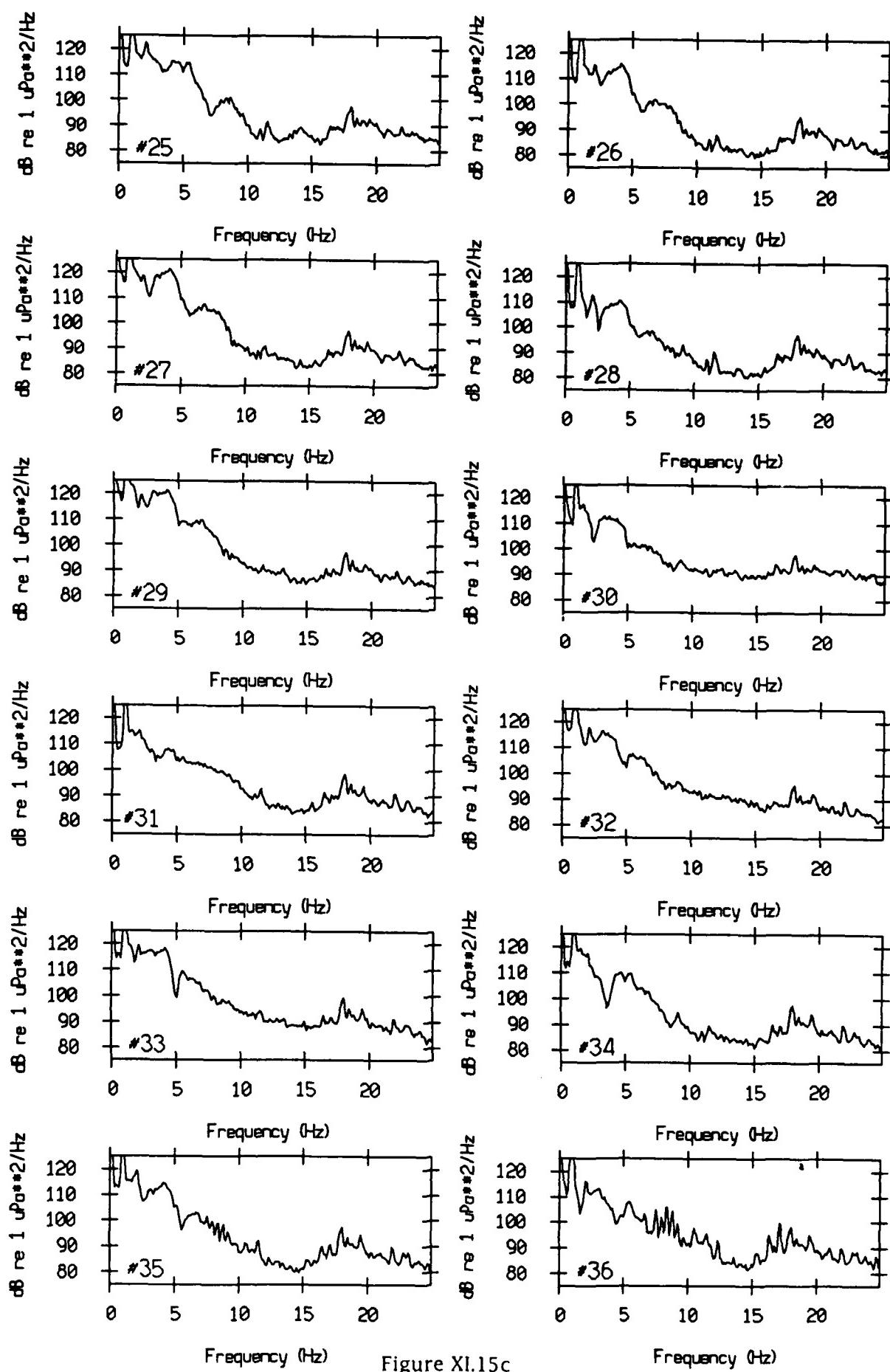


Figure XI.15c

VLA Tape 442, Sept, 1987 - Time 12:01:00.000 Cal. Pressure Spectra
Data dur.: 163.84 sec. FFT Length: 10.24 sec. Samp Freq: 50 Hz

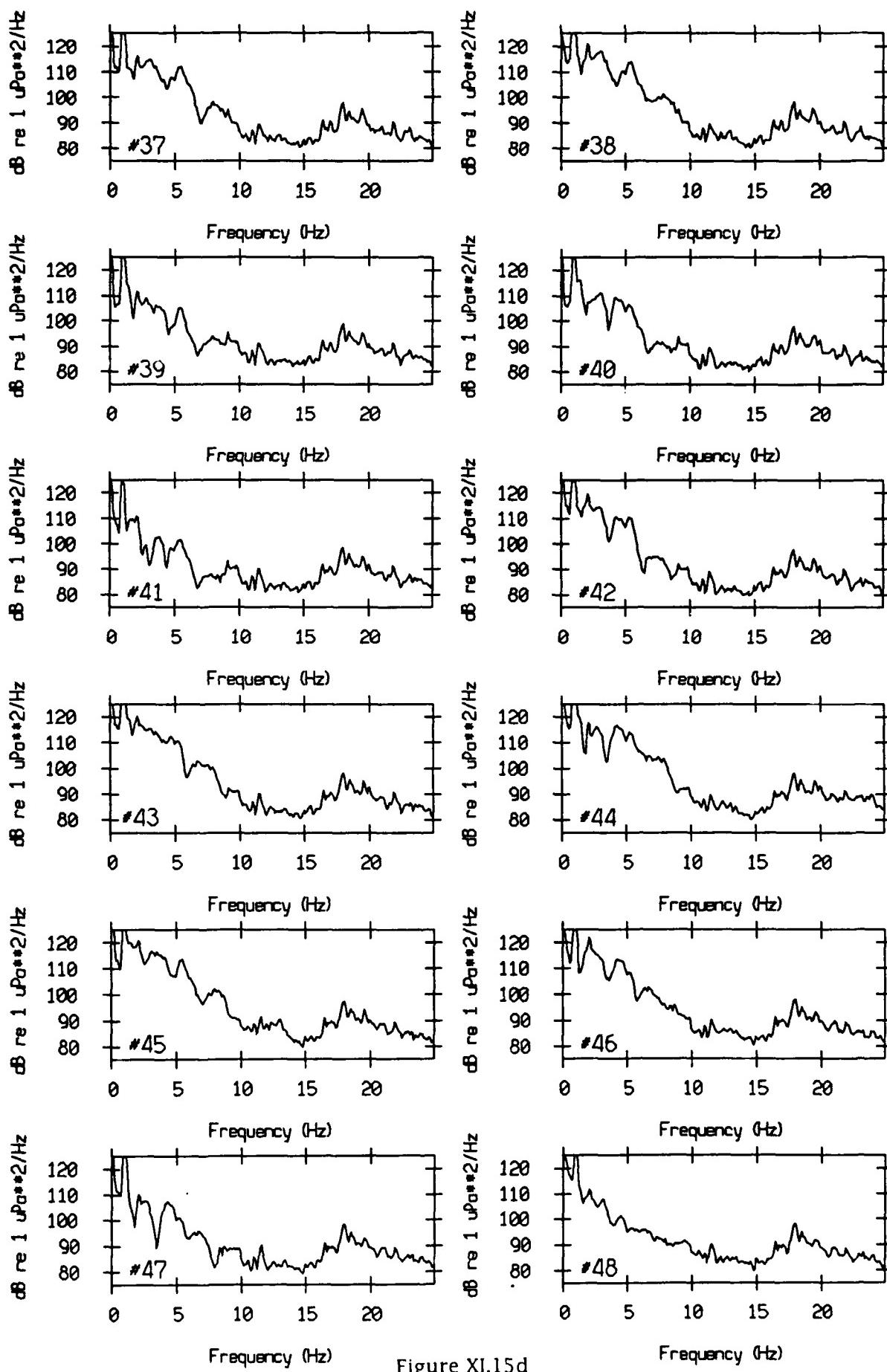


Figure XI.15d

VLA Tape 442, Sept, 1987 - Time 12:01:00.000 Cal. Pressure Spectra
Data dur.: 163.84 sec. FFT Length: 10.24 sec. Samp Freq: 50 Hz

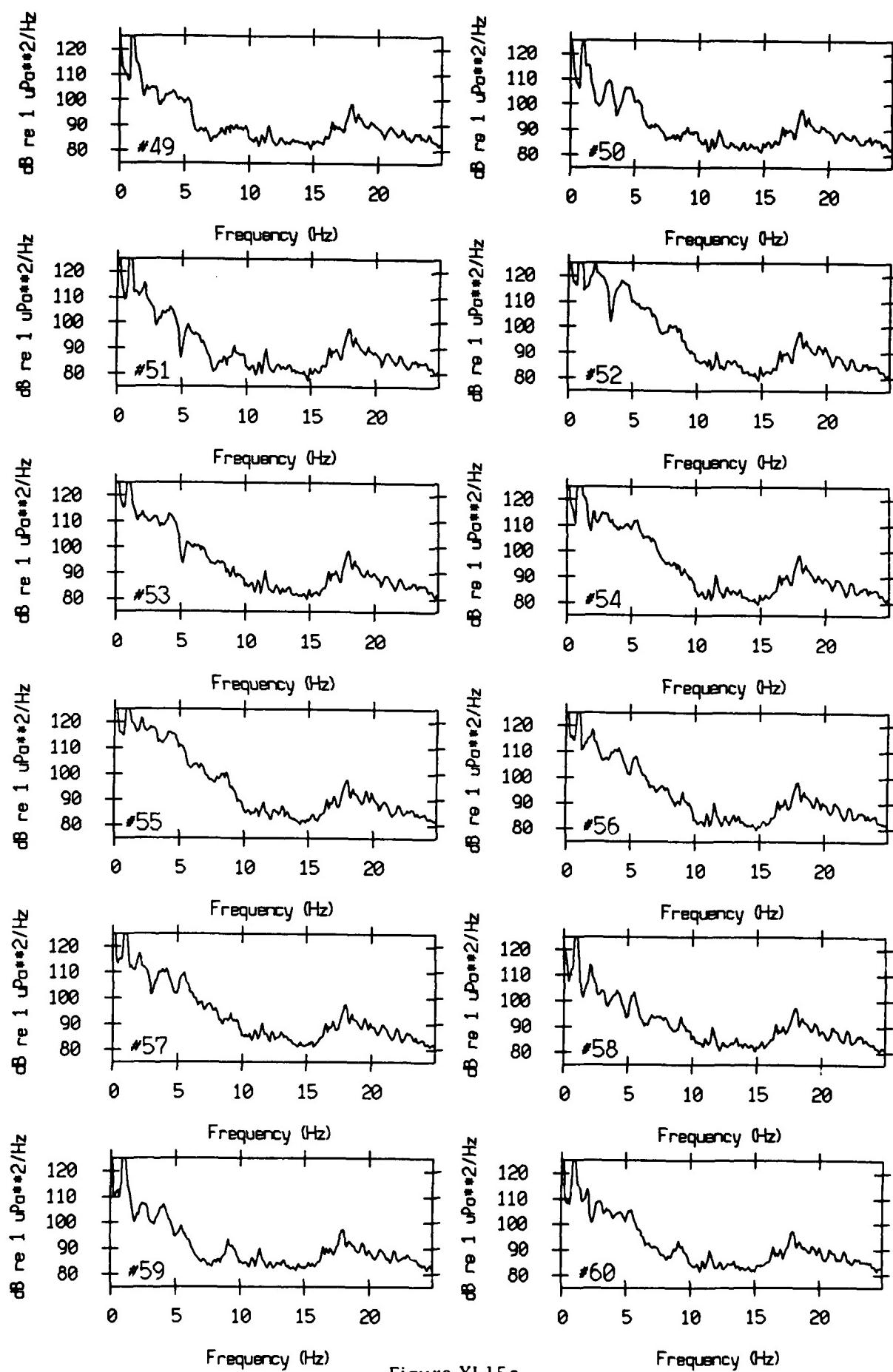


Figure XI.15e

VLA Tape 442, Sept, 1987 - Time 12:01:00.000 Col. Pressure Spectra
Data dur.: 163.84 sec. FFT Length: 10.24 sec. Samp Freq: 50 Hz

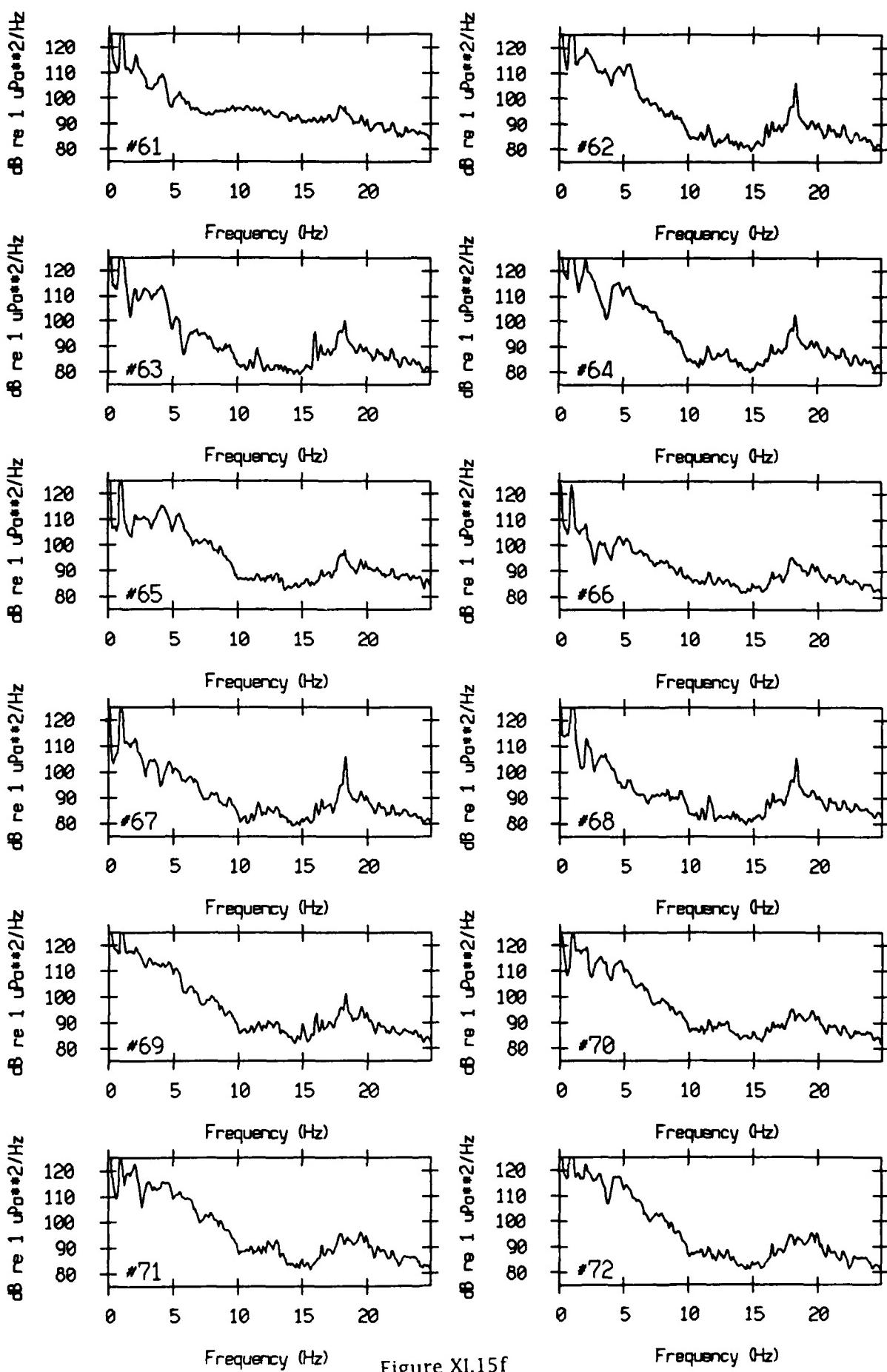


Figure XI.15f

VLA Tape 442, Sept, 1987 - Time 12:01:00.000 Cal. Pressure Spectra
Data dur.: 163.84 sec. FFT Length: 10.24 sec. Samp Freq: 50 Hz

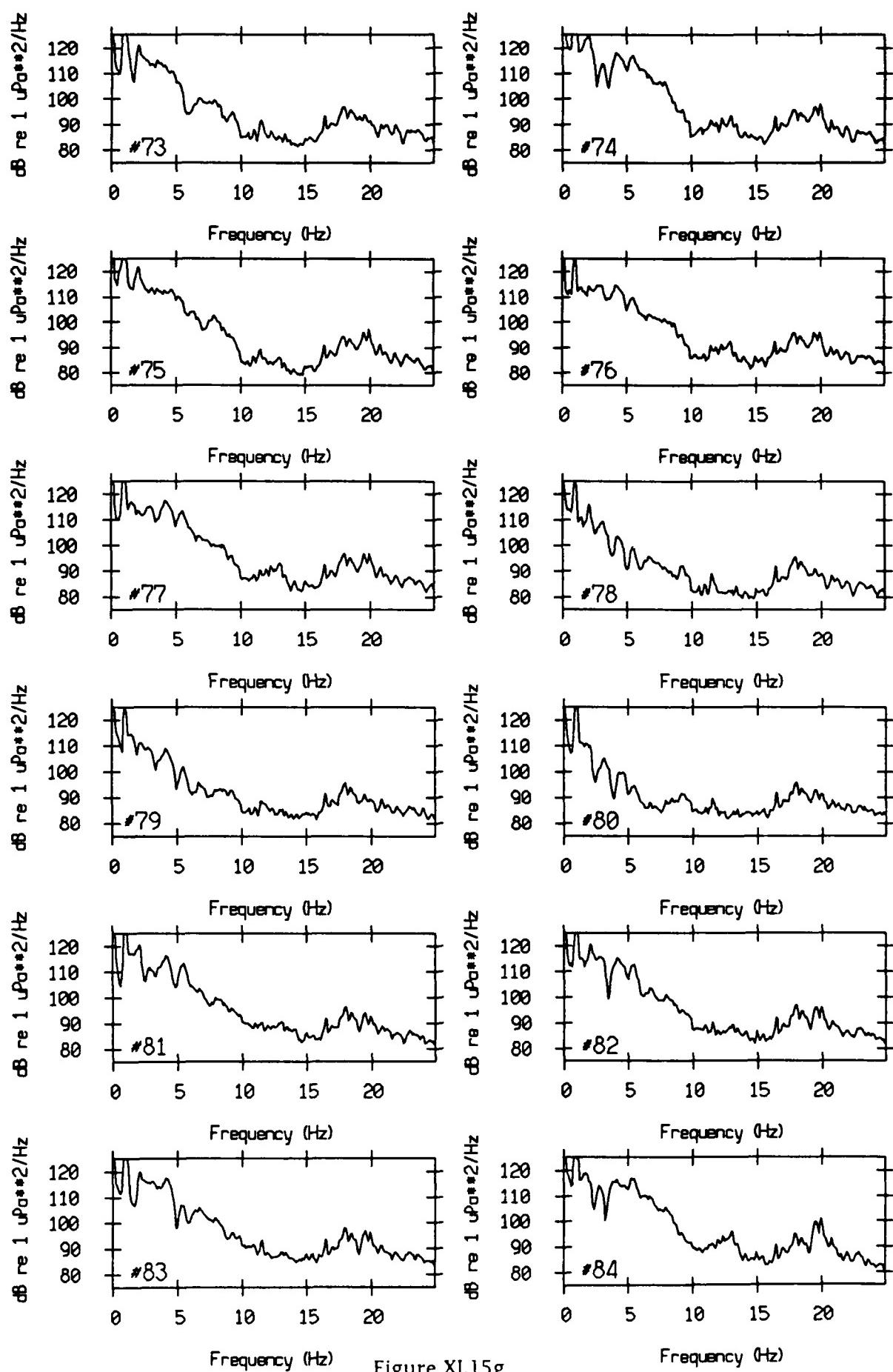


Figure XI.15g

VLA Tape 442, Sept, 1987 - Time 12:01:00.000 Col. Pressure Spectra
Data dur.: 163.84 sec. FFT Length: 10.24 sec. Samp Freq: 50 Hz

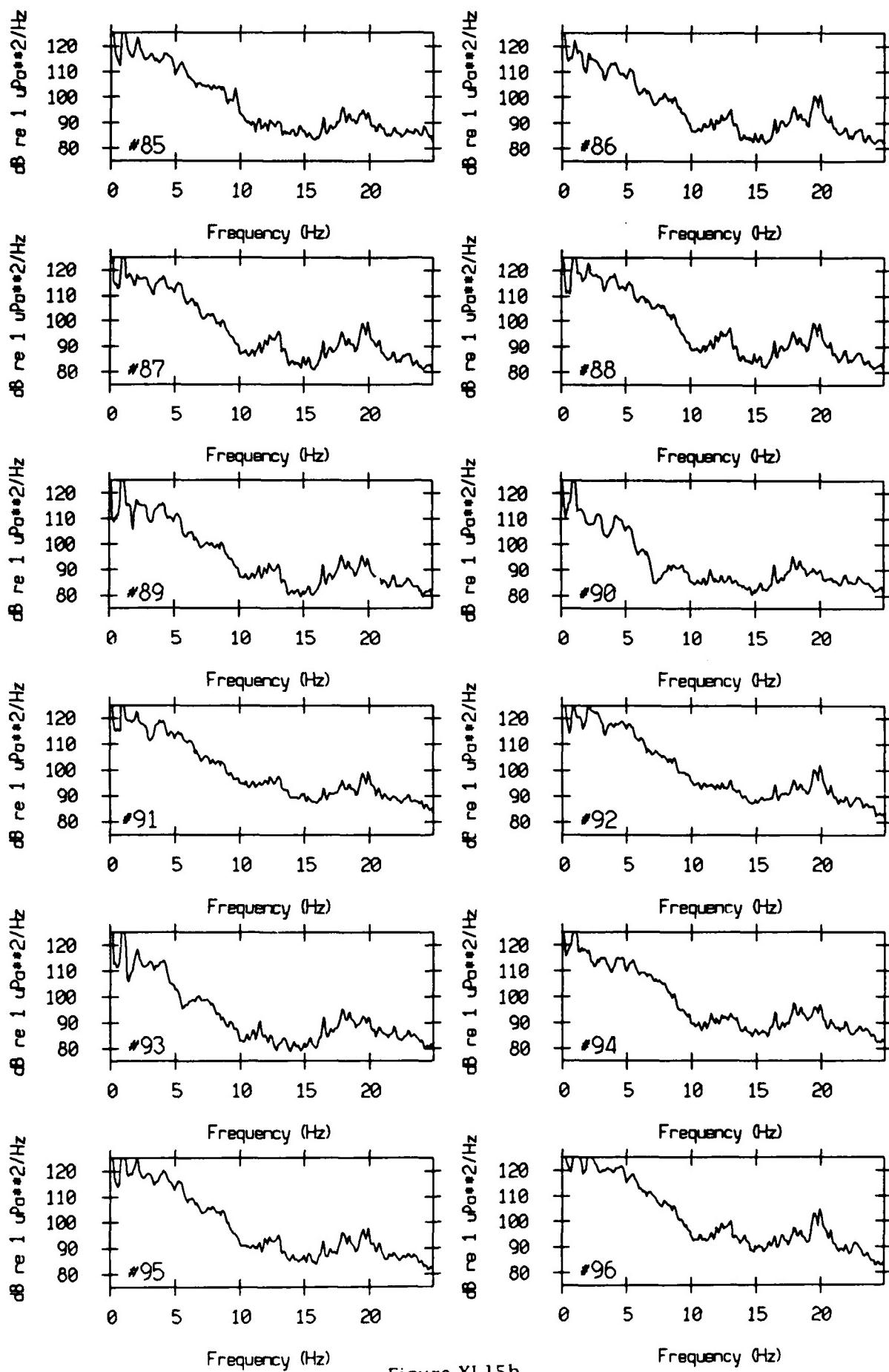


Figure XI.15h

VLA Tape 442, Sept, 1987 - Time 12:01:00.000 Col. Pressure Spectra
Data dur.: 163.84 sec. FFT Length: 10.24 sec. Samp Freq: 50 Hz

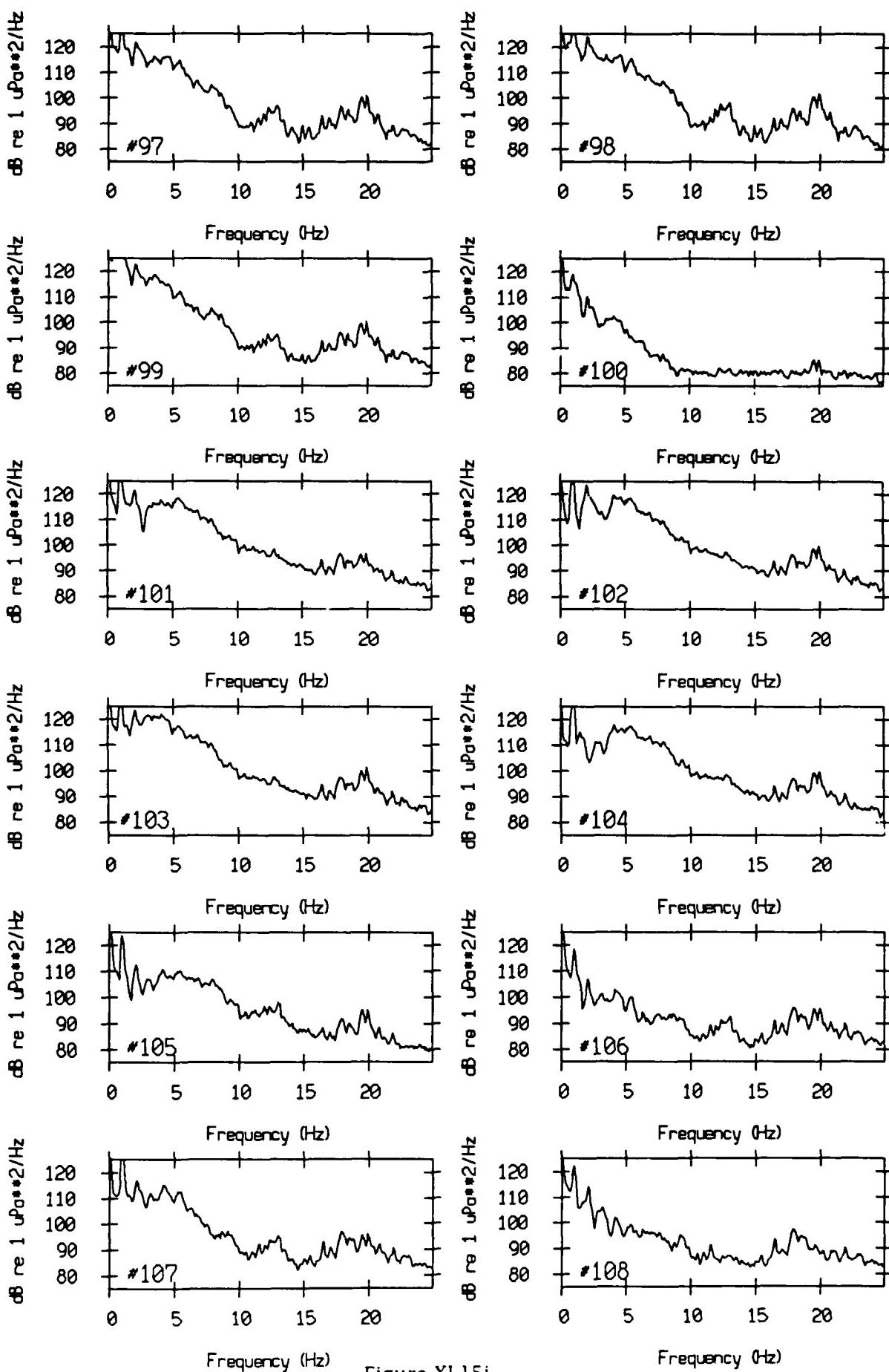


Figure XI.15i

VLA Tape 442, Sept, 1987 - Time 12:01:00.000 Cal. Pressure Spectra
Data dur.: 163.84 sec. FFT Length: 10.24 sec. Samp Freq: 50 Hz

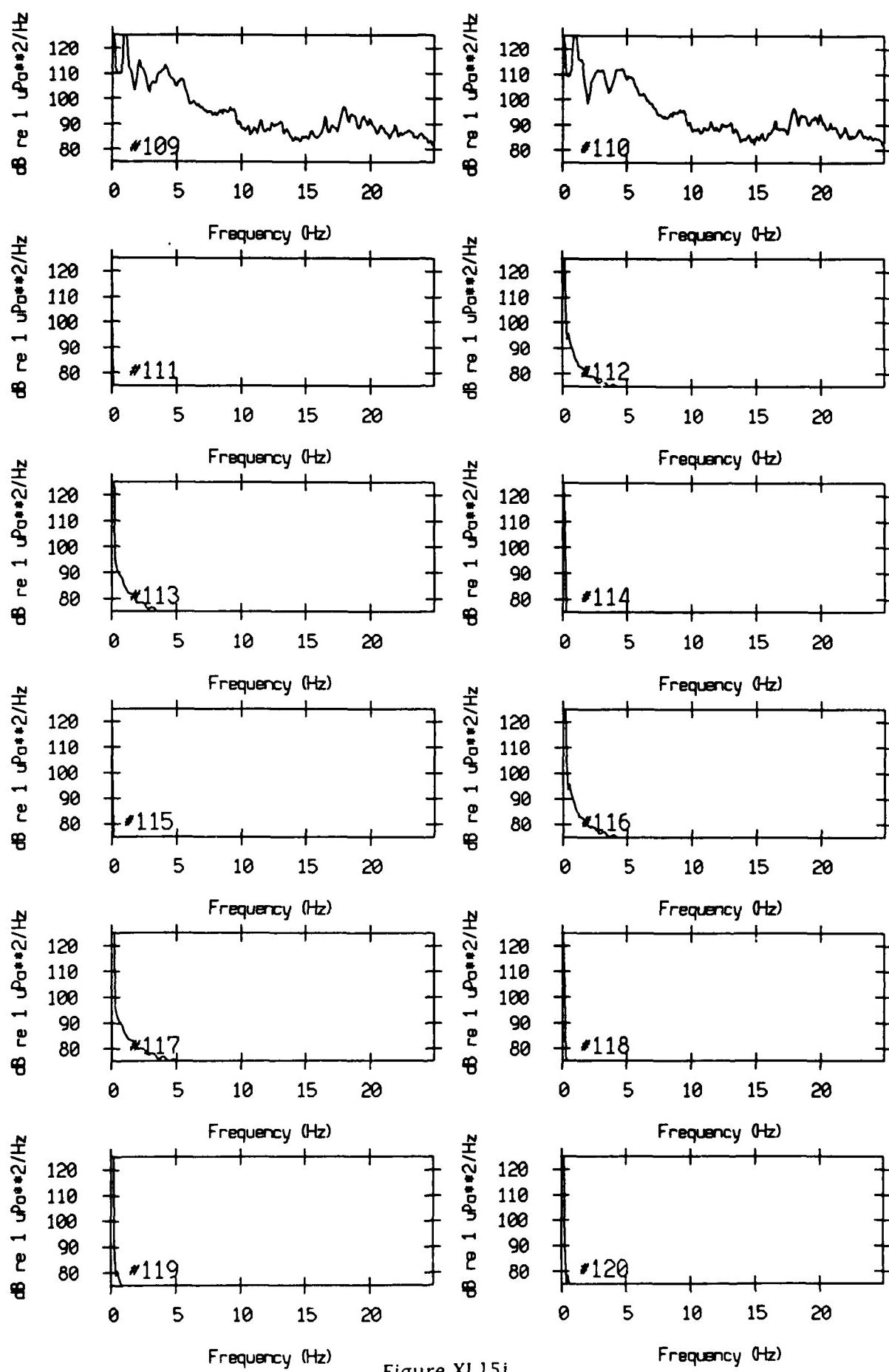


Figure XI.15j

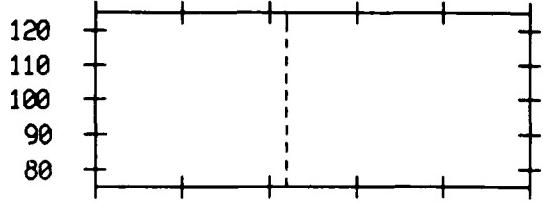
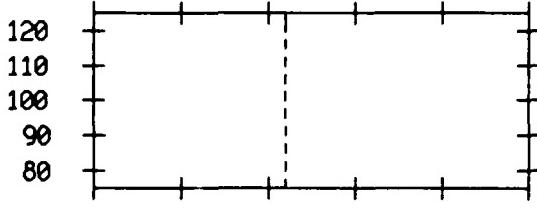
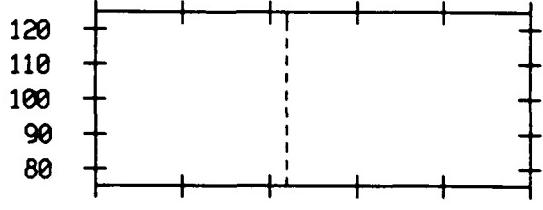
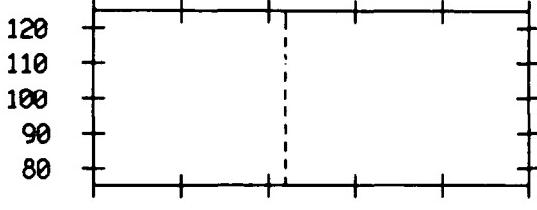
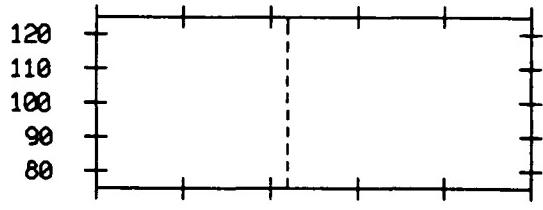
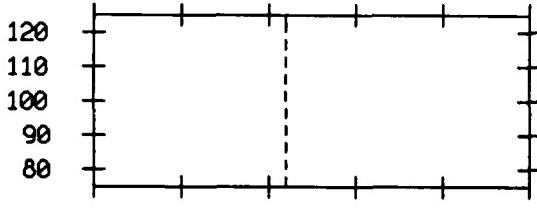
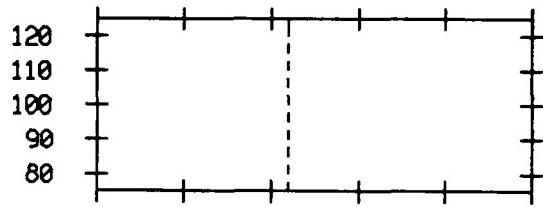
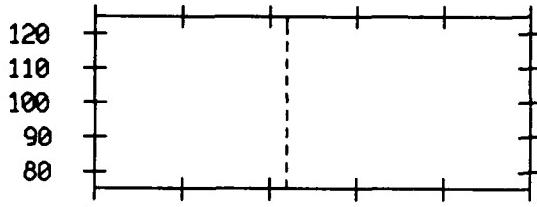
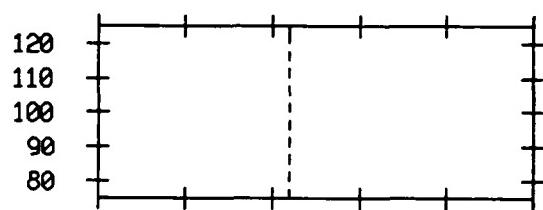
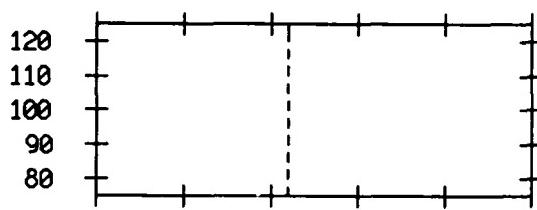
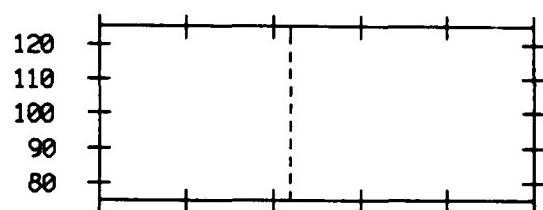
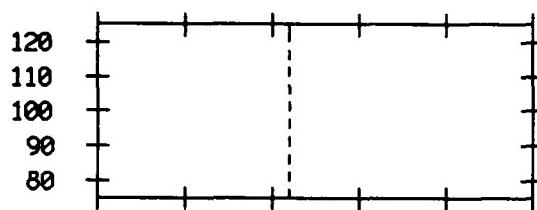


Figure XI.16a

VLA Tape 447, Sept, 1987 - Time 13:50:00.000 Cal. Pressure Spectra
Data dur.: 491.52 sec. FFT Length: 163.84 sec. Samp Freq: 50 Hz

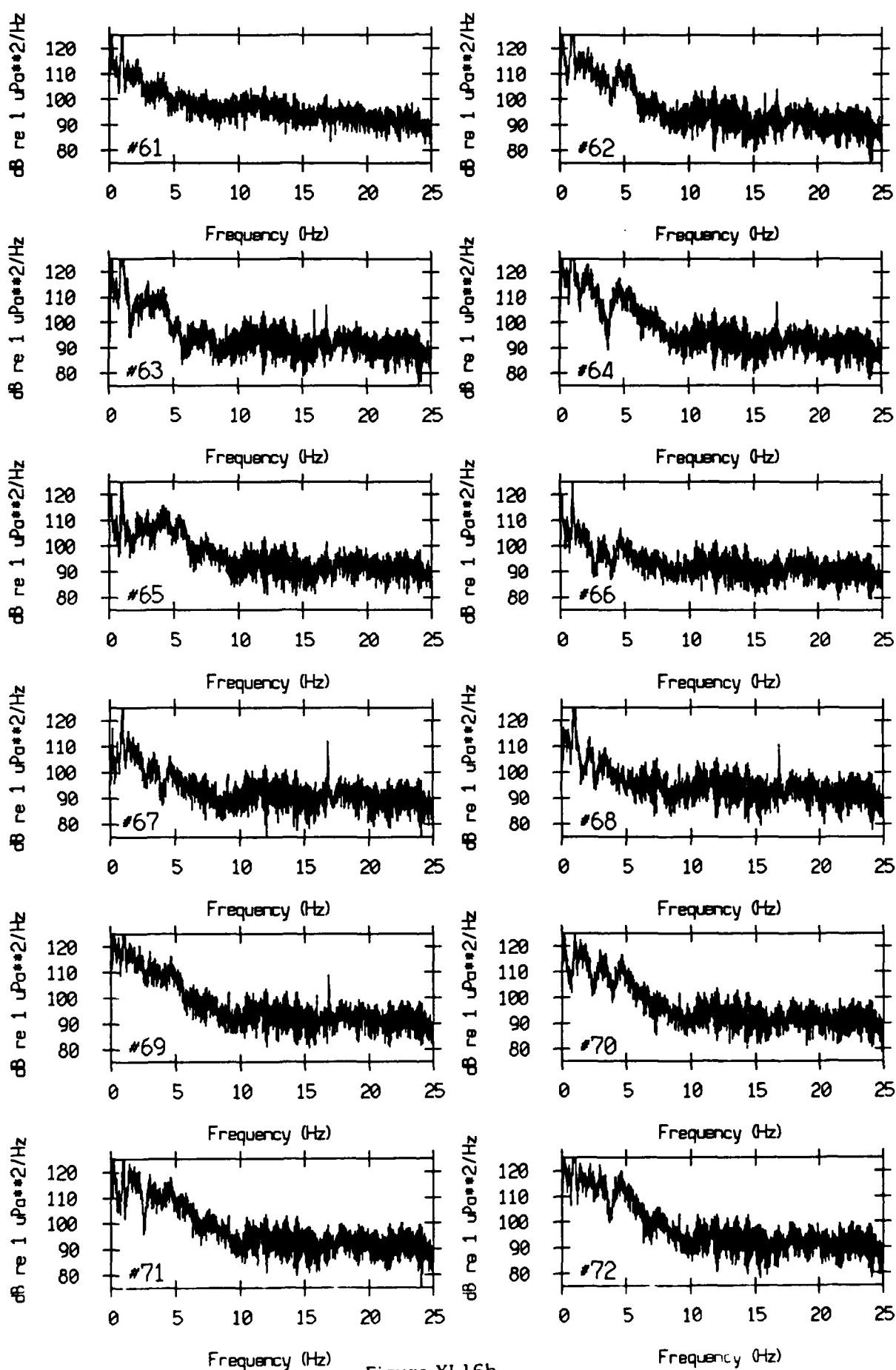


Figure XI.16b

VLA Tape 447, Sept, 1987 - Time 13:50:00.000 Cal. Pressure Spectra
Data dur.: 491.52 sec. FFT Length: 163.84 sec. Samp Freq: 50 Hz

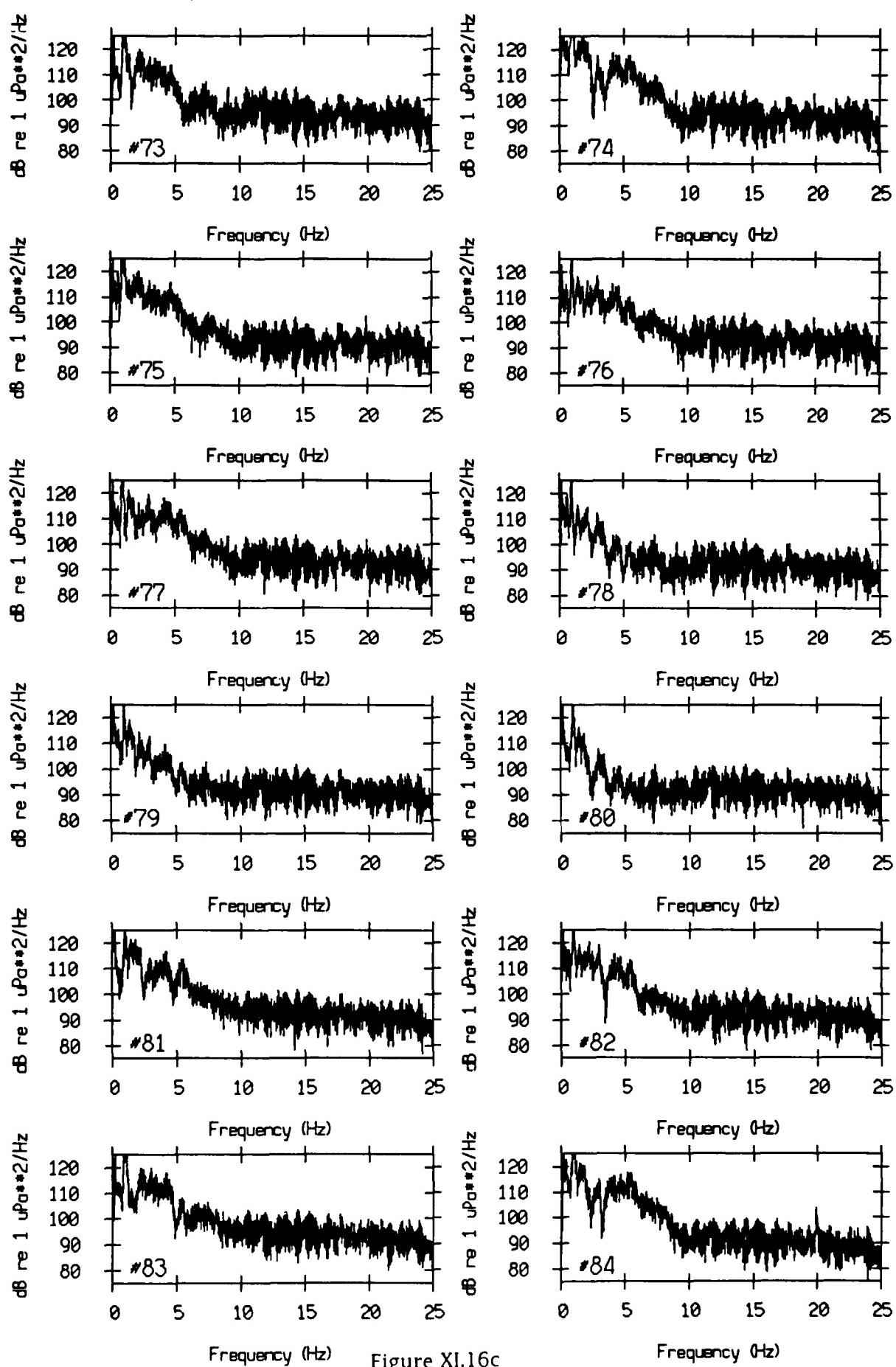


Figure XI.16c

VLA Tape 447, Sept, 1987 - Time 13:50:00.000 Cal. Pressure Spectra
Data dur.: 491.52 sec. FFT Length: 163.84 sec. Samp Freq: 50 Hz

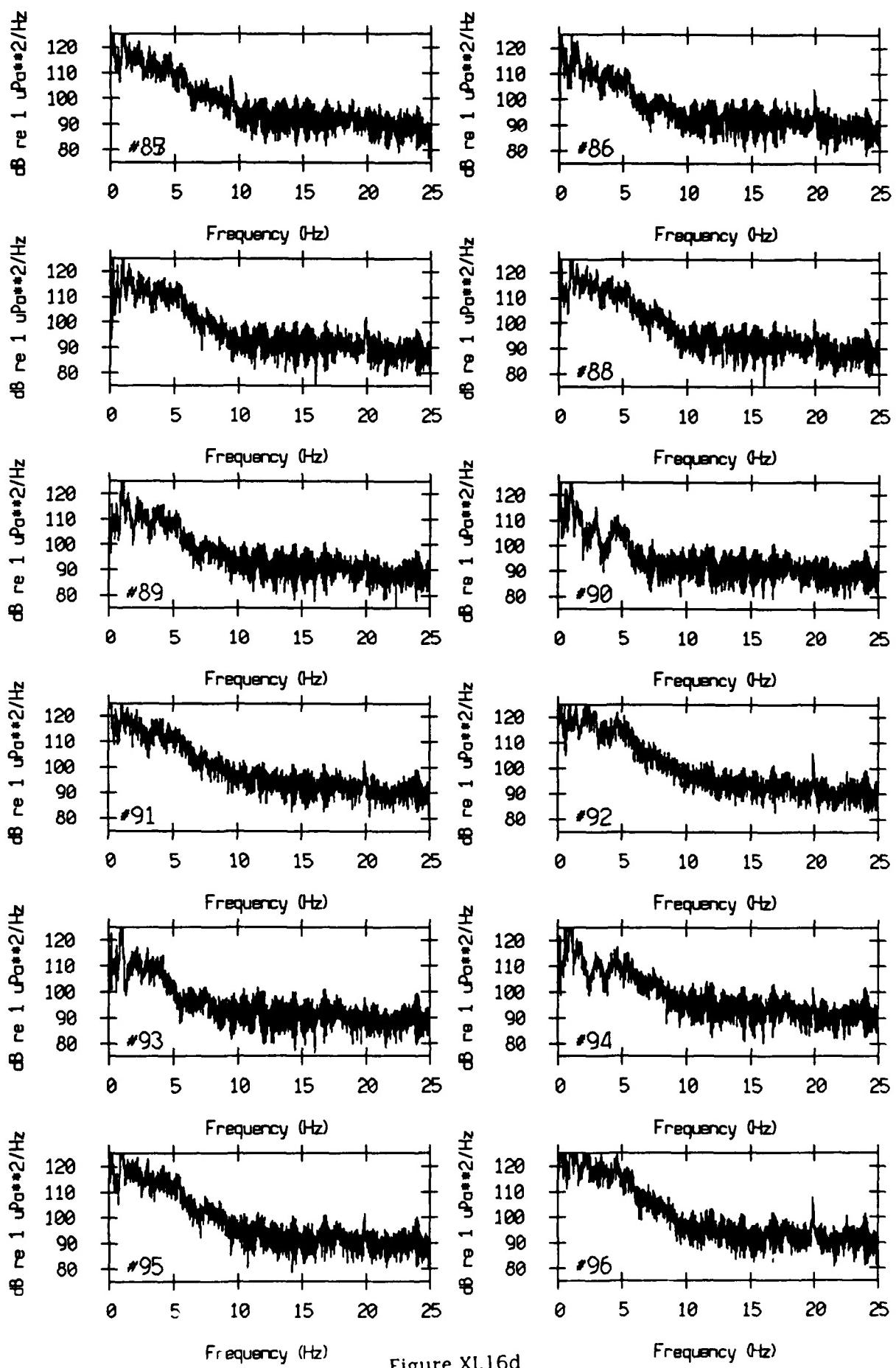


Figure XI.16d

VLA Tape 447, Sept, 1987 - Time 13:50:00.000 Cal. Pressure Spectra
Data dur.: 491.52 sec. FFT Length: 163.84 sec. Samp Freq: 50 Hz

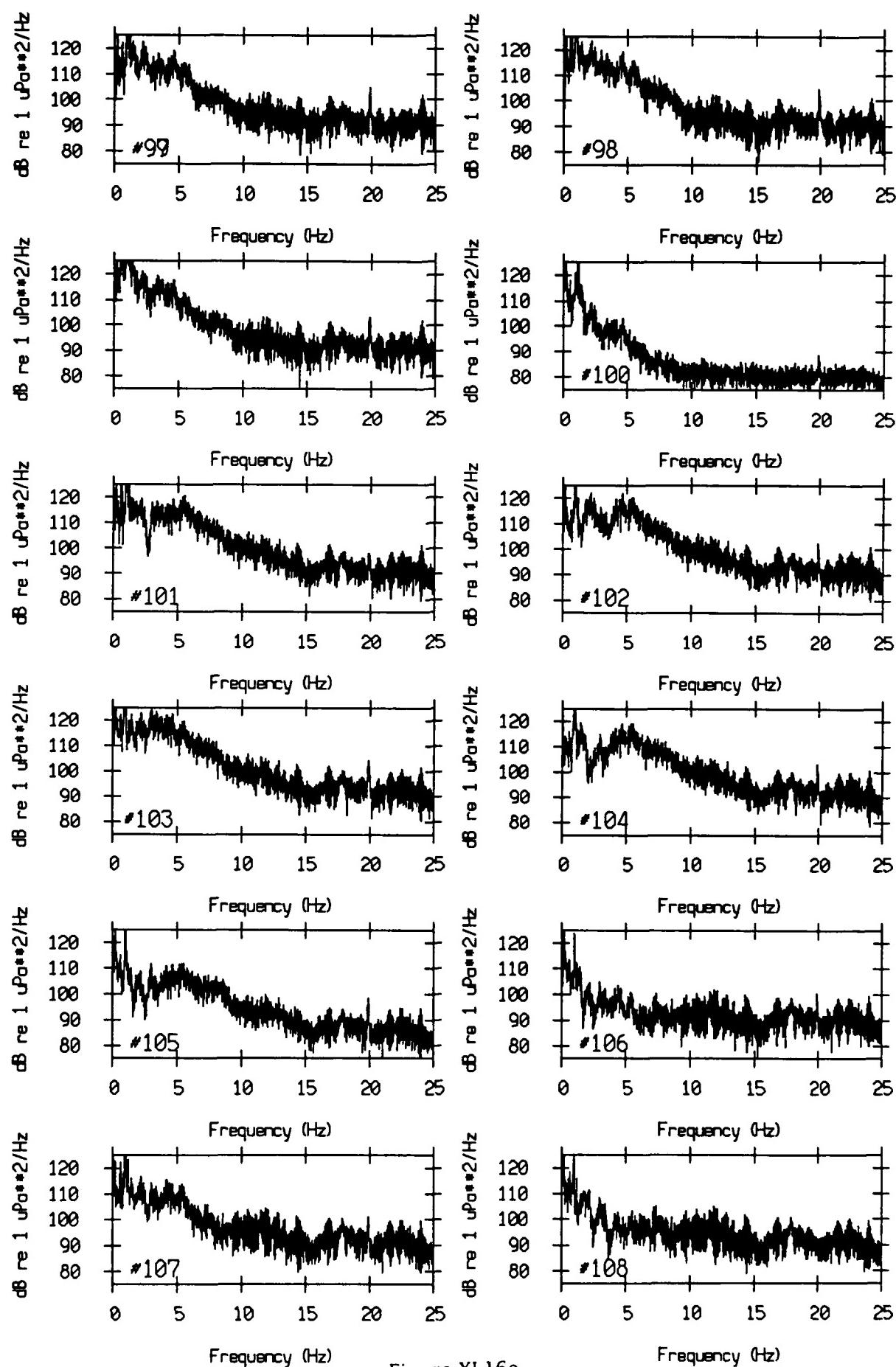


Figure XI.16e

VLA Tape 447, Sept, 1987 - Time 13:50:00.000 Col. Pressure Spectra
Data dur.: 491.52 sec. FFT Length: 163.84 sec. Samp Freq: 50 Hz

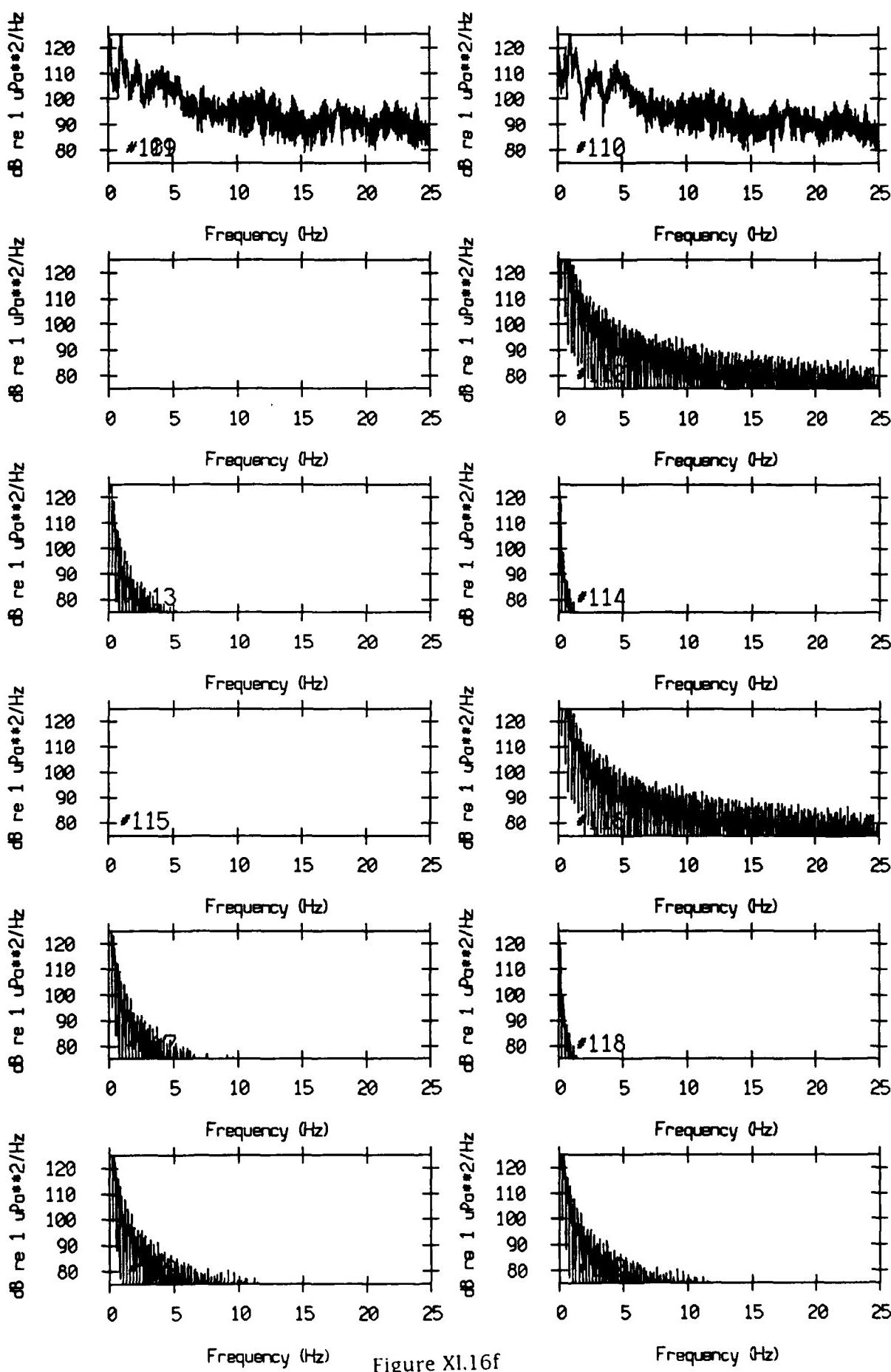


Figure XI.16f

VLA Tape 453, Sept, 1987 - Time 16:30:00.000 Cal. Pressure Spectra
Data dur.: 138.24 sec. FFT Length: 10.24 sec. Samp Freq: 50 Hz

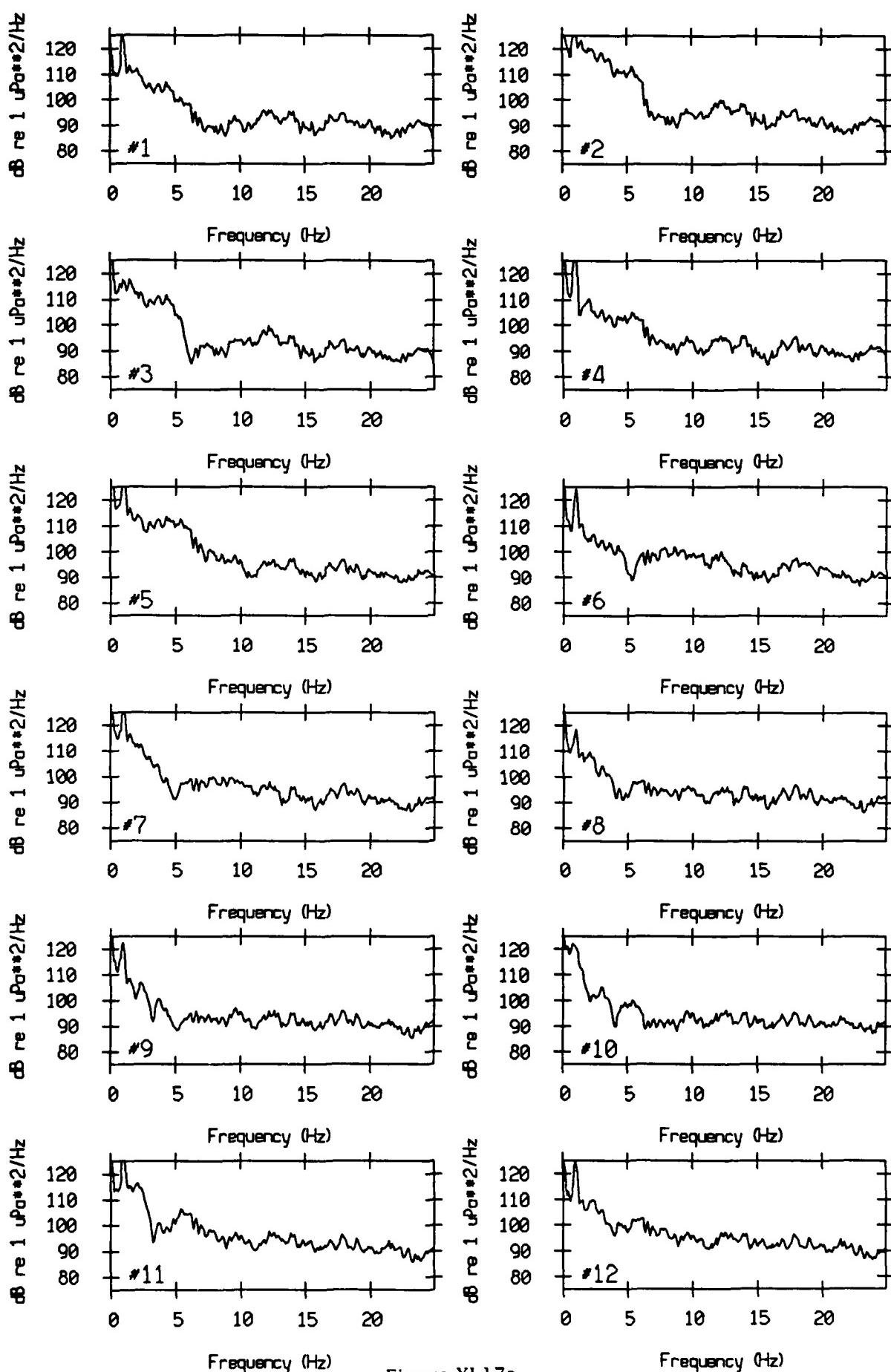


Figure XI.17a

VLA Tape 453, Sept, 1987 - Time 16:30:00.000 Cal. Pressure Spectra
Data dur.: 138.24 sec. FFT Length: 10.24 sec. Samp Freq: 50 Hz

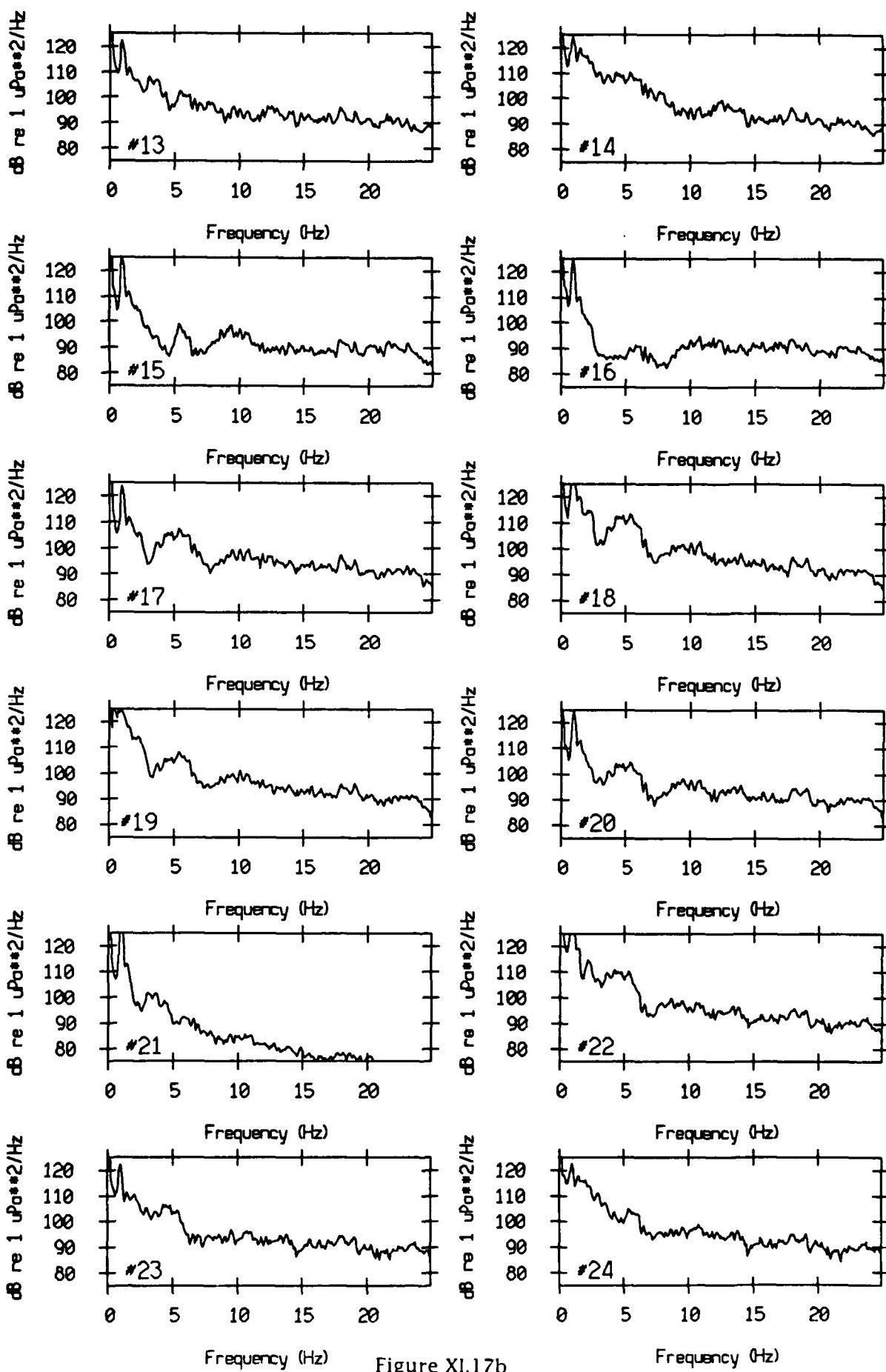


Figure XI.17b

VLA Tape 453, Sept, 1987 - Time 16:30:00.000 Cal. Pressure Spectra
Data dur.: 138.24 sec. FFT Length: 10.24 sec. Samp Freq: 50 Hz

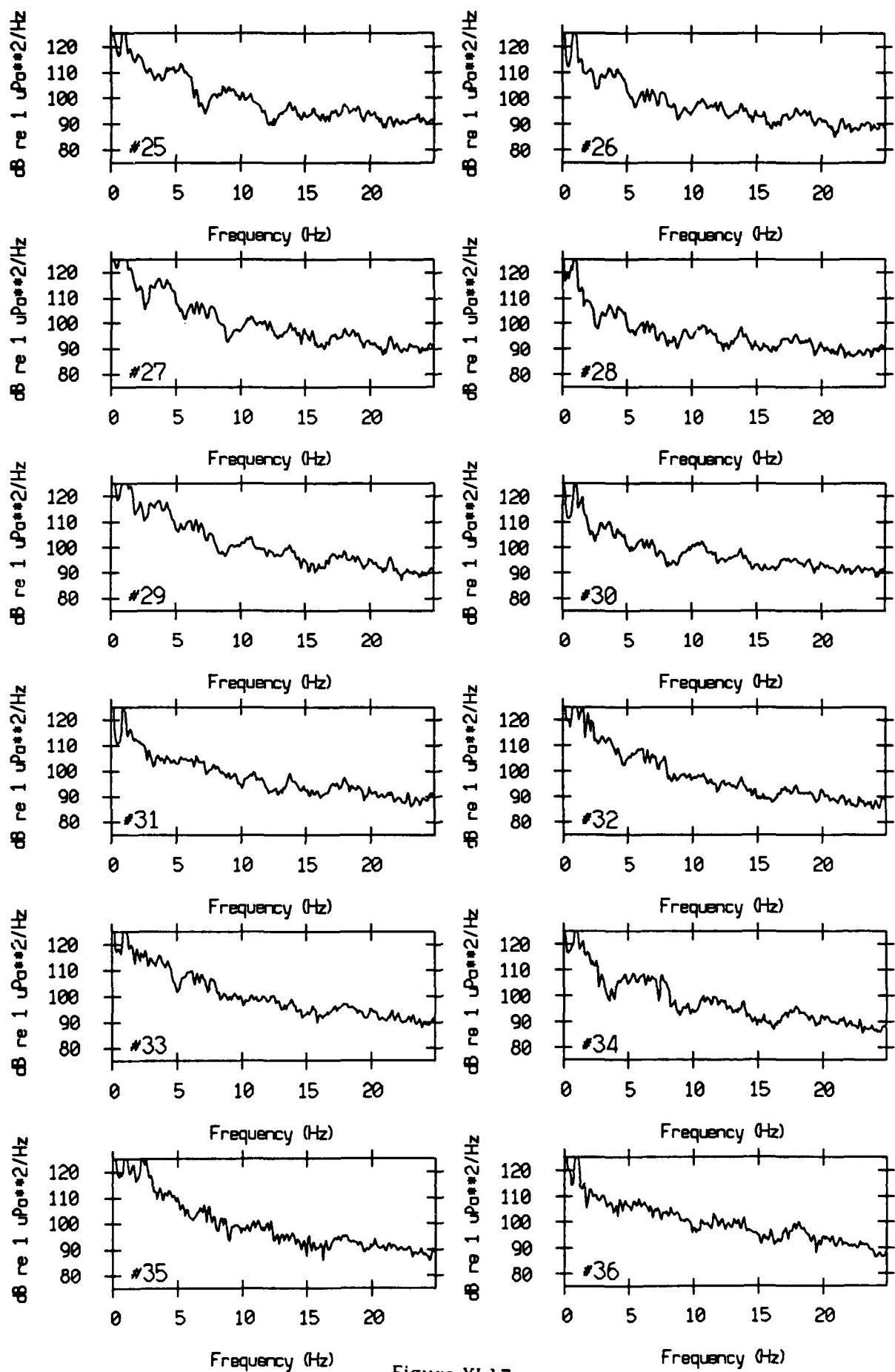


Figure XI.17c

VLA Tape 453, Sept, 1987 - Time 16:30:00.000 Cal. Pressure Spectra
Data dur.: 138.24 sec. FFT Length: 10.24 sec. Samp Freq: 50 Hz

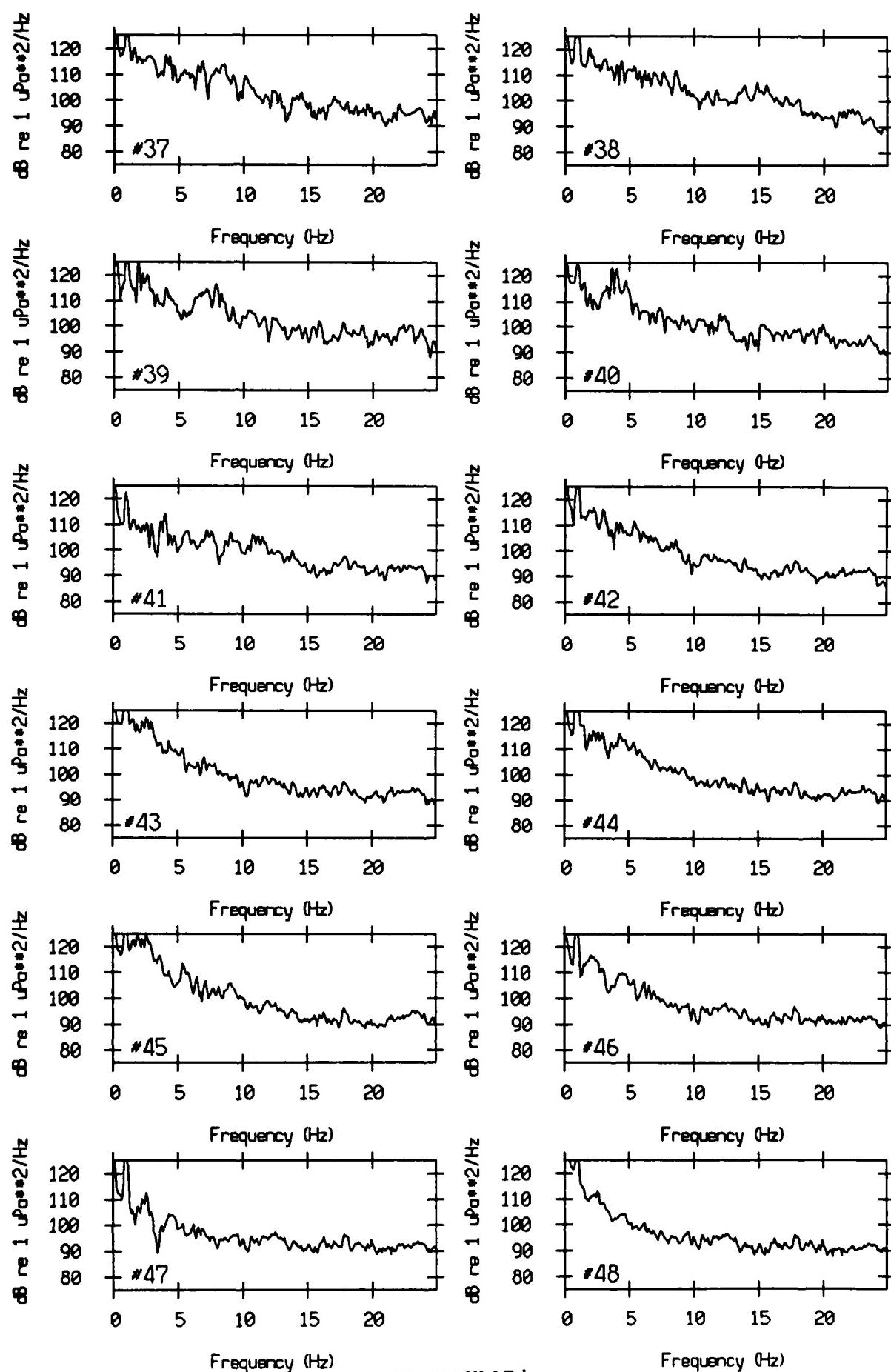


Figure XI.17d

VLA Tape 453, Sept, 1987 - Time 16:30:00.000 Cal. Pressure Spectra
Data dur.: 138.24 sec. FFT Length: 10.24 sec. Samp Freq: 50 Hz

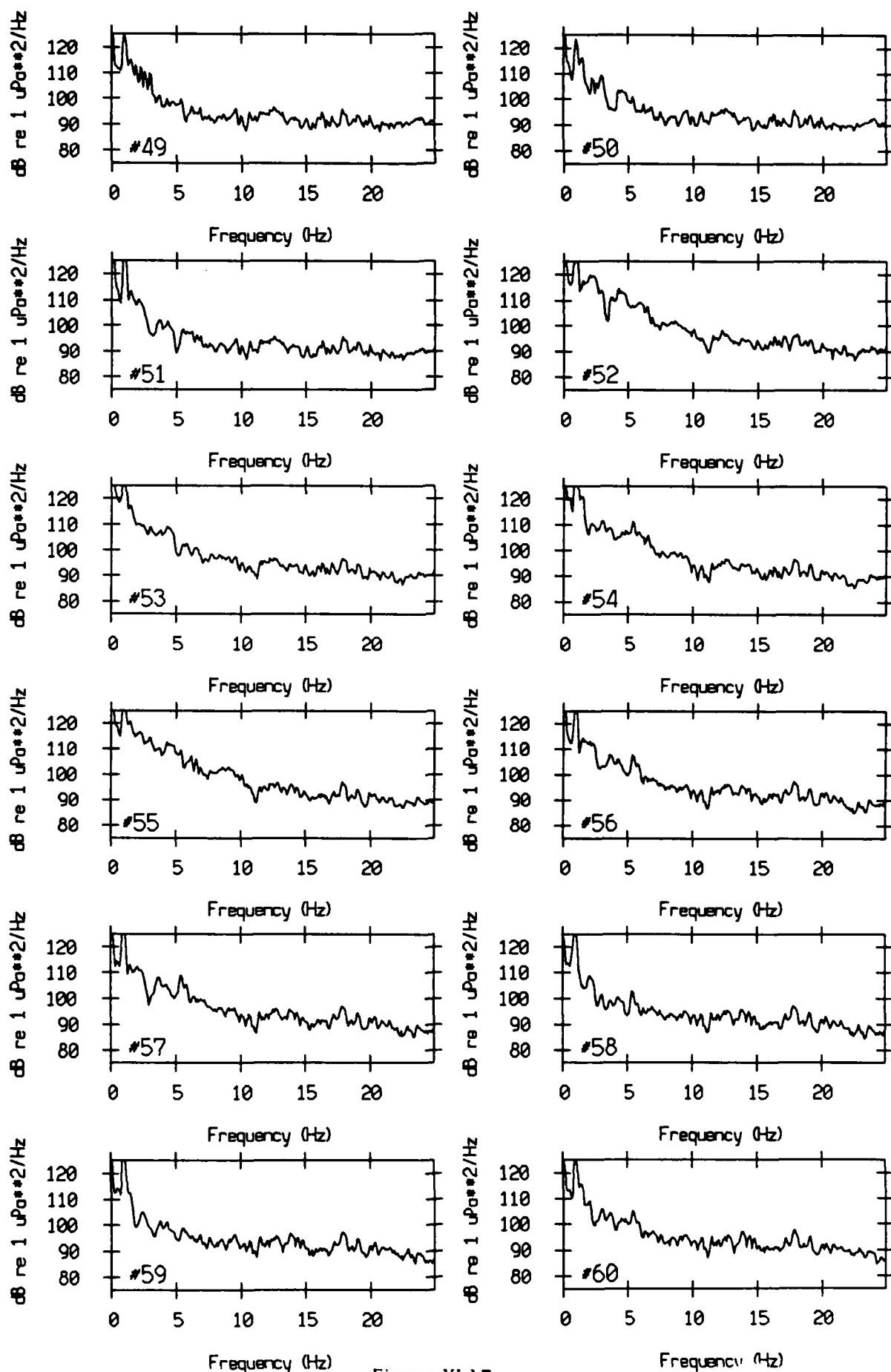


Figure XI.17e

VLA Tape 453, Sept, 1987 - Time 16:30:00.000 Cal. Pressure Spectra
Data dur.: 138.24 sec. FFT Length: 10.24 sec. Samp Freq: 50 Hz

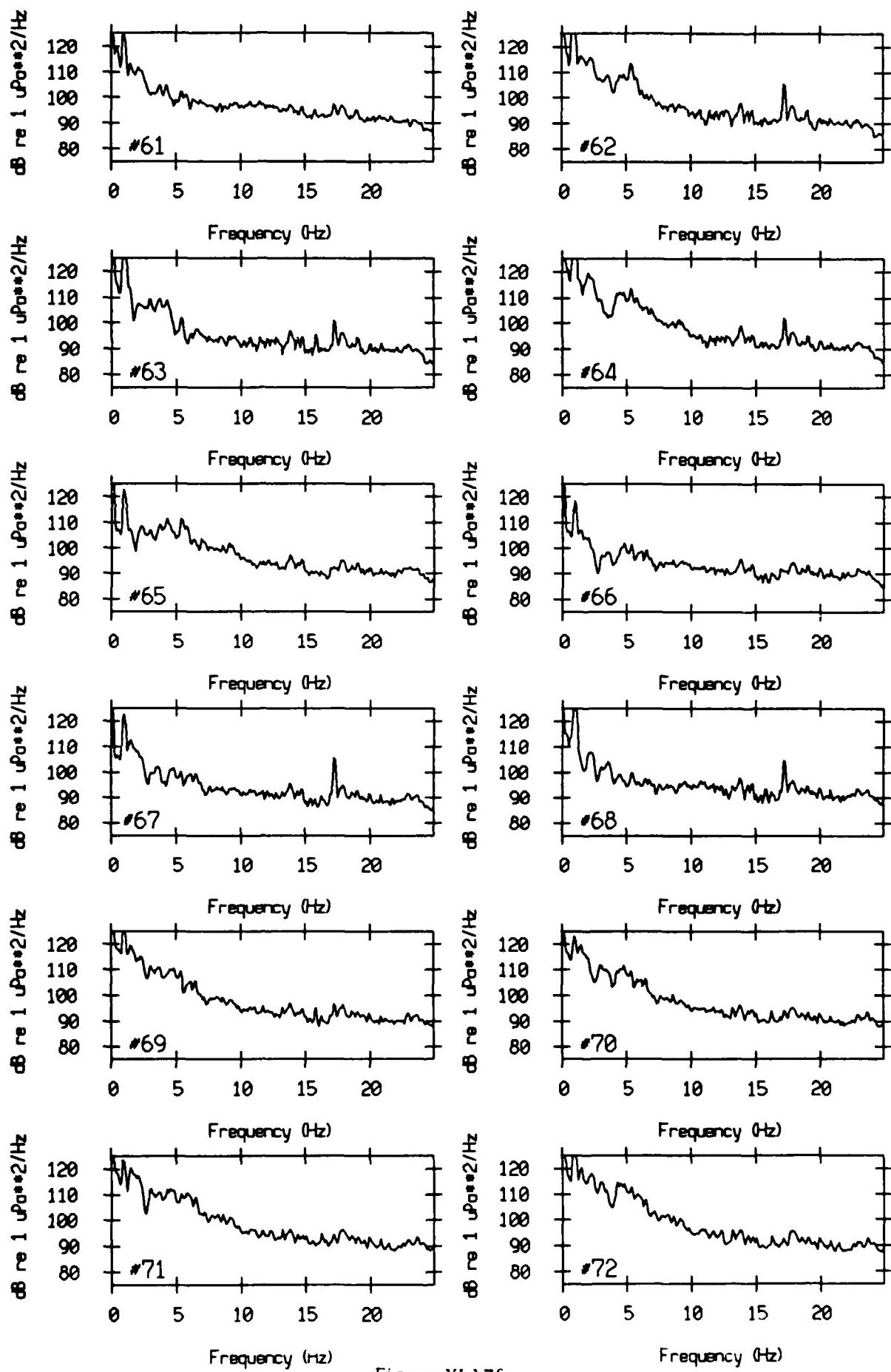


Figure XI.17f

VLA Tape 453, Sept, 1987 - Time 16:30:00.000 Cal. Pressure Spectra
Data dur.: 138.24 sec. FFT Length: 10.24 sec. Samp Freq: 50 Hz

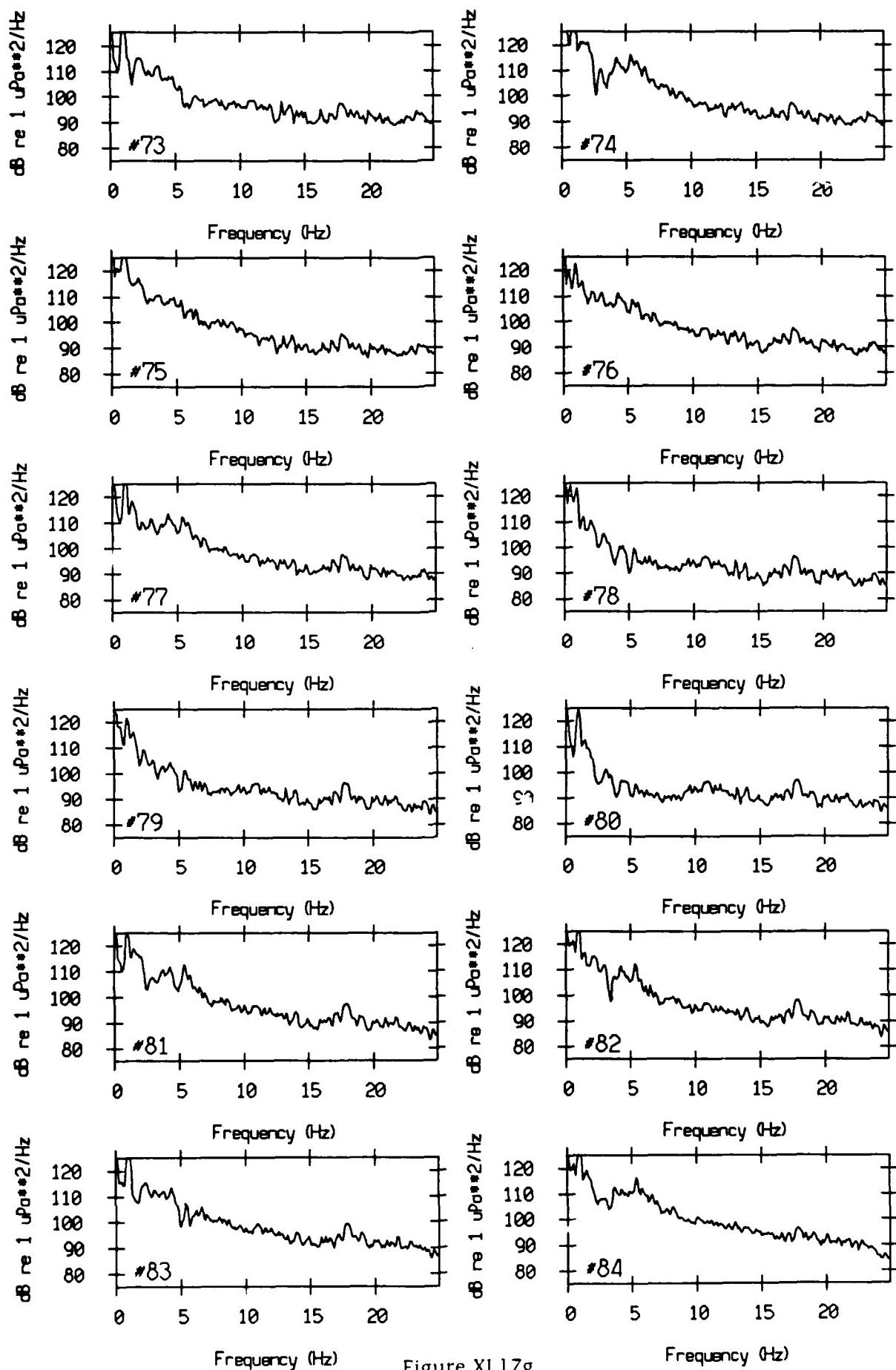
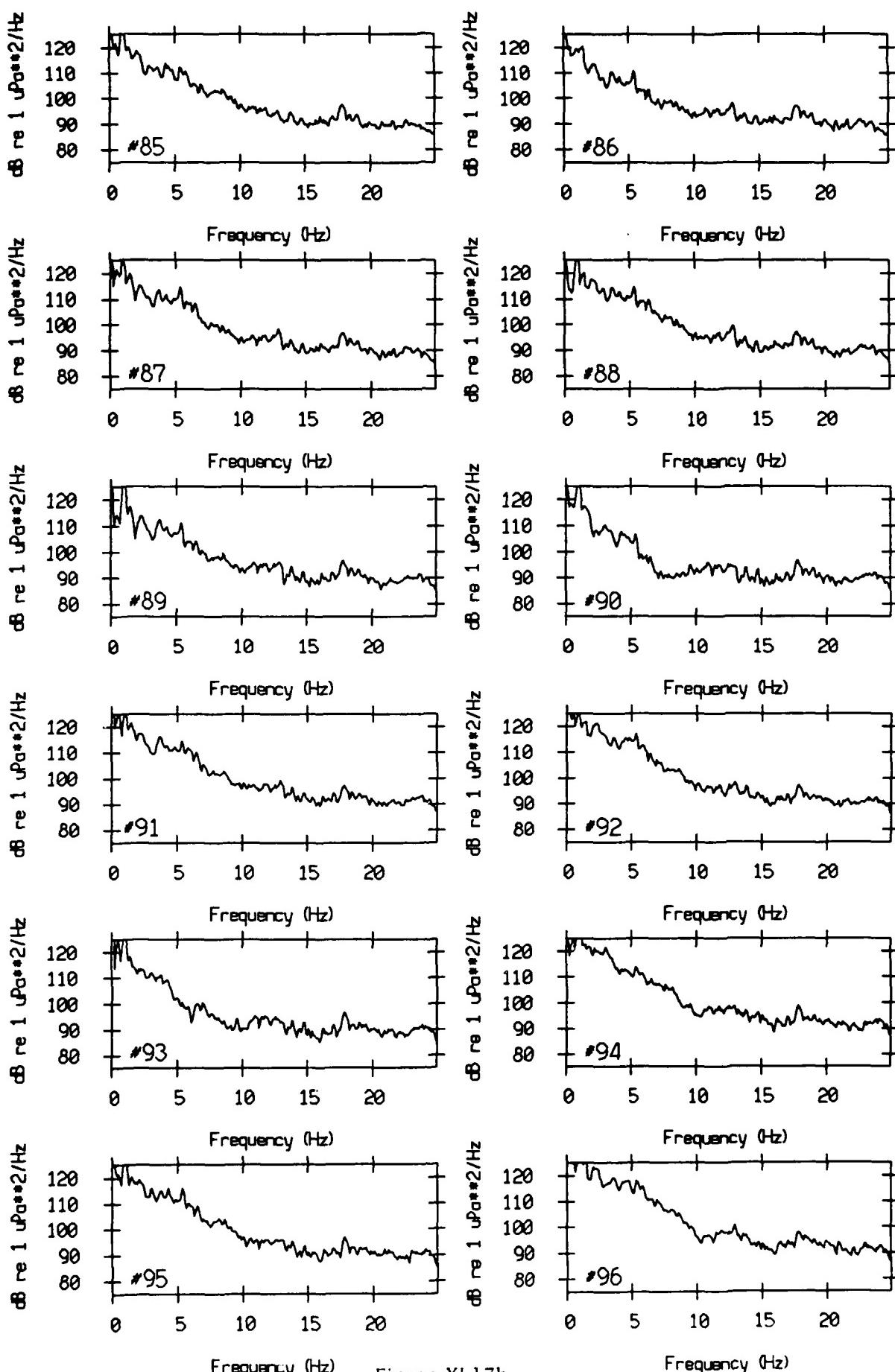


Figure XI.17g

VLA Tape 453, Sept, 1987 - Time 16:30:00.000 Col. Pressure Spectra
Data dur.: 138.24 sec. FFT Length: 10.24 sec. Samp Freq: 50 Hz



Frequency (Hz)

Figure XI.17h

VLA Tape 453, Sept, 1987 - Time 16:30:00.000 Col. Pressure Spectra
Data dur.: 138.24 sec. FFT Length: 10.24 sec. Samp Freq: 50 Hz

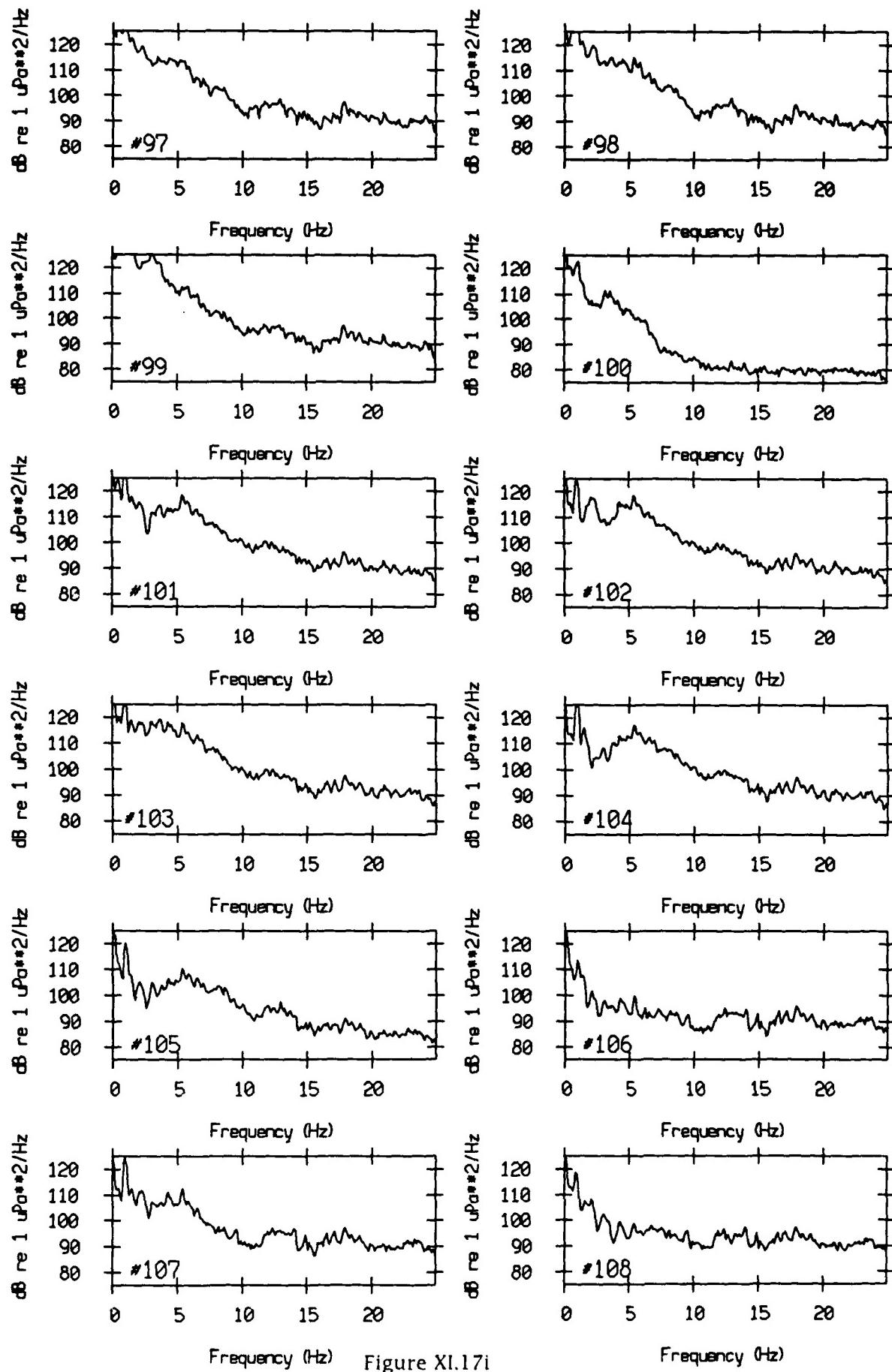
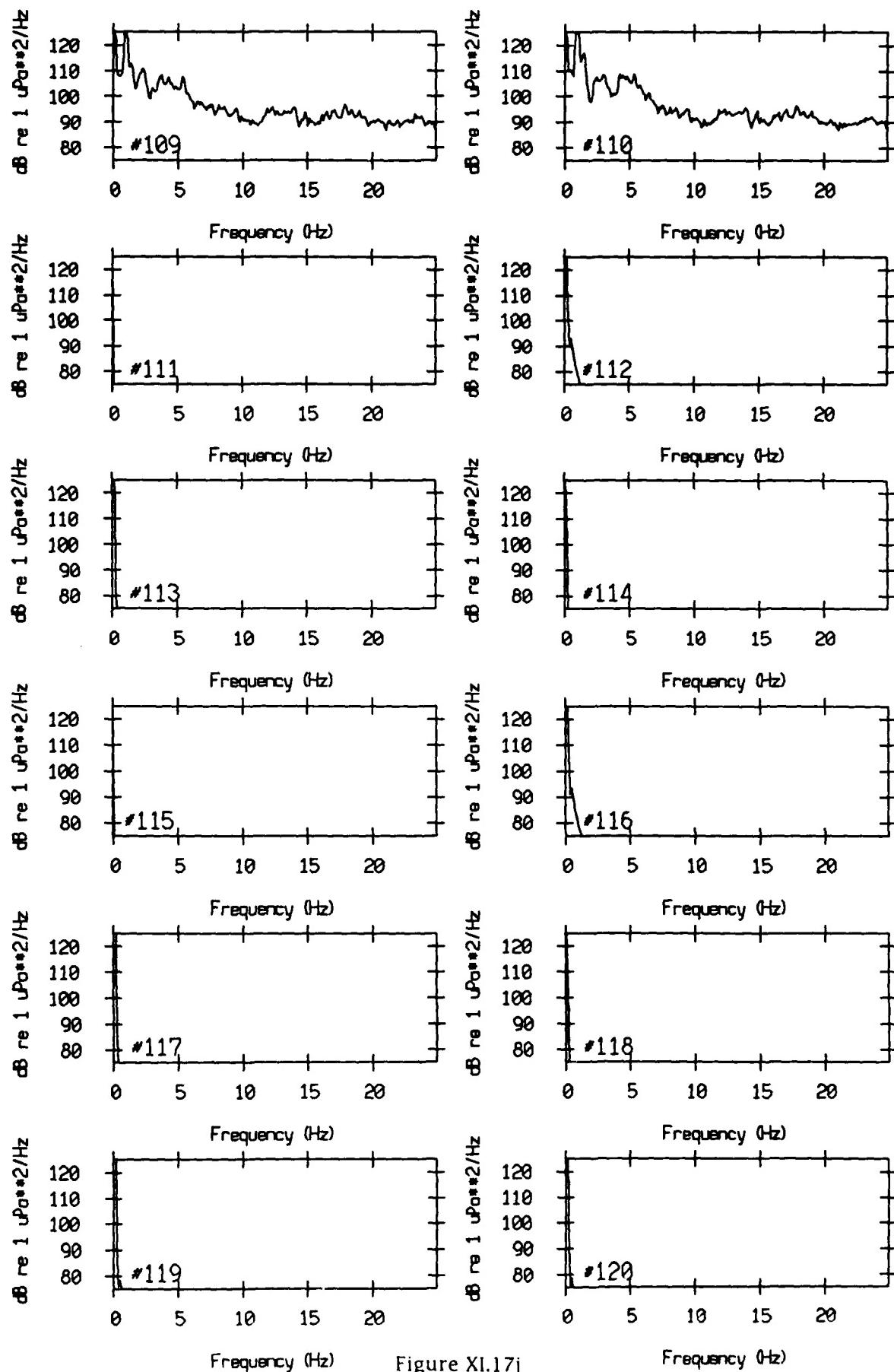


Figure XI.17i

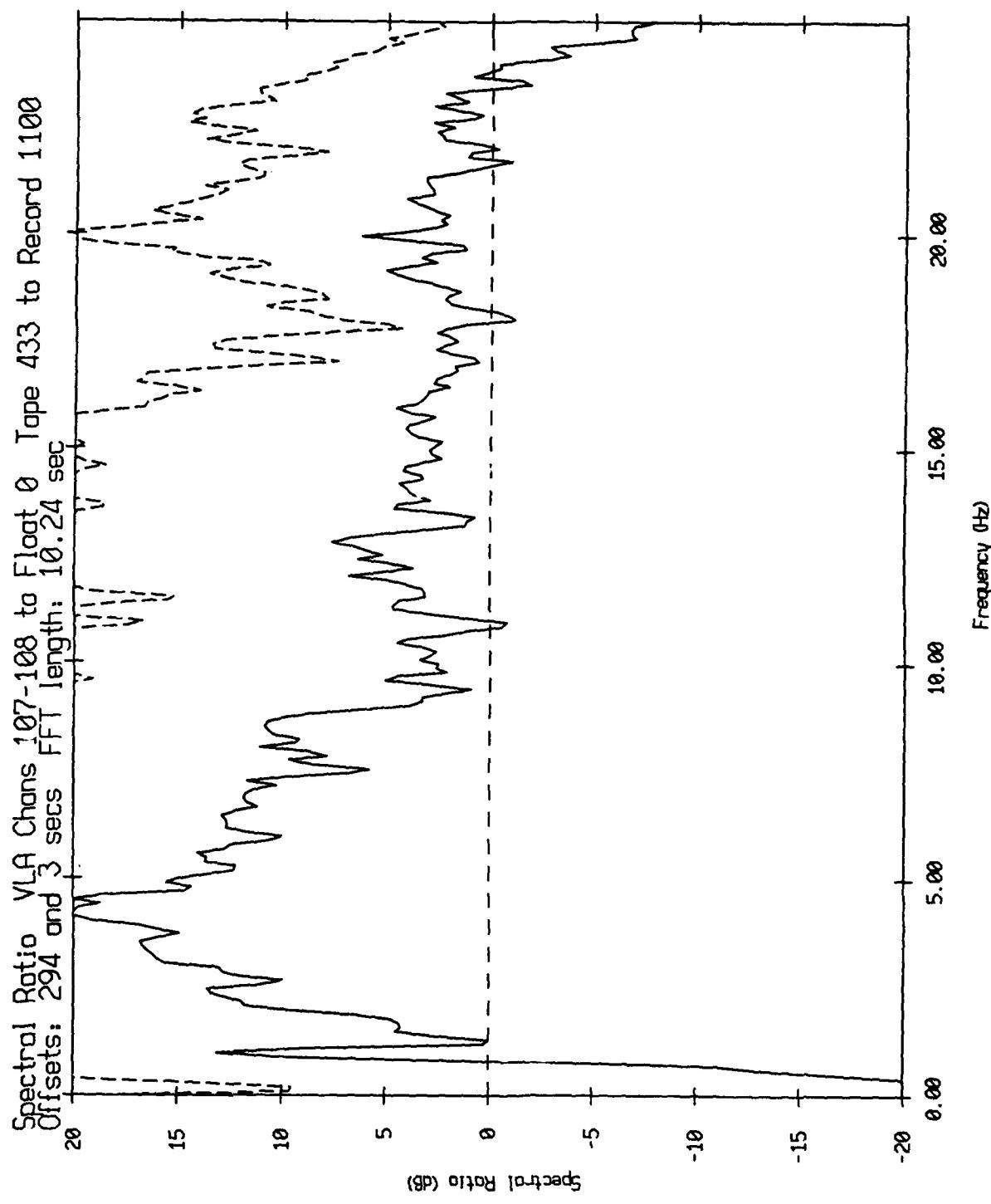
VLA Tape 453, Sept., 1987 - Time 16:30:00.000 Col. Pressure Spectra
Data dur.: 138.24 sec. FFT Length: 10.24 sec. Samp Freq: 50 Hz



Frequency (Hz)

Figure XI.17j

Frequency (Hz)



VLA Spectra over Small Float Spectra

Figure XI.18a

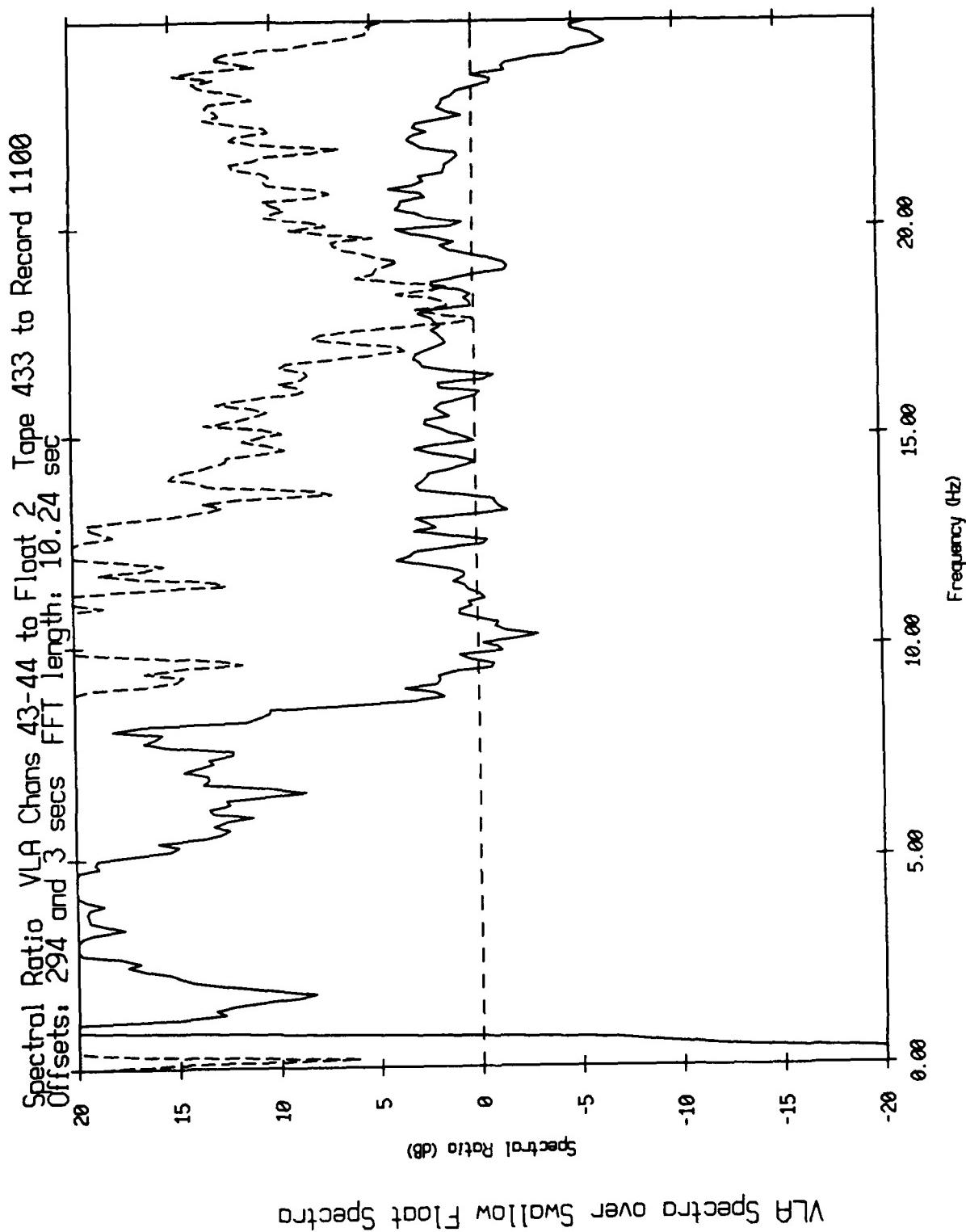


Figure XI.18b

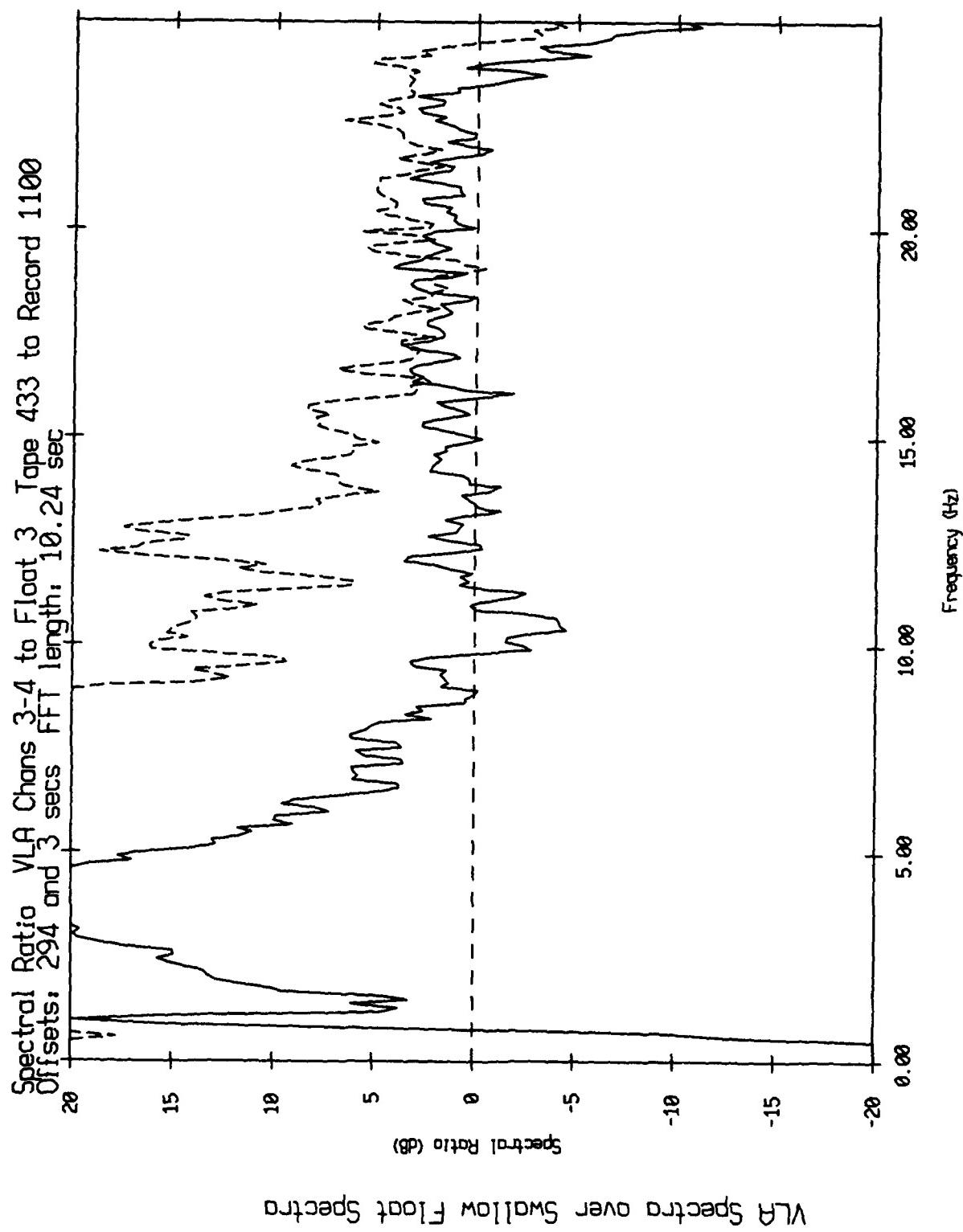
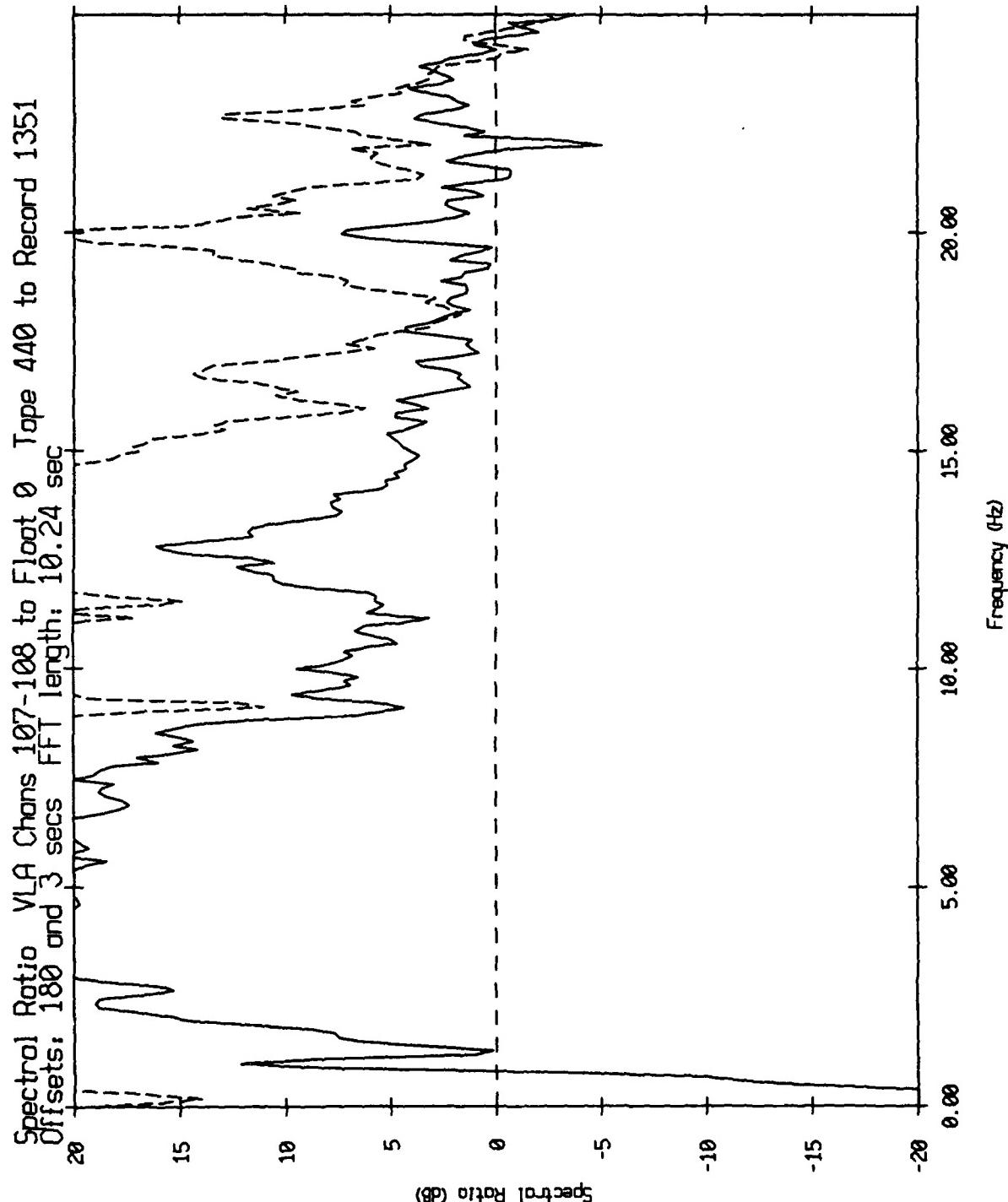


Figure XI.18c



VLA Spectra over Small Low Float Spectra

Figure XI.19a

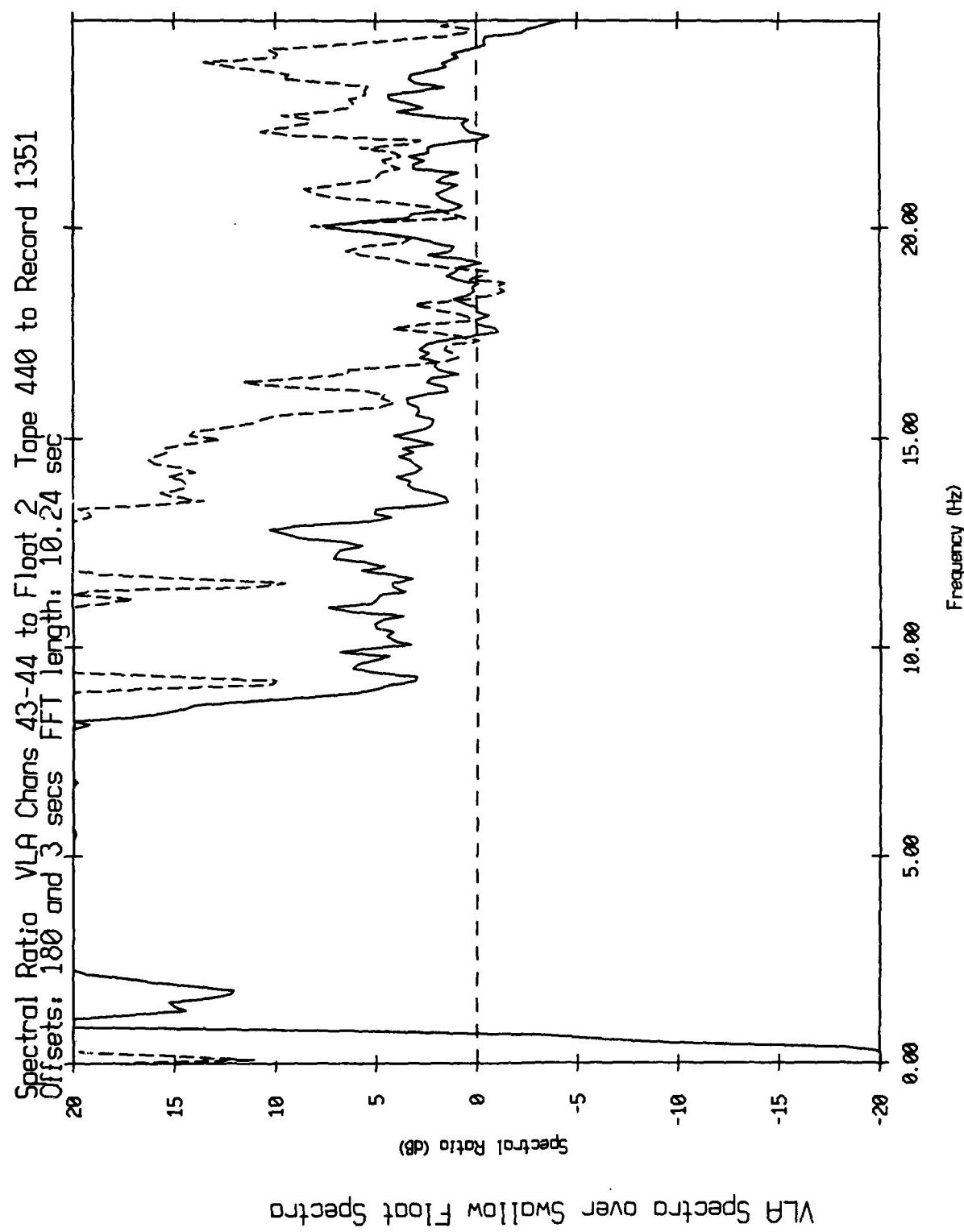


Figure XI.19b

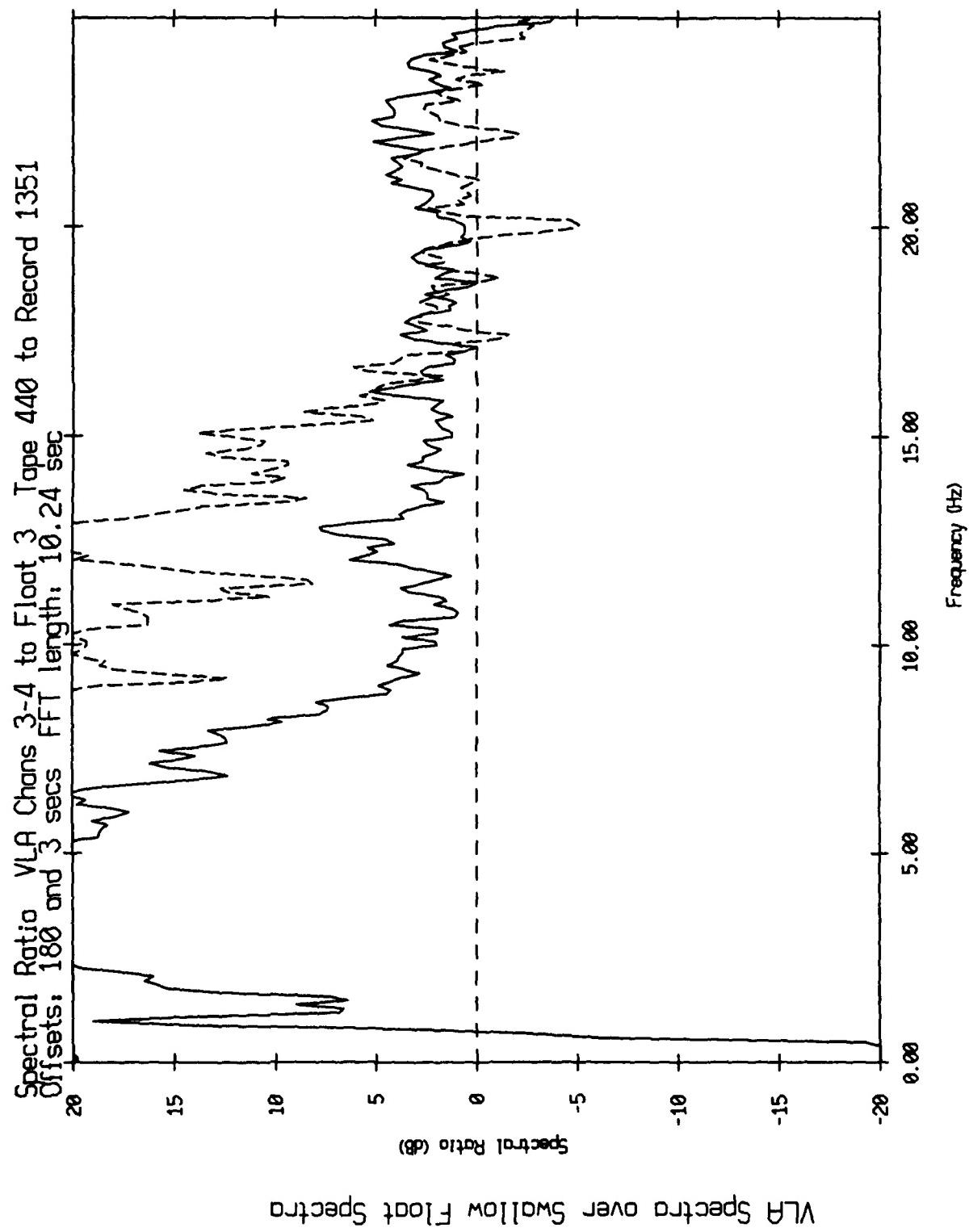
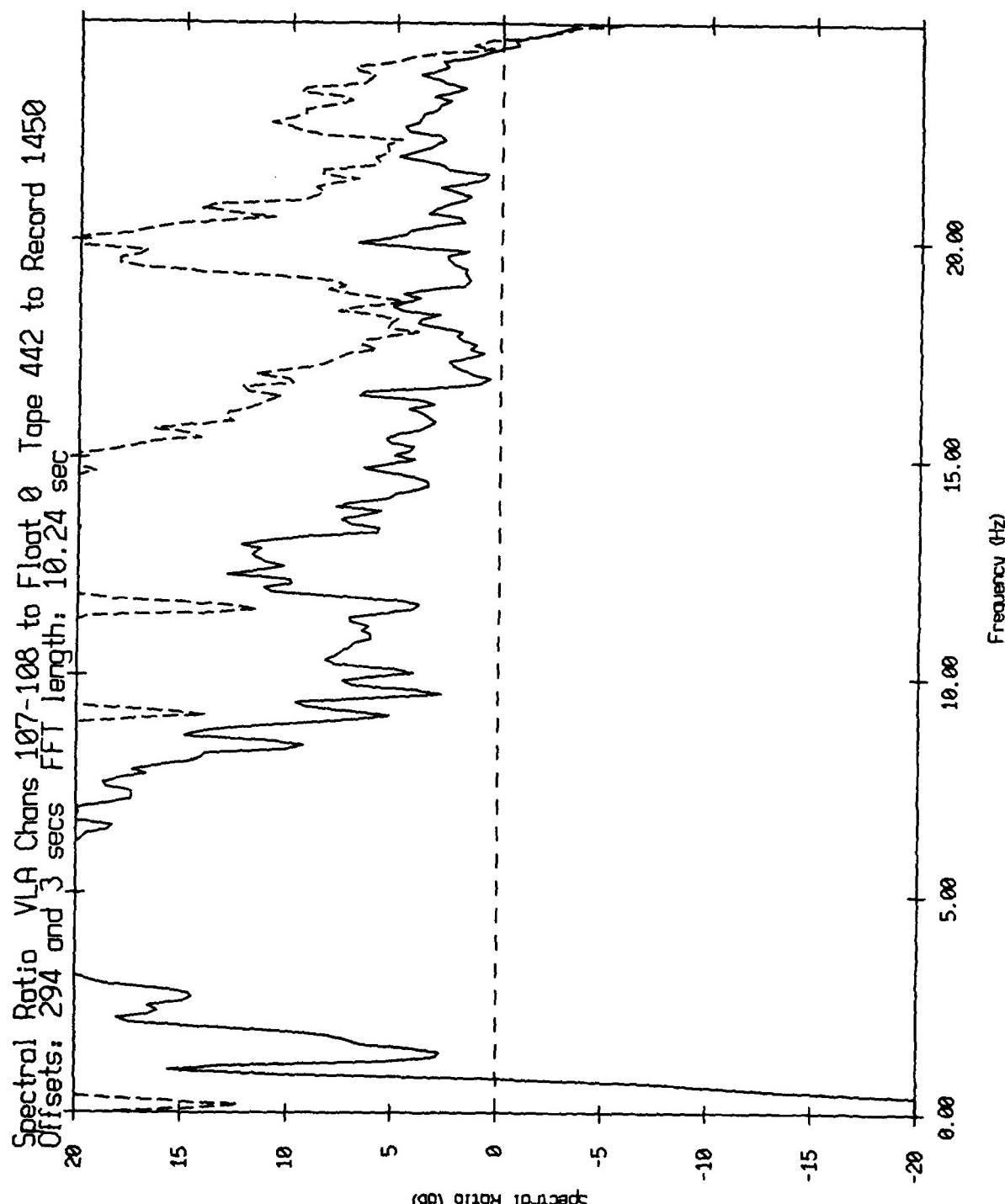
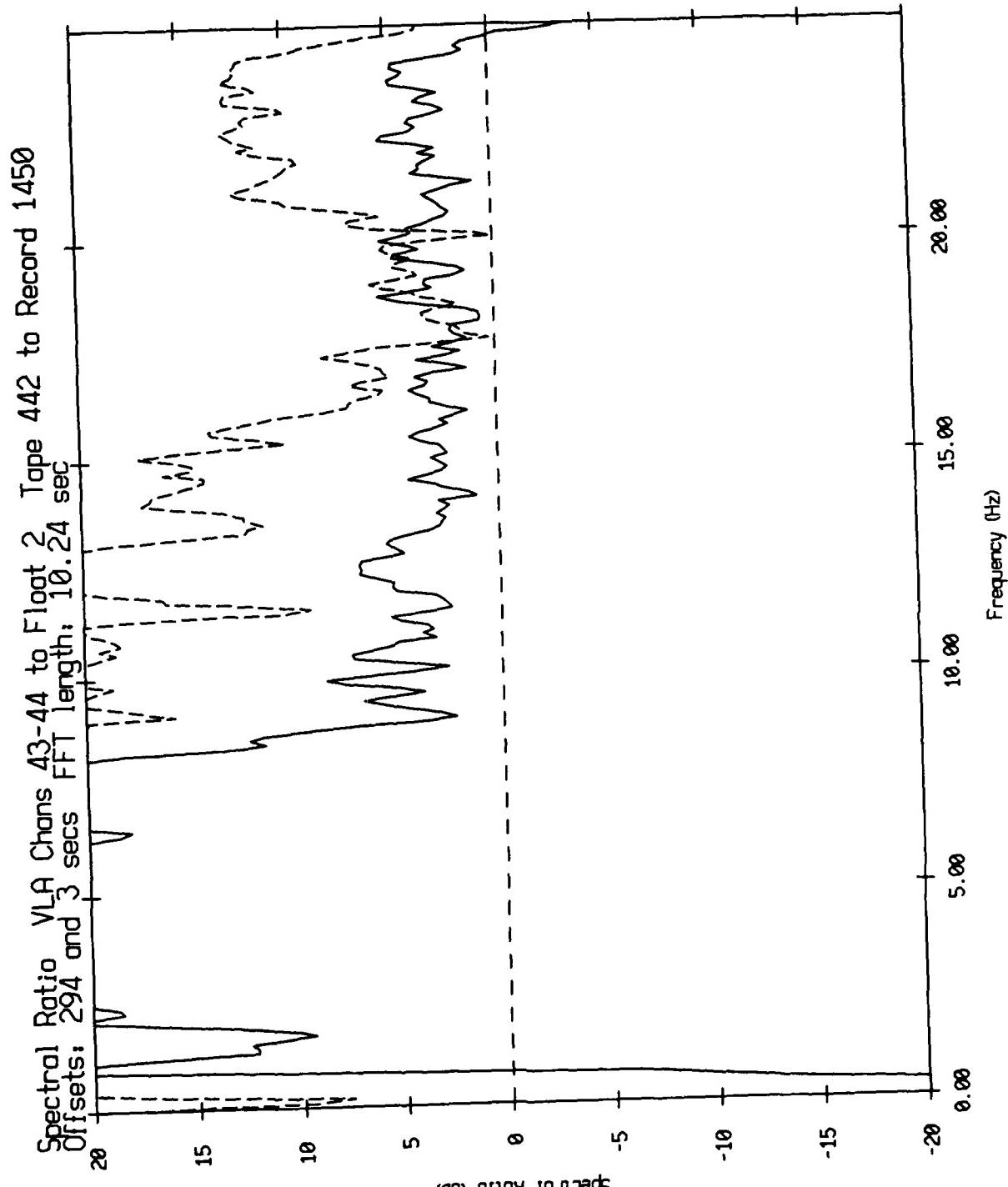


Figure XI.19c



VLA Spectra over Small Float Spectra

Figure XI.20a



VLA Spectra over Small Window Float Spectra

Figure XI.20b

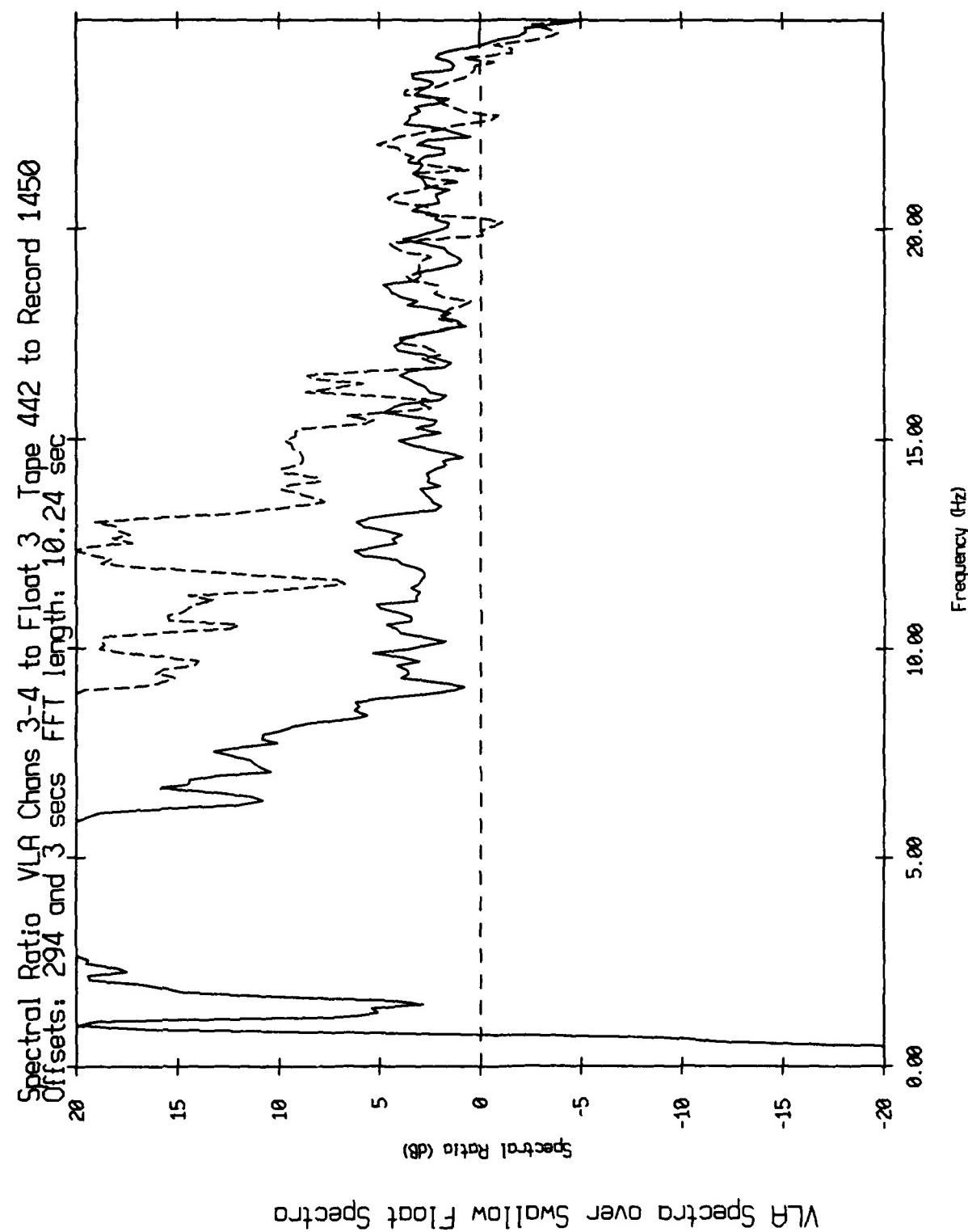


Figure XI.20c

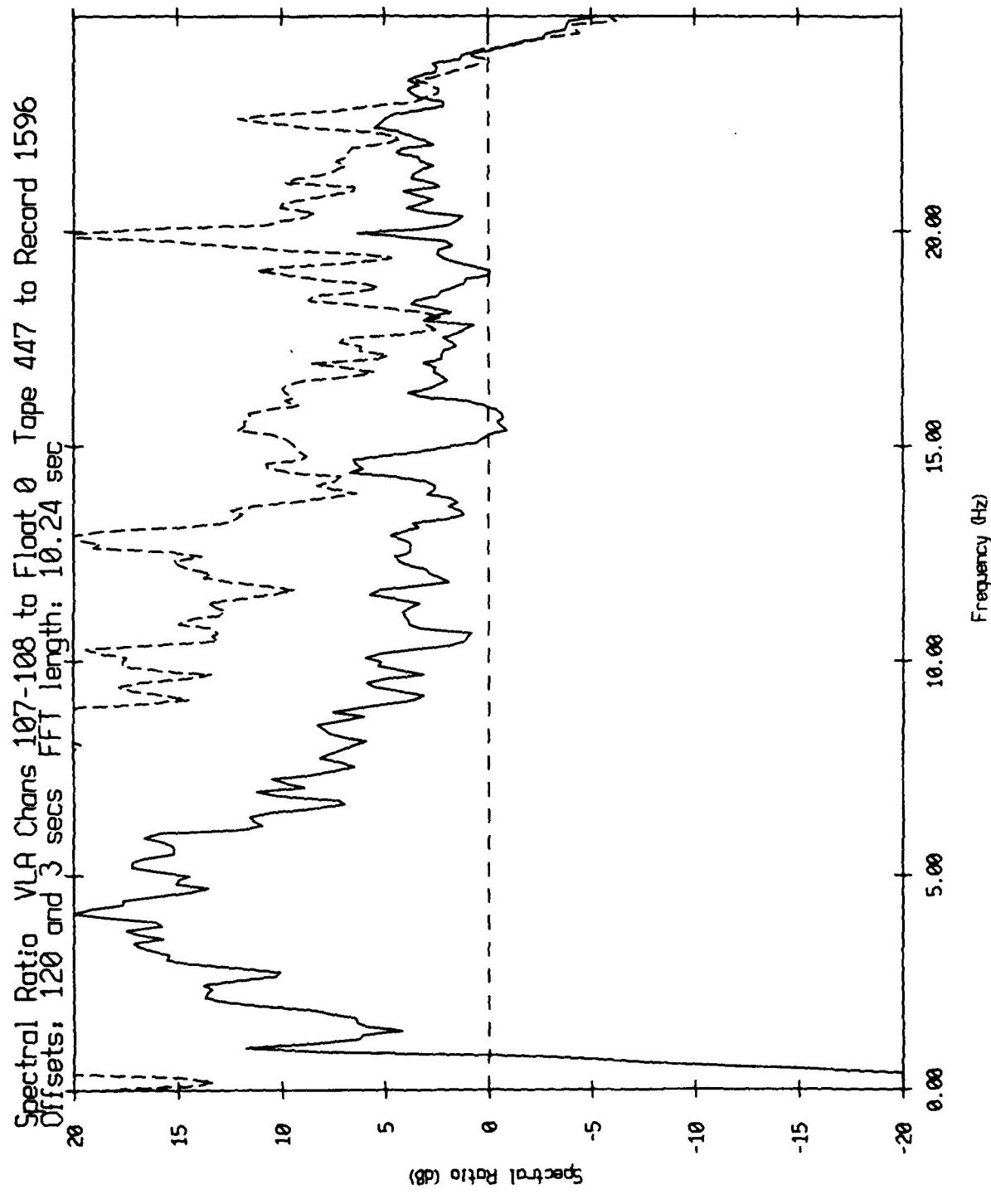
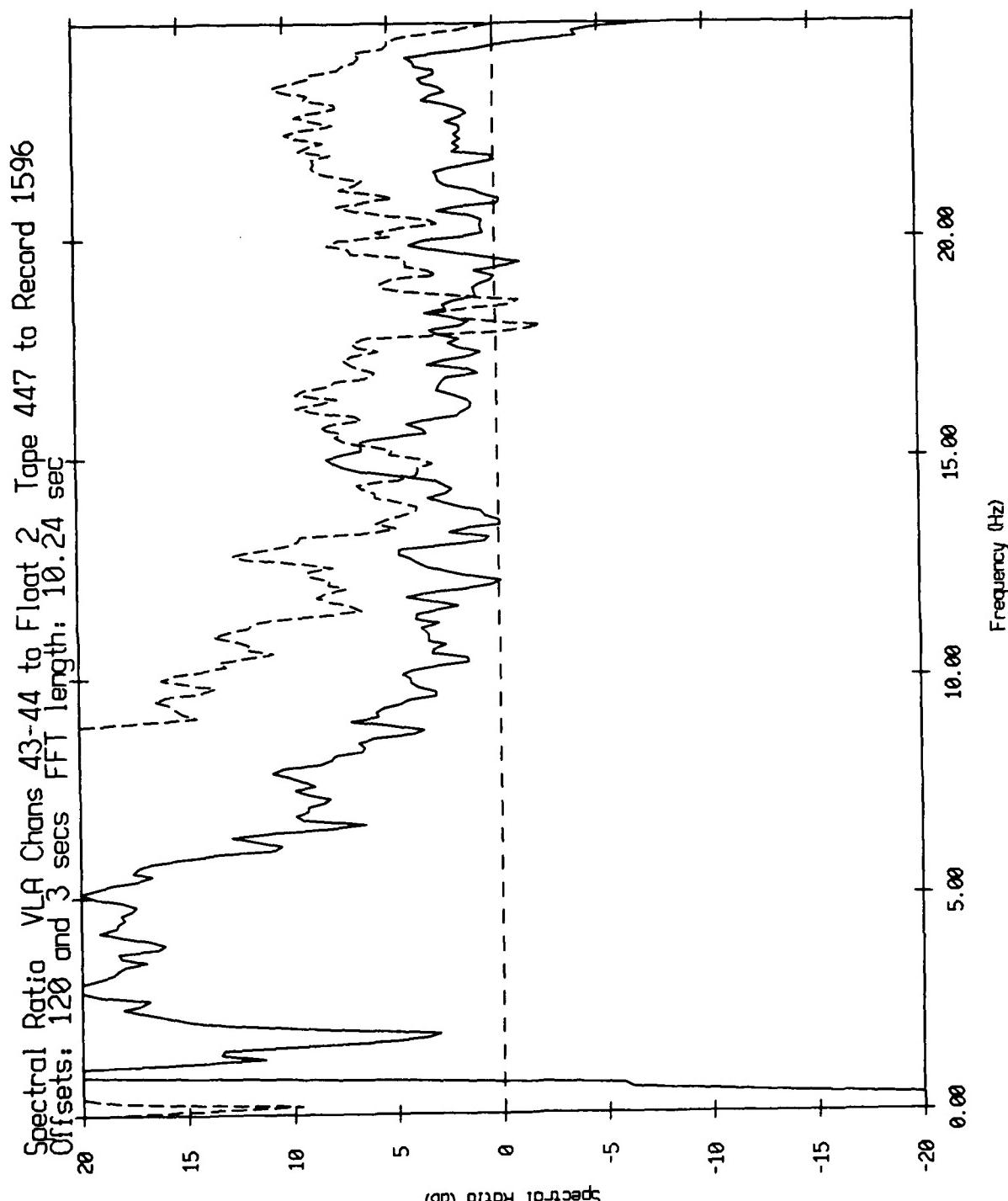
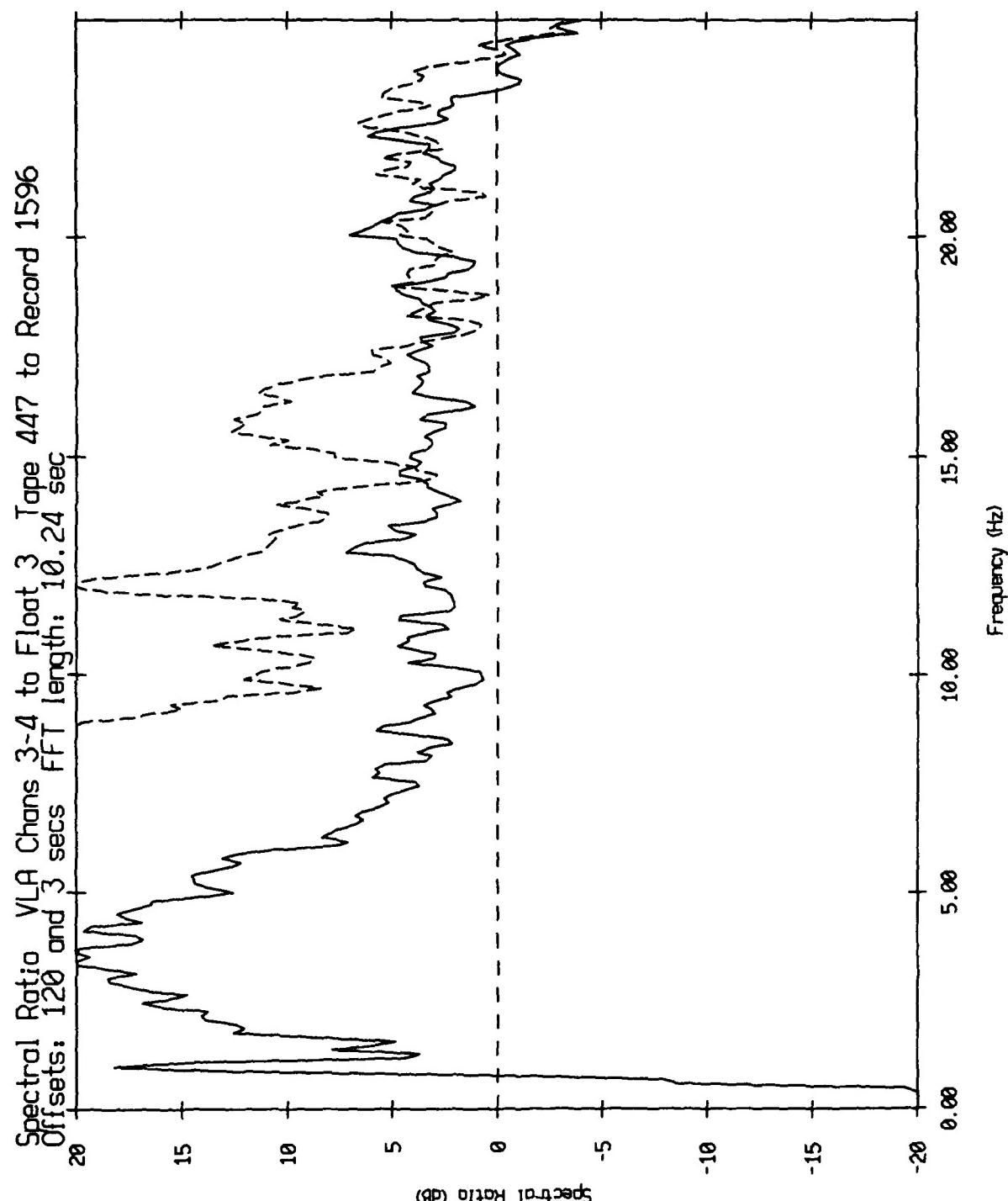


Figure XI.21a



VLA Spectra over Small Low Float Spectra

Figure XI.21b



VLA Spectra over 5wallow Float Spectra

Figure XI.21c

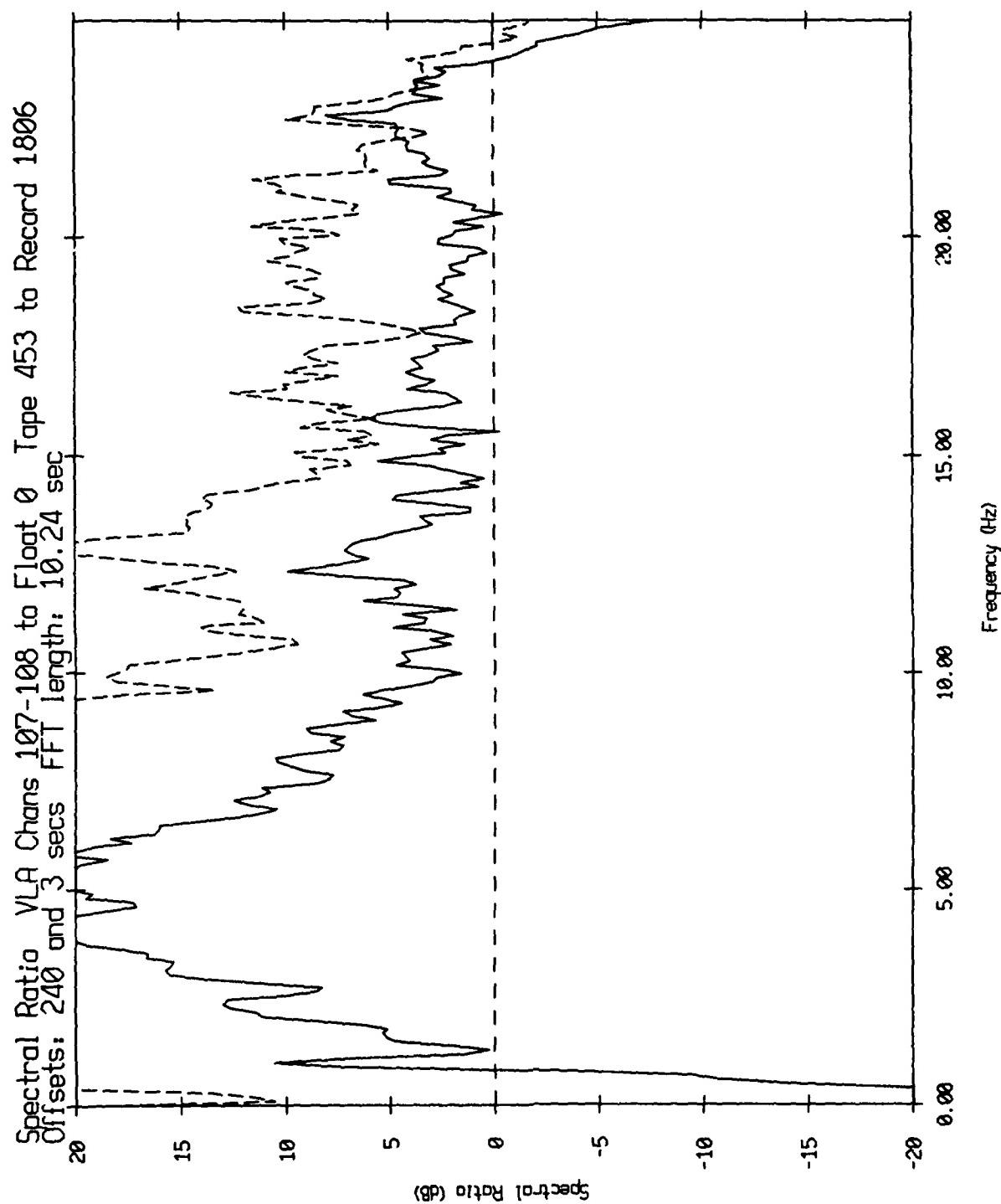
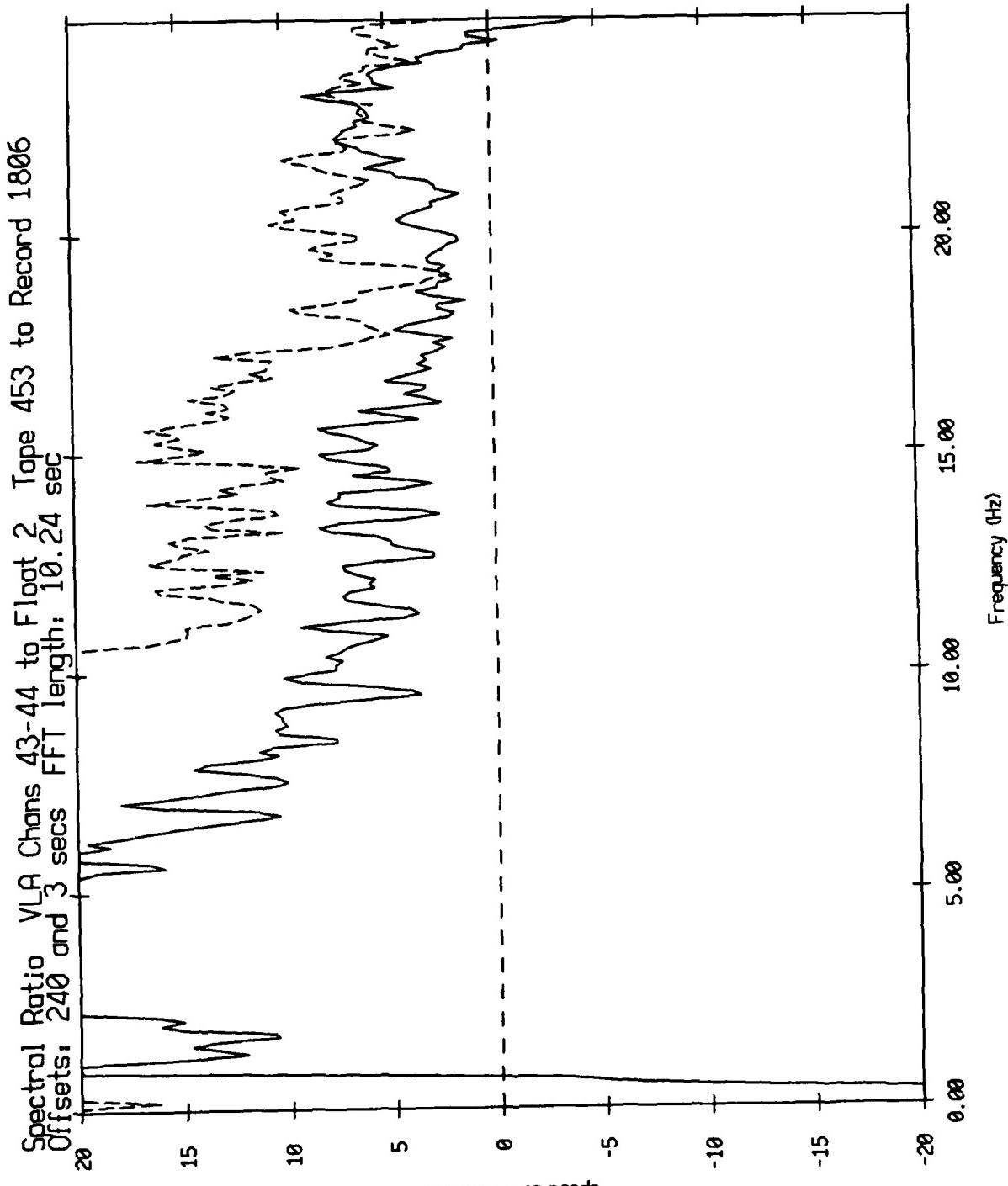


Figure XI.22a



VLA Spectra over 5wallow Float Spectra

Figure XI.22b

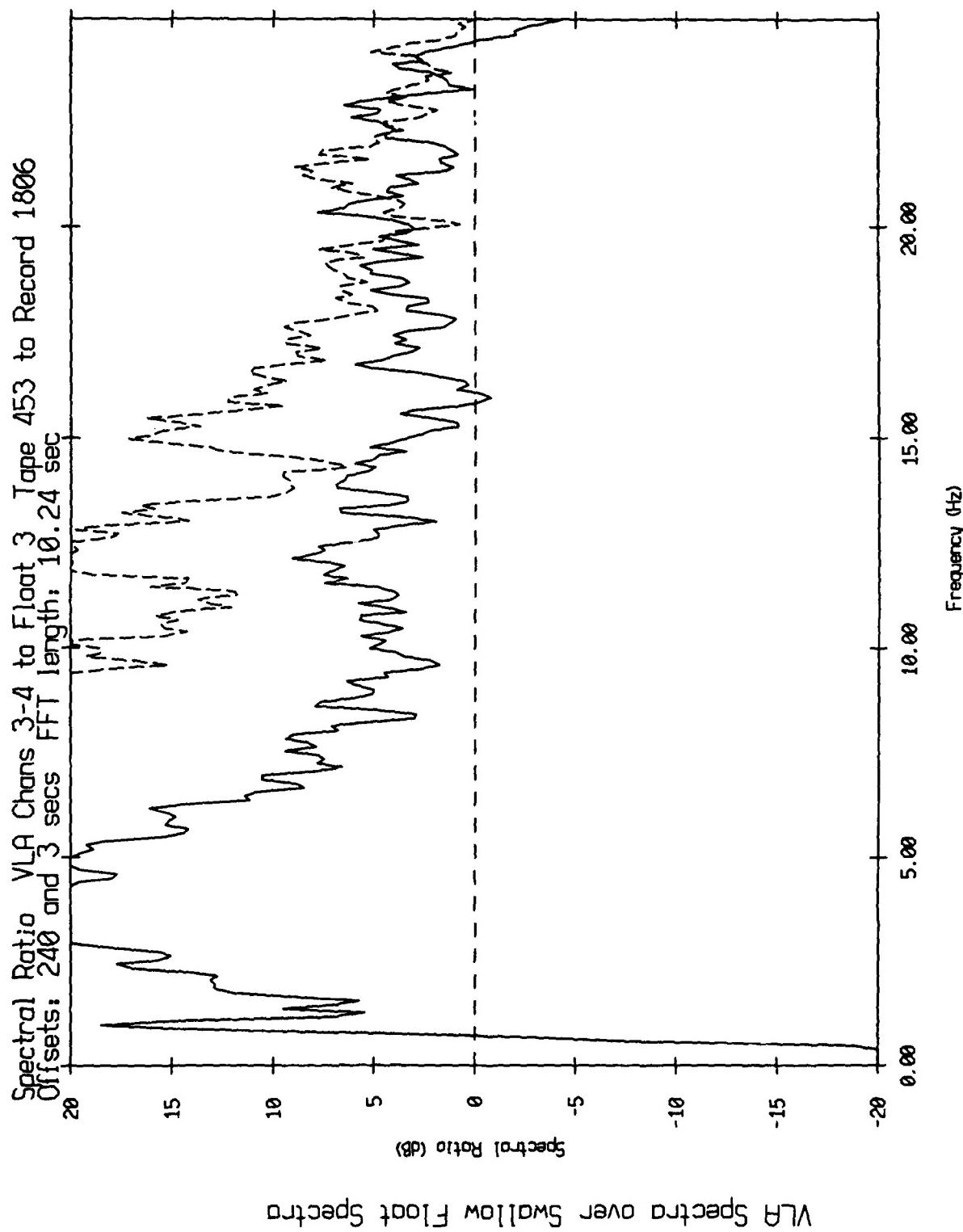


Figure XI.22c

BLOCK DIAGRAM OF THE GEOPHONE DATA ACQUISITION SYSTEM

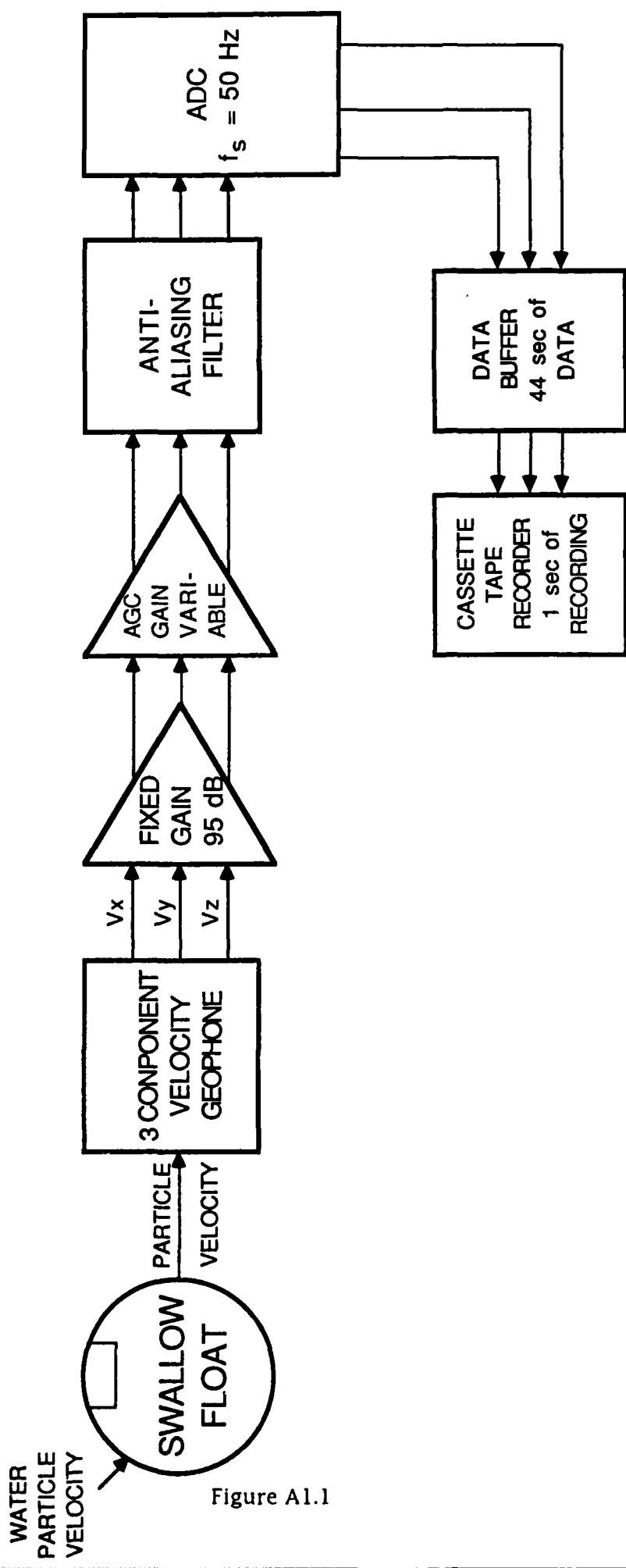


Figure A1.1

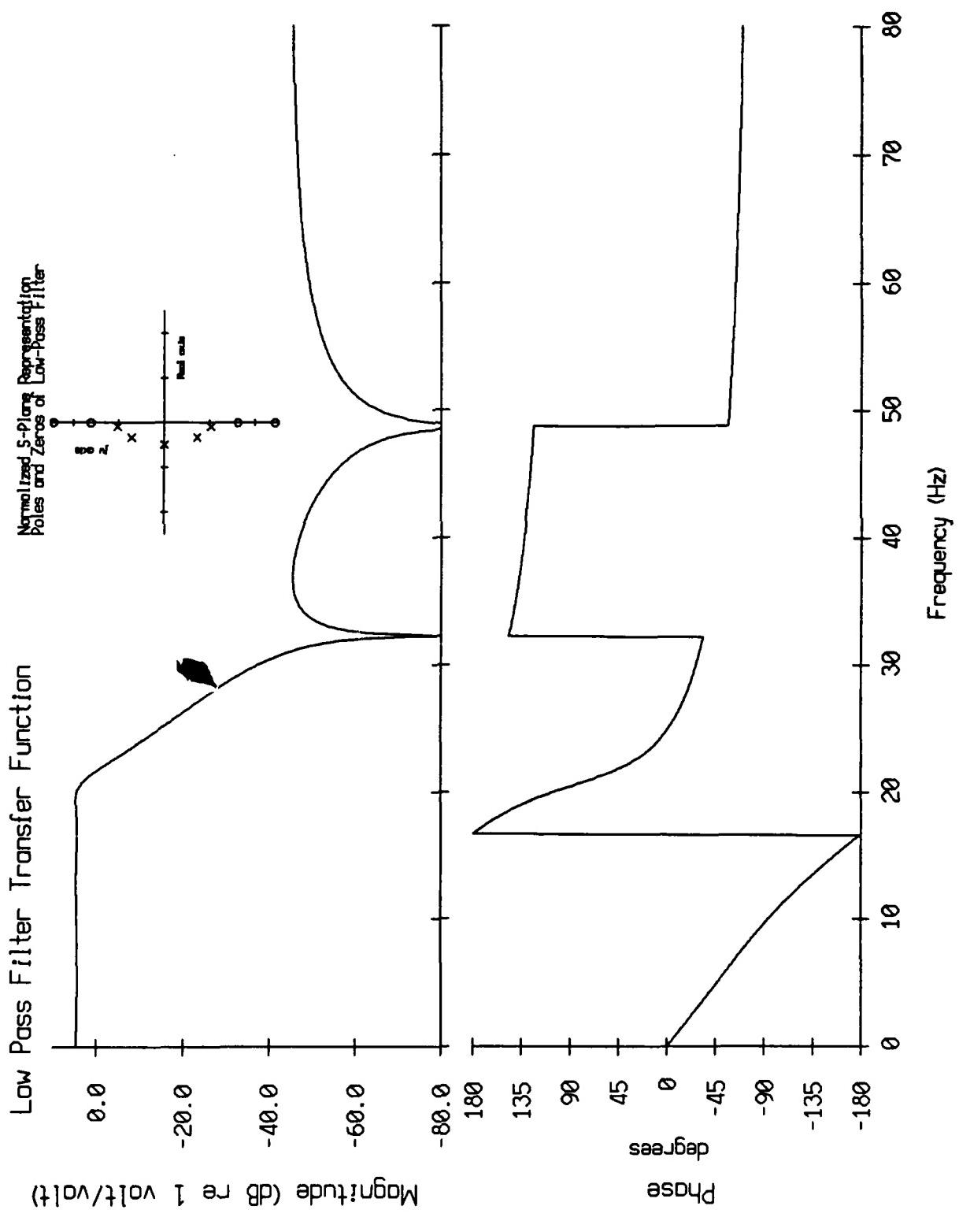


Figure A1.2

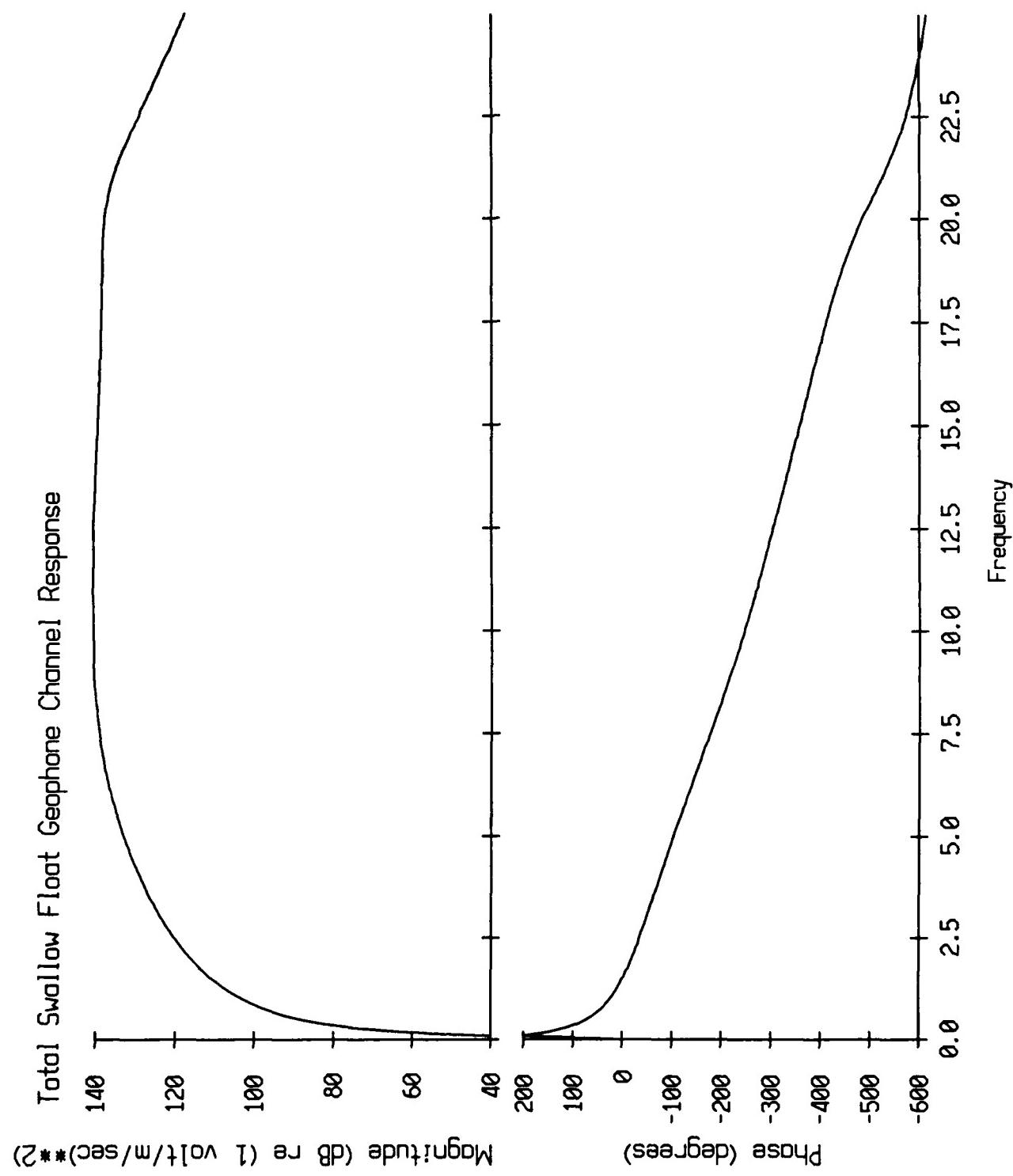


Figure A1.3

Geophone Channel Transfer Function Error
amount to be added to old spectra to get true spectra

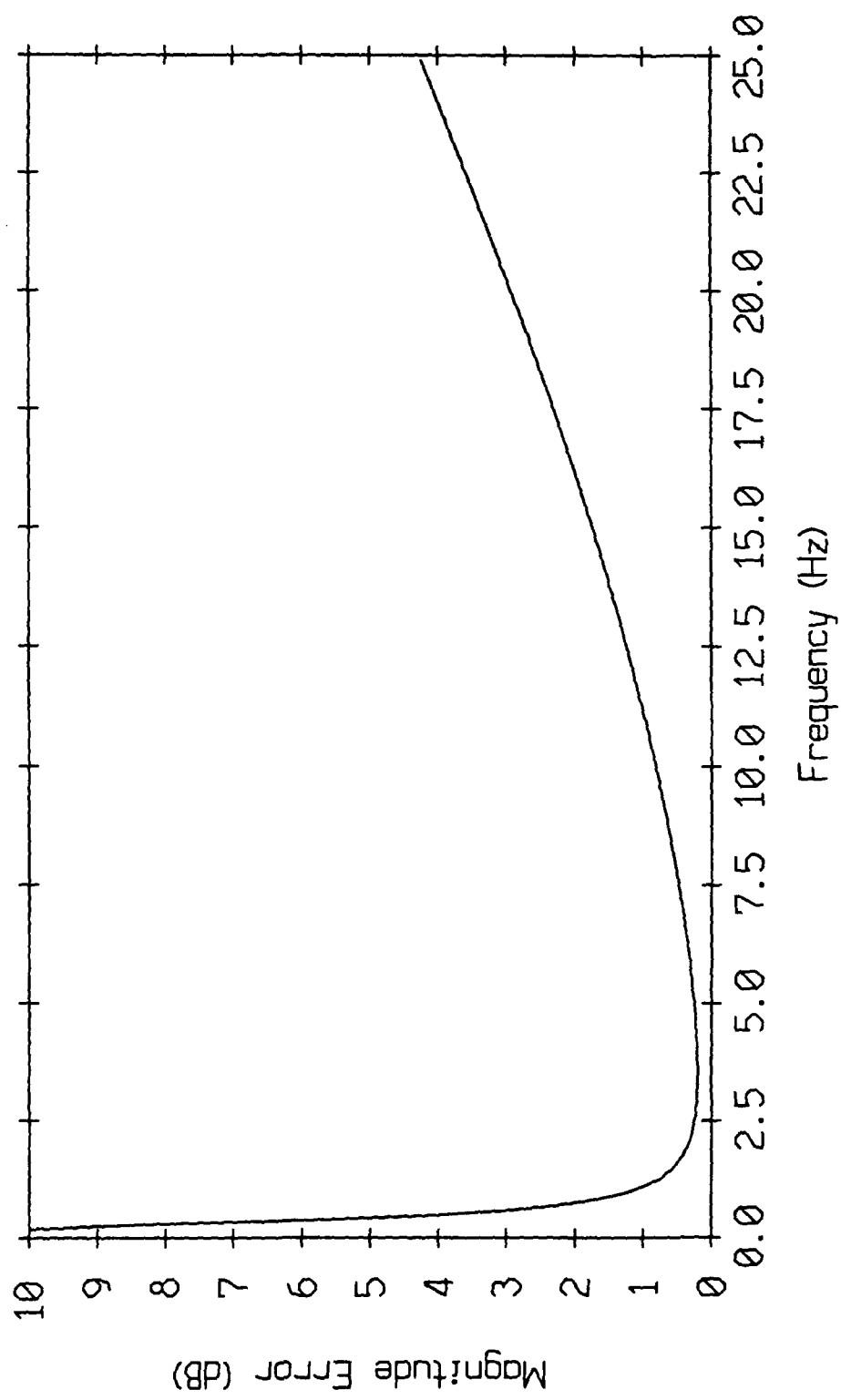


Figure A1.4

1	RECORD # (LB)	H	527	RESYNC (AA)	V
	RECORD # (HB)	E		RESYNC (AA)	L
	AGC CODE	A		RESYNC (01)	F
	COMPASS	D		CHAN X	
	BUOY ID	E		CHAN Y	A
	BATTERY	R		CHAN Z	C
	TAPE TRACK			CHAN X	O
	CHECKSUM (LB)			CHAN Y	U
	CHECKSUM (HB)			CHAN Z	S
10	RESYNC (AA)				T
	RESYNC (AA)				I
	RESYNC (01)			CHECKSUM (LB)	C
13	RANGE INDEX 1	R	607	CHECKSUM (HB)	
	DETECTION	A		RESYNC (AA)	D
	TIME (LB)	N		RESYNC (AA)	A
	TIME (HB)	G		RESYNC (01)	T
	DETECTION	E		CHAN X	A
	TIME (LB)			CHAN Y	
	TIME (HB)	P		CHAN Z	
		U			
		L			
	DETECTION	S		CHECKSUM (LB)	
	TIME (LB)	E	7646	CHECKSUM (HB)	
	TIME (HB)				G
269	RANGE INDEX 2	D			A
	DETECTION	A			P
	TIME (LB)	T	1	RECORD # (LB)	
	TIME (HB)	A			N
	DETECTION				E
	TIME (LB)				X
	TIME (HB)				T
	DETECTION				R
	TIME (LB)				E
	TIME (HB)				C
	CHKSUM (LB)				O
526	CHKSUM (HB)				D

FIG. SWALLOW DATA RECORD FORMAT

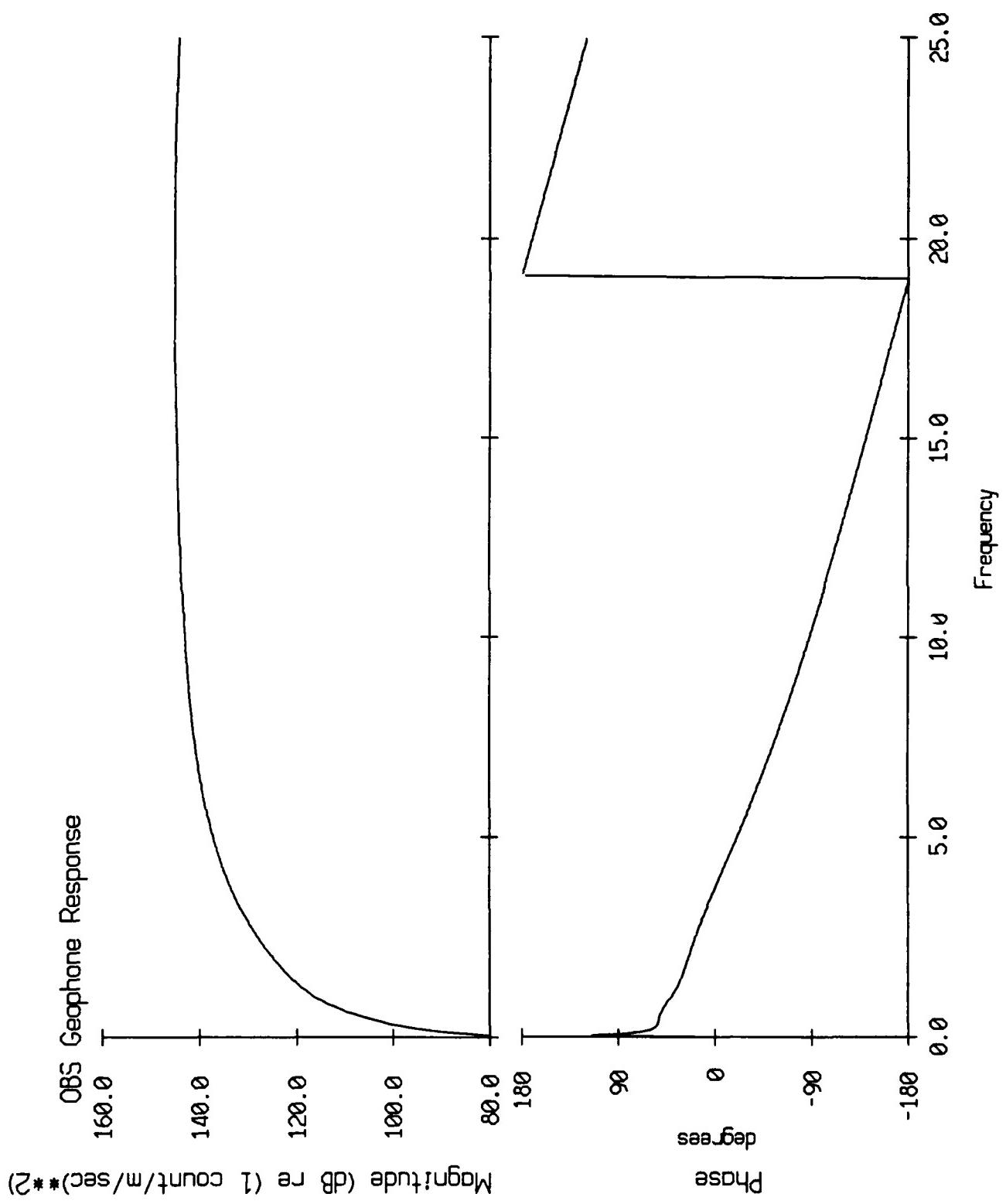


Figure A2.1

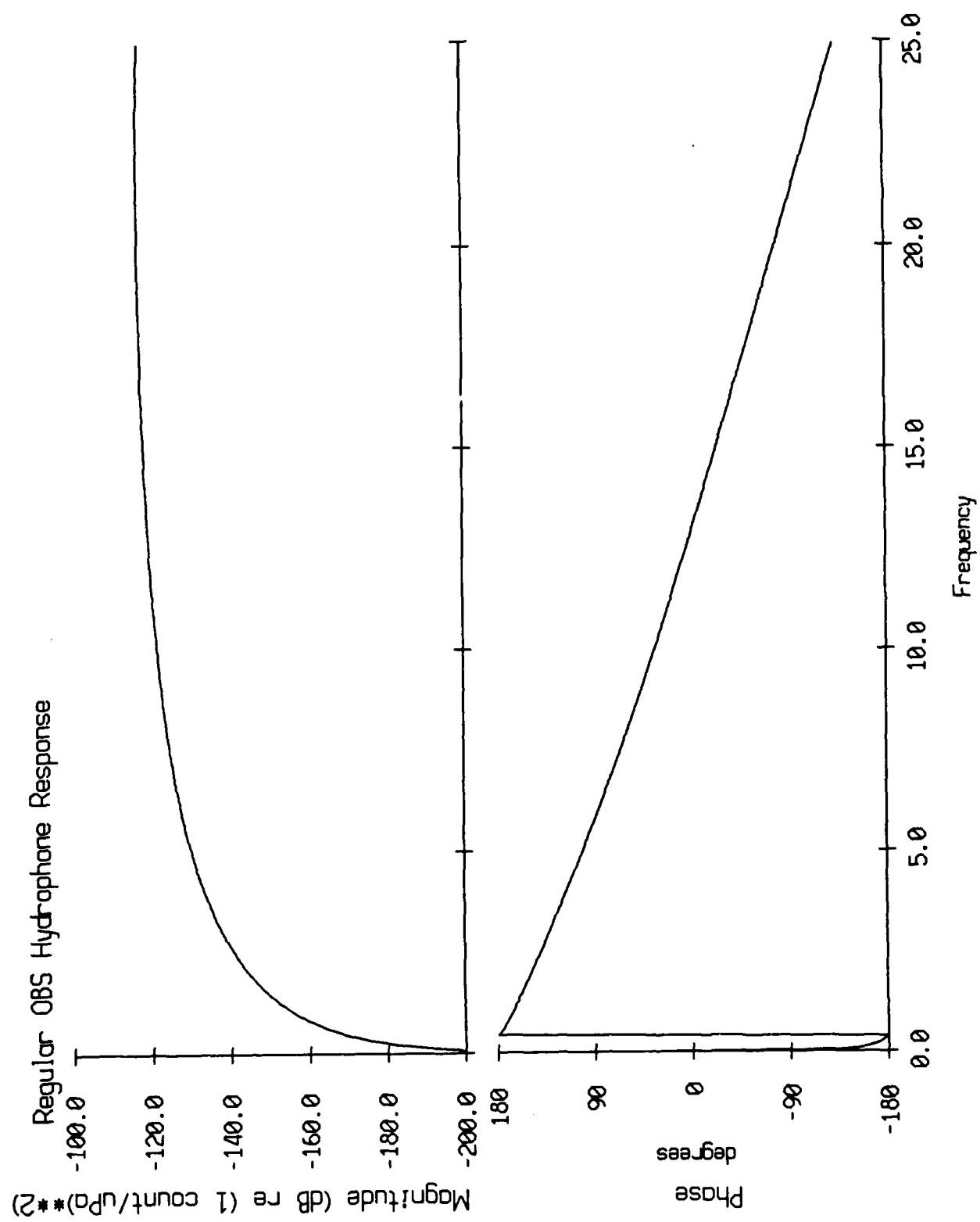


Figure A2.2

September 1987 SVLA Experiment

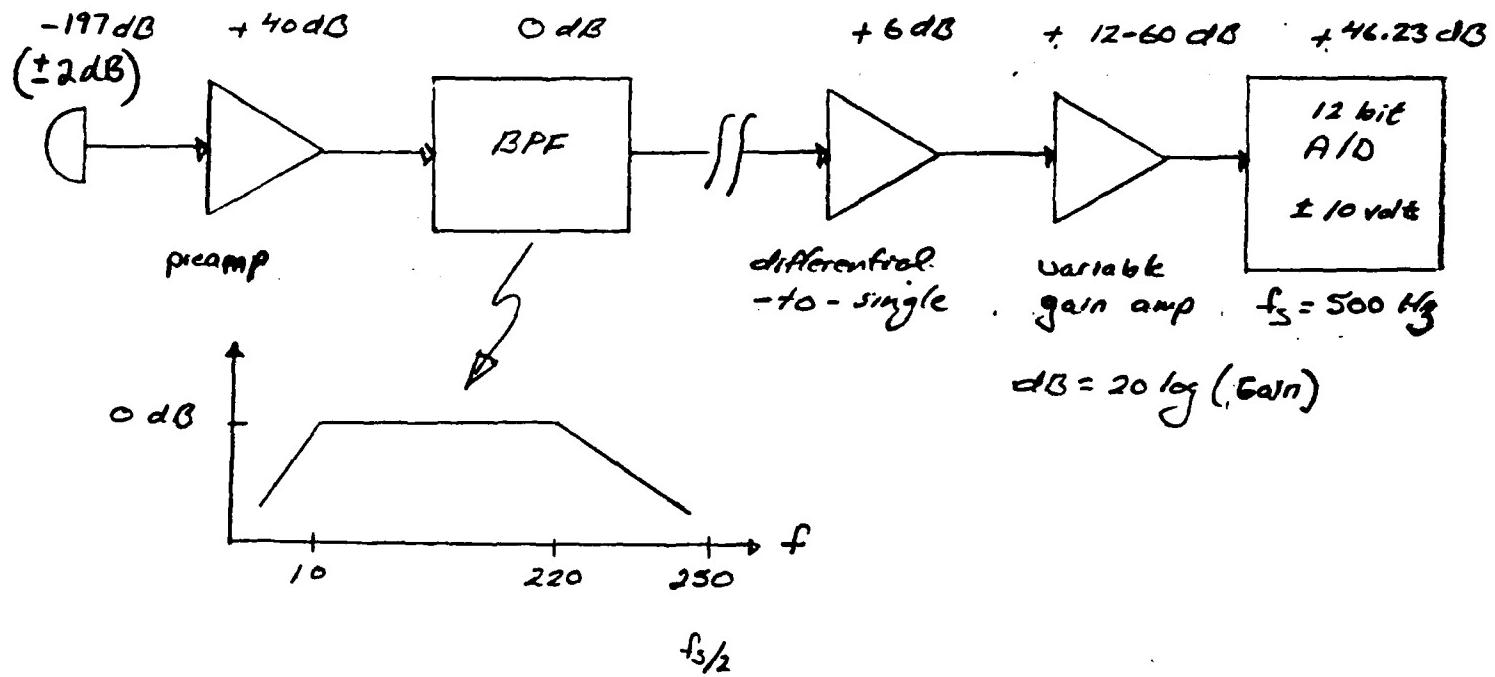


Figure A3.1

Vertical Line Array Channel Amplitude Response
September, 1987 Experiment

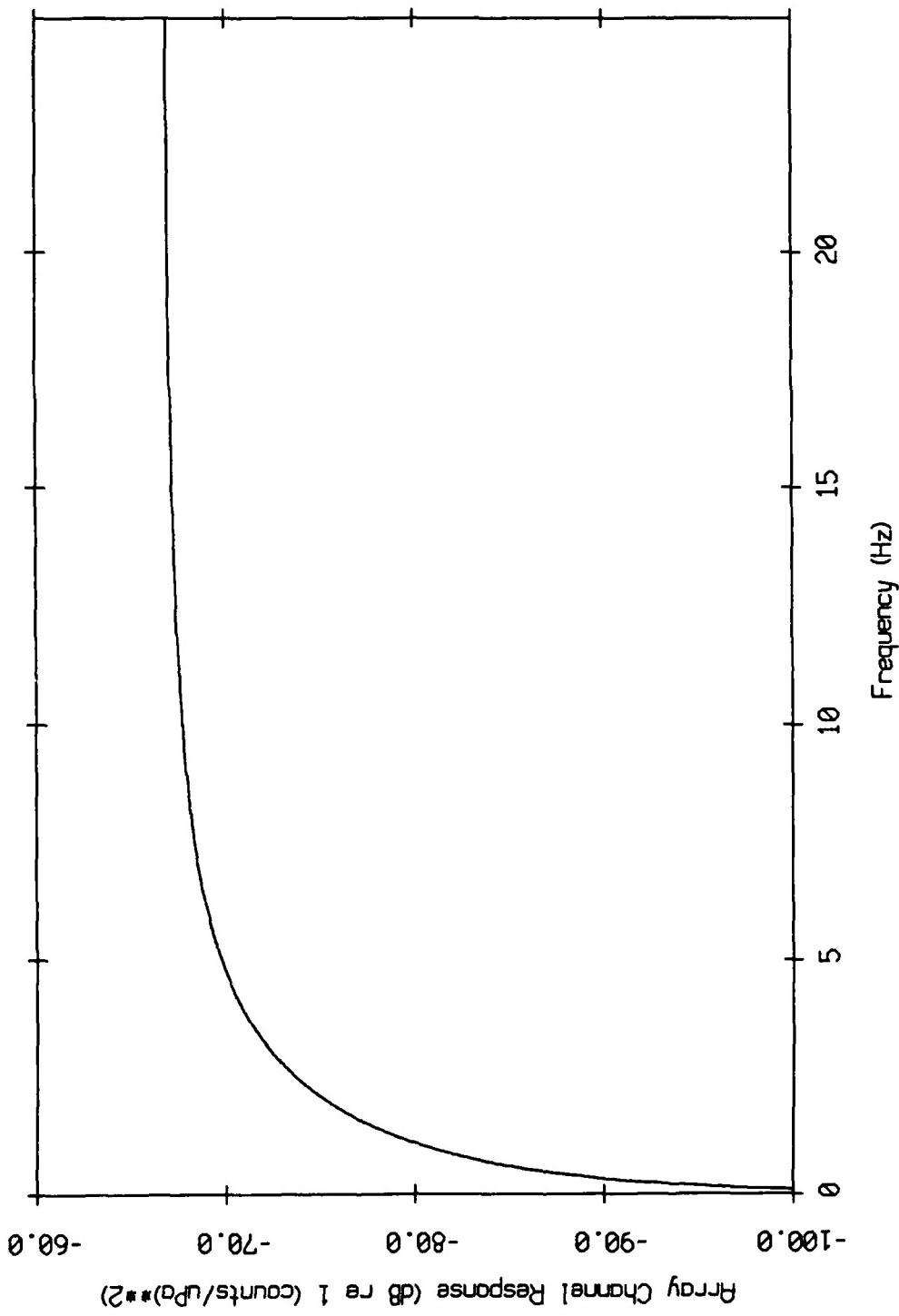


Figure A3.2

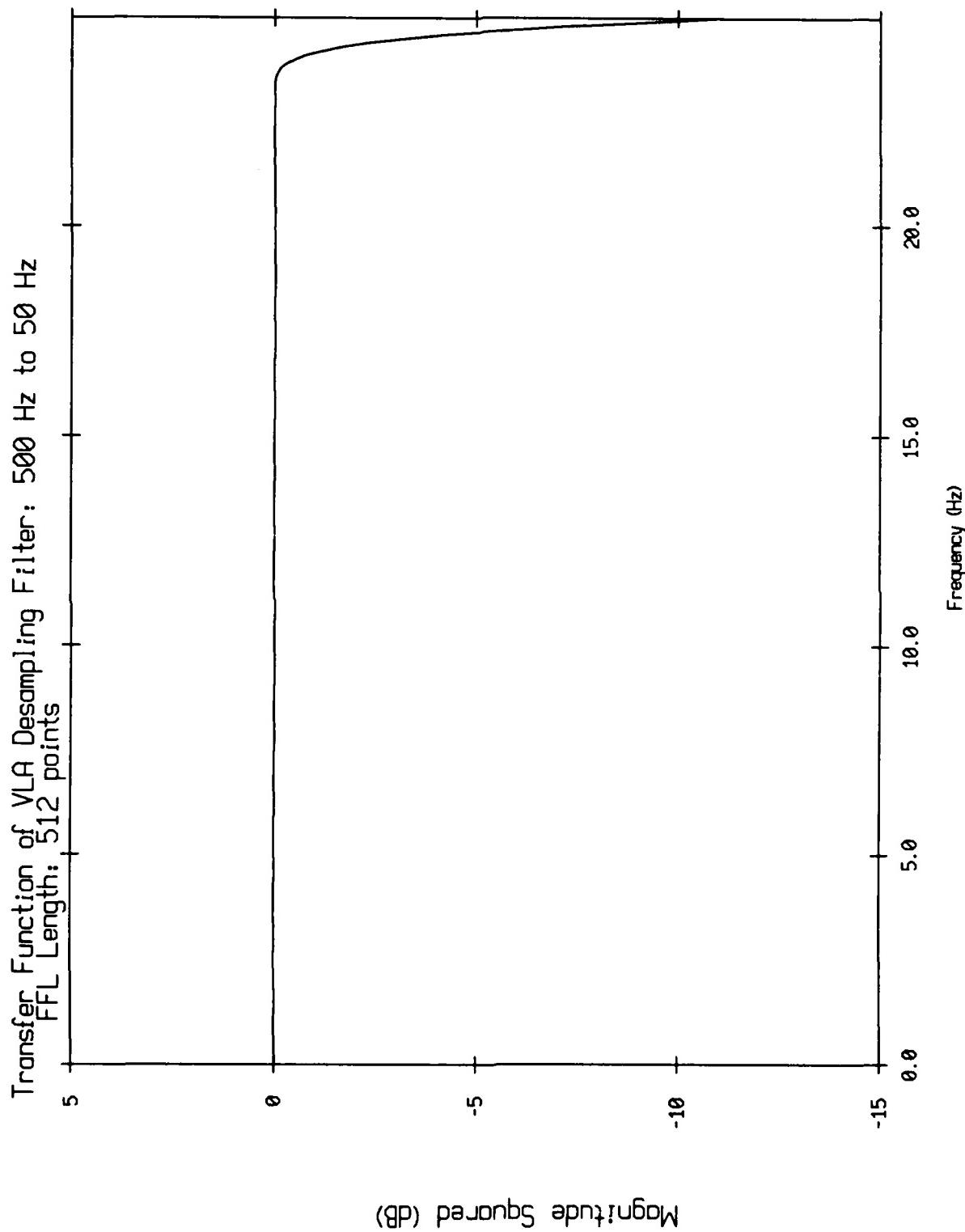


Figure A3.3